This publication is available free of charge from: https://doi.org/10.6028/NIST.IR.8271

NISTIR 8271 DRAFT SUPPLEMENT

Face Recognition Technology Evaluation (FRTE)

Part 2: Identification

Patrick Grother
Mei Ngan
Kayee Hanaoka
Information Access Division
Information Technology Laboratory

This document is a draft supplement of NIST Interagency Report 8271

2026/01/09

National Institute of Standards and Technology
U.S. Department of Commerce

This publication is available free of charge from: https://doi.org/10.6028/NIST.IR.8271

NISTIR 8271 DRAFT SUPPLEMENT

Face Recognition Technology Evaluation (FRTE)

Part 2: Identification

Patrick Grother
Mei Ngan
Kayee Hanaoka

Information Access Division
Information Technology Laboratory

This document is a draft supplement of NIST Interagency Report 8271

January, 2026

U.S. Department of Commerce
Howard Lutnick, Secretary

National Institute of Standards and Technology
Craig Burkhardt, Acting Under Secretary of Commerce for Standards and Technology and Acting NIST Director

RELEASE NOTES

2026-01-09: The 1:N track of the FRTE remains open.

- ▷ This document is the forty eighth draft update to NIST Interagency Report 8271. It contains results for three new developer: Biometrik Systems Private Limited, FAST-NUCES Lahore Campus, and Sparktek International Pte Ltd.
- ▷ The document also includes results for algorithms for seven returning developers: Clearview AI Inc, Compal Electronics, Hyundai Motor Company, Innovatrics, NEC, Panasonic R+D Center Singapore, and VDF Software.

2025-09-30: The 1:N track of the FRTE remains open.

- ▷ This document is the forty seventh draft update to NIST Interagency Report 8271. It contains results for three new developer: LightVision Inc, Protenet Soluções em Segurança, and Toss.
- ▷ The document also includes results for algorithms for one returning developers: Dermalog.

2025-08-27: The 1:N track of the FRTE remains open.

- ▷ This document is the forty sixth draft update to NIST Interagency Report 8271. It contains results for one new developer: Private Identity LLC.
- ▷ The document also includes results for algorithms for thirteen returning developers: AllGoVision, DAON, Incode Technologies Inc, Metsakuur, NextMedia Labs, Neurotechnology, Omnigarde, Panasonic R+D Center Singapore, Pentacomp Systemy Informatyczne, ROC, TigerIT Americas LLC, Toshiba, and VinBigData.

2025-07-17: The 1:N track of the FRTE remains open.

- ▷ This document is the forty fifth draft update to NIST Interagency Report 8271. It contains results for one new developers: IDENTY.
- ▷ The document also includes results for algorithms for six returning developers: Hyundai Motor Company, Idemia, Innovatrics, Paravision, STCON LLC, and Universidade de Coimbra.

2025-05-28: The 1:N track of the FRTE remains open.

- ▷ This document is the forty fourth draft update to NIST Interagency Report 8271. It contains results for three new developers: Adiance Technologies, RNIT Solutions and Services, and VDF Software.
- ▷ The document also includes results for algorithms for four returning developers: Cubox, Dermalog, QazSmartVision.AI, and Samsung S1.

2025-04-25: The 1:N track of the FRTE remains open.

- ▷ This document is the forty third draft update to NIST Interagency Report 8271. It contains results for five new developers: Compal Electronics, FCI Vietnam, GTEL OTS JSC, i2V Systems, and ioNetworks.
- ▷ The document also includes results for algorithms for five returning developers: Intel Research Group, Mobbeel Solutions, Pyramid Cyber Security + Forensic (P), Viante.AI, and Viettel Cyberspace Center.

2025-03-18: The 1:N track of the FRTE remains open.

- ▷ This document is the forty second draft update to NIST Interagency Report 8271. It contains results for two new developers: Algorithms Inc, and Maverick Research.
- ▷ The document also includes results for algorithms for four returning developers: AFR Engine, Akuvox, EI Networks, and VinBigData.

2025-03-05: The 1:N track of the FRTE remains open.

This publication is available free of charge from: https://doi.org/10.6028/NIST.IR.8271

- ▷ This document is the forty first draft update to NIST Interagency Report 8271. It contains results for three new developers: Awidit Systems, Hyundai Motor Company, and Kloudspot.
- ▷ The document also includes results for algorithms for seven returning developers: Innovatrics, Inspur (Beijing) Electronic Information Industry, NEC, Nominder, ROC, STCON, and Viettel Group

2025-02-05: The 1:N track of the FRTE remains open.

- ▷ This document is the fortieth draft update to NIST Interagency Report 8271. It contains results for three new developers: Keyless Technologies, Pentacomp Systemy Informatyczne, and TTI Group.
- ▷ The document also includes results for algorithms for four returning developers: DAON, Hangzhuo AIlu Network Information Technology, Unissey and useB.

2024-12-18: The 1:N track of the FRTE remains open.

- ▷ This document is the thirty nine draft update to NIST Interagency Report 8271. It contains results for two new developers: Pyramid Cyber Security + Forensic, and Shennona.
- ▷ The document also includes results for algorithms for nine returning developers: Alchera, Cubox, IMDS Software, Paravision, QazSmartVision.AI, Samsung S1, Sensetime, Vietnam Posts and Telecommunications Group, and Vision-Box.

2024-11-08: The 1:N track of the FRTE remains open.

- ▷ This document is the thirty eighth draft update to NIST Interagency Report 8271. It contains results for six new developers: FacePhi, Metsakuur, Nextmeta Labs, Scylla Technologies, Seventh Sense Artificial Intelligence, and Vietnam Payment Solution.
- ▷ The document also includes results for algorithms for four returning developers: EI Networks, Innovatrics, Nominder, STCON, Viettel Group, VinBigData, and WINK.

2024-09-18: The 1:N track of the FRTE remains open.

- ▷ This document is the thirty seventh draft update to NIST Interagency Report 8271. It contains results for three new developers: Antheus Technologia, Beijing Hisign Technology, and PT Ice House.
- ▷ The document also includes results for algorithms for four returning developers: Cognitec Systems, Neurotechnology, Qnap Security, and useB.
- ▷ In addition, many graphs for algorithms submitted between June 2023 and August 2024 have been included for the first time. They had incorrectly been omitted from several reports issued in that timeframe.

2024-08-09: The 1:N track of the FRTE remains open.

- ▷ This document is the thirty sixth draft update to NIST Interagency Report 8271. It contains results for one new developer: NextMedia Labs, OptiExacta and Universidade de Coimbra.
- ▷ The document also includes results for algorithms for seven returning developers: AFR Engine, Incode, Panasonic R+D Center Singapore and QazSmartVision.AI.

2024-07-03: The 1:N track of the FRTE remains open.

- ▷ This document is the thirty fifth draft update to NIST Interagency Report 8271. It contains results for one new developer: Sansap Technology.
- ▷ The document also includes results for algorithms for seven returning developers: Alchera, Clearview AI, Cyberlink Corp, Dermalog, Nominder, Omnigarde, and ROC.

2024-05-30: The 1:N track of the FRTE remains open.

This publication is available free of charge from: https://doi.org/10.6028/NIST.IR.8271

- ▷ This document is the thirty forth draft update to NIST Interagency Report 8271. It contains results for seven new developers: ALTTEKGlobal, Aratek Biometrics, BioID Technologies, EI Networks Private, Kogniza Technology, STCON, and VinBigData.
- ▷ The document also includes results for algorithms for five returning developers: AadiSysTech, Cognitec Systems, Hangzhuo AIlu Network Information Technology, Innovatrics, and Mobbeel Solutions.

2024-04-29: The 1:N track of the FRTE remains open.

- ▷ This document is the thirty third draft update to NIST Interagency Report 8271. It contains results for one new developer: FPT Smart Cloud
- ▷ The document also includes results for algorithms for one returning developer: Vision-Box

2024-03-26: The 1:N track of the FRTE remains open.

- ▷ This document is the thirty second draft update to NIST Interagency Report 8271. It contains results for one new developer: QazSmartVision.AI
- ▷ The document also includes results for algorithms for eight returning developers: AFR Engine, Corsight AI, Dactionable Technologies, Idemia, IMDS Software, Megvii/Face++, Panasonic R+D Center, and Unissey.

2024-02-21: The 1:N track of the FRTE remains open.

- ▷ This document is the thirty first draft update to NIST Interagency Report 8271. It contains results for one new developer: Yuan High-Tech Development.
- ▷ The document also includes results for algorithms for two returning developers: Clearview AI, and useB.

2024-01-22: The 1:N track of the FRTE remains open.

- ▷ This document is the thirtieth draft update to NIST Interagency Report 8271. It contains results for two new developer: Sparsh CCTV, and VNIS Joint Stock.
- ▷ The document also includes results for algorithms for ten returning developer: Dermalog, ICM Airport Technics, Innovatrics, Maxvision, Viettel Cyberspace Center, NEC, Neurotechnology, Nominder, ROC, and WINK.

2023-12-18: The 1:N track of the FRTE remains open.

- ▷ This document is the twenty nineth draft update to NIST Interagency Report 8271. It contains results for one new developer: Mobbeel Solutions.
- ▷ The document also includes results for algorithms for seven returning developer: AadiSysTech, Alchera, Aware, Cognitec Systems, Inspur (Beijing) Electronic Information, Qnap Security, and Vietnam Posts and Telecommunications Group.

2023-11-20: The 1:N track of the FRTE remains open.

- ▷ This document is the twenty eighth draft update to NIST Interagency Report 8271. It contains results for four new developer: Dactionable Technologies, IMDS Software Inc, Luxand Inc, and Unissey.
- ▷ The document also includes results for algorithms for seven returning developer: AllGoVision, Hangzhuo AIlu Network Information Technology, Kakao Brain, Megvii/Face++, Recognito, Verigram, and Viante.AI.

2023-09-29: The 1:N track of the FRTE remains open.

- ▷ This document is the twenty seventh draft update to NIST Interagency Report 8271. It contains results for one new developer: Nominder.

This publication is available free of charge from: https://doi.org/10.6028/NIST.IR.8271

- ▷ The document also includes results for algorithms for one returning developer: useB.

2023-09-09: The 1:N track of the FRTE remains open.

- ▷ We have renamed and split FRVT into two sets of technology evaluations: The Face Recognition Technology Evaluation (FRTE) is the umbrella for the ongoing 1:1, 1:N and twins disambiguation tracks; the Face Analysis Technology Evaluation (FATE) holds the morph and attacked detection tracks, the quality assessment tracks, and the new age estimation tracks.
- ▷ This document is the twenty sixth draft update to NIST Interagency Report 8271. It contains results for two new developers: ICM Airport Technics and Papilon Savunma.
- ▷ The document also includes results for algorithms for two returning developers: Canon and Tripleize.

2023-08-16: The 1:N track of the FRVT remains open.

- ▷ This document is the twenty fifth draft update to NIST Interagency Report 8271. It contains results for two new developers: Panasonic and Sumsub.
- ▷ The document also includes results for algorithms for two returning developers: Maxvision and Innovatrics.

2023-07-28: The 1:N track of the FRVT remains open.

- ▷ This document is the twenty fourth draft update to NIST Interagency Report 8271. It contains results for four new developers: AFR Engine, Corsight, Wink and Viettel Cyberspace Center.
- ▷ The document also includes results for algorithms for seven returning developers: Alchera, Cubox (cubox.aero), NEC, Rank One Computing, Samsung S-1, Tech5 SA, and Verihubs Inteligensia.

2023-07-05: The 1:N track of the FRVT remains open.

- ▷ This document corrects mugshot-mugshot results for algorithms submitted to FRVT 2023-02 to 2023-06. The prior report's FNIR values were uniformly approximately 0.003 higher due to a bug introduced into a script by changes to the FRVT API.

2023-07-03: The 1:N track of the FRVT remains open.

- ▷ This document is the twenty third draft update to NIST Interagency Report 8271. It contains results for eight first-time participants: Advance.AI, AFIS and Biometrics Consulting, Inspur (Beijing) Electronic Information Industry, Know U Tech, Omnigarde, Serendipity, useB, and Verigram.
- ▷ The document also includes results for algorithms for four returning developers: Hangzhuo AIlu Network Information Technology, Megvii/Face++, Paravision, and Qnap Security.

2023-04-20: The 1:N track of the FRVT is closed until 2023-05-01.

- ▷ This document is the twenty third draft update to NIST Interagency Report 8271. It contains results for one first-time participant: Armatura LLC.
- ▷ The document also includes results for algorithms for two returning developers: HyperVerge, Maxvision.

2023-03-29: The 1:N track of the FRVT remains open.

- ▷ This document is the twenty third draft update to NIST Interagency Report 8271. It contains results for one first-time participant: Recognito.
- ▷ The document also includes results for algorithms for one returning developer: AllGoVision Technologies.

2023-03-14: The 1:N track of the FRVT remains open.

This publication is available free of charge from: https://doi.org/10.6028/NIST.IR.8271

- ▷ This document is the twenty second draft update to NIST Interagency Report 8271. It contains results for no first-time participants.
- ▷ The document also includes results for algorithms from nine returning developers: Cloudwalk - Moontime Smart Technology, Line Corporation, Intema-LGL Group Neurotechnology, NEC, Paravision, Samsung S1, Veridas Digital Authentication Solutions, and Thales Group

2023-02-06: The 1:N track of the FRVT remains open.

- ▷ This document is the twenty first draft update to NIST Interagency Report 8271. It contains results for no first-time participants.
- ▷ The document also includes results for algorithms from seven returning developers: Dermalog, DiluSense Technology, Hangzhuo AIlu Network Information Technology, Idemia, Innovatrics, Rank One Computing, and Sensetime Group.

2022-12-15: The 1:N track of the FRVT remains open.

- ▷ This document is the twentieth draft update to NIST Interagency Report 8271. It contains results for one first-time participant: First Credit Bureau Kazakhstan.
- ▷ The document also includes results for algorithms from five returning developers: Gorilla Technology, Pangiam, Qnap Scurity, SQIsoft, Vixvizion (formerly known as Imagus).

2022-11-09: The 1:N track of the FRVT remains open.

- ▷ This document is the nineteenth draft update to NIST Interagency Report 8271. It contains results for four first-time participant: Mukh, Turing Technology VIP, Verijelas and Verihubs Inteligensia
- ▷ The document also includes results for algorithms from two returning developers: Maxvision and Samsung S1.

2022-09-23: The 1:N track of the FRVT remains open.

- ▷ This document is the eighteenth draft update to NIST Interagency Report 8271. It contains results for two first-time participants: Intema-LGL Group and T4iSB.
- ▷ The document also includes results for algorithms from two returning developers: Cloudwalk - Moontime Smart Technology, Dermalog, Griaule, Hangzhuo AIlu Network Information Technology, Intellivision, Line Corporation, NEC, Sensetime Group, Realnetworks Inc and Vietnam Posts and Telecommunications Group.

2022-07-28: The 1:N track of the FRVT remains open.

- ▷ This document is the seventeenth draft update to NIST Interagency Report 8271. It contains results for one first-time participant: Maxvision.
- ▷ The document also includes results for algorithms from two returning developers: Rank One Computing, and Viettel Group.
- ▷ We have replaced the probe set used in the visa-border benchmark. It was previously comprised of 80 000 images; it now has size 1 212 892 - see amended entries in Table 1. False negative identification rates have increased.
- ▷ We have added images to the probe set used in the visa-kiosk benchmark. It was previously comprised of 21 016 mates and the same number of non-mates; it now has 31 579 mates and 45 460 non-mates - see amended and entries in Table 1. False negative identification rates are improved (reduced) slightly.

2022-06-08: The 1:N track of the FRVT remains open.

This publication is available free of charge from: https://doi.org/10.6028/NIST.IR.8271

- This document is the seventeenth draft update to NIST Interagency Report 8271. It includes results for algorithms submitted by three first-time participants: Digidata, DiluSense Technology, and Vietnam Posts and Telecommunications Group.
- The document also includes results for algorithms from five returning developers: Canon Inc, Imagus Technology, Neurotechnology, Thales, and Samsung S1.

2022-04-28: The 1:N track of the FRVT remains open.

- This document is the sixteenth draft update to NIST Interagency Report 8271. It includes results for algorithms submitted by one first-time participants: Hangzhuo AIlu Network Information Technology.
- The document also includes results for algorithms from three returning developers: HyperVerge Inc, Qnap Security, and Realnetworks Inc.
- The 1:N results page has been updated.

2022-03-30: The 1:N track of the FRVT remains open.

- This document is the sixteenth draft update to NIST Interagency Report 8271. It includes results for algorithms submitted by two first-time participants: Intellivision, and Pangiam.
- The document also includes results for algorithms from three returning developers: Fujitsu Research and Development Center, Idemia, and Gorilla Technology.
- The 1:N results page has been updated.

2022-02-23: The 1:N track of the FRVT remains open.

- This document is the fifteenth draft update to NIST Interagency Report 8271. It includes results for algorithms submitted by four first-time participants: Cloudwalk - Moontime Smart Technology, Decatur Industries Inc, NotionTag Technologies Private Limited, and Reveal Media Ltd.
- The document also includes results for algorithms from three returning developers: Cognitec Systems GmbH, Sensetime Group, and Viettel Group
- The 1:N results page has been updated.

2022-01-20: The 1:N track of the FRVT remains open.

- This document is the fourteenth draft update to NIST Interagency Report 8271. It includes results for algorithms recently submitted by two first-time participants: Daon and SQIsoft.
- The document also includes results for algorithms from five returning developers: Cyberlink Corp, NEC, Neurotechnology, Paravision, and Rank One Computing.
- The 1:N results page has been updated.

2021-12-16: The 1:N track of the FRVT remains open.

- This document is the thirteenth draft update to NIST Interagency Report 8271. It includes results for algorithms from six returning developers: Dahua Technology, Imagus Technology, Line Corporation, N-Tech Lab, Qnap Security, and Realnetworks Inc.
- The 1:N results page has been updated.

2021-11-22: The 1:N track of the FRVT remains open.

- This document is the twelfth draft update to NIST Interagency Report 8271. It includes results for algorithms recently submitted by three first-time participants Clearview AI, Griaule, and Mantra Softech India.

This publication is available free of charge from: https://doi.org/10.6028/NIST.IR.8271

- This document and the 1:N results page also include results for algorithms from six returning developers: Acer Incorporated, Canon, Dermalog, Samsung S1, VisionLabs, and Veridas Digital Authentication.

2021-10-28: The 1:N track of the FRVT remains open.

- This document is the eleventh draft update to NIST Interagency Report 8271. It includes results for algorithms recently submitted by three first-time participants (20Face, Fujitsu Research and Development Center, and Vision-Box), and five returning participants (Alchera, Gorilla Technology, Tevian, Thales-Cogent, and Visidon). Visidon
- Both the main 1:N results page and the small-gallery paperless travel page have been updated.

2021-09-21: The 1:N track of the FRVT remains open. Three news items:

- This document is the tenth draft update to NIST Interagency Report 8271. It includes results for algorithms recently submitted by six first-time developers: Cubox, Fincore, HyperVerge, Qnap Security, Staqu Technologies, and Tripleize (Aize, 3-ize).
- It includes results also for four returning developers: Cognitec Systems, Incode Technologies, Innovatrics, Neurotechnology, and Rank One Computing.

2021-08-02: The 1:N track of the FRVT remains open. Three news items:

- This document is the nineth draft update to NIST Interagency Report 8271. It includes results for algorithms recently submitted by eight participants: Cyberlink Corp, NEC Corp, N-Tech Lab, Realnetworks Inc., Sensetime Group, Veridas Digital, Viettel Group, and Vigilant Solutions.
- Algorithms submitted since July 24 will be included in the next update scheduled for September 9, 2021.
- A new report, NIST Interagency Report 8381 - FRVT Part 7: Identification for Paperless Travel and Immigration, has been released [PDF, webpage]. It documents the use of FRVT 1:N algorithms in positive access control and immigration status update travel applications where the enrolled population size is as low as 420 people for aircraft boarding, and 42 000 for an airport security line. These population sizes are much smaller than those used in the main 1:N evaluation. Going forward, we will update the report and webpage with results for new algorithms.

2021-07-07: The 1:N track of the FRVT remains open. One update:

- This document is the eighth draft update to NIST Interagency Report 8271. It include results for an algorithm from one participant: Kakao Enterprises.

2021-06-22: The 1:N track of the FRVT remains open. Three updates:

- This is the seventh draft of the update to NIST Interagency Report 8271. It includes results for algorithms from three new participants: Line Corporation, Rendip, and Samsung S1 Corp.
- We have also added results for algorithms from five returning developers: Imagus Technology, Kneron, Tevian, Visidon, and Xforward AI Technology.
- The algorithm-specific report cards (examples: 1, 2, and 3) now include figures showing how low threshold values can be used to reduce candidate list lengths for human review, while (usually) elevating miss rates (FNIR) only modestly. The reports also feature some minor additions and clarifications.

2021-03-26: The 1:N track of the FRVT remains open. Three updates:

- This is the sixth draft of the update to NIST Interagency Report 8271. It includes results for algorithms from three returning developers: Neurotechnology, Guangzhou Pixel Solutions, and Tech5 SA.

This publication is available free of charge from: https://doi.org/10.6028/NIST.IR.8271

- ▷ We have added results on the webpage and in the report for a new ageing dataset in which border crossing photos are searched against a gallery of border crossing photos collected between 10 and 15 years prior to the mated search photos. See section 2 for a description of the images. Table 1 has a new entry describing the experiment.
- ▷ We will mostly discontinue running the mugshot ageing test, reserving it for algorithms that show high accuracy on the new border-crossing set.

2021-03-26: Regarding the fifth draft of the update to NIST Interagency Report 8271:

- ▷ In addition have added results for first algorithms from two new participants: Viettel Group and Veridas Digital Authentication Solutions.
- ▷ We have added results for algorithms from two returning developers: Idemia and Cognitec Systems.
- ▷ In addition to the report, the results page and its hyperlinked report cards have been updated.

2021-02-08: Regarding the fourth draft of the update to NIST Interagency Report 8271:

- ▷ We have added results for eight algorithms submitted by eight developers: Cyberlink, Dermalog, Imagus, Paravision, Sensetime, Trueface, Vigilant Solutions, and X-Forward AI. With the exception of Trueface, all of these developers have participated previously.
- ▷ We anticipate updating this report again in the first week of March 2021.
- ▷ The main results page has been revised with tabs for the investigative and lights-out identification tables, and a new tab dedicated to speed and resource consumption.
- ▷ The report cards (example here) hyperlinked from the results page have been revised to improve content and format.

2020-12-14: Regarding third draft of the update to NIST Interagency Report 8271:

- ▷ We have added results for fifteen algorithms submitted by thirteen developers. The four first-time participants are: Acer, Akurat Satu Indonesia, Canon, and Xforward AI Technology. The ten returning developers are: AllGoVision, Cyberlink Corp, Dahua Technology, Deepglint, Guangzhou Pixel Solutions, IIT Vision, Innovatrics, Rank One Computing, Scanovate, Sensetime Group, Synesis, and VisionLabs.
- ▷ We have added two new datasets to the evaluation: First a set of "visa-border" photos, representing search of an airport immigration lane photo against a database of closely ISO standard portraits; second a "visa-kiosk" set representing search of a photo collected in a registered traveller kiosk against the same ISO portrait gallery. The images are described in section 2.1.
- ▷ As in previous reports, we include results for searching mugshots against a mugshot gallery containing a single image of each of 12 million people. However we have suspending running searches against a gallery in which multiple lifetime photos per person are present, because this is computationally expensive. We retain a N = 3 million search test dedicated to ageing in which mugshots taken up to 18 years after the first photograph are searched - see Table 12.
- ▷ Tables containing computational resource information, Table 2. . ., now include duration of the finalization step, in which search algorithms can, at their option, build fast-search data structures.
- ▷ We have linked revised per-algorithm PDF report cards from the main results page.
- ▷ We have regenerated all figures and tables to drop algorithms submitted before June 2018. Results for prior algorithms appear in archived editions of this report.
- ▷ Going forward, we anticipate producing more frequent updates to this report. Developers may submit one algorithm to this evaluation every four calendar months.

2020-03-24: Regarding the second draft of the update to NIST Interagency Report 8271:

This publication is available free of charge from: https://doi.org/10.6028/NIST.IR.8271

- ▷ Adds results for three algorithms from three developers, Dermalog, Innovatrics, and Synesis.
- ▷ Adds Table 12 on ageing showing the increase in false negative rates with time elapsed between two photos. Some of the results were contained in graphs in prior editions of this report, but the table adds results for some newly submitted algorithms.
- ▷ Adjusts frontal mugshot results (for recent and lifetime consolidated galleries) to include the effect of removing some images that should not have been included in image test sets. These images were mostly profile views, images of tattoos containing faces, images of faces on tee shirts, and images of photographs on walls behind the intended subject. This affects many tables and reduces false negative identification rates for all algorithms. The reduction is larger for "recent" enrollments than for "lifetime consolidated" ones with the consequence that accuracy on recent images is now superior.

2020-02-26: Regarding the first draft of the update to NIST Interagency Report 8271:

- ▷ Adds results for 38 algorithms from 31 different developers, eleven of whom are entirely new to the 1:N track of FRVT. These are Allgovision, Cyberlink, Deepsea Tencent, Farbar F8, Imperial College London, Intsys MSU, Kedacom, Kneron, Pixelall, and Scanovate.

This publication is available free of charge from: https://doi.org/10.6028/NIST.IR.8271

DISCLAIMER

Specific hardware and software products identified in this report were used in order to perform the evaluations described in this document. In no case does identification of any commercial product, trade name, or vendor, imply recommendation or endorsement by the National Institute of Standards and Technology, nor does it imply that the products and equipment identified are necessarily the best available for the purpose.

INSTITUTIONAL REVIEW BOARD

The National Institute of Standards and Technology's Research Protections Office reviewed the protocol for this project and determined it is not human subjects research as defined in Department of Commerce Regulations, 15 CFR 27, also known as the Common Rule for the Protection of Human Subjects (45 CFR 46, Subpart A).

ACKNOWLEDGMENTS

The authors are grateful for the support and collaboration of the the Department of Homeland Security's Science & Technology Directorate (S&T), Office of Biometric Identity Management (OBIM), and Customs and Border Protection (CBP).

Additionally, the authors are grateful to staff in the NIST Biometrics Research Laboratory for infrastructure supporting rapid evaluation of algorithms.

This publication is available free of charge from: https://doi.org/10.6028/NIST.IR.8271

Executive Summary

This document is a draft revision of the September 2019 report NIST Interagency Report 8271. That report gave extensive documentation of face recognition applied to mugshots. This report extends that by adding more two more challenging datasets containing images with serious departures from canonical frontal image standards. The report also adds results for algorithms submitted to NIST since in 2019 and 2020. The algorithms, which implement one-to-many identification of faces appearing in two-dimensional images, are prototypes from the research and development laboratories of mostly commercial suppliers, and are submitted to NIST as compiled black-box libraries implementing a NIST-specified C++ test interface. The report therefore does not describe how algorithms operate. The report lists accuracy results alongside developer names and will therefore be useful for comparison of face recognition algorithms and assessment of absolute capability. The report is accompanied by a webpage with sortable results.

The evaluation uses six datasets: frontal mugshots, profile view mugshots, desktop webcam photos, visa-like immigration application photos, immigration lane photos, and registered traveler kiosk photos. These datasets are sequestered at NIST, meaning that developers do not have access to them for training or testing. This aspect is important because face recognition algorithms are very often deployed without the developer having access to the customers image data. A possible exception to this would be in a cloud-based application where the operational image data is uploaded to a cloud operated by a face recognition developer.

The major result in NIST IR 8271 was that massive gains in accuracy have been achieved in the years 2013 to 2018 and these far exceed improvements made in the prior period, 2010 to 2013. While the industry gains were broad - at least 30 developers' algorithms outperformed the most accurate algorithm from late 2013, there remains a wide range of capability. While this report shows accuracy gains only over the period 2018-2020, the most accurate algorithm reported here is substantially more accurate than anything reported in NIST IR 8271. This is evidence that face recognition development continues apace, and that FRVT reports are but a snapshot of contemporary capability.

From discussion with developers, the accuracy gains stem from the adoption of deep convolutional neural networks. As such, face recognition has undergone an industrial revolution, with algorithms increasingly tolerant of poorly illuminated and other low quality images, and poorly posed subjects. One related result is that a few algorithms correctly match side-view photographs to galleries of frontal photos, with search accuracy approaching that of the best c. 2010 algorithms operating on purely frontal images. The capability to recognize under a 90-degree change in viewpoint - pose invariance - has been a long-sought milestone in face recognition research.

With good quality portrait photos, the most accurate algorithms will find matching entries, when present, in galleries containing 12 million individuals, with rank one miss rates of approaching 0.1%. The remaining errors are in large part attributable to long-run ageing, facial injury and poor image quality. Given this impressive achievement - close to perfect recognition - an advocate might claim that cooperative face recognition is a solved problem, a statement that can be refuted with the following context and caveats:

- **Mugshots vs. less constrained captures:** The low error rates reported here are attained using mostly excellent cooperative live-capture mugshot images collected with an attendant present. Recognition in other circumstances, particularly those without a dedicated photographic environment and human or automated quality control checks, will lead to declines in accuracy. This is documented here for side-view images, poorer quality webcam images, and, particularly, for newly introduced ATM-style kiosk photos that were not originally intended for automated face recognition. In this case, recognition error rates are much higher, often in excess of 20% even with the more accurate algorithms which variously remain intolerant of face cropping (at image edge) and of large downward head pitch.
- **Algorithm accuracy spectrum:** Recognition accuracy is very strongly dependent on the algorithm and, more

This publication is available free of charge from: https://doi.org/10.6028/NIST.IR.8271

This publication is available free of charge from: https://doi.org/10.6028/NIST.IR.8271

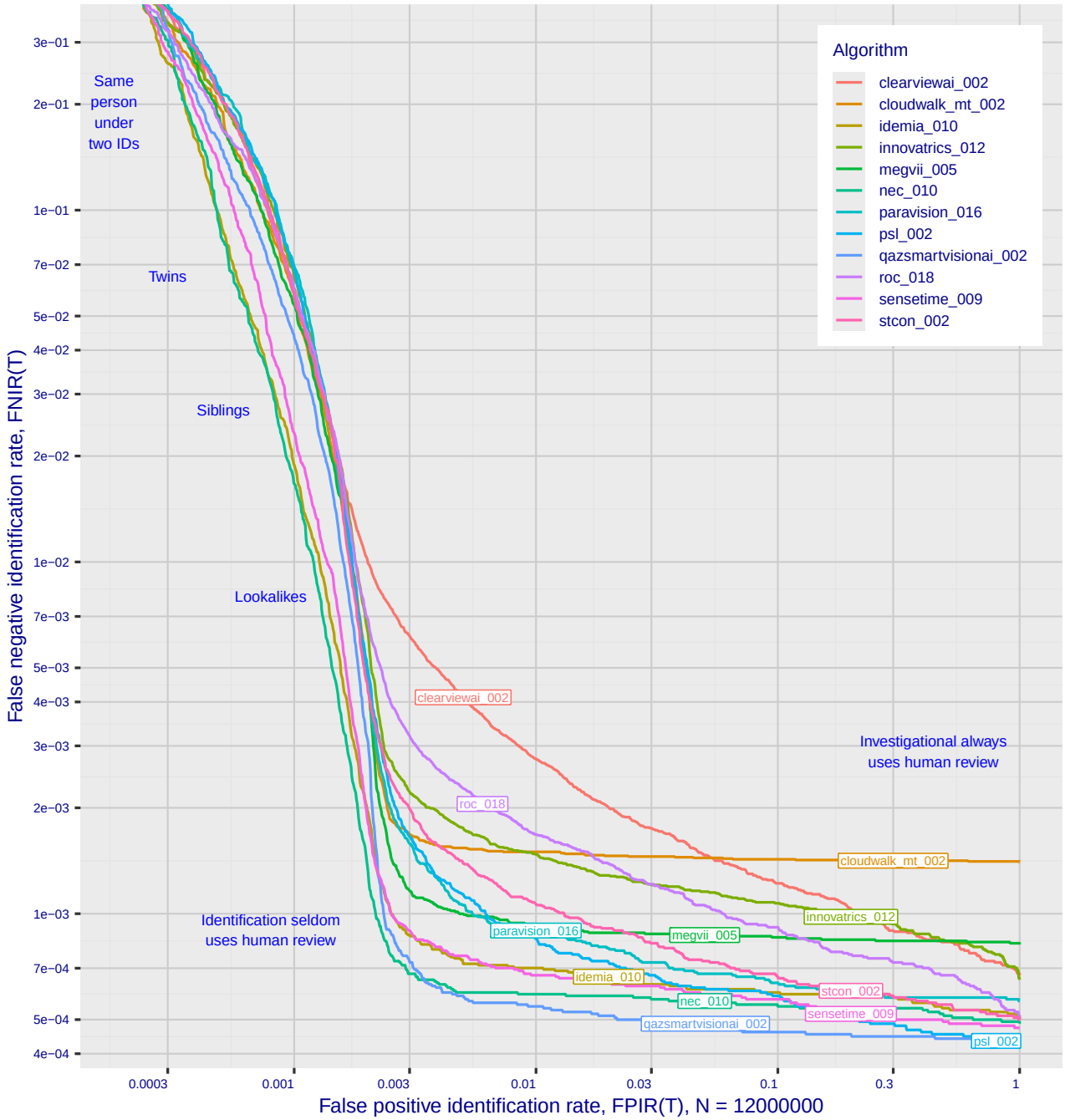

Figure 1: Identification miss rates across the false positive range. N = 12 million individuals are enrolled with one recent image.

generally, on the developer of the algorithm. False negative error rates in a particular scenario range from a few tenths of one percent to beyond fifty percent. This is tabulated exhaustively later: For example Table 20 shows accuracy across datasets. Figure 1 here compares algorithms on mugshot searches in a consolidated gallery of 12 million subjects and 12 million photos. Many algorithms do not achieve the low error rates noted above, and while many of those may still be useful and valuable to end-users, only the most accurate excel on poor quality images and those collected long after the initial enrollment sample.

▷ **Versioning:** While results for up to ten algorithms from each developer are reported here, the intra-provider

accuracy variations are usually smaller than the inter-provider variations. That said different versions give an order of magnitude fewer misses. Some developers demonstrate speed-accuracy tradeoffs[1]. See Figs. 18, 19.

- **Low similarity scores:** In thousands of mugshot cases the correct gallery image is returned at rank 1 but its similarity score is nevertheless low, below some operationally required score threshold. This is not so important when face recognition is used for "lead generation" in investigational applications because human reviewers are specifically required to review potentially long candidate lists and the threshold is effectively 0. In applications where search volumes are higher and labor is not available to review the results from searches, a higher threshold must be applied. This reduces the length of candidate lists and false positive identification rates at the expense of increased false negative miss rates. The tradeoff between the two error rates is reported extensively later.

- **Population size:** As the number of enrolled subjects grows, some mates are displaced from rank one, decreasing accuracy. As tabulated later for N up to 12 million, false negative rates generally rise slowly with population size. This enables use of face recognition in very large populations. However in most positive and negative identification applications[2], a score threshold is set to limit the rate at which non-mate searches produce false positives. This has the consequence that some mated searches will report the mate below threshold, i.e. a miss, even if it is at rank 1. The utility of this is that many non-mated searches will return no candidate identities at all. As the error-tradeoff characteristic shows, investigational miss rates on the right side are very low but then rise steadily (in the center region) as threshold is increased to support "lights-out" applications, and ultimately rise quickly (left side) as discussed below. Thus, if we demand that just one in one thousand non-mate searches produce any false positives, the most accurate algorithms there (Sensetime-004 and NEC-3) would fail on between 3 and 5% of mated searches. Even though the graph shows results for the most accurate algorithms, all but two would fail to find the mate in more than 8% of mated searches. While the two most accurate algorithms produce a relatively flat error tradeoff until the threshold is raised to limit false positives to about 1 in 400 non-mated searches[3]

  Thereafter, as the threshold is raised to further reduce false positives, miss rates rise rapidly. This means that low false positive identification rates are inaccesible with these algorithms, a result that does not apply for ten-finger identification algorithms. The rapid rise occurs because the lower mate scores are mixed with very high non-mate scores, the low scores from poor image quality and ageing, the high non-mates from the presence of lookalikes persons (doppelgangers), twins (discussed next) and, ultimately, the presence of a few unconsolidated subjects i.e. persons present under multiple IDs.

- **False negatives from ageing:** A large source of error in long-run applications where subjects are not re-enrolled on a set schedule is ageing. Changes in facial appearance increase with the time elapsed between photographs. These will depress similarity scores and eventually cause false negatives. All faces age and while this usually proceeds in a graceful and progressive manner, drug use can accelerate this [28]. Elective surgery may be effective in delaying it although this has not been formally quantified with face recognition. As ageing is essentially unavoidable, it can only be mitigated by scheduled re-capture, as in passport re-issuance. To quantify ageing effects, we used the more accurate algorithms to enroll the earliest image of 3.1 million adults and then search

[1] For example, NEC-0 prepares templates much faster than NEC-2 but gives twenty times more misses. Dermalog-5 executes a template search much more quickly than Dermalog-6 but is also much less accurate.

[2] In a positive identification application such as a registered traveler system, a user is making an implicit claim to be enrolled in the system - most users will be. In a negative application, such as with deportees, the implicit claim is that the subejct is not enrolled - most will not be.

[3] The gallery size here is 12 million people, one image per person. Given 331 201 non-mated searches, an exhaustive implementation of one-too-many search would execute almost 4 trillion comparisons. At a false positive identification rate of 0.0025 the number of false positives is, to first order, 828 corresponding to single-comparison false match rate of 828 / 4 trillion = 2.1 10^{-10} i.e. about 1 in 5 billion. Strictly this FMR computation is meaningful only for algorithms that implement 1:N search using N 1:1 comparisons, which is not always the case.

This publication is available free of charge from: https://doi.org/10.6028/NIST.IR.8271

with 10.3 million newer photos taken up to 18 years after the the initial enrollment photo. Figure 2 puts ageing into context by contrasting it with the increase in false negatives that occurs when the number of individuals in an enrollment database becomes larger and the chance of a false positive increases such that higher thresholds may become necessary[4].

The Figure shows, from to bottom, increases in false negative identification rates (FNIR) with the algorithm being tested. This applies to increases due to N on the left side, and increases due to ageing on the right side. The relative spacing of the dots shows that for all algorithms the dependency of FNIR on N (up to 12 million) is considerably less than on ΔT (up to 18 years). The figure additionally shows the most accurate nine algorithms for each year in which they were submitted, limiting to only one per developer.

In the inset table, accuracy is seen to degrade progressively with time, as mate scores decline and non-mates displace mates from rank 1 position. More accurate algorithms tend to be less sensitive to ageing. The more accurate algorithms give fewer errors after 18 years of ageing than middle tier algorithms give after four. Note also we do not quantify an ageing rate - more formal methods [2] borrowed from the longitudinal analysis literature have been published for doing so (given suitable repeated measures data). See Figures 148, 207 and 236.

This publication is available free of charge from: https://doi.org/10.6028/NIST.IR.8271

[4]Some algorithms implement stragegies to automatically adjust scores to account for increased population size. This relieves the system owner of having to increase thresholds as N increases.

This publication is available free of charge from: https://doi.org/10.6028/NIST.IR.8271

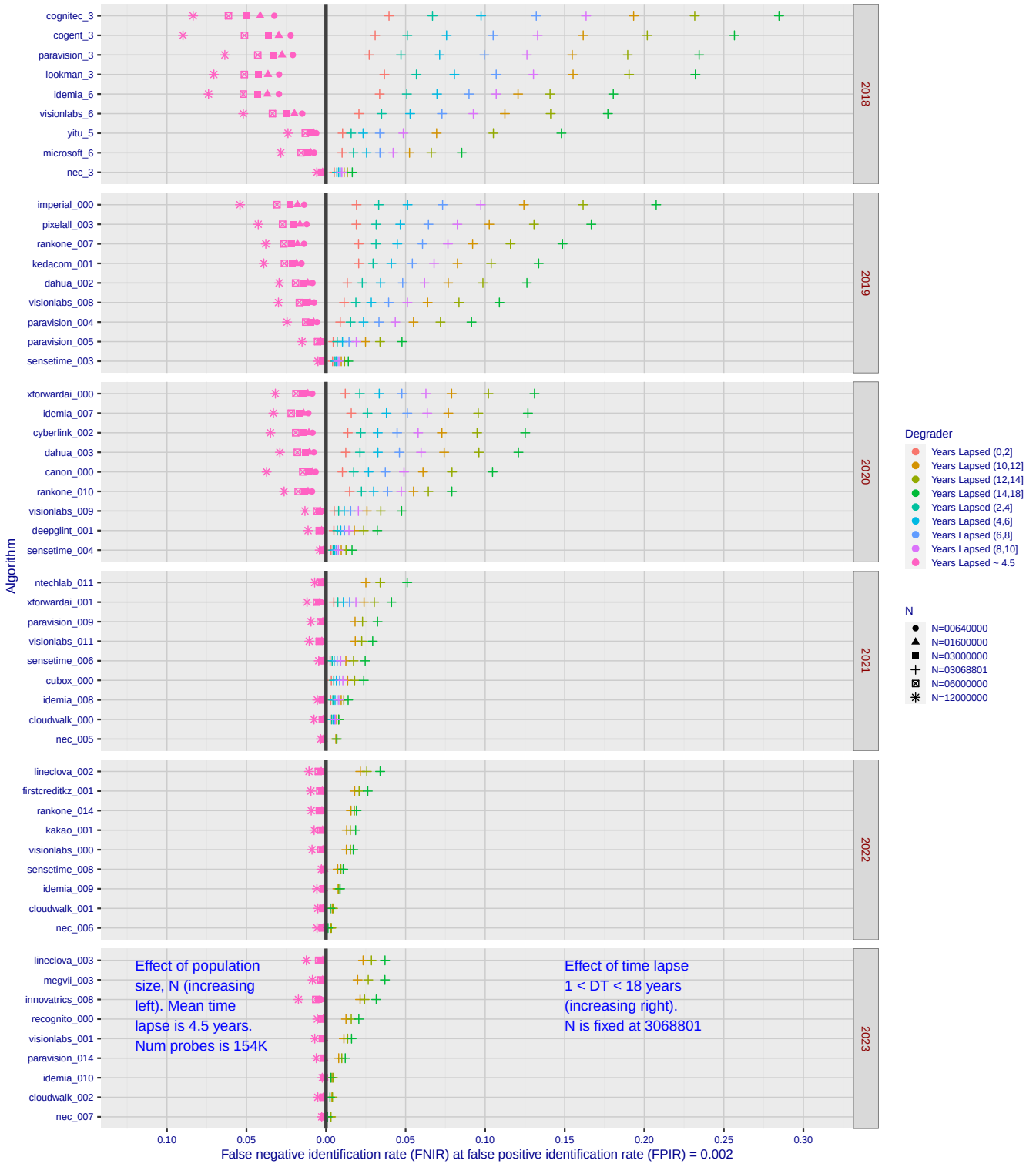

Figure 2: Identification miss rates as a function of enrolled population size, N, and time-lapse, ΔT.

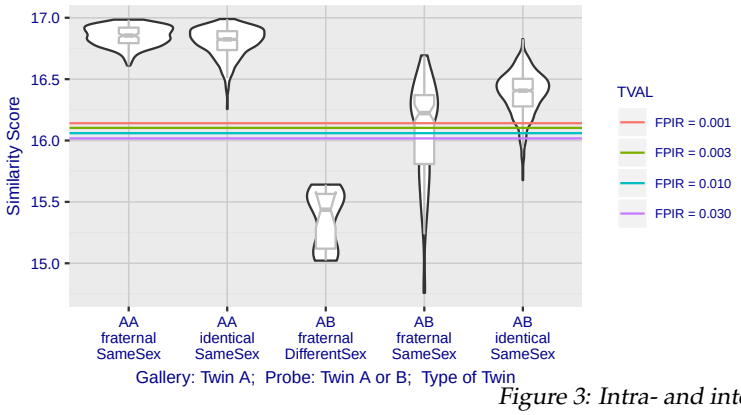

Figure 3: Intra- and inter-twin scores

This publication is available free of charge from: https://doi.org/10.6028/NIST.IR.8271

- **False positives from twins:** By enrolling 640 000 mugshots, adding photos of one twin, and then searching photos of those subjects and their twin the inset figure shows, for one typical algorithm, the similarity is generally greater when searching twins against themselves (A) than when searching twins against their sibling (B) but very often still above even stringent thresholds i.e. those corresponding to one in one thousand searches producing a false positive. Thus twins will very often produce a high-scoring non-match on a candidate list and a false alarm in an online identification system. The plot of Fig. 3 shows that fraternal twins are sometimes correctly rejected at those thresholds - including most different sex twins (at center). Figure **??** shows substantially similar behavior for all algorithms tested. In an investigative search, a twin would typically appear at rank 1, or rank 2 if their sibling happened to also be the gallery. Twins (and triplets etc.) constituted 3.3% of all live births [17] in recent years[5], and because that number is higher today than when the individuals in current adult databases were born, the false positives that arise from twins are now, and will increasingly be, an operational problem. Relative to the United States, twins are born with considerable regional variation. For example they are much less common in East Asia, and much more common in Sub-Saharan Africa [21].

  The presence of twins in the mugshot database is inevitable given its size, around 12.3 million people. As this is not an insignificant sample of the domestic United States population, people with other familial ties will be present also. The data was collected over an extended period and because location information is not available, we are unable to estimate the proportion of the domestic population that is present in the dataset. However, if we assume twins are neither more or less disposed to arrest than the general population, we can estimate that hundreds of thousands of individuals in the dataset are twins. This will affect false positive rates because we randomly set aside 331 201 individuals for nonmate searches, and some proportion of those will be twins with siblings in the gallery.

- **Database integrity:** An operational error rate should be added to all false negative rates in this report reflecting the proportion of images in a real database that are un-matchable. Such anomalies arise from images that: do not contain a face; include multiple persons; cannot be decoded; are rotated by 90° or 180°; depict a face on clothing; and others introduced by a long tail of various clerical errors. While the mugshot trials in this report have been constructed to minimize such effects, they are a real problem in actual operations.

This report is being updated continuously as new algorithms are submitted to FRVT, and run on new datasets. Participation in the one-to-many identification track is independent of participation in the one-to-one verification track of FRVT.

[5]See the CDC's National Vital Statistics Report for 2017: https://www.cdc.gov/nchs/data/nvsr/nvsr67/nvsr67_08-508.pdf

This publication is available free of charge from: https://doi.org/10.6028/NIST.IR.8271

Scope and Context

Audience: This report is intended for developers, integrators, end users, policy makers and others who have some familiarity with biometrics applications. The methods and metrics documented here will be of interest to organizations engaged in tests of face recognition algorithms. Some of these have been incorporated in the ISO/IEC 19795 Part 1 Biometric Testing and Reporting Framework standard, now nearing publication.

Prior benchmarks: Automated face recognition accuracy has improved massively in the two decades since initial commercialization of the various technologies. NIST has tracked that improvement through its conduct of regular independent, free, open, and public evaluations. These have fostered improvements in the state of the art. This report serves as an update to the NIST Interagency Report 8271 on performance of face identification algorithms, published in September 2019.

Demographics: In December 2019, NIST published a first report on demographic dependencies in face recognition, NIST Interagency Report 8280 that documented age, sex and race differentials in one-to-one and one-to-many false positive and false negative rates.

Scope: NIST IR 8271 documented recognition results for four databases containing in excess of 30.2 million still photographs of 14.4 million individuals. That constituted the largest public and independent evaluation of face recognition ever conducted. It includes results for accuracy, speed, investigative vs. identification applications, scalability to large populations, use of multiple images per person, images of cooperative and non-cooperative subjects.

The report also includes results for ageing, recognition of twins, and recognition of profile-view images against frontal galleries. It otherwise does not address causes of recognition failure, neither image-specific problems nor subject-specific factors including demographics. Separate reports on demographic dependencies in face recognition will be published in the future. Additionally out of scope are: performance of live human-in-the-loop transactional systems like automated border control gates; human recognition accuracy as used in forensic applications; and recognition of persons in video sequences (which NIST evaluated separately [9]). Some of those applications share core matching technologies that *are* tested in this report.

Images: Five kinds of images are employed; these are either compared with images of the same kind, or against others from different capture environments as follows. The primary dataset is a set of law enforcement mugshot images (Fig. 5) which are enrolled and then searched with three kinds of images: other mugshots (i.e. within-domain); profile-view photographs (90 degree cross-view); and lower quality webcam images (Fig. 6) collected in similar detention operations (cross-domain). Additionally we compare high quality visa-like photos collected in immigration offices, with: medium quality border crossing images collected in primary immigration lanes; poor quality images collected in ATM-like registered traveller kiosks.

Participation and industry coverage: The report includes performance figures for prototype algorithms from the research laboratories of commercial developers and a few universities. This represents a substantial majority of the face recognition industry, but only a tiny minority of the academic community. Participation was open worldwide. While there is no charge for participation, developers incur some software engineering expense in implementing their algorithms behind the NIST application programming interface (API). The test is a black-box test where the function of the algorithm, and the intellectual property associated with it, is hidden inside pre-compiled libraries.

Recent technology development: Most face recognition research with deep convolutional neural networks (CNNs) has been aimed at achieving invariance to pose, illumination and expression variations that characterize photojournalism and social media images. The initial research [18, 22] employed large numbers of images of relatively few ($\sim 10^4$) individuals to learn invariance. Inevitably much larger populations ($\sim 10^7$) were employed for training [11, 20] but the benchmark, Labeled Faces in the Wild with (essentially) an equal error rate metric [12], represents an easy task,

one-to-one verification at very high false match rates. While a larger scale identification benchmark duly followed, Megaface [15], its primary metric, rank one hit rate, contrasts with the high threshold discrimination task required in most large-population applications of face recognition, namely credential de-duplication, and background checks. There, identification in galleries containing up to 10^8 individuals must be performed using a) very few images per individual and b) stringent thresholds to afford very low false positive identification rates. This track of FRVT was launched to measure the capability of the new technologies, including in these two cases. FRVT has included open-set identification tests since 2002, reporting both false negative and positive identification rates [7].

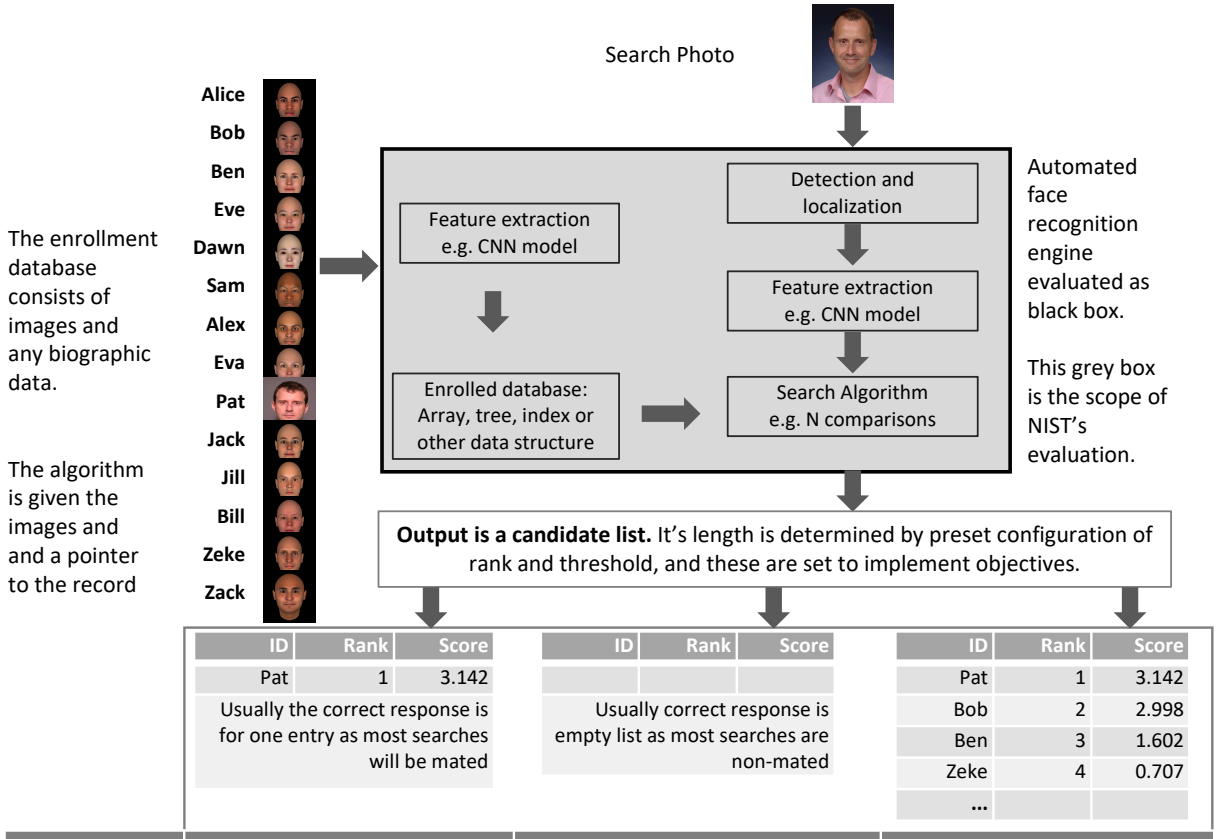

	Positive identification	Negative identification	Post-event investigation
Example	Access to a gym or cruise ship	Watchlist e.g. Detection of deportee or duplicate drivers license applications	Crime scene photos, or of detainee without ID documents.
Claim of identity	Implicit claim to be enrolled	Implicit claim to not be enrolled	No claim: Inquiry
Threshold	High, to implement security objective	High, to limit false positives	Zero
Num. candidates	1	0	L, set by request to algorithm
Human role	Review candidate to assist user in resolution of false negatives, or to detect impostor	Review candidate to determine false positive or correct hit	Review multiple candidates, refer possible hits to examiners see [26]
Intended human involvement frequency	Rare – approx. the false negative identification rate plus prior probability of impostor	Rare – approx. the false positive identification rate plus prior probability of an actual mate	Always
Performance metric of interest	**FNIR at low FPIR. See sec. 3.1, 3.2 and Tables 10, 19**	**FNIR at low FPIR. See sec. 3.1, 3.2 and Tables 10, 19**	**FNIR at ranks 1... 50, say. FPIR = 1. See sec. 3.2 and Table 12, 14, 16**

Performance metrics for applications: This report documents the performance of one-to-many face recognition algorithms. The word "performance" here refers to recognition accuracy and computational resource usage, as measured

This publication is available free of charge from: https://doi.org/10.6028/NIST.IR.8271

by executing those algorithms on massive sequestered datasets.

This report includes extensive tabulation of recognition error rates germane to the main use-cases for face search technology. The Figure below, inspired by the Figure 1 in [23] differentiates different applications of the technolgy. The last row directs readers to the main tables relevant to those applications, respectively threshold-based and rank-based metrics that are special cases of the metrics given in section 3. The terms negative identification and positive identification are taken from the ISO/IEC 2382-37:2017 standardized biometrics vocabulary.

The algorithms are specifically configured for these applications by setting thresholds and candidate list lengths. Both rank-based metrics and threshold-based metrics include tradeoffs. In investigation, overall accuracy will be reduced if labor is only available to review a few candidates from the automated system. Note that when a fixed number of candidates are returned, the false positive identification rate of the automated face recognition engine will be 100%, because a probe image of anyone not enrolled will still return candidates. In identification applications where false positives must be limited to satisfy reviewer labor availability or a security objective, higher false negative rates are implied. This report includes extensive quantification of this threshold-based tradeoff. See Sec. 3

Template diversity: The FRVT is designed to evaluate black-box technologies with the consequence that the templates that hold features extracted from face images are entirely proprietary opaque binary data that embed considerable intellectual property of the developer. Despite migration to CNN-based technologies there is no consensus on the optimal feature vector dimension. This is evidenced by template sizes ranging from below 100 bytes to more than four kilobytes. This diversity of approaches, suggests there is no prospect of a standard template something that would require a common feature set to be extracted from faces. Interoperability in automated face recognition remains solidly based on images and documentary standards for those, in particular the ICAO portrait [27] specification deriving from the ISO/IEC 19794-5 Token frontal [24] standard, which are similar to certain ANSI/NIST Type 10 [26] formats.

Training: The algorithms submitted to NIST have been developed using image datasets that developers do not disclose. The development will often include application of machine learning techniques and will additionally involve iterative training and testing cycles. NIST itself does not perform any training and does not refine or alter the algorithm in any way. Thus the model, data files, and libraries that define an algorithm are fixed for the duration of the tests. This reflects typical operational reality where recognition software, once installed, is fixed and constant until upgraded. This situation persists because on-site training of algorithms on customer data is atypical essentially because training is not a turnkey process.

Automated search and human review: Virtually all applications using automated face search require human review of the outputs at some frequency: Always for investigational applications; rarely in positive identification applications, after rejection (false or otherwise); and rarely in negative identification applications, after an alarm (false or otherwise). The human role is usually to compare a reference image with the query image or the live-subject if present, to render either a definitive decision on "exclusion" (different subjects), or "identification" (same subject), or a declaration that one or both images have "no value" and that no decision can be made. Note that automated face recognition algorithms are not built to do exclusion - low scores from a face comparison arise from different faces *and* poor quality images of the same face.

Human reviewers make recognition errors [5, 19, 25] and are sensitive to image acquisition and quality. Accurate human review is supported by high resolution - as specified in the Type 50, 51 acquisition profiles of the ANSI/NIST Type 10 record [26], and by multiple non-frontal views as specified in the same standard. These often afford views of the ear. Organizations involved in image collection should consider supporting human adjudication by collecting high-resolution frontal and non-frontal views, preparing low resolution versions for automated face recognition [24], and retaining both for any subsequent resolution of candidate matches. Along these lines, the ISO/IEC Joint Technical

This publication is available free of charge from: https://doi.org/10.6028/NIST.IR.8271

Committee 1 subcommittee 37 on biometrics has just initiated projects on image quality assessment and face-aware capture.

This publication is available free of charge from: https://doi.org/10.6028/NIST.IR.8271

Release Notes

FRVT Activities: Since February 2017, NIST has been evaluating one-to-one verification algorithms on an ongoing basis. NIST then restarted FRVT's one-to-many track in February 2018, inviting participants to send up to prototype algorithms. Both tracks allows developers to submit updated algorithms to NIST at any time but no more frequently than four calendar months. This more closely aligns development and evaluation schedules. Results are posted to the web within a few weeks of submission. Details and full report are linked from the Ongoing FRVT site.

FRVT Reports: The results of the FRVT appear in the series NIST Interagency Reports tabulated below. The reports were developed separately and released on different schedules. In prior years NIST has mostly reported FRVT results as a single report; this had the disadvantage that results from completed sub-studies were not published until all other studies were complete.

Date	Link	Title	No.
2014-03-20	PDF	FRVT Performance of Automated Age Estimation Algorithms	7995
2015-04-20	PDF	Face Recognition Vendor Test (FRVT) Performance of Automated Gender Classification Algorithms	8052
2014-05-21	PDF	FRVT Performance of face identification algorithms	8009
2017-03-07	PDF	Face In Video Evaluation (FIVE) Face Recognition of Non-Cooperative Subjects	8173
2017-11-23	PDF	The 2017 IARPA Face Recognition Prize Challenge (FRPC)	8197
2018-11-27	PDF	Face Recognition Vendor Test - Part 2: Identification	8271
2019-09-11	PDF	Face Recognition Vendor Test - Part 2: Identification	8271
2019-12-11	PDF	Face Recognition Vendor Test - Part 3: Demographic Effects	8280
2020-01-03	WWW	Face Recognition Vendor Test (FRVT) - Part 1 Verification	Draft

Details appear on pages linked from `https://www.nist.gov/programs-projects/face-projects`.

Appendices: This report is accompanied by appendices which present exhaustive results on a per-algorithm basis. These are machine-generated and are included because the authors believe that visualization of such data is broadly informative and vital to understanding the context of the report.

Typesetting: Virtually all of the tabulated content in this report was produced automatically. This involved the use of scripting tools to generate directly type-settable LaTeX content. This improves timeliness, flexibility, maintainability, and reduces transcription errors.

Graphics: Many of the Figures in this report were produced using the ggplot2 package running under R, the capabilities of which extend beyond those evident in this document.

This publication is available free of charge from: https://doi.org/10.6028/NIST.IR.8271

Contents

Release Notes 1

Disclaimer 10

Institutional Review Board 10

Acknowledgments 10

Executive Summary 11

Scope and Context 17

Release Notes 21

1 Introduction 23

2 Evaluation datasets 24

3 Performance metrics 30

4 Results 46

Appendices 115

A Accuracy on large-population FRVT 2018 mugshots 115

B Effect of time-lapse: Accuracy after face ageing 248

C Effect of enrolling multiple images 398

D Accuracy with poor quality webcam images 405

E Accuracy for profile-view to frontal recognition 415

F Search duration 419

G Gallery Insertion Timing 454

This publication is available free of charge from: https://doi.org/10.6028/NIST.IR.8271

1 Introduction

One-to-many identification represents the largest market for face recognition technology. Algorithms are used across the world in a diverse range of biometric applications: detection of duplicates in databases, detection of fraudulent applications for credentials such as passports and driving licenses, token-less access control, surveillance, social media tagging, lookalike discovery, criminal investigation, and forensic clustering.

This report contains a breadth of performance measurements relevant to many applications. Performance here refers to accuracy and resource consumption. In most applications, the core accuracy of a facial recognition algorithm is the most important performance variable. Resource consumption will be important also as it drives the amount of hardware, power, and cooling necessary to accommodate high volume workflows. Algorithms consume processing time, they require computer memory, and their static template data requires storage space. This report documents these variables.

1.1 Open-set searches

FRVT tested open-set identification algorithms. Real-world applications are almost always "open-set", meaning that some searches have an enrolled mate, but some do not. For example, some subjects have truly not been issued a visa or drivers license before; some law enforcement searches are from first-time arrestees[6]. In an "open-set" application, algorithms make no prior assumption about whether or not to return a high-scoring result, and for a mated search, the ideal behaviour is that the search produces the correct mate at high score and first rank. For a non-mate search, the ideal behavior is that the search produces zero high-scoring candidates.

Many academic benchmarks execute only closed-set searches. The proportion of mates found in the rank one position is the default accuracy metric. This hit rate metric ignores the score with which a mate is found; weak hits count as much as strong hits. This ignores the real-world imperative that in many applications it is necessary to elevate a threshold to reduce the number of false positives.

[6]Operationally closed-set applications are rare because it is usually not the case that all searches have an enrolled mate. One counter-example, however, is a cruise ship in which all passengers are enrolled and all searches should produce exactly one identity. Another example is forensic identification of dental records from an aircraft crash.

This publication is available free of charge from: https://doi.org/10.6028/NIST.IR.8271

2 Evaluation datasets

This report documents accuracy for four kinds of images - mugshots, webcam, profiles and wild - as described in the following sections.

2.1 Immigration-related images

This report includes benchmark tests sharing a common enrollment of high quality frontal portrait images collected while subject make applications for various immigration benefits. We then search that with two kinds of images, webcam images collected during in-bound immigration and also images collected from registered travelers using a ATM-style kiosk. These are described below and depicted in Figure 4.

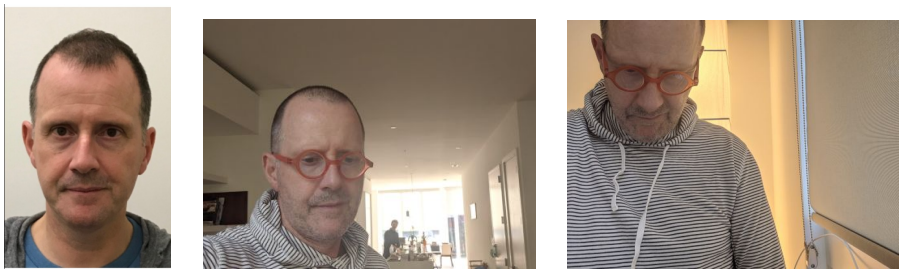

a) Application b) Immigration Lane c) Kiosk

Figure 4: Example photos.

- **Application reference photos**: The images are collected in an attended interview setting using dedicated capture equipment and lighting. The images, at size 300x300 pixels, are smaller than normally indicated by ISO. The images are all high-quality frontal portraits collected in immigration offices and with a white background. As such, potential quality related drivers of high false match rates (such as blur) can be expected to be absent. The images are encoded as ISO/IEC 10918-1 i.e. JPEG. Older images had a compression ration of about 16:1, while newer images, since 2010, are more lightly compressed at 4:1. When these images are provided as input into the algorithm, they are labeled with the type "iso". This report enrols 1 600 000 application images, one per person.

- **Border crossing photos**: Most images are have width 320 and height 240 pixels. They are JPEG compressed at 16:1 i.e. filesize just below 15KB. The images present challenges for face recognition in that subjects often exhibit non-zero yaw and pitch (associated with the rotational degrees of freedom of the camera mount), low contrast (due to varying and intense background lights), and poor spatial resolution (due to inexpensive cameras). There are often subjects standing in the background, usually at very low resolution (see Figure 4b). In such cases, algorithms should detect all faces and determine which is the largest and most centered. When these images are provided as input into the algorithm, they are labeled with the type "wild".

- **Kiosk photos**: These photos were collected from subjects whose attention was focused on interaction with an immigration kiosk. They images were not intended for use with automated face recognition. The camera is situated above a display which the user touches, and is triggered either without directing the subject to look at it, or without waiting for the subject to comply. The images are therefore characterized by pitch-down pose, sometimes exceeding 45 degrees, as in Figure 4c. Yaw-angle variation is mild, with most images close to frontal. The images

This publication is available free of charge from: https://doi.org/10.6028/NIST.IR.8271

have width 320 pixels and height 240 pixels and therefore tall individuals are sometimes cropped. This is often just above the eyes and can occur at the nose or mouth. Conversely, short individuals are sometimes cropped such that only the top part of the face is visible. In a quite small number of cases, there other subjects standing just behind the primary subject such that algoriths should detect all faces and determine which is the largest and most centered. Background ceiling lighting is often visible and this sometimes leads to under-exposure of the face When these images are provided as input into the algorithm, they are labeled with the type "wild".

2.2 Law enforcement images

The main mugshot dataset used is referred to as the FRVT 2018 set. This set was collected over the period 2002 to 2017 in routine United States law enforcement operations. This set yields three subsets

- **Mugshots**: Mugshots comprise about 86% of the database. They have reasonable compliance with the ANSI/NIST ITL1-2011 Type 10 standard's subject acquisition profiles levels 10-20 for frontal images [26]. The most common departure from the standard's requirements is the presence of mild pose variations around frontal - the images of Figure 5 are typical. The images vary in size, with many being 480x600 pixels with JPEG compression applied to produce filesizes of between 18 and 36KB with many images outside this range, implying that about 0.5 bits are being encoded per pixel. When these images are provided as input into the algorithm, they are labeled with the type "mugshot". Example images appear in Fig. 5

  NIST Interagency Report 8238 includes a comparison of this set of mugshots with the smaller and easier sets of mugshots used in tests run in 2010 and 2014.

- **Profile images**: Profile-view images have been collected in law enforcement for more than 100 years, as human capability is improved with orthogonal information. The profile images used in this report were collected during the same session as the frontal mugshot photograph, in the same standardized photographic setup. These would not therefore be used with automated face recognition. A small subset, 200 000 images, were set aside for testing. When these images are provided as input into the algorithm, they are labeled with the type "wild". Example images appear in Fig. 7

- **Webcam images**: The remaining 14% of the images were collected using an inexpensive webcam attached to a flexible operator-directed mount. These images are all of size 240x240 pixels, that are in considerable violation of most quality-related clauses of all face recognition standards. As evident in the figure, the most common defects are non-frontal pose (associated with the rotational degrees of freedom of the camera mount), low contrast (due to varying and intense background lights), and poor spatial resolution (due to inexpensive camera optics) - see examples in Fig 6. The images are overly JPEG compressed, to between 4 and 7KB, implying that only 0.5 to 1 bits are being encoded per color pixel. When these images are provided as input into the algorithm, they are labeled with the type "wild". Example images appear in Fig. 6

These are drawn from NIST Special Database 32 which may be downloaded here.

These images were partitioned in galleries and probesets for the various experiment listed in Table 1.

This publication is available free of charge from: https://doi.org/10.6028/NIST.IR.8271

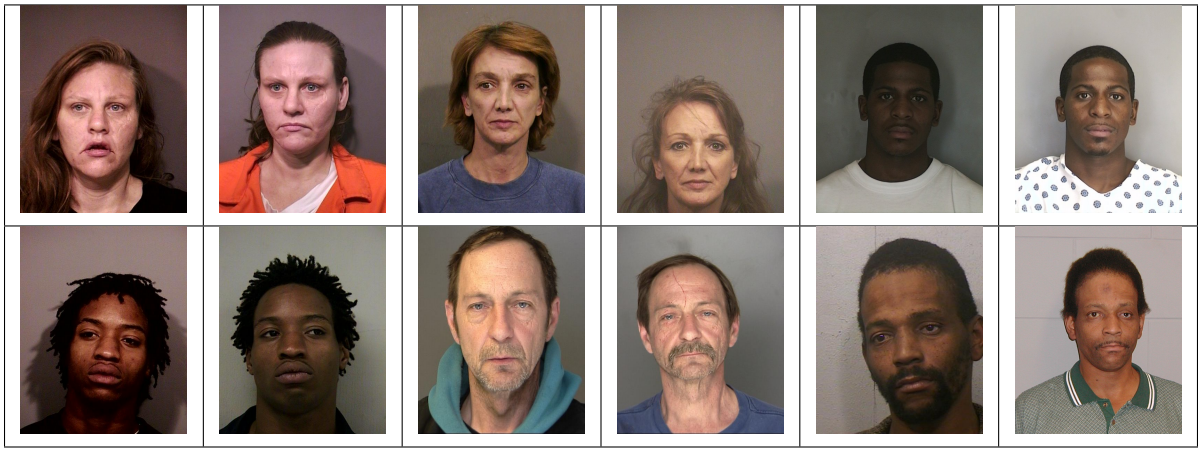

Figure 5: Six mated mugshot pairs representative of the FRVT-2014 (LEO) and FRVT-2018 datasets. The images are collected live, i.e. not scanned from paper. Image source: NIST Special Database 32 the Multiple Encounter Deceased Subjects dataset.

Figure 6: Twelve webcam images representative of probes against the FRVT-2018 mugshot gallery. The first eight images are four mated pairs. Such images present challenges to recognition including pose, non-uniform illumination, low contrast, compression, cropping, and low spatial sampling rate. Image source: NIST Special Database 32 the Multiple Encounter Deceased Subjects dataset.

Figure 7: **[Profile views]** *The three images are a frontal enrollment, subsequent frontal probe, and same-session ninety degree profile view. While collection of both frontal and profile views has been typical in law enforcement for more than a century, the recognition of profile to frontal views has essentially been impossible. However, reasonbly high accuracy results is now possible - see section E.*

This publication is available free of charge from: https://doi.org/10.6028/NIST.IR.8271

Image		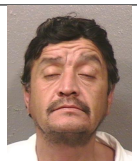		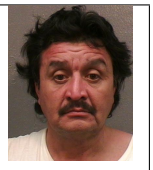
Encounter	1	...	$K_i - 1$	K_i
Capture Time	T_1	...	T_{K_i-1}	T_{K_i}
Role RECENT	Not used	Not used	Enrolled	Search
Role LIFETIME	Enrolled	Enrolled	Enrolled	Search

Figure 8: Depiction of the "recent" and "lifetime" enrollment types. Image source: NIST Special Database 32

This publication is available free of charge from: https://doi.org/10.6028/NIST.IR.8271

2.3 Enrollment strategies

Many operational applications include collection and enrollment of biometric data from subjects on more than one occasion. This might be done on a regular basis, as might occur in credential (re-)issuance, or irregularly, as might happen in a criminal recidivist situation [4]. The number of images per person will depend on the application area. In civil identity credentialing (e.g. passports, driver's licenses), the images will be acquired approximately uniformly over time (e.g. ten years for a passport). While the distribution of dates for such images of a person might be assumed uniform, a number of factors might undermine this assumption[7]. In criminal applications, the number of images would depend on the number of arrests. The distribution of dates for arrest records for a person (i.e. the recidivism distribution) has been modeled using the exponential distribution but is recognized to be more complicated[8].

In any case, the 2010 NIST evaluation of face recognition showed that considerable accuracy benefits accrue with retention and use of *all* historical images [6].

To this end, the FRVT API document provides $K \geq 1$ images of an individual to the enrollment software. The software is tasked with producing a single proprietary undocumented "black-box" template[9] from the K images. This affords the algorithm an ability to generate a *model* of the individual, rather than to simply extract features from each image on a sequential basis.

As depicted in Figure 8, the i-th individual in the FRVT 2018 dataset has K_i images. These are labelled as x_k for $k = 1 \ldots K_i$ in chronological order of capture date. To measure the utility of having multiple enrollment images, this report evaluates three kinds of enrollment:

- ▷ **Recent**: Only the second most recent image, x_{K_i-1} is enrolled. This strategy of enrollment mimics the operational policy of retaining the imagery from the most recent encounter. This might be done operationally to ameliorate the effects of face ageing. Obviously retaining only the most recent image should only be done if the identity of the person is trusted to be correct. For example, in an access control situation retention of the most recent successful *authentication* image would be hazardous if it could be a false positive.

- ▷ **Lifetime-consolidated**: All but the most recent image are enrolled, $x_1 \ldots x_{K_i-1}$. This subject-centric strategy might be adopted if quality variations exist where an older image might be more suitable for matching, despite the ageing effect.

[7] For example, a person might skip applying for a passport for one cycle, letting it expire. In addition, a person might submit identical images (from the same photography session) to consecutive passport applications at five year intervals.
[8] A number of distributions have been considered to model recidivism, see for example [3].
[9] There are no formal face template standards. Template standards only exist for fingerprint minutiae - see ISO/IEC 19794-2:2011.

This publication is available free of charge from: https://doi.org/10.6028/NIST.IR.8271

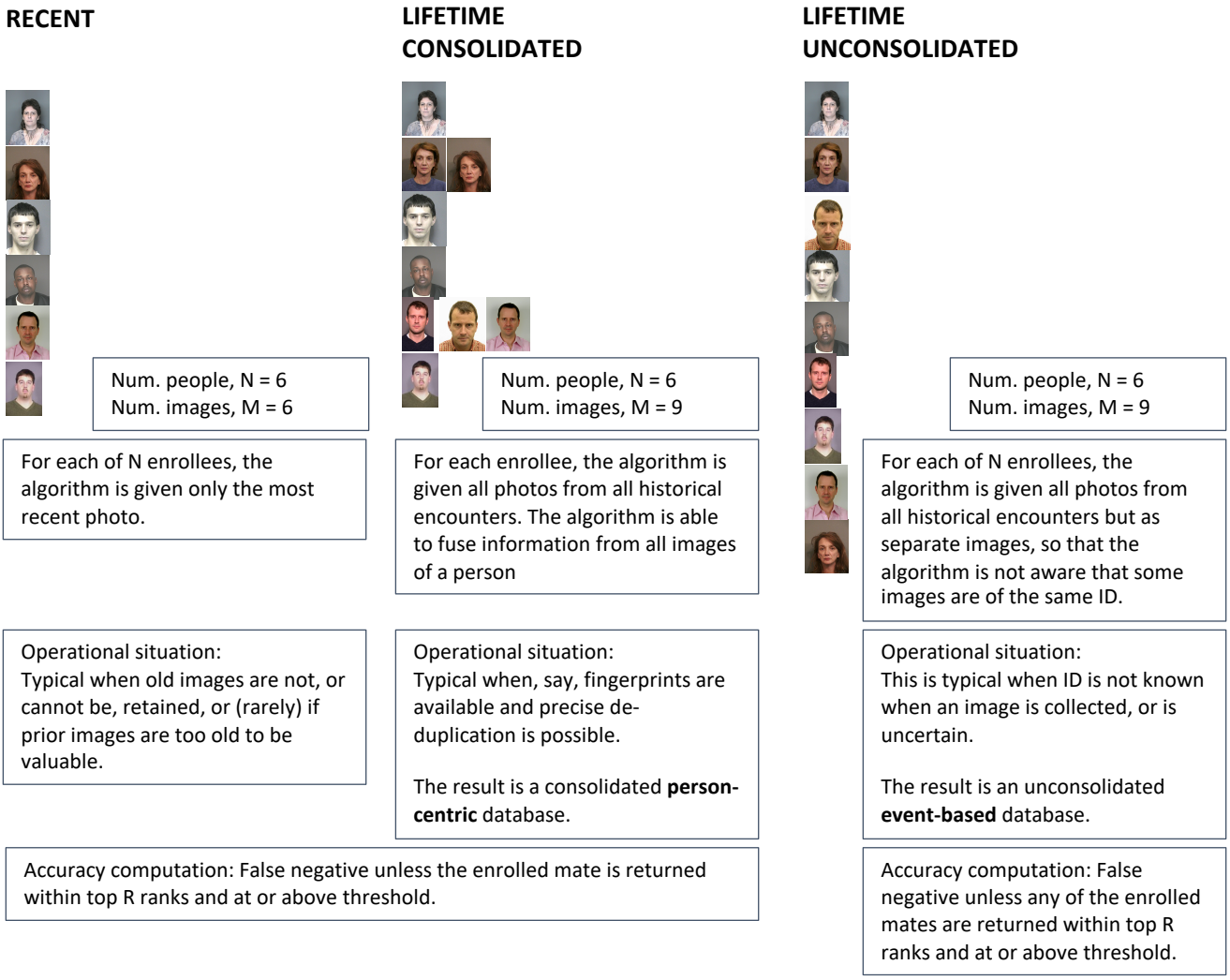

Figure 9: **Enrollment strategies**. *The figure shows the three kinds of enrollment databases examined in this report. Image source: NIST Special Database 32*

	ENROLLMENT				SEARCH			
	TYPE SEE	POPULATION			MATE		NON-MATE	
	SECTION 2.3	FILTER	N-SUBJECTS	N-IMAGES	N-SUBJECTS	N-IMAGES	N-SUBJECTS	N-IMAGES
Mugshot trials from enrollment of single images								
1	RECENT	NATURAL	640 000	640 000	154 549	154 549	331 254	331 254
2	RECENT	NATURAL	1 600 000	1 600 000				
3	RECENT	NATURAL	3 000 000	3 000 000				
4	RECENT	NATURAL	6 000 000	6 000 000				
5	RECENT	NATURAL	12 000 000	12 000 000				
Cross-domain								
13	MUGSHOTS AS ON ROW 2				82 106 WEBCAM	82 106 WEBCAM	331 254 WEBCAM	331 254 WEBCAM
Cross-view								
14	MUGSHOTS AS ON ROW 2				100 000 PROFILE	100 000 PROFILE	100 000 PROFILE	100 000 PROFILE
Mugshot ageing								
17	OLDEST	NATURAL	3 068 801	3 068 801	2 853 221	10 951 064	0	0
Border crossing ageing								
18	OLDEST	NATURAL	1 600 000	1 600 000	903 655	1 922 393	1 393 076	1 680 000
Visa-border								
19	PRIOR	NATURAL	1 600 000 VISA	1 600 000 VISA	577 444 BORDER	1 212 892 BORDER	79 769 BORDER	80 000 BORDER
20	VISA AS ON ROW 18				14 004 BORDER	31 579 BORDER	42 474 BORDER	45 460 BORDER

Table 1: **Enrollment and search sets**. *Each row summarizes one identification trial. Unless stated otherwise, all entries refer to mugshot images. The term "natural" means that subjects were selected without heed to demographics, i.e. in the distribution native to this dataset. The probe images were collected in a different calendar year to the enrollment image. Missing values in rows 2-12 are the same as in row 1.*

- **Lifetime-unconsolidated**: Again all but the most recent image are enrolled $x_1 \ldots x_{K_i-1}$ but now separately, with different identifiers, such that the algorithm is not aware that the images are from the same face. This kind of event- or encounter-centric enrollment is very common when operational constraints preclude reliable consolidation of the historical encounters into a single identity. This aspect also prevents the recognition algorithm from a) building a holistic model of identity (as is common in speaker recognition systems) and b) implementing fusion, for example template-level fusion of feature vectors, or post-search score-level fusion. The result is that searches will typically yield more than one image of a person in the top ranks. This has consequences for appropriate metrics, as detailed in section 3.2.1

  NIST first evaluated this kind of enrollment in mid 2018, and the results tables include some comparison of accuracy available from all three enrollment styles.

In all cases, the most recent image, x_{K_i}, is reserved as the search image. For the 1.6 million subject enrollment partition of the FRVT 2018 data, $1 \leq K_i \leq 33$ with $K_i = 1$ in 80.1% of the individuals, $K_i = 2$ in 13.4%, $K_i = 3$ in 3.7%, $K_i = 4$ in 1.4%, $K_i = 5$ in 0.6%, $K_i = 6$ in 0.3%, and $K_i > 6$ is 0.2% for everyone else. This distribution is substantially dependent on United States recidivism rates.

We did not evaluate the case of retaining only the highest quality image, since automated quality assessment is out of scope for this report. We do not anticipate that such strategies will prove beneficial when the quality assessment apparatus is imperfect and unvalidated.

This publication is available free of charge from: https://doi.org/10.6028/NIST.IR.8271

3 Performance metrics

This section gives specific definitions for accuracy and timing metrics. Tests of open-set biometric algorithms must quantify frequency of two error conditions:

- **False positives**: Type I errors occur when search data from a person who has never been seen before is incorrectly associated with one or more enrollees' data.
- **Misses**: Type II errors arise when a search of an enrolled person's biometric does not return the correct identity.

Many practitioners prefer to talk about "hit rates" instead of "miss rates" - the first is simply one minus the other as detailed below. Sections 3.1 and 3.2 define metrics for the Type I and Type II performance variables.

Additionally, because recognition algorithms sometimes fail to produce a template from an image, or fail to execute a one-to-many search, the occurrence of such events must be recorded. Further because algorithms might elect to not produce a template from, for example, a poor quality image, these failure rates must be combined with the recognition error rates to support algorithm comparison. This is addressed in section 3.5.

Finally, section 3.7 discusses measurement of computation duration, and section 3.8 addresses the uncertainty associated with various measurements. Template size measurement is included with the results.

This publication is available free of charge from: https://doi.org/10.6028/NIST.IR.8271

3.1 Quantifying false positives

It is typical for a search to be conducted into an enrolled population of N identities, and for the algorithm to be configured to return the closest L candidate identities. These candidates are ranked by their score, in descending order, with all scores required to be greater than or equal to zero. A human analyst might examine either all L candidates, or just the top $R \leq L$ identities, or only those with score greater than threshold, T. The workload associated with such examination is discussed later, in 3.6.

False alarm performance is quantified in two related ways. These express how many searches produces false positives, and then, how many false positives are produced in a search.

False positive identification rate: The first quantity, FPIR, is the proportion of non-mate searches that produce an adverse outcome:

$$\text{FPIR}(N,T) = \frac{\text{Num. non-mate searches where one or more enrolled candidates are returned with score at or above threshold}}{\text{Num. non-mate searches attempted.}} \tag{1}$$

Under this definition, FPIR can be computed from the highest non-mate candidate produced in a search - it is not necessary to consider candidates at rank 2 and above. FPIR is the primary measure of Type I errors in this report.

Selectivity: However, note that in any given search, several non-mate may be returned above threshold. In order to quantify such events, a second quantity, selectivity (SEL), is defined as the *number* of non-mates returned on a candidate list, averaged over all searches.

$$\text{SEL}(N,T) = \frac{\text{Num. non-mate enrolled candidates returned with score at or above threshold}}{\text{Num. non-mate searches attempted.}} \tag{2}$$

where $0 \leq$ SEL(N, T) $\leq$L. Both of these metrics are useful operationally. FPIR is useful for targeting how often an

adverse false positive outcome can occur, while SEL as a number is related to workload associated with adjudicating candidate lists. The relationship between the two quantities is complicated - it depends on whether an algorithm concentrates the false alarms in the results of a few searches or whether it disburses them across many. This was detailed in FRVT 2014, NISTIR 8009. It has not yet been detailed in FRVT 2018.

3.2 Quantifying hits and misses

If L candidates are returned in a search, a shorter candidate list can be prepared by taking the top $R \leq L$ candidates for which the score is above some threshold, $T \geq 0$. This reduction of the candidate list is done because thresholds may be applied, and only short lists might be reviewed (according to policy or labor availability, for example). It is useful then to state accuracy in terms of R and T, so we define a "miss rate" with the general name **false negative identification rate** (FNIR), as follows:

$$\text{FNIR}(N, R, T) = \frac{\text{Num. mate searches with enrolled mate found outside top R ranks or score below threshold}}{\text{Num. mate searches attempted.}} \quad (3)$$

This formulation is simple for evaluation in that it does not distinguish between causes of misses. Thus a mate that is not reported on a candidate list is treated the same as a miss arising from face finding failure, algorithm intolerance of poor quality, or software crashes. Thus if the algorithm fails to produce a candidate list, either because the search failed, or because a search template was not made, the result is regarded as a miss, adding to FNIR.

Hit rates, and true positive identification rates: While FNIR states the "miss rate" as how often the correct candidate is either not above threshold or not at good rank, many communities prefer to talk of "hit rates". This is simply the **true positive identification rate**(TPIR) which is the complement of FNIR giving a positive statement of how often mated searches are successful:

$$\text{TPIR}(N, R, T) = 1 - \text{FNIR}(N, R, T) \quad (4)$$

This report does not report true positive "hit" rates, preferring false negative miss rates for two reasons. First, costs rise linearly with error rates. For example, if we double FNIR in an access control system, then we double user inconvenience and delay. If we express that as decrease of TPIR from, say 98.5% to 97%, then we mentally have to invert the scale to see a doubling in costs. More subtly, readers don't perceive differences in numbers near 100% well, becoming inured to the "high nineties" effect where numbers close to 100 are perceived indifferently.

Reliability is a corresponding term, typically being identical to TPIR, and often cited in automated (fingerprint) identification system (AFIS) evaluations.

An important special case is the **cumulative match characteristic**(CMC) which summarizes accuracy of mated-searches only. It ignores similarity scores by relaxing the threshold requirement, and just reports the fraction of mated searches returning the mate at rank R or better.

$$\text{CMC}(N, R) = 1 - \text{FNIR}(N, R, 0) \quad (5)$$

We primarily cite the complement of this quantity, $\text{FNIR}(N, R, 0)$, the fraction of mates *not* in the top R ranks.

The **rank one hit rate** is the fraction of mated searches yielding the correct candidate at best rank, i.e. CMC(N, 1). While this quantity is the most common summary indicator of an algorithm's efficacy, it is not dependent on similarity scores, so it does not distinguish between strong (high scoring) and weak hits. It also ignores that an adjudicating reviewer is often willing to look at many candidates.

This publication is available free of charge from: https://doi.org/10.6028/NIST.IR.8271

3.2.1 False negative rates for unconsolidated galleries

As detailed in section 2.3 a common type of gallery, here referred to as the lifetime unconsolidate type, is populated with all images of an individual without any association between them. That is, the gallery construction algorithm is not provided with any ID labels that would support processing of a person's images jointly. This constrasts with the lifetime consolidate type where an algorithm may explicitly fuse features from multiple images of a person, or select a best image. In such cases, where the number of enrolled images is a random variable, we define two false negative rates as follows.

The first demands that the algorithm place any of the K_i mates in the top $R \geq 1$ ranks. The proportion of searches for which this does not occur forms a false negative identification rate:

$$\text{FNIR}_{\text{any}}(N, R, T) = 1 - \frac{\text{Num. mate searches where any enrolled mate is found in the top R ranks and at-or-above threshold}}{\text{Num. mate searches attempted.}} \tag{6}$$

The second demands that the algorithm place all K_i mates in the top $R \geq K_i$ ranks. The proportion of searches for which this does not occur forms a false negative identification rate:

$$\text{FNIR}_{\text{all}}(N, R, T) = 1 - \frac{\text{Num. mate searches where all enrolled mates are found in the top R ranks and at-or-above threshold}}{\text{Num. mate searches attempted.}} \tag{7}$$

Placing all mates in the top ranks is a more difficult task than correctly retrieving any image, so it holds that: $\text{FNIR}_{\text{all}} \geq \text{FNIR}_{\text{any}}$. This is evident in the results presented for November 2018 algorithms in Tables starting at **??**.

The information retrieval community might prefer to compute and plot *precision* and *recall*; this is a valid approach, but we advance the two metrics above because they relate to our normal definition of consolidated FNIR, and they cover the two extreme use-cases of wanting any hit vs. all hits.

3.3 DET interpretation

In biometrics, a false negative occurs when an algorithm fails to match two samples of one person – a Type II error. Correspondingly, a false positive occurs when samples from two persons are improperly associated – a Type I error.

Matches are declared by a biometric system when the native comparison score from the recognition algorithm meets some threshold. Comparison scores can be either similarity scores, in which case higher values indicate that the samples are more likely to come from the same person, or dissimilarity scores, in which case higher values indicate different people. Similarity scores are traditionally computed by fingerprint and face recognition algorithms, while dissimilarities are used in iris recognition. In some cases, the dissimilarity score is a distance possessing metric properties. In any case, scores can be either mate scores, coming from a comparison of one person's samples, or nonmate scores, coming from comparison of different persons' samples.

The words "genuine" or "authentic" are synonyms for mate, and the word "impostor" is used as a synonym for nonmate. The words "mate" and "nonmate" are traditionally used in identification applications (such as law enforcement search, or background checks) while genuine and impostor are used in verification applications (such as access control).

An error tradeoff characteristic represents the tradeoff between Type II and Type I classification errors. For identification this plots false negative vs. false positive identification rates i.e. FNIR vs. FPIR parametrically with T. Such plots

This publication is available free of charge from: https://doi.org/10.6028/NIST.IR.8271

are often called detection error tradeoff (DET) characteristics or receiver operating characteristic (ROC). These serve the same function − to show error tradeoff − but differ, for example, in plotting the complement of an error rate (e.g. TPIR = 1 − FNIR) and in transforming the axes, most commonly using logarithms, to show multiple decades of FPIR. More rarely, the function might be the inverse of the Gaussian cumulative distribution function.

The slides of Figures 10 through 15 discuss presentation and interpretation of DETs used in this document for reporting face identification accuracy. Further detail is provided in formal biometrics testing standards, see the various parts of ISO/IEC 19795 Biometrics Testing and Reporting. More terms, including and beyond those to do with accuracy, appear in ISO/IEC 2382-37 Information technology – Vocabulary – Part 37: Harmonized biometric vocabulary.

This publication is available free of charge from: https://doi.org/10.6028/NIST.IR.8271

This publication is available free of charge from: https://doi.org/10.6028/NIST.IR.8271

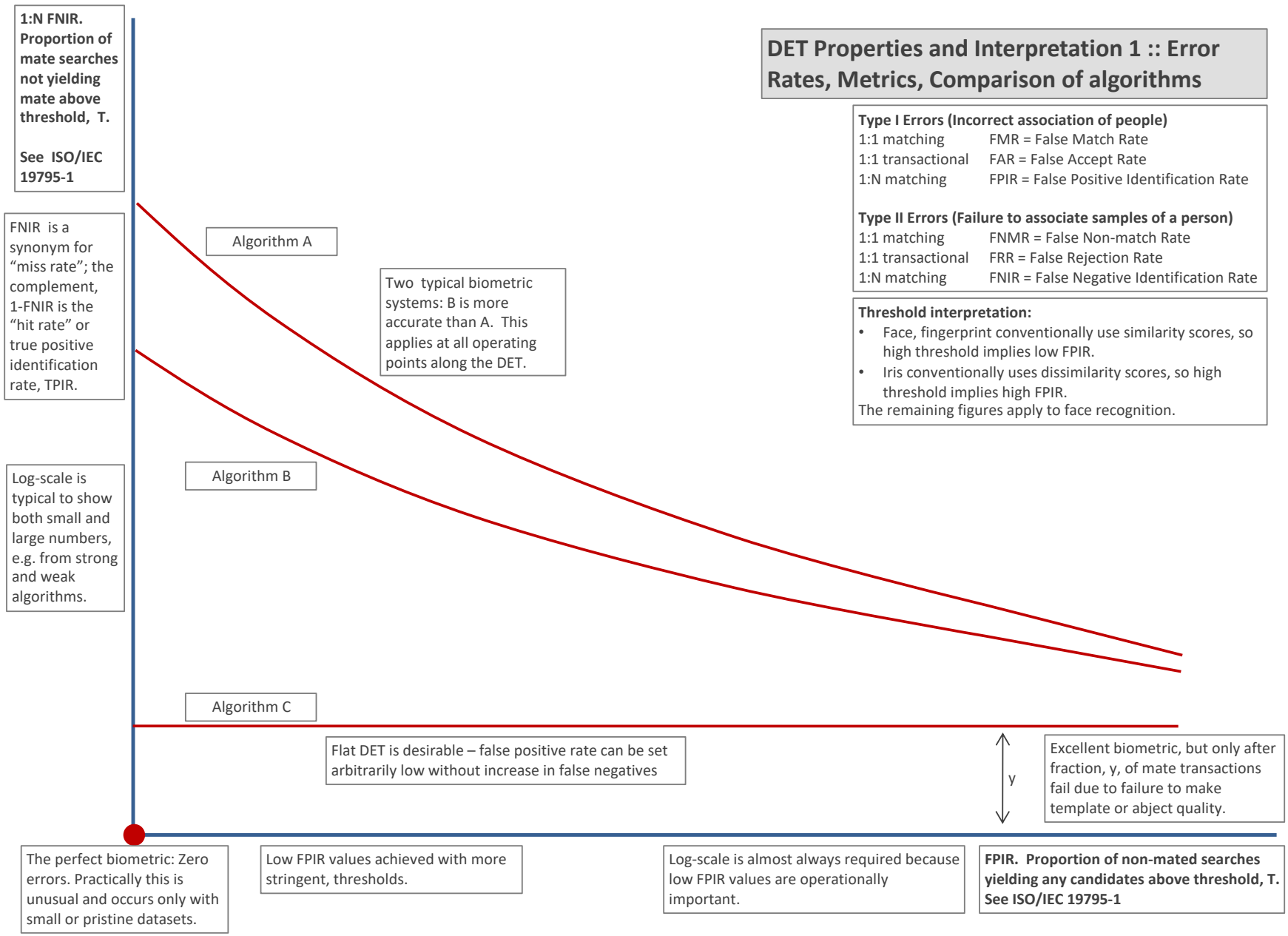

Figure 10: **DET as the primary performance reporting mechanism**.

This publication is available free of charge from: https://doi.org/10.6028/NIST.IR.8271

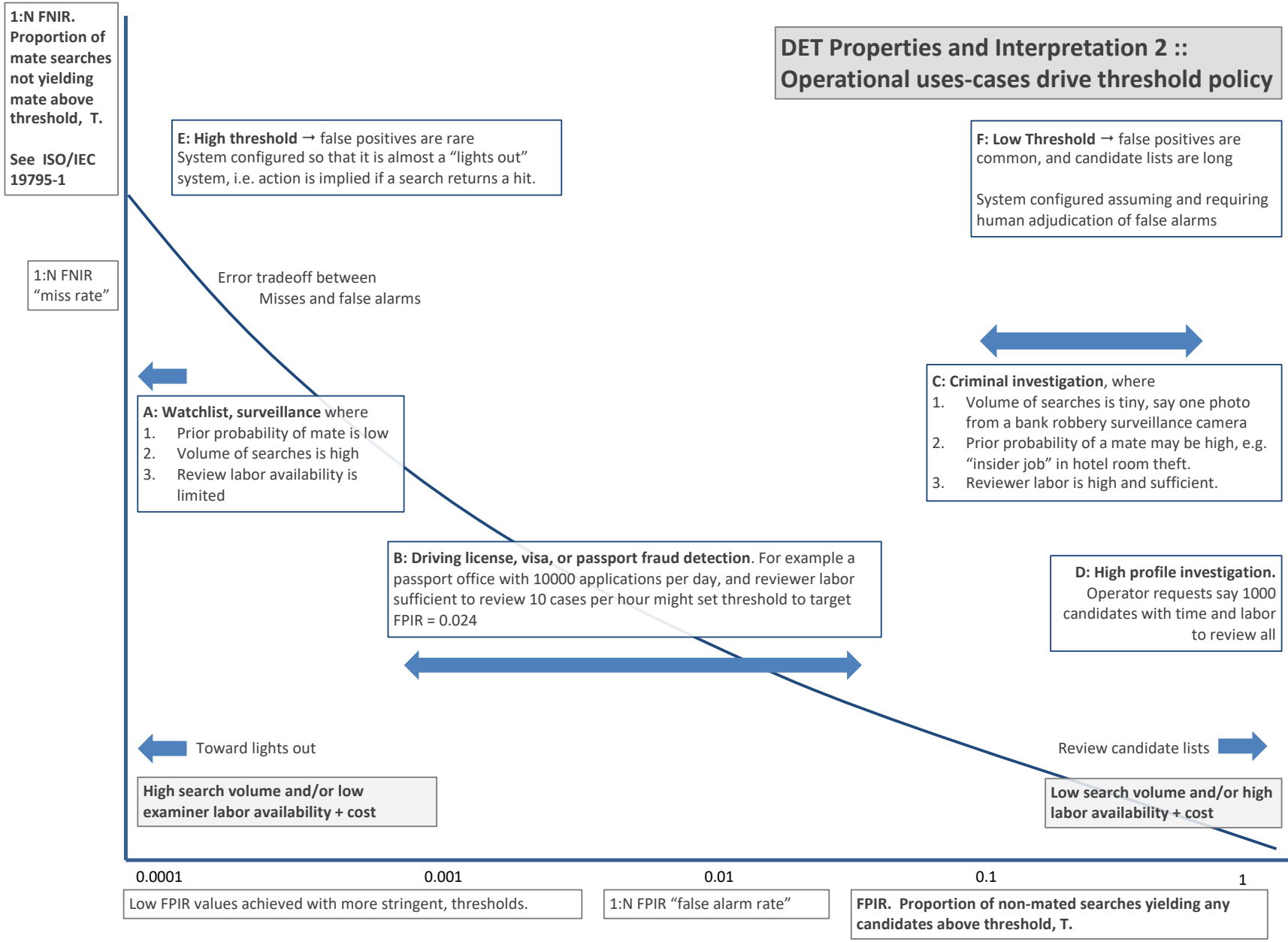

Figure 11: **DET as the primary performance reporting mechanism**.

2026/01/09 20:40:38

FNIR(N, R, T) = False neg. identification rate
FPIR(N, T) = False pos. identification rate
N = Num. enrolled subjects
R = Num. candidates examined
T = Threshold
T = 0 → Investigation
T > 0 → Identification

This publication is available free of charge from: https://doi.org/10.6028/NIST.IR.8271

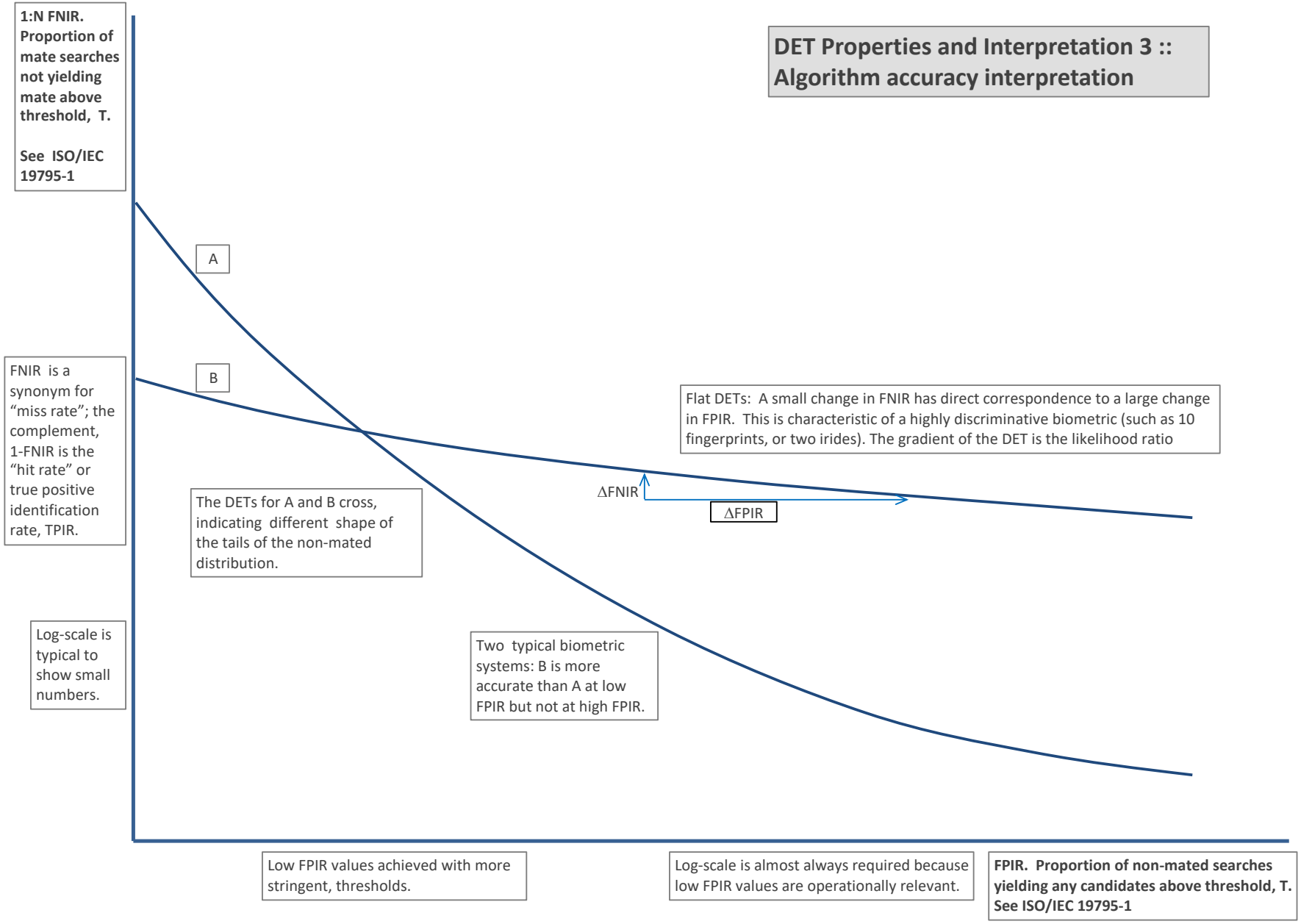

Figure 12: **DET as the primary performance reporting mechanism**.

2026/01/09 20:40:38

FNIR(N, R, T) = False neg. identification rate
FPIR(N, T) = False pos. identification rate

N = Num. enrolled subjects
R = Num. candidates examined

T = Threshold

T = 0 → Investigation
T > 0 → Identification

This publication is available free of charge from: https://doi.org/10.6028/NIST.IR.8271

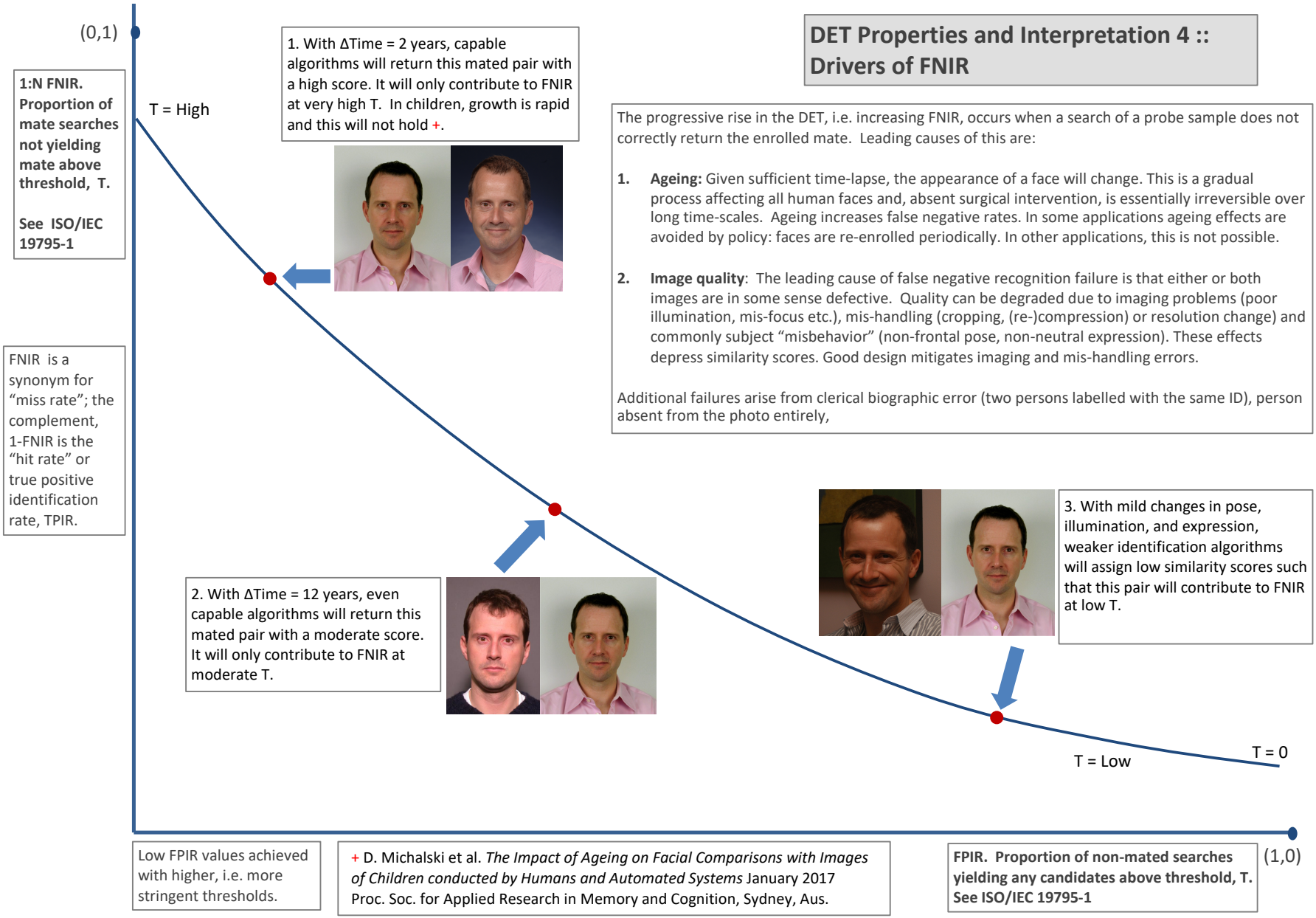

Figure 13: **DET as the primary performance reporting mechanism**.

2026/01/09 20:40:38
FNIR(N, R, T) = False neg. identification rate
FPIR(N, T) = False pos. identification rate
N = Num. enrolled subjects
R = Num. candidates examined
T = Threshold
T = 0 → Investigation
T > 0 → Identification

This publication is available free of charge from: https://doi.org/10.6028/NIST.IR.8271

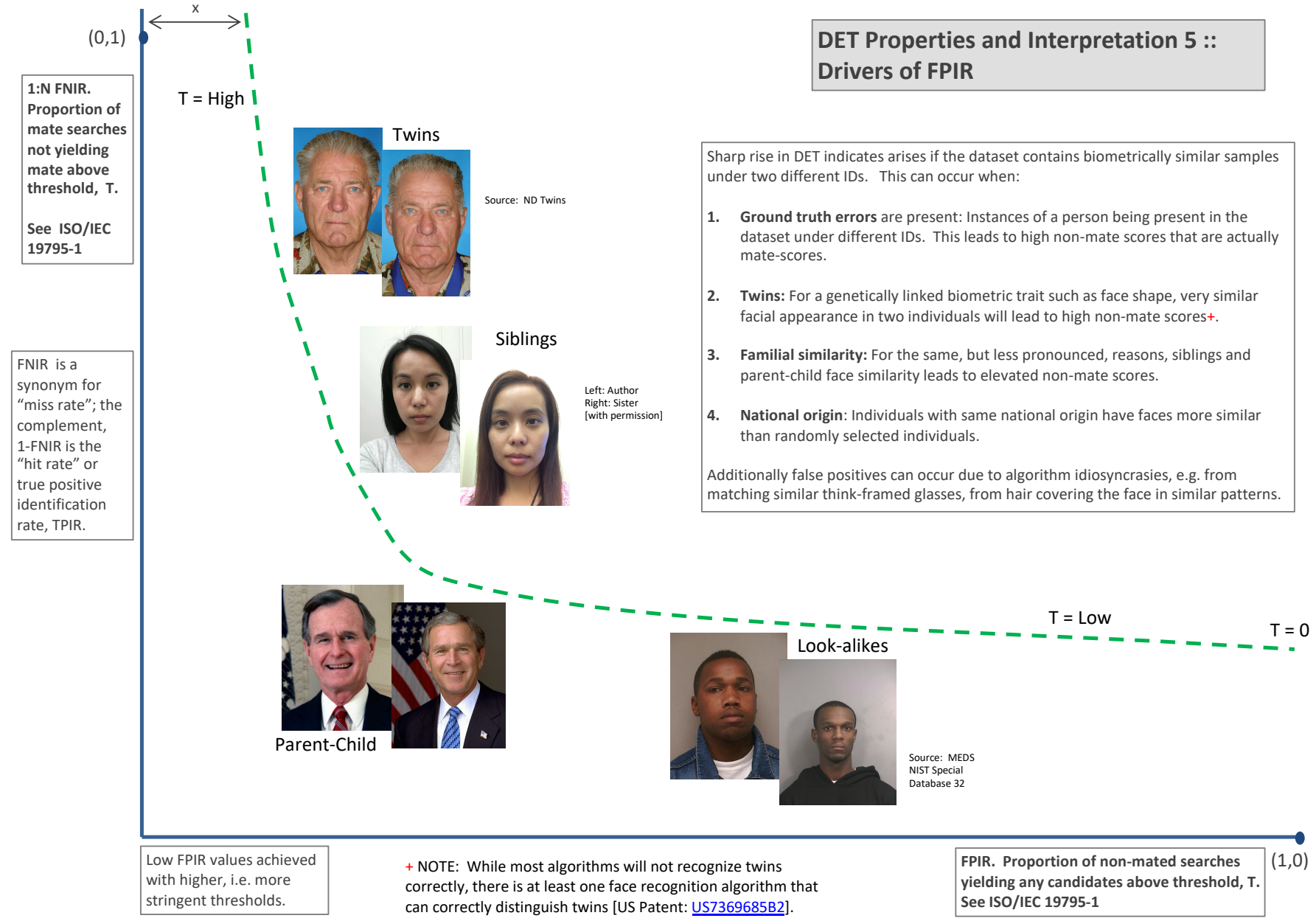

Figure 14: **DET as the primary performance reporting mechanism**.

2026/01/09 20:40:38
FNIR(N, R, T) = False neg. identification rate
FPIR(N, T) = False pos. identification rate
N = Num. enrolled subjects
R = Num. candidates examined
T = Threshold
T = 0 → Investigation
T > 0 → Identification

This publication is available free of charge from: https://doi.org/10.6028/NIST.IR.8271

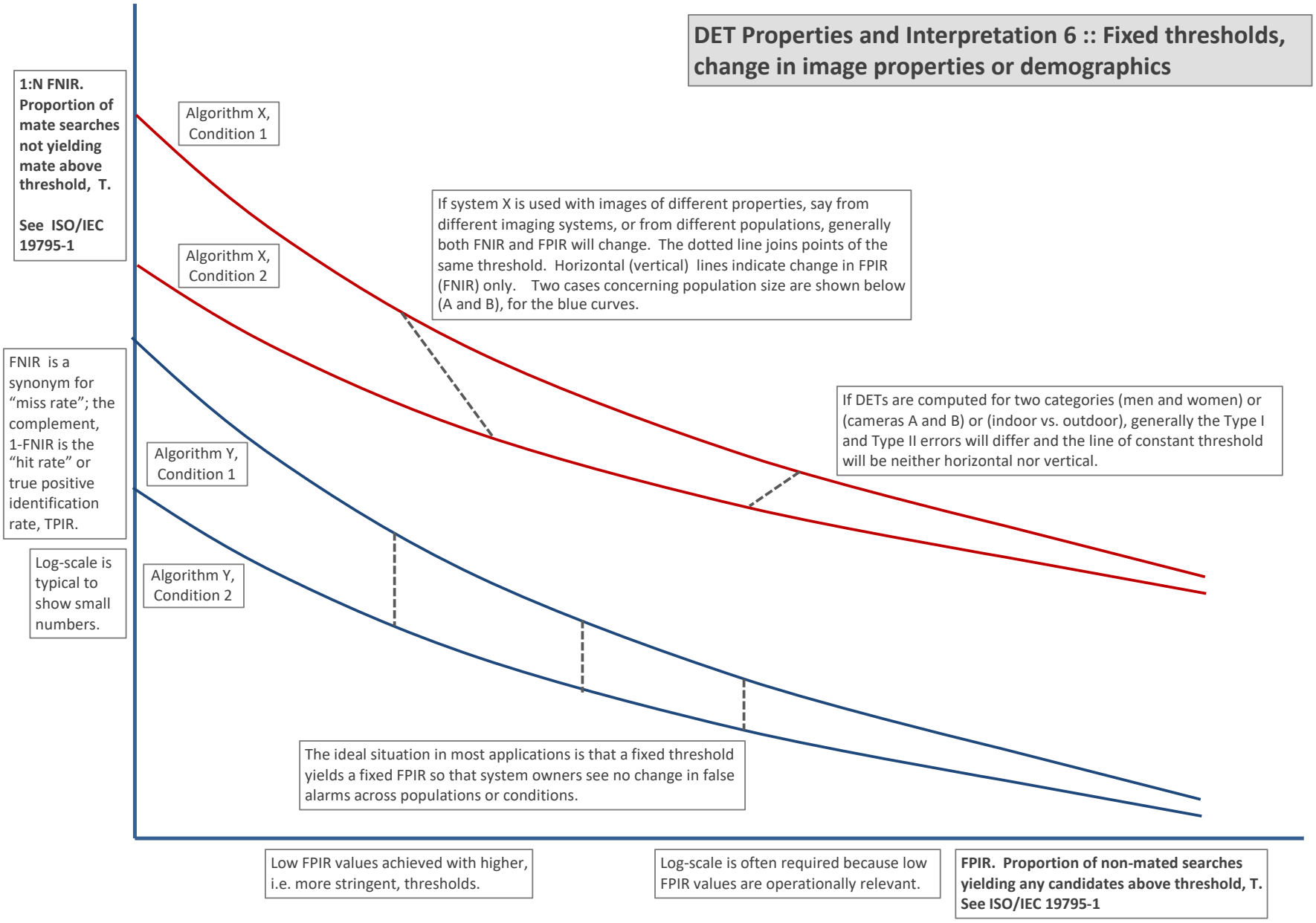

Figure 15: **DET as the primary performance reporting mechanism**.

2026/01/09 20:40:38

FNIR(N, R, T) = False neg. identification rate
FPIR(N, T) = False pos. identification rate
N = Num. enrolled subjects
R = Num. candidates examined
T = Threshold
T = 0 → Investigation
T > 0 → Identification

This publication is available free of charge from: https://doi.org/10.6028/NIST.IR.8271

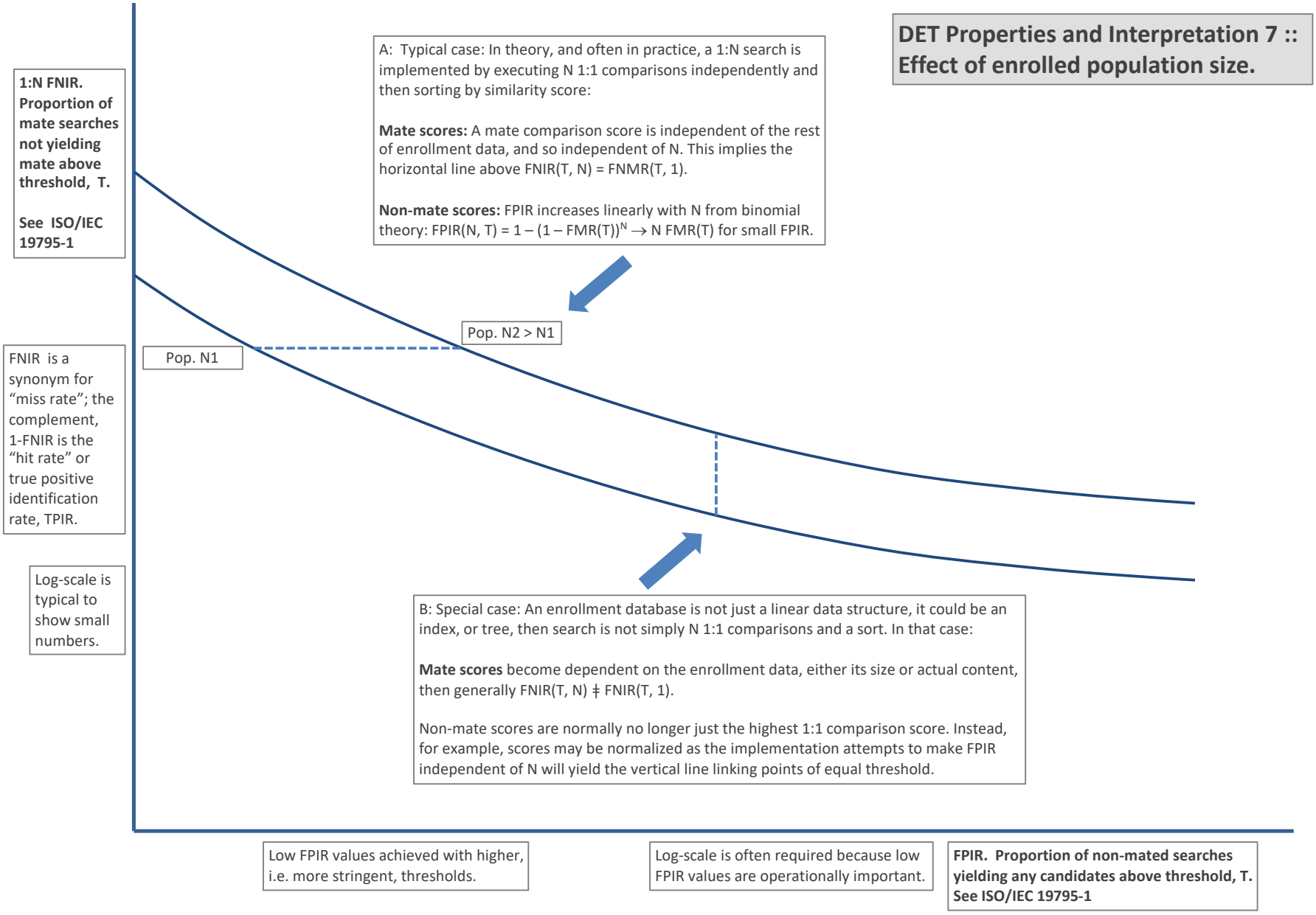

Figure 16: **DET as the primary performance reporting mechanism**.

2026/01/09 20:40:38

FNIR(N, R, T) = False neg. identification rate
FPIR(N, T) = False pos. identification rate
N = Num. enrolled subjects
R = Num. candidates examined
T = Threshold
T = 0 → Investigation
T > 0 → Identification

This publication is available free of charge from: https://doi.org/10.6028/NIST.IR.8271

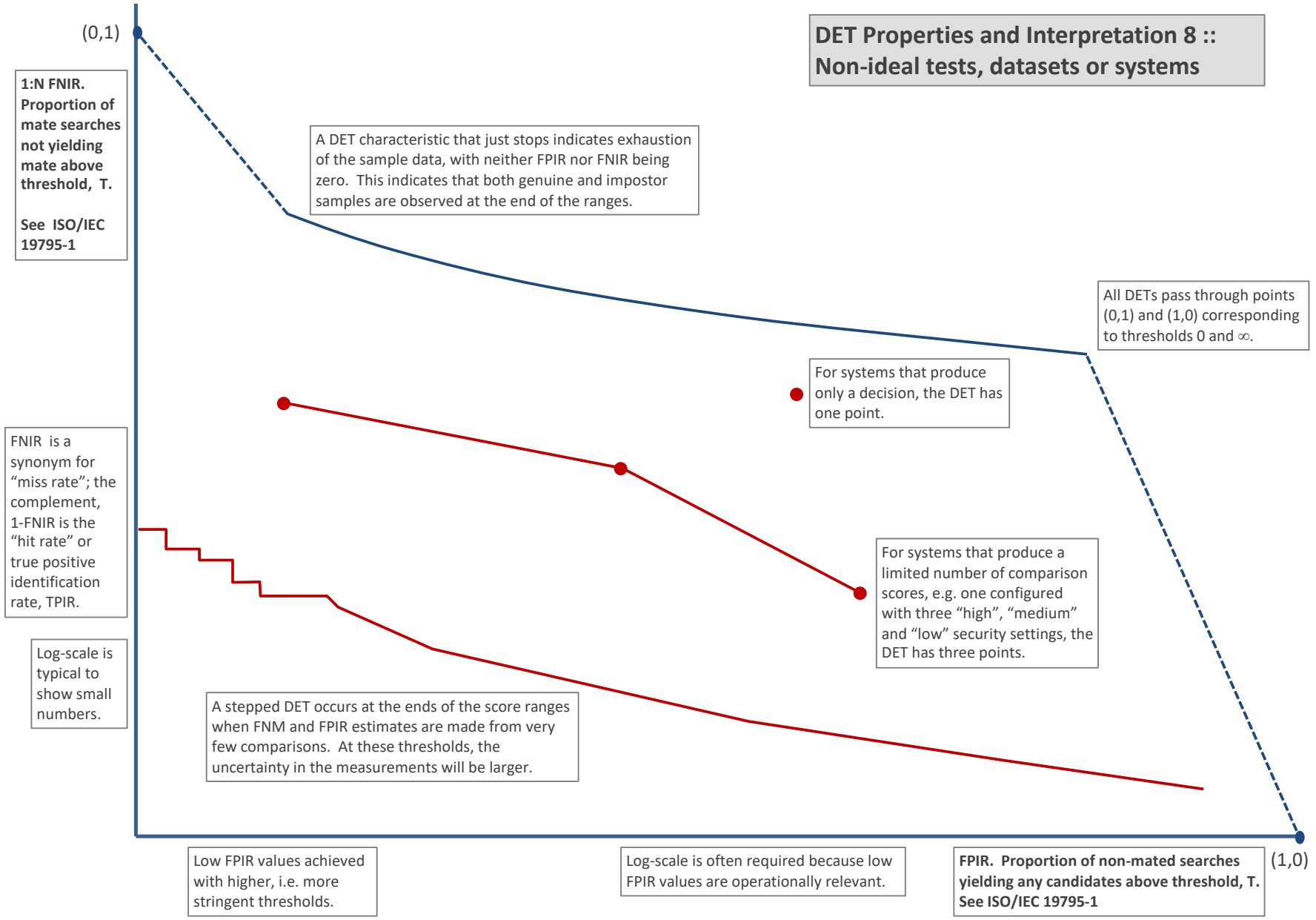

Figure 17: **DET as the primary performance reporting mechanism**.

2026/01/09 20:40:38

FNIR(N, R, T) = False neg. identification rate
FPIR(N, T) = False pos. identification rate
N = Num. enrolled subjects
R = Num. candidates examined
T = Threshold
T = 0 → Investigation
T > 0 → Identification

3.4 Best practice testing requires execution of searches with and without mates

FRVT embeds 1:N searches of two kinds: Those for which there is an enrolled mate, and those for which there is not. The respective numbers for these types of searches appear in Table 1. However, it is common to conduct only mated searches[10]. The cumulative match characteristic is computed from candidate lists produced in mated searches. Even if the CMC is the only metric of interest, the actual trials executed in a test should nevertheless include searches for which no mate exists. As detailed in Table 1 the FRVT reserved disjoint populations of subjects for executing true non-mate searches.

3.5 Failure to extract features

During enrollment some algorithms fail to convert a face image to a template. The proportion of failures is the failure-to-enroll rate, denoted by FTE. Similarly, some search images are not converted to templates. The corresponding proportion is termed failure-to-extract, denoted by FTX.

We do not report FTX because we assume that the same underlying algorithm is used for template generation for enrollment and search.

Failure to extract rates are incorporated into FNIR and FPIR measurements as follows.

- **Enrollment templates**: Any failed enrollment is regarded as producing a zero length template. Algorithms are required by the API [10] to transparently process zero length templates. The effect of template generation failure on search accuracy depends on whether subsequent searches are mated, or non-mated: Mated searches will fail giving elevated FNIR; non-mated searches will not produce false positives so, to first order, FPIR will be reduced by a factor of $1-\text{FTE}$.

- **Search templates and 1:N search**: In cases where the algorithm fails to produce a search template from input imagery, the result is taken to be a candidate list whose entries have no hypothesized identities and zero score. The effect of template generation failure on search accuracy depends on whether searches are mated, or non-mated: Mated searches will fail giving elevated FNIR; Non-mated searches will not produce false positives, so FPIR will be reduced. Thus given a measurement of false negative and positive rates made over only those where failures-to-extract did not occur, those rates - call them $\text{FNIR}^\dagger$ and $\text{FPIR}^\dagger$ - could be adjusted by an explicit measurement of FTX as follows

$$\text{FNIR} = \text{FTX} + (1 - \text{FTX})\text{FNIR}^\dagger \tag{8}$$

$$\text{FPIR} = (1 - \text{FTX})\text{FPIR}^\dagger \tag{9}$$

This approach is the correct treatment for positive-identification applications such as access control where cooperative users are enrolled and make attempts at recognition. This approach is not appropriate to negative identification applications, such as visa fraud detection, in which hostile individuals may attempt to evade detection by submitting poor quality samples. In those cases, template generation failures should be investigated as though a false alarm had occurred.

[10]For example, the Megaface benchmark. This is bad practice for several reasons: First, if a developer knows, or can reasonably assume, that a mate always exists, then unrealistic gaming of the test is possible. A second reason is that it does not put FPIR on equal footing with FNIR and that matters because in most applications, not all searches have mates - not everyone has been previously enrolled in a driving license issuance or a criminal justice system - so addressing between-class separation becomes necessary.

This publication is available free of charge from: https://doi.org/10.6028/NIST.IR.8271

3.6 Fixed length candidate lists, threshold independent workload

Suppose an automated face identification algorithm returns L candidates, and a human reviewer is retained to examine up to R candidates, where $R \leq L$ might be set by policy, preference or labor availability. For now, assume also that the reviewer is not provided with, or ignores, similarity scores, and thresholds are not applied. Given the algorithm typically places mates at low (good) ranks, the number of candidates a reviewer can be expected to review can be derived as follows. Note that the reviewer will:

- ▷ Always inspect the first ranked image — Frac. reviewed = 1
- ▷ Then inspect those candidates where mate not confirmed at rank 1 — Frac. reviewed = 1-CMC(1)
- ▷ Then inspect those candidates where mate not confirmed at rank 1 or 2 — Frac. reviewed = 1-CMC(2)

etc. Thus if the reviewer will stop after a maximum of R candidates, the expected number of candidate reviews is

$$M(R) = 1 + (1 - CMC(1)) + (1 - CMC(2)) + \ldots + (1 - CMC(R-1)) \tag{10}$$

$$= R - \sum_{r=1}^{R-1} CMC(r) \tag{11}$$

A recognition algorithm that front-loads the cumulative match characteristic will offer reduced workload for the reviewer. This workload is defined only over the searches for which a mate exists. In the cases where there truly is no mate, the reviewer would review all R candidates. Thus, if the proportion of searches for which a mate does exist is β, which in the law enforcement context would be the recidivism rate [3], the full expression for workload becomes:

$$M(R) = \beta \left(R - \sum_{r=1}^{R-1} CMC(r) \right) \quad + \quad (1 - \beta)R \tag{12}$$

$$= R - \beta \sum_{r=1}^{R-1} CMC(r) \tag{13}$$

3.7 Timing measurement

Algorithms were submitted to NIST as implementations of the application programming interface(API) specified by NIST in the Evaluation Plan [10]. The API includes functions for initialization, template generation, finalization, search, gallery insert, and gallery delete. Two template generation functions are required, one for the preparation of an enrollment template, and one for a search template.

In NIST's test harness, all functions were wrapped by calls to the C++ std::chrono::high resolution clock which on the dedicated timing machine counts 1ns clock ticks. Precision is somewhat worse than that however.

This publication is available free of charge from: https://doi.org/10.6028/NIST.IR.8271

3.8 Uncertainty estimation

3.8.1 Random error

This study leverages operational datasets for measurement of recognition error rates. This affords several advantages. First, large numbers of searches are conducted (see Table 1) giving precision to the measurements. Moreover, for the two mugshot datasets, these do not involve reuse of individuals so binomial statistics can be expected to apply to recognition error counts. In that case, an observed count of a particular recognition outcome (i.e. a false negative or false positive) in M trials will sustain 95% confidence that the actual error rate is no larger than some value.

As an example, the minimum number of mugshot searches conducted in this report is M =154 549, and for an observed FNIR around 0.002, the measurement supports a conclusion that the actual FNIR is no higher than 0.00228 at 99% confidence level. On the false positive side, we tabulate FNIR at FPIR values as low as 0.001. Given estimates based on 331 254 non-mate trials, the actual FPIR values will be below 0.00115 at 99% confidence. In conclusion, large scale evaluation, without reuse of subjects, supports tight uncertainty bounds on the measured error rates.

3.8.2 Systematic error

The FRVT 2018 dataset includes anomalies discovered as a result of inspecting images involved in recognition failures from the most accurate algorithms. Two kinds of failure occur: False negatives (which, for the purpose here, include failures to make templates) and false positives.

False negative errors: We reviewed 600 false negative pairs for which either or both of the leading two algorithms did not put the correct mate in the top 50 candidates. Given 154 549 searches, this number represents 0.39% of the total, resulting in FNIR ~ 0.0039. Of the 600 pairs:

- **A: Poor quality**: About 20% of the pairs included images of very low quality, often greyscale, low resolution, blurred, low contrast, partially cropped, interlaced, or noisy scans of paper images. Additionally, in a few cases, the face is injured or occluded by bandages or heavy cosmetics.
- **B: Ground truth identity label bugs**: About 15% of the pairs are not actually mated. We only assigned this outcome when a pair is clearly not mated.
- **C: Profile views**: About 35% included an image of a profile (side) view of the face, or, more rarely, an image that was rotated 90 degrees in-plane (roll).
- **D: Tattoos**: About 30% included an image of a tattoo that contained a face image. These arise from mis-labelling in the parent dataset metadata.
- **E: Ageing**: There is considerable time-lapse between the two captures.

All these estimates are approximate. Of these, the tattoo and mislabled images can never be matched. These constitute an accuracy floor in the sample implying that FNIR cannot be below 0.0018[11]. The profile-views, low-quality images, and images with considerable ageing can, in principle, be successfully matched - indeed some algorithms do so - so are not part of the accuracy floor.

[11] This value is the sum of two partial false negative rates: FNIR_B = 0.15 * 0.0039 plus FNIR_D = 0.3 * 0.0039

This publication is available free of charge from: https://doi.org/10.6028/NIST.IR.8271

For the microsoft-4 algorithm the lowest miss rate from (recent entry in Table 45) is FNIR(640 000, 50, 0) = 0.0018. This is close to the value estimated from the inspection of misses. It is below the 0.0039 figure because the algorithm does match some profile and poor quality images, that the yitu-2 algorithm does not.

For many tables (e.g. Table 45), the FNIR values obtained for the FRVT-2018 mugshots could be corrected by reducing them by 0.0018. The best values would then be indistinct from zero. The results in this report *were not* adjusted to account for this systematic error.

False positive errors: As shown in Figure 1 and discussed in Figure 14 many of the DET characteristics in this report exhibit a pronounced turn upward at low false positive rates. The shape can be caused by identity labelling errors in the ground truth of a dataset, specifically persons present in the database under two IDs such that some proportion of non-mate pairs are actually mated. To look for such possibilities, we merged the highest 1000 non-mate pairs produced by three different algorithms which resulted in 1839 unique pairs. This constitutes 0.56% of all non-mate searches. We assert that it is *very* difficult for human reviewers to assign the pairs into the following three categories: twins; doppelgangers; or ground-truth errors (instances of the same person under two IDs). Given this difficulty we made no attempt to correct any possible ground truth errors except by removing 57 pairs in the following categories:

- **A: Profile views**: Thirteen pairs included one or two profile-view images. As described in Figure 310, these can cause false positives.
- **B: Same-session photographs**: For twelve pairs, the images were identical or trivially altered (e.g. cropped) versions of the same photo. These were present under a different ID likely due to some clerical or procedural mistake.
- **C: Tattoos of faces**: There were fourteen instances of tattoo photographs that contained faces causing false matches.
- **D: T-shirt faces**: There were six instances of T-shirt photographs (of Bob Marley and Che Guevara) being detected instead of the face and causing false positives.
- **E: Background faces**: There were twelve instances of one subject appearing in the background of two otherwise correct portrait photos.

Note we did not remove any images where there was a chance that the pair was actually a different person.

In any case, the results in this report have not been adjusted for this systematic error.

This publication is available free of charge from: https://doi.org/10.6028/NIST.IR.8271

4 Results

This section gives extensive results for algorithms submitted to FRVT 2018. Three page "report cards" for each algorithm are contained in a separate supplement. Performance metrics were described in section 3. The main results are summarized in tabular form with more exhaustive data included as DET, CMC and related graphs in appendices as follows:

- The three tables 2-4 list algorithms alongside full developer names, acceptance date, size of the provided configuration data, template size and generation time, and search duration data.
  - The **template generation duration** is most important to applications that require fast response. For example, an eGate taking more than two seconds to produce a template might be unacceptable. Note that GPUs may be of utility in expediting this operation for some algorithms, though at additional expense. Two additional factors should be considered[12][13].
  - The **search duration** is the time taken for a search of a search template into a gallery of N enrollment templates. This performance variable, together with the volume of searches, is influential on the amount of hardware needed to sustain an operational deployment. This is measured here with the algorithm running on a single core of a contemporary CPU. Search is most simply implemented as N computations of a distance metric followed by a sort operation to find the closest enrollments. However, considerable optimization of this process is possible, up to and including fast-search algorithms that, by various means, avoid computation of all N distances.
  - The **template size** is the size of the extracted feature vector (or vectors) and any needed header information. Large template sizes may be influential on bus or network bandwidth, storage requirements, and on search duration. While the template itself is an opaque data blob, the feature dimensionality might be estimated by assuming a four-bytes-per-float encoding. There is a wide range of encodings. For the more accurate algorithm, sizes range from 256 bytes to about 2KB bytes, indicating essentially no consensus on face modeling and template design.
  - The **template size multiplier** column shows how, given k input images, the size of the template grows. Most implementations internally extract features from each image and concatenate them, and implement some score-level fusion logic during search. Other implementations, including many of the most accurate algorithms, produce templates whose size does not grow with k. This could be achieved via selection of the best quality image - but this is not optimal in handling ageing where the oldest image could be the best quality. Another mechanism would be feature-level fusion where information is fused from all k inputs. In any case, as a black-box test, the fusion scheme is proprietary and unknown.
  - The size of the **configuration data** is the total size of all files resident in a vendor-provided directory that contains arbitrary read-only files such as parameters, recognition models (e.g caffe). Generally a large value for this quantity may prohibit the use of the algorithm on a resource-constrained device.

[12] The FRVT 2018 API prohibited threading, so some gains from parallelism may be available on multiple-cores or multiple processors, if the feature extraction code could be distributed across them.

[13] Note also that factors of two or more may be realizable by exploiting modern vector processing instructions on CPUs. It is not clear in our measurements whether all developers exploited Intel's AVX2 instructions, for example. Our machine was so equipped, but we insisted that the same compiled library should also run on older machines lacking that instruction. The more sophisticated implementations may have detected AVX2 presence and branched accordingly. The less sophisticated may be defaulted to the reduced instruction set. Readers should see the FRVT 2018 API document for the specific chip details.

This publication is available free of charge from: https://doi.org/10.6028/NIST.IR.8271

This publication is available free of charge from: https://doi.org/10.6028/NIST.IR.8271

▷ Tables 45-46 report core rank-based accuracy for mugshot images. The population size is limited to N = 1.6 million identities because this is the largest gallery size on which all algorithms were executed. Notable observations from these tables are as follows:

- **Accuracy gains since 2018**: NIST Interagency Report 8238 documented massive gains over those reported in the FRVT 2014 report, NIST Interagency Report 8009. Further gains are documented in this report. Comparing the most accurate algorithm in November 2018, NEC-3, the value of FNIR(N, L, T) reduced from 0.0031 to 0.0024 for the Sensetime-004 algorithm with N = 12 million recent images. The tables show broader gains: many developers have made advances since 2018 with between two and five-fold reduction in errors.
- **Wide range in accuracy**: The rank-1 miss rates vary from FNIR(N, 1, 0) = 0.0012 for sensetime-004 up to about 0.5 for the very fast but inaccurate microfocus-x algorithms. Among the developers who are superior to NEC in 2013, the range is from 0.002 to 0.035 for camvi-3. This large accuracy range is consistent with the buyer-beware maxim, and indicates that face recognition software is far from being commoditized.

▷ Tables 53-54 report threshold-based error rates, FNIR(N, L, T), for N = 1.6 million for mugshot-mugshot accuracy on FRVT 2014, FRVT 2018, and also (in pink) mugshot-webcam accuracy using FRVT 2018 enrollments. Notable observations from these tables are as follows:

- **Order of magnitude accuracy gains since 2014**: As with rank-based results, the gains in accuracy are substantial, though somewhat reduced. At FPIR = 0.01, the best improvement over NEC in 2014 is a 27 fold reduction in FNIR using the NEC_2 algorithm. At FPIR = 0.001, the largest gain is a six-fold reduction in FNIR via the NEC_3 algorithm.
- **Broad gains across the industry**: About 19 companies realize accuracy better than the NEC benchmark from 2014. This is somewhat lower than the 28 developers who succeeded on the rank-1 metric. This may be due to the ubiquity of, and emphasis on, the rank-1 metric in many published algorithm development papers.
- **Webcam images**: Searches of webcam images give FNIR(N, T) values around 2 to 3 times higher than mugshot searches. Notably the leading developers with mugshots are approximately the same with poorer quality webcams. But some developers e.g. Camvi, Megvii, TongYi, and Neurotechnology do improve their relative rankings on webcams, perhaps indicating their algorithms were tailored to less constrained images.

▷ Tables 33, 39, 40 and show, respectively, high-threshold, rank 1, and rank 50 FNIR values for all algorithms performing searches into five different gallery sizes, N = 640 000, N = 1 600 000, N = 3 000 000, N = 6 000 000 and 12 000 000. The FPIR = 0.001 table is included to inform high-volume duplicate detection applications. The Rank-1 table is included as a primary accuracy indicator. The Rank-50 table is included to inform agencies who routinely produce 50 candidates for human-review. The notable results are:

- **Slow growth in rank-based miss rates:** FNIR(N, R) generally grows as a power law, aN^b. From the straight lines of many graphs of Figure 20 this is clearly a reasonable model for most, but not all, algorithms. The coefficient a can be interpreted as FNIR in a gallery of size 1. The more important coefficient b indicates scalability, and often, $b \ll 1$, implies very benign growth in FNIR. The coefficients of the models appear in the Tables 39 and 40.
- **Slow growth in threshold-based miss rates:** FNIR(N, T) also generally grows as a power law, aN^b except at the high threshold values corresponding to low FPIR values. This is visible in the plots of Figure 84 which

show straight lines except for FPIR = 0.001, which increase more rapidly with N above 3 000 000. Each trace in those figures shows FNIR(N, T) at fixed FPIR with both N and T varying. Thus at large N, it is usually necessary to elevate T to maintain fixed FPIR. This causes increased FNIR. Why that would no-longer obey a power-law is not known. However, if we expect large galleries to contain individuals with familial relations to the non-mate search images - in the most extreme case, twins - then suppression of false positives becomes more difficult. This is discussed in the Figures starting at Fig. 10

▷ Figure **??** shows false positives from twins against their enrolled siblings, broken out by type of twin: fraternal or identical. The Figure is based on the enrollment of 104 single images on one of a pair of twins, and then the search of 2354 second images. Note that the dataset is heavily skewed towards identical twins which is not representative of the true population. There is also a skew towards same sex fraternal twin pairs compared to different sex fraternal twin pairs again not representative of the true population.

The notable results are:

- For all algorithms tested, the 1087 mated searches (Twin A vs. Twin A) produce scores almost always above typical operational thresholds, with (not shown) matches at rank 1. The images are of good quality, so this is the result expected from the rest of this report.
- For the 1066 identical twin searches (AB), almost all produce the twin at rank 1, with a few producing the mate at further down the candidate lists rank and low score.
- For the 169 fraternal searches (AB) from same sex pairs, most algorithms give a large number of very high scores, implying false positives at all thresholds. However, there there are long tails containing lower scores that are correctly below threshold. In general, scores that are higher in this distribution are all rank 1 whereas the lower scores have much higher ranks.
- (Not shown) Of the 169, there are 24 fraternal searches (AB) involving different sex twins. Here most algorithms correctly report scores well below the lowest threshold, and usually not on the candidate list at all.

This publication is available free of charge from: https://doi.org/10.6028/NIST.IR.8271

This publication is available free of charge from: https://doi.org/10.6028/NIST.IR.8271

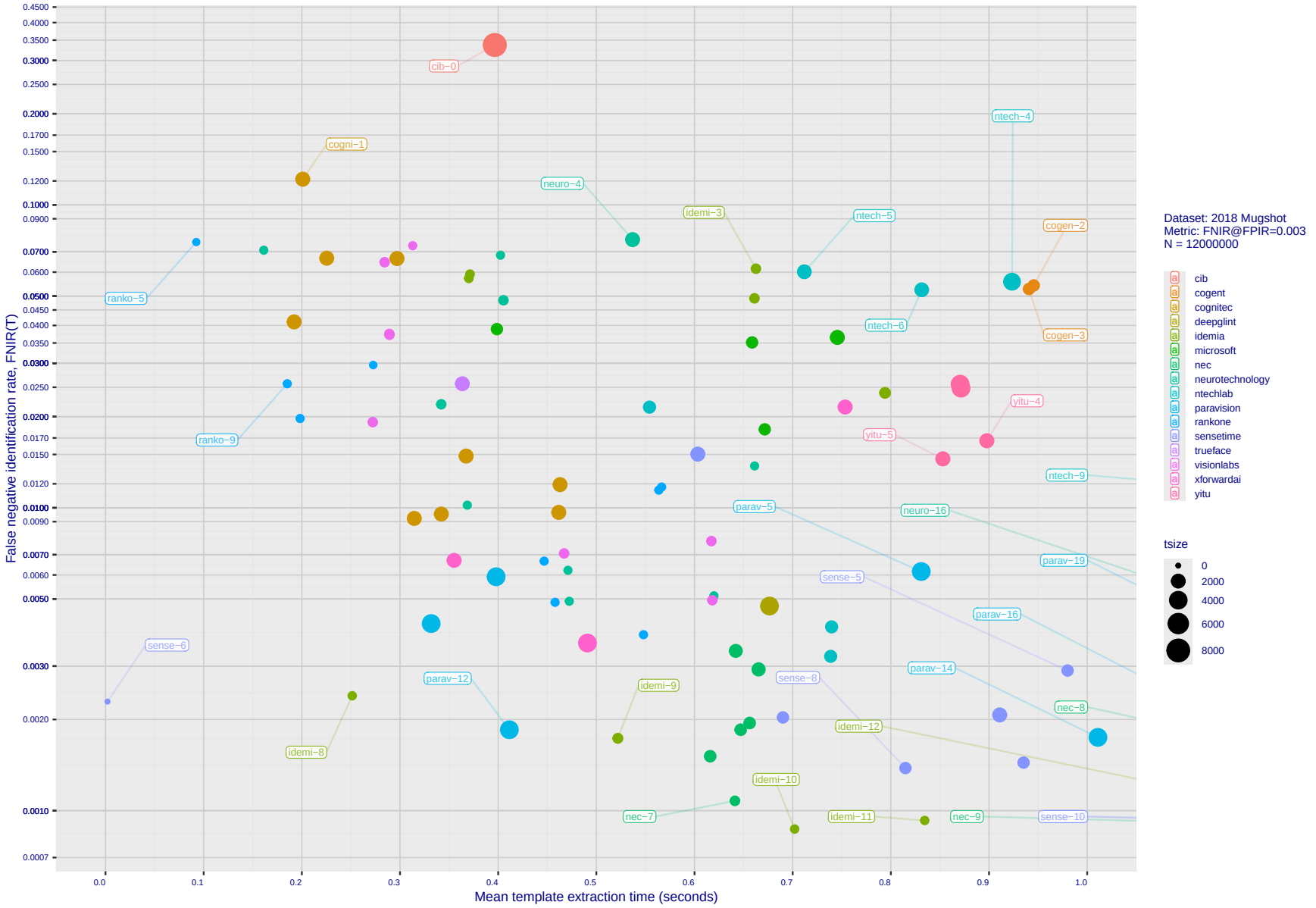

Figure 18: **[Mugshot Dataset] Speed-accuracy tradeoff**. *For developers of the more accurate algorithms the plot shows the tradeoff of high-threshold recognition miss-rates, FNIR(N, N, T) for FPIR(N, T) = 0.003, and template generation time. Developers are coded by color. Template size is encoded by the size of the circle. Some labels are quite distant from the respective point, to avoid superposing text. Without any other influences, the assumption would be that taking time to localize the face, and extract features, would lead to better accuracy. The most notable result, for NEC, is that their slower algorithms are much more accurate than the version that extract features in fewer than 90 milliseconds.*

2026/01/09 20:40:38
FNIR(N, R, T) = False neg. identification rate
FPIR(N, T) = False pos. identification rate
N = Num. enrolled subjects
R = Num. candidates examined
T = Threshold
T = 0 → Investigation
T > 0 → Identification

This publication is available free of charge from: https://doi.org/10.6028/NIST.IR.8271

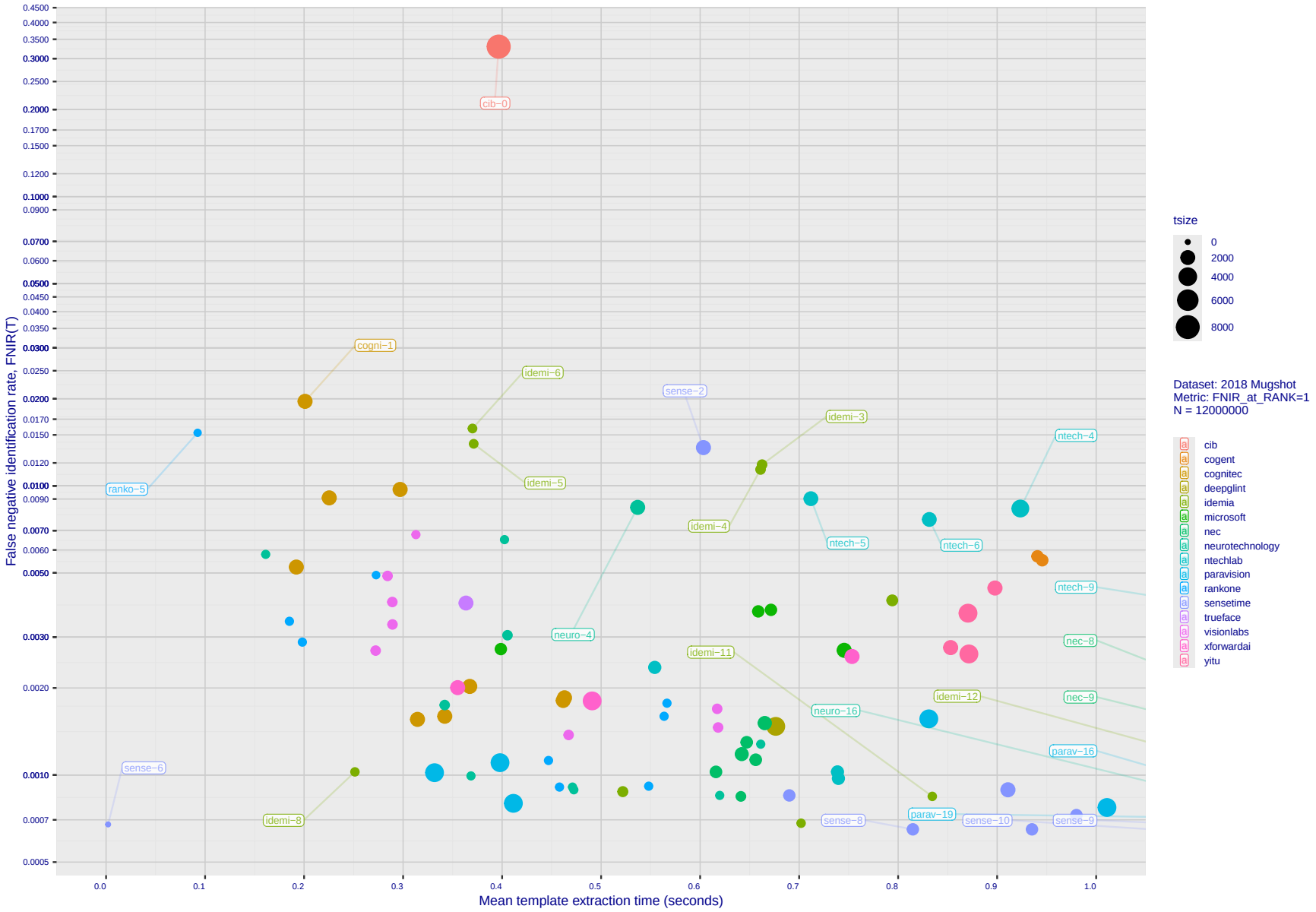

Figure 19: **[Mugshot Dataset] Speed-accuracy tradeoff**. *For developers of the more accurate algorithms the plot shows the tradeoff of rank-one recognition miss-rates, FNIR(N, 1, 0), and template generation time. Developers are coded by color. Template size is encoded by the size of the circle. Some labels are quite distant from the respective point, to avoid superposing text. Without any other influences, the assumption would be that taking time to localize the face, and extract features, would lead to better accuracy. This occurs for NEC with their slower algorithm being much accurate than the version that extract features in fewer than 90 milliseconds.*

2026/01/09 20:40:38
FNIR(N, R, T) = False neg. identification rate
FPIR(N, T) = False pos. identification rate
N = Num. enrolled subjects
R = Num. candidates examined
T = Threshold
T = 0 → Investigation
T > 0 → Identification

This publication is available free of charge from: https://doi.org/10.6028/NIST.IR.8271

	DEVELOPER	DEVELOPER	SHORT	SEQ.	VALIDATION	CONFIG[1]	LIB[1]	TEMPLATE GENERATION			FINALIZE[2]	SEARCH DURATION[5] MILLISEC					
	FULL NAME	LOCATION	NAME	NUM.	DATE	DATA (MB)	DATA (MB)	SIZE (B)	MULT[3]	TIME (MS)[4]	TIME (S)	L=1	L=50	L=50	L=50	L=50	POWER LAW
											N=1.6M	N=1.6M	N=1.6M	N=3M	N=6M	N=12M	(μs)
1	20Face	NL	20face	000	2021-10-01	112	319	[302]2048	-	[28]184	[119]9	[431]5679	[449]6341	-	-	-	
2	3Divi	RU	3divi	5	2018-10-26	186	51	[421]4096	k	[265]638	[382]28	[179]538	[179]537	[172]1377	[162]2614	[156]5530	$[353]0.07N^{1.1}$
3	3Divi	RU	3divi	6	2018-10-26	187	51	[81]528	k	[266]640	[55]5	[24]33	[22]33	-	-	-	
4	AFIS and Biometrics Consulting	US	afisbiometrics	000	2023-06-07	533	34	[38]265	-	[272]650	[8]2	[323]1718	[311]1563	[275]3063	[279]6541	[280]13588	$[276]0.46N^{1.1}$
5	AFR Engine	US	afrengine	000	2023-07-14	566	24	[329]2048	-	[357]818	[187]12	[419]4542	[426]4973	[367]9473	[366]20213	[361]45388	$[284]1.38N^{1.1}$
6	AFR Engine	US	afrengine	001	2024-03-15	565	24	[177]2048	-	[400]973	[233]13	[415]4505	[417]4444	[362]8555	[362]18109	[359]42844	$[314]0.89N^{1.1}$
7	AFR Engine	US	afrengine	002	2024-07-22	566	24	[189]2048	-	[421]1110	[208]12	[407]4324	[412]4120	[364]8653	[361]17832	[354]35825	$[333]0.61N^{1.1}$
8	AFR Engine	US	afrengine	003	2025-02-18	678	24	[257]2048	-	[404]1006	[237]13	[399]3803	[407]4034	[349]7389	[360]17642	[353]35554	$[299]0.90N^{1.1}$
9	ALTTEKGlobal	VN	alttekglobal	000	2024-04-12	634	2988	[193]2048	-	[419]1108	[211]13	[95]255	[96]257	-	-	-	
10	AadiSysTech	IN	aadi	000	2023-06-27	95	83	[56]512	-	[88]346	[33]3	[345]2024	[328]1754	-	-	-	
11	AadiSysTech	IN	aadi	001	2023-12-08	307	787	[310]2048	-	[15]127	[137]10	[383]3144	[381]2850	-	-	-	
12	AadiSysTech	IN	aadi	002	2024-04-17	95	567	[201]2048	-	[10]96	[234]13	[376]2992	[380]2794	-	-	-	
13	Acer Incorporated	TW	acer	000	2020-08-12	35	67	[67]512	-	[36]198	[45]4	[111]295	[110]295	[95]623	[150]2302	[146]4915	$[397]0.00N^{1.3}$
14	Acer Incorporated	TW	acer	001	2021-11-08	42	610	[186]2048	-	[8]92	[116]9	[155]444	[189]575	-	-	-	
15	Adiance Technologies Pvt Ltd	IN	adiance	001	2025-04-28	261	332	[209]2048	-	[329]887	[361]22	[351]2096	[348]2048	-	-	-	
16	Advance.AI	SG	advance	000	2023-05-30	271	825	[175]2048	-	[232]573	[166]12	[355]2268	[361]2271	[314]4338	[311]8690	[312]17842	$[151]1.15N^{1.0}$
17	Akurat Satu Indonesia	ID	ptakuratsatu	000	2020-10-23	0	572	[82]538	-	[389]929	[485]28633	[14]18	[11]16	[7]17	[6]17	[5]17	$[3]6827.74N^{0.1}$
18	Akuvox	CN	akuvox	001	2025-02-14	0	213	[467]4843	-	[14]114	[392]30	[360]2434	[376]2613	[325]4738	[325]10025	[325]19681	$[128]1.39N^{1.0}$
19	Alchera Inc	KR	alchera	2	2018-10-30	7	14	[218]2048	k	[13]114	[442]63	[374]2923	[383]2929	-	-	-	
20	Alchera Inc	KR	alchera	3	2018-10-30	251	14	[205]2048	k	[211]531	[443]63	[375]2955	[384]2956	[341]6546	[346]15013	[352]35262	$[390]0.10N^{1.2}$
21	Alchera Inc	KR	alchera	004	2021-09-17	476	24	[198]2048	-	[343]786	[405]35	[436]5801	[457]6851	-	-	-	
22	Alchera Inc	KR	alchera	005	2023-07-18	977	482	[166]2048	-	[208]527	[407]35	[439]6123	[439]6035	-	-	-	
23	Alchera Inc	KR	alchera	006	2023-11-22	977	482	[194]2048	-	[220]546	[165]12	[455]8046	[458]6865	[375]11609	[382]27328	[377]59209	$[165]3.40N^{1.0}$
24	Alchera Inc	KR	alchera	007	2024-06-17	978	482	[221]2048	-	[226]558	[181]12	[477]20981	[486]20564	-	-	-	
25	Alchera Inc	KR	alchera	008	2024-10-25	2037	443	[231]2048	-	[478]1429	[161]12	[448]6350	[441]6134	[378]11940	[375]25274	[375]56159	$[322]1.03N^{1.1}$
26	Algorithms Inc	AE	algorithmsinc	000	2025-02-26	255	79	[219]2048	-	[156]452	[261]14	[236]903	[238]924	[233]2153	[217]4199	[213]8654	$[375]0.06N^{1.2}$
27	Alivia / Innovation Sys	RU	isystems	3	2018-10-30	350	784	[197]2048	1	[358]825	[318]16	[134]385	[146]389	[136]979	[133]1822	[227]9348	$[399]0.00N^{1.3}$
28	AllGoVision	IN	allgovision	000	2019-07-30	168	150	[157]2048	k	[128]404	[192]12	[387]3226	[391]3193	[335]6129	[335]12449	[332]25835	$[193]1.40N^{1.0}$
29	AllGoVision	IN	allgovision	001	2020-07-14	283	126	[227]2048	-	[339]777	[224]13	[385]3174	[390]3183	[333]6073	[332]12284	[330]25701	$[188]1.42N^{1.0}$
30	AllGoVision	IN	allgovision	002	2023-03-13	284	797	[203]2048	-	[162]459	[244]13	[380]3112	[398]3454	-	-	-	
31	AllGoVision	IN	allgovision	003	2023-09-19	264	799	[230]2048	-	[424]1128	[197]12	[384]3171	[388]3100	[331]5906	[338]13318	-	$[264]0.97N^{1.1}$
32	AllGoVision	IN	allgovision	004	2025-07-11	704	34	[229]2048	-	[285]669	[191]12	[300]1480	[303]1492	-	-	-	
33	Anke Investments	CN	anke	0	2018-10-30	779	27	[398]2072	k	[145]429	[311]16	[198]675	[215]748	[180]1483	[176]2968	[173]6148	$[277]0.21N^{1.1}$
34	Anke Investments	CN	anke	1	2018-10-30	779	27	[399]2072	k	[146]430	[297]15	[203]707	[219]769	-	-	-	
35	Anke Investments	CN	anke	002	2019-06-27	341	401	[389]2056	k	[256]623	[256]13	[191]624	[203]682	[163]1306	[154]2403	[151]5082	$[173]0.30N^{1.0}$
36	Antheus Technologia	BR	antheus	000	2024-08-19	264	185	[211]2048	-	[460]1273	[203]12	[329]1781	[332]1788	-	-	-	
37	Aratek Biometrics Co Ltd	CN	aratek	001	2024-04-18	248	15	[286]2048	-	[42]232	[176]12	[457]8371	[466]8210	[399]16858	[394]33012	[382]68839	$[266]2.54N^{1.1}$
38	Armatura LLC	US	armatura	000	2023-04-13	0	935	[472]6144	-	[277]655	[444]66	[443]6211	[442]6138	[373]11533	[369]23189	[364]46629	$[93]3.59N^{1.0}$
39	Aware	US	aware	5	2018-10-30	368	27	[414]3100	k	[347]792	[402]34	[36]95	[44]98	[39]203	[36]371	[18]252	$[19]4.13N^{0.7}$
40	Aware	US	aware	6	2018-10-30	368	27	[5]124	k	[346]789	[13]2	[67]158	[65]162	-	-	-	
41	Aware	US	aware	007	2023-11-27	132	18	[52]480	-	[317]719	[140]11	[53]131	[53]131	[54]320	[54]655	[49]1324	$[355]0.02N^{1.1}$
42	Awidit Systems	IN	awiros	000	2025-02-10	478	584	[304]2048	-	[197]508	[236]13	[316]1628	[338]1931	-	-	-	
43	Ayonix	JP	ayonix	1	2018-10-29	74	2	[122]1036	k	[5]12	[148]11	[106]279	[103]279	-	-	-	
44	Ayonix	JP	ayonix	2	2018-10-30	74	2	[121]1036	1	[4]11	[273]14	[105]279	[102]276	[80]535	[82]1087	[79]2284	$[218]0.11N^{1.0}$
45	Beijing Hisign Technology	CN	hisign	001	2024-08-09	466	152	[402]2080	-	[255]620	[303]15	[241]926	[276]1179	[206]1855	[207]3910	[200]7639	$[37]2.25N^{0.9}$
46	BioID Technologies SA	CH	bioidtechswiss	001	2024-04-19	0	345	[64]512	-	[250]614	[42]4	[103]278	[109]294	[74]470	[75]944	[77]2141	$[232]0.10N^{1.0}$
47	Biometrik Systems Private Limited	ID	biometrik	001	2025-11-24	167	82	[278]2048	-	[485]1492	[292]15	[308]1543	[301]1486	[263]2813	[259]5694	[263]11840	$[210]0.59N^{1.0}$
48	Camvi Technologies	US	camvitech	4	2018-10-30	233	220	[101]1024	1	[297]686	[400]31	[25]33	[21]32	[15]38	[14]40	[9]48	$[4]8492.66N^{0.1}$
49	Camvi Technologies	US	camvitech	5	2018-10-30	257	220	[110]1024	1	[331]751	[397]31	[23]31	[19]30	-	-	-	
50	Canon Inc	CN	cib	000	2020-10-19	426	127	[486]8196	-	[120]396	[457]113	[390]3316	[401]3604	[343]6738	[341]13495	[335]27114	$[72]2.33N^{1.0}$
51	Canon Inc	JP	canon	001	2021-10-27	1139	91	[444]4096	-	[175]480	[357]21	[430]5489	[454]6789	[387]12741	[378]25650	[370]51922	$[115]3.82N^{1.0}$
52	Canon Inc	JP	canon	002	2022-04-26	1231	111	[475]6200	-	[229]565	[439]58	[453]7673	[452]6416	[380]12178	[373]24806	[368]49653	$[146]3.28N^{1.0}$

Notes	
1	Configuration size does not capture static data present in libraries. Libraries are included but the size also includes any ancillary libraries for image processing (e.g. openCV) or numerical computation (e.g. blas).
2	Finalization is the processing of converting N = 1600000 templates into a searchable data structure an operation which can be a simple copy, or the building of an index or tree, for example. The duration of the operation may be data dependent, and may not be linear in the number of input templates.
3	This multiplier expresses the increase in template size when k images are passed to the template generation function.
4	All durations are measured on Intel®Xeon®CPU E5-2630 v4 @ 2.20GHz processors. Estimates are made by wrapping the API function call in calls to std::chrono::high_resolution_clock which on the machine in (3) counts 1ns clock ticks. Precision is somewhat worse than that however.
5	Search durations are measured as in the prior note. The power-law model in the final column mostly fits the empirical results in Figure 311. However in certain cases the model is not correct and should not be used numerically.

Table 2: Summary of algorithms and properties included in this report. The blue superscripts give ranking for the quantity in that column. Missing search durations, denoted by "-", are absent because those runs were not executed, usually because we did not run on the larger galleries. Caution: The power-law model is sometimes an incorrect model. It is included here only to show broad sublinear behavior, which is flagged in green. The models should not be used for prediction.

2026/01/09 20:40:38

FNIR(N, R, T) = False neg. identification rate
FPIR(N, T) = False pos. identification rate

N = Num. enrolled subjects
R = Num. candidates examined

T = Threshold

T = 0 → Investigation
T > 0 → Identification

This publication is available free of charge from: https://doi.org/10.6028/NIST.IR.8271

	DEVELOPER	DEVELOPER	SHORT	SEQ.	VALIDATION	CONFIG[1]	LIB[1]	TEMPLATE GENERATION			FINALIZE[2]	SEARCH DURATION[5] MILLISEC					
	FULL NAME	LOCATION	NAME	NUM.	DATE	DATA (MB)	DATA (MB)	SIZE (B)	MULT[3]	TIME (MS)[4]	TIME (S)	L=1	L=50	L=50	L=50	L=50	POWER LAW
											N=1.6M	N=1.6M	N=1.6M	N=3M	N=6M	N=12M	(μs)
53	Canon Inc	JP	canon	003	2023-09-05	2462	78	[463]4148	-	[446]1211	[388]29	[342]2012	[341]1966	[301]3819	[298]7679	[306]16096	[212]$0.80N^{1.0}$
54	Clearview AI Inc	US	clearviewai	000	2021-11-12	358	316	[440]4096	-	[119]393	[394]30	[193]639	[199]657	[151]1134	[138]1939	[130]3889	[29]$1.59N^{0.9}$
55	Clearview AI Inc	US	clearviewai	001	2024-02-16	696	499	[338]2048	-	[327]743	[349]20	[140]394	[143]384	[112]722	[108]1451	[99]2919	[102]$0.22N^{1.0}$
56	Clearview AI Inc	US	clearviewai	002	2024-06-18	696	497	[266]2048	-	[344]786	[353]20	[176]517	[172]516	[134]969	[139]1946	[132]3931	[107]$0.29N^{1.0}$
57	Clearview AI Inc	US	clearviewai	003	2025-11-24	696	527	[337]2048	-	[420]1108	[346]20	[167]498	[132]362	[115]743	[132]1780	[126]3720	[356]$0.04N^{1.1}$
58	Cloudwalk - Hengrui AI Technology	CN	hr	000	2021-02-10	501	392	[220]2048	-	[305]701	[286]15	[149]420	[101]276	[82]539	[94]1268	[111]3177	[362]$0.03N^{1.1}$
59	Cloudwalk Moontime Smart Technology	CN	cloudwalk	000	2022-01-31	716	573	[254]2048	-	[376]869	[136]10	[153]440	[138]371	[84]547	[80]1065	[98]2902	[42]$0.53N^{0.9}$
60	Cloudwalk Moontime Smart Technology	CN	cloudwalk	001	2022-07-27	797	574	[307]2048	-	[210]529	[279]14	[99]273	[127]349	[101]658	[111]1492	[108]3026	[282]$0.10N^{1.1}$
61	Cloudwalk Moontime Smart Technology	CN	cloudwalk	002	2023-02-24	431	514	[293]2048	-	[212]531	[284]14	[213]767	[223]826	[185]1586	[187]3311	[172]6070	[198]$0.35N^{1.0}$
62	Cognitec Systems GmbH	DE	cognitec	2	2018-10-30	463	26	[373]2052	k	[41]225	[374]27	[325]1733	[331]1763	[295]3660	[290]7279	[282]13895	[184]$0.83N^{1.0}$
63	Cognitec Systems GmbH	DE	cognitec	3	2018-10-30	465	26	[369]2052	k	[65]297	[308]16	[324]1719	[333]1791	[293]3638	[289]7277	[291]14904	[237]$0.66N^{1.0}$
64	Cognitec Systems GmbH	DE	cognitec	004	2021-03-08	384	60	[360]2052	-	[33]192	[252]13	[320]1673	[326]1727	[266]2904	[261]5801	[260]11707	[62]$1.15N^{1.0}$
65	Cognitec Systems GmbH	DE	cognitec	005	2021-07-30	460	61	[372]2052	-	[100]367	[122]9	[310]1556	[309]1551	[268]2916	[280]6561	[283]13958	[293]$0.38N^{1.1}$
66	Cognitec Systems GmbH	DE	cognitec	006	2022-02-10	689	61	[362]2052	-	[167]463	[133]10	[257]1006	[255]1002	[226]2097	[223]4312	[199]7624	[270]$0.30N^{1.1}$
67	Cognitec Systems GmbH	DE	cognitec	007	2023-12-01	319	194	[367]2052	-	[71]314	[270]14	[266]1069	[266]1051	[236]2232	[219]4244	[206]7943	[147]$0.55N^{1.0}$
68	Cognitec Systems GmbH	DE	cognitec	008	2024-04-29	359	39	[336]2048	-	[87]342	[260]14	[283]1258	[262]1017	[245]2433	[240]4887	[246]9888	[340]$0.15N^{1.1}$
69	Cognitec Systems GmbH	DE	cognitec	009	2024-08-29	359	39	[315]2048	-	[166]461	[242]13	[264]1045	[264]1025	[227]2117	[220]4267	[209]8147	[213]$0.42N^{1.0}$
70	Compal Electronics	TW	compal	000	2025-03-20	980	182	[108]1024	-	[457]1256	[71]7	[425]4960	[432]5503	[344]6929	[286]6915	[188]6911	[16]$17496.15N^{0.4}$
71	Compal Electronics	TW	compal	001	2025-11-25	605	199	[356]2049	-	[387]910	[330]17	[479]22511	[487]22297	-	-	-	
72	Corsight AI	IL	corsight	000	2023-07-13	1277	31	[400]2080	-	[219]546	[160]12	[249]960	[284]1299	[230]2145	[204]3828	[247]9998	[291]$0.26N^{1.1}$
73	Corsight AI	IL	corsight	001	2024-03-14	1172	30	[401]2080	-	[215]543	[243]13	[258]1011	[260]1011	[218]1951	[211]4004	[232]9391	[297]$0.23N^{1.1}$
74	Cubox	KR	cubox	000	2021-08-24	529	298	[246]2048	-	[148]440	[131]10	[391]3410	[410]4076	[351]7605	[351]15871	-	[274]$1.16N^{1.1}$
75	Cubox	KR	cubox	001	2023-07-05	1654	342	[321]2048	-	[257]624	[183]12	[388]3268	[399]3476	[334]6097	[333]12320	[334]27074	[133]$1.78N^{1.0}$
76	Cubox	KR	cubox	002	2024-11-29	1273	342	[306]2048	-	[398]962	[175]12	[400]3809	[403]3859	[347]7095	[343]13774	[340]28747	[57]$3.02N^{1.0}$
77	Cubox	KR	cubox	003	2025-05-14	219	342	[309]2048	-	[102]369	[216]13	[402]3920	[404]3915	[348]7262	[347]15013	[342]29855	[172]$1.80N^{1.0}$
78	Cyberlink Corp	TW	cyberlink	000	2019-06-12	217	93	[366]2052	1	[276]654	[393]30	[200]696	[206]701	[173]1379	[163]2639	[175]6214	[224]$0.28N^{1.0}$
79	Cyberlink Corp	TW	cyberlink	001	2019-10-07	459	102	[363]2052	1	[140]423	[383]28	[201]698	[205]700	[168]1350	[256]5524	[267]12031	[396]$0.00N^{1.3}$
80	Cyberlink Corp	TW	cyberlink	002	2020-07-31	333	109	[460]4140	-	[320]724	[472]6875	[292]1353	[392]3198	[336]6138	[331]12205	[274]13106	[25]$16.71N^{0.8}$
81	Cyberlink Corp	TW	cyberlink	003	2021-01-05	333	100	[478]6212	-	[105]370	[409]35	[234]886	[211]723	[177]1415	[173]2886	[157]5643	[319]$0.12N^{1.1}$
82	Cyberlink Corp	TW	cyberlink	004	2021-07-16	371	100	[477]6212	-	[114]386	[363]23	[240]924	[171]504	[132]923	[107]1448	[114]3350	[41]$0.73N^{0.9}$
83	Cyberlink Corp	TW	cyberlink	005	2022-01-07	371	100	[476]6212	-	[323]733	[396]30	[169]501	[167]498	[158]1193	[164]2672	[161]5693	[385]$0.03N^{1.2}$
84	Cyberlink Corp	TW	cyberlink	006	2024-06-12	1163	99	[489]8260	-	[318]722	[436]54	[347]2068	[305]1498	[300]3804	[300]7796	[301]15790	[369]$0.13N^{1.1}$
85	DAON	IE	daon	000	2021-12-23	274	2	[395]2069	-	[207]526	[94]8	[261]1029	[195]625	[178]1454	[182]3097	[178]6316	[386]$0.03N^{1.2}$
86	DAON	IE	daon	001	2025-01-03	289	64	[170]2048	-	[281]661	[172]12	[282]1242	[280]1211	-	-	-	
87	DAON	IE	daon	002	2025-07-07	288	65	[332]2048	-	[330]751	[162]12	[290]1318	[310]1552	[248]2462	[253]5452	[253]11007	[221]$0.53N^{1.0}$
88	Dactionable Technologies	VN	datech	000	2023-10-24	603	178	[426]4096	-	[436]1176	[463]1282	[79]194	[99]262	[78]499	[78]998	[74]2029	[303]$0.05N^{1.1}$
89	Dactionable Technologies	VN	datech	001	2024-03-14	709	178	[422]4096	-	[396]953	[447]75	[208]753	[216]751	[183]1537	[174]2946	[167]5802	[152]$0.38N^{1.0}$
90	Dahua Technology Co	CN	dahua	0	2018-10-29	276	167	[343]2048	k	[109]374	[359]22	-	[92]258	-	-	-	
91	Dahua Technology Co	CN	dahua	1	2018-10-29	276	167	[272]2048	k	[103]369	[378]28	-	[95]257	[91]602	[90]1202	[103]3007	[372]$0.02N^{1.2}$
92	Dahua Technology Co	CN	dahua	002	2019-12-02	607	137	[300]2048	k	[296]685	[344]19	[91]243	[100]269	[156]1189	[175]2950	[182]6732	[403]$0.00N^{1.5}$
93	Dahua Technology Co	CN	dahua	003	2020-11-18	889	154	[313]2048	-	[319]723	[331]18	[107]283	[94]249	[73]468	[74]935	[71]1871	[75]$0.16N^{1.0}$
94	Dahua Technology Co	CN	dahua	004	2021-11-18	812	116	[301]2048	-	[334]758	[139]11	[150]423	[151]411	[127]871	[117]1568	[110]3174	[202]$0.17N^{1.0}$
95	Decatur Industries Inc	US	decatur	000	2022-02-09	411	383	[361]2052	-	[325]863	[124]9	[327]1761	[344]2023	[289]3361	[291]7283	[288]14592	[120]$1.06N^{1.0}$
96	Deepglint	CN	deepglint	001	2019-11-15	448	265	[427]4096	-	[289]676	[404]35	[199]677	[304]1495	[199]1724	[168]2747	[176]6246	[22]$25.27N^{0.8}$
97	Dermalog	DE	dermalog	5	2018-10-26	0	440	[6]128	1	[209]528	[467]3155	[1]0	[1]0	[1]0	[1]0	[1]0	[5]$66.21N^{0.2}$
98	Dermalog	DE	dermalog	6	2018-10-26	0	453	[21]256	1	[194]507	[17]2	[60]142	[58]144	[47]269	[46]531	[48]1294	[244]$0.05N^{1.0}$
99	Dermalog	DE	dermalog	007	2020-02-12	0	424	[10]128	1	[132]410	[3]1	[44]98	[40]96	[41]218	[39]429	[40]1013	[338]$0.01N^{1.1}$
100	Dermalog	DE	dermalog	008	2021-01-25	0	531	[69]512	-	[35]198	[47]4	[88]227	[90]246	[72]462	[73]924	[70]1849	[82]$0.15N^{1.0}$
101	Dermalog	DE	dermalog	009	2021-11-09	0	318	[74]512	-	[26]180	[31]3	[89]227	[91]246	[71]461	[72]923	[69]1846	[77]$0.16N^{1.0}$
102	Dermalog	DE	dermalog	010	2022-07-25	0	514	[71]512	-	[77]322	[41]3	[90]241	[81]210	[63]394	[65]789	[60]1580	[80]$0.13N^{1.0}$
103	Dermalog	DE	dermalog	011	2022-12-12	0	272	[7]128	-	[47]248	[4]1	[35]87	[34]88	[27]165	[27]331	[27]664	[93]$0.05N^{1.0}$
104	Dermalog	DE	dermalog	012	2023-12-19	0	287	[11]128	-	[25]177	[2]1	[40]95	[43]97	[29]177	[29]353	[29]709	[63]$0.07N^{1.0}$

Notes	
1	Configuration size does not capture static data present in libraries. Libraries are included but the size also includes any ancillary libraries for image processing (e.g. openCV) or numerical computation (e.g. blas).
2	Finalization is the processing of converting N = 1600000 templates into a searchable data structure an operation which can be a simple copy, or the building of an index or tree, for example. The duration of the operation may be data dependent, and may not be linear in the number of input templates.
3	This multiplier expresses the increase in template size when k images are passed to the template generation function.
4	All durations are measured on Intel®Xeon®CPU E5-2630 v4 @ 2.20GHz processors. Estimates are made by wrapping the API function call in calls to std::chrono::high_resolution_clock which on the machine in (3) counts 1ns clock ticks. Precision is somewhat worse than that however.
5	Search durations are measured as in the prior note. The power-law model in the final column mostly fits the empirical results in Figure 311. However in certain cases the model is not correct and should not be used numerically.

Table 3: Summary of algorithms and properties included in this report. The blue superscripts give ranking for the quantity in that column. Missing search durations, denoted by "-", are absent because those runs were not executed, usually because we did not run on the larger galleries. Caution: The power-law model is sometimes an incorrect model. It is included here only to show broad sublinear behavior, which is flagged in green. The models should not be used for prediction.

2026/01/09 20:40:38

FNIR(N, R, T) = False neg. identification rate
FPIR(N, T) = False pos. identification rate
N = Num. enrolled subjects
R = Num. candidates examined
T = Threshold
T = 0 → Investigation
T > 0 → Identification

This publication is available free of charge from: https://doi.org/10.6028/NIST.IR.8271

2026/01/09 20:40:38

FNIR(N, R, T) = FPIR(N, T) =

False neg. identification rate
False pos. identification rate

N = Num. enrolled subjects
R = Num. candidates examined

T = Threshold

T = 0 → Investigation
T > 0 → Identification

	DEVELOPER	DEVELOPER	SHORT	SEQ.	VALIDATION	CONFIG[1]	LIB[1]	TEMPLATE GENERATION			FINALIZE[2]	SEARCH DURATION[5] MILLISEC					
	FULL NAME	LOCATION	NAME	NUM.	DATE	DATA (MB)	DATA (MB)	SIZE (B)	MULT[3]	TIME (MS)[4]	TIME (S)	L=1	L=50	L=50	L=50	L=50	POWER LAW
												N=1.6M	N=1.6M	N=1.6M	N=3M	N=6M	N=12M	(μs)
105	Dermalog	DE	dermalog	013	2024-06-18	0	287	[8]128	-	[27]182	[1]1	[39]95	[39]95	[32]180	[31]361	[33]724	$[108]0.05N^{1.0}$
106	Dermalog	DE	dermalog	014	2025-05-09	0	289	[9]128	-	[24]177	[468]3293	[2]0	[2]0	[2]0	[2]1	[2]1	$[12]26.41N^{0.2}$
107	Dermalog	DE	dermalog	015	2025-09-12	0	683	[103]1024	-	[408]1033	[112]9	[87]217	[86]218	[65]410	[67]823	[63]1647	$[97]0.13N^{1.0}$
108	Digidata	IN	digidata	000	2022-06-03	248	33	[283]2048	-	[26]320	[465]2444	[3]0	[77]198	-	-	-	
109	DiluSense Technology	CN	dilusense	000	2022-05-26	311	56	[187]2048	-	[39]219	[372]26	[335]1904	[306]1498	[279]3116	[270]6126	[269]12046	$[219]0.61N^{1.0}$
110	DiluSense Technology	CN	dilusense	001	2022-12-24	599	5	[442]4096	-	[373]860	[412]38	[377]3026	[386]3042	[326]4738	[319]9473	[319]19026	$[38]5.36N^{0.9}$
111	EI Networks Private Ltd	IN	einetworksindia	000	2024-04-17	444	128	[296]2048	-	[89]347	[340]19	[160]470	[124]342	[131]915	[135]1844	[125]3719	$[374]0.03N^{1.2}$
112	EI Networks Private Ltd	IN	einetworksindia	001	2024-10-24	444	197	[190]2048	-	[84]341	[336]18	[143]402	[125]343	[100]656	[124]1714	[123]3659	$[363]0.03N^{1.1}$
113	EI Networks Private Ltd	IN	einetworksindia	002	2025-02-21	1186	141	[222]2048	-	[413]1076	[352]20	[117]327	[144]387	[98]651	[97]1310	[95]2872	$[164]0.17N^{1.0}$
114	FAST-NUCES Lahore Campus	PK	fastlahore	000	2025-09-26	186	138	[179]2048	-	[55]278	[289]15	[358]2432	[362]2272	-	-	-	
115	FCI Vietnam	VN	fci	000	2025-04-02	1452	444	[333]2048	-	[484]1466	[210]12	[472]13182	[479]13125	-	-	-	
116	FPT Smart Cloud	VN	fpt	000	2024-03-28	595	444	[188]2048	-	[369]850	[268]14	[471]13085	[478]13114	-	-	-	
117	FacePhi	ES	facephi	000	2024-10-03	134	182	[55]512	-	[54]275	[62]6	[85]214	[355]2087	[304]3854	[299]7745	[297]15540	$[394]0.01N^{1.3}$
118	FarBar Inc	TW	f8	001	2019-10-03	266	19	[162]2048	k	[352]810	[266]14	-	-	-	-	-	
119	Fincore	UK	fincore	000	2021-08-18	250	224	[180]2048	-	[150]443	[108]9	[250]971	[185]560	-	-	-	
120	First Credit Bureau Kazakhstan	KZ	firstcreditkz	001	2022-11-22	548	24	[40]288	-	[190]495	[14]2	[28]46	[26]38	[20]72	[20]150	[20]297	$[124]0.02N^{1.0}$
121	Fujitsu Research and Development Center	CN	fujitsulab	000	2021-10-12	497	337	[112]1032	-	[248]613	[58]5	[333]1864	[319]1657	[280]3140	[275]6320	[272]12723	$[171]0.78N^{1.0}$
122	Fujitsu Research and Development Center	CN	fujitsulab	001	2022-03-15	675	386	[120]1032	-	[214]535	[109]9	[332]1854	[327]1740	[288]3324	[284]6730	[293]14943	$[286]0.45N^{1.1}$
123	GTEL OTS JSC	VN	gtelots	000	2025-04-14	246	58	[53]512	-	[345]788	[483]21132	[5]3	[3]3	-	-	-	
124	Gorilla Technology	TW	gorilla	2	2018-10-29	91	1252	[130]1132	k	[82]338	[367]24	[61]145	[59]146	[49]293	[51]612	[57]1509	$[332]0.02N^{1.1}$
125	Gorilla Technology	TW	gorilla	3	2018-10-26	94	1252	[404]2156	k	[227]559	[477]12020	-	[346]2047	-	-	-	
126	Gorilla Technology	TW	gorilla	004	2020-01-06	182	1244	[405]2192	k	[115]388	[418]41	[108]286	[106]285	[157]1191	[156]2416	[150]5036	$[395]0.00N^{1.3}$
127	Gorilla Technology	TW	gorilla	005	2021-02-22	306	1420	[479]6288	-	[67]303	[448]78	[267]1070	[221]799	[182]1514	[230]4454	[217]8820	$[378]0.05N^{1.2}$
128	Gorilla Technology	TW	gorilla	006	2021-09-30	377	691	[490]8336	-	[139]422	[456]99	[305]1504	[315]1612	[244]2422	[227]4422	[228]9363	$[170]0.59N^{1.0}$
129	Gorilla Technology	TW	gorilla	007	2022-02-16	392	322	[480]6290	-	[73]315	[455]89	[211]765	[214]745	[176]1408	[171]2823	[164]5764	$[117]0.42N^{1.0}$
130	Gorilla Technology	TW	gorilla	008	2022-10-31	321	290	[465]4242	-	[204]521	[435]54	[172]513	[246]972	[194]1699	[160]2469	[183]6768	$[229]0.30N^{1.0}$
131	Griaule	US	griaule	000	2021-11-01	0	584	[368]2052	-	[46]247	[87]8	[422]4868	[444]6150	[372]11473	[368]22952	[362]46070	$[73]3.89N^{1.0}$
132	Griaule	US	griaule	001	2022-07-26	0	615	[375]2052	-	[294]684	[157]12	[437]5866	[438]6010	[376]11627	[371]24207	[363]46343	$[158]3.02N^{1.0}$
133	Guangzhou Pixel Solutions Co	CN	pixelall	002	2019-07-01	0	165	[407]2560	k	[32]190	[291]15	[289]1296	[291]1334	[253]2526	[246]5136	[254]11045	$[220]0.52N^{1.0}$
134	Guangzhou Pixel Solutions Co	CN	pixelall	003	2019-11-05	0	690	[408]2560	k	[308]703	[360]22	[285]1273	[286]1307	[250]2474	[247]5198	[255]11141	$[246]0.46N^{1.0}$
135	Guangzhou Pixel Solutions Co	CN	pixelall	004	2020-07-02	0	538	[409]2560	k	[154]449	[329]17	[284]1259	[285]1300	[249]2465	[254]5492	[256]11443	$[287]0.34N^{1.1}$
136	Guangzhou Pixel Solutions Co	CN	pixelall	005	2021-03-23	0	717	[406]2560	-	[366]840	[144]11	[314]1606	[308]1528	[256]2609	[242]4926	[262]11770	$[144]0.73N^{1.0}$
137	Hangzhuo Allu Network Information Technology	CN	hzailu	000	2022-03-18	855	97	[109]1024	-	[161]457	[145]11	[369]2609	[360]2251	[318]4612	[326]10075	[310]17156	$[197]1.01N^{1.0}$
138	Hangzhuo Allu Network Information Technology	CN	hzailu	001	2022-08-18	273	162	[344]2048	-	[110]377	[168]12	[418]4537	[421]4511	[361]8462	[364]19463	[358]42527	$[312]0.92N^{1.1}$
139	Hangzhuo Allu Network Information Technology	CN	hzailu	002	2023-01-12	302	293	[171]2048	-	[225]555	[194]12	[413]4481	[420]4509	[359]8413	[355]16568	[356]39517	$[240]1.59N^{1.0}$
140	Hangzhuo Allu Network Information Technology	CN	hzailu	003	2023-05-22	1434	293	[428]4096	-	[288]675	[365]24	[466]10145	[469]9351	[402]17922	[400]40619	[389]83432	$[262]3.03N^{1.0}$
141	Hangzhuo Allu Network Information Technology	CN	hzailu	004	2023-10-13	1902	293	[471]5120	-	[397]956	[386]29	[452]7508	[461]7639	[390]13673	[377]25457	[381]66435	$[288]1.83N^{1.1}$
142	Hangzhuo Allu Network Information Technology	CN	hzailu	005	2024-04-26	2201	293	[485]7168	-	[476]1389	[420]41	[467]11242	[474]10996	-	-	-	
143	Hangzhuo Allu Network Information Technology	CN	hzailu	006	2025-01-03	2866	293	[484]7168	-	[480]1455	[414]38	[469]12514	[476]11557	-	-	-	
144	Hikvision Research Institute	CN	hikvision	5	2018-10-29	593	9	[138]1408	1	[246]607	[304]16	[233]883	[232]895	[214]1908	[202]3792	[231]9387	$[354]0.10N^{1.1}$
145	Hikvision Research Institute	CN	hikvision	6	2018-10-29	593	9	[137]1408	1	[241]598	[309]16	[228]871	[231]877	-	-	-	
146	HyperVerge Inc	IN	hyperverge	001	2021-08-11	1791	212	[105]1024	-	[186]490	[53]5	[202]703	[202]681	[167]1346	[165]2681	[160]5680	$[187]0.32N^{1.0}$
147	HyperVerge Inc	IN	hyperverge	002	2022-04-13	1140	1118	[106]1024	-	[149]440	[115]9	[163]484	[173]518	[147]1099	[123]1690	[72]1953	$[23]6.15N^{0.8}$
148	HyperVerge Inc	IN	hyperverge	003	2023-04-04	2089	1118	[303]2048	-	[157]452	[226]13	[212]766	[237]921	[213]1900	[183]3198	[171]6065	$[121]0.48N^{1.0}$
149	Hyundai Motor Company	KR	hyundai	000	2025-02-03	352	104	[160]2048	-	[98]366	[249]13	[404]4258	[409]4068	[353]7815	[349]15618	[350]33716	$[233]1.52N^{1.0}$
150	Hyundai Motor Company	KR	hyundai	001	2025-06-23	176	104	[154]2048	-	[91]351	[189]12	[408]4329	[415]4382	[354]7827	[353]16459	[349]33035	$[140]2.22N^{1.0}$
151	Hyundai Motor Company	KR	hyundai	002	2025-11-14	472	104	[202]2048	-	[486]1802	[301]15	[458]8376	[465]8199	[395]15300	[392]31477	-	$[181]3.74N^{1.0}$
152	ICM Airport Technics	AU	icm	000	2023-08-14	991	1	[346]2048	-	[31]186	[190]12	[454]7990	[463]7943	-	-	-	
153	ICM Airport Technics	AU	icm	001	2023-12-12	858	1	[274]2048	-	[19]164	[185]12	[450]7124	[459]7219	[396]15370	[387]29562	[384]70229	$[331]1.10N^{1.1}$
154	IDENTY	UK	identy	000	2025-06-18	376	38	[213]2048	-	[282]662	[411]37	[129]366	[121]330	-	-	-	
155	IMDS Software Inc	CA	imds	000	2023-10-20	364	344	[295]2048	-	[63]296	[182]12	[464]10077	[473]10387	-	-	-	
156	IMDS Software Inc	CA	imds	001	2024-03-14	362	344	[161]2048	-	[392]943	[300]15	[164]485	[165]489	[133]924	[143]1970	[136]4100	$[243]0.17N^{1.0}$

Notes	
1	Configuration size does not capture static data present in libraries. Libraries are included but the size also includes any ancillary libraries for image processing (e.g. openCV) or numerical computation (e.g. blas).
2	Finalization is the processing of converting N = 1600000 templates into a searchable data structure an operation which can be a simple copy, or the building of an index or tree, for example. The duration of the operation may be data dependent, and may not be linear in the number of input templates.
3	This multiplier expresses the increase in template size when k images are passed to the template generation function.
4	All durations are measured on Intel®Xeon®CPU E5-2630 v4 @ 2.20GHz processors. Estimates are made by wrapping the API function call in calls to std::chrono::high_resolution_clock which on the machine in (3) counts 1ns clock ticks. Precision is somewhat worse than that however.
5	Search durations are measured as in the prior note. The power-law model in the final column mostly fits the empirical results in Figure 311. However in certain cases the model is not correct and should not be used numerically.

Table 4: Summary of algorithms and properties included in this report. The blue superscripts give ranking for the quantity in that column. Missing search durations, denoted by "-", are absent because those runs were not executed, usually because we did not run on the larger galleries. Caution: The power-law model is sometimes an incorrect model. It is included here only to show broad sublinear behavior, which is flagged in green. The models should not be used for prediction.

This publication is available free of charge from: https://doi.org/10.6028/NIST.IR.8271

	DEVELOPER	DEVELOPER	SHORT	SEQ.	VALIDATION	CONFIG[1]	LIB[1]	TEMPLATE GENERATION			FINALIZE[2]	SEARCH DURATION[5] MILLISEC					
	FULL NAME	LOCATION	NAME	NUM.	DATE	DATA (MB)	DATA (MB)	SIZE (B)	MULT[3]	TIME (MS)[4]	TIME (S)	L=1	L=50	L=50	L=50	L=50	POWER LAW
												N=1.6M	N=1.6M	N=3M	N=6M	N=12M	(μs)
157	IMDS Software Inc	CA	imds	002	2024-11-01	364	344	[235]2048	-	[69]311	[207]12	[190]622	[194]622	[150]1132	[141]1962	[135]4000	[43]$0.86N^{0.9}$
158	Idemia	FR	idemia	5	2018-10-29	417	48	[47]352	1	[108]371	[54]5	[55]137	[55]138	[68]437	[61]724	[61]1630	[387]$0.01N^{1.2}$
159	Idemia	FR	idemia	6	2018-10-29	417	48	[48]352	1	[106]370	[51]4	[56]137	[54]138	[69]442	[68]827	[62]1646	[389]$0.01N^{1.2}$
160	Idemia	FR	idemia	007	2020-01-17	738	113	[100]860	1	[348]794	[267]14	[62]151	[60]152	[103]683	[110]1481	[106]3022	[401]$0.00N^{1.4}$
161	Idemia	FR	idemia	008	2021-03-15	378	65	[46]300	-	[48]251	[32]3	[54]137	[52]131	[44]247	[43]501	[41]1013	[122]$0.07N^{1.0}$
162	Idemia	FR	idemia	009	2022-03-01	735	68	[96]636	-	[203]521	[77]7	[83]211	[87]221	[75]473	[81]1070	[80]2352	[364]$0.02N^{1.1}$
163	Idemia	FR	idemia	010	2023-01-11	942	71	[44]300	-	[306]701	[24]2	[81]197	[78]200	[61]380	[63]766	[59]1561	[179]$0.09N^{1.0}$
164	Idemia	FR	idemia	011	2024-03-05	776	63	[45]300	-	[364]834	[22]2	[80]196	[75]193	[60]368	[62]746	[58]1525	[203]$0.08N^{1.0}$
165	Idemia	FR	idemia	012	2025-07-02	758	66	[131]1212	-	[456]1255	[82]7	[120]343	[122]335	[96]643	[116]1544	[128]3849	[373]$0.02N^{1.2}$
166	Imagus Technology Pty	AU	imagus	005	2021-01-15	222	311	[287]2048	-	[189]491	[265]14	[114]302	[115]313	[99]651	[100]1361	[85]2461	[351]$0.03N^{1.1}$
167	Imagus Technology Pty	AU	imagus	006	2021-05-27	248	369	[185]2048	-	[191]505	[125]9	[115]303	[88]234	[77]499	[95]1273	[91]2727	[384]$0.01N^{1.2}$
168	Imagus Technology Pty	AU	imagus	007	2021-11-16	248	366	[240]2048	-	[491]32200	[102]9	[113]301	[89]238	[70]442	[71]881	[68]1765	[64]$0.16N^{1.0}$
169	Imagus Technology Pty	AU	imagus	008	2022-05-26	204	335	[264]2048	-	[56]284	[327]17	[184]560	[158]441	-	-	-	
170	Imperial College London	GB	imperial	000	2019-08-28	461	15	[208]2048	1	[235]577	[219]13	[125]360	[142]379	[189]1626	[212]4057	[250]10291	[404]$0.00N^{1.5}$
171	Incode Technologies Inc	US	incode	2	2018-10-29	71	31	[184]2048	1	[59]289	[299]15	[148]411	[147]404	-	-	-	
172	Incode Technologies Inc	US	incode	3	2018-10-29	133	31	[239]2048	1	[303]697	[285]15	[147]408	[152]412	[123]847	[119]1608	[141]4486	[344]$0.05N^{1.1}$
173	Incode Technologies Inc	US	incode	004	2019-06-24	254	50	[192]2048	1	[173]475	[163]12	[128]365	[140]378	[179]1482	[121]1660	[102]2954	[281]$0.12N^{1.1}$
174	Incode Technologies Inc	US	incode	005	2021-07-29	259	21	[181]2048	-	[57]285	[130]10	[151]427	[160]454	[128]890	[134]1843	[121]3640	[318]$0.07N^{1.1}$
175	Incode Technologies Inc	US	incode	006	2024-07-15	2309	41	[487]8196	-	[411]1071	[428]47	[322]1706	[323]1713	[238]2241	[263]5891	[237]9528	[34]$3.19N^{0.9}$
176	Incode Technologies Inc	US	incode	007	2025-07-30	1766	69	[474]6148	-	[410]1047	[406]35	[276]1172	[282]1256	[210]1873	[231]4462	[207]7970	[159]$0.53N^{1.0}$
177	Innovatrics	SK	innovatrics	4	2018-10-30	0	400	[126]1076	k	[123]399	[474]10902	[11]8	[6]8	[5]11	[3]9	[4]13	[10]$668.38N^{0.2}$
178	Innovatrics	SK	innovatrics	005	2019-09-30	0	455	[83]538	1	[359]827	[476]11897	[10]8	[7]8	[4]9	[4]9	[3]9	[1]$4055.65N^{0.1}$
179	Innovatrics	SK	innovatrics	007	2021-08-16	175	58	[84]538	-	[234]577	[272]14	[48]105	[46]100	[36]188	[38]378	[37]788	[54]$0.09N^{1.0}$
180	Innovatrics	SK	innovatrics	008	2023-01-12	609	102	[457]4136	-	[269]647	[421]42	[222]823	[226]864	[187]1610	[186]3271	[192]6943	[153]$0.43N^{1.0}$
181	Innovatrics	SK	innovatrics	009	2023-08-01	590	108	[459]4136	-	[172]474	[440]60	[239]924	[247]975	[200]1759	[195]3496	[190]6926	[55]$0.81N^{1.0}$
182	Innovatrics	SK	innovatrics	010	2024-01-09	797	42	[458]4136	-	[240]595	[438]56	[226]850	[235]907	[198]1724	[193]3444	[196]7470	[189]$0.41N^{1.0}$
183	Innovatrics	SK	innovatrics	011	2024-05-14	628	48	[464]4209	-	[243]600	[452]86	[465]10112	[472]10087	[405]18636	[396]37591	[387]75468	[114]$5.61N^{1.0}$
184	Innovatrics	SK	innovatrics	012	2024-09-20	0	1938	[466]4779	-	[482]1462	[377]28	[288]1295	[288]1312	[239]2250	[235]4635	[243]9711	[50]$1.14N^{1.0}$
185	Innovatrics	SK	innovatrics	013	2025-01-28	0	2784	[481]6845	-	[426]1133	[415]38	[303]1495	[313]1581	[269]2929	[262]5827	[259]11658	[51]$1.40N^{1.0}$
186	Innovatrics	SK	innovatrics	014	2025-05-28	0	3178	[482]6870	-	[472]1359	[416]39	[293]1405	[294]1405	[254]2556	[243]4929	[234]9479	[46]$1.49N^{1.0}$
187	Innovatrics	SK	innovatrics	015	2025-09-29	0	3057	[483]6870	-	[489]2124	[433]50	[312]1580	[312]1568	[271]2944	[264]5942	[265]11998	[112]$0.89N^{1.0}$
188	Inspur (Beijing) Electronic Information Industry Co	CN	inspur	000	2023-05-30	356	88	[232]2048	-	[385]898	[320]16	[394]3574	[393]3248	[342]6610	[339]13468	[336]27332	[259]$1.04N^{1.0}$
189	Inspur (Beijing) Electronic Information Industry Co	CN	inspur	001	2023-12-07	437	88	[236]2048	-	[406]1025	[317]16	[393]3483	[394]3254	[340]6520	[337]13141	[331]25818	[205]$1.36N^{1.0}$
190	Inspur (Beijing) Electronic Information Industry Co	CN	inspur	002	2025-02-11	434	88	[282]2048	-	[451]1222	[316]16	[389]3313	[395]3259	[337]6169	[344]13863	[337]27477	[272]$0.98N^{1.1}$
191	Intel Research Group	IS	intelresearch	001	2025-03-31	309	118	[247]2048	-	[447]1219	[247]13	[235]886	[228]866	[190]1652	[189]3339	[187]6862	[154]$0.44N^{1.0}$
192	Intellivision	IN	intellivision	001	2022-03-08	62	130	[379]2056	-	[78]325	[351]20	[135]388	[484]18764	-	-	-	
193	Intellivision	IN	intellivision	002	2022-07-28	114	128	[384]2056	-	[66]301	[231]13	[476]20542	[485]18784	-	-	-	
194	Intema-LGL Group	LU	intema	000	2022-08-24	1042	20	[57]512	-	[260]629	[481]13809	[22]27	[23]35	[16]39	[16]46	[10]51	[8]$3478.46N^{0.2}$
195	Intema-LGL Group	LU	intema	001	2023-02-22	723	20	[60]512	-	[350]802	[470]4808	[18]23	[16]24	[12]31	[10]38	[13]54	[13]$567.10N^{0.3}$
196	IrexAI	US	irex	000	2021-02-09	724	46	[413]3080	-	[213]532	[343]19	[230]873	[190]600	[149]1120	[161]2477	[169]5863	[302]$0.13N^{1.1}$
197	Kakao Brain	KR	kakao	000	2021-06-23	404	124	[371]2052	-	[124]399	[89]8	[231]876	[83]215	[79]510	[76]971	[73]1955	[308]$0.05N^{1.1}$
198	Kakao Brain	KR	kakao	001	2022-06-08	615	102	[183]2048	-	[198]509	[333]18	[159]469	[153]418	[135]977	[122]1661	[131]3898	[271]$0.13N^{1.1}$
199	Kakao Brain	KR	kakao	002	2023-11-07	749	102	[245]2048	-	[239]594	[174]12	[162]478	[162]466	[143]1055	[158]2443	[145]4801	[352]$0.06N^{1.1}$
200	Kedacom International Pte	SG	kedacom	001	2019-09-16	239	36	[41]292	1	[193]507	[19]2	[210]764	[217]760	[216]1940	[177]2983	[181]6623	[227]$0.31N^{1.0}$
201	Keyless Technologies	GB	keyless	000	2025-01-16	538	35	[244]2048	-	[242]600	[153]11	[121]355	[129]356	[119]811	-	-	[337]$0.05N^{1.1}$
202	Kloudspot Inc	US	kloudspot	001	2025-01-21	575	237	[359]2052	-	[428]1138	[218]13	[392]3435	[397]3438	[339]6477	[342]13716	[339]28709	[257]$1.11N^{1.0}$
203	Kneron	US	kneron	000	2020-03-03	366	13	[251]2048	k	[205]523	[230]13	[368]2535	[373]2506	[327]4752	[324]9696	[327]20926	[228]$0.95N^{1.0}$
204	Kneron	US	kneron	001	2021-06-10	270	69	[214]2048	-	[61]291	[110]9	[382]3141	[377]2642	-	-	-	
205	Know U Tech LLC	US	knowutech	000	2023-06-05	789	34	[98]781	-	[363]831	[56]5	[398]3773	[396]3411	[338]6413	[336]12847	[338]27685	[190]$1.50N^{1.0}$
206	Kogniza Technology	US	kogniza	000	2024-05-14	0	385	[139]1536	-	[467]1336	[114]9	[451]7385	[460]7272	[391]13740	[384]28092	[376]57099	[183]$3.33N^{1.0}$
207	LightVision Inc	KR	lightvision	000	2025-09-11	260	61	[267]2048	-	[374]862	[332]18	[428]5166	[428]5161	[368]9698	[365]19472	[355]39233	[109]$2.93N^{1.0}$
208	Line Corporation	JP	line	000	2021-06-02	138	397	[351]2048	-	[74]317	[95]8	[421]4637	[430]5418	[369]10144	-	-	[68]$3.65N^{1.0}$

Notes	
1	Configuration size does not capture static data present in libraries. Libraries are included but the size also includes any ancillary libraries for image processing (e.g. openCV) or numerical computation (e.g. blas).
2	Finalization is the processing of converting N = 1600000 templates into a searchable data structure an operation which can be a simple copy, or the building of an index or tree, for example. The duration of the operation may be data dependent, and may not be linear in the number of input templates.
3	This multiplier expresses the increase in template size when k images are passed to the template generation function.
4	All durations are measured on Intel®Xeon®CPU E5-2630 v4 @ 2.20GHz processors. Estimates are made by wrapping the API function call in calls to std::chrono::high_resolution_clock which on the machine in (3) counts 1ns clock ticks. Precision is somewhat worse than that however.
5	Search durations are measured as in the prior note. The power-law model in the final column mostly fits the empirical results in Figure 311. However in certain cases the model is not correct and should not be used numerically.

Table 5: Summary of algorithms and properties included in this report. The blue superscripts give ranking for the quantity in that column. Missing search durations, denoted by "-", are absent because those runs were not executed, usually because we did not run on the larger galleries. Caution: The power-law model is sometimes an incorrect model. It is included here only to show broad sublinear behavior, which is flagged in green. The models should not be used for prediction.

2026/01/09 20:40:38

FNIR(N, R, T) = False neg. identification rate
FPIR(N, T) = False pos. identification rate

N = Num. enrolled subjects
R = Num. candidates examined

T = Threshold

T = 0 → Investigation
T > 0 → Identification

This publication is available free of charge from: https://doi.org/10.6028/NIST.IR.8271

	DEVELOPER	DEVELOPER	SHORT	SEQ.	VALIDATION	CONFIG[1]	LIB[1]	TEMPLATE GENERATION			FINALIZE[2]	SEARCH DURATION[5] MILLISEC					
	FULL NAME	LOCATION	NAME	NUM.	DATE	DATA (MB)	DATA (MB)	SIZE (B)	MULT[3]	TIME (MS)[4]	TIME (S)	L=1	L=50	L=50	L=50	L=50	POWER LAW
												N=1.6M	N=1.6M	N=3M	N=6M	N=12M	(μs)
209	Line Corporation	JP	line	001	2021-11-21	471	396	[243]2048	-	[176]485	[96]8	[330]1815	[340]1934	[294]3647	[297]7675	-	[252]$0.64N^{1.0}$
210	Line Corporation	JP	lineclova	002	2022-07-29	560	72	[328]2048	-	[142]425	[241]13	[97]262	[117]321	[92]604	[113]1534	[107]3023	[325]$0.05N^{1.1}$
211	Line Corporation	JP	lineclova	003	2023-01-19	574	397	[249]2048	-	[134]412	[78]7	[63]156	[76]195	[141]1018	[140]1956	[116]3405	[342]$0.05N^{1.1}$
212	Lomonosov Moscow State University	RU	intsysmsu	000	2019-08-19	375	168	[207]2048	1	[249]614	[245]13	[152]430	[156]431	[126]860	[125]1730	[154]5353	[370]$0.03N^{1.1}$
213	Lookman Electroplast Industries	IN	lookman	3	2018-10-28	203	24	[42]292	1	[81]336	[30]3	[206]739	[213]745	[175]1394	[170]2817	[210]8286	[324]$0.13N^{1.1}$
214	Lookman Electroplast Industries	IN	lookman	4	2018-10-28	184	24	[89]548	1	[75]320	[50]4	[252]981	[253]998	-	-	-	
215	Lookman Electroplast Industries	IN	lookman	005	2019-09-16	239	36	[88]548	1	[192]506	[46]4	[256]1005	[256]1008	[255]2597	[252]5446	[220]8939	[321]$0.19N^{1.1}$
216	Luxand Inc	US	luxand	001	2023-10-17	83	70	[294]2048	-	[143]425	[173]12	[367]2523	[379]2713	[322]4690	[321]9543	[321]19507	[56]$2.11N^{1.0}$
217	Mantra Softech India	IN	mantra	000	2021-10-28	460	61	[370]2052	-	[136]412	[129]10	[238]916	[236]910	[196]1714	[192]3411	[185]6841	[78]$0.57N^{1.0}$
218	Maverick Research	AE	maverickresearch	000	2025-02-25	250	96	[339]2048	-	[402]995	[169]12	[131]372	[159]443	-	-	-	
219	Maxvision	CN	maxvision	000	2022-06-17	167	60	[159]2048	-	[16]139	[491]-	[426]5044	[277]1195	[234]2163	[225]4380	[219]8914	[169]$0.55N^{1.0}$
220	Maxvision	CN	maxvision	001	2022-10-28	228	63	[341]2048	-	[92]351	[239]13	[277]1173	[270]1061	[237]2233	[222]4311	[223]9084	[226]$0.42N^{1.0}$
221	Maxvision	CN	maxvision	002	2023-04-12	391	63	[311]2048	-	[258]626	[302]15	[278]1180	[267]1052	[235]2213	[218]4234	[226]9310	[253]$0.37N^{1.0}$
222	Maxvision	CN	maxvision	003	2023-08-11	228	62	[233]2048	-	[90]348	[159]12	[265]1049	[268]1052	[221]2006	[216]4177	[229]9366	[247]$0.37N^{1.0}$
223	Maxvision	CN	maxvision	004	2023-12-12	308	62	[191]2048	-	[442]1202	[228]13	[269]1094	[271]1088	[222]2044	[213]4067	[218]8836	[174]$0.51N^{1.0}$
224	Megvii/Face++	CN	megvii	1	2018-10-28	1703	41	[437]4096	1	[261]631	[401]32	[181]552	[186]561	[161]1222	[152]2321	[170]5968	[341]$0.08N^{1.1}$
225	Megvii/Face++	CN	megvii	2	2018-10-28	1735	42	[434]4096	1	[262]635	[399]31	[182]553	[183]558	-	-	-	
226	Megvii/Face++	CN	megvii	003	2023-05-11	1335	43	[355]2049	-	[459]1263	[312]16	[339]1972	[334]1854	[270]2942	[285]6803	[285]14061	[261]$0.52N^{1.0}$
227	Megvii/Face++	CN	megvii	004	2023-10-18	1605	43	[353]2049	-	[465]1303	[271]14	[326]1735	[321]1694	[285]3217	[278]6495	[290]14865	[256]$0.56N^{1.0}$
228	Megvii/Face++	CN	megvii	005	2024-02-20	1605	43	[354]2049	-	[469]1348	[282]14	[328]1764	[325]1721	[287]3261	[281]6584	[279]13376	[139]$0.90N^{1.0}$
229	Metsakuur	KR	metsakuurcompany	000	2024-10-24	0	1011	[378]2056	-	[360]830	[155]12	[378]3068	[456]6828	[403]18336	[397]38444	[390]89809	[391]$0.13N^{1.2}$
230	Metsakuur	KR	metsakuurcompany	001	2025-07-30	0	299	[285]2048	-	[185]490	[209]12	[456]8191	[464]8027	[394]15224	[391]31411	[383]69959	[290]$1.96N^{1.1}$
231	MicroFocus	GB	microfocus	5	2018-10-29	94	26	[23]256	k	[51]262	[25]2	[73]182	[73]186	[59]354	[59]708	[54]1425	[101]$0.11N^{1.0}$
232	MicroFocus	GB	microfocus	6	2018-10-29	94	26	[18]256	k	[50]262	[27]2	[74]183	[72]186	-	-	-	
233	Microsoft	US	microsoft	5	2018-10-29	381	155	[104]1024	1	[279]658	[152]11	[313]1606	[320]1673	[277]3076	[274]6302	[276]13160	[168]$0.79N^{1.0}$
234	Microsoft	US	microsoft	6	2018-10-29	478	155	[107]1024	1	[286]671	[290]15	[317]1642	[318]1618	[296]3710	[276]6401	[273]12892	[209]$0.68N^{1.0}$
235	Mobbeel Solutions	ES	mobbl	000	2023-11-30	168	157	[234]2048	-	[233]577	[487]34082	[338]1958	[368]2444	[366]9181	[327]11242	[197]7502	[30]$4.56N^{0.9}$
236	Mobbeel Solutions	ES	mobbl	001	2024-05-14	168	158	[308]2048	-	[231]568	[484]22755	[403]3993	[423]4689	-	-	-	
237	Mobbeel Solutions	ES	mobbl	002	2025-04-09	344	555	[291]2048	-	[418]1088	[171]12	[12]11	[8]11	-	-	-	
238	Mukh Technologies	US	mukh	002	2022-09-16	693	442	[225]2048	-	[340]780	[469]4261	[7]5	[33]82	[26]137	[26]319	[26]612	[91]$0.05N^{1.0}$
239	N-Tech Lab	RU	ntech	5	2018-10-30	1685	113	[152]1940	k	[314]711	[437]55	[93]243	[93]246	[81]538	[83]1100	[94]2867	[365]$0.02N^{1.1}$
240	N-Tech Lab	RU	ntech	6	2018-10-30	1686	117	[151]1940	k	[362]831	[441]63	[92]243	[92]246	[83]546	[84]1104	[96]2873	[367]$0.02N^{1.1}$
241	N-Tech Lab	RU	ntechlab	007	2019-06-25	2450	51	[417]3348	k	[349]795	[446]73	[139]393	[155]427	[118]780	[130]1768	[120]3499	[225]$0.16N^{1.0}$
242	N-Tech Lab	RU	ntechlab	008	2020-01-06	1111	51	[135]1300	k	[224]554	[410]36	[72]179	[70]184	[57]341	[57]683	[53]1395	[92]$0.11N^{1.0}$
243	N-Tech Lab	RU	ntechlab	009	2021-03-01	1208	42	[136]1300	-	[488]1936	[408]35	[78]193	[71]184	[55]336	[56]676	[65]1704	[283]$0.05N^{1.1}$
244	N-Tech Lab	RU	ntechlab	010	2021-06-24	351	213	[132]1280	-	[325]738	[61]6	[197]666	[157]435	[120]821	[120]1645	[113]3337	[149]$0.22N^{1.0}$
245	N-Tech Lab	RU	ntechlab	011	2021-12-07	679	208	[134]1280	-	[326]739	[65]6	[223]827	[164]483	[130]912	[137]1869	[148]5003	[330]$0.07N^{1.1}$
246	NEC	JP	nec	2	2018-10-30	705	35	[146]1616	k	[268]642	[339]18	[144]405	[150]409	[145]1072	[128]1755	[140]4255	[347]$0.06N^{1.1}$
247	NEC	JP	nec	3	2018-10-30	774	110	[148]1712	k	[283]665	[355]21	[9]7	[5]7	[6]14	[13]40	[15]82	[379]$0.00N^{1.2}$
248	NEC	JP	nec	004	2021-07-19	971	63	[129]1104	-	[270]647	[66]7	[158]468	[128]351	[102]662	[99]1330	[89]2685	[110]$0.20N^{1.0}$
249	NEC	JP	nec	005	2021-12-13	922	88	[127]1104	-	[251]615	[72]7	[146]407	[181]551	[140]1017	[145]2091	[138]4242	[141]$0.28N^{1.0}$
250	NEC	JP	nec	006	2022-08-10	701	54	[128]1104	-	[278]656	[107]9	[122]358	[149]409	[117]765	[115]1543	[129]3878	[295]$0.10N^{1.1}$
251	NEC	JP	nec	007	2023-03-03	632	56	[93]560	-	[267]641	[63]6	[86]216	[82]214	[67]423	[69]853	[66]1720	[335]$0.03N^{1.1}$
252	NEC	JP	nec	008	2023-07-03	1380	50	[147]1648	-	[475]1381	[146]11	[178]532	[180]548	[174]1384	[79]999	[142]4757	[31]$1.39N^{0.9}$
253	NEC	JP	nec	009	2023-12-21	1688	51	[92]560	-	[481]1462	[59]5	[58]138	[56]139	[45]261	[44]523	[43]1056	[118]$0.08N^{1.0}$
254	NEC	JP	nec	010	2025-01-24	2015	53	[95]560	-	[474]1373	[60]5	[57]138	[66]177	[48]270	[60]712	[55]1455	[230]$0.06N^{1.0}$
255	NEC	JP	nec	011	2025-10-16	1966	52	[94]560	-	[490]2362	[67]7	[75]184	[69]184	[58]346	[58]692	[52]1389	[113]$0.10N^{1.0}$
256	Neurotechnology	LT	neurotech	5	2018-10-30	266	53	[25]256	k	[126]402	[26]2	[224]835	[224]839	[191]1690	[185]3219	[221]8955	[304]$0.19N^{1.1}$
257	Neurotechnology	LT	neurotech	6	2018-10-30	564	53	[15]256	k	[321]726	[23]2	[225]839	[225]842	-	-	-	
258	Neurotechnology	LT	neurotech	007	2019-10-03	57	51	[20]256	k	[18]161	[20]2	[272]1118	[272]1110	[229]2143	[226]4397	[222]9045	[167]$0.55N^{1.0}$
259	Neurotechnology	LT	neurotechnology	008	2021-03-22	355	49	[77]514	-	[130]405	[49]4	[271]1100	[275]1149	[240]2266	[234]4573	[239]9586	[178]$0.55N^{1.0}$
260	Neurotechnology	LT	neurotechnology	009	2021-09-01	246	82	[75]513	-	[85]341	[28]3	[244]941	[265]1049	[219]1977	[221]4270	[214]8756	[265]$0.32N^{1.1}$

Notes	
1	Configuration size does not capture static data present in libraries. Libraries are included but the size also includes any ancillary libraries for image processing (e.g. openCV) or numerical computation (e.g. blas).
2	Finalization is the processing of converting N = 1600000 templates into a searchable data structure an operation which can be a simple copy, or the building of an index or tree, for example. The duration of the operation may be data dependent, and may not be linear in the number of input templates.
3	This multiplier expresses the increase in template size when k images are passed to the template generation function.
4	All durations are measured on Intel®Xeon®CPU E5-2630 v4 @ 2.20GHz processors. Estimates are made by wrapping the API function call in calls to std::chrono::high_resolution_clock which on the machine in (3) counts 1ns clock ticks. Precision is somewhat worse than that however.
5	Search durations are measured as in the prior note. The power-law model in the final column mostly fits the empirical results in Figure 311. However in certain cases the model is not correct and should not be used numerically.

Table 6: Summary of algorithms and properties included in this report. The blue superscripts give ranking for the quantity in that column. Missing search durations, denoted by "-", are absent because those runs were not executed, usually because we did not run on the larger galleries. Caution: The power-law model is sometimes an incorrect model. It is included here only to show broad sublinear behavior, which is flagged in green. The models should not be used for prediction.

2026/01/09 20:40:38

FNIR(N, R, T) = False neg. identification rate
FPIR(N, T) = False pos. identification rate

N = Num. enrolled subjects
R = Num. candidates examined

T = Threshold

T = 0 → Investigation
T > 0 → Identification

This publication is available free of charge from: https://doi.org/10.6028/NIST.IR.8271

	DEVELOPER	DEVELOPER	SHORT	SEQ.	VALIDATION	CONFIG[1]	LIB[1]	TEMPLATE GENERATION			FINALIZE[2]	SEARCH DURATION[5] MILLISEC					
	FULL NAME	LOCATION	NAME	NUM.	DATE	DATA (MB)	DATA (MB)	SIZE (B)	MULT[3]	TIME (MS)[4]	TIME (S)	L=1	L=50	L=50	L=50	L=50	POWER LAW
											N=1.6M	N=1.6M	N=1.6M	N=3M	N=6M	N=12M	(μs)
261	Neurotechnology	LT	neurotechnology	010	2022-01-07	247	83	[17]256	-	[280]661	[7]2	[253]988	[250]984	[211]1897	[209]3977	[208]8048	$[236]0.36N^{1.0}$
262	Neurotechnology	LT	neurotechnology	012	2022-06-07	247	84	[24]256	-	[101]368	[29]3	[263]1036	[244]945	[204]1828	[201]3787	[204]7838	$[250]0.32N^{1.0}$
263	Neurotechnology	LT	neurotechnology	013	2023-02-03	364	87	[22]256	-	[169]471	[10]2	[424]4935	[424]4812	[371]10461	[389]30539	[386]73417	$[398]0.03N^{1.3}$
264	Neurotechnology	LT	neurotechnology	014	2023-12-27	362	95	[19]256	-	[170]472	[5]2	[84]212	[84]215	[66]414	[70]854	[67]1763	$[239]0.08N^{1.0}$
265	Neurotechnology	LT	neurotechnology	015	2024-08-27	357	100	[16]256	-	[254]619	[18]2	[82]203	[80]207	[64]398	[66]821	[64]1690	$[238]0.07N^{1.0}$
266	Neurotechnology	LT	neurotechnology	016	2025-08-01	788	100	[73]512	-	[429]1146	[43]4	[110]293	[107]287	[89]594	[88]1187	[82]2408	$[268]0.09N^{1.1}$
267	Newland Computer Co	CN	newland	2	2018-10-30	96	27	[217]2048	-	[371]855	[293]15	[460]8741	[468]8854	[401]17892	[399]39356	-	$[334]1.32N^{1.1}$
268	NextMedia Labs	IN	nextmetalabs	001	2024-09-20	353	8204	[275]2048	-	[395]948	[246]13	[434]5732	[436]5897	-	-	-	
269	NextMedia Labs	IN	nextmetalabs	002	2025-07-07	1079	6593	[276]2048	-	[440]1197	[215]13	[449]6479	[447]6259	[377]11828	[380]26060	[371]52936	$[275]1.84N^{1.1}$
270	Noblis	US	noblis	1	2018-10-30	114	176	[158]2048	1	[37]206	[287]15	[286]1273	[283]1272	-	-	-	
271	Noblis	US	noblis	2	2018-10-30	153	176	[473]6144	1	[202]517	[422]43	[366]2513	[374]2522	[329]5649	[334]12432	[360]44262	$[392]0.04N^{1.3}$
272	Nominder	LT	nominder	000	2023-09-07	534	100	[30]258	-	[112]384	[6]2	[31]48	[30]49	[23]92	[23]186	[22]376	$[157]0.02N^{1.0}$
273	Nominder	LT	nominder	001	2024-01-08	243	114	[28]258	-	[117]390	[15]2	[30]48	[29]48	[22]92	[22]186	[21]375	$[162]0.02N^{1.0}$
274	Nominder	LT	nominder	002	2024-06-05	243	111	[29]258	-	[116]388	[21]2	[33]61	[27]47	[24]107	[25]234	[24]483	$[360]0.00N^{1.1}$
275	Nominder	LT	nominder	003	2024-10-07	244	111	[26]258	-	[304]697	[12]2	[29]46	[28]47	[21]89	[21]180	[23]400	$[254]0.02N^{1.0}$
276	Nominder	LT	nominder	004	2025-02-10	312	111	[27]258	-	[462]1294	[16]2	[32]50	[31]50	[25]116	[24]193	[25]507	$[316]0.01N^{1.1}$
277	NotionTag Technologies Private Limited	IN	notiontag	000	2022-01-14	265	945	[403]2120	-	[158]453	[134]10	[459]8619	[467]8705	[398]16652	[398]38794	[391]90607	$[345]1.15N^{1.1}$
278	Omnigarde	US	omnigarde	000	2023-05-22	417	34	[79]517	-	[310]705	[39]3	[340]1983	[339]1933	[290]3430	[288]7224	[298]15597	$[215]0.75N^{1.0}$
279	Omnigarde	US	omnigarde	001	2024-06-25	971	34	[78]517	-	[443]1205	[37]3	[344]2017	[353]2079	[308]3941	[305]7908	[305]15974	$[105]1.20N^{1.0}$
280	Omnigarde	US	omnigarde	002	2025-07-28	1285	34	[80]525	-	[435]1168	[38]3	[365]2512	[375]2534	[324]4734	[322]9553	[320]19203	$[67]1.72N^{1.0}$
281	OptiExacta	IN	optiexacta	000	2024-07-23	505	2446	[410]2564	-	[431]1149	[294]15	[246]954	[243]944	[201]1780	[197]3583	[194]7238	$[208]0.38N^{1.0}$
282	PT Ice House	ID	icehouse	000	2024-08-30	62	58	[347]2048	-	[7]46	[180]12	[474]15996	[482]16117	-	-	-	
283	Panasonic R+D Center Singapore	SG	psl	000	2023-08-08	795	607	[488]8248	-	[416]1085	[424]43	[397]3678	[402]3669	[346]7080	[340]13494	[333]26559	$[163]1.74N^{1.0}$
284	Panasonic R+D Center Singapore	SG	psl	001	2024-02-22	894	607	[461]4144	-	[422]1114	[371]25	[354]2250	[363]2288	[313]4316	[309]8577	[323]19561	$[231]0.86N^{1.0}$
285	Panasonic R+D Center Singapore	SG	psl	002	2024-07-26	992	607	[462]4148	-	[464]1300	[364]23	[370]2731	[378]2704	[328]4953	[320]9531	[326]20015	$[61]1.95N^{1.0}$
286	Panasonic R+D Center Singapore	SG	psl	003	2025-07-07	1585	607	[416]3124	-	[444]1207	[338]18	[352]2146	[365]2399	[317]4575	[316]9364	[311]17474	$[200]0.98N^{1.0}$
287	Panasonic R+D Center Singapore	SG	psl	004	2025-11-28	1088	607	[415]3124	-	[487]1824	[369]24	[386]3213	[389]3150	[332]5926	[330]12019	[343]31019	$[296]0.74N^{1.1}$
288	Pangiam	US	pangiam	000	2022-02-22	453	23	[314]2048	-	[263]636	[328]17	[101]276	[116]319	[90]601	[91]1210	[84]2443	$[103]0.18N^{1.0}$
289	Pangiam	US	pangiam	001	2022-11-17	991	36	[290]2048	-	[236]577	[263]14	[100]275	[141]378	[114]724	[106]1436	[124]3676	$[300]0.08N^{1.1}$
290	Papilon Savunma	TR	papsav1923	000	2023-08-22	923	24	[39]288	-	[337]767	[9]2	[27]37	[25]38	[18]72	[19]143	[19]286	$[74]0.02N^{1.0}$
291	Paravision (EverAI)	US	everai	2	2018-10-30	224	304	[327]2048	1	[99]366	[395]30	[104]278	[105]283	-	-	-	
292	Paravision (EverAI)	US	everai	3	2018-10-30	438	304	[292]2048	1	[316]717	[381]28	[102]278	[104]281	[86]572	[85]1146	[78]2278	$[214]0.12N^{1.0}$
293	Paravision (EverAI)	US	everai-paravision	004	2019-06-19	527	128	[438]4096	1	[287]672	[427]45	[183]559	[184]559	[257]2611	[277]6445	[287]14519	$[402]0.00N^{1.5}$
294	Paravision (EverAI)	US	paravision	005	2019-12-11	543	154	[443]4096	1	[361]830	[431]48	[185]561	[187]564	[144]1056	[148]2298	[147]4966	$[278]0.16N^{1.1}$
295	Paravision (EverAI)	US	paravision	007	2021-02-01	529	235	[432]4096	-	[122]397	[432]48	[215]786	[182]558	[146]1086	[146]2111	[139]4254	$[39]1.11N^{0.9}$
296	Paravision	US	paravision	009	2021-12-14	672	300	[445]4100	-	[79]331	[449]82	[414]4495	[413]4230	[357]8037	[354]16532	[344]31422	$[217]1.62N^{1.0}$
297	Paravision	US	paravision	012	2023-02-07	762	182	[448]4100	-	[133]411	[451]85	[406]4313	[422]4534	[363]8651	[356]16582	[347]32114	$[71]2.87N^{1.0}$
298	Paravision	US	paravision	014	2023-06-08	1501	182	[446]4100	-	[405]1010	[454]86	[416]4524	[418]4454	[356]7993	[352]16169	[345]31691	$[185]1.88N^{1.0}$
299	Paravision	US	paravision	016	2024-12-04	1546	250	[447]4100	-	[441]1200	[450]84	[412]4436	[406]4006	[355]7861	[357]16711	[348]32464	$[177]1.94N^{1.0}$
300	Paravision	US	paravision	019	2025-07-03	1558	250	[449]4100	-	[477]1415	[453]86	[405]4304	[414]4301	[352]7639	[348]15454	[346]31978	$[191]1.78N^{1.0}$
301	Pentacomp Systemy Informatyczne	PL	pentacomp	000	2025-01-10	255	187	[349]2048	-	[171]473	[235]13	[171]511	[177]534	-	-	-	
302	Pentacomp Systemy Informatyczne	PL	pentacomp	001	2025-07-28	255	187	[167]2048	-	[163]459	[269]14	[302]1485	[297]1447	[243]2408	[237]4708	[235]9479	$[35]2.83N^{0.9}$
303	Private Identity LLC		privid	000	2025-08-01	0	975	[342]2048	-	[463]1296	[458]226	[15]20	[12]19	-	-	-	
304	Protenet Soluções em Segurança	BR	protenet	000	2025-09-17	182	173	[182]2048	-	[329]748	[460]389	[71]178	[67]178	-	-	-	
305	Pyramid Cyber Security + Forensic (P)	IN	pyramid	000	2024-11-19	1016	141	[298]2048	-	[365]837	[345]20	[161]473	[166]489	[122]844	[118]1587	[117]3408	$[47]0.50N^{1.0}$
306	Pyramid Cyber Security + Forensic (P)	IN	pyramid	001	2025-04-01	1023	140	[320]2048	-	[372]857	[348]20	[118]336	[126]345	[97]649	[96]1303	[105]3008	$[249]0.12N^{1.0}$
307	QazSmartVision.AI	KZ	qazsmartvisionai	000	2024-03-15	547	95	[66]512	-	[307]701	[68]7	[66]157	[62]157	[52]296	[48]597	[47]1220	$[166]0.07N^{1.0}$
308	QazSmartVision.AI	KZ	qazsmartvisionai	001	2024-07-16	1383	98	[85]544	-	[454]1245	[75]7	[51]124	[50]125	[42]234	[41]473	[39]957	$[125]0.07N^{1.0}$
309	QazSmartVision.AI	KZ	qazsmartvisionai	002	2024-12-03	1333	98	[86]544	-	[449]1221	[70]7	[64]156	[63]157	[51]294	[47]591	[51]1369	$[251]0.05N^{1.0}$
310	QazSmartVision.AI	KZ	qazsmartvisionai	003	2025-04-24	1358	98	[87]544	-	[453]1238	[69]7	[65]156	[61]156	[53]297	[49]598	[45]1204	$[135]0.08N^{1.0}$
311	Qnap Security	TW	qnap	000	2021-07-28	182	15	[280]2048	-	[125]401	[117]9	[295]1427	[330]1763	-	-	-	
312	Qnap Security	TW	qnap	001	2021-12-09	191	13	[172]2048	-	[179]487	[90]8	[298]1449	[296]1429	[291]3472	[292]7375	[295]15159	$[376]0.11N^{1.2}$

Notes	
1	Configuration size does not capture static data present in libraries. Libraries are included but the size also includes any ancillary libraries for image processing (e.g. openCV) or numerical computation (e.g. blas).
2	Finalization is the processing of converting N = 1600000 templates into a searchable data structure an operation which can be a simple copy, or the building of an index or tree, for example. The duration of the operation may be data dependent, and may not be linear in the number of input templates.
3	This multiplier expresses the increase in template size when k images are passed to the template generation function.
4	All durations are measured on Intel®Xeon®CPU E5-2630 v4 @ 2.20GHz processors. Estimates are made by wrapping the API function call in calls to std::chrono::high_resolution_clock which on the machine in (3) counts 1ns clock ticks. Precision is somewhat worse than that however.
5	Search durations are measured as in the prior note. The power-law model in the final column mostly fits the empirical results in Figure 311. However in certain cases the model is not correct and should not be used numerically.

Table 7: Summary of algorithms and properties included in this report. The blue superscripts give ranking for the quantity in that column. Missing search durations, denoted by "-", are absent because those runs were not executed, usually because we did not run on the larger galleries. Caution: The power-law model is sometimes an incorrect model. It is included here only to show broad sublinear behavior, which is flagged in green. The models should not be used for prediction.

2026/01/09 20:40:38

FNIR(N, R, T) = FPIR(N, T) = False neg. identification rate / False pos. identification rate

N = Num. enrolled subjects
R = Num. candidates examined

T = Threshold

T = 0 → Investigation
T > 0 → Identification

This publication is available free of charge from: https://doi.org/10.6028/NIST.IR.8271

	DEVELOPER	DEVELOPER	SHORT	SEQ.	VALIDATION	CONFIG[1]	LIB[1]	TEMPLATE GENERATION			FINALIZE[2]	SEARCH DURATION[5] MILLISEC					
	FULL NAME	LOCATION	NAME	NUM.	DATE	DATA (MB)	DATA (MB)	SIZE (B)	MULT[3]	TIME (MS)[4]	TIME (S)	L=1	L=50	L=50	L=50	L=50	POWER LAW
											N=1.6M	N=1.6M	N=1.6M	N=3M	N=6M	N=12M	(μs)
313	Qnap Security	TW	qnap	002	2022-04-15	338	32	[334]2048	-	[182]489	[324]17	[248]958	[241]938	[207]1866	[224]4359	[215]8792	[346]$0.12N^{1.1}$
314	Qnap Security	TW	qnap	003	2022-12-09	239	60	[271]2048	-	[44]244	[258]13	[319]1671	[345]2039	[309]4010	[307]8379	[292]14911	[195]$0.87N^{1.0}$
315	Qnap Security	TW	qnap	004	2023-05-05	362	60	[223]2048	-	[97]365	[151]11	[334]1885	[356]2096	[284]3191	[282]6601	[286]14490	[52]$1.66N^{1.0}$
316	Qnap Security	TW	qnap	005	2023-11-16	954	60	[176]2048	-	[399]971	[179]12	[304]1499	[358]2151	[286]3232	[306]7969	[296]15499	[142]$1.02N^{1.0}$
317	Qnap Security	TW	qnap	006	2024-08-09	1178	60	[364]2052	-	[403]1005	[214]13	[337]1908	[335]1894	[278]3098	[272]6263	[284]14003	[201]$0.72N^{1.0}$
318	Quantasoft	CZ	quantasoft	1	2018-10-30	276	452	[195]2048	k	[113]385	[64]6	[473]15422	[480]14858	[393]14717	-	[313]18323	
319	RNIT Solutions and Servies Ltd	IN	rnit	000	2025-05-08	490	33	[43]296	-	[448]1220	[11]2	[136]389	[145]387	[116]752	[112]1524	[109]3098	[211]$0.16N^{1.0}$
320	ROC	US	rankone	4	2018-10-09	0	101	[4]85	k	[6]36	[73]7	[45]101	[47]101	[38]190	-	-	[65]$0.07N^{1.0}$
321	ROC	US	rankone	5	2018-10-24	0	101	[12]133	k	[9]92	[74]7	[59]140	[57]144	[46]266	[45]525	[42]1049	[60]$0.11N^{1.0}$
322	ROC	US	rankone	006	2019-06-03	0	133	[14]165	k	[45]245	[88]8	-	-	-	-	-	
323	ROC	US	rankone	007	2019-11-12	0	137	[13]165	k	[53]272	[80]7	[49]116	[48]115	[40]215	[40]439	[38]877	[100]$0.07N^{1.0}$
324	ROC	US	rankone	009	2020-06-26	0	105	[31]260	k	[29]185	[143]11	[37]95	[41]96	[33]181	[33]362	[34]727	[81]$0.06N^{1.0}$
325	ROC	US	rankone	010	2020-11-05	0	135	[34]261	-	[34]198	[135]10	[38]95	[36]95	[30]178	[30]357	[31]714	[76]$0.06N^{1.0}$
326	ROC	US	rankone	011	2021-08-27	0	175	[32]261	-	[230]566	[97]8	[42]96	[37]95	[35]183	[35]370	[30]714	[89]$0.06N^{1.0}$
327	ROC	US	rankone	012	2021-12-27	0	257	[33]261	-	[228]563	[83]8	[41]95	[38]95	[31]179	[32]361	[32]718	[79]$0.06N^{1.0}$
328	ROC	US	rankone	013	2022-07-21	0	223	[35]261	-	[152]446	[313]16	[46]101	[35]89	[28]167	[28]335	[28]672	[87]$0.06N^{1.0}$
329	ROC	US	rankone	014	2022-12-21	0	237	[37]261	-	[160]457	[86]8	[47]101	[45]100	[37]188	[37]376	[36]775	[123]$0.06N^{1.0}$
330	ROC	US	rankone	015	2023-07-20	0	282	[36]261	-	[221]548	[101]9	[43]97	[42]97	[34]183	[34]366	[35]734	[95]$0.06N^{1.0}$
331	ROC	US	roc	016	2023-12-20	0	659	[49]392	-	[223]552	[91]8	[52]131	[51]130	[43]245	[42]491	[44]1084	[207]$0.05N^{1.0}$
332	ROC	US	roc	017	2024-06-24	0	552	[50]396	-	[274]651	[104]9	[69]158	[64]159	[50]294	[50]601	[46]1204	[106]$0.09N^{1.0}$
333	ROC	US	roc	018	2025-01-31	0	910	[99]792	-	[452]1235	[132]10	[109]290	[108]290	[85]550	[92]1222	[86]2527	[279]$0.08N^{1.1}$
334	ROC	US	roc	019	2025-08-04	0	924	[51]444	-	[425]1131	[486]31194	[76]185	[68]183	[56]340	[55]669	[50]1338	[48]$0.19N^{1.0}$
335	Realnetworks Inc	US	realnetworks	2	2018-10-30	105	104	[454]4104	k	[43]241	[380]28	[341]2008	[347]2048	[311]4194	[310]8642	[294]15035	[143]$1.08N^{1.0}$
336	Realnetworks Inc	US	realnetworks	003	2019-06-12	93	102	[149]1848	k	[23]173	[213]13	[275]1145	[273]1132	[228]2142	[248]5241	[251]10495	[315]$0.21N^{1.1}$
337	Realnetworks Inc	US	realnetworks	004	2019-10-17	94	102	[150]1848	1	[21]171	[142]11	[274]1143	[274]1137	[231]2149	[239]4740	[242]9693	[260]$0.36N^{1.0}$
338	Realnetworks Inc	US	realnetworks	005	2021-06-23	168	209	[381]2056	-	[80]332	[106]9	[318]1654	[317]1616	[273]3030	[268]6068	[270]12134	[85]$1.01N^{1.0}$
339	Realnetworks Inc	US	realnetworks	006	2021-12-02	250	56	[391]2056	-	[22]172	[92]8	[218]791	[175]531	[137]996	[144]1998	[134]3991	[84]$0.33N^{1.0}$
340	Realnetworks Inc	US	realnetworks	007	2022-04-11	455	99	[382]2056	-	[86]342	[325]17	[221]815	[201]674	[186]1597	[199]3683	[163]5729	[317]$0.13N^{1.1}$
341	Realnetworks Inc	US	realnetworks	008	2022-08-29	557	99	[380]2056	-	[206]524	[170]12	[180]538	[200]673	[162]1264	[178]3011	[166]5801	[289]$0.18N^{1.1}$
342	Recognito	AE	recognito	000	2023-02-17	350	242	[133]1280	-	[338]775	[120]9	[214]780	[191]605	[153]1152	[151]2320	[162]5707	[320]$0.10N^{1.1}$
343	Recognito	AE	recognito	001	2023-06-23	536	242	[411]2564	-	[417]1086	[296]15	[273]1128	[251]989	[225]2078	[210]3978	[137]4107	[28]$2.45N^{0.9}$
344	Recognito	AE	recognito	002	2023-11-09	505	61	[412]2564	-	[412]1075	[306]16	[247]957	[245]945	[202]1791	[228]4437	[224]9161	[357]$0.10N^{1.1}$
345	Remark Holdings	CN	remarkai	0	2018-10-30	187	847	[215]2048	k	[238]593	[276]14	[433]5685	[434]5723	-	-	-	
346	Remark Holdings	CN	remarkai	000	2019-06-12	234	1092	[350]2048	k	[273]650	[200]12	[435]5776	[433]5703	[374]11604	[393]32133	[392]91436	[393]$0.05N^{1.3}$
347	Remark Holdings	CN	remarkai	1	2018-10-30	187	847	[255]2048	k	[144]427	[283]14	[432]5680	[435]5761	[384]12475	[386]28726	[378]59618	[381]$0.37N^{1.2}$
348	Rendip	SG	rendip	000	2021-05-21	0	416	[324]2048	-	[247]611	[121]9	[112]299	[135]368	[107]697	[109]1452	[101]2926	[294]$0.08N^{1.1}$
349	Reveal Media	UK	revealmedia	000	2022-02-02	287	196	[374]2052	-	[111]383	[128]10	[356]2322	[343]2019	[303]3838	[301]7816	[309]16559	[223]$0.78N^{1.0}$
350	SQIsoft	KR	sqisoft	001	2021-12-20	271	377	[386]2056	-	[70]312	[118]9	[336]1907	[289]1319	[247]2456	[241]4906	[245]9755	[66]$0.90N^{1.0}$
351	SQIsoft	KR	sqisoft	002	2022-10-26	354	593	[390]2056	-	[141]425	[238]13	[301]1480	[314]1596	[274]3044	[269]6111	[275]13138	[199]$0.68N^{1.0}$
352	STCON LLC	SA	stcon	000	2024-04-10	1999	62	[439]4096	-	[351]804	[354]20	[379]3092	[400]3527	-	-	-	
353	STCON LLC	SA	stcon	001	2024-09-23	2973	49	[423]4096	-	[468]1343	[387]29	[219]794	[254]998	[181]1495	[179]3016	[202]7739	[44]$1.36N^{0.9}$
354	STCON LLC	SA	stcon	002	2025-01-31	2973	49	[433]4096	-	[473]1369	[398]31	[217]790	[220]791	[205]1838	[198]3602	[193]7108	[307]$0.18N^{1.1}$
355	STCON LLC	SA	stcon	003	2025-06-24	2973	49	[420]4096	-	[471]1359	[391]29	[255]1005	[248]977	[208]1870	[203]3795	[195]7362	[131]$0.52N^{1.0}$
356	Samsung S1 Corp	KR	s1	000	2021-06-03	257	196	[419]4096	-	[178]487	[347]20	[427]5149	[455]6794	[389]13032	[381]26372	[374]55723	[206]$2.82N^{1.0}$
357	Samsung S1 Corp	KR	s1	001	2021-11-01	240	198	[340]2048	-	[188]491	[98]8	[357]2366	[372]2491	[323]4718	[323]9614	[329]24472	[306]$0.53N^{1.1}$
358	Samsung S1 Corp	KR	s1	002	2022-05-04	244	93	[174]2048	-	[181]488	[305]16	[280]1234	[298]1450	[259]2729	[265]5945	[264]11923	[241]$0.51N^{1.0}$
359	Samsung S1 Corp	KR	s1	003	2022-09-27	471	93	[156]2048	-	[180]487	[255]13	[315]1620	[299]1454	[260]2740	[267]6025	[258]11644	[222]$0.57N^{1.0}$
360	Samsung S1 Corp	KR	s1	004	2023-02-03	471	58	[277]2048	-	[183]489	[232]13	[309]1554	[300]1481	[282]3184	[283]6701	[268]12044	[267]$0.47N^{1.1}$
361	Samsung S1 Corp	KR	s1	005	2023-07-03	770	58	[284]2048	-	[367]847	[206]12	[297]1445	[302]1491	[264]2844	[258]5691	[277]13208	[273]$0.44N^{1.1}$
362	Samsung S1 Corp	KR	s1	006	2024-11-29	768	172	[242]2048	-	[368]849	[217]13	[307]1534	[316]1613	[276]3063	[273]6271	[261]11735	[45]$1.84N^{1.0}$
363	Samsung S1 Corp	KR	s1	007	2025-04-29	1439	172	[317]2048	-	[415]1083	[223]13	[299]1465	[307]1520	[265]2848	[257]5688	[278]13337	[245]$0.53N^{1.0}$
364	Sansap Technology	IN	sansap	001	2024-06-07	0	357	[173]2048	-	[293]684	[240]13	[270]1098	[259]1010	[224]2066	[215]4160	[211]8363	[248]$0.35N^{1.0}$

Notes	
1	Configuration size does not capture static data present in libraries. Libraries are included but the size also includes any ancillary libraries for image processing (e.g. openCV) or numerical computation (e.g. blas).
2	Finalization is the processing of converting N = 1600000 templates into a searchable data structure an operation which can be a simple copy, or the building of an index or tree, for example. The duration of the operation may be data dependent, and may not be linear in the number of input templates.
3	This multiplier expresses the increase in template size when k images are passed to the template generation function.
4	All durations are measured on Intel®Xeon®CPU E5-2630 v4 @ 2.20GHz processors. Estimates are made by wrapping the API function call in calls to std::chrono::high_resolution_clock which on the machine in (3) counts 1ns clock ticks. Precision is somewhat worse than that however.
5	Search durations are measured as in the prior note. The power-law model in the final column mostly fits the empirical results in Figure 311. However in certain cases the model is not correct and should not be used numerically.

Table 8: Summary of algorithms and properties included in this report. The blue superscripts give ranking for the quantity in that column. Missing search durations, denoted by "-", are absent because those runs were not executed, usually because we did not run on the larger galleries. Caution: The power-law model is sometimes an incorrect model. It is included here only to show broad sublinear behavior, which is flagged in green. The models should not be used for prediction.

2026/01/09 20:40:38

FNIR(N, R, T) = FPIR(N, T) = False neg. identification rate / False pos. identification rate

N = Num. enrolled subjects
R = Num. candidates examined

T = Threshold

T = 0 → Investigation
T > 0 → Identification

This publication is available free of charge from: https://doi.org/10.6028/NIST.IR.8271

	DEVELOPER	DEVELOPER	SHORT	SEQ.	VALIDATION	CONFIG[1]	LIB[1]	TEMPLATE GENERATION			FINALIZE[2]	SEARCH DURATION[5] MILLISEC					
	FULL NAME	LOCATION	NAME	NUM.	DATE	DATA (MB)	DATA (MB)	SIZE (B)	MULT[3]	TIME (MS)[4]	TIME (S)	L=1	L=50	L=50	L=50	L=50	POWER LAW
											N=1.6M	N=1.6M	N=1.6M	N=3M	N=6M	N=12M	(μs)
365	Scanovate	IL	scanovate	000	2020-01-15	250	446	165 2048	-	309 705	280 14	(294) 1419	(295) 1412	(272) 3008	(329) 11616	(266) 12012	382 $0.10N^{1.2}$
366	Scanovate	IL	scanovate	001	2020-09-10	250	446	352 2048	-	217 545	229 13	(306) 1520	(290) 1320	(251) 2502	(245) 5047	(248) 10163	155 $0.65N^{1.0}$
367	Scylla Technologies Inc	US	scylla	001	2024-10-09	450	1789	268 2048	-	382 891	461 467	(462) 9267	(470) 9373	(400) 17883	(395) 37069	(388) 76927	263 $2.84N^{1.0}$
368	Sensetime Group	CN	sensetime	0	2018-10-30	525	6	451 4104	k	301 693	419 41	(168) 498	(168) 501	(159) 1212	(147) 2281	(149) 5032	326 $0.09N^{1.1}$
369	Sensetime Group	CN	sensetime	1	2018-10-30	525	6	452 4104	k	259 628	430 48	(174) 516	(169) 502	(152) 1146	(149) 2301	(143) 4765	323 $0.09N^{1.1}$
370	Sensetime Group	CN	sensetime	002	2019-06-03	523	6	383 2056	k	244 603	335 18	(123) 359	(136) 370	(212) 1897	(232) 4508	(238) 9543	405 $0.00N^{1.5}$
371	Sensetime Group	CN	sensetime	003	2019-12-02	769	76	387 2056	1	388 910	342 19	(423) 4885	(427) 4989	(382) 12325	(372) 24712	(366) 49445	350 $0.67N^{1.1}$
372	Sensetime Group	CN	sensetime	004	2020-08-10	456	29	118 1032	-	300 690	198 12	(364) 2490	(369) 2477	(320) 4654	(318) 9402	(324) 19651	161 $1.22N^{1.0}$
373	Sensetime Group	CN	sensetime	005	2020-12-17	631	39	114 1032	-	401 980	141 11	-	(405) 3939	(350) 7398	(345) 14768	(318) 19016	26 $14.03N^{0.9}$
374	Sensetime Group	CN	sensetime	006	2021-07-26	526	54	1 -	-	3 -	81 7	-	(367) 2422	(316) 4527	(313) 9128	(314) 18640	119 $1.35N^{1.0}$
375	Sensetime Group	CN	sensetime	007	2022-01-15	526	37	111 1032	-	390 935	99 8	(359) 2432	(366) 2406	(315) 4513	(312) 8998	(316) 18796	132 $1.28N^{1.0}$
376	Sensetime Group	CN	sensetime	008	2022-08-17	567	37	119 1032	-	354 814	113 9	(361) 2444	(342) 2012	(299) 3785	(296) 7551	(302) 15799	138 $1.05N^{1.0}$
377	Sensetime Group	CN	sensetime	009	2023-01-04	883	59	116 1032	-	466 1320	100 9	(346) 2031	(349) 2062	(298) 3747	(295) 7543	(300) 15781	136 $1.06N^{1.0}$
378	Sensetime Group	CN	sensetime	010	2024-12-03	1148	60	113 1032	-	432 1156	85 8	(96) 262	(98) 259	(76) 481	(77) 981	(75) 2031	150 $0.13N^{1.0}$
379	Serendipity	UZ	serendipity	000	2023-06-20	0	366	262 2048	-	383 894	220 13	(142) 400	(137) 371	(121) 827	(89) 1188	(81) 2386	40 $0.60N^{0.9}$
380	Seventh Sense Artificial Intelligence	SG	seventhsense	001	2024-09-12	1410	633	436 4096	-	423 1127	462 890	(4) 2	(13) 22	(9) 23	(8) 32	(7) 40	14 $381.33N^{0.3}$
381	Shaman Software	US	shaman	6	2018-10-26	0	200	226 2048	k	311 706	277 14	(189) 603	(192) 612	-	-	-	
382	Shaman Software	US	shaman	7	2018-10-26	0	200	258 2048	k	312 707	281 14	(188) 602	(193) 614	(155) 1187	(159) 2448	(152) 5083	216 $0.25N^{1.0}$
383	Shanghai Yitu Technology	CN	yitu	4	2018-10-30	2119	136	396 2070	1	384 897	426 45	(287) 1288	(279) 1203	(246) 2440	(249) 5241	(241) 9671	204 $0.52N^{1.0}$
384	Shanghai Yitu Technology	CN	yitu	5	2018-10-30	2043	136	397 2070	1	370 853	425 44	(281) 1237	(278) 1199	(252) 2513	(244) 5013	(240) 9620	192 $0.55N^{1.0}$
385	Shennona Co Ltd	TW	shennona	000	2024-11-20	977	72	102 1024	-	461 1290	76 7	(429) 5286	(429) 5244	-	-	-	
386	Smilart	DE	smilart	4	2018-10-30	65	89	68 512	k	20 167	48 4	(475) 16137	(481) 15633	-	-	-	
387	Smilart	DE	smilart	5	2018-10-30	562	89	169 2048	k	155 450	274 14	-	-	-	-	-	
388	Sparktek International Pte Ltd	CN	sparktek	000	2025-11-24	785	116	212 2048	-	271 649	326 17	(166) 495	(163) 467	(142) 1031	(136) 1856	(122) 3658	134 $0.26N^{1.0}$
389	Sparsh CCTV	IN	sparsh	001	2024-01-12	0	357	238 2048	-	291 684	147 11	(262) 1036	(258) 1008	(215) 1908	(208) 3927	(203) 7764	148 $0.51N^{1.0}$
390	Staqu Technologies	IN	staqu	000	2021-08-30	1018	690	431 4096	-	292 684	368 24	(417) 4527	(425) 4933	-	-	-	
391	Sum and Substance	UK	sumsub	000	2023-08-18	169	108	250 2048	-	62 292	199 12	(132) 380	(139) 372	-	-	-	
392	Synesis	RU	synesis	3	2018-10-30	237	150	425 4096	k	11 99	385 29	(216) 789	(222) 801	(217) 1941	(206) 3888	(216) 8810	366 $0.07N^{1.1}$
393	Synesis	RU	synesis	003	2019-07-04	143	17	297 2048	k	38 211	188 12	(170) 507	(170) 502	(241) 2297	(233) 4564	(233) 9452	400 $0.00N^{1.4}$
394	Synesis	RU	synesis	005	2020-09-08	494	24	450 4104	-	333 756	366 24	(232) 877	(227) 865	(281) 3182	(236) 4658	(244) 9750	383 $0.06N^{1.2}$
395	T4iSB	BR	t4isb	000	2022-08-17	228	15	316 2048	-	322 729	250 13	(94) 250	(113) 311	-	-	-	
396	TTI Group	VN	ttigroup	000	2024-12-16	455	444	204 2048	-	380 887	177 12	(470) 13054	(477) 12894	-	-	-	
397	Tech5 SA	CH	tech5	001	2019-08-19	1394	116	140 1536	k	381 887	127 10	(133) 383	(218) 766	(261) 2767	(271) 6149	(174) 6178	349 $0.12N^{1.1}$
398	Tech5 SA	CH	tech5	002	2021-04-07	727	112	76 513	-	298 687	44 4	(401) 3816	(453) 6689	(385) 12541	(374) 25145	(369) 50239	83 $4.18N^{1.0}$
399	Tech5 SA	CH	tech5	003	2023-07-14	0	357	261 2048	-	275 653	201 12	(260) 1025	(261) 1013	(223) 2050	(214) 4126	(205) 7935	196 $0.45N^{1.0}$
400	Tencent Deepsea Lab	CN	deepsea	001	2019-07-29	250	323	163 2048	1	324 737	196 12	(259) 1021	(263) 1020	(262) 2774	(260) 5767	(271) 12341	388 $0.06N^{1.2}$
401	Tevian	RU	tevian	5	2018-10-30	773	15	161 2048	1	129 405	288 15	(145) 405	(148) 408	(124) 854	(129) 1757	(115) 3380	258 $0.14N^{1.0}$
402	Tevian	RU	tevian	006	2021-04-16	769	19	117 1032	-	218 546	126 10	(119) 343	(111) 295	(87) 578	(87) 1187	(93) 2741	301 $0.06N^{1.1}$
403	Tevian	RU	tevian	007	2021-10-12	703	19	115 1032	-	328 747	52 4	(130) 369	(112) 298	(88) 579	(86) 1179	(83) 2418	235 $0.11N^{1.0}$
404	Thales Group	US	cogent	2	2018-10-30	681	39	124 1043	k	393 945	375 27	(343) 2017	(357) 2144	(312) 4298	(308) 8472	(308) 16429	156 $1.08N^{1.0}$
405	Thales Group	US	cogent	3	2018-10-30	681	39	123 1043	k	391 940	123 9	(279) 1230	(287) 1311	(258) 2687	(250) 5398	(249) 10184	182 $0.62N^{1.0}$
406	Thales Group	US	cogent	004	2021-02-10	1376	59	377 2053	-	394 947	262 14	(372) 2903	(336) 1911	(292) 3566	(293) 7498	(307) 16370	255 $0.64N^{1.0}$
407	Thales Group	US	cogent	005	2021-09-13	1043	56	125 1062	-	137 418	57 5	(195) 648	(252) 996	(209) 1872	(205) 3845	(198) 7555	186 $0.44N^{1.0}$
408	Thales Group	US	cogent	006	2022-05-14	508	70	91 550	-	135 412	84 8	(187) 587	(207) 706	(166) 1328	(169) 2767	(159) 5675	145 $0.37N^{1.0}$
409	Thales Group	US	cogent	007	2023-01-30	597	72	90 550	-	177 485	40 3	(175) 516	(208) 708	(165) 1321	(172) 2839	(165) 5789	175 $0.34N^{1.0}$
410	TigerIT Americas LLC	US	tiger	2	2018-10-29	416	518	358 2052	k	165 461	295 15	(331) 1816	(337) 1921	(302) 3833	(294) 7526	(289) 14820	194 $0.83N^{1.0}$
411	TigerIT Americas LLC	US	tiger	3	2018-10-30	416	518	357 2052	k	164 461	489 37431	(77) 191	(74) 189	-	-	-	
412	TigerIT Americas LLC	US	tiger	004	2025-08-04	248	194	252 2048	-	159 456	278 14	(251) 976	(249) 982	(220) 1997	(200) 3773	(212) 8432	339 $0.13N^{1.1}$
413	Toshiba	JP	toshiba	0	2018-10-30	961	105	145 1548	k	378 876	156 12	(440) 6153	(446) 6236	(381) 12221	(376) 25355	(367) 49448	377 $0.36N^{1.2}$
414	Toshiba	JP	toshiba	1	2018-10-30	961	105	394 2060	k	372 875	490 44701	(438) 6007	(450) 6355	-	-	-	
415	Toshiba	JP	toshiba	002	2025-07-08	1080	75	385 2056	-	470 1348	193 12	(321) 1685	(329) 1757	(283) 3185	(287) 6968	(281) 13797	242 $0.60N^{1.0}$
416	Toss	KR	toss	000	2025-09-22	970	91	305 2048	-	407 1028	334 18	(186) 572	(188) 571	(148) 1119	(155) 2413	(158) 5647	298 $0.13N^{1.1}$

Notes	
1	Configuration size does not capture static data present in libraries. Libraries are included but the size also includes any ancillary libraries for image processing (e.g. openCV) or numerical computation (e.g. blas).
2	Finalization is the processing of converting N = 1600000 templates into a searchable data structure an operation which can be a simple copy, or the building of an index or tree, for example. The duration of the operation may be data dependent, and may not be linear in the number of input templates.
3	This multiplier expresses the increase in template size when k images are passed to the template generation function.
4	All durations are measured on Intel®Xeon®CPU E5-2630 v4 @ 2.20GHz processors. Estimates are made by wrapping the API function call in calls to std::chrono::high_resolution_clock which on the machine in (3) counts 1ns clock ticks. Precision is somewhat worse than that however.
5	Search durations are measured as in the prior note. The power-law model in the final column mostly fits the empirical results in Figure 311. However in certain cases the model is not correct and should not be used numerically.

Table 9: Summary of algorithms and properties included in this report. The blue superscripts give ranking for the quantity in that column. Missing search durations, denoted by "-", are absent because those runs were not executed, usually because we did not run on the larger galleries. Caution: The power-law model is sometimes an incorrect model. It is included here only to show broad sublinear behavior, which is flagged in green. The models should not be used for prediction.

2026/01/09 20:40:38

FNIR(N, R, T) = False neg. identification rate
FPIR(N, T) = False pos. identification rate

N = Num. enrolled subjects
R = Num. candidates examined

T = Threshold

T = 0 → Investigation
T > 0 → Identification

This publication is available free of charge from: https://doi.org/10.6028/NIST.IR.8271

	DEVELOPER	DEVELOPER	SHORT	SEQ.	VALIDATION	CONFIG[1]	LIB[1]	TEMPLATE GENERATION			FINALIZE[2]	SEARCH DURATION[5] MILLISEC					
	FULL NAME	LOCATION	NAME	NUM.	DATE	DATA (MB)	DATA (MB)	SIZE (B)	MULT[3]	TIME (MS)[4]	TIME (S)	L=1	L=50	L=50	L=50	L=50	POWER LAW
											N=1.6M	N=1.6M	N=1.6M	N=3M	N=6M	N=12M	(μs)
417	Tripleize	JP	aize	001	2021-08-06	262	150	[253]2048	-	[40]222	[111]9	[371]2870	[387]3080	-	-	-	
418	Tripleize	JP	aize	002	2023-08-30	251	32	[272]2048	-	[30]185	[202]12	[381]3119	[385]3037	[330]5662	[328]11312	[328]22897	$^{70}2.00N^{1.0}$
419	Trueface.ai	US	trueface	000	2021-01-27	247	119	[153]2000	-	[96]363	[225]13	[98]271	[120]327	[93]614	[93]1239	[88]2678	$^{176}0.15N^{1.0}$
420	TuringTech.vip	CN	turingtechvip	001	2022-09-29	151	161	[200]2048	-	[295]685	[257]13	[478]22085	[483]17480	-	-	-	
421	Unissey	FR	unissey	001	2023-10-24	0	1052	[430]4096	-	[104]370	[473]7732	[13]15	[9]14	-	-	-	
422	Unissey	FR	unissey	002	2024-02-23	0	1055	[429]4096	-	[107]371	[471]5962	[50]119	[49]117	-	-	-	
423	Unissey	FR	unissey	003	2025-01-17	0	1100	[418]4096	-	[94]359	[429]47	[116]318	[114]312	[110]701	[114]1536	[97]2892	$^{327}0.05N^{1.1}$
424	Universidade de Coimbra	PT	visteam	000	2024-07-26	569	46	[299]2048	-	[438]1187	[212]13	[395]3619	[408]4053	[345]7043	[350]15723	[341]28968	$^{127}2.11N^{1.0}$
425	Universidade de Coimbra	PT	visteam	001	2025-05-28	569	46	[319]2048	-	[445]1207	[221]13	[396]3635	[411]4113	-	-	-	
426	VDF Software	CA	vdfsoftware	001	2025-04-25	5949	0	[330]2048	-	[83]339	[314]16	[373]2912	[382]2917	-	-	-	
427	VDF Software	CA	vdfsoftware	002	2025-10-01	5989	5	[365]2052	-	[409]1044	[362]23	-	-	[358]8209	[358]16739	[385]71934	$^{53}5.47N^{1.0}$
428	VNIS Joint Stock	VN	vnis	000	2024-01-05	278	2988	[325]2048	-	[147]435	[186]12	[196]648	[196]633	-	-	-	
429	Veridas Digital Authentication Solutions S.L.	ES	veridas	001	2021-03-05	347	875	[260]2048	-	[199]509	[227]13	[411]4407	[431]5469	[370]10350	[367]20655	[357]41264	$^{86}3.40N^{1.0}$
430	Veridas Digital Authentication Solutions S.L.	ES	veridas	002	2021-07-06	347	870	[279]2048	-	[195]507	[138]10	[157]459	[118]325	[106]685	[101]1365	[92]2730	$^{280}0.09N^{1.1}$
431	Veridas Digital Authentication Solutions S.L.	ES	veridas	003	2021-11-09	346	870	[326]2048	-	[196]508	[103]9	[156]457	[119]327	[108]699	[104]1401	[133]3954	$^{380}0.02N^{1.2}$
432	Veridas Digital Authentication Solutions S.L.	ES	veridas	004	2023-02-03	1074	608	[224]2048	-	[237]579	[253]13	[154]440	[154]426	[94]618	[52]620	[127]3775	$^{69}0.22N^{1.0}$
433	Verigram	KZ	verigram	000	2023-05-17	1553	20	[435]4096	-	[290]681	[445]68	[204]710	[204]688	[111]706	[98]1312	[90]2696	$^{20}16.28N^{0.7}$
434	Verigram	KZ	verigram	001	2023-10-26	1553	20	[453]4104	-	[302]696	[434]51	[242]929	[239]929	[164]1315	[166]2698	[168]5822	$^{36}1.67N^{0.9}$
435	Verijelas	ID	verijelas	000	2022-10-11	248	11	[237]2048	-	[68]310	[264]14	[16]20	[17]26	-	-	-	
436	Viante.AI	AE	viante	000	2023-10-02	1234	19	[392]2056	-	[414]1079	[164]12	[291]1336	[281]1249	[297]3733	[251]5411	[252]10878	$^{313}0.27N^{1.1}$
437	Viante.AI	AE	viante	001	2025-04-18	2541	19	[388]2056	-	[434]1160	[184]12	[268]1072	[257]1008	[232]2151	[229]4443	[230]9382	$^{328}0.16N^{1.1}$
438	Vietnam Payment Solution	VN	vnpay	001	2024-10-15	566	3948	[178]2048	-	[430]1148	[154]12	[192]638	[198]637	[160]1214	[157]2440	[179]6391	$^{310}0.13N^{1.1}$
439	Vietnam Posts and Telecommunications Group	VN	vnpt	001	2022-05-05	361	235	[241]2048	-	[187]491	[350]20	[220]813	[229]867	[188]1626	[190]3346	[184]6808	$^{160}0.43N^{1.0}$
440	Vietnam Posts and Telecommunications Group	VN	vnpt	002	2022-09-08	547	235	[256]2048	-	[264]636	[323]16	[227]857	[233]897	[195]1700	[188]3320	[180]6622	$^{98}0.52N^{1.0}$
441	Vietnam Posts and Telecommunications Group	VN	vnpt	003	2023-06-26	547	235	[345]2048	-	[355]816	[307]16	[237]904	[240]933	[197]1719	[196]3498	[191]6933	$^{96}0.55N^{1.0}$
442	Vietnam Posts and Telecommunications Group	VN	vnpt	004	2023-12-05	1088	351	[199]2048	-	[458]1263	[319]16	[245]941	[234]904	[193]1698	[194]3485	[189]6918	$^{126}0.50N^{1.0}$
443	Vietnam Posts and Telecommunications Group	VN	vnpt	005	2024-11-12	1088	351	[248]2048	-	[439]1189	[310]16	[243]940	[242]939	[192]1697	[191]3404	[186]6845	$^{58}0.69N^{1.0}$
444	Viettel Cyberspace Center	VN	vtcc	000	2023-07-11	277	312	[470]4861	-	[72]315	[376]27	[138]392	[178]537	[139]1012	[127]1753	[118]3437	$^{32}1.28N^{0.9}$
445	Viettel Cyberspace Center	VN	vtcc	001	2023-12-18	515	313	[468]4858	-	[313]710	[379]28	[165]494	[161]459	[138]1010	[142]1967	-	$^{130}0.27N^{1.0}$
446	Viettel Cyberspace Center	VN	vtcc	002	2025-04-14	515	259	[469]4858	-	[315]714	[373]27	[141]397	[176]532	[129]905	[131]1771	[104]3007	$^{27}1.40N^{0.9}$
447	Viettel Group	VN	vts	000	2021-03-12	250	257	[331]2048	-	[153]447	[464]2295	[6]3	[4]4	[3]6	[5]11	-	$^{18}0.61N^{0.6}$
448	Viettel Group	VN	vts	001	2021-07-16	352	600	[259]2048	-	[151]444	[358]21	[350]2081	[371]2487	[319]4644	[315]9313	[315]18713	$^{88}1.53N^{1.0}$
449	Viettel Group	VN	vts	002	2022-02-08	244	600	[312]2048	-	[386]903	[389]29	[363]2485	[370]2485	[321]4678	[317]9370	[317]18833	$^{94}1.49N^{1.0}$
450	Viettel Group	VN	vts	003	2022-07-14	493	468	[318]2048	-	[118]393	[403]34	[362]2482	[351]2075	[305]3894	[302]7883	[304]15891	$^{111}1.18N^{1.0}$
451	Viettel Group	VN	vts	004	2024-09-03	491	887	[216]2048	-	[138]420	[384]29	[349]2073	[352]2075	[307]3925	[303]7883	[299]15770	$^{104}1.19N^{1.0}$
452	Viettel Group	VN	vts	005	2025-01-21	491	887	[288]2048	-	[127]402	[390]29	[348]2070	[350]2071	[306]3917	[304]7893	[303]15828	$^{116}1.16N^{1.0}$
453	Vigilant Solutions	US	vigilant	5	2018-10-30	335	122	[141]1544	k	[335]762	[341]19	-	[324]1720	-	-	-	
454	Vigilant Solutions	US	vigilant	6	2018-10-30	337	122	[142]1544	k	[356]816	[356]21	-	[322]1713	-	-	-	
455	Vigilant Solutions	US	vigilantsolutions	007	2021-01-08	340	51	[143]1544	-	[222]552	[322]16	[311]1570	[292]1352	[267]2911	[266]5966	[257]11466	$^{311}0.27N^{1.1}$
456	Vigilant Solutions	US	vigilantsolutions	008	2021-07-23	340	51	[144]1544	-	[95]360	[248]13	[296]1442	[269]1061	[242]2330	[255]5520	[236]9499	$^{358}0.11N^{1.1}$
457	VinBigData	VN	vinbigdata	001	2024-05-07	1534	268	[441]4096	-	[427]1136	[370]25	[254]990	[293]1384	[203]1810	[238]4715	[225]9281	$^{59}0.91N^{1.0}$
458	VinBigData	VN	vinbigdata	002	2024-10-16	1080	268	[323]2048	-	[450]1222	[158]12	[209]756	[210]721	[170]1369	[167]2745	[155]5514	$^{137}0.38N^{1.0}$
459	VinBigData	VN	vinbigdata	003	2025-02-19	1080	268	[348]2048	-	[433]1157	[222]13	[205]738	[212]731	[169]1366	[184]3199	[177]6303	$^{285}0.20N^{1.1}$
460	VinBigData	VN	vinbigdata	004	2025-07-24	1080	270	[168]2048	-	[437]1179	[251]13	[207]748	[209]717	[171]1377	[180]3024	[201]7726	$^{348}0.09N^{1.1}$
461	Visidon	FI	visidon	1	2018-10-30	166	42	[376]2052	k	[284]667	[298]15	[410]4370	[419]4472	[360]8454	[359]17262	[351]34288	$^{129}2.40N^{1.0}$
462	Visidon	FI	vd	002	2021-05-18	248	42	[2]-	-	[1]-	[105]9	-	[364]2336	-	-	-	
463	Visidon	FI	vd	003	2021-10-12	497	43	[3]-	-	[2]-	[93]8	-	[354]2082	-	-	-	
464	Vision-Box	PT	visionbox	000	2021-09-17	252	274	[393]2059	-	[299]687	[321]16	[173]515	[130]359	[125]855	[53]631	[76]2096	$^{24}2.46N^{0.8}$
465	Vision-Box	PT	visionbox	001	2024-03-19	301	191	[455]4116	-	[64]297	[423]43	[194]640	[197]634	[154]1181	[153]2380	[153]5276	$^{234}0.23N^{1.0}$
466	Vision-Box	PT	visionbox	002	2024-10-31	468	166	[456]4116	-	[121]397	[417]40	[229]872	[230]874	[184]1573	[181]3057	[144]4801	$^{33}1.76N^{0.9}$
467	VisionLabs	RU	visionlabs	6	2018-10-30	360	17	[62]512	1	[58]289	[482]20290	[26]36	[24]36	[17]39	[15]44	[12]53	$^{9}3211.93N^{0.2}$
468	VisionLabs	RU	visionlabs	7	2018-10-30	360	17	[63]512	1	[60]289	[488]34666	[34]63	[32]63	[19]72	[18]80	[16]115	$^{11}2076.32N^{0.2}$

Notes	
1	Configuration size does not capture static data present in libraries. Libraries are included but the size also includes any ancillary libraries for image processing (e.g. openCV) or numerical computation (e.g. blas).
2	Finalization is the processing of converting N = 1600000 templates into a searchable data structure an operation which can be a simple copy, or the building of an index or tree, for example. The duration of the operation may be data dependent, and may not be linear in the number of input templates.
3	This multiplier expresses the increase in template size when k images are passed to the template generation function.
4	All durations are measured on Intel®Xeon®CPU E5-2630 v4 @ 2.20GHz processors. Estimates are made by wrapping the API function call in calls to std::chrono::high_resolution_clock which on the machine in (3) counts 1ns clock ticks. Precision is somewhat worse than that however.
5	Search durations are measured as in the prior note. The power-law model in the final column mostly fits the empirical results in Figure 311. However in certain cases the model is not correct and should not be used numerically.

Table 10: Summary of algorithms and properties included in this report. The blue superscripts give ranking for the quantity in that column. Missing search durations, denoted by "-", are absent because those runs were not executed, usually because we did not run on the larger galleries. Caution: The power-law model is sometimes an incorrect model. It is included here only to show broad sublinear behavior, which is flagged in green. The models should not be used for prediction.

2026/01/09 20:40:38

FNIR(N, R, T) = FPIR(N, T) =

False neg. identification rate
False pos. identification rate

N = Num. enrolled subjects
R = Num. candidates examined

T = Threshold

T = 0 → Investigation
T > 0 → Identification

This publication is available free of charge from: https://doi.org/10.6028/NIST.IR.8271

	DEVELOPER	DEVELOPER	SHORT	SEQ.	VALIDATION	CONFIG[1]	LIB[1]	TEMPLATE GENERATION			FINALIZE[2]	SEARCH DURATION[5] MILLISEC					
	FULL NAME	LOCATION	NAME	NUM.	DATE	DATA (MB)	DATA (MB)	SIZE (B)	MULT[3]	TIME (MS)[4]	TIME (S)	L=1	L=50	L=50	L=50	L=50	POWER LAW
											N=1.6M	N=1.6M	N=1.6M	N=3M	N=6M	N=12M	(μs)
469	VisionLabs	RU	visionlabs	008	2019-06-18	348	17	[59]512	1	[52]272	[479]12747	[19]23	[15]24	[10]26	[7]29	[6]33	[6]$2539.61N^{0.2}$
470	VisionLabs	RU	visionlabs	009	2020-08-04	689	20	[58]512	-	[168]467	[480]13245	[20]23	[18]29	[13]34	[17]61	[17]145	[17]$8.88N^{0.6}$
471	VisionLabs	RU	visionlabs	010	2021-02-05	1042	20	[61]512	-	[252]617	[475]11837	[17]21	[20]32	[14]36	[12]39	[8]43	[7]$3183.79N^{0.2}$
472	VisionLabs	RU	visionlabs	011	2021-10-20	1042	20	[72]512	-	[253]618	[478]12255	[21]23	[14]23	[11]26	[9]34	[11]51	[15]$301.26N^{0.3}$
473	Vixvizon	AU	vixvizion	009	2022-11-28	580	460	[289]2048	-	[201]516	[259]14	[137]389	[123]339	[113]724	[126]1750	[87]2622	[269]$0.11N^{1.1}$
474	Vocord	RU	vocord	5	2018-10-30	1035	185	[97]768	k	[341]780	[79]7	[68]158	[79]204	[62]383	[64]767	[56]1466	[90]$0.12N^{1.0}$
475	Vocord	RU	vocord	6	2018-10-30	1035	185	[491]10240	k	[342]785	[459]243	[70]170	[85]216	-	-	-	
476	WINK	US	wink	000	2023-07-18	507	552	[65]512	-	[12]101	[36]3	[124]360	[131]359	-	-	-	
477	WINK	US	wink	001	2023-12-21	685	552	[54]512	-	[17]144	[35]3	[126]364	[133]363	[104]683	[102]1373	[100]2921	[180]$0.17N^{1.0}$
478	WINK	US	wink	002	2024-10-18	376	552	[70]512	-	[353]811	[34]3	[127]364	[134]363	[105]684	[103]1375	[119]3459	[292]$0.09N^{1.1}$
479	Xforward AI Technology	CN	xforwardai	000	2020-07-24	236	171	[269]2048	-	[332]753	[254]13	[420]4603	[462]7647	[397]15723	[370]23900	[372]53729	[361]$0.56N^{1.1}$
480	Xforward AI Technology	CN	xforwardai	001	2021-01-21	332	50	[196]2048	-	[93]355	[315]16	[409]4338	[416]4384	[365]8798	[363]18553	[365]48993	[371]$0.32N^{1.1}$
481	Xforward AI Technology	CN	xforwardai	002	2021-05-24	691	50	[424]4096	-	[184]490	[337]18	[447]6340	[451]6400	[386]12659	[390]31077	[380]65158	[368]$0.52N^{1.1}$
482	Yuan High-Tech Development	TW	yuan	000	2024-01-23	356	206	[206]2048	-	[131]408	[167]12	[177]522	[174]521	[109]700	[105]1411	[112]3308	[49]$0.38N^{1.0}$
483	i2V Systems Pvt Ltd	IN	i2v	001	2025-04-17	331	249	[228]2048	-	[479]1433	[205]12	[353]2207	[359]2161	[310]4133	[314]9212	[322]19528	[305]$0.46N^{1.1}$
484	ioNetworks Inc	TW	ionetworks	001	2025-05-09	302	99	[322]2048	-	[336]766	[466]2884	[8]6	[10]14	[8]22	[11]39	[14]73	[21]$0.35N^{0.7}$
485	useB	KR	useb	000	2023-05-08	979	482	[270]2048	-	[245]606	[413]38	[445]6280	[445]6158	-	-	-	
486	useB	KR	useb	001	2023-09-12	977	482	[155]2048	-	[216]545	[149]11	[441]6159	[437]5936	[379]12125	[385]28466	[379]62969	[359]$0.58N^{1.1}$
487	useB	KR	useb	002	2024-01-19	977	482	[335]2048	-	[200]513	[150]11	[444]6231	[440]6094	[392]13842	[388]29794	[373]54153	[336]$0.88N^{1.1}$
488	useB	KR	useb	003	2024-08-22	2023	482	[281]2048	-	[455]1248	[204]12	[446]6295	[448]6316	[388]12799	[379]25794	-	[329]$0.94N^{1.1}$
489	useB	KR	useb	004	2024-12-23	2037	443	[210]2048	-	[483]1464	[195]12	[442]6168	[443]6139	[383]12391	[383]27431	-	[343]$0.81N^{1.1}$
490	verihubs-inteligensia	ID	verihubs-inteligensia	000	2022-09-29	204	75	[265]2048	-	[49]260	[275]14	[463]9715	[471]9677	[404]18417	[401]41160	[393]95915	[309]$2.05N^{1.1}$
491	verihubs-inteligensia	ID	verihubs-inteligensia	001	2023-06-27	352	16	[263]2048	-	[174]475	[178]12	[468]11526	[475]11418	-	-	-	

Notes	
1	Configuration size does not capture static data present in libraries. Libraries are included but the size also includes any ancillary libraries for image processing (e.g. openCV) or numerical computation (e.g. blas).
2	Finalization is the processing of converting N = 1600000 templates into a searchable data structure an operation which can be a simple copy, or the building of an index or tree, for example. The duration of the operation may be data dependent, and may not be linear in the number of input templates.
3	This multiplier expresses the increase in template size when k images are passed to the template generation function.
4	All durations are measured on Intel®Xeon®CPU E5-2630 v4 @ 2.20GHz processors. Estimates are made by wrapping the API function call in calls to std::chrono::high_resolution_clock which on the machine in (3) counts 1ns clock ticks. Precision is somewhat worse than that however.
5	Search durations are measured as in the prior note. The power-law model in the final column mostly fits the empirical results in Figure 311. However in certain cases the model is not correct and should not be used numerically.

Table 11: Summary of algorithms and properties included in this report. The blue superscripts give ranking for the quantity in that column. Missing search durations, denoted by "-", are absent because those runs were not executed, usually because we did not run on the larger galleries. Caution: The power-law model is sometimes an incorrect model. It is included here only to show broad sublinear behavior, which is flagged in green. The models should not be used for prediction.

2026/01/09 20:40:38

FNIR(N, R, T) = FPIR(N, T) = False neg. identification rate / False pos. identification rate

N = Num. enrolled subjects
R = Num. candidates examined

T = Threshold

T = 0 → Investigation
T > 0 → Identification

This publication is available free of charge from: https://doi.org/10.6028/NIST.IR.8271

MISS RATES		INVESTIGATION, FNIR(N, R = 1, T = 0)								IDENTIFICATION, FNIR(N, R = L, T $\geq$ 0) FOR FPIR = 0.001							
#	ALGORITHM	(0, 2]	(2, 4]	(4, 6]	(6, 8]	(8, 10]	(10, 12]	(12, 14]	(14, 18]	(0, 2]	(2, 4]	(4, 6]	(6, 8]	(8, 10]	(10, 12]	(12, 14]	(14, 18]
1	3DIVI-005	[98]0.0207	[97]0.0304	[97]0.0415	[97]0.0533	[97]0.0646	[323]0.0735	[323]0.0884	[324]0.1148	[101]0.1580	[98]0.2316	[98]0.3033	[98]0.3740	[98]0.4285	[320]0.4742	[321]0.5329	[318]0.5975
2	ADVANCE-000						[218]0.0087	[221]0.0099	[221]0.0111						[232]0.1275	[231]0.1527	[228]0.1920
3	AFISBIOMETRICS-000						[249]0.0118	[250]0.0146	[256]0.0185						[276]0.2012	[275]0.2397	[276]0.3004
4	AFRENGINE-000						[256]0.0129	[254]0.0150	[258]0.0187						[211]0.0958	[208]0.1152	[207]0.1469
5	AFRENGINE-001						[136]0.0048	[117]0.0050	[130]0.0039						[76]0.0200	[74]0.0233	[76]0.0313
6	AFRENGINE-002						[108]0.0045	[97]0.0048	[136]0.0041						[64]0.0168	[61]0.0192	[65]0.0273
7	AFRENGINE-003						[155]0.0052	[147]0.0056	[165]0.0052						[86]0.0239	[86]0.0286	[87]0.0398
8	AIZE-002						[273]0.0152	[268]0.0174	[260]0.0203						[288]0.2500	[283]0.2854	[281]0.3438
9	AKUVOX-001						[208]0.0079	[215]0.0093	[214]0.0102						[217]0.1009	[213]0.1240	[214]0.1609
10	ALCHERA-006						[128]0.0046	[122]0.0051	[132]0.0040						[143]0.0419	[142]0.0535	[145]0.0737
11	ALCHERA-008						[98]0.0044	[104]0.0049	[109]0.0035						[97]0.0280	[96]0.0348	[97]0.0469
12	ALGORITHMSINC-000						[264]0.0137	[263]0.0164	[263]0.0205						[236]0.1349	[235]0.1654	[237]0.2137
13	ANKE-000	[95]0.0162	[95]0.0245	[95]0.0333	[95]0.0428	[95]0.0515	[321]0.0615	[321]0.0780	[320]0.1028	[96]0.1132	[96]0.1761	[96]0.2402	[96]0.3057	[95]0.3640	[316]0.4200	[316]0.4928	[316]0.5680
14	ANKE-002	[49]0.0055	[50]0.0074	[50]0.0090	[49]0.0103	[48]0.0116	[262]0.0135	[262]0.0162	[259]0.0202	[54]0.0329	[54]0.0560	[56]0.0843	[57]0.1169	[57]0.1481	[269]0.1820	[270]0.2280	[269]0.2831
15	ARATEK-001						[149]0.0050	[143]0.0055	[157]0.0049						[192]0.0686	[193]0.0843	[192]0.1082
16	ARMATURA-000						[76]0.0041	[86]0.0047	[117]0.0037						[113]0.0344	[113]0.0428	[110]0.0555
17	AWARE-005	[106]0.0328	[106]0.0519	[106]0.0712	[104]0.0910	[104]0.1078	[330]0.1235	[330]0.1457	[331]0.1831	[106]0.3605	[107]0.4949	[107]0.5948	[107]0.6783	[108]0.7393	[332]0.7905	[332]0.8408	[333]0.8831
18	AWARE-006	[110]0.0702	[110]0.1110	[110]0.1502	[110]0.1899	[110]0.2253	[339]0.2614	[338]0.3045	[339]0.3659								
19	AWARE-007						[279]0.0162	[274]0.0189	[277]0.0257						[221]0.1053	[215]0.1246	[218]0.1676
20	AYONIX-002	[113]0.3360	[114]0.4389	[114]0.5144	[114]0.5814	[114]0.6340	[343]0.6818	[343]0.7297	[344]0.7774	[110]0.8288	[111]0.9013	[111]0.9375	[111]0.9603	[111]0.9744	[337]0.9837	[337]0.9893	[337]0.9927
21	BIOIDTECHSWISS-001						[126]0.0046	[124]0.0051	[103]0.0034						[118]0.0355	[114]0.0429	[109]0.0548
22	BIOMETRIK-001						[305]0.0281	[303]0.0319	[303]0.0413						[298]0.2812	[294]0.3249	[292]0.3882
23	CAMVI-004	[109]0.0623	[109]0.0944	[109]0.1243	[109]0.1548	[108]0.1812	[336]0.2056	[336]0.2344	[334]0.2672	[91]0.0810	[91]0.1267	[88]0.1721	[88]0.2203	[88]0.2619	[306]0.3040	[305]0.3543	[302]0.4124
24	CAMVI-005	[111]0.0849	[111]0.1255	[111]0.1631	[111]0.1989	[111]0.2298	[338]0.2585	[337]0.2915	[338]0.3246								
25	CANON-001						[156]0.0052	[151]0.0057	[139]0.0042						[159]0.0491	[157]0.0606	[163]0.0826
26	CANON-002						[186]0.0062	[187]0.0070	[189]0.0070						[152]0.0472	[152]0.0582	[158]0.0792
27	CANON-003						[138]0.0049	[137]0.0053	[141]0.0043						[78]0.0209	[79]0.0257	[80]0.0358
28	CIB-000	[14]0.0022	[14]0.0030	[15]0.0037	[15]0.0044	[17]0.0049	[178]0.0057	[183]0.0069	[181]0.0062	[25]0.0139	[26]0.0240	[27]0.0373	[28]0.0525	[28]0.0689	[202]0.0859	[206]0.1109	[206]0.1454
29	CLEARVIEWAI-000	[4]0.0017	[4]0.0023	[4]0.0028	[9]0.0034	[11]0.0039	[122]0.0046	[148]0.0056	[155]0.0047	[16]0.0066	[18]0.0121	[18]0.0194	[19]0.0287	[19]0.0385	[161]0.0493	[175]0.0662	[174]0.0873
30	CLEARVIEWAI-001						[105]0.0044	[91]0.0047	[93]0.0032						[130]0.0389	[131]0.0497	[133]0.0676
31	CLEARVIEWAI-002						[101]0.0044	[95]0.0048	[110]0.0036						[147]0.0438	[148]0.0566	[154]0.0778
32	CLEARVIEWAI-003						[72]0.0041	[51]0.0042	[65]0.0024						[84]0.0224	[85]0.0285	[84]0.0370
33	CLOUDWALK-HR-000	[8]0.0019	[7]0.0024	[8]0.0029	[6]0.0032	[5]0.0032	[29]0.0036	[48]0.0041	[41]0.0020	[1]0.0029	[1]0.0041	[1]0.0054	[1]0.0064	[2]0.0073	[23]0.0085	[23]0.0102	[23]0.0112
34	CLOUDWALK-MT-000						[44]0.0037	[19]0.0038	[14]0.0013						[16]0.0065	[15]0.0072	[15]0.0075
35	CLOUDWALK-MT-001						[36]0.0037	[13]0.0037	[12]0.0012						[13]0.0045	[9]0.0051	[8]0.0042
36	CLOUDWALK-MT-002						[35]0.0036	[15]0.0038	[11]0.0012						[7]0.0042	[7]0.0048	[7]0.0034
37	COGENT-000	[91]0.0128	[90]0.0184	[93]0.0250	[92]0.0327	[93]0.0407	[315]0.0488	[315]0.0611	[313]0.0794	[77]0.0559	[78]0.0923	[77]0.1342	[77]0.1812	[76]0.2243	[293]0.2675	[292]0.3240	[298]0.3992
38	COGENT-001	[90]0.0128	[91]0.0184	[92]0.0250	[93]0.0327	[92]0.0407	[316]0.0488	[314]0.0611	[314]0.0794	[78]0.0559	[79]0.0923	[76]0.1342	[76]0.1812	[75]0.2243	[292]0.2675	[291]0.3240	[295]0.3992
39	COGENT-002	[69]0.0081	[66]0.0105	[63]0.0123	[64]0.0137	[62]0.0157	[281]0.0175	[279]0.0215	[280]0.0280	[69]0.0499	[68]0.0827	[67]0.1207	[67]0.1639	[67]0.2037	[283]0.2432	[285]0.2972	[286]0.3638
40	COGENT-003	[71]0.0082	[67]0.0108	[65]0.0128	[67]0.0145	[66]0.0168	[289]0.0191	[290]0.0239	[287]0.0312	[80]0.0582	[80]0.0971	[80]0.1417	[80]0.1918	[80]0.2380	[301]0.2836	[303]0.3440	[305]0.4207
41	COGENT-004	[59]0.0066	[53]0.0080	[45]0.0085	[39]0.0080	[31]0.0083	[229]0.0092	[228]0.0106	[234]0.0130	[63]0.0410	[65]0.0720	[65]0.1099	[65]0.1539	[64]0.1974	[284]0.2443	[288]0.3043	[288]0.3757
42	COGENT-006						[113]0.0045	[114]0.0049	[127]0.0038						[127]0.0370	[121]0.0448	[121]0.0602
43	COGENT-007						[103]0.0044	[105]0.0049	[111]0.0036						[110]0.0332	[110]0.0415	[114]0.0566
44	COGNITEC-000	[105]0.0265	[103]0.0423	[103]0.0588	[103]0.0757	[102]0.0894	[328]0.1014	[328]0.1169	[327]0.1381	[100]0.1522	[99]0.2330	[99]0.3051	[99]0.3751	[99]0.4300	[321]0.4779	[320]0.5307	[317]0.5913

Table 12: **Accuracy for the FRVT 2018 mugshot sets under ageing**. *The second row shows the time lapse between gallery and subsequent probe images, in years. The first two columns identify the algorithm The next 8 values give rank-based FNIR with R = 1, T = 0 and FPIR = 1. All these are relevant to investigational uses where candidates from all searches would need human review. The second 8 values give threshold-based FNIR with T $\geq$ 0, FPIR = 0.001 and no rank criterion. The shaded cells indictate indicate the three most accurate algorithms for that elapsed time. The gallery size is 3068801. The total number of searches is 10951064.*

2026/01/09 20:40:38

FNIR(N, R, T) = False neg. identification rate
FPIR(N, T) = False pos. identification rate

N = Num. enrolled subjects
R = Num. candidates examined

T = Threshold

T = 0 → Investigation
T > 0 → Identification

This publication is available free of charge from: https://doi.org/10.6028/NIST.IR.8271

MISS RATES		INVESTIGATION, FNIR(N, R = 1, T = 0)								IDENTIFICATION, FNIR(N, R = L, T $\geq$ 0) FOR FPIR = 0.001							
#	ALGORITHM	(0, 2]	(2, 4]	(4, 6]	(6, 8]	(8, 10]	(10, 12]	(12, 14]	(14, 18]	(0, 2]	(2, 4]	(4, 6]	(6, 8]	(8, 10]	(10, 12]	(12, 14]	(14, 18]
45	COGNITEC-001	93 0.0149	94 0.0228	94 0.0312	94 0.0399	94 0.0479	318 0.0546	317 0.0656	315 0.0806	93 0.0963	93 0.1562	93 0.2157	93 0.2771	93 0.3287	314 0.3771	313 0.4343	312 0.4959
46	COGNITEC-002	77 0.0101	80 0.0138	81 0.0170	81 0.0201	81 0.0237	303 0.0264	300 0.0309	299 0.0389	72 0.0517	71 0.0879	72 0.1269	73 0.1707	71 0.2098	285 0.2463	284 0.2919	284 0.3535
47	COGNITEC-003	78 0.0104	81 0.0140	82 0.0174	82 0.0205	82 0.0238	304 0.0266	301 0.0311	301 0.0401	71 0.0504	70 0.0855	69 0.1235	69 0.1662	68 0.2045	282 0.2403	282 0.2854	282 0.3451
48	COGNITEC-004	64 0.0073	63 0.0099	62 0.0118	59 0.0130	59 0.0147	280 0.0163	275 0.0189	274 0.0239	53 0.0325	53 0.0548	52 0.0798	51 0.1074	50 0.1325	257 0.1591	254 0.1952	253 0.2414
49	COGNITEC-006						211 0.0081	207 0.0086	208 0.0090						197 0.0777	197 0.0926	197 0.1274
50	COGNITEC-007						193 0.0066	191 0.0072	183 0.0066						168 0.0507	163 0.0616	164 0.0826
51	COGNITEC-008						199 0.0067	193 0.0074	192 0.0071						169 0.0508	159 0.0607	167 0.0836
52	COGNITEC-009						203 0.0069	195 0.0075	194 0.0073						170 0.0510	160 0.0609	169 0.0838
53	COMPAL-000						340 0.3198	339 0.3198	337 0.3206						311 0.3559	307 0.3655	291 0.3844
54	CORSIGHT-000						152 0.0051	152 0.0057	142 0.0043						172 0.0523	170 0.0641	165 0.0829
55	CORSIGHT-001						140 0.0049	136 0.0053	146 0.0044						179 0.0556	179 0.0688	177 0.0893
56	CUBOX-000	7 0.0019	5 0.0024	5 0.0028	4 0.0031	4 0.0032	37 0.0037	72 0.0044	72 0.0027	6 0.0039	6 0.0059	7 0.0083	8 0.0111	8 0.0141	73 0.0185	77 0.0252	76 0.0339
57	CUBOX-001						65 0.0040	62 0.0044	76 0.0028						83 0.0223	83 0.0276	82 0.0361
58	CUBOX-002						60 0.0039	69 0.0044	101 0.0033						85 0.0237	87 0.0293	86 0.0396
59	CUBOX-003						86 0.0043	94 0.0048	137 0.0041						91 0.0254	88 0.0317	89 0.0422
60	CYBERLINK-002	50 0.0055	45 0.0068	41 0.0075	35 0.0078	32 0.0084	231 0.0094	231 0.0107	224 0.0114	32 0.0180	33 0.0302	33 0.0460	32 0.0643	33 0.0837	222 0.1058	222 0.1370	223 0.1787
61	CYBERLINK-003	35 0.0041	34 0.0052	27 0.0057	25 0.0058	25 0.0061	200 0.0068	200 0.0078	203 0.0078	19 0.0109	19 0.0175	20 0.0259	21 0.0356	21 0.0468	181 0.0594	186 0.0787	190 0.1072
62	CYBERLINK-006						69 0.0040	63 0.0043	57 0.0023						74 0.0188	71 0.0219	70 0.0291
63	DAHUA-002	30 0.0035	28 0.0047	28 0.0058	27 0.0067	28 0.0074	212 0.0082	222 0.0100	218 0.0108	30 0.0169	32 0.0294	31 0.0449	30 0.0635	30 0.0817	218 0.1013	218 0.1291	216 0.1638
64	DAHUA-003	19 0.0026	19 0.0036	19 0.0043	20 0.0050	20 0.0055	185 0.0062	203 0.0080	196 0.0073	29 0.0160	30 0.0280	29 0.0432	29 0.0615	29 0.0794	215 0.0987	217 0.1270	213 0.1587
65	DAON-002						190 0.0064	198 0.0077	199 0.0076						195 0.0693	195 0.0889	195 0.1147
66	DATECH-001						158 0.0052	163 0.0059	162 0.0050						188 0.0641	187 0.0794	185 0.1011
67	DEEPGLINT-001	17 0.0024	16 0.0032	14 0.0037	13 0.0040	13 0.0043	142 0.0049	167 0.0060	167 0.0052	12 0.0058	10 0.0087	11 0.0119	11 0.0155	11 0.0199	89 0.0249	91 0.0338	95 0.0463
68	DEEPSEA-001	70 0.0081	70 0.0116	73 0.0149	76 0.0182	76 0.0216	301 0.0260	305 0.0332	305 0.0432	66 0.0458	66 0.0752	64 0.1086	63 0.1460	63 0.1812	278 0.2186	278 0.2663	277 0.3213
69	DERMALOG-006	82 0.0113	82 0.0142	78 0.0163	77 0.0183	74 0.0200	294 0.0218	292 0.0251	290 0.0329	75 0.0545	73 0.0889	73 0.1271	72 0.1697	70 0.2090	287 0.2498	287 0.3028	287 0.3670
70	DERMALOG-007	88 0.0125	88 0.0170	88 0.0214	88 0.0264	87 0.0309	310 0.0356	311 0.0432	311 0.0579	92 0.0910	92 0.1453	92 0.2009	92 0.2602	92 0.3134	313 0.3649	312 0.4289	313 0.5007
71	DERMALOG-008	52 0.0057	52 0.0077	54 0.0095	54 0.0110	53 0.0128	271 0.0148	271 0.0180	272 0.0223	70 0.0501	69 0.0850	70 0.1247	71 0.1692	72 0.2105	289 0.2541	289 0.3102	289 0.3762
72	DERMALOG-010						174 0.0056	162 0.0059	140 0.0043						171 0.0519	171 0.0643	171 0.0843
73	DERMALOG-011						222 0.0089	232 0.0107	232 0.0128						252 0.1543	248 0.1833	249 0.2314
74	DERMALOG-012						226 0.0090	230 0.0107	236 0.0133						249 0.1497	244 0.1783	243 0.2238
75	DERMALOG-013						224 0.0089	229 0.0106	235 0.0132						251 0.1516	245 0.1803	245 0.2264
76	DERMALOG-014						296 0.0232	296 0.0279	296 0.0358						253 0.1544	247 0.1833	247 0.2295
77	DERMALOG-015						130 0.0047	103 0.0049	118 0.0037						132 0.0392	127 0.0481	125 0.0634
78	DILUSENSE-000						251 0.0123	249 0.0146	254 0.0180						268 0.1814	264 0.2149	261 0.2644
79	DILUSENSE-001						191 0.0065	182 0.0069	187 0.0069						186 0.0632	184 0.0778	184 0.1006
80	EINETWORKSINDIA-000						228 0.0091	227 0.0105	225 0.0115						227 0.1139	223 0.1413	222 0.1785
81	EINETWORKSINDIA-001						227 0.0090	223 0.0103	223 0.0113						230 0.1196	228 0.1476	226 0.1889
82	EINETWORKSINDIA-002						112 0.0045	118 0.0050	99 0.0033						123 0.0361	123 0.0463	124 0.0634
83	FACEPHI-000						168 0.0054	159 0.0059	163 0.0050						151 0.0468	149 0.0575	149 0.0748
84	FIRSTCREDITKZ-001						176 0.0057	177 0.0066	173 0.0055						88 0.0240	84 0.0284	83 0.0368
85	FUJITSULAB-001						225 0.0089	219 0.0098	220 0.0111						241 0.1403	240 0.1723	238 0.2165
86	GORILLA-002	100 0.0213	100 0.0359	101 0.0528	102 0.0716	103 0.0895	329 0.1088	329 0.1367	329 0.1765	103 0.1828	104 0.2787	104 0.3654	104 0.4485	104 0.5168	325 0.5823	325 0.6508	325 0.7180
87	GORILLA-005	38 0.0044	47 0.0070	58 0.0102	62 0.0136	67 0.0170	292 0.0204	295 0.0272	298 0.0373	79 0.0566	81 0.0973	82 0.1432	81 0.1937	81 0.2398	303 0.2862	302 0.3437	303 0.4150
88	GORILLA-007						244 0.0108	240 0.0128	237 0.0145						271 0.1862	269 0.2198	265 0.2716

Table 13: **Accuracy for the FRVT 2018 mugshot sets under ageing**. *The second row shows the time lapse between gallery and subsequent probe images, in years. The first two columns identify the algorithm The next 8 values give rank-based FNIR with R = 1, T = 0 and FPIR = 1. All these are relevant to investigational uses where candidates from all searches would need human review. The second 8 values give threshold-based FNIR with T $\geq$ 0, FPIR = 0.001 and no rank criterion. The shaded cells indictate indicate the three most accurate algorithms for that elapsed time. The gallery size is 3068801. The total number of searches is 10951064.*

2026/01/09 20:40:38

FNIR(N, R, T) = False neg. identification rate
FPIR(N, T) = False pos. identification rate

N = Num. enrolled subjects
R = Num. candidates examined

T = Threshold

T = 0 → Investigation
T > 0 → Identification

This publication is available free of charge from: https://doi.org/10.6028/NIST.IR.8271

MISS RATES		INVESTIGATION, FNIR(N, R = 1, T = 0)								IDENTIFICATION, FNIR(N, R = L, T $\geq$ 0) FOR FPIR = 0.001							
#	ALGORITHM	(0, 2]	(2, 4]	(4, 6]	(6, 8]	(8, 10]	(10, 12]	(12, 14]	(14, 18]	(0, 2]	(2, 4]	(4, 6]	(6, 8]	(8, 10]	(10, 12]	(12, 14]	(14, 18]
89	GORILLA-008						206 0.0071	204 0.0081	207 0.0089						255 0.1557	250 0.1847	251 0.2340
90	GRIAULE-001						120 0.0046	116 0.0050	123 0.0038						135 0.0402	130 0.0487	126 0.0636
91	HISIGN-001						188 0.0063	186 0.0070	188 0.0070						184 0.0613	183 0.0754	182 0.0969
92	HYPERVERGE-003						161 0.0053	159 0.0058	180 0.0059						194 0.0689	190 0.0826	191 0.1081
93	HYUNDAI-ROBOTICSLAB-000						223 0.0089	220 0.0099	227 0.0119						205 0.0872	202 0.1082	202 0.1405
94	HYUNDAI-ROBOTICSLAB-001						214 0.0084	213 0.0092	216 0.0104						207 0.0928	207 0.1151	208 0.1482
95	HYUNDAI-ROBOTICSLAB-002						117 0.0045	100 0.0048	105 0.0034						154 0.0481	156 0.0598	155 0.0784
96	HZAILU-001						179 0.0058	160 0.0059	160 0.0049						173 0.0524	168 0.0630	157 0.0791
97	HZAILU-002						180 0.0058	176 0.0064	166 0.0052						158 0.0488	154 0.0597	144 0.0728
98	HZAILU-003						189 0.0063	188 0.0071	185 0.0067						189 0.0668	194 0.0850	193 0.1136
99	HZAILU-004						148 0.0050	144 0.0055	158 0.0049						166 0.0503	172 0.0655	179 0.0902
100	I2V-001						201 0.0068	189 0.0071	186 0.0069						319 0.4618	318 0.5191	319 0.6022
101	ICM-001						250 0.0122	246 0.0138	246 0.0164						279 0.1997	274 0.2375	272 0.2940
102	IDEMIA-003	81 0.0110	86 0.0151	86 0.0196	85 0.0238	84 0.0281	308 0.0313	308 0.0368	307 0.0504	87 0.0717	86 0.1147	86 0.1614	86 0.2113	85 0.2553	305 0.2976	304 0.3537	306 0.4334
103	IDEMIA-004	80 0.0107	84 0.0148	85 0.0192	84 0.0233	83 0.0277	307 0.0312	307 0.0367	308 0.0512	58 0.0373	55 0.0587	54 0.0833	53 0.1100	52 0.1340	256 0.1580	253 0.1911	255 0.2482
104	IDEMIA-005	84 0.0118	87 0.0167	90 0.0218	89 0.0270	88 0.0317	311 0.0357	310 0.0425	310 0.0579	65 0.0440	64 0.0689	60 0.0964	59 0.1254	58 0.1513	266 0.1762	261 0.2113	263 0.2698
105	IDEMIA-006	87 0.0124	89 0.0171	89 0.0218	89 0.0263	86 0.0302	309 0.0321	306 0.0356	306 0.0471	62 0.0409	59 0.0620	57 0.0850	52 0.1097	49 0.1309	245 0.1486	242 0.1738	242 0.2200
106	IDEMIA-007	47 0.0050	48 0.0071	48 0.0089	50 0.0106	51 0.0124	266 0.0142	267 0.0171	270 0.0220	36 0.0202	36 0.0335	34 0.0491	33 0.0663	31 0.0825	216 0.0999	214 0.1240	217 0.1645
107	IDEMIA-008	5 0.0018	6 0.0024	6 0.0029	5 0.0032	7 0.0035	55 0.0039	83 0.0046	97 0.0033	3 0.0034	3 0.0051	5 0.0069	5 0.0087	5 0.0102	48 0.0123	44 0.0146	45 0.0186
108	IDEMIA-009						66 0.0040	52 0.0042	61 0.0024						24 0.0094	24 0.0103	24 0.0123
109	IDEMIA-010						11 0.0034	9 0.0036	9 0.0011						12 0.0045	12 0.0052	11 0.0043
110	IDEMIA-011						8 0.0033	5 0.0035	8 0.0011						8 0.0043	10 0.0051	12 0.0044
111	IDEMIA-012						10 0.0033	4 0.0034	7 0.0011						10 0.0043	8 0.0049	13 0.0048
112	IMAGUS-005	33 0.0039	33 0.0052	31 0.0061	29 0.0067	30 0.0077	221 0.0088	224 0.0103	219 0.0109	39 0.0212	39 0.0357	40 0.0539	40 0.0755	38 0.0967	229 0.1183	229 0.1485	227 0.1893
113	IMAGUS-008						333 0.1625	331 0.1704	330 0.1823								
114	IMDS-SOFTWARE-001						159 0.0052	166 0.0060	164 0.0050						180 0.0569	180 0.0693	180 0.0903
115	IMDS-SOFTWARE-002						166 0.0054	161 0.0059	159 0.0049						177 0.0541	174 0.0661	170 0.0838
116	IMPERIAL-000	34 0.0040	35 0.0054	36 0.0067	38 0.0079	40 0.0093	245 0.0112	247 0.0139	251 0.0178	49 0.0286	51 0.0503	51 0.0779	54 0.1116	56 0.1455	270 0.1844	273 0.2341	273 0.2951
117	INCODE-003	94 0.0155	96 0.0247	96 0.0348	96 0.0463	96 0.0571	322 0.0674	322 0.0856	323 0.1114	102 0.1627	102 0.2507	102 0.3322	100 0.4122	100 0.4772	324 0.5368	324 0.6059	324 0.6766
118	INCODE-004	56 0.0061	59 0.0087	59 0.0110	61 0.0136	64 0.0161	284 0.0185	288 0.0236	286 0.0309	73 0.0532	74 0.0908	75 0.1334	75 0.1809	77 0.2245	294 0.2675	295 0.3249	295 0.3932
119	INCODE-006						56 0.0039	77 0.0045	77 0.0028						61 0.0160	68 0.0212	74 0.0298
120	INCODE-007						41 0.0037	44 0.0041	50 0.0021						40 0.0114	51 0.0155	57 0.0229
121	INNOVATRICS-004	114 0.3594	113 0.3629	113 0.3688	112 0.3754	112 0.3813	341 0.3870	341 0.3960	341 0.4135	107 0.4234	106 0.4642	106 0.5073	106 0.5522	105 0.5902	328 0.6274	326 0.6736	326 0.7253
122	INNOVATRICS-005	41 0.0046	41 0.0063	42 0.0078	45 0.0092	45 0.0106	252 0.0124	253 0.0149	252 0.0178	55 0.0343	56 0.0590	58 0.0886	58 0.1222	59 0.1544	273 0.1881	272 0.2321	270 0.2874
123	INNOVATRICS-008						132 0.0047	107 0.0049	88 0.0031						104 0.0309	97 0.0353	94 0.0463
124	INNOVATRICS-009						90 0.0043	74 0.0044	71 0.0027						58 0.0154	56 0.0170	52 0.0214
125	INNOVATRICS-010						91 0.0043	79 0.0045	81 0.0030						63 0.0167	60 0.0192	63 0.0265
126	INNOVATRICS-011						79 0.0042	73 0.0044	59 0.0023						38 0.0109	27 0.0122	28 0.0153
127	INNOVATRICS-012						64 0.0040	55 0.0042	58 0.0023						27 0.0099	25 0.0110	25 0.0138
128	INNOVATRICS-013						34 0.0036	33 0.0040	24 0.0017						29 0.0100	26 0.0116	27 0.0142
129	INNOVATRICS-014						13 0.0034	12 0.0037	13 0.0013						14 0.0055	14 0.0059	14 0.0061
130	INSPUR-000						137 0.0048	135 0.0053	129 0.0039						176 0.0539	176 0.0665	173 0.0865
131	INSPUR-001						121 0.0046	119 0.0050	112 0.0036						153 0.0478	153 0.0588	152 0.0763
132	INSPUR-002						95 0.0043	96 0.0048	89 0.0031						160 0.0493	165 0.0619	161 0.0820

Table 14: **Accuracy for the FRVT 2018 mugshot sets under ageing**. *The second row shows the time lapse between gallery and subsequent probe images, in years. The first two columns identify the algorithm The next 8 values give rank-based FNIR with R = 1, T = 0 and FPIR = 1. All these are relevant to investigational uses where candidates from all searches would need human review. The second 8 values give threshold-based FNIR with T $\geq$ 0, FPIR = 0.001 and no rank criterion. The shaded cells indictate indicate the three most accurate algorithms for that elapsed time. The gallery size is 3068801. The total number of searches is 10951064.*

FNIR(N, R, T) = False neg. identification rate
FPIR(N, T) = False pos. identification rate
N = Num. enrolled subjects
R = Num. candidates examined
T = Threshold
T = 0 → Investigation
T > 0 → Identification

This publication is available free of charge from: https://doi.org/10.6028/NIST.IR.8271

MISS RATES		INVESTIGATION, FNIR(N, R = 1, T = 0)								IDENTIFICATION, FNIR(N, R = L, T $\geq$ 0) FOR FPIR = 0.001							
#	ALGORITHM	(0, 2]	(2, 4]	(4, 6]	(6, 8]	(8, 10]	(10, 12]	(12, 14]	(14, 18]	(0, 2]	(2, 4]	(4, 6]	(6, 8]	(8, 10]	(10, 12]	(12, 14]	(14, 18]
133	INTELLIVISION-002						[319]0.0577	[318]0.0694	[317]0.0881								
134	INTELRESEARCH-001						[73]0.0041	[65]0.0043	[63]0.0024						[53]0.0132	[46]0.0149	[42]0.0181
135	INTEMA-000						[67]0.0040	[59]0.0043	[66]0.0024						[75]0.0193	[75]0.0235	[73]0.0294
136	INTEMA-001						[62]0.0039	[37]0.0040	[39]0.0020						[60]0.0157	[62]0.0194	[61]0.0246
137	IONETWORKS-001						[302]0.0261	[302]0.0313	[302]0.0404						[225]0.1113	[221]0.1349	[221]0.1723
138	IREX-000	[24]0.0031	[24]0.0042	[25]0.0051	[26]0.0060	[26]0.0068	[209]0.0080	[217]0.0095	[217]0.0107	[52]0.0313	[52]0.0539	[53]0.0815	[56]0.1137	[55]0.1442	[265]0.1755	[268]0.2181	[266]0.2718
139	ISYSTEMS-002	[76]0.0101	[79]0.0135	[80]0.0169	[79]0.0197	[80]0.0228	[299]0.0256	[299]0.0304	[300]0.0398	[90]0.0779	[90]0.1258	[91]0.1759	[90]0.2299	[90]0.2758	[309]0.3204	[310]0.3763	[308]0.4401
140	ISYSTEMS-003	[75]0.0089	[69]0.0115	[69]0.0139	[69]0.0158	[70]0.0177	[291]0.0198	[287]0.0234	[284]0.0303	[84]0.0647	[84]0.1056	[84]0.1502	[84]0.1986	[83]0.2402	[299]0.2819	[298]0.3351	[297]0.3976
141	KAKAO-001						[59]0.0039	[60]0.0043	[53]0.0022						[70]0.0182	[72]0.0220	[71]0.0291
142	KAKAO-002						[39]0.0037	[28]0.0039	[30]0.0018						[43]0.0119	[39]0.0141	[39]0.0174
143	KEDACOM-001	[83]0.0116	[75]0.0130	[67]0.0135	[60]0.0133	[57]0.0135	[265]0.0141	[255]0.0151	[250]0.0176	[41]0.0241	[41]0.0360	[39]0.0513	[34]0.0689	[34]0.0866	[223]0.1060	[219]0.1327	[219]0.1694
144	KLOUDSPOT-001						[246]0.0113	[241]0.0130	[239]0.0148						[264]0.1730	[260]0.2071	[257]0.2534
145	KNOWUTECH-000						[183]0.0061	[190]0.0072	[190]0.0070						[199]0.0805	[198]0.0995	[199]0.1329
146	KOGNIZA-000						[134]0.0048	[139]0.0053	[149]0.0045						[157]0.0486	[162]0.0615	[153]0.0776
147	LIGHTVISION-000						[263]0.0136	[261]0.0158	[261]0.0204						[259]0.1646	[255]0.1959	[254]0.2422
148	LINECLOVA-002						[116]0.0045	[106]0.0049	[80]0.0030						[103]0.0307	[101]0.0374	[99]0.0497
149	LINECLOVA-003						[97]0.0044	[98]0.0048	[84]0.0030						[119]0.0356	[119]0.0443	[117]0.0586
150	LOOKMAN-003	[86]0.0123	[83]0.0144	[77]0.0158	[70]0.0168	[71]0.0178	[286]0.0188	[278]0.0212	[278]0.0260	[64]0.0438	[62]0.0687	[61]0.0978	[61]0.1296	[60]0.1581	[272]0.1879	[271]0.2294	[268]0.2756
151	LOOKMAN-005	[85]0.0118	[77]0.0134	[70]0.0142	[66]0.0144	[61]0.0150	[277]0.0160	[269]0.0176	[267]0.0213	[51]0.0310	[49]0.0480	[46]0.0698	[46]0.0954	[46]0.1216	[247]0.1491	[252]0.1890	[252]0.2381
152	LUXAND-001						[267]0.0144	[265]0.0166	[265]0.0207						[297]0.2802	[293]0.3247	[294]0.3916
153	MAXVISION-000						[255]0.0128	[252]0.0146	[249]0.0169						[262]0.1706	[257]0.2023	[258]0.2550
154	MAXVISION-001						[124]0.0046	[110]0.0049	[100]0.0033						[116]0.0351	[116]0.0435	[115]0.0581
155	MAXVISION-002						[129]0.0047	[109]0.0049	[85]0.0030						[106]0.0318	[104]0.0385	[100]0.0500
156	MAXVISION-003						[131]0.0047	[133]0.0052	[125]0.0038						[156]0.0485	[158]0.0606	[160]0.0812
157	MAXVISION-004						[52]0.0038	[54]0.0042	[42]0.0020						[71]0.0182	[70]0.0217	[72]0.0293
158	MEGVII-003						[151]0.0051	[168]0.0060	[168]0.0052						[94]0.0277	[102]0.0376	[105]0.0520
159	MEGVII-004						[33]0.0036	[38]0.0040	[34]0.0018						[15]0.0062	[17]0.0078	[17]0.0084
160	MEGVII-005						[32]0.0036	[39]0.0040	[35]0.0018						[18]0.0067	[19]0.0084	[18]0.0094
161	METSAKUURCOMPANY-000						[171]0.0055	[174]0.0062	[177]0.0057						[185]0.0632	[188]0.0795	[188]0.1043
162	METSAKUURCOMPANY-001						[182]0.0063	[181]0.0069	[184]0.0067						[200]0.0821	[200]0.1024	[201]0.1363
163	MICROFOCUS-005	[115]0.4269	[115]0.5527	[115]0.6355	[116]0.7024	[116]0.7503	[345]0.7876	[345]0.8234	[346]0.8601	[111]0.8338	[112]0.9113	[112]0.9468	[112]0.9667	[112]0.9771	[336]0.9836	[336]0.9880	[336]0.9924
164	MICROSOFT-003	[28]0.0034	[32]0.0050	[33]0.0064	[36]0.0078	[38]0.0092	[241]0.0107	[245]0.0135	[247]0.0166	[50]0.0288	[50]0.0503	[50]0.0763	[50]0.1067	[54]0.1359	[260]0.1680	[263]0.2116	[262]0.2644
165	MICROSOFT-004	[25]0.0032	[27]0.0047	[29]0.0060	[32]0.0075	[35]0.0087	[236]0.0103	[242]0.0131	[244]0.0159	[47]0.0268	[48]0.0470	[49]0.0716	[48]0.1007	[48]0.1291	[258]0.1610	[259]0.2052	[259]0.2590
166	MICROSOFT-005	[22]0.0031	[29]0.0047	[35]0.0066	[43]0.0084	[43]0.0103	[259]0.0131	[264]0.0164	[255]0.0185	[43]0.0243	[44]0.0432	[44]0.0658	[44]0.0913	[45]0.1172	[244]0.1476	[251]0.1874	[246]0.2272
167	MICROSOFT-006	[26]0.0032	[31]0.0049	[34]0.0065	[42]0.0081	[42]0.0096	[248]0.0117	[248]0.0144	[245]0.0160	[24]0.0134	[24]0.0233	[25]0.0346	[23]0.0462	[22]0.0578	[196]0.0713	[196]0.0903	[196]0.1156
168	MOBBL-000						[247]0.0116	[243]0.0132	[243]0.0156						[263]0.1709	[256]0.2020	[256]0.2507
169	MUKH-002						[331]0.1394	[332]0.1754	[332]0.2335						[335]0.9761	[335]0.9840	[335]0.9899
170	NEC-000	[97]0.0195	[99]0.0316	[99]0.0445	[99]0.0581	[98]0.0699	[325]0.0817	[325]0.0998	[325]0.1237	[89]0.0759	[89]0.1245	[89]0.1729	[89]0.2240	[89]0.2671	[308]0.3117	[306]0.3639	[307]0.4348
171	NEC-001	[104]0.0246	[102]0.0382	[100]0.0524	[100]0.0672	[101]0.0793	[327]0.0904	[326]0.1076	[326]0.1317	[94]0.1019	[94]0.1623	[94]0.2214	[94]0.2834	[94]0.3341	[315]0.3844	[315]0.4440	[314]0.5183
172	NEC-002	[27]0.0033	[22]0.0041	[18]0.0043	[16]0.0044	[15]0.0045	[141]0.0049	[146]0.0056	[138]0.0041	[15]0.0066	[11]0.0090	[10]0.0111	[10]0.0131	[9]0.0149	[65]0.0171	[65]0.0207	[64]0.0267
173	NEC-003	[31]0.0036	[26]0.0046	[24]0.0051	[24]0.0055	[24]0.0059	[194]0.0067	[197]0.0077	[198]0.0073	[9]0.0056	[9]0.0076	[9]0.0091	[7]0.0105	[6]0.0119	[55]0.0137	[53]0.0162	[51]0.0209
174	NEC-004	[32]0.0039	[25]0.0045	[22]0.0047	[18]0.0046	[14]0.0044	[127]0.0046	[134]0.0052	[115]0.0036	[7]0.0046	[5]0.0057	[2]0.0063	[2]0.0066	[1]0.0069	[21]0.0076	[21]0.0090	[21]0.0105
175	NEC-005						[47]0.0037	[43]0.0041	[43]0.0020						[22]0.0080	[22]0.0091	[22]0.0107
176	NEC-006						[58]0.0039	[56]0.0042	[49]0.0021						[6]0.0030	[6]0.0033	[6]0.0012

Table 15: **Accuracy for the FRVT 2018 mugshot sets under ageing**. *The second row shows the time lapse between gallery and subsequent probe images, in years. The first two columns identify the algorithm The next 8 values give rank-based FNIR with R = 1, T = 0 and FPIR = 1. All these are relevant to investigational uses where candidates from all searches would need human review. The second 8 values give threshold-based FNIR with T $\geq$ 0, FPIR = 0.001 and no rank criterion. The shaded cells indictate indicate the three most accurate algorithms for that elapsed time. The gallery size is 3068801. The total number of searches is 10951064.*

2026/01/09 20:40:38

FNIR(N, R, T) = False neg. identification rate
FPIR(N, T) = False pos. identification rate
N = Num. enrolled subjects
R = Num. candidates examined
T = Threshold
T = 0 → Investigation
T > 0 → Identification

This publication is available free of charge from: https://doi.org/10.6028/NIST.IR.8271

MISS RATES		INVESTIGATION, FNIR(N, R = 1, T = 0)								IDENTIFICATION, FNIR(N, R = L, T $\geq$ 0) FOR FPIR = 0.001							
#	ALGORITHM	(0, 2]	(2, 4]	(4, 6]	(6, 8]	(8, 10]	(10, 12]	(12, 14]	(14, 18]	(0, 2]	(2, 4]	(4, 6]	(6, 8]	(8, 10]	(10, 12]	(12, 14]	(14, 18]
177	NEC-007						[12]0.0034	[11]0.0036	[18]0.0016						[4]0.0027	[4]0.0031	[4]0.0010
178	NEC-008						[38]0.0037	[23]0.0038	[28]0.0018						[5]0.0030	[5]0.0033	[5]0.0012
179	NEC-009						[3]0.0032	[3]0.0034	[3]0.0010						[3]0.0027	[2]0.0030	[2]0.0007
180	NEC-010						[2]0.0031	[1]0.0034	[5]0.0010						[2]0.0027	[1]0.0030	[3]0.0007
181	NEC-011						[1]0.0031	[2]0.0034	[2]0.0009						[1]0.0027	[3]0.0030	[1]0.0007
182	NEUROTECHNOLOGY-003	[101]0.0234	[101]0.0379	[102]0.0549	[101]0.0682	[100]0.0720	[324]0.0747	[324]0.0886	[322]0.1066	[109]0.6802	[109]0.8187	[110]0.8920	[110]0.9355	[110]0.9594	[334]0.9738	[334]0.9828	[334]0.9885
183	NEUROTECHNOLOGY-004	[79]0.0104	[78]0.0134	[76]0.0156	[73]0.0173	[72]0.0195	[293]0.0212	[291]0.0245	[288]0.0320	[83]0.0642	[82]0.1015	[81]0.1426	[79]0.1881	[78]0.2299	[295]0.2722	[296]0.3269	[296]0.3943
184	NEUROTECHNOLOGY-005	[74]0.0089	[71]0.0116	[68]0.0136	[68]0.0152	[69]0.0173	[290]0.0196	[286]0.0233	[285]0.0306	[76]0.0556	[76]0.0913	[74]0.1315	[74]0.1766	[74]0.2192	[291]0.2617	[290]0.3174	[290]0.3843
185	NEUROTECHNOLOGY-007	[66]0.0078	[65]0.0103	[64]0.0124	[65]0.0140	[63]0.0161	[283]0.0185	[283]0.0225	[282]0.0290	[82]0.0641	[85]0.1069	[85]0.1546	[85]0.2075	[86]0.2572	[307]0.3081	[309]0.3713	[309]0.4421
186	NEUROTECHNOLOGY-010						[162]0.0053	[173]0.0061	[170]0.0053						[203]0.0863	[201]0.1050	[200]0.1333
187	NEUROTECHNOLOGY-012						[106]0.0044	[121]0.0051	[119]0.0038						[187]0.0638	[185]0.0783	[186]0.1027
188	NEUROTECHNOLOGY-013						[87]0.0043	[88]0.0047	[91]0.0032						[139]0.0406	[132]0.0498	[128]0.0654
189	NEUROTECHNOLOGY-014						[94]0.0043	[80]0.0046	[69]0.0027						[105]0.0312	[103]0.0380	[101]0.0501
190	NEUROTECHNOLOGY-015						[78]0.0042	[70]0.0044	[55]0.0023						[107]0.0322	[107]0.0391	[102]0.0502
191	NEUROTECHNOLOGY-016						[77]0.0041	[68]0.0044	[74]0.0028						[115]0.0349	[118]0.0438	[116]0.0584
192	NEXTMETALABS-002						[92]0.0043	[102]0.0049	[102]0.0033						[131]0.0391	[135]0.0500	[138]0.0691
193	NOBLIS-002	[112]0.1520	[112]0.2419	[112]0.3296	[113]0.4114	[113]0.4856	[342]0.5528	[342]0.6061	[342]0.6532	[113]0.9984	[113]0.9996	[113]0.9998	[113]0.9999	[113]0.9999	[338]1.0000	[344]1.0000	[338]1.0000
194	NOMINDER-000						[144]0.0050	[154]0.0057	[126]0.0038						[148]0.0443	[145]0.0545	[143]0.0727
195	NOMINDER-001						[157]0.0052	[150]0.0056	[147]0.0044						[146]0.0436	[144]0.0544	[140]0.0709
196	NOMINDER-002						[135]0.0048	[142]0.0055	[135]0.0041						[144]0.0425	[140]0.0521	[137]0.0690
197	NOMINDER-003						[110]0.0045	[125]0.0051	[120]0.0038						[134]0.0401	[134]0.0499	[129]0.0657
198	NOMINDER-004						[107]0.0045	[126]0.0051	[134]0.0041						[138]0.0406	[137]0.0505	[130]0.0662
199	NTECHLAB-003	[65]0.0078	[76]0.0131	[87]0.0202	[90]0.0295	[91]0.0405	[317]0.0543	[320]0.0761	[321]0.1035	[68]0.0491	[72]0.0881	[79]0.1384	[83]0.1985	[87]0.2594	[310]0.3270	[311]0.4065	[311]0.4891
200	NTECHLAB-004	[62]0.0068	[68]0.0110	[79]0.0167	[86]0.0239	[89]0.0330	[314]0.0447	[316]0.0641	[318]0.0891	[60]0.0379	[63]0.0688	[66]0.1108	[66]0.1629	[73]0.2192	[302]0.2846	[308]0.3657	[310]0.4524
201	NTECHLAB-006	[51]0.0056	[62]0.0095	[72]0.0148	[83]0.0218	[85]0.0301	[312]0.0413	[313]0.0591	[316]0.0814	[56]0.0349	[60]0.0636	[63]0.1023	[64]0.1506	[66]0.2024	[290]0.2617	[299]0.3374	[304]0.4185
202	NTECHLAB-007	[37]0.0044	[43]0.0066	[49]0.0089	[57]0.0118	[60]0.0150	[287]0.0189	[293]0.0255	[293]0.0342	[45]0.0256	[46]0.0450	[48]0.0705	[49]0.1012	[51]0.1334	[261]0.1692	[265]0.2170	[267]0.2752
203	NTECHLAB-008	[18]0.0025	[21]0.0038	[26]0.0052	[31]0.0074	[44]0.0104	[268]0.0146	[289]0.0236	[294]0.0348	[26]0.0143	[28]0.0267	[32]0.0459	[37]0.0733	[40]0.1062	[243]0.1469	[258]0.2044	[264]0.2698
204	NTECHLAB-009	[13]0.0022	[15]0.0031	[16]0.0038	[17]0.0045	[19]0.0055	[196]0.0067	[209]0.0088	[213]0.0100	[18]0.0073	[17]0.0117	[17]0.0170	[17]0.0238	[18]0.0319	[142]0.0419	[150]0.0577	[166]0.0833
205	NTECHLAB-011						[175]0.0056	[178]0.0066	[195]0.0073						[117]0.0351	[124]0.0475	[142]0.0724
206	OMNIGARDE-000						[147]0.0050	[155]0.0057	[156]0.0048						[141]0.0413	[141]0.0531	[147]0.0741
207	OMNIGARDE-001						[54]0.0039	[62]0.0043	[64]0.0024						[68]0.0178	[69]0.0215	[66]0.0275
208	OMNIGARDE-002						[68]0.0040	[71]0.0044	[62]0.0024						[45]0.0120	[43]0.0146	[43]0.0182
209	OPTIEXACTA-000						[45]0.0037	[49]0.0042	[46]0.0021						[26]0.0099	[31]0.0125	[33]0.0157
210	PANGIAM-000						[150]0.0051	[145]0.0055	[150]0.0046						[165]0.0503	[164]0.0617	[159]0.0810
211	PANGIAM-001						[260]0.0132	[258]0.0153	[242]0.0153						[178]0.0545	[178]0.0685	[178]0.0894
212	PAPSAV1923-000						[146]0.0050	[149]0.0056	[131]0.0040						[98]0.0280	[93]0.0344	[92]0.0447
213	PARAVISION-002	[53]0.0058	[58]0.0083	[60]0.0111	[63]0.0137	[65]0.0162	[285]0.0187	[285]0.0229	[283]0.0295								
214	PARAVISION-003	[44]0.0048	[44]0.0067	[51]0.0090	[52]0.0109	[54]0.0128	[269]0.0148	[270]0.0178	[269]0.0219	[57]0.0354	[58]0.0618	[59]0.0931	[60]0.1290	[61]0.1625	[274]0.1964	[276]0.2408	[271]0.2924
215	PARAVISION-004	[16]0.0024	[17]0.0032	[17]0.0040	[19]0.0047	[18]0.0053	[184]0.0061	[192]0.0073	[193]0.0072	[20]0.0118	[23]0.0209	[24]0.0327	[24]0.0465	[24]0.0613	[198]0.0779	[199]0.1008	[198]0.1285
216	PARAVISION-005	[12]0.0021	[13]0.0028	[13]0.0035	[14]0.0041	[16]0.0046	[167]0.0054	[179]0.0067	[191]0.0070	[11]0.0057	[12]0.0093	[12]0.0144	[14]0.0207	[15]0.0278	[125]0.0368	[138]0.0508	[141]0.0715
217	PARAVISION-007	[6]0.0019	[8]0.0025	[7]0.0029	[8]0.0033	[8]0.0036	[82]0.0042	[112]0.0049	[86]0.0030	[10]0.0057	[13]0.0094	[14]0.0144	[13]0.0206	[14]0.0275	[120]0.0357	[129]0.0485	[127]0.0652
218	PARAVISION-009						[74]0.0041	[81]0.0046	[68]0.0026						[99]0.0283	[100]0.0371	[107]0.0525
219	PARAVISION-012						[42]0.0037	[45]0.0041	[40]0.0020						[54]0.0137	[54]0.0167	[55]0.0219
220	PARAVISION-014						[31]0.0036	[34]0.0040	[32]0.0018						[44]0.0119	[45]0.0148	[48]0.0195

Table 16: **Accuracy for the FRVT 2018 mugshot sets under ageing**. *The second row shows the time lapse between gallery and subsequent probe images, in years. The first two columns identify the algorithm The next 8 values give rank-based FNIR with R = 1, T = 0 and FPIR = 1. All these are relevant to investigational uses where candidates from all searches would need human review. The second 8 values give threshold-based FNIR with T $\geq$ 0, FPIR = 0.001 and no rank criterion. The shaded cells indictate indicate the three most accurate algorithms for that elapsed time. The gallery size is 3068801. The total number of searches is 10951064.*

2026/01/09 20:40:38

FNIR(N, R, T) = False neg. identification rate
FPIR(N, T) = False pos. identification rate

N = Num. enrolled subjects
R = Num. candidates examined

T = Threshold

T = 0 → Investigation
T > 0 → Identification

This publication is available free of charge from: https://doi.org/10.6028/NIST.IR.8271

MISS RATES		INVESTIGATION, FNIR(N, R = 1, T = 0)								IDENTIFICATION, FNIR(N, R = L, T $\geq$ 0) FOR FPIR = 0.001							
#	ALGORITHM	(0, 2]	(2, 4]	(4, 6]	(6, 8]	(8, 10]	(10, 12]	(12, 14]	(14, 18]	(0, 2]	(2, 4]	(4, 6]	(6, 8]	(8, 10]	(10, 12]	(12, 14]	(14, 18]
221	PARAVISION-016						[28]0.0036	[29]0.0039	[23]0.0016						[30]0.0100	[32]0.0125	[30]0.0156
222	PARAVISION-019						[24]0.0035	[25]0.0039	[16]0.0015						[31]0.0100	[33]0.0125	[31]0.0157
223	PENTACOMP-000						[347]0.9396	[347]0.9391	[347]0.9364								
224	PENTACOMP-001						[230]0.0094	[233]0.0108	[233]0.0130								
225	PIXELALL-002	[72]0.0085	[73]0.0119	[71]0.0147	[72]0.0172	[73]0.0198	[295]0.0225	[294]0.0270	[295]0.0349	[97]0.1193	[97]0.1900	[97]0.2601	[92]0.3332	[97]0.3955	[318]0.4565	[319]0.5268	[320]0.6030
226	PIXELALL-003	[46]0.0050	[42]0.0063	[39]0.0072	[34]0.0077	[33]0.0085	[232]0.0095	[235]0.0113	[228]0.0119	[44]0.0248	[43]0.0418	[43]0.0622	[43]0.0861	[43]0.1104	[238]0.1364	[239]0.1723	[239]0.2167
227	PIXELALL-004	[45]0.0049	[40]0.0063	[40]0.0072	[37]0.0079	[36]0.0089	[238]0.0103	[238]0.0127	[238]0.0146	[38]0.0211	[40]0.0360	[42]0.0553	[42]0.0792	[39]0.1045	[234]0.1317	[238]0.1700	[244]0.2246
228	PSL-000						[48]0.0038	[57]0.0042	[56]0.0023						[90]0.0252	[89]0.0324	[91]0.0436
229	PSL-001						[30]0.0036	[27]0.0039	[38]0.0019						[77]0.0202	[76]0.0248	[78]0.0337
230	PSL-002						[21]0.0035	[22]0.0038	[27]0.0017						[49]0.0124	[52]0.0160	[54]0.0218
231	PSL-003						[17]0.0035	[16]0.0038	[20]0.0016						[42]0.0118	[49]0.0152	[50]0.0197
232	PSL-004						[14]0.0034	[20]0.0038	[26]0.0017						[35]0.0105	[42]0.0142	[47]0.0190
233	PTAKURATSATU-000	[54]0.0061	[55]0.0082	[55]0.0097	[53]0.0109	[49]0.0120	[258]0.0131	[251]0.0146	[253]0.0180	[59]0.0375	[57]0.0596	[55]0.0842	[55]0.1116	[53]0.1357	[254]0.1553	[246]0.1820	[250]0.2326
234	PYRAMID-000						[114]0.0045	[130]0.0052	[128]0.0039						[108]0.0325	[111]0.0415	[119]0.0588
235	PYRAMID-001						[133]0.0047	[138]0.0053	[121]0.0038						[129]0.0384	[128]0.0482	[134]0.0676
236	QAZSMARTVISIONAI-000						[15]0.0034	[14]0.0037	[15]0.0015						[32]0.0102	[28]0.0123	[26]0.0142
237	QAZSMARTVISIONAI-001						[9]0.0033	[10]0.0036	[6]0.0010						[17]0.0066	[16]0.0077	[16]0.0081
238	QAZSMARTVISIONAI-002						[4]0.0032	[6]0.0035	[1]0.0009						[9]0.0043	[11]0.0051	[9]0.0042
239	QAZSMARTVISIONAI-003						[5]0.0033	[7]0.0035	[4]0.0010						[11]0.0045	[13]0.0052	[10]0.0043
240	QNAP-004						[239]0.0105	[244]0.0133	[248]0.0167						[231]0.1243	[232]0.1556	[233]0.2050
241	QNAP-005						[217]0.0084	[212]0.0091	[222]0.0113						[183]0.0612	[181]0.0724	[187]0.1031
242	QNAP-006						[205]0.0071	[206]0.0082	[205]0.0084						[190]0.0676	[191]0.0838	[194]0.1137
243	RANKONE-002	[99]0.0212	[98]0.0313	[98]0.0431	[98]0.0562	[99]0.0712	[326]0.0881	[327]0.1130	[328]0.1543	[95]0.1111	[95]0.1707	[95]0.2305	[95]0.2968	[96]0.3646	[317]0.4345	[317]0.5172	[321]0.6110
244	RANKONE-004	[108]0.0424	[107]0.0643	[107]0.0875	[107]0.1127	[107]0.1364	[332]0.1579	[333]0.1914	[333]0.2378	[104]0.1855	[103]0.2681	[103]0.3431	[101]0.4155	[101]0.4785	[323]0.5350	[323]0.5980	[323]0.6722
245	RANKONE-005	[92]0.0136	[93]0.0192	[91]0.0246	[91]0.0303	[90]0.0362	[313]0.0422	[312]0.0521	[312]0.0694	[81]0.0582	[75]0.0910	[71]0.1260	[68]0.1645	[65]0.2005	[281]0.2353	[281]0.2816	[283]0.3522
246	RANKONE-007	[67]0.0078	[64]0.0099	[61]0.0113	[58]0.0123	[58]0.0139	[276]0.0156	[277]0.0191	[275]0.0242	[42]0.0242	[42]0.0376	[41]0.0542	[38]0.0737	[37]0.0935	[226]0.1130	[225]0.1416	[225]0.1811
247	RANKONE-009	[48]0.0054	[49]0.0072	[46]0.0085	[47]0.0098	[47]0.0113	[257]0.0130	[266]0.0169	[271]0.0220	[37]0.0208	[38]0.0345	[37]0.0504	[36]0.0706	[36]0.0930	[228]0.1174	[230]0.1504	[230]0.2002
248	RANKONE-010	[42]0.0047	[38]0.0061	[38]0.0070	[33]0.0076	[34]0.0087	[234]0.0098	[236]0.0113	[229]0.0120	[31]0.0177	[29]0.0269	[26]0.0368	[26]0.0479	[23]0.0590	[193]0.0688	[189]0.0803	[183]0.0991
249	RANKONE-011	[23]0.0031	[23]0.0041	[23]0.0047	[23]0.0053	[22]0.0058	[197]0.0067	[196]0.0077	[197]0.0073	[23]0.0127	[20]0.0194	[21]0.0265	[20]0.0345	[20]0.0422	[163]0.0499	[161]0.0611	[151]0.0756
250	RANKONE-012						[192]0.0065	[184]0.0069	[169]0.0053						[149]0.0460	[145]0.0540	[132]0.0672
251	RANKONE-013						[153]0.0051	[127]0.0051	[108]0.0035						[102]0.0306	[98]0.0355	[88]0.0405
252	RANKONE-014						[99]0.0044	[85]0.0047	[78]0.0029						[82]0.0222	[78]0.0255	[69]0.0287
253	RANKONE-015						[75]0.0041	[66]0.0044	[60]0.0024						[62]0.0162	[59]0.0187	[53]0.0218
254	REALNETWORKS-002	[107]0.0381	[108]0.0687	[108]0.1062	[108]0.1495	[109]0.1963	[337]0.2513	[340]0.3206	[340]0.3927	[105]0.2153	[105]0.3323	[105]0.4444	[105]0.5485	[106]0.6355	[330]0.7132	[331]0.7855	[331]0.8437
255	REALNETWORKS-003	[103]0.0245	[105]0.0437	[105]0.0686	[106]0.0975	[106]0.1312	[335]0.1719	[335]0.2294	[336]0.2907	[98]0.1468	[100]0.2370	[101]0.3313	[103]0.4269	[103]0.5142	[327]0.5979	[328]0.6815	[328]0.7567
256	REALNETWORKS-004	[102]0.0244	[104]0.0428	[104]0.0663	[105]0.0939	[105]0.1251	[334]0.1634	[334]0.2170	[335]0.2785	[99]0.1484	[101]0.2377	[100]0.3303	[102]0.4249	[102]0.5106	[326]0.5924	[327]0.6758	[327]0.7534
257	REALNETWORKS-006						[204]0.0069	[199]0.0077	[204]0.0080						[219]0.1022	[216]0.1253	[215]0.1622
258	REALNETWORKS-008						[143]0.0049	[141]0.0054	[153]0.0047						[150]0.0462	[151]0.0577	[148]0.0745
259	RECOGNITO-000						[83]0.0042	[92]0.0047	[79]0.0030						[66]0.0176	[73]0.0221	[75]0.0306
260	RECOGNITO-001						[43]0.0037	[47]0.0041	[44]0.0021						[34]0.0105	[37]0.0135	[38]0.0172
261	RECOGNITO-002						[46]0.0037	[50]0.0042	[47]0.0021						[25]0.0099	[30]0.0125	[32]0.0157
262	RNIT-000						[169]0.0054	[172]0.0061	[151]0.0046						[242]0.1456	[243]0.1739	[241]0.2192
263	ROC-016						[53]0.0038	[53]0.0042	[29]0.0018						[51]0.0130	[48]0.0152	[46]0.0187
264	ROC-017						[70]0.0040	[61]0.0043	[70]0.0027						[69]0.0181	[66]0.0209	[60]0.0238

Table 17: **Accuracy for the FRVT 2018 mugshot sets under ageing**. *The second row shows the time lapse between gallery and subsequent probe images, in years. The first two columns identify the algorithm The next 8 values give rank-based FNIR with R = 1, T = 0 and FPIR = 1. All these are relevant to investigational uses where candidates from all searches would need human review. The second 8 values give threshold-based FNIR with T $\geq$ 0, FPIR = 0.001 and no rank criterion. The shaded cells indictate indicate the three most accurate algorithms for that elapsed time. The gallery size is 3068801. The total number of searches is 10951064.*

2026/01/09 20:40:38

FNIR(N, R, T) = False neg. identification rate
FPIR(N, T) = False pos. identification rate

N = Num. enrolled subjects
R = Num. candidates examined

T = Threshold

T = 0 → Investigation
T > 0 → Identification

This publication is available free of charge from: https://doi.org/10.6028/NIST.IR.8271

MISS RATES		INVESTIGATION, FNIR(N, R = 1, T = 0)								IDENTIFICATION, FNIR(N, R = L, T $\geq$ 0) FOR FPIR = 0.001							
#	ALGORITHM	(0, 2]	(2, 4]	(4, 6]	(6, 8]	(8, 10]	(10, 12]	(12, 14]	(14, 18]	(0, 2]	(2, 4]	(4, 6]	(6, 8]	(8, 10]	(10, 12]	(12, 14]	(14, 18]
265	ROC-018						[49] 0.0038	[32] 0.0039	[36] 0.0018						[52] 0.0131	[47] 0.0151	[37] 0.0171
266	ROC-019						[20] 0.0035	[17] 0.0038	[22] 0.0016						[46] 0.0121	[41] 0.0142	[36] 0.0164
267	S1-002						[123] 0.0046	[123] 0.0051	[124] 0.0038						[155] 0.0482	[155] 0.0597	[156] 0.0788
268	S1-003						[177] 0.0057	[175] 0.0063	[176] 0.0056						[191] 0.0681	[192] 0.0839	[189] 0.1061
269	S1-004						[80] 0.0042	[78] 0.0045	[94] 0.0032						[122] 0.0360	[120] 0.0448	[120] 0.0598
270	S1-005						[84] 0.0042	[76] 0.0045	[83] 0.0030						[136] 0.0403	[139] 0.0515	[139] 0.0695
271	S1-006						[51] 0.0038	[41] 0.0041	[54] 0.0022						[67] 0.0176	[67] 0.0211	[68] 0.0280
272	S1-007						[50] 0.0038	[36] 0.0040	[45] 0.0021						[57] 0.0152	[57] 0.0177	[59] 0.0230
273	SANSAP-001						[170] 0.0054	[171] 0.0061	[161] 0.0050						[133] 0.0395	[126] 0.0479	[123] 0.0632
274	SCANOVATE-001	[68] 0.0079	[72] 0.0117	[75] 0.0151	[78] 0.0185	[78] 0.0221	[300] 0.0259	[304] 0.0321	[304] 0.0427	[88] 0.0727	[88] 0.1169	[87] 0.1650	[87] 0.2115	[84] 0.2528	[304] 0.2925	[301] 0.3437	[301] 0.4084
275	SCYLLA-001						[233] 0.0097	[234] 0.0112	[231] 0.0124						[233] 0.1292	[233] 0.1600	[234] 0.2093
276	SENSETIME-002	[96] 0.0186	[92] 0.0191	[84] 0.0183	[75] 0.0179	[68] 0.0173	[261] 0.0133	[210] 0.0089	[179] 0.0059	[40] 0.0220	[25] 0.0236	[19] 0.0237	[18] 0.0240	[12] 0.0245	[81] 0.0219	[63] 0.0195	[56] 0.0222
277	SENSETIME-003	[11] 0.0021	[12] 0.0028	[11] 0.0031	[7] 0.0033	[6] 0.0035	[63] 0.0040	[93] 0.0047	[95] 0.0033	[8] 0.0046	[8] 0.0064	[6] 0.0076	[4] 0.0086	[4] 0.0101	[47] 0.0122	[50] 0.0155	[49] 0.0196
278	SENSETIME-004	[3] 0.0016	[3] 0.0022	[3] 0.0025	[3] 0.0028	[3] 0.0030	[23] 0.0035	[64] 0.0043	[67] 0.0025	[4] 0.0036	[4] 0.0052	[3] 0.0066	[3] 0.0081	[3] 0.0099	[50] 0.0126	[55] 0.0169	[58] 0.0230
279	SENSETIME-005	[2] 0.0015	[2] 0.0020	[2] 0.0024	[2] 0.0026	[2] 0.0029	[19] 0.0035	[58] 0.0043	[75] 0.0028	[5] 0.0036	[7] 0.0059	[8] 0.0089	[9] 0.0128	[10] 0.0177	[87] 0.0240	[94] 0.0345	[98] 0.0493
280	SENSETIME-006	[1] 0.0015	[1] 0.0019	[1] 0.0022	[1] 0.0025	[1] 0.0027	[6] 0.0033	[40] 0.0040	[51] 0.0021	[2] 0.0031	[2] 0.0049	[4] 0.0068	[6] 0.0097	[7] 0.0132	[72] 0.0184	[81] 0.0262	[81] 0.0359
281	SENSETIME-007						[18] 0.0035	[18] 0.0038	[17] 0.0015						[39] 0.0112	[38] 0.0140	[40] 0.0176
282	SENSETIME-008						[16] 0.0034	[24] 0.0039	[25] 0.0017						[33] 0.0103	[35] 0.0127	[35] 0.0163
283	SENSETIME-010						[7] 0.0033	[8] 0.0036	[10] 0.0012						[20] 0.0071	[20] 0.0086	[20] 0.0099
284	SERENDIPITY-000						[215] 0.0084	[214] 0.0092	[210] 0.0094						[214] 0.0981	[211] 0.1180	[211] 0.1519
285	SEVENTHSENSE-001						[254] 0.0128	[260] 0.0156	[264] 0.0206						[128] 0.0383	[125] 0.0476	[136] 0.0688
286	SIAT-002	[117] 0.8309	[117] 0.8310	[117] 0.8311	[117] 0.8306	[117] 0.8296	[346] 0.8302	[346] 0.8300	[345] 0.8301	[112] 0.8340	[110] 0.8368	[109] 0.8404	[109] 0.8445	[109] 0.8480	[333] 0.8532	[333] 0.8595	[332] 0.8691
287	SPARKTEK-000						[182] 0.0060	[180] 0.0068	[172] 0.0054						[96] 0.0279	[92] 0.0344	[93] 0.0451
288	SPARSH-001						[118] 0.0046	[111] 0.0049	[92] 0.0032						[124] 0.0362	[117] 0.0435	[112] 0.0557
289	STCON-001						[40] 0.0037	[46] 0.0041	[33] 0.0018						[56] 0.0146	[58] 0.0186	[62] 0.0254
290	STCON-002						[22] 0.0035	[31] 0.0039	[21] 0.0016						[41] 0.0115	[40] 0.0142	[44] 0.0182
291	STCON-003						[25] 0.0035	[26] 0.0039	[19] 0.0016						[28] 0.0100	[29] 0.0124	[29] 0.0154
292	SYNESIS-003	[89] 0.0125	[85] 0.0151	[83] 0.0174	[80] 0.0199	[79] 0.0223	[297] 0.0240	[299] 0.0279	[291] 0.0331	[85] 0.0658	[83] 0.1052	[83] 0.1483	[82] 0.1968	[82] 0.2399	[300] 0.2834	[300] 0.3405	[300] 0.4046
293	SYNESIS-005	[40] 0.0044	[37] 0.0058	[37] 0.0070	[40] 0.0080	[37] 0.0091	[237] 0.0103	[237] 0.0125	[241] 0.0152	[46] 0.0262	[45] 0.0444	[45] 0.0666	[45] 0.0923	[44] 0.1156	[240] 0.1399	[241] 0.1736	[240] 0.2185
294	T4ISB-000						[320] 0.0606	[319] 0.0748	[319] 0.0970								
295	TECH5-001	[57] 0.0061	[61] 0.0093	[66] 0.0128	[71] 0.0171	[77] 0.0221	[306] 0.0289	[309] 0.0412	[309] 0.0560	[86] 0.0660	[87] 0.1156	[90] 0.1733	[91] 0.2385	[91] 0.2998	[312] 0.3629	[314] 0.4424	[315] 0.5284
296	TECH5-003						[125] 0.0046	[115] 0.0050	[90] 0.0032						[114] 0.0345	[109] 0.0414	[108] 0.0529
297	TIGER-004						[240] 0.0106	[239] 0.0127	[240] 0.0152						[235] 0.1350	[236] 0.1654	[236] 0.2136
298	TOSHIBA-001	[73] 0.0086	[74] 0.0119	[74] 0.0150	[74] 0.0178	[75] 0.0209	[298] 0.0241	[298] 0.0292	[297] 0.0365								
299	TOSHIBA-002						[57] 0.0039	[35] 0.0040	[48] 0.0021						[36] 0.0105	[36] 0.0130	[41] 0.0179
300	TOSS-000						[27] 0.0036	[30] 0.0039	[37] 0.0019						[37] 0.0109	[34] 0.0126	[34] 0.0163
301	TRUEFACE-000	[36] 0.0043	[36] 0.0057	[30] 0.0061	[28] 0.0067	[27] 0.0073	[216] 0.0084	[216] 0.0097	[212] 0.0099	[35] 0.0200	[37] 0.0338	[38] 0.0504	[35] 0.0705	[35] 0.0904	[224] 0.1112	[223] 0.1401	[224] 0.1792
302	UNISSEY-003						[213] 0.0083	[211] 0.0090	[209] 0.0091						[212] 0.0963	[212] 0.1181	[209] 0.1516
303	USEB-001						[102] 0.0044	[99] 0.0048	[107] 0.0035						[101] 0.0305	[106] 0.0389	[104] 0.0516
304	USEB-002						[111] 0.0045	[108] 0.0049	[104] 0.0034						[109] 0.0328	[112] 0.0417	[111] 0.0556
305	USEB-003						[100] 0.0044	[89] 0.0047	[96] 0.0033						[100] 0.0305	[105] 0.0387	[106] 0.0522
306	USEB-004						[85] 0.0043	[90] 0.0047	[106] 0.0035						[95] 0.0279	[95] 0.0347	[96] 0.0467
307	VDFSOFTWARE-002						[282] 0.0182	[280] 0.0221	[279] 0.0276						[279] 0.2342	[279] 0.2744	[279] 0.3298
308	VERIDAS-001	[58] 0.0063	[56] 0.0083	[56] 0.0099	[56] 0.0113	[56] 0.0132	[270] 0.0148	[272] 0.0184	[268] 0.0219	[61] 0.0403	[61] 0.0684	[62] 0.1012	[62] 0.1386	[62] 0.1741	[277] 0.2113	[277] 0.2611	[278] 0.3233

Table 18: **Accuracy for the FRVT 2018 mugshot sets under ageing**. *The second row shows the time lapse between gallery and subsequent probe images, in years. The first two columns identify the algorithm The next 8 values give rank-based FNIR with R = 1, T = 0 and FPIR = 1. All these are relevant to investigational uses where candidates from all searches would need human review. The second 8 values give threshold-based FNIR with T $\geq$ 0, FPIR = 0.001 and no rank criterion. The shaded cells indictate indicate the three most accurate algorithms for that elapsed time. The gallery size is 3068801. The total number of searches is 10951064.*

This publication is available free of charge from: https://doi.org/10.6028/NIST.IR.8271

MISS RATES		INVESTIGATION, FNIR(N, R = 1, T = 0)								IDENTIFICATION, FNIR(N, R = L, T $\geq$ 0) FOR FPIR = 0.001							
#	ALGORITHM	(0, 2]	(2, 4]	(4, 6]	(6, 8]	(8, 10]	(10, 12]	(12, 14]	(14, 18]	(0, 2]	(2, 4]	(4, 6]	(6, 8]	(8, 10]	(10, 12]	(12, 14]	(14, 18]
309	VERIDAS-004						[160] 0.0052	[165] 0.0059	[143] 0.0043						[167] 0.0506	[169] 0.0634	[168] 0.0836
310	VERIGRAM-001						[154] 0.0051	[140] 0.0053	[178] 0.0058						[112] 0.0336	[108] 0.0413	[113] 0.0561
311	VIANTE-000						[71] 0.0040	[75] 0.0045	[73] 0.0028						[79] 0.0210	[80] 0.0259	[77] 0.0315
312	VIANTE-001						[26] 0.0036	[21] 0.0038	[31] 0.0018						[19] 0.0070	[18] 0.0082	[19] 0.0095
313	VINBIGDATA-001						[202] 0.0068	[202] 0.0079	[201] 0.0077						[239] 0.1383	[237] 0.1670	[235] 0.2134
314	VINBIGDATA-002						[89] 0.0043	[84] 0.0047	[82] 0.0030						[80] 0.0213	[82] 0.0271	[85] 0.0372
315	VINBIGDATA-003						[93] 0.0043	[87] 0.0047	[87] 0.0031						[93] 0.0273	[99] 0.0357	[103] 0.0503
316	VINBIGDATA-004						[61] 0.0039	[42] 0.0041	[52] 0.0022						[59] 0.0156	[64] 0.0197	[67] 0.0280
317	VISIONBOX-001						[235] 0.0099	[225] 0.0103	[226] 0.0117						[329] 0.6689	[329] 0.7251	[329] 0.7917
318	VISIONBOX-002						[210] 0.0080	[208] 0.0088	[211] 0.0097						[208] 0.0937	[210] 0.1170	[212] 0.1531
319	VISIONLABS-004	[43] 0.0048	[46] 0.0069	[52] 0.0091	[55] 0.0111	[55] 0.0130	[274] 0.0152	[273] 0.0187	[276] 0.0242	[74] 0.0540	[77] 0.0916	[78] 0.1358	[78] 0.1855	[79] 0.2303	[296] 0.2745	[297] 0.3312	[293] 0.3913
320	VISIONLABS-005	[39] 0.0044	[39] 0.0063	[43] 0.0081	[46] 0.0095	[46] 0.0109	[253] 0.0125	[256] 0.0151	[257] 0.0187	[67] 0.0479	[67] 0.0812	[68] 0.1212	[70] 0.1664	[69] 0.2078	[286] 0.2473	[286] 0.2999	[285] 0.3577
321	VISIONLABS-006	[29] 0.0035	[30] 0.0048	[32] 0.0061	[30] 0.0069	[29] 0.0077	[219] 0.0087	[226] 0.0105	[230] 0.0120	[48] 0.0273	[47] 0.0465	[47] 0.0702	[47] 0.0970	[47] 0.1228	[246] 0.1486	[249] 0.1847	[248] 0.2295
322	VISIONLABS-008	[21] 0.0028	[20] 0.0037	[21] 0.0047	[22] 0.0053	[23] 0.0058	[195] 0.0067	[205] 0.0081	[206] 0.0085	[27] 0.0143	[27] 0.0241	[28] 0.0373	[27] 0.0519	[27] 0.0677	[201] 0.0850	[204] 0.1104	[205] 0.1444
323	VISIONLABS-009	[10] 0.0020	[10] 0.0026	[10] 0.0030	[10] 0.0034	[10] 0.0038	[104] 0.0044	[131] 0.0052	[152] 0.0046	[14] 0.0065	[15] 0.0105	[15] 0.0156	[15] 0.0217	[16] 0.0289	[126] 0.0368	[133] 0.0499	[135] 0.0681
324	VISIONLABS-010	[9] 0.0020	[9] 0.0025	[9] 0.0030	[11] 0.0034	[9] 0.0036	[88] 0.0043	[120] 0.0051	[154] 0.0047	[17] 0.0069	[16] 0.0113	[16] 0.0170	[16] 0.0238	[17] 0.0316	[140] 0.0411	[147] 0.0557	[146] 0.0740
325	VISIONLABS-011						[81] 0.0042	[82] 0.0046	[114] 0.0036						[92] 0.0270	[90] 0.0337	[90] 0.0432
326	VIXVIZION-009						[278] 0.0161	[276] 0.0190	[273] 0.0238						[267] 0.1787	[262] 0.2116	[260] 0.2595
327	VNPAY-001						[163] 0.0053	[156] 0.0058	[144] 0.0043						[164] 0.0501	[166] 0.0619	[162] 0.0822
328	VNPT-002						[164] 0.0053	[164] 0.0059	[148] 0.0044						[175] 0.0534	[177] 0.0670	[175] 0.0882
329	VNPT-003						[145] 0.0050	[153] 0.0057	[133] 0.0041						[174] 0.0532	[173] 0.0658	[176] 0.0883
330	VNPT-004						[139] 0.0049	[132] 0.0052	[122] 0.0038						[145] 0.0432	[146] 0.0549	[150] 0.0754
331	VNPT-005						[109] 0.0045	[101] 0.0048	[98] 0.0033						[121] 0.0357	[122] 0.0456	[122] 0.0623
332	VTCC-000						[207] 0.0072	[194] 0.0074	[202] 0.0077						[322] 0.5122	[322] 0.5689	[322] 0.6493
333	VTCC-001						[173] 0.0056	[169] 0.0060	[174] 0.0055								
334	VTCC-002						[172] 0.0056	[170] 0.0060	[175] 0.0055						[206] 0.0902	[205] 0.1106	[204] 0.1438
335	VTS-000	[116] 0.5878	[116] 0.6312	[116] 0.6602	[115] 0.6863	[115] 0.7073	[344] 0.7246	[344] 0.7458	[343] 0.7747	[108] 0.5929	[108] 0.6397	[108] 0.6729	[108] 0.7034	[107] 0.7279	[331] 0.7493	[330] 0.7739	[330] 0.8076
336	VTS-003						[165] 0.0054	[158] 0.0059	[171] 0.0054						[182] 0.0597	[182] 0.0731	[181] 0.0950
337	VTS-004						[119] 0.0046	[128] 0.0051	[116] 0.0037						[137] 0.0405	[136] 0.0505	[131] 0.0671
338	VTS-005						[96] 0.0044	[113] 0.0049	[113] 0.0036						[162] 0.0497	[167] 0.0625	[172] 0.0849
339	WINK-001						[288] 0.0190	[281] 0.0223	[281] 0.0286						[280] 0.2344	[280] 0.2754	[280] 0.3370
340	WINK-002						[220] 0.0087	[216] 0.0095	[215] 0.0103						[213] 0.0966	[209] 0.1168	[210] 0.1518
341	XFORWARDAI-000	[20] 0.0027	[18] 0.0034	[20] 0.0044	[21] 0.0052	[21] 0.0058	[198] 0.0067	[201] 0.0079	[200] 0.0076	[28] 0.0157	[31] 0.0281	[30] 0.0443	[31] 0.0635	[32] 0.0834	[220] 0.1050	[220] 0.1330	[220] 0.1714
342	XFORWARDAI-001	[15] 0.0023	[11] 0.0028	[12] 0.0034	[12] 0.0037	[12] 0.0039	[115] 0.0045	[129] 0.0052	[145] 0.0043	[13] 0.0060	[14] 0.0096	[13] 0.0144	[12] 0.0200	[13] 0.0260	[111] 0.0334	[115] 0.0435	[118] 0.0586
343	YITU-002	[60] 0.0066	[57] 0.0083	[53] 0.0094	[48] 0.0101	[50] 0.0121	[272] 0.0150	[282] 0.0223	[289] 0.0328	[33] 0.0189	[34] 0.0317	[35] 0.0494	[39] 0.0750	[41] 0.1066	[248] 0.1494	[266] 0.2171	[274] 0.2958
344	YITU-003	[63] 0.0072	[60] 0.0089	[57] 0.0100	[51] 0.0107	[52] 0.0125	[275] 0.0153	[284] 0.0226	[292] 0.0334	[34] 0.0194	[35] 0.0321	[36] 0.0500	[41] 0.0756	[42] 0.1071	[250] 0.1500	[267] 0.2177	[275] 0.2964
345	YITU-004	[55] 0.0061	[51] 0.0075	[44] 0.0081	[41] 0.0081	[39] 0.0092	[242] 0.0107	[259] 0.0154	[266] 0.0207	[22] 0.0125	[22] 0.0204	[23] 0.0314	[25] 0.0469	[26] 0.0671	[210] 0.0955	[227] 0.1421	[231] 0.2006
346	YITU-005	[61] 0.0067	[54] 0.0080	[47] 0.0087	[44] 0.0085	[41] 0.0094	[243] 0.0108	[257] 0.0151	[262] 0.0204	[21] 0.0124	[21] 0.0198	[22] 0.0308	[22] 0.0462	[25] 0.0667	[209] 0.0953	[226] 0.1418	[229] 0.1930
347	YUAN-000						[181] 0.0059	[185] 0.0070	[182] 0.0063						[204] 0.0864	[203] 0.1083	[203] 0.1406

Table 19: **Accuracy for the FRVT 2018 mugshot sets under ageing**. *The second row shows the time lapse between gallery and subsequent probe images, in years. The first two columns identify the algorithm The next 8 values give rank-based FNIR with R = 1, T = 0 and FPIR = 1. All these are relevant to investigational uses where candidates from all searches would need human review. The second 8 values give threshold-based FNIR with T $\geq$ 0, FPIR = 0.001 and no rank criterion. The shaded cells indictate indicate the three most accurate algorithms for that elapsed time. The gallery size is 3068801. The total number of searches is 10951064.*

FNIR(N, R, T) = False neg. identification rate
FPIR(N, T) = False pos. identification rate

N = Num. enrolled subjects
R = Num. candidates examined

T = Threshold

T = 0 → Investigation
T > 0 → Identification

This publication is available free of charge from: https://doi.org/10.6028/NIST.IR.8271

#	ALGORITHM	INVESTIGATION MODE						IDENTIFICATION MODE						FAILURE TO EXTRACT					
		RANK ONE MISS RATE, FNIR(N, 0, 1)						HIGH T ⟶ FPIR = 0.001, FNIR(N, T, L)						FEATURES					
		N=1.6M						N=1.6M											
	GALLERY	MUGSHOT	MUGSHOT	MUGSHOT	VISA	BORDER	VISA	MUGSHOT	MUGSHOT	MUGSHOT	VISA	BORDER	VISA	MUGSHOT	MUGSHOT	MUGSHOT	VISA	BORDER	KIOSK
	PROBE	MUGSHOT	WEBCAM	PROFILE	BORDER	BOR¿10YR	KIOSK	MUGSHOT	WEBCAM	PROFILE	BORDER	BOR¿10YR	KIOSK	MUGSHOT	WEBCAM	PROFILE	BORDER	BOR¿10YR	KIOSK
1	20FACE-000	[500] 0.055	[481] 0.085	[398] 0.733	[420] 0.056	[344] 0.239	[414] 0.243	[499] 0.347	[466] 0.450	[473] 1.000	[412] 0.424	[265] 0.772	[410] 0.938	0.000	0.000	0.000		0.000	
2	3DIVI-003	[510] 0.083	[507] 0.206		[438] 0.141		[447] 0.474	[508] 0.400	[488] 0.626		[431] 0.605		[377] 0.821	0.002	0.005				
3	3DIVI-004	[460] 0.017	[469] 0.062		[409] 0.035		[419] 0.279	[466] 0.168	[451] 0.343		[390] 0.277		[336] 0.607	0.002	0.005				
4	3DIVI-005	[461] 0.017	[468] 0.062	[450] 0.929	[467] 0.821		[420] 0.279	[463] 0.166	[449] 0.339	[357] 0.996	[449] 0.864		[334] 0.597	0.002	0.005	0.442			
5	3DIVI-006	[472] 0.024	[476] 0.074		[415] 0.047		[432] 0.312	[465] 0.167	[450] 0.342		[391] 0.283		[339] 0.615	0.002	0.005				
6	AADI-000	[551] 0.999	[548] 1.000	[530] 1.000	[532] 1.000	[370] 1.000	[537] 1.000	[547] 1.000	[549] 1.000	[552] 1.000	[531] 1.000	[418] 1.000	[520] 1.000	0.028	0.154	0.990		0.274	
7	AADI-001	[547] 0.789	[543] 0.944	[506] 0.999	[471] 0.967	[365] 0.988	[472] 0.985			[429] 1.000				0.160	0.278	0.991		0.473	
8	AADI-002	[546] 0.699	[542] 0.915	[505] 0.999	[469] 0.898	[363] 0.955	[471] 0.982	[536] 0.939	[531] 0.992	[395] 0.999	[462] 0.995	[308] 0.999	[437] 0.998	0.008	0.047	0.919		0.047	
9	ACER-000	[434] 0.010	[426] 0.036	[429] 0.825	[391] 0.025		[401] 0.209	[455] 0.145	[421] 0.246	[283] 0.981	[381] 0.201		[312] 0.490	0.000	0.000	0.042			
10	ACER-001	[378] 0.005	[355] 0.020	[329] 0.416	[334] 0.008	[286] 0.050	[268] 0.098	[388] 0.056	[336] 0.109	[406] 0.999	[319] 0.068	[233] 0.406	[311] 0.479	0.001	0.001	0.041		0.000	
11	ADIANCE-001	[555] 1.000	[547] 1.000	[529] 1.000	[468] 0.823	[368] 1.000	[466] 0.837	[554] 1.000	[538] 1.000	[550] 1.000	[446] 0.833	[317] 1.000	[407] 0.931	0.001	0.000	0.043		0.000	
12	ADVANCE-000	[259] 0.002	[265] 0.013	[256] 0.177	[225] 0.003	[296] 0.060	[215] 0.081	[289] 0.020	[435] 0.270	[265] 0.973	[368] 0.163	[277] 0.884	[262] 0.326	0.000	0.000	0.043		0.000	
13	AFISBIOMETRICS-000	[205] 0.001	[145] 0.009	[222] 0.115	[228] 0.003	[199] 0.015	[225] 0.083	[336] 0.029	[296] 0.081	[152] 0.511	[269] 0.034	[173] 0.154	[195] 0.172	0.000	0.000	0.041		0.000	
14	AFRENGINE-000	[337] 0.003	[437] 0.038	[221] 0.114	[408] 0.035	[251] 0.028	[329] 0.121	[285] 0.019	[436] 0.271	[120] 0.360	[382] 0.206	[260] 0.743	[254] 0.308	0.001	0.000	0.042		0.000	
15	AFRENGINE-001	[219] 0.001	[257] 0.013	[133] 0.060	[340] 0.010	[211] 0.018	[186] 0.073	[102] 0.003	[166] 0.031	[92] 0.227	[208] 0.018	[147] 0.113	[138] 0.120	0.001	0.001	0.042		0.009	
16	AFRENGINE-002	[220] 0.001	[245] 0.012	[120] 0.058	[146] 0.001	[140] 0.008	[86] 0.054	[93] 0.003	[132] 0.026	[116] 0.344	[149] 0.008	[284] 0.926	[113] 0.102	0.001	0.000	0.042		0.000	
17	AFRENGINE-003	[316] 0.002	[263] 0.013	[134] 0.061	[149] 0.002	[131] 0.007	[128] 0.060	[144] 0.004	[177] 0.033	[67] 0.183	[172] 0.011	[140] 0.097	[129] 0.111	0.002	0.000	0.044		0.001	
18	AIZE-001	[384] 0.005	[374] 0.022	[386] 0.679	[373] 0.016	[288] 0.050	[372] 0.165	[411] 0.076	[368] 0.143	[331] 0.994	[340] 0.101	[223] 0.364	[278] 0.387	0.001	0.001	0.047		0.000	
19	AIZE-002	[346] 0.003	[344] 0.019	[305] 0.311	[317] 0.007	[281] 0.043	[260] 0.096	[374] 0.051	[530] 0.981	[464] 1.000	[402] 0.355	[330] 1.000	[481] 1.000	0.000	0.000	0.000		0.000	
20	AKUVOX-001	[226] 0.001	[248] 0.012	[225] 0.118	[186] 0.002	[228] 0.022	[161] 0.069	[246] 0.013	[229] 0.050	[251] 0.964	[214] 0.019	[257] 0.737	[164] 0.141	0.001	0.000	0.044		0.000	
21	ALCHERA-000	[456] 0.016	[452] 0.047	[437] 0.869	[414] 0.046		[427] 0.292	[452] 0.138	[405] 0.216	[381] 0.999	[374] 0.176		[373] 0.803	0.006	0.014	0.328			
22	ALCHERA-001	[550] 0.987	[549] 1.000		[474] 1.000		[506] 1.000	[544] 0.999	[543] 1.000		[505] 1.000		[483] 1.000	0.006	0.013	0.324			
23	ALCHERA-002	[512] 0.095	[501] 0.166	[467] 0.954	[461] 0.668		[444] 0.446	[516] 0.485	[483] 0.591	[414] 1.000	[445] 0.827		[374] 0.811	0.001	0.002	0.106			
24	ALCHERA-003	[433] 0.010	[424] 0.035	[400] 0.738	[374] 0.016		[399] 0.206	[457] 0.155	[417] 0.239	[398] 0.999	[373] 0.172		[304] 0.464	0.001	0.002	0.106			
25	ALCHERA-004	[438] 0.011	[430] 0.038	[316] 0.338	[375] 0.017	[311] 0.088	[362] 0.144	[507] 0.394	[478] 0.529	[319] 0.991	[413] 0.424	[252] 0.708	[326] 0.546	0.001	0.001	0.046		0.000	
26	ALCHERA-005	[405] 0.007	[402] 0.027	[286] 0.265	[356] 0.012	[306] 0.081	[324] 0.118	[495] 0.314	[464] 0.439	[297] 0.985	[397] 0.305	[281] 0.908	[300] 0.455	0.000	0.001	0.042		0.000	
27	ALCHERA-006	[135] 0.001	[162] 0.009	[205] 0.096	[55] 0.001	[136] 0.008	[79] 0.052	[154] 0.005	[124] 0.025	[286] 0.982	[90] 0.006	[242] 0.493	[92] 0.094	0.000	0.001	0.042		0.000	
28	ALCHERA-007	[129] 0.001	[159] 0.009	[200] 0.095	[81] 0.001	[139] 0.008	[77] 0.052	[115] 0.004	[110] 0.023	[289] 0.982	[74] 0.005	[261] 0.743	[70] 0.087	0.000	0.001	0.042		0.000	
29	ALCHERA-008	[153] 0.001	[154] 0.009	[67] 0.049	[38] 0.001	[313] 0.096	[73] 0.052	[108] 0.003	[99] 0.022	[62] 0.177	[169] 0.010	[321] 1.000	[208] 0.186	0.000	0.000	0.040		0.000	
30	ALGORITHMSINC-000	[251] 0.002	[202] 0.011	[258] 0.181	[235] 0.003	[315] 0.107	[227] 0.083	[268] 0.016	[357] 0.130	[150] 0.507	[342] 0.108	[335] 1.000	[294] 0.433	0.000	0.000	0.041		0.000	
31	ALLGOVISION-000	[440] 0.011	[420] 0.033	[440] 0.893	[384] 0.021		[423] 0.282	[425] 0.088	[385] 0.166	[315] 0.990	[345] 0.117		[321] 0.526	0.002	0.003	0.122			
32	ALLGOVISION-001	[419] 0.009	[436] 0.038	[381] 0.657	[382] 0.021		[412] 0.241	[432] 0.101	[409] 0.221	[299] 0.986	[362] 0.150		[313] 0.491	0.001	0.001	0.042			
33	ALLGOVISION-002	[357] 0.004	[383] 0.023	[371] 0.580	[336] 0.008	[332] 0.161	[350] 0.132	[402] 0.065	[477] 0.520	[240] 0.950	[384] 0.232	[475] 1.000	[358] 0.716	0.000	0.000	0.041		0.000	
34	ALLGOVISION-003	[278] 0.002	[276] 0.014	[255] 0.175	[223] 0.003	[200] 0.015	[224] 0.082	[272] 0.017	[253] 0.059	[167] 0.566	[225] 0.021	[165] 0.147	[310] 0.478	0.001	0.000	0.042		0.000	
35	ALLGOVISION-004	[430] 0.010	[398] 0.026	[311] 0.321	[361] 0.013	[295] 0.059	[339] 0.127	[437] 0.114	[397] 0.190	[197] 0.747	[346] 0.121	[235] 0.418	[287] 0.412	0.001	0.000	0.042		0.000	
36	ALTTEKGLOBAL-000	[533] 0.274	[513] 0.255	[357] 0.526	[452] 0.380	[352] 0.419	[455] 0.632	[489] 0.278	[432] 0.267	[174] 0.617	[407] 0.383	[245] 0.536	[344] 0.641	0.000	0.001	0.048		0.001	
37	ANKE-000	[451] 0.013	[431] 0.038	[454] 0.930	[500] 1.000		[484] 1.000	[439] 0.117	[408] 0.220	[330] 0.994	[475] 1.000		[461] 1.000	0.000	0.001	0.080			
38	ANKE-001	[452] 0.013	[432] 0.038	[461] 0.945	[504] 1.000		[479] 1.000	[442] 0.119	[407] 0.220	[338] 0.994	[469] 1.000		[449] 1.000	0.000	0.001	0.080			
39	ANKE-002	[321] 0.002	[320] 0.016	[353] 0.516	[281] 0.005		[326] 0.119	[341] 0.031	[292] 0.079	[239] 0.947	[270] 0.034		[230] 0.245	0.001	0.001	0.049			
40	ANTHEUS-000	[404] 0.007	[412] 0.029	[299] 0.297	[393] 0.027	[330] 0.152	[379] 0.167	[355] 0.041	[494] 0.664	[204] 0.793	[448] 0.862	[406] 1.000	[422] 0.972	0.003	0.006	0.042		0.000	
41	ARATEK-001	[100] 0.001	[120] 0.008	[248] 0.152	[187] 0.002	[148] 0.009	[147] 0.065	[206] 0.008	[226] 0.050	[474] 1.000	[333] 0.086	[293] 0.971	[553] 1.000	0.000	0.000	0.000		0.000	
42	ARMATURA-000	[244] 0.002	[261] 0.013	[129] 0.060	[159] 0.002	[83] 0.005	[132] 0.062	[131] 0.004	[125] 0.025	[85] 0.214	[92] 0.006	[78] 0.048	[82] 0.090	0.001	0.001	0.056		0.001	
43	AWARE-003	[483] 0.030	[483] 0.090	[480] 0.966	[450] 0.316		[425] 0.290	[446] 0.128	[443] 0.298	[294] 0.984	[414] 0.428		[322] 0.530	0.004	0.003	0.874			
44	AWARE-004	[505] 0.068	[503] 0.176	[490] 0.975	[435] 0.122		[441] 0.414	[487] 0.268	[475] 0.509	[416] 1.000	[408] 0.397		[375] 0.816	0.003	0.003	0.776			
45	AWARE-005	[484] 0.031	[470] 0.067	[491] 0.978	[417] 0.048		[431] 0.308	[502] 0.363	[424] 0.253	[428] 1.000	[388] 0.255		[398] 0.916	0.001	0.002	0.189			
46	AWARE-006	[507] 0.069	[495] 0.128	[494] 0.983	[434] 0.111		[443] 0.421	[488] 0.275	[457] 0.398	[409] 0.999	[404] 0.368		[363] 0.749	0.001	0.002	0.189			

Table 20: **Miss rates by dataset:** *At left, rank 1 miss rates relevant to investigations; at right, with threshold set to target FPIR = 0.01 for higher volume, low prior, uses. Yellow indicates most accurate algorithm. Throughout blue superscripts indicate the rank of the algorithm for that column.*

2026/01/09 20:40:38

FNIR(N, R, T) = False neg. identification rate
FPIR(N, T) = False pos. identification rate
N = Num. enrolled subjects
R = Num. candidates examined
T = Threshold
T = 0 → Investigation
T > 0 → Identification

This publication is available free of charge from: https://doi.org/10.6028/NIST.IR.8271

#	ALGORITHM	INVESTIGATION MODE						IDENTIFICATION MODE						FAILURE TO EXTRACT					
		RANK ONE MISS RATE, FNIR(N, 0, 1)						HIGH T ⟶ FPIR = 0.001, FNIR(N, T, L)						FEATURES					
		N=1.6M						N=1.6M											
	GALLERY	MUGSHOT	MUGSHOT	MUGSHOT	VISA	BORDER	VISA	MUGSHOT	MUGSHOT	MUGSHOT	VISA	BORDER	VISA	MUGSHOT	MUGSHOT	MUGSHOT	VISA	BORDER	KIOSK
	PROBE	MUGSHOT	WEBCAM	PROFILE	BORDER	BOR¿10YR	KIOSK	MUGSHOT	WEBCAM	PROFILE	BORDER	BOR¿10YR	KIOSK	MUGSHOT	WEBCAM	PROFILE	BORDER	BOR¿10YR	KIOSK
47	AWARE-007	303 0.002	321 0.016	317 0.339	311 0.007	276 0.038	319 0.116	267 0.016	274 0.070	322 0.992	290 0.044	296 0.982	233 0.250	0.000	0.000	0.043		0.000	
48	AWIROS-000	408 0.007	417 0.031	453 0.930	379 0.018	318 0.109	376 0.165	491 0.291	471 0.471	443 1.000	458 0.976	368 1.000	441 0.999	0.000	0.000	0.000		0.000	
49	AYONIX-000	540 0.450	537 0.685	504 0.996	459 0.607		467 0.867	530 0.811	524 0.939	368 0.998	455 0.954		425 0.982	0.010	0.031	0.939			
50	AYONIX-001	534 0.341	524 0.527	500 0.993	473 0.994		463 0.778	532 0.824	519 0.920	407 0.999	464 0.999		420 0.969	0.010	0.031	0.939			
51	AYONIX-002	535 0.341	525 0.527	499 0.993	455 0.464		462 0.778	531 0.824	520 0.920	404 0.999	451 0.915		419 0.969	0.010	0.031	0.939			
52	BIOIDTECHSWISS-001	107 0.001	329 0.017	139 0.062	294 0.005	218 0.018	380 0.168	125 0.004	162 0.030	304 0.987	166 0.010	116 0.067	203 0.179	0.000	0.009	0.042		0.004	
53	BIOMETRIK-001	370 0.004	310 0.015	399 0.734	322 0.007	274 0.038	279 0.101	376 0.052	325 0.098	422 1.000	303 0.054	221 0.341	340 0.618	0.000	0.000	0.000		0.000	
54	CAMVI-003	499 0.052	484 0.090	443 0.910	429 0.093		437 0.360	406 0.071	359 0.132	259 0.970	344 0.114		283 0.402	0.006	0.013	0.675			
55	CAMVI-004	497 0.047	477 0.077	402 0.741	427 0.072		429 0.296	407 0.071	361 0.136	403 0.999	339 0.100		370 0.787	0.000	0.000	0.000			
56	CAMVI-005	504 0.065	492 0.103	404 0.743	432 0.098		436 0.341	430 0.099	394 0.179	413 1.000	365 0.156		438 0.999	0.000	0.000	0.000			
57	CANON-001	80 0.001	48 0.006	176 0.077	142 0.001	107 0.007	137 0.062	162 0.005	116 0.023	118 0.357	133 0.008	119 0.068	159 0.139	0.001	0.000	0.042		0.000	
58	CANON-002	111 0.001	53 0.006	203 0.095	111 0.001	114 0.007	127 0.059	140 0.004	90 0.020	128 0.400	190 0.013	127 0.075	211 0.188	0.001	0.000	0.042		0.000	
59	CANON-003	37 0.001	118 0.008	153 0.067	246 0.004	103 0.006	68 0.051	71 0.002	51 0.012	76 0.199	89 0.006	39 0.030	40 0.076	0.000	0.003	0.041		0.003	
60	CIB-000	196 0.001	127 0.008	191 0.090	189 0.002	175 0.011	167 0.069	239 0.012	218 0.045	438 1.000	207 0.017	158 0.141	393 0.894	0.000	0.000	0.000		0.000	
61	CLEARVIEWAI-000	82 0.001	80 0.007	80 0.051	137 0.001	92 0.006	109 0.056	171 0.005	131 0.025	266 0.974	134 0.008	98 0.057	243 0.268	0.000	0.000	0.037		0.000	
62	CLEARVIEWAI-001	83 0.001	91 0.007	31 0.044	57 0.001	35 0.004	94 0.054	112 0.003	89 0.020	55 0.167	82 0.005	70 0.042	54 0.079	0.000	0.000	0.040		0.000	
63	CLEARVIEWAI-002	93 0.001	93 0.007	32 0.044	60 0.001	36 0.004	88 0.054	123 0.004	98 0.022	58 0.170	83 0.006	69 0.041	48 0.078	0.000	0.000	0.040		0.000	
64	CLEARVIEWAI-003	90 0.001	83 0.007	22 0.043	53 0.001	31 0.003	98 0.055	70 0.002	68 0.015	33 0.128	69 0.005	60 0.038	50 0.079	0.000	0.000	0.040		0.000	
65	CLOUDWALK-HR-000	186 0.001	179 0.010	91 0.053	178 0.002	102 0.006	115 0.057	59 0.002	57 0.013	31 0.123	70 0.005	47 0.033	105 0.099	0.001	0.000	0.042		0.000	
66	CLOUDWALK-MT-000	231 0.001	217 0.011	43 0.047	92 0.001	40 0.004	64 0.051	57 0.002	56 0.013	18 0.099	33 0.002	14 0.018	33 0.072	0.001	0.000	0.042		0.000	
67	CLOUDWALK-MT-001	229 0.001	218 0.011	19 0.043	11 0.001	16 0.003	10 0.042	52 0.002	44 0.012	4 0.059	8 0.001	10 0.015	7 0.056	0.001	0.000	0.042		0.000	
68	CLOUDWALK-MT-002	230 0.001	216 0.011	12 0.041	9 0.001	10 0.002	8 0.041	49 0.002	41 0.011	2 0.053	5 0.001	6 0.013	6 0.055	0.001	0.000	0.042		0.000	
69	COGENT-000	431 0.010	450 0.046	479 0.965				378 0.052	365 0.140	343 0.995				0.000	0.000	0.000			
70	COGENT-001	432 0.010	449 0.046	478 0.965				379 0.052	364 0.140	344 0.995				0.000	0.000	0.000			
71	COGENT-002	349 0.003	358 0.020	448 0.924				362 0.044	324 0.098	366 0.998				0.000	0.000	0.000			
72	COGENT-003	351 0.003	365 0.021	459 0.938				365 0.045	318 0.095	370 0.998				0.000	0.000	0.000			
73	COGENT-004	260 0.002	269 0.013	447 0.921	257 0.004	222 0.019	314 0.113	342 0.033	230 0.051	364 0.997	229 0.022	151 0.126	301 0.456	0.000	0.000	0.000		0.000	
74	COGENT-005	216 0.001	196 0.010	223 0.116	190 0.002	170 0.010	327 0.120	214 0.009	193 0.037	309 0.989	174 0.011	132 0.082	396 0.905	0.000	0.000	0.000		0.000	
75	COGENT-006	132 0.001	95 0.007	116 0.056	121 0.001	123 0.007	280 0.101	134 0.004	117 0.023	95 0.229	103 0.006	236 0.422	150 0.130	0.000	0.000	0.041		0.000	
76	COGENT-007	85 0.001	126 0.008	96 0.053	114 0.001	98 0.006	285 0.103	109 0.003	96 0.021	68 0.185	105 0.006	76 0.047	170 0.144	0.000	0.000	0.043		0.000	
77	COGNITEC-000	474 0.025	464 0.059	476 0.963				461 0.160	444 0.303	320 0.992				0.003	0.002	0.924			
78	COGNITEC-001	442 0.011	422 0.034	470 0.957				431 0.101	413 0.230	486 1.000				0.003	0.002	0.924			
79	COGNITEC-002	386 0.005	392 0.025	463 0.948				381 0.053	393 0.178	439 1.000				0.003	0.002	0.924			
80	COGNITEC-003	390 0.006	391 0.025	452 0.929				377 0.052	383 0.162	444 1.000				0.004	0.002	0.878			
81	COGNITEC-004	336 0.003	318 0.016	426 0.811	359 0.013	293 0.057	361 0.143	340 0.031	322 0.097	312 0.990	317 0.068	215 0.316	248 0.288	0.002	0.001	0.635		0.006	
82	COGNITEC-005	213 0.001	189 0.010	395 0.710	386 0.021	273 0.037	318 0.115	219 0.009	207 0.041	511 1.000	285 0.041	175 0.157	202 0.179	0.002	0.001	0.614		0.017	
83	COGNITEC-006	200 0.001	175 0.010	392 0.699	320 0.007	241 0.024	308 0.111	201 0.007	205 0.040	487 1.000	256 0.030	181 0.171	352 0.681	0.002	0.001	0.568		0.003	
84	COGNITEC-007	168 0.001	139 0.009	290 0.275	295 0.005	231 0.022	267 0.098	169 0.005	181 0.034	177 0.621	241 0.026	195 0.210	187 0.160	0.000	0.001	0.100		0.002	
85	COGNITEC-008	154 0.001	155 0.009	273 0.216	274 0.004	217 0.018	257 0.095	175 0.006	185 0.035	166 0.564	242 0.026	161 0.142	179 0.155	0.000	0.001	0.091		0.001	
86	COGNITEC-009	192 0.001	164 0.009	274 0.219	270 0.004	204 0.016	282 0.102	179 0.006	186 0.035	165 0.554	238 0.025	149 0.124	181 0.156	0.001	0.001	0.106		0.001	
87	COMPAL-000	228 0.001	345 0.019	138 0.062	424 0.065	298 0.063	334 0.125	204 0.008	199 0.038		321 0.072	142 0.104	171 0.147	0.000	0.012	0.000		0.067	
88	COMPAL-001	401 0.007	290 0.014	132 0.060	310 0.006	167 0.010	148 0.065	242 0.012	176 0.033	132 0.422	188 0.013	135 0.090	134 0.117	0.004	0.002	0.049		0.005	
89	CORSIGHT-000	89 0.001	79 0.007	148 0.065	112 0.001	106 0.007	114 0.057	180 0.006	155 0.029	154 0.517	158 0.009	117 0.067	333 0.594	0.000	0.000	0.000		0.000	
90	CORSIGHT-001	94 0.001	78 0.007	131 0.060	106 0.001	93 0.006	103 0.055	188 0.006	178 0.034	142 0.460	144 0.008	104 0.062	158 0.138	0.000	0.000	0.000		0.000	
91	CUBOX-000	173 0.001	183 0.010	52 0.048	151 0.002	61 0.004	54 0.049	84 0.002	83 0.019	50 0.158	62 0.004	36 0.028	34 0.073	0.001	0.000	0.042		0.000	
92	CUBOX-001	137 0.001	131 0.008	68 0.049	97 0.001	68 0.004	39 0.047	89 0.003	93 0.021	84 0.212	113 0.007	121 0.068	64 0.085	0.001	0.001	0.041		0.000	

Table 21: **Miss rates by dataset:** *At left, rank 1 miss rates relevant to investigations; at right, with threshold set to target FPIR = 0.01 for higher volume, low prior, uses. Yellow indicates most accurate algorithm. Throughout blue superscripts indicate the rank of the algorithm for that column.*

2026/01/09 20:40:38

FNIR(N, R, T) = False neg. identification rate
FPIR(N, T) = False pos. identification rate

N = Num. enrolled subjects
R = Num. candidates examined

T = Threshold

T = 0 → Investigation
T > 0 → Identification

This publication is available free of charge from: https://doi.org/10.6028/NIST.IR.8271

#	ALGORITHM	INVESTIGATION MODE						IDENTIFICATION MODE						FAILURE TO EXTRACT					
		RANK ONE MISS RATE, FNIR(N, 0, 1)						HIGH T ⟶ FPIR = 0.001, FNIR(N, T, L)						FEATURES					
		N=1.6M						N=1.6M											
	GALLERY	MUGSHOT	MUGSHOT	MUGSHOT	VISA	BORDER	VISA	MUGSHOT	MUGSHOT	MUGSHOT	VISA	BORDER	VISA	MUGSHOT	MUGSHOT	MUGSHOT	VISA	BORDER	KIOSK
	PROBE	MUGSHOT	WEBCAM	PROFILE	BORDER	BOR¿10YR	KIOSK	MUGSHOT	WEBCAM	PROFILE	BORDER	BOR¿10YR	KIOSK	MUGSHOT	WEBCAM	PROFILE	BORDER	BOR¿10YR	KIOSK
93	CUBOX-002	189 0.001	224 0.011	76 0.050	99 0.001	51 0.004	27 0.046	100 0.003	106 0.022	63 0.181	65 0.004	62 0.038	45 0.077	0.001	0.001	0.040		0.000	
94	CUBOX-003	202 0.001	239 0.012	110 0.056	109 0.001	71 0.005	51 0.048	105 0.003	111 0.023	88 0.219	93 0.006	86 0.051	59 0.082	0.001	0.001	0.040		0.000	
95	CYBERLINK-000	353 0.004	354 0.020	396 0.713	326 0.007		352 0.134	389 0.056	340 0.116	347 0.995	314 0.063		267 0.339	0.001	0.001	0.063			
96	CYBERLINK-001	347 0.003	337 0.018	397 0.728	315 0.007		351 0.133	382 0.053	337 0.109	342 0.995	311 0.062		347 0.652	0.000	0.000	0.040			
97	CYBERLINK-002	312 0.002	241 0.012	369 0.572	250 0.004		299 0.107	257 0.014	240 0.053	308 0.988	236 0.024		249 0.288	0.001	0.000	0.042			
98	CYBERLINK-003	201 0.001	152 0.009	343 0.468	218 0.003	176 0.012	221 0.082	202 0.007	184 0.035	263 0.972	181 0.012	141 0.100	273 0.368	0.000	0.000	0.039		0.000	
99	CYBERLINK-004	215 0.001	234 0.011	330 0.416	216 0.003	171 0.011	290 0.104	194 0.007	188 0.036	456 1.000	187 0.013	143 0.109	416 0.954	0.000	0.000	0.011		0.000	
100	CYBERLINK-005	236 0.001	207 0.011	265 0.200	197 0.002	161 0.010	269 0.098	223 0.010	204 0.041	424 1.000	193 0.014	134 0.089	405 0.926	0.000	0.000	0.034		0.000	
101	CYBERLINK-006	103 0.001	72 0.007	186 0.085	65 0.001	54 0.004	171 0.071	82 0.002	79 0.018	300 0.986	66 0.004	125 0.073	207 0.186	0.000	0.000	0.034		0.000	
102	DAHUA-000	421 0.009	397 0.026					421 0.086	360 0.135					0.004	0.003				
103	DAHUA-001	396 0.006	386 0.024	391 0.699				409 0.072	348 0.122	279 0.980				0.002	0.002	0.346			
104	DAHUA-002	239 0.001	238 0.012	298 0.296	213 0.003		228 0.084	258 0.015	221 0.046	178 0.634	204 0.017		185 0.159	0.001	0.000	0.099			
105	DAHUA-003	120 0.001	84 0.007	263 0.197	180 0.002	154 0.009	185 0.073	249 0.014	206 0.041	169 0.574	184 0.013	130 0.081	153 0.134	0.000	0.000	0.000		0.000	
106	DAHUA-004	77 0.001	100 0.008	234 0.134	154 0.002	113 0.007	162 0.069	193 0.007	135 0.026	147 0.479	146 0.008	87 0.051	133 0.113	0.000	0.000	0.000		0.000	
107	DAON-000	356 0.004	330 0.017	356 0.525	282 0.005	226 0.020	335 0.125	304 0.022	257 0.061	420 1.000	239 0.025	183 0.173	383 0.846	0.002	0.002	0.108		0.001	
108	DAON-001	475 0.025	461 0.057	464 0.951	412 0.040	284 0.046	226 0.083	357 0.043	363 0.140	241 0.952	315 0.064	172 0.154	188 0.161	0.014	0.042	0.950		0.034	
109	DAON-002	142 0.001	166 0.009	216 0.109	176 0.002	188 0.013	155 0.067	195 0.007	215 0.044		197 0.015	156 0.141	470 1.000	0.000	0.001	0.000		0.000	
110	DATECH-000	155 0.001	133 0.008	253 0.168	134 0.001	282 0.045	96 0.055	203 0.007	197 0.038	356 0.996	201 0.016	283 0.926	256 0.311	0.000	0.000	0.039		0.000	
111	DATECH-001	91 0.001	125 0.008	233 0.132	104 0.001	290 0.052	112 0.056	189 0.006	259 0.062	327 0.993	281 0.039	307 0.998	271 0.360	0.000	0.000	0.038		0.000	
112	DECATUR-000	275 0.002	236 0.011	275 0.220	264 0.004	221 0.019	304 0.109	307 0.023	265 0.066	183 0.671	246 0.027	182 0.173	227 0.239	0.001	0.000	0.044		0.001	
113	DEEPGLINT-001	181 0.001	77 0.007	259 0.190	205 0.002		187 0.073	99 0.003	59 0.014	411 1.000	108 0.006		184 0.159	0.000	0.000	0.038			
114	DEEPSEA-001	361 0.004	316 0.016	427 0.812	339 0.010		359 0.140	367 0.046	328 0.101	296 0.984	327 0.077		263 0.326	0.000	0.001	0.047			
115	DERMALOG-003	517 0.126	510 0.217		449 0.296		453 0.560	515 0.482	491 0.655		438 0.677		388 0.870	0.002	0.002	0.103			
116	DERMALOG-004	516 0.125	508 0.215	451 0.929	437 0.135		446 0.467	514 0.479	492 0.657	348 0.995	429 0.603		385 0.856	0.001	0.002	0.107			
117	DERMALOG-005	455 0.015	429 0.037	390 0.697	444 0.242		440 0.384	424 0.088	375 0.154	314 0.990	396 0.300		338 0.614	0.001	0.002	0.102			
118	DERMALOG-006	414 0.008	390 0.024	378 0.615	343 0.010		371 0.155	375 0.051	330 0.105	282 0.981	309 0.059		261 0.318	0.003	0.006	0.181			
119	DERMALOG-007	421 0.009	400 0.027	384 0.671	369 0.014		381 0.170	422 0.086	373 0.152	313 0.990	338 0.099		328 0.557	0.001	0.002	0.102			
120	DERMALOG-008	323 0.003	301 0.015	351 0.511	312 0.007	259 0.029	358 0.139	364 0.045	315 0.094	451 1.000	305 0.057	228 0.382	411 0.940	0.000	0.000	0.002		0.000	
121	DERMALOG-009	322 0.002	289 0.014	250 0.157	321 0.007	367 0.999	293 0.106	292 0.020	266 0.066	440 1.000	258 0.031	310 0.999	380 0.840	0.001	0.001	0.018		0.003	
122	DERMALOG-010	283 0.002	231 0.011	111 0.056	411 0.038	325 0.124	315 0.113	192 0.007	244 0.055	390 0.999	335 0.089	316 1.000	319 0.522	0.001	0.001	0.018		0.003	
123	DERMALOG-011	204 0.001	191 0.010	188 0.086	234 0.003	261 0.031	248 0.092	297 0.021	304 0.087	376 0.998	351 0.129	300 0.991	366 0.764	0.000	0.000	0.013		0.000	
124	DERMALOG-012	270 0.002	267 0.013	206 0.096	221 0.003	194 0.014	176 0.071	296 0.021	268 0.067	148 0.505	231 0.023	166 0.147	286 0.409	0.001	0.000	0.040		0.000	
125	DERMALOG-013	252 0.002	262 0.013	207 0.096	230 0.003	195 0.014	178 0.071	295 0.021	271 0.068	232 0.908	232 0.024	171 0.153	324 0.541	0.000	0.000	0.038		0.000	
126	DERMALOG-014	343 0.003	315 0.016	228 0.123	338 0.009	235 0.023	300 0.107	299 0.021	272 0.069	231 0.907	249 0.028	174 0.156	293 0.432	0.000	0.000	0.038		0.000	
127	DERMALOG-015	203 0.001	214 0.011	115 0.056	175 0.002	117 0.007	107 0.056	156 0.005	167 0.031	109 0.313	152 0.009	110 0.065	183 0.158	0.001	0.000	0.040		0.000	
128	DIGIDATA-000	543 0.590	526 0.548	441 0.894	460 0.642	359 0.707	465 0.813	521 0.610	482 0.577	335 0.994	434 0.646	268 0.789	378 0.824	0.002	0.001	0.070		0.001	
129	DILUSENSE-000	285 0.002	247 0.012	294 0.289	329 0.008	255 0.028	273 0.099	338 0.030	291 0.078	179 0.651	279 0.039	251 0.664	215 0.203	0.001	0.001	0.219		0.006	
130	DILUSENSE-001	182 0.001	171 0.010	281 0.241	303 0.006	203 0.016	240 0.088	208 0.008	182 0.034	137 0.450	198 0.015	244 0.511	157 0.137	0.001	0.001	0.219		0.007	
131	EINETWORKSINDIA-000	234 0.001	142 0.009	327 0.386	241 0.004	190 0.013	289 0.104	262 0.015	216 0.044	363 0.997	218 0.020	240 0.455	186 0.159	0.001	0.001	0.055		0.002	
132	EINETWORKSINDIA-001	222 0.001	141 0.009	324 0.375	220 0.003	196 0.014	261 0.096	266 0.016	223 0.048	361 0.997	322 0.072	291 0.957	369 0.782	0.001	0.000	0.043		0.000	
133	EINETWORKSINDIA-002	101 0.001	58 0.007	72 0.050	44 0.001	267 0.033	63 0.050	121 0.004	103 0.022	71 0.188	131 0.007	289 0.953	145 0.127	0.000	0.000	0.041		0.000	
134	EYEDEA-003	509 0.080	498 0.148	474 0.960	433 0.101		439 0.379	505 0.387	480 0.543	339 0.994	427 0.570		371 0.792	0.001	0.003	0.161			
135	F8-001	446 0.012		382 0.665	538 1.000		530 1.000	462 0.166		379 0.998				0.004	1.000	0.158			
136	FACEPHI-000	242 0.002	294 0.014	194 0.093	229 0.003	156 0.009	288 0.104	187 0.006	183 0.034	121 0.367	163 0.009	113 0.066	154 0.135	0.001	0.007	0.049		0.001	
137	FASTLAHORE-000	478 0.026	500 0.154	458 0.938	445 0.277	371 1.000	449 0.499	477 0.214	540 1.000	442 1.000	486 1.000	506 1.000	475 1.000	0.000	0.064	0.000		0.000	
138	FCI-000	241 0.002	252 0.012	135 0.061	107 0.001	294 0.057	66 0.051	183 0.006	138 0.026	243 0.957	150 0.008	266 0.777	115 0.103	0.000	0.000	0.000		0.000	

Table 22: **Miss rates by dataset:** *At left, rank 1 miss rates relevant to investigations; at right, with threshold set to target FPIR = 0.01 for higher volume, low prior, uses. Yellow indicates most accurate algorithm. Throughout blue superscripts indicate the rank of the algorithm for that column.*

FNIR(N, R, T) = FPIR(N, T) =

False neg. identification rate
False pos. identification rate

N = Num. enrolled subjects
R = Num. candidates examined

T = Threshold

T = 0 → Investigation
T > 0 → Identification

This publication is available free of charge from: https://doi.org/10.6028/NIST.IR.8271

2026/01/09 20:40:38

FNIR(N, R, T) = False neg. identification rate
FPIR(N, T) = False pos. identification rate
N = Num. enrolled subjects
R = Num. candidates examined
T = Threshold
T = 0 → Investigation
T > 0 → Identification

#	ALGORITHM	INVESTIGATION MODE						IDENTIFICATION MODE						FAILURE TO EXTRACT					
		RANK ONE MISS RATE, FNIR(N, 0, 1)						HIGH T ⟶ FPIR = 0.001, FNIR(N, T, L)						FEATURES					
		N=1.6M						N=1.6M											
	GALLERY	MUGSHOT	MUGSHOT	MUGSHOT	VISA	BORDER	VISA	MUGSHOT	MUGSHOT	MUGSHOT	VISA	BORDER	VISA	MUGSHOT	MUGSHOT	MUGSHOT	VISA	BORDER	KIOSK
	PROBE	MUGSHOT	WEBCAM	PROFILE	BORDER	BOR¿10YR	KIOSK	MUGSHOT	WEBCAM	PROFILE	BORDER	BOR¿10YR	KIOSK	MUGSHOT	WEBCAM	PROFILE	BORDER	BOR¿10YR	KIOSK
139	FINCORE-000	[437] 0.010	[423] 0.034	[410] 0.764	[402] 0.032	[323] 0.117	[394] 0.191	[451] 0.133	[406] 0.217	[431] 1.000	[376] 0.187	[247] 0.598	[302] 0.458	0.000	0.001	0.043		0.000	
140	FIRSTCREDITKZ-001	[123] 0.001	[130] 0.008	[185] 0.084	[182] 0.002	[163] 0.010	[144] 0.065	[87] 0.003	[84] 0.019	[104] 0.282	[126] 0.007	[103] 0.061	[101] 0.097	0.000	0.001	0.047		0.001	
141	FPT-000	[250] 0.002	[296] 0.014	[157] 0.068	[285] 0.005	[340] 0.210	[276] 0.100	[217] 0.009	[453] 0.372	[380] 0.999	[403] 0.360	[383] 1.000	[408] 0.935	0.000	0.000	0.000		0.000	
142	FUJITSULAB-000	[286] 0.002	[282] 0.014	[335] 0.434	[255] 0.004	[233] 0.023	[270] 0.098	[293] 0.020	[247] 0.056		[233] 0.024	[184] 0.177	[228] 0.240	0.000	0.001	0.016		0.000	
143	FUJITSULAB-001	[243] 0.002	[274] 0.013	[338] 0.449	[259] 0.004	[245] 0.026	[295] 0.106	[280] 0.018	[249] 0.058	[324] 0.992	[235] 0.024	[258] 0.739	[232] 0.247	0.000	0.003	0.150		0.002	
144	GLORY-000	[521] 0.178	[517] 0.320	[503] 0.993	[443] 0.228		[456] 0.678	[503] 0.367	[481] 0.547	[341] 0.995	[418] 0.453		[379] 0.839	0.011	0.013	0.985			
145	GLORY-001	[518] 0.126	[514] 0.267	[498] 0.992	[441] 0.178		[454] 0.594	[492] 0.305	[479] 0.537	[328] 0.993	[410] 0.408		[376] 0.819	0.011	0.013	0.988			
146	GORILLA-001	[501] 0.060	[488] 0.095	[456] 0.936	[425] 0.069		[434] 0.329	[509] 0.406	[468] 0.453	[478] 1.000	[419] 0.468		[532] 1.000	0.001	0.001	0.069			
147	GORILLA-002	[467] 0.019	[446] 0.044	[406] 0.751	[392] 0.027		[406] 0.214	[471] 0.188	[433] 0.268	[470] 1.000	[387] 0.250		[444] 1.000	0.001	0.001	0.069			
148	GORILLA-003	[487] 0.036	[472] 0.070	[428] 0.818	[416] 0.048		[417] 0.265	[496] 0.317	[463] 0.434	[492] 1.000	[409] 0.407		[446] 1.000	0.001	0.001	0.069			
149	GORILLA-004	[391] 0.006	[387] 0.024	[388] 0.693	[351] 0.012		[375] 0.162	[428] 0.089	[381] 0.160	[244] 0.958	[356] 0.135		[296] 0.438	0.000	0.001	0.042			
150	GORILLA-005	[335] 0.003	[338] 0.018	[264] 0.199	[302] 0.006		[332] 0.124	[394] 0.058	[367] 0.142	[187] 0.697	[334] 0.088		[259] 0.315	0.000	0.000	0.040			
151	GORILLA-006	[227] 0.001	[243] 0.012	[217] 0.112	[233] 0.003	[212] 0.018	[292] 0.105	[326] 0.027	[308] 0.089	[160] 0.525	[247] 0.028	[179] 0.166	[220] 0.218	0.000	0.000	0.041		0.000	
152	GORILLA-007	[218] 0.001	[204] 0.011	[209] 0.103	[201] 0.002	[206] 0.016	[239] 0.088	[323] 0.027	[290] 0.077	[162] 0.529	[240] 0.026	[204] 0.264	[200] 0.178	0.000	0.000	0.041		0.000	
153	GORILLA-008	[188] 0.001	[177] 0.010	[174] 0.075	[163] 0.002	[182] 0.012	[222] 0.082	[308] 0.024	[299] 0.083	[139] 0.457	[255] 0.030	[218] 0.319	[199] 0.178	0.000	0.000	0.041		0.000	
154	GRIAULE-000	[305] 0.002	[275] 0.014	[309] 0.319	[346] 0.011	[264] 0.031	[337] 0.126	[290] 0.020	[261] 0.063	[345] 0.995	[265] 0.033	[188] 0.185	[213] 0.198	0.000	0.002	0.090		0.001	
155	GRIAULE-001	[117] 0.001	[115] 0.008	[227] 0.123	[84] 0.001	[237] 0.023	[145] 0.065	[141] 0.004	[149] 0.028	[216] 0.863	[121] 0.007	[302] 0.995	[104] 0.099	0.000	0.000	0.000		0.000	
156	GTELOTS-000	[525] 0.194	[509] 0.217	[368] 0.558	[446] 0.278	[353] 0.446	[452] 0.560	[475] 0.206	[426] 0.256	[191] 0.727	[394] 0.292	[554] 1.000	[335] 0.603	0.001	0.000	0.043		0.000	
157	HIK-003	[443] 0.011	[404] 0.027	[387] 0.685	[354] 0.012		[368] 0.151	[433] 0.102	[377] 0.158	[257] 0.968	[359] 0.142		[299] 0.445	0.000	0.000	0.048			
158	HIK-004	[441] 0.011	[401] 0.027	[401] 0.740	[352] 0.012		[370] 0.152	[429] 0.098	[374] 0.153	[267] 0.976	[357] 0.137		[295] 0.434	0.000	0.000	0.048			
159	HIK-005	[369] 0.004	[323] 0.017	[359] 0.530	[318] 0.007		[307] 0.111	[359] 0.043	[289] 0.077	[408] 0.999	[316] 0.068		[323] 0.541	0.000	0.000	0.000			
160	HIK-006	[368] 0.004	[322] 0.017	[360] 0.530				[368] 0.047	[303] 0.086	[472] 1.000				0.000	0.000	0.000			
161	HISIGN-001	[124] 0.001	[132] 0.008	[247] 0.150	[171] 0.002	[207] 0.016	[200] 0.076	[199] 0.007	[192] 0.037	[310] 0.990	[191] 0.013	[273] 0.824	[169] 0.143	0.000	0.000	0.041		0.000	
162	HYPERVERGE-001	[167] 0.001	[223] 0.011	[112] 0.056	[148] 0.002	[111] 0.007	[131] 0.061	[136] 0.004	[164] 0.031	[82] 0.210	[123] 0.007	[91] 0.053	[111] 0.101	0.001	0.000	0.041		0.000	
163	HYPERVERGE-002	[162] 0.001	[215] 0.011	[82] 0.052	[126] 0.001	[96] 0.006	[123] 0.058	[110] 0.003	[143] 0.027	[77] 0.201	[88] 0.006	[80] 0.048	[91] 0.093	0.001	0.000	0.041		0.000	
164	HYPERVERGE-003	[178] 0.001	[237] 0.011	[150] 0.065	[170] 0.002	[135] 0.008	[134] 0.062	[198] 0.007	[208] 0.042	[101] 0.274	[176] 0.012	[109] 0.065	[119] 0.106	0.001	0.000	0.041		0.000	
165	HYUNDAI-ROBOTICSLAB-000	[317] 0.002	[308] 0.015	[262] 0.195	[380] 0.020	[329] 0.133	[430] 0.298	[248] 0.013	[462] 0.452	[184] 0.672	[422] 0.492	[326] 1.000	[382] 0.870	0.001	0.001	0.045		0.009	
166	HYUNDAI-ROBOTICSLAB-001	[225] 0.001	[367] 0.021	[260] 0.192	[396] 0.029	[345] 0.252	[389] 0.178	[243] 0.013	[503] 0.774	[213] 0.839	[441] 0.699	[517] 1.000	[409] 0.937	0.000	0.001	0.041		0.001	
167	HYUNDAI-ROBOTICSLAB-002	[75] 0.001	[66] 0.007	[74] 0.050	[131] 0.001	[320] 0.112	[143] 0.064	[165] 0.005	[396] 0.189	[94] 0.228	[318] 0.068	[327] 1.000	[298] 0.440	0.000	0.000	0.040		0.000	
168	HZAILU-000	[284] 0.002	[273] 0.013	[270] 0.235	[219] 0.003	[201] 0.015	[244] 0.090	[288] 0.019	[231] 0.051	[254] 0.967	[221] 0.020	[214] 0.316	[175] 0.153	0.001	0.001	0.054		0.001	
169	HZAILU-001	[257] 0.002	[221] 0.011	[204] 0.095	[196] 0.002	[321] 0.113	[247] 0.092	[209] 0.008	[395] 0.183	[303] 0.986	[380] 0.196	[550] 1.000	[351] 0.679	0.000	0.000	0.039		0.000	
170	HZAILU-002	[261] 0.002	[220] 0.011	[218] 0.112	[169] 0.002	[164] 0.010	[199] 0.076	[205] 0.008	[200] 0.039	[188] 0.701	[177] 0.012	[115] 0.066	[265] 0.330	0.001	0.000	0.041		0.000	
171	HZAILU-003	[212] 0.001	[210] 0.011	[197] 0.094	[120] 0.001	[118] 0.007	[182] 0.072	[207] 0.008	[196] 0.038	[163] 0.545	[162] 0.009	[106] 0.062	[137] 0.119	0.001	0.000	0.041		0.000	
172	HZAILU-004	[146] 0.001	[192] 0.010	[180] 0.079	[87] 0.001	[75] 0.005	[174] 0.071	[135] 0.004	[168] 0.031	[126] 0.390	[86] 0.006	[74] 0.045	[112] 0.102	0.001	0.000	0.041		0.000	
173	HZAILU-005	[144] 0.001	[186] 0.010	[151] 0.065	[68] 0.001	[43] 0.004	[156] 0.067	[106] 0.003	[123] 0.025	[113] 0.329	[55] 0.004	[46] 0.033	[93] 0.094	0.001	0.000	0.041		0.000	
174	HZAILU-006	[139] 0.001	[185] 0.010	[142] 0.063	[63] 0.001	[38] 0.004	[153] 0.066	[104] 0.003	[102] 0.022	[112] 0.325	[52] 0.004	[40] 0.030	[85] 0.091	0.001	0.000	0.041		0.000	
175	I2V-001	[326] 0.003	[309] 0.015	[193] 0.092	[290] 0.005	[209] 0.017	[152] 0.066	[371] 0.049	[526] 0.966	[417] 1.000	[450] 0.905	[466] 1.000	[426] 0.983	0.000	0.001	0.040		0.000	
176	ICEHOUSE-000	[371] 0.004	[409] 0.028	[416] 0.793	[341] 0.010	[326] 0.125	[373] 0.158	[427] 0.089	[515] 0.852	[423] 1.000	[343] 0.111	[387] 1.000	[307] 0.470	0.001	0.002	0.053		0.000	
177	ICM-000	[380] 0.005	[415] 0.031	[468] 0.957	[349] 0.012	[278] 0.040	[382] 0.174	[317] 0.026	[314] 0.092	[252] 0.965	[274] 0.036	[202] 0.241	[229] 0.242	0.005	0.014	0.949		0.006	
178	ICM-001	[332] 0.003	[319] 0.016	[325] 0.375	[291] 0.005	[256] 0.028	[312] 0.112	[335] 0.029	[422] 0.251	[433] 1.000	[398] 0.307	[332] 1.000	[389] 0.878	0.001	0.002	0.096		0.001	
179	IDEMIA-003	[400] 0.007	[421] 0.034	[469] 0.957	[377] 0.018		[402] 0.210	[369] 0.047	[384] 0.165		[348] 0.123		[367] 0.766	0.000	0.000	0.041			
180	IDEMIA-004	[395] 0.006	[418] 0.032	[462] 0.947	[378] 0.018		[403] 0.210	[352] 0.037	[344] 0.118	[264] 0.973	[349] 0.123		[368] 0.766	0.000	0.000	0.041			
181	IDEMIA-005	[413] 0.008	[438] 0.039	[466] 0.953	[388] 0.021		[407] 0.217	[361] 0.044	[372] 0.150	[272] 0.977	[352] 0.130		[390] 0.879	0.000	0.000	0.041			
182	IDEMIA-006	[427] 0.009	[474] 0.072	[483] 0.969	[398] 0.030		[415] 0.253	[358] 0.043	[411] 0.226	[289] 0.982	[360] 0.144		[360] 0.733	0.000	0.000	0.041			
183	IDEMIA-007	[309] 0.002	[307] 0.015	[554] 1.000	[304] 0.006	[270] 0.036	[347] 0.131	[279] 0.018	[243] 0.055	[527] 1.000	[298] 0.052	[186] 0.182	[514] 1.000	0.000	0.000	0.040		0.000	
184	IDEMIA-008	[72] 0.001	[59] 0.007	[160] 0.069	[145] 0.001	[115] 0.007	[198] 0.075	[51] 0.002	[55] 0.013	[74] 0.195	[68] 0.005	[55] 0.036	[120] 0.106	0.000	0.000	0.040		0.000	

Table 23: **Miss rates by dataset:** *At left, rank 1 miss rates relevant to investigations; at right, with threshold set to target FPIR = 0.01 for higher volume, low prior, uses. Yellow indicates most accurate algorithm. Throughout blue superscripts indicate the rank of the algorithm for that column.*

This publication is available free of charge from: https://doi.org/10.6028/NIST.IR.8271

#	ALGORITHM	INVESTIGATION MODE						IDENTIFICATION MODE						FAILURE TO EXTRACT					
		RANK ONE MISS RATE, FNIR(N, 0, 1)						HIGH T → FPIR = 0.001, FNIR(N, T, L)						FEATURES					
		N=1.6M						N=1.6M											
	GALLERY	MUGSHOT	MUGSHOT	MUGSHOT	VISA	BORDER	VISA	MUGSHOT	MUGSHOT	MUGSHOT	VISA	BORDER	VISA	MUGSHOT	MUGSHOT	MUGSHOT	VISA	BORDER	KIOSK
	PROBE	MUGSHOT	WEBCAM	PROFILE	BORDER	BORˌ10YR	KIOSK	MUGSHOT	WEBCAM	PROFILE	BORDER	BORˌ10YR	KIOSK	MUGSHOT	WEBCAM	PROFILE	BORDER	BORˌ10YR	KIOSK
185	IDEMIA-009	[50] 0.001	[55] 0.006	[105] 0.055	[88] 0.001	[74] 0.005	[71] 0.051	[35] 0.001	[32] 0.011	[36] 0.131	[39] 0.003	[30] 0.027	[37] 0.074	0.000	0.000	0.040		0.000	
186	IDEMIA-010	[27] 0.001	[50] 0.006	[53] 0.048	[45] 0.001	[39] 0.004	[55] 0.049	[7] 0.001	[11] 0.008	[27] 0.120	[25] 0.002	[33] 0.028	[28] 0.070	0.000	0.000	0.037		0.000	
187	IDEMIA-011	[68] 0.001	[102] 0.008	[16] 0.042	[42] 0.001	[29] 0.003	[14] 0.043	[11] 0.001	[26] 0.009	[9] 0.070	[11] 0.002	[25] 0.025	[9] 0.061	0.000	0.000	0.036		0.000	
188	IDEMIA-012	[73] 0.001	[89] 0.007	[8] 0.041	[28] 0.001	[15] 0.003	[6] 0.041	[10] 0.001	[16] 0.009	[7] 0.069	[23] 0.002	[13] 0.016	[11] 0.061	0.000	0.000	0.036		0.000	
189	IDENTY-000	[554] 1.000	[546] 0.999	[549] 1.000	[472] 0.991	[369] 1.000	[473] 0.992	[551] 1.000	[534] 0.999	[525] 1.000	[461] 0.991	[318] 1.000	[431] 0.992	0.001	0.001	0.052		0.000	
190	IMAGUS-002	[530] 0.220	[515] 0.301	[496] 0.988				[526] 0.749	[509] 0.816	[476] 1.000				0.004	0.008	0.550			
191	IMAGUS-003	[537] 0.356	[522] 0.513	[501] 0.993				[529] 0.807	[517] 0.909	[445] 1.000				0.004	0.008	0.550			
192	IMAGUS-005	[256] 0.002	[242] 0.012	[306] 0.311	[301] 0.006	[229] 0.022	[349] 0.132	[283] 0.018	[264] 0.066	[212] 0.836	[250] 0.029	[178] 0.161	[224] 0.231	0.000	0.000	0.000		0.000	
193	IMAGUS-006	[262] 0.002	[279] 0.014	[293] 0.285	[260] 0.004	[224] 0.019	[311] 0.112	[287] 0.019	[273] 0.069	[227] 0.896	[248] 0.028	[177] 0.161	[237] 0.260	0.000	0.000	0.000		0.000	
194	IMAGUS-007	[266] 0.002	[270] 0.013	[307] 0.313	[251] 0.004	[230] 0.022	[325] 0.117	[306] 0.022	[281] 0.073	[225] 0.892	[259] 0.031	[180] 0.169	[242] 0.265	0.000	0.000	0.000		0.000	
195	IMAGUS-008	[511] 0.086	[486] 0.093	[300] 0.297	[387] 0.021	[302] 0.081	[325] 0.119	[538] 0.974	[504] 0.774	[351] 0.996	[425] 0.520	[319] 1.000	[318] 0.518	0.000	0.000	0.000		0.000	
196	IMDS-SOFTWARE-000	[97] 0.001	[89] 0.007	[167] 0.071	[144] 0.001	[142] 0.008	[189] 0.073	[186] 0.006	[175] 0.033	[471] 1.000	[186] 0.013	[196] 0.216	[538] 1.000	0.000	0.000	0.000		0.000	
197	IMDS-SOFTWARE-001	[102] 0.001	[65] 0.007	[144] 0.064	[139] 0.001	[158] 0.009	[262] 0.096	[190] 0.006	[179] 0.034	[429] 1.000	[216] 0.019	[237] 0.424	[530] 1.000	0.000	0.000	0.000		0.000	
198	IMDS-SOFTWARE-002	[99] 0.001	[88] 0.007	[166] 0.071	[143] 0.001	[143] 0.008	[188] 0.073	[185] 0.006	[174] 0.033	[459] 1.000	[185] 0.013	[197] 0.216	[486] 1.000	0.000	0.000	0.000		0.000	
199	IMPERIAL-000	[300] 0.002	[302] 0.015	[288] 0.272	[273] 0.004		[263] 0.097	[315] 0.026	[269] 0.068	[385] 0.999	[286] 0.042		[231] 0.245	0.000	0.000	0.000			
200	INCODE-000	[498] 0.049	[490] 0.100	[465] 0.951				[493] 0.310	[461] 0.420	[374] 0.998				0.001	0.004	0.173			
201	INCODE-001	[458] 0.016	[451] 0.046	[407] 0.759				[476] 0.211	[439] 0.296	[466] 1.000				0.001	0.004	0.173			
202	INCODE-002	[462] 0.017	[453] 0.048	[431] 0.841				[468] 0.184	[434] 0.269	[329] 0.993				0.000	0.001	0.066			
203	INCODE-003	[450] 0.013	[440] 0.040	[408] 0.762				[464] 0.167	[429] 0.264	[405] 0.999				0.000	0.001	0.066			
204	INCODE-004	[348] 0.003	[335] 0.017	[344] 0.468	[335] 0.008		[354] 0.135	[385] 0.053	[347] 0.120	[340] 0.994	[313] 0.063		[257] 0.313	0.000	0.001	0.066			
205	INCODE-005	[214] 0.001	[232] 0.011	[237] 0.138	[204] 0.002	[186] 0.013	[213] 0.079	[232] 0.011	[213] 0.043	[156] 0.522	[206] 0.017	[163] 0.145	[180] 0.155	0.000	0.000	0.042		0.000	
206	INCODE-006	[76] 0.001	[122] 0.008	[97] 0.053	[191] 0.002	[76] 0.005	[124] 0.058	[38] 0.001	[34] 0.011	[51] 0.159	[46] 0.003	[26] 0.026	[53] 0.079	0.000	0.000	0.041		0.000	
207	INCODE-007	[22] 0.001	[21] 0.006	[103] 0.054	[66] 0.001	[47] 0.004	[111] 0.056	[33] 0.001	[17] 0.009	[46] 0.146	[21] 0.002	[37] 0.028	[78] 0.089	0.000	0.000	0.043		0.000	
208	INNOVATRICS-002	[495] 0.045	[475] 0.074	[435] 0.851				[485] 0.233	[445] 0.310	[457] 1.000				0.000	0.001	0.046			
209	INNOVATRICS-003	[477] 0.026	[459] 0.055	[433] 0.843				[480] 0.221	[440] 0.297	[419] 1.000				0.000	0.001	0.046			
210	INNOVATRICS-004	[448] 0.012	[442] 0.040	[471] 0.957				[448] 0.131	[410] 0.222	[278] 0.980				0.000	0.001	0.046			
211	INNOVATRICS-005	[301] 0.002	[288] 0.014	[328] 0.400	[279] 0.005		[303] 0.109	[343] 0.034	[307] 0.089	[214] 0.845	[294] 0.047		[234] 0.251	0.000	0.001	0.041			
212	INNOVATRICS-007	[217] 0.001	[229] 0.011	[280] 0.239	[206] 0.002	[189] 0.013	[203] 0.077	[241] 0.012	[232] 0.051	[194] 0.740	[205] 0.017	[138] 0.093	[177] 0.154	0.000	0.001	0.041		0.000	
213	INNOVATRICS-008	[147] 0.001	[137] 0.008	[171] 0.072	[161] 0.002	[227] 0.021	[183] 0.072	[155] 0.005	[189] 0.036	[458] 1.000	[189] 0.013	[278] 0.886	[160] 0.139	0.000	0.000	0.004		0.000	
214	INNOVATRICS-009	[161] 0.001	[194] 0.010	[164] 0.070	[157] 0.002	[101] 0.006	[180] 0.072	[91] 0.003	[125] 0.025	[114] 0.338	[120] 0.007	[85] 0.050	[121] 0.106	0.000	0.001	0.040		0.001	
215	INNOVATRICS-010	[172] 0.001	[195] 0.010	[123] 0.074	[150] 0.002	[99] 0.006	[181] 0.072	[101] 0.003	[126] 0.025	[117] 0.347	[127] 0.007	[94] 0.054	[128] 0.110	0.000	0.001	0.040		0.001	
216	INNOVATRICS-011	[87] 0.001	[81] 0.007	[162] 0.070	[95] 0.001	[84] 0.005	[62] 0.050	[62] 0.002	[63] 0.014	[157] 0.523	[58] 0.004	[63] 0.039	[69] 0.087	0.000	0.000	0.012		0.000	
217	INNOVATRICS-012	[84] 0.001	[46] 0.006	[109] 0.056	[46] 0.001	[55] 0.004	[50] 0.048	[53] 0.002	[36] 0.011	[56] 0.168	[40] 0.003	[29] 0.027	[61] 0.083	0.000	0.000	0.016		0.000	
218	INNOVATRICS-013	[46] 0.001	[40] 0.006	[73] 0.050	[90] 0.001	[57] 0.004	[22] 0.045	[41] 0.001	[71] 0.015	[48] 0.147	[96] 0.006	[81] 0.048	[76] 0.088	0.000	0.000	0.016		0.000	
219	INNOVATRICS-014	[32] 0.001	[8] 0.005	[40] 0.045	[15] 0.001	[13] 0.003	[48] 0.048	[22] 0.001	[8] 0.008	[22] 0.106	[17] 0.002	[11] 0.015	[18] 0.066	0.000	0.000	0.041		0.000	
220	INNOVATRICS-015	[33] 0.001	[7] 0.005	[30] 0.044	[8] 0.001	[8] 0.002	[33] 0.046	[12] 0.001	[7] 0.007	[32] 0.126	[12] 0.002	[9] 0.015	[49] 0.078	0.000	0.000	0.039		0.000	
221	INSPUR-000	[55] 0.001	[532] 0.606	[81] 0.052	[397] 0.030	[351] 0.395	[396] 0.195	[182] 0.006	[518] 0.915	[427] 1.000	[454] 0.936	[551] 1.000	[436] 0.998	0.000	0.000	0.000		0.000	
222	INSPUR-001	[48] 0.001	[43] 0.006	[100] 0.054	[122] 0.001	[89] 0.006	[105] 0.056	[161] 0.005	[141] 0.027	[441] 1.000	[143] 0.008	[99] 0.057	[406] 0.931	0.000	0.000	0.000		0.000	
223	INSPUR-002	[39] 0.001	[39] 0.006	[61] 0.049	[128] 0.001	[79] 0.005	[91] 0.054	[167] 0.005	[158] 0.029	[392] 0.999	[137] 0.008	[90] 0.052	[417] 0.957	0.000	0.000	0.000		0.000	
224	INTELIGENSIA-000	[264] 0.002	[254] 0.012	[266] 0.201	[269] 0.004	[268] 0.033	[330] 0.124	[309] 0.024	[288] 0.077	[203] 0.784	[302] 0.053	[200] 0.235	[235] 0.255	0.001	0.000	0.046		0.001	
225	INTELIGENSIA-001	[71] 0.001	[64] 0.007	[117] 0.057	[162] 0.002	[141] 0.008	[286] 0.103	[166] 0.005	[147] 0.028	[138] 0.451	[135] 0.008	[118] 0.067	[149] 0.129	0.001	0.000	0.046		0.001	
226	INTELLIVISION-001	[488] 0.036	[491] 0.102	[485] 0.971	[421] 0.057	[342] 0.222	[435] 0.333	[490] 0.279	[458] 0.404	[426] 1.000	[400] 0.328	[262] 0.749	[354] 0.685	0.001	0.000	0.044		0.000	
227	INTELLIVISION-002	[435] 0.010	[416] 0.031	[460] 0.942	[376] 0.018	[305] 0.080	[397] 0.200	[456] 0.154	[398] 0.196	[388] 0.999	[355] 0.134	[239] 0.437	[303] 0.460	0.001	0.000	0.043		0.000	
228	INTELRESEARCH-001	[60] 0.001	[68] 0.007	[154] 0.067	[124] 0.001	[86] 0.005	[83] 0.053	[46] 0.001	[49] 0.012	[102] 0.276	[72] 0.005	[41] 0.030	[56] 0.080	0.000	0.000	0.041		0.000	
229	INTEMA-000	[98] 0.001	[135] 0.008	[48] 0.047	[93] 0.001	[88] 0.005	[65] 0.051	[67] 0.002	[75] 0.017	[448] 1.000	[71] 0.005	[210] 0.288	[57] 0.081	0.000	0.000	0.040		0.000	
230	INTEMA-001	[8] 0.000	[529] 0.601	[14] 0.042	[48] 0.001	[177] 0.012	[29] 0.046	[24] 0.001	[485] 0.603	[12] 0.092	[56] 0.004	[253] 0.715	[43] 0.076	0.001	0.000	0.041		0.000	

Table 24: **Miss rates by dataset:** *At left, rank 1 miss rates relevant to investigations; at right, with threshold set to target FPIR = 0.01 for higher volume, low prior, uses. Yellow indicates most accurate algorithm. Throughout blue superscripts indicate the rank of the algorithm for that column.*

2026/01/09 20:40:38

FNIR(N, R, T) = False neg. identification rate
FPIR(N, T) = False pos. identification rate

N = Num. enrolled subjects
R = Num. candidates examined

T = Threshold

T = 0 → Investigation
T > 0 → Identification

This publication is available free of charge from: https://doi.org/10.6028/NIST.IR.8271

#	ALGORITHM	INVESTIGATION MODE						IDENTIFICATION MODE						FAILURE TO EXTRACT					
		RANK ONE MISS RATE, FNIR(N, 0, 1)						HIGH T ⟶ FPIR = 0.001, FNIR(N, T, L)						FEATURES					
		N=1.6M						N=1.6M											
	GALLERY	MUGSHOT	MUGSHOT	MUGSHOT	VISA	BORDER	VISA	MUGSHOT	MUGSHOT	MUGSHOT	VISA	BORDER	VISA	MUGSHOT	MUGSHOT	MUGSHOT	VISA	BORDER	KIOSK
	PROBE	MUGSHOT	WEBCAM	PROFILE	BORDER	BOR¿10YR	KIOSK	MUGSHOT	WEBCAM	PROFILE	BORDER	BOR¿10YR	KIOSK	MUGSHOT	WEBCAM	PROFILE	BORDER	BOR¿10YR	KIOSK
231	INTSYSMSU-000	519 0.145	384 0.023	367 0.557	426 0.072		348 0.132	542 0.998	535 1.000	418 1.000	463 0.999		439 0.999	0.000	0.000	0.050			
232	IONETWORKS-001	350 0.003	253 0.012	226 0.118	261 0.004	223 0.019	217 0.082	254 0.014	219 0.045	421 1.000	199 0.016	152 0.129	251 0.294	0.000	0.000	0.000		0.000	
233	IREX-000	364 0.004	168 0.010	385 0.677	203 0.002	128 0.012	219 0.082	331 0.028	256 0.060	242 0.956	289 0.044	213 0.302	194 0.170	0.000	0.000	0.042		0.000	
234	ISYSTEMS-002	394 0.006	396 0.026	432 0.842				413 0.078	352 0.126	365 0.998				0.002	0.002	0.142			
235	ISYSTEMS-003	381 0.005	380 0.023	414 0.789				395 0.058	335 0.107	425 1.000				0.002	0.002	0.142			
236	KAKAO-000	184 0.001	201 0.011	214 0.109	208 0.002	184 0.013	208 0.078	260 0.015	246 0.056	143 0.462	217 0.019	157 0.141	182 0.158	0.000	0.000	0.041		0.000	
237	KAKAO-001	166 0.001	156 0.009	42 0.047	64 0.001	65 0.004	41 0.047	78 0.002	78 0.017	49 0.150	61 0.004	71 0.042	36 0.074	0.000	0.000	0.040		0.000	
238	KAKAO-002	159 0.001	144 0.009	38 0.045	32 0.001	34 0.004	21 0.045	60 0.002	64 0.014	37 0.134	41 0.003	59 0.037	31 0.070	0.000	0.000	0.040		0.000	
239	KEDACOM-001	409 0.007	425 0.036	487 0.972	404 0.034		409 0.237	305 0.022	279 0.072	302 0.986	304 0.055		253 0.305	0.000	0.000	0.000			
240	KEYLESS-000	74 0.001	37 0.006	152 0.066	103 0.001	269 0.034	190 0.073	174 0.006	154 0.029	305 0.987	175 0.011	301 0.994	173 0.149	0.000	0.000	0.041		0.000	
241	KLOUDSPOT-001	295 0.002	361 0.021	244 0.145	330 0.008	333 0.170	274 0.100	310 0.024		164 0.550				0.001	0.000	0.042		0.000	
242	KNERON-000	389 0.006	403 0.027	365 0.547	394 0.028		395 0.195							0.000	0.000	0.000			
243	KNERON-001	482 0.029	534 0.621	278 0.228	439 0.144	339 0.207	422 0.280							0.000	0.000	0.000		0.000	
244	KNOWUTECH-000	92 0.001	69 0.007	161 0.069	153 0.002	145 0.008	170 0.070	215 0.009	198 0.038	107 0.310	182 0.012	136 0.091	147 0.129	0.000	0.000	0.041		0.000	
245	KOGNIZA-000	207 0.001	199 0.010	179 0.078	83 0.001	48 0.004	110 0.056	176 0.006	148 0.028	136 0.444	78 0.005	84 0.050	71 0.087	0.001	0.001	0.041		0.000	
246	LIGHTVISION-000	331 0.003	407 0.028	373 0.585	277 0.005	328 0.129	266 0.098	325 0.027	505 0.797	432 1.000	266 0.033	390 1.000	218 0.214	0.000	0.000	0.000		0.000	
247	LINE-000	288 0.002	280 0.014	272 0.214	292 0.005	257 0.029	297 0.107	339 0.030	319 0.095		292 0.046	207 0.278	544 1.000	0.000	0.000	0.000		0.000	
248	LINE-001	96 0.001	92 0.007	89 0.053	172 0.002	146 0.008	235 0.085	146 0.004	140 0.027	469 1.000	157 0.009	122 0.072	501 1.000	0.000	0.000	0.000		0.000	
249	LINECLOVA-002	149 0.001	98 0.008	127 0.059	156 0.002	172 0.011	121 0.058	118 0.004	354 0.130	281 0.980	283 0.040	324 1.000	356 0.700	0.000	0.001	0.040		0.001	
250	LINECLOVA-003	52 0.001	531 0.601	190 0.089	89 0.001	149 0.009	233 0.085	80 0.002	486 0.606		84 0.006	294 0.974	127 0.110	0.000	0.000	0.024		0.000	
251	LOOKMAN-003	418 0.008	435 0.038		407 0.035		411 0.239	360 0.043	339 0.112		332 0.084		270 0.355	0.000	0.000				
252	LOOKMAN-004	420 0.009	439 0.039	489 0.973				363 0.044	332 0.105	269 0.977				0.000	0.000	0.000			
253	LOOKMAN-005	412 0.008	428 0.036	488 0.972	406 0.035		410 0.237	337 0.030	301 0.086	271 0.977	312 0.062		255 0.308	0.000	0.000	0.000			
254	LUXAND-001	334 0.003	357 0.020	304 0.305	348 0.012	299 0.068	341 0.127	391 0.057	455 0.385	349 0.995	435 0.662	282 0.909	395 0.903	0.001	0.002	0.088		0.001	
255	MANTRA-000	223 0.001	184 0.010	394 0.705	314 0.007	242 0.024	309 0.112	224 0.010	205 0.041	555 1.000	252 0.029	169 0.152	443 1.000	0.002	0.001	0.591		0.003	
256	MAVERICKRESEARCH-000	436 0.010	393 0.025	332 0.419	365 0.014	283 0.045	363 0.144	417 0.084	391 0.176	321 0.992	347 0.122	229 0.394	325 0.546	0.004	0.001	0.055		0.005	
257	MAXVISION-000	298 0.002	297 0.015	310 0.319	265 0.004	289 0.051	277 0.101	332 0.028	414 0.237	200 0.764	361 0.149	305 0.997	329 0.557	0.000	0.000	0.042		0.000	
258	MAXVISION-001	122 0.001	103 0.008	99 0.054	100 0.001	215 0.018	118 0.057	130 0.004	129 0.025	81 0.210	115 0.007	288 0.951	109 0.100	0.000	0.000	0.042		0.000	
259	MAXVISION-002	130 0.001	75 0.007	90 0.053	119 0.001	157 0.009	166 0.069	113 0.004	105 0.022	70 0.188	111 0.007	279 0.895	117 0.104	0.001	0.000	0.044		0.000	
260	MAXVISION-003	136 0.001	101 0.008	101 0.054	132 0.001	185 0.013	125 0.059	173 0.006	201 0.039	96 0.237	173 0.011	222 0.348	130 0.111	0.000	0.000	0.042		0.000	
261	MAXVISION-004	121 0.001	151 0.009	29 0.044	40 0.001	272 0.037	104 0.055	69 0.002	87 0.020	29 0.122	54 0.004	298 0.990	60 0.082	0.001	0.000	0.042		0.000	
262	MEGVII-001	445 0.012	334 0.017		483 1.000			408 0.072	323 0.097					0.002	0.000				
263	MEGVII-002	447 0.012	336 0.017	336 0.444	488 1.000			412 0.077	321 0.096	378 0.998				0.002	0.000	0.033			
264	MEGVII-003	134 0.001	121 0.008	78 0.050	80 0.001	62 0.004	116 0.057	75 0.002	38 0.011	45 0.145	45 0.003	32 0.027	47 0.078	0.001	0.000	0.044		0.000	
265	MEGVII-004	119 0.001	110 0.008	26 0.044	59 0.001	19 0.003	93 0.054	18 0.001	13 0.008	10 0.072	7 0.001	4 0.009	17 0.065	0.001	0.000	0.044		0.000	
266	MEGVII-005	118 0.001	112 0.008	27 0.044	31 0.001	105 0.007	13 0.042	19 0.001	25 0.009	64 0.181	87 0.006	333 1.000	135 0.117	0.001	0.000	0.044		0.000	
267	METSAKUURCOMPANY-000	105 0.001	70 0.007	140 0.063	152 0.002	309 0.083	126 0.059	197 0.007	187 0.036	391 0.999	329 0.081	304 0.995	353 0.683	0.000	0.000	0.000		0.000	
268	METSAKUURCOMPANY-001	163 0.001	106 0.008	208 0.097	165 0.002	144 0.008	184 0.072	216 0.009	165 0.031	412 1.000	167 0.010	124 0.073	382 0.841	0.000	0.000	0.000		0.000	
269	MICROFOCUS-003	545 0.594	541 0.781		466 0.708		469 0.907	535 0.931	529 0.979		460 0.982		430 0.991	0.001	0.005				
270	MICROFOCUS-004	542 0.576	540 0.758		465 0.701		468 0.904	543 0.999	527 0.975		457 0.974		428 0.989	0.001	0.005				
271	MICROFOCUS-005	538 0.424	530 0.601		457 0.494		461 0.777	533 0.835	522 0.928		453 0.935		427 0.985	0.001	0.005				
272	MICROFOCUS-006	539 0.427	528 0.583		456 0.490		464 0.782	539 0.978	521 0.923		452 0.923		421 0.971	0.001	0.005				
273	MICROSOFT-003	248 0.002	249 0.012		249 0.004		305 0.109	328 0.027	311 0.091		275 0.036		226 0.233	0.000	0.001				
274	MICROSOFT-004	233 0.001	246 0.012		240 0.004		306 0.109	316 0.026	305 0.087		267 0.033		221 0.222	0.000	0.001				
275	MICROSOFT-005	287 0.002	213 0.011	235 0.134	227 0.003		271 0.099	313 0.025	276 0.070	170 0.582	243 0.027		204 0.180	0.000	0.001	0.049			
276	MICROSOFT-006	292 0.002	235 0.011	239 0.140	245 0.004		275 0.100	237 0.012	190 0.037	123 0.379	262 0.032		198 0.178	0.000	0.001	0.049			

Table 25: **Miss rates by dataset:** *At left, rank 1 miss rates relevant to investigations; at right, with threshold set to target FPIR = 0.01 for higher volume, low prior, uses. Yellow indicates most accurate algorithm. Throughout blue superscripts indicate the rank of the algorithm for that column.*

This publication is available free of charge from: https://doi.org/10.6028/NIST.IR.8271

#	ALGORITHM	INVESTIGATION MODE						IDENTIFICATION MODE						FAILURE TO EXTRACT					
		RANK ONE MISS RATE, FNIR(N, 0, 1)						HIGH T → FPIR = 0.001, FNIR(N, T, L)						FEATURES					
		N=1.6M						N=1.6M											
	GALLERY	MUGSHOT	MUGSHOT	MUGSHOT	VISA	BORDER	VISA	MUGSHOT	MUGSHOT	MUGSHOT	VISA	BORDER	VISA	MUGSHOT	MUGSHOT	MUGSHOT	VISA	BORDER	KIOSK
	PROBE	MUGSHOT	WEBCAM	PROFILE	BORDER	BOR¿10YR	KIOSK	MUGSHOT	WEBCAM	PROFILE	BORDER	BOR¿10YR	KIOSK	MUGSHOT	WEBCAM	PROFILE	BORDER	BOR¿10YR	KIOSK
277	MOBBL-000	315 0.002	271 0.013	334 0.431	272 0.004	244 0.026	317 0.114	330 0.028	286 0.077	295 0.984	273 0.036	248 0.621	223 0.228	0.000	0.002	0.088		0.001	
278	MOBBL-001	444 0.012	348 0.019	337 0.446	395 0.029	285 0.047	387 0.178	345 0.035	295 0.080	291 0.983	308 0.058	249 0.622	246 0.275	0.000	0.002	0.088		0.001	
279	MOBBL-002	528 0.212	506 0.193	393 0.701	447 0.282	356 0.500	451 0.550	479 0.215	403 0.207	311 0.990	392 0.285	306 0.997	330 0.558	0.000	0.000	0.042		0.000	
280	MUKH-002	476 0.025	427 0.036	329 0.633	350 0.012	304 0.079	343 0.129	519 0.594	420 0.242	437 1.000	371 0.170	259 0.741	279 0.389	0.000	0.000	0.042		0.000	
281	NEC-000	459 0.017	444 0.041	423 0.958	390 0.025		413 0.243	415 0.079	366 0.140	275 0.979			309 0.474	0.001	0.002	0.890			
282	NEC-001	468 0.021	460 0.056	481 0.967	403 0.033		418 0.277	435 0.105	400 0.197	301 0.986	354 0.133		306 0.468	0.005	0.003	0.934			
283	NEC-002	140 0.001	146 0.009	320 0.355	237 0.003		320 0.117	81 0.002	88 0.020	401 0.999	140 0.008		350 0.676	0.000	0.001	0.041			
284	NEC-003	211 0.001	181 0.010	319 0.345	244 0.004	183 0.013	328 0.120	76 0.002	77 0.017	209 0.822	145 0.008	56 0.036	349 0.668	0.000	0.001	0.041		0.001	
285	NEC-004	176 0.001	140 0.009	361 0.533	224 0.003	128 0.007	197 0.075	45 0.001	54 0.013	175 0.618	63 0.004	16 0.019	108 0.100	0.000	0.001	0.041		0.001	
286	NEC-005	113 0.001	104 0.008	168 0.071	166 0.002	73 0.005	192 0.073	40 0.001	45 0.012	182 0.669	48 0.003	15 0.019	103 0.099	0.000	0.001	0.040		0.001	
287	NEC-006	141 0.001	128 0.008	106 0.055	177 0.002	78 0.005	150 0.065	55 0.002	81 0.018	140 0.457	53 0.004	28 0.026	96 0.094	0.000	0.001	0.040		0.001	
288	NEC-007	64 0.001	38 0.006	57 0.048	85 0.001	18 0.003	58 0.049	21 0.001	19 0.009	41 0.137	18 0.002	5 0.010	16 0.065	0.000	0.000	0.040		0.000	
289	NEC-008	81 0.001	57 0.006	28 0.044	78 0.001	12 0.003	38 0.047	29 0.001	15 0.009	11 0.089	15 0.002	3 0.008	13 0.062	0.000	0.000	0.040		0.000	
290	NEC-009	49 0.001	36 0.006	7 0.040	58 0.001	5 0.002	18 0.044	9 0.001	5 0.007	8 0.070	6 0.001	2 0.005	4 0.052	0.000	0.000	0.040		0.000	
291	NEC-010	15 0.000	6 0.005	2 0.039	50 0.001	3 0.002	15 0.043	4 0.001	2 0.006	6 0.067	4 0.001	1 0.004	1 0.050	0.000	0.000	0.040		0.000	
292	NEC-011	9 0.000	2 0.005	4 0.039	4 0.001	180 0.012	3 0.037	3 0.001	4 0.006	42 0.140	1 0.001	267 0.789	3 0.052	0.000	0.000	0.039		0.000	
293	NEUROTECHNOLOGY-003	470 0.022	445 0.042	425 0.960				523 0.631	431 0.266	551 1.000				0.000	0.001	0.131			
294	NEUROTECHNOLOGY-004	383 0.005	353 0.020	484 0.970				401 0.062	341 0.117	334 0.994				0.000	0.001	0.131			
295	NEUROTECHNOLOGY-005	362 0.004	389 0.024	439 0.892				386 0.054	355 0.130	369 0.998				0.000	0.000	0.030			
296	NEUROTECHNOLOGY-006	463 0.018	448 0.045	376 0.602				486 0.249	459 0.418					0.000	0.000				
297	NEUROTECHNOLOGY-007	352 0.004	363 0.021	418 0.794	337 0.009		390 0.180	400 0.062	389 0.173	436 1.000	401 0.339		500 1.000	0.001	0.001	0.041			
298	NEUROTECHNOLOGY-008	281 0.002	287 0.014	340 0.451	253 0.004	238 0.023	281 0.101	380 0.053	294 0.080	468 1.000	272 0.035	212 0.293	214 0.203	0.000	0.001	0.052		0.001	
299	NEUROTECHNOLOGY-009	179 0.001	209 0.011	254 0.169	194 0.002	187 0.013	212 0.079	261 0.015	236 0.052	171 0.583	220 0.020	170 0.153	191 0.165	0.001	0.000	0.046		0.000	
300	NEUROTECHNOLOGY-010	131 0.001	167 0.009	128 0.060	130 0.001	125 0.007	160 0.068	222 0.010	194 0.037	99 0.269	168 0.010	129 0.075	142 0.126	0.000	0.000	0.041		0.000	
301	NEUROTECHNOLOGY-012	63 0.001	113 0.008	85 0.052	56 0.001	85 0.005	117 0.057	191 0.006	172 0.032	246 0.959	151 0.008	102 0.061	399 0.916	0.000	0.000	0.039		0.000	
302	NEUROTECHNOLOGY-013	65 0.001	109 0.008	51 0.047	51 0.001	67 0.004	106 0.056	129 0.004	113 0.023	110 0.316	106 0.006	75 0.046	343 0.641	0.000	0.000	0.039		0.000	
303	NEUROTECHNOLOGY-014	41 0.001	49 0.006	62 0.049	70 0.001	70 0.005	100 0.055	97 0.003	104 0.022	86 0.215	97 0.006	89 0.052	93 0.094	0.000	0.000	0.039		0.000	
304	NEUROTECHNOLOGY-015	28 0.001	31 0.006	50 0.047	26 0.001	56 0.004	44 0.048	103 0.003	119 0.024	57 0.170	98 0.006	83 0.049	68 0.086	0.000	0.000	0.039		0.000	
305	NEUROTECHNOLOGY-016	21 0.001	18 0.006	41 0.046	19 0.001	46 0.004	52 0.048	96 0.003	95 0.021	65 0.182	122 0.007	92 0.054	90 0.093	0.000	0.000	0.039		0.000	
306	NEWLAND-002	508 0.078	494 0.117	455 0.935				511 0.437	469 0.466	393 0.999				0.007	0.012	0.200			
307	NEXTMETALABS-001	485 0.031	480 0.090	349 0.510	440 0.154	357 0.550	442 0.419	482 0.233	537 1.000	462 1.000	492 1.000	521 1.000	465 1.000	0.000	0.000	0.000		0.000	
308	NEXTMETALABS-002	54 0.001	73 0.007	75 0.050	195 0.002	336 0.182	204 0.077	122 0.004	351 0.125	75 0.198	353 0.131	329 1.000	316 0.510	0.000	0.000	0.041		0.000	
309	NOBLIS-001	532 0.249	523 0.522	502 0.993				545 1.000	547 1.000	449 1.000				0.000	0.000	0.000			
310	NOBLIS-002	522 0.179	520 0.392	493 0.981				541 0.997	548 1.000	452 1.000				0.000	0.000	0.000			
311	NOMINDER-000	67 0.001	138 0.009	240 0.142	262 0.004	331 0.155	243 0.090	147 0.004	437 0.280	236 0.929	405 0.370	484 1.000	372 0.799	0.000	0.000	0.040		0.000	
312	NOMINDER-001	190 0.001	222 0.011	211 0.104	73 0.001	225 0.020	122 0.058	160 0.005	302 0.086	185 0.675	138 0.008	325 1.000	176 0.154	0.000	0.000	0.040		0.000	
313	NOMINDER-002	194 0.001	211 0.011	79 0.051	76 0.001	120 0.007	47 0.048	158 0.005	157 0.029	90 0.223	107 0.006	276 0.867	80 0.089	0.001	0.000	0.040		0.000	
314	NOMINDER-003	193 0.001	205 0.011	64 0.049	71 0.001	97 0.006	24 0.045	151 0.005	145 0.027	79 0.208	95 0.006	272 0.816	66 0.085	0.001	0.000	0.040		0.000	
315	NOMINDER-004	177 0.001	187 0.010	66 0.049	77 0.001	72 0.005	46 0.048	145 0.004	134 0.026	80 0.208	101 0.006	219 0.331	79 0.089	0.001	0.000	0.040		0.000	
316	NOTIONTAG-000	299 0.002	250 0.012	261 0.195	256 0.004	202 0.016	256 0.095	274 0.017	252 0.059	173 0.606	226 0.021	165 0.150	197 0.176	0.000	0.000	0.000		0.000	
317	NTECHLAB-003	393 0.006	377 0.023	346 0.498				384 0.053	342 0.118	211 0.835				0.000	0.000	0.040			
318	NTECHLAB-004	376 0.005	340 0.019	347 0.500	328 0.008		344 0.129	354 0.040	331 0.105	210 0.831	301 0.053		239 0.263	0.000	0.000	0.040			
319	NTECHLAB-005	374 0.005	339 0.018	321 0.360	333 0.008		323 0.118	356 0.042	329 0.102	201 0.769	323 0.073		250 0.294	0.000	0.000	0.040			
320	NTECHLAB-006	363 0.004	327 0.017	318 0.340	324 0.007		316 0.113	348 0.036	316 0.094	199 0.751	306 0.057		238 0.260	0.000	0.000	0.040			
321	NTECHLAB-007	313 0.002	255 0.012	308 0.318	271 0.004		296 0.107	312 0.025	267 0.067	198 0.747	263 0.032		222 0.223	0.000	0.000	0.042			
322	NTECHLAB-008	221 0.001	169 0.010	245 0.147	236 0.003		229 0.084	252 0.014	220 0.045	158 0.524	268 0.033		205 0.183	0.000	0.000	0.044			

Table 26: **Miss rates by dataset:** *At left, rank 1 miss rates relevant to investigations; at right, with threshold set to target FPIR = 0.01 for higher volume, low prior, uses. Yellow indicates most accurate algorithm. Throughout blue superscripts indicate the rank of the algorithm for that column.*

2026/01/09 20:40:38

FNIR(N, R, T) = False neg. identification rate
FPIR(N, T) = False pos. identification rate
N = Num. enrolled subjects
R = Num. candidates examined
T = Threshold
T = 0 → Investigation
T > 0 → Identification

This publication is available free of charge from: https://doi.org/10.6028/NIST.IR.8271

#	ALGORITHM	INVESTIGATION MODE						IDENTIFICATION MODE						FAILURE TO EXTRACT					
		RANK ONE MISS RATE, FNIR(N, 0, 1)						HIGH T ⟶ FPIR = 0.001, FNIR(N, T, L)						FEATURES					
		N=1.6M						N=1.6M											
	GALLERY	MUGSHOT	MUGSHOT	MUGSHOT	VISA	BORDER	VISA	MUGSHOT	MUGSHOT	MUGSHOT	VISA	BORDER	VISA	MUGSHOT	MUGSHOT	MUGSHOT	VISA	BORDER	KIOSK
	PROBE	MUGSHOT	WEBCAM	PROFILE	BORDER	BOR¿10YR	KIOSK	MUGSHOT	WEBCAM	PROFILE	BORDER	BOR¿10YR	KIOSK	MUGSHOT	WEBCAM	PROFILE	BORDER	BOR¿10YR	KIOSK
323	NTECHLAB-009	143 0.001	114 0.008	230 0.128	192 0.002	191 0.013	194 0.074	153 0.005	107 0.022	133 0.423	195 0.015	144 0.109	165 0.142	0.000	0.000	0.041		0.001	
324	NTECHLAB-010	88 0.001	129 0.008	175 0.075	164 0.002	137 0.008	119 0.057	74 0.002	66 0.015	98 0.243	112 0.007	101 0.059	102 0.098	0.001	0.001	0.043		0.000	
325	NTECHLAB-011	66 0.001	67 0.007	136 0.062	136 0.001	132 0.007	72 0.051	86 0.003	65 0.015	87 0.219	156 0.009	126 0.074	84 0.091	0.000	0.000	0.040		0.000	
326	OMNIGARDE-000	70 0.001	60 0.007	141 0.063	127 0.001	110 0.007	158 0.068	126 0.004	114 0.023	97 0.243	128 0.007	95 0.055	155 0.136	0.000	0.000	0.041		0.000	
327	OMNIGARDE-001	31 0.001	30 0.006	46 0.047	52 0.001	45 0.004	99 0.055	61 0.002	70 0.015	40 0.135	50 0.003	42 0.030	46 0.078	0.000	0.000	0.041		0.000	
328	OMNIGARDE-002	43 0.001	33 0.006	47 0.047	41 0.001	52 0.004	108 0.056	39 0.001	31 0.011	24 0.111	31 0.002	19 0.022	52 0.079	0.000	0.000	0.041		0.000	
329	OPTIEXACTA-000	26 0.001	34 0.006	69 0.049	98 0.001	41 0.004	59 0.049	15 0.001	12 0.008	39 0.135	42 0.003	49 0.033	30 0.070	0.000	0.000	0.040		0.000	
330	PANGIAM-000	114 0.001	105 0.008	143 0.064	179 0.002	130 0.007	146 0.065	177 0.006	160 0.030	108 0.310	161 0.009	155 0.136	118 0.105	0.000	0.001	0.044		0.001	
331	PANGIAM-001	397 0.007	266 0.013	153 0.067	105 0.001	159 0.009	142 0.064	233 0.011	159 0.030	122 0.376	155 0.009	275 0.860	163 0.141	0.003	0.000	0.040		0.000	
332	PAPSAV1923-000	109 0.001	117 0.008	169 0.071	278 0.005	165 0.010	139 0.063	94 0.003	92 0.021	91 0.226	164 0.009	82 0.049	94 0.094	0.000	0.001	0.052		0.003	
333	PARAVISION-000	464 0.019	434 0.038	358 0.529	454 0.423		450 0.529	426 0.088	386 0.170	396 0.999	420 0.470		404 0.926	0.000	0.000	0.000			
334	PARAVISION-001	354 0.004	359 0.020	312 0.322	453 0.414		448 0.484	370 0.049	353 0.128	382 0.999	417 0.444		361 0.739	0.000	0.000	0.000			
335	PARAVISION-002	360 0.004	370 0.022	314 0.328	371 0.015		384 0.175	372 0.050	345 0.119	290 0.983	328 0.080		314 0.497	0.000	0.000	0.032			
336	PARAVISION-003	344 0.003	349 0.019	282 0.244	372 0.015		378 0.167	344 0.035	320 0.096	336 0.994	307 0.058		252 0.296	0.000	0.000	0.032			
337	PARAVISION-004	209 0.001	190 0.010	196 0.094	299 0.006		310 0.112	225 0.010	195 0.038	461 1.000	211 0.018		397 0.908	0.000	0.000	0.032			
338	PARAVISION-005	198 0.001	176 0.010	159 0.068	316 0.007		294 0.106	124 0.004	120 0.024	277 0.980	171 0.011		151 0.132	0.000	0.000	0.038			
339	PARAVISION-007	112 0.001	124 0.008	107 0.055	287 0.005	166 0.010	278 0.101	119 0.004	128 0.025	454 1.000	153 0.009	146 0.113	453 1.000	0.000	0.000	0.000		0.000	
340	PARAVISION-009	62 0.001	86 0.007	113 0.056	129 0.001	53 0.004	87 0.054	79 0.002	85 0.019	193 0.732	43 0.003	48 0.033	35 0.073	0.000	0.001	0.025		0.000	
341	PARAVISION-012	42 0.001	76 0.007	77 0.050	125 0.001	42 0.004	75 0.052	34 0.001	50 0.012	144 0.469	35 0.002	24 0.025	25 0.068	0.000	0.001	0.025		0.000	
342	PARAVISION-014	40 0.001	74 0.007	58 0.048	47 0.001	30 0.003	34 0.047	26 0.001	40 0.011	161 0.527	22 0.002	50 0.033	12 0.061	0.000	0.001	0.025		0.000	
343	PARAVISION-016	45 0.001	56 0.006	39 0.045	29 0.001	28 0.003	67 0.051	17 0.001	37 0.011	25 0.112	13 0.002	34 0.028	14 0.065	0.000	0.000	0.040		0.000	
344	PARAVISION-019	16 0.000	25 0.006	37 0.045	23 0.001	20 0.003	19 0.044	13 0.001	28 0.010	61 0.176	10 0.002	38 0.028	10 0.061	0.000	0.000	0.003		0.000	
345	PENTACOMP-000	549 0.975	545 0.978	486 0.972	470 0.948	364 0.980	470 0.951	540 0.996	533 0.998	317 0.990	456 0.955	370 1.000	418 0.960	0.000	0.000	0.041		0.000	
346	PENTACOMP-001	232 0.001	240 0.012	241 0.142	202 0.002	324 0.123	163 0.069	270 0.016	382 0.172	153 0.517	326 0.076	356 1.000	292 0.430	0.000	0.000	0.041		0.000	
347	PIXELALL-002	366 0.004	373 0.022	424 0.808	345 0.011		392 0.187	434 0.105	456 0.388	475 1.000	428 0.602		552 1.000	0.000	0.000	0.000			
348	PIXELALL-003	229 0.002	286 0.014	350 0.510	309 0.006		367 0.151	300 0.021	280 0.073	415 1.000	278 0.037		327 0.554	0.000	0.000	0.000			
349	PIXELALL-004	269 0.002	298 0.015	354 0.518	296 0.005		369 0.152	282 0.018	293 0.079	446 1.000	296 0.051		432 0.994	0.000	0.000	0.000			
350	PIXELALL-005	247 0.002	212 0.011	284 0.256	353 0.012	252 0.028	365 0.146	235 0.012	227 0.050	450 1.000	244 0.027	190 0.203	442 1.000	0.000	0.000	0.000		0.000	
351	PRIVID-000	469 0.021	364 0.021	187 0.086	410 0.037	349 0.369	391 0.181	321 0.027	511 0.825	220 0.882	430 0.603	445 1.000	423 0.972	0.000	0.000	0.039		0.000	
352	PROTENET-000	503 0.063	505 0.190	374 0.597	430 0.096	354 0.448	445 0.462	527 0.794	512 0.834	226 0.980	444 0.804	449 1.000	391 0.890	0.015	0.111	0.216		0.015	
353	PSL-000	18 0.000	29 0.006	87 0.053	62 0.001	60 0.004	82 0.053	77 0.002	94 0.021	78 0.208	79 0.005	93 0.054	100 0.097	0.000	0.000	0.040		0.000	
354	PSL-001	11 0.000	13 0.005	11 0.041	3 0.001	17 0.003	20 0.045	68 0.002	74 0.017	30 0.122	47 0.003	35 0.028	39 0.075	0.000	0.000	0.040		0.000	
355	PSL-002	5 0.000	4 0.005	10 0.041	7 0.001	6 0.002	28 0.046	25 0.001	39 0.011	15 0.095	26 0.002	22 0.023	51 0.079	0.000	0.000	0.040		0.000	
356	PSL-003	6 0.000	10 0.005	20 0.043	16 0.001	7 0.002	37 0.047	27 0.001	35 0.011	20 0.102	24 0.002	20 0.022	114 0.102	0.000	0.000	0.040		0.000	
357	PSL-004	4 0.000	5 0.005	18 0.043	18 0.001	9 0.002	43 0.047	16 0.001	22 0.009	19 0.101	14 0.002	21 0.022	42 0.076	0.000	0.000	0.040		0.000	
358	PTAKURATSATU-000	330 0.003	326 0.017	375 0.600	293 0.005	248 0.027	291 0.105	347 0.036	350 0.124	234 0.923	293 0.046	193 0.206	225 0.232	0.000	0.001	0.039		0.000	
359	PYRAMID-000	86 0.001	54 0.006	86 0.052	72 0.001	126 0.007	101 0.055	116 0.004	91 0.021	72 0.190	116 0.007	238 0.433	97 0.095	0.001	0.000	0.042		0.000	
360	PYRAMID-001	115 0.001	419 0.032	88 0.053	389 0.021	232 0.022	138 0.063	143 0.004	222 0.047	73 0.193	245 0.027	128 0.075	107 0.100	0.000	0.037	0.041		0.018	
361	QAZSMARTVISIONAI-000	10 0.000	16 0.005	15 0.042	13 0.001	25 0.003	12 0.042	28 0.001	29 0.010	14 0.094	34 0.002	62 0.041	20 0.067	0.000	0.000	0.035		0.000	
362	QAZSMARTVISIONAI-001	3 0.000	11 0.005	5 0.040	5 0.001	4 0.002	4 0.039	5 0.001	9 0.008	5 0.065	16 0.002	27 0.026	8 0.058	0.000	0.000	0.031		0.000	
363	QAZSMARTVISIONAI-002	1 0.000	3 0.005	1 0.039	1 0.001	1 0.002	2 0.037	1 0.001	3 0.006	1 0.052	3 0.001	7 0.014	5 0.052	0.000	0.000	0.031		0.000	
364	QAZSMARTVISIONAI-003	2 0.000	1 0.005	3 0.039	2 0.001	2 0.002	1 0.036	2 0.001	1 0.006	3 0.053	2 0.001	12 0.016	2 0.052	0.000	0.000	0.031		0.000	
365	QNAP-000	410 0.007	406 0.027	352 0.516	363 0.013	291 0.054	372 0.158	447 0.129	418 0.238	480 1.000	377 0.191	246 0.539	435 0.998	0.001	0.000	0.054		0.000	
366	QNAP-001	358 0.004	371 0.022	345 0.492	308 0.006	279 0.041	313 0.112	383 0.053	362 0.137	235 0.927	330 0.081	225 0.368	266 0.331	0.000	0.000	0.004		0.000	
367	QNAP-002	373 0.005	362 0.021	252 0.163	263 0.004	263 0.031	336 0.125	318 0.026	333 0.106	202 0.769	300 0.052	208 0.281	244 0.272	0.001	0.004	0.057		0.001	
368	QNAP-003	320 0.002	332 0.017	242 0.142	331 0.008	297 0.061	253 0.093	286 0.019	513 0.835	323 0.992	424 0.502	341 1.000	386 0.865	0.000	0.001	0.002		0.001	

Table 27: **Miss rates by dataset:** *At left, rank 1 miss rates relevant to investigations; at right, with threshold set to target FPIR = 0.01 for higher volume, low prior, uses. Yellow indicates most accurate algorithm. Throughout blue superscripts indicate the rank of the algorithm for that column.*

2026/01/09 20:40:38

FNIR(N, R, T) = False neg. identification rate
FPIR(N, T) = False pos. identification rate

N = Num. enrolled subjects
R = Num. candidates examined

T = Threshold

T = 0 → Investigation
T > 0 → Identification

This publication is available free of charge from: https://doi.org/10.6028/NIST.IR.8271

#	ALGORITHM	INVESTIGATION MODE						IDENTIFICATION MODE						FAILURE TO EXTRACT					
		RANK ONE MISS RATE, FNIR(N, 0, 1)						HIGH T ⟶ FPIR = 0.001, FNIR(N, T, L)						FEATURES					
		N=1.6M						N=1.6M											
	GALLERY	MUGSHOT	MUGSHOT	MUGSHOT	VISA	BORDER	VISA	MUGSHOT	MUGSHOT	MUGSHOT	VISA	BORDER	VISA	MUGSHOT	MUGSHOT	MUGSHOT	VISA	BORDER	KIOSK
	PROBE	MUGSHOT	WEBCAM	PROFILE	BORDER	BOR¿10YR	KIOSK	MUGSHOT	WEBCAM	PROFILE	BORDER	BOR¿10YR	KIOSK	MUGSHOT	WEBCAM	PROFILE	BORDER	BOR¿10YR	KIOSK
369	QNAP-004	[249]0.002	[293]0.014	[215]0.109	[284]0.005	[280]0.041	[237]0.086	[250]0.014	[516]0.890	[358]0.996	[423]0.501	[462]1.000	[401]0.922	0.000	0.001	0.002		0.001	
370	QNAP-005	[338]0.003	[394]0.026	[192]0.091	[323]0.007	[219]0.019	[232]0.085	[227]0.010	[263]0.066	[119]0.359	[234]0.024	[145]0.110	[143]0.127	0.005	0.015	0.054		0.005	
371	QNAP-006	[187]0.001	[225]0.011	[201]0.095	[181]0.002	[197]0.014	[159]0.068	[210]0.008	[211]0.042	[125]0.388	[215]0.019	[153]0.131	[156]0.137	0.000	0.000	0.046		0.000	
372	QUANTASOFT-001	[529]0.217	[539]0.727					[524]0.638						0.000	0.000				
373	RANKONE-002	[466]0.019	[473]0.071					[440]0.117	[427]0.261					0.000	0.000				
374	RANKONE-003	[465]0.019	[471]0.068					[441]0.117	[425]0.255					0.000	0.000				
375	RANKONE-004	[494]0.041	[496]0.141					[472]0.193	[462]0.426					0.000	0.000				
376	RANKONE-005	[423]0.009	[443]0.041	[495]0.986				[397]0.059	[390]0.173	[371]0.998				0.000	0.000	0.489			
377	RANKONE-006	[377]0.005		[420]0.795				[349]0.037		[270]0.977				0.002		0.167			
378	RANKONE-007	[340]0.003	[341]0.019	[417]0.793				[303]0.022	[317]0.095	[253]0.967				0.001	0.001	0.102			
379	RANKONE-009	[294]0.002	[258]0.013	[362]0.544	[298]0.006		[353]0.134	[277]0.017	[284]0.076	[258]0.969	[310]0.062		[264]0.328	0.000	0.000	0.000			
380	RANKONE-010	[289]0.002	[178]0.010	[322]0.367	[283]0.005	[246]0.027	[338]0.126	[247]0.013	[250]0.058	[207]0.799	[299]0.052	[194]0.208	[236]0.259	0.000	0.000	0.000		0.000	
381	RANKONE-011	[191]0.001	[233]0.011	[271]0.214	[243]0.004	[220]0.019	[223]0.082	[211]0.008	[224]0.048		[277]0.037	[185]0.182	[424]0.977	0.000	0.000	0.000		0.000	
382	RANKONE-012	[165]0.001	[198]0.010	[224]0.117	[226]0.003	[193]0.014	[165]0.069	[200]0.007	[241]0.053		[253]0.029	[162]0.144	[305]0.465	0.000	0.000	0.000		0.000	
383	RANKONE-013	[69]0.001	[63]0.007	[149]0.065	[110]0.001	[147]0.008	[85]0.054	[137]0.004	[180]0.034	[354]0.996	[212]0.018	[159]0.141	[166]0.142	0.000	0.000	0.033		0.000	
384	RANKONE-014	[53]0.001	[47]0.006	[118]0.057	[74]0.001	[87]0.005	[60]0.050	[95]0.003	[121]0.024		[159]0.009	[131]0.081	[491]1.000	0.000	0.000	0.006		0.000	
385	RANKONE-015	[57]0.001	[42]0.006	[84]0.052	[27]0.001	[82]0.005	[90]0.054	[83]0.002	[82]0.018		[117]0.007	[72]0.042	[126]0.109	0.000	0.000	0.000		0.000	
386	REALNETWORKS-000	[492]0.040	[479]0.078					[484]0.233	[448]0.319					0.001	0.000				
387	REALNETWORKS-001	[493]0.040	[480]0.078					[483]0.233	[447]0.319					0.001	0.000				
388	REALNETWORKS-002	[489]0.039	[478]0.078					[481]0.231	[446]0.315					0.001	0.000				
389	REALNETWORKS-003	[473]0.024	[467]0.062	[411]0.768	[401]0.031		[400]0.209	[460]0.159	[430]0.266	[377]0.998	[369]0.164		[315]0.500	0.001	0.000	0.009			
390	REALNETWORKS-004	[471]0.023	[465]0.059	[419]0.794	[400]0.031		[405]0.213	[459]0.158	[428]0.263	[397]0.999	[372]0.170		[337]0.613	0.001	0.000	0.009			
391	REALNETWORKS-005	[293]0.002	[272]0.013	[333]0.427	[267]0.004	[234]0.023	[284]0.102	[327]0.027	[282]0.074	[260]0.970	[276]0.037	[198]0.223	[219]0.215	0.000	0.000	0.006		0.000	
392	REALNETWORKS-006	[170]0.001	[180]0.010	[291]0.279	[210]0.002	[168]0.010	[209]0.078	[253]0.014	[238]0.053	[280]0.980	[200]0.016	[148]0.120	[178]0.154	0.000	0.000	0.009		0.000	
393	REALNETWORKS-007	[156]0.001	[165]0.009	[285]0.258	[158]0.002	[150]0.009	[179]0.072	[220]0.009	[214]0.043	[274]0.979	[179]0.012	[241]0.463	[162]0.140	0.000	0.000	0.009		0.000	
394	REALNETWORKS-008	[106]0.001	[107]0.008	[177]0.078	[167]0.002	[122]0.007	[245]0.091	[178]0.006	[156]0.029	[255]0.967	[147]0.008	[120]0.068	[146]0.129	0.000	0.000	0.042		0.000	
395	RECOGNITO-000	[38]0.001	[51]0.006	[93]0.053	[43]0.001	[249]0.028	[23]0.045	[56]0.002	[43]0.012	[60]0.175	[129]0.007	[256]0.730	[87]0.092	0.000	0.000	0.040		0.000	
396	RECOGNITO-001	[35]0.001	[32]0.006	[56]0.048	[116]0.001	[44]0.004	[61]0.050	[30]0.001	[18]0.009	[229]0.899	[49]0.003	[51]0.033	[38]0.075	0.000	0.000	0.032		0.000	
397	RECOGNITO-002	[25]0.001	[35]0.006	[70]0.049	[22]0.001	[210]0.017	[17]0.044	[14]0.001	[14]0.008	[38]0.135	[38]0.003	[243]0.510	[23]0.068	0.000	0.000	0.040		0.000	
398	REMARKAI-000	[342]0.003	[340]0.018	[380]0.656	[327]0.008		[366]0.148	[387]0.055	[346]0.120	[394]0.999	[320]0.069		[359]0.717	0.000	0.000	0.000			
399	REMARKAI-000	[417]0.008	[414]0.030					[445]0.127	[401]0.203					0.000	0.001				
400	REMARKAI-002	[415]0.008	[413]0.029	[422]0.800				[444]0.123	[399]0.196	[318]0.991				0.000	0.001	0.017			
401	RENDIP-000	[199]0.001	[300]0.015	[331]0.417	[305]0.006	[250]0.028	[230]0.084	[234]0.012	[251]0.059	[226]0.892	[227]0.022	[182]0.185	[192]0.167	0.000	0.000	0.041		0.000	
402	REVEALMEDIA-000	[240]0.001	[174]0.010	[287]0.266	[193]0.002	[181]0.012	[193]0.074	[236]0.012	[210]0.042	[186]0.677	[224]0.021	[139]0.093	[168]0.143	0.000	0.000	0.041		0.000	
403	RNIT-000	[185]0.001	[108]0.008	[220]0.114	[135]0.001	[109]0.007	[113]0.056	[230]0.011	[136]0.026	[151]0.510	[180]0.012	[201]0.239	[140]0.123	0.000	0.001	0.076		0.000	
404	ROC-016	[59]0.001	[44]0.006	[71]0.050	[20]0.001	[80]0.005	[36]0.047	[73]0.002	[76]0.017		[132]0.008	[73]0.045	[123]0.108	0.000	0.000	0.001		0.000	
405	ROC-017	[47]0.001	[45]0.006	[63]0.049	[37]0.001	[59]0.004	[26]0.046	[90]0.003	[101]0.022	[59]0.174	[110]0.006	[64]0.039	[86]0.092	0.000	0.000	0.032		0.000	
406	ROC-018	[29]0.001	[15]0.005	[35]0.045	[14]0.001	[32]0.003	[16]0.043	[65]0.002	[80]0.018	[44]0.142	[85]0.006	[58]0.037	[63]0.085	0.000	0.000	0.039		0.000	
407	ROC-019	[17]0.000	[9]0.005	[17]0.042	[12]0.001	[26]0.003	[9]0.042	[32]0.001	[21]0.009	[17]0.098	[28]0.002	[31]0.027	[29]0.070	0.000	0.000	0.041		0.000	
408	S1-000	[296]0.002	[325]0.017	[283]0.250	[297]0.005	[243]0.025	[242]0.090	[329]0.028	[300]0.085	[482]1.000	[295]0.047	[358]1.000	[495]1.000	0.000	0.000	0.040		0.000	
409	S1-001	[333]0.003	[283]0.014	[269]0.206	[215]0.003	[213]0.018	[201]0.077	[263]0.015	[235]0.052	[298]0.985	[213]0.019	[154]0.136	[172]0.148	0.001	0.000	0.035		0.000	
410	S1-002	[174]0.001	[161]0.009	[184]0.083	[101]0.001	[169]0.010	[102]0.055	[168]0.005	[163]0.031	[69]0.186	[124]0.007	[269]0.792	[381]0.841	0.000	0.000	0.028		0.000	
411	S1-003	[183]0.001	[170]0.010	[210]0.103	[140]0.001	[119]0.007	[120]0.060	[212]0.008	[191]0.037	[434]1.000	[194]0.014	[230]0.396	[543]1.000	0.000	0.000	0.033		0.000	
412	S1-004	[157]0.001	[158]0.009	[94]0.053	[69]0.001	[77]0.005	[57]0.049	[120]0.004	[122]0.025	[360]0.997	[100]0.006	[108]0.064	[487]1.000	0.000	0.000	0.033		0.000	
413	S1-005	[169]0.001	[150]0.009	[54]0.048	[34]0.001	[66]0.004	[45]0.048	[132]0.004	[108]0.022	[337]0.994	[91]0.006	[112]0.065	[394]0.895	0.000	0.000	0.033		0.000	
414	S1-006	[151]0.001	[148]0.009	[45]0.047	[94]0.001	[69]0.005	[56]0.049	[66]0.002	[73]0.016	[402]0.999	[75]0.005	[66]0.040	[291]0.423	0.000	0.000	0.033		0.000	

Table 28: **Miss rates by dataset:** *At left, rank 1 miss rates relevant to investigations; at right, with threshold set to target FPIR = 0.01 for higher volume, low prior, uses. Yellow indicates most accurate algorithm. Throughout blue superscripts indicate the rank of the algorithm for that column.*

2026/01/09 20:40:38

FNIR(N, R, T) = False neg. identification rate
FPIR(N, T) = False pos. identification rate

N = Num. enrolled subjects
R = Num. candidates examined

T = Threshold

T = 0 → Investigation
T > 0 → Identification

This publication is available free of charge from: https://doi.org/10.6028/NIST.IR.8271

#	ALGORITHM	INVESTIGATION MODE						IDENTIFICATION MODE						FAILURE TO EXTRACT					
		RANK ONE MISS RATE, FNIR(N, 0, 1)						HIGH T ⟶ FPIR = 0.001, FNIR(N, T, L)						FEATURES					
		N=1.6M						N=1.6M											
	GALLERY	MUGSHOT	MUGSHOT	MUGSHOT	VISA	BORDER	VISA	MUGSHOT	MUGSHOT	MUGSHOT	VISA	BORDER	VISA	MUGSHOT	MUGSHOT	MUGSHOT	VISA	BORDER	KIOSK
	PROBE	MUGSHOT	WEBCAM	PROFILE	BORDER	BOR¿10YR	KIOSK	MUGSHOT	WEBCAM	PROFILE	BORDER	BOR¿10YR	KIOSK	MUGSHOT	WEBCAM	PROFILE	BORDER	BOR¿10YR	KIOSK
415	S1-007	125 0.001	111 0.008	44 0.047	86 0.001	49 0.004	31 0.046	54 0.002	61 0.014	54 0.165	60 0.004	52 0.034	44 0.077	0.000	0.001	0.039		0.000	
416	SANSAP-001	110 0.001	173 0.010	156 0.068	138 0.001	310 0.087	130 0.061	133 0.004	473 0.480	245 0.958	237 0.024	322 1.000	247 0.280	0.000	0.000	0.041		0.000	
417	SCANOVATE-000	375 0.005	447 0.045	366 0.555	405 0.035		404 0.211	405 0.066	419 0.240	224 0.892	383 0.215		281 0.400	0.000	0.001	0.057			
418	SCANOVATE-001	382 0.005	441 0.040	372 0.580	399 0.031		388 0.178	416 0.081	412 0.227	233 0.910	378 0.192		285 0.404	0.000	0.001	0.044			
419	SCYLLA-001	282 0.002	408 0.028	213 0.107	385 0.021	343 0.231	364 0.146	271 0.016	532 0.995	141 0.457	415 0.431		414 0.953	0.000	0.000	0.041		0.000	
420	SENSETIME-000	307 0.002	314 0.016	355 0.523				294 0.020	260 0.063	530 1.000				0.004	0.000	0.042			
421	SENSETIME-001	308 0.002	313 0.016					301 0.022	262 0.064					0.004	0.000				
422	SENSETIME-002	453 0.013	350 0.020	326 0.377	344 0.011		287 0.104	256 0.014	150 0.028	333 0.994	261 0.032		320 0.523	0.009	0.000	0.040			
423	SENSETIME-003	58 0.001	61 0.007	238 0.140	214 0.003		246 0.091	47 0.001	47 0.012	145 0.471	141 0.008		152 0.133	0.000	0.000	0.041			
424	SENSETIME-004	56 0.001	71 0.007	137 0.062	200 0.002		231 0.084	42 0.001	52 0.013	89 0.220	94 0.006		132 0.113	0.000	0.000	0.041			
425	SENSETIME-005	20 0.001	41 0.006	60 0.048	199 0.002	116 0.007	218 0.082	64 0.002	60 0.014	53 0.163	114 0.007	88 0.051	116 0.104	0.000	0.000	0.041		0.000	
426	SENSETIME-006	19 0.001	27 0.006	33 0.044	67 0.001	33 0.004	141 0.064	44 0.001	48 0.012	373 0.998	57 0.004	53 0.034	88 0.093	0.000	0.000	0.025		0.000	
427	SENSETIME-007	14 0.000	20 0.006	13 0.041	33 0.001	23 0.003	133 0.062	23 0.001	24 0.009	400 0.999	36 0.003	23 0.024	65 0.085	0.000	0.000	0.025		0.000	
428	SENSETIME-008	13 0.000	17 0.006	21 0.043	21 0.001	22 0.003	154 0.067	20 0.001	20 0.009	127 0.398	29 0.002	18 0.021	55 0.080	0.000	0.000	0.039		0.000	
429	SENSETIME-009	12 0.000	12 0.005	9 0.041	24 0.001	21 0.003	206 0.078	6 0.001	6 0.007	217 0.866	9 0.001	8 0.015	67 0.085	0.000	0.000	0.039		0.000	
430	SENSETIME-010	7 0.000	14 0.005	6 0.040	25 0.001	24 0.003	207 0.078	8 0.001	10 0.008	16 0.096	19 0.002	17 0.020	75 0.087	0.000	0.000	0.039		0.000	
431	SERENDIPITY-000	195 0.001	299 0.015	296 0.291	266 0.004	316 0.108	191 0.073	240 0.012	404 0.213	196 0.745	209 0.018	336 1.000	167 0.142	0.000	0.000	0.041		0.000	
432	SEVENTHSENSE-001	267 0.002	149 0.009	147 0.064	185 0.002	266 0.032	169 0.070	142 0.004	212 0.043	93 0.228	165 0.010	250 0.643	144 0.127	0.000	0.000	0.039		0.000	
433	SHAMAN-003	514 0.124	502 0.172					513 0.451	484 0.597					0.020	0.011				
434	SHAMAN-004	531 0.222	516 0.319					522 0.615	501 0.754					0.020	0.011				
435	SHAMAN-006	491 0.039	463 0.058	457 0.938				453 0.141	415 0.237	262 0.971				0.020	0.011	0.869			
436	SHAMAN-007	490 0.039	462 0.057					454 0.141	418 0.240					0.020	0.010				
437	SHENNONA-000	449 0.012	482 0.086	189 0.088	364 0.014	346 0.257	255 0.094	302 0.022	382 0.160	124 0.383	367 0.160	503 1.000	331 0.558	0.007	0.063	0.041		0.000	
438	SIAT-001	265 0.002	518 0.333		268 0.004		272 0.099	276 0.017	452 0.365		257 0.031			0.000	0.000				
439	SIAT-002	271 0.002	521 0.446		451 0.348		283 0.102	298 0.021	472 0.478		406 0.372		402 0.923	0.000	0.000				
440	SMILART-004	548 0.965	544 0.974					537 0.968	528 0.976					0.011	0.013				
441	SMILART-005													0.011	0.013				
442	SPARKTEK-000	95 0.001	94 0.007	249 0.154	168 0.002	124 0.007	164 0.069	92 0.003	67 0.015	130 0.414	99 0.006	79 0.048	122 0.106	0.000	0.000	0.062		0.001	
443	SPARSH-001	79 0.001	200 0.010	121 0.058	173 0.002	308 0.082	149 0.065	128 0.004	502 0.759	268 0.976	370 0.166	467 1.000	341 0.633	0.000	0.000	0.041		0.000	
444	SQISOFT-001	359 0.004	347 0.019	289 0.273	289 0.005	247 0.027	264 0.097	449 0.132	423 0.252	205 0.794	282 0.040	217 0.317	289 0.420	0.000	0.000	0.039		0.000	
445	SQISOFT-002	148 0.001	395 0.026	181 0.080	286 0.005	347 0.282	211 0.078	334 0.029		230 0.903	433 0.621		415 0.953	0.000	0.000	0.039		0.000	
446	STAQU-000	403 0.007	356 0.020	377 0.609	381 0.020	292 0.055	374 0.159	398 0.061	465 0.443	430 1.000	426 0.535	292 0.961	549 1.000	0.000	0.000	0.000		0.000	
447	STCON-000	524 0.183	536 0.675	293 0.284	463 0.674	358 0.704	458 0.709	469 0.184	495 0.678	111 0.318	437 0.674	286 0.941	357 0.709	0.000	0.000	0.041		0.000	
448	STCON-001	30 0.001	22 0.006	36 0.045	17 0.001	153 0.009	11 0.042	43 0.001	46 0.012	35 0.131	37 0.003	226 0.370	26 0.069	0.000	0.000	0.041		0.000	
449	STCON-002	23 0.001	19 0.006	25 0.043	10 0.001	162 0.010	7 0.041	36 0.001	33 0.011	26 0.115	30 0.002	234 0.415	22 0.067	0.000	0.000	0.041		0.000	
450	STCON-003	24 0.001	23 0.006	24 0.043	6 0.001	11 0.003	5 0.041	31 0.001	27 0.010	23 0.110	27 0.002	43 0.031	15 0.065	0.000	0.000	0.041		0.000	
451	SUMSUB-000	496 0.045	493 0.106	497 0.989	431 0.097	366 0.999	433 0.313	512 0.445	499 0.742	463 1.000	447 0.852	524 1.000	434 0.996	0.000	0.000	0.000		0.000	
452	SYNESIS-003	520 0.170	511 0.235					518 0.582	490 0.646					0.006	0.015				
453	SYNESIS-003	457 0.016	381 0.023	430 0.825	357 0.013		356 0.136	403 0.065	349 0.123	247 0.960	325 0.075		258 0.314	0.000	0.001	0.063			
454	SYNESIS-005	416 0.008	260 0.013	403 0.741	232 0.003		249 0.092	311 0.024	277 0.072	293 0.983	264 0.032		217 0.214	0.001	0.000	0.135			
455	T4ISB-000	429 0.010	385 0.023	341 0.456	211 0.003	322 0.115	216 0.081	264 0.015	239 0.053	149 0.505	222 0.021	263 0.759	189 0.161	0.000	0.000	0.000		0.000	
456	TECH5-001	355 0.004	324 0.017	370 0.579	313 0.007		298 0.107	390 0.057	523 0.935	481 1.000	386 0.244		433 0.994	0.000	0.000	0.006			
457	TECH5-002	314 0.002	208 0.011	303 0.304	231 0.003	258 0.029	241 0.089	322 0.027	275 0.070	208 0.803	280 0.039	191 0.205	297 0.440	0.001	0.000	0.041		0.000	
458	TECH5-003	78 0.001	219 0.011	122 0.058	183 0.002	312 0.089	151 0.066	117 0.004	506 0.801	288 0.982	375 0.179	409 1.000	348 0.656	0.000	0.000	0.041		0.000	
459	TEVIAN-003	454 0.015	455 0.052					467 0.177	441 0.298					0.001	0.002				
460	TEVIAN-004	439 0.011	433 0.038					438 0.117	392 0.176					0.001	0.002				

Table 29: **Miss rates by dataset:** *At left, rank 1 miss rates relevant to investigations; at right, with threshold set to target FPIR = 0.01 for higher volume, low prior, uses. Yellow indicates most accurate algorithm. Throughout blue superscripts indicate the rank of the algorithm for that column.*

2026/01/09 20:40:38

FNIR(N, R, T) = False neg. identification rate
FPIR(N, T) = False pos. identification rate

N = Num. enrolled subjects
R = Num. candidates examined

T = Threshold

T = 0 → Investigation
T > 0 → Identification

This publication is available free of charge from: https://doi.org/10.6028/NIST.IR.8271

#	ALGORITHM	INVESTIGATION MODE						IDENTIFICATION MODE						FAILURE TO EXTRACT					
		RANK ONE MISS RATE, FNIR(N, 0, 1)						HIGH T → FPIR = 0.001, FNIR(N, T, L)						FEATURES					
		N=1.6M						N=1.6M											
	GALLERY	MUGSHOT	MUGSHOT	MUGSHOT	VISA	BORDER	VISA	MUGSHOT	MUGSHOT	MUGSHOT	VISA	BORDER	VISA	MUGSHOT	MUGSHOT	MUGSHOT	VISA	BORDER	KIOSK
	PROBE	MUGSHOT	WEBCAM	PROFILE	BORDER	BOR¿10YR	KIOSK	MUGSHOT	WEBCAM	PROFILE	BORDER	BOR¿10YR	KIOSK	MUGSHOT	WEBCAM	PROFILE	BORDER	BOR¿10YR	KIOSK
461	TEVIAN-005	[406]0.007	[410]0.028	[342]0.460				[423]0.087	[369]0.144	[250]0.961				0.001	0.002	0.116			
462	TEVIAN-006	[297]0.002	[227]0.011	[219]0.113	[217]0.003	[192]0.013	[173]0.071	[221]0.009	[170]0.032	[131]0.418	[202]0.016	[137]0.093	[413]0.951	0.001	0.000	0.062		0.000	
463	TEVIAN-007	[235]0.001	[163]0.009	[183]0.082	[184]0.002	[160]0.009	[157]0.067	[159]0.005	[100]0.022	[106]0.293	[160]0.009	[111]0.065	[139]0.122	0.000	0.000	0.062		0.000	
464	TIGER-000	[502]0.061	[489]0.095					[506]0.390	[474]0.500					0.000	0.000				
465	TIGER-002	[387]0.005	[378]0.023	[348]0.509				[420]0.086	[379]0.158	[387]0.999				0.000	0.000	0.056			
466	TIGER-003	[388]0.005	[379]0.023					[419]0.086	[378]0.158					0.000	0.000				
467	TIGER-004	[310]0.002	[328]0.017	[212]0.106	[325]0.007	[303]0.076	[195]0.075	[273]0.017	[278]0.072	[129]0.410	[337]0.095	[331]1.000	[282]0.402	0.001	0.009	0.041		0.004	
468	TONGYITRANS-000	[398]0.007	[375]0.022					[410]0.074	[338]0.112					0.003	0.001				
469	TONGYITRANS-001	[399]0.007	[376]0.022					[404]0.066	[329]0.101					0.003	0.001				
470	TOSHIBA-000	[367]0.004	[368]0.022	[409]0.764				[399]0.062	[343]0.118	[346]0.995				0.000	0.000	0.070			
471	TOSHIBA-001	[372]0.005	[372]0.022					[393]0.057	[312]0.092					0.000	0.000				
472	TOSHIBA-002	[145]0.001	[203]0.011	[23]0.043	[30]0.001	[14]0.003	[35]0.047	[48]0.001	[69]0.015	[13]0.094	[20]0.002	[44]0.031	[19]0.066	0.001	0.000	0.040		0.000	
473	TOSS-000	[158]0.001	[143]0.009	[34]0.045	[35]0.001	[37]0.004	[25]0.046	[58]0.002	[62]0.014	[28]0.121	[51]0.003	[57]0.037	[27]0.069	0.000	0.000	0.040		0.000	
474	TRUEFACE-000	[339]0.003	[277]0.014	[276]0.221	[319]0.007	[240]0.024	[250]0.092	[281]0.018	[258]0.062	[219]0.881	[254]0.030	[187]0.194	[210]0.188	0.001	0.001	0.047		0.003	
475	TTIGROUP-000	[253]0.002	[291]0.014	[158]0.068	[254]0.004	[341]0.213	[252]0.093	[213]0.009	[442]0.298	[375]0.998	[393]0.286	[334]1.000	[384]0.855	0.000	0.000	0.000		0.000	
476	TURINGTECHVIP-001	[425]0.009	[399]0.026	[163]0.070	[413]0.045	[338]0.199	[408]0.220	[497]0.345	[514]0.850	[325]0.993	[459]0.978	[435]1.000	[440]0.999	0.001	0.003	0.044		0.000	
477	UNISSEY-001	[527]0.210	[538]0.692	[339]0.449	[464]0.690	[362]0.731	[459]0.737	[478]0.214	[499]0.700	[176]0.619	[440]0.693	[312]0.999	[362]0.748	0.000	0.000	0.041		0.000	
478	UNISSEY-002	[523]0.181	[535]0.673	[297]0.291	[462]0.674	[360]0.710	[457]0.703	[470]0.187	[496]0.685	[168]0.571	[443]0.724	[313]1.000	[392]0.891	0.000	0.000	0.041		0.000	
479	UNISSEY-003	[345]0.003	[311]0.016	[232]0.131	[366]0.014	[236]0.023	[196]0.075	[255]0.014	[228]0.050	[159]0.524	[251]0.029	[192]0.205	[196]0.173	0.001	0.006	0.042		0.011	
480	USEB-000	[486]0.034	[457]0.054	[323]0.373	[383]0.021	[334]0.172	[355]0.135	[525]0.715	[498]0.722	[256]0.968	[421]0.490	[270]0.804	[345]0.648	0.000	0.001	0.042		0.000	
481	USEB-001	[127]0.001	[160]0.009	[198]0.094	[82]0.001	[134]0.008	[80]0.052	[114]0.004	[112]0.023	[285]0.982	[73]0.005	[254]0.728	[72]0.087	0.000	0.001	0.042		0.000	
482	USEB-002	[175]0.001	[172]0.010	[202]0.095	[79]0.001	[133]0.008	[81]0.052	[127]0.004	[118]0.023	[284]0.982	[81]0.005	[255]0.728	[77]0.088	0.000	0.001	0.042		0.000	
483	USEB-003	[128]0.001	[157]0.009	[199]0.094	[61]0.001	[108]0.007	[70]0.051	[111]0.003	[97]0.021	[261]0.971	[80]0.005	[232]0.398	[73]0.087	0.000	0.001	0.042		0.000	
484	USEB-004	[150]0.001	[153]0.009	[65]0.049	[39]0.001	[314]0.096	[74]0.052	[107]0.003	[109]0.022	[66]0.182	[170]0.010	[320]1.000	[209]0.186	0.000	0.000	0.040		0.000	
485	VD-000	[541]0.474	[527]0.551					[534]0.917	[525]0.946					0.011	0.013				
486	VD-001	[480]0.027	[456]0.053					[473]0.201	[438]0.281					0.005	0.001				
487	VD-002	[426]0.009	[405]0.027	[438]0.892	[362]0.013	[287]0.050	[385]0.176	[414]0.078	[371]0.148	[350]0.995	[336]0.095	[224]0.367	[275]0.372	0.004	0.003	0.156		0.002	
488	VD-003	[407]0.007	[369]0.022	[412]0.770	[332]0.008	[260]0.030	[357]0.137	[366]0.045	[326]0.100	[389]0.999	[297]0.051	[203]0.244	[260]0.315	0.003	0.003	0.144		0.002	
489	VDFSOFTWARE-001	[526]0.206	[504]0.179	[421]0.799	[342]0.010	[327]0.128	[321]0.117	[546]1.000	[476]0.518	[460]1.000	[439]0.680	[314]1.000	[412]0.948	0.000	0.000	0.000		0.000	
490	VDFSOFTWARE-002	[277]0.002	[206]0.011	[246]0.148	[258]0.004	[301]0.071	[238]0.087	[353]0.038	[334]0.107	[189]0.713	[324]0.075	[328]1.000	[290]0.423	0.000	0.000	0.040		0.000	
491	VERIDAS-001	[319]0.002	[284]0.014	[363]0.545	[306]0.006	[254]0.028	[346]0.131	[351]0.037	[297]0.082	[307]0.987	[288]0.044	[205]0.266	[241]0.264	0.000	0.002	0.093		0.001	
492	VERIDAS-002	[318]0.002	[285]0.014	[364]0.545	[307]0.006	[253]0.028	[345]0.131	[350]0.037	[298]0.082	[306]0.987	[287]0.044	[206]0.266	[240]0.264	0.000	0.002	0.093		0.001	
493	VERIDAS-003	[237]0.001	[226]0.011	[295]0.289	[252]0.004	[205]0.016	[302]0.108	[269]0.016	[245]0.055	[359]0.997	[219]0.020	[167]0.150	[201]0.178	0.000	0.002	0.093		0.001	
494	VERIDAS-004	[160]0.001	[119]0.008	[257]0.177	[212]0.003	[155]0.009	[265]0.097	[170]0.005	[130]0.025	[273]0.978	[139]0.008	[100]0.058	[136]0.118	0.000	0.002	0.094		0.001	
495	VERIGRAM-000	[306]0.002	[312]0.016	[98]0.053	[174]0.002	[129]0.007	[76]0.052	[150]0.005	[151]0.028	[83]0.212	[104]0.006	[133]0.088	[62]0.083	0.001	0.004	0.046		0.001	
496	VERIGRAM-001	[304]0.002	[305]0.015	[92]0.053	[160]0.002	[121]0.007	[40]0.047	[152]0.005	[202]0.039	[172]0.584	[102]0.006	[297]0.988	[58]0.082	0.001	0.003	0.045		0.001	
497	VERIJELAS-000	[536]0.354	[519]0.369	[482]0.968	[428]0.086	[337]0.191	[428]0.292	[528]0.799	[508]0.813	[384]0.999	[399]0.324	[285]0.933	[332]0.589	0.002	0.001	0.070		0.001	
498	VIANTE-000	[138]0.001	[123]0.008	[170]0.072	[118]0.001	[58]0.004	[97]0.055	[85]0.003	[58]0.014	[47]0.147	[109]0.006	[61]0.038	[74]0.087	0.001	0.000	0.073		0.001	
499	VIANTE-001	[133]0.001	[116]0.008	[165]0.071	[36]0.001	[27]0.003	[53]0.049	[37]0.001	[23]0.009	[21]0.105	[32]0.002	[211]0.293	[21]0.067	0.001	0.000	0.073		0.001	
500	VIGILANTSOLUTIONS-003	[506]0.069	[499]0.151	[472]0.957				[510]0.408	[493]0.660	[383]0.999				0.000	0.001	0.127			
501	VIGILANTSOLUTIONS-004	[515]0.125	[512]0.244	[477]0.965				[517]0.549	[510]0.817	[353]0.996				0.000	0.001	0.127			
502	VIGILANTSOLUTIONS-005	[422]0.009		[445]0.919				[504]0.386		[453]1.000				0.000	0.001	0.127			
503	VIGILANTSOLUTIONS-006	[428]0.010		[446]0.920				[500]0.349		[465]1.000				0.000	0.001	0.127			
504	VIGILANTSOLUTIONS-007	[341]0.003	[331]0.017	[449]0.924	[358]0.013	[300]0.068	[383]0.175	[333]0.028	[306]0.088	[352]0.996	[331]0.081	[227]0.371	[280]0.391	0.000	0.001	0.127		0.001	
505	VIGILANTSOLUTIONS-008	[327]0.003	[333]0.017	[444]0.912	[368]0.014	[302]0.072	[386]0.178	[291]0.020	[287]0.077	[386]0.999	[341]0.104	[231]0.398	[317]0.511	0.000	0.001	0.127		0.001	
506	VINBIGDATA-001	[126]0.001	[85]0.007	[195]0.093	[147]0.001	[173]0.011	[120]0.057	[265]0.016	[254]0.059	[237]0.931	[210]0.018	[287]0.944	[245]0.274	0.000	0.000	0.041		0.000	

Table 30: **Miss rates by dataset:** *At left, rank 1 miss rates relevant to investigations; at right, with threshold set to target FPIR = 0.01 for higher volume, low prior, uses. Yellow indicates most accurate algorithm. Throughout blue superscripts indicate the rank of the algorithm for that column.*

2026/01/09 20:40:38

FNIR(N, R, T) = False neg. identification rate
FPIR(N, T) = False pos. identification rate

N = Num. enrolled subjects
R = Num. candidates examined

T = Threshold

T = 0 → Investigation
T > 0 → Identification

This publication is available free of charge from: https://doi.org/10.6028/NIST.IR.8271

#	ALGORITHM	INVESTIGATION MODE						IDENTIFICATION MODE						FAILURE TO EXTRACT					
		RANK ONE MISS RATE, FNIR(N, 0, 1)						HIGH T ⟶ FPIR = 0.001, FNIR(N, T, L)						FEATURES					
		N=1.6M						N=1.6M											
	GALLERY	MUGSHOT	MUGSHOT	MUGSHOT	VISA	BORDER	VISA	MUGSHOT	MUGSHOT	MUGSHOT	VISA	BORDER	VISA	MUGSHOT	MUGSHOT	MUGSHOT	VISA	BORDER	KIOSK
	PROBE	MUGSHOT	WEBCAM	PROFILE	BORDER	BOR¿10YR	KIOSK	MUGSHOT	WEBCAM	PROFILE	BORDER	BOR¿10YR	KIOSK	MUGSHOT	WEBCAM	PROFILE	BORDER	BOR¿10YR	KIOSK
507	VINBIGDATA-002	[44]0.001	[24]0.006	[102]0.054	[75]0.001	[91]0.006	[69]0.051	[63]0.002	[42]0.012	[52]0.160	[62]0.005	[216]0.317	[41]0.076	0.000	0.000	0.040		0.000	
508	VINBIGDATA-003	[34]0.001	[28]0.006	[59]0.048	[54]0.001	[63]0.004	[32]0.046	[72]0.002	[53]0.013	[43]0.141	[59]0.004	[65]0.039	[32]0.070	0.000	0.000	0.040		0.000	
509	VINBIGDATA-004	[36]0.001	[26]0.006	[49]0.047	[49]0.001	[50]0.004	[30]0.046	[50]0.002	[30]0.010	[34]0.130	[44]0.003	[45]0.032	[24]0.068	0.000	0.000	0.041		0.000	
510	VISIONBOX-000	[254]0.002	[228]0.011	[405]0.750	[276]0.005	[208]0.017	[210]0.078	[278]0.017	[248]0.057	[316]0.990	[230]0.023	[164]0.146	[190]0.162	0.000	0.001	0.043		0.001	
511	VISIONBOX-001	[328]0.003	[304]0.015	[434]0.848	[239]0.003	[216]0.018	[360]0.140	[450]0.133	[255]0.060	[467]1.000	[363]0.152	[309]0.999	[403]0.924	0.002	0.000	0.264		0.001	
512	VISIONBOX-002	[238]0.001	[193]0.010	[243]0.143	[188]0.002	[174]0.011	[136]0.062	[231]0.011	[209]0.042	[192]0.730	[196]0.015	[150]0.125	[161]0.140	0.001	0.001	0.056		0.001	
513	VISIONLABS-004	[329]0.003	[352]0.020	[315]0.335				[392]0.057	[380]0.159	[223]0.888				0.001	0.001	0.046			
514	VISIONLABS-005	[311]0.002	[342]0.019	[313]0.326				[373]0.050	[370]0.147	[222]0.886				0.001	0.001	0.046			
515	VISIONLABS-006	[276]0.002	[306]0.015	[268]0.202	[247]0.004		[259]0.096	[320]0.026	[310]0.090	[180]0.668				0.001	0.001	0.051			
516	VISIONLABS-007	[274]0.002	[303]0.015	[267]0.202	[242]0.004		[258]0.095	[319]0.026	[309]0.090	[181]0.668	[260]0.031		[206]0.185	0.001	0.001	0.051			
517	VISIONLABS-008	[263]0.002	[278]0.014	[231]0.131	[198]0.002		[214]0.081	[244]0.013	[234]0.051	[146]0.475	[203]0.017		[174]0.151	0.001	0.000	0.075			
518	VISIONLABS-009	[104]0.001	[136]0.008	[182]0.081	[133]0.001		[172]0.071	[138]0.004	[132]0.025	[206]0.797	[148]0.008		[131]0.113	0.000	0.000	0.060			
519	VISIONLABS-010	[171]0.001	[197]0.010	[125]0.058	[123]0.001	[95]0.006	[168]0.069	[157]0.005	[146]0.027		[136]0.008	[96]0.055	[124]0.109	0.000	0.000	0.040		0.000	
520	VISIONLABS-011	[116]0.001	[147]0.009	[95]0.053	[115]0.001	[64]0.004	[140]0.063	[98]0.003	[86]0.020		[64]0.004	[54]0.034	[83]0.090	0.000	0.000	0.032		0.000	
521	VISTEAM-000	[379]0.005	[351]0.020	[301]0.301	[347]0.011	[317]0.108	[331]0.124	[418]0.085	[402]0.205	[221]0.886	[350]0.128	[323]1.000	[269]0.345	0.000	0.000	0.040		0.000	
522	VISTEAM-001	[385]0.005	[366]0.021	[302]0.302	[360]0.013	[319]0.110	[342]0.127	[436]0.109	[470]0.469	[218]0.878	[364]0.154	[339]1.000	[276]0.374	0.000	0.000	0.040		0.000	
523	VIXVIZION-009	[290]0.002	[259]0.013	[270]0.210	[275]0.005	[262]0.031	[301]0.107	[324]0.027	[285]0.077	[195]0.742	[284]0.041	[209]0.286	[308]0.472	0.000	0.000	0.000		0.000	
524	VNIS-000	[513]0.105	[497]0.143	[383]0.671	[436]0.127	[355]0.448	[421]0.279	[494]0.311	[460]0.418	[326]0.993	[442]0.701	[274]0.838	[355]0.696	0.012	0.019	0.098		0.062	
525	VNPAY-001	[180]0.001	[99]0.008	[145]0.064	[280]0.005	[176]0.012	[234]0.085	[172]0.006	[139]0.026	[103]0.280	[178]0.012	[114]0.066	[125]0.109	0.001	0.001	0.048		0.006	
526	VNPT-001	[280]0.002	[292]0.014	[236]0.135	[209]0.002	[239]0.023	[175]0.071	[251]0.014	[270]0.068	[190]0.715	[271]0.035	[299]0.990	[272]0.362	0.001	0.000	0.042		0.000	
527	VNPT-002	[246]0.002	[251]0.012	[119]0.058	[108]0.001	[104]0.006	[89]0.054	[184]0.006	[169]0.032	[105]0.284	[130]0.007	[123]0.072	[98]0.096	0.001	0.000	0.042		0.000	
528	VNPT-003	[206]0.001	[97]0.007	[130]0.060	[113]0.001	[100]0.006	[95]0.054	[181]0.006	[152]0.028	[248]0.960	[125]0.007	[105]0.062	[99]0.096	0.001	0.000	0.041		0.000	
529	VNPT-004	[208]0.001	[96]0.007	[126]0.059	[102]0.001	[90]0.006	[92]0.054	[163]0.005	[133]0.026	[228]0.899	[119]0.007	[97]0.057	[89]0.093	0.001	0.000	0.041		0.000	
530	VNPT-005	[210]0.001	[90]0.007	[108]0.056	[91]0.001	[81]0.005	[78]0.052	[139]0.004	[115]0.023	[215]0.853	[77]0.005	[77]0.047	[81]0.090	0.001	0.000	0.041		0.000	
531	VOCORD-003	[392]0.006	[388]0.024	[423]0.802	[423]0.061		[393]0.188	[443]0.122	[376]0.155	[372]0.998	[366]0.157		[284]0.404	0.001	0.011	0.425			
532	VOCORD-004	[411]0.008	[360]0.021	[415]0.789	[355]0.012		[340]0.127	[501]0.353	[388]0.173	[435]1.000	[379]0.193		[429]0.991	0.000	0.000	0.000			
533	VOCORD-005	[402]0.007	[382]0.023	[425]0.810	[419]0.055		[398]0.206	[458]0.156	[356]0.130	[362]0.997	[358]0.138		[277]0.381	0.001	0.009	0.554			
534	VOCORD-006	[553]1.000	[551]1.000	[551]1.000	[544]1.000		[522]1.000	[552]1.000	[553]1.000	[519]1.000	[518]1.000		[509]1.000	0.001	0.009	0.554			
535	VTCC-000	[365]0.004	[343]0.019	[172]0.073	[238]0.003	[265]0.032	[177]0.071	[396]0.058	[500]0.753	[455]1.000	[416]0.435	[303]0.995	[454]1.000	0.000	0.000	0.000		0.000	
536	VTCC-001	[273]0.002	[230]0.011	[123]0.058	[367]0.014	[271]0.036	[236]0.086							0.000	0.000	0.040		0.001	
537	VTCC-002	[268]0.002	[411]0.028	[124]0.058	[288]0.005	[277]0.040	[251]0.092	[229]0.010	[489]0.631	[100]0.269	[411]0.421	[311]0.999	[364]0.750	0.000	0.000	0.040		0.001	
538	VTS-000	[544]0.594	[533]0.608	[442]0.908	[458]0.607	[361]0.724	[460]0.739	[520]0.598	[487]0.619	[399]0.999	[432]0.613	[264]0.760	[365]0.761	0.000	0.001	0.047		0.000	
539	VTS-001	[197]0.001	[182]0.010	[251]0.158	[300]0.006	[214]0.018	[205]0.077	[245]0.013	[233]0.051	[332]0.994	[228]0.022	[160]0.141	[212]0.192	0.000	0.000	0.040		0.000	
540	VTS-002	[255]0.002	[268]0.013	[277]0.224	[370]0.014	[275]0.038	[335]0.125	[314]0.026	[283]0.075	[410]1.000	[291]0.045	[199]0.231	[288]0.417	0.000	0.000	0.029		0.000	
541	VTS-003	[108]0.001	[82]0.007	[146]0.064	[155]0.002	[151]0.009	[84]0.053	[196]0.007	[173]0.033	[447]1.000	[192]0.014	[290]0.954	[342]0.635	0.000	0.001	0.029		0.000	
542	VTS-004	[61]0.001	[62]0.007	[104]0.055	[117]0.001	[127]0.007	[49]0.048	[148]0.004	[144]0.027	[477]1.000	[154]0.009	[315]1.000	[216]0.203	0.000	0.001	0.029		0.000	
543	VTS-005	[51]0.001	[52]0.006	[83]0.052	[96]0.001	[94]0.006	[42]0.047	[164]0.005	[161]0.030	[367]0.998	[118]0.007	[271]0.811	[110]0.100	0.000	0.001	0.029		0.000	
544	WINK-000	[481]0.029	[487]0.095	[492]0.979	[418]0.049	[335]0.176	[438]0.366	[474]0.203	[454]0.377	[292]0.983	[389]0.261	[494]1.000	[346]0.649	0.007	0.001	0.979		0.000	
545	WINK-001	[324]0.003	[454]0.049	[413]0.785	[442]0.206	[348]0.296	[416]0.253	[346]0.036	[358]0.131	[355]0.996	[385]0.237	[280]0.903	[274]0.372	0.001	0.036	0.043		0.169	
546	WINK-002	[152]0.001	[458]0.055	[389]0.696	[448]0.285	[350]0.386	[426]0.291	[238]0.012	[313]0.092	[249]0.961	[395]0.294	[295]0.978	[268]0.342	0.000	0.048	0.041		0.247	
547	XFORWARDAI-000	[291]0.002	[281]0.014	[178]0.078	[248]0.004	[198]0.015	[254]0.094	[259]0.015	[242]0.053	[134]0.434	[223]0.021	[176]0.159	[193]0.169	0.000	0.000	0.000		0.000	
548	XFORWARDAI-001	[272]0.002	[256]0.013	[114]0.056	[222]0.003	[152]0.009	[220]0.082	[149]0.005	[153]0.028	[135]0.441	[142]0.008	[107]0.062	[141]0.123	0.000	0.000	0.000		0.000	
549	XFORWARDAI-002	[258]0.002	[244]0.012	[55]0.048	[207]0.002	[112]0.007	[202]0.077	[88]0.003	[72]0.016	[155]0.519	[76]0.005	[68]0.041	[106]0.099	0.000	0.000	0.000		0.000	
550	YISHENG-001	[479]0.026	[466]0.060		[422]0.058		[424]0.287	[498]0.346	[507]0.808		[436]0.666		[400]0.919	0.002	0.005				
551	YITU-002	[245]0.002	[188]0.010					[275]0.017	[225]0.049					0.000	0.000				
552	YITU-003	[325]0.003	[317]0.016					[284]0.018	[237]0.052					0.003	0.001				

Table 31: **Miss rates by dataset:** *At left, rank 1 miss rates relevant to investigations; at right, with threshold set to target FPIR = 0.01 for higher volume, low prior, uses. Yellow indicates most accurate algorithm. Throughout blue superscripts indicate the rank of the algorithm for that column.*

2026/01/09 20:40:38

FNIR(N, R, T) = FPIR(N, T) =

False neg. identification rate
False pos. identification rate

N = Num. enrolled subjects
R = Num. candidates examined

T = Threshold

T = 0 → Investigation
T > 0 → Identification

This publication is available free of charge from: https://doi.org/10.6028/NIST.IR.8271

#	ALGORITHM	INVESTIGATION MODE						IDENTIFICATION MODE						FAILURE TO EXTRACT					
		RANK ONE MISS RATE, FNIR(N, 0, 1)						HIGH T → FPIR = 0.001, FNIR(N, T, L)						FEATURES					
		N=1.6M						N=1.6M											
	GALLERY	MUGSHOT	MUGSHOT	MUGSHOT	VISA	BORDER	VISA	MUGSHOT	MUGSHOT	MUGSHOT	VISA	BORDER	VISA	MUGSHOT	MUGSHOT	MUGSHOT	VISA	BORDER	KIOSK
	PROBE	MUGSHOT	WEBCAM	PROFILE	BORDER	BOR¿10YR	KIOSK	MUGSHOT	WEBCAM	PROFILE	BORDER	BOR¿10YR	KIOSK	MUGSHOT	WEBCAM	PROFILE	BORDER	BOR¿10YR	KIOSK
553	YITU-004	[164]0.001	[134]0.008	[436]0.864				[218]0.009	[142]0.027	[238]0.936				0.000	0.000	0.000			
554	YITU-005	[302]0.002	[295]0.014					[226]0.010	[171]0.032					0.003	0.001				
555	YUAN-000	[224]0.001	[264]0.013	[229]0.128	[141]0.001	[138]0.008	[135]0.062	[228]0.010	[217]0.045	[115]0.342	[183]0.012	[220]0.333	[148]0.129	0.001	0.006	0.071		0.000	

Table 32: **Miss rates by dataset:** *At left, rank 1 miss rates relevant to investigations; at right, with threshold set to target FPIR = 0.01 for higher volume, low prior, uses. Yellow indicates most accurate algorithm. Throughout blue superscripts indicate the rank of the algorithm for that column.*

2026/01/09 20:40:38

FNIR(N, R, T) = False neg. identification rate
FPIR(N, T) = False pos. identification rate

N = Num. enrolled subjects
R = Num. candidates examined

T = Threshold

T = 0 → Investigation
T > 0 → Identification

This publication is available free of charge from: https://doi.org/10.6028/NIST.IR.8271

MISSES BELOW THRESHOLD, T FNIR(N, T> 0, R >L)		ENROL MOST RECENT DATASET: FRVT 2018 MUGSHOTS				
#	ALGORITHM	N=0.64M	N=1.6M	N=3.0M	N=6.0M	N=12.0M
1	3DIVI-005	464 0.1353	463 0.1661	412 0.1907	398 0.2339	387 0.2995
2	ACER-000	456 0.1182	455 0.1452	406 0.1711	392 0.2071	380 0.2534
3	ADVANCE-000	287 0.0138	289 0.0195	274 0.0243	263 0.0401	264 0.1278
4	AFISBIOMETRICS-000	334 0.0201	336 0.0295	319 0.0378	311 0.0559	246 0.1173
5	AFRENGINE-000	283 0.0134	285 0.0185	275 0.0245	283 0.0461	328 0.1717
6	AFRENGINE-001	111 0.0025	102 0.0030	98 0.0040	114 0.0115	163 0.0919
7	AFRENGINE-002	101 0.0023	93 0.0028	87 0.0034	122 0.0117	151 0.0901
8	AFRENGINE-003	166 0.0036	144 0.0044	129 0.0054	113 0.0115	165 0.0921
9	AIZE-002	377 0.0374	374 0.0508	350 0.0653	352 0.1022	365 0.2232
10	AKUVOX-001	244 0.0093	246 0.0130	234 0.0168	234 0.0317	253 0.1234
11	ALCHERA-003	454 0.1172	457 0.1550	408 0.1834	401 0.2389	396 0.3457
12	ALCHERA-006	154 0.0034	154 0.0046	145 0.0060	170 0.0166	203 0.1034
13	ALCHERA-008	108 0.0025	108 0.0032	104 0.0042	97 0.0098	117 0.0815
14	ALGORITHMSINC-000	278 0.0132	268 0.0160	267 0.0235	265 0.0404	239 0.1156
15	ALLGOVISION-000	425 0.0684	425 0.0878	387 0.1081	376 0.1386	360 0.2126
16	ALLGOVISION-001	432 0.0782	432 0.1014	395 0.1215	384 0.1581	368 0.2270
17	ANKE-000	441 0.0939	439 0.1166	401 0.1394	389 0.1767	378 0.2486
18	ANKE-002	342 0.0225	341 0.0315	325 0.0402	314 0.0602	300 0.1463
19	ARATEK-001	203 0.0053	206 0.0078	201 0.0109	251 0.0367	293 0.1433
20	ARMATURA-000	142 0.0031	131 0.0039	118 0.0051	93 0.0095	61 0.0613
21	AWARE-003	451 0.1094	446 0.1279	402 0.1438	387 0.1754	371 0.2325
22	AWARE-005	504 0.3375	502 0.3633	420 0.3963	411 0.4470	379 0.2519
23	AWARE-007	267 0.0117	267 0.0158	251 0.0199	236 0.0319	235 0.1146
24	AYONIX-002	531 0.7859	531 0.8241	427 0.8500	417 0.8697	409 0.8927
25	BIOIDTECHSWISS-001	126 0.0028	125 0.0038	123 0.0053	132 0.0125	190 0.0991
26	BIOMETRIK-001	379 0.0385	376 0.0520	360 0.0675	351 0.0984	336 0.2062
27	CAMVI-004	373 0.0363	407 0.0713	381 0.0976	403 0.2503	385 0.2679
28	CANON-001	165 0.0036	162 0.0051	162 0.0070	160 0.0154	164 0.0920
29	CANON-002	147 0.0033	140 0.0043	140 0.0058	128 0.0121	113 0.0805
30	CANON-003	65 0.0015	71 0.0021	72 0.0028	62 0.0068	71 0.0660
31	CIB-000	234 0.0082	239 0.0121	229 0.0156	229 0.0299	398 0.3606
32	CLEARVIEWAI-000	169 0.0037	171 0.0055	168 0.0074	164 0.0155	177 0.0968
33	CLEARVIEWAI-001	105 0.0024	112 0.0035	115 0.0049	96 0.0096	47 0.0556
34	CLEARVIEWAI-002	119 0.0027	123 0.0038	130 0.0054	103 0.0102	60 0.0605
35	CLEARVIEWAI-003	73 0.0016	70 0.0021	71 0.0027	56 0.0065	40 0.0522
36	CLOUDWALK-HR-000	67 0.0015	59 0.0017	52 0.0020	63 0.0068	83 0.0698
37	CLOUDWALK-MT-000	71 0.0016	57 0.0017	47 0.0018	27 0.0046	28 0.0463
38	CLOUDWALK-MT-001	62 0.0015	52 0.0016	41 0.0017	33 0.0048	46 0.0551
39	CLOUDWALK-MT-002	61 0.0015	49 0.0015	37 0.0016	32 0.0047	55 0.0583
40	COGENT-000	395 0.0426	378 0.0523	361 0.0688	361 0.1106	342 0.1872
41	COGENT-001	394 0.0426	379 0.0523	362 0.0688	362 0.1106	341 0.1872
42	COGENT-002	359 0.0318	362 0.0441	345 0.0587	356 0.1077	358 0.2080
43	COGENT-003	360 0.0324	365 0.0453	355 0.0667	368 0.1241	372 0.2341
44	COGENT-004	339 0.0206	342 0.0327	340 0.0523	363 0.1135	359 0.2116
45	COGENT-005	214 0.0061	214 0.0087	207 0.0119	230 0.0299	252 0.1230
46	COGENT-006	130 0.0029	134 0.0040	127 0.0053	120 0.0117	126 0.0827
47	COGENT-007	109 0.0025	109 0.0033	111 0.0046	107 0.0107	101 0.0753
48	COGNITEC-000	467 0.1374	461 0.1602	411 0.1858	394 0.2154	386 0.2784
49	COGNITEC-001	435 0.0803	431 0.1013	394 0.1204	379 0.1495	361 0.2159
50	COGNITEC-002	387 0.0402	381 0.0527	351 0.0654	341 0.0910	339 0.1810
51	COGNITEC-003	384 0.0395	377 0.0520	348 0.0642	338 0.0874	319 0.1648
52	COGNITEC-004	341 0.0219	340 0.0310	321 0.0385	304 0.0537	221 0.1100
53	COGNITEC-005	212 0.0060	219 0.0093	219 0.0140	220 0.0284	175 0.0964
54	COGNITEC-006	196 0.0049	201 0.0073	205 0.0113	205 0.0251	159 0.0916
55	COGNITEC-007	164 0.0036	169 0.0053	175 0.0079	163 0.0155	116 0.0812
56	COGNITEC-008	168 0.0036	175 0.0056	172 0.0077	158 0.0152	122 0.0822
57	COGNITEC-009	171 0.0038	179 0.0059	177 0.0080	167 0.0158	129 0.0829
58	COMPAL-000	204 0.0053	204 0.0075	497 1.0000	509 1.0000	489 1.0000
59	CORSIGHT-000	180 0.0042	180 0.0059	178 0.0080	174 0.0176	204 0.1039
60	CORSIGHT-001	187 0.0045	188 0.0064	181 0.0084	176 0.0180	169 0.0945
61	CUBOX-001	89 0.0020	89 0.0027	84 0.0034	67 0.0071	52 0.0575
62	CUBOX-002	99 0.0023	100 0.0030	92 0.0037	68 0.0072	34 0.0493
63	CUBOX-003	106 0.0024	105 0.0032	100 0.0040	73 0.0074	35 0.0506
64	CYBERLINK-000	389 0.0411	389 0.0561	367 0.0704	354 0.1028	354 0.2047
65	CYBERLINK-001	380 0.0389	382 0.0532	364 0.0691	349 0.0969	335 0.1791
66	CYBERLINK-002	253 0.0102	257 0.0145	250 0.0198	262 0.0395	259 0.1252
67	CYBERLINK-003	202 0.0052	202 0.0074	193 0.0097	200 0.0232	254 0.1234
68	CYBERLINK-004	193 0.0048	194 0.0068	196 0.0099	281 0.0458	304 0.1509
69	CYBERLINK-005	220 0.0063	223 0.0096	217 0.0134	259 0.0391	313 0.1563
70	CYBERLINK-006	80 0.0018	82 0.0023	80 0.0030	77 0.0078	51 0.0571
71	DAHUA-001	411 0.0566	409 0.0724	375 0.0868	364 0.1138	333 0.1773
72	DAHUA-002	258 0.0105	258 0.0148	245 0.0188	225 0.0288	236 0.1150

Table 33: **Identification-mode: Effect of N on FNIR at high threshold.** *Values are threshold-based miss rates i.e.* FNIR *at* FPIR = *0.001 for five enrollment population sizes, N. The right six columns apply for enrollment of one image. Missing entries usually apply because another algorithm from the same developer was run instead. Some developers are missing because less accurate algorithms were not run on galleries with* $N \geq 3\,000\,000$. *Throughout blue superscripts indicate the rank of the algorithm for that column.*

This publication is available free of charge from: https://doi.org/10.6028/NIST.IR.8271

MISSES BELOW THRESHOLD, T		ENROL MOST RECENT				
FNIR(N, T> 0, R >L)		DATASET: FRVT 2018 MUGSHOTS				
#	ALGORITHM	N=0.64M	N=1.6M	N=3.0M	N=6.0M	N=12.0M
73	DAHUA-003	[248]0.0097	[249]0.0135	[239]0.0177	[227]0.0293	[229]0.1127
74	DAHUA-004	[186]0.0044	[193]0.0065	[183]0.0086	[169]0.0160	[131]0.0850
75	DAON-000	[305]0.0157	[304]0.0223	[292]0.0289	[310]0.0558	[324]0.1699
76	DAON-002	[194]0.0048	[195]0.0069	[190]0.0095	[190]0.0212	[211]0.1072
77	DATECH-000	[200]0.0051	[203]0.0074	[197]0.0099	[221]0.0284	[258]0.1244
78	DATECH-001	[191]0.0046	[189]0.0064	[191]0.0096	[206]0.0253	[234]0.1145
79	DECATUR-000	[308]0.0170	[307]0.0226	[295]0.0302	[282]0.0460	[292]0.1430
80	DEEPGLINT-001	[102]0.0023	[99]0.0030	[99]0.0040	[123]0.0118	[162]0.0919
81	DEEPSEA-001	[369]0.0343	[367]0.0459	[344]0.0583	[336]0.0799	[327]0.1705
82	DERMALOG-005	[429]0.0696	[424]0.0876	[389]0.1135	[383]0.1550	[373]0.2356
83	DERMALOG-006	[382]0.0392	[375]0.0514	[349]0.0651	[347]0.0951	[320]0.1664
84	DERMALOG-007	[426]0.0687	[422]0.0859	[388]0.1104	[380]0.1501	[370]0.2296
85	DERMALOG-008	[365]0.0334	[364]0.0452	[347]0.0622	[355]0.1057	[369]0.2273
86	DERMALOG-009	[296]0.0144	[292]0.0202	[281]0.0265	[270]0.0413	[280]0.1371
87	DERMALOG-010	[195]0.0048	[192]0.0065	[182]0.0084	[184]0.0203	[178]0.0968
88	DERMALOG-011	[298]0.0145	[297]0.0212	[289]0.0276	[279]0.0457	[249]0.1188
89	DERMALOG-012	[290]0.0141	[296]0.0207	[285]0.0272	[273]0.0425	[215]0.1083
90	DERMALOG-013	[292]0.0142	[295]0.0207	[288]0.0275	[274]0.0435	[222]0.1105
91	DERMALOG-014	[295]0.0144	[299]0.0214	[293]0.0291	[286]0.0472	[243]0.1168
92	DERMALOG-015	[152]0.0033	[156]0.0047	[151]0.0062	[133]0.0125	[141]0.0871
93	DILUSENSE-000	[337]0.0205	[338]0.0301	[318]0.0374	[306]0.0540	[290]0.1426
94	DILUSENSE-001	[207]0.0057	[208]0.0082	[199]0.0106		[240]0.1158
95	EINETWORKSINDIA-000	[262]0.0107	[262]0.0150	[252]0.0203	[256]0.0385	[287]0.1402
96	EINETWORKSINDIA-001	[264]0.0110	[266]0.0157	[257]0.0218	[278]0.0451	[314]0.1569
97	EINETWORKSINDIA-002	[114]0.0026	[121]0.0037	[119]0.0052	[106]0.0107	[111]0.0797
98	FACEPHI-000	[188]0.0045	[187]0.0063	[176]0.0079	[146]0.0141	[70]0.0657
99	FIRSTCREDITKZ-001	[85]0.0019	[87]0.0026	[90]0.0036	[88]0.0090	[102]0.0756
100	FUJITSULAB-000	[297]0.0144	[293]0.0203	[287]0.0274	[305]0.0538	[331]0.1736
101	FUJITSULAB-001	[270]0.0122	[280]0.0178	[276]0.0247	[317]0.0642	[357]0.2076
102	GORILLA-002	[420]0.1534	[471]0.1877	[416]0.2172	[405]0.2586	[395]0.3357
103	GORILLA-004	[428]0.0696	[428]0.0889	[384]0.1045	[375]0.1367	[345]0.1967
104	GORILLA-005	[399]0.0450	[394]0.0579	[366]0.0701	[350]0.0971	[301]0.1471
105	GORILLA-006	[325]0.0192	[326]0.0271	[302]0.0328	[295]0.0513	[226]0.1110
106	GORILLA-007	[322]0.0187	[323]0.0267	[309]0.0345	[298]0.0516	[228]0.1126
107	GORILLA-008	[307]0.0167	[308]0.0235	[296]0.0305	[284]0.0465	[227]0.1117
108	GRIAULE-000	[291]0.0141	[290]0.0198	[277]0.0250	[264]0.0404	[294]0.1437
109	GRIAULE-001	[137]0.0030	[141]0.0043	[149]0.0061	[155]0.0150	[154]0.0907
110	HIK-003	[436]0.0824	[433]0.1023	[393]0.1194	[382]0.1513	[375]0.2401
111	HIK-004	[433]0.0792	[429]0.0984	[390]0.1142	[378]0.1460	[376]0.2403
112	HIK-005	[356]0.0309	[359]0.0432	[343]0.0555	[340]0.0894	[350]0.2000
113	HISIGN-001	[199]0.0051	[199]0.0073	[188]0.0093	[181]0.0189	[195]0.1011
114	HYPERVERGE-001	[135]0.0030	[136]0.0041	[135]0.0056	[111]0.0113	[138]0.0869
115	HYPERVERGE-002	[112]0.0025	[110]0.0034	[106]0.0043	[49]0.0060	[41]0.0535
116	HYPERVERGE-003	[201]0.0052	[198]0.0071	[192]0.0096	[180]0.0185	[185]0.0983
117	HYUNDAI-ROBOTICSLAB-000	[249]0.0097	[248]0.0135	[235]0.0169	[219]0.0284	[199]0.1016
118	HYUNDAI-ROBOTICSLAB-001	[241]0.0091	[243]0.0125	[237]0.0171	[222]0.0284	[209]0.1071
119	HYUNDAI-ROBOTICSLAB-002	[155]0.0034	[165]0.0052	[161]0.0070	[138]0.0130	[93]0.0720
120	HZAILU-000	[289]0.0140	[288]0.0194	[278]0.0252	[266]0.0408	[245]0.1170
121	HZAILU-001	[219]0.0062	[209]0.0082	[198]0.0105	[186]0.0204	[205]0.1049
122	HZAILU-002	[209]0.0057	[205]0.0076	[195]0.0098	[178]0.0184	[156]0.0911
123	HZAILU-003	[206]0.0057	[207]0.0078	[200]0.0108	[175]0.0179	[176]0.0966
124	HZAILU-004	[136]0.0030	[135]0.0041	[142]0.0058	[109]0.0111	[85]0.0702
125	I2V-001	[304]0.0157	[371]0.0488	[391]0.1152	[400]0.2377	[397]0.3600
126	ICM-001	[338]0.0206	[335]0.0287	[326]0.0405	[335]0.0792	[367]0.2254
127	IDEMIA-003	[367]0.0343	[369]0.0468	[376]0.0869	[406]0.2689	[403]0.4184
128	IDEMIA-004	[355]0.0296	[352]0.0370	[330]0.0441	[315]0.0607	[311]0.1545
129	IDEMIA-005	[372]0.0356	[361]0.0436	[342]0.0532	[331]0.0745	[337]0.1797
130	IDEMIA-006	[370]0.0348	[358]0.0429	[339]0.0520	[326]0.0722	[355]0.2062
131	IDEMIA-007	[279]0.0133	[279]0.0177	[260]0.0224	[247]0.0353	[286]0.1399
132	IDEMIA-008	[51]0.0013	[51]0.0016	[55]0.0020	[35]0.0049	[29]0.0466
133	IDEMIA-009	[34]0.0010	[35]0.0012	[30]0.0014	[44]0.0058	[43]0.0547
134	IDEMIA-010	[8]0.0007	[7]0.0007	[7]0.0008	[8]0.0023	[4]0.0190
135	IDEMIA-011	[18]0.0008	[11]0.0009	[11]0.0009	[7]0.0022	[9]0.0258
136	IDEMIA-012	[13]0.0008	[10]0.0008	[10]0.0009	[5]0.0021	[11]0.0266
137	IMAGUS-005	[281]0.0133	[283]0.0181	[265]0.0234	[250]0.0364	[207]0.1064
138	IMAGUS-006	[282]0.0134	[287]0.0187	[271]0.0241	[260]0.0392	[238]0.1156
139	IMAGUS-007	[302]0.0157	[306]0.0224	[290]0.0280	[275]0.0441	[247]0.1176
140	IMDS-SOFTWARE-001	[189]0.0045	[190]0.0064	[185]0.0091	[185]0.0204	[250]0.1190
141	IMDS-SOFTWARE-002	[185]0.0044	[185]0.0063	[184]0.0087	[182]0.0192	[214]0.1083
142	IMPERIAL-000	[317]0.0183	[315]0.0256	[315]0.0354	[329]0.0730	[336]0.1791
143	INCODE-003	[462]0.1321	[464]0.1668	[413]0.1951	[396]0.2319	[388]0.3041
144	INCODE-004	[385]0.0400	[385]0.0535	[354]0.0658	[343]0.0914	[318]0.1616

Table 34: **Identification-mode: Effect of N on FNIR at high threshold.** *Values are threshold-based miss rates i.e.* FNIR *at* FPIR *= 0.001 for five enrollment population sizes, N. The right six columns apply for enrollment of one image. Missing entries usually apply because another algorithm from the same developer was run instead. Some developers are missing because less accurate algorithms were not run on galleries with $N \geq 3\,000\,000$. Throughout blue superscripts indicate the rank of the algorithm for that column.*

This publication is available free of charge from: https://doi.org/10.6028/NIST.IR.8271

MISSES BELOW THRESHOLD, T		ENROL MOST RECENT				
FNIR(N, T> 0, R >L)		DATASET: FRVT 2018 MUGSHOTS				
#	ALGORITHM	N=0.64M	N=1.6M	N=3.0M	N=6.0M	N=12.0M
145	INCODE-005	232 0.0079	232 0.0109	220 0.0141	205 0.0244	155 0.0909
146	INCODE-006	37 0.0011	38 0.0013	42 0.0017	24 0.0041	31 0.0485
147	INCODE-007	22 0.0009	33 0.0011	29 0.0014	20 0.0036	44 0.0549
148	INNOVATRICS-007	239 0.0090	241 0.0122	228 0.0156	207 0.0256	216 0.1089
149	INNOVATRICS-008	153 0.0034	155 0.0046	152 0.0062	183 0.0203	217 0.1090
150	INNOVATRICS-009	103 0.0023	91 0.0028	89 0.0035	102 0.0102	91 0.0714
151	INNOVATRICS-010	104 0.0023	101 0.0030	93 0.0037	101 0.0102	110 0.0783
152	INNOVATRICS-011	64 0.0015	62 0.0018	61 0.0023	66 0.0071	77 0.0685
153	INNOVATRICS-012	54 0.0014	53 0.0016	51 0.0019	59 0.0065	66 0.0649
154	INNOVATRICS-013	44 0.0012	41 0.0014	45 0.0018	53 0.0062	45 0.0550
155	INNOVATRICS-014	20 0.0008	22 0.0010	16 0.0011	37 0.0050	32 0.0486
156	INSPUR-000	181 0.0042	182 0.0060	180 0.0083	177 0.0181	183 0.0977
157	INSPUR-001	161 0.0035	161 0.0050	160 0.0070	141 0.0132	132 0.0851
158	INSPUR-002	160 0.0034	167 0.0052	159 0.0069	137 0.0129	98 0.0742
159	INTELRESEARCH-001	42 0.0011	46 0.0015	54 0.0020	74 0.0074	104 0.0765
160	INTEMA-000	72 0.0016	67 0.0021	75 0.0028	91 0.0094	97 0.0741
161	INTEMA-001	36 0.0010	24 0.0010	48 0.0019	61 0.0068	74 0.0675
162	INTSYSMSU-000	545 0.9982	542 0.9984	431 0.9985	420 0.9987	412 0.9988
163	IONETWORKS-001	247 0.0095	254 0.0142	253 0.0207	280 0.0457	312 0.1556
164	IREX-000	323 0.0187	331 0.0277	322 0.0388	320 0.0674	302 0.1476
165	ISYSTEMS-002	413 0.0579	413 0.0779	380 0.0963	374 0.1360	364 0.2221
166	ISYSTEMS-003	397 0.0434	395 0.0585	370 0.0792	367 0.1224	366 0.2243
167	KAKAO-000	259 0.0105	260 0.0148	247 0.0192	239 0.0321	194 0.1007
168	KAKAO-001	77 0.0017	78 0.0022	76 0.0029	79 0.0081	81 0.0689
169	KAKAO-002	56 0.0014	60 0.0018	58 0.0022	43 0.0057	48 0.0559
170	KEDACOM-001	312 0.0177	305 0.0223	279 0.0262	271 0.0419	274 0.1337
171	KLOUDSPOT-001	310 0.0176	310 0.0243	308 0.0343	321 0.0685	272 0.1319
172	KNOWUTECH-000	216 0.0061	215 0.0089	206 0.0118	191 0.0214	183 0.0982
173	KOGNIZA-000	179 0.0041	176 0.0056	167 0.0073	149 0.0144	94 0.0723
174	LIGHTVISION-000	326 0.0193	325 0.0270	316 0.0355	313 0.0591	332 0.1742
175	LINECLOVA-002	110 0.0025	118 0.0036	110 0.0046	121 0.0117	120 0.0821
176	LINECLOVA-003	92 0.0022	80 0.0022	109 0.0045	161 0.0154	186 0.0986
177	LOOKMAN-003	368 0.0343	360 0.0433	337 0.0509	325 0.0712	306 0.1530
178	LOOKMAN-005	344 0.0237	337 0.0298	314 0.0352	293 0.0509	273 0.1331
179	LUXAND-001	402 0.0465	391 0.0573	359 0.0674	348 0.0954	322 0.1681
180	MANTRA-000	217 0.0062	224 0.0097	222 0.0147	231 0.0304	201 0.1032
181	MAXVISION-000	335 0.0202	332 0.0278	311 0.0351	296 0.0514	275 0.1337
182	MAXVISION-001	125 0.0028	130 0.0039	117 0.0051	125 0.0119	147 0.0891
183	MAXVISION-002	123 0.0027	113 0.0035	112 0.0047	127 0.0120	170 0.0946
184	MAXVISION-003	175 0.0039	123 0.0055	163 0.0071	151 0.0145	80 0.0688
185	MAXVISION-004	75 0.0016	69 0.0021	66 0.0027	81 0.0084	99 0.0743
186	MEGVII-001	409 0.0558	408 0.0719	374 0.0861	370 0.1281	384 0.2600
187	MEGVII-003	78 0.0017	75 0.0022	74 0.0028	80 0.0082	108 0.0781
188	MEGVII-004	27 0.0009	18 0.0010	13 0.0011	23 0.0040	39 0.0521
189	MEGVII-005	28 0.0009	19 0.0010	14 0.0011	51 0.0061	42 0.0540
190	METSAKUURCOMPANY-000	197 0.0049	197 0.0070	187 0.0093	189 0.0209	208 0.1065
191	METSAKUURCOMPANY-001	218 0.0062	216 0.0089	211 0.0126	290 0.0498	329 0.1724
192	MICROFOCUS-005	540 0.9732	533 0.8352	428 0.8550	418 0.8748	410 0.8941
193	MICROSOFT-003	328 0.0196	328 0.0274	312 0.0351	302 0.0526	296 0.1440
194	MICROSOFT-004	315 0.0182	316 0.0256	303 0.0329	294 0.0509	289 0.1415
195	MICROSOFT-005	313 0.0180	313 0.0254	300 0.0317	291 0.0499	279 0.1368
196	MICROSOFT-006	240 0.0090	237 0.0119	230 0.0158	226 0.0292	283 0.1395
197	MOBBL-000	327 0.0195	330 0.0276	317 0.0364	272 0.0424	22 0.0424
198	MUKH-002	519 0.5039	519 0.5941	425 0.6673	415 0.7313	408 0.8275
199	NEC-000	412 0.0634	415 0.0786	379 0.0928	365 0.1150	340 0.1862
200	NEC-001	437 0.0859	435 0.1050	396 0.1237	381 0.1511	363 0.2196
201	NEC-002	79 0.0018	81 0.0023	78 0.0030	126 0.0119	57 0.0594
202	NEC-003	83 0.0019	76 0.0022	64 0.0026	40 0.0053	33 0.0492
203	NEC-004	53 0.0013	45 0.0015	40 0.0016	18 0.0033	16 0.0326
204	NEC-005	43 0.0012	40 0.0013	36 0.0015	50 0.0061	14 0.0304
205	NEC-006	60 0.0015	55 0.0017	59 0.0022	99 0.0099	50 0.0570
206	NEC-007	30 0.0009	21 0.0010	15 0.0011	9 0.0025	10 0.0265
207	NEC-008	35 0.0010	29 0.0011	22 0.0012	14 0.0030	13 0.0292
208	NEC-009	9 0.0007	9 0.0008	9 0.0008	6 0.0022	5 0.0191
209	NEC-010	4 0.0006	4 0.0006	4 0.0007	3 0.0019	3 0.0167
210	NEC-011	3 0.0005	3 0.0006	3 0.0006	1 0.0018	2 0.0164
211	NEUROTECHNOLOGY-003	522 0.5681	523 0.6312	426 0.6951	416 0.7551	407 0.8014
212	NEUROTECHNOLOGY-004	401 0.0462	401 0.0625	368 0.0772	360 0.1101	352 0.2008
213	NEUROTECHNOLOGY-005	381 0.0390	386 0.0535	357 0.0672	344 0.0934	343 0.1874
214	NEUROTECHNOLOGY-007	396 0.0433	400 0.0619	371 0.0799	372 0.1317	374 0.2391
215	NEUROTECHNOLOGY-008	366 0.0335	380 0.0527	377 0.0889	388 0.1766	394 0.3286
216	NEUROTECHNOLOGY-009	257 0.0104	261 0.0148	248 0.0192	237 0.0320	220 0.1099

Table 35: **Identification-mode: Effect of N on FNIR at high threshold.** *Values are threshold-based miss rates i.e.* FNIR *at* FPIR = *0.001 for five enrollment population sizes, N. The right six columns apply for enrollment of one image. Missing entries usually apply because another algorithm from the same developer was run instead. Some developers are missing because less accurate algorithms were not run on galleries with $N \geq 3\,000\,000$. Throughout blue superscripts indicate the rank of the algorithm for that column.*

This publication is available free of charge from: https://doi.org/10.6028/NIST.IR.8271

MISSES BELOW THRESHOLD, T		ENROL MOST RECENT				
FNIR(N, T> 0, R >L)		DATASET: FRVT 2018 MUGSHOTS				
#	ALGORITHM	N=0.64M	N=1.6M	N=3.0M	N=6.0M	N=12.0M
217	NEUROTECHNOLOGY-010	[224] 0.0066	[222] 0.0096	[218] 0.0135	[227] 0.0445	[330] 0.1724
218	NEUROTECHNOLOGY-012	[183] 0.0044	[191] 0.0065	[189] 0.0094	[211] 0.0261	[277] 0.1340
219	NEUROTECHNOLOGY-013	[113] 0.0026	[129] 0.0039	[131] 0.0054	[187] 0.0205	[251] 0.1199
220	NEUROTECHNOLOGY-014	[91] 0.0020	[97] 0.0029	[105] 0.0042	[105] 0.0103	[139] 0.0870
221	NEUROTECHNOLOGY-015	[87] 0.0020	[103] 0.0030	[102] 0.0041	[95] 0.0096	[173] 0.0951
222	NEUROTECHNOLOGY-016	[90] 0.0020	[96] 0.0029	[96] 0.0039	[84] 0.0087	[114] 0.0807
223	NEXTMETALABS-002	[124] 0.0027	[122] 0.0037	[126] 0.0053	[116] 0.0116	[118] 0.0818
224	NOMINDER-000	[145] 0.0032	[147] 0.0045	[147] 0.0060	[159] 0.0152	[153] 0.0906
225	NOMINDER-001	[163] 0.0036	[160] 0.0049	[155] 0.0064	[150] 0.0145	[171] 0.0947
226	NOMINDER-002	[162] 0.0035	[158] 0.0047	[153] 0.0063	[147] 0.0141	[157] 0.0913
227	NOMINDER-003	[146] 0.0033	[151] 0.0045	[146] 0.0060	[131] 0.0125	[150] 0.0900
228	NOMINDER-004	[144] 0.0031	[145] 0.0044	[143] 0.0058	[140] 0.0130	[168] 0.0943
229	NOTIONTAG-000	[272] 0.0124	[274] 0.0171	[261] 0.0224	[248] 0.0354	[263] 0.1267
230	NTECHLAB-003	[391] 0.0417	[384] 0.0534	[356] 0.0667	[339] 0.0893	[303] 0.1508
231	NTECHLAB-004	[357] 0.0309	[354] 0.0402	[338] 0.0514	[324] 0.0705	[295] 0.1440
232	NTECHLAB-005	[363] 0.0331	[356] 0.0420	[341] 0.0530	[332] 0.0748	[299] 0.1459
233	NTECHLAB-006	[353] 0.0285	[348] 0.0364	[332] 0.0464	[319] 0.0660	[298] 0.1445
234	NTECHLAB-007	[319] 0.0184	[312] 0.0252	[298] 0.0314	[289] 0.0492	[270] 0.1303
235	NTECHLAB-008	[255] 0.0103	[252] 0.0141	[243] 0.0184	[218] 0.0282	[191] 0.0991
236	NTECHLAB-009	[150] 0.0033	[153] 0.0045	[144] 0.0059	[129] 0.0121	[96] 0.0731
237	NTECHLAB-010	[74] 0.0016	[74] 0.0022	[68] 0.0027	[72] 0.0074	[88] 0.0707
238	NTECHLAB-011	[82] 0.0019	[86] 0.0026	[88] 0.0034	[69] 0.0072	[63] 0.0622
239	OMNIGARDE-000	[128] 0.0028	[126] 0.0039	[121] 0.0052	[135] 0.0127	[143] 0.0875
240	OMNIGARDE-001	[55] 0.0014	[61] 0.0018	[62] 0.0024	[58] 0.0066	[90] 0.0711
241	OMNIGARDE-002	[40] 0.0011	[39] 0.0013	[39] 0.0016	[47] 0.0060	[89] 0.0708
242	OPTIEXACTA-000	[11] 0.0008	[15] 0.0009	[18] 0.0011	[11] 0.0027	[21] 0.0372
243	PANGIAM-000	[174] 0.0039	[177] 0.0057	[171] 0.0076	[165] 0.0156	[142] 0.0873
244	PANGIAM-001	[246] 0.0094	[233] 0.0110	[213] 0.0130	[197] 0.0229	[136] 0.0862
245	PAPSAV1923-000	[95] 0.0021	[94] 0.0029	[95] 0.0038	[83] 0.0087	[87] 0.0705
246	PARAVISION-003	[347] 0.0257	[344] 0.0347	[329] 0.0441	[318] 0.0646	[309] 0.1539
247	PARAVISION-004	[226] 0.0070	[225] 0.0098	[216] 0.0133	[212] 0.0263	[260] 0.1253
248	PARAVISION-005	[129] 0.0029	[124] 0.0038	[125] 0.0053	[173] 0.0171	[202] 0.1034
249	PARAVISION-007	[115] 0.0026	[119] 0.0036	[120] 0.0052	[188] 0.0207	[219] 0.1094
250	PARAVISION-009	[76] 0.0016	[79] 0.0022	[85] 0.0034	[92] 0.0094	[133] 0.0854
251	PARAVISION-012	[32] 0.0009	[34] 0.0012	[35] 0.0015	[52] 0.0061	[105] 0.0767
252	PARAVISION-014	[25] 0.0009	[26] 0.0011	[27] 0.0013	[42] 0.0056	[92] 0.0717
253	PARAVISION-016	[24] 0.0009	[17] 0.0010	[24] 0.0013	[34] 0.0049	[84] 0.0699
254	PARAVISION-019	[14] 0.0008	[13] 0.0009	[19] 0.0012	[30] 0.0047	[82] 0.0696
255	PENTACOMP-001	[286] 0.0136	[270] 0.0162	[270] 0.0238	[269] 0.0412	[237] 0.1156
256	PIXELALL-002	[430] 0.0713	[434] 0.1049	[404] 0.1472	[402] 0.2487	[401] 0.3902
257	PIXELALL-003	[300] 0.0155	[300] 0.0215	[291] 0.0285	[285] 0.0470	[232] 0.1135
258	PIXELALL-004	[275] 0.0126	[282] 0.0179	[272] 0.0242	[312] 0.0573	[321] 0.1678
259	PIXELALL-005	[235] 0.0084	[235] 0.0117	[233] 0.0168	[255] 0.0380	[266] 0.1290
260	PSL-000	[67] 0.0014	[77] 0.0022	[79] 0.0030	[78] 0.0078	[167] 0.0937
261	PSL-001	[66] 0.0015	[68] 0.0021	[73] 0.0028	[76] 0.0075	[72] 0.0663
262	PSL-002	[17] 0.0008	[25] 0.0011	[26] 0.0013	[45] 0.0058	[79] 0.0687
263	PSL-003	[23] 0.0009	[27] 0.0011	[34] 0.0015	[48] 0.0060	[76] 0.0685
264	PSL-004	[10] 0.0007	[16] 0.0009	[20] 0.0012	[28] 0.0046	[49] 0.0560
265	PTAKURATSATU-000	[350] 0.0272	[347] 0.0363	[331] 0.0455	[299] 0.0520	[38] 0.0520
266	PYRAMID-000	[117] 0.0026	[116] 0.0036	[114] 0.0047	[89] 0.0092	[78] 0.0686
267	PYRAMID-001	[140] 0.0031	[143] 0.0044	[141] 0.0058	[110] 0.0111	[107] 0.0780
268	QAZSMARTVISIONAI-000	[21] 0.0009	[28] 0.0011	[25] 0.0013	[26] 0.0043	[54] 0.0582
269	QAZSMARTVISIONAI-001	[5] 0.0006	[5] 0.0007	[5] 0.0008	[19] 0.0035	[27] 0.0453
270	QAZSMARTVISIONAI-002	[2] 0.0005	[1] 0.0006	[2] 0.0006	[17] 0.0033	[23] 0.0444
271	QAZSMARTVISIONAI-003	[1] 0.0005	[2] 0.0006	[1] 0.0006	[15] 0.0032	[26] 0.0453
272	QNAP-001	[386] 0.0400	[383] 0.0533	[353] 0.0658	[342] 0.0912	[316] 0.1592
273	QNAP-002	[329] 0.0197	[318] 0.0261	[301] 0.0324	[288] 0.0487	[276] 0.1338
274	QNAP-003	[285] 0.0136	[286] 0.0186	[268] 0.0235	[252] 0.0376	[288] 0.1411
275	QNAP-004	[243] 0.0092	[250] 0.0136	[241] 0.0180	[245] 0.0342	[271] 0.1318
276	QNAP-005	[230] 0.0075	[227] 0.0098	[209] 0.0124	[194] 0.0219	[225] 0.1108
277	QNAP-006	[210] 0.0059	[210] 0.0083	[202] 0.0111	[195] 0.0224	[268] 0.1300
278	QUANTASOFT-001	[524] 0.6384	[524] 0.6384	[424] 0.6384		[405] 0.6384
279	RANKONE-002	[447] 0.0970	[440] 0.1170	[398] 0.1349	[386] 0.1697	[383] 0.2553
280	RANKONE-003	[446] 0.0970	[441] 0.1170	[397] 0.1349	[385] 0.1697	[382] 0.2553
281	RANKONE-005	[403] 0.0469	[397] 0.0588	[363] 0.0690	[345] 0.0934	[345] 0.1921
282	RANKONE-007	[306] 0.0164	[303] 0.0218	[280] 0.0262	[254] 0.0378	[230] 0.1129
283	RANKONE-009	[276] 0.0129	[277] 0.0174	[263] 0.0226	[244] 0.0341	[161] 0.0918
284	RANKONE-010	[254] 0.0102	[247] 0.0133	[236] 0.0170	[210] 0.0261	[109] 0.0782
285	RANKONE-011	[211] 0.0059	[211] 0.0084	[203] 0.0112	[213] 0.0266	[231] 0.1132
286	RANKONE-012	[205] 0.0054	[200] 0.0073	[194] 0.0097	[192] 0.0216	[224] 0.1107
287	RANKONE-013	[139] 0.0030	[137] 0.0042	[136] 0.0056	[130] 0.0124	[140] 0.0871
288	RANKONE-014	[92] 0.0021	[95] 0.0029	[97] 0.0039	[104] 0.0102	[67] 0.0652

Table 36: **Identification-mode: Effect of N on FNIR at high threshold.** *Values are threshold-based miss rates i.e.* FNIR *at* FPIR = *0.001 for five enrollment population sizes, N. The right six columns apply for enrollment of one image. Missing entries usually apply because another algorithm from the same developer was run instead. Some developers are missing because less accurate algorithms were not run on galleries with* $N \geq 3\,000\,000$. *Throughout blue superscripts indicate the rank of the algorithm for that column.*

This publication is available free of charge from: https://doi.org/10.6028/NIST.IR.8271

MISSES BELOW THRESHOLD, T		ENROL MOST RECENT				
FNIR(N, T> 0, R >L)		DATASET: FRVT 2018 MUGSHOTS				
#	ALGORITHM	N=0.64M	N=1.6M	N=3.0M	N=6.0M	N=12.0M
289	RANKONE-015	[81] 0.0018	[83] 0.0024	[82] 0.0031	[64] 0.0071	[65] 0.0628
290	REALNETWORKS-002	[481] 0.1939	[481] 0.2308	[419] 0.2647	[410] 0.3110	[392] 0.3185
291	REALNETWORKS-003	[461] 0.1296	[460] 0.1591	[410] 0.1855	[395] 0.2243	[389] 0.3074
292	REALNETWORKS-004	[460] 0.1276	[459] 0.1578	[409] 0.1854	[397] 0.2326	[391] 0.3177
293	REALNETWORKS-005	[330] 0.0198	[327] 0.0273	[313] 0.0352	[309] 0.0557	[291] 0.1428
294	REALNETWORKS-006	[245] 0.0094	[253] 0.0142	[240] 0.0178	[232] 0.0305	[189] 0.0988
295	REALNETWORKS-007	[222] 0.0064	[220] 0.0093	[208] 0.0121	[198] 0.0230	[158] 0.0913
296	REALNETWORKS-008	[178] 0.0041	[178] 0.0058	[174] 0.0079	[142] 0.0135	[119] 0.0821
297	RECOGNITO-000	[50] 0.0013	[56] 0.0017	[60] 0.0023	[38] 0.0053	[36] 0.0516
298	RECOGNITO-001	[29] 0.0009	[30] 0.0011	[28] 0.0014	[13] 0.0029	[18] 0.0368
299	RECOGNITO-002	[12] 0.0008	[14] 0.0009	[17] 0.0011	[10] 0.0027	[20] 0.0372
300	REMARKAI-000	[388] 0.0402	[387] 0.0549	[358] 0.0673	[353] 0.1025	[351] 0.2000
301	RENDIP-000	[233] 0.0081	[234] 0.0117	[224] 0.0153	[217] 0.0274	[248] 0.1179
302	REVEALMEDIA-000	[236] 0.0086	[236] 0.0118	[225] 0.0154	[216] 0.0274	[198] 0.1016
303	RNIT-000	[213] 0.0061	[230] 0.0109	[294] 0.0292	[366] 0.1179	[381] 0.2553
304	ROC-016	[70] 0.0016	[73] 0.0021	[67] 0.0027	[85] 0.0088	[64] 0.0626
305	ROC-017	[86] 0.0020	[90] 0.0027	[91] 0.0036	[87] 0.0088	[69] 0.0655
306	ROC-018	[69] 0.0015	[65] 0.0020	[65] 0.0026	[65] 0.0071	[59] 0.0599
307	ROC-019	[19] 0.0008	[32] 0.0011	[32] 0.0014	[54] 0.0063	[37] 0.0519
308	S1-000	[333] 0.0200	[329] 0.0276	[320] 0.0378	[316] 0.0627	[326] 0.1704
309	S1-001	[265] 0.0112	[263] 0.0153	[249] 0.0195	[257] 0.0388	[261] 0.1253
310	S1-002	[167] 0.0036	[168] 0.0053	[165] 0.0073	[209] 0.0261	[265] 0.1282
311	S1-003	[208] 0.0057	[212] 0.0084	[204] 0.0112	[214] 0.0273	[267] 0.1295
312	S1-004	[120] 0.0027	[120] 0.0037	[124] 0.0053	[168] 0.0159	[187] 0.0986
313	S1-005	[127] 0.0028	[132] 0.0040	[128] 0.0053	[148] 0.0143	[148] 0.0896
314	S1-006	[68] 0.0015	[66] 0.0020	[69] 0.0027	[112] 0.0114	[124] 0.0824
315	S1-007	[52] 0.0013	[54] 0.0016	[57] 0.0021	[60] 0.0067	[58] 0.0598
316	SANSAP-001	[132] 0.0029	[133] 0.0040	[133] 0.0055	[166] 0.0157	[181] 0.0975
317	SCANOVATE-000	[405] 0.0494	[405] 0.0664	[372] 0.0801	[358] 0.1094	[223] 0.1105
318	SCANOVATE-001	[416] 0.0626	[416] 0.0812	[382] 0.0989	[371] 0.1289	[346] 0.1958
319	SCYLLA-001	[271] 0.0123	[271] 0.0164	[254] 0.0211	[243] 0.0340	[262] 0.1261
320	SENSETIME-000	[301] 0.0155	[294] 0.0204	[282] 0.0266	[258] 0.0389	[233] 0.1135
321	SENSETIME-001	[303] 0.0157	[301] 0.0216	[286] 0.0273	[268] 0.0410	[255] 0.1238
322	SENSETIME-002	[293] 0.0142	[256] 0.0145	[223] 0.0149	[199] 0.0230	[68] 0.0654
323	SENSETIME-003	[47] 0.0012	[47] 0.0015	[44] 0.0018	[36] 0.0050	[24] 0.0448
324	SENSETIME-004	[45] 0.0012	[42] 0.0014	[43] 0.0017	[21] 0.0037	[17] 0.0350
325	SENSETIME-005	[49] 0.0013	[64] 0.0019	[70] 0.0027	[82] 0.0085	[25] 0.0451
326	SENSETIME-006	[38] 0.0011	[44] 0.0015	[53] 0.0020	[25] 0.0043	[19] 0.0369
327	SENSETIME-007	[26] 0.0009	[23] 0.0010	[23] 0.0012	[16] 0.0032	[15] 0.0312
328	SENSETIME-008	[15] 0.0008	[20] 0.0010	[21] 0.0012	[12] 0.0027	[12] 0.0285
329	SENSETIME-009	[7] 0.0006	[6] 0.0007	[8] 0.0008	[4] 0.0020	[7] 0.0234
330	SENSETIME-010	[6] 0.0006	[8] 0.0007	[6] 0.0008	[2] 0.0019	[8] 0.0241
331	SERENDIPITY-000	[238] 0.0088	[240] 0.0121	[227] 0.0156	[215] 0.0274	[196] 0.1013
332	SEVENTHSENSE-001	[134] 0.0029	[142] 0.0044	[158] 0.0067	[156] 0.0150	[127] 0.0828
333	SHAMAN-007	[458] 0.1209	[454] 0.1410	[405] 0.1577	[391] 0.1864	[377] 0.2404
334	SIAT-001	[280] 0.0133	[276] 0.0173	[262] 0.0225	[240] 0.0337	[172] 0.0950
335	SIAT-002	[299] 0.0151	[298] 0.0213	[284] 0.0270	[261] 0.0392	[244] 0.1169
336	SPARKTEK-000	[93] 0.0021	[92] 0.0028	[94] 0.0037	[90] 0.0093	[130] 0.0831
337	SPARSH-001	[131] 0.0029	[128] 0.0039	[134] 0.0055	[139] 0.0130	[146] 0.0890
338	SQISOFT-001	[439] 0.0918	[449] 0.1319	[407] 0.1778	[399] 0.2345	[390] 0.3174
339	SQISOFT-002	[309] 0.0173	[334] 0.0286	[327] 0.0411	[330] 0.0736	[278] 0.1347
340	STCON-001	[46] 0.0012	[43] 0.0015	[49] 0.0019	[46] 0.0058	[73] 0.0670
341	STCON-002	[33] 0.0010	[36] 0.0012	[38] 0.0016	[29] 0.0046	[53] 0.0579
342	STCON-003	[31] 0.0009	[31] 0.0011	[31] 0.0014	[22] 0.0040	[56] 0.0590
343	SYNESIS-003	[520] 0.5339	[518] 0.5817	[423] 0.6099	[414] 0.6473	[406] 0.6801
344	SYNESIS-003	[406] 0.0496	[403] 0.0649	[373] 0.0801	[357] 0.1092	[344] 0.1913
345	SYNESIS-005	[311] 0.0177	[311] 0.0245	[299] 0.0316	[297] 0.0515	[315] 0.1577
346	TECH5-001	[390] 0.0417	[390] 0.0571	[378] 0.0907	[393] 0.2103	[399] 0.3723
347	TECH5-002	[324] 0.0190	[322] 0.0266	[307] 0.0343	[303] 0.0534	[317] 0.1604
348	TECH5-003	[116] 0.0026	[117] 0.0036	[116] 0.0050	[134] 0.0125	[166] 0.0931
349	TEVIAN-005	[427] 0.0687	[423] 0.0870	[385] 0.1053	[369] 0.1279	[338] 0.1798
350	TEVIAN-006	[229] 0.0074	[221] 0.0095	[212] 0.0127	[208] 0.0258	[269] 0.1302
351	TEVIAN-007	[159] 0.0034	[159] 0.0048	[150] 0.0062	[157] 0.0151	[174] 0.0954
352	TIGER-002	[419] 0.0643	[420] 0.0857	[383] 0.1027	[373] 0.1317	[362] 0.2175
353	TIGER-004	[288] 0.0140	[273] 0.0168	[273] 0.0242	[267] 0.0410	[241] 0.1159
354	TOSHIBA-000	[400] 0.0457	[399] 0.0616	[369] 0.0776	[359] 0.1097	[353] 0.2014
355	TOSHIBA-002	[48] 0.0012	[48] 0.0015	[46] 0.0018	[70] 0.0073	[95] 0.0727
356	TOSS-000	[58] 0.0014	[58] 0.0017	[56] 0.0020	[41] 0.0056	[30] 0.0476
357	TRUEFACE-000	[277] 0.0130	[281] 0.0178	[266] 0.0235	[253] 0.0377	[282] 0.1382
358	UNISSEY-003	[263] 0.0107	[255] 0.0144	[242] 0.0183	[233] 0.0306	[218] 0.1090
359	USEB-001	[122] 0.0027	[114] 0.0036	[113] 0.0047	[124] 0.0118	[123] 0.0822
360	USEB-002	[133] 0.0029	[127] 0.0039	[122] 0.0052	[162] 0.0154	[152] 0.0901

Table 37: **Identification-mode: Effect of N on FNIR at high threshold.** *Values are threshold-based miss rates i.e.* FNIR *at* FPIR = *0.001 for five enrollment population sizes, N. The right six columns apply for enrollment of one image. Missing entries usually apply because another algorithm from the same developer was run instead. Some developers are missing because less accurate algorithms were not run on galleries with $N \geq 3\,000\,000$. Throughout blue superscripts indicate the rank of the algorithm for that column.*

This publication is available free of charge from: https://doi.org/10.6028/NIST.IR.8271

MISSES BELOW THRESHOLD, T		ENROL MOST RECENT				
FNIR(N, T> 0, R >L)		DATASET: FRVT 2018 MUGSHOTS				
#	ALGORITHM	N=0.64M	N=1.6M	N=3.0M	N=6.0M	N=12.0M
361	USEB-003	[118] 0.0026	[111] 0.0034	[107] 0.0044	[108] 0.0111	[134] 0.0854
362	USEB-004	[107] 0.0025	[107] 0.0032	[103] 0.0042	[94] 0.0095	[106] 0.0774
363	VD-001	[472] 0.1639	[473] 0.2010	[418] 0.2344	[407] 0.2719	[393] 0.3253
364	VDFSOFTWARE-002	[349] 0.0267	[353] 0.0376	[334] 0.0482	[322] 0.0685	[305] 0.1523
365	VERIDAS-001	[351] 0.0275	[351] 0.0369	[336] 0.0488	[334] 0.0749	[308] 0.1538
366	VERIDAS-002	[352] 0.0275	[350] 0.0369	[335] 0.0488	[333] 0.0749	[307] 0.1538
367	VERIDAS-003	[266] 0.0114	[269] 0.0162	[256] 0.0215	[276] 0.0443	[310] 0.1540
368	VERIDAS-004	[173] 0.0038	[170] 0.0054	[166] 0.0073	[71] 0.0073	[6] 0.0229
369	VERIGRAM-000	[156] 0.0034	[150] 0.0045	[108] 0.0045	[39] 0.0053	[1] 0.0111
370	VERIGRAM-001	[157] 0.0034	[152] 0.0045	[132] 0.0054	[136] 0.0129	[115] 0.0811
371	VIANTE-000	[84] 0.0019	[85] 0.0025	[86] 0.0034	[119] 0.0116	[103] 0.0763
372	VIANTE-001	[39] 0.0011	[37] 0.0012	[33] 0.0015	[59] 0.0067	[62] 0.0614
373	VIGILANTSOLUTIONS-008	[294] 0.0143	[291] 0.0202	[283] 0.0266	[287] 0.0485	[242] 0.1161
374	VINBIGDATA-001	[260] 0.0106	[265] 0.0157	[253] 0.0213	[242] 0.0339	[184] 0.0983
375	VINBIGDATA-002	[59] 0.0015	[63] 0.0019	[63] 0.0024	[100] 0.0101	[125] 0.0824
376	VINBIGDATA-003	[63] 0.0015	[72] 0.0021	[77] 0.0029	[98] 0.0099	[135] 0.0860
377	VINBIGDATA-004	[41] 0.0011	[50] 0.0015	[50] 0.0019	[86] 0.0088	[100] 0.0744
378	VISIONBOX-000	[268] 0.0119	[278] 0.0174	[269] 0.0236		[411] 0.9538
379	VISIONBOX-001	[431] 0.0757	[450] 0.1326	[414] 0.2095	[409] 0.3064	[402] 0.4116
380	VISIONBOX-002	[231] 0.0078	[231] 0.0109	[221] 0.0145	[202] 0.0242	[212] 0.1079
381	VISIONLABS-004	[393] 0.0424	[392] 0.0575	[365] 0.0697	[346] 0.0940	[334] 0.1785
382	VISIONLABS-005	[375] 0.0366	[373] 0.0498	[346] 0.0620	[337] 0.0831	[325] 0.1701
383	VISIONLABS-006	[321] 0.0186	[320] 0.0262	[305] 0.0331	[301] 0.0525	[283] 0.1392
384	VISIONLABS-007	[320] 0.0186	[319] 0.0262	[304] 0.0330	[300] 0.0523	[284] 0.1393
385	VISIONLABS-008	[242] 0.0092	[244] 0.0127	[232] 0.0162	[224] 0.0288	[257] 0.1244
386	VISIONLABS-009	[143] 0.0031	[138] 0.0042	[138] 0.0056	[143] 0.0136	[144] 0.0878
387	VISIONLABS-010	[158] 0.0034	[157] 0.0047	[157] 0.0066	[152] 0.0145	[160] 0.0917
388	VISIONLABS-011	[94] 0.0021	[98] 0.0030	[101] 0.0040	[118] 0.0116	[121] 0.0822
389	VISTEAM-000	[422] 0.0656	[418] 0.0852	[386] 0.1072	[377] 0.1387	[349] 0.1987
390	VIXVIZION-009	[332] 0.0199	[324] 0.0270	[310] 0.0345	[307] 0.0541	[281] 0.1374
391	VNPAY-001	[176] 0.0039	[172] 0.0055	[169] 0.0075	[154] 0.0149	[128] 0.0829
392	VNPT-001	[251] 0.0100	[251] 0.0140	[244] 0.0186	[228] 0.0293	[200] 0.1025
393	VNPT-002	[192] 0.0047	[184] 0.0062	[179] 0.0080	[172] 0.0169	[193] 0.1002
394	VNPT-003	[190] 0.0046	[181] 0.0060	[173] 0.0078	[171] 0.0168	[188] 0.0987
395	VNPT-004	[172] 0.0038	[163] 0.0051	[154] 0.0064	[153] 0.0148	[145] 0.0885
396	VNPT-005	[148] 0.0033	[139] 0.0042	[137] 0.0056	[115] 0.0115	[137] 0.0866
397	VOCORD-005	[455] 0.1174	[458] 0.1559	[415] 0.2152	[408] 0.3062	[404] 0.4354
398	VTCC-000	[343] 0.0227	[396] 0.0585	[400] 0.1394	[404] 0.2506	[400] 0.3742
399	VTCC-002	[227] 0.0070	[229] 0.0102	[226] 0.0156	[328] 0.0724	[347] 0.1964
400	VTS-001	[250] 0.0099	[245] 0.0130	[238] 0.0172	[235] 0.0319	[256] 0.1240
401	VTS-002	[314] 0.0181	[314] 0.0255	[306] 0.0341	[308] 0.0546	[297] 0.1444
402	VTS-003	[198] 0.0050	[196] 0.0069	[186] 0.0092	[179] 0.0184	[197] 0.1014
403	VTS-004	[141] 0.0031	[148] 0.0045	[148] 0.0061	[145] 0.0140	[149] 0.0896
404	VTS-005	[151] 0.0033	[164] 0.0051	[164] 0.0071	[144] 0.0138	[75] 0.0680
405	WINK-001	[345] 0.0244	[346] 0.0359	[333] 0.0481	[327] 0.0724	[323] 0.1692
406	WINK-002	[237] 0.0086	[238] 0.0121	[231] 0.0159	[223] 0.0285	[179] 0.0968
407	XFORWARDAI-000	[256] 0.0103	[259] 0.0148	[246] 0.0192	[238] 0.0321	[206] 0.1054
408	XFORWARDAI-001	[149] 0.0033	[149] 0.0045	[139] 0.0057	[117] 0.0116	[112] 0.0797
409	XFORWARDAI-002	[100] 0.0023	[88] 0.0027	[83] 0.0031	[75] 0.0074	[86] 0.0702
410	YITU-002	[274] 0.0125	[275] 0.0173	[259] 0.0223	[241] 0.0337	[210] 0.1071
411	YITU-003	[284] 0.0134	[284] 0.0181	[264] 0.0232	[246] 0.0345	[213] 0.1079
412	YITU-004	[221] 0.0064	[218] 0.0092	[210] 0.0124	[193] 0.0219	[180] 0.0973
413	YITU-005	[228] 0.0071	[226] 0.0098	[214] 0.0131	[201] 0.0242	[192] 0.0993
414	YUAN-000	[225] 0.0067	[228] 0.0099	[215] 0.0132	[196] 0.0227	[543] 1.0000

Table 38: **Identification-mode: Effect of N on FNIR at high threshold.** *Values are threshold-based miss rates i.e.* FNIR *at* FPIR = *0.001 for five enrollment population sizes, N. The right six columns apply for enrollment of one image. Missing entries usually apply because another algorithm from the same developer was run instead. Some developers are missing because less accurate algorithms were not run on galleries with* $N \geq 3\,000\,000$. *Throughout blue superscripts indicate the rank of the algorithm for that column.*

This publication is available free of charge from: https://doi.org/10.6028/NIST.IR.8271

MISSES AT GIVEN RANK FNIR(N, T= 0, R)		ENROL MOST RECENT											
		RANK 1						RANK 50					
#	ALGORITHM	N=0.64M	N=1.6M	N=3.0M	N=6.0M	N=12.0M	aN^b	N=0.64M	N=1.6M	N=3.0M	N=6.0M	N=12.0M	aN^b
1	3DIVI-005	464 0.0134	461 0.0173	407 0.0207	399 0.0250	391 0.0298	336 0.0003 $N^{0.275}$ 354	438 0.0038	437 0.0046	395 0.0054	389 0.0065	381 0.0079	72 0.0001 $N^{0.251}$ 372
2	ACER-000	426 0.0077	434 0.0102	395 0.0124	391 0.0153	381 0.0191	220 0.0001 $N^{0.308}$ 390	363 0.0016	389 0.0022	369 0.0027	367 0.0034	361 0.0042	19 0.0000 $N^{0.324}$ 394
3	ADVANCE-000	249 0.0014	259 0.0016	258 0.0018	254 0.0022	249 0.0025	164 0.0001 $N^{0.206}$ 281	269 0.0010	266 0.0011	259 0.0011	259 0.0012	254 0.0013	228 0.0004 $N^{0.064}$ 268
4	AFISBIOMETRICS-000	164 0.0010	205 0.0012	227 0.0016	243 0.0020	248 0.0025	13 0.0000 $N^{0.336}$ 400	68 0.0005	77 0.0006	98 0.0006	105 0.0007	109 0.0007	77 0.0001 $N^{0.097}$ 309
5	AFRENGINE-000	333 0.0023	337 0.0029	329 0.0034	325 0.0041	321 0.0052	83 0.0001 $N^{0.275}$ 357	334 0.0013	327 0.0014	312 0.0015	304 0.0016	295 0.0017	224 0.0004 $N^{0.084}$ 292
6	AFRENGINE-001	233 0.0013	219 0.0013	210 0.0014	205 0.0016	198 0.0018	327 0.0003 $N^{0.106}$ 88	325 0.0012	301 0.0013	288 0.0013	276 0.0013	257 0.0013	367 0.0011 $N^{0.007}$ 47
7	AFRENGINE-002	234 0.0013	220 0.0013	205 0.0014	197 0.0015	190 0.0017	356 0.0004 $N^{0.087}$ 53	324 0.0012	304 0.0013	289 0.0013	275 0.0013	256 0.0013	372 0.0012 $N^{0.005}$ 33
8	AFRENGINE-003	330 0.0023	316 0.0023	293 0.0024	277 0.0025	257 0.0027	387 0.0010 $N^{0.063}$ 23	402 0.0022	385 0.0022	355 0.0022	345 0.0022	327 0.0022	393 0.0021 $N^{0.002}$ 9
9	AIZE-002	343 0.0025	346 0.0031	334 0.0036	330 0.0043	323 0.0052	163 0.0001 $N^{0.251}$ 334	333 0.0013	336 0.0014	321 0.0015	313 0.0017	304 0.0018	141 0.0003 $N^{0.106}$ 313
10	AKUVOX-001	230 0.0013	226 0.0014	221 0.0016	222 0.0018	215 0.0020	253 0.0002 $N^{0.154}$ 182	263 0.0010	263 0.0011	253 0.0011	233 0.0011	226 0.0011	308 0.0007 $N^{0.031}$ 181
11	ALCHERA-003	425 0.0077	433 0.0102	393 0.0120	390 0.0145	380 0.0177	267 0.0002 $N^{0.282}$ 369	415 0.0025	414 0.0030	379 0.0033	374 0.0040	363 0.0046	81 0.0002 $N^{0.206}$ 364
12	ALCHERA-006	140 0.0009	135 0.0009	134 0.0010	129 0.0011	137 0.0013	232 0.0001 $N^{0.132}$ 149	154 0.0007	152 0.0007	147 0.0007	140 0.0008	134 0.0008	244 0.0005 $N^{0.032}$ 189
13	ALCHERA-008	162 0.0009	153 0.0010	140 0.0010	141 0.0011	131 0.0012	310 0.0003 $N^{0.095}$ 73	216 0.0009	203 0.0009	190 0.0009	178 0.0009	168 0.0009	344 0.0008 $N^{0.004}$ 28
14	ALGORITHMSINC-000	219 0.0012	251 0.0016	254 0.0018	260 0.0022	267 0.0029	25 0.0000 $N^{0.293}$ 378	283 0.0011	315 0.0013	320 0.0015	326 0.0018	330 0.0023	26 0.0000 $N^{0.256}$ 374
15	ALLGOVISION-000	444 0.0097	440 0.0111	394 0.0124	388 0.0142	379 0.0162	385 0.0009 $N^{0.176}$ 229	460 0.0059	456 0.0064	402 0.0067	392 0.0072	380 0.0078	388 0.0017 $N^{0.091}$ 302
16	ALLGOVISION-001	411 0.0066	419 0.0086	388 0.0103	383 0.0124	376 0.0154	237 0.0001 $N^{0.287}$ 375	391 0.0020	396 0.0023	370 0.0028	360 0.0032	358 0.0040	52 0.0001 $N^{0.238}$ 368
17	ANKE-000	447 0.0099	451 0.0129	403 0.0152	396 0.0185	386 0.0222	308 0.0003 $N^{0.275}$ 355	423 0.0029	427 0.0037	390 0.0044	380 0.0053	371 0.0063	56 0.0001 $N^{0.261}$ 377
18	ANKE-002	319 0.0021	321 0.0024	315 0.0029	310 0.0034	304 0.0040	175 0.0001 $N^{0.228}$ 306	320 0.0012	310 0.0013	298 0.0014	293 0.0014	288 0.0016	199 0.0004 $N^{0.085}$ 293
19	ARATEK-001	104 0.0007	100 0.0008	94 0.0008	103 0.0010	107 0.0011	159 0.0001 $N^{0.159}$ 190	112 0.0006	97 0.0006	95 0.0006	96 0.0006	90 0.0006	197 0.0004 $N^{0.031}$ 186
20	ARMATURA-000	273 0.0015	244 0.0015	226 0.0016	214 0.0017	201 0.0018	372 0.0007 $N^{0.061}$ 20	345 0.0015	337 0.0015	313 0.0015	297 0.0015	276 0.0015	383 0.0014 $N^{0.004}$ 23
21	AWARE-003	483 0.0235	483 0.0303	419 0.0358	411 0.0427	405 0.0503	379 0.0007 $N^{0.260}$ 342	453 0.0052	467 0.0072	413 0.0088	405 0.0109	400 0.0140	41 0.0001 $N^{0.335}$ 399
22	AWARE-005	486 0.0241	484 0.0308	420 0.0363	412 0.0431	395 0.0309	408 0.0055 $N^{0.120}$ 117	458 0.0058	470 0.0079	415 0.0098	408 0.0125	383 0.0086	298 0.0006 $N^{0.176}$ 353
23	AWARE-007	294 0.0017	303 0.0021	302 0.0025	300 0.0031	299 0.0038	42 0.0000 $N^{0.282}$ 368	167 0.0008	189 0.0009	224 0.0010	242 0.0011	261 0.0013	42 0.0001 $N^{0.187}$ 357
24	AYONIX-002	534 0.2933	535 0.3412	430 0.3734	420 0.4099	412 0.4463	413 0.0439 $N^{0.143}$ 168	527 0.0947	529 0.1271	430 0.1522	419 0.1825	410 0.2147	397 0.0023 $N^{0.279}$ 384
25	BIOIDTECHSWISS-001	117 0.0008	107 0.0008	96 0.0009	89 0.0009	87 0.0011	249 0.0002 $N^{0.118}$ 114	127 0.0006	114 0.0006	111 0.0007	111 0.0007	111 0.0007	237 0.0004 $N^{0.027}$ 161
26	BIOMETRIK-001	363 0.0033	370 0.0044	357 0.0052	347 0.0062	341 0.0075	154 0.0001 $N^{0.278}$ 362	310 0.0012	328 0.0014	325 0.0016	323 0.0018	319 0.0021	59 0.0001 $N^{0.191}$ 360
27	CAMVI-004	457 0.0122	497 0.0466	424 0.0717	419 0.2360	410 0.2365	6 0.0000 $N^{1.059}$ 412	495 0.0116	513 0.0462	426 0.0713	420 0.2358	411 0.2362	7 0.0000 $N^{1.075}$ 412
28	CANON-001	85 0.0007	80 0.0007	85 0.0008	95 0.0010	91 0.0011	148 0.0001 $N^{0.159}$ 191	74 0.0005	74 0.0006	76 0.0006	80 0.0006	78 0.0006	132 0.0003 $N^{0.042}$ 218
29	CANON-002	96 0.0007	111 0.0008	126 0.0009	133 0.0011	135 0.0012	70 0.0001 $N^{0.196}$ 267	77 0.0005	71 0.0006	71 0.0006	70 0.0006	74 0.0006	193 0.0004 $N^{0.025}$ 156
30	CANON-003	37 0.0005	37 0.0006	46 0.0007	53 0.0008	43 0.0009	73 0.0001 $N^{0.173}$ 215	28 0.0005	27 0.0005	23 0.0005	20 0.0005	25 0.0005	175 0.0004 $N^{0.017}$ 117
31	CIB-000	196 0.0011	196 0.0012	196 0.0013	202 0.0016	411 0.3301	4 0.0000 $N^{1.598}$ 413	182 0.0008	172 0.0008	174 0.0008	180 0.0009	413 0.3295	4 0.0000 $N^{1.644}$ 413
32	CLEARVIEWAI-000	76 0.0007	82 0.0007	87 0.0008	104 0.0010	101 0.0011	80 0.0001 $N^{0.183}$ 247	80 0.0006	72 0.0006	74 0.0006	78 0.0006	76 0.0006	171 0.0004 $N^{0.031}$ 180
33	CLEARVIEWAI-001	98 0.0007	83 0.0007	75 0.0008	73 0.0009	72 0.0010	230 0.0001 $N^{0.121}$ 124	136 0.0007	122 0.0007	112 0.0007	112 0.0007	105 0.0007	284 0.0006 $N^{0.011}$ 71
34	CLEARVIEWAI-002	101 0.0007	93 0.0008	86 0.0008	87 0.0009	81 0.0010	212 0.0001 $N^{0.132}$ 147	135 0.0007	129 0.0007	116 0.0007	110 0.0007	99 0.0007	288 0.0006 $N^{0.008}$ 53
35	CLEARVIEWAI-003	107 0.0007	90 0.0008	78 0.0008	72 0.0009	68 0.0010	256 0.0002 $N^{0.107}$ 92	134 0.0006	124 0.0007	113 0.0007	102 0.0007	96 0.0007	297 0.0006 $N^{0.003}$ 16
36	CLOUDWALK-HR-000	203 0.0011	186 0.0011	173 0.0012	156 0.0012	150 0.0014	359 0.0004 $N^{0.069}$ 28	268 0.0010	255 0.0010	243 0.0011	232 0.0011	213 0.0011	342 0.0008 $N^{0.016}$ 113
37	CLOUDWALK-MT-000	256 0.0014	231 0.0014	214 0.0015	196 0.0015	180 0.0016	381 0.0008 $N^{0.045}$ 11	338 0.0014	329 0.0014	303 0.0014	285 0.0014	271 0.0014	380 0.0014 $N^{0.002}$ 10
38	CLOUDWALK-MT-001	253 0.0014	229 0.0014	207 0.0014	190 0.0015	176 0.0016	383 0.0009 $N^{0.036}$ 8	337 0.0014	326 0.0014	302 0.0014	288 0.0014	267 0.0014	378 0.0013 $N^{0.003}$ 20
39	CLOUDWALK-MT-002	254 0.0014	230 0.0014	208 0.0014	191 0.0015	170 0.0016	384 0.0009 $N^{0.034}$ 6	339 0.0014	325 0.0014	304 0.0014	286 0.0014	269 0.0014	381 0.0014 $N^{0.002}$ 11
40	COGENT-000	445 0.0098	431 0.0101	389 0.0106	378 0.0112	369 0.0122	405 0.0036 $N^{0.073}$ 30	378 0.0018	382 0.0021	362 0.0024	364 0.0033	386 0.0092	11 0.0000 $N^{0.507}$ 405
41	COGENT-001	446 0.0098	432 0.0101	390 0.0106	379 0.0112	368 0.0122	404 0.0036 $N^{0.073}$ 31	379 0.0018	381 0.0021	361 0.0024	363 0.0033	387 0.0092	12 0.0000 $N^{0.507}$ 406
42	COGENT-002	344 0.0025	349 0.0033	338 0.0038	333 0.0046	327 0.0055	134 0.0001 $N^{0.264}$ 348	298 0.0011	302 0.0013	296 0.0014	303 0.0016	301 0.0018	68 0.0001 $N^{0.163}$ 347
43	COGENT-003	350 0.0027	351 0.0035	341 0.0040	336 0.0048	330 0.0057	182 0.0001 $N^{0.249}$ 332	309 0.0012	324 0.0014	322 0.0015	314 0.0017	311 0.0019	74 0.0001 $N^{0.165}$ 348
44	COGENT-004	258 0.0014	260 0.0016	253 0.0018	253 0.0021	242 0.0025	196 0.0001 $N^{0.190}$ 261	250 0.0010	252 0.0010	252 0.0011	246 0.0011	236 0.0012	203 0.0004 $N^{0.067}$ 273
45	COGENT-005	216 0.0012	216 0.0013	215 0.0015	210 0.0016	199 0.0018	277 0.0002 $N^{0.134}$ 152	253 0.0010	241 0.0010	227 0.0010	216 0.0010	205 0.0010	315 0.0007 $N^{0.023}$ 149
46	COGENT-006	134 0.0008	132 0.0009	128 0.0009	121 0.0011	115 0.0012	255 0.0002 $N^{0.120}$ 118	146 0.0007	154 0.0007	145 0.0007	128 0.0007	125 0.0008	255 0.0005 $N^{0.028}$ 167
47	COGENT-007	83 0.0007	85 0.0007	102 0.0009	101 0.0010	102 0.0011	111 0.0001 $N^{0.172}$ 210	103 0.0006	100 0.0006	94 0.0006	93 0.0006	92 0.0006	173 0.0004 $N^{0.035}$ 199
48	COGNITEC-000	475 0.0192	474 0.0249	415 0.0294	408 0.0349	399 0.0414	370 0.0006 $N^{0.262}$ 347	449 0.0046	454 0.0062	409 0.0074	403 0.0093	395 0.0118	44 0.0001 $N^{0.319}$ 392
49	COGNITEC-001	438 0.0087	442 0.0114	400 0.0136	394 0.0163	383 0.0196	284 0.0002 $N^{0.278}$ 361	418 0.0027	416 0.0031	385 0.0036	378 0.0043	366 0.0051	73 0.0001 $N^{0.224}$ 367
50	COGNITEC-002	390 0.0045	386 0.0053	366 0.0063	357 0.0075	352 0.0091	258 0.0002 $N^{0.244}$ 327	396 0.0021	394 0.0023	365 0.0025	357 0.0027	345 0.0030	163 0.0004 $N^{0.131}$ 327
51	COGNITEC-003	393 0.0049	390 0.0059	371 0.0069	364 0.0082	355 0.0097	291 0.0002 $N^{0.232}$ 309	414 0.0025	406 0.0028	371 0.0029	359 0.0032	351 0.0034	296 0.0006 $N^{0.105}$ 312
52	COGNITEC-004	332 0.0023	336 0.0028	330 0.0034	325 0.0042	322 0.0052	76 0.0001 $N^{0.280}$ 365	246 0.0010	259 0.0010	265 0.0011	278 0.0013	280 0.0015	66 0.0001 $N^{0.160}$ 344
53	COGNITEC-005	200 0.0011	213 0.0013	217 0.0015	216 0.0017	217 0.0020	106 0.0001 $N^{0.210}$ 287	162 0.0007	163 0.0008	160 0.0008	167 0.0008	158 0.0009	176 0.0004 $N^{0.053}$ 242
54	COGNITEC-006	193 0.0011	200 0.0012	197 0.0013	203 0.0016	204 0.0018	142 0.0001 $N^{0.194}$ 265	165 0.0007	161 0.0008	159 0.0008	162 0.0008	161 0.0009	178 0.0004 $N^{0.052}$ 241
55	COGNITEC-007	152 0.0009	168 0.0010	161 0.0011	167 0.0013	173 0.0016	124 0.0001 $N^{0.186}$ 253	122 0.0006	125 0.0007	122 0.0007	121 0.0007	122 0.0007	130 0.0003 $N^{0.056}$ 246
56	COGNITEC-008	139 0.0008	154 0.0010	156 0.0011	166 0.0013	177 0.0016	56 0.0000 $N^{0.218}$ 294	117 0.0006	112 0.0006	110 0.0006	103 0.0007	102 0.0007	220 0.0004 $N^{0.028}$ 168
57	COGNITEC-009	189 0.0010	192 0.0012	189 0.0013	195 0.0015	202 0.0018	152 0.0001 $N^{0.189}$ 258	190 0.0008	177 0.0008	172 0.0008	169 0.0008	160 0.0009	293 0.0006 $N^{0.022}$ 143
58	COMPAL-000	235 0.0013	228 0.0014	511 1.0000	510 1.0000	467 1.0000	2 0.0000 $N^{2.726}$ 416	294 0.0011	285 0.0011	554 1.0000	468 1.0000	507 1.0000	2 0.0000 $N^{2.800}$ 415
59	CORSIGHT-000	93 0.0007	89 0.0008	95 0.0008	109 0.0010	109 0.0011	108 0.0001 $N^{0.173}$ 221	115 0.0006	111 0.0006	100 0.0006	91 0.0006	83 0.0006	285 0.0006 $N^{0.006}$ 46
60	CORSIGHT-001	103 0.0007	94 0.0008	101 0.0009	100 0.0010	99 0.0011	168 0.0001 $N^{0.155}$ 185	107 0.0006	107 0.0006	102 0.0006	99 0.0006	100 0.0007	165 0.0004 $N^{0.038}$ 209
61	CUBOX-001	147 0.0009	137 0.0009	127 0.0009	127 0.0011	118 0.0012	278 0.0002 $N^{0.107}$ 91	194 0.0008	176 0.0008	168 0.0008	157 0.0008	147 0.0008	332 0.0008 $N^{0.004}$ 30
62	CUBOX-002	205 0.0011	189 0.0011	182 0.0012	168 0.0013	156 0.0014	343 0.0004 $N^{0.082}$ 41	276 0.0010	261 0.0011	246 0.0011	230 0.0011	210 0.0011	360 0.0010 $N^{0.007}$ 48
63	CUBOX-003	220 0.0012	202 0.0012	190 0.0013	179 0.0014	171 0.0016	350 0.0004 $N^{0.085}$ 50	295 0.0011	280 0.0011	268 0.0011	257 0.0012	234 0.0012	356 0.0009 $N^{0.014}$ 101
64	CYBERLINK-000	359 0.0031	353 0.0036	346 0.0042	339 0.0050	332 0.0059	242 0.0001 $N^{0.227}$ 304	374 0.0017	367 0.0019	349 0.0020	344 0.0022	333 0.0024	205 0.0004 $N^{0.108}$ 315
65	CYBERLINK-001	347 0.0026	347 0.0032	339 0.0038	335 0.0047	329 0.0057	126 0.0001 $N^{0.266}$ 349	322 0.0012	321 0.0013	308 0.0014	307 0.0016	305 0.0018	95 0.0002 $N^{0.135}$ 330
66	CYBERLINK-002	320 0.0021	312 0.0023	298 0.0025	285 0.0027	276 0.0031	333 0.0003 $N^{0.138}$ 159	365 0.0017	357 0.0017	338 0.0018	325 0.0018	308 0.0019	358 0.0009 $N^{0.043}$ 221
67	CYBERLINK-003	201 0.0011	201 0.0012	198 0.0013	187 0.0015	186 0.0017	259 0.0002 $N^{0.139}$ 162	172 0.0008	168 0.0008	166 0.0008	175 0.0009	175 0.0009	133 0.0003 $N^{0.067}$ 274
68	CYBERLINK-004	228 0.0012	215 0.0013	211 0.0014	209 0.0016	193 0.0018	304 0.0002 $N^{0.122}$ 126	264 0.0010	262 0.0011	247 0.0011	236 0.0011	227 0.0011	306 0.0007 $N^{0.032}$ 187
69	CYBERLINK-005	241 0.0013	236 0.0015	219 0.0015	218 0.0017	211 0.0019	311 0.0003 $N^{0.121}$ 125	275 0.0010	267 0.0011	261 0.0011	252 0.0011	237 0.0012	289 0.0006 $N^{0.042}$ 216
70	CYBERLINK-006	113 0.0008	103 0.0008	84 0.0008	81 0.0009	78 0.0010	269 0.0002 $N^{0.104}$ 85	138 0.0007	130 0.0007	120 0.0007	116 0.0007	107 0.0007	283 0.0006 $N^{0.012}$ 81
71	DAHUA-001	399 0.0051	396 0.0064	377 0.0077	369 0.0090	360 0.0109	251 0.0002 $N^{0.261}$ 343	413 0.0025	407 0.0028	373 0.0030	362 0.0033	353 0.0036	250 0.0005 $N^{0.124}$ 325
72	DAHUA-002	239 0.0013	239 0.0015	238 0.0017	235 0.0019	236 0.0023	189 0.0001 $N^{0.188}$ 257	241 0.0009	239 0.0010	232 0.0010	225 0.0011	222 0.0011	221 0.0004 $N^{0.059}$ 253

Table 39: **Investigation-mode: Effect of N on FNIR on recent images** *For five enrollment population sizes, N, with T = 0 and FPIR = 1. The left five columns are rank 1 miss rates The right five columns are rank 50 miss rates Missing entries usually apply because another algorithm from the same developer was run instead. Some developers are missing because less accurate algorithms were not run on galleries with $N > 1\,600\,000$. Throughout blue superscripts indicate the rank of the algorithm for that column, and yellow highlighting indicates the most accurate value. Caution: The Power-low models are mostly intended to draw attention to the kind of behavior, not as a model to be used for prediction.*

This publication is available free of charge from: https://doi.org/10.6028/NIST.IR.8271

MISSES AT GIVEN RANK FNIR(N, T= 0, R)		ENROL MOST RECENT											
		RANK 1						RANK 50					
#	ALGORITHM	N=0.64M	N=1.6M	N=3.0M	N=6.0M	N=12.0M	aN^b	N=0.64M	N=1.6M	N=3.0M	N=6.0M	N=12.0M	aN^b
73	DAHUA-003	82 0.0007	120 0.0008	148 0.0011	157 0.0012	163 0.0015	20 0.0000 $N^{0.270\ 353}$	64 0.0005	54 0.0005	54 0.0005	66 0.0006	64 0.0006	122 0.0003 $N^{0.044\ 224}$
74	DAHUA-004	79 0.0007	77 0.0007	81 0.0008	79 0.0009	94 0.0011	139 0.0001 $N^{0.161\ 196}$	67 0.0005	69 0.0005	67 0.0005	72 0.0006	70 0.0006	139 0.0003 $N^{0.037\ 206}$
75	DAON-000	373 0.0035	356 0.0037	340 0.0039	324 0.0042	317 0.0045	390 0.0011 $N^{0.084\ 48}$	428 0.0032	421 0.0033	377 0.0033	366 0.0033	350 0.0034	399 0.0027 $N^{0.014\ 100}$
76	DAON-002	122 0.0008	142 0.0009	153 0.0011	164 0.0013	178 0.0016	31 0.0000 $N^{0.239\ 321}$	106 0.0006	109 0.0006	105 0.0006	106 0.0007	106 0.0007	137 0.0003 $N^{0.047\ 230}$
77	DATECH-000	123 0.0008	155 0.0010	154 0.0011	163 0.0013	174 0.0016	50 0.0000 $N^{0.223\ 301}$	120 0.0006	145 0.0007	131 0.0007	126 0.0007	121 0.0007	134 0.0003 $N^{0.055\ 243}$
78	DATECH-001	90 0.0007	91 0.0008	91 0.0008	102 0.0010	100 0.0011	141 0.0001 $N^{0.163\ 203}$	92 0.0006	91 0.0006	87 0.0006	89 0.0006	82 0.0006	157 0.0003 $N^{0.036\ 204}$
79	DECATUR-000	267 0.0015	275 0.0017	272 0.0021	270 0.0024	268 0.0029	100 0.0001 $N^{0.236\ 315}$	221 0.0009	231 0.0009	226 0.0010	237 0.0011	241 0.0012	109 0.0002 $N^{0.097\ 308}$
80	DEEPGLINT-001	191 0.0011	181 0.0011	170 0.0012	162 0.0013	162 0.0015	290 0.0002 $N^{0.115\ 108}$	240 0.0009	223 0.0009	215 0.0010	205 0.0010	197 0.0010	309 0.0007 $N^{0.023\ 150}$
81	DEEPSEA-001	355 0.0029	361 0.0040	351 0.0048	348 0.0062	343 0.0077	33 0.0000 $N^{0.335\ 399}$	218 0.0009	249 0.0010	275 0.0012	281 0.0014	290 0.0016	40 0.0001 $N^{0.204\ 363}$
82	DERMALOG-005	458 0.0112	455 0.0147	405 0.0198	404 0.0287	403 0.0445	17 0.0000 $N^{0.475\ 406}$	485 0.0092	489 0.0120	421 0.0169	413 0.0252	406 0.0403	14 0.0000 $N^{0.510\ 407}$
83	DERMALOG-006	420 0.0073	414 0.0079	383 0.0084	370 0.0091	358 0.0101	398 0.0017 $N^{0.110\ 96}$	461 0.0061	453 0.0062	399 0.0063	387 0.0064	373 0.0066	405 0.0042 $N^{0.027\ 165}$
84	DERMALOG-007	424 0.0076	421 0.0089	387 0.0099	381 0.0115	372 0.0136	369 0.0005 $N^{0.197\ 268}$	450 0.0048	441 0.0050	394 0.0053	381 0.0055	370 0.0059	389 0.0018 $N^{0.072\ 280}$
85	DERMALOG-008	318 0.0021	323 0.0025	318 0.0030	318 0.0036	315 0.0045	82 0.0001 $N^{0.268\ 351}$	292 0.0011	290 0.0012	286 0.0012	280 0.0014	283 0.0015	106 0.0002 $N^{0.113\ 319}$
86	DERMALOG-009	329 0.0022	323 0.0024	305 0.0027	296 0.0029	283 0.0033	339 0.0004 $N^{0.137\ 155}$	377 0.0018	368 0.0019	341 0.0019	329 0.0019	314 0.0020	369 0.0012 $N^{0.034\ 194}$
87	DERMALOG-010	302 0.0018	283 0.0018	266 0.0019	242 0.0020	227 0.0021	380 0.0008 $N^{0.064\ 24}$	367 0.0017	355 0.0017	333 0.0017	316 0.0017	296 0.0017	387 0.0015 $N^{0.010\ 69}$
88	DERMALOG-011	198 0.0011	204 0.0012	213 0.0015	215 0.0017	216 0.0020	81 0.0001 $N^{0.219\ 295}$	144 0.0007	143 0.0007	150 0.0008	151 0.0008	142 0.0008	125 0.0003 $N^{0.065\ 271}$
89	DERMALOG-012	259 0.0014	270 0.0017	260 0.0019	245 0.0021	239 0.0024	240 0.0001 $N^{0.172\ 213}$	290 0.0011	279 0.0011	266 0.0011	254 0.0012	248 0.0012	313 0.0007 $N^{0.032\ 188}$
90	DERMALOG-013	238 0.0013	252 0.0016	243 0.0018	238 0.0020	233 0.0023	208 0.0001 $N^{0.182\ 242}$	260 0.0010	251 0.0010	237 0.0010	229 0.0011	224 0.0011	301 0.0006 $N^{0.034\ 196}$
91	DERMALOG-014	307 0.0019	343 0.0030	355 0.0050	375 0.0095	384 0.0197	8 0.0000 $N^{0.807\ 409}$	360 0.0016	401 0.0026	392 0.0045	402 0.0089	402 0.0190	8 0.0000 $N^{0.855\ 409}$
92	DERMALOG-015	204 0.0011	203 0.0012	185 0.0012	177 0.0014	169 0.0015	317 0.0003 $N^{0.105\ 86}$	267 0.0010	254 0.0010	240 0.0010	220 0.0010	208 0.0011	357 0.0009 $N^{0.008\ 52}$
93	DILUSENSE-000	280 0.0016	288 0.0018	274 0.0021	272 0.0025	270 0.0030	157 0.0001 $N^{0.219\ 297}$	203 0.0009	204 0.0009	204 0.0009	215 0.0010	216 0.0011	116 0.0003 $N^{0.086\ 295}$
94	DILUSENSE-001	174 0.0010	182 0.0011	181 0.0012		182 0.0016	178 0.0001 $N^{0.172\ 211}$	177 0.0008	166 0.0008	162 0.0008		155 0.0009	252 0.0005 $N^{0.036\ 203}$
95	EINETWORKSINDIA-000	231 0.0013	234 0.0014	234 0.0016	231 0.0019	229 0.0022	204 0.0001 $N^{0.180\ 234}$	277 0.0011	263 0.0011	254 0.0011	238 0.0011	223 0.0011	335 0.0008 $N^{0.021\ 135}$
96	EINETWORKSINDIA-001	226 0.0012	222 0.0014	220 0.0016	220 0.0017	219 0.0020	213 0.0001 $N^{0.172\ 214}$	247 0.0010	237 0.0010	229 0.0010	219 0.0010	212 0.0011	286 0.0006 $N^{0.038\ 208}$
97	EINETWORKSINDIA-002	108 0.0007	101 0.0008	88 0.0008	83 0.0009	80 0.0010	238 0.0001 $N^{0.120\ 119}$	124 0.0006	117 0.0006	108 0.0006	101 0.0006	98 0.0007	270 0.0005 $N^{0.014\ 98}$
98	FACEPHI-000	263 0.0015	242 0.0015	225 0.0016	213 0.0017	205 0.0019	367 0.0005 $N^{0.077\ 36}$	331 0.0013	322 0.0014	297 0.0014	284 0.0014	270 0.0014	366 0.0011 $N^{0.017\ 118}$
99	FIRSTCREDITKZ-001	130 0.0008	123 0.0008	115 0.0009	106 0.0010	96 0.0011	280 0.0002 $N^{0.101\ 79}$	189 0.0008	174 0.0008	169 0.0008	159 0.0008	143 0.0008	325 0.0008 $N^{0.006\ 39}$
100	FUJITSULAB-000	281 0.0016	286 0.0018	279 0.0022	278 0.0026	269 0.0030	150 0.0001 $N^{0.222\ 299}$	251 0.0010	246 0.0010	245 0.0011	243 0.0011	247 0.0012	151 0.0003 $N^{0.079\ 286}$
101	FUJITSULAB-001	240 0.0013	243 0.0015	240 0.0017	236 0.0019	232 0.0023	210 0.0001 $N^{0.180\ 235}$	249 0.0010	250 0.0010	242 0.0010	239 0.0011	232 0.0012	226 0.0004 $N^{0.060\ 259}$
102	GORILLA-002	466 0.0145	467 0.0194	411 0.0235	403 0.0285	396 0.0348	315 0.0003 $N^{0.299\ 383}$	425 0.0030	432 0.0039	393 0.0047	385 0.0060	379 0.0078	31 0.0000 $N^{0.321\ 393}$
103	GORILLA-004	389 0.0045	391 0.0059	373 0.0072	368 0.0088	361 0.0111	128 0.0001 $N^{0.307\ 389}$	311 0.0012	335 0.0014	340 0.0018	343 0.0021	339 0.0026	25 0.0000 $N^{0.269\ 382}$
104	GORILLA-005	327 0.0022	335 0.0028	333 0.0035	327 0.0043	324 0.0053	48 0.0000 $N^{0.301\ 386}$	211 0.0009	222 0.0009	236 0.0010	263 0.0012	268 0.0014	55 0.0001 $N^{0.168\ 350}$
105	GORILLA-006	207 0.0011	227 0.0014	237 0.0017	240 0.0020	247 0.0025	29 0.0000 $N^{0.275\ 356}$	145 0.0007	155 0.0007	156 0.0008	158 0.0008	159 0.0009	104 0.0002 $N^{0.081\ 290}$
106	GORILLA-007	190 0.0010	218 0.0013	222 0.0016	239 0.0020	244 0.0025	21 0.0000 $N^{0.295\ 381}$	142 0.0007	140 0.0007	136 0.0007	134 0.0008	145 0.0008	126 0.0003 $N^{0.063\ 264}$
107	GORILLA-008	165 0.0010	188 0.0011	195 0.0013	206 0.0016	206 0.0019	55 0.0000 $N^{0.229\ 307}$	140 0.0007	139 0.0007	135 0.0007	129 0.0007	130 0.0008	155 0.0003 $N^{0.050\ 235}$
108	GRIAULE-000	305 0.0018	305 0.0021	294 0.0024	281 0.0027	278 0.0031	264 0.0002 $N^{0.175\ 225}$	323 0.0012	307 0.0013	305 0.0014	296 0.0015	282 0.0015	233 0.0004 $N^{0.078\ 284}$
109	GRIAULE-001	116 0.0008	117 0.0008	111 0.0009	113 0.0010	111 0.0012	193 0.0001 $N^{0.144\ 169}$	128 0.0006	134 0.0007	121 0.0007	115 0.0007	115 0.0007	235 0.0004 $N^{0.029\ 172}$
110	HIK-003	439 0.0089	443 0.0115	401 0.0137	395 0.0167	385 0.0201	287 0.0002 $N^{0.278\ 364}$	403 0.0022	412 0.0029	382 0.0034	372 0.0042	368 0.0052	37 0.0001 $N^{0.283\ 386}$
111	HIK-004	437 0.0086	441 0.0111	398 0.0132	392 0.0160	382 0.0192	285 0.0002 $N^{0.276\ 359}$	407 0.0023	408 0.0028	380 0.0033	375 0.0040	365 0.0050	43 0.0001 $N^{0.267\ 379}$
112	HIK-005	369 0.0034	369 0.0044	356 0.0051	349 0.0063	344 0.0079	144 0.0001 $N^{0.283\ 370}$	303 0.0011	331 0.0014	317 0.0015	322 0.0018	321 0.0021	53 0.0001 $N^{0.198\ 362}$
113	HISIGN-001	111 0.0007	124 0.0009	139 0.0010	146 0.0012	147 0.0013	65 0.0000 $N^{0.206\ 278}$	104 0.0006	101 0.0006	93 0.0006	98 0.0006	88 0.0006	168 0.0004 $N^{0.037\ 205}$
114	HYPERVERGE-001	171 0.0010	162 0.0010	155 0.0011	150 0.0012	149 0.0014	286 0.0002 $N^{0.111\ 102}$	239 0.0009	228 0.0009	209 0.0009	193 0.0009	182 0.0009	347 0.0009 $N^{0.006\ 45}$
115	HYPERVERGE-002	173 0.0010	162 0.0010	151 0.0011	136 0.0011	121 0.0012	357 0.0004 $N^{0.062\ 22}$	230 0.0009	215 0.0009	205 0.0009	192 0.0009	179 0.0009	333 0.0008 $N^{0.012\ 78}$
116	HYPERVERGE-003	181 0.0010	178 0.0011	168 0.0012	165 0.0013	168 0.0015	252 0.0002 $N^{0.136\ 154}$	227 0.0009	229 0.0009	211 0.0009	194 0.0009	184 0.0010	331 0.0008 $N^{0.013\ 89}$
117	HYUNDAI-ROBOTICSLAB-000	328 0.0022	317 0.0023	301 0.0025	284 0.0027	273 0.0030	368 0.0005 $N^{0.107\ 89}$	380 0.0018	370 0.0019	346 0.0019	330 0.0019	315 0.0020	374 0.0012 $N^{0.030\ 177}$
118	HYUNDAI-ROBOTICSLAB-001	227 0.0012	225 0.0014	224 0.0016	224 0.0018	220 0.0021	200 0.0001 $N^{0.178\ 232}$	209 0.0009	205 0.0009	210 0.0009	210 0.0010	209 0.0011	158 0.0003 $N^{0.067\ 275}$
119	HYUNDAI-ROBOTICSLAB-002	69 0.0006	75 0.0007	72 0.0008	76 0.0009	92 0.0011	84 0.0001 $N^{0.178\ 233}$	82 0.0006	78 0.0006	77 0.0006	75 0.0006	68 0.0006	216 0.0004 $N^{0.021\ 133}$
120	HZAILU-000	285 0.0016	284 0.0018	275 0.0021	273 0.0025	272 0.0030	162 0.0001 $N^{0.216\ 291}$	280 0.0011	270 0.0011	256 0.0011	255 0.0012	243 0.0012	294 0.0006 $N^{0.042\ 215}$
121	HZAILU-001	268 0.0015	257 0.0016	239 0.0017	228 0.0018	223 0.0021	332 0.0003 $N^{0.114\ 107}$	286 0.0011	287 0.0011	278 0.0012	269 0.0012	258 0.0013	246 0.0005 $N^{0.063\ 261}$
122	HZAILU-002	269 0.0015	261 0.0016	244 0.0018	237 0.0020	231 0.0022	301 0.0002 $N^{0.137\ 157}$	287 0.0011	286 0.0011	276 0.0012	271 0.0013	259 0.0013	245 0.0005 $N^{0.063\ 262}$
123	HZAILU-003	213 0.0012	212 0.0013	206 0.0014	208 0.0016	203 0.0018	243 0.0001 $N^{0.153\ 181}$	208 0.0009	212 0.0009	223 0.0010	213 0.0010	204 0.0010	181 0.0004 $N^{0.064\ 267}$
124	HZAILU-004	153 0.0009	146 0.0009	138 0.0010	139 0.0011	134 0.0012	275 0.0002 $N^{0.111\ 101}$	207 0.0009	191 0.0009	179 0.0009	174 0.0009	163 0.0009	326 0.0008 $N^{0.009\ 62}$
125	I2V-001	340 0.0025	328 0.0026	306 0.0027	289 0.0028	271 0.0030	389 0.0011 $N^{0.059\ 19}$	409 0.0024	398 0.0024	360 0.0024	350 0.0024	335 0.0024	395 0.0022 $N^{0.006\ 44}$
126	ICM-001	342 0.0025	332 0.0028	320 0.0030	306 0.0033	298 0.0038	348 0.0004 $N^{0.141\ 164}$	376 0.0018	372 0.0019	348 0.0020	339 0.0020	325 0.0021	346 0.0009 $N^{0.056\ 245}$
127	IDEMIA-003	398 0.0050	400 0.0066	380 0.0080	376 0.0098	367 0.0118	185 0.0001 $N^{0.293\ 379}$	390 0.0020	399 0.0024	368 0.0027	361 0.0033	354 0.0038	62 0.0001 $N^{0.224\ 366}$
128	IDEMIA-004	398 0.0051	395 0.0063	376 0.0076	373 0.0094	363 0.0114	207 0.0001 $N^{0.281\ 366}$	349 0.0015	360 0.0018	357 0.0022	353 0.0027	348 0.0033	29 0.0000 $N^{0.272\ 383}$
129	IDEMIA-005	405 0.0061	413 0.0077	385 0.0093	380 0.0115	373 0.0140	226 0.0001 $N^{0.287\ 374}$	388 0.0019	405 0.0027	376 0.0033	376 0.0041	367 0.0051	22 0.0000 $N^{0.329\ 397}$
130	IDEMIA-006	419 0.0072	427 0.0092	392 0.0109	385 0.0132	377 0.0158	279 0.0002 $N^{0.267\ 350}$	411 0.0025	423 0.0034	389 0.0043	382 0.0055	377 0.0073	17 0.0000 $N^{0.369\ 402}$
131	IDEMIA-007	299 0.0017	309 0.0022	304 0.0026	304 0.0032	305 0.0040	44 0.0000 $N^{0.284\ 371}$	163 0.0007	179 0.0008	186 0.0009	217 0.0010	233 0.0012	61 0.0001 $N^{0.153\ 339}$
132	IDEMIA-008	63 0.0006	72 0.0007	77 0.0008	75 0.0009	76 0.0010	85 0.0001 $N^{0.176\ 227}$	71 0.0005	70 0.0005	68 0.0005	67 0.0006	62 0.0006	185 0.0004 $N^{0.026\ 157}$
133	IDEMIA-009	54 0.0006	50 0.0006	50 0.0007	47 0.0008	45 0.0009	147 0.0001 $N^{0.146\ 172}$	52 0.0005	49 0.0005	46 0.0005	45 0.0005	42 0.0005	214 0.0004 $N^{0.013\ 86}$
134	IDEMIA-010	28 0.0005	27 0.0005	27 0.0006	23 0.0006	13 0.0007	236 0.0001 $N^{0.095\ 71}$	51 0.0005	50 0.0005	45 0.0005	44 0.0005	33 0.0005	249 0.0005 $N^{0.004\ 25}$
135	IDEMIA-011	77 0.0007	68 0.0007	63 0.0007	50 0.0008	38 0.0008	300 0.0002 $N^{0.077\ 34}$	131 0.0006	128 0.0007	118 0.0007	109 0.0007	101 0.0007	282 0.0006 $N^{0.011\ 74}$
136	IDEMIA-012	80 0.0007	73 0.0007	68 0.0007	52 0.0008	36 0.0008	312 0.0003 $N^{0.070\ 29}$	123 0.0006	115 0.0006	109 0.0006	104 0.0007	94 0.0007	275 0.0005 $N^{0.011\ 77}$
137	IMAGUS-005	255 0.0014	256 0.0016	251 0.0018	248 0.0021	241 0.0024	194 0.0001 $N^{0.189\ 259}$	225 0.0009	240 0.0010	230 0.0010	228 0.0011	242 0.0012	120 0.0003 $N^{0.089\ 299}$
138	IMAGUS-006	261 0.0014	262 0.0016	250 0.0018	247 0.0021	246 0.0025	209 0.0001 $N^{0.185\ 251}$	261 0.0010	273 0.0011	262 0.0011	248 0.0011	253 0.0012	219 0.0004 $N^{0.065\ 270}$
139	IMAGUS-007	250 0.0014	266 0.0016	262 0.0019	265 0.0023	253 0.0026	114 0.0001 $N^{0.224\ 302}$	195 0.0008	207 0.0009	198 0.0009	198 0.0010	220 0.0011	114 0.0003 $N^{0.088\ 298}$
140	IMDS-SOFTWARE-001	91 0.0007	102 0.0008	120 0.0009	126 0.0011	133 0.0012	64 0.0000 $N^{0.201\ 272}$	94 0.0006	86 0.0006	85 0.0006	83 0.0006	85 0.0006	152 0.0003 $N^{0.039\ 210}$
141	IMDS-SOFTWARE-002	88 0.0007	99 0.0008	110 0.0009	123 0.0011	127 0.0012	63 0.0000 $N^{0.200\ 271}$	76 0.0005	79 0.0006	79 0.0006	76 0.0006	79 0.0006	149 0.0003 $N^{0.037\ 207}$
142	IMPERIAL-000	304 0.0018	300 0.0021	289 0.0023	282 0.0027	279 0.0031	254 0.0002 $N^{0.181\ 239}$	327 0.0013	314 0.0013	299 0.0014	291 0.0014	277 0.0015	300 0.0006 $N^{0.052\ 240}$
143	INCODE-003	443 0.0096	450 0.0127	402 0.0151	397 0.0188	387 0.0230	266 0.0002 $N^{0.299\ 384}$	406 0.0023	413 0.0029	384 0.0035	379 0.0044	369 0.0054	33 0.0000 $N^{0.295\ 390}$
144	INCODE-004	346 0.0026	348 0.0032	337 0.0038	334 0.0046	328 0.0056	119 0.0001 $N^{0.268\ 352}$	343 0.0014	341 0.0015	327 0.0016	319 0.0017	306 0.0018	201 0.0004 $N^{0.094\ 305}$

Table 40: **Investigation-mode: Effect of N on FNIR on recent images** *For five enrollment population sizes, N, with T = 0 and FPIR = 1. The left five columns are rank 1 miss rates The right five columns are rank 50 miss rates Missing entries usually apply because another algorithm from the same developer was run instead. Some developers are missing because less accurate algorithms were not run on galleries with $N > 1\,600\,000$. Throughout blue superscripts indicate the rank of the algorithm for that column, and yellow highlighting indicates the most accurate value. Caution: The Power-low models are mostly intended to draw attention to the kind of behavior, not as a model to be used for prediction.*

This publication is available free of charge from: https://doi.org/10.6028/NIST.IR.8271

MISSES AT GIVEN RANK FNIR(N, T= 0, R)		ENROL MOST RECENT											
		RANK 1						RANK 50					
#	ALGORITHM	N=0.64M	N=1.6M	N=3.0M	N=6.0M	N=12.0M	aN^b	N=0.64M	N=1.6M	N=3.0M	N=6.0M	N=12.0M	aN^b
145	INCODE-005	211 0.0012	214 0.0013	209 0.0014	211 0.0016	212 0.0019	197 0.0001 N^0.174 222	204 0.0009	210 0.0009	201 0.0009	201 0.0010	201 0.0010	206 0.0004 N^0.056 247
146	INCODE-006	92 0.0007	76 0.0007	70 0.0008	61 0.0008	56 0.0009	283 0.0002 N^0.088 55	141 0.0007	138 0.0007	130 0.0007	120 0.0007	110 0.0007	292 0.0006 N^0.009 65
147	INCODE-007	21 0.0005	22 0.0005	23 0.0006	16 0.0006	21 0.0007	176 0.0001 N^0.120 120	24 0.0005	16 0.0005	15 0.0005	22 0.0005	21 0.0005	144 0.0003 N^0.025 155
148	INNOVATRICS-007	218 0.0012	217 0.0013	218 0.0015	217 0.0017	218 0.0020	199 0.0001 N^0.176 230	202 0.0009	198 0.0009	191 0.0009	195 0.0009	194 0.0010	218 0.0004 N^0.052 239
149	INNOVATRICS-008	146 0.0009	147 0.0009	144 0.0010	144 0.0011	142 0.0013	229 0.0001 N^0.137 156	147 0.0007	146 0.0007	138 0.0007	131 0.0007	126 0.0008	260 0.0005 N^0.027 162
150	INNOVATRICS-009	163 0.0010	161 0.0010	152 0.0011	151 0.0012	148 0.0013	273 0.0002 N^0.117 112	210 0.0009	197 0.0009	182 0.0009	176 0.0009	167 0.0009	327 0.0008 N^0.010 68
151	INNOVATRICS-010	177 0.0010	172 0.0010	162 0.0011	148 0.0012	144 0.0013	318 0.0003 N^0.095 68	217 0.0009	201 0.0009	192 0.0009	186 0.0009	180 0.0009	299 0.0006 N^0.024 152
152	INNOVATRICS-011	94 0.0007	87 0.0008	93 0.0008	80 0.0009	82 0.0010	206 0.0001 N^0.133 151	105 0.0006	106 0.0006	101 0.0006	100 0.0006	103 0.0007	150 0.0003 N^0.043 222
153	INNOVATRICS-012	84 0.0007	84 0.0007	83 0.0008	88 0.0009	88 0.0011	166 0.0001 N^0.153 180	111 0.0006	98 0.0006	96 0.0006	97 0.0006	89 0.0006	196 0.0004 N^0.031 185
154	INNOVATRICS-013	38 0.0005	46 0.0006	45 0.0007	56 0.0008	58 0.0009	52 0.0000 N^0.186 252	20 0.0005	34 0.0005	34 0.0005	24 0.0005	20 0.0005	172 0.0004 N^0.018 121
155	INNOVATRICS-014	30 0.0005	32 0.0006	31 0.0006	34 0.0007	31 0.0008	137 0.0001 N^0.142 165	23 0.0005	24 0.0005	20 0.0005	37 0.0005	41 0.0005	115 0.0003 N^0.039 211
156	INSPUR-000	48 0.0006	55 0.0006	54 0.0007	64 0.0008	75 0.0010	34 0.0000 N^0.205 277	35 0.0005	40 0.0005	43 0.0005	40 0.0005	38 0.0005	153 0.0003 N^0.024 154
157	INSPUR-001	47 0.0006	48 0.0006	64 0.0007	66 0.0008	62 0.0010	47 0.0000 N^0.195 266	36 0.0005	39 0.0005	38 0.0005	26 0.0005	31 0.0005	184 0.0004 N^0.017 119
158	INSPUR-002	36 0.0005	39 0.0006	48 0.0007	45 0.0008	46 0.0009	72 0.0001 N^0.173 220	26 0.0005	22 0.0005	19 0.0005	17 0.0005	16 0.0005	189 0.0004 N^0.014 95
159	INTELRESEARCH-001	55 0.0006	60 0.0006	55 0.0007	55 0.0008	59 0.0009	116 0.0001 N^0.158 188	53 0.0005	52 0.0005	49 0.0005	48 0.0005	47 0.0005	200 0.0004 N^0.017 120
160	INTEMA-000	102 0.0007	98 0.0008	97 0.0009	98 0.0010	120 0.0012	113 0.0001 N^0.173 216	129 0.0006	137 0.0007	149 0.0008	142 0.0008	173 0.0009	75 0.0001 N^0.116 321
161	INTEMA-001	9 0.0005	8 0.0005	19 0.0006	27 0.0007	57 0.0009	16 0.0000 N^0.237 318	14 0.0004	10 0.0004	29 0.0005	43 0.0005	116 0.0007	38 0.0001 N^0.151 338
162	INTSYSMSU-000	520 0.1392	519 0.1454	426 0.1495	416 0.1541	407 0.1588	415 0.0765 N^0.045 12	529 0.1095	527 0.1160	429 0.1203	418 0.1248	409 0.1293	415 0.0516 N^0.057 248
163	IONETWORKS-001	288 0.0016	350 0.0034	369 0.0066	389 0.0142	389 0.0263	5 0.0000 N^0.974 411	341 0.0014	417 0.0031	398 0.0062	410 0.0138	404 0.0257	5 0.0000 N^1.013 411
164	IREX-000	379 0.0040	364 0.0040	342 0.0041	326 0.0042	313 0.0044	400 0.0024 N^0.035 7	440 0.0039	431 0.0039	388 0.0039	371 0.0039	357 0.0039	402 0.0038 N^0.002 13
165	ISYSTEMS-002	391 0.0050	394 0.0061	372 0.0070	362 0.0080	353 0.0093	328 0.0003 N^0.209 284	426 0.0031	420 0.0032	381 0.0034	368 0.0035	353 0.0038	370 0.0012 N^0.072 279
166	ISYSTEMS-003	386 0.0043	381 0.0049	358 0.0055	350 0.0063	340 0.0073	351 0.0004 N^0.181 237	422 0.0029	415 0.0031	374 0.0031	365 0.0033	352 0.0035	375 0.0012 N^0.063 263
167	KAKAO-000	157 0.0009	184 0.0011	188 0.0013	201 0.0016	208 0.0019	35 0.0000 N^0.245 328	96 0.0006	105 0.0006	104 0.0006	118 0.0007	117 0.0007	96 0.0002 N^0.079 287
168	KAKAO-001	180 0.0010	166 0.0010	158 0.0011	147 0.0012	140 0.0013	337 0.0003 N^0.079 39	237 0.0009	226 0.0009	214 0.0010	200 0.0010	188 0.0010	321 0.0007 N^0.016 115
169	KAKAO-002	175 0.0010	159 0.0010	149 0.0011	143 0.0011	124 0.0012	341 0.0004 N^0.074 33	233 0.0009	218 0.0009	207 0.0009	196 0.0010	186 0.0010	320 0.0007 N^0.016 112
170	KEDACOM-001	418 0.0072	409 0.0074	375 0.0076	361 0.0079	345 0.0083	406 0.0037 N^0.049 14	469 0.0068	461 0.0068	406 0.0069	390 0.0069	374 0.0070	409 0.0060 N^0.010 66
171	KLOUDSPOT-001	298 0.0017	295 0.0020	292 0.0024	292 0.0028	289 0.0035	109 0.0001 N^0.241 324	273 0.0010	264 0.0011	257 0.0011	251 0.0011	250 0.0012	259 0.0005 N^0.055 244
172	KNERON-000	387 0.0044	389 0.0056	367 0.0064	358 0.0075	350 0.0089	270 0.0002 N^0.239 320	445 0.0044	446 0.0056	400 0.0064	395 0.0075	385 0.0089	89 0.0002 N^0.239 369
173	KNOWUTECH-000	73 0.0007	92 0.0008	118 0.0009	128 0.0011	125 0.0012	38 0.0000 N^0.216 292	48 0.0005	57 0.0005	55 0.0005	50 0.0005	53 0.0005	136 0.0003 N^0.034 195
174	KOGNIZA-000	217 0.0012	207 0.0013	204 0.0014	199 0.0015	187 0.0017	309 0.0003 N^0.115 109	279 0.0011	274 0.0011	260 0.0011	240 0.0011	225 0.0011	341 0.0008 N^0.019 125
175	LIGHTVISION-000	337 0.0024	331 0.0027	319 0.0030	309 0.0034	303 0.0040	305 0.0002 N^0.170 208	387 0.0019	374 0.0019	347 0.0019	335 0.0020	318 0.0021	382 0.0014 N^0.024 153
176	LINECLOVA-002	156 0.0009	149 0.0009	142 0.0010	140 0.0011	138 0.0013	288 0.0002 N^0.106 87	191 0.0008	182 0.0008	171 0.0008	161 0.0008	153 0.0009	312 0.0007 N^0.011 73
177	LINECLOVA-003	61 0.0006	52 0.0006	67 0.0007	68 0.0009	63 0.0010	88 0.0001 N^0.171 209	18 0.0005	20 0.0005	39 0.0005	41 0.0005	44 0.0005	103 0.0002 N^0.050 233
178	LOOKMAN-003	430 0.0080	418 0.0084	384 0.0087	372 0.0093	357 0.0101	402 0.0027 N^0.079 38	473 0.0069	464 0.0070	408 0.0071	393 0.0072	378 0.0074	407 0.0051 N^0.023 146
179	LOOKMAN-005	422 0.0075	412 0.0077	379 0.0080	365 0.0082	349 0.0088	403 0.0035 N^0.056 15	470 0.0068	462 0.0069	407 0.0069	391 0.0070	375 0.0071	408 0.0056 N^0.014 97
180	LUXAND-001	336 0.0024	334 0.0028	325 0.0032	319 0.0037	310 0.0043	250 0.0002 N^0.203 274	354 0.0015	351 0.0016	332 0.0017	320 0.0017	307 0.0019	303 0.0006 N^0.064 265
181	MANTRA-000	212 0.0012	223 0.0014	223 0.0016	225 0.0018	228 0.0022	118 0.0001 N^0.210 285	193 0.0008	183 0.0008	183 0.0009	184 0.0009	187 0.0010	180 0.0004 N^0.058 252
182	MAXVISION-000	297 0.0017	298 0.0021	290 0.0024	290 0.0028	288 0.0035	122 0.0001 N^0.237 316	226 0.0009	244 0.0010	244 0.0011	261 0.0012	265 0.0013	78 0.0002 N^0.132 328
183	MAXVISION-001	124 0.0008	122 0.0008	123 0.0009	111 0.0010	106 0.0011	248 0.0002 N^0.122 128	157 0.0007	151 0.0007	144 0.0007	137 0.0008	127 0.0008	273 0.0005 N^0.021 139
184	MAXVISION-002	127 0.0008	130 0.0009	125 0.0009	115 0.0010	113 0.0012	246 0.0001 N^0.124 132	175 0.0008	165 0.0008	158 0.0008	145 0.0008	133 0.0008	328 0.0008 N^0.002 15
185	MAXVISION-003	142 0.0009	136 0.0009	132 0.0010	132 0.0011	128 0.0012	249 0.0002 N^0.126 134	150 0.0007	153 0.0007	146 0.0007	138 0.0008	129 0.0008	254 0.0005 N^0.029 174
186	MAXVISION-004	136 0.0008	121 0.0008	108 0.0009	91 0.0009	84 0.0011	314 0.0003 N^0.082 42	179 0.0008	169 0.0008	161 0.0008	149 0.0008	137 0.0008	338 0.0008 N^0.000 4
187	MEGVII-001	451 0.0104	445 0.0116	396 0.0127	387 0.0140	378 0.0158	396 0.0015 N^0.142 167	476 0.0077	472 0.0080	412 0.0082	400 0.0085	384 0.0088	404 0.0041 N^0.046 227
188	MEGVII-003	143 0.0009	134 0.0009	117 0.0009	105 0.0010	98 0.0011	316 0.0003 N^0.084 47	188 0.0008	175 0.0008	170 0.0008	155 0.0008	148 0.0008	314 0.0007 N^0.010 67
189	MEGVII-004	129 0.0008	119 0.0008	98 0.0009	78 0.0009	66 0.0010	345 0.0004 N^0.059 17	185 0.0008	171 0.0008	164 0.0008	153 0.0008	140 0.0008	323 0.0007 N^0.006 41
190	MEGVII-005	131 0.0008	118 0.0008	99 0.0009	77 0.0009	65 0.0010	346 0.0004 N^0.059 18	184 0.0008	173 0.0008	163 0.0008	154 0.0008	139 0.0008	322 0.0007 N^0.006 40
191	METSAKUURCOMPANY-000	87 0.0007	105 0.0008	109 0.0009	117 0.0010	136 0.0013	59 0.0000 N^0.202 273	61 0.0005	65 0.0005	59 0.0005	58 0.0005	58 0.0006	160 0.0003 N^0.029 173
192	METSAKUURCOMPANY-001	154 0.0009	163 0.0010	157 0.0011	160 0.0013	166 0.0015	177 0.0001 N^0.166 205	155 0.0007	157 0.0008	152 0.0008	148 0.0008	141 0.0008	210 0.0004 N^0.042 217
193	MICROFOCUS-005	538 0.3698	538 0.4240	431 0.4608	421 0.4998	413 0.5390	414 0.0673 N^0.128 139	533 0.1298	532 0.1721	431 0.2043	421 0.2423	412 0.2808	403 0.0039 N^0.263 378
194	MICROSOFT-003	215 0.0012	248 0.0015	249 0.0018	257 0.0022	256 0.0027	30 0.0000 N^0.276 360	85 0.0006	102 0.0006	134 0.0007	147 0.0008	157 0.0009	46 0.0001 N^0.158 342
195	MICROSOFT-004	210 0.0011	233 0.0014	242 0.0017	244 0.0021	255 0.0027	26 0.0000 N^0.287 376	83 0.0006	88 0.0006	107 0.0006	122 0.0007	144 0.0008	54 0.0001 N^0.139 333
196	MICROSOFT-005	260 0.0014	287 0.0018	287 0.0023	297 0.0030	295 0.0037	18 0.0000 N^0.326 396	97 0.0006	110 0.0006	129 0.0007	136 0.0008	151 0.0009	58 0.0001 N^0.137 332
197	MICROSOFT-006	274 0.0015	292 0.0019	299 0.0025	298 0.0030	296 0.0037	24 0.0000 N^0.310 391	102 0.0006	120 0.0007	133 0.0007	163 0.0008	200 0.0010	34 0.0000 N^0.188 358
198	MOBBL-000	316 0.0020	315 0.0023	303 0.0026	287 0.0027	258 0.0027	366 0.0005 N^0.107 90	316 0.0012	303 0.0013	291 0.0013	282 0.0014	266 0.0014	304 0.0007 N^0.046 228
199	MUKH-002	429 0.0200	426 0.0255	416 0.0301	409 0.0358	402 0.0427	371 0.0006 N^0.258 340	452 0.0051	460 0.0066	410 0.0079	404 0.0097	396 0.0120	65 0.0001 N^0.293 389
200	NEC-000	460 0.0128	459 0.0167	406 0.0199	398 0.0241	390 0.0291	325 0.0003 N^0.281 367	416 0.0026	424 0.0035	391 0.0044	383 0.0056	376 0.0071	23 0.0000 N^0.344 400
201	NEC-001	472 0.0177	468 0.0206	410 0.0230	402 0.0262	392 0.0300	397 0.0016 N^0.181 238	493 0.0106	483 0.0109	416 0.0113	406 0.0118	397 0.0125	406 0.0049 N^0.057 249
202	NEC-002	137 0.0008	140 0.0009	135 0.0010	131 0.0011	116 0.0012	262 0.0002 N^0.117 111	149 0.0007	150 0.0007	143 0.0007	133 0.0008	131 0.0008	238 0.0004 N^0.034 197
203	NEC-003	222 0.0012	211 0.0013	200 0.0013	181 0.0014	167 0.0015	362 0.0005 N^0.074 32	300 0.0011	282 0.0011	270 0.0011	256 0.0012	238 0.0012	359 0.0009 N^0.013 90
204	NEC-004	186 0.0010	176 0.0011	165 0.0011	152 0.0012	143 0.0013	340 0.0004 N^0.078 37	236 0.0009	224 0.0009	213 0.0009	208 0.0010	191 0.0010	309 0.0007 N^0.023 145
205	NEC-005	121 0.0008	113 0.0008	105 0.0009	90 0.0009	77 0.0010	293 0.0002 N^0.092 62	153 0.0007	142 0.0007	139 0.0007	132 0.0007	124 0.0008	274 0.0005 N^0.020 128
206	NEC-006	144 0.0009	141 0.0009	130 0.0009	124 0.0011	105 0.0011	303 0.0002 N^0.095 72	170 0.0008	164 0.0008	165 0.0008	156 0.0008	152 0.0009	251 0.0005 N^0.036 202
207	NEC-007	71 0.0006	64 0.0007	56 0.0007	48 0.0008	39 0.0008	263 0.0002 N^0.095 70	98 0.0006	95 0.0006	90 0.0006	84 0.0006	80 0.0006	232 0.0004 N^0.021 138
208	NEC-008	100 0.0007	81 0.0007	73 0.0008	69 0.0009	50 0.0009	294 0.0002 N^0.085 49	116 0.0006	113 0.0006	106 0.0006	94 0.0006	93 0.0006	264 0.0005 N^0.016 110
209	NEC-009	56 0.0006	49 0.0006	42 0.0006	35 0.0007	27 0.0008	265 0.0002 N^0.088 56	100 0.0006	92 0.0006	83 0.0006	77 0.0006	69 0.0006	279 0.0006 N^0.003 21
210	NEC-010	19 0.0005	15 0.0005	15 0.0005	10 0.0006	11 0.0007	217 0.0001 N^0.100 78	17 0.0004	21 0.0005	18 0.0005	33 0.0005	23 0.0005	129 0.0003 N^0.031 179
211	NEC-011	4 0.0004	9 0.0005	7 0.0005	4 0.0005	4 0.0006	183 0.0001 N^0.110 99	5 0.0004	7 0.0004	7 0.0004	9 0.0004	9 0.0004	143 0.0003 N^0.019 127
212	NEUROTECHNOLOGY-003	471 0.0175	470 0.0222	412 0.0259	405 0.0302	397 0.0358	378 0.0007 N^0.242 325	441 0.0039	445 0.0054	405 0.0069	401 0.0087	393 0.0109	28 0.0000 N^0.348 401
213	NEUROTECHNOLOGY-004	382 0.0043	383 0.0052	365 0.0061	355 0.0071	348 0.0084	274 0.0002 N^0.231 308	383 0.0019	387 0.0022	363 0.0025	358 0.0028	346 0.0031	92 0.0002 N^0.173 351
214	NEUROTECHNOLOGY-005	362 0.0033	362 0.0040	349 0.0046	342 0.0054	334 0.0065	233 0.0001 N^0.235 314	384 0.0019	379 0.0021	354 0.0022	347 0.0023	338 0.0025	267 0.0005 N^0.097 310
215	NEUROTECHNOLOGY-007	352 0.0028	352 0.0036	343 0.0041	337 0.0049	331 0.0058	198 0.0001 N^0.242 326	368 0.0017	361 0.0018	344 0.0019	336 0.0020	328 0.0022	261 0.0005 N^0.091 300
216	NEUROTECHNOLOGY-008	275 0.0015	281 0.0018	273 0.0021	276 0.0025	274 0.0030	96 0.0001 N^0.240 323	245 0.0009	232 0.0010	225 0.0010	222 0.0010	221 0.0011	223 0.0004 N^0.058 251

Table 41: **Investigation-mode: Effect of N on FNIR on recent images** *For five enrollment population sizes, N, with T = 0 and FPIR = 1. The left five columns are rank 1 miss rates The right five columns are rank 50 miss rates Missing entries usually apply because another algorithm from the same developer was run instead. Some developers are missing because less accurate algorithms were not run on galleries with N > 1 600 000. Throughout blue superscripts indicate the rank of the algorithm for that column, and yellow highlighting indicates the most accurate value. Caution: The Power-low models are mostly intended to draw attention to the kind of behavior, not as a model to be used for prediction.*

This publication is available free of charge from: https://doi.org/10.6028/NIST.IR.8271

MISSES AT GIVEN RANK FNIR(N, T= 0, R)		ENROL MOST RECENT											
		RANK 1						RANK 50					
#	ALGORITHM	N=0.64M	N=1.6M	N=3.0M	N=6.0M	N=12.0M	aN^b	N=0.64M	N=1.6M	N=3.0M	N=6.0M	N=12.0M	aN^b
217	NEUROTECHNOLOGY-009	166 0.0010	179 0.0011	178 0.0012	189 0.0015	192 0.0017	87 0.0001 N^0.207 282	160 0.0007	158 0.0008	153 0.0008	150 0.0008	146 0.0008	212 0.0004 N^0.043 219
218	NEUROTECHNOLOGY-010	120 0.0008	131 0.0009	133 0.0010	138 0.0011	141 0.0013	146 0.0001 N^0.170 206	132 0.0006	133 0.0007	117 0.0007	113 0.0007	113 0.0007	256 0.0005 N^0.021 140
219	NEUROTECHNOLOGY-012	70 0.0006	63 0.0007	57 0.0007	62 0.0008	70 0.0010	155 0.0001 N^0.149 176	99 0.0006	93 0.0006	80 0.0006	81 0.0006	77 0.0006	253 0.0005 N^0.014 96
220	NEUROTECHNOLOGY-013	68 0.0006	65 0.0007	60 0.0007	57 0.0008	52 0.0009	205 0.0001 N^0.124 133	109 0.0006	99 0.0006	92 0.0006	90 0.0006	87 0.0006	231 0.0004 N^0.023 148
221	NEUROTECHNOLOGY-014	43 0.0006	41 0.0006	40 0.0006	41 0.0007	48 0.0009	93 0.0001 N^0.162 200	54 0.0005	53 0.0005	57 0.0005	55 0.0005	63 0.0006	118 0.0003 N^0.045 226
222	NEUROTECHNOLOGY-015	25 0.0005	28 0.0005	30 0.0006	33 0.0007	41 0.0009	62 0.0000 N^0.175 224	33 0.0005	41 0.0005	53 0.0005	62 0.0006	72 0.0006	80 0.0002 N^0.080 289
223	NEUROTECHNOLOGY-016	24 0.0005	21 0.0005	20 0.0006	26 0.0006	32 0.0008	95 0.0001 N^0.154 183	31 0.0005	37 0.0005	42 0.0005	54 0.0005	48 0.0005	98 0.0002 N^0.058 250
224	NEXTMETALABS-002	45 0.0006	54 0.0006	49 0.0007	42 0.0007	47 0.0009	121 0.0001 N^0.152 179	29 0.0005	33 0.0005	35 0.0005	28 0.0005	35 0.0005	146 0.0003 N^0.026 160
225	NOMINDER-000	66 0.0006	67 0.0007	69 0.0007	71 0.0009	79 0.0010	89 0.0001 N^0.174 223	50 0.0005	51 0.0005	51 0.0005	51 0.0005	49 0.0005	142 0.0003 N^0.031 182
226	NOMINDER-001	206 0.0011	190 0.0011	176 0.0012	171 0.0013	164 0.0015	323 0.0003 N^0.096 75	222 0.0010	258 0.0010	241 0.0010	223 0.0010	207 0.0011	362 0.0010 N^0.005 37
227	NOMINDER-002	208 0.0011	194 0.0012	179 0.0012	174 0.0013	157 0.0014	344 0.0004 N^0.082 43	270 0.0010	257 0.0010	238 0.0010	227 0.0011	211 0.0011	353 0.0009 N^0.009 63
228	NOMINDER-003	209 0.0011	193 0.0012	177 0.0012	176 0.0013	158 0.0014	342 0.0004 N^0.084 46	281 0.0011	269 0.0011	250 0.0011	231 0.0011	215 0.0011	364 0.0010 N^0.003 19
229	NOMINDER-004	188 0.0010	177 0.0011	159 0.0011	155 0.0012	148 0.0014	324 0.0003 N^0.091 61	252 0.0010	236 0.0010	220 0.0010	209 0.0010	193 0.0010	350 0.0009 N^0.007 50
230	NOTIONTAG-000	312 0.0019	299 0.0021	281 0.0022	274 0.0025	264 0.0029	329 0.0003 N^0.135 153	358 0.0016	349 0.0016	328 0.0016	311 0.0016	297 0.0017	363 0.0010 N^0.032 190
231	NTECHLAB-003	388 0.0045	393 0.0060	374 0.0074	371 0.0092	362 0.0112	107 0.0001 N^0.315 392	318 0.0012	340 0.0015	334 0.0017	340 0.0021	337 0.0025	35 0.0000 N^0.241 370
232	NTECHLAB-004	372 0.0035	376 0.0046	361 0.0056	353 0.0069	346 0.0083	112 0.0001 N^0.296 382	274 0.0010	299 0.0012	310 0.0014	306 0.0016	312 0.0019	45 0.0001 N^0.207 365
233	NTECHLAB-005	365 0.0034	374 0.0046	362 0.0057	356 0.0071	351 0.0090	41 0.0000 N^0.337 401	176 0.0008	248 0.0010	271 0.0011	294 0.0015	302 0.0018	16 0.0000 N^0.288 387
234	NTECHLAB-006	354 0.0029	363 0.0040	353 0.0049	346 0.0061	342 0.0077	36 0.0000 N^0.330 398	156 0.0007	194 0.0009	235 0.0010	264 0.0012	286 0.0015	20 0.0000 N^0.260 376
235	NTECHLAB-007	305 0.0018	313 0.0023	307 0.0027	308 0.0034	306 0.0041	53 0.0000 N^0.278 363	171 0.0008	188 0.0008	200 0.0009	224 0.0011	240 0.0012	64 0.0001 N^0.150 337
236	NTECHLAB-008	197 0.0011	221 0.0014	233 0.0016	241 0.0020	238 0.0024	27 0.0000 N^0.275 358	126 0.0006	135 0.0007	132 0.0007	144 0.0008	149 0.0008	86 0.0002 N^0.096 307
237	NTECHLAB-009	126 0.0008	143 0.0009	143 0.0010	149 0.0012	152 0.0014	102 0.0001 N^0.187 255	101 0.0006	94 0.0006	99 0.0006	108 0.0007	108 0.0007	110 0.0002 N^0.064 266
238	NTECHLAB-010	95 0.0007	88 0.0008	82 0.0008	86 0.0009	74 0.0010	214 0.0001 N^0.130 145	133 0.0006	132 0.0007	115 0.0007	107 0.0007	104 0.0007	287 0.0006 N^0.008 57
239	NTECHLAB-011	67 0.0006	66 0.0007	62 0.0007	65 0.0008	67 0.0010	151 0.0001 N^0.151 177	66 0.0005	67 0.0005	66 0.0005	64 0.0006	59 0.0006	166 0.0004 N^0.028 170
240	OMNIGARDE-000	60 0.0006	70 0.0007	74 0.0008	85 0.0009	93 0.0011	46 0.0000 N^0.203 275	32 0.0005	47 0.0005	52 0.0005	52 0.0005	50 0.0005	112 0.0002 N^0.049 232
241	OMNIGARDE-001	35 0.0005	31 0.0005	36 0.0006	40 0.0007	35 0.0008	101 0.0001 N^0.157 186	15 0.0004	14 0.0004	14 0.0005	18 0.0005	26 0.0005	121 0.0003 N^0.035 198
242	OMNIGARDE-002	39 0.0005	43 0.0006	41 0.0006	39 0.0007	40 0.0009	117 0.0001 N^0.151 178	12 0.0004	13 0.0004	22 0.0005	29 0.0005	36 0.0005	99 0.0002 N^0.052 237
243	OPTIEXACTA-000	27 0.0005	26 0.0005	24 0.0006	19 0.0006	15 0.0007	224 0.0001 N^0.101 82	47 0.0005	44 0.0005	35 0.0005	32 0.0005	24 0.0005	242 0.0005 N^0.004 27
244	PANGIAM-000	119 0.0008	114 0.0008	121 0.0009	118 0.0010	132 0.0012	160 0.0001 N^0.162 199	125 0.0006	131 0.0007	123 0.0007	119 0.0007	118 0.0007	177 0.0004 N^0.041 214
245	PANGIAM-001	410 0.0065	397 0.0065	370 0.0066	352 0.0068	337 0.0069	407 0.0049 N^0.021 4	465 0.0064	457 0.0064	401 0.0064	388 0.0064	372 0.0064	410 0.0063 N^0.002 8
246	PAPSAV1923-000	118 0.0008	109 0.0008	92 0.0008	74 0.0009	71 0.0010	282 0.0002 N^0.095 69	161 0.0007	156 0.0007	142 0.0007	127 0.0007	119 0.0007	318 0.0007 N^-0.000 1
247	PARAVISION-003	345 0.0026	344 0.0031	331 0.0034	321 0.0041	318 0.0047	244 0.0001 N^0.212 289	359 0.0016	354 0.0017	339 0.0018	328 0.0019	316 0.0020	257 0.0005 N^0.087 296
248	PARAVISION-004	214 0.0012	209 0.0013	203 0.0014	198 0.0015	194 0.0018	268 0.0002 N^0.139 160	238 0.0009	230 0.0009	216 0.0010	202 0.0010	202 0.0010	302 0.0006 N^0.027 163
249	PARAVISION-005	202 0.0011	198 0.0012	183 0.0012	180 0.0014	175 0.0016	289 0.0002 N^0.120 122	244 0.0009	234 0.0010	222 0.0010	206 0.0010	199 0.0010	316 0.0007 N^0.020 132
250	PARAVISION-007	114 0.0008	112 0.0008	107 0.0009	93 0.0010	97 0.0011	228 0.0001 N^0.126 135	130 0.0006	127 0.0007	119 0.0007	117 0.0007	114 0.0007	236 0.0004 N^0.028 166
251	PARAVISION-009	65 0.0006	62 0.0006	66 0.0007	67 0.0009	73 0.0010	92 0.0001 N^0.172 212	87 0.0006	89 0.0006	84 0.0006	88 0.0006	91 0.0006	123 0.0003 N^0.051 236
252	PARAVISION-012	53 0.0006	42 0.0006	34 0.0006	32 0.0007	33 0.0008	218 0.0001 N^0.111 100	90 0.0006	75 0.0006	70 0.0006	69 0.0006	60 0.0006	269 0.0005 N^0.005 35
253	PARAVISION-014	51 0.0006	40 0.0006	35 0.0006	36 0.0007	30 0.0008	223 0.0001 N^0.109 95	75 0.0005	73 0.0006	69 0.0006	65 0.0006	57 0.0006	258 0.0005 N^0.008 55
254	PARAVISION-016	52 0.0006	45 0.0006	39 0.0006	31 0.0007	28 0.0008	235 0.0001 N^0.101 83	84 0.0006	81 0.0006	75 0.0006	68 0.0006	61 0.0006	271 0.0005 N^0.003 22
255	PARAVISION-019	18 0.0005	16 0.0005	16 0.0005	15 0.0006	14 0.0007	174 0.0001 N^0.121 123	19 0.0005	25 0.0005	27 0.0005	25 0.0005	19 0.0005	156 0.0003 N^0.021 137
256	PENTACOMP-001	228 0.0012	232 0.0014	230 0.0016	230 0.0019	234 0.0023	133 0.0001 N^0.208 283	200 0.0008	202 0.0009	195 0.0009	207 0.0010	206 0.0011	135 0.0003 N^0.073 281
257	PIXELALL-002	366 0.0034	366 0.0041	352 0.0048	345 0.0059	339 0.0071	192 0.0001 N^0.256 337	335 0.0014	348 0.0016	335 0.0017	337 0.0020	331 0.0023	67 0.0001 N^0.185 356
258	PIXELALL-003	279 0.0015	279 0.0018	270 0.0021	268 0.0024	265 0.0029	169 0.0001 N^0.213 290	262 0.0010	260 0.0011	251 0.0011	247 0.0011	246 0.0012	239 0.0004 N^0.060 258
259	PIXELALL-004	242 0.0013	269 0.0017	264 0.0019	267 0.0023	259 0.0027	71 0.0001 N^0.245 329	243 0.0009	238 0.0010	233 0.0010	235 0.0011	230 0.0011	182 0.0004 N^0.069 276
260	PIXELALL-005	251 0.0014	247 0.0015	235 0.0016	226 0.0018	221 0.0021	302 0.0002 N^0.132 150	307 0.0012	297 0.0012	284 0.0012	267 0.0012	255 0.0013	340 0.0008 N^0.026 159
261	PSL-000	10 0.0005	18 0.0005	17 0.0005	25 0.0006	29 0.0008	57 0.0000 N^0.173 217	7 0.0004	5 0.0004	10 0.0004	7 0.0004	7 0.0004	167 0.0004 N^0.012 84
262	PSL-001	11 0.0005	11 0.0005	14 0.0005	18 0.0006	22 0.0007	98 0.0001 N^0.149 175	8 0.0004	8 0.0004	6 0.0004	10 0.0004	10 0.0004	140 0.0003 N^0.021 134
263	PSL-002	6 0.0004	5 0.0004	8 0.0005	11 0.0006	19 0.0007	68 0.0000 N^0.161 198	6 0.0004	4 0.0004	3 0.0004	4 0.0004	5 0.0004	170 0.0004 N^0.010 70
264	PSL-003	7 0.0004	6 0.0004	6 0.0005	8 0.0006	8 0.0006	138 0.0001 N^0.128 140	4 0.0004	9 0.0004	8 0.0004	5 0.0004	6 0.0004	183 0.0004 N^0.009 60
265	PSL-004	5 0.0004	4 0.0004	5 0.0005	5 0.0005	3 0.0006	172 0.0001 N^0.115 110	11 0.0004	6 0.0004	5 0.0004	6 0.0004	4 0.0004	225 0.0004 N^-0.000 2
266	PTAKURATSATU-000	326 0.0021	330 0.0027	328 0.0033	317 0.0036	291 0.0036	272 0.0002 N^0.188 256	306 0.0012	306 0.0013	314 0.0015	308 0.0016	291 0.0016	105 0.0002 N^0.121 322
267	PYRAMID-000	81 0.0007	86 0.0007	89 0.0008	94 0.0010	86 0.0011	145 0.0001 N^0.160 193	108 0.0006	104 0.0006	92 0.0006	92 0.0006	84 0.0006	243 0.0005 N^0.019 124
268	PYRAMID-001	115 0.0008	115 0.0008	103 0.0009	97 0.0010	95 0.0011	239 0.0001 N^0.123 131	137 0.0007	119 0.0007	114 0.0007	114 0.0007	112 0.0007	263 0.0005 N^0.020 129
269	QAZSMARTVISIONAI-000	13 0.0005	10 0.0005	12 0.0005	13 0.0006	16 0.0007	156 0.0001 N^0.128 137	9 0.0004	12 0.0004	11 0.0004	12 0.0005	11 0.0005	128 0.0003 N^0.028 169
270	QAZSMARTVISIONAI-001	3 0.0004	3 0.0004	4 0.0005	6 0.0006	6 0.0006	97 0.0001 N^0.141 163	3 0.0004	3 0.0004	4 0.0004	3 0.0004	3 0.0004	164 0.0004 N^0.011 75
271	QAZSMARTVISIONAI-002	1 0.0004	1 0.0004	1 0.0005	1 0.0005	2 0.0006	140 0.0001 N^0.123 130	1 0.0004	2 0.0004	2 0.0004	1 0.0004	1 0.0004	192 0.0004 N^0.004 32
272	QAZSMARTVISIONAI-003	2 0.0004	2 0.0004	2 0.0005	2 0.0005	1 0.0006	173 0.0001 N^0.112 104	2 0.0004	1 0.0004	1 0.0004	2 0.0004	2 0.0004	162 0.0004 N^0.011 72
273	QNAP-001	360 0.0031	358 0.0038	347 0.0043	338 0.0050	333 0.0059	260 0.0002 N^0.216 293	382 0.0019	376 0.0020	353 0.0021	346 0.0022	334 0.0024	290 0.0006 N^0.085 294
274	QNAP-002	384 0.0043	373 0.0045	350 0.0048	340 0.0051	326 0.0055	393 0.0014 N^0.085 51	435 0.0038	429 0.0038	387 0.0039	373 0.0039	359 0.0040	400 0.0028 N^0.021 136
275	QNAP-003	325 0.0021	320 0.0024	308 0.0027	302 0.0031	292 0.0036	271 0.0002 N^0.182 244	289 0.0011	295 0.0012	290 0.0013	289 0.0014	292 0.0016	88 0.0002 N^0.133 329
276	QNAP-004	247 0.0014	249 0.0016	248 0.0018	246 0.0021	245 0.0025	165 0.0001 N^0.204 276	257 0.0010	247 0.0010	234 0.0010	234 0.0011	228 0.0011	268 0.0005 N^0.047 229
277	QNAP-005	353 0.0028	338 0.0029	317 0.0030	303 0.0032	287 0.0034	388 0.0011 N^0.069 26	419 0.0027	404 0.0027	367 0.0027	356 0.0027	342 0.0027	398 0.0025 N^0.006 42
278	QNAP-006	194 0.0011	187 0.0011	184 0.0012	186 0.0015	191 0.0017	184 0.0001 N^0.173 219	192 0.0008	180 0.0008	178 0.0009	172 0.0009	169 0.0009	272 0.0005 N^0.030 176
279	QUANTASOFT-001	533 0.2174	529 0.2174	429 0.2174		408 0.2174	416 0.2174 N^0.000 1	530 0.1113	526 0.1113	428 0.1113		408 0.1113	416 0.1113 N^0.000 3
280	RANKONE-002	468 0.0151	466 0.0191	409 0.0221	401 0.0259	393 0.0300	325 0.0007 N^0.233 311	447 0.0045	449 0.0057	404 0.0068	398 0.0081	391 0.0098	69 0.0001 N^0.268 380
281	RANKONE-003	467 0.0151	465 0.0191	408 0.0221	400 0.0259	394 0.0300	376 0.0007 N^0.233 312	448 0.0045	447 0.0057	403 0.0068	399 0.0081	390 0.0098	70 0.0001 N^0.268 381
282	RANKONE-005	417 0.0072	423 0.0090	391 0.0106	384 0.0129	375 0.0153	292 0.0002 N^0.259 341	408 0.0023	409 0.0028	378 0.0033	372 0.0039	364 0.0047	57 0.0001 N^0.242 371
283	RANKONE-007	339 0.0025	340 0.0030	332 0.0035	322 0.0041	320 0.0049	195 0.0001 N^0.233 310	301 0.0011	308 0.0013	306 0.0014	302 0.0016	299 0.0018	76 0.0001 N^0.154 340
284	RANKONE-009	290 0.0016	294 0.0020	288 0.0023	293 0.0028	286 0.0034	78 0.0001 N^0.253 336	254 0.0010	256 0.0010	258 0.0011	253 0.0012	251 0.0012	154 0.0003 N^0.079 285
285	RANKONE-010	293 0.0017	289 0.0019	276 0.0022	275 0.0025	266 0.0029	219 0.0001 N^0.192 263	278 0.0011	273 0.0011	274 0.0012	262 0.0012	262 0.0013	187 0.0004 N^0.076 282
286	RANKONE-011	179 0.0010	191 0.0011	192 0.0013	192 0.0015	197 0.0018	143 0.0001 N^0.191 262	178 0.0008	167 0.0008	167 0.0008	165 0.0008	156 0.0009	266 0.0005 N^0.033 191
287	RANKONE-012	155 0.0009	165 0.0010	172 0.0012	169 0.0013	179 0.0016	125 0.0001 N^0.187 254	164 0.0007	159 0.0008	154 0.0008	143 0.0008	136 0.0008	276 0.0006 N^0.023 147
288	RANKONE-013	64 0.0006	69 0.0007	80 0.0008	92 0.0010	104 0.0011	43 0.0000 N^0.206 279	62 0.0005	60 0.0005	58 0.0005	57 0.0005	56 0.0006	159 0.0003 N^0.028 171

Table 42: **Investigation-mode: Effect of N on FNIR on recent images** *For five enrollment population sizes, N, with T = 0 and FPIR = 1. The left five columns are rank 1 miss rates The right five columns are rank 50 miss rates Missing entries usually apply because another algorithm from the same developer was run instead. Some developers are missing because less accurate algorithms were not run on galleries with $N > 1\,600\,000$. Throughout blue superscripts indicate the rank of the algorithm for that column, and yellow highlighting indicates the most accurate value. Caution: The Power-low models are mostly intended to draw attention to the kind of behavior, not as a model to be used for prediction.*

This publication is available free of charge from: https://doi.org/10.6028/NIST.IR.8271

MISSES AT GIVEN RANK		ENROL MOST RECENT											
FNIR(N, T= 0, R)		RANK 1						RANK 50					
#	ALGORITHM	N=0.64M	N=1.6M	N=3.0M	N=6.0M	N=12.0M	aN^b	N=0.64M	N=1.6M	N=3.0M	N=6.0M	N=12.0M	aN^b
289	RANKONE-014	[49] 0.0006	[53] 0.0006	[51] 0.0007	[54] 0.0008	[51] 0.0009	[99] 0.0001 $N^{0.164}$ [204]	[60] 0.0005	[64] 0.0005	[56] 0.0005	[53] 0.0005	[51] 0.0005	[215] 0.0004 $N^{0.016}$ [109]
290	RANKONE-015	[59] 0.0006	[57] 0.0006	[53] 0.0007	[58] 0.0008	[55] 0.0009	[158] 0.0001 $N^{0.146}$ [170]	[69] 0.0005	[66] 0.0005	[61] 0.0005	[59] 0.0005	[54] 0.0006	[217] 0.0004 $N^{0.017}$ [116]
291	REALNETWORKS-002	[493] 0.0297	[489] 0.0391	[422] 0.0467	[414] 0.0560	[406] 0.0577	[392] 0.0013 $N^{0.237}$ [317]	[454] 0.0053	[466] 0.0075	[414] 0.0095	[407] 0.0124	[398] 0.0130	[49] 0.0001 $N^{0.324}$ [395]
292	REALNETWORKS-003	[473] 0.0179	[473] 0.0238	[414] 0.0287	[407] 0.0349	[401] 0.0420	[349] 0.0004 $N^{0.291}$ [377]	[436] 0.0038	[440] 0.0050	[392] 0.0061	[396] 0.0077	[389] 0.0098	[36] 0.0000 $N^{0.325}$ [396]
293	REALNETWORKS-004	[470] 0.0172	[471] 0.0233	[413] 0.0280	[406] 0.0344	[398] 0.0413	[334] 0.0003 $N^{0.299}$ [385]	[433] 0.0036	[438] 0.0047	[396] 0.0058	[394] 0.0074	[388] 0.0095	[30] 0.0000 $N^{0.335}$ [398]
294	REALNETWORKS-005	[289] 0.0016	[293] 0.0019	[283] 0.0022	[279] 0.0026	[284] 0.0033	[103] 0.0001 $N^{0.240}$ [322]	[183] 0.0008	[192] 0.0009	[208] 0.0009	[218] 0.0010	[218] 0.0011	[87] 0.0002 $N^{0.111}$ [317]
295	REALNETWORKS-006	[161] 0.0009	[170] 0.0010	[180] 0.0012	[185] 0.0015	[188] 0.0017	[77] 0.0001 $N^{0.210}$ [288]	[119] 0.0006	[126] 0.0007	[127] 0.0007	[135] 0.0008	[138] 0.0008	[90] 0.0002 $N^{0.091}$ [301]
296	REALNETWORKS-007	[151] 0.0009	[156] 0.0010	[150] 0.0011	[154] 0.0012	[159] 0.0014	[181] 0.0001 $N^{0.163}$ [201]	[110] 0.0006	[116] 0.0006	[124] 0.0007	[123] 0.0007	[128] 0.0008	[91] 0.0002 $N^{0.087}$ [297]
297	REALNETWORKS-008	[89] 0.0007	[106] 0.0008	[114] 0.0009	[110] 0.0010	[122] 0.0012	[94] 0.0001 $N^{0.182}$ [245]	[56] 0.0005	[55] 0.0005	[72] 0.0006	[71] 0.0006	[73] 0.0006	[101] 0.0002 $N^{0.061}$ [260]
298	RECOGNITO-000	[33] 0.0005	[38] 0.0006	[33] 0.0006	[38] 0.0007	[34] 0.0008	[120] 0.0001 $N^{0.148}$ [174]	[41] 0.0005	[30] 0.0005	[30] 0.0005	[34] 0.0005	[27] 0.0005	[194] 0.0004 $N^{0.015}$ [102]
299	RECOGNITO-001	[44] 0.0006	[35] 0.0006	[28] 0.0006	[28] 0.0007	[23] 0.0007	[241] 0.0001 $N^{0.097}$ [76]	[58] 0.0005	[56] 0.0005	[50] 0.0005	[49] 0.0005	[45] 0.0005	[240] 0.0005 $N^{0.009}$ [59]
300	RECOGNITO-002	[26] 0.0005	[25] 0.0005	[22] 0.0006	[17] 0.0006	[17] 0.0007	[225] 0.0001 $N^{0.101}$ [81]	[46] 0.0005	[45] 0.0005	[36] 0.0005	[35] 0.0005	[22] 0.0005	[241] 0.0005 $N^{0.004}$ [26]
301	REMARKAI-000	[334] 0.0024	[342] 0.0030	[336] 0.0037	[332] 0.0045	[325] 0.0055	[74] 0.0001 $N^{0.286}$ [373]	[284] 0.0011	[293] 0.0012	[282] 0.0013	[290] 0.0014	[289] 0.0016	[84] 0.0002 $N^{0.137}$ [331]
302	RENDIP-000	[195] 0.0011	[199] 0.0012	[201] 0.0014	[204] 0.0016	[207] 0.0019	[123] 0.0001 $N^{0.198}$ [269]	[186] 0.0008	[184] 0.0008	[176] 0.0008	[171] 0.0009	[170] 0.0009	[265] 0.0005 $N^{0.035}$ [200]
303	REVEALMEDIA-000	[237] 0.0013	[240] 0.0015	[232] 0.0016	[234] 0.0019	[224] 0.0021	[245] 0.0001 $N^{0.163}$ [202]	[196] 0.0008	[196] 0.0009	[188] 0.0009	[183] 0.0009	[185] 0.0010	[230] 0.0004 $N^{0.048}$ [231]
304	RNIT-000	[169] 0.0010	[185] 0.0011	[187] 0.0013	[183] 0.0014	[185] 0.0016	[167] 0.0001 $N^{0.180}$ [236]	[212] 0.0009	[225] 0.0009	[228] 0.0010	[221] 0.0010	[217] 0.0011	[131] 0.0003 $N^{0.079}$ [288]
305	ROC-016	[50] 0.0006	[59] 0.0006	[59] 0.0007	[60] 0.0008	[53] 0.0009	[105] 0.0001 $N^{0.161}$ [197]	[63] 0.0005	[59] 0.0005	[64] 0.0005	[60] 0.0005	[52] 0.0005	[186] 0.0004 $N^{0.024}$ [151]
306	ROC-017	[41] 0.0006	[47] 0.0006	[61] 0.0007	[70] 0.0009	[69] 0.0010	[32] 0.0000 $N^{0.210}$ [286]	[55] 0.0005	[61] 0.0005	[60] 0.0005	[56] 0.0005	[55] 0.0006	[145] 0.0003 $N^{0.033}$ [192]
307	ROC-018	[32] 0.0005	[29] 0.0005	[37] 0.0006	[46] 0.0008	[44] 0.0009	[54] 0.0000 $N^{0.181}$ [240]	[49] 0.0005	[46] 0.0005	[42] 0.0005	[39] 0.0005	[32] 0.0005	[234] 0.0004 $N^{0.007}$ [51]
308	ROC-019	[20] 0.0005	[17] 0.0005	[21] 0.0006	[24] 0.0006	[26] 0.0008	[104] 0.0001 $N^{0.147}$ [173]	[34] 0.0005	[28] 0.0005	[24] 0.0005	[14] 0.0005	[15] 0.0005	[247] 0.0005 $N^{0.000}$ [5]
309	S1-000	[296] 0.0017	[296] 0.0021	[297] 0.0024	[294] 0.0029	[285] 0.0034	[132] 0.0001 $N^{0.234}$ [313]	[288] 0.0011	[283] 0.0011	[277] 0.0012	[270] 0.0012	[263] 0.0013	[213] 0.0004 $N^{0.071}$ [278]
310	S1-001	[349] 0.0027	[333] 0.0028	[321] 0.0030	[305] 0.0033	[294] 0.0037	[374] 0.0007 $N^{0.103}$ [84]	[389] 0.0019	[375] 0.0020	[350] 0.0020	[341] 0.0021	[324] 0.0021	[379] 0.0013 $N^{0.027}$ [164]
311	S1-002	[183] 0.0010	[174] 0.0011	[167] 0.0011	[159] 0.0012	[155] 0.0014	[297] 0.0002 $N^{0.110}$ [97]	[242] 0.0009	[235] 0.0010	[218] 0.0010	[199] 0.0010	[195] 0.0010	[329] 0.0008 $N^{0.015}$ [108]
312	S1-003	[182] 0.0010	[183] 0.0011	[174] 0.0012	[172] 0.0013	[165] 0.0015	[261] 0.0002 $N^{0.131}$ [146]	[206] 0.0009	[206] 0.0009	[193] 0.0009	[191] 0.0009	[181] 0.0009	[278] 0.0006 $N^{0.033}$ [193]
313	S1-004	[170] 0.0010	[157] 0.0010	[146] 0.0010	[142] 0.0011	[139] 0.0013	[319] 0.0003 $N^{0.089}$ [59]	[220] 0.0009	[209] 0.0009	[196] 0.0009	[188] 0.0009	[176] 0.0009	[319] 0.0007 $N^{0.015}$ [104]
314	S1-005	[172] 0.0010	[169] 0.0010	[160] 0.0011	[153] 0.0012	[146] 0.0013	[298] 0.0002 $N^{0.107}$ [93]	[234] 0.0009	[220] 0.0009	[206] 0.0009	[190] 0.0009	[183] 0.0009	[339] 0.0008 $N^{0.009}$ [58]
315	S1-006	[158] 0.0009	[151] 0.0010	[141] 0.0010	[134] 0.0011	[117] 0.0012	[321] 0.0003 $N^{0.086}$ [52]	[214] 0.0009	[199] 0.0009	[189] 0.0009	[179] 0.0009	[171] 0.0009	[330] 0.0008 $N^{0.009}$ [61]
316	S1-007	[135] 0.0008	[125] 0.0009	[113] 0.0009	[99] 0.0010	[90] 0.0011	[306] 0.0002 $N^{0.088}$ [58]	[123] 0.0008	[162] 0.0008	[152] 0.0008	[146] 0.0008	[135] 0.0008	[311] 0.0007 $N^{0.008}$ [54]
317	SANSAP-001	[110] 0.0007	[110] 0.0008	[112] 0.0009	[119] 0.0010	[129] 0.0012	[110] 0.0001 $N^{0.176}$ [228]	[88] 0.0006	[87] 0.0006	[86] 0.0006	[79] 0.0006	[86] 0.0006	[148] 0.0003 $N^{0.039}$ [212]
318	SCANOVATE-000	[371] 0.0035	[375] 0.0046	[360] 0.0055	[354] 0.0069	[338] 0.0070	[222] 0.0001 $N^{0.252}$ [335]	[265] 0.0010	[294] 0.0012	[294] 0.0014	[312] 0.0017	[294] 0.0017	[60] 0.0001 $N^{0.180}$ [354]
319	SCANOVATE-001	[376] 0.0037	[382] 0.0050	[364] 0.0060	[359] 0.0076	[354] 0.0095	[75] 0.0001 $N^{0.317}$ [393]	[256] 0.0010	[292] 0.0012	[295] 0.0014	[317] 0.0017	[322] 0.0021	[24] 0.0000 $N^{0.259}$ [375]
320	SCYLLA-001	[278] 0.0015	[282] 0.0018	[268] 0.0020	[263] 0.0023	[262] 0.0028	[203] 0.0001 $N^{0.194}$ [264]	[255] 0.0010	[253] 0.0010	[249] 0.0011	[241] 0.0011	[245] 0.0012	[207] 0.0004 $N^{0.066}$ [272]
321	SENSETIME-000	[314] 0.0020	[307] 0.0022	[295] 0.0024	[280] 0.0027	[275] 0.0031	[330] 0.0003 $N^{0.139}$ [161]	[355] 0.0015	[350] 0.0016	[330] 0.0016	[318] 0.0017	[303] 0.0018	[310] 0.0007 $N^{0.059}$ [256]
322	SENSETIME-001	[315] 0.0020	[308] 0.0022	[291] 0.0024	[286] 0.0027	[290] 0.0036	[257] 0.0002 $N^{0.183}$ [248]	[350] 0.0015	[345] 0.0015	[326] 0.0016	[315] 0.0017	[329] 0.0023	[113] 0.0003 $N^{0.128}$ [326]
323	SENSETIME-002	[462] 0.0133	[453] 0.0133	[399] 0.0133	[386] 0.0134	[371] 0.0136	[411] 0.0120 $N^{0.007}$ [2]	[500] 0.0132	[491] 0.0132	[418] 0.0132	[409] 0.0132	[399] 0.0132	[412] 0.0131 $N^{0.001}$ [7]
324	SENSETIME-003	[62] 0.0006	[58] 0.0006	[52] 0.0007	[51] 0.0008	[49] 0.0009	[191] 0.0001 $N^{0.127}$ [136]	[93] 0.0006	[90] 0.0006	[81] 0.0006	[82] 0.0006	[75] 0.0006	[229] 0.0004 $N^{0.020}$ [131]
325	SENSETIME-004	[58] 0.0006	[56] 0.0006	[43] 0.0006	[49] 0.0008	[42] 0.0009	[202] 0.0001 $N^{0.122}$ [127]	[42] 0.0005	[48] 0.0005	[48] 0.0005	[47] 0.0005	[46] 0.0005	[138] 0.0003 $N^{0.031}$ [183]
326	SENSETIME-005	[16] 0.0005	[20] 0.0005	[18] 0.0006	[22] 0.0006	[24] 0.0007	[135] 0.0001 $N^{0.137}$ [158]	[27] 0.0005	[15] 0.0005	[13] 0.0005	[11] 0.0005	[12] 0.0005	[227] 0.0004 $N^{0.004}$ [24]
327	SENSETIME-006	[17] 0.0005	[19] 0.0005	[13] 0.0005	[14] 0.0006	[12] 0.0007	[188] 0.0001 $N^{0.112}$ [105]	[25] 0.0005	[23] 0.0005	[16] 0.0005	[21] 0.0005	[18] 0.0005	[161] 0.0003 $N^{0.019}$ [126]
328	SENSETIME-007	[14] 0.0005	[14] 0.0005	[10] 0.0005	[9] 0.0006	[9] 0.0006	[211] 0.0001 $N^{0.101}$ [80]	[21] 0.0005	[26] 0.0005	[17] 0.0005	[15] 0.0005	[17] 0.0005	[188] 0.0004 $N^{0.014}$ [94]
329	SENSETIME-008	[12] 0.0005	[13] 0.0005	[11] 0.0005	[12] 0.0006	[10] 0.0006	[187] 0.0001 $N^{0.111}$ [103]	[13] 0.0004	[17] 0.0005	[12] 0.0005	[13] 0.0005	[13] 0.0005	[147] 0.0003 $N^{0.022}$ [144]
330	SENSETIME-009	[15] 0.0005	[12] 0.0005	[9] 0.0005	[7] 0.0006	[7] 0.0006	[227] 0.0001 $N^{0.093}$ [65]	[16] 0.0004	[19] 0.0005	[25] 0.0005	[16] 0.0005	[14] 0.0005	[174] 0.0004 $N^{0.016}$ [111]
331	SENSETIME-010	[8] 0.0005	[7] 0.0005	[3] 0.0005	[3] 0.0005	[5] 0.0006	[186] 0.0001 $N^{0.108}$ [94]	[10] 0.0004	[11] 0.0004	[9] 0.0004	[8] 0.0004	[8] 0.0004	[190] 0.0004 $N^{0.008}$ [56]
332	SERENDIPITY-000	[184] 0.0010	[195] 0.0012	[191] 0.0013	[194] 0.0015	[195] 0.0018	[161] 0.0001 $N^{0.184}$ [249]	[181] 0.0008	[181] 0.0008	[181] 0.0009	[181] 0.0009	[174] 0.0009	[211] 0.0004 $N^{0.050}$ [234]
333	SEVENTHSENSE-001	[199] 0.0011	[267] 0.0016	[324] 0.0031	[344] 0.0058	[363] 0.0117	[7] 0.0000 $N^{0.832}$ [410]	[228] 0.0009	[343] 0.0015	[372] 0.0030	[384] 0.0056	[394] 0.0115	[6] 0.0000 $N^{0.880}$ [410]
334	SHAMAN-007	[498] 0.0368	[490] 0.0393	[421] 0.0413	[413] 0.0439	[404] 0.0470	[410] 0.0120 $N^{0.083}$ [45]	[514] 0.0306	[508] 0.0311	[424] 0.0316	[414] 0.0323	[405] 0.0334	[413] 0.0205 $N^{0.029}$ [175]
335	SIAT-001	[271] 0.0015	[265] 0.0016	[256] 0.0018	[252] 0.0021	[250] 0.0026	[216] 0.0001 $N^{0.185}$ [250]	[231] 0.0009	[242] 0.0010	[239] 0.0010	[244] 0.0011	[244] 0.0012	[119] 0.0003 $N^{0.091}$ [303]
336	SIAT-002	[262] 0.0014	[271] 0.0017	[257] 0.0018	[251] 0.0021	[243] 0.0025	[221] 0.0001 $N^{0.182}$ [243]	[259] 0.0010	[268] 0.0011	[263] 0.0011	[258] 0.0012	[249] 0.0012	[222] 0.0004 $N^{0.064}$ [269]
337	SPARKTEK-000	[105] 0.0007	[95] 0.0008	[106] 0.0009	[96] 0.0010	[110] 0.0011	[153] 0.0001 $N^{0.161}$ [194]	[95] 0.0006	[96] 0.0006	[91] 0.0006	[85] 0.0006	[81] 0.0006	[209] 0.0004 $N^{0.026}$ [158]
338	SPARSH-001	[75] 0.0007	[79] 0.0007	[79] 0.0008	[82] 0.0009	[83] 0.0011	[149] 0.0001 $N^{0.157}$ [187]	[91] 0.0006	[84] 0.0006	[78] 0.0006	[73] 0.0006	[66] 0.0006	[262] 0.0005 $N^{0.009}$ [64]
339	SQISOFT-001	[341] 0.0025	[359] 0.0038	[359] 0.0055	[363] 0.0081	[366] 0.0118	[10] 0.0000 $N^{0.537}$ [408]	[114] 0.0006	[136] 0.0007	[148] 0.0008	[168] 0.0008	[189] 0.0010	[48] 0.0001 $N^{0.160}$ [345]
340	SQISOFT-002	[125] 0.0008	[148] 0.0009	[169] 0.0012	[195] 0.0015	[209] 0.0019	[15] 0.0000 $N^{0.301}$ [387]	[79] 0.0006	[82] 0.0006	[88] 0.0006	[86] 0.0006	[95] 0.0007	[111] 0.0002 $N^{0.060}$ [257]
341	STCON-001	[29] 0.0005	[30] 0.0005	[32] 0.0006	[30] 0.0007	[25] 0.0007	[171] 0.0001 $N^{0.129}$ [142]	[39] 0.0005	[32] 0.0005	[31] 0.0005	[23] 0.0005	[30] 0.0005	[202] 0.0004 $N^{0.013}$ [88]
342	STCON-002	[22] 0.0005	[23] 0.0005	[25] 0.0006	[20] 0.0006	[20] 0.0007	[180] 0.0001 $N^{0.119}$ [116]	[37] 0.0005	[42] 0.0005	[33] 0.0005	[38] 0.0005	[34] 0.0005	[179] 0.0004 $N^{0.018}$ [123]
343	STCON-003	[23] 0.0005	[24] 0.0005	[26] 0.0006	[21] 0.0006	[18] 0.0007	[190] 0.0001 $N^{0.114}$ [106]	[45] 0.0005	[38] 0.0005	[32] 0.0005	[27] 0.0005	[39] 0.0005	[204] 0.0004 $N^{0.013}$ [85]
344	SYNESIS-003	[821] 0.1453	[520] 0.1697	[427] 0.1873	[417] 0.2085	[409] 0.2315	[412] 0.0176 $N^{0.158}$ [189]	[523] 0.0825	[523] 0.0866	[427] 0.0917	[417] 0.0995	[407] 0.1101	[414] 0.0216 $N^{0.098}$ [311]
345	SYNESIS-003	[469] 0.0157	[457] 0.0159	[404] 0.0160	[393] 0.0162	[388] 0.0250	[401] 0.0026 $N^{0.129}$ [141]	[503] 0.0156	[497] 0.0156	[420] 0.0156	[412] 0.0156	[403] 0.0242	[349] 0.0009 $N^{0.196}$ [361]
346	SYNESIS-005	[432] 0.0081	[416] 0.0082	[381] 0.0082	[366] 0.0083	[347] 0.0084	[409] 0.0069 $N^{0.012}$ [3]	[480] 0.0081	[473] 0.0081	[411] 0.0081	[397] 0.0081	[382] 0.0081	[411] 0.0081 $N^{0.000}$ [6]
347	TECH5-001	[351] 0.0028	[355] 0.0036	[348] 0.0044	[341] 0.0053	[335] 0.0067	[79] 0.0001 $N^{0.294}$ [380]	[319] 0.0012	[316] 0.0013	[309] 0.0014	[305] 0.0016	[309] 0.0019	[82] 0.0002 $N^{0.148}$ [335]
348	TECH5-002	[292] 0.0017	[314] 0.0023	[311] 0.0028	[307] 0.0034	[312] 0.0044	[23] 0.0000 $N^{0.324}$ [394]	[81] 0.0006	[123] 0.0007	[140] 0.0007	[160] 0.0008	[190] 0.0010	[32] 0.0000 $N^{0.190}$ [359]
349	TECH5-003	[74] 0.0007	[78] 0.0007	[76] 0.0008	[84] 0.0009	[85] 0.0011	[136] 0.0001 $N^{0.161}$ [195]	[89] 0.0006	[80] 0.0006	[73] 0.0006	[74] 0.0006	[65] 0.0006	[248] 0.0005 $N^{0.013}$ [87]
350	TEVIAN-005	[401] 0.0055	[406] 0.0071	[382] 0.0082	[377] 0.0103	[370] 0.0128	[215] 0.0001 $N^{0.285}$ [372]	[386] 0.0019	[384] 0.0022	[364] 0.0025	[355] 0.0027	[345] 0.0033	[83] 0.0002 $N^{0.181}$ [355]
351	TEVIAN-006	[309] 0.0019	[297] 0.0021	[286] 0.0023	[269] 0.0024	[260] 0.0027	[347] 0.0004 $N^{0.123}$ [129]	[321] 0.0012	[309] 0.0013	[292] 0.0013	[283] 0.0014	[274] 0.0014	[295] 0.0006 $N^{0.052}$ [238]
352	TEVIAN-007	[243] 0.0014	[235] 0.0014	[216] 0.0015	[212] 0.0016	[196] 0.0018	[355] 0.0004 $N^{0.090}$ [60]	[219] 0.0009	[219] 0.0009	[212] 0.0009	[204] 0.0010	[198] 0.0010	[281] 0.0006 $N^{0.035}$ [201]
353	TIGER-002	[383] 0.0043	[387] 0.0054	[368] 0.0066	[367] 0.0084	[359] 0.0102	[131] 0.0001 $N^{0.302}$ [388]	[317] 0.0012	[332] 0.0014	[331] 0.0016	[332] 0.0020	[340] 0.0026	[27] 0.0000 $N^{0.256}$ [373]
354	TIGER-004	[310] 0.0019	[310] 0.0022	[296] 0.0024	[283] 0.0027	[277] 0.0031	[295] 0.0002 $N^{0.160}$ [192]	[369] 0.0017	[363] 0.0018	[342] 0.0019	[334] 0.0020	[328] 0.0022	[277] 0.0006 $N^{0.083}$ [291]
355	TOSHIBA-000	[364] 0.0033	[367] 0.0043	[354] 0.0050	[343] 0.0058	[374] 0.0151	[11] 0.0000 $N^{0.462}$ [405]	[344] 0.0014	[353] 0.0016	[332] 0.0017	[331] 0.0019	[392] 0.0103	[9] 0.0000 $N^{0.568}$ [408]
356	TOSHIBA-002	[160] 0.0009	[145] 0.0009	[131] 0.0010	[112] 0.0010	[103] 0.0011	[354] 0.0004 $N^{0.062}$ [21]	[229] 0.0009	[211] 0.0009	[194] 0.0009	[185] 0.0009	[172] 0.0009	[351] 0.0009 $N^{0.002}$ [12]
357	TOSS-000	[168] 0.0010	[158] 0.0010	[145] 0.0010	[135] 0.0011	[114] 0.0012	[392] 0.0004 $N^{0.069}$ [27]	[235] 0.0009	[217] 0.0009	[192] 0.0009	[189] 0.0009	[177] 0.0009	[348] 0.0009 $N^{0.005}$ [36]
358	TRUEFACE-000	[348] 0.0027	[339] 0.0029	[326] 0.0032	[314] 0.0035	[301] 0.0039	[365] 0.0005 $N^{0.128}$ [138]	[400] 0.0022	[388] 0.0022	[358] 0.0023	[349] 0.0024	[338] 0.0024	[373] 0.0012 $N^{0.044}$ [225]
359	UNISSEY-003	[357] 0.0029	[345] 0.0031	[327] 0.0032	[313] 0.0034	[297] 0.0038	[386] 0.0009 $N^{0.083}$ [44]	[417] 0.0026	[402] 0.0026	[366] 0.0026	[354] 0.0027	[343] 0.0027	[394] 0.0022 $N^{0.014}$ [93]
360	USEB-001	[132] 0.0008	[127] 0.0009	[124] 0.0009	[125] 0.0011	[126] 0.0012	[231] 0.0001 $N^{0.132}$ [148]	[158] 0.0007	[149] 0.0007	[137] 0.0007	[125] 0.0007	[120] 0.0007	[305] 0.0007 $N^{0.007}$ [49]

Table 43: **Investigation-mode: Effect of N on FNIR on recent images** *For five enrollment population sizes, N, with T = 0 and FPIR = 1. The left five columns are rank 1 miss rates The right five columns are rank 50 miss rates Missing entries usually apply because another algorithm from the same developer was run instead. Some developers are missing because less accurate algorithms were not run on galleries with N > 1 600 000. Throughout blue superscripts indicate the rank of the algorithm for that column, and yellow highlighting indicates the most accurate value. Caution: The Power-low models are mostly intended to draw attention to the kind of behavior, not as a model to be used for prediction.*

MISSES AT GIVEN RANK FNIR(N, T= 0, R)		ENROL MOST RECENT											
		RANK 1						RANK 50					
#	ALGORITHM	N=0.64M	N=1.6M	N=3.0M	N=6.0M	N=12.0M	aN^b	N=0.64M	N=1.6M	N=3.0M	N=6.0M	N=12.0M	aN^b
361	USEB-002	185 0.0010	175 0.0011	163 0.0011	161 0.0013	153 0.0014	296 0.0002 $N^{0.110}$ 98	232 0.0009	216 0.0009	199 0.0009	187 0.0009	178 0.0009	345 0.0009 $N^{0.006}$ 43
362	USEB-003	128 0.0008	128 0.0009	119 0.0009	116 0.0010	123 0.0012	234 0.0001 $N^{0.129}$ 143	152 0.0007	144 0.0007	141 0.0007	130 0.0007	123 0.0008	280 0.0006 $N^{0.018}$ 122
363	USEB-004	159 0.0009	150 0.0010	137 0.0010	137 0.0011	130 0.0012	307 0.0002 $N^{0.096}$ 74	213 0.0009	200 0.0009	187 0.0009	177 0.0009	165 0.0009	343 0.0008 $N^{0.004}$ 29
364	VD-001	482 0.0227	480 0.0272	417 0.0312	410 0.0360	400 0.0414	394 0.0014 $N^{0.206}$ 280	497 0.0117	490 0.0127	419 0.0137	411 0.0151	401 0.0167	396 0.0022 $N^{0.123}$ 324
365	VDFSOFTWARE-002	245 0.0014	277 0.0018	285 0.0023	295 0.0029	300 0.0038	14 0.0000 $N^{0.358}$ 402	73 0.0005	103 0.0006	128 0.0007	139 0.0008	164 0.0009	39 0.0001 $N^{0.168}$ 349
366	VERIDAS-001	311 0.0019	319 0.0024	313 0.0028	312 0.0034	308 0.0041	90 0.0001 $N^{0.261}$ 344	271 0.0010	277 0.0011	273 0.0012	273 0.0013	275 0.0014	108 0.0002 $N^{0.107}$ 314
367	VERIDAS-002	308 0.0019	318 0.0024	312 0.0028	311 0.0034	307 0.0041	86 0.0001 $N^{0.261}$ 345	266 0.0010	276 0.0011	272 0.0012	272 0.0013	273 0.0014	107 0.0002 $N^{0.108}$ 316
368	VERIDAS-003	232 0.0013	237 0.0015	231 0.0016	229 0.0019	230 0.0022	201 0.0001 $N^{0.181}$ 241	224 0.0009	227 0.0009	217 0.0010	212 0.0010	214 0.0011	208 0.0004 $N^{0.059}$ 255
369	VERIDAS-004	167 0.0010	160 0.0010	147 0.0011	120 0.0011	112 0.0012	360 0.0004 $N^{0.058}$ 16	199 0.0008	195 0.0009	184 0.0009	173 0.0009	162 0.0009	317 0.0007 $N^{0.012}$ 80
370	VERIGRAM-000	324 0.0021	306 0.0022	277 0.0022	288 0.0022	235 0.0023	395 0.0015 $N^{0.025}$ 5	395 0.0021	380 0.0021	352 0.0021	342 0.0021	320 0.0021	392 0.0020 $N^{0.002}$ 14
371	VERIGRAM-001	322 0.0021	304 0.0021	278 0.0022	264 0.0023	237 0.0023	391 0.0012 $N^{0.042}$ 10	394 0.0020	378 0.0020	351 0.0020	338 0.0020	317 0.0020	391 0.0019 $N^{0.003}$ 17
372	VIANTE-000	148 0.0009	138 0.0009	129 0.0009	114 0.0010	108 0.0011	313 0.0003 $N^{0.088}$ 57	198 0.0008	187 0.0008	175 0.0008	170 0.0009	154 0.0009	334 0.0008 $N^{0.005}$ 38
373	VIANTE-001	145 0.0009	133 0.0009	122 0.0009	108 0.0010	89 0.0011	322 0.0003 $N^{0.079}$ 40	197 0.0008	186 0.0008	177 0.0008	166 0.0008	150 0.0008	337 0.0008 $N^{0.003}$ 18
374	VIGILANTSOLUTIONS-008	323 0.0021	327 0.0026	322 0.0031	320 0.0037	311 0.0044	127 0.0001 $N^{0.250}$ 333	180 0.0008	221 0.0009	248 0.0011	260 0.0012	264 0.0013	51 0.0001 $N^{0.175}$ 352
375	VINBIGDATA-001	109 0.0007	126 0.0009	136 0.0010	145 0.0011	154 0.0014	39 0.0000 $N^{0.223}$ 300	57 0.0005	63 0.0005	63 0.0005	61 0.0006	67 0.0006	124 0.0003 $N^{0.043}$ 223
376	VINBIGDATA-002	40 0.0006	44 0.0006	44 0.0006	44 0.0008	61 0.0009	58 0.0000 $N^{0.183}$ 246	38 0.0005	35 0.0005	40 0.0005	30 0.0005	29 0.0005	198 0.0004 $N^{0.015}$ 105
377	VINBIGDATA-003	34 0.0005	34 0.0006	47 0.0007	43 0.0008	54 0.0009	49 0.0000 $N^{0.190}$ 260	44 0.0005	43 0.0005	44 0.0005	42 0.0005	35 0.0005	191 0.0004 $N^{0.016}$ 114
378	VINBIGDATA-004	42 0.0006	36 0.0006	38 0.0006	37 0.0007	37 0.0008	129 0.0001 $N^{0.146}$ 171	40 0.0005	31 0.0005	26 0.0005	36 0.0005	40 0.0005	169 0.0004 $N^{0.020}$ 130
379	VISIONBOX-000	248 0.0014	254 0.0016	255 0.0018	494 1.0000	414 0.9526	1 0.0000 $N^{2.661}$ 415	215 0.0009	214 0.0009	219 0.0010	423 1.0000	414 0.9525	1 0.0000 $N^{2.857}$ 416
380	VISIONBOX-001	338 0.0025	328 0.0026	310 0.0027	299 0.0030	280 0.0033	377 0.0007 $N^{0.094}$ 66	404 0.0023	393 0.0023	359 0.0023	348 0.0023	332 0.0024	390 0.0019 $N^{0.015}$ 107
381	VISIONBOX-002	246 0.0014	238 0.0015	228 0.0016	223 0.0018	222 0.0021	276 0.0002 $N^{0.142}$ 166	302 0.0011	296 0.0012	282 0.0012	266 0.0012	252 0.0012	324 0.0008 $N^{0.031}$ 184
382	VISIONLABS-004	321 0.0021	329 0.0026	323 0.0031	328 0.0043	336 0.0068	12 0.0000 $N^{0.395}$ 404	314 0.0012	318 0.0013	329 0.0016	351 0.0024	362 0.0044	13 0.0000 $N^{0.440}$ 403
383	VISIONLABS-005	306 0.0019	311 0.0023	309 0.0027	315 0.0035	319 0.0049	22 0.0000 $N^{0.328}$ 397	308 0.0012	300 0.0013	318 0.0015	327 0.0019	344 0.0029	18 0.0000 $N^{0.303}$ 391
384	VISIONLABS-006	277 0.0015	276 0.0018	271 0.0021	288 0.0027	302 0.0040	19 0.0000 $N^{0.324}$ 395	305 0.0011	298 0.0012	307 0.0014	324 0.0018	341 0.0026	21 0.0000 $N^{0.281}$ 385
385	VISIONLABS-007	272 0.0015	274 0.0017	263 0.0019	261 0.0023	281 0.0033	60 0.0000 $N^{0.256}$ 339	299 0.0011	291 0.0012	281 0.0012	274 0.0013	310 0.0019	71 0.0001 $N^{0.156}$ 341
386	VISIONLABS-008	270 0.0015	263 0.0016	245 0.0018	255 0.0022	254 0.0027	179 0.0001 $N^{0.199}$ 270	328 0.0013	320 0.0013	300 0.0014	309 0.0016	313 0.0020	93 0.0002 $N^{0.140}$ 334
387	VISIONLABS-009	106 0.0007	104 0.0008	104 0.0009	122 0.0011	151 0.0014	37 0.0000 $N^{0.219}$ 296	118 0.0006	118 0.0006	125 0.0007	141 0.0008	203 0.0010	47 0.0001 $N^{0.158}$ 343
388	VISIONLABS-010	178 0.0010	171 0.0010	171 0.0012	175 0.0013	189 0.0017	170 0.0001 $N^{0.176}$ 226	223 0.0009	208 0.0009	221 0.0010	226 0.0011	260 0.0013	85 0.0002 $N^{0.121}$ 323
389	VISIONLABS-011	112 0.0008	116 0.0008	116 0.0009	130 0.0011	160 0.0015	40 0.0000 $N^{0.219}$ 298	143 0.0007	141 0.0007	151 0.0008	164 0.0008	229 0.0011	50 0.0001 $N^{0.162}$ 346
390	VISTEAM-000	367 0.0034	379 0.0048	363 0.0060	360 0.0077	356 0.0097	28 0.0000 $N^{0.361}$ 403	168 0.0008	245 0.0010	285 0.0012	292 0.0014	298 0.0018	15 0.0000 $N^{0.288}$ 388
391	VIXVIZION-009	282 0.0016	290 0.0019	284 0.0023	291 0.0028	282 0.0033	66 0.0000 $N^{0.262}$ 346	148 0.0007	185 0.0008	202 0.0009	211 0.0010	219 0.0011	63 0.0001 $N^{0.148}$ 336
392	VNPAY-001	192 0.0011	180 0.0011	175 0.0012	170 0.0013	161 0.0015	281 0.0002 $N^{0.118}$ 113	222 0.0009	213 0.0009	203 0.0009	203 0.0010	192 0.0010	291 0.0006 $N^{0.030}$ 178
393	VNPT-001	295 0.0017	280 0.0018	265 0.0019	249 0.0021	240 0.0024	335 0.0003 $N^{0.119}$ 115	340 0.0014	334 0.0014	311 0.0015	295 0.0015	278 0.0015	365 0.0010 $N^{0.022}$ 141
394	VNPT-002	265 0.0015	246 0.0015	229 0.0016	221 0.0017	210 0.0019	363 0.0005 $N^{0.087}$ 54	336 0.0014	323 0.0014	301 0.0014	287 0.0014	272 0.0014	371 0.0012 $N^{0.012}$ 79
395	VNPT-003	223 0.0012	206 0.0013	202 0.0014	188 0.0015	183 0.0016	331 0.0003 $N^{0.100}$ 77	297 0.0011	281 0.0011	267 0.0011	249 0.0011	239 0.0012	354 0.0009 $N^{0.015}$ 106
396	VNPT-004	224 0.0012	208 0.0013	194 0.0013	182 0.0014	181 0.0016	338 0.0003 $N^{0.092}$ 63	296 0.0011	284 0.0011	269 0.0011	250 0.0011	235 0.0012	361 0.0010 $N^{0.011}$ 76
397	VNPT-005	221 0.0012	210 0.0013	193 0.0013	178 0.0014	172 0.0016	358 0.0004 $N^{0.077}$ 35	293 0.0011	278 0.0011	264 0.0011	245 0.0011	231 0.0011	355 0.0009 $N^{0.014}$ 92
398	VOCORD-005	402 0.0057	402 0.0068	378 0.0079	374 0.0095	364 0.0114	299 0.0002 $N^{0.238}$ 319	427 0.0031	422 0.0033	383 0.0034	369 0.0038	360 0.0041	352 0.0009 $N^{0.092}$ 304
399	VTCC-000	380 0.0040	365 0.0041	345 0.0042	329 0.0043	316 0.0045	399 0.0024 $N^{0.039}$ 9	437 0.0038	428 0.0038	386 0.0038	370 0.0039	356 0.0039	401 0.0031 $N^{0.013}$ 91
400	VTCC-001	287 0.0016	273 0.0017	246 0.0018	233 0.0019	226 0.0021	364 0.0005 $N^{0.093}$ 64	348 0.0015	339 0.0015	315 0.0015	298 0.0015	285 0.0015	376 0.0013 $N^{0.012}$ 82
401	VTCC-002	286 0.0016	268 0.0017	247 0.0018	232 0.0019	225 0.0021	361 0.0004 $N^{0.094}$ 67	347 0.0015	338 0.0015	316 0.0015	299 0.0015	284 0.0015	377 0.0013 $N^{0.012}$ 83
402	VTS-001	176 0.0010	197 0.0012	199 0.0013	207 0.0016	213 0.0019	67 0.0000 $N^{0.226}$ 303	121 0.0006	121 0.0007	126 0.0007	124 0.0007	132 0.0008	100 0.0002 $N^{0.077}$ 283
403	VTS-002	236 0.0013	255 0.0016	259 0.0019	262 0.0023	263 0.0028	51 0.0000 $N^{0.256}$ 338	151 0.0007	160 0.0008	173 0.0008	182 0.0009	196 0.0010	79 0.0002 $N^{0.113}$ 318
404	VTS-003	99 0.0007	108 0.0008	100 0.0009	107 0.0010	119 0.0012	115 0.0001 $N^{0.173}$ 218	65 0.0005	62 0.0005	63 0.0005	63 0.0006	71 0.0006	122 0.0003 $N^{0.043}$ 220
405	VTS-004	57 0.0006	61 0.0006	65 0.0007	63 0.0008	64 0.0010	91 0.0001 $N^{0.170}$ 207	30 0.0005	36 0.0005	41 0.0005	46 0.0005	43 0.0005	117 0.0003 $N^{0.041}$ 213
406	VTS-005	46 0.0006	51 0.0006	58 0.0007	59 0.0008	60 0.0009	69 0.0001 $N^{0.177}$ 231	43 0.0005	29 0.0005	28 0.0005	31 0.0005	28 0.0005	195 0.0004 $N^{0.015}$ 103
407	WINK-001	317 0.0021	324 0.0026	316 0.0030	316 0.0035	309 0.0043	130 0.0001 $N^{0.249}$ 331	282 0.0011	288 0.0011	283 0.0012	277 0.0013	279 0.0015	102 0.0002 $N^{0.114}$ 320
408	WINK-002	138 0.0008	152 0.0010	166 0.0011	173 0.0013	184 0.0016	45 0.0000 $N^{0.227}$ 305	72 0.0005	83 0.0006	89 0.0006	87 0.0006	97 0.0007	97 0.0002 $N^{0.069}$ 277
409	XFORWARDAI-000	301 0.0018	291 0.0019	269 0.0020	266 0.0023	251 0.0026	326 0.0003 $N^{0.130}$ 144	357 0.0016	347 0.0016	324 0.0016	310 0.0016	293 0.0017	368 0.0011 $N^{0.022}$ 142
410	XFORWARDAI-001	291 0.0017	272 0.0017	241 0.0017	227 0.0018	214 0.0020	373 0.0007 $N^{0.066}$ 25	356 0.0015	346 0.0015	323 0.0015	301 0.0015	287 0.0016	386 0.0014 $N^{0.005}$ 34
411	XFORWARDAI-002	284 0.0016	258 0.0016	236 0.0017	219 0.0017	200 0.0018	382 0.0008 $N^{0.047}$ 13	352 0.0015	344 0.0015	319 0.0015	300 0.0015	281 0.0015	385 0.0014 $N^{0.004}$ 31
412	YITU-002	229 0.0013	245 0.0015	252 0.0018	250 0.0021	252 0.0026	61 0.0000 $N^{0.247}$ 330	139 0.0007	147 0.0007	155 0.0008	152 0.0008	166 0.0009	94 0.0002 $N^{0.095}$ 306
413	YITU-003	331 0.0023	325 0.0026	314 0.0028	301 0.0031	293 0.0036	320 0.0003 $N^{0.154}$ 184	375 0.0018	364 0.0018	343 0.0019	333 0.0020	323 0.0021	336 0.0008 $N^{0.059}$ 254
414	YITU-004	141 0.0009	164 0.0010	186 0.0012	184 0.0015	314 0.0044	9 0.0000 $N^{0.500}$ 407	113 0.0006	108 0.0006	103 0.0006	95 0.0006	349 0.0033	10 0.0000 $N^{0.470}$ 404
415	YITU-005	313 0.0019	302 0.0021	282 0.0022	271 0.0024	261 0.0028	353 0.0004 $N^{0.120}$ 121	371 0.0017	358 0.0017	336 0.0017	321 0.0017	300 0.0018	384 0.0014 $N^{0.014}$ 99
416	YUAN-000	244 0.0014	224 0.0014	212 0.0014	200 0.0015	418 1.0000	3 0.0000 $N^{1.807}$ 414	332 0.0013	319 0.0013	293 0.0013	279 0.0013	415 1.0000	3 0.0000 $N^{1.793}$ 414

Table 44: **Investigation-mode: Effect of N on FNIR on recent images** *For five enrollment population sizes, N, with T = 0 and FPIR = 1. The left five columns are rank 1 miss rates The right five columns are rank 50 miss rates Missing entries usually apply because another algorithm from the same developer was run instead. Some developers are missing because less accurate algorithms were not run on galleries with $N > 1\,600\,000$. Throughout blue superscripts indicate the rank of the algorithm for that column, and yellow highlighting indicates the most accurate value. Caution: The Power-low models are mostly intended to draw attention to the kind of behavior, not as a model to be used for prediction.*

This publication is available free of charge from: https://doi.org/10.6028/NIST.IR.8271

This publication is available free of charge from: https://doi.org/10.6028/NIST.IR.8271

MISSES OUTSIDE RANK R		RESOURCE USAGE		ENROL MOST RECENT, N = 1.6M					
FNIR(N, T=0, R)		TEMPLATE		FRVT 2018 MUGSHOTS					
#	ALGORITHM	BYTES	MSEC	R=1	R=5	R=10	R=20	R=50	WORK-10
1	20FACE-000	555 -	555 -	500 0.0549	493 0.0265	490 0.0194	486 0.0143	477 0.0095	495 1.272
2	3DIVI-003	555 -	555 -	510 0.0830	504 0.0441	504 0.0346	500 0.0267	499 0.0188	506 1.444
3	3DIVI-004	555 -	555 -	460 0.0172	449 0.0088	446 0.0072	441 0.0058	436 0.0046	454 1.089
4	3DIVI-005	555 -	555 -	461 0.0173	450 0.0088	445 0.0071	439 0.0058	437 0.0046	455 1.090
5	3DIVI-006	555 -	555 -	472 0.0237	480 0.0168	486 0.0157	488 0.0151	495 0.0145	478 1.160
6	AADI-000	555 -	555 -	551 0.9991	551 0.9987	551 0.9984	551 0.9979	551 0.9969	551 9.988
7	AADI-001	555 -	555 -	547 0.7887	547 0.7331	547 0.7098	548 0.6856	548 0.6528	547 7.655
8	AADI-002	555 -	555 -	546 0.6994	546 0.6287	546 0.5993	544 0.5688	545 0.5255	546 6.734
9	ACER-000	555 -	555 -	434 0.0102	412 0.0048	406 0.0037	401 0.0030	389 0.0022	414 1.050
10	ACER-001	555 -	555 -	378 0.0047	380 0.0029	376 0.0024	372 0.0021	366 0.0019	376 1.028
11	ADIANCE-001	555 -	555 -	555 1.0000	553 1.0000	555 1.0000	554 1.0000	552 1.0000	553 10.000
12	ADVANCE-000	555 -	555 -	259 0.0016	269 0.0013	270 0.0012	266 0.0011	266 0.0011	262 1.012
13	AFISBIOMETRICS-000	555 -	555 -	205 0.0012	126 0.0008	106 0.0007	104 0.0006	77 0.0006	144 1.007
14	AFRENGINE-000	555 -	555 -	337 0.0029	326 0.0019	325 0.0017	330 0.0015	327 0.0014	328 1.018
15	AFRENGINE-001	555 -	555 -	219 0.0013	266 0.0013	279 0.0013	290 0.0013	301 0.0013	254 1.012
16	AFRENGINE-002	555 -	555 -	220 0.0013	264 0.0013	278 0.0013	291 0.0013	304 0.0013	253 1.012
17	AFRENGINE-003	555 -	555 -	316 0.0023	351 0.0022	363 0.0022	374 0.0022	385 0.0022	344 1.020
18	AIZE-001	555 -	555 -	384 0.0053	384 0.0033	389 0.0030	390 0.0027	395 0.0023	384 1.032
19	AIZE-002	555 -	555 -	346 0.0031	330 0.0019	332 0.0017	333 0.0016	336 0.0014	333 1.019
20	AKUVOX-001	555 -	555 -	226 0.0014	236 0.0012	244 0.0011	251 0.0011	263 0.0011	230 1.011
21	ALCHERA-000	555 -	555 -	456 0.0159	465 0.0122	470 0.0114	475 0.0108	481 0.0102	464 1.114
22	ALCHERA-001	555 -	555 -	550 0.9869	550 0.9782	550 0.9735	550 0.9679	549 0.9589	550 9.811
23	ALCHERA-002	555 -	555 -	512 0.0946	510 0.0552	508 0.0440	507 0.0351	503 0.0251	510 1.542
24	ALCHERA-003	555 -	555 -	433 0.0102	418 0.0051	417 0.0043	415 0.0036	414 0.0030	420 1.053
25	ALCHERA-004	555 -	555 -	438 0.0106	410 0.0045	401 0.0035	394 0.0028	386 0.0022	412 1.048
26	ALCHERA-005	555 -	555 -	405 0.0070	381 0.0030	372 0.0023	359 0.0019	342 0.0015	383 1.032
27	ALCHERA-006	555 -	555 -	135 0.0009	139 0.0008	145 0.0008	150 0.0008	152 0.0007	137 1.007
28	ALCHERA-007	555 -	555 -	129 0.0009	128 0.0008	133 0.0007	132 0.0007	148 0.0007	128 1.007
29	ALCHERA-008	555 -	555 -	153 0.0010	174 0.0009	184 0.0009	191 0.0009	203 0.0009	167 1.008
30	ALGORITHMSINC-000	555 -	555 -	251 0.0016	276 0.0013	288 0.0013	299 0.0013	315 0.0013	272 1.012
31	ALLGOVISION-000	555 -	555 -	440 0.0111	443 0.0080	449 0.0074	450 0.0069	456 0.0064	443 1.076
32	ALLGOVISION-001	555 -	555 -	419 0.0086	408 0.0045	404 0.0036	400 0.0030	396 0.0023	407 1.045
33	ALLGOVISION-002	555 -	555 -	357 0.0037	352 0.0022	340 0.0018	335 0.0016	317 0.0013	351 1.022
34	ALLGOVISION-003	555 -	555 -	278 0.0018	272 0.0013	272 0.0012	285 0.0012	289 0.0011	275 1.012
35	ALLGOVISION-004	555 -	555 -	430 0.0101	407 0.0044	392 0.0033	382 0.0025	371 0.0019	411 1.046
36	ALTTEKGLOBAL-000	555 -	555 -	533 0.2740	536 0.2740	539 0.2740	540 0.2740	542 0.2740	536 3.466
37	ANKE-000	555 -	555 -	451 0.0129	434 0.0070	428 0.0057	429 0.0047	427 0.0037	439 1.070
38	ANKE-001	555 -	555 -	452 0.0129	435 0.0070	430 0.0058	430 0.0047	426 0.0037	440 1.070
39	ANKE-002	555 -	555 -	321 0.0024	314 0.0016	310 0.0015	314 0.0014	310 0.0013	315 1.016
40	ANTHEUS-000	555 -	555 -	404 0.0069	426 0.0060	433 0.0059	440 0.0058	450 0.0057	421 1.055
41	ARATEK-001	555 -	555 -	100 0.0008	95 0.0007	94 0.0006	95 0.0006	97 0.0006	98 1.006
42	ARMATURA-000	555 -	555 -	244 0.0015	296 0.0015	309 0.0015	322 0.0015	337 0.0015	293 1.013
43	AWARE-003	555 -	555 -	483 0.0303	478 0.0158	475 0.0124	470 0.0097	465 0.0072	479 1.160
44	AWARE-004	555 -	555 -	505 0.0676	501 0.0345	498 0.0271	496 0.0205	494 0.0142	501 1.351
45	AWARE-005	555 -	555 -	484 0.0308	479 0.0164	477 0.0130	472 0.0104	470 0.0079	481 1.164
46	AWARE-006	555 -	555 -	507 0.0694	503 0.0366	499 0.0284	498 0.0220	496 0.0155	503 1.368
47	AWARE-007	555 -	555 -	303 0.0021	258 0.0012	235 0.0011	213 0.0010	189 0.0009	270 1.012
48	AWIROS-000	555 -	555 -	408 0.0073	413 0.0048	418 0.0044	425 0.0041	430 0.0039	409 1.046
49	AYONIX-000	555 -	555 -	540 0.4503	541 0.3538	541 0.3174	541 0.2831	540 0.2379	541 4.286
50	AYONIX-001	555 -	555 -	534 0.3412	533 0.2335	531 0.1974	528 0.1649	528 0.1271	533 3.223
51	AYONIX-002	555 -	555 -	535 0.3412	534 0.2336	532 0.1975	527 0.1649	529 0.1271	534 3.224
52	BIOIDTECHSWISS-001	555 -	555 -	107 0.0008	117 0.0007	120 0.0007	113 0.0007	114 0.0006	111 1.006
53	BIOMETRIK-001	555 -	555 -	370 0.0044	354 0.0023	349 0.0019	341 0.0016	328 0.0014	358 1.023
54	CAMVI-003	555 -	555 -	499 0.0517	509 0.0514	510 0.0514	513 0.0514	514 0.0514	508 1.463
55	CAMVI-004	555 -	555 -	497 0.0466	507 0.0463	509 0.0463	510 0.0462	513 0.0462	504 1.417
56	CAMVI-005	555 -	555 -	504 0.0650	511 0.0646	515 0.0646	516 0.0645	519 0.0645	511 1.582
57	CANON-001	555 -	555 -	80 0.0007	89 0.0006	84 0.0006	80 0.0006	74 0.0006	87 1.006
58	CANON-002	555 -	555 -	111 0.0008	85 0.0006	78 0.0006	70 0.0006	71 0.0006	83 1.006
59	CANON-003	555 -	555 -	37 0.0006	32 0.0005	24 0.0005	25 0.0005	27 0.0005	33 1.005
60	CIB-000	555 -	555 -	196 0.0012	193 0.0010	180 0.0009	175 0.0008	172 0.0008	193 1.009
61	CLEARVIEWAI-000	555 -	555 -	82 0.0007	86 0.0006	88 0.0006	77 0.0006	72 0.0006	86 1.006
62	CLEARVIEWAI-001	555 -	555 -	83 0.0007	101 0.0007	111 0.0007	120 0.0007	122 0.0007	105 1.006
63	CLEARVIEWAI-002	555 -	555 -	93 0.0008	105 0.0007	112 0.0007	115 0.0007	129 0.0007	106 1.006
64	CLEARVIEWAI-003	555 -	555 -	90 0.0008	104 0.0007	109 0.0007	112 0.0007	124 0.0007	104 1.006
65	CLOUDWALK-HR-000	555 -	555 -	186 0.0011	227 0.0011	236 0.0011	245 0.0011	255 0.0010	219 1.010
66	CLOUDWALK-MT-000	555 -	555 -	231 0.0014	288 0.0014	298 0.0014	311 0.0014	329 0.0014	281 1.013
67	CLOUDWALK-MT-001	555 -	555 -	229 0.0014	290 0.0014	294 0.0014	310 0.0014	326 0.0014	279 1.013
68	CLOUDWALK-MT-002	555 -	555 -	230 0.0014	289 0.0014	296 0.0014	312 0.0014	325 0.0014	280 1.013
69	COGENT-000	555 -	555 -	431 0.0101	456 0.0093	459 0.0092	396 0.0028	382 0.0021	450 1.085
70	COGENT-001	555 -	555 -	432 0.0101	455 0.0093	460 0.0092	395 0.0028	381 0.0021	449 1.085
71	COGENT-002	555 -	555 -	349 0.0033	331 0.0019	327 0.0017	321 0.0015	302 0.0013	332 1.019
72	COGENT-003	555 -	555 -	351 0.0035	344 0.0021	336 0.0018	336 0.0016	324 0.0014	348 1.020

Table 45: **Rank-based accuracy for the FRVT 2018 mugshot sets**. *In columns 3 and 4 are template size and template generation duration. Thereafter values are rank-based FNIR with T = 0 and FPIR = 1. This is appropriate to investigational uses but not those with higher volumes where candidates from all searches would need review. The next column is a workload statistic, a small value shows an algorithm front-loads mates into the first 10 candidates. Throughout, blue superscripts indicate the rank of the algorithm for that column, and the best value is highlighted in yellow.*

This publication is available free of charge from: https://doi.org/10.6028/NIST.IR.8271

MISSES OUTSIDE RANK R		RESOURCE USAGE		ENROL MOST RECENT, N = 1.6M					
FNIR(N, T=0, R)		TEMPLATE		FRVT 2018 MUGSHOTS					
#	ALGORITHM	BYTES	MSEC	R=1	R=5	R=10	R=20	R=50	WORK-10
73	COGENT-004	555 -	555 -	260 0.0016	253 0.0012	248 0.0011	256 0.0011	252 0.0010	250 1.011
74	COGENT-005	555 -	555 -	216 0.0013	221 0.0011	220 0.0010	231 0.0010	241 0.0010	220 1.010
75	COGENT-006	555 -	555 -	132 0.0009	138 0.0008	134 0.0007	145 0.0007	154 0.0007	132 1.007
76	COGENT-007	555 -	555 -	85 0.0007	90 0.0006	95 0.0006	99 0.0006	100 0.0006	94 1.006
77	COGNITEC-000	555 -	555 -	474 0.0249	471 0.0133	467 0.0104	462 0.0082	454 0.0062	472 1.133
78	COGNITEC-001	555 -	555 -	442 0.0114	424 0.0058	423 0.0047	424 0.0039	416 0.0031	425 1.059
79	COGNITEC-002	555 -	555 -	386 0.0053	385 0.0033	383 0.0028	383 0.0026	394 0.0023	385 1.032
80	COGNITEC-003	555 -	555 -	390 0.0059	392 0.0037	393 0.0033	402 0.0030	406 0.0028	394 1.036
81	COGNITEC-004	555 -	555 -	336 0.0028	316 0.0017	300 0.0014	276 0.0012	259 0.0010	320 1.016
82	COGNITEC-005	555 -	555 -	213 0.0013	179 0.0009	174 0.0009	164 0.0008	163 0.0008	184 1.009
83	COGNITEC-006	555 -	555 -	200 0.0012	173 0.0009	166 0.0008	162 0.0008	161 0.0008	174 1.008
84	COGNITEC-007	555 -	555 -	168 0.0010	131 0.0008	129 0.0007	129 0.0007	125 0.0007	139 1.007
85	COGNITEC-008	555 -	555 -	154 0.0010	115 0.0007	108 0.0007	111 0.0007	112 0.0006	121 1.007
86	COGNITEC-009	555 -	555 -	192 0.0012	175 0.0009	175 0.0009	174 0.0008	177 0.0008	175 1.008
87	COMPAL-000	555 -	555 -	228 0.0014	252 0.0012	266 0.0012	274 0.0012	285 0.0011	246 1.011
88	COMPAL-001	555 -	555 -	401 0.0067	432 0.0066	439 0.0066	446 0.0065	459 0.0065	427 1.059
89	CORSIGHT-000	555 -	555 -	89 0.0008	88 0.0006	93 0.0006	98 0.0006	111 0.0006	89 1.006
90	CORSIGHT-001	555 -	555 -	94 0.0008	98 0.0007	107 0.0007	105 0.0006	107 0.0006	102 1.006
91	CUBOX-000	555 -	555 -	173 0.0011	211 0.0010	221 0.0010	233 0.0010	243 0.0010	203 1.009
92	CUBOX-001	555 -	555 -	137 0.0009	154 0.0008	159 0.0008	169 0.0008	176 0.0008	151 1.008
93	CUBOX-002	555 -	555 -	189 0.0011	218 0.0011	234 0.0011	246 0.0011	261 0.0011	215 1.010
94	CUBOX-003	555 -	555 -	202 0.0012	241 0.0012	258 0.0012	272 0.0011	280 0.0011	232 1.011
95	CYBERLINK-000	555 -	555 -	353 0.0036	363 0.0024	367 0.0022	371 0.0021	367 0.0019	362 1.023
96	CYBERLINK-001	555 -	555 -	347 0.0032	335 0.0020	329 0.0017	320 0.0015	321 0.0013	339 1.019
97	CYBERLINK-002	555 -	555 -	312 0.0023	332 0.0019	342 0.0019	349 0.0018	357 0.0017	327 1.018
98	CYBERLINK-003	555 -	555 -	201 0.0012	195 0.0010	189 0.0009	176 0.0008	168 0.0008	196 1.009
99	CYBERLINK-004	555 -	555 -	215 0.0013	234 0.0011	247 0.0011	249 0.0011	262 0.0011	228 1.011
100	CYBERLINK-005	555 -	555 -	236 0.0015	254 0.0012	260 0.0012	263 0.0011	267 0.0011	247 1.011
101	CYBERLINK-006	555 -	555 -	103 0.0008	124 0.0007	116 0.0007	118 0.0007	130 0.0007	116 1.007
102	DAHUA-000	555 -	555 -	424 0.0091	429 0.0064	432 0.0059	437 0.0056	444 0.0052	430 1.061
103	DAHUA-001	555 -	555 -	396 0.0064	395 0.0039	400 0.0034	405 0.0031	407 0.0028	397 1.038
104	DAHUA-002	555 -	555 -	239 0.0015	230 0.0011	239 0.0011	238 0.0010	239 0.0010	237 1.011
105	DAHUA-003	555 -	555 -	120 0.0008	70 0.0006	66 0.0006	59 0.0005	54 0.0005	81 1.006
106	DAHUA-004	555 -	555 -	77 0.0007	74 0.0006	71 0.0006	67 0.0006	69 0.0005	73 1.006
107	DAON-000	555 -	555 -	356 0.0037	382 0.0034	396 0.0033	408 0.0033	421 0.0033	382 1.031
108	DAON-001	555 -	555 -	475 0.0252	491 0.0249	496 0.0249	499 0.0248	502 0.0248	491 1.225
109	DAON-002	555 -	555 -	142 0.0009	111 0.0007	110 0.0007	109 0.0006	109 0.0006	119 1.007
110	DATECH-000	555 -	555 -	155 0.0010	130 0.0008	135 0.0007	140 0.0007	145 0.0007	136 1.007
111	DATECH-001	555 -	555 -	91 0.0008	93 0.0006	89 0.0006	88 0.0006	91 0.0006	90 1.006
112	DECATUR-000	555 -	555 -	275 0.0017	255 0.0012	251 0.0011	243 0.0011	231 0.0009	261 1.012
113	DEEPGLINT-001	555 -	555 -	181 0.0011	208 0.0010	207 0.0010	214 0.0010	223 0.0009	202 1.009
114	DEEPSEA-001	555 -	555 -	361 0.0040	327 0.0019	306 0.0015	286 0.0012	249 0.0010	340 1.019
115	DERMALOG-003	555 -	555 -	517 0.1256	515 0.0741	513 0.0600	512 0.0477	511 0.0345	515 1.729
116	DERMALOG-004	555 -	555 -	516 0.1248	514 0.0737	512 0.0595	511 0.0473	510 0.0341	514 1.725
117	DERMALOG-005	555 -	555 -	455 0.0147	468 0.0127	474 0.0123	480 0.0121	489 0.0120	465 1.116
118	DERMALOG-006	555 -	555 -	414 0.0079	433 0.0067	437 0.0064	443 0.0063	453 0.0062	432 1.062
119	DERMALOG-007	555 -	555 -	421 0.0089	428 0.0063	427 0.0057	435 0.0054	441 0.0050	426 1.059
120	DERMALOG-008	555 -	555 -	323 0.0025	313 0.0016	305 0.0014	295 0.0013	290 0.0012	314 1.016
121	DERMALOG-009	555 -	555 -	322 0.0024	341 0.0020	350 0.0020	357 0.0019	368 0.0019	338 1.019
122	DERMALOG-010	555 -	555 -	283 0.0018	320 0.0017	328 0.0017	343 0.0017	355 0.0017	313 1.016
123	DERMALOG-011	555 -	555 -	204 0.0012	164 0.0009	156 0.0008	152 0.0008	145 0.0007	164 1.008
124	DERMALOG-012	555 -	555 -	270 0.0017	259 0.0012	268 0.0012	269 0.0011	279 0.0011	259 1.012
125	DERMALOG-013	555 -	555 -	252 0.0016	238 0.0012	242 0.0011	240 0.0010	251 0.0010	239 1.011
126	DERMALOG-014	555 -	555 -	343 0.0030	373 0.0027	379 0.0026	389 0.0026	401 0.0026	368 1.025
127	DERMALOG-015	555 -	555 -	203 0.0012	216 0.0011	230 0.0011	237 0.0010	254 0.0010	217 1.010
128	DIGIDATA-000	555 -	555 -	543 0.5896	544 0.5890	544 0.5889	545 0.5889	546 0.5889	544 6.302
129	DILUSENSE-000	555 -	555 -	285 0.0018	249 0.0012	229 0.0011	225 0.0010	204 0.0009	251 1.011
130	DILUSENSE-001	555 -	555 -	182 0.0011	169 0.0009	164 0.0008	170 0.0008	166 0.0008	168 1.008
131	EINETWORKSINDIA-000	555 -	555 -	234 0.0014	232 0.0011	245 0.0011	254 0.0011	265 0.0011	234 1.011
132	EINETWORKSINDIA-001	555 -	555 -	222 0.0014	219 0.0011	226 0.0010	230 0.0010	237 0.0010	224 1.010
133	EINETWORKSINDIA-002	555 -	555 -	101 0.0008	106 0.0007	101 0.0006	108 0.0006	117 0.0006	101 1.006
134	EYEDEA-003	555 -	555 -	509 0.0797	505 0.0447	505 0.0359	501 0.0286	501 0.0208	507 1.445
135	F8-001	555 -	555 -	446 0.0116	458 0.0101	463 0.0099	469 0.0097	476 0.0095	457 1.093
136	FACEPHI-000	555 -	555 -	242 0.0015	291 0.0014	297 0.0014	306 0.0014	322 0.0014	286 1.013
137	FASTLAHORE-000	555 -	555 -	478 0.0261	484 0.0178	483 0.0155	484 0.0138	486 0.0115	483 1.169
138	FCI-000	555 -	555 -	241 0.0015	280 0.0013	284 0.0013	294 0.0013	305 0.0013	274 1.012
139	FINCORE-000	555 -	555 -	437 0.0105	415 0.0049	409 0.0038	403 0.0030	392 0.0023	416 1.051
140	FIRSTCREDITKZ-001	555 -	555 -	123 0.0008	152 0.0008	157 0.0008	167 0.0008	174 0.0008	147 1.007
141	FPT-000	555 -	555 -	250 0.0016	285 0.0014	293 0.0014	302 0.0013	313 0.0013	285 1.013
142	FUJITSULAB-000	555 -	555 -	286 0.0018	268 0.0013	262 0.0012	253 0.0011	246 0.0010	268 1.012
143	FUJITSULAB-001	555 -	555 -	243 0.0015	244 0.0012	253 0.0011	242 0.0011	250 0.0010	242 1.011
144	GLORY-000	555 -	555 -	521 0.1778	523 0.1388	523 0.1263	523 0.1151	524 0.1004	522 2.295

Table 46: **Rank-based accuracy for the FRVT 2018 mugshot sets**. *In columns 3 and 4 are template size and template generation duration. Thereafter values are rank-based FNIR with T = 0 and FPIR = 1. This is appropriate to investigational uses but not those with higher volumes where candidates from all searches would need review. The next column is a workload statistic, a small value shows an algorithm front-loads mates into the first 10 candidates. Throughout, blue superscripts indicate the rank of the algorithm for that column, and the best value is highlighted in yellow.*

This publication is available free of charge from: https://doi.org/10.6028/NIST.IR.8271

MISSES OUTSIDE RANK R		RESOURCE USAGE		ENROL MOST RECENT, N = 1.6M					
FNIR(N, T=0, R)		TEMPLATE		FRVT 2018 MUGSHOTS					
#	ALGORITHM	BYTES	MSEC	R=1	R=5	R=10	R=20	R=50	WORK-10
145	GLORY-001	555 -	555 -	518 0.1265	518 0.0964	518 0.0866	519 0.0775	520 0.0670	518 1.900
146	GORILLA-001	555 -	555 -	501 0.0600	496 0.0300	494 0.0227	492 0.0171	485 0.0114	496 1.306
147	GORILLA-002	555 -	555 -	467 0.0194	451 0.0090	440 0.0068	433 0.0052	432 0.0039	458 1.094
148	GORILLA-003	555 -	555 -	487 0.0359	474 0.0144	466 0.0103	458 0.0076	443 0.0052	476 1.156
149	GORILLA-004	555 -	555 -	391 0.0059	379 0.0028	370 0.0023	358 0.0019	335 0.0014	381 1.030
150	GORILLA-005	555 -	555 -	335 0.0028	298 0.0015	285 0.0013	259 0.0011	222 0.0009	310 1.015
151	GORILLA-006	555 -	555 -	227 0.0014	167 0.0009	165 0.0008	160 0.0008	155 0.0007	191 1.009
152	GORILLA-007	555 -	555 -	218 0.0013	160 0.0009	153 0.0008	139 0.0007	140 0.0007	172 1.008
153	GORILLA-008	555 -	555 -	188 0.0011	147 0.0008	140 0.0008	133 0.0007	139 0.0007	153 1.008
154	GRIAULE-000	555 -	555 -	305 0.0021	310 0.0016	314 0.0015	315 0.0014	309 0.0013	307 1.015
155	GRIAULE-001	555 -	555 -	117 0.0008	120 0.0007	123 0.0007	125 0.0007	134 0.0007	118 1.007
156	GTELOTS-000	555 -	555 -	525 0.1940	529 0.1938	530 0.1938	533 0.1938	537 0.1938	529 2.745
157	HIK-003	555 -	555 -	443 0.0115	423 0.0058	421 0.0046	419 0.0038	412 0.0029	428 1.059
158	HIK-004	555 -	555 -	441 0.0111	422 0.0057	420 0.0045	412 0.0035	408 0.0028	423 1.058
159	HIK-005	555 -	555 -	369 0.0044	358 0.0024	347 0.0019	338 0.0016	331 0.0014	361 1.023
160	HIK-006	555 -	555 -	368 0.0044	359 0.0024	346 0.0019	337 0.0016	330 0.0014	360 1.023
161	HISIGN-001	555 -	555 -	124 0.0009	102 0.0007	99 0.0006	96 0.0006	101 0.0006	109 1.006
162	HYPERVERGE-001	555 -	555 -	167 0.0010	185 0.0009	200 0.0009	207 0.0009	228 0.0009	183 1.009
163	HYPERVERGE-002	555 -	555 -	162 0.0010	187 0.0009	195 0.0009	204 0.0009	215 0.0009	182 1.009
164	HYPERVERGE-003	555 -	555 -	178 0.0011	196 0.0010	198 0.0009	208 0.0009	229 0.0009	189 1.009
165	HYUNDAI-ROBOTICSLAB-000	555 -	555 -	317 0.0023	339 0.0020	352 0.0020	361 0.0019	370 0.0019	331 1.019
166	HYUNDAI-ROBOTICSLAB-001	555 -	555 -	225 0.0014	225 0.0011	219 0.0010	223 0.0010	205 0.0009	225 1.010
167	HYUNDAI-ROBOTICSLAB-002	555 -	555 -	75 0.0007	72 0.0006	76 0.0006	75 0.0006	78 0.0006	76 1.006
168	HZAILU-000	555 -	555 -	284 0.0018	261 0.0013	264 0.0012	258 0.0011	270 0.0011	265 1.012
169	HZAILU-001	555 -	555 -	257 0.0016	281 0.0014	281 0.0013	287 0.0012	287 0.0011	278 1.012
170	HZAILU-002	555 -	555 -	261 0.0016	278 0.0013	277 0.0013	282 0.0012	286 0.0011	277 1.012
171	HZAILU-003	555 -	555 -	212 0.0013	215 0.0011	222 0.0010	232 0.0010	212 0.0009	216 1.010
172	HZAILU-004	555 -	555 -	146 0.0009	166 0.0009	178 0.0009	186 0.0009	191 0.0009	161 1.008
173	HZAILU-005	555 -	555 -	144 0.0009	161 0.0009	173 0.0009	181 0.0009	193 0.0009	160 1.008
174	HZAILU-006	555 -	555 -	139 0.0009	162 0.0009	172 0.0009	182 0.0009	190 0.0009	159 1.008
175	I2V-001	555 -	555 -	326 0.0026	364 0.0024	377 0.0024	378 0.0024	398 0.0024	353 1.022
176	ICEHOUSE-000	555 -	555 -	371 0.0044	371 0.0026	366 0.0022	365 0.0020	359 0.0017	374 1.026
177	ICM-000	555 -	555 -	380 0.0049	405 0.0043	415 0.0042	426 0.0042	434 0.0041	400 1.040
178	ICM-001	555 -	555 -	332 0.0028	349 0.0022	356 0.0021	364 0.0020	372 0.0019	345 1.020
179	IDEMIA-003	555 -	555 -	400 0.0066	402 0.0041	402 0.0035	404 0.0031	399 0.0024	401 1.040
180	IDEMIA-004	555 -	555 -	395 0.0063	390 0.0035	384 0.0029	379 0.0024	360 0.0018	389 1.035
181	IDEMIA-005	555 -	555 -	413 0.0077	400 0.0041	394 0.0033	398 0.0029	405 0.0027	403 1.042
182	IDEMIA-006	555 -	555 -	427 0.0092	414 0.0048	410 0.0039	413 0.0035	423 0.0034	413 1.049
183	IDEMIA-007	555 -	555 -	309 0.0022	257 0.0012	232 0.0011	200 0.0009	179 0.0008	271 1.012
184	IDEMIA-008	555 -	555 -	72 0.0007	65 0.0006	70 0.0006	74 0.0006	70 0.0005	67 1.005
185	IDEMIA-009	555 -	555 -	50 0.0006	48 0.0005	49 0.0005	49 0.0005	49 0.0005	48 1.005
186	IDEMIA-010	555 -	555 -	27 0.0005	41 0.0005	40 0.0005	47 0.0005	50 0.0005	34 1.005
187	IDEMIA-011	555 -	555 -	68 0.0007	100 0.0007	113 0.0007	116 0.0007	128 0.0007	96 1.006
188	IDEMIA-012	555 -	555 -	73 0.0007	97 0.0007	103 0.0007	107 0.0006	115 0.0006	95 1.006
189	IDENTY-000	555 -	555 -	554 1.0000	552 1.0000	552 1.0000	552 1.0000	553 1.0000	552 10.000
190	IMAGUS-002	555 -	555 -	530 0.2200	522 0.1339	521 0.1087	520 0.0868	518 0.0629	523 2.305
191	IMAGUS-003	555 -	555 -	537 0.3557	535 0.2489	535 0.2129	529 0.1788	530 0.1394	535 3.360
192	IMAGUS-005	555 -	555 -	256 0.0016	260 0.0012	249 0.0011	236 0.0010	240 0.0010	252 1.012
193	IMAGUS-006	555 -	555 -	262 0.0016	271 0.0013	263 0.0012	261 0.0011	273 0.0011	263 1.012
194	IMAGUS-007	555 -	555 -	266 0.0016	235 0.0011	224 0.0010	210 0.0009	207 0.0009	240 1.011
195	IMAGUS-008	555 -	555 -	511 0.0857	512 0.0698	514 0.0643	514 0.0587	515 0.0514	512 1.646
196	IMDS-SOFTWARE-000	555 -	555 -	97 0.0008	83 0.0006	79 0.0006	79 0.0006	76 0.0006	84 1.006
197	IMDS-SOFTWARE-001	555 -	555 -	102 0.0008	92 0.0006	92 0.0006	93 0.0006	86 0.0006	92 1.006
198	IMDS-SOFTWARE-002	555 -	555 -	99 0.0008	82 0.0006	80 0.0006	81 0.0006	79 0.0006	85 1.006
199	IMPERIAL-000	555 -	555 -	300 0.0021	299 0.0015	308 0.0015	313 0.0014	314 0.0013	303 1.014
200	INCODE-000	555 -	555 -	498 0.0486	492 0.0258	491 0.0201	490 0.0157	484 0.0114	492 1.259
201	INCODE-001	555 -	555 -	458 0.0164	445 0.0082	438 0.0065	434 0.0053	435 0.0041	447 1.084
202	INCODE-002	555 -	555 -	462 0.0175	448 0.0088	441 0.0068	436 0.0054	433 0.0041	453 1.089
203	INCODE-003	555 -	555 -	450 0.0127	427 0.0062	424 0.0049	420 0.0038	413 0.0029	434 1.064
204	INCODE-004	555 -	555 -	348 0.0032	332 0.0020	338 0.0018	340 0.0016	341 0.0015	341 1.019
205	INCODE-005	555 -	555 -	214 0.0013	209 0.0010	217 0.0010	209 0.0009	210 0.0009	210 1.010
206	INCODE-006	555 -	555 -	76 0.0007	114 0.0007	122 0.0007	128 0.0007	138 0.0007	108 1.006
207	INCODE-007	555 -	555 -	22 0.0005	23 0.0005	17 0.0005	16 0.0005	16 0.0005	21 1.004
208	INNOVATRICS-002	555 -	555 -	495 0.0448	499 0.0340	501 0.0319	503 0.0306	506 0.0295	500 1.319
209	INNOVATRICS-003	555 -	555 -	477 0.0260	467 0.0124	461 0.0092	452 0.0072	442 0.0051	469 1.127
210	INNOVATRICS-004	555 -	555 -	448 0.0120	425 0.0059	422 0.0047	418 0.0037	410 0.0029	431 1.061
211	INNOVATRICS-005	555 -	555 -	301 0.0021	293 0.0015	286 0.0013	280 0.0012	271 0.0011	295 1.014
212	INNOVATRICS-007	555 -	555 -	217 0.0013	213 0.0010	208 0.0010	194 0.0009	198 0.0009	213 1.010
213	INNOVATRICS-008	555 -	555 -	147 0.0009	136 0.0008	138 0.0008	143 0.0007	146 0.0007	135 1.007
214	INNOVATRICS-009	555 -	555 -	161 0.0010	170 0.0009	176 0.0009	185 0.0009	197 0.0009	169 1.008
215	INNOVATRICS-010	555 -	555 -	172 0.0010	188 0.0009	190 0.0009	195 0.0009	201 0.0009	180 1.009
216	INNOVATRICS-011	555 -	555 -	87 0.0008	109 0.0007	105 0.0007	101 0.0006	106 0.0006	107 1.006

Table 47: **Rank-based accuracy for the FRVT 2018 mugshot sets**. *In columns 3 and 4 are template size and template generation duration. Thereafter values are rank-based FNIR with T = 0 and FPIR = 1. This is appropriate to investigational uses but not those with higher volumes where candidates from all searches would need review. The next column is a workload statistic, a small value shows an algorithm front-loads mates into the first 10 candidates. Throughout, blue superscripts indicate the rank of the algorithm for that column, and the best value is highlighted in yellow.*

This publication is available free of charge from: https://doi.org/10.6028/NIST.IR.8271

MISSES OUTSIDE RANK R		RESOURCE USAGE		ENROL MOST RECENT, N = 1.6M					
FNIR(N, T=0, R)		TEMPLATE		FRVT 2018 MUGSHOTS					
#	ALGORITHM	BYTES	MSEC	R=1	R=5	R=10	R=20	R=50	WORK-10
217	INNOVATRICS-012	555 -	555 -	84 0.0007	96 0.0007	100 0.0006	102 0.0006	98 0.0006	97 1.006
218	INNOVATRICS-013	555 -	555 -	46 0.0006	39 0.0005	23 0.0005	24 0.0005	34 0.0005	40 1.005
219	INNOVATRICS-014	555 -	555 -	32 0.0006	35 0.0005	46 0.0005	37 0.0005	24 0.0005	39 1.005
220	INNOVATRICS-015	555 -	555 -	33 0.0006	29 0.0005	31 0.0005	22 0.0005	18 0.0005	30 1.005
221	INSPUR-000	555 -	555 -	55 0.0006	36 0.0005	44 0.0005	44 0.0005	40 0.0005	43 1.005
222	INSPUR-001	555 -	555 -	48 0.0006	43 0.0005	39 0.0005	39 0.0005	39 0.0005	44 1.005
223	INSPUR-002	555 -	555 -	39 0.0006	40 0.0005	18 0.0005	17 0.0005	22 0.0005	36 1.005
224	INTELIGENSIA-000	555 -	555 -	264 0.0016	229 0.0011	212 0.0010	193 0.0009	178 0.0008	229 1.011
225	INTELIGENSIA-001	555 -	555 -	71 0.0007	68 0.0006	64 0.0006	69 0.0006	68 0.0005	70 1.005
226	INTELLIVISION-001	555 -	555 -	488 0.0361	488 0.0195	484 0.0156	482 0.0123	475 0.0091	487 1.196
227	INTELLIVISION-002	555 -	555 -	435 0.0103	416 0.0051	413 0.0040	409 0.0034	403 0.0027	418 1.052
228	INTELRESEARCH-001	555 -	555 -	60 0.0006	52 0.0005	52 0.0005	53 0.0005	52 0.0005	53 1.005
229	INTEMA-000	555 -	555 -	98 0.0008	119 0.0007	124 0.0007	126 0.0007	137 0.0007	113 1.006
230	INTEMA-001	555 -	555 -	8 0.0005	10 0.0005	11 0.0005	11 0.0004	10 0.0004	10 1.004
231	INTSYSMSU-000	555 -	555 -	519 0.1454	521 0.1317	524 0.1269	524 0.1222	527 0.1160	521 2.200
232	IONETWORKS-001	555 -	555 -	350 0.0034	382 0.0032	391 0.0032	406 0.0031	417 0.0031	380 1.029
233	IREX-000	555 -	555 -	364 0.0040	397 0.0039	411 0.0039	422 0.0039	431 0.0039	393 1.036
234	ISYSTEMS-002	555 -	555 -	394 0.0061	401 0.0041	405 0.0037	410 0.0034	420 0.0032	399 1.039
235	ISYSTEMS-003	555 -	555 -	381 0.0049	391 0.0037	399 0.0034	407 0.0032	415 0.0031	388 1.034
236	KAKAO-000	555 -	555 -	184 0.0011	133 0.0008	125 0.0007	110 0.0007	105 0.0006	140 1.007
237	KAKAO-001	555 -	555 -	166 0.0010	199 0.0010	206 0.0010	216 0.0010	226 0.0009	190 1.009
238	KAKAO-002	555 -	555 -	159 0.0010	197 0.0010	204 0.0010	205 0.0009	218 0.0009	187 1.009
239	KEDACOM-001	555 -	555 -	409 0.0074	436 0.0070	442 0.0069	449 0.0068	461 0.0068	433 1.064
240	KEYLESS-000	555 -	555 -	74 0.0007	66 0.0006	61 0.0006	64 0.0005	58 0.0005	66 1.005
241	KLOUDSPOT-001	555 -	555 -	295 0.0020	275 0.0013	261 0.0012	267 0.0011	264 0.0011	282 1.013
242	KNERON-000	555 -	555 -	389 0.0056	419 0.0056	426 0.0056	438 0.0056	446 0.0056	415 1.050
243	KNERON-001	555 -	555 -	482 0.0292	495 0.0292	500 0.0292	502 0.0292	505 0.0291	493 1.262
244	KNOWUTECH-000	555 -	555 -	92 0.0008	57 0.0006	53 0.0005	55 0.0005	57 0.0005	63 1.005
245	KOGNIZA-000	555 -	555 -	207 0.0013	231 0.0011	246 0.0011	255 0.0011	274 0.0011	226 1.010
246	LIGHTVISION-000	555 -	555 -	331 0.0027	345 0.0021	353 0.0020	362 0.0020	374 0.0019	342 1.020
247	LINE-000	555 -	555 -	288 0.0019	248 0.0012	223 0.0010	192 0.0009	170 0.0008	249 1.011
248	LINE-001	555 -	555 -	96 0.0008	87 0.0006	90 0.0006	84 0.0006	85 0.0006	88 1.006
249	LINECLOVA-002	555 -	555 -	149 0.0009	159 0.0009	162 0.0008	173 0.0008	182 0.0008	157 1.008
250	LINECLOVA-003	555 -	555 -	52 0.0006	45 0.0005	29 0.0005	41 0.0005	20 0.0005	45 1.005
251	LOOKMAN-003	555 -	555 -	418 0.0084	440 0.0075	448 0.0073	454 0.0072	464 0.0070	437 1.068
252	LOOKMAN-004	555 -	555 -	420 0.0087	441 0.0075	447 0.0073	453 0.0072	463 0.0070	438 1.069
253	LOOKMAN-005	555 -	555 -	412 0.0077	437 0.0071	444 0.0070	451 0.0069	462 0.0069	435 1.065
254	LUXAND-001	555 -	555 -	334 0.0028	334 0.0020	339 0.0018	344 0.0017	351 0.0016	335 1.019
255	MANTRA-000	555 -	555 -	223 0.0014	202 0.0010	197 0.0009	188 0.0009	183 0.0008	207 1.009
256	MAVERICKRESEARCH-000	555 -	555 -	436 0.0104	447 0.0085	450 0.0081	460 0.0080	469 0.0078	444 1.079
257	MAXVISION-000	555 -	555 -	298 0.0021	282 0.0014	271 0.0012	262 0.0011	244 0.0010	291 1.013
258	MAXVISION-001	555 -	555 -	122 0.0008	137 0.0008	141 0.0008	148 0.0008	151 0.0007	131 1.007
259	MAXVISION-002	555 -	555 -	130 0.0009	140 0.0008	148 0.0008	158 0.0008	165 0.0008	134 1.007
260	MAXVISION-003	555 -	555 -	136 0.0009	135 0.0008	143 0.0008	149 0.0008	153 0.0007	133 1.007
261	MAXVISION-004	555 -	555 -	121 0.0008	144 0.0008	151 0.0008	163 0.0008	169 0.0008	141 1.007
262	MEGVII-001	555 -	555 -	445 0.0116	453 0.0092	453 0.0086	464 0.0083	472 0.0080	451 1.085
263	MEGVII-002	555 -	555 -	447 0.0117	454 0.0092	455 0.0087	463 0.0083	471 0.0079	452 1.086
264	MEGVII-003	555 -	555 -	134 0.0009	153 0.0008	161 0.0008	172 0.0008	175 0.0008	149 1.008
265	MEGVII-004	555 -	555 -	119 0.0008	151 0.0008	158 0.0008	168 0.0008	171 0.0008	145 1.007
266	MEGVII-005	555 -	555 -	118 0.0008	150 0.0008	155 0.0008	166 0.0008	173 0.0008	146 1.007
267	METSAKUURCOMPANY-000	555 -	555 -	105 0.0008	79 0.0006	65 0.0006	60 0.0005	65 0.0005	77 1.006
268	METSAKUURCOMPANY-001	555 -	555 -	163 0.0010	146 0.0008	149 0.0008	154 0.0008	157 0.0008	154 1.008
269	MICROFOCUS-003	555 -	555 -	543 0.5940	543 0.4690	543 0.4202	543 0.3722	544 0.3093	543 5.359
270	MICROFOCUS-004	555 -	555 -	542 0.5762	542 0.4517	542 0.4024	542 0.3558	543 0.2954	542 5.198
271	MICROFOCUS-005	555 -	555 -	538 0.4240	538 0.3025	536 0.2604	536 0.2206	532 0.1721	538 3.859
272	MICROFOCUS-006	555 -	555 -	539 0.4266	539 0.3046	537 0.2621	538 0.2230	533 0.1743	539 3.878
273	MICROSOFT-003	555 -	555 -	248 0.0015	181 0.0009	163 0.0008	144 0.0007	102 0.0006	198 1.009
274	MICROSOFT-004	555 -	555 -	233 0.0014	168 0.0009	136 0.0008	122 0.0007	88 0.0006	179 1.009
275	MICROSOFT-005	555 -	555 -	287 0.0018	177 0.0009	154 0.0008	137 0.0007	110 0.0006	208 1.009
276	MICROSOFT-006	555 -	555 -	292 0.0019	228 0.0011	191 0.0009	153 0.0008	120 0.0007	238 1.011
277	MOBBL-000	555 -	555 -	315 0.0023	309 0.0016	303 0.0014	305 0.0014	303 0.0013	311 1.015
278	MOBBL-001	555 -	555 -	444 0.0115	462 0.0109	468 0.0108	474 0.0108	482 0.0107	459 1.099
279	MOBBL-002	555 -	555 -	528 0.2119	532 0.2119	534 0.2119	535 0.2119	539 0.2119	532 2.907
280	MUKH-002	555 -	555 -	476 0.0255	472 0.0136	469 0.0109	465 0.0086	460 0.0066	473 1.136
281	NEC-000	555 -	555 -	459 0.0167	446 0.0083	434 0.0063	431 0.0049	424 0.0035	448 1.084
282	NEC-001	555 -	555 -	468 0.0206	473 0.0138	476 0.0125	478 0.0115	483 0.0109	471 1.132
283	NEC-002	555 -	555 -	140 0.0009	142 0.0008	142 0.0008	147 0.0008	150 0.0007	142 1.007
284	NEC-003	555 -	555 -	211 0.0013	247 0.0012	256 0.0012	271 0.0011	282 0.0011	236 1.011
285	NEC-004	555 -	555 -	176 0.0011	204 0.0010	213 0.0010	212 0.0010	224 0.0009	201 1.009
286	NEC-005	555 -	555 -	113 0.0008	132 0.0008	137 0.0008	142 0.0007	142 0.0007	125 1.007
287	NEC-006	555 -	555 -	141 0.0009	158 0.0009	167 0.0008	165 0.0008	164 0.0008	155 1.008
288	NEC-007	555 -	555 -	64 0.0007	81 0.0006	87 0.0006	89 0.0006	95 0.0006	78 1.006

Table 48: **Rank-based accuracy for the FRVT 2018 mugshot sets**. *In columns 3 and 4 are template size and template generation duration. Thereafter values are rank-based FNIR with T = 0 and FPIR = 1. This is appropriate to investigational uses but not those with higher volumes where candidates from all searches would need review. The next column is a workload statistic, a small value shows an algorithm front-loads mates into the first 10 candidates. Throughout, blue superscripts indicate the rank of the algorithm for that column, and the best value is highlighted in yellow.*

This publication is available free of charge from: https://doi.org/10.6028/NIST.IR.8271

MISSES OUTSIDE RANK R		RESOURCE USAGE		ENROL MOST RECENT, N = 1.6M					
FNIR(N, T=0, R)		TEMPLATE		FRVT 2018 MUGSHOTS					
#	ALGORITHM	BYTES	MSEC	R=1	R=5	R=10	R=20	R=50	WORK-10
289	NEC-008	555 -	555 -	81 0.0007	99 0.0007	102 0.0006	106 0.0006	113 0.0006	99 1.006
290	NEC-009	555 -	555 -	49 0.0006	67 0.0006	77 0.0006	83 0.0006	92 0.0006	65 1.005
291	NEC-010	555 -	555 -	15 0.0005	21 0.0005	27 0.0005	26 0.0005	21 0.0005	22 1.004
292	NEC-011	555 -	555 -	9 0.0005	9 0.0004	8 0.0004	6 0.0004	7 0.0004	8 1.004
293	NEUROTECHNOLOGY-003	555 -	555 -	470 0.0222	466 0.0123	462 0.0096	457 0.0075	445 0.0054	468 1.122
294	NEUROTECHNOLOGY-004	555 -	555 -	383 0.0052	386 0.0033	388 0.0029	388 0.0026	387 0.0022	386 1.032
295	NEUROTECHNOLOGY-005	555 -	555 -	362 0.0040	370 0.0026	375 0.0024	375 0.0022	379 0.0021	372 1.025
296	NEUROTECHNOLOGY-006	555 -	555 -	463 0.0178	442 0.0078	429 0.0058	422 0.0045	419 0.0032	446 1.082
297	NEUROTECHNOLOGY-007	555 -	555 -	352 0.0036	355 0.0023	359 0.0021	360 0.0019	361 0.0018	354 1.022
298	NEUROTECHNOLOGY-008	555 -	555 -	281 0.0018	237 0.0012	238 0.0011	234 0.0010	232 0.0010	248 1.011
299	NEUROTECHNOLOGY-009	555 -	555 -	179 0.0011	157 0.0009	160 0.0008	157 0.0008	158 0.0008	162 1.008
300	NEUROTECHNOLOGY-010	555 -	555 -	131 0.0009	112 0.0007	119 0.0007	117 0.0007	133 0.0007	117 1.007
301	NEUROTECHNOLOGY-012	555 -	555 -	63 0.0007	80 0.0006	81 0.0006	82 0.0006	93 0.0006	74 1.006
302	NEUROTECHNOLOGY-013	555 -	555 -	65 0.0007	76 0.0006	86 0.0006	91 0.0006	99 0.0006	72 1.005
303	NEUROTECHNOLOGY-014	555 -	555 -	41 0.0006	37 0.0005	47 0.0005	50 0.0005	53 0.0005	38 1.005
304	NEUROTECHNOLOGY-015	555 -	555 -	28 0.0005	17 0.0005	22 0.0005	33 0.0005	41 0.0005	20 1.004
305	NEUROTECHNOLOGY-016	555 -	555 -	21 0.0005	28 0.0005	34 0.0005	42 0.0005	37 0.0005	25 1.004
306	NEWLAND-002	555 -	555 -	508 0.0783	508 0.0477	506 0.0394	506 0.0329	504 0.0261	509 1.466
307	NEXTMETALABS-001	555 -	555 -	485 0.0312	476 0.0156	472 0.0116	466 0.0087	452 0.0061	477 1.159
308	NEXTMETALABS-002	555 -	555 -	54 0.0006	46 0.0005	43 0.0005	38 0.0005	33 0.0005	49 1.005
309	NOBLIS-001	555 -	555 -	532 0.2489	526 0.1769	526 0.1539	526 0.1336	525 0.1109	528 2.676
310	NOBLIS-002	555 -	555 -	522 0.1791	519 0.1104	519 0.0900	517 0.0719	517 0.0532	519 2.074
311	NOMINDER-000	555 -	555 -	67 0.0007	53 0.0005	54 0.0005	54 0.0005	51 0.0005	56 1.005
312	NOMINDER-001	555 -	555 -	190 0.0011	217 0.0011	227 0.0011	239 0.0010	258 0.0010	214 1.010
313	NOMINDER-002	555 -	555 -	194 0.0012	220 0.0011	233 0.0011	241 0.0011	257 0.0010	218 1.010
314	NOMINDER-003	555 -	555 -	193 0.0012	226 0.0011	240 0.0011	248 0.0011	269 0.0011	221 1.010
315	NOMINDER-004	555 -	555 -	177 0.0011	205 0.0010	214 0.0010	221 0.0010	236 0.0010	199 1.009
316	NOTIONTAG-000	555 -	555 -	299 0.0021	322 0.0017	326 0.0017	342 0.0016	349 0.0016	317 1.016
317	NTECHLAB-003	555 -	555 -	393 0.0060	375 0.0028	365 0.0022	352 0.0018	340 0.0015	379 1.029
318	NTECHLAB-004	555 -	555 -	376 0.0046	350 0.0022	335 0.0018	326 0.0015	299 0.0012	355 1.023
319	NTECHLAB-005	555 -	555 -	374 0.0046	346 0.0021	323 0.0016	289 0.0013	248 0.0010	352 1.022
320	NTECHLAB-006	555 -	555 -	363 0.0040	324 0.0018	302 0.0014	260 0.0011	194 0.0009	336 1.019
321	NTECHLAB-007	555 -	555 -	313 0.0023	273 0.0013	237 0.0011	226 0.0010	188 0.0008	284 1.013
322	NTECHLAB-008	555 -	555 -	221 0.0014	155 0.0008	150 0.0008	146 0.0007	135 0.0007	173 1.008
323	NTECHLAB-009	555 -	555 -	143 0.0009	121 0.0007	115 0.0007	103 0.0006	94 0.0006	123 1.007
324	NTECHLAB-010	555 -	555 -	88 0.0008	103 0.0007	114 0.0007	114 0.0007	132 0.0007	103 1.006
325	NTECHLAB-011	555 -	555 -	66 0.0007	64 0.0006	62 0.0006	65 0.0005	67 0.0005	64 1.005
326	OMNIGARDE-000	555 -	555 -	70 0.0007	55 0.0005	55 0.0005	52 0.0005	47 0.0005	58 1.005
327	OMNIGARDE-001	555 -	555 -	31 0.0005	26 0.0005	32 0.0005	18 0.0005	14 0.0004	26 1.004
328	OMNIGARDE-002	555 -	555 -	43 0.0006	38 0.0005	30 0.0005	23 0.0005	13 0.0004	37 1.005
329	OPTIEXACTA-000	555 -	555 -	26 0.0005	22 0.0005	28 0.0005	34 0.0005	44 0.0005	23 1.004
330	PANGIAM-000	555 -	555 -	114 0.0008	123 0.0007	126 0.0007	124 0.0007	131 0.0007	122 1.007
331	PANGIAM-001	555 -	555 -	397 0.0065	430 0.0064	436 0.0064	444 0.0064	457 0.0064	424 1.058
332	PAPSAV1923-000	555 -	555 -	109 0.0008	125 0.0007	128 0.0007	141 0.0007	156 0.0007	124 1.007
333	PARAVISION-000	555 -	555 -	464 0.0187	482 0.0170	488 0.0166	491 0.0164	498 0.0163	475 1.155
334	PARAVISION-001	555 -	555 -	354 0.0036	356 0.0023	361 0.0021	363 0.0020	362 0.0018	356 1.023
335	PARAVISION-002	555 -	555 -	360 0.0039	365 0.0025	364 0.0022	366 0.0020	365 0.0018	363 1.024
336	PARAVISION-003	555 -	555 -	344 0.0031	348 0.0021	351 0.0020	354 0.0018	354 0.0017	346 1.020
337	PARAVISION-004	555 -	555 -	209 0.0013	212 0.0010	216 0.0010	222 0.0010	230 0.0009	212 1.010
338	PARAVISION-005	555 -	555 -	198 0.0012	210 0.0010	215 0.0010	224 0.0010	234 0.0010	205 1.009
339	PARAVISION-007	555 -	555 -	112 0.0008	122 0.0007	121 0.0007	123 0.0007	127 0.0007	115 1.006
340	PARAVISION-009	555 -	555 -	62 0.0006	71 0.0006	83 0.0006	86 0.0006	89 0.0006	69 1.005
341	PARAVISION-012	555 -	555 -	42 0.0006	62 0.0006	67 0.0006	72 0.0006	75 0.0006	60 1.005
342	PARAVISION-014	555 -	555 -	40 0.0006	59 0.0006	63 0.0006	68 0.0006	73 0.0006	55 1.005
343	PARAVISION-016	555 -	555 -	45 0.0006	61 0.0006	69 0.0006	73 0.0006	81 0.0006	59 1.005
344	PARAVISION-019	555 -	555 -	16 0.0005	16 0.0005	21 0.0005	32 0.0005	25 0.0005	19 1.004
345	PENTACOMP-000	555 -	555 -	549 0.9751	548 0.8897	548 0.7909	547 0.5980	312 0.0013	548 9.021
346	PENTACOMP-001	555 -	555 -	232 0.0014	223 0.0011	218 0.0010	218 0.0010	202 0.0009	223 1.010
347	PIXELALL-002	555 -	555 -	366 0.0041	367 0.0025	362 0.0021	350 0.0018	348 0.0016	367 1.025
348	PIXELALL-003	555 -	555 -	279 0.0018	265 0.0013	263 0.0012	252 0.0011	260 0.0011	266 1.012
349	PIXELALL-004	555 -	555 -	269 0.0017	245 0.0012	243 0.0011	244 0.0011	238 0.0010	245 1.011
350	PIXELALL-005	555 -	555 -	247 0.0015	274 0.0013	274 0.0012	288 0.0012	297 0.0012	264 1.012
351	PRIVID-000	555 -	555 -	469 0.0208	489 0.0207	492 0.0207	492 0.0207	500 0.0207	485 1.186
352	PROTENET-000	555 -	555 -	503 0.0632	506 0.0461	507 0.0426	508 0.0400	512 0.0377	505 1.436
353	PSL-000	555 -	555 -	18 0.0005	7 0.0004	9 0.0004	10 0.0004	5 0.0004	9 1.004
354	PSL-001	555 -	555 -	11 0.0005	11 0.0005	10 0.0004	8 0.0004	8 0.0004	11 1.004
355	PSL-002	555 -	555 -	5 0.0004	6 0.0004	4 0.0004	2 0.0004	4 0.0004	4 1.004
356	PSL-003	555 -	555 -	6 0.0004	4 0.0004	6 0.0004	7 0.0004	9 0.0004	6 1.004
357	PSL-004	555 -	555 -	4 0.0004	5 0.0004	5 0.0004	5 0.0004	6 0.0004	5 1.004
358	PTAKURATSATU-000	555 -	555 -	330 0.0027	321 0.0017	320 0.0016	309 0.0014	306 0.0013	322 1.017
359	PYRAMID-000	555 -	555 -	86 0.0007	91 0.0006	97 0.0006	92 0.0006	104 0.0006	93 1.006
360	PYRAMID-001	555 -	555 -	115 0.0008	118 0.0007	117 0.0007	119 0.0007	119 0.0007	114 1.006

Table 49: **Rank-based accuracy for the FRVT 2018 mugshot sets**. *In columns 3 and 4 are template size and template generation duration. Thereafter values are rank-based FNIR with T = 0 and FPIR = 1. This is appropriate to investigational uses but not those with higher volumes where candidates from all searches would need review. The next column is a workload statistic, a small value shows an algorithm front-loads mates into the first 10 candidates. Throughout, blue superscripts indicate the rank of the algorithm for that column, and the best value is highlighted in yellow.*

This publication is available free of charge from: https://doi.org/10.6028/NIST.IR.8271

MISSES OUTSIDE RANK R		RESOURCE USAGE		ENROL MOST RECENT, N = 1.6M					
FNIR(N, T=0, R)		TEMPLATE		FRVT 2018 MUGSHOTS					
#	ALGORITHM	BYTES	MSEC	R=1	R=5	R=10	R=20	R=50	WORK-10
361	QAZSMARTVISIONAI-000	[555] -	[555] -	[10] 0.0005	[13] 0.0005	[13] 0.0005	[12] 0.0004	[12] 0.0004	[13] 1.004
362	QAZSMARTVISIONAI-001	[555] -	[555] -	[3] 0.0004	[2] 0.0004	[3] 0.0004	[4] 0.0004	[3] 0.0004	[3] 1.004
363	QAZSMARTVISIONAI-002	[555] -	[555] -	[1] 0.0004	[1] 0.0004	[2] 0.0004	[1] 0.0004	[2] 0.0004	[1] 1.004
364	QAZSMARTVISIONAI-003	[555] -	[555] -	[2] 0.0004	[3] 0.0004	[1] 0.0004	[3] 0.0004	[1] 0.0004	[2] 1.004
365	QNAP-000	[555] -	[555] -	[410] 0.0074	[399] 0.0040	[397] 0.0033	[399] 0.0029	[400] 0.0025	[402] 1.040
366	QNAP-001	[555] -	[555] -	[358] 0.0038	[368] 0.0025	[371] 0.0023	[373] 0.0021	[376] 0.0020	[365] 1.024
367	QNAP-002	[555] -	[555] -	[373] 0.0045	[398] 0.0040	[412] 0.0040	[423] 0.0039	[429] 0.0038	[395] 1.037
368	QNAP-003	[555] -	[555] -	[320] 0.0024	[317] 0.0017	[313] 0.0015	[298] 0.0013	[295] 0.0012	[318] 1.016
369	QNAP-004	[555] -	[555] -	[249] 0.0016	[246] 0.0012	[252] 0.0011	[235] 0.0010	[247] 0.0010	[243] 1.011
370	QNAP-005	[555] -	[555] -	[338] 0.0029	[374] 0.0027	[381] 0.0027	[392] 0.0027	[404] 0.0027	[369] 1.025
371	QNAP-006	[555] -	[555] -	[187] 0.0011	[178] 0.0009	[179] 0.0009	[180] 0.0009	[180] 0.0008	[177] 1.009
372	QUANTASOFT-001	[555] -	[555] -	[529] 0.2174	[525] 0.1641	[525] 0.1465	[525] 0.1309	[526] 0.1113	[525] 2.537
373	RANKONE-002	[555] -	[555] -	[466] 0.0191	[459] 0.0108	[457] 0.0089	[456] 0.0074	[449] 0.0057	[462] 1.108
374	RANKONE-003	[555] -	[555] -	[465] 0.0191	[460] 0.0108	[456] 0.0089	[455] 0.0074	[447] 0.0057	[461] 1.108
375	RANKONE-004	[555] -	[555] -	[494] 0.0412	[490] 0.0222	[489] 0.0174	[485] 0.0138	[478] 0.0098	[490] 1.222
376	RANKONE-005	[555] -	[555] -	[423] 0.0090	[417] 0.0051	[416] 0.0043	[411] 0.0035	[409] 0.0028	[417] 1.051
377	RANKONE-006	[555] -	[555] -	[377] 0.0047	[372] 0.0027	[373] 0.0023	[369] 0.0020	[356] 0.0017	[375] 1.027
378	RANKONE-007	[555] -	[555] -	[340] 0.0030	[333] 0.0020	[330] 0.0017	[323] 0.0015	[308] 0.0013	[334] 1.019
379	RANKONE-009	[555] -	[555] -	[294] 0.0020	[267] 0.0013	[267] 0.0012	[265] 0.0011	[256] 0.0010	[273] 1.012
380	RANKONE-010	[555] -	[555] -	[289] 0.0019	[287] 0.0014	[280] 0.0013	[279] 0.0012	[275] 0.0011	[290] 1.013
381	RANKONE-011	[555] -	[555] -	[191] 0.0011	[165] 0.0009	[171] 0.0009	[171] 0.0008	[167] 0.0008	[170] 1.008
382	RANKONE-012	[555] -	[555] -	[165] 0.0010	[149] 0.0008	[146] 0.0008	[155] 0.0008	[159] 0.0008	[148] 1.008
383	RANKONE-013	[555] -	[555] -	[69] 0.0007	[63] 0.0006	[57] 0.0005	[57] 0.0005	[60] 0.0005	[62] 1.005
384	RANKONE-014	[555] -	[555] -	[53] 0.0006	[54] 0.0005	[56] 0.0005	[56] 0.0005	[64] 0.0005	[54] 1.005
385	RANKONE-015	[555] -	[555] -	[57] 0.0006	[58] 0.0006	[59] 0.0005	[62] 0.0005	[66] 0.0005	[61] 1.005
386	REALNETWORKS-000	[555] -	[555] -	[492] 0.0399	[487] 0.0193	[481] 0.0147	[476] 0.0109	[467] 0.0075	[488] 1.199
387	REALNETWORKS-001	[555] -	[555] -	[493] 0.0399	[486] 0.0193	[482] 0.0147	[477] 0.0109	[468] 0.0075	[489] 1.199
388	REALNETWORKS-002	[555] -	[555] -	[489] 0.0391	[485] 0.0187	[479] 0.0140	[473] 0.0106	[466] 0.0075	[486] 1.193
389	REALNETWORKS-003	[555] -	[555] -	[473] 0.0238	[463] 0.0113	[454] 0.0086	[448] 0.0067	[440] 0.0050	[466] 1.117
390	REALNETWORKS-004	[555] -	[555] -	[471] 0.0233	[461] 0.0109	[452] 0.0084	[445] 0.0065	[438] 0.0047	[463] 1.113
391	REALNETWORKS-005	[555] -	[555] -	[293] 0.0019	[251] 0.0012	[225] 0.0010	[227] 0.0010	[192] 0.0009	[257] 1.012
392	REALNETWORKS-006	[555] -	[555] -	[170] 0.0010	[148] 0.0008	[144] 0.0008	[131] 0.0007	[126] 0.0007	[150] 1.008
393	REALNETWORKS-007	[555] -	[555] -	[156] 0.0010	[143] 0.0008	[130] 0.0007	[127] 0.0007	[116] 0.0006	[143] 1.007
394	REALNETWORKS-008	[555] -	[555] -	[106] 0.0008	[75] 0.0006	[72] 0.0006	[76] 0.0006	[55] 0.0005	[79] 1.006
395	RECOGNITO-000	[555] -	[555] -	[38] 0.0006	[33] 0.0005	[33] 0.0005	[27] 0.0005	[30] 0.0005	[35] 1.005
396	RECOGNITO-001	[555] -	[555] -	[35] 0.0006	[49] 0.0005	[50] 0.0005	[51] 0.0005	[56] 0.0005	[47] 1.005
397	RECOGNITO-002	[555] -	[555] -	[25] 0.0005	[24] 0.0005	[26] 0.0005	[36] 0.0005	[45] 0.0005	[24] 1.004
398	REMARKAI-000	[555] -	[555] -	[342] 0.0030	[318] 0.0017	[312] 0.0015	[297] 0.0013	[293] 0.0012	[324] 1.017
399	REMARKAI-000	[555] -	[555] -	[417] 0.0083	[404] 0.0042	[398] 0.0034	[397] 0.0029	[397] 0.0024	[405] 1.043
400	REMARKAI-002	[555] -	[555] -	[415] 0.0079	[394] 0.0037	[385] 0.0029	[381] 0.0024	[369] 0.0019	[398] 1.039
401	RENDIP-000	[555] -	[555] -	[199] 0.0012	[194] 0.0010	[182] 0.0009	[177] 0.0008	[184] 0.0008	[192] 1.009
402	REVEALMEDIA-000	[555] -	[555] -	[240] 0.0015	[200] 0.0010	[203] 0.0009	[196] 0.0009	[196] 0.0009	[211] 1.010
403	RNIT-000	[555] -	[555] -	[185] 0.0011	[203] 0.0010	[205] 0.0010	[217] 0.0010	[225] 0.0009	[200] 1.009
404	ROC-016	[555] -	[555] -	[59] 0.0006	[60] 0.0006	[58] 0.0005	[61] 0.0005	[59] 0.0005	[57] 1.005
405	ROC-017	[555] -	[555] -	[47] 0.0006	[56] 0.0006	[60] 0.0005	[58] 0.0005	[61] 0.0005	[53] 1.005
406	ROC-018	[555] -	[555] -	[29] 0.0005	[34] 0.0005	[41] 0.0005	[43] 0.0005	[46] 0.0005	[31] 1.005
407	ROC-019	[555] -	[555] -	[17] 0.0005	[18] 0.0005	[20] 0.0005	[20] 0.0005	[28] 0.0005	[17] 1.004
408	S1-000	[555] -	[555] -	[296] 0.0021	[286] 0.0014	[282] 0.0013	[281] 0.0012	[283] 0.0011	[294] 1.013
409	S1-001	[555] -	[555] -	[333] 0.0028	[345] 0.0021	[358] 0.0021	[368] 0.0020	[375] 0.0020	[343] 1.020
410	S1-002	[555] -	[555] -	[174] 0.0011	[201] 0.0010	[209] 0.0010	[219] 0.0010	[235] 0.0010	[195] 1.009
411	S1-003	[555] -	[555] -	[183] 0.0011	[198] 0.0010	[196] 0.0009	[199] 0.0009	[206] 0.0009	[194] 1.009
412	S1-004	[555] -	[555] -	[157] 0.0010	[184] 0.0009	[194] 0.0009	[201] 0.0009	[209] 0.0009	[178] 1.009
413	S1-005	[555] -	[555] -	[169] 0.0010	[186] 0.0009	[202] 0.0009	[206] 0.0009	[220] 0.0009	[181] 1.009
414	S1-006	[555] -	[555] -	[151] 0.0010	[176] 0.0009	[185] 0.0009	[190] 0.0009	[199] 0.0009	[166] 1.008
415	S1-007	[555] -	[555] -	[125] 0.0009	[141] 0.0008	[147] 0.0008	[156] 0.0008	[162] 0.0008	[138] 1.007
416	SANSAP-001	[555] -	[555] -	[110] 0.0008	[108] 0.0007	[85] 0.0006	[87] 0.0006	[89] 0.0006	[100] 1.006
417	SCANOVATE-000	[555] -	[555] -	[375] 0.0046	[353] 0.0023	[343] 0.0019	[319] 0.0015	[294] 0.0012	[359] 1.023
418	SCANOVATE-001	[555] -	[555] -	[382] 0.0050	[357] 0.0023	[345] 0.0019	[324] 0.0015	[292] 0.0012	[366] 1.024
419	SCYLLA-001	[555] -	[555] -	[282] 0.0018	[270] 0.0013	[255] 0.0012	[250] 0.0011	[253] 0.0010	[267] 1.012
420	SENSETIME-000	[555] -	[555] -	[307] 0.0022	[329] 0.0019	[337] 0.0018	[345] 0.0017	[350] 0.0016	[325] 1.017
421	SENSETIME-001	[555] -	[555] -	[308] 0.0022	[325] 0.0018	[333] 0.0018	[339] 0.0016	[345] 0.0015	[323] 1.017
422	SENSETIME-002	[555] -	[555] -	[453] 0.0133	[470] 0.0132	[478] 0.0132	[483] 0.0132	[491] 0.0132	[467] 1.119
423	SENSETIME-003	[555] -	[555] -	[58] 0.0006	[78] 0.0006	[82] 0.0006	[85] 0.0006	[90] 0.0006	[68] 1.005
424	SENSETIME-004	[555] -	[555] -	[56] 0.0006	[50] 0.0005	[51] 0.0005	[48] 0.0005	[48] 0.0005	[51] 1.005
425	SENSETIME-005	[555] -	[555] -	[20] 0.0005	[20] 0.0005	[14] 0.0005	[14] 0.0005	[15] 0.0005	[16] 1.004
426	SENSETIME-006	[555] -	[555] -	[19] 0.0005	[19] 0.0005	[19] 0.0005	[21] 0.0005	[23] 0.0005	[18] 1.004
427	SENSETIME-007	[555] -	[555] -	[14] 0.0005	[15] 0.0005	[16] 0.0005	[15] 0.0005	[26] 0.0005	[15] 1.004
428	SENSETIME-008	[555] -	[555] -	[13] 0.0005	[14] 0.0005	[12] 0.0005	[13] 0.0005	[17] 0.0005	[12] 1.004
429	SENSETIME-009	[555] -	[555] -	[12] 0.0005	[12] 0.0005	[15] 0.0005	[19] 0.0005	[19] 0.0005	[14] 1.004
430	SENSETIME-010	[555] -	[555] -	[7] 0.0005	[8] 0.0004	[7] 0.0004	[9] 0.0004	[11] 0.0004	[7] 1.004
431	SERENDIPITY-000	[555] -	[555] -	[195] 0.0012	[190] 0.0010	[186] 0.0009	[184] 0.0009	[181] 0.0008	[188] 1.009
432	SEVENTHSENSE-001	[555] -	[555] -	[267] 0.0016	[307] 0.0016	[321] 0.0016	[332] 0.0016	[343] 0.0015	[302] 1.014

Table 50: **Rank-based accuracy for the FRVT 2018 mugshot sets**. *In columns 3 and 4 are template size and template generation duration. Thereafter values are rank-based FNIR with T = 0 and FPIR = 1. This is appropriate to investigational uses but not those with higher volumes where candidates from all searches would need review. The next column is a workload statistic, a small value shows an algorithm front-loads mates into the first 10 candidates. Throughout, blue superscripts indicate the rank of the algorithm for that column, and the best value is highlighted in yellow.*

This publication is available free of charge from: https://doi.org/10.6028/NIST.IR.8271

MISSES OUTSIDE RANK R		RESOURCE USAGE		ENROL MOST RECENT, N = 1.6M					
FNIR(N, T=0, R)		TEMPLATE		FRVT 2018 MUGSHOTS					
#	ALGORITHM	BYTES	MSEC	R=1	R=5	R=10	R=20	R=50	WORK-10
433	SHAMAN-003	555 -	555 -	514 0.1240	516 0.0819	516 0.0704	515 0.0613	516 0.0515	516 1.786
434	SHAMAN-004	555 -	555 -	531 0.2218	524 0.1470	522 0.1238	522 0.1046	522 0.0822	524 2.409
435	SHAMAN-006	555 -	555 -	491 0.0395	500 0.0341	503 0.0329	505 0.0320	509 0.0312	498 1.313
436	SHAMAN-007	555 -	555 -	490 0.0393	498 0.0339	502 0.0328	504 0.0319	508 0.0311	497 1.312
437	SHENNONA-000	555 -	555 -	449 0.0120	464 0.0118	473 0.0118	479 0.0117	487 0.0117	460 1.106
438	SIAT-001	555 -	555 -	265 0.0016	263 0.0013	257 0.0012	249 0.0011	242 0.0010	258 1.012
439	SIAT-002	555 -	555 -	271 0.0017	256 0.0012	269 0.0012	273 0.0012	268 0.0011	260 1.012
440	SMILART-004	555 -	555 -	548 0.9648	549 0.9641	549 0.9640	549 0.9639	550 0.9637	549 9.678
441	SMILART-005	555 -	555 -						554 10.000
442	SPARKTEK-000	555 -	555 -	95 0.0008	94 0.0006	91 0.0006	92 0.0006	96 0.0006	91 1.006
443	SPARSH-001	555 -	555 -	79 0.0007	77 0.0006	75 0.0006	78 0.0006	84 0.0006	73 1.006
444	SQISOFT-001	555 -	555 -	359 0.0038	224 0.0011	187 0.0009	161 0.0008	136 0.0007	287 1.013
445	SQISOFT-002	555 -	555 -	148 0.0009	107 0.0007	98 0.0006	90 0.0006	82 0.0006	112 1.006
446	STAQU-000	555 -	555 -	403 0.0068	421 0.0057	425 0.0054	432 0.0052	439 0.0050	419 1.052
447	STCON-000	555 -	555 -	524 0.1826	528 0.1826	528 0.1826	531 0.1826	535 0.1825	527 2.643
448	STCON-001	555 -	555 -	30 0.0005	25 0.0005	25 0.0005	28 0.0005	32 0.0005	27 1.004
449	STCON-002	555 -	555 -	23 0.0005	31 0.0005	36 0.0005	31 0.0005	42 0.0005	28 1.004
450	STCON-003	555 -	555 -	24 0.0005	30 0.0005	38 0.0005	29 0.0005	38 0.0005	29 1.005
451	SUMSUB-000	555 -	555 -	496 0.0453	494 0.0270	493 0.0221	494 0.0182	492 0.0136	494 1.264
452	SYNESIS-003	555 -	555 -	520 0.1697	520 0.1169	520 0.1045	521 0.0950	523 0.0866	520 2.118
453	SYNESIS-003	555 -	555 -	457 0.0159	477 0.0156	485 0.0156	489 0.0156	497 0.0156	474 1.141
454	SYNESIS-005	555 -	555 -	416 0.0082	444 0.0081	451 0.0081	461 0.0081	473 0.0081	441 1.073
455	T4ISB-000	555 -	555 -	429 0.0100	457 0.0100	465 0.0100	471 0.0100	479 0.0100	456 1.090
456	TECH5-001	555 -	555 -	355 0.0036	338 0.0020	331 0.0017	325 0.0015	316 0.0013	347 1.020
457	TECH5-002	555 -	555 -	314 0.0023	222 0.0011	181 0.0009	151 0.0008	123 0.0007	244 1.011
458	TECH5-003	555 -	555 -	78 0.0007	69 0.0006	74 0.0006	71 0.0006	80 0.0006	71 1.005
459	TEVIAN-003	555 -	555 -	454 0.0145	438 0.0072	431 0.0058	428 0.0046	425 0.0036	442 1.074
460	TEVIAN-004	555 -	555 -	439 0.0111	420 0.0056	419 0.0045	417 0.0036	411 0.0029	422 1.057
461	TEVIAN-005	555 -	555 -	406 0.0071	393 0.0037	390 0.0030	386 0.0026	384 0.0022	396 1.037
462	TEVIAN-006	555 -	555 -	297 0.0021	294 0.0015	295 0.0014	304 0.0013	309 0.0013	296 1.014
463	TEVIAN-007	555 -	555 -	235 0.0014	206 0.0010	210 0.0010	220 0.0010	219 0.0009	209 1.010
464	TIGER-000	555 -	555 -	502 0.0613	497 0.0308	495 0.0234	493 0.0176	488 0.0118	499 1.313
465	TIGER-002	555 -	555 -	387 0.0054	377 0.0028	369 0.0023	347 0.0018	332 0.0014	377 1.029
466	TIGER-003	555 -	555 -	388 0.0054	378 0.0028	368 0.0022	348 0.0018	333 0.0014	378 1.029
467	TIGER-004	555 -	555 -	310 0.0022	328 0.0019	344 0.0019	355 0.0018	363 0.0018	326 1.017
468	TONGYITRANS-000	555 -	555 -	398 0.0066	388 0.0035	387 0.0029	384 0.0026	390 0.0023	390 1.035
469	TONGYITRANS-001	555 -	555 -	399 0.0066	389 0.0035	386 0.0029	385 0.0026	391 0.0023	391 1.035
470	TOSHIBA-000	555 -	555 -	367 0.0043	361 0.0024	354 0.0020	351 0.0018	353 0.0016	364 1.024
471	TOSHIBA-001	555 -	555 -	372 0.0045	369 0.0025	360 0.0021	353 0.0018	352 0.0016	371 1.025
472	TOSHIBA-002	555 -	555 -	145 0.0009	180 0.0009	188 0.0009	197 0.0009	211 0.0009	171 1.008
473	TOSS-000	555 -	555 -	158 0.0010	182 0.0009	192 0.0009	203 0.0009	217 0.0009	176 1.009
474	TRUEFACE-000	555 -	555 -	339 0.0029	366 0.0025	378 0.0024	376 0.0023	388 0.0022	357 1.023
475	TTIGROUP-000	555 -	555 -	253 0.0016	284 0.0014	292 0.0014	300 0.0013	311 0.0013	283 1.013
476	TURINGTECHVIP-001	555 -	555 -	425 0.0091	452 0.0090	458 0.0090	468 0.0089	474 0.0089	445 1.081
477	UNISSEY-001	555 -	555 -	527 0.2098	531 0.2097	533 0.2097	534 0.2097	538 0.2097	531 2.887
478	UNISSEY-002	555 -	555 -	523 0.1808	527 0.1805	527 0.1805	530 0.1805	534 0.1804	526 2.625
479	UNISSEY-003	555 -	555 -	345 0.0031	376 0.0028	380 0.0027	391 0.0027	402 0.0026	373 1.025
480	USEB-000	555 -	555 -	486 0.0342	475 0.0153	471 0.0115	467 0.0089	451 0.0060	480 1.162
481	USEB-001	555 -	555 -	127 0.0009	129 0.0008	131 0.0007	134 0.0007	149 0.0007	129 1.007
482	USEB-002	555 -	555 -	175 0.0011	189 0.0010	199 0.0009	202 0.0009	216 0.0009	186 1.009
483	USEB-003	555 -	555 -	128 0.0009	134 0.0008	132 0.0007	138 0.0007	144 0.0007	130 1.007
484	USEB-004	555 -	555 -	150 0.0010	171 0.0009	177 0.0009	189 0.0009	200 0.0009	163 1.008
485	VD-000	555 -	555 -	541 0.4735	540 0.3202	538 0.2693	537 0.2212	531 0.1675	540 4.056
486	VD-001	555 -	555 -	480 0.0272	483 0.0178	487 0.0158	487 0.0143	490 0.0127	484 1.171
487	VD-002	555 -	555 -	426 0.0092	439 0.0073	443 0.0070	447 0.0067	458 0.0064	436 1.068
488	VD-003	555 -	555 -	407 0.0073	431 0.0065	435 0.0064	442 0.0063	455 0.0062	429 1.059
489	VDFSOFTWARE-001	555 -	555 -	526 0.2055	530 0.1958	529 0.1926	532 0.1893	536 0.1853	530 2.773
490	VDFSOFTWARE-002	555 -	555 -	277 0.0018	192 0.0010	152 0.0008	130 0.0007	103 0.0006	206 1.009
491	VERIDAS-001	555 -	555 -	319 0.0024	305 0.0016	290 0.0013	278 0.0012	277 0.0011	306 1.015
492	VERIDAS-002	555 -	555 -	318 0.0024	302 0.0016	287 0.0013	277 0.0012	276 0.0011	305 1.015
493	VERIDAS-003	555 -	555 -	237 0.0015	233 0.0011	228 0.0011	228 0.0010	227 0.0009	227 1.011
494	VERIDAS-004	555 -	555 -	160 0.0010	172 0.0009	183 0.0009	187 0.0009	195 0.0009	165 1.008
495	VERIGRAM-000	555 -	555 -	306 0.0022	342 0.0021	357 0.0021	370 0.0021	380 0.0021	337 1.019
496	VERIGRAM-001	555 -	555 -	304 0.0021	340 0.0020	355 0.0020	367 0.0020	378 0.0020	329 1.018
497	VERIJELAS-000	555 -	555 -	536 0.3545	537 0.2973	540 0.2802	539 0.2652	541 0.2486	537 3.742
498	VIANTE-000	555 -	555 -	138 0.0009	163 0.0009	169 0.0009	178 0.0008	187 0.0008	158 1.008
499	VIANTE-001	555 -	555 -	133 0.0009	156 0.0008	168 0.0008	179 0.0008	186 0.0008	152 1.008
500	VIGILANTSOLUTIONS-003	555 -	555 -	506 0.0691	502 0.0346	497 0.0259	495 0.0198	493 0.0137	502 1.352
501	VIGILANTSOLUTIONS-004	555 -	555 -	515 0.1246	513 0.0702	511 0.0553	509 0.0431	507 0.0302	513 1.696
502	VIGILANTSOLUTIONS-005	555 -	555 -	422 0.0089	403 0.0042	395 0.0033	387 0.0026	373 0.0019	406 1.043
503	VIGILANTSOLUTIONS-006	555 -	555 -	428 0.0096	409 0.0045	403 0.0035	393 0.0028	377 0.0020	410 1.046
504	VIGILANTSOLUTIONS-007	555 -	555 -	341 0.0030	308 0.0016	289 0.0013	275 0.0012	233 0.0010	316 1.016

Table 51: **Rank-based accuracy for the FRVT 2018 mugshot sets**. *In columns 3 and 4 are template size and template generation duration. Thereafter values are rank-based FNIR with T = 0 and FPIR = 1. This is appropriate to investigational uses but not those with higher volumes where candidates from all searches would need review. The next column is a workload statistic, a small value shows an algorithm front-loads mates into the first 10 candidates. Throughout, blue superscripts indicate the rank of the algorithm for that column, and the best value is highlighted in yellow.*

This publication is available free of charge from: https://doi.org/10.6028/NIST.IR.8271

MISSES OUTSIDE RANK R		RESOURCE USAGE		ENROL MOST RECENT, N = 1.6M					
FNIR(N, T=0, R)		TEMPLATE		FRVT 2018 MUGSHOTS					
#	ALGORITHM	BYTES	MSEC	R=1	R=5	R=10	R=20	R=50	WORK-10
505	VIGILANTSOLUTIONS-008	555 -	555 -	327 0.0026	297 0.0015	275 0.0012	257 0.0011	221 0.0009	304 1.014
506	VINBIGDATA-001	555 -	555 -	126 0.0009	75 0.0006	68 0.0006	66 0.0005	63 0.0005	80 1.006
507	VINBIGDATA-002	555 -	555 -	44 0.0006	27 0.0005	37 0.0005	40 0.0005	35 0.0005	32 1.005
508	VINBIGDATA-003	555 -	555 -	34 0.0006	44 0.0005	42 0.0005	45 0.0005	43 0.0005	41 1.005
509	VINBIGDATA-004	555 -	555 -	36 0.0006	42 0.0005	45 0.0005	30 0.0005	31 0.0005	42 1.005
510	VISIONBOX-000	555 -	555 -	254 0.0016	239 0.0012	241 0.0011	229 0.0010	214 0.0009	241 1.011
511	VISIONBOX-001	555 -	555 -	328 0.0026	360 0.0024	374 0.0023	377 0.0023	393 0.0023	349 1.022
512	VISIONBOX-002	555 -	555 -	238 0.0015	262 0.0013	273 0.0012	284 0.0012	296 0.0012	256 1.012
513	VISIONLABS-004	555 -	555 -	329 0.0026	319 0.0017	319 0.0016	317 0.0015	318 0.0013	319 1.016
514	VISIONLABS-005	555 -	555 -	311 0.0023	311 0.0016	307 0.0015	301 0.0013	300 0.0013	308 1.015
515	VISIONLABS-006	555 -	555 -	276 0.0018	283 0.0014	283 0.0013	292 0.0013	298 0.0012	289 1.013
516	VISIONLABS-007	555 -	555 -	274 0.0017	277 0.0013	276 0.0013	283 0.0012	291 0.0012	276 1.012
517	VISIONLABS-008	555 -	555 -	263 0.0016	295 0.0015	304 0.0014	307 0.0014	320 0.0013	292 1.013
518	VISIONLABS-009	555 -	555 -	104 0.0008	116 0.0007	118 0.0007	121 0.0007	118 0.0006	110 1.006
519	VISIONLABS-010	555 -	555 -	171 0.0010	191 0.0010	201 0.0009	198 0.0009	208 0.0009	185 1.009
520	VISIONLABS-011	555 -	555 -	116 0.0008	127 0.0008	139 0.0008	135 0.0007	141 0.0007	126 1.007
521	VISTEAM-000	555 -	555 -	379 0.0048	343 0.0021	322 0.0016	296 0.0013	245 0.0010	350 1.022
522	VISTEAM-001	555 -	555 -	385 0.0053	362 0.0024	341 0.0018	316 0.0015	272 0.0011	370 1.025
523	VIXVIZION-009	555 -	555 -	290 0.0019	250 0.0012	231 0.0011	215 0.0010	185 0.0008	255 1.012
524	VNIS-000	555 -	555 -	513 0.1054	517 0.0880	517 0.0825	518 0.0771	521 0.0707	517 1.811
525	VNPAY-001	555 -	555 -	180 0.0011	207 0.0010	211 0.0010	211 0.0009	213 0.0009	197 1.009
526	VNPT-001	555 -	555 -	280 0.0018	300 0.0015	311 0.0015	318 0.0015	334 0.0014	298 1.014
527	VNPT-002	555 -	555 -	246 0.0015	292 0.0014	301 0.0014	308 0.0014	323 0.0014	288 1.013
528	VNPT-003	555 -	555 -	206 0.0013	240 0.0012	259 0.0012	268 0.0011	281 0.0011	235 1.011
529	VNPT-004	555 -	555 -	208 0.0013	243 0.0012	254 0.0011	270 0.0011	284 0.0011	233 1.011
530	VNPT-005	555 -	555 -	210 0.0013	242 0.0012	250 0.0011	264 0.0011	278 0.0011	231 1.011
531	VOCORD-003	555 -	555 -	392 0.0060	383 0.0032	382 0.0027	380 0.0024	383 0.0021	387 1.032
532	VOCORD-004	555 -	555 -	411 0.0077	411 0.0046	414 0.0040	416 0.0036	418 0.0032	408 1.045
533	VOCORD-005	555 -	555 -	402 0.0068	406 0.0044	409 0.0039	414 0.0036	422 0.0033	404 1.042
534	VOCORD-006	555 -	555 -	553 1.0000	555 1.0000	554 1.0000	553 1.0000	554 1.0000	555 10.000
535	VTCC-000	555 -	555 -	365 0.0041	396 0.0039	408 0.0039	421 0.0039	428 0.0038	392 1.036
536	VTCC-001	555 -	555 -	273 0.0017	304 0.0016	317 0.0015	328 0.0015	339 0.0015	300 1.014
537	VTCC-002	555 -	555 -	268 0.0017	303 0.0016	316 0.0015	327 0.0015	338 0.0015	299 1.014
538	VTS-000	555 -	555 -	544 0.5936	545 0.5935	545 0.5935	546 0.5935	547 0.5935	545 6.341
539	VTS-001	555 -	555 -	197 0.0012	145 0.0008	127 0.0007	130 0.0007	121 0.0007	156 1.008
540	VTS-002	555 -	555 -	255 0.0016	214 0.0010	193 0.0009	183 0.0009	160 0.0008	222 1.010
541	VTS-003	555 -	555 -	108 0.0008	84 0.0006	73 0.0006	63 0.0005	62 0.0005	82 1.006
542	VTS-004	555 -	555 -	61 0.0006	47 0.0005	48 0.0005	46 0.0005	36 0.0005	50 1.005
543	VTS-005	555 -	555 -	51 0.0006	51 0.0005	35 0.0005	35 0.0005	29 0.0005	46 1.005
544	WINK-000	555 -	555 -	481 0.0291	481 0.0170	480 0.0142	481 0.0121	480 0.0100	482 1.168
545	WINK-001	555 -	555 -	324 0.0026	312 0.0016	299 0.0014	293 0.0013	288 0.0011	312 1.016
546	WINK-002	555 -	555 -	152 0.0010	110 0.0007	96 0.0006	94 0.0006	83 0.0006	120 1.007
547	XFORWARDAI-000	555 -	555 -	291 0.0019	315 0.0017	324 0.0016	334 0.0016	347 0.0016	309 1.015
548	XFORWARDAI-001	555 -	555 -	272 0.0017	306 0.0016	318 0.0016	331 0.0015	346 0.0015	301 1.014
549	XFORWARDAI-002	555 -	555 -	258 0.0016	301 0.0015	315 0.0015	329 0.0015	344 0.0015	297 1.014
550	YISHENG-001	555 -	555 -	479 0.0262	469 0.0128	464 0.0099	459 0.0077	448 0.0057	470 1.131
551	YITU-002	555 -	555 -	245 0.0015	183 0.0009	170 0.0009	159 0.0008	147 0.0007	204 1.009
552	YITU-003	555 -	555 -	325 0.0026	336 0.0020	348 0.0019	356 0.0018	364 0.0018	330 1.019
553	YITU-004	555 -	555 -	164 0.0010	113 0.0007	104 0.0007	100 0.0006	108 0.0006	125 1.007
554	YITU-005	555 -	555 -	302 0.0021	323 0.0018	334 0.0018	346 0.0017	358 0.0017	321 1.017
555	YUAN-000	555 -	555 -	224 0.0014	279 0.0013	291 0.0013	303 0.0013	319 0.0013	269 1.012

Table 52: **Rank-based accuracy for the FRVT 2018 mugshot sets**. *In columns 3 and 4 are template size and template generation duration. Thereafter values are rank-based FNIR with T = 0 and FPIR = 1. This is appropriate to investigational uses but not those with higher volumes where candidates from all searches would need review. The next column is a workload statistic, a small value shows an algorithm front-loads mates into the first 10 candidates. Throughout, blue superscripts indicate the rank of the algorithm for that column, and the best value is highlighted in yellow.*

This publication is available free of charge from: https://doi.org/10.6028/NIST.IR.8271

MISSES BELOW THRESHOLD, T		ENROL RECENT MUGSHOT, N = 1.6M									ENROL APPLICATION PORTRAIT, N = 1.6M					
		ENROL: MUGSHOT			ENROL: MUGSHOT			ENROL: MUGSHOT			ENROL: VISA		ENROL: BORDER		ENROL: VISA	
		PROBE: MUGSHOT			PROBE: WEBCAM			PROBE: PROFILE			PROBE: BORDER		PROBE: BORDER 10+YR		PROBE: KIOSK	
#	ALGORITHM	FPIR=0.0003	FPIR=0.001	FPIR=0.01	FPIR=0.0003	FPIR=0.001	FPIR=0.01	FPIR=0.0003	FPIR=0.001	FPIR=0.01	FPIR=0.001	FPIR=0.01	FPIR=0.001	FPIR=0.01	FPIR=0.001	FPIR=0.01
1	20FACE-000	483 0.462	499 0.347	506 0.229	480 0.763	466 0.450	484 0.301	437 1.000	473 1.000	470 1.000	412 0.424	418 0.255	265 0.772	297 0.599	410 0.938	431 0.836
2	3DIVI-003	486 0.481	508 0.400	514 0.281	469 0.685	488 0.626	504 0.497				431 0.605	438 0.445			327 0.821	416 0.717
3	3DIVI-004	446 0.255	466 0.168	472 0.093	419 0.400	451 0.343	474 0.237				390 0.277	406 0.172			336 0.607	381 0.485
4	3DIVI-005	445 0.254	463 0.166	471 0.092	418 0.395	449 0.339	473 0.234	341 0.998	352 0.996	383 0.990	449 0.864	456 0.846			334 0.597	380 0.484
5	3DIVI-006	443 0.252	465 0.167	474 0.095	422 0.403	450 0.342	475 0.238				391 0.283	407 0.174			339 0.615	382 0.490
6	AADI-000	547 1.000	547 1.000	549 1.000	555 1.000	549 1.000	554 1.000	510 1.000	552 1.000	495 1.000	531 1.000	494 1.000	418 1.000	357 1.000	520 1.000	514 1.000
7	AADI-001								429 1.000	441 0.998						460 1.000
8	AADI-002	530 0.952	536 0.939	540 0.899	523 0.995	531 0.992	536 0.980	387 1.000	395 0.999	425 0.997	462 0.995	462 0.986	308 0.999	329 0.997	437 0.998	456 0.996
9	ACER-000	425 0.207	455 0.145	461 0.073	395 0.300	421 0.246	443 0.157	258 0.987	283 0.981	336 0.955	381 0.201	399 0.114			312 0.490	359 0.363
10	ACER-001	358 0.108	388 0.056	395 0.025	314 0.136	336 0.109	357 0.069	385 1.000	406 0.999	440 0.998	319 0.068	335 0.036	233 0.406	269 0.250	311 0.479	285 0.206
11	ADIANCE-001	548 1.000	554 1.000	552 1.000	531 1.000	536 1.000	540 1.000	507 1.000	550 1.000	555 1.000	446 0.833	454 0.828	317 1.000	342 1.000	407 0.931	433 0.852
12	ADVANCE-000	257 0.038	289 0.020	284 0.008	413 0.371	435 0.270	419 0.112	328 0.997	265 0.973	218 0.470	368 0.163	349 0.047	277 0.884	302 0.667	262 0.326	291 0.209
13	AFISBIOMETRICS-000	299 0.053	336 0.029	319 0.010	273 0.104	296 0.081	296 0.044	135 0.619	152 0.511	192 0.340	269 0.034	267 0.015	173 0.154	197 0.080	195 0.172	214 0.127
14	AFRENGINE-000	241 0.033	285 0.019	303 0.009	412 0.364	436 0.271	436 0.149	125 0.565	120 0.360	156 0.237	382 0.206	398 0.114	260 0.743	237 0.135	254 0.308	306 0.231
15	AFRENGINE-001	100 0.008	102 0.003	152 0.002	155 0.041	166 0.031	182 0.020	121 0.550	92 0.227	89 0.119	208 0.018	251 0.013	147 0.113	163 0.051	138 0.120	162 0.097
16	AFRENGINE-002	84 0.006	93 0.003	138 0.002	171 0.046	137 0.026	150 0.018	191 0.901	116 0.344	71 0.106	149 0.008	143 0.004	284 0.926	142 0.039	113 0.102	96 0.075
17	AFRENGINE-003	107 0.008	144 0.004	204 0.003	164 0.045	177 0.033	190 0.022	87 0.333	67 0.183	79 0.113	172 0.011	161 0.005	140 0.097	141 0.039	129 0.111	120 0.083
18	AIZE-001	371 0.126	411 0.076	412 0.033	350 0.187	368 0.143	385 0.087	306 0.995	331 0.994	368 0.983	340 0.101	356 0.052	223 0.364	262 0.216	278 0.387	333 0.289
19	AIZE-002	512 0.787	374 0.051	361 0.019	540 1.000	530 0.981	350 0.065	465 1.000	464 1.000	473 1.000	402 0.355	331 0.036	330 1.000	273 0.272	481 1.000	470 1.000
20	AKUVOX-001	222 0.026	246 0.013	242 0.005	219 0.067	229 0.050	238 0.031	230 0.979	251 0.964	287 0.844	214 0.019	215 0.009	257 0.737	274 0.275	164 0.141	181 0.110
21	ALCHERA-000	435 0.228	452 0.138	455 0.070	382 0.259	405 0.216	435 0.146	358 0.999	381 0.999	418 0.996	324 0.176	396 0.111			323 0.803	375 0.456
22	ALCHERA-001	544 1.000	544 0.999	547 0.999	539 1.000	543 1.000	545 1.000				505 1.000	522 1.000			483 1.000	486 1.000
23	ALCHERA-002	515 0.806	516 0.485	517 0.301	468 0.685	483 0.591	499 0.442	414 1.000	414 1.000	449 0.999	445 0.827	452 0.770			324 0.811	411 0.705
24	ALCHERA-003	478 0.449	457 0.155	456 0.070	396 0.304	417 0.239	441 0.152	400 1.000	398 0.999	424 0.997	373 0.172	388 0.097			304 0.464	358 0.362
25	ALCHERA-004	490 0.519	507 0.394	503 0.211	461 0.642	478 0.529	490 0.327	307 0.995	319 0.991	280 0.811	413 0.424	416 0.232	252 0.708	290 0.515	326 0.546	370 0.398
26	ALCHERA-005	476 0.432	495 0.314	491 0.145	445 0.534	464 0.439	477 0.258	277 0.991	297 0.985	319 0.935	397 0.305	404 0.144	281 0.908	289 0.502	300 0.455	343 0.309
27	ALCHERA-006	157 0.012	154 0.005	150 0.002	124 0.033	124 0.025	138 0.017	268 0.989	286 0.982	307 0.913	90 0.006	89 0.003	242 0.493	182 0.068	92 0.094	82 0.072
28	ALCHERA-007	117 0.009	115 0.004	120 0.002	107 0.029	110 0.023	123 0.016	278 0.991	289 0.982	299 0.885	74 0.005	77 0.003	261 0.743	211 0.086	70 0.087	73 0.069
29	ALCHERA-008	97 0.008	108 0.003	109 0.002	108 0.029	99 0.022	109 0.015	69 0.272	62 0.177	68 0.105	169 0.010	64 0.002	321 1.000	321 0.975	208 0.186	144 0.090
30	ALGORITHMSINC-000	245 0.034	268 0.016	279 0.007	417 0.394	357 0.130	256 0.033	160 0.760	150 0.507	200 0.367	342 0.108	260 0.014	335 1.000	330 0.997	294 0.433	244 0.153
31	ALLGOVISION-000	382 0.138	425 0.088	435 0.045	363 0.202	385 0.166	415 0.106	286 0.993	315 0.990	366 0.982	345 0.117	368 0.066			321 0.526	369 0.396
32	ALLGOVISION-001	397 0.154	432 0.101	442 0.052	388 0.275	409 0.221	434 0.141	292 0.993	299 0.986	316 0.932	362 0.150	381 0.081			313 0.491	367 0.389
33	ALLGOVISION-002	372 0.132	402 0.065	400 0.028	478 0.753	477 0.520	420 0.113	242 0.983	240 0.950	293 0.868	384 0.232	353 0.049	475 1.000	348 1.000	358 0.716	361 0.366
34	ALLGOVISION-003	239 0.032	272 0.017	274 0.007	232 0.075	253 0.059	271 0.037	144 0.656	167 0.566	208 0.423	225 0.021	228 0.010	165 0.147	208 0.082	310 0.478	223 0.133
35	ALLGOVISION-004	403 0.164	437 0.114	450 0.059	371 0.229	397 0.190	424 0.120	173 0.804	197 0.747	249 0.627	346 0.121	367 0.066	235 0.418	272 0.271	287 0.412	321 0.262
36	ALTTEKGLOBAL-000	454 0.282	489 0.278	512 0.275	387 0.272	432 0.267	478 0.259	141 0.646	174 0.617	237 0.571	407 0.383	431 0.381	245 0.536	285 0.434	344 0.641	405 0.636
37	ANKE-000	410 0.183	439 0.117	452 0.062	380 0.256	408 0.220	439 0.151	303 0.995	330 0.994	380 0.990	475 1.000	541 1.000			461 1.000	499 1.000
38	ANKE-001	409 0.183	442 0.119	453 0.062	381 0.256	407 0.220	440 0.151	308 0.995	338 0.994	395 0.992	469 1.000	554 1.000			449 1.000	493 1.000
39	ANKE-002	313 0.062	341 0.031	342 0.013	271 0.103	292 0.079	314 0.050	222 0.974	239 0.947	275 0.793	270 0.034	285 0.018			230 0.245	279 0.190
40	ANTHEUS-000	323 0.066	355 0.041	368 0.020	484 0.805	494 0.664	393 0.093	197 0.927	204 0.793	241 0.598	448 0.862	441 0.548	406 1.000	358 1.000	422 0.972	435 0.900
41	ARATEK-001	388 0.141	206 0.008	184 0.003	506 0.958	226 0.050	178 0.020	438 1.000	474 1.000	450 0.999	333 0.086	174 0.005	293 0.971	153 0.045	553 1.000	458 0.999
42	ARMATURA-000	111 0.008	131 0.004	161 0.002	120 0.031	127 0.025	158 0.018	73 0.283	85 0.214	93 0.124	92 0.006	99 0.003	78 0.048	73 0.019	82 0.090	87 0.073
43	AWARE-003	406 0.173	446 0.128	464 0.082	409 0.351	443 0.298	464 0.204	255 0.986	294 0.984	357 0.977	414 0.428	430 0.378			322 0.530	374 0.443
44	AWARE-004	466 0.354	487 0.268	496 0.174	457 0.619	475 0.509	495 0.375	407 1.000	416 1.000	452 0.999	408 0.397	421 0.279			375 0.816	402 0.631
45	AWARE-005	497 0.606	502 0.363	466 0.085	403 0.342	424 0.253	446 0.163	403 1.000	428 1.000	453 0.999	388 0.255	401 0.122			398 0.916	414 0.714
46	AWARE-006	484 0.470	488 0.275	497 0.175	438 0.466	457 0.398	481 0.283	381 1.000	409 0.999	444 0.999	404 0.368	417 0.254			363 0.749	399 0.623

Table 53: **Threshold-based accuracy**. *Values are FNIR(N, T, L) with N = 1.6 million with thresholds set to produce FPIR = 0.0003, 0.001, and 0.01 in non-mate searches. Throughout blue superscripts indicate the rank of the algorithm for that column. Caution: The Power-low models are mostly intended to draw attention to the kind of behavior, not as a model to be used for prediction.*

2026/01/09 20:40:38

FNIR(N, R, T) = FPIR(N, T) =

False neg. identification rate
False pos. identification rate

N = Num. enrolled subjects
R = Num. candidates examined

T = Threshold

T = 0 → Investigation
T > 0 → Identification

This publication is available free of charge from: https://doi.org/10.6028/NIST.IR.8271

MISSES BELOW THRESHOLD, T		ENROL RECENT MUGSHOT, N = 1.6M									ENROL APPLICATION PORTRAIT, N = 1.6M					
		ENROL: MUGSHOT			ENROL: MUGSHOT			ENROL: MUGSHOT			ENROL: VISA		ENROL: BORDER		ENROL: VISA	
		PROBE: MUGSHOT			PROBE: WEBCAM			PROBE: PROFILE			PROBE: BORDER		PROBE: BORDER 10+YR		PROBE: KIOSK	
#	ALGORITHM	FPIR=0.0003	FPIR=0.001	FPIR=0.01	FPIR=0.0003	FPIR=0.001	FPIR=0.01	FPIR=0.0003	FPIR=0.001	FPIR=0.01	FPIR=0.001	FPIR=0.01	FPIR=0.001	FPIR=0.01	FPIR=0.001	FPIR=0.01
47	AWARE-007	[231]0.029	[267]0.016	[275]0.007	[356]0.197	[274]0.070	[272]0.038	[335]0.998	[322]0.992	[262]0.694	[290]0.044	[298]0.021	[296]0.982	[278]0.338	[233]0.250	[265]0.177
48	AWIROS-000	[510]0.761	[491]0.291	[419]0.037	[492]0.909	[471]0.471	[417]0.109	[425]1.000	[443]1.000	[474]1.000	[458]0.976	[427]0.320	[368]1.000	[333]0.998	[441]0.999	[437]0.924
49	AYONIX-000	[518]0.846	[530]0.811	[536]0.724	[505]0.956	[524]0.939	[530]0.892	[342]0.998	[368]0.998	[416]0.995	[455]0.954	[458]0.891			[425]0.982	[443]0.959
50	AYONIX-001	[522]0.874	[532]0.824	[534]0.701	[499]0.946	[519]0.920	[526]0.845	[398]1.000	[407]0.999	[420]0.996	[464]0.999	[465]0.998			[420]0.969	[439]0.926
51	AYONIX-002	[523]0.874	[531]0.824	[535]0.701	[500]0.946	[520]0.920	[525]0.845	[399]1.000	[404]0.999	[419]0.996	[451]0.915	[453]0.821			[419]0.969	[438]0.926
52	BIOIDTECHSWISS-001	[121]0.009	[125]0.004	[111]0.002	[145]0.038	[162]0.030	[204]0.023	[324]0.997	[301]0.987	[149]0.207	[166]0.010	[194]0.007	[116]0.067	[136]0.036	[203]0.179	[260]0.172
53	BIOMETRIK-001	[362]0.115	[376]0.052	[384]0.023	[303]0.129	[325]0.098	[334]0.058	[455]1.000	[422]1.000	[423]0.997	[303]0.054	[319]0.027	[221]0.341	[256]0.183	[340]0.618	[276]0.188
54	CAMVI-003	[345]0.094	[406]0.071	[447]0.057	[326]0.152	[359]0.132	[416]0.108	[231]0.979	[259]0.970	[323]0.940	[344]0.114	[390]0.100			[283]0.402	[364]0.377
55	CAMVI-004	[356]0.106	[407]0.071	[445]0.054	[376]0.240	[361]0.136	[402]0.100	[383]1.000	[403]0.999	[429]0.998	[339]0.100	[380]0.081			[320]0.787	[384]0.507
56	CAMVI-005	[383]0.138	[430]0.099	[463]0.076	[434]0.451	[394]0.179	[429]0.132	[388]1.000	[413]1.000	[438]0.998	[365]0.156	[397]0.112			[438]0.999	[450]0.983
57	CANON-001	[147]0.012	[162]0.005	[159]0.002	[114]0.031	[116]0.023	[110]0.015	[137]0.629	[118]0.357	[150]0.208	[133]0.008	[141]0.004	[119]0.068	[129]0.034	[159]0.139	[150]0.092
58	CANON-002	[123]0.009	[140]0.004	[146]0.002	[93]0.027	[90]0.020	[82]0.013	[105]0.481	[128]0.400	[161]0.245	[190]0.013	[147]0.004	[127]0.075	[154]0.046	[211]0.188	[174]0.106
59	CANON-003	[63]0.005	[71]0.002	[57]0.001	[43]0.015	[51]0.012	[53]0.010	[20]0.274	[76]0.199	[97]0.127	[89]0.006	[157]0.004	[39]0.030	[48]0.014	[40]0.076	[45]0.063
60	CIB-000	[271]0.044	[239]0.012	[231]0.005	[234]0.077	[218]0.045	[215]0.025	[424]1.000	[438]1.000	[465]1.000	[207]0.017	[202]0.008	[158]0.141	[183]0.068	[393]0.894	[386]0.521
61	CLEARVIEWAI-000	[162]0.013	[171]0.005	[155]0.002	[142]0.036	[131]0.025	[121]0.016	[362]0.999	[266]0.974	[109]0.139	[134]0.008	[130]0.004	[98]0.057	[104]0.027	[243]0.268	[112]0.080
62	CLEARVIEWAI-001	[96]0.007	[112]0.003	[92]0.001	[88]0.026	[89]0.020	[81]0.013	[45]0.234	[55]0.167	[58]0.093	[82]0.005	[61]0.002	[70]0.042	[64]0.016	[54]0.079	[59]0.066
63	CLEARVIEWAI-002	[106]0.008	[123]0.004	[102]0.002	[103]0.029	[98]0.022	[89]0.013	[55]0.250	[58]0.170	[60]0.095	[83]0.006	[73]0.002	[69]0.041	[66]0.017	[48]0.078	[55]0.066
64	CLEARVIEWAI-003	[64]0.005	[70]0.002	[65]0.001	[70]0.019	[68]0.015	[58]0.010	[18]0.172	[33]0.128	[30]0.074	[69]0.005	[55]0.002	[60]0.038	[53]0.015	[50]0.079	[53]0.065
65	CLOUDWALK-HR-000	[50]0.004	[59]0.002	[84]0.001	[50]0.015	[57]0.013	[71]0.012	[22]0.179	[31]0.123	[46]0.085	[70]0.005	[110]0.003	[47]0.033	[70]0.018	[105]0.099	[97]0.075
66	CLOUDWALK-MT-000	[34]0.003	[57]0.002	[97]0.001	[44]0.015	[56]0.013	[75]0.012	[13]0.160	[18]0.099	[25]0.066	[33]0.002	[46]0.002	[14]0.018	[21]0.009	[33]0.072	[46]0.063
67	CLOUDWALK-MT-001	[28]0.003	[52]0.002	[91]0.001	[32]0.013	[44]0.012	[70]0.011	[3]0.093	[4]0.059	[8]0.049	[8]0.001	[6]0.001	[10]0.015	[9]0.006	[7]0.056	[8]0.049
68	CLOUDWALK-MT-002	[26]0.003	[49]0.002	[89]0.001	[27]0.012	[41]0.011	[67]0.011	[1]0.070	[2]0.053	[5]0.045	[5]0.001	[4]0.001	[6]0.013	[5]0.005	[6]0.055	[5]0.047
69	COGENT-000	[391]0.143	[378]0.052	[402]0.029	[341]0.175	[365]0.140	[404]0.100	[314]0.996	[343]0.995	[391]0.991						
70	COGENT-001	[390]0.143	[379]0.052	[401]0.029	[342]0.175	[364]0.140	[405]0.100	[315]0.996	[344]0.995	[392]0.991						
71	COGENT-002	[400]0.157	[362]0.044	[356]0.017	[298]0.124	[324]0.098	[347]0.063	[351]0.998	[366]0.998	[402]0.994						
72	COGENT-003	[423]0.199	[365]0.045	[349]0.015	[296]0.121	[318]0.095	[343]0.061	[352]0.999	[370]0.998	[412]0.995						
73	COGENT-004	[428]0.209	[342]0.033	[249]0.006	[217]0.067	[230]0.051	[242]0.031	[340]0.998	[364]0.997	[415]0.995	[229]0.022	[244]0.012	[151]0.126	[186]0.072	[301]0.456	[268]0.178
74	COGENT-005	[289]0.050	[214]0.009	[218]0.003	[181]0.050	[193]0.037	[206]0.023	[311]0.996	[309]0.989	[186]0.315	[174]0.011	[185]0.006	[132]0.082	[149]0.043	[396]0.905	[281]0.202
75	COGENT-006	[134]0.010	[134]0.004	[132]0.002	[127]0.033	[117]0.023	[115]0.015	[95]0.376	[95]0.229	[104]0.135	[103]0.006	[116]0.003	[236]0.422	[110]0.028	[150]0.130	[197]0.120
76	COGENT-007	[101]0.008	[109]0.003	[103]0.002	[96]0.027	[96]0.021	[106]0.014	[49]0.241	[68]0.185	[85]0.116	[105]0.006	[112]0.003	[76]0.047	[81]0.022	[170]0.144	[217]0.129
77	COGNITEC-000	[433]0.225	[461]0.160	[473]0.095	[430]0.439	[444]0.303	[462]0.200	[310]0.995	[320]0.992	[345]0.971						
78	COGNITEC-001	[421]0.191	[431]0.101	[443]0.052	[525]0.997	[413]0.230	[431]0.135	[519]1.000	[486]1.000	[341]0.965						
79	COGNITEC-002	[367]0.120	[381]0.053	[390]0.024	[520]0.990	[393]0.178	[409]0.101	[511]1.000	[439]1.000	[337]0.956						
80	COGNITEC-003	[350]0.099	[377]0.052	[392]0.025	[370]0.222	[383]0.162	[403]0.100	[480]1.000	[444]1.000	[326]0.945						
81	COGNITEC-004	[301]0.055	[340]0.031	[343]0.013	[301]0.127	[322]0.097	[335]0.058	[305]0.995	[312]0.990	[310]0.918	[317]0.068	[336]0.038	[215]0.316	[261]0.196	[248]0.288	[298]0.218
82	COGNITEC-005	[303]0.055	[219]0.009	[210]0.003	[201]0.058	[207]0.041	[199]0.022	[545]1.000	[511]1.000	[296]0.877	[285]0.041	[320]0.028	[175]0.157	[216]0.092	[202]0.179	[237]0.145
83	COGNITEC-006	[230]0.029	[201]0.007	[194]0.003	[211]0.065	[203]0.040	[193]0.022	[520]1.000	[487]1.000	[445]0.999	[256]0.030	[256]0.013	[181]0.171	[202]0.081	[352]0.681	[295]0.214
84	COGNITEC-007	[167]0.013	[169]0.005	[165]0.002	[183]0.051	[181]0.034	[171]0.019	[156]0.735	[177]0.621	[220]0.483	[241]0.026	[243]0.012	[195]0.210	[210]0.085	[187]0.160	[208]0.124
85	COGNITEC-008	[171]0.014	[175]0.006	[171]0.002	[177]0.048	[185]0.035	[181]0.020	[143]0.653	[166]0.564	[206]0.414	[242]0.026	[239]0.011	[161]0.142	[181]0.068	[179]0.155	[205]0.122
86	COGNITEC-009	[172]0.014	[179]0.006	[183]0.003	[175]0.048	[186]0.035	[180]0.020	[138]0.633	[165]0.554	[207]0.415	[238]0.025	[240]0.011	[149]0.124	[169]0.059	[181]0.156	[211]0.126
87	COMPAL-000	[461]0.323	[204]0.008	[196]0.003	[170]0.046	[199]0.038	[229]0.028			[483]1.000	[321]0.072	[371]0.068	[142]0.104	[201]0.081	[171]0.147	[228]0.135
88	COMPAL-001	[469]0.366	[242]0.012	[285]0.008	[169]0.046	[176]0.033	[200]0.023	[288]0.993	[132]0.422	[105]0.136	[188]0.013	[213]0.009	[135]0.090	[124]0.033	[134]0.117	[126]0.084
89	CORSIGHT-000	[180]0.016	[180]0.006	[172]0.002	[146]0.038	[155]0.029	[151]0.018	[217]0.971	[154]0.517	[132]0.173	[158]0.009	[153]0.004	[117]0.067	[125]0.033	[333]0.594	[136]0.088
90	CORSIGHT-001	[178]0.015	[188]0.006	[170]0.002	[162]0.043	[178]0.034	[174]0.020	[192]0.903	[142]0.460	[131]0.171	[144]0.008	[146]0.004	[104]0.062	[116]0.030	[158]0.138	[116]0.082
91	CUBOX-000	[57]0.004	[84]0.002	[101]0.002	[79]0.022	[83]0.019	[97]0.014	[65]0.267	[50]0.158	[59]0.093	[62]0.004	[82]0.003	[36]0.028	[49]0.014	[34]0.073	[43]0.062
92	CUBOX-001	[65]0.005	[89]0.003	[93]0.001	[89]0.026	[93]0.021	[98]0.014	[81]0.311	[84]0.212	[88]0.118	[113]0.007	[108]0.003	[121]0.068	[86]0.023	[64]0.085	[60]0.067

Table 54: **Threshold-based accuracy**. *Values are FNIR(N, T, L) with N = 1.6 million with thresholds set to produce FPIR = 0.0003, 0.001, and 0.01 in non-mate searches. Throughout blue superscripts indicate the rank of the algorithm for that column. Caution: The Power-low models are mostly intended to draw attention to the kind of behavior, not as a model to be used for prediction.*

FNIR(N, R, T) = False neg. identification rate
FPIR(N, T) = False pos. identification rate
N = Num. enrolled subjects
R = Num. candidates examined
T = Threshold
T = 0 → Investigation
T > 0 → Identification

This publication is available free of charge from: https://doi.org/10.6028/NIST.IR.8271

MISSES BELOW THRESHOLD, T		ENROL RECENT MUGSHOT, N = 1.6M									ENROL APPLICATION PORTRAIT, N = 1.6M					
		ENROL: MUGSHOT			ENROL: MUGSHOT			ENROL: MUGSHOT			ENROL: VISA		ENROL: BORDER		ENROL: VISA	
		PROBE: MUGSHOT			PROBE: WEBCAM			PROBE: PROFILE			PROBE: BORDER		PROBE: BORDER 10+YR		PROBE: KIOSK	
#	ALGORITHM	FPIR=0.0003	FPIR=0.001	FPIR=0.01	FPIR=0.0003	FPIR=0.001	FPIR=0.01	FPIR=0.0003	FPIR=0.001	FPIR=0.01	FPIR=0.001	FPIR=0.01	FPIR=0.001	FPIR=0.01	FPIR=0.001	FPIR=0.01
93	CUBOX-002	74 0.006	100 0.003	106 0.002	94 0.027	106 0.022	133 0.016	67 0.270	63 0.181	65 0.103	65 0.004	60 0.002	62 0.038	60 0.016	45 0.077	40 0.061
94	CUBOX-003	76 0.006	105 0.003	137 0.002	95 0.027	111 0.023	136 0.017	84 0.321	88 0.219	100 0.131	93 0.006	105 0.003	86 0.051	80 0.021	59 0.082	56 0.066
95	CYBERLINK-000	381 0.137	389 0.056	380 0.022	334 0.162	340 0.116	360 0.070	331 0.997	347 0.995	365 0.981	314 0.063	328 0.032			267 0.339	308 0.232
96	CYBERLINK-001	348 0.096	382 0.053	378 0.022	318 0.138	337 0.109	353 0.067	330 0.997	342 0.995	369 0.983	311 0.062	324 0.031			347 0.652	310 0.239
97	CYBERLINK-002	258 0.038	257 0.014	257 0.006	222 0.068	240 0.053	248 0.032	295 0.994	308 0.988	338 0.957	236 0.024	247 0.013			249 0.288	249 0.157
98	CYBERLINK-003	275 0.045	202 0.007	207 0.003	166 0.045	184 0.035	187 0.021	297 0.994	263 0.972	286 0.843	181 0.012	195 0.007	141 0.100	162 0.051	273 0.368	199 0.120
99	CYBERLINK-004	418 0.188	194 0.007	192 0.003	209 0.063	188 0.036	197 0.022	471 1.000	456 1.000	456 0.999	187 0.013	193 0.007	143 0.109	158 0.050	416 0.954	336 0.291
100	CYBERLINK-005	426 0.208	223 0.010	222 0.004	190 0.054	204 0.041	220 0.026	415 1.000	424 1.000	300 0.887	193 0.014	197 0.007	134 0.089	147 0.043	405 0.926	324 0.266
101	CYBERLINK-006	108 0.008	82 0.002	72 0.001	78 0.022	79 0.018	76 0.012	285 0.992	300 0.986	191 0.339	66 0.004	70 0.002	125 0.073	54 0.015	207 0.186	159 0.096
102	DAHUA-000	372 0.127	421 0.086	432 0.044	345 0.179	360 0.135	383 0.083									
103	DAHUA-001	355 0.105	409 0.072	416 0.036	325 0.151	348 0.122	373 0.075	257 0.987	279 0.980	317 0.933						
104	DAHUA-002	220 0.026	258 0.015	254 0.006	204 0.060	221 0.046	231 0.029	150 0.678	178 0.634	229 0.517	204 0.017	209 0.008			185 0.159	209 0.125
105	DAHUA-003	217 0.025	249 0.014	240 0.005	189 0.054	206 0.041	209 0.024	139 0.643	169 0.574	213 0.441	184 0.013	191 0.006	130 0.081	148 0.043	153 0.134	179 0.109
106	DAHUA-004	168 0.014	193 0.007	185 0.003	130 0.033	135 0.026	126 0.016	120 0.547	147 0.479	190 0.337	146 0.008	152 0.004	87 0.051	101 0.027	133 0.113	154 0.094
107	DAON-000	379 0.135	304 0.022	304 0.009	238 0.079	257 0.061	275 0.039	412 1.000	420 1.000	437 0.998	239 0.025	248 0.013	183 0.173	215 0.091	383 0.846	259 0.172
108	DAON-001	318 0.063	357 0.043	405 0.031	340 0.173	363 0.140	398 0.096	211 0.953	241 0.952	330 0.951	315 0.064	352 0.048	172 0.154	222 0.098	188 0.161	219 0.129
109	DAON-002	187 0.018	195 0.007	201 0.003	319 0.139	215 0.044	212 0.024			489 1.000	197 0.015	189 0.006	156 0.141	152 0.044	470 1.000	368 0.395
110	DATECH-000	264 0.041	203 0.007	198 0.003	272 0.104	197 0.038	175 0.020	337 0.998	356 0.996	367 0.982	201 0.016	177 0.005	283 0.926	300 0.632	256 0.311	184 0.111
111	DATECH-001	256 0.037	189 0.006	175 0.002	337 0.168	259 0.062	153 0.018	320 0.996	327 0.993	346 0.971	281 0.039	199 0.007	307 0.998	314 0.875	271 0.360	274 0.184
112	DECATUR-000	267 0.043	307 0.023	310 0.010	246 0.085	265 0.066	283 0.040	159 0.754	183 0.671	224 0.503	246 0.027	261 0.014	182 0.173	223 0.098	227 0.239	247 0.156
113	DEEPGLINT-001	128 0.010	99 0.003	114 0.002	63 0.018	59 0.014	54 0.010	427 1.000	411 1.000	222 0.498	108 0.006	150 0.004			184 0.159	160 0.097
114	DEEPSEA-001	329 0.073	367 0.046	376 0.021	305 0.129	328 0.101	338 0.059	263 0.988	296 0.984	351 0.973	327 0.077	342 0.041			263 0.326	315 0.251
115	DERMALOG-003	494 0.549	515 0.482	520 0.360	475 0.715	491 0.655	508 0.526				438 0.677	442 0.554			388 0.870	426 0.791
116	DERMALOG-004	495 0.553	514 0.479	519 0.358	473 0.711	492 0.657	506 0.526	322 0.997	348 0.995	394 0.991	429 0.603	440 0.458			385 0.856	421 0.751
117	DERMALOG-005	419 0.189	424 0.088	427 0.043	359 0.201	375 0.154	399 0.096	317 0.996	314 0.990	329 0.949	396 0.300	419 0.267			338 0.614	376 0.459
118	DERMALOG-006	347 0.095	375 0.051	394 0.025	316 0.137	330 0.105	352 0.067	266 0.989	282 0.981	318 0.933	309 0.059	326 0.031			261 0.318	305 0.230
119	DERMALOG-007	417 0.188	422 0.086	424 0.040	358 0.200	373 0.152	395 0.093	316 0.996	313 0.990	328 0.949	338 0.099	354 0.052			328 0.557	340 0.299
120	DERMALOG-008	448 0.267	364 0.045	355 0.017	373 0.231	315 0.094	327 0.054	446 1.000	451 1.000	467 1.000	305 0.057	314 0.025	228 0.382	250 0.158	411 0.940	409 0.678
121	DERMALOG-009	262 0.041	292 0.020	301 0.009	248 0.086	266 0.066	286 0.040	417 1.000	440 1.000	461 1.000	258 0.031	272 0.016	310 0.999	334 0.999	380 0.840	299 0.222
122	DERMALOG-010	192 0.018	192 0.007	206 0.003	312 0.134	244 0.055	203 0.023	382 1.000	390 0.999	332 0.951	335 0.089	344 0.041	316 1.000	319 0.971	319 0.522	294 0.211
123	DERMALOG-011	278 0.046	297 0.021	276 0.007	354 0.193	304 0.087	278 0.039	361 0.999	376 0.998	370 0.985	351 0.129	253 0.013	300 0.991	295 0.567	366 0.764	304 0.228
124	DERMALOG-012	265 0.041	296 0.021	280 0.007	251 0.089	268 0.067	281 0.040	201 0.932	148 0.505	178 0.294	231 0.023	234 0.011	166 0.147	190 0.076	286 0.409	206 0.123
125	DERMALOG-013	263 0.041	295 0.021	278 0.007	257 0.095	271 0.068	280 0.040	299 0.995	232 0.908	183 0.306	232 0.024	237 0.011	171 0.153	191 0.076	324 0.541	215 0.128
126	DERMALOG-014	266 0.042	299 0.021	296 0.008	258 0.095	272 0.069	288 0.041	300 0.995	231 0.907	185 0.312	249 0.028	276 0.016	174 0.156	198 0.080	293 0.432	236 0.144
127	DERMALOG-015	138 0.011	156 0.005	167 0.002	148 0.039	167 0.031	184 0.021	174 0.809	109 0.313	115 0.143	152 0.009	162 0.005	110 0.065	126 0.033	183 0.158	121 0.083
128	DIGIDATA-000	498 0.619	521 0.610	531 0.598	453 0.588	482 0.577	510 0.560	365 0.999	335 0.994	325 0.941	434 0.646	446 0.643	268 0.789	307 0.722	378 0.824	429 0.816
129	DILUSENSE-000	294 0.053	338 0.030	336 0.012	267 0.100	291 0.078	306 0.047	180 0.850	179 0.651	219 0.482	279 0.039	304 0.022	251 0.664	266 0.242	215 0.203	246 0.154
130	DILUSENSE-001	189 0.018	208 0.008	209 0.003	172 0.046	182 0.034	191 0.022	165 0.769	137 0.450	188 0.332	198 0.015	223 0.010	244 0.511	227 0.109	157 0.137	185 0.112
131	EINETWORKSINDIA-000	302 0.055	262 0.015	253 0.006	206 0.063	210 0.044	222 0.026	350 0.998	363 0.997	388 0.991	218 0.020	218 0.010	240 0.455	168 0.057	186 0.159	221 0.132
132	EINETWORKSINDIA-001	349 0.096	266 0.016	251 0.006	240 0.080	223 0.048	221 0.026	345 0.998	361 0.997	384 0.990	322 0.072	216 0.009	291 0.957	193 0.077	369 0.782	267 0.178
133	EINETWORKSINDIA-002	104 0.008	121 0.004	107 0.002	98 0.028	103 0.022	92 0.014	51 0.243	71 0.188	82 0.114	131 0.007	93 0.003	289 0.953	306 0.701	145 0.127	91 0.074
134	EYEDEA-003	488 0.507	505 0.387	511 0.265	459 0.625	480 0.543	497 0.404	321 0.997	339 0.994	379 0.989	427 0.570	433 0.392			371 0.792	407 0.658
135	F8-001	481 0.458	462 0.166	413 0.035				360 0.999	379 0.998	417 0.995						
136	FACEPHI-000	153 0.012	187 0.006	192 0.003	152 0.042	183 0.034	211 0.024	106 0.487	121 0.367	155 0.236	163 0.009	186 0.006	113 0.066	115 0.030	154 0.135	203 0.121
137	FASTLAHORE-000	480 0.457	477 0.214	476 0.098	542 1.000	540 1.000	541 1.000	467 1.000	442 1.000	462 1.000	486 1.000	531 1.000	506 1.000	533 1.000	475 1.000	466 1.000
138	FCI-000	240 0.033	183 0.006	199 0.003	126 0.033	138 0.026	164 0.019	232 0.979	243 0.957	282 0.820	150 0.008	144 0.004	266 0.777	292 0.538	115 0.103	109 0.079

Table 55: **Threshold-based accuracy**. *Values are FNIR(N, T, L) with N = 1.6 million with thresholds set to produce FPIR = 0.0003, 0.001, and 0.01 in non-mate searches. Throughout blue superscripts indicate the rank of the algorithm for that column. Caution: The Power-low models are mostly intended to draw attention to the kind of behavior, not as a model to be used for prediction.*

2026/01/09 20:40:38

FNIR(N, R, T) = FPIR(N, T) = False neg. identification rate / False pos. identification rate

N = Num. enrolled subjects
R = Num. candidates examined

T = Threshold

T = 0 → Investigation
T > 0 → Identification

This publication is available free of charge from: https://doi.org/10.6028/NIST.IR.8271

MISSES BELOW THRESHOLD, T		ENROL RECENT MUGSHOT, N = 1.6M									ENROL APPLICATION PORTRAIT, N = 1.6M					
		ENROL: MUGSHOT			ENROL: MUGSHOT			ENROL: MUGSHOT			ENROL: VISA		ENROL: BORDER		ENROL: VISA	
		PROBE: MUGSHOT			PROBE: WEBCAM			PROBE: PROFILE			PROBE: BORDER		PROBE: BORDER 10+YR		PROBE: KIOSK	
#	ALGORITHM	FPIR=0.0003	FPIR=0.001	FPIR=0.01	FPIR=0.0003	FPIR=0.001	FPIR=0.01	FPIR=0.0003	FPIR=0.001	FPIR=0.01	FPIR=0.001	FPIR=0.01	FPIR=0.001	FPIR=0.01	FPIR=0.001	FPIR=0.01
139	FINCORE-000	416 0.187	451 0.133	459 0.071	386 0.267	406 0.217	432 0.140	401 1.000	431 1.000	407 0.995	376 0.187	395 0.108	247 0.598	283 0.418	302 0.458	352 0.349
140	FIRSTCREDITKZ-001	79 0.006	87 0.003	79 0.001	85 0.025	84 0.019	86 0.013	94 0.372	104 0.282	129 0.167	126 0.007	140 0.004	103 0.061	111 0.028	101 0.097	108 0.079
141	FPT-000	376 0.129	217 0.009	219 0.004	462 0.643	453 0.372	268 0.036	363 0.999	380 0.999	387 0.991	403 0.360	389 0.100	383 1.000	345 1.000	408 0.935	408 0.668
142	FUJITSULAB-000	439 0.246	293 0.020	294 0.008	225 0.070	247 0.056	261 0.035				233 0.024	255 0.013	184 0.177	220 0.093	228 0.240	248 0.156
143	FUJITSULAB-001	502 0.655	280 0.018	264 0.006	284 0.112	249 0.058	250 0.033	313 0.996	324 0.992	324 0.940	235 0.024	241 0.011	258 0.739	277 0.310	232 0.247	240 0.146
144	GLORY-000	477 0.440	503 0.367	516 0.294	452 0.586	481 0.547	502 0.470	301 0.995	341 0.995	399 0.993	418 0.453	432 0.381			379 0.839	427 0.795
145	GLORY-001	465 0.354	492 0.305	508 0.236	451 0.582	479 0.537	500 0.448	293 0.994	328 0.993	386 0.991	410 0.408	428 0.336			376 0.819	422 0.753
146	GORILLA-001	509 0.743	509 0.406	509 0.246	454 0.590	468 0.453	487 0.314	444 1.000	478 1.000	494 1.000	419 0.468	425 0.299			532 1.000	413 0.710
147	GORILLA-002	447 0.265	471 0.188	479 0.105	405 0.342	433 0.268	452 0.170	433 1.000	470 1.000	400 0.993	387 0.250	402 0.137			444 1.000	379 0.466
148	GORILLA-003	507 0.690	496 0.317	493 0.157	467 0.684	463 0.434	476 0.247	525 1.000	492 1.000	471 1.000	409 0.407	411 0.213			446 1.000	393 0.562
149	GORILLA-004	378 0.135	428 0.089	428 0.043	360 0.202	381 0.160	407 0.101	218 0.972	244 0.958	302 0.902	356 0.135	374 0.072			296 0.438	342 0.309
150	GORILLA-005	341 0.086	394 0.058	396 0.026	344 0.179	367 0.142	387 0.088	164 0.768	187 0.697	234 0.548	334 0.088	340 0.040			259 0.315	300 0.223
151	GORILLA-006	280 0.046	326 0.027	320 0.010	291 0.118	308 0.089	323 0.053	131 0.597	160 0.525	195 0.361	247 0.028	250 0.013	179 0.166	219 0.093	220 0.218	245 0.154
152	GORILLA-007	276 0.046	323 0.027	313 0.010	268 0.101	290 0.077	300 0.045	136 0.622	162 0.529	196 0.361	240 0.026	242 0.012	204 0.264	226 0.108	200 0.178	230 0.138
153	GORILLA-008	269 0.043	308 0.024	295 0.008	282 0.111	299 0.083	309 0.048	118 0.536	139 0.457	174 0.286	255 0.030	238 0.011	218 0.319	214 0.090	199 0.178	222 0.132
154	GRIAULE-000	270 0.043	290 0.020	297 0.008	242 0.082	261 0.063	274 0.038	333 0.997	345 0.995	331 0.951	265 0.033	295 0.020	188 0.185	225 0.107	213 0.198	253 0.166
155	GRIAULE-001	160 0.012	141 0.004	129 0.002	184 0.051	149 0.028	131 0.016	198 0.927	216 0.863	245 0.621	121 0.007	107 0.003	302 0.995	299 0.610	104 0.099	114 0.081
156	GTELOTS-000	429 0.217	475 0.206	500 0.198	397 0.307	426 0.256	472 0.232	166 0.770	191 0.727	256 0.651	394 0.292	422 0.282	554 1.000	519 1.000	335 0.603	397 0.577
157	HIK-003	399 0.156	433 0.102	446 0.057	353 0.190	377 0.158	412 0.105	234 0.980	257 0.968	312 0.924	359 0.142	329 0.080			299 0.445	356 0.359
158	HIK-004	398 0.155	429 0.098	444 0.054	348 0.182	374 0.153	408 0.101	245 0.983	267 0.976	327 0.946	357 0.137	378 0.077			295 0.434	354 0.353
159	HIK-005	352 0.102	359 0.043	362 0.019	262 0.098	289 0.077	310 0.048	389 1.000	408 0.999	432 0.998	316 0.068	333 0.036			323 0.541	318 0.258
160	HIK-006	389 0.141	368 0.047	365 0.020	281 0.111	303 0.086	321 0.052	435 1.000	472 1.000	458 0.999						
161	HISIGN-001	179 0.015	199 0.007	200 0.003	202 0.058	192 0.037	195 0.022	354 0.999	310 0.990	204 0.397	191 0.013	192 0.007	273 0.824	260 0.194	169 0.143	180 0.109
162	HYPERVERGE-001	120 0.009	136 0.004	149 0.002	149 0.039	164 0.031	179 0.020	64 0.267	82 0.210	106 0.136	123 0.007	139 0.004	91 0.053	106 0.027	111 0.101	122 0.083
163	HYPERVERGE-002	105 0.008	110 0.003	118 0.002	133 0.034	143 0.027	155 0.018	68 0.270	77 0.201	90 0.120	88 0.006	98 0.003	80 0.048	89 0.023	91 0.093	104 0.077
164	HYPERVERGE-003	178 0.015	198 0.007	195 0.003	188 0.053	208 0.042	225 0.026	89 0.346	101 0.274	135 0.174	176 0.012	179 0.005	109 0.065	123 0.033	119 0.106	129 0.085
165	HYUNDAI-ROBOTICSLAB-000	214 0.025	248 0.013	263 0.006	464 0.673	467 0.452	362 0.070	187 0.876	184 0.672	210 0.439	422 0.492	410 0.197	326 1.000	337 0.999	387 0.870	406 0.654
166	HYUNDAI-ROBOTICSLAB-001	224 0.027	243 0.013	248 0.005	494 0.921	503 0.774	488 0.322	238 0.981	213 0.839	214 0.444	441 0.699	435 0.404	517 1.000	355 1.000	409 0.937	428 0.807
167	HYUNDAI-ROBOTICSLAB-002	143 0.011	165 0.005	134 0.002	437 0.463	396 0.189	185 0.021	88 0.344	94 0.228	98 0.129	318 0.068	208 0.008	327 1.000	322 0.981	298 0.440	258 0.171
168	HZAILU-000	248 0.035	288 0.019	300 0.008	210 0.064	231 0.051	241 0.031	243 0.983	254 0.967	281 0.811	221 0.020	220 0.010	214 0.316	194 0.077	175 0.153	202 0.120
169	HZAILU-001	182 0.016	209 0.008	226 0.004	423 0.414	395 0.183	213 0.024	348 0.998	303 0.986	167 0.273	380 0.196	300 0.021	550 1.000	331 0.997	351 0.679	357 0.360
170	HZAILU-002	173 0.015	205 0.008	223 0.004	182 0.050	200 0.039	214 0.024	270 0.990	188 0.701	175 0.291	177 0.012	182 0.006	115 0.066	131 0.034	265 0.330	182 0.110
171	HZAILU-003	174 0.015	207 0.008	224 0.004	185 0.051	196 0.038	198 0.022	154 0.711	163 0.545	169 0.278	162 0.009	158 0.004	106 0.062	121 0.031	137 0.119	158 0.096
172	HZAILU-004	119 0.009	135 0.004	136 0.002	159 0.042	168 0.031	163 0.019	116 0.528	126 0.390	159 0.241	86 0.006	86 0.003	74 0.045	79 0.021	112 0.102	133 0.087
173	HZAILU-005	87 0.007	106 0.003	100 0.002	125 0.033	123 0.025	120 0.015	103 0.463	113 0.329	144 0.199	55 0.004	52 0.002	46 0.033	52 0.015	93 0.094	106 0.078
174	HZAILU-006	92 0.007	104 0.003	96 0.001	99 0.028	102 0.022	107 0.015	111 0.497	112 0.325	143 0.198	52 0.004	48 0.002	40 0.030	47 0.014	85 0.091	103 0.077
175	I2V-001	520 0.851	371 0.049	230 0.004	522 0.994	526 0.966	363 0.071	411 1.000	417 1.000	359 0.977	450 0.905	264 0.014	466 1.000	303 0.683	426 0.983	348 0.328
176	ICEHOUSE-000	458 0.298	427 0.089	411 0.033	493 0.917	515 0.852	471 0.223	397 1.000	423 1.000	446 0.999	343 0.111	355 0.052	387 1.000	354 1.000	307 0.470	350 0.346
177	ICM-000	307 0.058	317 0.026	339 0.012	285 0.113	314 0.092	346 0.062	253 0.984	252 0.965	340 0.960	274 0.036	306 0.022	202 0.241	238 0.136	229 0.242	290 0.208
178	ICM-001	475 0.421	335 0.029	312 0.010	497 0.942	422 0.251	317 0.051	451 1.000	433 1.000	397 0.993	398 0.307	268 0.015	332 1.000	240 0.145	389 0.878	261 0.173
179	IDEMIA-003	493 0.541	369 0.047	371 0.021	537 1.000	384 0.165	377 0.079			507 1.000	348 0.123	361 0.061			367 0.766	400 0.630
180	IDEMIA-004	300 0.054	352 0.037	370 0.021	321 0.144	344 0.118	376 0.079	226 0.975	264 0.973	342 0.967	349 0.123	360 0.061			368 0.766	401 0.630
181	IDEMIA-005	321 0.065	361 0.044	393 0.025	347 0.181	372 0.150	410 0.102	233 0.979	272 0.977	350 0.973	352 0.130	372 0.070			390 0.879	418 0.743
182	IDEMIA-006	319 0.064	358 0.043	391 0.025	385 0.266	411 0.226	445 0.161	248 0.984	287 0.982	363 0.980	360 0.144	385 0.090			360 0.733	388 0.531
183	IDEMIA-007	250 0.035	279 0.018	287 0.008	230 0.073	243 0.055	251 0.033	482 1.000	527 1.000	523 1.000	298 0.052	307 0.022	186 0.182	228 0.109	514 1.000	448 0.982
184	IDEMIA-008	40 0.003	51 0.002	54 0.001	56 0.016	55 0.013	50 0.009	66 0.267	74 0.195	96 0.126	68 0.005	88 0.003	55 0.036	75 0.019	120 0.106	148 0.092

Table 56: **Threshold-based accuracy**. *Values are FNIR(N, T, L) with N = 1.6 million with thresholds set to produce FPIR = 0.0003, 0.001, and 0.01 in non-mate searches. Throughout blue superscripts indicate the rank of the algorithm for that column. Caution: The Power-low models are mostly intended to draw attention to the kind of behavior, not as a model to be used for prediction.*

2026/01/09 20:40:38

FNIR(N, R, T) = FPIR(N, T) =

False neg. identification rate
False pos. identification rate

N = Num. enrolled subjects
R = Num. candidates examined

T = Threshold

T = 0 → Investigation
T > 0 → Identification

This publication is available free of charge from: https://doi.org/10.6028/NIST.IR.8271

MISSES BELOW THRESHOLD, T		ENROL RECENT MUGSHOT, N = 1.6M									ENROL APPLICATION PORTRAIT, N = 1.6M					
		ENROL: MUGSHOT			ENROL: MUGSHOT			ENROL: MUGSHOT			ENROL: VISA		ENROL: BORDER		ENROL: VISA	
		PROBE: MUGSHOT			PROBE: WEBCAM			PROBE: PROFILE			PROBE: BORDER		PROBE: BORDER 10+YR		PROBE: KIOSK	
#	ALGORITHM	FPIR=0.0003	FPIR=0.001	FPIR=0.01	FPIR=0.0003	FPIR=0.001	FPIR=0.01	FPIR=0.0003	FPIR=0.001	FPIR=0.01	FPIR=0.001	FPIR=0.01	FPIR=0.001	FPIR=0.01	FPIR=0.001	FPIR=0.01
185	IDEMIA-009	[38]0.003	[35]0.001	[33]0.001	[28]0.012	[32]0.011	[32]0.008	[30]0.193	[36]0.131	[50]0.088	[39]0.003	[45]0.002	[30]0.027	[42]0.013	[37]0.074	[50]0.064
186	IDEMIA-010	[15]0.002	[7]0.001	[10]0.001	[11]0.009	[11]0.008	[19]0.007	[38]0.219	[27]0.120	[26]0.068	[25]0.002	[28]0.001	[33]0.028	[20]0.009	[28]0.070	[31]0.058
187	IDEMIA-011	[12]0.002	[11]0.001	[31]0.001	[18]0.010	[26]0.009	[37]0.008	[28]0.192	[9]0.070	[10]0.050	[11]0.002	[19]0.001	[25]0.025	[16]0.008	[9]0.061	[12]0.052
188	IDEMIA-012	[7]0.002	[10]0.001	[29]0.001	[15]0.010	[16]0.009	[30]0.008	[6]0.116	[7]0.069	[7]0.048	[23]0.002	[25]0.001	[13]0.016	[10]0.007	[11]0.061	[10]0.051
189	IDENTY-000	[552]1.000	[551]1.000	[555]1.000	[530]0.999	[534]0.999	[539]0.999	[475]1.000	[525]1.000	[528]1.000	[461]0.991	[464]0.991	[318]1.000	[346]1.000	[431]0.992	[455]0.992
190	IMAGUS-002	[527]0.907	[526]0.749	[529]0.564	[498]0.944	[509]0.816	[515]0.645	[442]1.000	[476]1.000	[477]1.000						
191	IMAGUS-003	[526]0.897	[529]0.807	[532]0.669	[504]0.954	[517]0.909	[524]0.809	[436]1.000	[445]1.000	[468]1.000						
192	IMAGUS-005	[244]0.034	[283]0.018	[288]0.008	[249]0.088	[264]0.066	[284]0.040	[196]0.925	[212]0.836	[253]0.642	[250]0.029	[273]0.016	[178]0.161	[221]0.094	[224]0.231	[277]0.189
193	IMAGUS-006	[259]0.039	[287]0.019	[290]0.008	[254]0.093	[273]0.069	[293]0.042	[236]0.980	[227]0.896	[243]0.617	[248]0.028	[265]0.015	[177]0.161	[217]0.092	[237]0.260	[271]0.181
194	IMAGUS-007	[268]0.043	[306]0.022	[309]0.009	[266]0.100	[281]0.073	[299]0.045	[220]0.973	[225]0.892	[254]0.647	[259]0.031	[270]0.016	[180]0.169	[224]0.098	[242]0.265	[270]0.181
195	IMAGUS-008	[537]0.995	[538]0.974	[527]0.523	[507]0.958	[504]0.774	[482]0.285	[392]1.000	[351]0.996	[263]0.697	[425]0.520	[373]0.071	[319]1.000	[293]0.540	[318]0.518	[313]0.246
196	IMDS-SOFTWARE-000	[191]0.018	[186]0.006	[181]0.003	[416]0.389	[175]0.033	[166]0.019	[434]1.000	[471]1.000	[492]1.000	[186]0.013	[168]0.005	[196]0.216	[144]0.041	[538]1.000	[534]1.000
197	IMDS-SOFTWARE-001	[216]0.025	[190]0.006	[179]0.003	[486]0.834	[179]0.034	[154]0.018	[445]1.000	[479]1.000	[476]1.000	[216]0.019	[164]0.005	[237]0.424	[167]0.055	[530]1.000	[509]1.000
198	IMDS-SOFTWARE-002	[190]0.018	[185]0.006	[178]0.003	[415]0.389	[174]0.033	[165]0.019	[460]1.000	[459]1.000	[485]1.000	[185]0.013	[170]0.005	[197]0.216	[143]0.041	[486]1.000	[479]1.000
199	IMPERIAL-000	[394]0.154	[315]0.026	[306]0.009	[252]0.089	[269]0.068	[290]0.041	[440]1.000	[385]0.999	[406]0.995	[286]0.042	[296]0.020			[231]0.245	[254]0.168
200	INCODE-000	[474]0.421	[493]0.310	[501]0.199	[443]0.486	[461]0.420	[486]0.304	[395]1.000	[374]0.998	[404]0.994						
201	INCODE-001	[460]0.317	[476]0.211	[481]0.111	[408]0.348	[439]0.296	[460]0.198	[423]1.000	[466]1.000	[464]1.000						
202	INCODE-002	[456]0.285	[468]0.184	[478]0.100	[401]0.333	[434]0.269	[455]0.176	[336]0.998	[329]0.993	[356]0.975						
203	INCODE-003	[455]0.282	[464]0.167	[465]0.083	[414]0.372	[429]0.264	[448]0.164	[408]1.000	[405]0.999	[421]0.996						
204	INCODE-004	[351]0.099	[385]0.053	[383]0.023	[336]0.167	[347]0.120	[361]0.070	[332]0.997	[340]0.994	[314]0.928	[313]0.063	[325]0.031			[257]0.313	[302]0.226
205	INCODE-005	[198]0.020	[232]0.011	[228]0.004	[197]0.055	[213]0.043	[223]0.026	[134]0.609	[156]0.522	[197]0.365	[206]0.017	[211]0.009	[163]0.145	[187]0.073	[180]0.155	[191]0.116
206	INCODE-006	[36]0.003	[38]0.001	[44]0.001	[29]0.013	[34]0.011	[45]0.009	[42]0.230	[51]0.159	[57]0.093	[46]0.003	[65]0.002	[26]0.026	[40]0.013	[53]0.079	[62]0.067
207	INCODE-007	[25]0.003	[33]0.001	[18]0.001	[24]0.012	[17]0.009	[9]0.006	[35]0.205	[46]0.146	[55]0.092	[21]0.002	[20]0.001	[37]0.028	[31]0.011	[28]0.089	[49]0.064
208	INNOVATRICS-002	[471]0.374	[485]0.233	[490]0.139	[421]0.403	[445]0.310	[467]0.209	[458]1.000	[457]1.000	[460]0.999						
209	INNOVATRICS-003	[457]0.296	[480]0.221	[486]0.131	[410]0.351	[440]0.297	[463]0.203	[405]1.000	[419]1.000	[435]0.998						
210	INNOVATRICS-004	[412]0.183	[448]0.131	[462]0.073	[383]0.262	[410]0.222	[437]0.149	[247]0.983	[278]0.980	[348]0.972						
211	INNOVATRICS-005	[305]0.056	[343]0.034	[345]0.014	[287]0.114	[307]0.089	[322]0.052	[188]0.889	[214]0.845	[264]0.720	[294]0.047	[305]0.022			[234]0.251	[272]0.182
212	INNOVATRICS-007	[205]0.023	[241]0.012	[241]0.005	[212]0.065	[232]0.051	[244]0.032	[172]0.803	[194]0.740	[235]0.562	[205]0.017	[217]0.009	[138]0.093	[166]0.053	[177]0.154	[201]0.120
213	INNOVATRICS-008	[212]0.024	[155]0.005	[153]0.002	[317]0.138	[189]0.036	[152]0.018	[459]1.000	[458]1.000	[414]0.995	[189]0.013	[198]0.007	[278]0.886	[284]0.430	[160]0.139	[178]0.108
214	INNOVATRICS-009	[86]0.007	[91]0.003	[117]0.002	[117]0.031	[125]0.025	[148]0.018	[104]0.475	[114]0.338	[142]0.197	[120]0.007	[149]0.004	[85]0.050	[98]0.025	[121]0.106	[146]0.090
215	INNOVATRICS-010	[88]0.007	[101]0.003	[130]0.002	[123]0.032	[126]0.025	[147]0.018	[113]0.500	[117]0.347	[148]0.206	[127]0.007	[148]0.004	[94]0.054	[107]0.027	[128]0.110	[152]0.093
216	INNOVATRICS-011	[62]0.005	[62]0.002	[69]0.001	[61]0.017	[63]0.014	[63]0.010	[151]0.684	[157]0.523	[146]0.204	[58]0.004	[78]0.003	[63]0.039	[68]0.017	[69]0.087	[75]0.069
217	INNOVATRICS-012	[46]0.004	[53]0.002	[63]0.001	[36]0.014	[36]0.011	[38]0.008	[53]0.247	[56]0.168	[67]0.104	[40]0.003	[43]0.002	[29]0.027	[38]0.012	[61]0.083	[54]0.066
218	INNOVATRICS-013	[41]0.004	[41]0.001	[41]0.001	[74]0.022	[71]0.015	[49]0.009	[43]0.230	[48]0.147	[49]0.088	[96]0.006	[66]0.002	[81]0.048	[65]0.016	[76]0.088	[47]0.063
219	INNOVATRICS-014	[23]0.002	[22]0.001	[30]0.001	[8]0.009	[8]0.008	[6]0.006	[50]0.241	[22]0.106	[24]0.066	[17]0.002	[18]0.001	[11]0.015	[14]0.007	[18]0.066	[22]0.056
220	INNOVATRICS-015	[22]0.002	[12]0.001	[23]0.001	[7]0.008	[7]0.007	[5]0.006	[133]0.604	[32]0.126	[22]0.065	[12]0.002	[7]0.001	[9]0.015	[11]0.007	[49]0.078	[21]0.056
221	INSPUR-000	[176]0.015	[182]0.006	[162]0.002	[508]0.963	[518]0.915	[523]0.740	[413]1.000	[427]1.000	[443]0.999	[454]0.936	[443]0.584	[551]1.000	[529]1.000	[436]0.998	[445]0.966
222	INSPUR-001	[145]0.011	[161]0.005	[139]0.002	[160]0.043	[141]0.027	[122]0.016	[462]1.000	[441]1.000	[455]0.999	[143]0.008	[137]0.004	[99]0.057	[105]0.027	[406]0.931	[204]0.121
223	INSPUR-002	[152]0.012	[167]0.005	[133]0.002	[161]0.043	[158]0.029	[134]0.016	[428]1.000	[392]0.999	[364]0.980	[137]0.008	[129]0.004	[90]0.052	[96]0.024	[417]0.957	[157]0.095
224	INTELIGENSIA-000	[292]0.050	[309]0.024	[318]0.010	[260]0.097	[288]0.077	[313]0.049	[239]0.981	[203]0.784	[223]0.501	[302]0.053	[332]0.036	[200]0.235	[241]0.145	[235]0.255	[289]0.208
225	INTELIGENSIA-001	[155]0.012	[166]0.005	[143]0.002	[144]0.037	[147]0.028	[139]0.017	[168]0.787	[138]0.451	[102]0.132	[135]0.008	[151]0.004	[118]0.067	[122]0.031	[149]0.129	[188]0.115
226	INTELLIVISION-001	[489]0.508	[490]0.279	[494]0.158	[436]0.459	[458]0.404	[485]0.302	[419]1.000	[426]1.000	[457]0.999	[400]0.328	[413]0.219	[262]0.749	[296]0.598	[354]0.685	[394]0.562
227	INTELLIVISION-002	[453]0.281	[456]0.154	[460]0.072	[374]0.236	[398]0.196	[427]0.127	[370]0.999	[388]0.999	[428]0.997	[355]0.134	[375]0.073	[239]0.437	[276]0.297	[303]0.460	[351]0.348
228	INTELRESEARCH-001	[55]0.004	[46]0.001	[42]0.001	[45]0.015	[49]0.012	[47]0.009	[98]0.396	[102]0.276	[101]0.132	[72]0.005	[94]0.003	[41]0.030	[56]0.015	[56]0.080	[61]0.067
229	INTEMA-000	[110]0.008	[67]0.002	[64]0.001	[80]0.022	[75]0.017	[77]0.012		[448]1.000	[52]0.090	[71]0.005	[67]0.002	[210]0.288	[146]0.042	[57]0.081	[63]0.067
230	INTEMA-001	[8]0.002	[24]0.001	[21]0.001	[455]0.604	[485]0.603	[511]0.602	[7]0.127	[12]0.092	[19]0.062	[56]0.004	[49]0.002	[253]0.715	[275]0.294	[43]0.076	[41]0.062

Table 57: **Threshold-based accuracy**. *Values are FNIR(N, T, L) with N = 1.6 million with thresholds set to produce FPIR = 0.0003, 0.001, and 0.01 in non-mate searches. Throughout blue superscripts indicate the rank of the algorithm for that column. Caution: The Power-low models are mostly intended to draw attention to the kind of behavior, not as a model to be used for prediction.*

2026/01/09 20:40:38

FNIR(N, R, T) = FPIR(N, T) = False neg. identification rate / False pos. identification rate

N = Num. enrolled subjects
R = Num. candidates examined

T = Threshold

T = 0 → Investigation
T > 0 → Identification

This publication is available free of charge from: https://doi.org/10.6028/NIST.IR.8271

MISSES BELOW THRESHOLD, T		ENROL RECENT MUGSHOT, N = 1.6M									ENROL APPLICATION PORTRAIT, N = 1.6M					
		ENROL: MUGSHOT			ENROL: MUGSHOT			ENROL: MUGSHOT			ENROL: VISA		ENROL: BORDER		ENROL: VISA	
		PROBE: MUGSHOT			PROBE: WEBCAM			PROBE: PROFILE			PROBE: BORDER		PROBE: BORDER 10+YR		PROBE: KIOSK	
#	ALGORITHM	FPIR=0.0003	FPIR=0.001	FPIR=0.01	FPIR=0.0003	FPIR=0.001	FPIR=0.01	FPIR=0.0003	FPIR=0.001	FPIR=0.01	FPIR=0.001	FPIR=0.01	FPIR=0.001	FPIR=0.01	FPIR=0.001	FPIR=0.01
231	INTSYSMSU-000	[539]0.999	[542]0.998	[544]0.990	[532]1.000	[535]1.000	[537]0.998	[404]1.000	[418]1.000	[430]0.998	[463]0.999	[463]0.989			[439]0.999	[453]0.988
232	IONETWORKS-001	[357]0.108	[254]0.014	[266]0.007	[200]0.057	[219]0.045	[232]0.029	[402]1.000	[421]1.000	[436]0.998	[199]0.016	[212]0.009	[152]0.129	[180]0.065	[251]0.294	[186]0.112
233	IREX-000	[325]0.068	[331]0.028	[286]0.008	[265]0.099	[256]0.060	[246]0.032	[262]0.988	[242]0.956	[260]0.676	[289]0.044	[233]0.011	[213]0.302	[175]0.062	[194]0.170	[227]0.135
234	ISYSTEMS-002	[396]0.154	[413]0.078	[408]0.032	[331]0.161	[352]0.126	[379]0.080	[346]0.998	[365]0.998	[398]0.993						
235	ISYSTEMS-003	[424]0.203	[395]0.058	[386]0.024	[313]0.135	[335]0.107	[355]0.068	[418]1.000	[425]1.000	[427]0.997						
236	KAKAO-000	[228]0.028	[260]0.015	[260]0.006	[228]0.071	[246]0.056	[259]0.034	[117]0.534	[143]0.462	[187]0.319	[217]0.019	[219]0.010	[157]0.141	[188]0.075	[182]0.158	[200]0.120
237	KAKAO-001	[72]0.006	[78]0.002	[90]0.001	[76]0.022	[78]0.017	[85]0.013	[37]0.218	[49]0.150	[54]0.090	[61]0.004	[54]0.002	[71]0.042	[62]0.016	[36]0.074	[44]0.063
238	KAKAO-002	[56]0.004	[60]0.002	[74]0.001	[58]0.017	[64]0.014	[68]0.011	[36]0.217	[32]0.134	[41]0.083	[41]0.003	[40]0.002	[59]0.037	[36]0.012	[31]0.070	[32]0.058
239	KEDACOM-001	[261]0.040	[305]0.022	[341]0.013	[259]0.096	[279]0.072	[326]0.054	[267]0.989	[302]0.986	[352]0.973	[304]0.055	[345]0.043			[253]0.305	[322]0.264
240	KEYLESS-000	[159]0.012	[174]0.006	[160]0.002	[154]0.041	[154]0.029	[140]0.017	[296]0.994	[305]0.987	[215]0.455	[175]0.011	[135]0.004	[301]0.994	[315]0.888	[173]0.149	[166]0.099
241	KLOUDSPOT-001	[326]0.069	[310]0.024	[311]0.010			[428]0.128	[158]0.752	[164]0.550	[202]0.381		[387]0.094				[371]0.406
242	KNERON-000			[410]0.033			[401]0.099									
243	KNERON-001			[440]0.051												
244	KNOWUTECH-000	[184]0.017	[215]0.009	[214]0.003	[180]0.049	[198]0.038	[201]0.023	[97]0.392	[107]0.310	[141]0.196	[182]0.012	[190]0.006	[136]0.091	[156]0.046	[147]0.129	[173]0.103
245	KOGNIZA-000	[151]0.012	[176]0.006	[182]0.003	[140]0.036	[148]0.028	[162]0.019	[152]0.692	[136]0.444	[162]0.255	[78]0.005	[83]0.003	[84]0.050	[74]0.019	[71]0.087	[70]0.069
246	LIGHTVISION-000	[342]0.086	[325]0.027	[322]0.010	[495]0.925	[505]0.797	[365]0.072	[406]1.000	[432]1.000	[442]0.998	[266]0.033	[277]0.017	[390]1.000	[356]1.000	[218]0.214	[243]0.153
247	LINE-000	[314]0.062	[339]0.030	[337]0.012	[309]0.132	[319]0.095	[328]0.054			[493]1.000	[292]0.046	[301]0.021	[207]0.278	[247]0.151	[544]1.000	[325]0.268
248	LINE-001	[234]0.030	[146]0.004	[126]0.002	[213]0.066	[140]0.027	[119]0.015	[429]1.000	[469]1.000	[491]1.000	[157]0.009	[145]0.004	[122]0.072	[132]0.034	[501]1.000	[434]0.858
249	LINECLOVA-002	[126]0.009	[118]0.004	[113]0.002	[444]0.508	[354]0.130	[99]0.014	[284]0.992	[281]0.980	[238]0.572	[283]0.040	[123]0.004	[324]1.000	[304]0.690	[356]0.700	[147]0.091
250	LINECLOVA-003	[51]0.004	[80]0.002	[62]0.001	[456]0.612	[486]0.606	[512]0.603			[480]1.000	[84]0.006	[75]0.002	[294]0.974	[251]0.158	[127]0.110	[163]0.097
251	LOOKMAN-003	[320]0.065	[360]0.043	[389]0.024	[308]0.131	[339]0.112	[380]0.082				[332]0.084	[362]0.061			[270]0.355	[341]0.304
252	LOOKMAN-004	[330]0.073	[363]0.044	[385]0.024	[297]0.123	[332]0.105	[371]0.075	[229]0.978	[269]0.977	[354]0.974						
253	LOOKMAN-005	[288]0.050	[337]0.030	[353]0.017	[269]0.102	[301]0.086	[348]0.063	[235]0.980	[271]0.977	[349]0.973	[312]0.062	[347]0.047			[255]0.308	[328]0.273
254	LUXAND-001	[386]0.140	[391]0.057	[360]0.019	[447]0.553	[455]0.385	[444]0.161	[479]1.000	[349]0.995	[265]0.723	[435]0.662	[415]0.222	[282]0.909	[305]0.698	[395]0.903	[395]0.562
255	MANTRA-000	[322]0.066	[224]0.010	[212]0.003	[205]0.063	[205]0.041	[196]0.022	[512]1.000	[553]1.000	[454]0.999	[252]0.029	[257]0.014	[169]0.152	[203]0.081	[443]1.000	[241]0.151
256	MAVERICKRESEARCH-000	[384]0.138	[417]0.084	[425]0.040	[327]0.245	[391]0.176	[413]0.105	[326]0.997	[321]0.992	[274]0.785	[347]0.122	[359]0.058	[229]0.394	[263]0.220	[325]0.546	[329]0.279
257	MAXVISION-000	[283]0.048	[332]0.028	[338]0.012	[439]0.468	[414]0.237	[329]0.054	[177]0.825	[200]0.764	[248]0.626	[361]0.149	[302]0.022	[305]0.997	[313]0.872	[329]0.557	[312]0.245
258	MAXVISION-001	[124]0.009	[130]0.004	[122]0.002	[163]0.044	[129]0.025	[117]0.015	[71]0.274	[81]0.210	[95]0.126	[115]0.007	[102]0.003	[288]0.951	[288]0.485	[109]0.100	[105]0.078
259	MAXVISION-002	[103]0.008	[113]0.004	[124]0.002	[105]0.029	[105]0.022	[100]0.014	[52]0.246	[70]0.188	[86]0.116	[111]0.007	[103]0.003	[279]0.895	[160]0.050	[117]0.104	[131]0.086
260	MAXVISION-003	[149]0.012	[173]0.006	[164]0.002	[186]0.051	[201]0.039	[194]0.022	[80]0.304	[96]0.237	[114]0.142	[173]0.011	[173]0.005	[222]0.348	[242]0.145	[130]0.111	[132]0.086
261	MAXVISION-004	[66]0.005	[69]0.002	[66]0.001	[86]0.025	[87]0.020	[102]0.014	[16]0.171	[29]0.122	[35]0.078	[54]0.004	[58]0.002	[298]0.990	[311]0.846	[60]0.082	[80]0.071
262	MEGVII-001	[425]0.209	[408]0.072	[415]0.036	[293]0.119	[323]0.097	[340]0.061									
263	MEGVII-002	[442]0.251	[412]0.077	[417]0.037	[294]0.120	[321]0.096	[337]0.059	[359]0.999	[378]0.998	[295]0.870						
264	MEGVII-003	[70]0.006	[75]0.002	[82]0.001	[33]0.013	[38]0.011	[46]0.009	[63]0.265	[45]0.145	[53]0.090	[45]0.003	[47]0.002	[32]0.027	[46]0.014	[47]0.078	[69]0.069
265	MEGVII-004	[11]0.002	[18]0.001	[38]0.001	[10]0.009	[13]0.008	[31]0.008	[32]0.196	[10]0.072	[11]0.053	[7]0.001	[17]0.001	[4]0.009	[7]0.005	[17]0.065	[36]0.060
266	MEGVII-005	[82]0.006	[19]0.001	[37]0.001	[60]0.017	[25]0.009	[33]0.008	[128]0.580	[64]0.181	[12]0.053	[87]0.006	[15]0.001	[333]1.000	[259]0.190	[135]0.117	[34]0.058
267	METSAKUURCOMPANY-000	[183]0.017	[197]0.007	[190]0.003	[244]0.084	[187]0.036	[160]0.018	[367]0.999	[391]0.999	[411]0.995	[329]0.081	[225]0.010	[304]0.995	[316]0.915	[353]0.683	[323]0.264
268	METSAKUURCOMPANY-001	[395]0.154	[216]0.009	[208]0.003	[203]0.059	[165]0.031	[159]0.018	[431]1.000	[412]1.000	[431]0.998	[167]0.010	[171]0.005	[124]0.073	[135]0.036	[382]0.841	[372]0.416
269	MICROFOCUS-003	[532]0.958	[535]0.931	[539]0.866	[519]0.988	[529]0.979	[534]0.948				[460]0.982	[460]0.945			[430]0.991	[447]0.977
270	MICROFOCUS-004	[541]0.999	[543]0.999	[548]0.999	[518]0.984	[527]0.975	[533]0.940				[457]0.974	[459]0.935			[428]0.989	[446]0.976
271	MICROFOCUS-005	[525]0.882	[533]0.835	[537]0.736	[502]0.951	[522]0.928	[528]0.865				[453]0.935	[457]0.848			[427]0.985	[444]0.965
272	MICROFOCUS-006	[535]0.983	[539]0.978	[541]0.963	[501]0.950	[521]0.923	[527]0.858				[452]0.923	[455]0.843			[421]0.971	[440]0.939
273	MICROSOFT-003	[284]0.048	[328]0.027	[330]0.011	[288]0.117	[311]0.091	[332]0.056				[275]0.036	[292]0.019			[226]0.233	[263]0.176
274	MICROSOFT-004	[279]0.046	[316]0.026	[323]0.010	[283]0.111	[305]0.087	[325]0.053				[267]0.033	[286]0.018			[221]0.222	[257]0.170
275	MICROSOFT-005	[281]0.047	[313]0.025	[317]0.010	[253]0.090	[276]0.070	[291]0.041	[375]0.999	[170]0.582	[193]0.347	[243]0.027	[252]0.013			[204]0.180	[226]0.134
276	MICROSOFT-006	[213]0.025	[237]0.012	[258]0.006	[176]0.048	[190]0.037	[210]0.024	[100]0.446	[123]0.379	[166]0.272	[262]0.032	[266]0.015			[198]0.178	[229]0.138

Table 58: **Threshold-based accuracy**. *Values are FNIR(N, T, L) with N = 1.6 million with thresholds set to produce FPIR = 0.0003, 0.001, and 0.01 in non-mate searches. Throughout blue superscripts indicate the rank of the algorithm for that column. Caution: The Power-low models are mostly intended to draw attention to the kind of behavior, not as a model to be used for prediction.*

This publication is available free of charge from: https://doi.org/10.6028/NIST.IR.8271

MISSES BELOW THRESHOLD, T		ENROL RECENT MUGSHOT, N = 1.6M									ENROL APPLICATION PORTRAIT, N = 1.6M					
		ENROL: MUGSHOT			ENROL: MUGSHOT			ENROL: MUGSHOT			ENROL: VISA		ENROL: BORDER		ENROL: VISA	
		PROBE: MUGSHOT			PROBE: WEBCAM			PROBE: PROFILE			PROBE: BORDER		PROBE: BORDER 10+YR		PROBE: KIOSK	
#	ALGORITHM	FPIR=0.0003	FPIR=0.001	FPIR=0.01	FPIR=0.0003	FPIR=0.001	FPIR=0.01	FPIR=0.0003	FPIR=0.001	FPIR=0.01	FPIR=0.001	FPIR=0.01	FPIR=0.001	FPIR=0.01	FPIR=0.001	FPIR=0.01
277	MOBBL-000	309 0.059	330 0.028	329 0.011	278 0.107	286 0.077	297 0.045	273 0.990	295 0.984	309 0.918	273 0.036	282 0.017	248 0.621	239 0.145	223 0.228	256 0.170
278	MOBBL-001	317 0.063	345 0.035	367 0.020	279 0.109	295 0.080	311 0.049	272 0.990	291 0.983	305 0.911	308 0.058	341 0.040	249 0.622	252 0.160	246 0.275	301 0.225
279	MOBBL-002	431 0.218	479 0.215	505 0.213	368 0.217	403 0.207	459 0.197	312 0.996	311 0.990	266 0.729	392 0.285	423 0.283	306 0.997	312 0.866	330 0.558	390 0.553
280	MUKH-002	542 0.999	519 0.594	480 0.110	399 0.326	420 0.242	442 0.153	456 1.000	437 1.000	374 0.987	371 0.170	384 0.089	259 0.741	281 0.382	279 0.389	331 0.286
281	NEC-000	361 0.111	415 0.079	437 0.046	338 0.171	366 0.140	391 0.093	244 0.983	275 0.979	344 0.968					309 0.474	365 0.377
282	NEC-001	393 0.148	435 0.105	451 0.060	325 0.238	400 0.197	430 0.133	279 0.991	301 0.986	347 0.972	354 0.133	382 0.082			306 0.468	366 0.378
283	NEC-002	185 0.017	81 0.002	94 0.001	110 0.029	88 0.020	90 0.013	386 1.000	401 0.999	408 0.995	140 0.008	180 0.005			350 0.676	337 0.292
284	NEC-003	54 0.004	76 0.002	112 0.002	72 0.021	77 0.017	88 0.013	190 0.901	209 0.822	247 0.623	145 0.008	183 0.006	56 0.036	85 0.023	349 0.668	319 0.261
285	NEC-004	21 0.002	45 0.001	73 0.001	49 0.015	54 0.013	59 0.010	142 0.649	175 0.618	236 0.570	63 0.004	124 0.004	16 0.019	37 0.012	108 0.100	138 0.088
286	NEC-005	83 0.006	40 0.001	53 0.001	40 0.014	45 0.012	51 0.009	189 0.900	182 0.669	128 0.168	48 0.003	72 0.002	15 0.019	27 0.011	103 0.099	135 0.087
287	NEC-006	125 0.009	55 0.002	68 0.001	83 0.024	81 0.018	83 0.013	181 0.855	140 0.457	78 0.112	53 0.004	84 0.003	28 0.026	41 0.013	96 0.094	115 0.081
288	NEC-007	9 0.002	21 0.001	34 0.001	20 0.010	19 0.009	22 0.007	44 0.232	41 0.137	36 0.078	18 0.002	30 0.001	5 0.010	8 0.006	16 0.065	26 0.057
289	NEC-008	14 0.002	29 0.001	43 0.001	16 0.010	15 0.009	25 0.008	12 0.157	11 0.089	16 0.060	15 0.002	29 0.001	3 0.008	6 0.005	13 0.062	17 0.055
290	NEC-009	13 0.002	9 0.001	20 0.001	5 0.007	5 0.007	11 0.007	15 0.165	8 0.070	6 0.048	6 0.001	14 0.001	2 0.005	2 0.003	4 0.052	6 0.048
291	NEC-010	6 0.002	4 0.001	6 0.001	1 0.006	2 0.006	4 0.006	25 0.184	6 0.067	1 0.043	4 0.001	5 0.001	1 0.004	1 0.003	1 0.050	4 0.046
292	NEC-011	4 0.001	3 0.001	4 0.001	4 0.007	4 0.006	2 0.005	96 0.380	42 0.140	2 0.043	1 0.001	1 0.001	267 0.789	280 0.354	3 0.052	1 0.043
293	NEUROTECHNOLOGY-003	540 0.999	523 0.631	477 0.098	481 0.773	431 0.266	447 0.164	509 1.000	551 1.000	554 1.000						
294	NEUROTECHNOLOGY-004	365 0.119	401 0.062	398 0.027	322 0.146	341 0.117	362 0.073	318 0.996	334 0.994	382 0.990						
295	NEUROTECHNOLOGY-005	363 0.116	386 0.054	377 0.022	379 0.252	355 0.130	370 0.074	355 0.999	369 0.998	377 0.988						
296	NEUROTECHNOLOGY-006	536 0.987	486 0.249	483 0.121	551 1.000	459 0.418	465 0.206									
297	NEUROTECHNOLOGY-007	444 0.252	400 0.062	374 0.021	524 0.996	389 0.173	354 0.068	430 1.000	436 1.000	426 0.997	401 0.339	334 0.036			500 1.000	454 0.989
298	NEUROTECHNOLOGY-008	514 0.797	380 0.053	334 0.012	280 0.110	294 0.080	305 0.047	422 1.000	468 1.000	490 1.000	272 0.035	281 0.017	212 0.293	245 0.149	214 0.203	242 0.152
299	NEUROTECHNOLOGY-009	221 0.026	261 0.015	250 0.006	215 0.066	236 0.052	245 0.032	145 0.657	171 0.583	209 0.430	220 0.020	226 0.010	170 0.153	207 0.082	191 0.165	218 0.129
300	NEUROTECHNOLOGY-010	463 0.346	222 0.010	203 0.003	174 0.047	194 0.037	207 0.023	93 0.370	99 0.269	123 0.160	168 0.010	163 0.005	129 0.075	140 0.039	142 0.126	164 0.097
301	NEUROTECHNOLOGY-012	344 0.092	191 0.006	154 0.002	167 0.045	172 0.032	169 0.019	409 1.000	246 0.959	108 0.139	151 0.008	132 0.004	102 0.061	112 0.028	399 0.916	139 0.088
302	NEUROTECHNOLOGY-013	308 0.058	129 0.004	88 0.001	113 0.030	113 0.023	105 0.014	223 0.974	110 0.316	73 0.107	106 0.006	91 0.003	75 0.046	83 0.022	343 0.641	125 0.083
303	NEUROTECHNOLOGY-014	95 0.007	97 0.003	83 0.001	115 0.031	104 0.022	87 0.013	126 0.568	86 0.215	72 0.107	97 0.006	90 0.003	89 0.052	92 0.024	95 0.094	95 0.075
304	NEUROTECHNOLOGY-015	90 0.007	103 0.003	70 0.001	121 0.032	119 0.024	101 0.014	58 0.254	57 0.170	66 0.104	98 0.006	85 0.003	83 0.049	84 0.023	68 0.086	65 0.068
305	NEUROTECHNOLOGY-016	93 0.007	96 0.003	71 0.001	100 0.028	95 0.021	84 0.013	47 0.238	65 0.182	76 0.109	122 0.007	113 0.003	92 0.054	97 0.025	90 0.093	85 0.073
306	NEWLAND-002	491 0.522	511 0.437	515 0.294	446 0.535	469 0.466	491 0.335	372 0.999	393 0.999	434 0.998						
307	NEXTMETALABS-001	459 0.305	482 0.233	492 0.145	546 1.000	537 1.000	532 0.933	463 1.000	462 1.000	488 1.000	492 1.000	466 0.999	521 1.000	547 1.000	465 1.000	472 1.000
308	NEXTMETALABS-002	109 0.008	122 0.004	108 0.002	392 0.285	351 0.125	167 0.019	61 0.260	75 0.198	87 0.118	353 0.131	308 0.023	329 1.000	336 0.999	316 0.510	317 0.257
309	NOBLIS-001	545 1.000	545 1.000	545 0.991	534 1.000	547 1.000	542 1.000	445 1.000	449 1.000	479 1.000						
310	NOBLIS-002	543 1.000	541 0.997	524 0.488	533 1.000	548 1.000	543 1.000	448 1.000	452 1.000	478 1.000						
311	NOMINDER-000	154 0.012	147 0.004	127 0.002	441 0.481	437 0.280	233 0.029	240 0.982	236 0.929	213 0.441	405 0.370	383 0.088	484 1.000	347 1.000	372 0.799	391 0.557
312	NOMINDER-001	158 0.012	160 0.005	166 0.002	329 0.156	302 0.086	177 0.020	180 0.875	185 0.675	170 0.282	138 0.008	109 0.003	325 1.000	317 0.948	176 0.154	118 0.082
313	NOMINDER-002	146 0.011	158 0.005	158 0.002	165 0.045	157 0.029	161 0.019	83 0.317	90 0.223	91 0.121	107 0.006	100 0.003	276 0.867	174 0.062	80 0.089	74 0.069
314	NOMINDER-003	132 0.010	151 0.005	147 0.002	150 0.039	145 0.027	145 0.018	78 0.299	79 0.208	81 0.114	95 0.006	92 0.003	272 0.816	130 0.034	66 0.085	52 0.065
315	NOMINDER-004	135 0.010	145 0.004	148 0.002	137 0.035	134 0.026	144 0.017	77 0.296	80 0.208	84 0.116	101 0.006	95 0.003	219 0.331	103 0.027	79 0.089	68 0.068
316	NOTIONTAG-000	238 0.032	274 0.017	272 0.007	233 0.076	252 0.059	266 0.036	147 0.667	173 0.606	217 0.460	226 0.021	236 0.011	168 0.150	209 0.084	197 0.176	231 0.140
317	NTECHLAB-003	334 0.079	384 0.053	399 0.028	323 0.148	342 0.118	372 0.075	184 0.872	211 0.835	273 0.749						
318	NTECHLAB-004	315 0.062	354 0.040	372 0.021	307 0.131	331 0.105	351 0.065	183 0.866	210 0.831	271 0.743	301 0.053	323 0.030			239 0.263	297 0.214
319	NTECHLAB-005	312 0.062	356 0.042	373 0.021	306 0.130	329 0.102	349 0.063	175 0.813	201 0.769	257 0.657	323 0.073	338 0.039			250 0.294	303 0.227
320	NTECHLAB-006	304 0.056	348 0.036	358 0.018	295 0.121	316 0.094	336 0.059	171 0.799	199 0.751	251 0.631	306 0.057	327 0.032			238 0.260	287 0.207
321	NTECHLAB-007	260 0.040	312 0.025	331 0.012	245 0.085	267 0.067	289 0.041	170 0.793	193 0.747	252 0.638	263 0.032	283 0.017			222 0.223	262 0.176
322	NTECHLAB-008	210 0.024	252 0.014	265 0.006	199 0.057	220 0.045	234 0.029	130 0.596	158 0.524	203 0.384	268 0.033	287 0.018			205 0.183	232 0.140

Table 59: **Threshold-based accuracy**. *Values are FNIR(N, T, L) with N = 1.6 million with thresholds set to produce FPIR = 0.0003, 0.001, and 0.01 in non-mate searches. Throughout blue superscripts indicate the rank of the algorithm for that column. Caution: The Power-low models are mostly intended to draw attention to the kind of behavior, not as a model to be used for prediction.*

This publication is available free of charge from: https://doi.org/10.6028/NIST.IR.8271

MISSES BELOW THRESHOLD, T		ENROL RECENT MUGSHOT, N = 1.6M									ENROL APPLICATION PORTRAIT, N = 1.6M					
		ENROL: MUGSHOT			ENROL: MUGSHOT			ENROL: MUGSHOT			ENROL: VISA		ENROL: BORDER		ENROL: VISA	
		PROBE: MUGSHOT			PROBE: WEBCAM			PROBE: PROFILE			PROBE: BORDER		PROBE: BORDER 10+YR		PROBE: KIOSK	
#	ALGORITHM	FPIR=0.0003	FPIR=0.001	FPIR=0.01	FPIR=0.0003	FPIR=0.001	FPIR=0.01	FPIR=0.0003	FPIR=0.001	FPIR=0.01	FPIR=0.001	FPIR=0.01	FPIR=0.001	FPIR=0.01	FPIR=0.001	FPIR=0.01
323	NTECHLAB-009	[127] 0.009	[153] 0.005	[169] 0.002	[101] 0.028	[107] 0.022	[103] 0.014	[114] 0.517	[133] 0.423	[181] 0.303	[195] 0.015	[205] 0.008	[144] 0.109	[172] 0.061	[165] 0.142	[187] 0.114
324	NTECHLAB-010	[60] 0.005	[74] 0.002	[67] 0.001	[66] 0.018	[66] 0.015	[65] 0.011	[86] 0.327	[98] 0.243	[121] 0.159	[112] 0.007	[138] 0.004	[101] 0.059	[119] 0.031	[102] 0.098	[101] 0.077
325	NTECHLAB-011	[69] 0.006	[86] 0.003	[77] 0.001	[65] 0.018	[65] 0.015	[61] 0.010	[72] 0.282	[87] 0.219	[112] 0.140	[156] 0.009	[155] 0.004	[126] 0.074	[139] 0.038	[84] 0.091	[94] 0.075
326	OMNIGARDE-000	[131] 0.010	[126] 0.004	[128] 0.002	[106] 0.029	[114] 0.023	[104] 0.014	[85] 0.324	[97] 0.243	[117] 0.150	[128] 0.007	[121] 0.003	[95] 0.055	[109] 0.027	[155] 0.136	[149] 0.092
327	OMNIGARDE-001	[53] 0.004	[61] 0.002	[48] 0.001	[71] 0.019	[70] 0.015	[56] 0.010	[31] 0.193	[40] 0.135	[47] 0.087	[50] 0.003	[51] 0.002	[42] 0.030	[51] 0.015	[46] 0.078	[66] 0.068
328	OMNIGARDE-002	[39] 0.003	[39] 0.001	[40] 0.001	[34] 0.013	[31] 0.011	[34] 0.008	[11] 0.156	[24] 0.111	[37] 0.079	[31] 0.002	[36] 0.001	[19] 0.022	[34] 0.012	[52] 0.079	[64] 0.068
329	OPTIEXACTA-000	[17] 0.002	[15] 0.001	[14] 0.001	[12] 0.010	[12] 0.008	[14] 0.007	[27] 0.186	[39] 0.135	[44] 0.085	[42] 0.003	[53] 0.002	[49] 0.033	[55] 0.015	[30] 0.070	[35] 0.059
330	PANGIAM-000	[165] 0.013	[177] 0.006	[163] 0.002	[152] 0.039	[160] 0.030	[157] 0.018	[221] 0.974	[108] 0.310	[125] 0.165	[161] 0.009	[159] 0.005	[155] 0.136	[128] 0.033	[118] 0.105	[124] 0.083
331	PANGIAM-001	[201] 0.023	[233] 0.011	[289] 0.008	[147] 0.039	[159] 0.030	[176] 0.020	[140] 0.646	[122] 0.376	[129] 0.171	[155] 0.009	[136] 0.004	[275] 0.860	[200] 0.081	[163] 0.141	[128] 0.085
332	PAPSAV1923-000	[89] 0.007	[94] 0.003	[78] 0.001	[91] 0.027	[92] 0.021	[94] 0.014	[79] 0.300	[91] 0.226	[111] 0.140	[164] 0.009	[187] 0.006	[82] 0.049	[91] 0.024	[94] 0.094	[100] 0.076
333	PARAVISION-000	[450] 0.271	[426] 0.088	[434] 0.045	[432] 0.447	[386] 0.170	[406] 0.100	[439] 1.000	[396] 0.999	[422] 0.997	[420] 0.470	[437] 0.443			[404] 0.926	[425] 0.779
334	PARAVISION-001	[385] 0.139	[370] 0.049	[369] 0.020	[365] 0.207	[353] 0.128	[369] 0.074	[426] 1.000	[382] 0.999	[403] 0.994	[417] 0.444	[436] 0.428			[361] 0.739	[396] 0.573
335	PARAVISION-002	[340] 0.085	[372] 0.050	[379] 0.022	[327] 0.152	[345] 0.119	[374] 0.076	[283] 0.992	[290] 0.983	[272] 0.746	[328] 0.080	[346] 0.043			[314] 0.497	[326] 0.268
336	PARAVISION-003	[316] 0.063	[344] 0.035	[350] 0.015	[300] 0.124	[320] 0.096	[339] 0.060	[329] 0.997	[336] 0.994	[267] 0.730	[307] 0.058	[330] 0.034			[252] 0.296	[307] 0.232
337	PARAVISION-004	[215] 0.025	[225] 0.010	[227] 0.004	[179] 0.049	[195] 0.038	[208] 0.024	[457] 1.000	[461] 1.000	[278] 0.794	[211] 0.018	[231] 0.011			[397] 0.908	[293] 0.211
338	PARAVISION-005	[170] 0.014	[124] 0.004	[144] 0.002	[118] 0.031	[120] 0.024	[132] 0.016	[325] 0.997	[277] 0.980	[130] 0.171	[171] 0.011	[206] 0.008			[151] 0.132	[198] 0.120
339	PARAVISION-007	[282] 0.047	[119] 0.004	[98] 0.002	[440] 0.560	[128] 0.025	[116] 0.015	[453] 1.000	[454] 1.000	[482] 1.000	[153] 0.009	[188] 0.006	[146] 0.113	[93] 0.024	[453] 1.000	[488] 1.000
340	PARAVISION-009	[85] 0.007	[79] 0.002	[52] 0.001	[87] 0.026	[85] 0.019	[72] 0.012	[167] 0.775	[193] 0.732	[233] 0.545	[43] 0.003	[41] 0.002	[48] 0.033	[57] 0.015	[35] 0.073	[39] 0.061
341	PARAVISION-012	[47] 0.004	[34] 0.001	[25] 0.001	[53] 0.016	[50] 0.012	[43] 0.009	[119] 0.541	[144] 0.469	[165] 0.263	[35] 0.002	[37] 0.002	[24] 0.025	[35] 0.012	[25] 0.068	[25] 0.057
342	PARAVISION-014	[33] 0.003	[26] 0.001	[24] 0.001	[39] 0.014	[40] 0.011	[36] 0.008	[129] 0.595	[161] 0.527	[153] 0.235	[22] 0.002	[23] 0.001	[50] 0.033	[39] 0.012	[12] 0.061	[11] 0.052
343	PARAVISION-016	[24] 0.002	[17] 0.001	[17] 0.001	[42] 0.015	[37] 0.011	[29] 0.008	[10] 0.156	[25] 0.112	[27] 0.068	[13] 0.002	[10] 0.001	[34] 0.028	[29] 0.011	[14] 0.065	[15] 0.055
344	PARAVISION-019	[29] 0.003	[13] 0.001	[8] 0.001	[38] 0.014	[28] 0.010	[20] 0.007	[40] 0.226	[61] 0.176	[75] 0.108	[10] 0.002	[8] 0.001	[38] 0.028	[28] 0.011	[10] 0.061	[7] 0.049
345	PENTACOMP-000	[538] 0.996	[540] 0.996	[546] 0.996	[527] 0.998	[533] 0.998	[538] 0.998	[274] 0.991	[317] 0.990	[381] 0.990	[456] 0.955	[461] 0.955	[370] 1.000	[351] 1.000	[418] 0.960	[442] 0.958
346	PENTACOMP-001	[246] 0.034	[270] 0.016	[283] 0.008	[429] 0.436	[387] 0.172	[265] 0.036	[148] 0.667	[153] 0.517	[201] 0.374	[326] 0.076	[254] 0.013	[356] 1.000	[332] 0.998	[292] 0.430	[264] 0.177
347	PIXELALL-002	[503] 0.664	[434] 0.105	[403] 0.029	[514] 0.974	[456] 0.388	[382] 0.083		[475] 1.000	[475] 1.000	[428] 0.602	[350] 0.047			[552] 1.000	[461] 1.000
348	PIXELALL-003	[285] 0.048	[300] 0.021	[302] 0.009	[270] 0.102	[280] 0.073	[294] 0.043		[415] 1.000	[433] 0.998	[278] 0.037	[293] 0.020			[327] 0.554	[316] 0.255
349	PIXELALL-004	[366] 0.120	[282] 0.018	[270] 0.007	[482] 0.783	[293] 0.079	[270] 0.037		[446] 1.000	[448] 0.999	[296] 0.051	[269] 0.015			[432] 0.994	[441] 0.942
350	PIXELALL-005	[333] 0.078	[235] 0.012	[229] 0.004	[435] 0.456	[227] 0.050	[228] 0.027		[450] 1.000	[459] 0.999	[244] 0.027	[278] 0.017	[190] 0.203	[184] 0.071	[442] 1.000	[449] 0.983
351	PRIVID-000	[293] 0.036	[321] 0.027	[381] 0.022	[512] 0.968	[511] 0.825	[466] 0.207	[393] 1.000	[220] 0.882	[145] 0.199	[430] 0.603	[409] 0.195	[445] 1.000	[431] 1.000	[423] 0.972	[432] 0.842
352	PROTENET-000	[524] 0.875	[527] 0.794	[526] 0.540	[490] 0.884	[512] 0.834	[519] 0.682	[261] 0.988	[276] 0.980	[315] 0.930	[444] 0.804	[444] 0.587	[449] 1.000	[353] 1.000	[391] 0.890	[419] 0.747
353	PSL-000	[75] 0.006	[77] 0.002	[50] 0.001	[109] 0.029	[94] 0.021	[78] 0.012	[76] 0.295	[78] 0.208	[83] 0.115	[79] 0.005	[63] 0.002	[93] 0.054	[100] 0.026	[100] 0.097	[89] 0.074
354	PSL-001	[59] 0.005	[68] 0.002	[45] 0.001	[77] 0.022	[74] 0.017	[64] 0.011	[19] 0.173	[30] 0.122	[31] 0.075	[47] 0.003	[38] 0.002	[35] 0.028	[44] 0.013	[39] 0.075	[37] 0.060
355	PSL-002	[35] 0.003	[25] 0.001	[12] 0.001	[47] 0.015	[39] 0.011	[24] 0.008	[9] 0.155	[15] 0.095	[15] 0.059	[26] 0.002	[13] 0.001	[22] 0.023	[26] 0.010	[51] 0.079	[38] 0.060
356	PSL-003	[48] 0.004	[27] 0.001	[11] 0.001	[37] 0.014	[35] 0.011	[18] 0.007	[33] 0.202	[20] 0.102	[21] 0.064	[24] 0.002	[22] 0.001	[20] 0.022	[23] 0.010	[114] 0.102	[29] 0.058
357	PSL-004	[37] 0.003	[16] 0.001	[7] 0.001	[25] 0.012	[22] 0.009	[10] 0.007	[20] 0.174	[19] 0.101	[23] 0.065	[14] 0.002	[9] 0.001	[21] 0.022	[25] 0.010	[42] 0.076	[27] 0.058
358	PTAKURATSATU-000	[306] 0.057	[347] 0.036	[354] 0.017	[335] 0.165	[350] 0.124	[364] 0.071	[209] 0.947	[234] 0.923	[292] 0.867	[293] 0.046	[303] 0.022	[193] 0.206	[232] 0.120	[225] 0.232	[269] 0.179
359	PYRAMID-000	[102] 0.008	[116] 0.004	[105] 0.002	[92] 0.027	[91] 0.021	[91] 0.013	[48] 0.241	[72] 0.190	[92] 0.122	[116] 0.007	[101] 0.003	[238] 0.433	[165] 0.051	[97] 0.095	[90] 0.074
360	PYRAMID-001	[112] 0.008	[143] 0.004	[145] 0.002	[192] 0.054	[222] 0.047	[276] 0.039	[62] 0.262	[73] 0.193	[94] 0.125	[245] 0.027	[312] 0.023	[128] 0.075	[150] 0.044	[107] 0.100	[123] 0.083
361	QAZSMARTVISIONAI-000	[19] 0.002	[28] 0.001	[22] 0.001	[30] 0.013	[29] 0.010	[28] 0.008	[8] 0.130	[14] 0.094	[20] 0.064	[34] 0.002	[34] 0.001	[67] 0.041	[52] 0.011	[20] 0.067	[19] 0.056
362	QAZSMARTVISIONAI-001	[10] 0.002	[5] 0.001	[3] 0.001	[9] 0.009	[9] 0.008	[7] 0.006	[4] 0.095	[5] 0.065	[9] 0.050	[16] 0.002	[11] 0.001	[27] 0.026	[13] 0.007	[8] 0.058	[9] 0.049
363	QAZSMARTVISIONAI-002	[1] 0.001	[1] 0.001	[1] 0.000	[3] 0.007	[3] 0.006	[3] 0.005	[5] 0.107	[1] 0.052	[3] 0.043	[3] 0.001	[3] 0.001	[7] 0.014	[3] 0.004	[5] 0.052	[3] 0.045
364	QAZSMARTVISIONAI-003	[3] 0.001	[2] 0.001	[2] 0.000	[2] 0.006	[1] 0.006	[1] 0.005	[2] 0.071	[3] 0.053	[4] 0.044	[2] 0.001	[2] 0.001	[12] 0.016	[4] 0.004	[2] 0.052	[2] 0.044
365	QNAP-000	[534] 0.971	[447] 0.129	[441] 0.052	[526] 0.998	[416] 0.238	[422] 0.117	[470] 1.000	[480] 1.000	[481] 1.000	[377] 0.191	[370] 0.068	[246] 0.539	[271] 0.263	[438] 0.998	[452] 0.985
366	QNAP-001	[339] 0.083	[383] 0.053	[388] 0.024	[343] 0.176	[362] 0.137	[384] 0.085	[204] 0.942	[235] 0.927	[294] 0.869	[330] 0.081	[343] 0.041	[225] 0.368	[265] 0.227	[266] 0.331	[314] 0.248
367	QNAP-002	[274] 0.044	[318] 0.026	[340] 0.013	[315] 0.136	[333] 0.106	[356] 0.068	[176] 0.818	[202] 0.769	[244] 0.617	[300] 0.052	[315] 0.025	[208] 0.281	[254] 0.171	[244] 0.272	[296] 0.214
368	QNAP-003	[252] 0.036	[286] 0.019	[297] 0.008	[516] 0.980	[513] 0.835	[333] 0.057	[410] 1.000	[323] 0.992	[198] 0.365	[424] 0.502	[369] 0.066	[341] 1.000	[350] 1.000	[386] 0.865	[363] 0.373

Table 60: **Threshold-based accuracy**. *Values are FNIR(N, T, L) with N = 1.6 million with thresholds set to produce FPIR = 0.0003, 0.001, and 0.01 in non-mate searches. Throughout blue superscripts indicate the rank of the algorithm for that column. Caution: The Power-low models are mostly intended to draw attention to the kind of behavior, not as a model to be used for prediction.*

This publication is available free of charge from: https://doi.org/10.6028/NIST.IR.8271

MISSES BELOW THRESHOLD, T		ENROL RECENT MUGSHOT, N = 1.6M									ENROL APPLICATION PORTRAIT, N = 1.6M					
		ENROL: MUGSHOT			ENROL: MUGSHOT			ENROL: MUGSHOT			ENROL: VISA		ENROL: BORDER		ENROL: VISA	
		PROBE: MUGSHOT			PROBE: WEBCAM			PROBE: PROFILE			PROBE: BORDER		PROBE: BORDER 10+YR		PROBE: KIOSK	
#	ALGORITHM	FPIR=0.0003	FPIR=0.001	FPIR=0.01	FPIR=0.0003	FPIR=0.001	FPIR=0.01	FPIR=0.0003	FPIR=0.001	FPIR=0.01	FPIR=0.001	FPIR=0.01	FPIR=0.001	FPIR=0.01	FPIR=0.001	FPIR=0.01
369	QNAP-004	242 0.034	250 0.014	245 0.005	529 0.999	516 0.890	273 0.038	454 1.000	358 0.996	179 0.295	423 0.501	358 0.056	462 1.000	339 0.999	401 0.922	387 0.530
370	QNAP-005	186 0.018	227 0.010	239 0.005	243 0.082	263 0.066	301 0.045	102 0.460	119 0.359	152 0.227	234 0.024	262 0.014	145 0.110	173 0.061	143 0.127	177 0.108
371	QNAP-006	188 0.018	210 0.008	213 0.003	194 0.055	211 0.042	224 0.026	108 0.488	125 0.388	160 0.244	215 0.019	214 0.009	153 0.131	179 0.065	156 0.137	172 0.102
372	QUANTASOFT-001	508 0.713	524 0.638	525 0.493												
373	RANKONE-002	408 0.182	440 0.117	457 0.070	398 0.308	427 0.261	458 0.190									
374	RANKONE-003	407 0.182	441 0.117	458 0.070	394 0.300	425 0.255	456 0.187									
375	RANKONE-004	441 0.250	472 0.193	485 0.124	442 0.482	462 0.426	489 0.324									
376	RANKONE-005	346 0.095	397 0.059	409 0.033	366 0.212	390 0.173	423 0.119	373 0.999	371 0.998	405 0.994						
377	RANKONE-006	311 0.060	349 0.037	363 0.019				256 0.987	270 0.977	320 0.936						
378	RANKONE-007	243 0.034	303 0.022	326 0.011	292 0.118	317 0.095	342 0.061	225 0.975	253 0.967	311 0.923						
379	RANKONE-009	235 0.030	277 0.017	291 0.008	261 0.098	284 0.076	298 0.045	241 0.982	258 0.969	290 0.857	310 0.062	322 0.029			264 0.328	286 0.206
380	RANKONE-010	202 0.023	247 0.013	271 0.007	235 0.077	250 0.058	264 0.036	193 0.904	207 0.799	255 0.648	299 0.052	318 0.027	194 0.208	231 0.119	236 0.259	280 0.194
381	RANKONE-011	359 0.109	211 0.008	221 0.004	239 0.079	224 0.048	235 0.029				277 0.037	284 0.017	185 0.182	218 0.092	424 0.977	378 0.465
382	RANKONE-012	197 0.020	200 0.007	215 0.003	229 0.072	241 0.053	237 0.030				253 0.029	259 0.014	162 0.144	185 0.072	305 0.465	216 0.128
383	RANKONE-013	133 0.010	137 0.004	142 0.002	173 0.046	180 0.034	173 0.020	343 0.998	354 0.996	147 0.205	212 0.018	203 0.008	159 0.141	161 0.050	166 0.142	165 0.097
384	RANKONE-014	98 0.008	95 0.003	87 0.001	128 0.033	121 0.024	111 0.015				159 0.009	142 0.004	131 0.081	99 0.026	491 1.000	119 0.083
385	RANKONE-015	67 0.005	83 0.002	81 0.001	84 0.024	82 0.018	79 0.012				117 0.007	114 0.003	72 0.042	77 0.020	126 0.109	137 0.088
386	REALNETWORKS-000	467 0.365	484 0.233	489 0.137	428 0.433	448 0.319	469 0.209									
387	REALNETWORKS-001	468 0.365	483 0.233	488 0.137	427 0.433	447 0.319	468 0.209									
388	REALNETWORKS-002	470 0.369	481 0.231	487 0.137	424 0.416	446 0.315	470 0.209									
389	REALNETWORKS-003	451 0.272	460 0.159	468 0.090	404 0.342	430 0.266	453 0.172	368 0.999	327 0.998	373 0.987	369 0.164	391 0.103			315 0.500	360 0.364
390	REALNETWORKS-004	438 0.242	459 0.158	467 0.090	411 0.353	428 0.263	450 0.169	391 1.000	397 0.999	396 0.992	372 0.170	392 0.103			337 0.613	362 0.370
391	REALNETWORKS-005	293 0.052	327 0.027	333 0.012	256 0.094	282 0.074	304 0.047	246 0.983	260 0.970	301 0.894	276 0.037	279 0.017	198 0.223	234 0.123	219 0.215	252 0.165
392	REALNETWORKS-006	218 0.025	253 0.014	246 0.005	223 0.068	238 0.053	249 0.032	287 0.993	280 0.980	285 0.836	200 0.016	209 0.008	148 0.120	176 0.063	178 0.154	190 0.116
393	REALNETWORKS-007	195 0.019	220 0.009	220 0.004	198 0.057	214 0.043	227 0.027	280 0.991	274 0.979	289 0.853	179 0.012	176 0.005	241 0.463	177 0.063	162 0.140	169 0.100
394	REALNETWORKS-008	156 0.012	178 0.006	187 0.003	143 0.037	156 0.029	156 0.018	264 0.988	255 0.967	164 0.262	147 0.008	156 0.004	120 0.068	134 0.035	146 0.129	183 0.110
395	RECOGNITO-000	44 0.004	56 0.002	51 0.001	46 0.015	43 0.012	44 0.009	59 0.257	60 0.175	80 0.113	129 0.007	120 0.003	256 0.730	286 0.437	87 0.092	79 0.070
396	RECOGNITO-001	20 0.002	30 0.001	27 0.001	19 0.010	18 0.009	17 0.007	216 0.971	229 0.899	62 0.099	49 0.003	56 0.002	51 0.033	58 0.016	38 0.075	48 0.063
397	RECOGNITO-002	18 0.002	14 0.001	15 0.001	14 0.010	14 0.008	15 0.007	26 0.186	38 0.135	43 0.085	38 0.003	39 0.002	243 0.510	268 0.248	25 0.068	18 0.055
398	REMARKAI-000	370 0.124	387 0.055	382 0.022	339 0.173	346 0.120	359 0.070	378 0.999	394 0.999	409 0.995	320 0.069	329 0.033			359 0.717	345 0.315
399	REMARKAI-000	422 0.196	445 0.127	449 0.059	384 0.263	401 0.203	426 0.123									
400	REMARKAI-002	415 0.186	444 0.123	448 0.058	378 0.248	399 0.196	425 0.122	291 0.993	318 0.991	362 0.980						
401	RENDIP-000	203 0.023	234 0.012	237 0.005	352 0.189	251 0.059	257 0.034	208 0.945	226 0.892	270 0.741	227 0.022	249 0.013	187 0.185	213 0.089	192 0.167	220 0.130
402	REVEALMEDIA-000	204 0.023	236 0.012	244 0.005	191 0.054	210 0.042	218 0.025	157 0.752	186 0.677	232 0.533	224 0.021	232 0.011	139 0.093	164 0.051	168 0.143	194 0.118
403	RNIT-000	472 0.388	230 0.011	186 0.003	158 0.042	136 0.026	125 0.016	149 0.672	151 0.510	173 0.285	180 0.012	166 0.005	201 0.239	145 0.041	140 0.123	127 0.084
404	ROC-016	71 0.006	73 0.002	61 0.001	75 0.022	76 0.017	74 0.012				132 0.008	131 0.004	73 0.045	78 0.020	123 0.108	111 0.079
405	ROC-017	81 0.006	90 0.003	80 0.001	102 0.028	101 0.022	95 0.014	57 0.253	59 0.174	70 0.105	110 0.006	97 0.003	64 0.039	59 0.016	86 0.092	84 0.073
406	ROC-018	77 0.006	65 0.002	55 0.001	81 0.023	80 0.018	69 0.011	39 0.223	44 0.142	51 0.089	85 0.006	76 0.002	58 0.037	50 0.015	63 0.085	58 0.066
407	ROC-019	43 0.004	32 0.001	16 0.001	22 0.011	21 0.009	13 0.007	34 0.203	17 0.098	18 0.062	28 0.002	26 0.001	31 0.027	24 0.010	29 0.070	23 0.057
408	S1-000	380 0.136	329 0.028	324 0.010	304 0.129	300 0.085	308 0.048	468 1.000	482 1.000	240 0.591	295 0.047	288 0.018	358 1.000	233 0.123	495 1.000	403 0.632
409	S1-001	298 0.053	263 0.015	268 0.007	214 0.066	235 0.052	254 0.033	281 0.992	298 0.985	333 0.952	213 0.019	224 0.010	154 0.136	189 0.075	172 0.148	195 0.119
410	S1-002	310 0.060	168 0.005	157 0.002	247 0.085	163 0.031	149 0.018	195 0.923	69 0.186	45 0.085	124 0.007	111 0.003	269 0.792	248 0.151	381 0.841	235 0.144
411	S1-003	290 0.050	212 0.008	205 0.003	187 0.052	191 0.037	192 0.022	432 1.000	434 1.000	378 0.989	194 0.014	184 0.006	230 0.396	137 0.037	543 1.000	292 0.209
412	S1-004	207 0.024	120 0.004	123 0.002	131 0.034	122 0.025	130 0.016	420 1.000	360 0.997	136 0.182	100 0.006	96 0.003	108 0.064	94 0.024	487 1.000	130 0.086
413	S1-005	211 0.024	132 0.004	131 0.002	116 0.031	108 0.022	118 0.015	327 0.999	337 0.994	107 0.138	91 0.006	68 0.002	112 0.065	88 0.023	394 0.895	99 0.076
414	S1-006	181 0.016	66 0.002	75 0.001	73 0.021	73 0.016	73 0.012	469 1.000	402 0.999	64 0.103	75 0.005	69 0.002	66 0.040	72 0.019	291 0.423	78 0.070

Table 61: **Threshold-based accuracy**. *Values are FNIR(N, T, L) with N = 1.6 million with thresholds set to produce FPIR = 0.0003, 0.001, and 0.01 in non-mate searches. Throughout blue superscripts indicate the rank of the algorithm for that column. Caution: The Power-low models are mostly intended to draw attention to the kind of behavior, not as a model to be used for prediction.*

FNIR(N, R, T) = False neg. identification rate
FPIR(N, T) = False pos. identification rate
N = Num. enrolled subjects
R = Num. candidates examined
T = Threshold
T = 0 → Investigation
T > 0 → Identification

This publication is available free of charge from: https://doi.org/10.6028/NIST.IR.8271

MISSES BELOW THRESHOLD, T		ENROL RECENT MUGSHOT, N = 1.6M									ENROL APPLICATION PORTRAIT, N = 1.6M					
		ENROL: MUGSHOT			ENROL: MUGSHOT			ENROL: MUGSHOT			ENROL: VISA		ENROL: BORDER		ENROL: VISA	
		PROBE: MUGSHOT			PROBE: WEBCAM			PROBE: PROFILE			PROBE: BORDER		PROBE: BORDER 10+YR		PROBE: KIOSK	
#	ALGORITHM	FPIR=0.0003	FPIR=0.001	FPIR=0.01	FPIR=0.0003	FPIR=0.001	FPIR=0.01	FPIR=0.0003	FPIR=0.001	FPIR=0.01	FPIR=0.001	FPIR=0.01	FPIR=0.001	FPIR=0.01	FPIR=0.001	FPIR=0.01
415	S1-007	61 0.005	54 0.002	60 0.001	64 0.018	61 0.014	62 0.010	92 0.367	54 0.165	48 0.088	60 0.004	59 0.002	52 0.034	61 0.016	44 0.077	42 0.062
416	SANSAP-001	148 0.012	133 0.004	135 0.002	479 0.755	473 0.480	217 0.025	265 0.989	245 0.958	137 0.184	237 0.024	181 0.006	322 1.000	327 0.991	247 0.280	207 0.124
417	SCANOVATE-000	353 0.102	405 0.066	404 0.030	393 0.296	419 0.240	438 0.150	200 0.930	224 0.892	279 0.800	383 0.215	400 0.118			281 0.400	339 0.299
418	SCANOVATE-001	374 0.128	416 0.081	418 0.037	391 0.281	412 0.227	433 0.140	202 0.934	233 0.910	284 0.832	378 0.192	393 0.103			285 0.404	335 0.290
419	SCYLLA-001	233 0.030	271 0.016	281 0.007	528 0.999	532 0.995	518 0.680	146 0.664	141 0.457	180 0.299	415 0.431	420 0.279		379 1.000	414 0.953	415 0.714
420	SENSETIME-000	251 0.035	294 0.020	305 0.009	236 0.078	260 0.063	285 0.040	483 1.000	530 1.000	375 0.987						
421	SENSETIME-001	254 0.036	301 0.022	308 0.009	241 0.080	262 0.064	292 0.041									
422	SENSETIME-002	255 0.036	256 0.014	346 0.014	299 0.124	150 0.028	205 0.023	322 0.997	333 0.994	360 0.978	261 0.032	280 0.017			320 0.523	251 0.160
423	SENSETIME-003	49 0.004	47 0.001	47 0.001	41 0.014	47 0.012	48 0.009	132 0.602	145 0.471	182 0.303	141 0.008	175 0.005			152 0.133	189 0.115
424	SENSETIME-004	32 0.003	42 0.001	46 0.001	48 0.015	52 0.013	55 0.010	75 0.293	89 0.220	110 0.140	94 0.006	128 0.004			132 0.113	168 0.100
425	SENSETIME-005	137 0.010	64 0.002	39 0.001	67 0.018	60 0.014	52 0.010	54 0.250	53 0.163	56 0.092	114 0.007	133 0.004	88 0.051	90 0.023	116 0.104	151 0.093
426	SENSETIME-006	52 0.004	44 0.001	32 0.001	51 0.016	48 0.012	40 0.009	353 0.999	373 0.998	259 0.676	57 0.004	50 0.002	53 0.034	63 0.016	88 0.093	110 0.079
427	SENSETIME-007	30 0.003	23 0.001	19 0.001	23 0.012	24 0.009	21 0.007	390 1.000	400 0.999	231 0.533	36 0.003	33 0.001	23 0.024	30 0.011	65 0.085	92 0.074
428	SENSETIME-008	16 0.002	20 0.001	13 0.001	21 0.011	20 0.009	16 0.007	269 0.990	127 0.398	32 0.075	29 0.002	24 0.001	18 0.021	19 0.009	55 0.080	88 0.074
429	SENSETIME-009	* 0.001	6 0.001	9 0.001	6 0.008	6 0.007	8 0.006	366 0.999	217 0.866	14 0.058	9 0.001	12 0.001	8 0.015	12 0.007	67 0.085	113 0.081
430	SENSETIME-010	5 0.001	8 0.001	5 0.001	13 0.010	10 0.008	12 0.007	21 0.176	16 0.096	13 0.058	19 0.002	16 0.001	17 0.020	17 0.008	75 0.087	117 0.082
431	SERENDIPITY-000	206 0.023	240 0.012	236 0.005	440 0.474	404 0.213	267 0.036	179 0.842	196 0.745	239 0.575	209 0.018	221 0.010	336 1.000	340 0.999	167 0.142	175 0.106
432	SEVENTHSENSE-001	113 0.009	142 0.004	180 0.003	195 0.055	212 0.043	216 0.025	90 0.346	93 0.228	99 0.130	163 0.010	165 0.005	250 0.643	279 0.351	144 0.127	155 0.095
433	SHAMAN-003	487 0.506	513 0.451	518 0.346	463 0.650	484 0.597	503 0.472									
434	SHAMAN-004	505 0.678	522 0.615	523 0.488	485 0.812	501 0.754	514 0.639									
435	SHAMAN-006	413 0.184	453 0.141	470 0.092	389 0.278	415 0.237	449 0.168	228 0.977	262 0.971	339 0.959						
436	SHAMAN-007	411 0.183	454 0.141	469 0.092	390 0.280	418 0.240	451 0.169									
437	SHENNONA-000	287 0.049	302 0.022	348 0.015	369 0.221	382 0.160	411 0.104	115 0.524	124 0.383	154 0.235	367 0.160	364 0.064	503 1.000	343 1.000	331 0.558	353 0.350
438	SIAT-001	373 0.127	276 0.017	267 0.007	460 0.641	452 0.365	492 0.348				257 0.031	258 0.014				
439	SIAT-002	473 0.417	298 0.021	273 0.007	496 0.942	472 0.478	501 0.460				406 0.372	429 0.356			402 0.923	255 0.169
440	SMILART-004	533 0.970	537 0.968	542 0.965	515 0.977	528 0.976	535 0.973									
441	SMILART-005															
442	SPARKTEK-000	91 0.007	92 0.003	95 0.001	69 0.018	67 0.015	60 0.010	107 0.487	130 0.414	177 0.294	99 0.006	119 0.003	79 0.048	82 0.022	122 0.106	134 0.087
443	SPARSH-001	122 0.009	128 0.004	104 0.002	503 0.952	502 0.759	279 0.039	282 0.992	268 0.976	124 0.164	370 0.166	294 0.020	467 1.000	338 0.999	341 0.633	349 0.340
444	SQISOFT-001	434 0.226	449 0.132	431 0.044	402 0.340	423 0.252	418 0.111	212 0.955	205 0.794	242 0.604	282 0.040	291 0.019	217 0.317	246 0.150	289 0.420	278 0.189
445	SQISOFT-002	331 0.074	334 0.029	252 0.006			531 0.908		230 0.903	163 0.258	433 0.621	377 0.074			415 0.953	373 0.435
446	STAQU-000	462 0.334	398 0.061	375 0.021	487 0.848	465 0.443	341 0.061	416 1.000	430 1.000	451 0.999	426 0.535	339 0.039	292 0.961	257 0.183	549 1.000	459 0.999
447	STCON-000	414 0.185	469 0.184	498 0.183	466 0.679	495 0.678	516 0.675	91 0.355	111 0.318	172 0.284	437 0.674	448 0.674	286 0.941	310 0.837	357 0.709	412 0.709
448	STCON-001	42 0.004	43 0.001	35 0.001	54 0.016	46 0.012	41 0.009	29 0.192	35 0.131	40 0.082	37 0.003	35 0.001	226 0.370	249 0.158	26 0.069	20 0.056
449	STCON-002	31 0.003	36 0.001	28 0.001	35 0.013	33 0.011	27 0.008	14 0.162	26 0.115	29 0.074	30 0.002	32 0.001	234 0.415	258 0.185	22 0.067	16 0.055
450	STCON-003	27 0.003	31 0.001	26 0.001	26 0.012	27 0.010	23 0.007	17 0.171	23 0.110	28 0.071	27 0.002	27 0.001	43 0.031	22 0.009	15 0.065	13 0.053
451	SUMSUB-000	504 0.675	512 0.445	495 0.173	491 0.888	499 0.742	493 0.348	464 1.000	463 1.000	487 1.000	447 0.852	439 0.453	524 1.000	546 1.000	434 0.996	436 0.901
452	SYNESIS-003	500 0.648	518 0.582	522 0.443	471 0.708	490 0.646	505 0.524									
453	SYNESIS-003	360 0.111	403 0.065	406 0.031	328 0.155	349 0.123	375 0.078	219 0.973	247 0.960	303 0.910	325 0.075	337 0.039			258 0.314	309 0.235
454	SYNESIS-005	286 0.049	311 0.024	328 0.011	250 0.088	277 0.072	295 0.043	304 0.995	293 0.983	276 0.793	264 0.032	271 0.016			217 0.214	250 0.158
455	T4ISB-000	223 0.027	264 0.015	321 0.010	221 0.068	239 0.053	258 0.034	123 0.561	149 0.505	216 0.457	222 0.021	227 0.010	263 0.759	255 0.177	189 0.161	210 0.125
456	TECH5-001	516 0.807	390 0.057	357 0.018	521 0.994	523 0.935	331 0.055	531 1.000	481 1.000	469 1.000	386 0.244	321 0.028			433 0.994	430 0.817
457	TECH5-002	297 0.053	322 0.027	332 0.012	255 0.094	275 0.070	287 0.040	185 0.872	208 0.803	246 0.622	280 0.039	290 0.019	191 0.205	229 0.111	297 0.440	273 0.182
458	TECH5-003	115 0.009	117 0.004	99 0.002	509 0.964	506 0.801	312 0.049	294 0.994	288 0.982	122 0.160	375 0.179	311 0.023	409 1.000	349 1.000	348 0.656	355 0.358
459	TEVIAN-003	437 0.238	467 0.177	475 0.096	407 0.346	441 0.298	461 0.198									
460	TEVIAN-004	404 0.169	438 0.117	454 0.063	367 0.216	392 0.176	421 0.115									

Table 62: **Threshold-based accuracy**. *Values are FNIR(N, T, L) with N = 1.6 million with thresholds set to produce FPIR = 0.0003, 0.001, and 0.01 in non-mate searches. Throughout blue superscripts indicate the rank of the algorithm for that column. Caution: The Power-low models are mostly intended to draw attention to the kind of behavior, not as a model to be used for prediction.*

This publication is available free of charge from: https://doi.org/10.6028/NIST.IR.8271

MISSES BELOW THRESHOLD, T		ENROL RECENT MUGSHOT, N = 1.6M									ENROL APPLICATION PORTRAIT, N = 1.6M					
		ENROL: MUGSHOT			ENROL: MUGSHOT			ENROL: MUGSHOT			ENROL: VISA		ENROL: BORDER		ENROL: VISA	
		PROBE: MUGSHOT			PROBE: WEBCAM			PROBE: PROFILE			PROBE: BORDER		PROBE: BORDER 10+YR		PROBE: KIOSK	
#	ALGORITHM	FPIR=0.0003	FPIR=0.001	FPIR=0.01	FPIR=0.0003	FPIR=0.001	FPIR=0.01	FPIR=0.0003	FPIR=0.001	FPIR=0.01	FPIR=0.001	FPIR=0.01	FPIR=0.001	FPIR=0.01	FPIR=0.001	FPIR=0.01
461	TEVIAN-005	375 0.128	423 0.087	433 0.044	346 0.180	369 0.144	388 0.089	259 0.987	250 0.961	277 0.793						
462	TEVIAN-006	209 0.024	221 0.009	235 0.005	156 0.041	170 0.032	189 0.021	122 0.556	131 0.418	171 0.282	202 0.016	210 0.009	137 0.093	159 0.050	413 0.951	193 0.117
463	TEVIAN-007	140 0.011	159 0.005	173 0.002	97 0.028	100 0.022	108 0.015	112 0.498	106 0.293	134 0.174	160 0.009	167 0.005	111 0.065	127 0.033	139 0.122	171 0.102
464	TIGER-000	482 0.461	506 0.390	510 0.261	450 0.565	474 0.500	493 0.366									
465	TIGER-002	402 0.157	420 0.086	423 0.039	362 0.202	379 0.158	392 0.095	380 0.999	387 0.999	355 0.975						
466	TIGER-003	401 0.157	419 0.086	422 0.039	361 0.202	378 0.158	396 0.095									
467	TIGER-004	249 0.035	273 0.017	293 0.008	274 0.105	278 0.072	282 0.040	109 0.489	129 0.410	168 0.278	337 0.095	274 0.016	331 1.000	324 0.990	282 0.402	234 0.143
468	TONGYITRANS-000	354 0.105	410 0.074	421 0.038	320 0.141	338 0.112	358 0.069									
469	TONGYITRANS-001	369 0.123	404 0.066	407 0.032	302 0.128	327 0.101	345 0.062									
470	TOSHIBA-000	368 0.122	399 0.062	397 0.026	324 0.150	343 0.118	368 0.074	327 0.997	346 0.995	376 0.988						
471	TOSHIBA-001	432 0.222	393 0.057	359 0.018	311 0.133	312 0.092	330 0.054									
472	TOSHIBA-002	58 0.005	48 0.001	58 0.001	59 0.017	69 0.015	80 0.012	23 0.179	13 0.094	17 0.060	20 0.002	21 0.001	44 0.031	15 0.008	19 0.066	14 0.054
473	TOSS-000	45 0.004	58 0.002	76 0.001	62 0.017	62 0.014	66 0.011	24 0.182	28 0.121	34 0.077	51 0.003	42 0.002	57 0.037	43 0.013	27 0.069	33 0.058
474	TRUEFACE-000	277 0.046	281 0.018	292 0.008	237 0.079	258 0.062	277 0.039	309 0.995	219 0.881	221 0.493	254 0.030	275 0.016	189 0.194	230 0.111	210 0.188	238 0.145
475	TTIGROUP-000	364 0.116	213 0.009	211 0.003	448 0.553	442 0.298	243 0.032	357 0.999	375 0.998	371 0.986	393 0.286	365 0.065	334 1.000	344 1.000	384 0.855	389 0.540
476	TURINGTECHVIP-001	521 0.865	497 0.345	325 0.011	510 0.967	514 0.850	454 0.173	379 0.999	325 0.993	140 0.196	459 0.978	451 0.754	438 1.000	352 1.000	440 0.999	451 0.984
477	UNISSEY-001	430 0.217	478 0.214	504 0.211	472 0.709	497 0.700	520 0.695	163 0.767	176 0.619	230 0.532	440 0.693	450 0.691	312 0.999	326 0.991	362 0.748	417 0.742
478	UNISSEY-002	420 0.190	470 0.187	499 0.183	470 0.703	496 0.685	517 0.677	169 0.792	168 0.571	211 0.441	443 0.724	449 0.678	313 1.000	328 0.992	392 0.891	423 0.769
479	UNISSEY-003	232 0.029	255 0.014	277 0.007	208 0.063	228 0.050	255 0.033	182 0.857	159 0.524	194 0.347	251 0.029	297 0.020	192 0.205	192 0.077	196 0.173	192 0.116
480	USEB-000	513 0.789	525 0.715	526 0.509	483 0.803	498 0.722	509 0.531	237 0.980	256 0.968	308 0.914	421 0.490	426 0.301	270 0.804	301 0.651	345 0.648	383 0.506
481	USEB-001	118 0.009	114 0.004	121 0.002	104 0.029	112 0.023	124 0.016	275 0.991	283 0.982	297 0.877	73 0.005	79 0.003	254 0.728	204 0.081	72 0.087	67 0.068
482	USEB-002	194 0.019	127 0.004	140 0.002	112 0.030	118 0.023	129 0.016	276 0.991	284 0.982	298 0.877	81 0.005	80 0.003	255 0.728	205 0.081	77 0.088	71 0.069
483	USEB-003	116 0.009	111 0.003	119 0.002	90 0.026	97 0.021	114 0.015	252 0.984	261 0.971	291 0.861	80 0.005	81 0.003	232 0.398	151 0.044	73 0.087	76 0.069
484	USEB-004	94 0.007	107 0.003	110 0.002	119 0.031	109 0.022	112 0.015	74 0.284	66 0.182	69 0.105	170 0.010	62 0.002	320 1.000	320 0.975	209 0.186	145 0.090
485	VD-000	529 0.949	534 0.917	538 0.827	511 0.968	525 0.946	529 0.871									
486	VD-001	452 0.278	473 0.201	482 0.115	400 0.331	438 0.281	457 0.188									
487	VD-002	392 0.144	414 0.078	414 0.036	351 0.188	371 0.148	389 0.092	339 0.998	350 0.995	372 0.987	336 0.095	351 0.048	221 0.367	264 0.220	275 0.372	330 0.280
488	VD-003	436 0.234	366 0.045	364 0.019	310 0.133	326 0.100	344 0.061	376 0.999	389 0.999	401 0.994	297 0.051	317 0.027	203 0.244	235 0.133	260 0.315	282 0.203
489	VDFSOFTWARE-001	546 1.000	546 1.000	543 0.990	477 0.746	476 0.518	483 0.301	461 1.000	460 1.000	472 1.000	439 0.680	403 0.144	314 1.000	323 0.989	412 0.948	398 0.608
490	VDFSOFTWARE-002	324 0.068	353 0.038	347 0.015	372 0.229	334 0.107	320 0.052	213 0.969	189 0.713	205 0.398	324 0.075	313 0.024	328 1.000	325 0.990	290 0.423	288 0.207
491	VERIDAS-001	335 0.080	351 0.037	351 0.016	277 0.106	297 0.082	316 0.051	290 0.993	307 0.987	321 0.937	288 0.044	309 0.023	205 0.266	243 0.146	241 0.264	283 0.204
492	VERIDAS-002	336 0.080	350 0.037	352 0.016	276 0.106	298 0.082	315 0.051	289 0.993	306 0.987	322 0.937	287 0.044	310 0.023	206 0.266	244 0.146	240 0.264	284 0.204
493	VERIDAS-003	327 0.072	269 0.016	256 0.006	226 0.071	245 0.055	252 0.033	349 0.998	359 0.997	313 0.927	219 0.020	230 0.011	167 0.150	195 0.078	201 0.178	233 0.142
494	VERIDAS-004	219 0.026	170 0.005	168 0.002	132 0.034	130 0.025	137 0.017	271 0.990	273 0.978	283 0.820	139 0.008	160 0.005	100 0.058	113 0.029	136 0.118	176 0.107
495	VERIGRAM-000	130 0.010	150 0.005	189 0.003	135 0.034	151 0.028	186 0.021	155 0.722	83 0.212	74 0.108	104 0.006	122 0.004	133 0.088	95 0.024	62 0.083	72 0.069
496	VERIGRAM-001	164 0.013	152 0.005	188 0.003	425 0.419	202 0.039	183 0.021	251 0.984	172 0.584	77 0.110	102 0.006	117 0.003	297 0.988	118 0.030	58 0.082	57 0.066
497	VERIJELAS-000	519 0.846	528 0.799	533 0.681	489 0.868	508 0.813	521 0.697	369 0.999	384 0.999	413 0.995	399 0.324	412 0.216	285 0.933	294 0.561	332 0.589	377 0.462
498	VIANTE-000	136 0.010	85 0.003	85 0.001	55 0.016	58 0.014	57 0.010	83 0.311	47 0.147	63 0.102	109 0.006	104 0.003	61 0.038	69 0.018	74 0.087	81 0.071
499	VIANTE-001	68 0.006	37 0.001	49 0.001	17 0.010	23 0.009	39 0.008	60 0.260	21 0.105	39 0.080	32 0.002	31 0.001	211 0.293	18 0.008	21 0.067	24 0.057
500	VIGILANTSOLUTIONS-003	485 0.481	510 0.408	513 0.281	476 0.730	493 0.660	507 0.526	371 0.999	383 0.999	410 0.995						
501	VIGILANTSOLUTIONS-004	499 0.623	517 0.549	521 0.422	488 0.858	510 0.817	522 0.709	344 0.998	353 0.996	390 0.991						
502	VIGILANTSOLUTIONS-005	528 0.934	504 0.386	426 0.042				450 1.000	453 1.000	484 1.000						
503	VIGILANTSOLUTIONS-006	531 0.955	500 0.349	429 0.043				466 1.000	465 1.000	486 1.000						
504	VIGILANTSOLUTIONS-007	332 0.075	333 0.028	327 0.011	286 0.113	306 0.088	324 0.053	334 0.997	352 0.996	393 0.991	331 0.081	348 0.047	227 0.371	267 0.242	280 0.391	338 0.295
505	VIGILANTSOLUTIONS-008	291 0.050	291 0.020	307 0.009	275 0.105	287 0.077	302 0.046	384 1.000	386 0.999	389 0.991	341 0.104	357 0.054	231 0.398	270 0.259	317 0.511	346 0.316
506	VINBIGDATA-001	227 0.028	265 0.016	238 0.005	364 0.204	254 0.059	236 0.029	302 0.995	237 0.931	176 0.293	210 0.018	200 0.007	287 0.944	171 0.061	245 0.274	156 0.095

Table 63: **Threshold-based accuracy**. *Values are FNIR(N, T, L) with N = 1.6 million with thresholds set to produce FPIR = 0.0003, 0.001, and 0.01 in non-mate searches. Throughout blue superscripts indicate the rank of the algorithm for that column. Caution: The Power-low models are mostly intended to draw attention to the kind of behavior, not as a model to be used for prediction.*

2026/01/09 20:40:38

FNIR(N, R, T) = FPIR(N, T) = False neg. identification rate / False pos. identification rate

N = Num. enrolled subjects
R = Num. candidates examined

T = Threshold

T = 0 → Investigation
T > 0 → Identification

This publication is available free of charge from: https://doi.org/10.6028/NIST.IR.8271

MISSES BELOW THRESHOLD, T		ENROL RECENT MUGSHOT, N = 1.6M									ENROL APPLICATION PORTRAIT, N = 1.6M					
		ENROL: MUGSHOT			ENROL: MUGSHOT			ENROL: MUGSHOT			ENROL: VISA		ENROL: BORDER		ENROL: VISA	
		PROBE: MUGSHOT			PROBE: WEBCAM			PROBE: PROFILE			PROBE: BORDER		PROBE: BORDER 10+YR		PROBE: KIOSK	
#	ALGORITHM	FPIR=0.0003	FPIR=0.001	FPIR=0.01	FPIR=0.0003	FPIR=0.001	FPIR=0.01	FPIR=0.0003	FPIR=0.001	FPIR=0.01	FPIR=0.001	FPIR=0.01	FPIR=0.001	FPIR=0.01	FPIR=0.001	FPIR=0.01
507	VINBIGDATA-002	78 0.006	63 0.002	59 0.001	52 0.016	42 0.012	35 0.008	46 0.237	52 0.160	61 0.095	67 0.005	71 0.002	216 0.317	76 0.019	41 0.076	51 0.064
508	VINBIGDATA-003	99 0.008	72 0.002	56 0.001	57 0.016	53 0.013	42 0.009	41 0.226	43 0.141	38 0.080	59 0.004	57 0.002	65 0.039	45 0.014	32 0.070	28 0.058
509	VINBIGDATA-004	73 0.006	50 0.002	36 0.001	31 0.013	30 0.010	26 0.008	56 0.251	34 0.130	33 0.076	44 0.003	44 0.002	45 0.032	33 0.012	24 0.068	30 0.058
510	VISIONBOX-000	328 0.073	278 0.017	269 0.007	227 0.071	248 0.057	262 0.035	298 0.994	316 0.990	353 0.973	230 0.023	245 0.012	164 0.146	199 0.081	190 0.162	212 0.126
511	VISIONBOX-001	501 0.649	450 0.133	261 0.006	431 0.441	255 0.060	239 0.031	421 1.000	467 1.000	466 1.000	363 0.152	222 0.010	309 0.999	212 0.087	403 0.924	327 0.269
512	VISIONBOX-002	200 0.022	231 0.011	233 0.005	193 0.055	209 0.042	219 0.025	249 0.984	192 0.730	189 0.336	196 0.015	201 0.007	150 0.125	178 0.063	161 0.140	167 0.099
513	VISIONLABS-004	343 0.090	392 0.057	387 0.024	357 0.199	380 0.159	400 0.097	205 0.943	223 0.888	269 0.739						
514	VISIONLABS-005	337 0.080	373 0.050	366 0.020	349 0.183	370 0.147	386 0.087	207 0.945	222 0.886	268 0.733						
515	VISIONLABS-006	273 0.044	320 0.026	316 0.010	290 0.117	310 0.090	319 0.051	162 0.762	180 0.668	227 0.506						
516	VISIONLABS-007	272 0.044	319 0.026	314 0.010	289 0.117	309 0.090	318 0.051	161 0.762	181 0.668	226 0.505	260 0.031	263 0.014			206 0.185	239 0.145
517	VISIONLABS-008	226 0.027	244 0.013	243 0.005	220 0.068	234 0.051	247 0.032	127 0.569	146 0.475	184 0.309	203 0.017	204 0.008			174 0.151	196 0.119
518	VISIONLABS-009	150 0.012	138 0.004	115 0.002	122 0.032	132 0.025	141 0.017	199 0.929	206 0.797	139 0.186	148 0.008	154 0.004			131 0.113	153 0.093
519	VISIONLABS-010	169 0.014	157 0.005	151 0.002	134 0.034	146 0.027	168 0.019			120 0.159	136 0.008	134 0.004	96 0.055	102 0.027	124 0.109	142 0.089
520	VISIONLABS-011	142 0.011	98 0.003	86 0.001	82 0.024	86 0.020	96 0.014			138 0.184	64 0.004	74 0.002	54 0.034	67 0.017	83 0.090	107 0.079
521	VISTEAM-000	387 0.140	418 0.085	420 0.038	465 0.674	402 0.205	392 0.093	215 0.970	221 0.886	258 0.666	350 0.128	363 0.062	323 1.000	335 0.999	269 0.345	311 0.240
522	VISTEAM-001	405 0.172	436 0.109	436 0.046	550 1.000	470 0.469	414 0.105	206 0.944	218 0.878	261 0.691	364 0.154	376 0.074	339 1.000	341 1.000	276 0.374	320 0.262
523	VIXVIZION-009	295 0.053	324 0.027	335 0.012	263 0.098	285 0.077	307 0.048	227 0.976	195 0.742	228 0.513	284 0.041	299 0.021	209 0.286	253 0.165	308 0.472	266 0.178
524	VNIS-000	492 0.541	494 0.311	507 0.234	433 0.448	460 0.418	496 0.383	319 0.996	326 0.993	335 0.953	442 0.701	447 0.663	274 0.838	309 0.782	355 0.696	404 0.635
525	VNPAY-001	161 0.013	172 0.006	174 0.002	136 0.035	139 0.026	128 0.016	110 0.491	103 0.280	119 0.156	178 0.012	196 0.007	114 0.066	133 0.034	125 0.109	161 0.097
526	VNPT-001	225 0.027	251 0.014	259 0.006	330 0.158	270 0.068	263 0.036	194 0.921	190 0.715	199 0.365	271 0.035	235 0.011	299 0.990	291 0.537	272 0.362	225 0.134
527	VNPT-002	163 0.013	184 0.006	202 0.003	153 0.040	169 0.032	188 0.021	124 0.563	105 0.284	116 0.144	130 0.007	126 0.004	123 0.072	120 0.031	98 0.096	98 0.075
528	VNPT-003	166 0.013	181 0.006	193 0.003	141 0.036	152 0.028	146 0.018	260 0.988	248 0.960	133 0.173	125 0.007	127 0.004	105 0.062	114 0.030	99 0.096	102 0.077
529	VNPT-004	141 0.011	163 0.005	177 0.002	129 0.033	133 0.026	135 0.016	214 0.969	228 0.899	126 0.166	119 0.007	118 0.003	97 0.057	108 0.027	89 0.093	93 0.075
530	VNPT-005	114 0.009	139 0.004	156 0.002	111 0.030	115 0.023	113 0.015	203 0.936	215 0.853	113 0.141	77 0.005	87 0.003	77 0.047	87 0.023	81 0.090	83 0.072
531	VOCORD-003	464 0.350	443 0.122	438 0.047	355 0.195	376 0.155	394 0.093	356 0.999	372 0.998	385 0.990	366 0.157	394 0.105			284 0.404	334 0.289
532	VOCORD-004	517 0.825	501 0.353	439 0.051	420 0.401	388 0.173	390 0.093	449 1.000	435 1.000	447 0.999	379 0.193	366 0.065			429 0.991	424 0.776
533	VOCORD-005	506 0.687	458 0.156	430 0.043	332 0.161	356 0.130	378 0.080	364 0.999	362 0.997	343 0.968	358 0.138	386 0.090			277 0.381	332 0.287
534	VOCORD-006	550 1.000	552 1.000	553 1.000	549 1.000	553 1.000	550 1.000	476 1.000	519 1.000	527 1.000	518 1.000	507 1.000			509 1.000	550 1.000
535	VTCC-000	511 0.784	396 0.058	255 0.006	513 0.972	500 0.753	269 0.036	452 1.000	455 1.000	463 1.000	416 0.435	289 0.018	303 0.995	298 0.601	454 1.000	457 0.997
536	VTCC-001															
537	VTCC-002	440 0.249	229 0.010	216 0.003	474 0.713	489 0.631	498 0.411	99 0.438	100 0.269	118 0.152	411 0.421	408 0.176	311 0.999	318 0.957	364 0.750	385 0.514
538	VTS-000	496 0.605	520 0.598	530 0.595	458 0.624	487 0.619	513 0.613	374 0.999	399 0.999	439 0.998	432 0.613	445 0.609	264 0.760	308 0.739	365 0.761	420 0.749
539	VTS-001	247 0.034	245 0.013	247 0.005	218 0.067	233 0.051	240 0.031	338 0.998	332 0.994	225 0.504	228 0.022	246 0.012	160 0.141	196 0.079	212 0.192	213 0.126
540	VTS-002	296 0.053	314 0.026	315 0.010	264 0.098	283 0.075	303 0.046	396 1.000	410 1.000	334 0.953	291 0.045	316 0.026	199 0.231	236 0.133	288 0.417	275 0.187
541	VTS-003	177 0.015	196 0.007	191 0.003	178 0.048	173 0.033	170 0.019	441 1.000	447 1.000	250 0.628	192 0.014	169 0.005	290 0.954	170 0.060	342 0.635	143 0.089
542	VTS-004	139 0.011	148 0.004	125 0.002	196 0.055	144 0.027	127 0.016	443 1.000	477 1.000	288 0.847	154 0.009	125 0.004	315 1.000	155 0.046	216 0.203	86 0.073
543	VTS-005	144 0.011	164 0.005	116 0.002	168 0.045	161 0.030	142 0.017	394 1.000	367 0.998	157 0.238	118 0.007	106 0.003	271 0.811	138 0.037	110 0.100	77 0.070
544	WINK-000	449 0.269	474 0.203	484 0.122	426 0.432	454 0.377	480 0.274	254 0.985	292 0.983	361 0.979	389 0.261	405 0.163	494 1.000	399 1.000	346 0.649	392 0.558
545	WINK-001	338 0.082	346 0.036	344 0.014	406 0.346	358 0.131	381 0.083	347 0.998	355 0.996	358 0.977	385 0.237	414 0.220	280 0.903	282 0.412	274 0.372	344 0.312
546	WINK-002	208 0.024	238 0.012	234 0.005	333 0.162	313 0.092	366 0.072	250 0.984	249 0.961	304 0.910	395 0.294	424 0.289	295 0.978	287 0.441	268 0.342	347 0.316
547	XFORWARDAI-000	229 0.028	259 0.015	262 0.006	224 0.070	242 0.053	260 0.034	153 0.694	134 0.434	158 0.241	223 0.021	229 0.011	176 0.159	206 0.082	193 0.169	224 0.134
548	XFORWARDAI-001	129 0.010	149 0.005	176 0.002	139 0.036	153 0.028	172 0.020	128 0.836	135 0.441	103 0.133	142 0.008	172 0.005	107 0.062	117 0.030	141 0.123	170 0.102
549	XFORWARDAI-002	80 0.006	88 0.003	141 0.002	68 0.018	72 0.016	93 0.014	224 0.974	155 0.519	42 0.084	76 0.005	115 0.003	68 0.041	71 0.018	106 0.099	141 0.089
550	YISHENG-001	479 0.451	498 0.346	502 0.206	517 0.983	507 0.808	479 0.269				436 0.666	434 0.396			400 0.919	410 0.695
551	YITU-002	236 0.031	275 0.017	282 0.008	207 0.063	225 0.049	230 0.028									
552	YITU-003	237 0.031	284 0.018	298 0.008	216 0.067	237 0.052	253 0.033									

Table 64: **Threshold-based accuracy**. *Values are FNIR(N, T, L) with N = 1.6 million with thresholds set to produce FPIR = 0.0003, 0.001, and 0.01 in non-mate searches. Throughout blue superscripts indicate the rank of the algorithm for that column. Caution: The Power-low models are mostly intended to draw attention to the kind of behavior, not as a model to be used for prediction.*

2026/01/09 20:40:38

FNIR(N, R, T) = False neg. identification rate
FPIR(N, T) = False pos. identification rate
N = Num. enrolled subjects
R = Num. candidates examined
T = Threshold
T = 0 → Investigation
T > 0 → Identification

This publication is available free of charge from: https://doi.org/10.6028/NIST.IR.8271

MISSES BELOW THRESHOLD, T		ENROL RECENT MUGSHOT, N = 1.6M									ENROL APPLICATION PORTRAIT, N = 1.6M					
		ENROL: MUGSHOT			ENROL: MUGSHOT			ENROL: MUGSHOT			ENROL: VISA		ENROL: BORDER		ENROL: VISA	
		PROBE: MUGSHOT			PROBE: WEBCAM			PROBE: PROFILE			PROBE: BORDER		PROBE: BORDER 10+YR		PROBE: KIOSK	
#	ALGORITHM	FPIR=0.0003	FPIR=0.001	FPIR=0.01	FPIR=0.0003	FPIR=0.001	FPIR=0.01	FPIR=0.0003	FPIR=0.001	FPIR=0.01	FPIR=0.001	FPIR=0.01	FPIR=0.001	FPIR=0.01	FPIR=0.001	FPIR=0.01
553	YITU-004	[193] 0.019	[218] 0.009	[225] 0.004	[138] 0.035	[142] 0.027	[143] 0.017	[210] 0.947	[238] 0.936	[306] 0.912						
554	YITU-005	[199] 0.021	[226] 0.010	[232] 0.005	[151] 0.039	[171] 0.032	[202] 0.023									
555	YUAN-000	[196] 0.019	[228] 0.010	[217] 0.003	[231] 0.073	[217] 0.045	[226] 0.027	[101] 0.454	[115] 0.342	[151] 0.210	[183] 0.012	[178] 0.005	[220] 0.333	[157] 0.048	[148] 0.129	[140] 0.088

Table 65: **Threshold-based accuracy**. *Values are FNIR(N, T, L) with N = 1.6 million with thresholds set to produce FPIR = 0.0003, 0.001, and 0.01 in non-mate searches. Throughout blue superscripts indicate the rank of the algorithm for that column. Caution: The Power-low models are mostly intended to draw attention to the kind of behavior, not as a model to be used for prediction.*

Appendices

Appendix A Accuracy on large-population FRVT 2018 mugshots

This publication is available free of charge from: https://doi.org/10.6028/NIST.IR.8271

2026/01/09 20:40:38	FNIR(N, R, T) = FPIR(N, T) =	False neg. identification rate False pos. identification rate	N = Num. enrolled subjects R = Num. candidates examined	T = Threshold	$T = 0 \rightarrow$ Investigation $T > 0 \rightarrow$ Identification

This publication is available free of charge from: https://doi.org/10.6028/NIST.IR.8271

This publication is available free of charge from: https://doi.org/10.6028/NIST.IR.8271

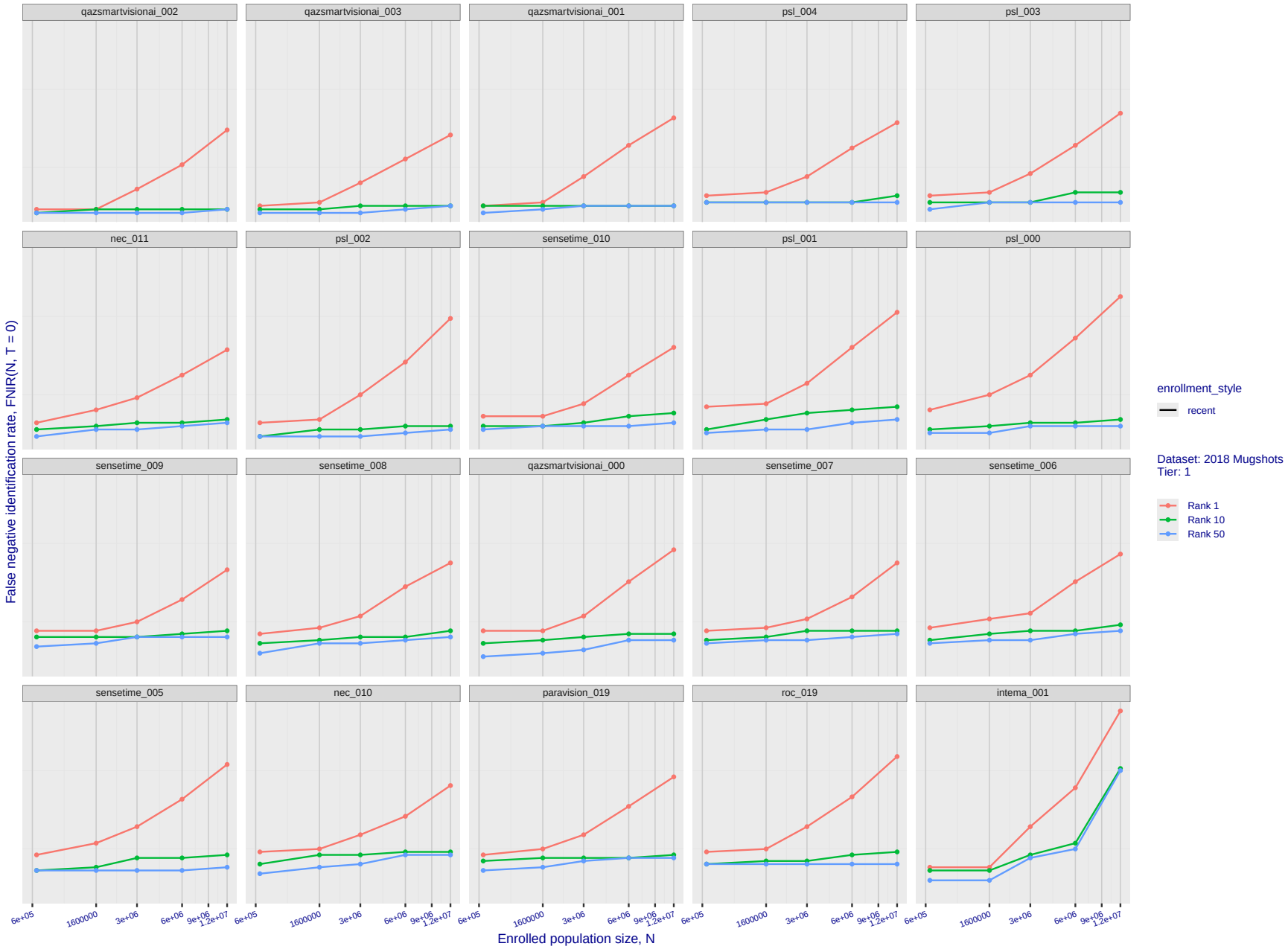

Figure 20: **[FRVT-2018 Mugshot Dataset] Rank-based identification miss rates vs. number of enrolled subjects**. *The figure shows false negative identification rates, FNIR(N, R), across various gallery sizes and ranks 1, 10 and 50. The threshold is set to zero, so this metric rewards even weak scoring rank 1 mates. This also means FPIR = 1, so any search without an enrolled mate will return non-mated candidates. For clarity, results are sorted and reported into tiers spanning multiple pages, the tiering criteria being rank 1 hit rate on a gallery size of 640 000.*

2026/01/09
20:40:38

FNIR(N, R, T) = False neg. identification rate
FPIR(N, T) = False pos. identification rate

N = Num. enrolled subjects
R = Num. candidates examined

T = Threshold

T = 0 → Investigation
T > 0 → Identification

This publication is available free of charge from: https://doi.org/10.6028/NIST.IR.8271

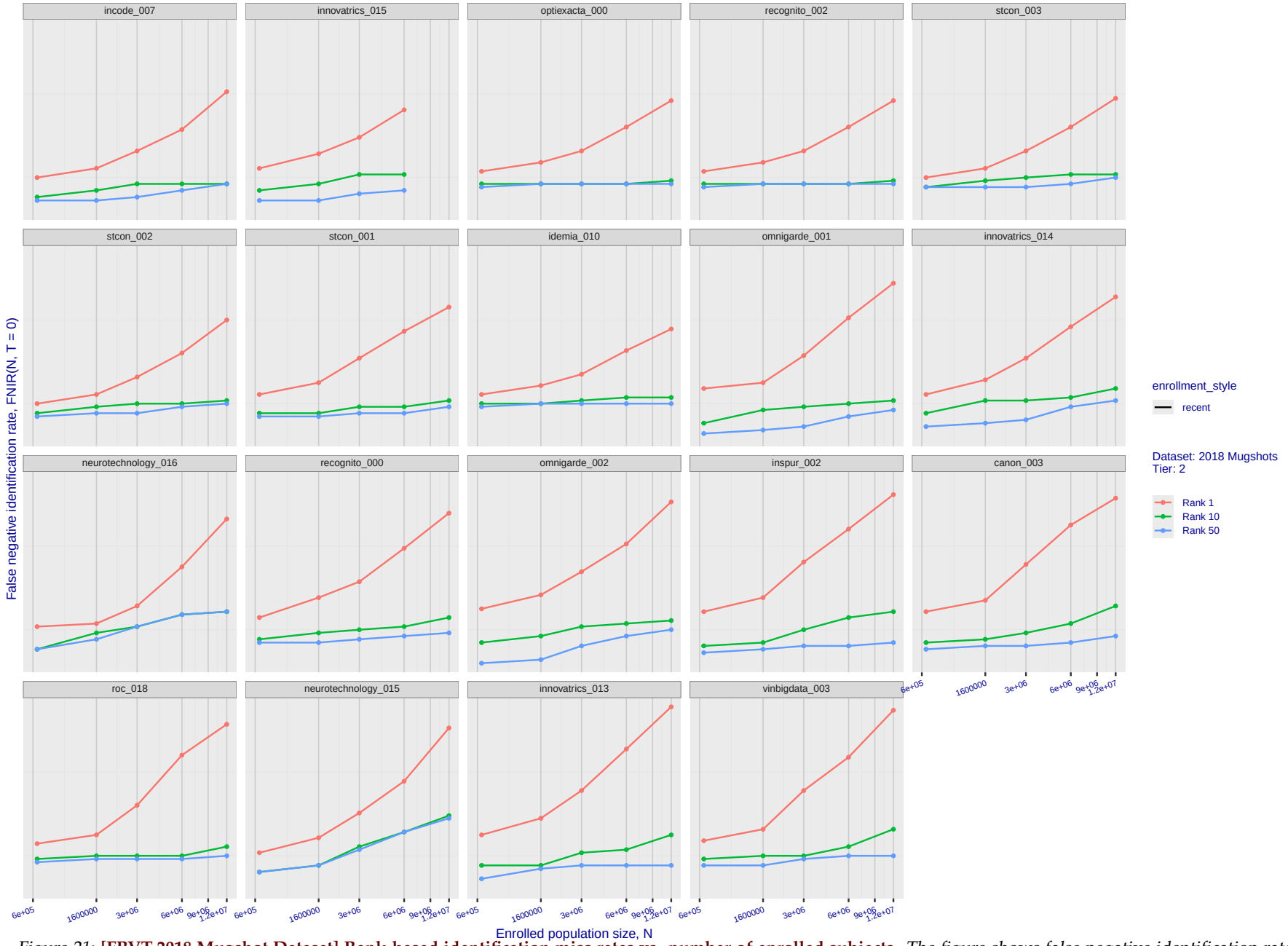

Figure 21: **[FRVT-2018 Mugshot Dataset] Rank-based identification miss rates vs. number of enrolled subjects**. *The figure shows false negative identification rates, FNIR(N, R), across various gallery sizes and ranks 1, 10 and 50. The threshold is set to zero, so this metric rewards even weak scoring rank 1 mates. This also means FPIR = 1, so any search without an enrolled mate will return non-mated candidates. For clarity, results are sorted and reported into tiers spanning multiple pages, the tiering criteria being rank 1 hit rate on a gallery size of 640 000.*

2026/01/09 20:40:38

FNIR(N, R, T) = False neg. identification rate
FPIR(N, T) = False pos. identification rate

N = Num. enrolled subjects
R = Num. candidates examined

T = Threshold

T = 0 → Investigation
T > 0 → Identification

This publication is available free of charge from: https://doi.org/10.6028/NIST.IR.8271

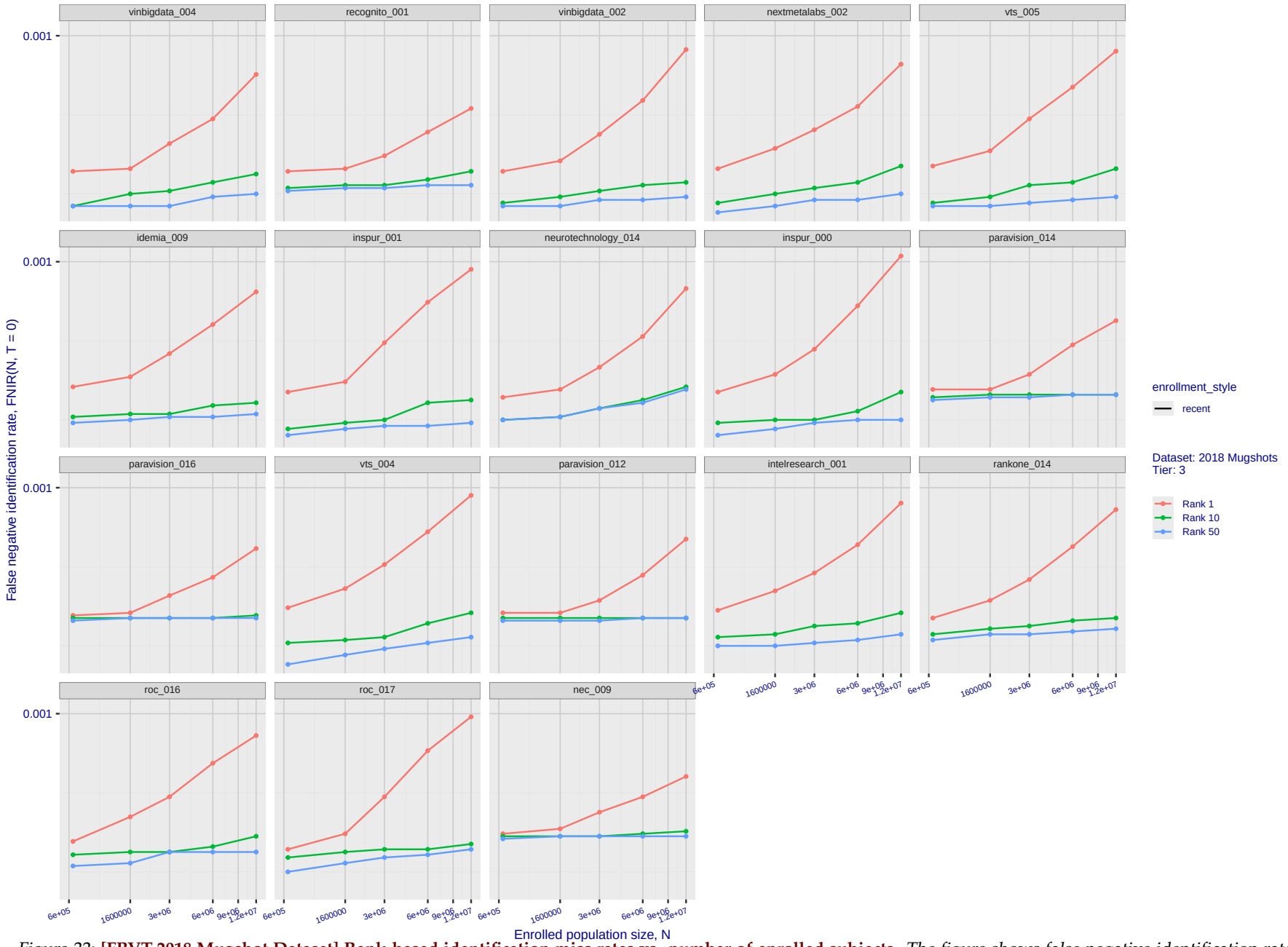

Figure 22: **[FRVT-2018 Mugshot Dataset] Rank-based identification miss rates vs. number of enrolled subjects**. *The figure shows false negative identification rates, FNIR(N, R), across various gallery sizes and ranks 1, 10 and 50. The threshold is set to zero, so this metric rewards even weak scoring rank 1 mates. This also means FPIR = 1, so any search without an enrolled mate will return non-mated candidates. For clarity, results are sorted and reported into tiers spanning multiple pages, the tiering criteria being rank 1 hit rate on a gallery size of 640 000.*

2026/01/09 20:40:38

FNIR(N, R, T) = False neg. identification rate
FPIR(N, T) = False pos. identification rate

N = Num. enrolled subjects
R = Num. candidates examined

T = Threshold

T = 0 → Investigation
T > 0 → Identification

This publication is available free of charge from: https://doi.org/10.6028/NIST.IR.8271

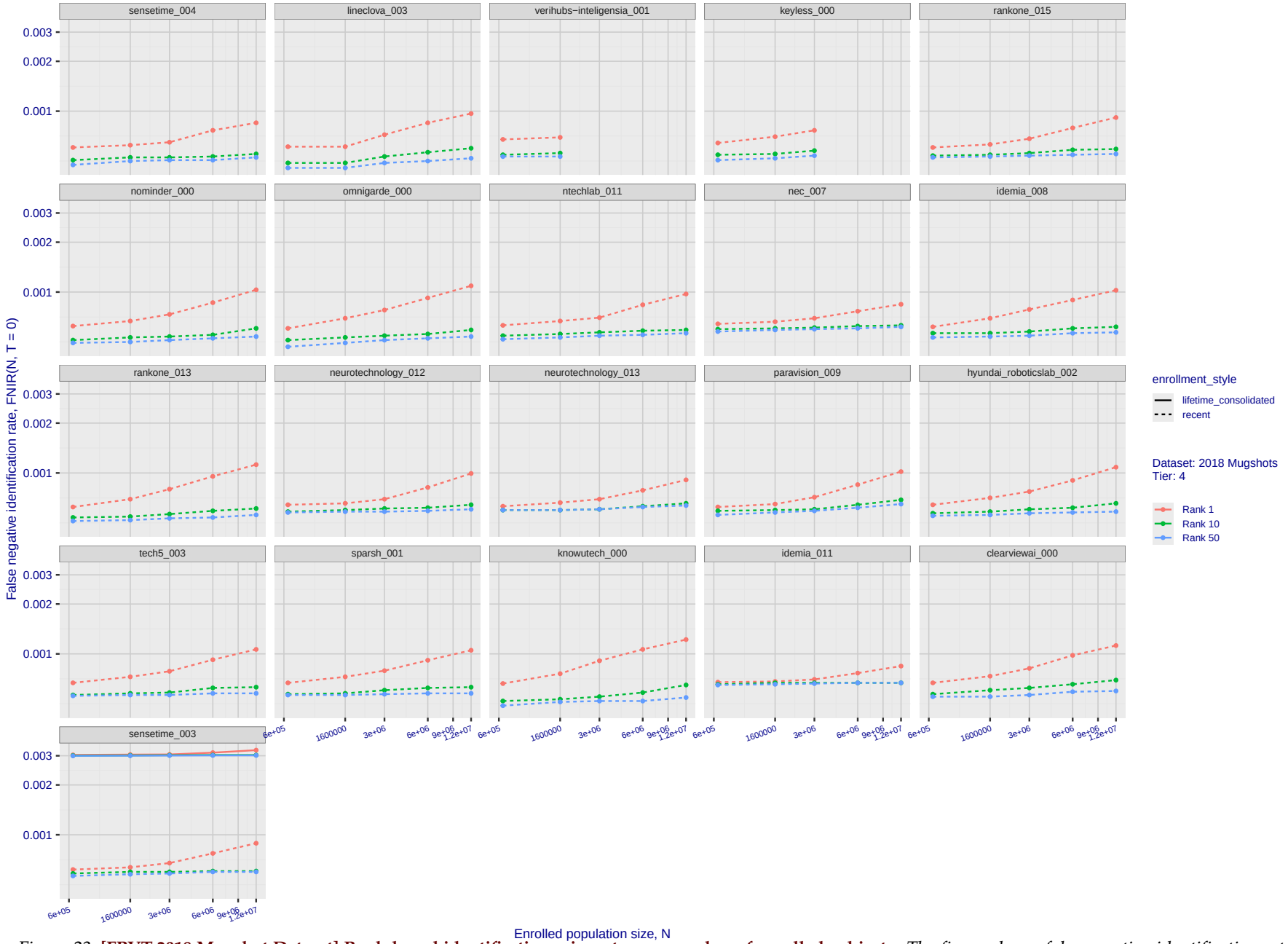

Figure 23: **[FRVT-2018 Mugshot Dataset] Rank-based identification miss rates vs. number of enrolled subjects**. *The figure shows false negative identification rates, FNIR(N, R), across various gallery sizes and ranks 1, 10 and 50. The threshold is set to zero, so this metric rewards even weak scoring rank 1 mates. This also means FPIR = 1, so any search without an enrolled mate will return non-mated candidates. For clarity, results are sorted and reported into tiers spanning multiple pages, the tiering criteria being rank 1 hit rate on a gallery size of 640 000.*

2026/01/09 20:40:38

FNIR(N, R, T) = False neg. identification rate
FPIR(N, T) = False pos. identification rate

N = Num. enrolled subjects
R = Num. candidates examined

T = Threshold

T = 0 → Investigation
T > 0 → Identification

This publication is available free of charge from: https://doi.org/10.6028/NIST.IR.8271

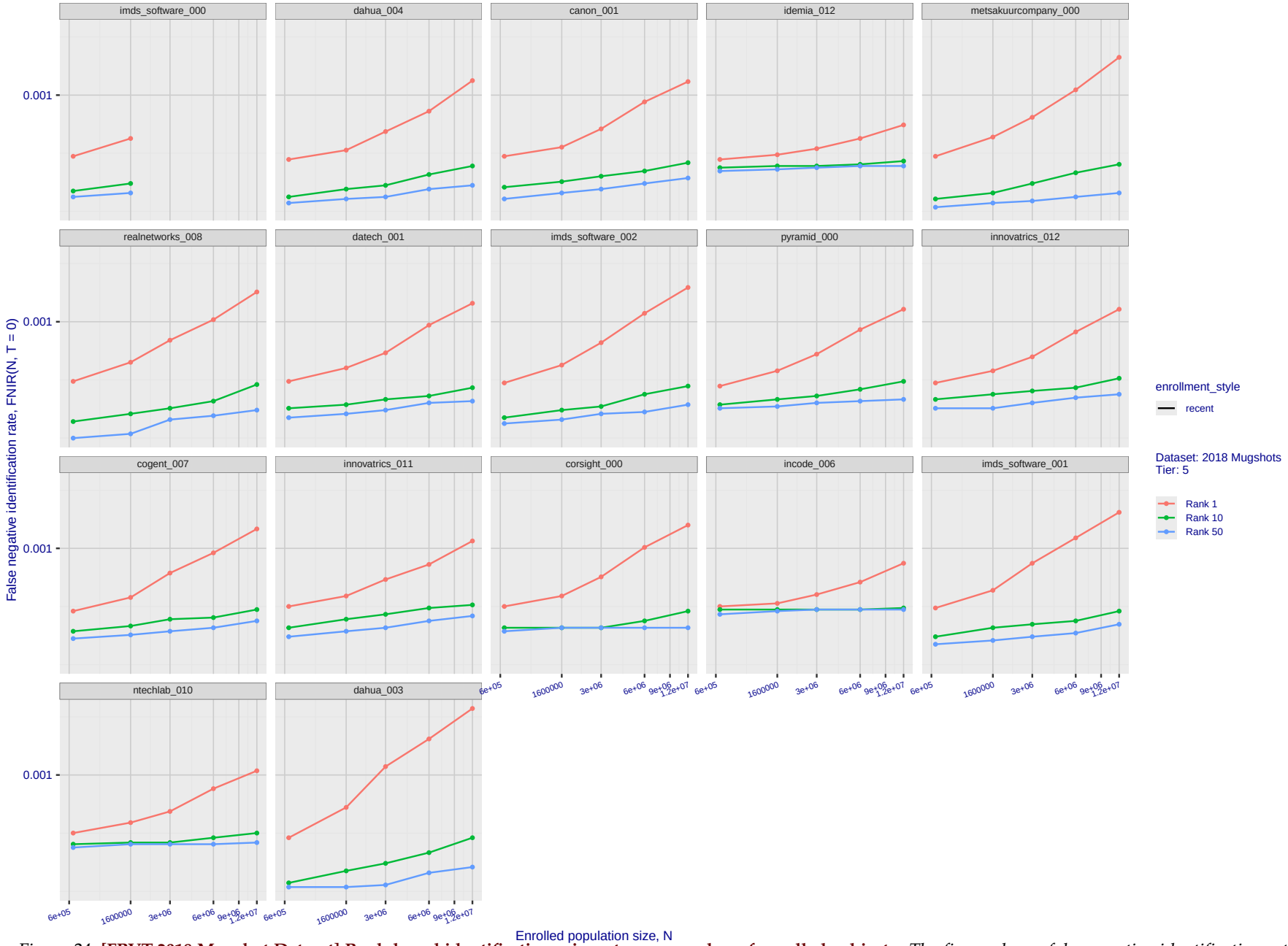

Figure 24: **[FRVT-2018 Mugshot Dataset] Rank-based identification miss rates vs. number of enrolled subjects**. *The figure shows false negative identification rates, FNIR(N, R), across various gallery sizes and ranks 1, 10 and 50. The threshold is set to zero, so this metric rewards even weak scoring rank 1 mates. This also means FPIR = 1, so any search without an enrolled mate will return non-mated candidates. For clarity, results are sorted and reported into tiers spanning multiple pages, the tiering criteria being rank 1 hit rate on a gallery size of 640 000.*

2026/01/09 20:40:38

FNIR(N, R, T) = False neg. identification rate
FPIR(N, T) = False pos. identification rate

N = Num. enrolled subjects
R = Num. candidates examined

T = Threshold

T = 0 → Investigation
T > 0 → Identification

This publication is available free of charge from: https://doi.org/10.6028/NIST.IR.8271

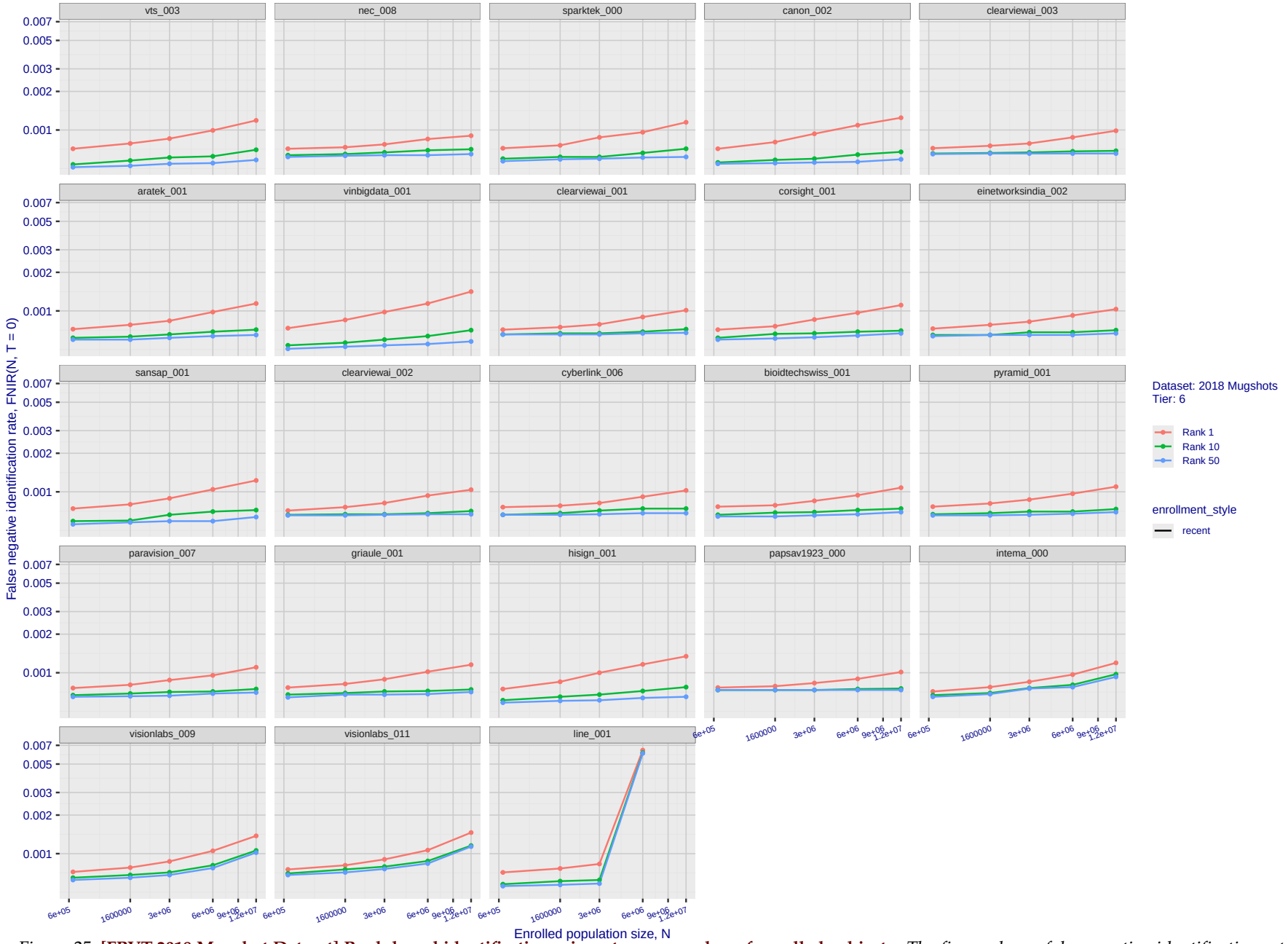

Figure 25: **[FRVT-2018 Mugshot Dataset] Rank-based identification miss rates vs. number of enrolled subjects**. *The figure shows false negative identification rates, FNIR(N, R), across various gallery sizes and ranks 1, 10 and 50. The threshold is set to zero, so this metric rewards even weak scoring rank 1 mates. This also means FPIR = 1, so any search without an enrolled mate will return non-mated candidates. For clarity, results are sorted and reported into tiers spanning multiple pages, the tiering criteria being rank 1 hit rate on a gallery size of 640 000.*

2026/01/09 20:40:38

FNIR(N, R, T) = False neg. identification rate
FPIR(N, T) = False pos. identification rate

N = Num. enrolled subjects
R = Num. candidates examined

T = Threshold

T = 0 → Investigation
T > 0 → Identification

This publication is available free of charge from: https://doi.org/10.6028/NIST.IR.8271

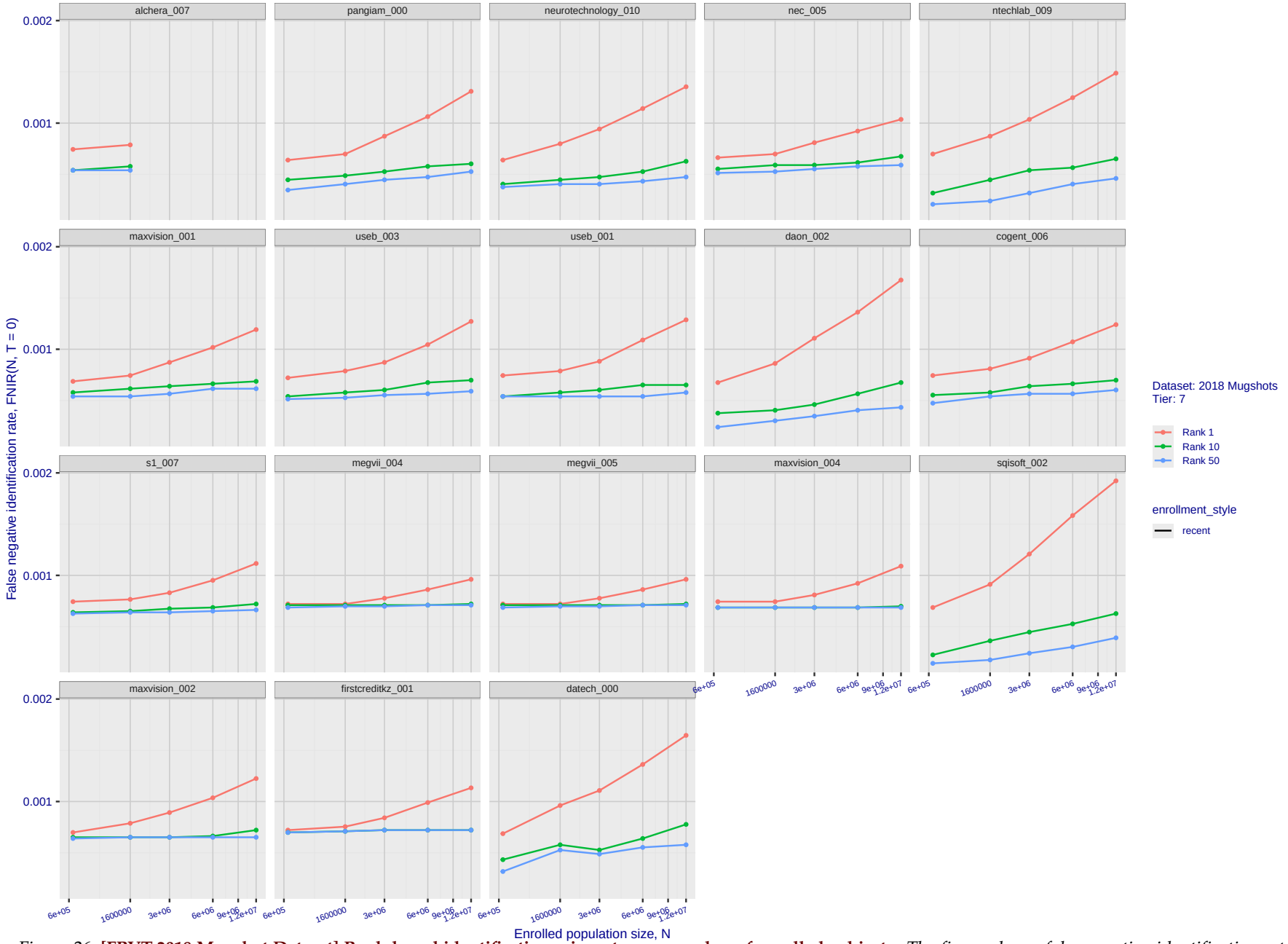

Figure 26: **[FRVT-2018 Mugshot Dataset] Rank-based identification miss rates vs. number of enrolled subjects**. *The figure shows false negative identification rates, FNIR(N, R), across various gallery sizes and ranks 1, 10 and 50. The threshold is set to zero, so this metric rewards even weak scoring rank 1 mates. This also means FPIR = 1, so any search without an enrolled mate will return non-mated candidates. For clarity, results are sorted and reported into tiers spanning multiple pages, the tiering criteria being rank 1 hit rate on a gallery size of 640 000.*

2026/01/09
20:40:38

FNIR(N, R, T) = False neg. identification rate
FPIR(N, T) = False pos. identification rate

N = Num. enrolled subjects
R = Num. candidates examined

T = Threshold

T = 0 → Investigation
T > 0 → Identification

This publication is available free of charge from: https://doi.org/10.6028/NIST.IR.8271

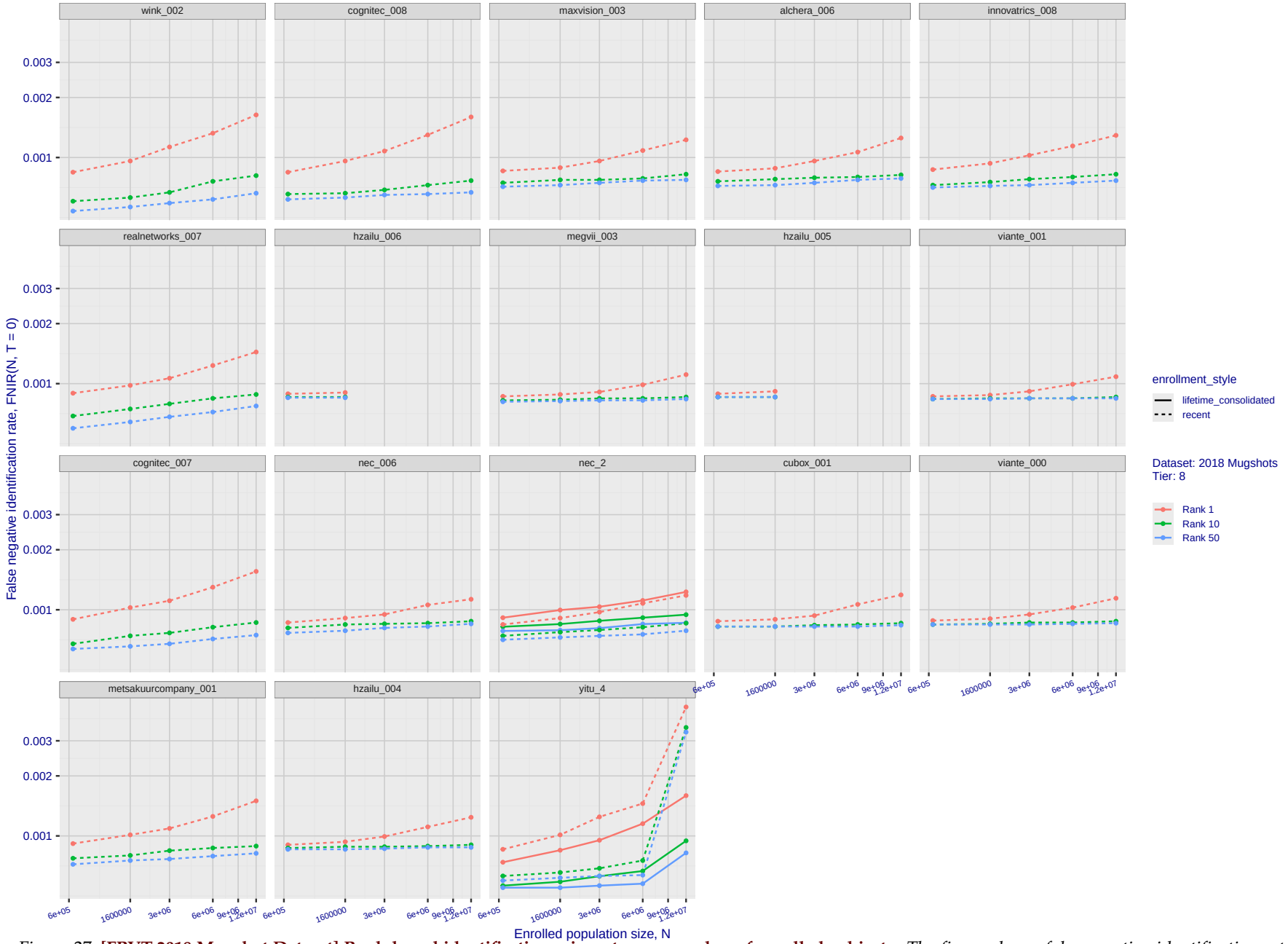

Figure 27: **[FRVT-2018 Mugshot Dataset] Rank-based identification miss rates vs. number of enrolled subjects**. *The figure shows false negative identification rates, FNIR(N, R), across various gallery sizes and ranks 1, 10 and 50. The threshold is set to zero, so this metric rewards even weak scoring rank 1 mates. This also means FPIR = 1, so any search without an enrolled mate will return non-mated candidates. For clarity, results are sorted and reported into tiers spanning multiple pages, the tiering criteria being rank 1 hit rate on a gallery size of 640 000.*

2026/01/09 20:40:38

FNIR(N, R, T) = False neg. identification rate
FPIR(N, T) = False pos. identification rate

N = Num. enrolled subjects
R = Num. candidates examined

T = Threshold

T = 0 → Investigation
T > 0 → Identification

This publication is available free of charge from: https://doi.org/10.6028/NIST.IR.8271

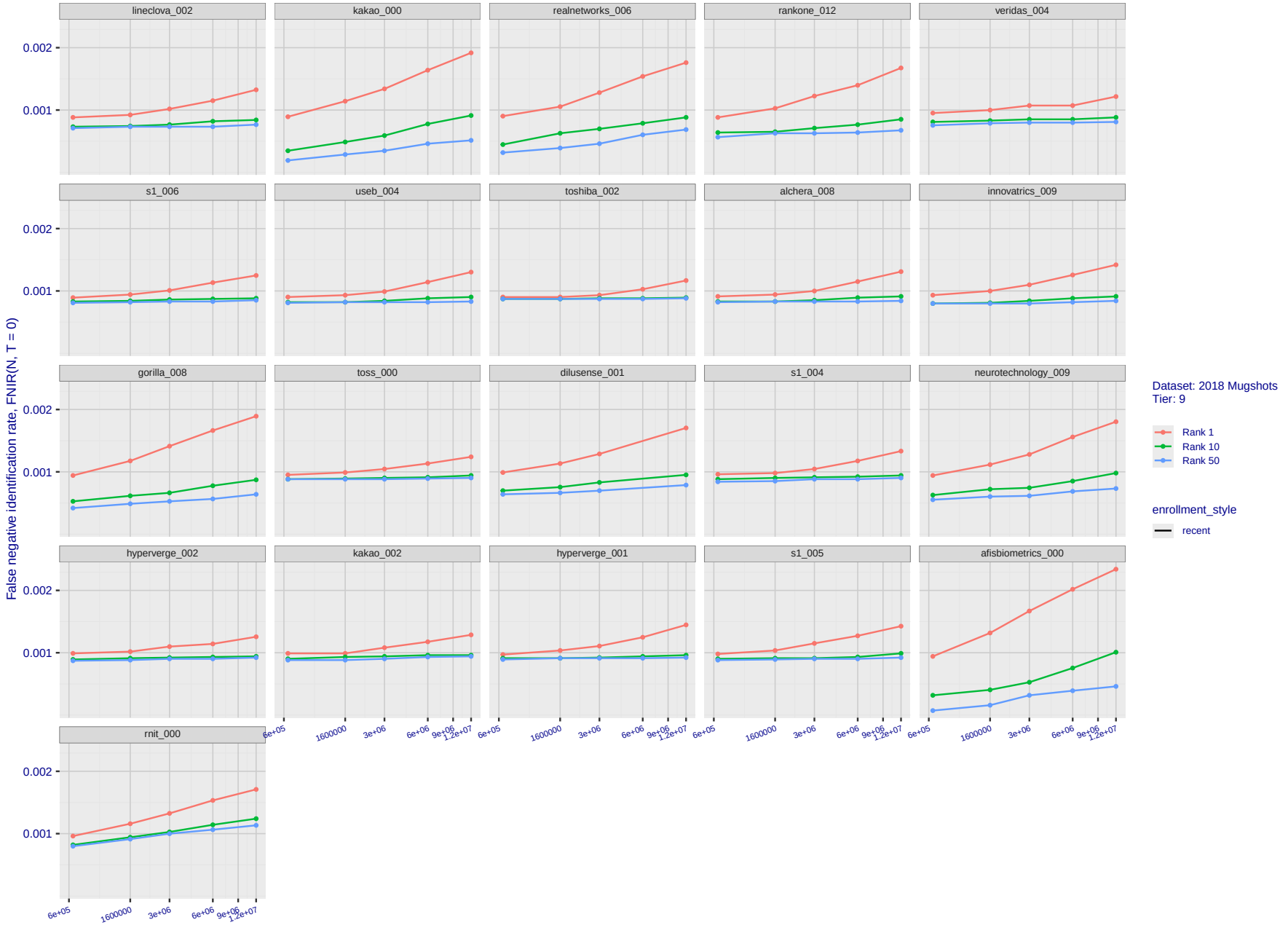

Figure 28: **[FRVT-2018 Mugshot Dataset] Rank-based identification miss rates vs. number of enrolled subjects**. *The figure shows false negative identification rates, FNIR(N, R), across various gallery sizes and ranks 1, 10 and 50. The threshold is set to zero, so this metric rewards even weak scoring rank 1 mates. This also means FPIR = 1, so any search without an enrolled mate will return non-mated candidates. For clarity, results are sorted and reported into tiers spanning multiple pages, the tiering criteria being rank 1 hit rate on a gallery size of 640 000.*

2026/01/09 20:40:38

FNIR(N, R, T) = False neg. identification rate
FPIR(N, T) = False pos. identification rate

N = Num. enrolled subjects
R = Num. candidates examined

T = Threshold

T = 0 → Investigation
T > 0 → Identification

This publication is available free of charge from: https://doi.org/10.6028/NIST.IR.8271

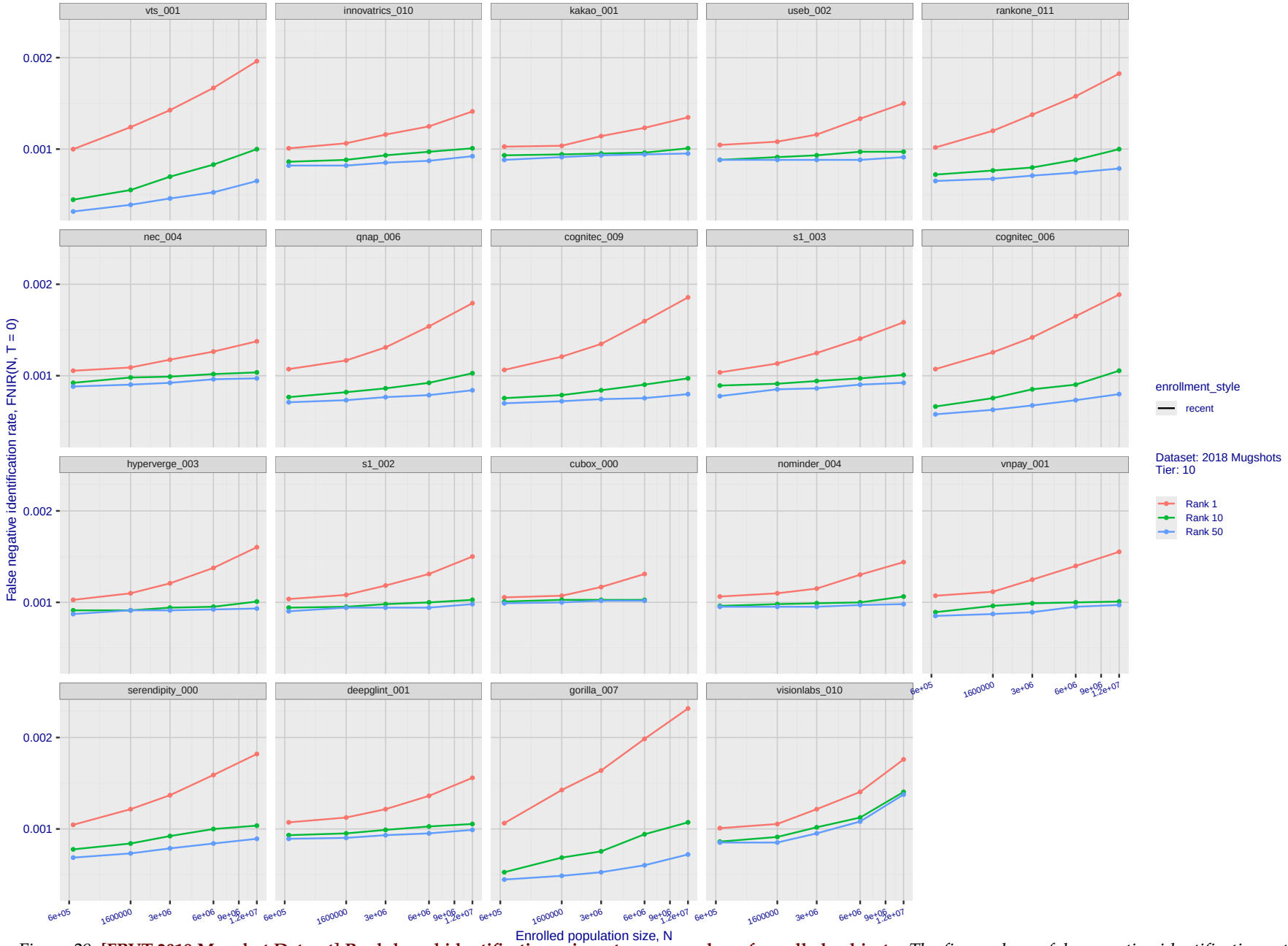

Figure 29: **[FRVT-2018 Mugshot Dataset] Rank-based identification miss rates vs. number of enrolled subjects**. *The figure shows false negative identification rates, FNIR(N, R), across various gallery sizes and ranks 1, 10 and 50. The threshold is set to zero, so this metric rewards even weak scoring rank 1 mates. This also means FPIR = 1, so any search without an enrolled mate will return non-mated candidates. For clarity, results are sorted and reported into tiers spanning multiple pages, the tiering criteria being rank 1 hit rate on a gallery size of 640 000.*

2026/01/09
20:40:38

FNIR(N, R, T) = False neg. identification rate
FPIR(N, T) = False pos. identification rate
N = Num. enrolled subjects
R = Num. candidates examined
T = Threshold
T = 0 → Investigation
T > 0 → Identification

This publication is available free of charge from: https://doi.org/10.6028/NIST.IR.8271

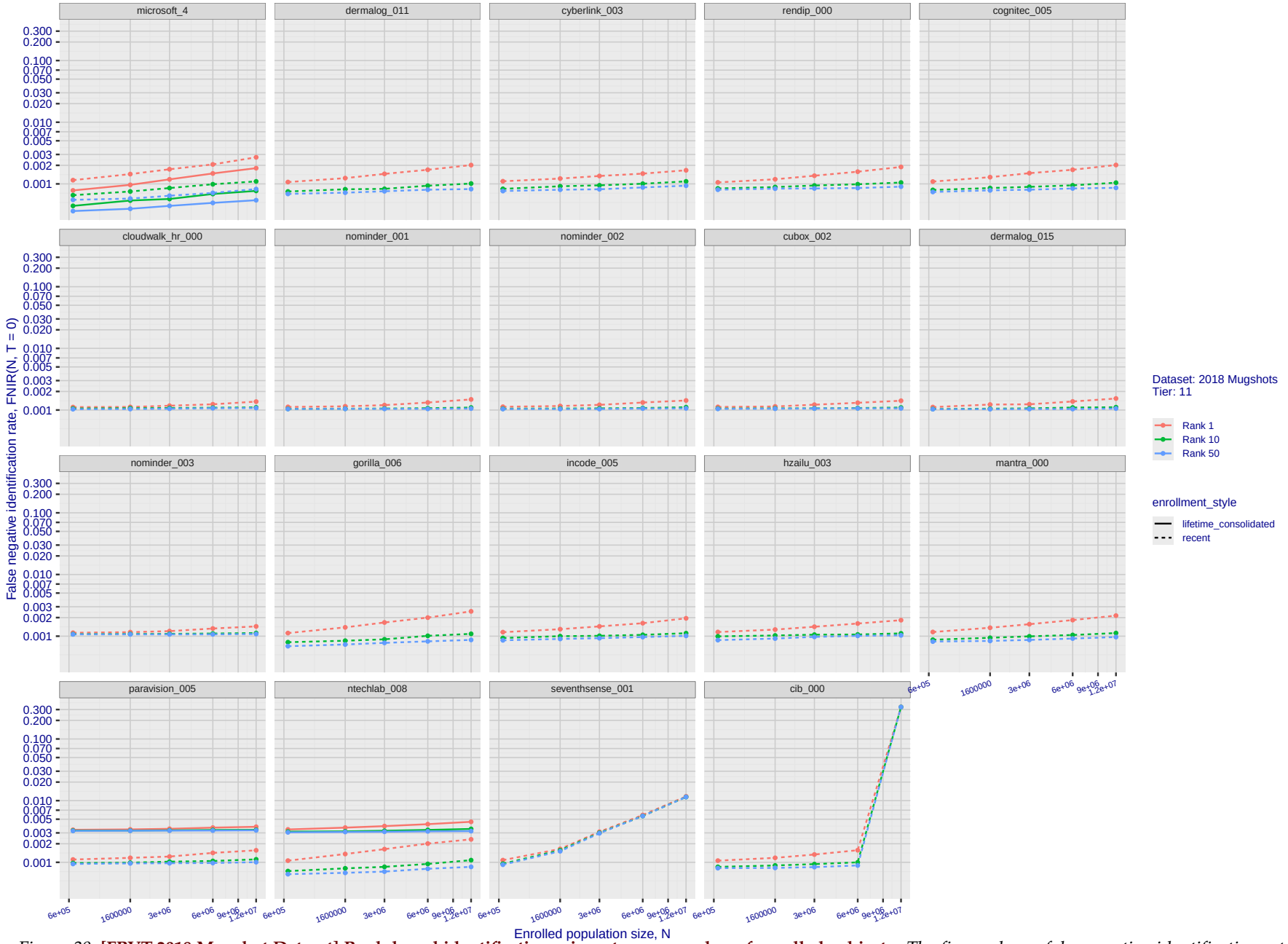

Figure 30: **[FRVT-2018 Mugshot Dataset] Rank-based identification miss rates vs. number of enrolled subjects**. *The figure shows false negative identification rates, FNIR(N, R), across various gallery sizes and ranks 1, 10 and 50. The threshold is set to zero, so this metric rewards even weak scoring rank 1 mates. This also means FPIR = 1, so any search without an enrolled mate will return non-mated candidates. For clarity, results are sorted and reported into tiers spanning multiple pages, the tiering criteria being rank 1 hit rate on a gallery size of 640 000.*

2026/01/09 20:40:38
FNIR(N, R, T) = False neg. identification rate
FPIR(N, T) = False pos. identification rate
N = Num. enrolled subjects
R = Num. candidates examined
T = Threshold
T = 0 → Investigation
T > 0 → Identification

This publication is available free of charge from: https://doi.org/10.6028/NIST.IR.8271

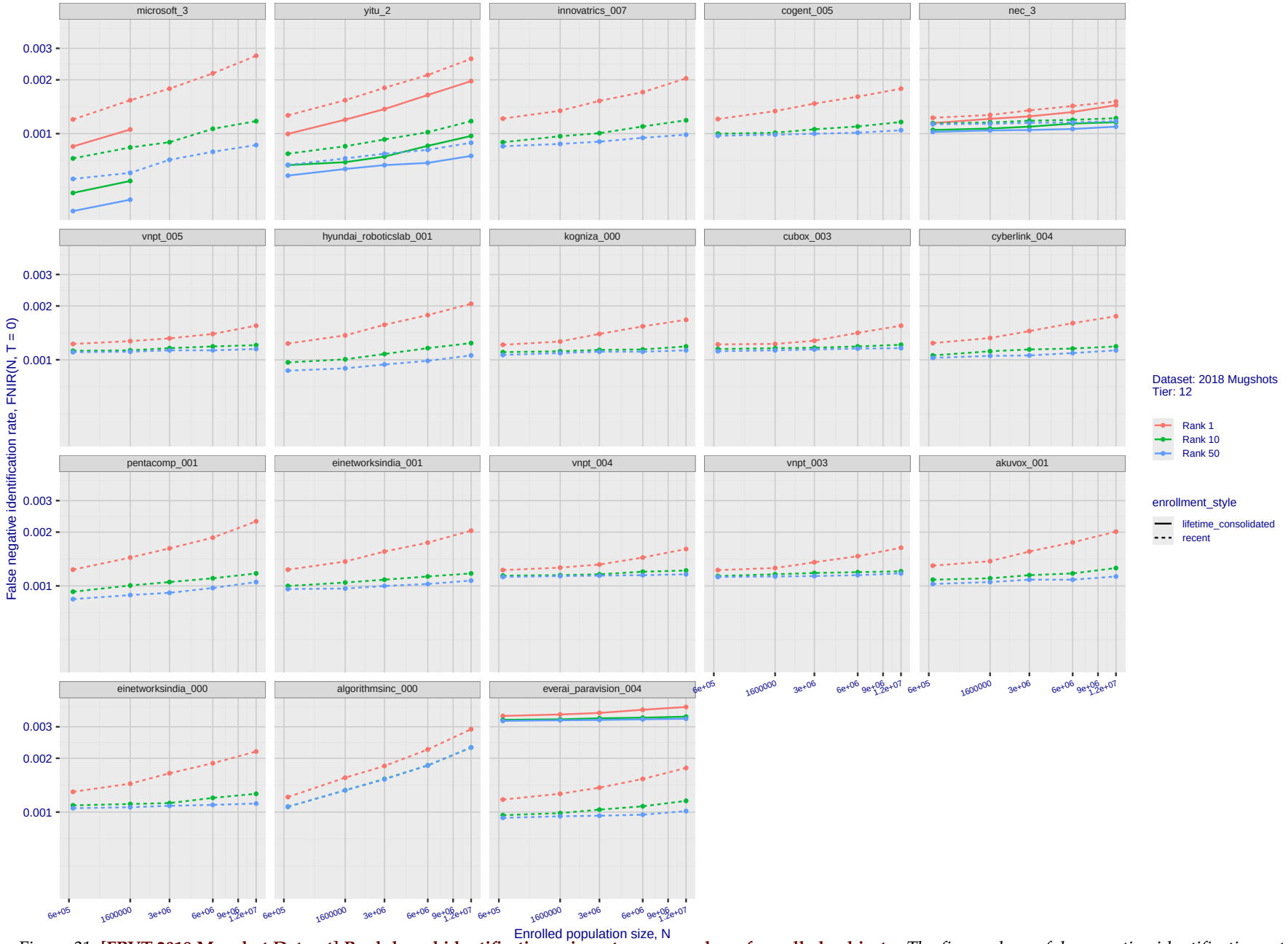

Figure 31: **[FRVT-2018 Mugshot Dataset] Rank-based identification miss rates vs. number of enrolled subjects**. *The figure shows false negative identification rates, FNIR(N, R), across various gallery sizes and ranks 1, 10 and 50. The threshold is set to zero, so this metric rewards even weak scoring rank 1 mates. This also means FPIR = 1, so any search without an enrolled mate will return non-mated candidates. For clarity, results are sorted and reported into tiers spanning multiple pages, the tiering criteria being rank 1 hit rate on a gallery size of 640 000.*

2026/01/09 20:40:38
FNIR(N, R, T) = False neg. identification rate
FPIR(N, T) = False pos. identification rate
N = Num. enrolled subjects
R = Num. candidates examined
T = Threshold
T = 0 → Investigation
T > 0 → Identification

This publication is available free of charge from: https://doi.org/10.6028/NIST.IR.8271

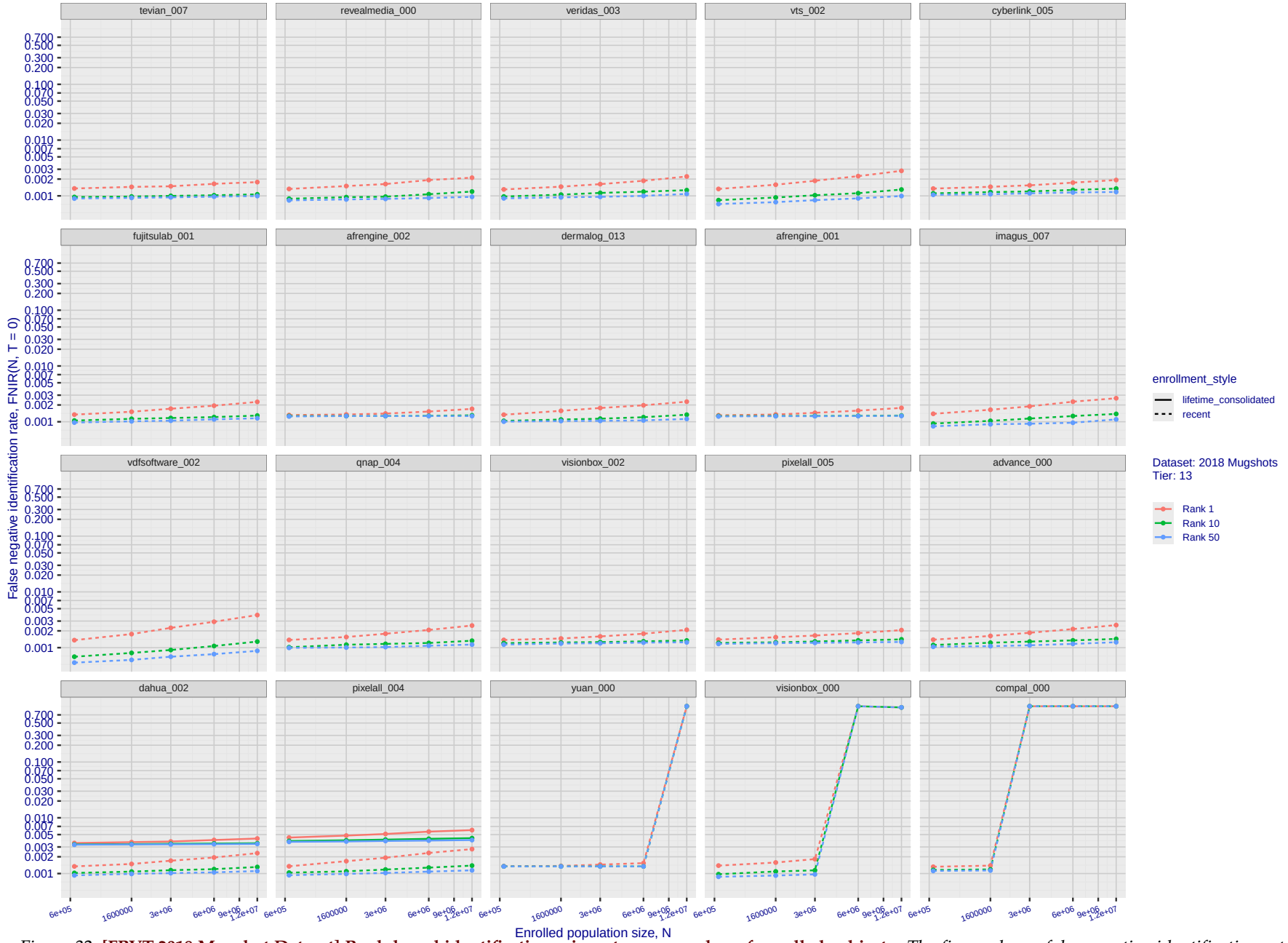

Figure 32: **[FRVT-2018 Mugshot Dataset] Rank-based identification miss rates vs. number of enrolled subjects**. *The figure shows false negative identification rates, FNIR(N, R), across various gallery sizes and ranks 1, 10 and 50. The threshold is set to zero, so this metric rewards even weak scoring rank 1 mates. This also means FPIR = 1, so any search without an enrolled mate will return non-mated candidates. For clarity, results are sorted and reported into tiers spanning multiple pages, the tiering criteria being rank 1 hit rate on a gallery size of 640 000.*

2026/01/09 20:40:38
FNIR(N, R, T) = False neg. identification rate
FPIR(N, T) = False pos. identification rate
N = Num. enrolled subjects
R = Num. candidates examined
T = Threshold
T = 0 → Investigation
T > 0 → Identification

This publication is available free of charge from: https://doi.org/10.6028/NIST.IR.8271

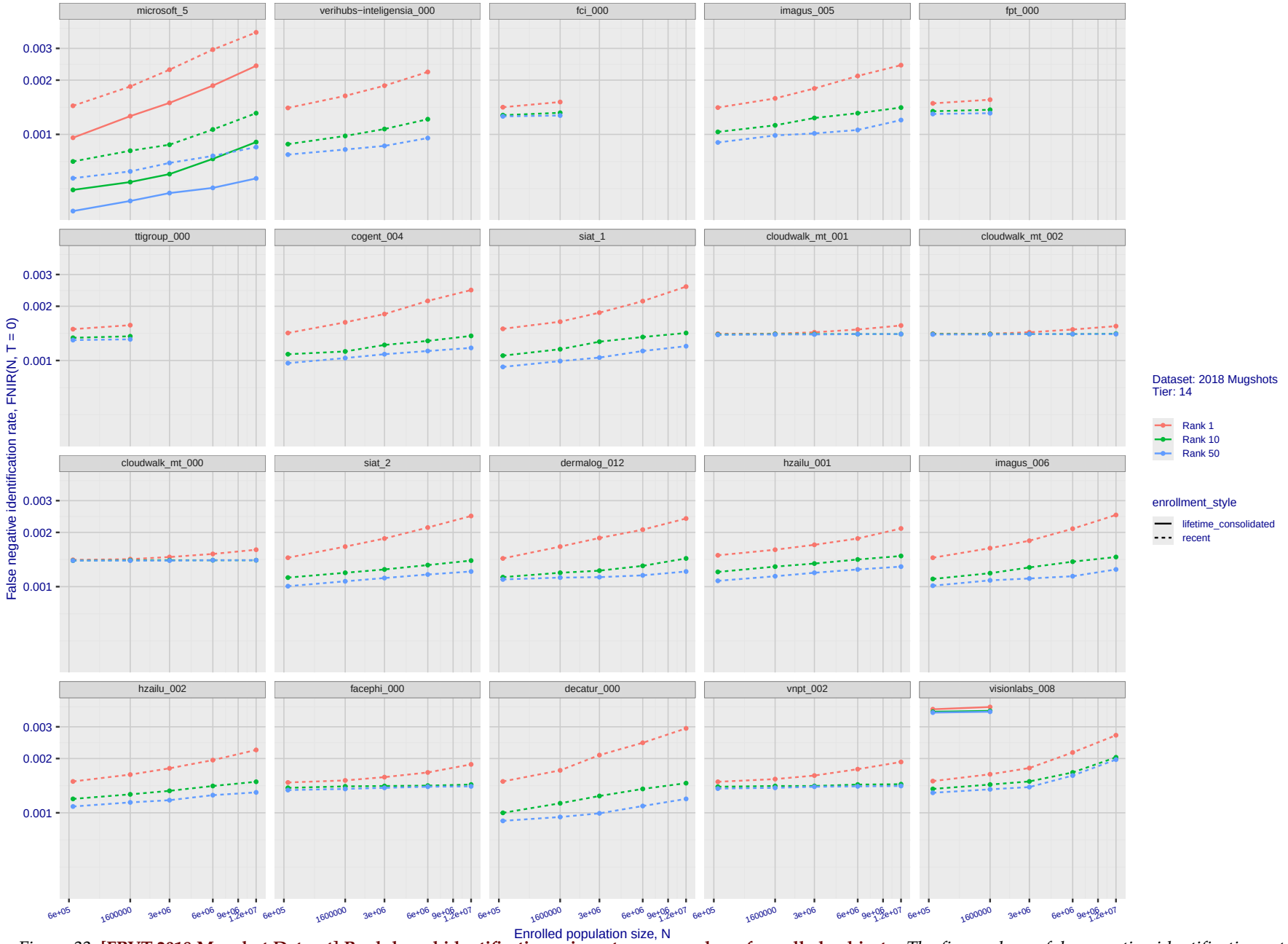

Figure 33: **[FRVT-2018 Mugshot Dataset] Rank-based identification miss rates vs. number of enrolled subjects**. *The figure shows false negative identification rates, FNIR(N, R), across various gallery sizes and ranks 1, 10 and 50. The threshold is set to zero, so this metric rewards even weak scoring rank 1 mates. This also means FPIR = 1, so any search without an enrolled mate will return non-mated candidates. For clarity, results are sorted and reported into tiers spanning multiple pages, the tiering criteria being rank 1 hit rate on a gallery size of 640 000.*

2026/01/09 20:40:38

FNIR(N, R, T) = False neg. identification rate
FPIR(N, T) = False pos. identification rate

N = Num. enrolled subjects
R = Num. candidates examined

T = Threshold

T = 0 → Investigation
T > 0 → Identification

This publication is available free of charge from: https://doi.org/10.6028/NIST.IR.8271

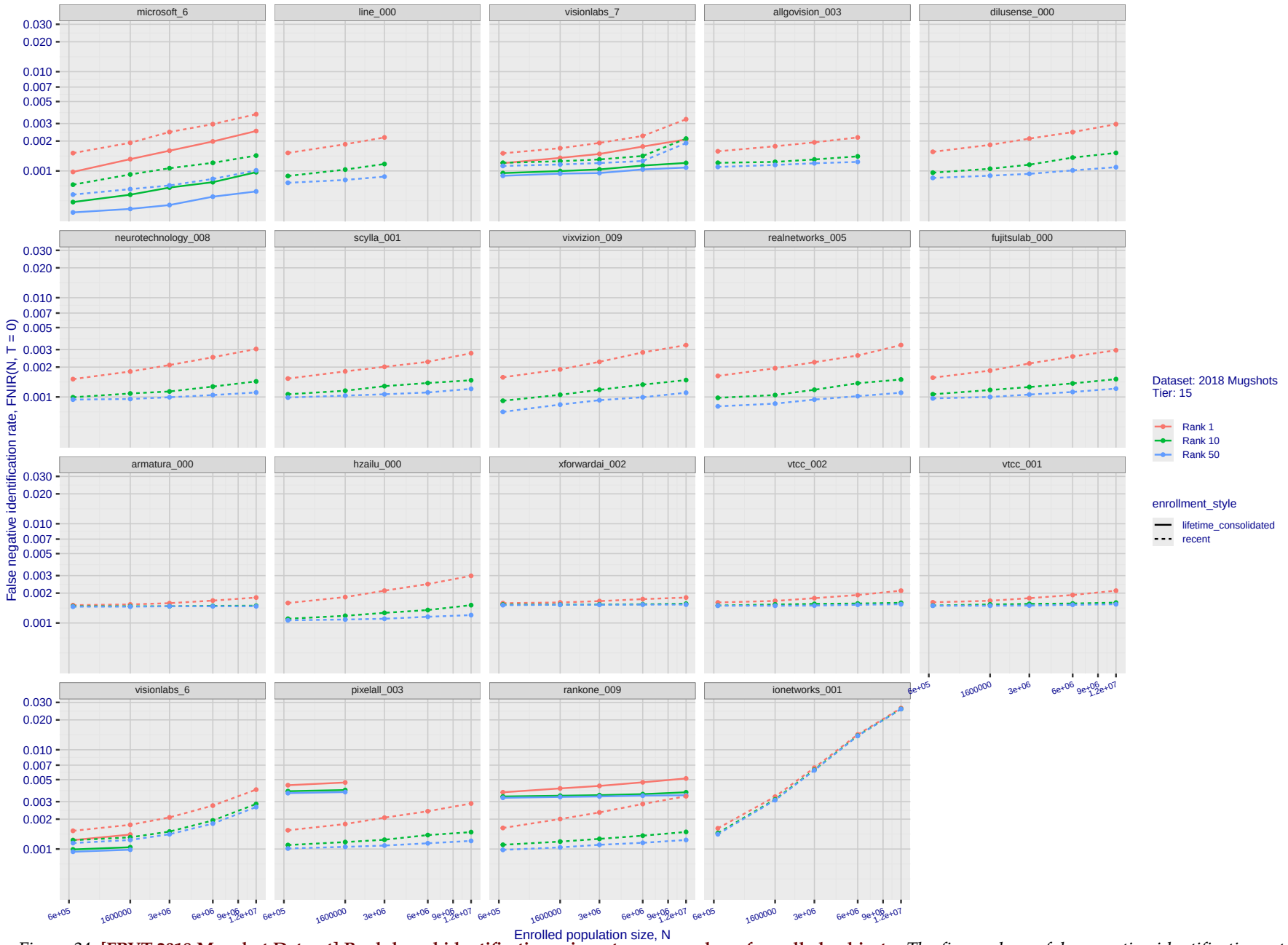

Figure 34: **[FRVT-2018 Mugshot Dataset] Rank-based identification miss rates vs. number of enrolled subjects**. *The figure shows false negative identification rates, FNIR(N, R), across various gallery sizes and ranks 1, 10 and 50. The threshold is set to zero, so this metric rewards even weak scoring rank 1 mates. This also means FPIR = 1, so any search without an enrolled mate will return non-mated candidates. For clarity, results are sorted and reported into tiers spanning multiple pages, the tiering criteria being rank 1 hit rate on a gallery size of 640 000.*

2026/01/09
20:40:38

FNIR(N, R, T) = False neg. identification rate
FPIR(N, T) = False pos. identification rate

N = Num. enrolled subjects
R = Num. candidates examined

T = Threshold

T = 0 → Investigation
T > 0 → Identification

This publication is available free of charge from: https://doi.org/10.6028/NIST.IR.8271

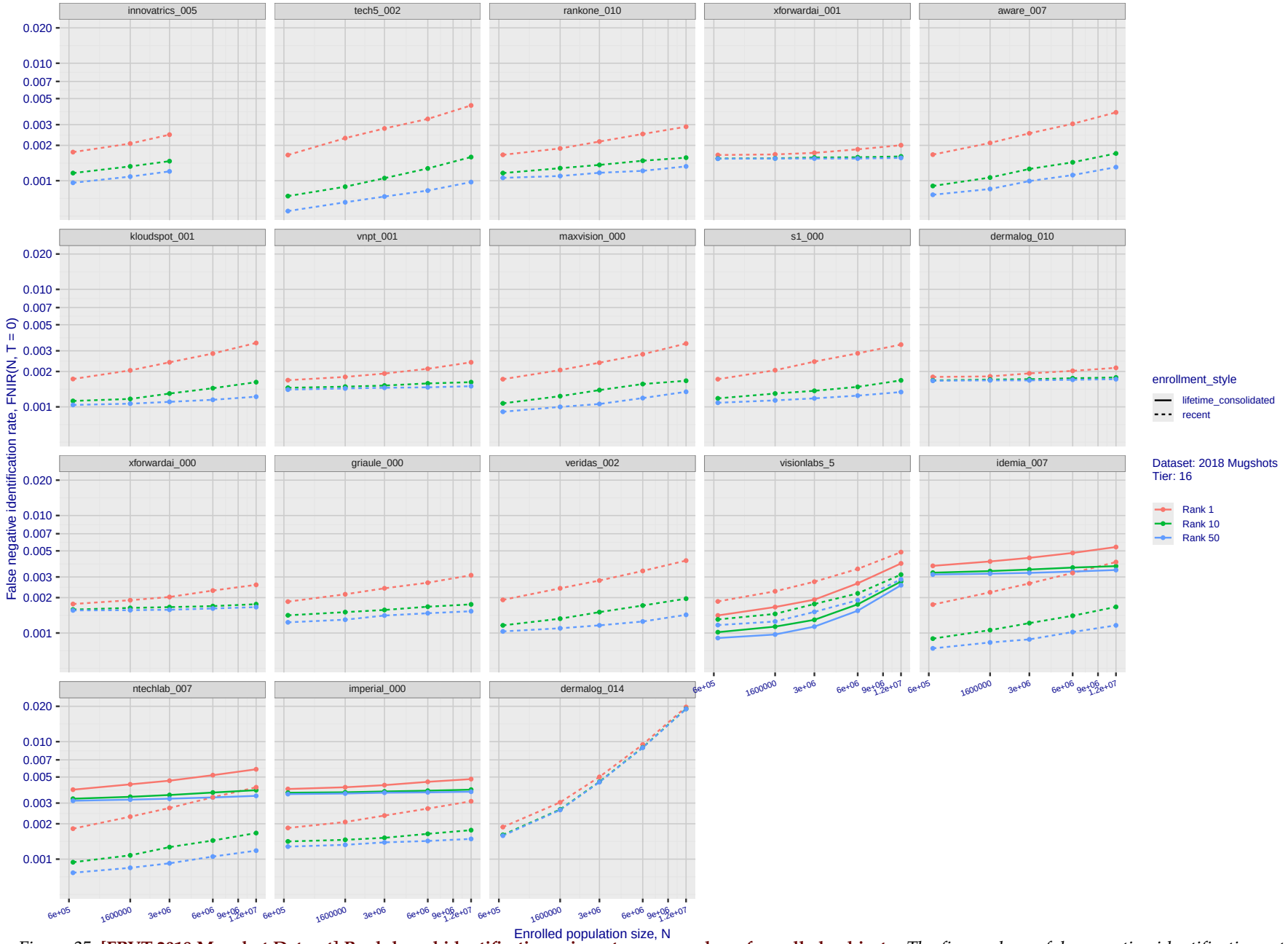

Figure 35: **[FRVT-2018 Mugshot Dataset] Rank-based identification miss rates vs. number of enrolled subjects**. *The figure shows false negative identification rates, FNIR(N, R), across various gallery sizes and ranks 1, 10 and 50. The threshold is set to zero, so this metric rewards even weak scoring rank 1 mates. This also means FPIR = 1, so any search without an enrolled mate will return non-mated candidates. For clarity, results are sorted and reported into tiers spanning multiple pages, the tiering criteria being rank 1 hit rate on a gallery size of 640 000.*

2026/01/09 20:40:38
FNIR(N, R, T) = False neg. identification rate
FPIR(N, T) = False pos. identification rate
N = Num. enrolled subjects
R = Num. candidates examined
T = Threshold
T = 0 → Investigation
T > 0 → Identification

This publication is available free of charge from: https://doi.org/10.6028/NIST.IR.8271

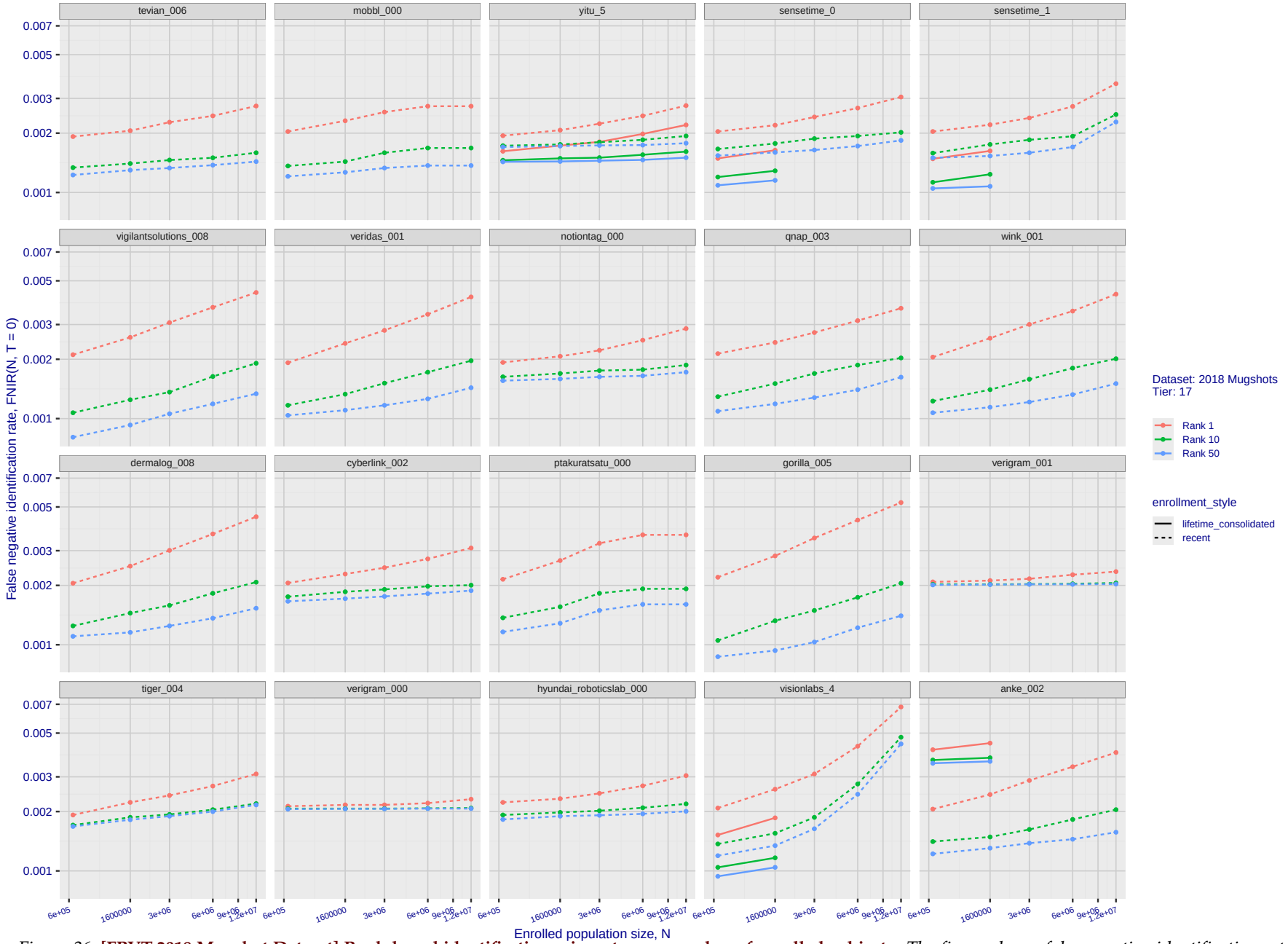

Figure 36: **[FRVT-2018 Mugshot Dataset] Rank-based identification miss rates vs. number of enrolled subjects**. *The figure shows false negative identification rates, FNIR(N, R), across various gallery sizes and ranks 1, 10 and 50. The threshold is set to zero, so this metric rewards even weak scoring rank 1 mates. This also means FPIR = 1, so any search without an enrolled mate will return non-mated candidates. For clarity, results are sorted and reported into tiers spanning multiple pages, the tiering criteria being rank 1 hit rate on a gallery size of 640 000.*

This publication is available free of charge from: https://doi.org/10.6028/NIST.IR.8271

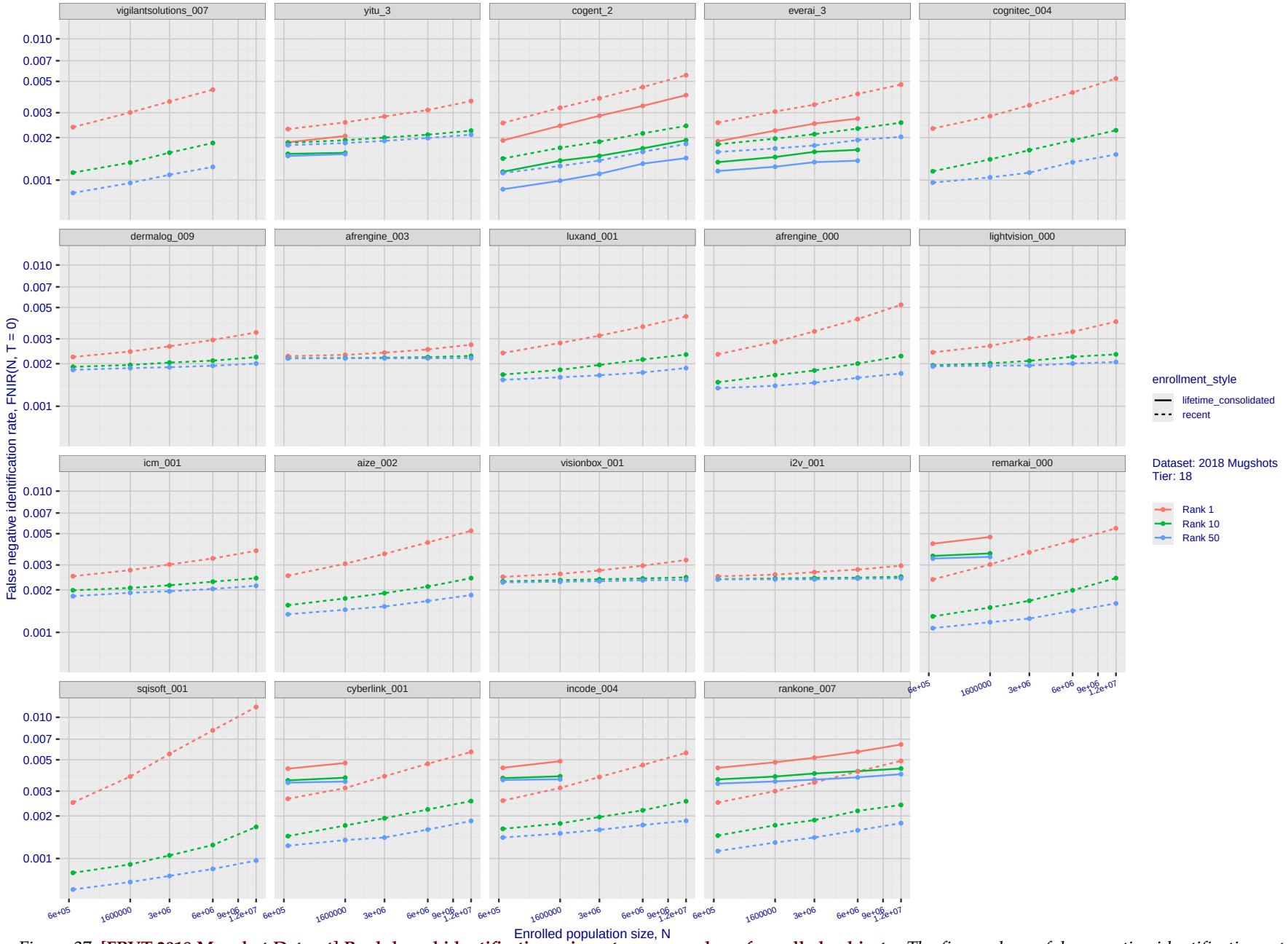

Figure 37: **[FRVT-2018 Mugshot Dataset] Rank-based identification miss rates vs. number of enrolled subjects**. *The figure shows false negative identification rates, FNIR(N, R), across various gallery sizes and ranks 1, 10 and 50. The threshold is set to zero, so this metric rewards even weak scoring rank 1 mates. This also means FPIR = 1, so any search without an enrolled mate will return non-mated candidates. For clarity, results are sorted and reported into tiers spanning multiple pages, the tiering criteria being rank 1 hit rate on a gallery size of 640 000.*

2026/01/09
20:40:38

FNIR(N, R, T) = False neg. identification rate
FPIR(N, T) = False pos. identification rate

N = Num. enrolled subjects
R = Num. candidates examined

T = Threshold

T = 0 → Investigation
T > 0 → Identification

This publication is available free of charge from: https://doi.org/10.6028/NIST.IR.8271

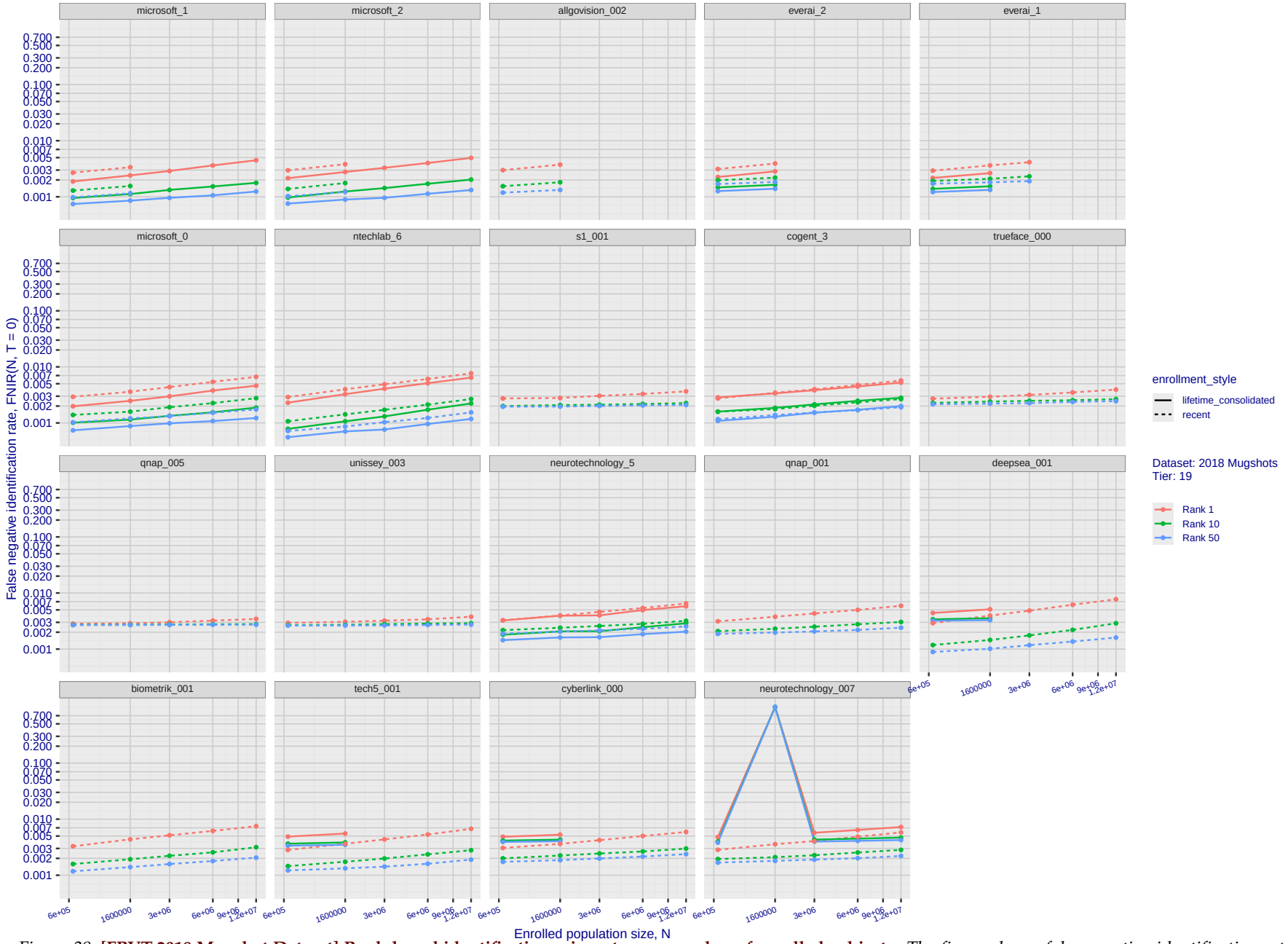

Figure 38: **[FRVT-2018 Mugshot Dataset] Rank-based identification miss rates vs. number of enrolled subjects**. *The figure shows false negative identification rates, FNIR(N, R), across various gallery sizes and ranks 1, 10 and 50. The threshold is set to zero, so this metric rewards even weak scoring rank 1 mates. This also means FPIR = 1, so any search without an enrolled mate will return non-mated candidates. For clarity, results are sorted and reported into tiers spanning multiple pages, the tiering criteria being rank 1 hit rate on a gallery size of 640 000.*

2026/01/09
20:40:38

FNIR(N, R, T) = False neg. identification rate
FPIR(N, T) = False pos. identification rate

N = Num. enrolled subjects
R = Num. candidates examined

T = Threshold

T = 0 → Investigation
T > 0 → Identification

This publication is available free of charge from: https://doi.org/10.6028/NIST.IR.8271

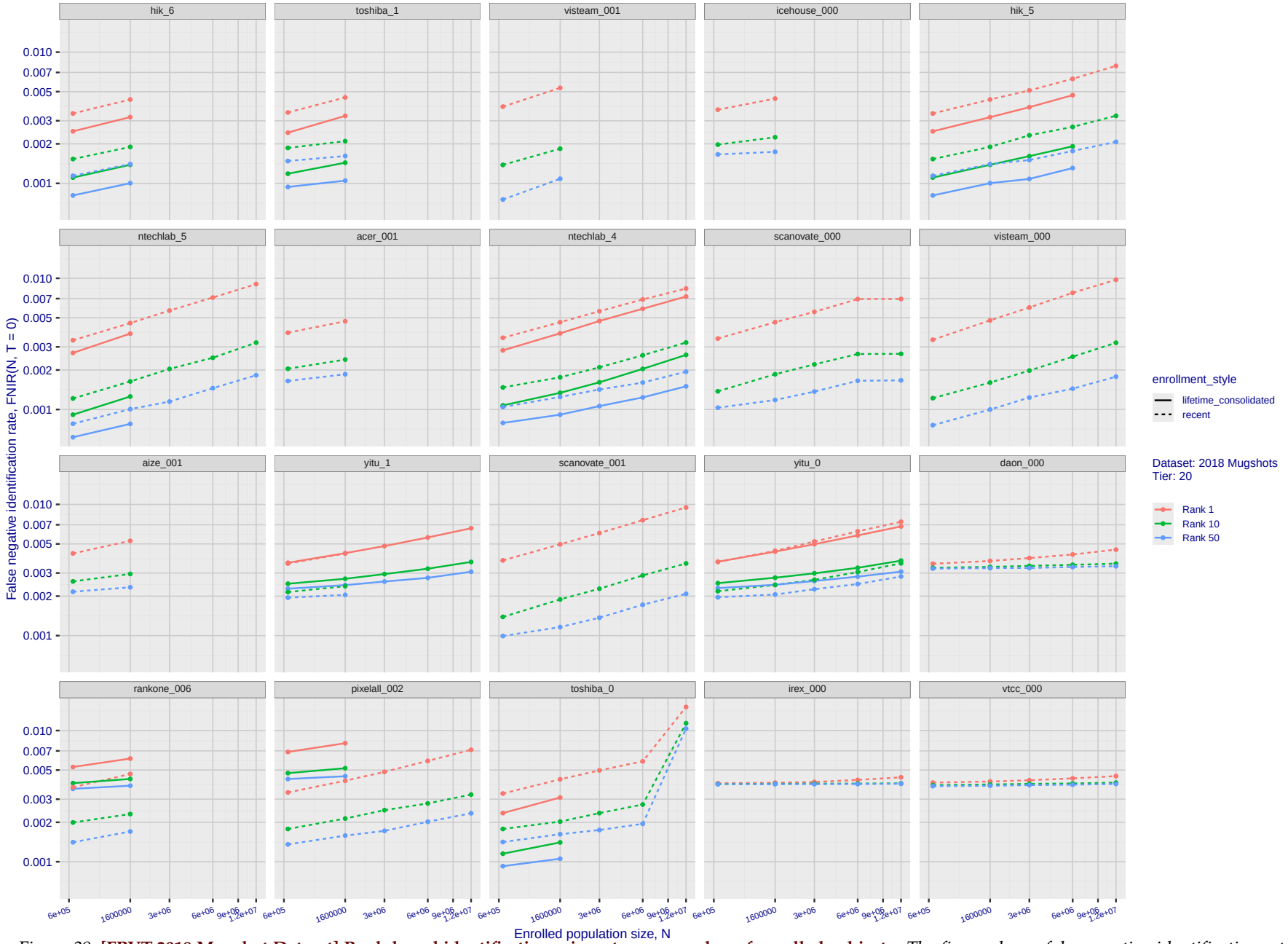

Figure 39: **[FRVT-2018 Mugshot Dataset] Rank-based identification miss rates vs. number of enrolled subjects**. *The figure shows false negative identification rates, FNIR(N, R), across various gallery sizes and ranks 1, 10 and 50. The threshold is set to zero, so this metric rewards even weak scoring rank 1 mates. This also means FPIR = 1, so any search without an enrolled mate will return non-mated candidates. For clarity, results are sorted and reported into tiers spanning multiple pages, the tiering criteria being rank 1 hit rate on a gallery size of 640 000.*

2026/01/09 20:40:38

FNIR(N, R, T) = False neg. identification rate
FPIR(N, T) = False pos. identification rate

N = Num. enrolled subjects
R = Num. candidates examined

T = Threshold

T = 0 → Investigation
T > 0 → Identification

This publication is available free of charge from: https://doi.org/10.6028/NIST.IR.8271

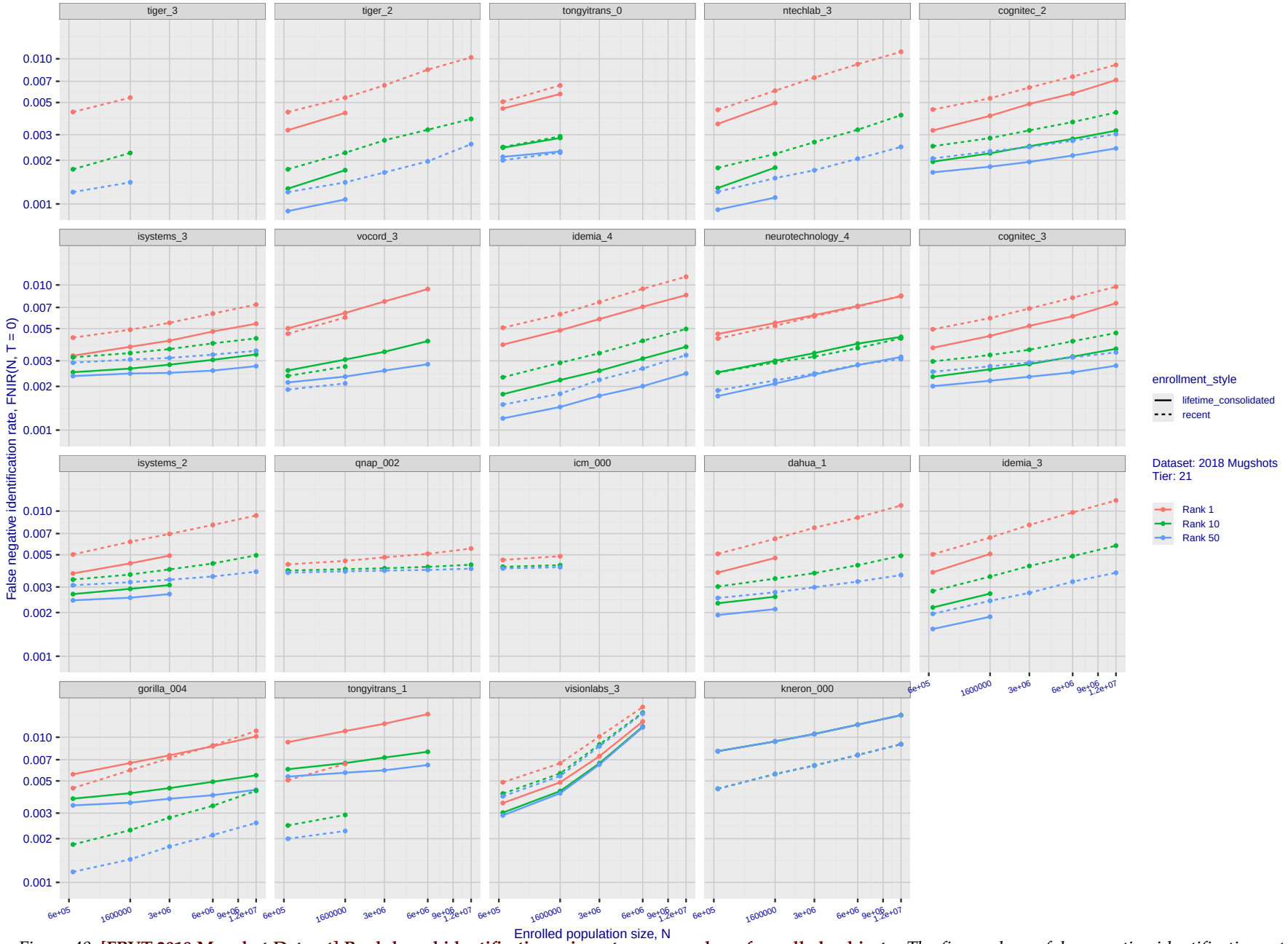

Figure 40: **[FRVT-2018 Mugshot Dataset] Rank-based identification miss rates vs. number of enrolled subjects**. *The figure shows false negative identification rates, FNIR(N, R), across various gallery sizes and ranks 1, 10 and 50. The threshold is set to zero, so this metric rewards even weak scoring rank 1 mates. This also means FPIR = 1, so any search without an enrolled mate will return non-mated candidates. For clarity, results are sorted and reported into tiers spanning multiple pages, the tiering criteria being rank 1 hit rate on a gallery size of 640 000.*

2026/01/09 20:40:38

FNIR(N, R, T) = False neg. identification rate
FPIR(N, T) = False pos. identification rate

N = Num. enrolled subjects
R = Num. candidates examined

T = Threshold

T = 0 → Investigation
T > 0 → Identification

This publication is available free of charge from: https://doi.org/10.6028/NIST.IR.8271

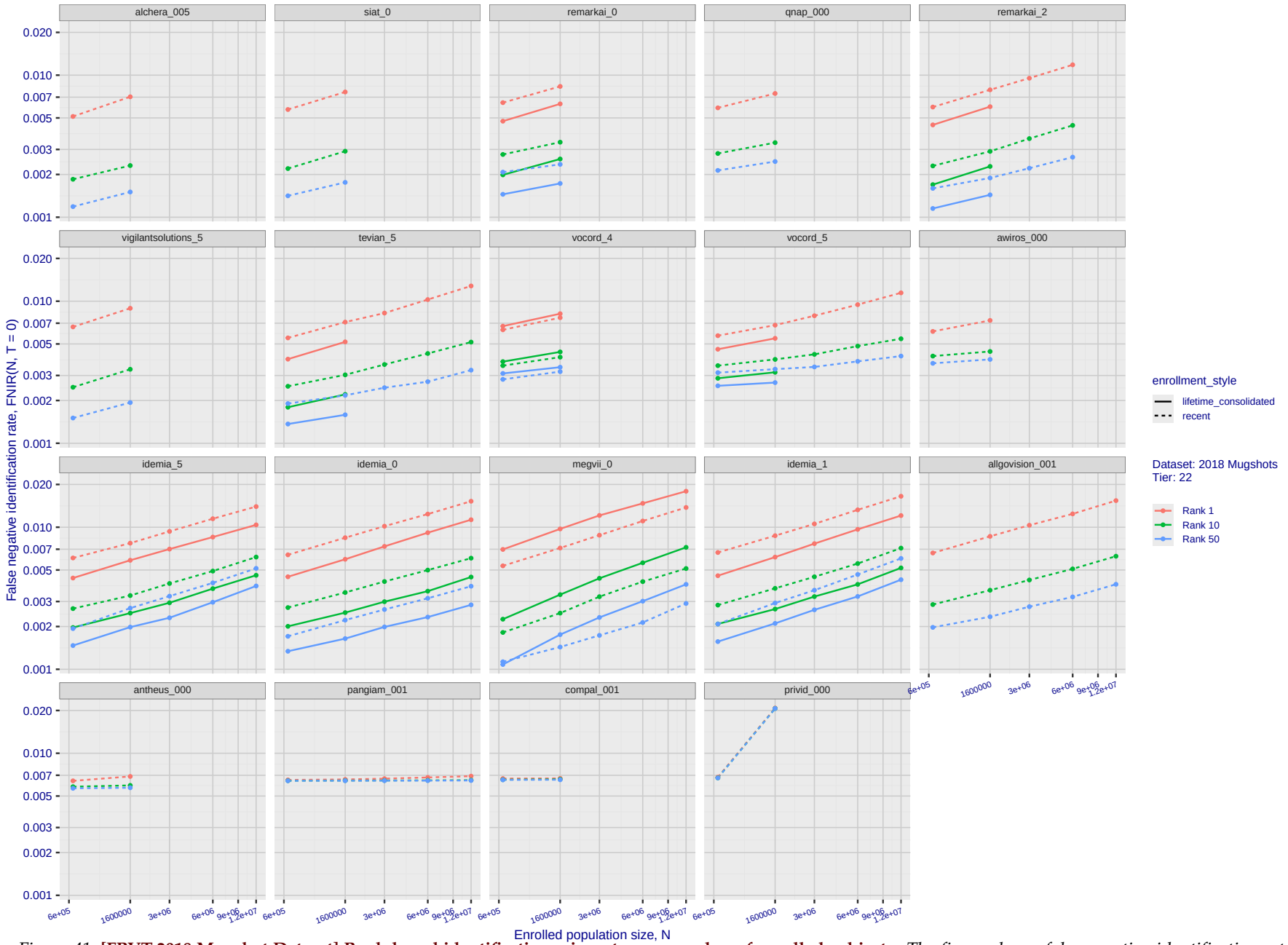

Figure 41: **[FRVT-2018 Mugshot Dataset] Rank-based identification miss rates vs. number of enrolled subjects**. *The figure shows false negative identification rates, FNIR(N, R), across various gallery sizes and ranks 1, 10 and 50. The threshold is set to zero, so this metric rewards even weak scoring rank 1 mates. This also means FPIR = 1, so any search without an enrolled mate will return non-mated candidates. For clarity, results are sorted and reported into tiers spanning multiple pages, the tiering criteria being rank 1 hit rate on a gallery size of 640 000.*

2026/01/09 20:40:38
FNIR(N, R, T) = False neg. identification rate
FPIR(N, T) = False pos. identification rate
N = Num. enrolled subjects
R = Num. candidates examined
T = Threshold
T = 0 → Investigation
T > 0 → Identification

This publication is available free of charge from: https://doi.org/10.6028/NIST.IR.8271

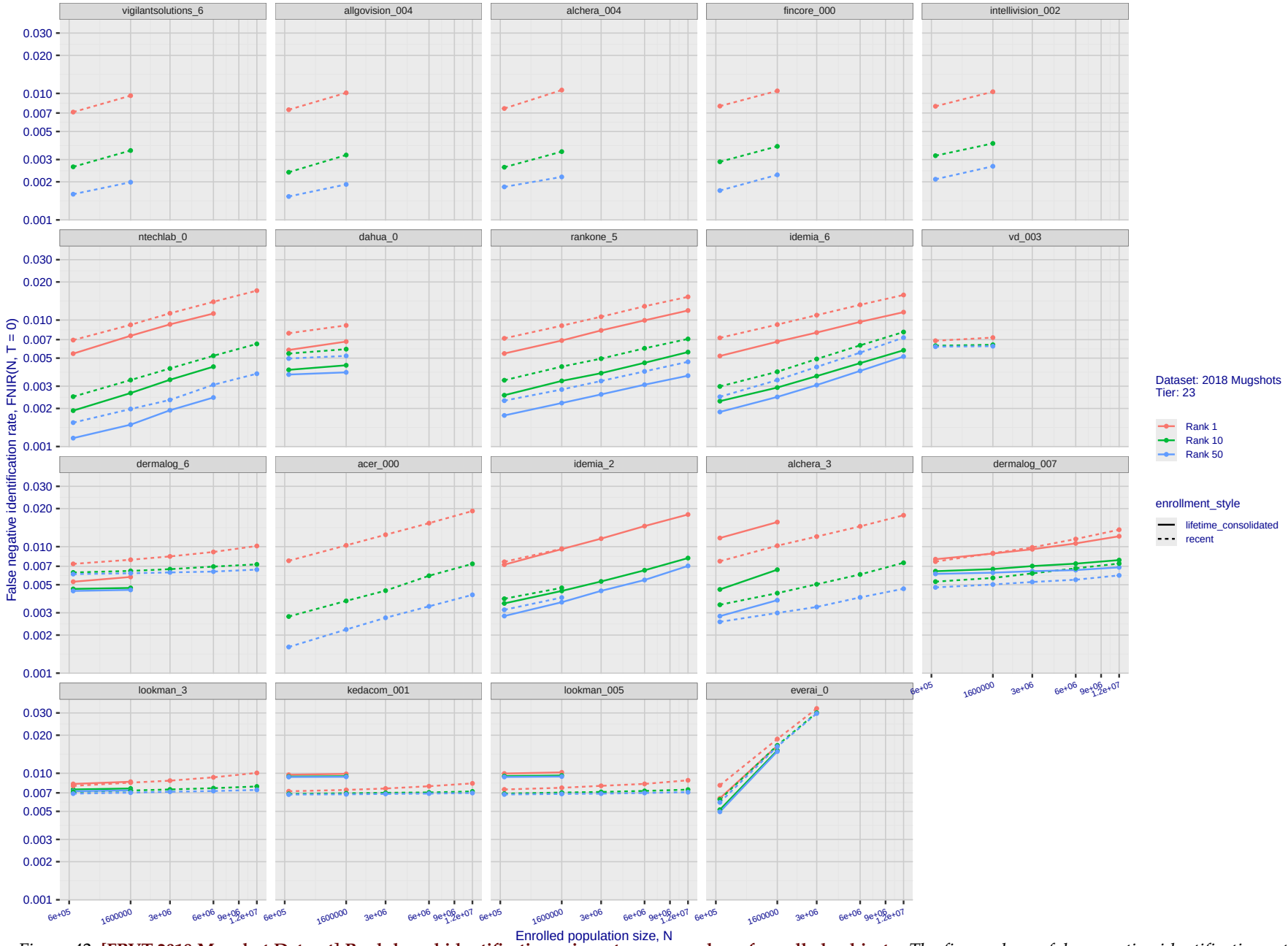

Figure 42: **[FRVT-2018 Mugshot Dataset] Rank-based identification miss rates vs. number of enrolled subjects**. *The figure shows false negative identification rates, FNIR(N, R), across various gallery sizes and ranks 1, 10 and 50. The threshold is set to zero, so this metric rewards even weak scoring rank 1 mates. This also means FPIR = 1, so any search without an enrolled mate will return non-mated candidates. For clarity, results are sorted and reported into tiers spanning multiple pages, the tiering criteria being rank 1 hit rate on a gallery size of 640 000.*

2026/01/09 20:40:38
FNIR(N, R, T) = False neg. identification rate
FPIR(N, T) = False pos. identification rate
N = Num. enrolled subjects
R = Num. candidates examined
T = Threshold
T = 0 → Investigation
T > 0 → Identification

This publication is available free of charge from: https://doi.org/10.6028/NIST.IR.8271

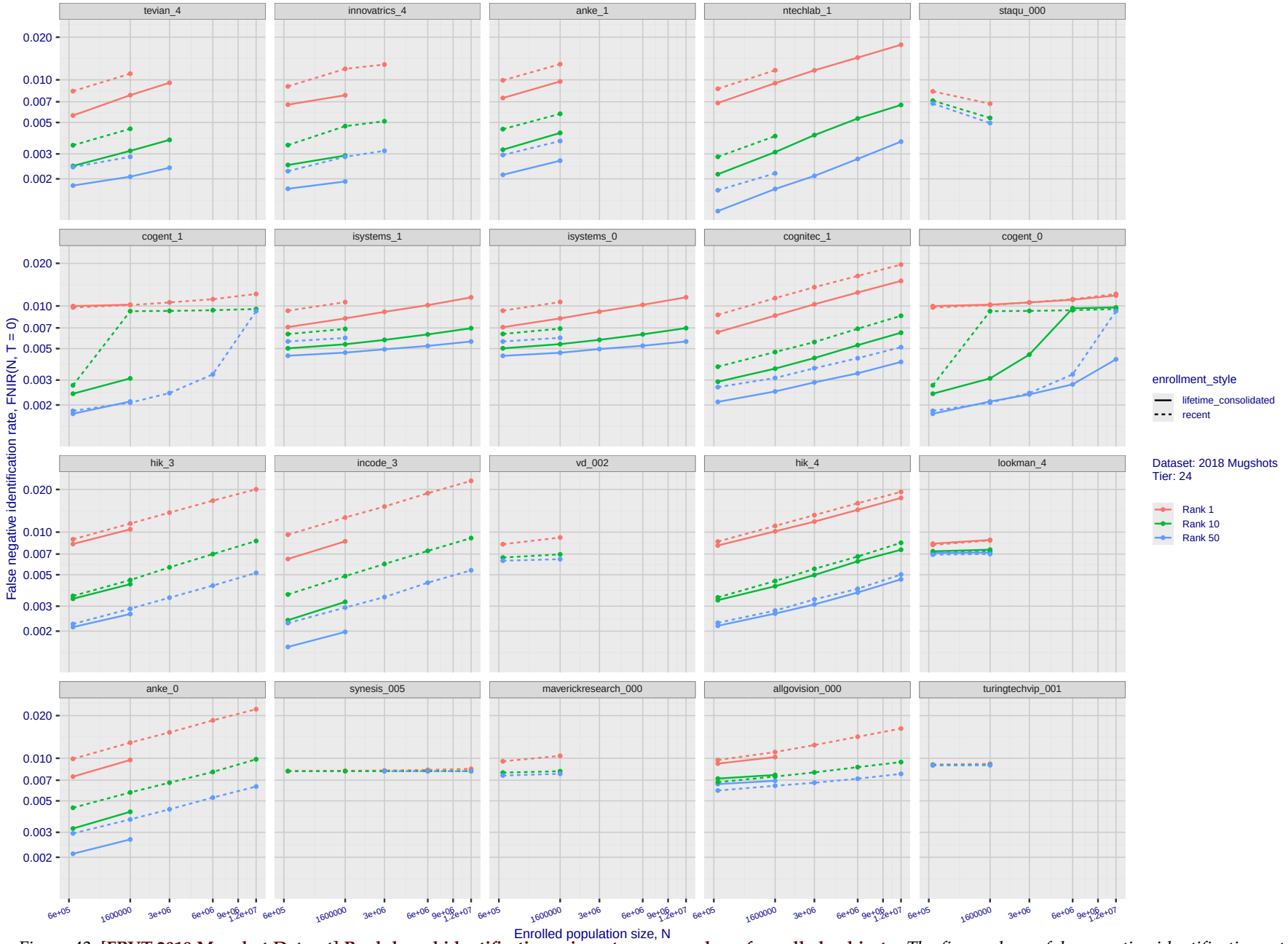

Figure 43: **[FRVT-2018 Mugshot Dataset] Rank-based identification miss rates vs. number of enrolled subjects**. *The figure shows false negative identification rates, FNIR(N, R), across various gallery sizes and ranks 1, 10 and 50. The threshold is set to zero, so this metric rewards even weak scoring rank 1 mates. This also means FPIR = 1, so any search without an enrolled mate will return non-mated candidates. For clarity, results are sorted and reported into tiers spanning multiple pages, the tiering criteria being rank 1 hit rate on a gallery size of 640 000.*

2026/01/09 20:40:38
FNIR(N, R, T) = False neg. identification rate
FPIR(N, T) = False pos. identification rate
N = Num. enrolled subjects
R = Num. candidates examined
T = Threshold
T = 0 → Investigation
T > 0 → Identification

This publication is available free of charge from: https://doi.org/10.6028/NIST.IR.8271

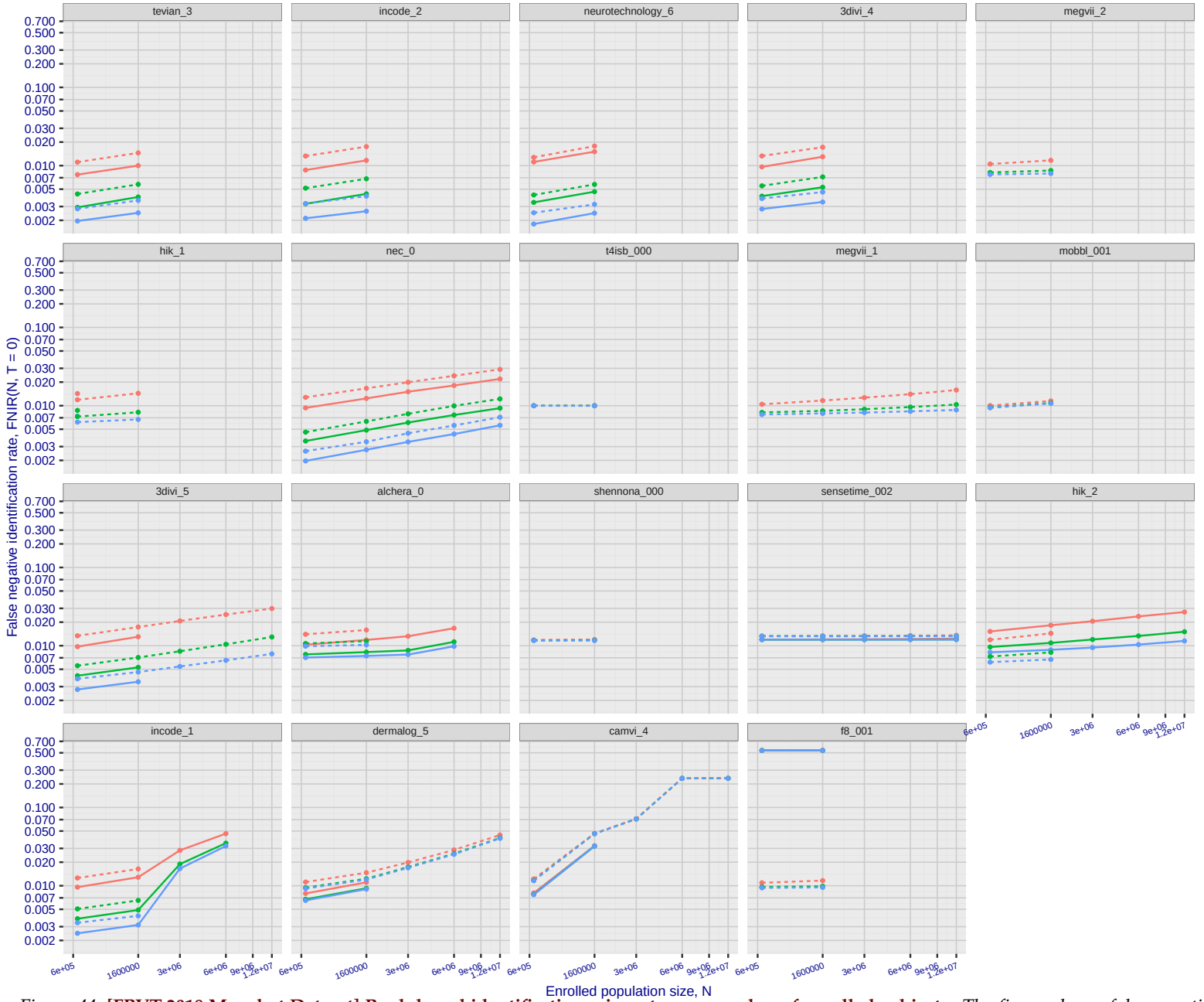

Figure 44: **[FRVT-2018 Mugshot Dataset] Rank-based identification miss rates vs. number of enrolled subjects**. *The figure shows false negative identification rates, FNIR(N, R), across various gallery sizes and ranks 1, 10 and 50. The threshold is set to zero, so this metric rewards even weak scoring rank 1 mates. This also means FPIR = 1, so any search without an enrolled mate will return non-mated candidates. For clarity, results are sorted and reported into tiers spanning multiple pages, the tiering criteria being rank 1 hit rate on a gallery size of 640 000.*

2026/01/09 20:40:38
FNIR(N, R, T) = False neg. identification rate
FPIR(N, T) = False pos. identification rate
N = Num. enrolled subjects
R = Num. candidates examined
T = Threshold
T = 0 → Investigation
T > 0 → Identification

This publication is available free of charge from: https://doi.org/10.6028/NIST.IR.8271

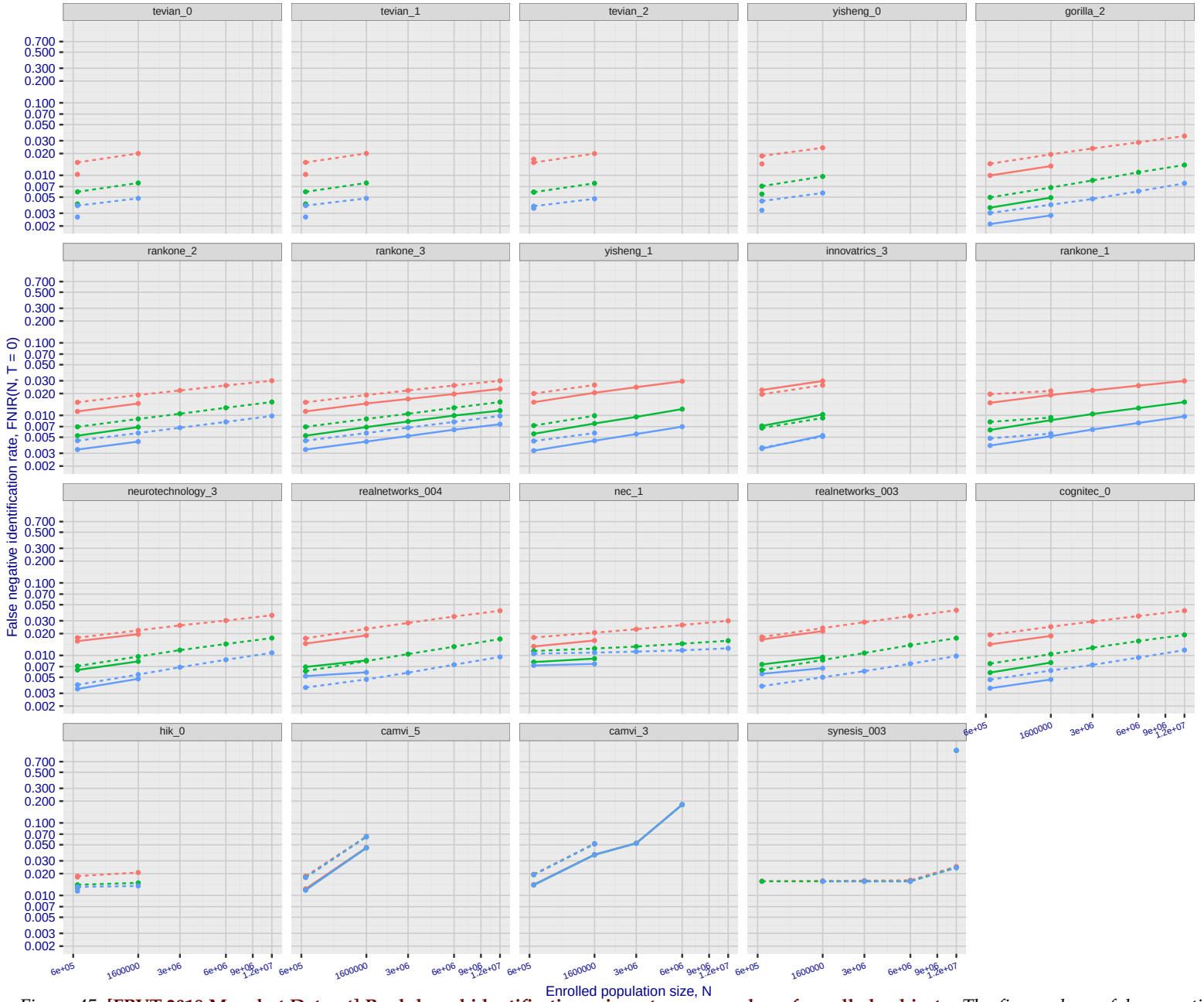

Figure 45: **[FRVT-2018 Mugshot Dataset] Rank-based identification miss rates vs. number of enrolled subjects**. *The figure shows false negative identification rates, FNIR(N, R), across various gallery sizes and ranks 1, 10 and 50. The threshold is set to zero, so this metric rewards even weak scoring rank 1 mates. This also means FPIR = 1, so any search without an enrolled mate will return non-mated candidates. For clarity, results are sorted and reported into tiers spanning multiple pages, the tiering criteria being rank 1 hit rate on a gallery size of 640 000.*

2026/01/09 20:40:38
FNIR(N, R, T) = False neg. identification rate
FPIR(N, T) = False pos. identification rate
N = Num. enrolled subjects
R = Num. candidates examined
T = Threshold
T = 0 → Investigation
T > 0 → Identification

This publication is available free of charge from: https://doi.org/10.6028/NIST.IR.8271

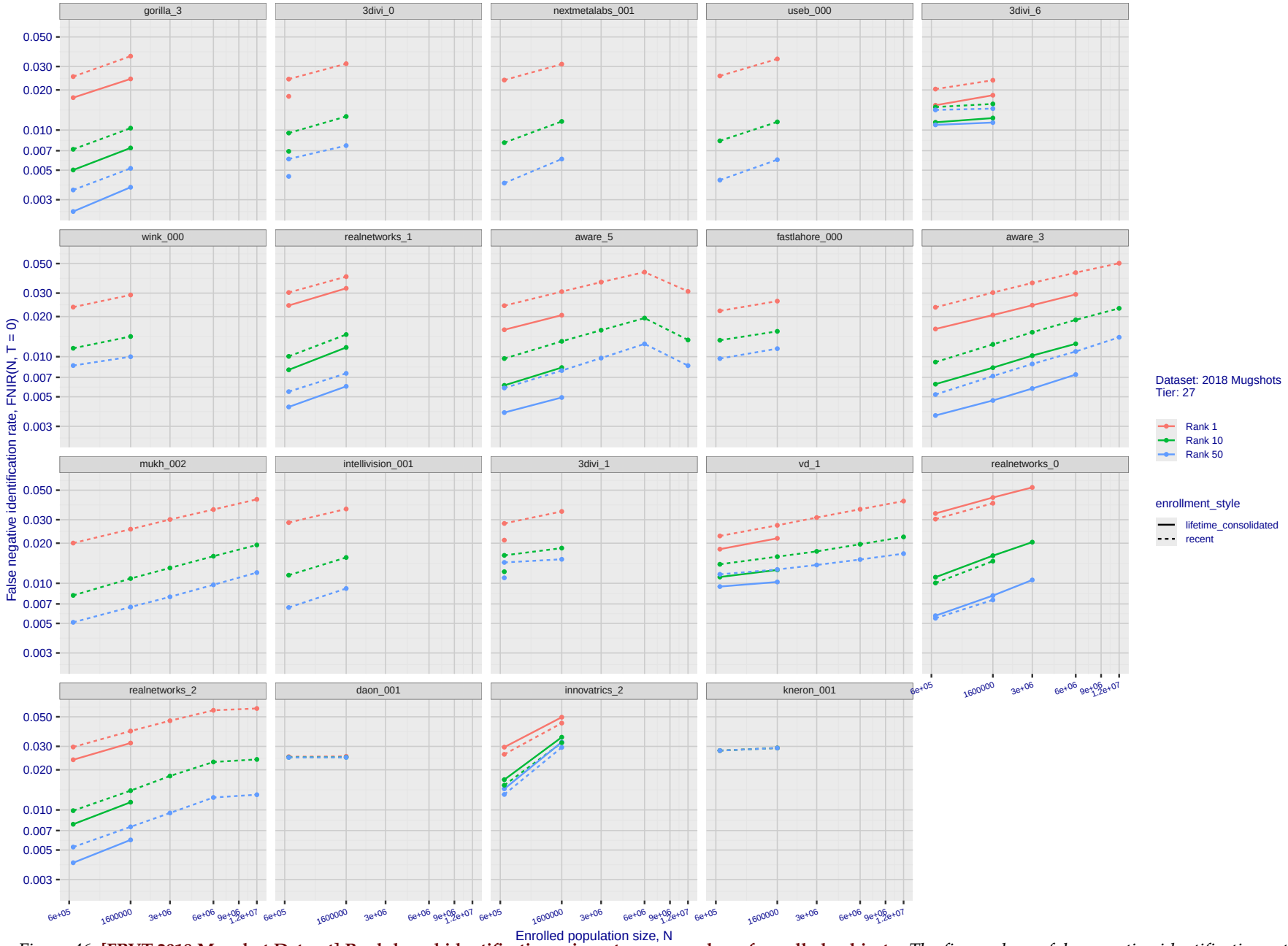

Figure 46: **[FRVT-2018 Mugshot Dataset] Rank-based identification miss rates vs. number of enrolled subjects**. *The figure shows false negative identification rates, FNIR(N, R), across various gallery sizes and ranks 1, 10 and 50. The threshold is set to zero, so this metric rewards even weak scoring rank 1 mates. This also means FPIR = 1, so any search without an enrolled mate will return non-mated candidates. For clarity, results are sorted and reported into tiers spanning multiple pages, the tiering criteria being rank 1 hit rate on a gallery size of 640 000.*

2026/01/09 20:40:38
FNIR(N, R, T) = False neg. identification rate
FPIR(N, T) = False pos. identification rate
N = Num. enrolled subjects
R = Num. candidates examined
T = Threshold
T = 0 → Investigation
T > 0 → Identification

This publication is available free of charge from: https://doi.org/10.6028/NIST.IR.8271

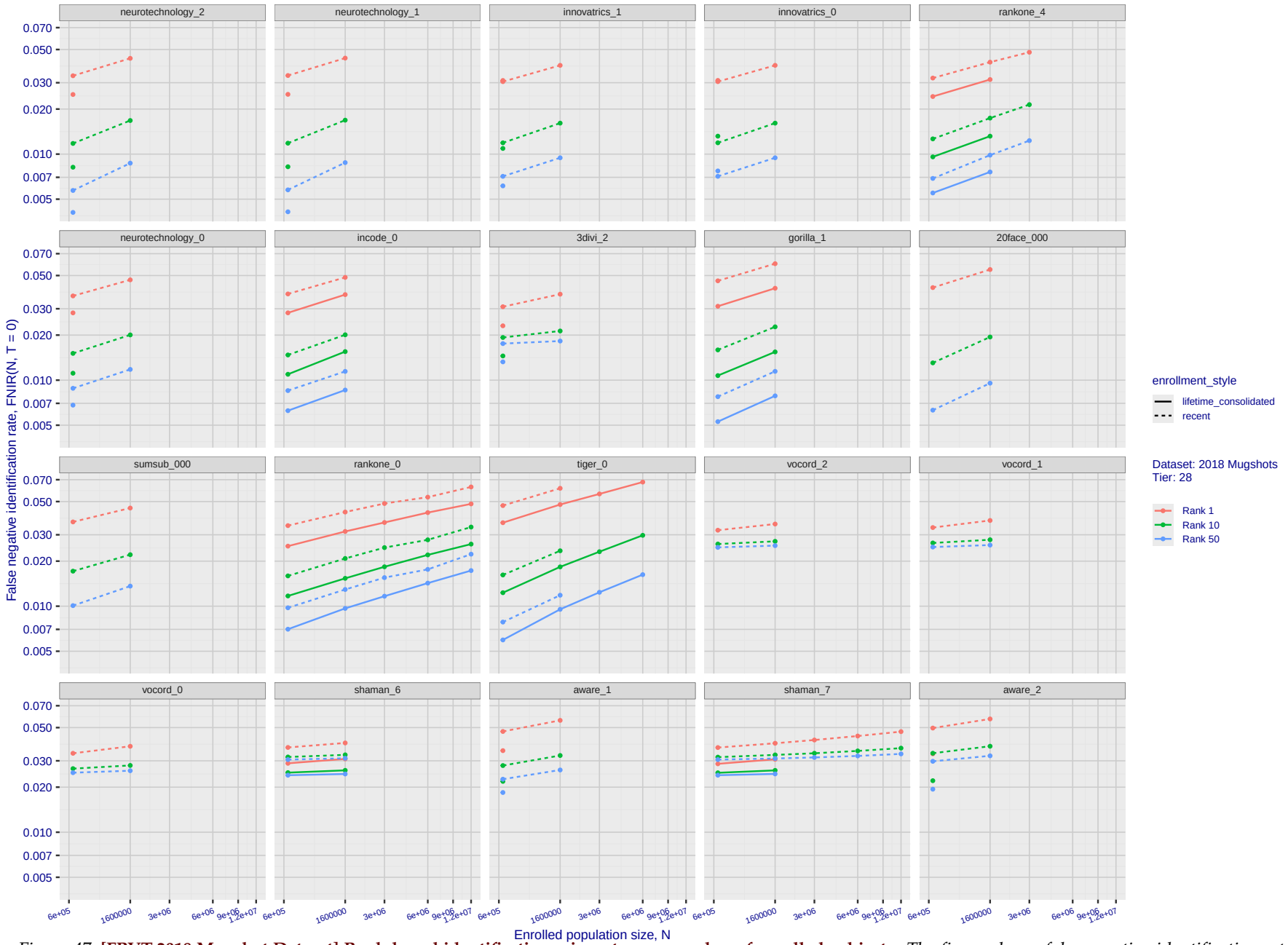

Figure 47: **[FRVT-2018 Mugshot Dataset] Rank-based identification miss rates vs. number of enrolled subjects**. *The figure shows false negative identification rates, FNIR(N, R), across various gallery sizes and ranks 1, 10 and 50. The threshold is set to zero, so this metric rewards even weak scoring rank 1 mates. This also means FPIR = 1, so any search without an enrolled mate will return non-mated candidates. For clarity, results are sorted and reported into tiers spanning multiple pages, the tiering criteria being rank 1 hit rate on a gallery size of 640 000.*

2026/01/09 20:40:38
FNIR(N, R, T) = False neg. identification rate
FPIR(N, T) = False pos. identification rate
N = Num. enrolled subjects
R = Num. candidates examined
T = Threshold
T = 0 → Investigation
T > 0 → Identification

This publication is available free of charge from: https://doi.org/10.6028/NIST.IR.8271

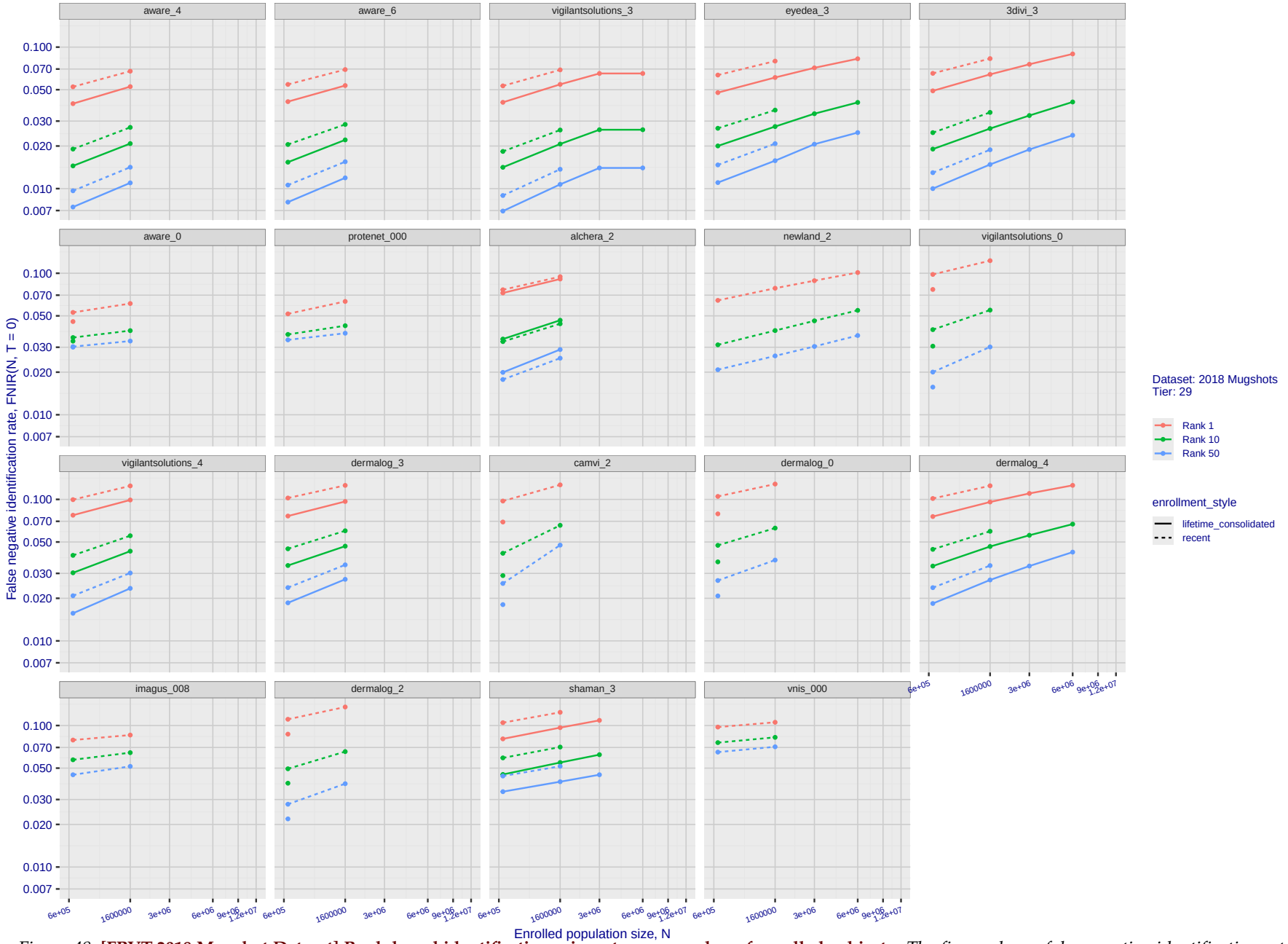

Figure 48: **[FRVT-2018 Mugshot Dataset] Rank-based identification miss rates vs. number of enrolled subjects**. *The figure shows false negative identification rates, FNIR(N, R), across various gallery sizes and ranks 1, 10 and 50. The threshold is set to zero, so this metric rewards even weak scoring rank 1 mates. This also means FPIR = 1, so any search without an enrolled mate will return non-mated candidates. For clarity, results are sorted and reported into tiers spanning multiple pages, the tiering criteria being rank 1 hit rate on a gallery size of 640 000.*

2026/01/09 20:40:38
FNIR(N, R, T) = False neg. identification rate
FPIR(N, T) = False pos. identification rate
N = Num. enrolled subjects
R = Num. candidates examined
T = Threshold
T = 0 → Investigation
T > 0 → Identification

This publication is available free of charge from: https://doi.org/10.6028/NIST.IR.8271

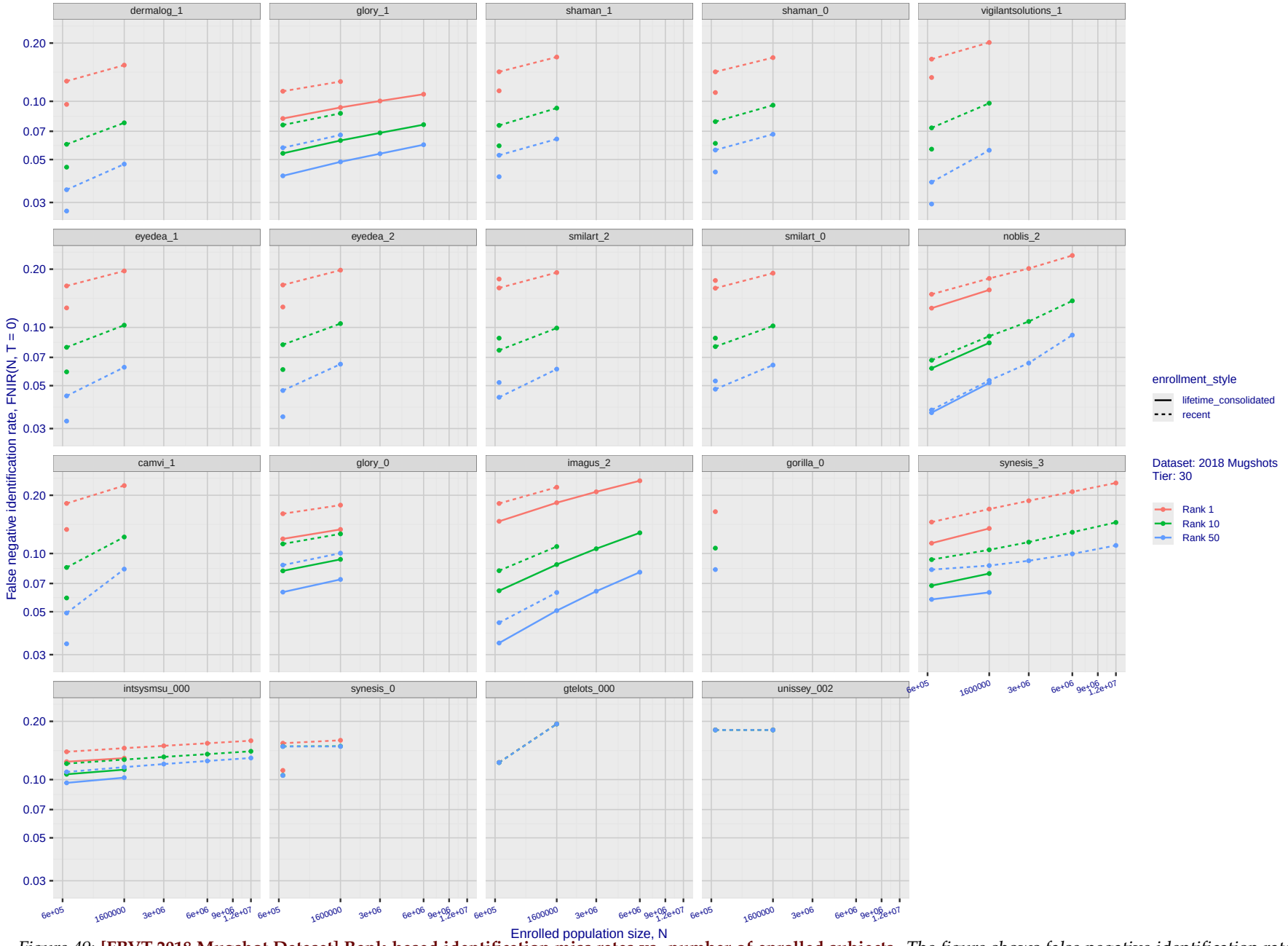

Figure 49: **[FRVT-2018 Mugshot Dataset] Rank-based identification miss rates vs. number of enrolled subjects**. *The figure shows false negative identification rates, FNIR(N, R), across various gallery sizes and ranks 1, 10 and 50. The threshold is set to zero, so this metric rewards even weak scoring rank 1 mates. This also means FPIR = 1, so any search without an enrolled mate will return non-mated candidates. For clarity, results are sorted and reported into tiers spanning multiple pages, the tiering criteria being rank 1 hit rate on a gallery size of 640 000.*

2026/01/09 20:40:38

FNIR(N, R, T) = False neg. identification rate
FPIR(N, T) = False pos. identification rate

N = Num. enrolled subjects
R = Num. candidates examined

T = Threshold

T = 0 → Investigation
T > 0 → Identification

This publication is available free of charge from: https://doi.org/10.6028/NIST.IR.8271

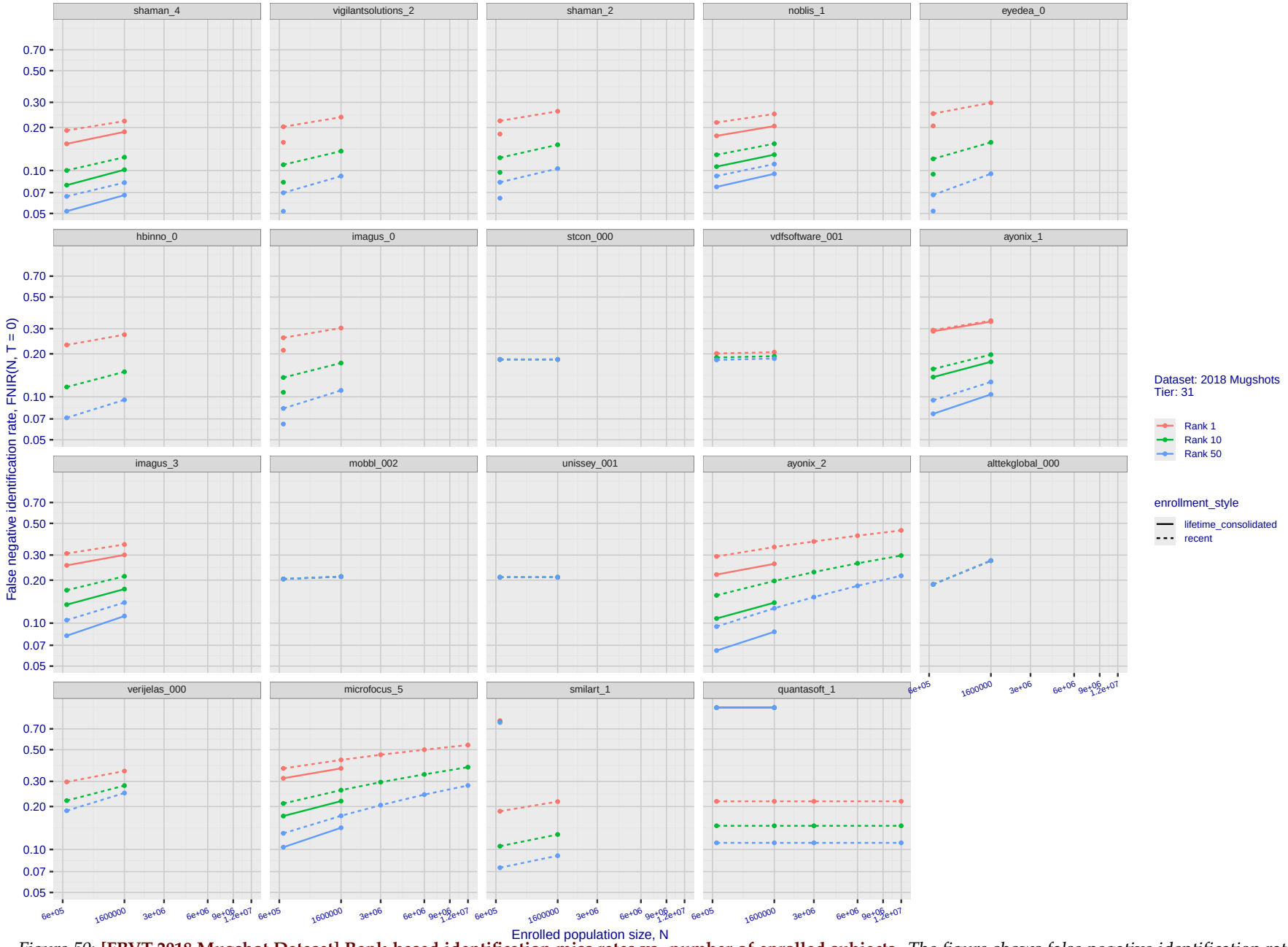

Figure 50: **[FRVT-2018 Mugshot Dataset] Rank-based identification miss rates vs. number of enrolled subjects**. *The figure shows false negative identification rates, FNIR(N, R), across various gallery sizes and ranks 1, 10 and 50. The threshold is set to zero, so this metric rewards even weak scoring rank 1 mates. This also means FPIR = 1, so any search without an enrolled mate will return non-mated candidates. For clarity, results are sorted and reported into tiers spanning multiple pages, the tiering criteria being rank 1 hit rate on a gallery size of 640 000.*

2026/01/09 20:40:38
FNIR(N, R, T) = False neg. identification rate
FPIR(N, T) = False pos. identification rate
N = Num. enrolled subjects
R = Num. candidates examined
T = Threshold
T = 0 → Investigation
T > 0 → Identification

This publication is available free of charge from: https://doi.org/10.6028/NIST.IR.8271

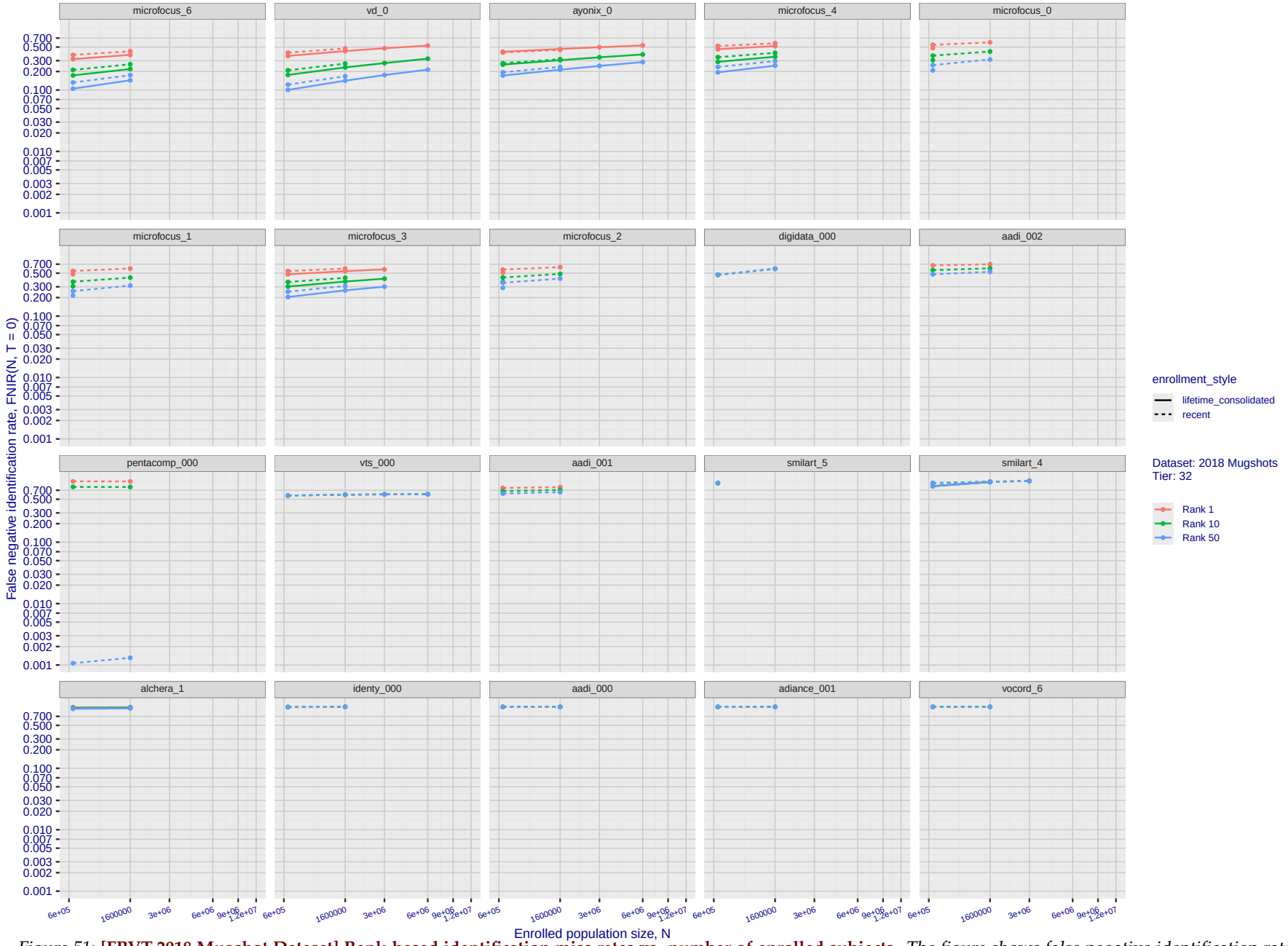

Figure 51: **[FRVT-2018 Mugshot Dataset] Rank-based identification miss rates vs. number of enrolled subjects**. *The figure shows false negative identification rates, FNIR(N, R), across various gallery sizes and ranks 1, 10 and 50. The threshold is set to zero, so this metric rewards even weak scoring rank 1 mates. This also means FPIR = 1, so any search without an enrolled mate will return non-mated candidates. For clarity, results are sorted and reported into tiers spanning multiple pages, the tiering criteria being rank 1 hit rate on a gallery size of 640 000.*

2026/01/09 20:40:38
FNIR(N, R, T) = False neg. identification rate
FPIR(N, T) = False pos. identification rate
N = Num. enrolled subjects
R = Num. candidates examined
T = Threshold
T = 0 → Investigation
T > 0 → Identification

2026/01/09	FNIR(N, R, T) =	False neg. identification rate	N = Num. enrolled subjects	T = Threshold	$T = 0 \rightarrow$ Investigation
20:40:38	FPIR(N, T) =	False pos. identification rate	R = Num. candidates examined		$T > 0 \rightarrow$ Identification

This publication is available free of charge from: https://doi.org/10.6028/NIST.IR.8271

This publication is available free of charge from: https://doi.org/10.6028/NIST.IR.8271

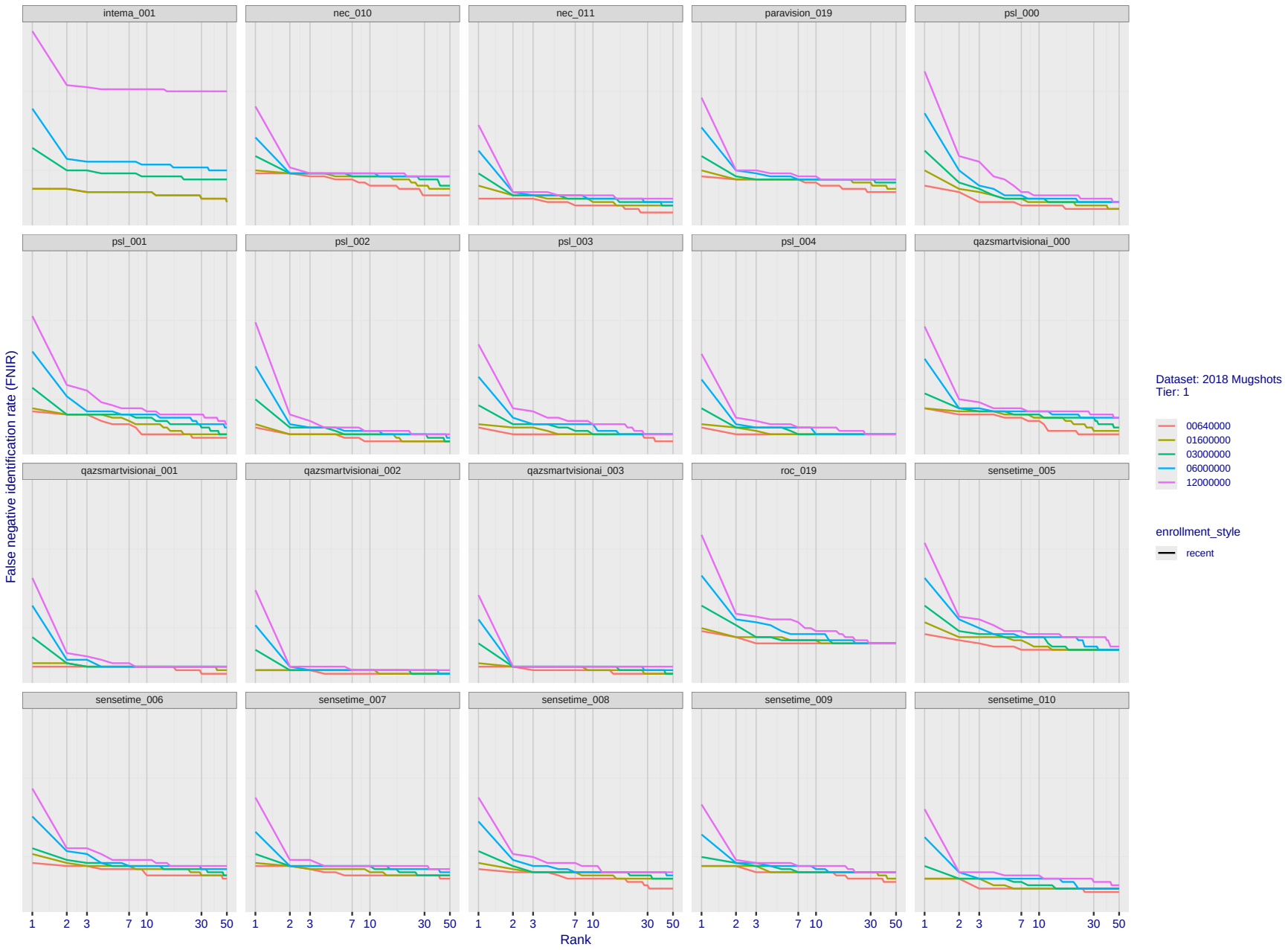

Figure 52: **[FRVT-2018 Mugshot Dataset] Rank-based identification miss rates vs. rank**. *The figure shows false negative identification rates (FNIR) for ranks up to 50. This metric is appropriate to investigational applications where human reviewers will adjudicate sorted candidate lists. Note that with threshold set to zero, FPIR = 1, i.e. any search without an enrolled mate will return non-mated candidates. Results are sorted and reported into tiers for clarity, with the tiering criteria being rank 1 hit rate on a gallery size of N = 640 000 subjects.*

2026/01/09 20:40:38
FNIR(N, R, T) = False neg. identification rate
FPIR(N, T) = False pos. identification rate
N = Num. enrolled subjects
R = Num. candidates examined
T = Threshold
T = 0 → Investigation
T > 0 → Identification

This publication is available free of charge from: https://doi.org/10.6028/NIST.IR.8271

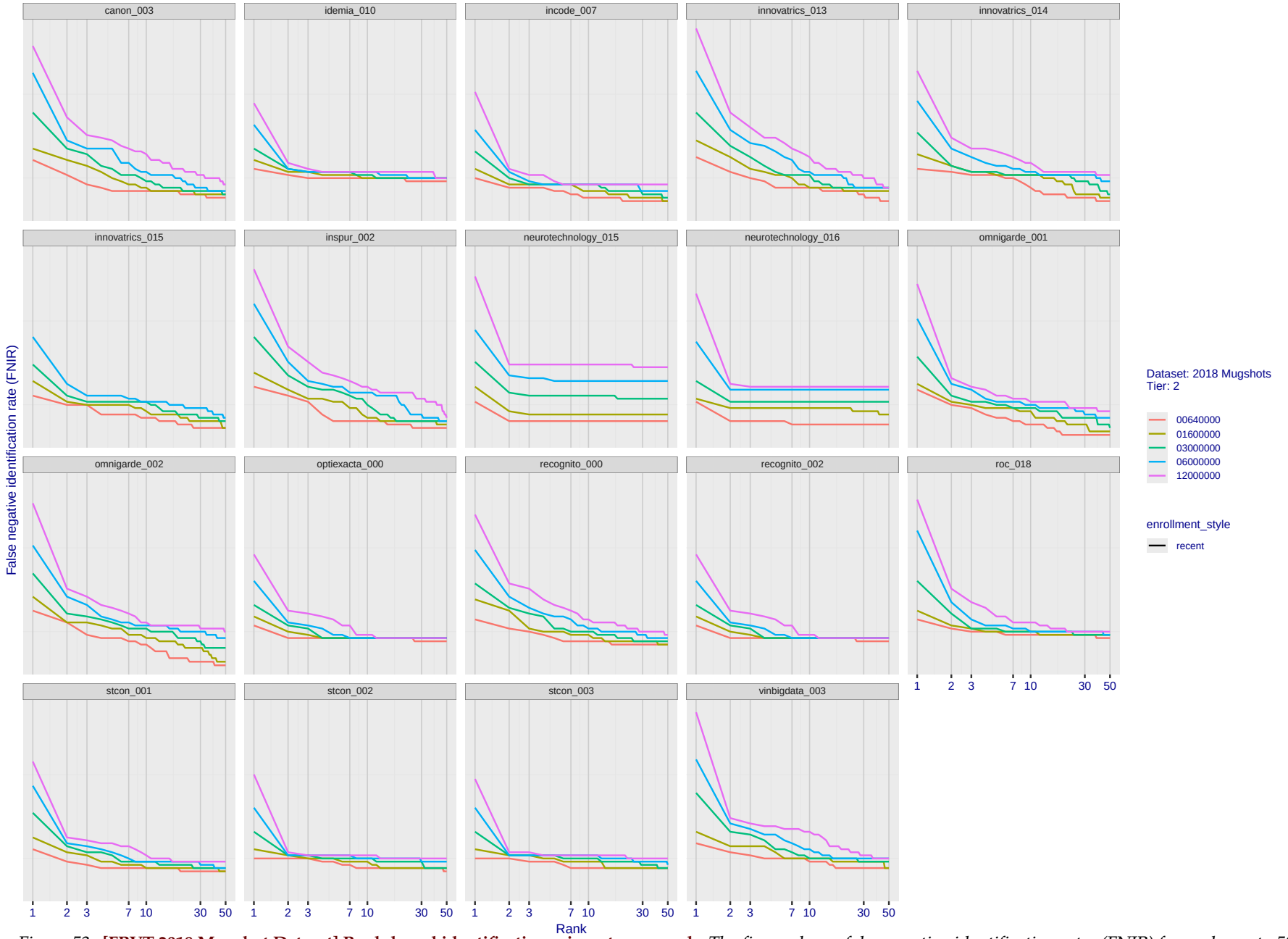

Figure 53: **[FRVT-2018 Mugshot Dataset] Rank-based identification miss rates vs. rank**. *The figure shows false negative identification rates (FNIR) for ranks up to 50. This metric is appropriate to investigational applications where human reviewers will adjudicate sorted candidate lists. Note that with threshold set to zero, FPIR = 1, i.e. any search without an enrolled mate will return non-mated candidates. Results are sorted and reported into tiers for clarity, with the tiering criteria being rank 1 hit rate on a gallery size of N = 640 000 subjects.*

This publication is available free of charge from: https://doi.org/10.6028/NIST.IR.8271

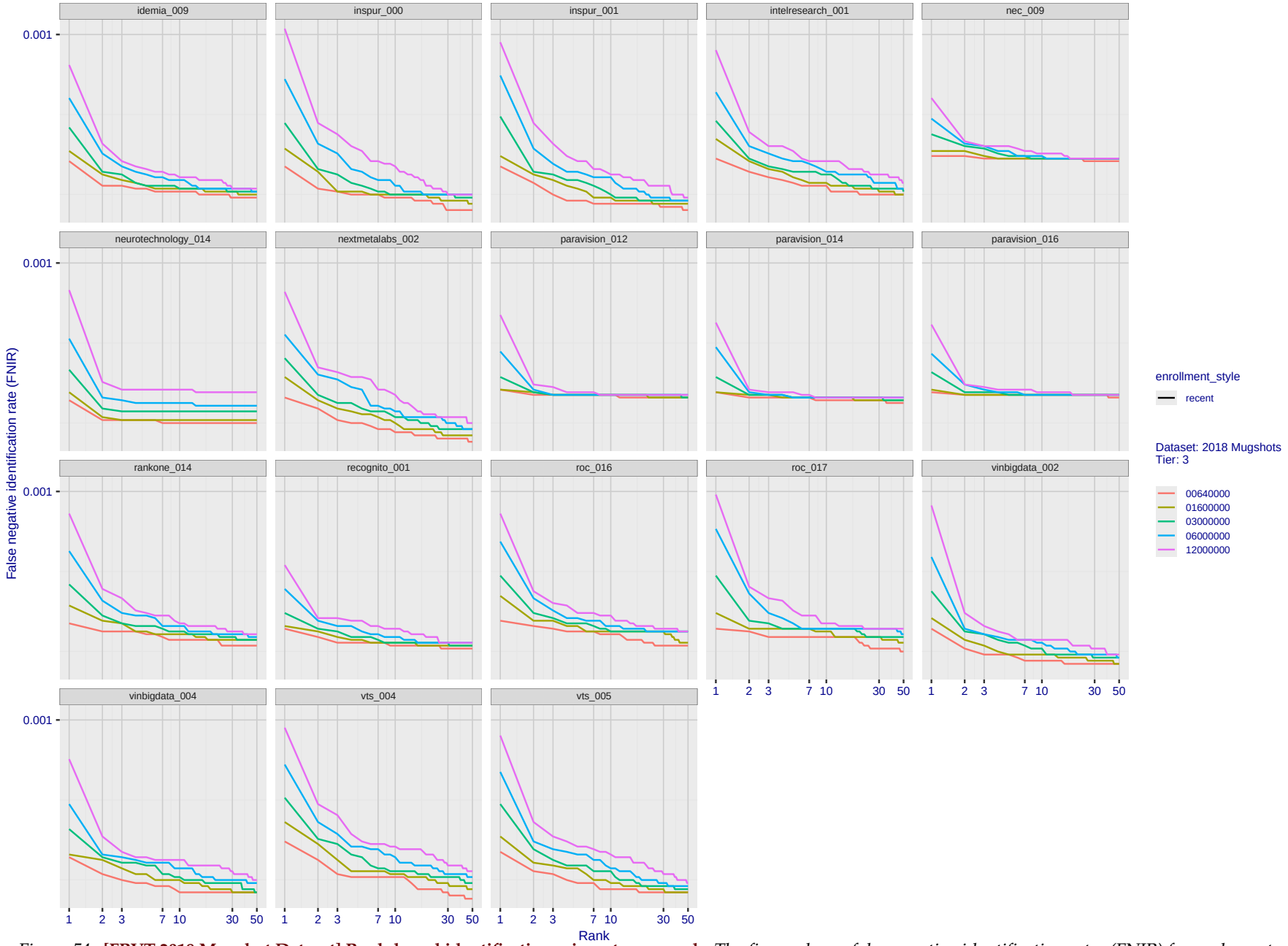

Figure 54: **[FRVT-2018 Mugshot Dataset] Rank-based identification miss rates vs. rank**. *The figure shows false negative identification rates (FNIR) for ranks up to 50. This metric is appropriate to investigational applications where human reviewers will adjudicate sorted candidate lists. Note that with threshold set to zero, FPIR = 1, i.e. any search without an enrolled mate will return non-mated candidates. Results are sorted and reported into tiers for clarity, with the tiering criteria being rank 1 hit rate on a gallery size of N = 640 000 subjects.*

2026/01/09 20:40:38

FNIR(N, R, T) = False neg. identification rate
FPIR(N, T) = False pos. identification rate

N = Num. enrolled subjects
R = Num. candidates examined

T = Threshold

T = 0 → Investigation
T > 0 → Identification

This publication is available free of charge from: https://doi.org/10.6028/NIST.IR.8271

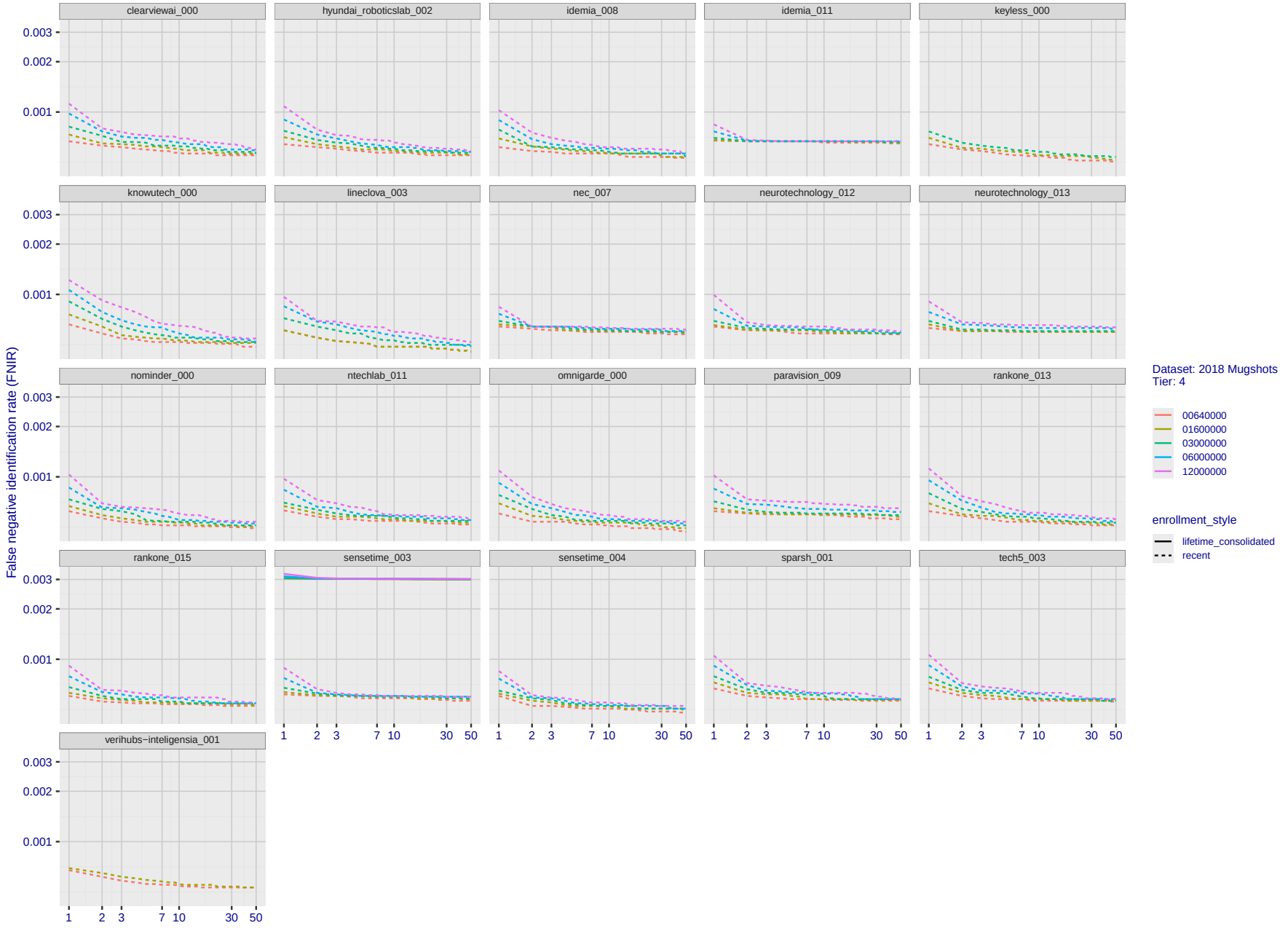

Figure 55: **[FRVT-2018 Mugshot Dataset] Rank-based identification miss rates vs. rank**. *The figure shows false negative identification rates (FNIR) for ranks up to 50. This metric is appropriate to investigational applications where human reviewers will adjudicate sorted candidate lists. Note that with threshold set to zero, FPIR = 1, i.e. any search without an enrolled mate will return non-mated candidates. Results are sorted and reported into tiers for clarity, with the tiering criteria being rank 1 hit rate on a gallery size of N = 640 000 subjects.*

2026/01/09 20:40:38
FNIR(N, R, T) = False neg. identification rate
FPIR(N, T) = False pos. identification rate
N = Num. enrolled subjects
R = Num. candidates examined
T = Threshold
T = 0 → Investigation
T > 0 → Identification

This publication is available free of charge from: https://doi.org/10.6028/NIST.IR.8271

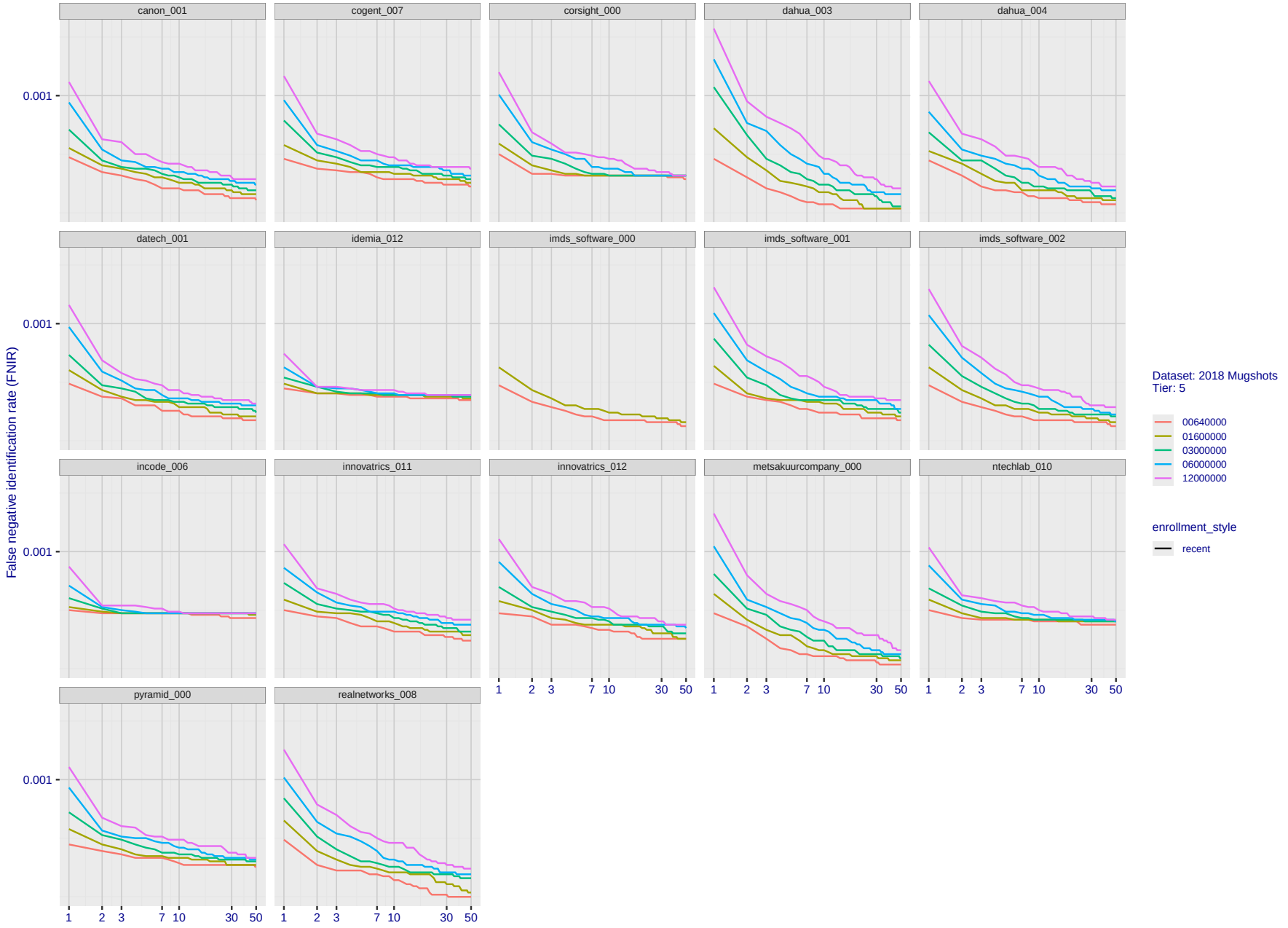

Figure 56: **[FRVT-2018 Mugshot Dataset] Rank-based identification miss rates vs. rank**. *The figure shows false negative identification rates (FNIR) for ranks up to 50. This metric is appropriate to investigational applications where human reviewers will adjudicate sorted candidate lists. Note that with threshold set to zero, FPIR = 1, i.e. any search without an enrolled mate will return non-mated candidates. Results are sorted and reported into tiers for clarity, with the tiering criteria being rank 1 hit rate on a gallery size of N = 640 000 subjects.*

2026/01/09 20:40:38
FNIR(N, R, T) = False neg. identification rate
FPIR(N, T) = False pos. identification rate
N = Num. enrolled subjects
R = Num. candidates examined
T = Threshold
T = 0 → Investigation
T > 0 → Identification

This publication is available free of charge from: https://doi.org/10.6028/NIST.IR.8271

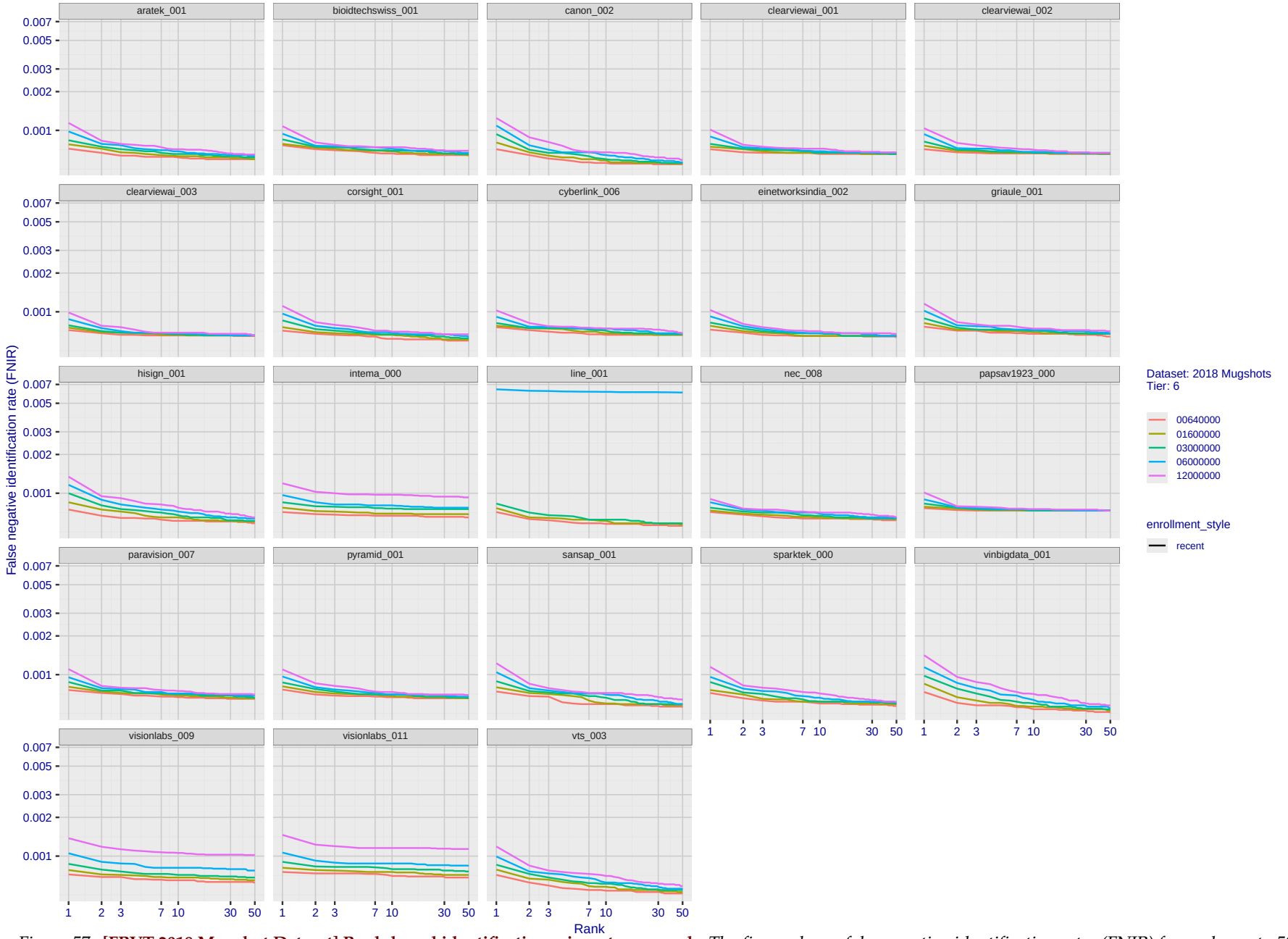

Figure 57: **[FRVT-2018 Mugshot Dataset] Rank-based identification miss rates vs. rank**. *The figure shows false negative identification rates (FNIR) for ranks up to 50. This metric is appropriate to investigational applications where human reviewers will adjudicate sorted candidate lists. Note that with threshold set to zero, FPIR = 1, i.e. any search without an enrolled mate will return non-mated candidates. Results are sorted and reported into tiers for clarity, with the tiering criteria being rank 1 hit rate on a gallery size of N = 640 000 subjects.*

2026/01/09 20:40:38

FNIR(N, R, T) = False neg. identification rate
FPIR(N, T) = False pos. identification rate

N = Num. enrolled subjects
R = Num. candidates examined

T = Threshold

T = 0 → Investigation
T > 0 → Identification

This publication is available free of charge from: https://doi.org/10.6028/NIST.IR.8271

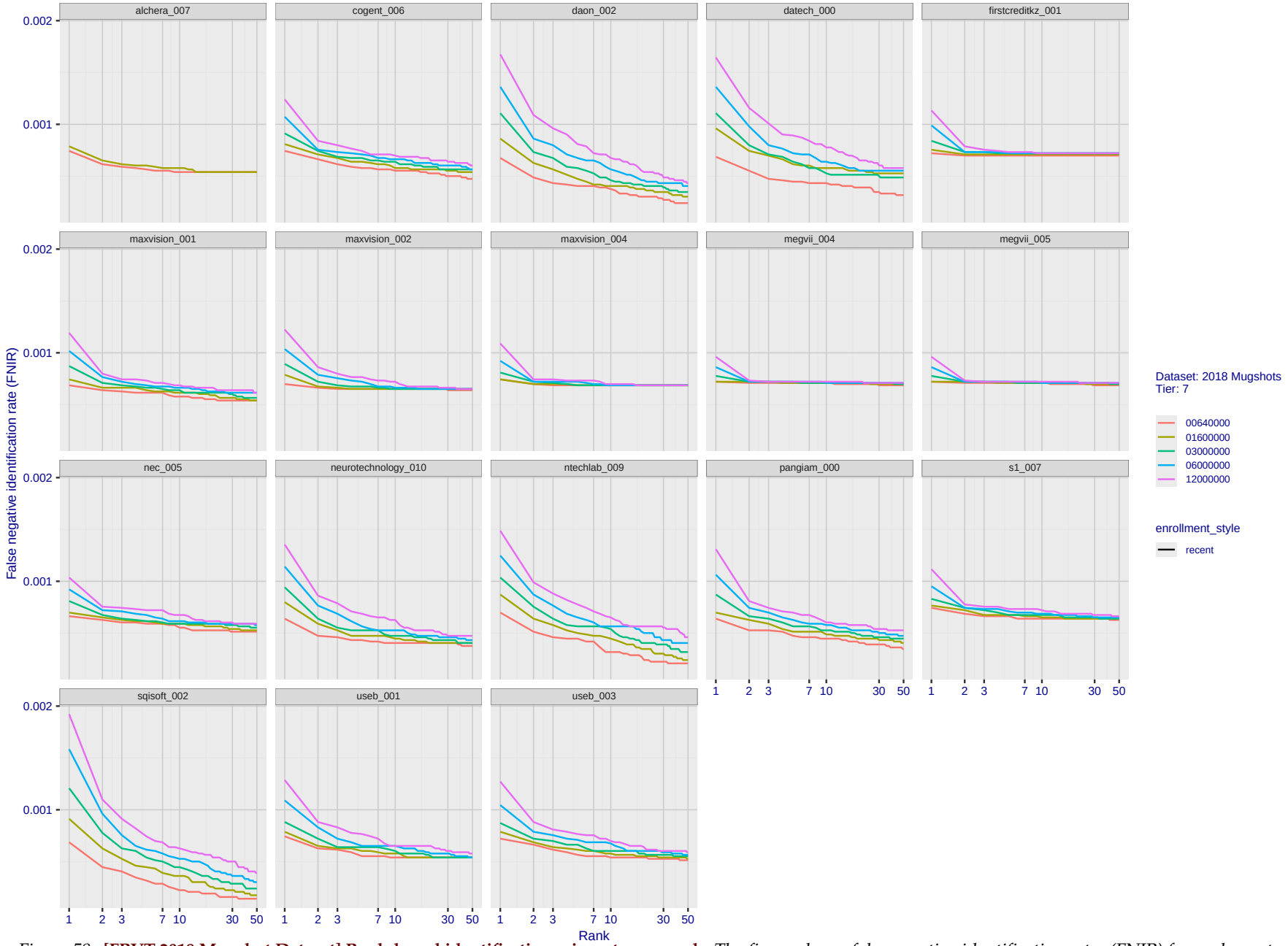

Figure 58: **[FRVT-2018 Mugshot Dataset] Rank-based identification miss rates vs. rank**. *The figure shows false negative identification rates (FNIR) for ranks up to 50. This metric is appropriate to investigational applications where human reviewers will adjudicate sorted candidate lists. Note that with threshold set to zero, FPIR = 1, i.e. any search without an enrolled mate will return non-mated candidates. Results are sorted and reported into tiers for clarity, with the tiering criteria being rank 1 hit rate on a gallery size of N = 640 000 subjects.*

2026/01/09 20:40:38

FNIR(N, R, T) = False neg. identification rate
FPIR(N, T) = False pos. identification rate

N = Num. enrolled subjects
R = Num. candidates examined

T = Threshold

T = 0 → Investigation
T > 0 → Identification

This publication is available free of charge from: https://doi.org/10.6028/NIST.IR.8271

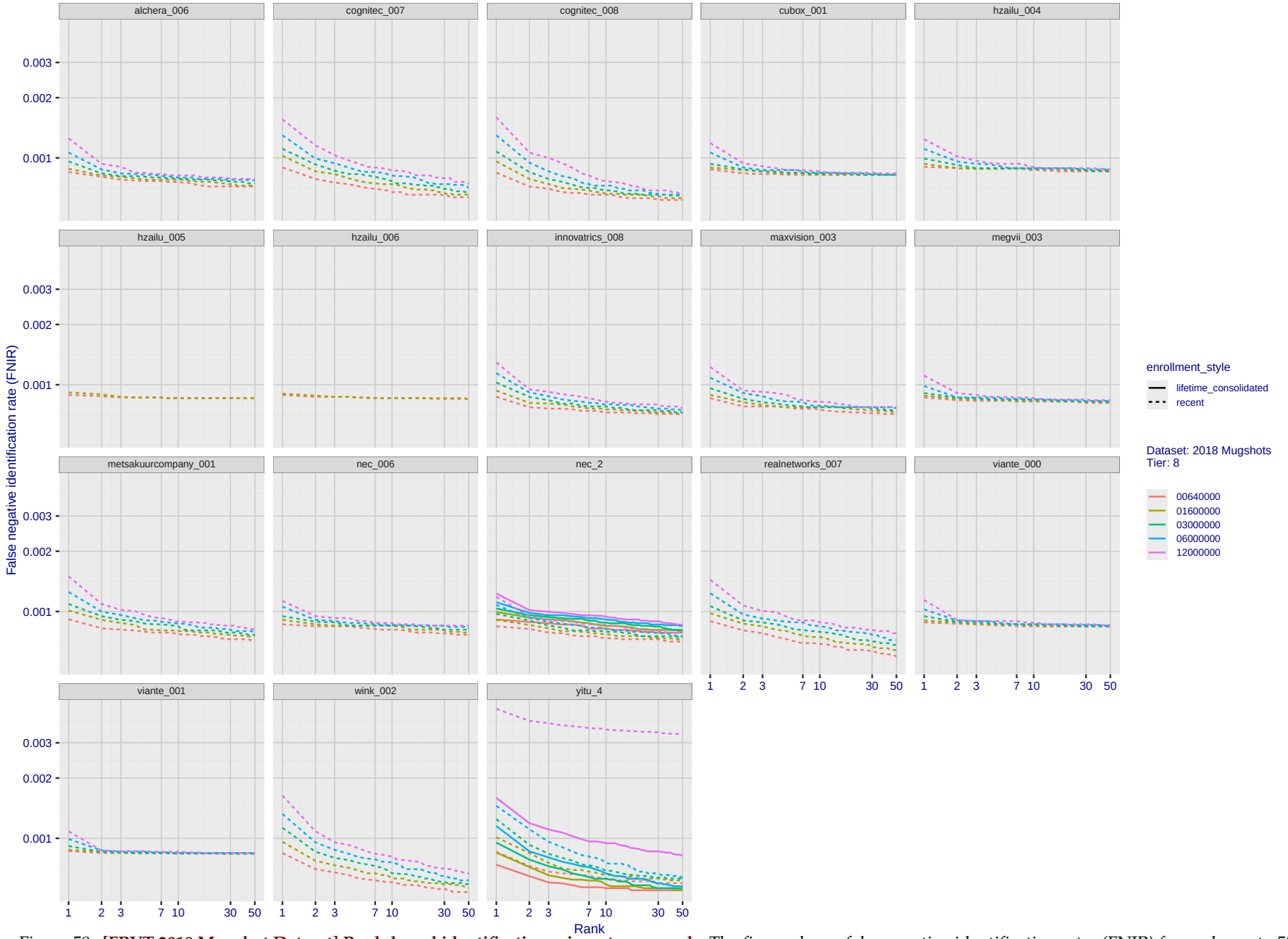

Figure 59: **[FRVT-2018 Mugshot Dataset] Rank-based identification miss rates vs. rank**. *The figure shows false negative identification rates (FNIR) for ranks up to 50. This metric is appropriate to investigational applications where human reviewers will adjudicate sorted candidate lists. Note that with threshold set to zero, FPIR = 1, i.e. any search without an enrolled mate will return non-mated candidates. Results are sorted and reported into tiers for clarity, with the tiering criteria being rank 1 hit rate on a gallery size of N = 640 000 subjects.*

2026/01/09 20:40:38

FNIR(N, R, T) = False neg. identification rate
FPIR(N, T) = False pos. identification rate

N = Num. enrolled subjects
R = Num. candidates examined

T = Threshold

T = 0 → Investigation
T > 0 → Identification

This publication is available free of charge from: https://doi.org/10.6028/NIST.IR.8271

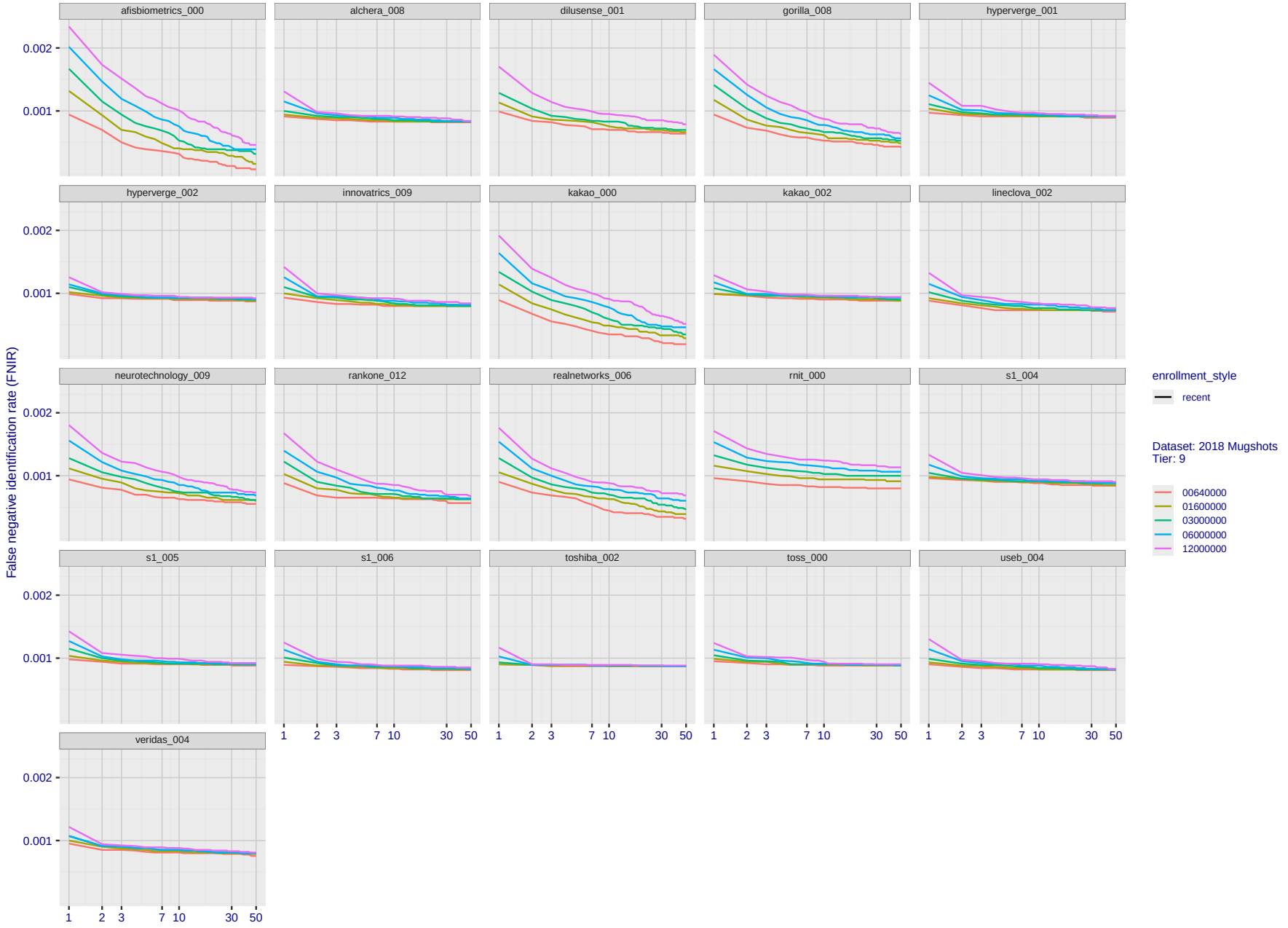

Figure 60: **[FRVT-2018 Mugshot Dataset] Rank-based identification miss rates vs. rank**. *The figure shows false negative identification rates (FNIR) for ranks up to 50. This metric is appropriate to investigational applications where human reviewers will adjudicate sorted candidate lists. Note that with threshold set to zero, FPIR = 1, i.e. any search without an enrolled mate will return non-mated candidates. Results are sorted and reported into tiers for clarity, with the tiering criteria being rank 1 hit rate on a gallery size of N = 640 000 subjects.*

2026/01/09 20:40:38
FNIR(N, R, T) = False neg. identification rate
FPIR(N, T) = False pos. identification rate
N = Num. enrolled subjects
R = Num. candidates examined
T = Threshold
T = 0 → Investigation
T > 0 → Identification

This publication is available free of charge from: https://doi.org/10.6028/NIST.IR.8271

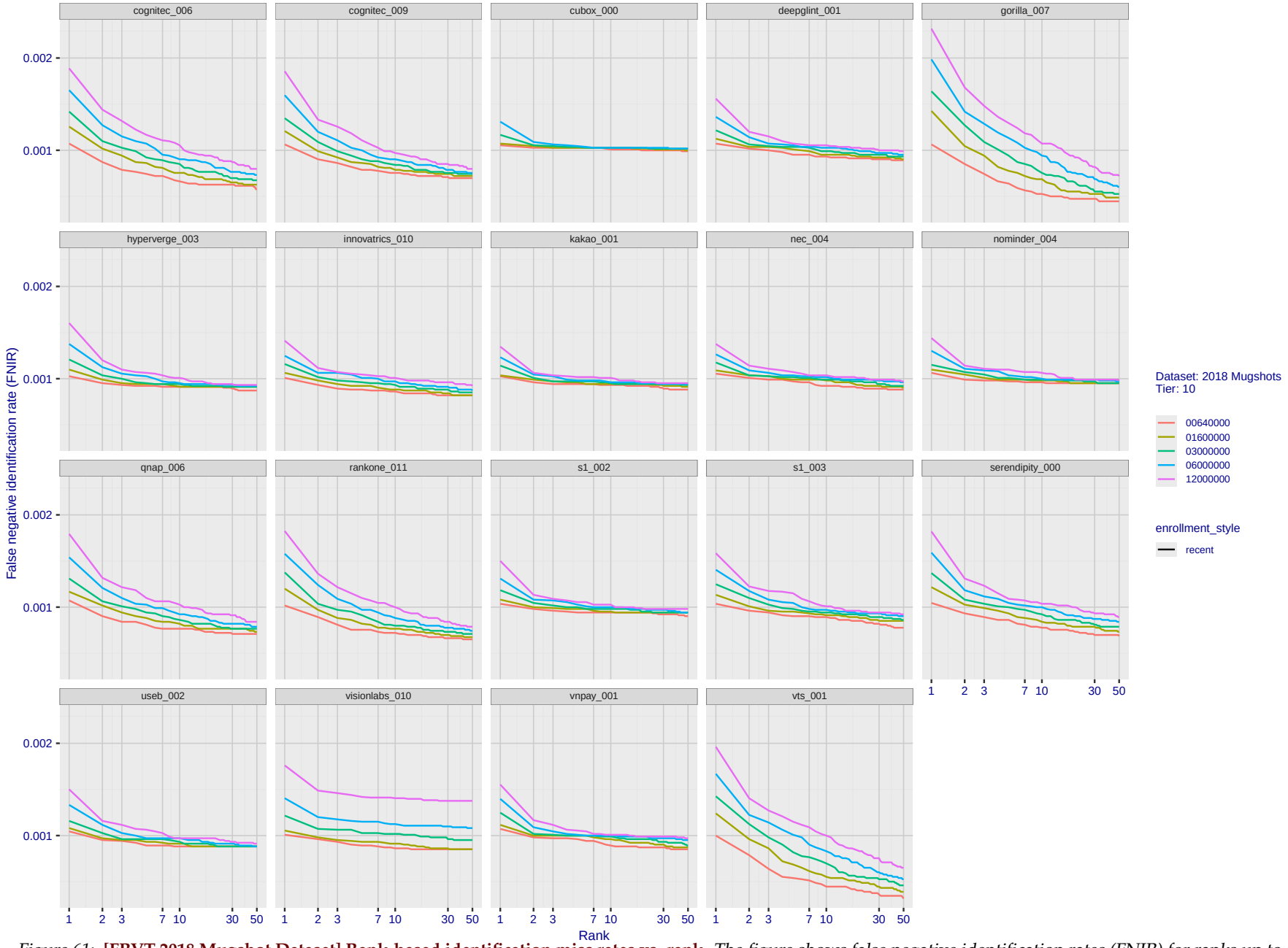

Figure 61: **[FRVT-2018 Mugshot Dataset] Rank-based identification miss rates vs. rank**. *The figure shows false negative identification rates (FNIR) for ranks up to 50. This metric is appropriate to investigational applications where human reviewers will adjudicate sorted candidate lists. Note that with threshold set to zero, FPIR = 1, i.e. any search without an enrolled mate will return non-mated candidates. Results are sorted and reported into tiers for clarity, with the tiering criteria being rank 1 hit rate on a gallery size of N = 640 000 subjects.*

2026/01/09 20:40:38
FNIR(N, R, T) = False neg. identification rate
FPIR(N, T) = False pos. identification rate
N = Num. enrolled subjects
R = Num. candidates examined
T = Threshold
T = 0 → Investigation
T > 0 → Identification

This publication is available free of charge from: https://doi.org/10.6028/NIST.IR.8271

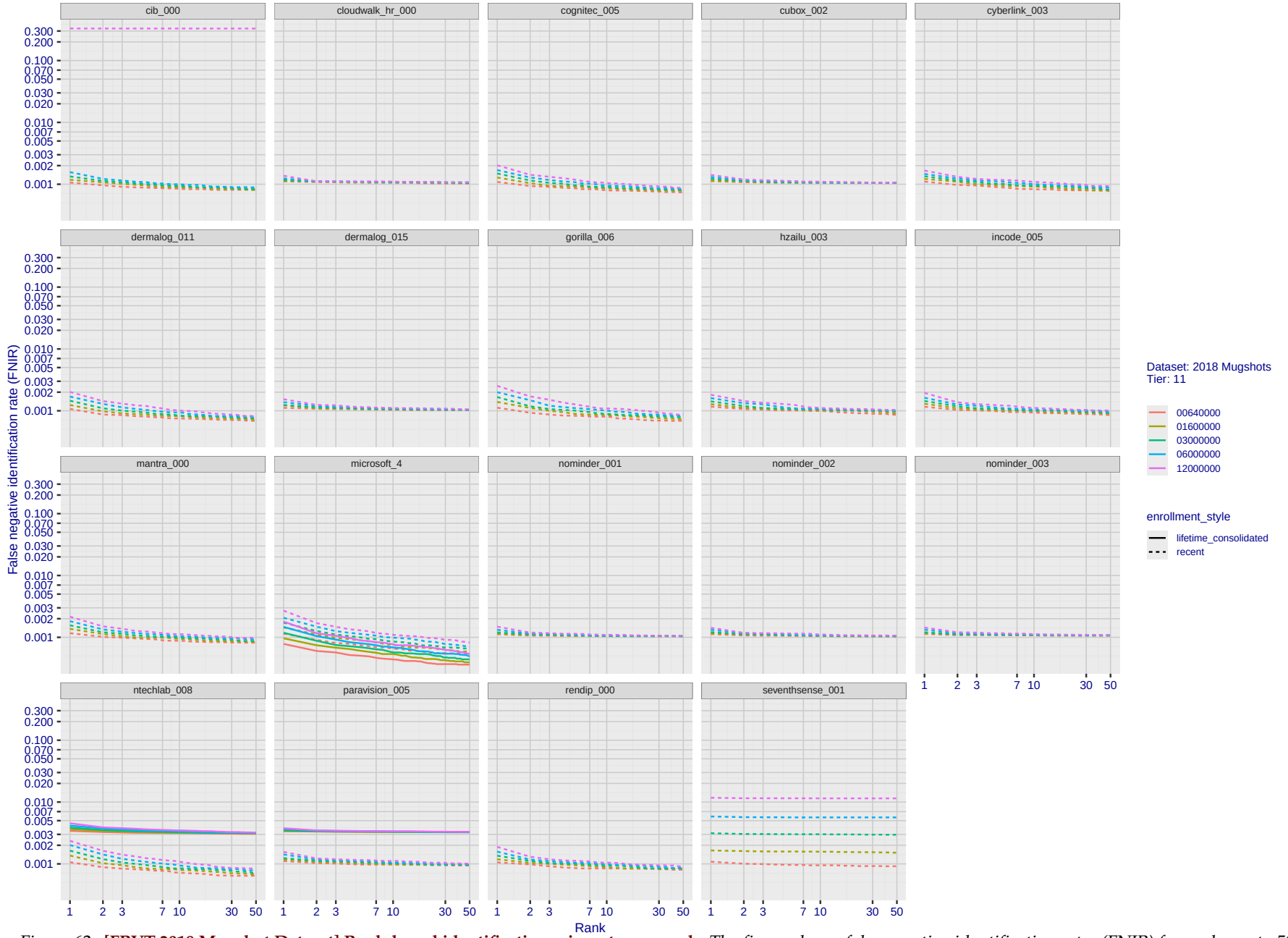

Figure 62: **[FRVT-2018 Mugshot Dataset] Rank-based identification miss rates vs. rank**. *The figure shows false negative identification rates (FNIR) for ranks up to 50. This metric is appropriate to investigational applications where human reviewers will adjudicate sorted candidate lists. Note that with threshold set to zero, FPIR = 1, i.e. any search without an enrolled mate will return non-mated candidates. Results are sorted and reported into tiers for clarity, with the tiering criteria being rank 1 hit rate on a gallery size of N = 640 000 subjects.*

2026/01/09 20:40:38
FNIR(N, R, T) = False neg. identification rate
FPIR(N, T) = False pos. identification rate
N = Num. enrolled subjects
R = Num. candidates examined
T = Threshold
T = 0 → Investigation
T > 0 → Identification

This publication is available free of charge from: https://doi.org/10.6028/NIST.IR.8271

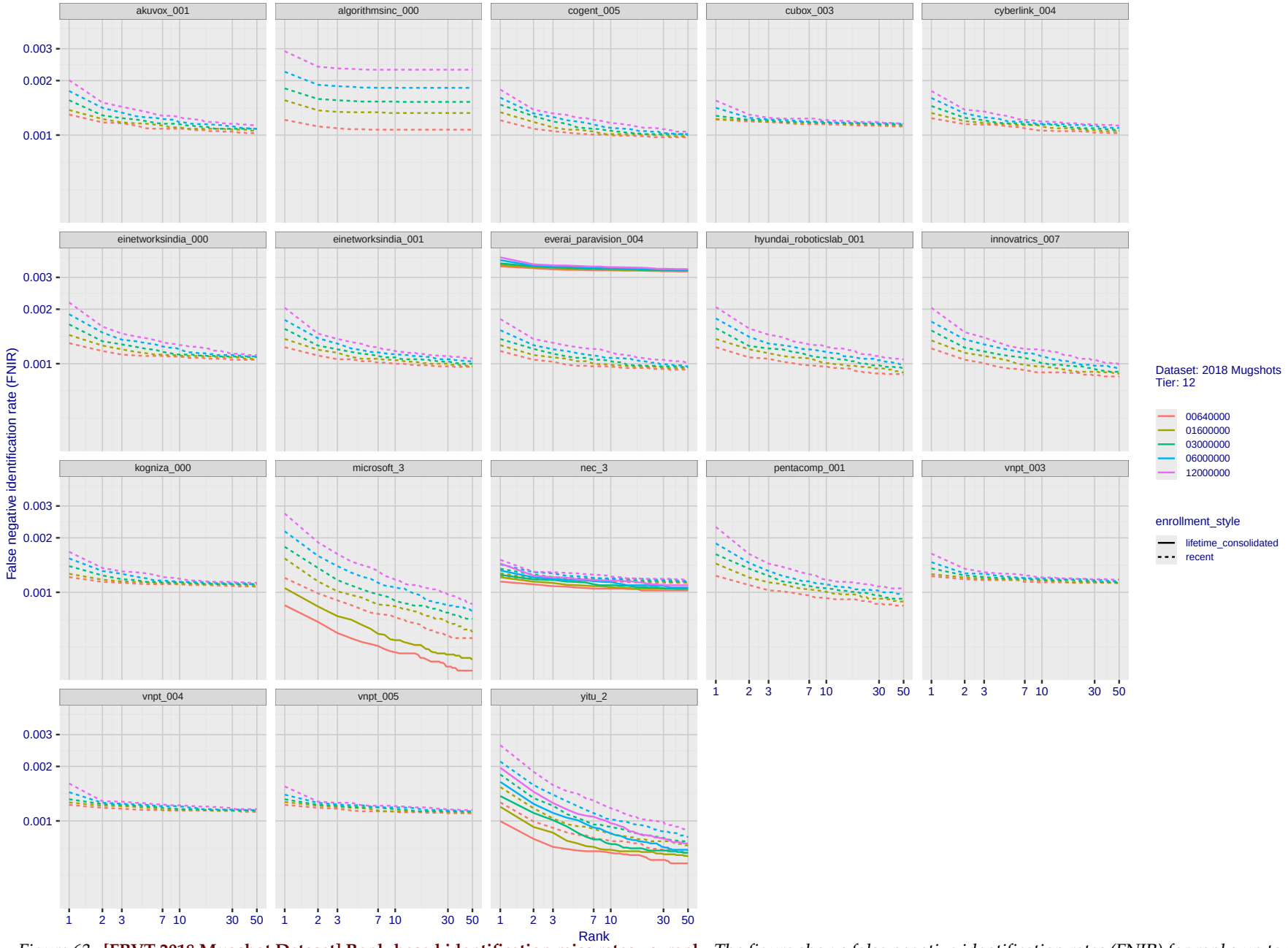

Figure 63: **[FRVT-2018 Mugshot Dataset] Rank-based identification miss rates vs. rank**. *The figure shows false negative identification rates (FNIR) for ranks up to 50. This metric is appropriate to investigational applications where human reviewers will adjudicate sorted candidate lists. Note that with threshold set to zero, FPIR = 1, i.e. any search without an enrolled mate will return non-mated candidates. Results are sorted and reported into tiers for clarity, with the tiering criteria being rank 1 hit rate on a gallery size of N = 640 000 subjects.*

2026/01/09 20:40:38
FNIR(N, R, T) = False neg. identification rate
FPIR(N, T) = False pos. identification rate
N = Num. enrolled subjects
R = Num. candidates examined
T = Threshold
T = 0 → Investigation
T > 0 → Identification

This publication is available free of charge from: https://doi.org/10.6028/NIST.IR.8271

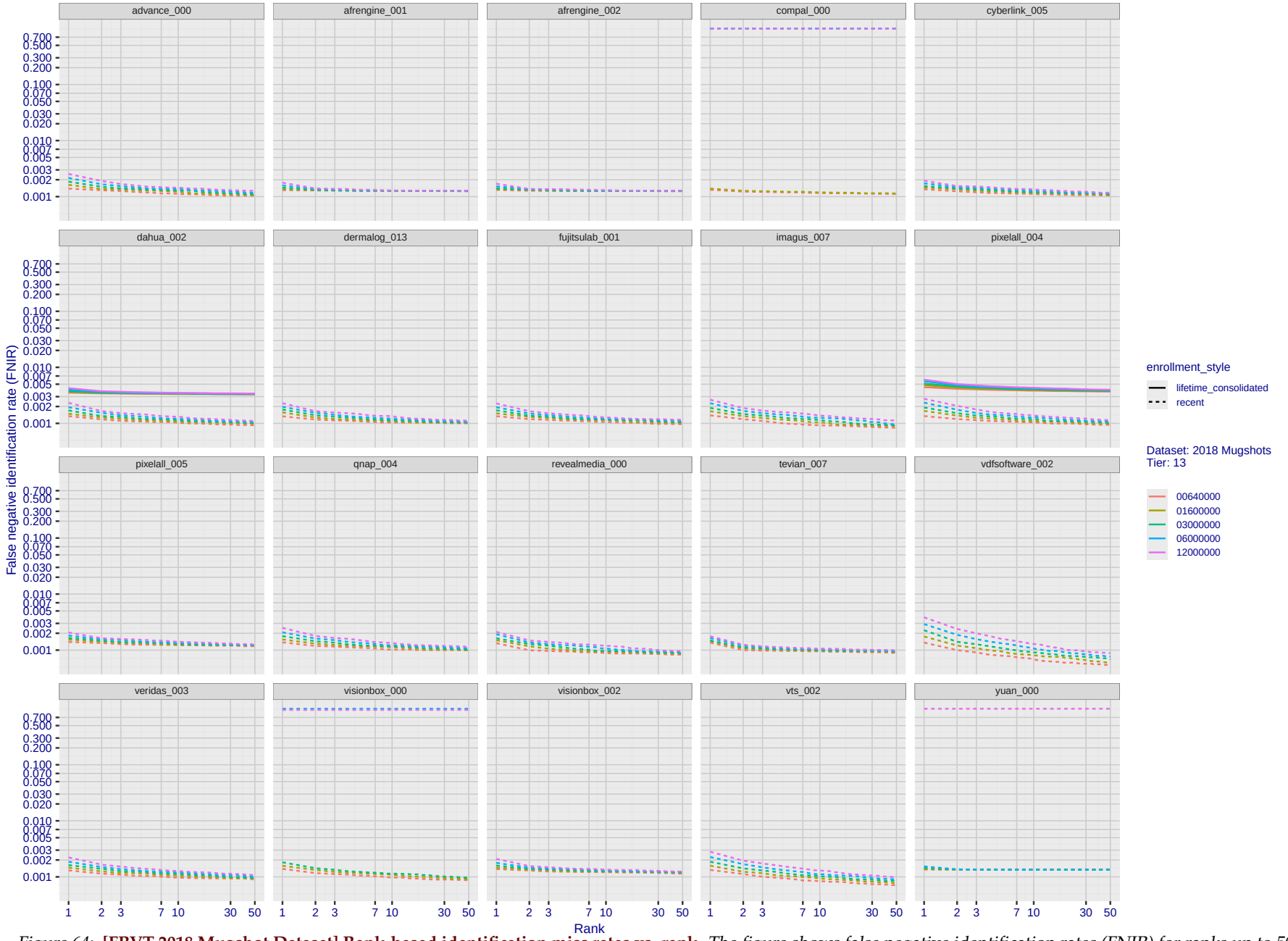

Figure 64: **[FRVT-2018 Mugshot Dataset] Rank-based identification miss rates vs. rank**. *The figure shows false negative identification rates (FNIR) for ranks up to 50. This metric is appropriate to investigational applications where human reviewers will adjudicate sorted candidate lists. Note that with threshold set to zero, FPIR = 1, i.e. any search without an enrolled mate will return non-mated candidates. Results are sorted and reported into tiers for clarity, with the tiering criteria being rank 1 hit rate on a gallery size of N = 640 000 subjects.*

FNIR(N, R, T) = False neg. identification rate
FPIR(N, T) = False pos. identification rate
N = Num. enrolled subjects
R = Num. candidates examined
T = Threshold
T = 0 → Investigation
T > 0 → Identification

This publication is available free of charge from: https://doi.org/10.6028/NIST.IR.8271

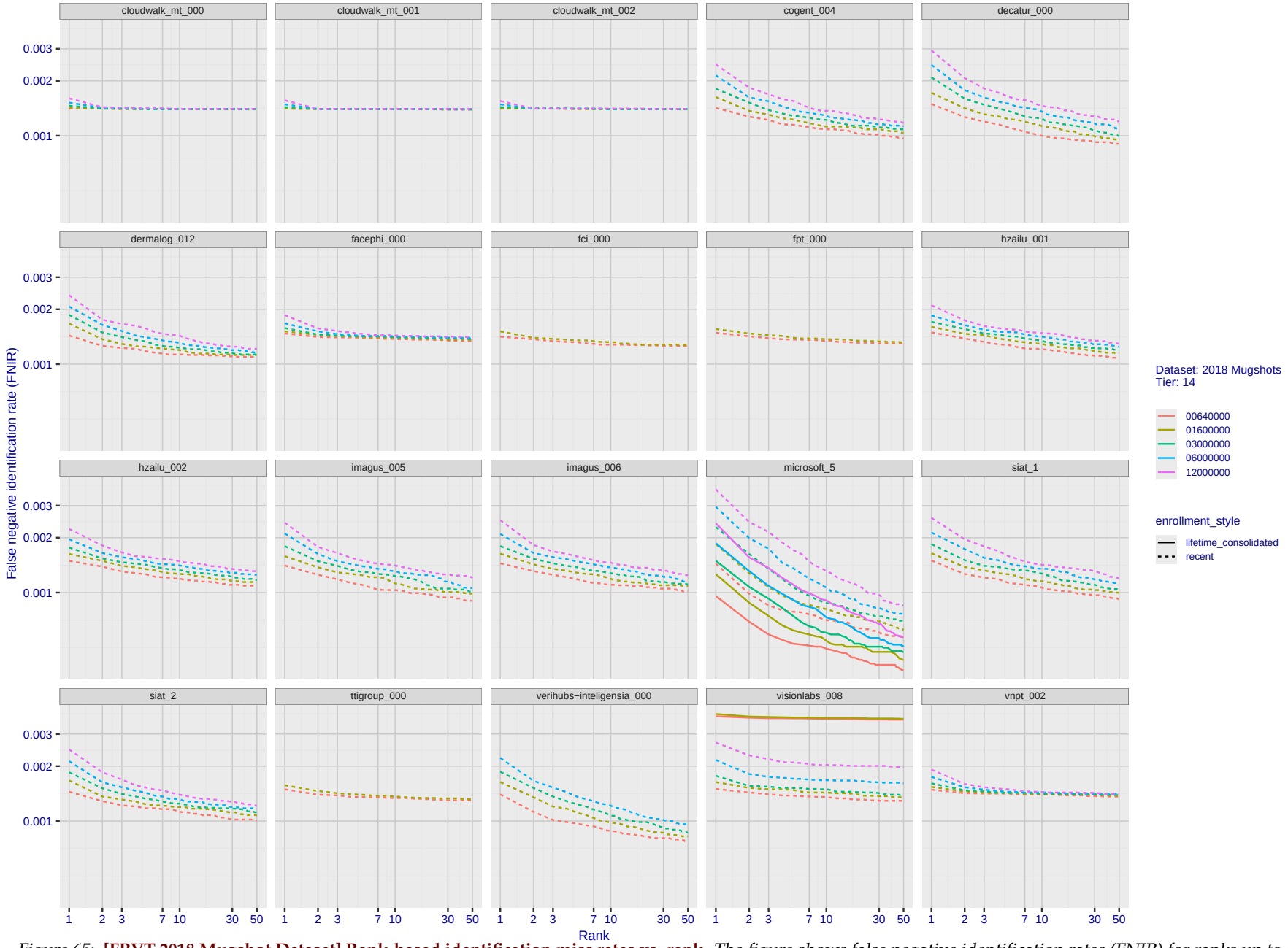

Figure 65: **[FRVT-2018 Mugshot Dataset] Rank-based identification miss rates vs. rank**. *The figure shows false negative identification rates (FNIR) for ranks up to 50. This metric is appropriate to investigational applications where human reviewers will adjudicate sorted candidate lists. Note that with threshold set to zero, FPIR = 1, i.e. any search without an enrolled mate will return non-mated candidates. Results are sorted and reported into tiers for clarity, with the tiering criteria being rank 1 hit rate on a gallery size of N = 640 000 subjects.*

This publication is available free of charge from: https://doi.org/10.6028/NIST.IR.8271

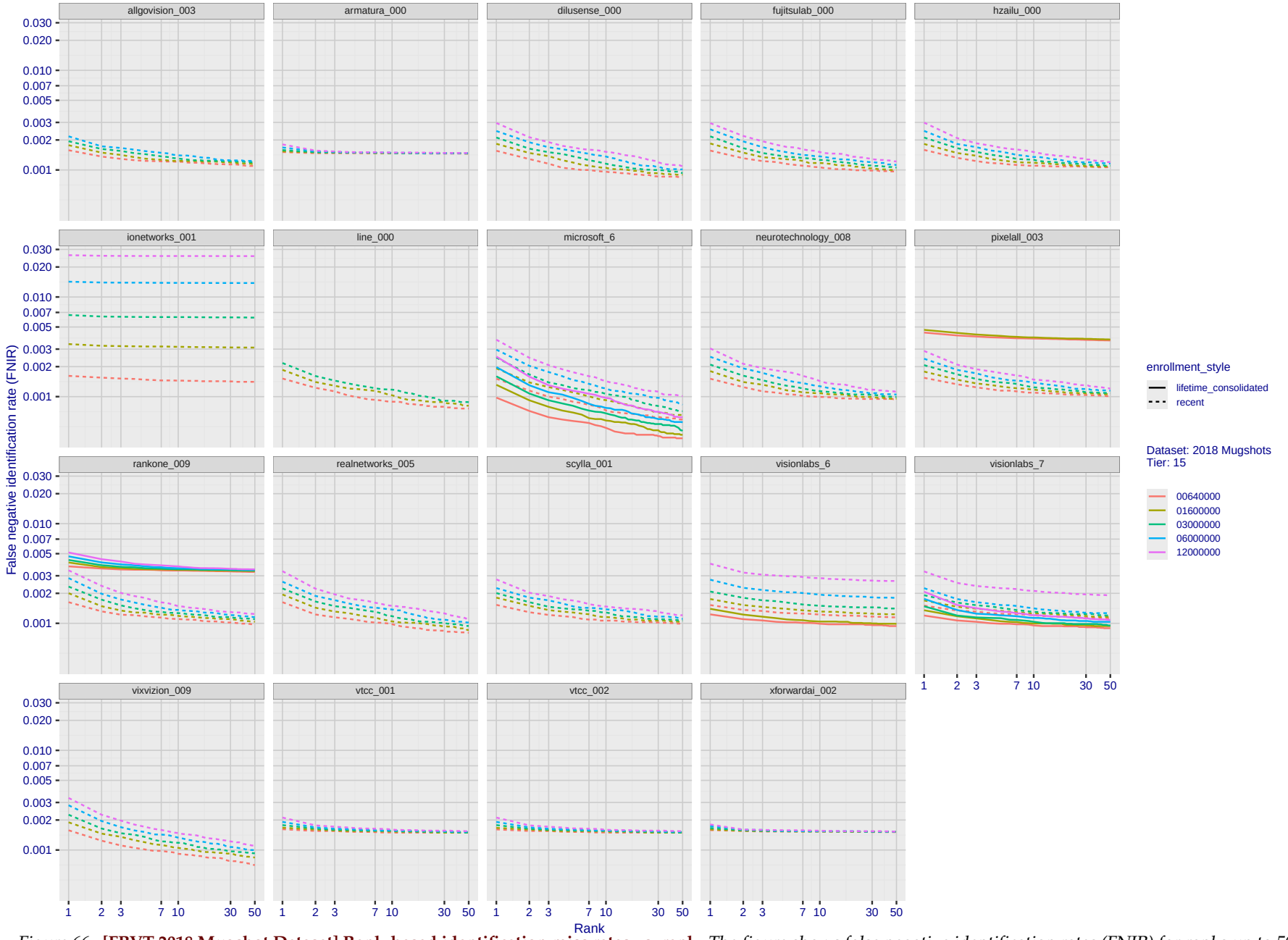

Figure 66: **[FRVT-2018 Mugshot Dataset] Rank-based identification miss rates vs. rank**. *The figure shows false negative identification rates (FNIR) for ranks up to 50. This metric is appropriate to investigational applications where human reviewers will adjudicate sorted candidate lists. Note that with threshold set to zero, FPIR = 1, i.e. any search without an enrolled mate will return non-mated candidates. Results are sorted and reported into tiers for clarity, with the tiering criteria being rank 1 hit rate on a gallery size of N = 640 000 subjects.*

This publication is available free of charge from: https://doi.org/10.6028/NIST.IR.8271

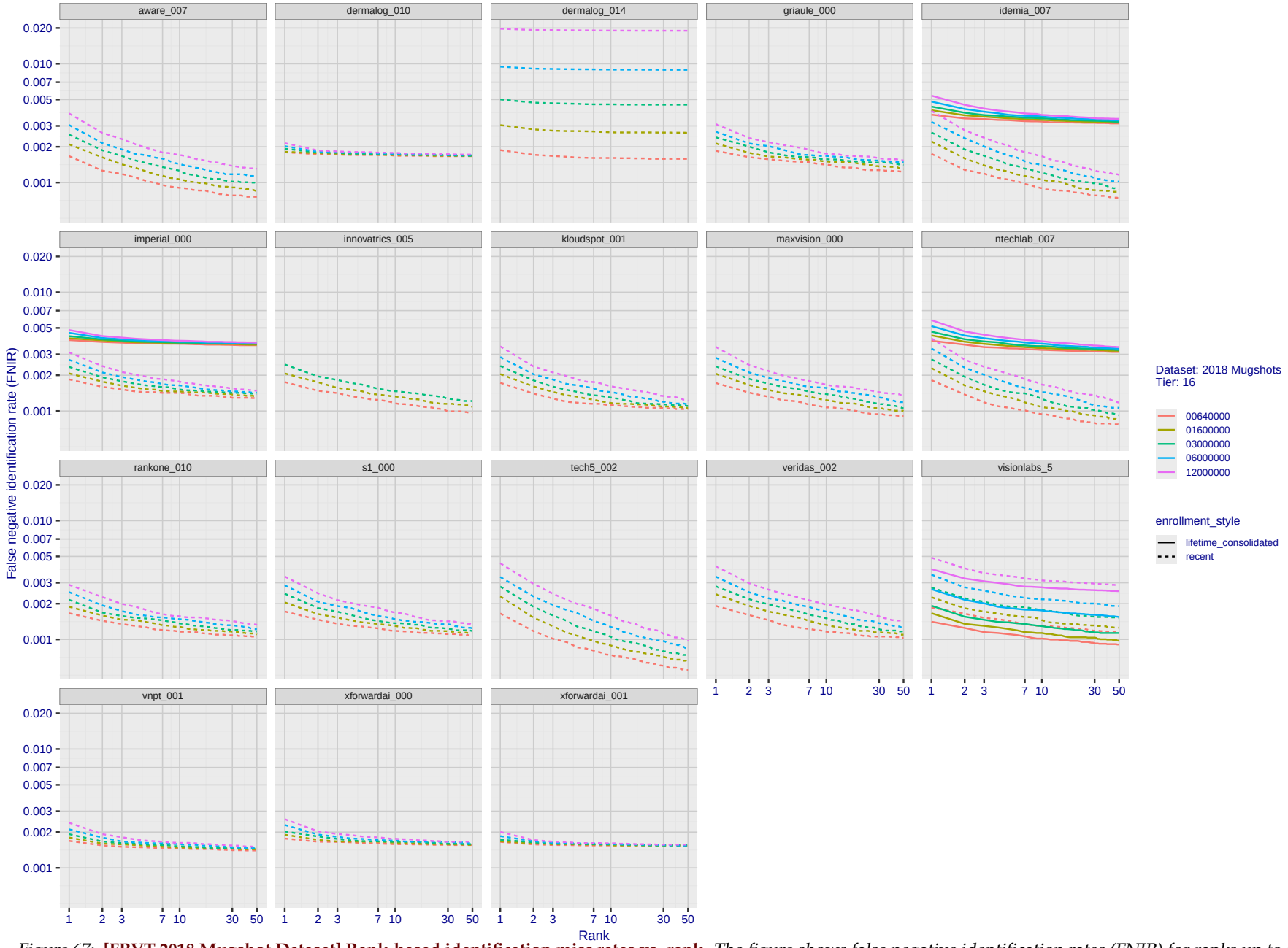

Figure 67: **[FRVT-2018 Mugshot Dataset] Rank-based identification miss rates vs. rank**. *The figure shows false negative identification rates (FNIR) for ranks up to 50. This metric is appropriate to investigational applications where human reviewers will adjudicate sorted candidate lists. Note that with threshold set to zero, FPIR = 1, i.e. any search without an enrolled mate will return non-mated candidates. Results are sorted and reported into tiers for clarity, with the tiering criteria being rank 1 hit rate on a gallery size of N = 640 000 subjects.*

2026/01/09 20:40:38
FNIR(N, R, T) = False neg. identification rate
FPIR(N, T) = False pos. identification rate
N = Num. enrolled subjects
R = Num. candidates examined
T = Threshold
T = 0 → Investigation
T > 0 → Identification

This publication is available free of charge from: https://doi.org/10.6028/NIST.IR.8271

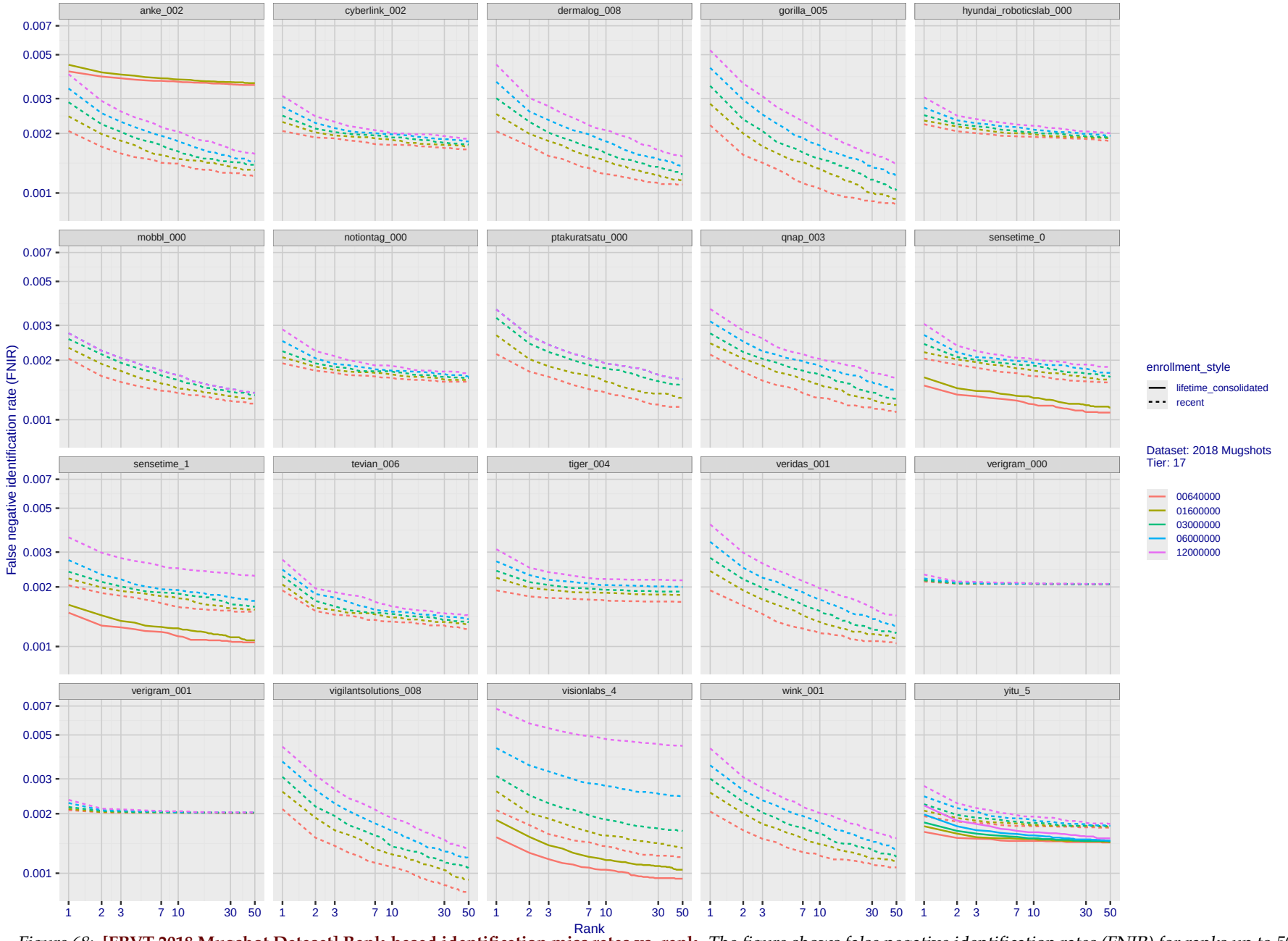

Figure 68: **[FRVT-2018 Mugshot Dataset] Rank-based identification miss rates vs. rank**. *The figure shows false negative identification rates (FNIR) for ranks up to 50. This metric is appropriate to investigational applications where human reviewers will adjudicate sorted candidate lists. Note that with threshold set to zero, FPIR = 1, i.e. any search without an enrolled mate will return non-mated candidates. Results are sorted and reported into tiers for clarity, with the tiering criteria being rank 1 hit rate on a gallery size of N = 640 000 subjects.*

This publication is available free of charge from: https://doi.org/10.6028/NIST.IR.8271

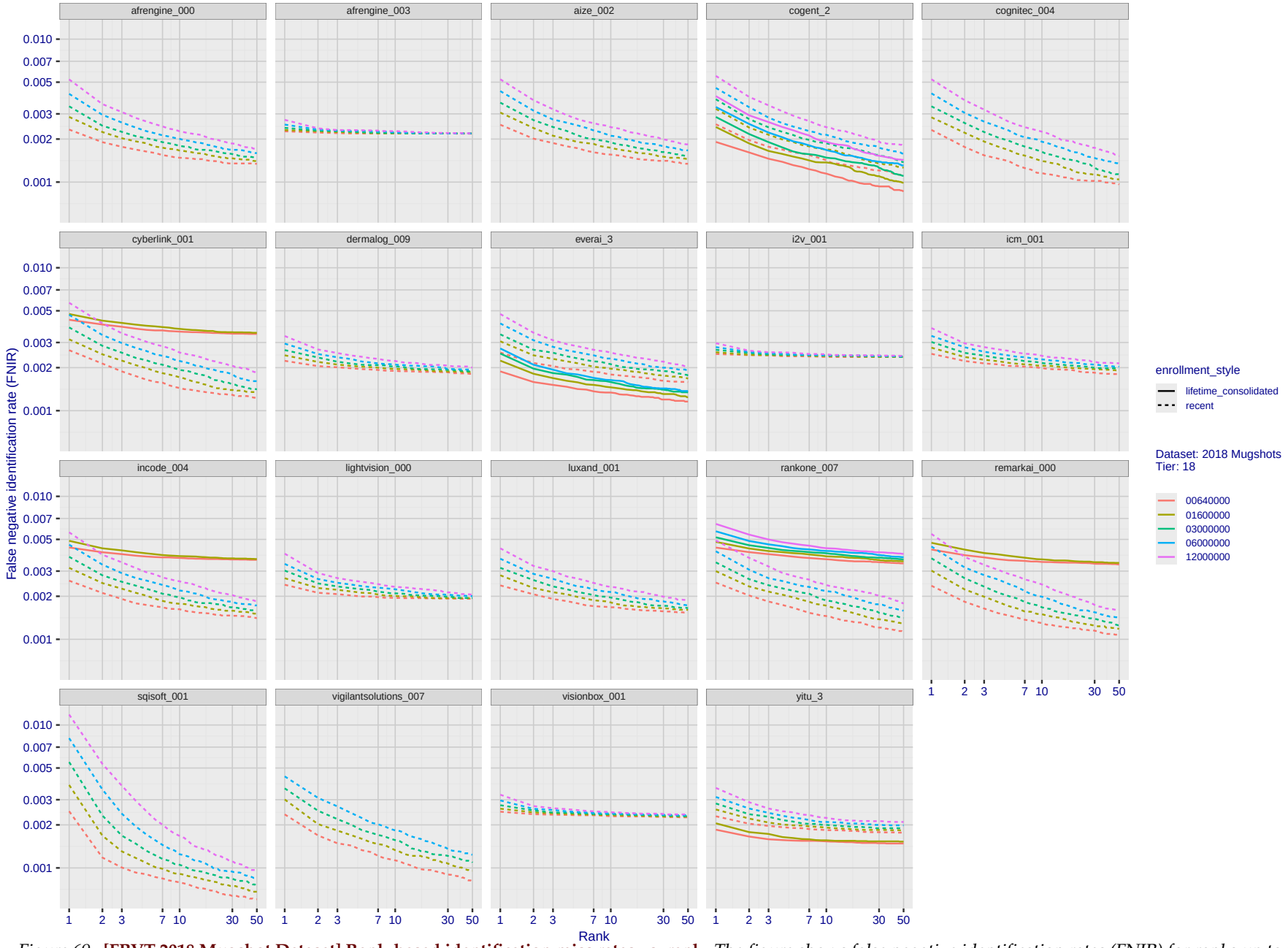

Figure 69: **[FRVT-2018 Mugshot Dataset] Rank-based identification miss rates vs. rank**. *The figure shows false negative identification rates (FNIR) for ranks up to 50. This metric is appropriate to investigational applications where human reviewers will adjudicate sorted candidate lists. Note that with threshold set to zero, FPIR = 1, i.e. any search without an enrolled mate will return non-mated candidates. Results are sorted and reported into tiers for clarity, with the tiering criteria being rank 1 hit rate on a gallery size of N = 640 000 subjects.*

This publication is available free of charge from: https://doi.org/10.6028/NIST.IR.8271

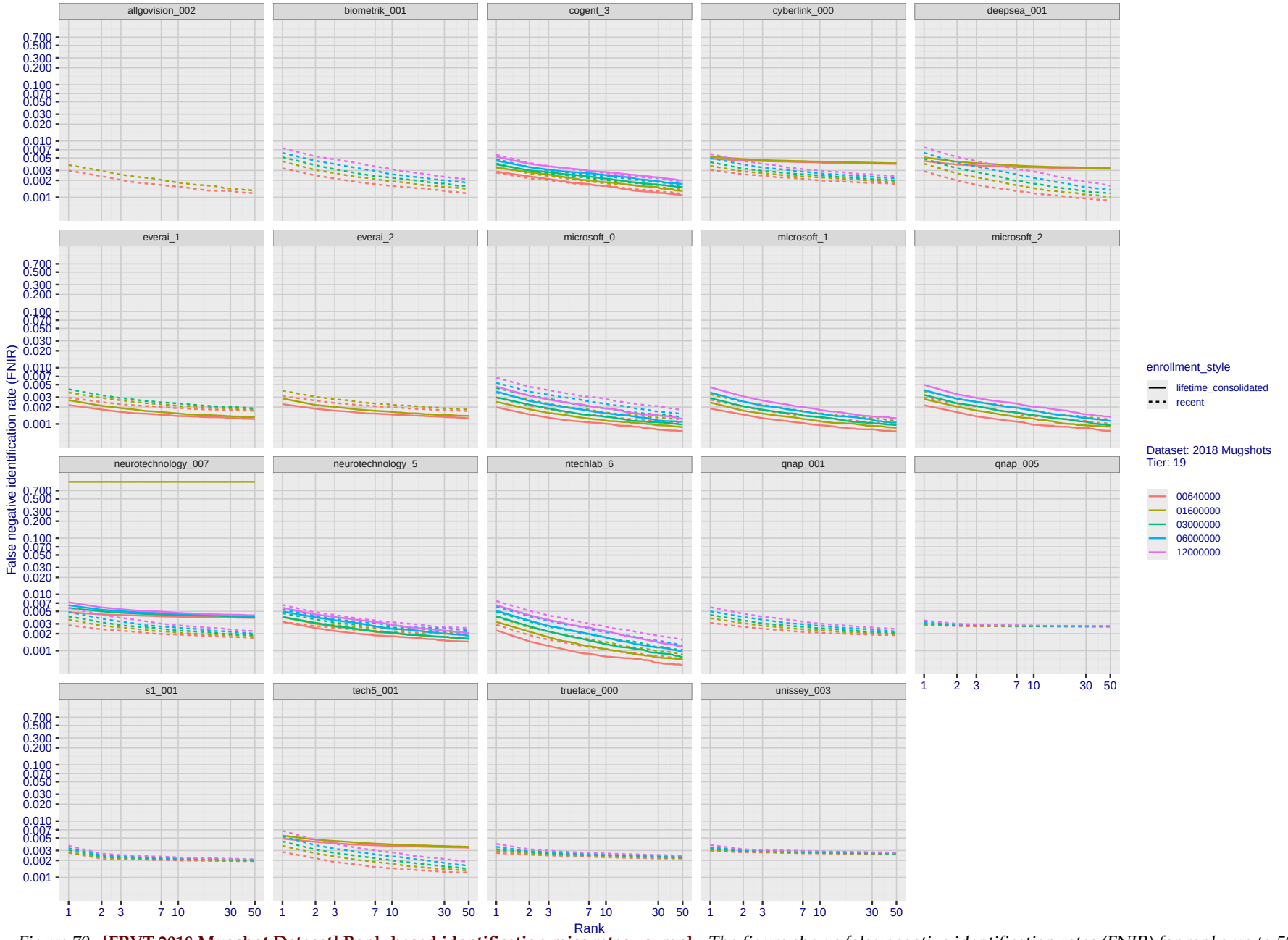

Figure 70: **[FRVT-2018 Mugshot Dataset] Rank-based identification miss rates vs. rank**. *The figure shows false negative identification rates (FNIR) for ranks up to 50. This metric is appropriate to investigational applications where human reviewers will adjudicate sorted candidate lists. Note that with threshold set to zero, FPIR = 1, i.e. any search without an enrolled mate will return non-mated candidates. Results are sorted and reported into tiers for clarity, with the tiering criteria being rank 1 hit rate on a gallery size of N = 640 000 subjects.*

2026/01/09 20:40:38
FNIR(N, R, T) = False neg. identification rate
FPIR(N, T) = False pos. identification rate
N = Num. enrolled subjects
R = Num. candidates examined
T = Threshold
T = 0 → Investigation
T > 0 → Identification

This publication is available free of charge from: https://doi.org/10.6028/NIST.IR.8271

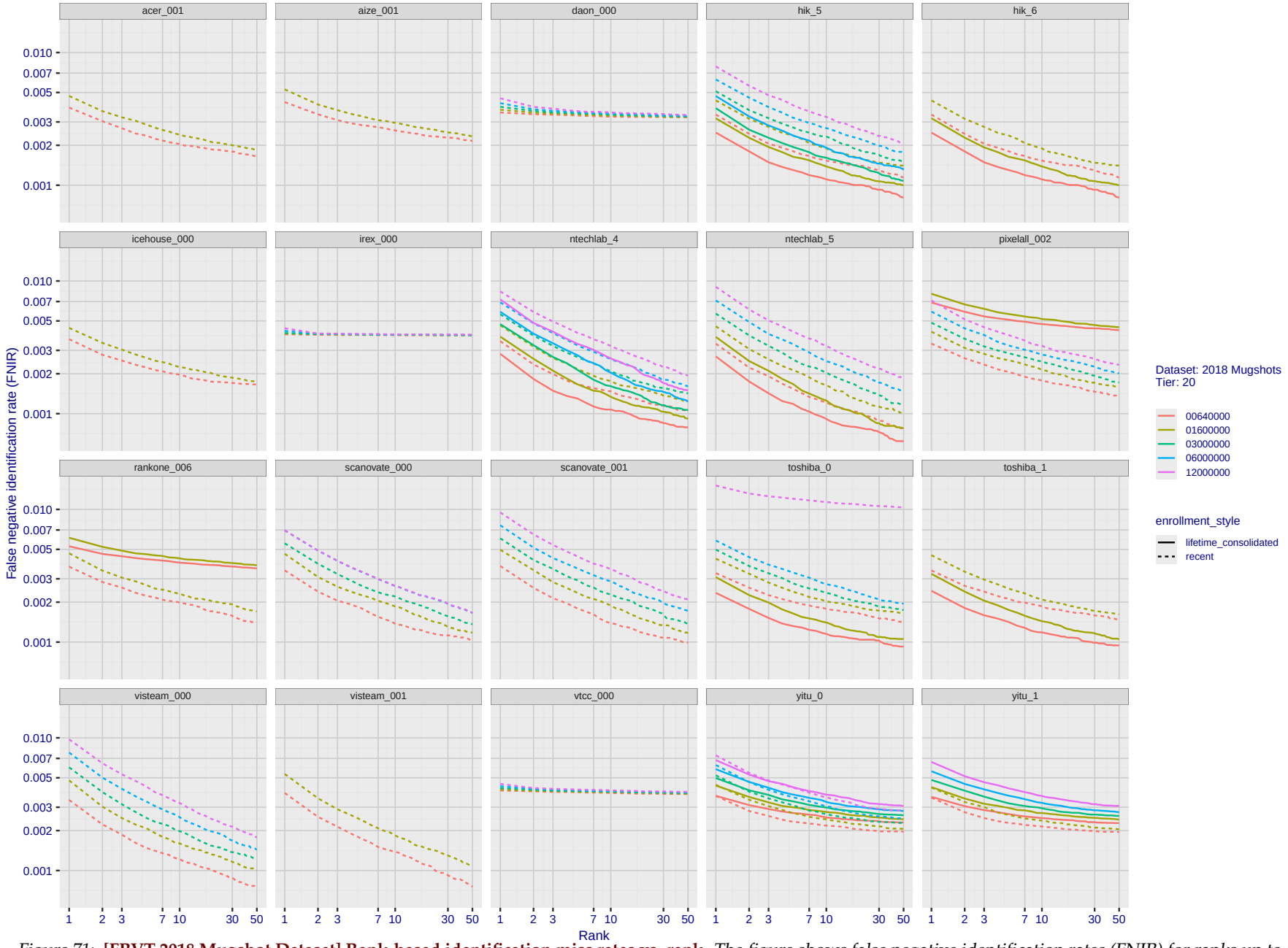

Figure 71: **[FRVT-2018 Mugshot Dataset] Rank-based identification miss rates vs. rank**. *The figure shows false negative identification rates (FNIR) for ranks up to 50. This metric is appropriate to investigational applications where human reviewers will adjudicate sorted candidate lists. Note that with threshold set to zero, FPIR = 1, i.e. any search without an enrolled mate will return non-mated candidates. Results are sorted and reported into tiers for clarity, with the tiering criteria being rank 1 hit rate on a gallery size of N = 640 000 subjects.*

This publication is available free of charge from: https://doi.org/10.6028/NIST.IR.8271

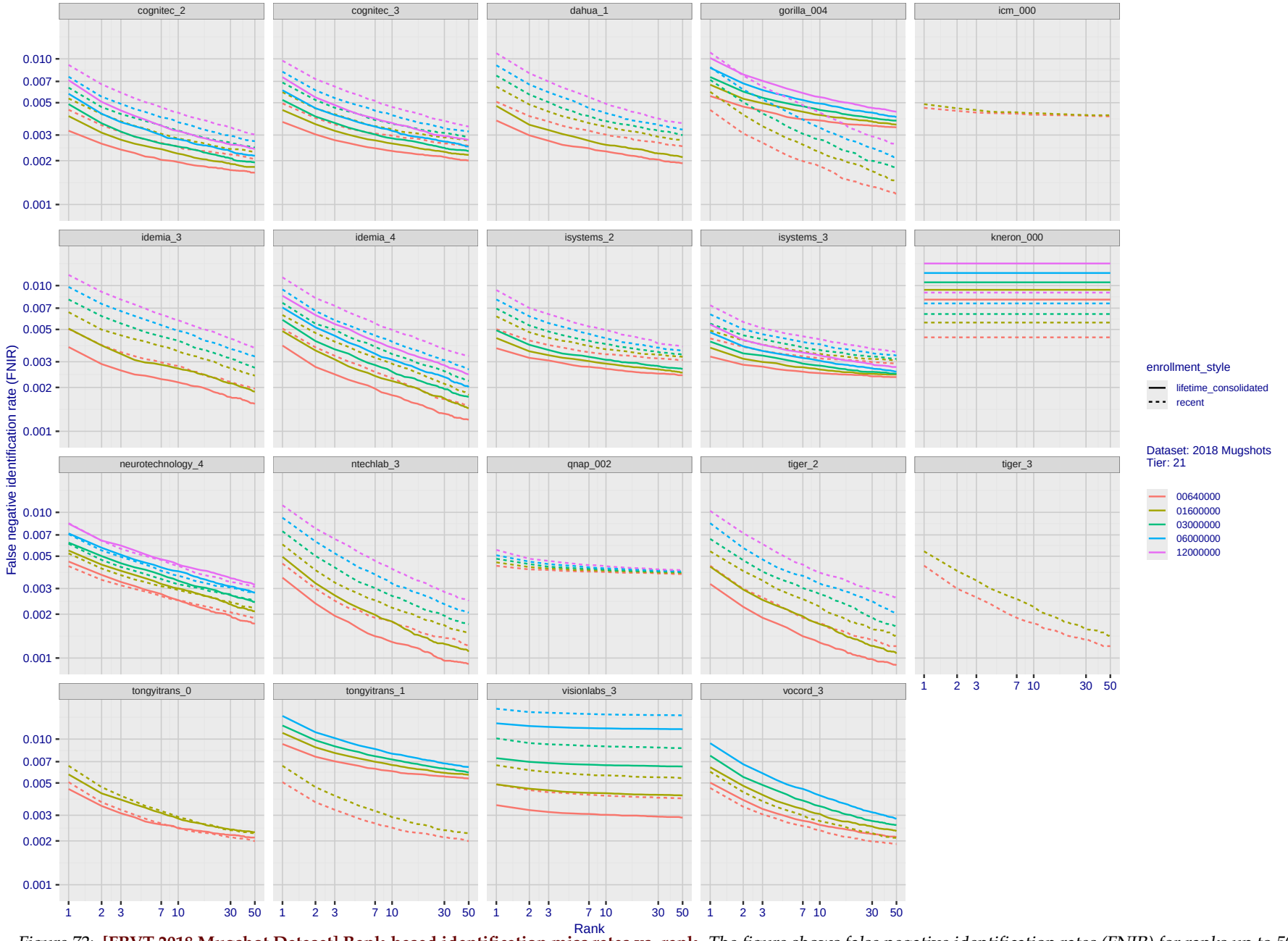

Figure 72: **[FRVT-2018 Mugshot Dataset] Rank-based identification miss rates vs. rank**. *The figure shows false negative identification rates (FNIR) for ranks up to 50. This metric is appropriate to investigational applications where human reviewers will adjudicate sorted candidate lists. Note that with threshold set to zero, FPIR = 1, i.e. any search without an enrolled mate will return non-mated candidates. Results are sorted and reported into tiers for clarity, with the tiering criteria being rank 1 hit rate on a gallery size of N = 640 000 subjects.*

2026/01/09 20:40:38

FNIR(N, R, T) = False neg. identification rate
FPIR(N, T) = False pos. identification rate

N = Num. enrolled subjects
R = Num. candidates examined

T = Threshold

T = 0 → Investigation
T > 0 → Identification

This publication is available free of charge from: https://doi.org/10.6028/NIST.IR.8271

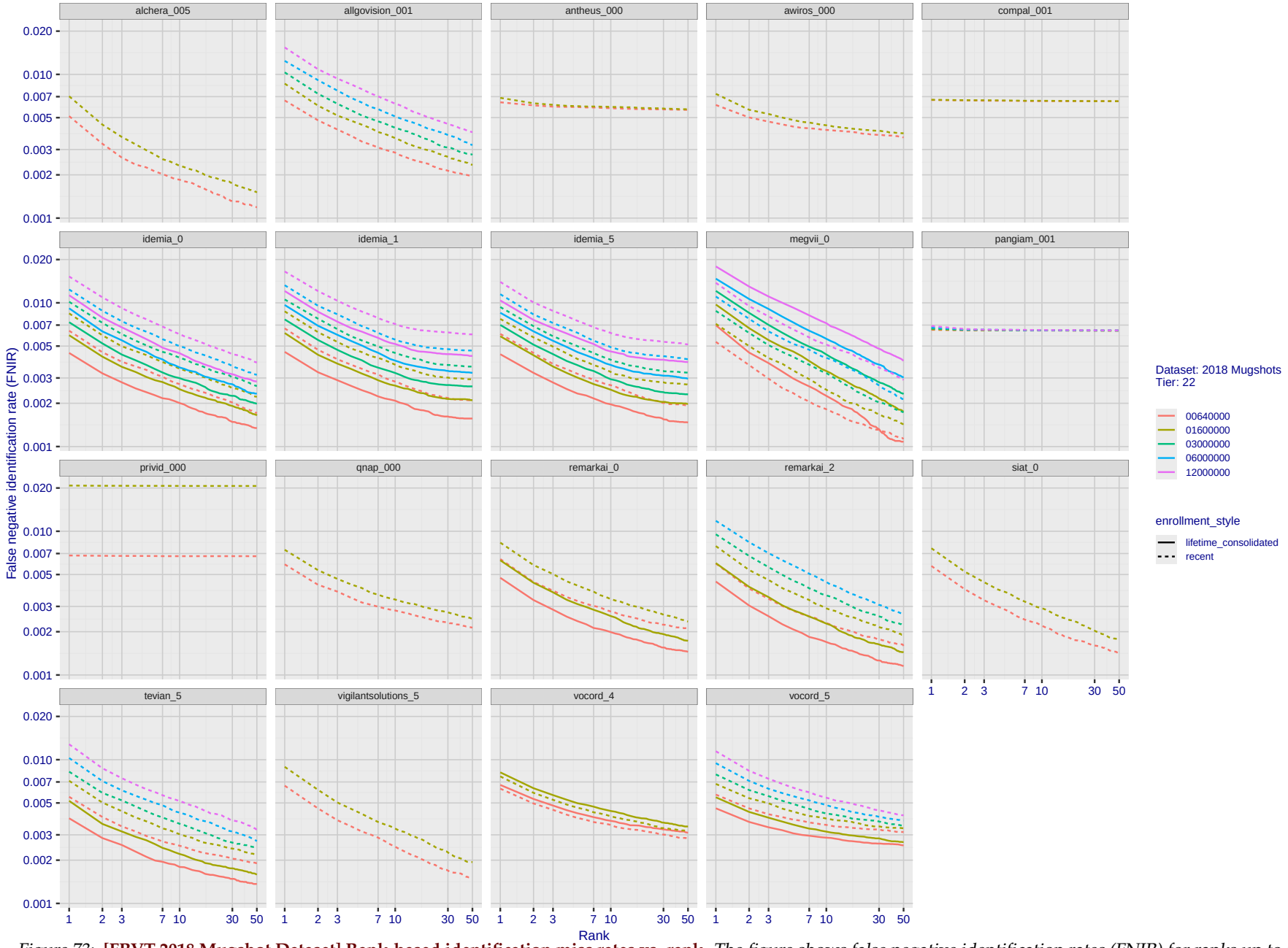

Figure 73: **[FRVT-2018 Mugshot Dataset] Rank-based identification miss rates vs. rank**. *The figure shows false negative identification rates (FNIR) for ranks up to 50. This metric is appropriate to investigational applications where human reviewers will adjudicate sorted candidate lists. Note that with threshold set to zero, FPIR = 1, i.e. any search without an enrolled mate will return non-mated candidates. Results are sorted and reported into tiers for clarity, with the tiering criteria being rank 1 hit rate on a gallery size of N = 640 000 subjects.*

2026/01/09 20:40:38
FNIR(N, R, T) = False neg. identification rate
FPIR(N, T) = False pos. identification rate
N = Num. enrolled subjects
R = Num. candidates examined
T = Threshold
T = 0 → Investigation
T > 0 → Identification

This publication is available free of charge from: https://doi.org/10.6028/NIST.IR.8271

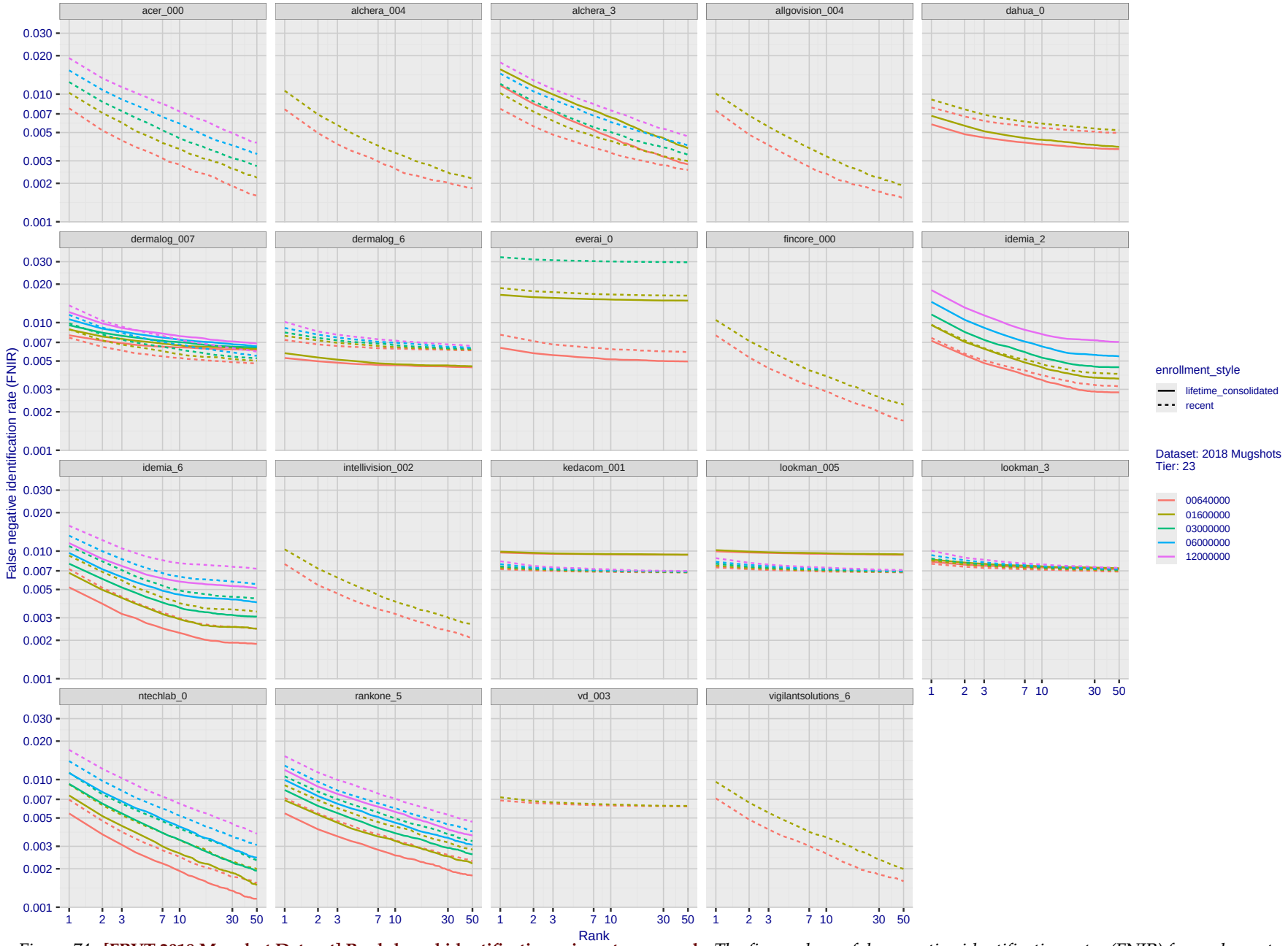

Figure 74: **[FRVT-2018 Mugshot Dataset] Rank-based identification miss rates vs. rank**. *The figure shows false negative identification rates (FNIR) for ranks up to 50. This metric is appropriate to investigational applications where human reviewers will adjudicate sorted candidate lists. Note that with threshold set to zero, FPIR = 1, i.e. any search without an enrolled mate will return non-mated candidates. Results are sorted and reported into tiers for clarity, with the tiering criteria being rank 1 hit rate on a gallery size of N = 640 000 subjects.*

This publication is available free of charge from: https://doi.org/10.6028/NIST.IR.8271

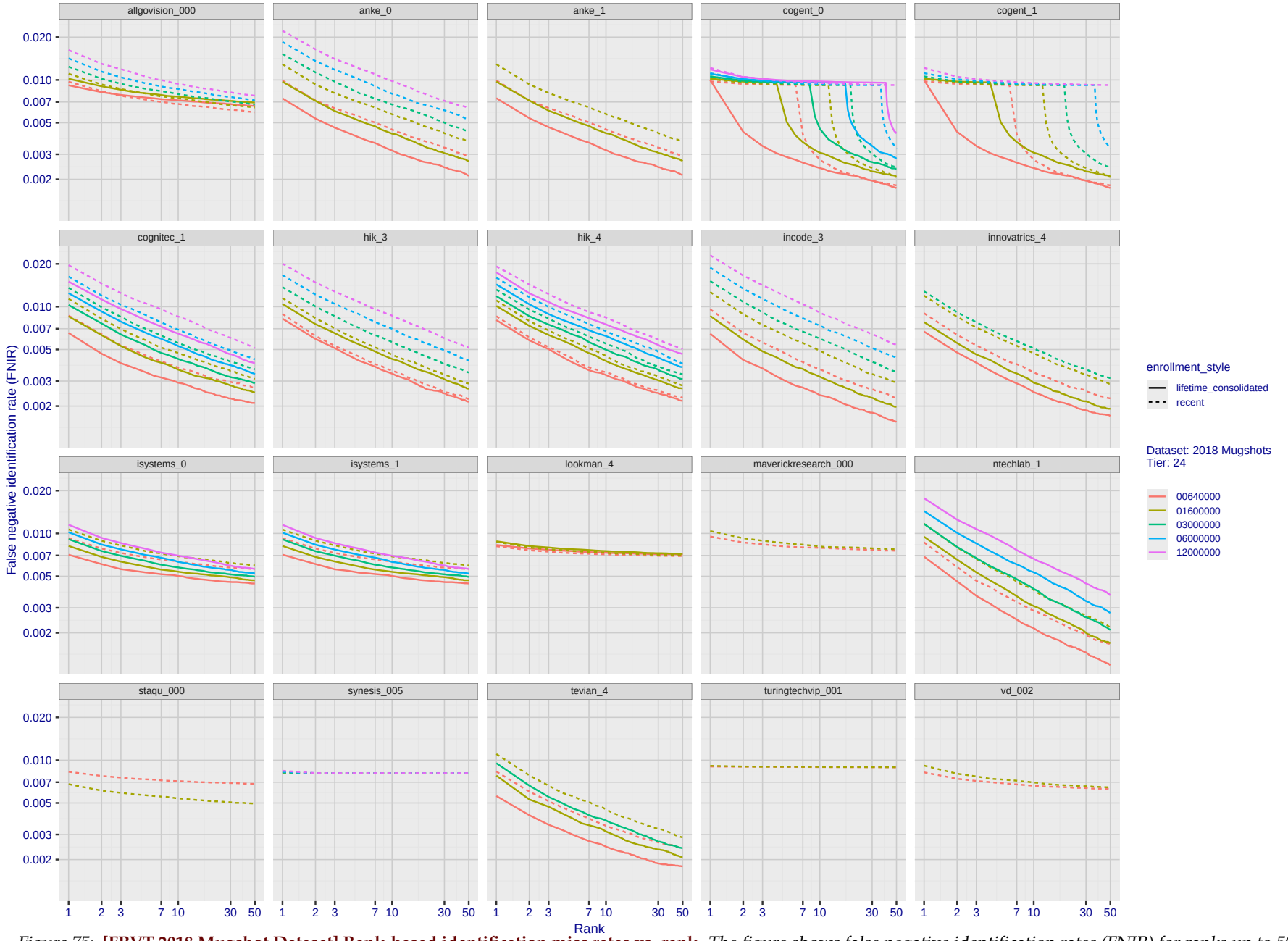

Figure 75: **[FRVT-2018 Mugshot Dataset] Rank-based identification miss rates vs. rank**. *The figure shows false negative identification rates (FNIR) for ranks up to 50. This metric is appropriate to investigational applications where human reviewers will adjudicate sorted candidate lists. Note that with threshold set to zero, FPIR = 1, i.e. any search without an enrolled mate will return non-mated candidates. Results are sorted and reported into tiers for clarity, with the tiering criteria being rank 1 hit rate on a gallery size of N = 640 000 subjects.*

2026/01/09 20:40:38
FNIR(N, R, T) = False neg. identification rate
FPIR(N, T) = False pos. identification rate
N = Num. enrolled subjects
R = Num. candidates examined
T = Threshold
T = 0 → Investigation
T > 0 → Identification

This publication is available free of charge from: https://doi.org/10.6028/NIST.IR.8271

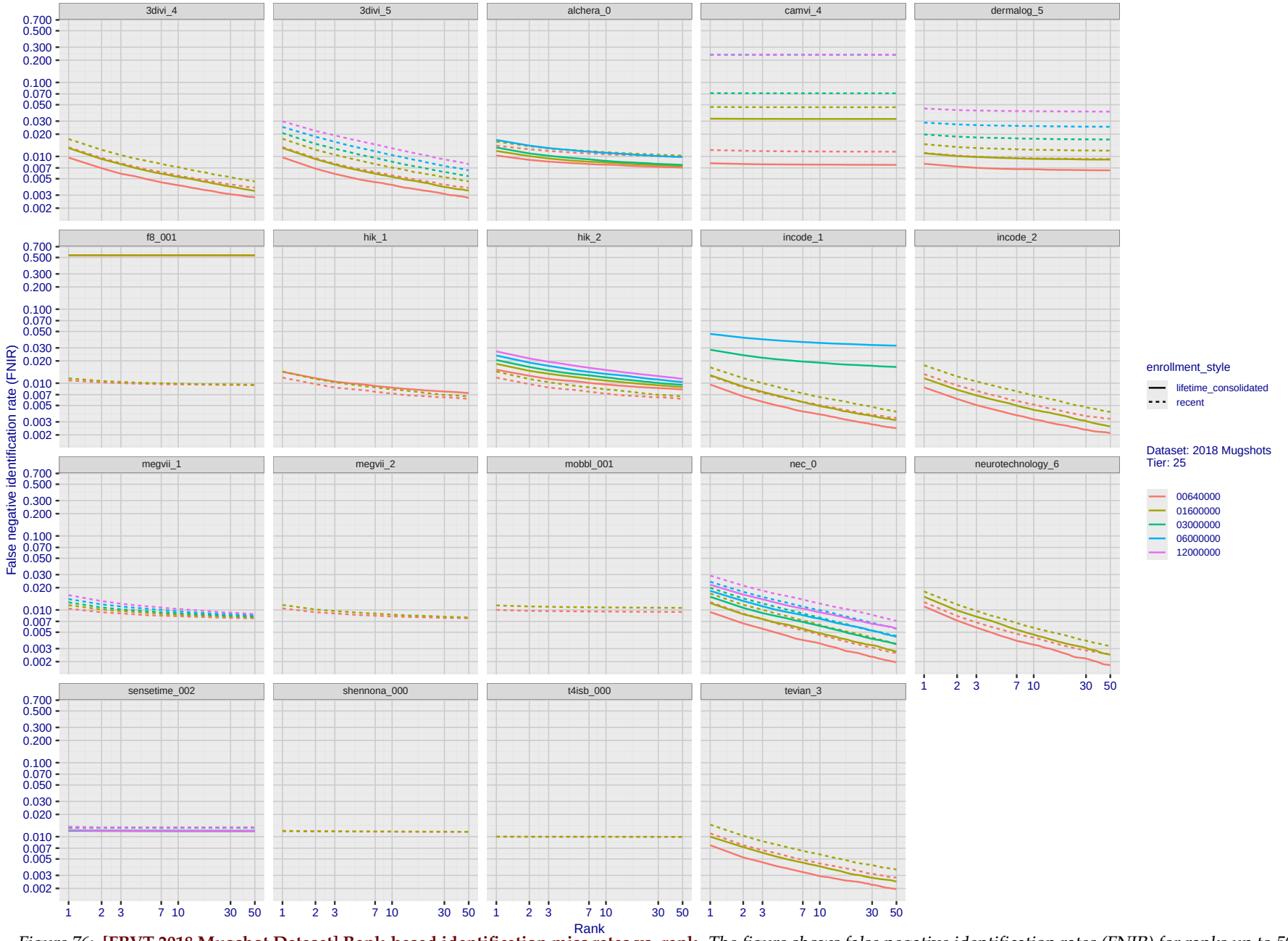

Figure 76: **[FRVT-2018 Mugshot Dataset] Rank-based identification miss rates vs. rank**. *The figure shows false negative identification rates (FNIR) for ranks up to 50. This metric is appropriate to investigational applications where human reviewers will adjudicate sorted candidate lists. Note that with threshold set to zero, FPIR = 1, i.e. any search without an enrolled mate will return non-mated candidates. Results are sorted and reported into tiers for clarity, with the tiering criteria being rank 1 hit rate on a gallery size of N = 640 000 subjects.*

This publication is available free of charge from: https://doi.org/10.6028/NIST.IR.8271

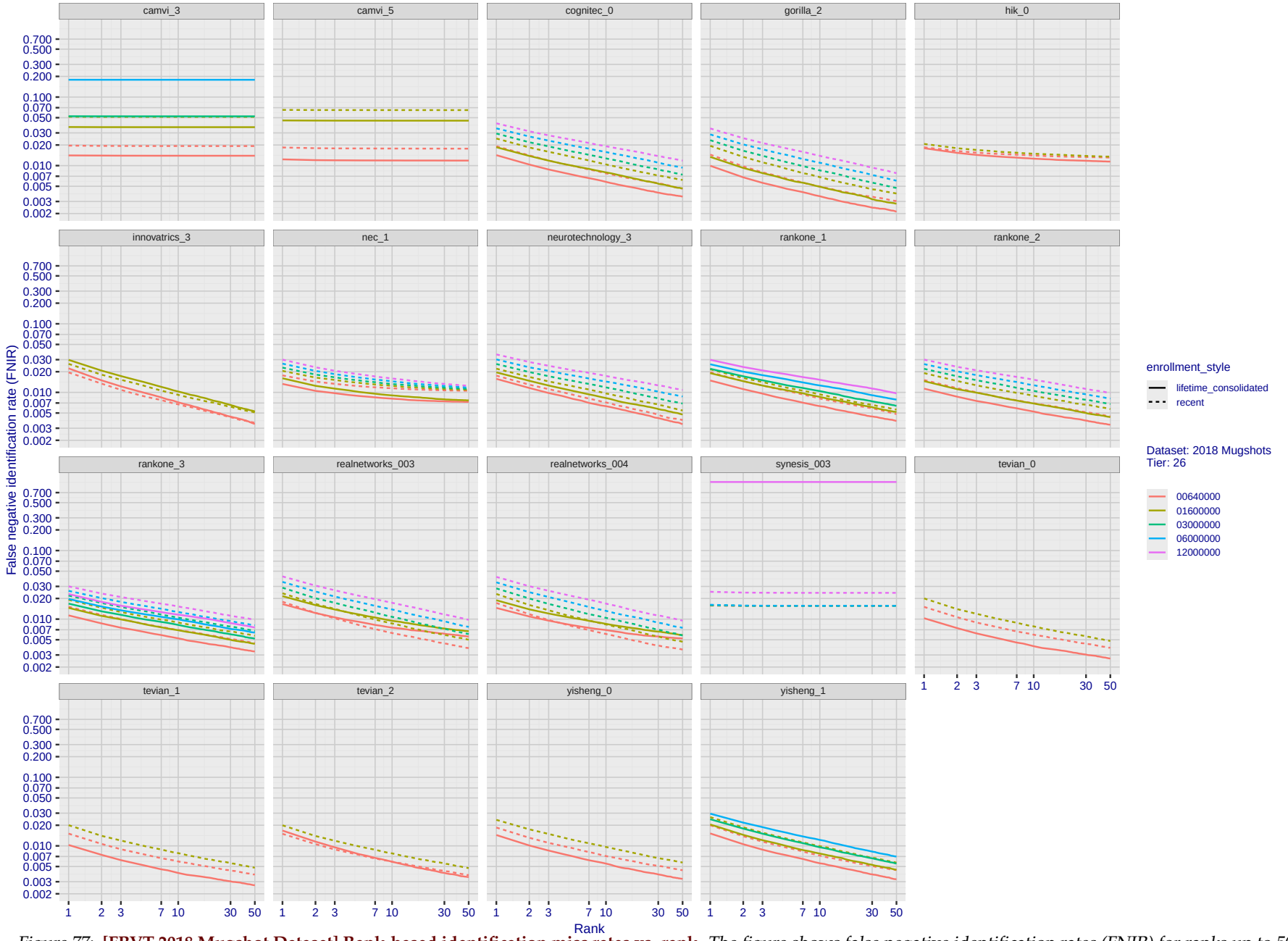

Figure 77: **[FRVT-2018 Mugshot Dataset] Rank-based identification miss rates vs. rank**. *The figure shows false negative identification rates (FNIR) for ranks up to 50. This metric is appropriate to investigational applications where human reviewers will adjudicate sorted candidate lists. Note that with threshold set to zero, FPIR = 1, i.e. any search without an enrolled mate will return non-mated candidates. Results are sorted and reported into tiers for clarity, with the tiering criteria being rank 1 hit rate on a gallery size of N = 640 000 subjects.*

This publication is available free of charge from: https://doi.org/10.6028/NIST.IR.8271

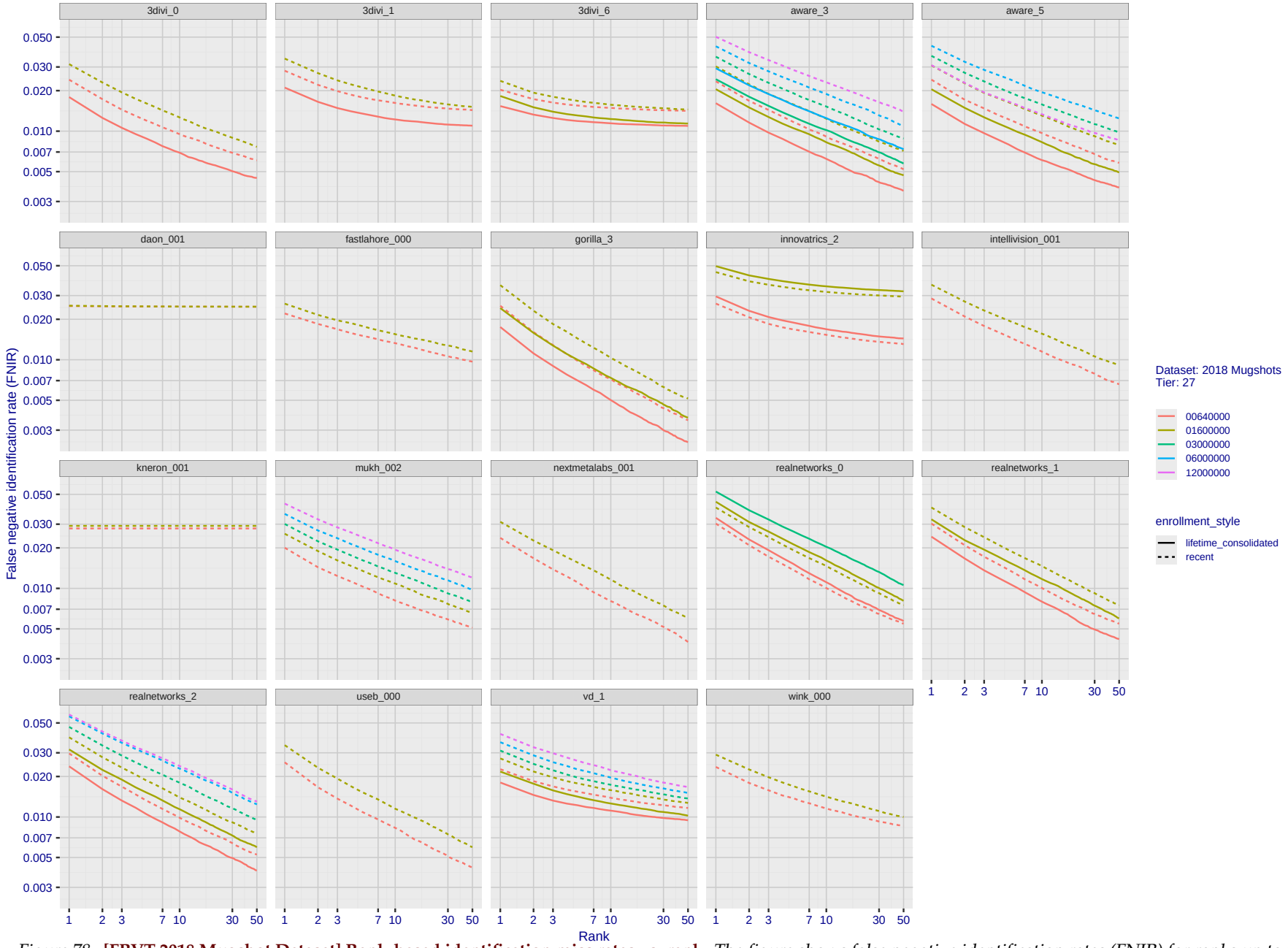

Figure 78: **[FRVT-2018 Mugshot Dataset] Rank-based identification miss rates vs. rank**. *The figure shows false negative identification rates (FNIR) for ranks up to 50. This metric is appropriate to investigational applications where human reviewers will adjudicate sorted candidate lists. Note that with threshold set to zero, FPIR = 1, i.e. any search without an enrolled mate will return non-mated candidates. Results are sorted and reported into tiers for clarity, with the tiering criteria being rank 1 hit rate on a gallery size of N = 640 000 subjects.*

2026/01/09 20:40:38
FNIR(N, R, T) = False neg. identification rate
FPIR(N, T) = False pos. identification rate
N = Num. enrolled subjects
R = Num. candidates examined
T = Threshold
T = 0 → Investigation
T > 0 → Identification

This publication is available free of charge from: https://doi.org/10.6028/NIST.IR.8271

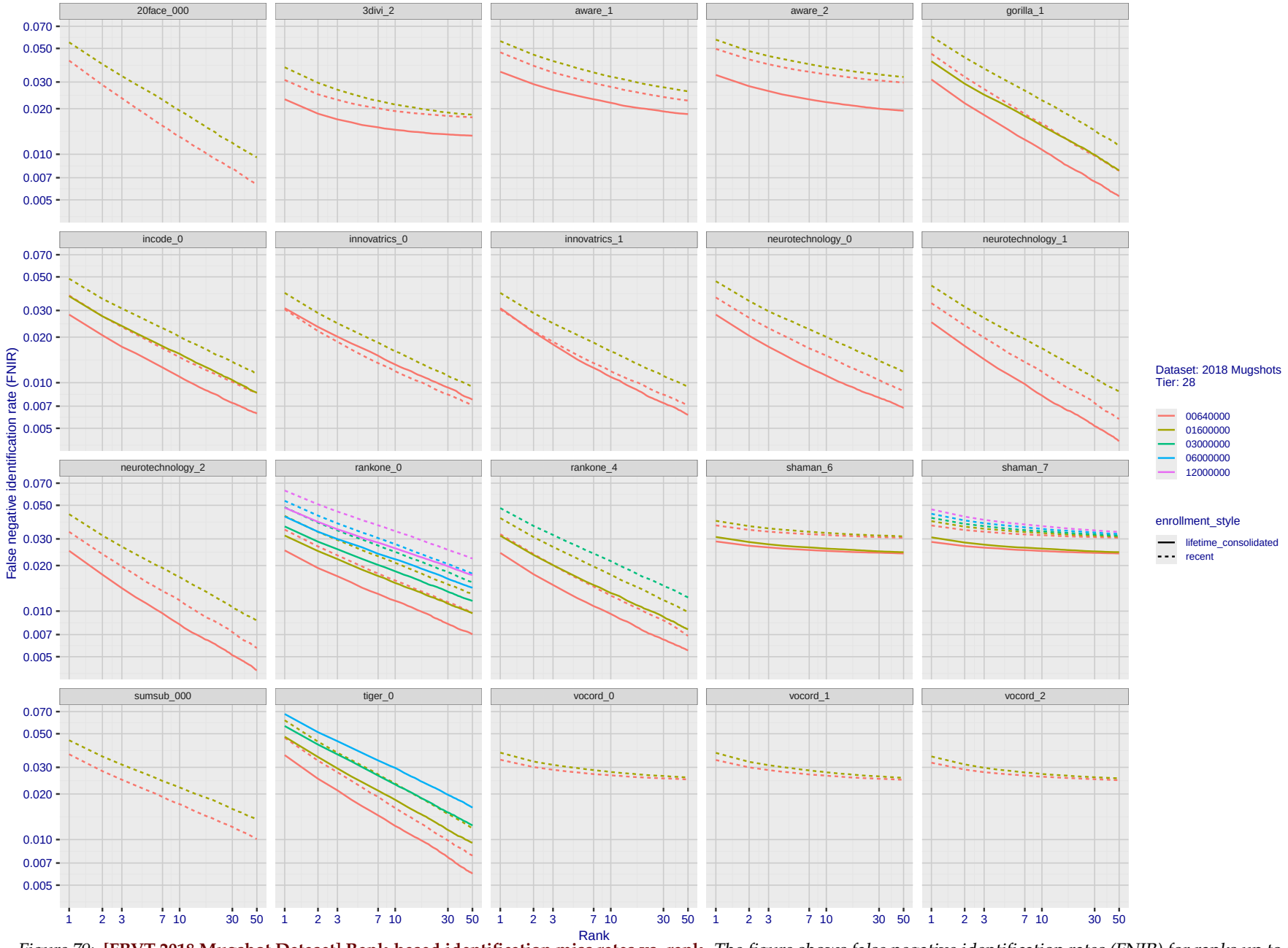

Figure 79: **[FRVT-2018 Mugshot Dataset] Rank-based identification miss rates vs. rank**. *The figure shows false negative identification rates (FNIR) for ranks up to 50. This metric is appropriate to investigational applications where human reviewers will adjudicate sorted candidate lists. Note that with threshold set to zero, FPIR = 1, i.e. any search without an enrolled mate will return non-mated candidates. Results are sorted and reported into tiers for clarity, with the tiering criteria being rank 1 hit rate on a gallery size of N = 640 000 subjects.*

2026/01/09 20:40:38

FNIR(N, R, T) = False neg. identification rate
FPIR(N, T) = False pos. identification rate

N = Num. enrolled subjects
R = Num. candidates examined

T = Threshold

T = 0 → Investigation
T > 0 → Identification

This publication is available free of charge from: https://doi.org/10.6028/NIST.IR.8271

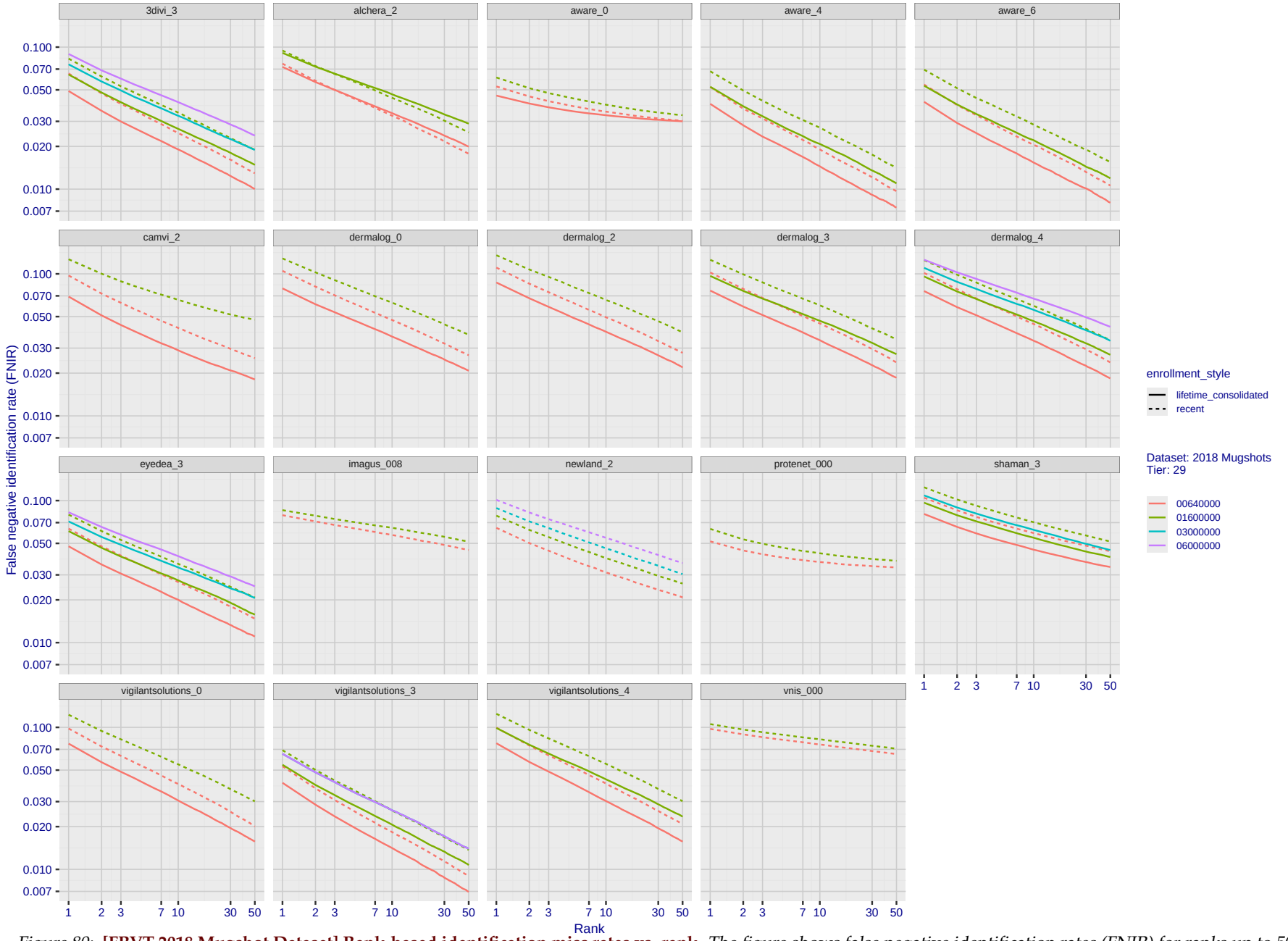

Figure 80: **[FRVT-2018 Mugshot Dataset] Rank-based identification miss rates vs. rank**. *The figure shows false negative identification rates (FNIR) for ranks up to 50. This metric is appropriate to investigational applications where human reviewers will adjudicate sorted candidate lists. Note that with threshold set to zero, FPIR = 1, i.e. any search without an enrolled mate will return non-mated candidates. Results are sorted and reported into tiers for clarity, with the tiering criteria being rank 1 hit rate on a gallery size of N = 640 000 subjects.*

2026/01/09
20:40:38

FNIR(N, R, T) = False neg. identification rate
FPIR(N, T) = False pos. identification rate

N = Num. enrolled subjects
R = Num. candidates examined

T = Threshold

T = 0 → Investigation
T > 0 → Identification

This publication is available free of charge from: https://doi.org/10.6028/NIST.IR.8271

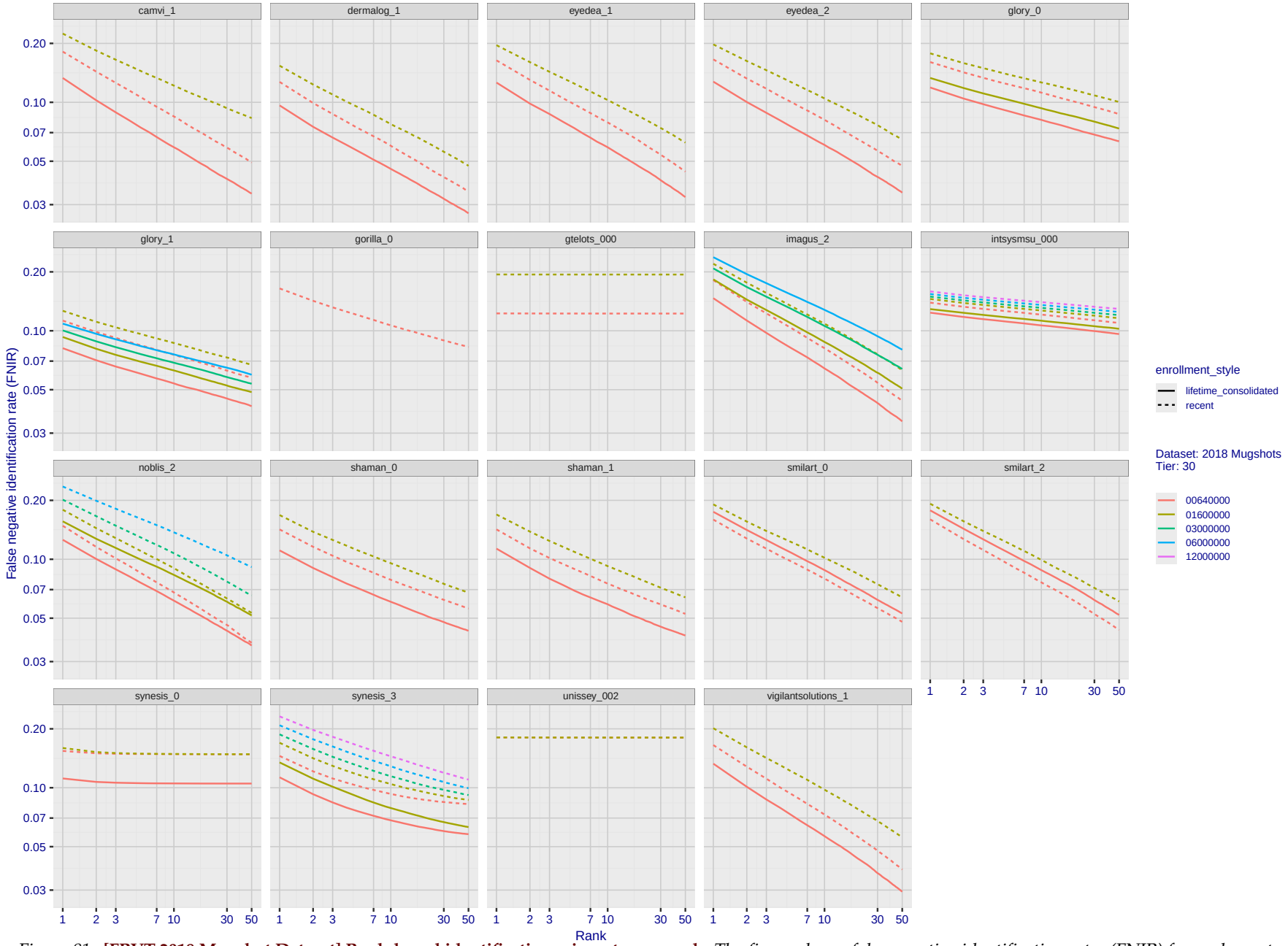

Figure 81: **[FRVT-2018 Mugshot Dataset] Rank-based identification miss rates vs. rank**. *The figure shows false negative identification rates (FNIR) for ranks up to 50. This metric is appropriate to investigational applications where human reviewers will adjudicate sorted candidate lists. Note that with threshold set to zero, FPIR = 1, i.e. any search without an enrolled mate will return non-mated candidates. Results are sorted and reported into tiers for clarity, with the tiering criteria being rank 1 hit rate on a gallery size of N = 640 000 subjects.*

2026/01/09 20:40:38
FNIR(N, R, T) = False neg. identification rate
FPIR(N, T) = False pos. identification rate
N = Num. enrolled subjects
R = Num. candidates examined
T = Threshold
T = 0 → Investigation
T > 0 → Identification

This publication is available free of charge from: https://doi.org/10.6028/NIST.IR.8271

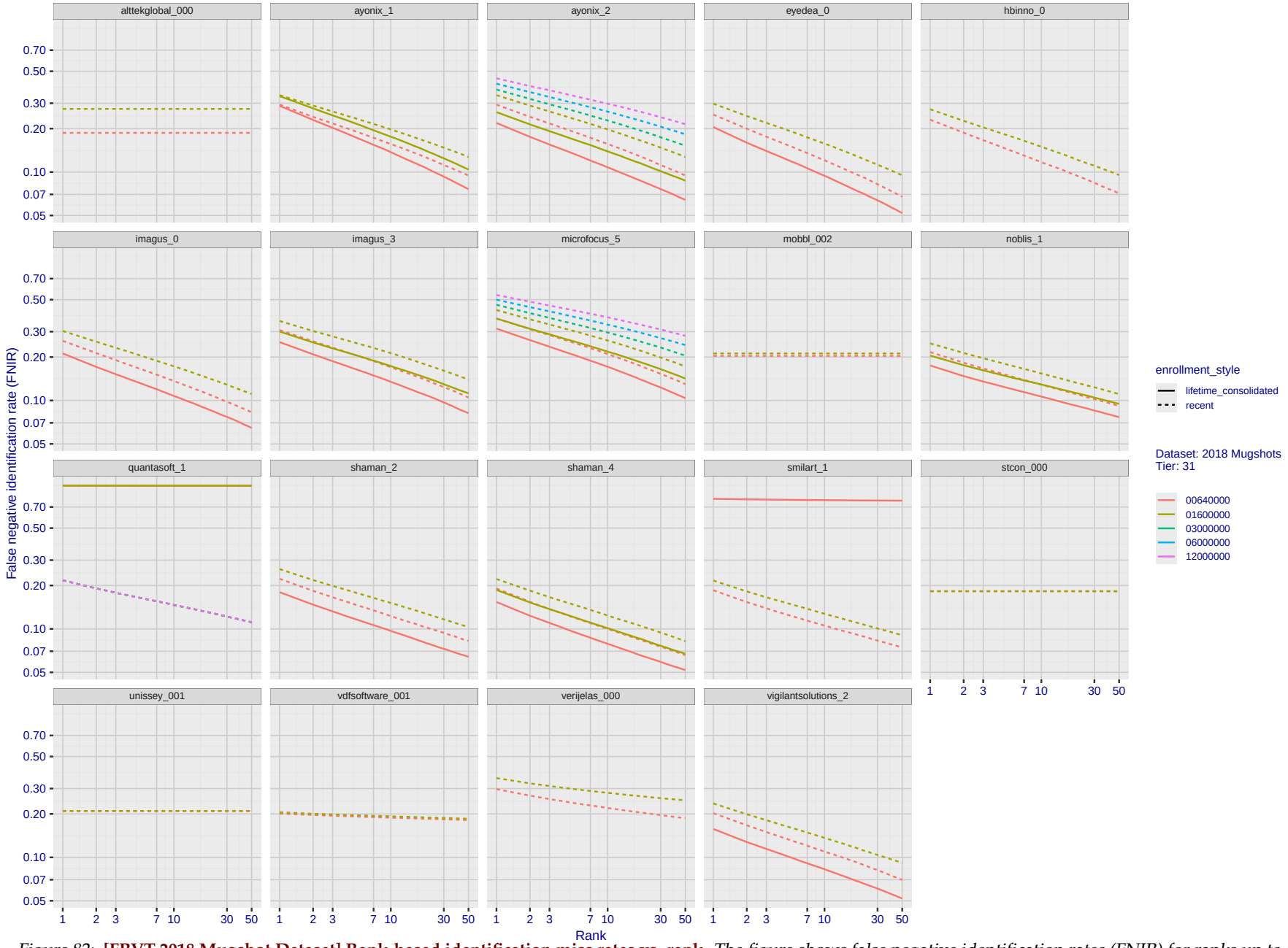

Figure 82: **[FRVT-2018 Mugshot Dataset] Rank-based identification miss rates vs. rank**. *The figure shows false negative identification rates (FNIR) for ranks up to 50. This metric is appropriate to investigational applications where human reviewers will adjudicate sorted candidate lists. Note that with threshold set to zero, FPIR = 1, i.e. any search without an enrolled mate will return non-mated candidates. Results are sorted and reported into tiers for clarity, with the tiering criteria being rank 1 hit rate on a gallery size of N = 640 000 subjects.*

2026/01/09 20:40:38

FNIR(N, R, T) = False neg. identification rate
FPIR(N, T) = False pos. identification rate

N = Num. enrolled subjects
R = Num. candidates examined

T = Threshold

T = 0 → Investigation
T > 0 → Identification

This publication is available free of charge from: https://doi.org/10.6028/NIST.IR.8271

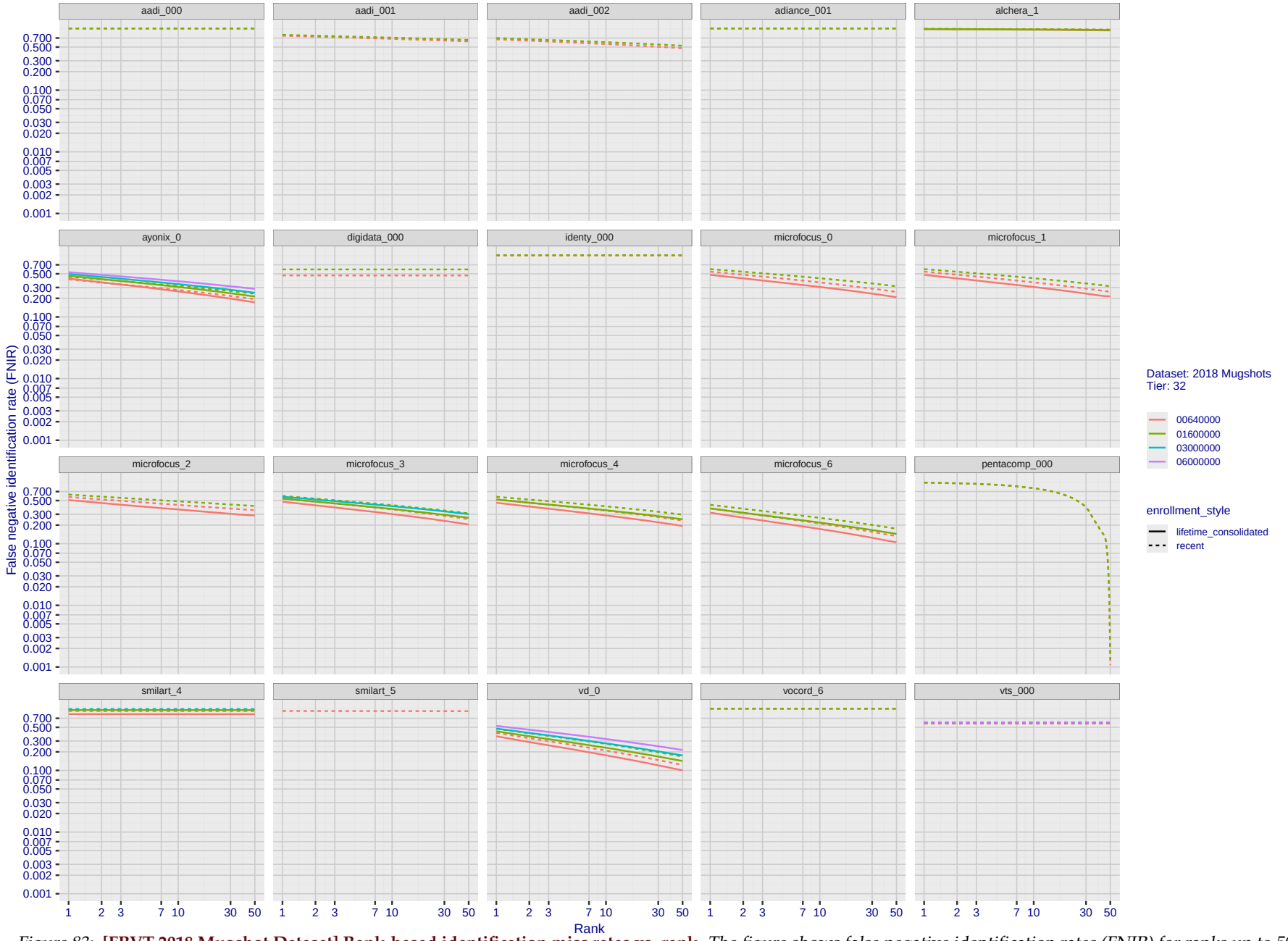

Figure 83: **[FRVT-2018 Mugshot Dataset] Rank-based identification miss rates vs. rank**. *The figure shows false negative identification rates (FNIR) for ranks up to 50. This metric is appropriate to investigational applications where human reviewers will adjudicate sorted candidate lists. Note that with threshold set to zero, FPIR = 1, i.e. any search without an enrolled mate will return non-mated candidates. Results are sorted and reported into tiers for clarity, with the tiering criteria being rank 1 hit rate on a gallery size of N = 640 000 subjects.*

2026/01/09 20:40:38
FNIR(N, R, T) = FPIR(N, T) = False neg. identification rate / False pos. identification rate
N = Num. enrolled subjects
R = Num. candidates examined
T = Threshold
T = 0 → Investigation
T > 0 → Identification

2026/01/09	FNIR(N, R, T) =	False neg. identification rate	N = Num. enrolled subjects	T = Threshold	$T = 0 \rightarrow$ Investigation
20:40:38	FPIR(N, T) =	False pos. identification rate	R = Num. candidates examined		$T > 0 \rightarrow$ Identification

This publication is available free of charge from: https://doi.org/10.6028/NIST.IR.8271

This publication is available free of charge from: https://doi.org/10.6028/NIST.IR.8271

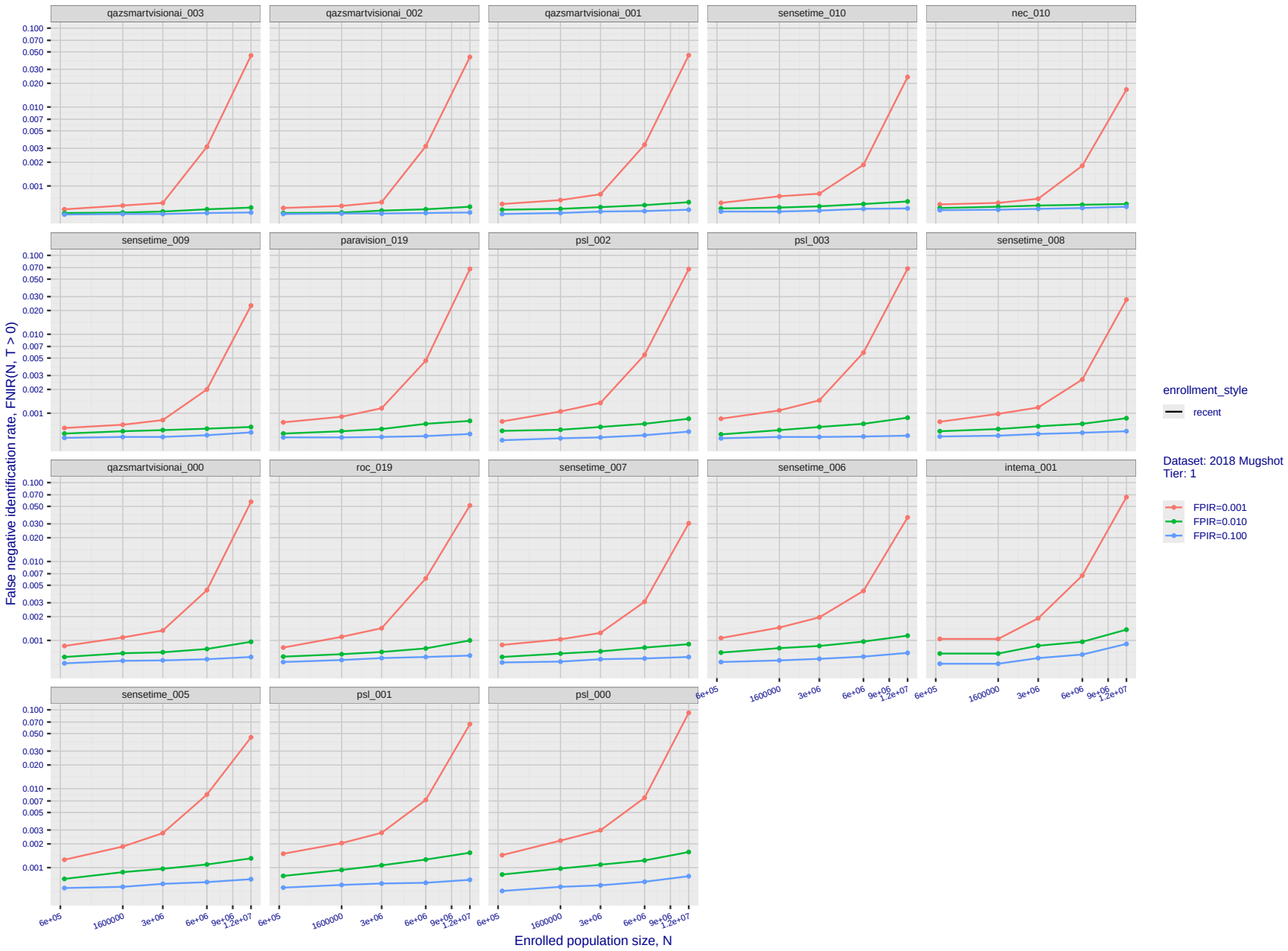

Figure 84: **[FRVT-2018 Mugshot Dataset] Threshold-based identification miss rates vs. number of enrolled subjects**. *The figure shows FNIR(N, T) across various gallery sizes when the threshold is set to achieve the given FPIRs. The rank criterion is irrelevant at high thresholds as mates are always at rank 1. The results are computed from the trials listed in rows 1-10 of Table 1. Less accurate algorithms were not run on large N, so results are missing. For clarity, results are sorted and reported into tiers spanning multiple pages. The tiering criteria is complicated: First paging by FNIR(N_b, 1, 0), then sorting by median FNIR(N_b, T), N_b = 640 000.*

2026/01/09 20:40:38
FNIR(N, R, T) = False neg. identification rate
FPIR(N, T) = False pos. identification rate
N = Num. enrolled subjects
R = Num. candidates examined
T = Threshold
T = 0 → Investigation
T > 0 → Identification

This publication is available free of charge from: https://doi.org/10.6028/NIST.IR.8271

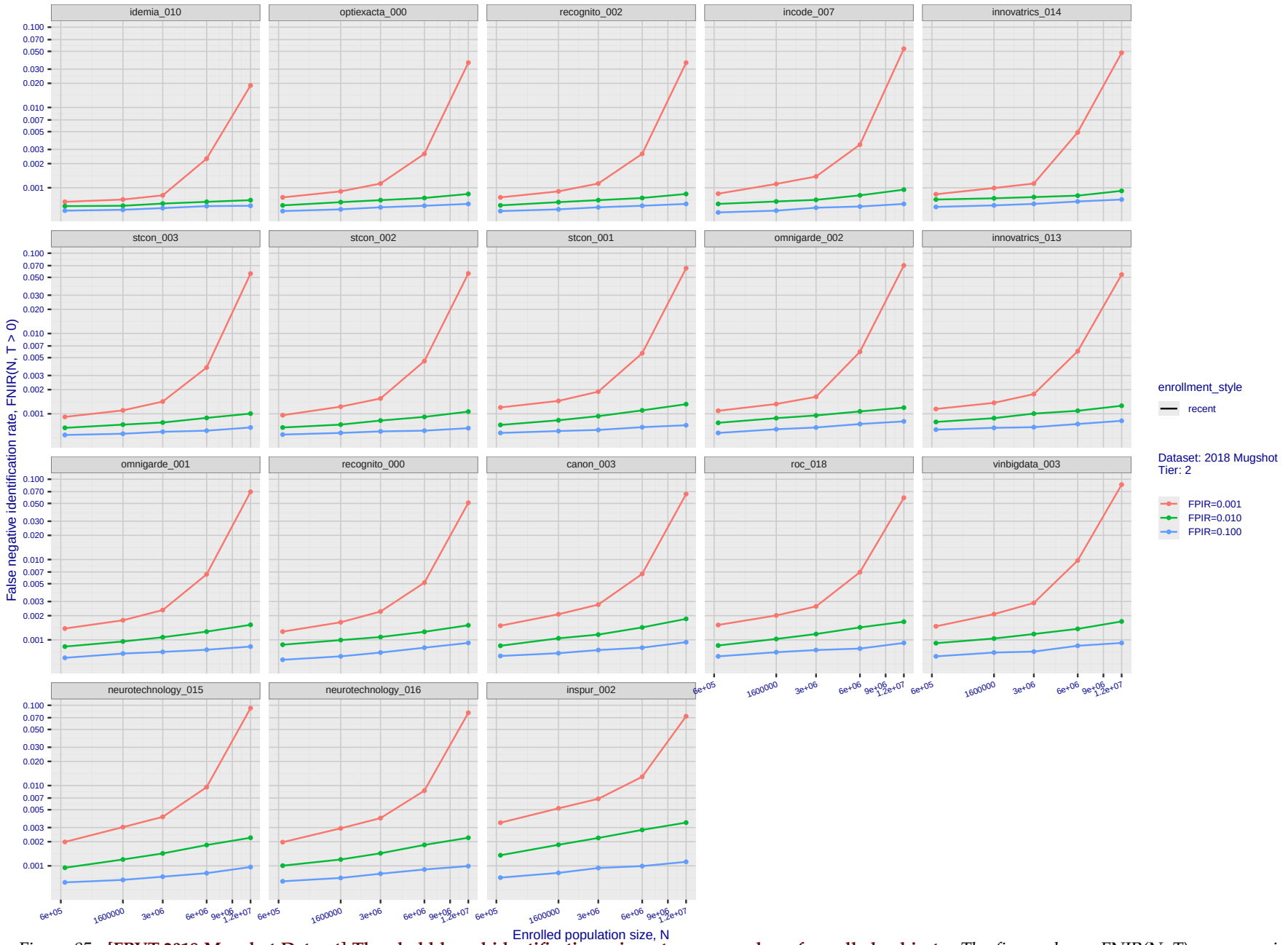

Figure 85: **[FRVT-2018 Mugshot Dataset] Threshold-based identification miss rates vs. number of enrolled subjects**. *The figure shows FNIR(N, T) across various gallery sizes when the threshold is set to achieve the given FPIRs. The rank criterion is irrelevant at high thresholds as mates are always at rank 1. The results are computed from the trials listed in rows 1-10 of Table 1. Less accurate algorithms were not run on large N, so results are missing. For clarity, results are sorted and reported into tiers spanning multiple pages. The tiering criteria is complicated: First paging by FNIR(N_b, 1, 0), then sorting by median FNIR(N_b, T), N_b = 640 000.*

2026/01/09 20:40:38

FNIR(N, R, T) = False neg. identification rate
FPIR(N, T) = False pos. identification rate
N = Num. enrolled subjects
R = Num. candidates examined
T = Threshold
T = 0 → Investigation
T > 0 → Identification

This publication is available free of charge from: https://doi.org/10.6028/NIST.IR.8271

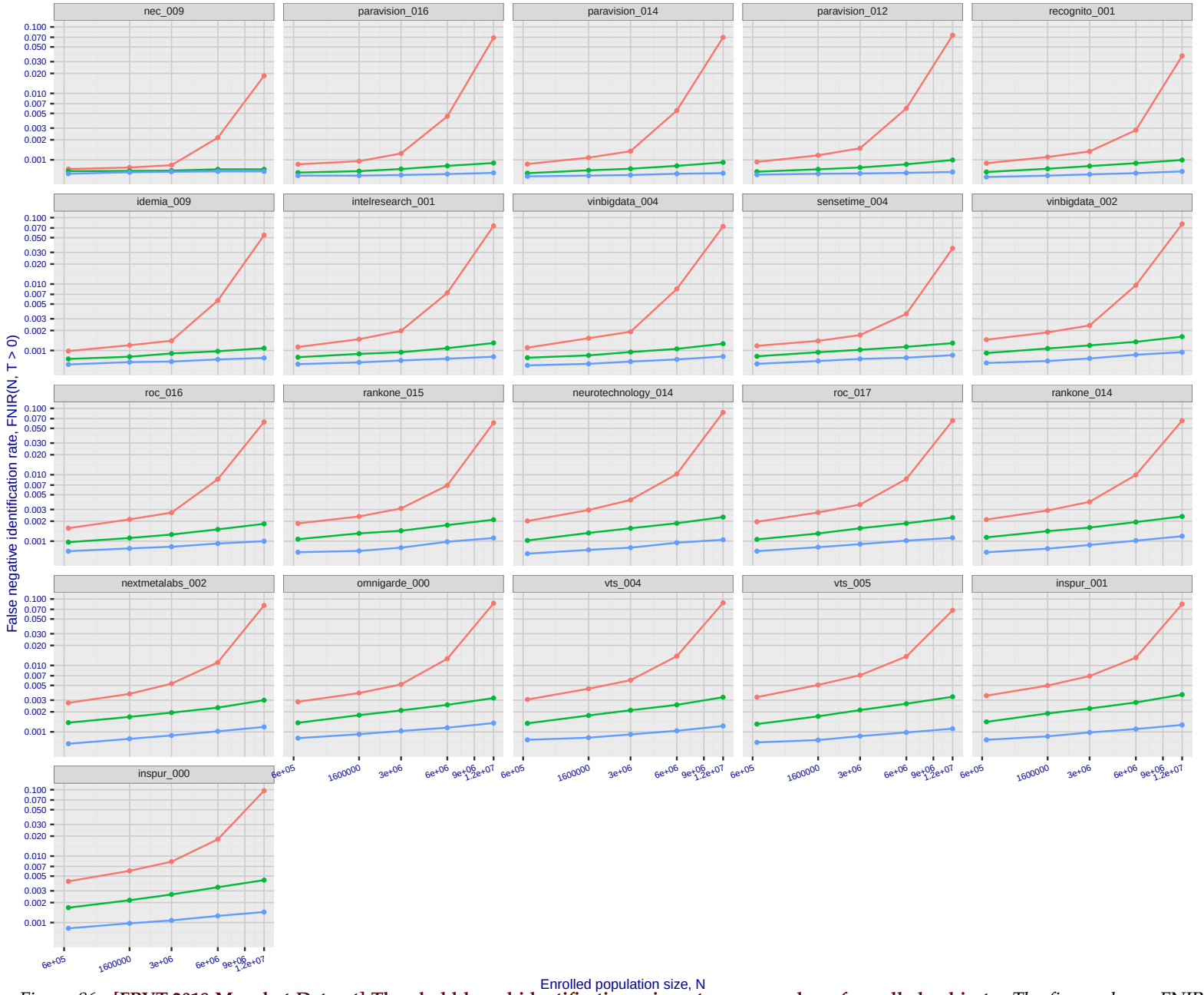

Figure 86: **[FRVT-2018 Mugshot Dataset] Threshold-based identification miss rates vs. number of enrolled subjects**. *The figure shows FNIR(N, T) across various gallery sizes when the threshold is set to achieve the given FPIRs. The rank criterion is irrelevant at high thresholds as mates are always at rank 1. The results are computed from the trials listed in rows 1-10 of Table 1. Less accurate algorithms were not run on large N, so results are missing. For clarity, results are sorted and reported into tiers spanning multiple pages. The tiering criteria is complicated: First paging by FNIR(N_b, 1, 0), then sorting by median FNIR(N_b, T), N_b = 640 000.*

2026/01/09 20:40:38
FNIR(N, R, T) = False neg. identification rate
FPIR(N, T) = False pos. identification rate
N = Num. enrolled subjects
R = Num. candidates examined
T = Threshold
T = 0 → Investigation
T > 0 → Identification

This publication is available free of charge from: https://doi.org/10.6028/NIST.IR.8271

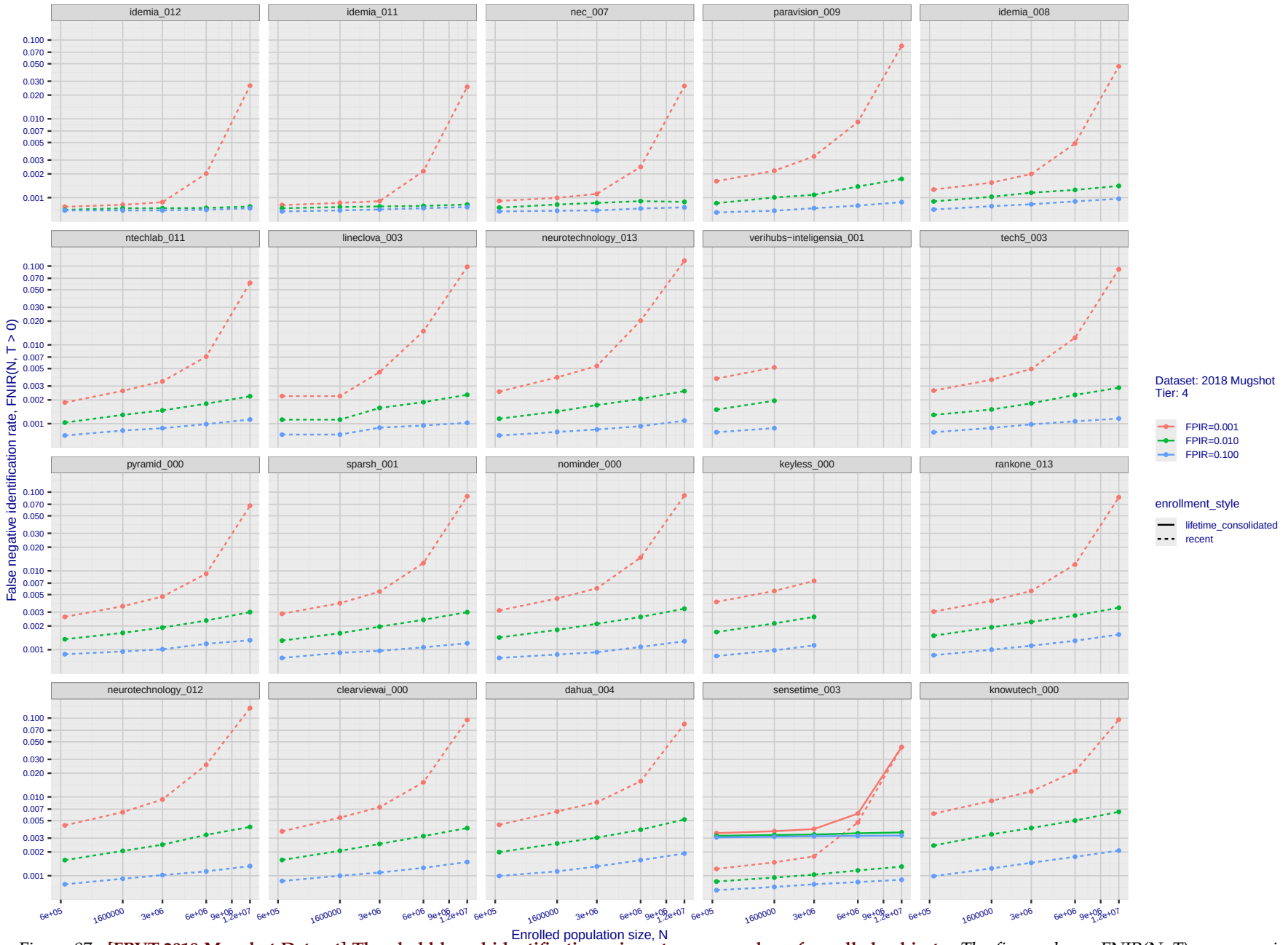

Figure 87: **[FRVT-2018 Mugshot Dataset] Threshold-based identification miss rates vs. number of enrolled subjects**. *The figure shows FNIR(N, T) across various gallery sizes when the threshold is set to achieve the given FPIRs. The rank criterion is irrelevant at high thresholds as mates are always at rank 1. The results are computed from the trials listed in rows 1-10 of Table 1. Less accurate algorithms were not run on large N, so results are missing. For clarity, results are sorted and reported into tiers spanning multiple pages. The tiering criteria is complicated: First paging by FNIR(N_b, 1, 0), then sorting by median FNIR(N_b, T), N_b = 640 000.*

2026/01/09 20:40:38

FNIR(N, R, T) = False neg. identification rate
FPIR(N, T) = False pos. identification rate
N = Num. enrolled subjects
R = Num. candidates examined
T = Threshold
T = 0 → Investigation
T > 0 → Identification

This publication is available free of charge from: https://doi.org/10.6028/NIST.IR.8271

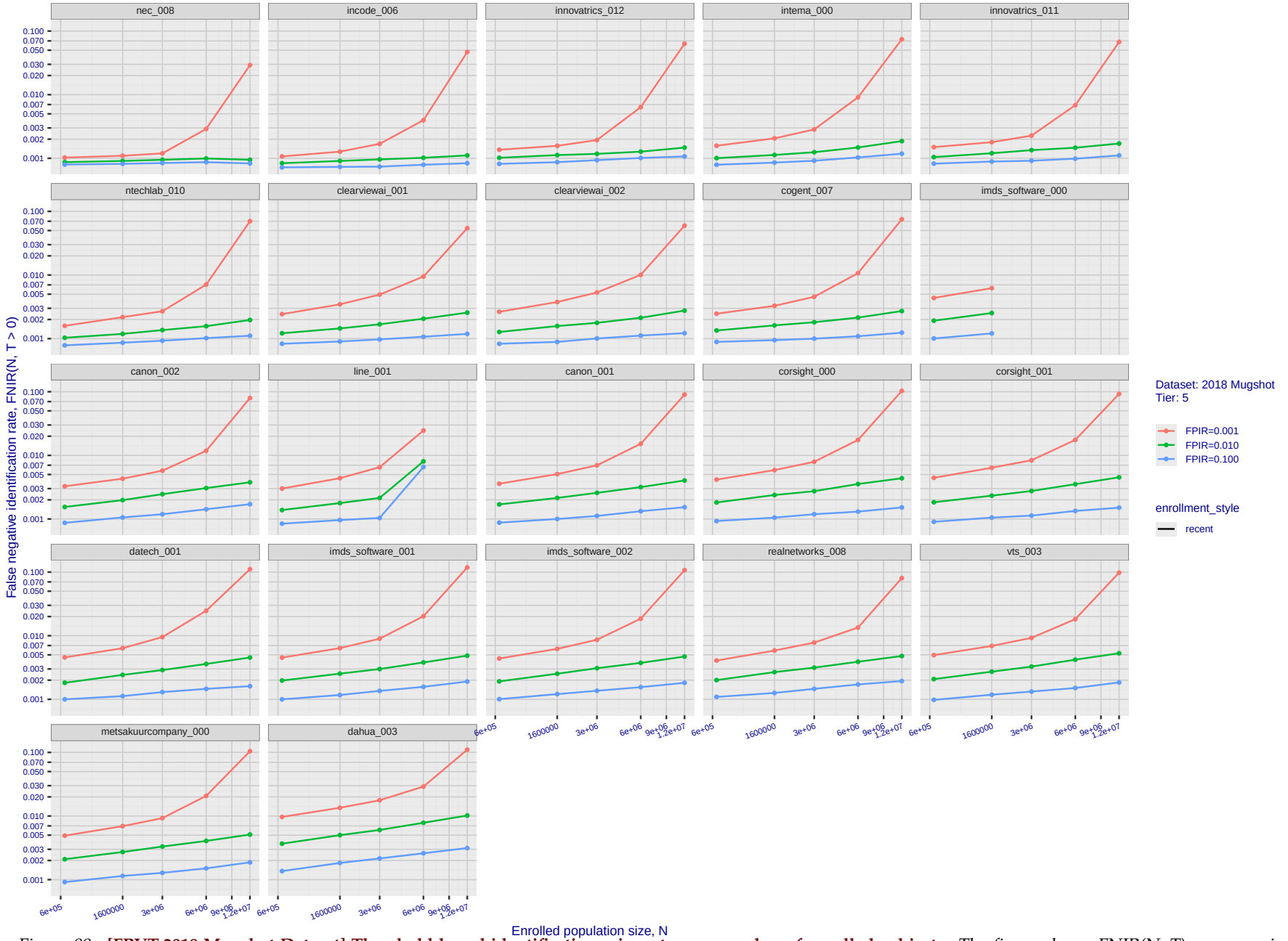

Figure 88: **[FRVT-2018 Mugshot Dataset] Threshold-based identification miss rates vs. number of enrolled subjects**. *The figure shows FNIR(N, T) across various gallery sizes when the threshold is set to achieve the given FPIRs. The rank criterion is irrelevant at high thresholds as mates are always at rank 1. The results are computed from the trials listed in rows 1-10 of Table 1. Less accurate algorithms were not run on large N, so results are missing. For clarity, results are sorted and reported into tiers spanning multiple pages. The tiering criteria is complicated: First paging by FNIR(N_b, 1, 0), then sorting by median FNIR(N_b, T), N_b = 640 000.*

2026/01/09 20:40:38
FNIR(N, R, T) = False neg. identification rate
FPIR(N, T) = False pos. identification rate
N = Num. enrolled subjects
R = Num. candidates examined
T = Threshold
T = 0 → Investigation
T > 0 → Identification

This publication is available free of charge from: https://doi.org/10.6028/NIST.IR.8271

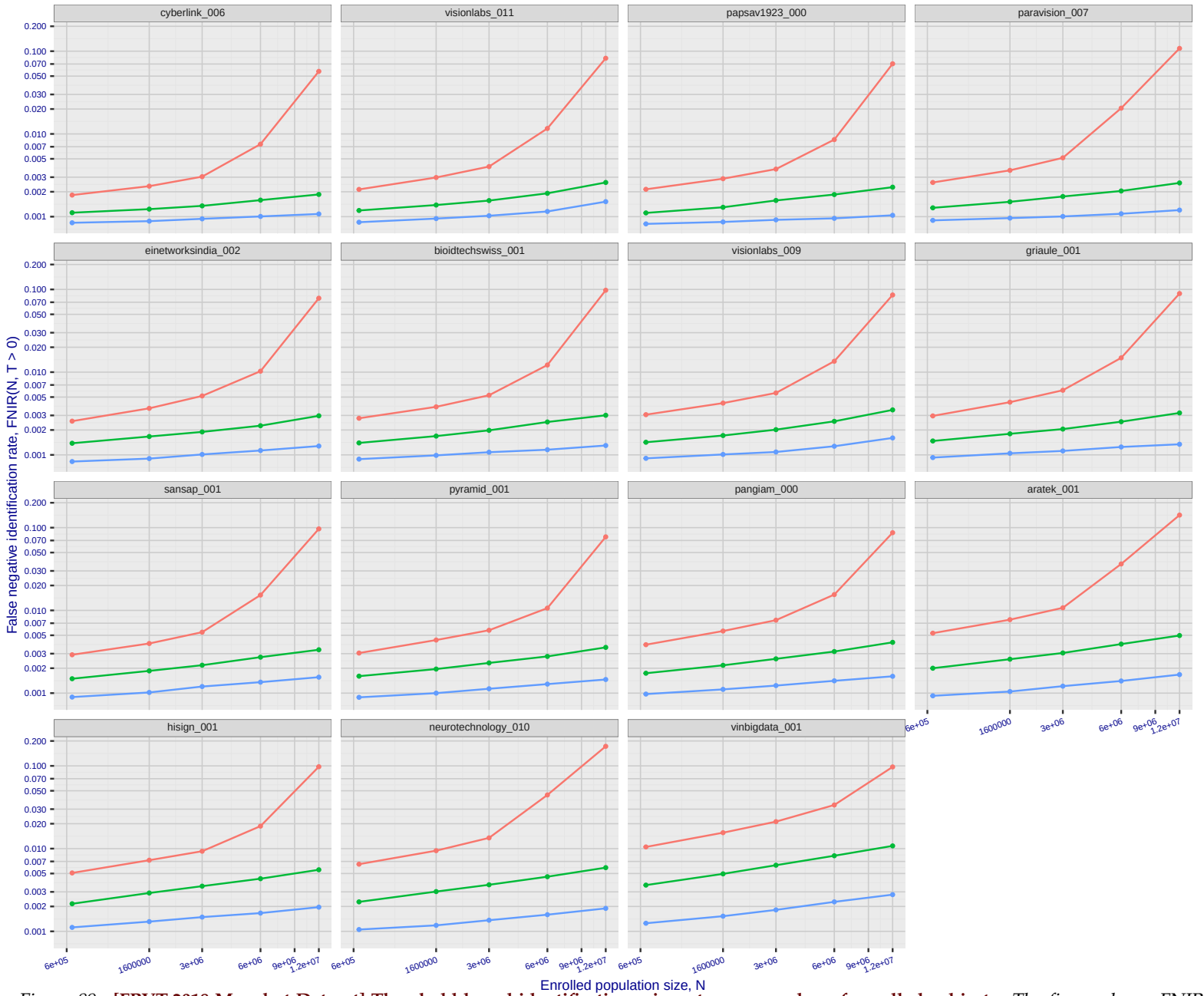

Figure 89: **[FRVT-2018 Mugshot Dataset] Threshold-based identification miss rates vs. number of enrolled subjects**. *The figure shows FNIR(N, T) across various gallery sizes when the threshold is set to achieve the given FPIRs. The rank criterion is irrelevant at high thresholds as mates are always at rank 1. The results are computed from the trials listed in rows 1-10 of Table 1. Less accurate algorithms were not run on large N, so results are missing. For clarity, results are sorted and reported into tiers spanning multiple pages. The tiering criteria is complicated: First paging by FNIR(N_b, 1, 0), then sorting by median FNIR(N_b, T), N_b = 640 000.*

2026/01/09 20:40:38

FNIR(N, R, T) = False neg. identification rate
FPIR(N, T) = False pos. identification rate
N = Num. enrolled subjects
R = Num. candidates examined
T = Threshold
T = 0 → Investigation
T > 0 → Identification

This publication is available free of charge from: https://doi.org/10.6028/NIST.IR.8271

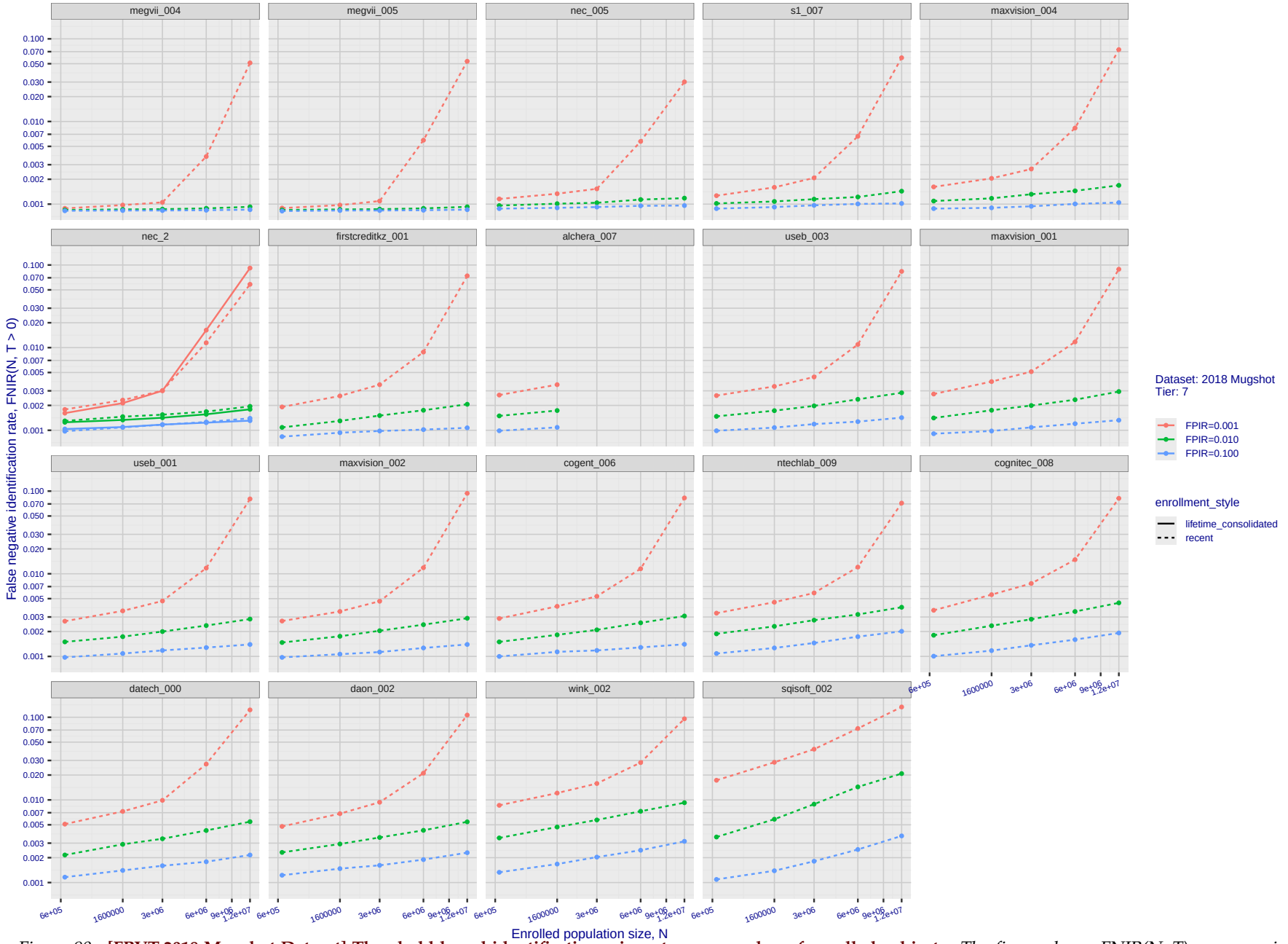

Figure 90: **[FRVT-2018 Mugshot Dataset] Threshold-based identification miss rates vs. number of enrolled subjects**. *The figure shows FNIR(N, T) across various gallery sizes when the threshold is set to achieve the given FPIRs. The rank criterion is irrelevant at high thresholds as mates are always at rank 1. The results are computed from the trials listed in rows 1-10 of Table 1. Less accurate algorithms were not run on large N, so results are missing. For clarity, results are sorted and reported into tiers spanning multiple pages. The tiering criteria is complicated: First paging by FNIR(N_b, 1, 0), then sorting by median FNIR(N_b, T), N_b = 640 000.*

2026/01/09 20:40:38

FNIR(N, R, T) = False neg. identification rate
FPIR(N, T) = False pos. identification rate
N = Num. enrolled subjects
R = Num. candidates examined
T = Threshold
T = 0 → Investigation
T > 0 → Identification

This publication is available free of charge from: https://doi.org/10.6028/NIST.IR.8271

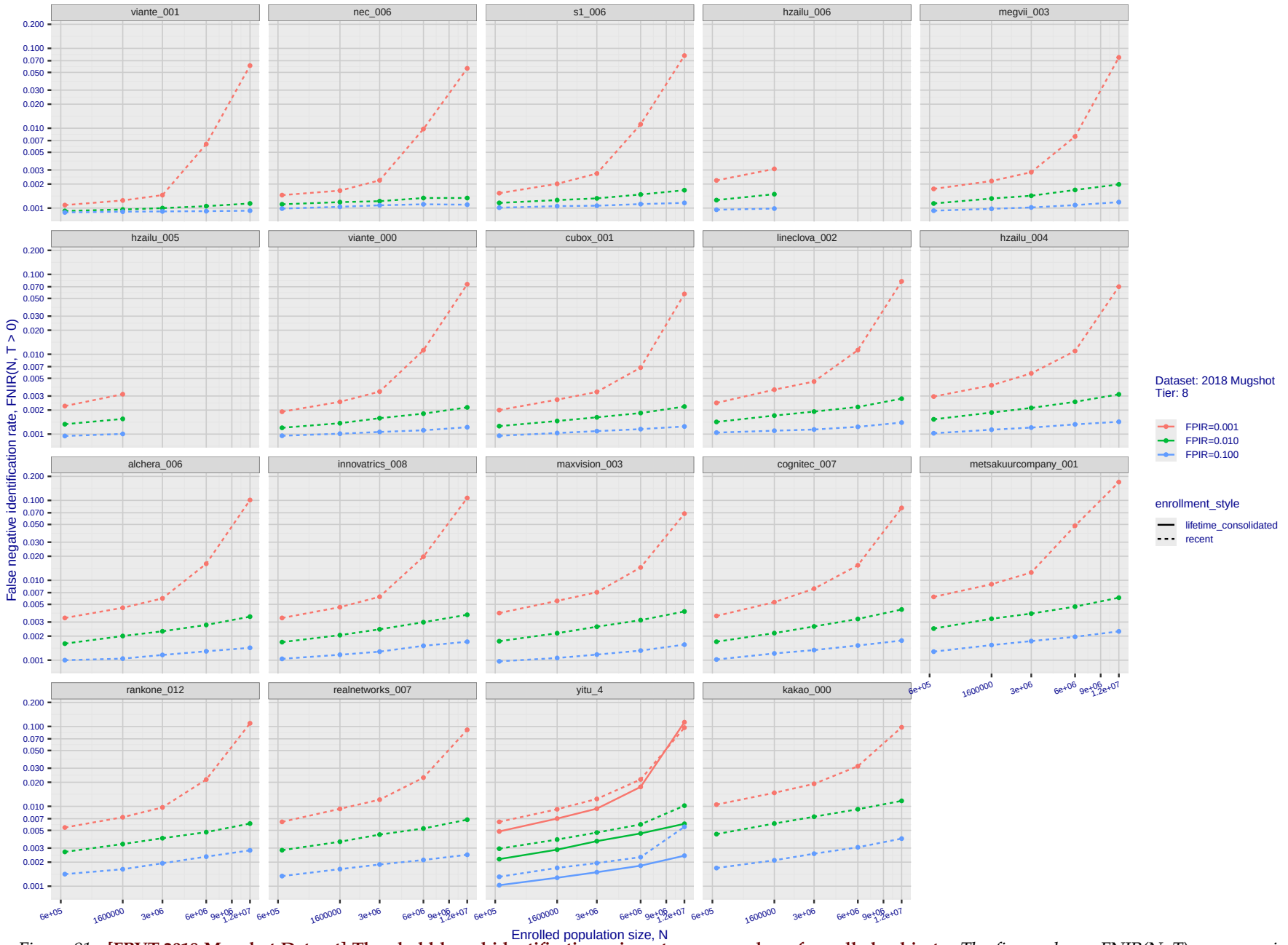

Figure 91: **[FRVT-2018 Mugshot Dataset] Threshold-based identification miss rates vs. number of enrolled subjects**. *The figure shows FNIR(N, T) across various gallery sizes when the threshold is set to achieve the given FPIRs. The rank criterion is irrelevant at high thresholds as mates are always at rank 1. The results are computed from the trials listed in rows 1-10 of Table 1. Less accurate algorithms were not run on large N, so results are missing. For clarity, results are sorted and reported into tiers spanning multiple pages. The tiering criteria is complicated: First paging by FNIR(N_b, 1, 0), then sorting by median FNIR(N_b, T), N_b = 640 000.*

2026/01/09
20:40:38

FNIR(N, R, T) = False neg. identification rate
FPIR(N, T) = False pos. identification rate

N = Num. enrolled subjects
R = Num. candidates examined

T = Threshold

T = 0 → Investigation
T > 0 → Identification

This publication is available free of charge from: https://doi.org/10.6028/NIST.IR.8271

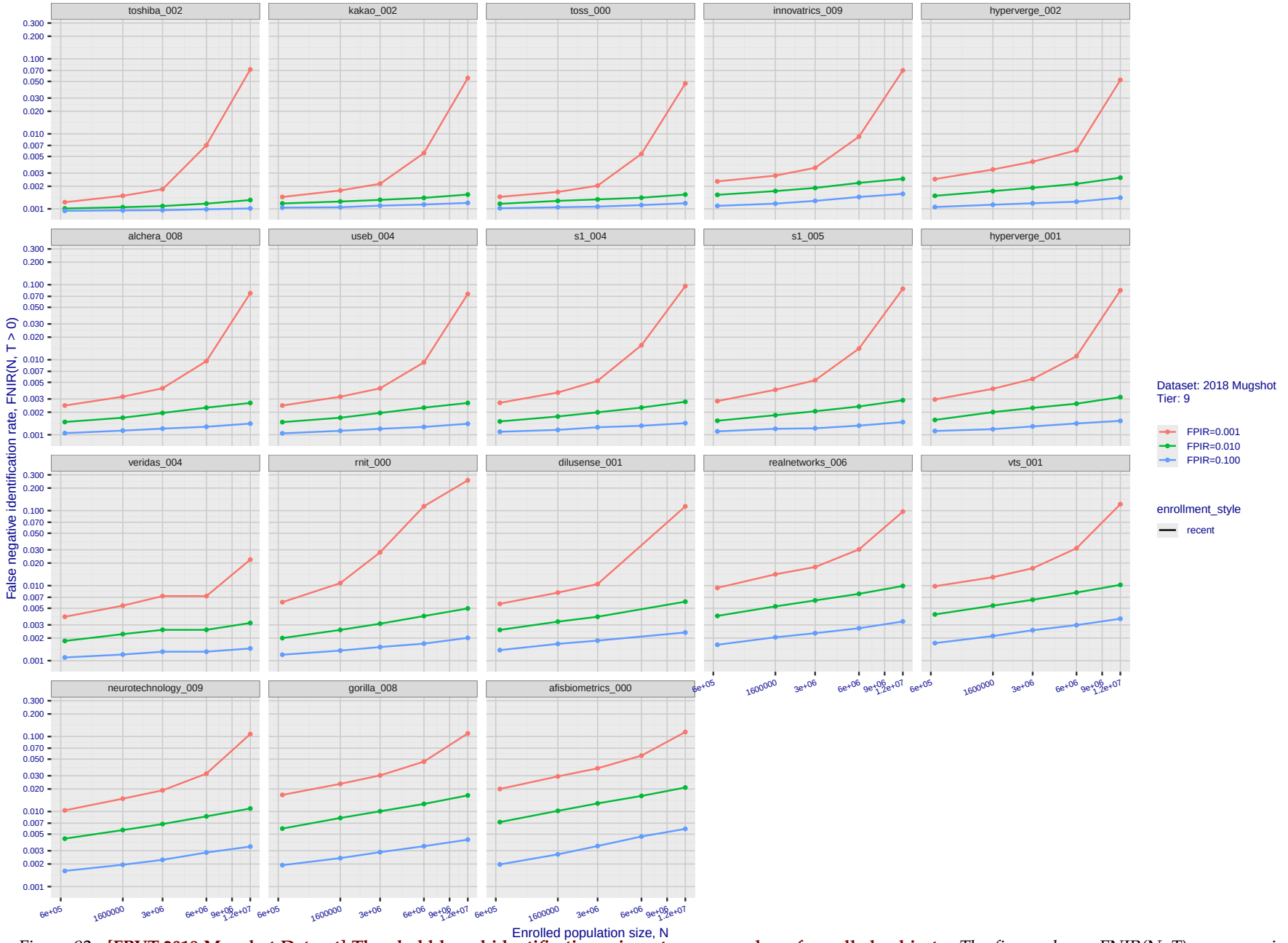

Figure 92: **[FRVT-2018 Mugshot Dataset] Threshold-based identification miss rates vs. number of enrolled subjects**. *The figure shows FNIR(N, T) across various gallery sizes when the threshold is set to achieve the given FPIRs. The rank criterion is irrelevant at high thresholds as mates are always at rank 1. The results are computed from the trials listed in rows 1-10 of Table 1. Less accurate algorithms were not run on large N, so results are missing. For clarity, results are sorted and reported into tiers spanning multiple pages. The tiering criteria is complicated: First paging by FNIR(N_b, 1, 0), then sorting by median FNIR(N_b, T), N_b = 640 000.*

2026/01/09 20:40:38

FNIR(N, R, T) = False neg. identification rate
FPIR(N, T) = False pos. identification rate
N = Num. enrolled subjects
R = Num. candidates examined
T = Threshold
T = 0 → Investigation
T > 0 → Identification

This publication is available free of charge from: https://doi.org/10.6028/NIST.IR.8271

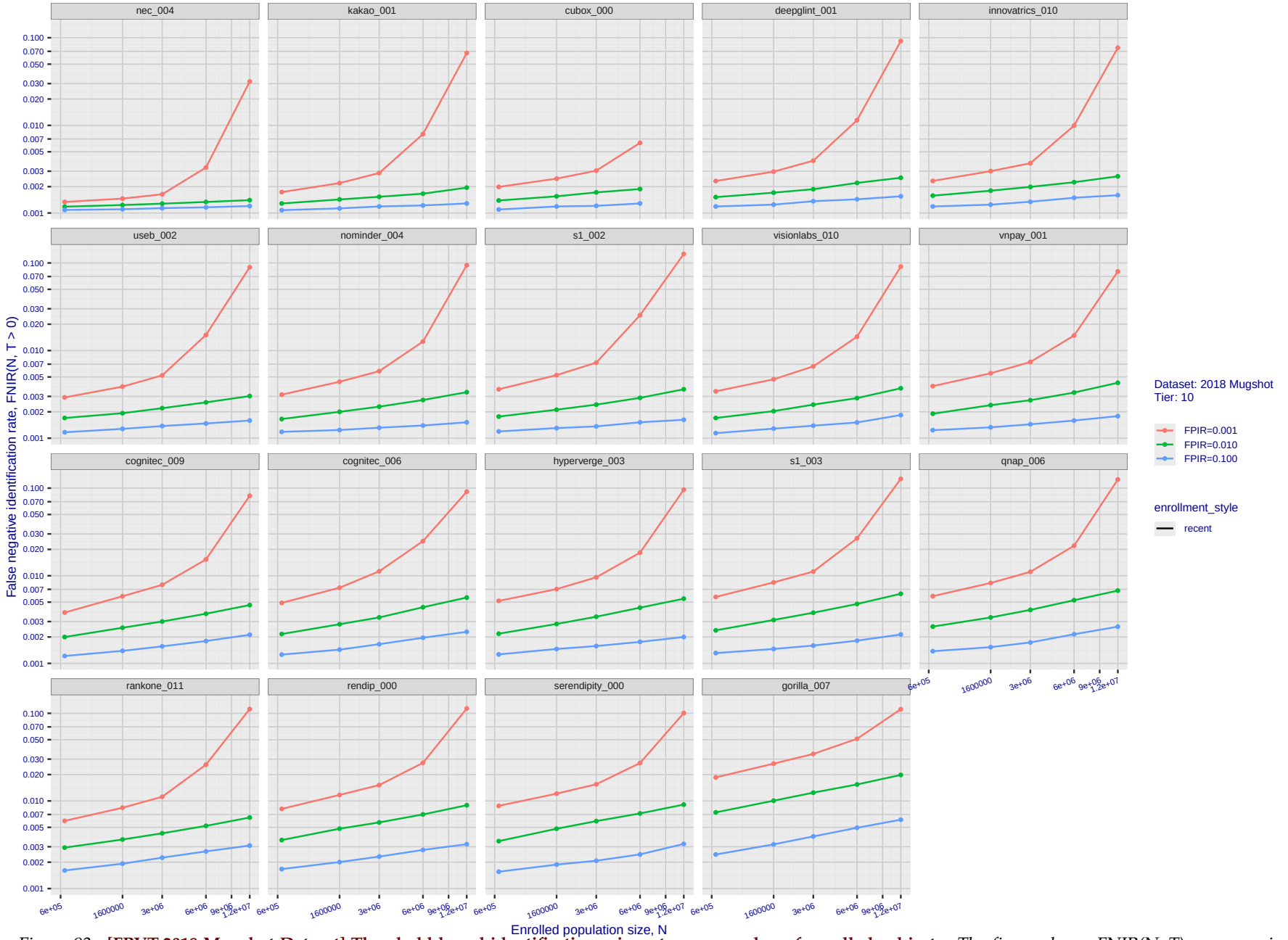

Figure 93: **[FRVT-2018 Mugshot Dataset] Threshold-based identification miss rates vs. number of enrolled subjects**. *The figure shows FNIR(N, T) across various gallery sizes when the threshold is set to achieve the given FPIRs. The rank criterion is irrelevant at high thresholds as mates are always at rank 1. The results are computed from the trials listed in rows 1-10 of Table 1. Less accurate algorithms were not run on large N, so results are missing. For clarity, results are sorted and reported into tiers spanning multiple pages. The tiering criteria is complicated: First paging by FNIR(N_b, 1, 0), then sorting by median FNIR(N_b, T), N_b = 640 000.*

This publication is available free of charge from: https://doi.org/10.6028/NIST.IR.8271

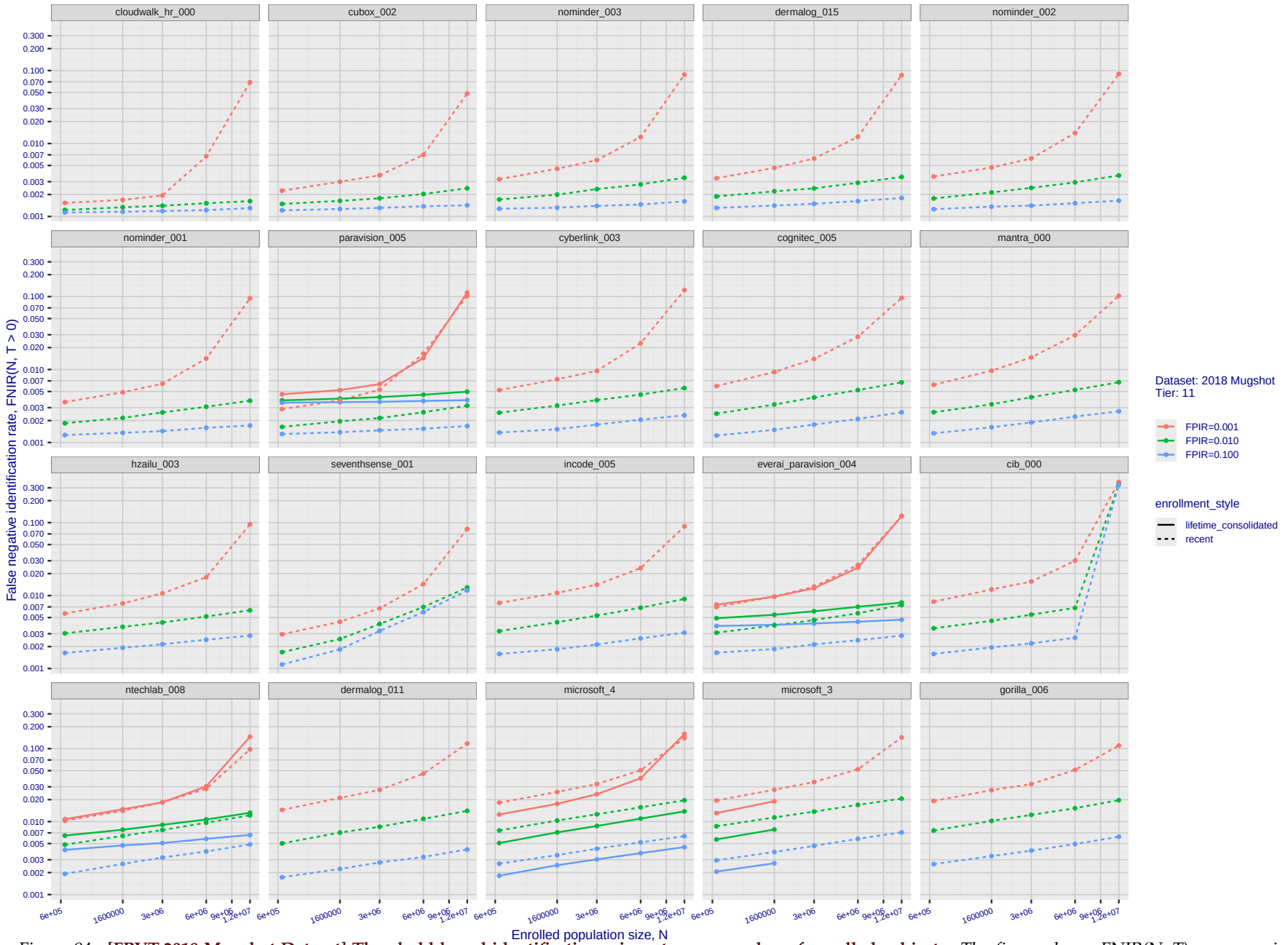

Figure 94: **[FRVT-2018 Mugshot Dataset] Threshold-based identification miss rates vs. number of enrolled subjects**. *The figure shows FNIR(N, T) across various gallery sizes when the threshold is set to achieve the given FPIRs. The rank criterion is irrelevant at high thresholds as mates are always at rank 1. The results are computed from the trials listed in rows 1-10 of Table 1. Less accurate algorithms were not run on large N, so results are missing. For clarity, results are sorted and reported into tiers spanning multiple pages. The tiering criteria is complicated: First paging by FNIR(N_b, 1, 0), then sorting by median FNIR(N_b, T), N_b = 640 000.*

This publication is available free of charge from: https://doi.org/10.6028/NIST.IR.8271

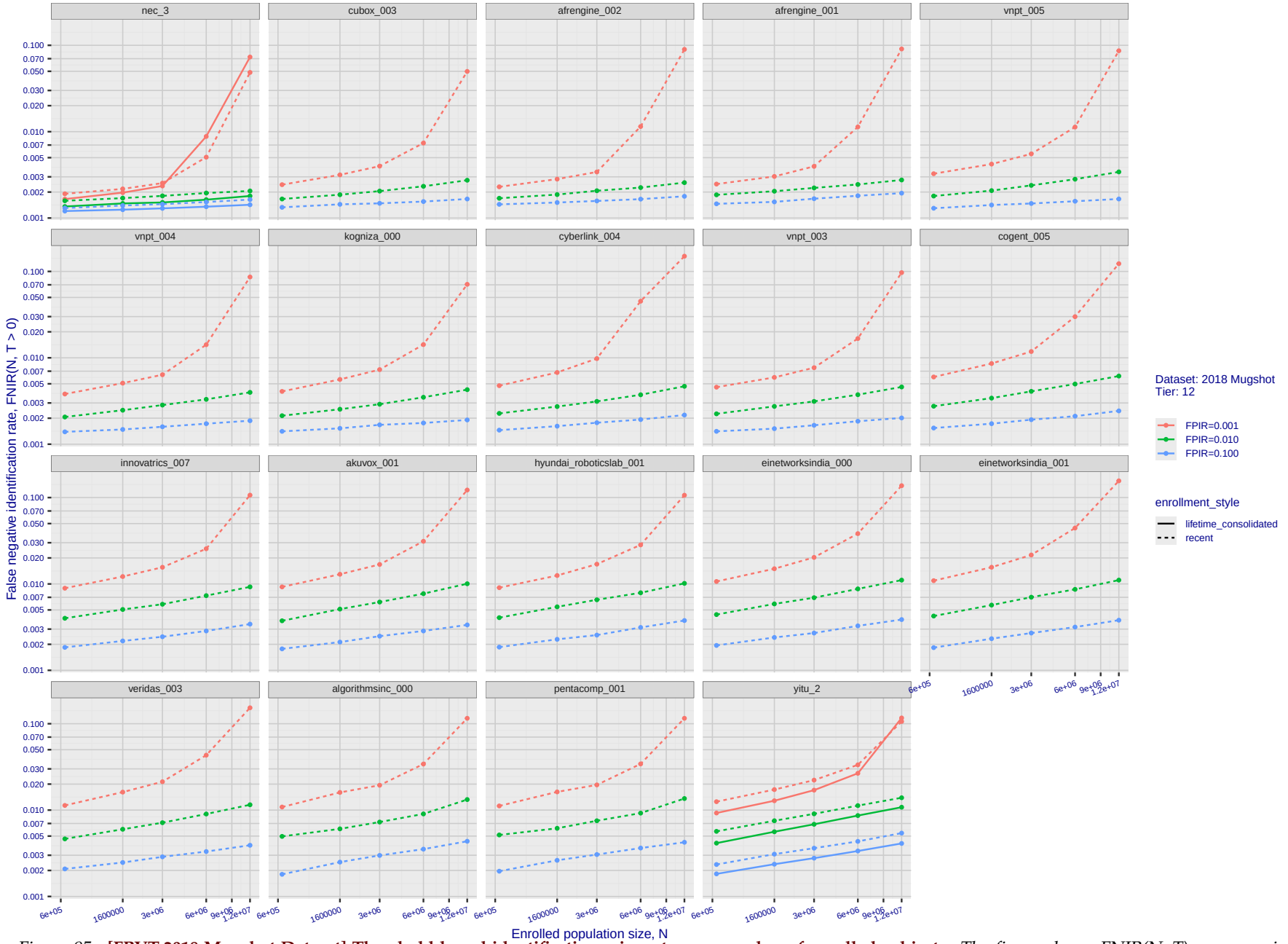

Figure 95: **[FRVT-2018 Mugshot Dataset] Threshold-based identification miss rates vs. number of enrolled subjects**. *The figure shows FNIR(N, T) across various gallery sizes when the threshold is set to achieve the given FPIRs. The rank criterion is irrelevant at high thresholds as mates are always at rank 1. The results are computed from the trials listed in rows 1-10 of Table 1. Less accurate algorithms were not run on large N, so results are missing. For clarity, results are sorted and reported into tiers spanning multiple pages. The tiering criteria is complicated: First paging by FNIR(N_b, 1, 0), then sorting by median FNIR(N_b, T), N_b = 640 000.*

2026/01/09 20:40:38

FNIR(N, R, T) = False neg. identification rate
FPIR(N, T) = False pos. identification rate
N = Num. enrolled subjects
R = Num. candidates examined
T = Threshold
T = 0 → Investigation
T > 0 → Identification

This publication is available free of charge from: https://doi.org/10.6028/NIST.IR.8271

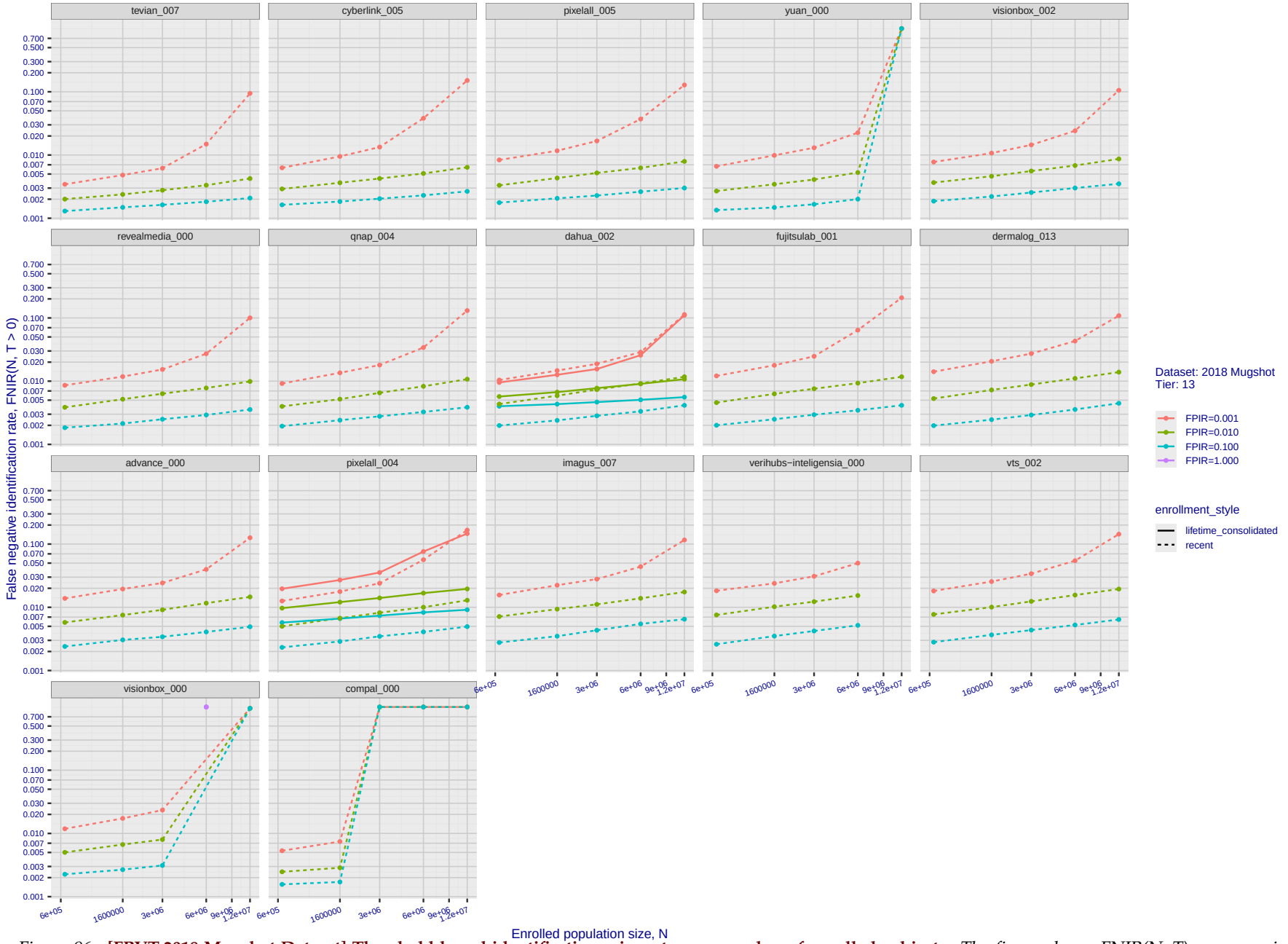

Figure 96: **[FRVT-2018 Mugshot Dataset] Threshold-based identification miss rates vs. number of enrolled subjects**. *The figure shows FNIR(N, T) across various gallery sizes when the threshold is set to achieve the given FPIRs. The rank criterion is irrelevant at high thresholds as mates are always at rank 1. The results are computed from the trials listed in rows 1-10 of Table 1. Less accurate algorithms were not run on large N, so results are missing. For clarity, results are sorted and reported into tiers spanning multiple pages. The tiering criteria is complicated: First paging by FNIR(N_b, 1, 0), then sorting by median FNIR(N_b, T), N_b = 640 000.*

2026/01/09 20:40:38

FNIR(N, R, T) = False neg. identification rate
FPIR(N, T) = False pos. identification rate
N = Num. enrolled subjects
R = Num. candidates examined
T = Threshold
T = 0 → Investigation
T > 0 → Identification

This publication is available free of charge from: https://doi.org/10.6028/NIST.IR.8271

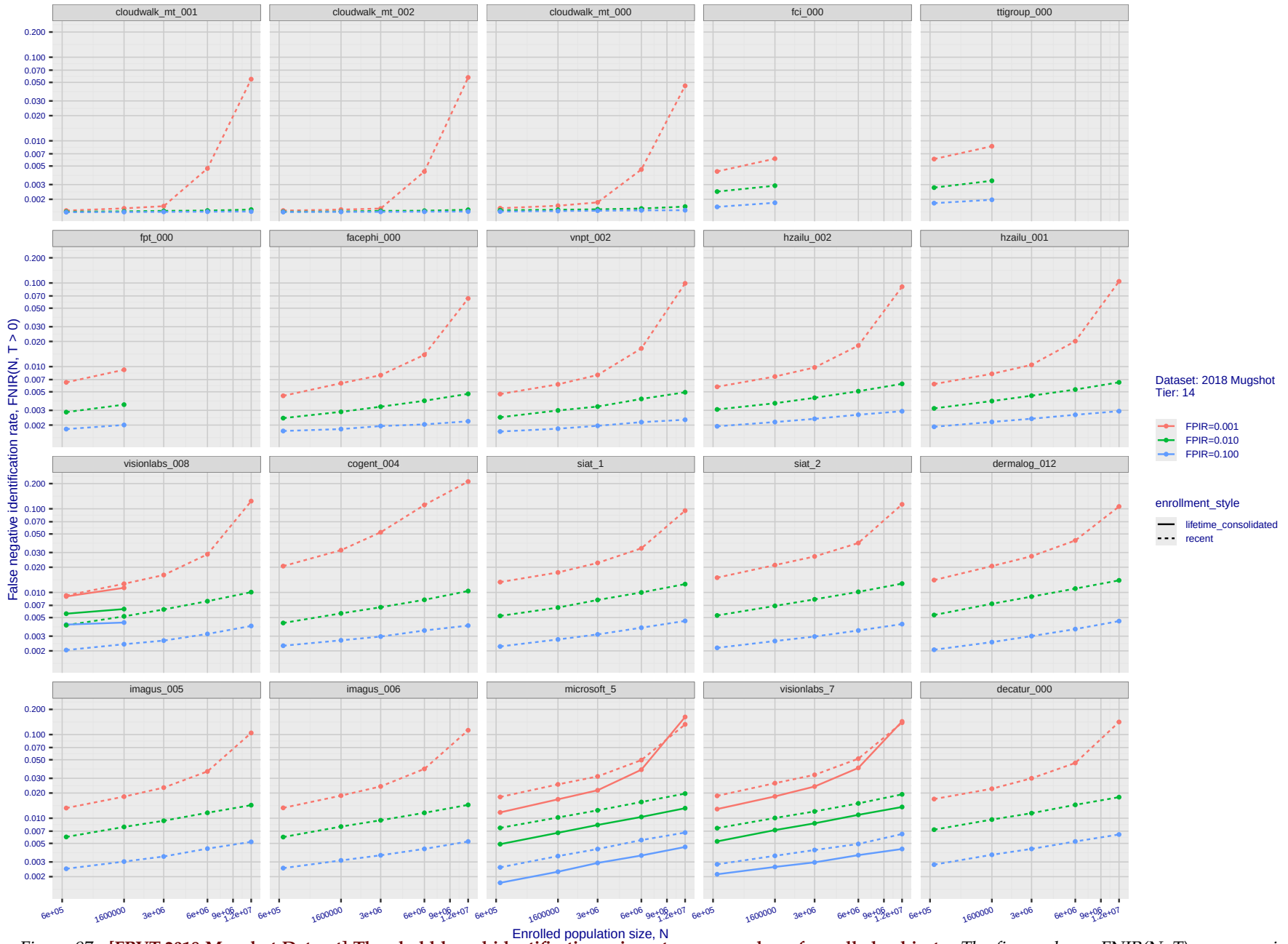

Figure 97: **[FRVT-2018 Mugshot Dataset] Threshold-based identification miss rates vs. number of enrolled subjects**. *The figure shows FNIR(N, T) across various gallery sizes when the threshold is set to achieve the given FPIRs. The rank criterion is irrelevant at high thresholds as mates are always at rank 1. The results are computed from the trials listed in rows 1-10 of Table 1. Less accurate algorithms were not run on large N, so results are missing. For clarity, results are sorted and reported into tiers spanning multiple pages. The tiering criteria is complicated: First paging by FNIR(N_b, 1, 0), then sorting by median FNIR(N_b, T), N_b = 640 000.*

2026/01/09 20:40:38
FNIR(N, R, T) = False neg. identification rate
FPIR(N, T) = False pos. identification rate
N = Num. enrolled subjects
R = Num. candidates examined
T = Threshold
T = 0 → Investigation
T > 0 → Identification

This publication is available free of charge from: https://doi.org/10.6028/NIST.IR.8271

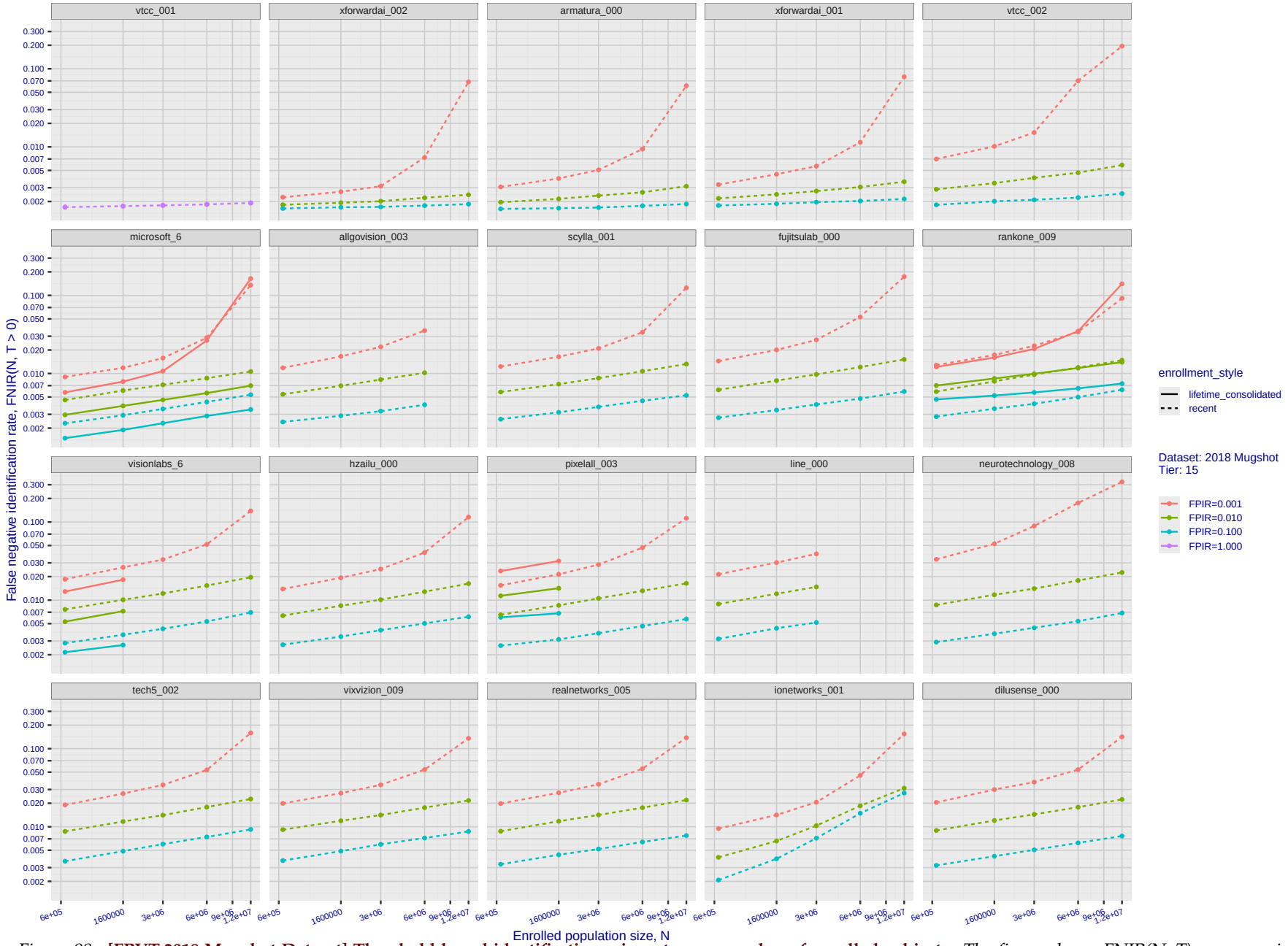

Figure 98: **[FRVT-2018 Mugshot Dataset] Threshold-based identification miss rates vs. number of enrolled subjects**. *The figure shows FNIR(N, T) across various gallery sizes when the threshold is set to achieve the given FPIRs. The rank criterion is irrelevant at high thresholds as mates are always at rank 1. The results are computed from the trials listed in rows 1-10 of Table 1. Less accurate algorithms were not run on large N, so results are missing. For clarity, results are sorted and reported into tiers spanning multiple pages. The tiering criteria is complicated: First paging by FNIR(N_b, 1, 0), then sorting by median FNIR(N_b, T), N_b = 640 000.*

This publication is available free of charge from: https://doi.org/10.6028/NIST.IR.8271

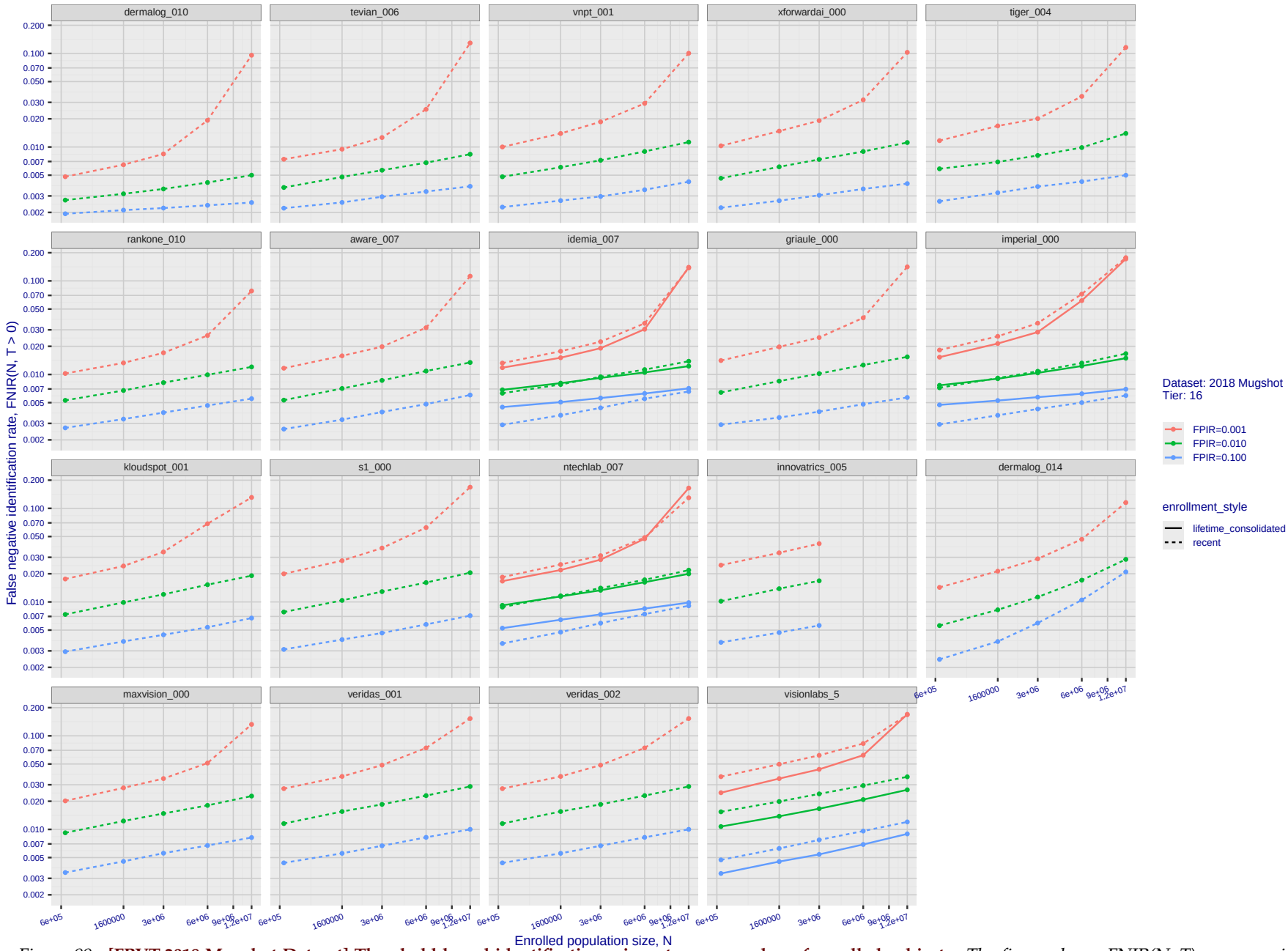

Figure 99: **[FRVT-2018 Mugshot Dataset] Threshold-based identification miss rates vs. number of enrolled subjects**. *The figure shows FNIR(N, T) across various gallery sizes when the threshold is set to achieve the given FPIRs. The rank criterion is irrelevant at high thresholds as mates are always at rank 1. The results are computed from the trials listed in rows 1-10 of Table 1. Less accurate algorithms were not run on large N, so results are missing. For clarity, results are sorted and reported into tiers spanning multiple pages. The tiering criteria is complicated: First paging by FNIR(N_b, 1, 0), then sorting by median FNIR(N_b, T), N_b = 640 000.*

2026/01/09 20:40:38

FNIR(N, R, T) = FPIR(N, T) =

False neg. identification rate
False pos. identification rate

N = Num. enrolled subjects
R = Num. candidates examined

T = Threshold

T = 0 → Investigation
T > 0 → Identification

This publication is available free of charge from: https://doi.org/10.6028/NIST.IR.8271

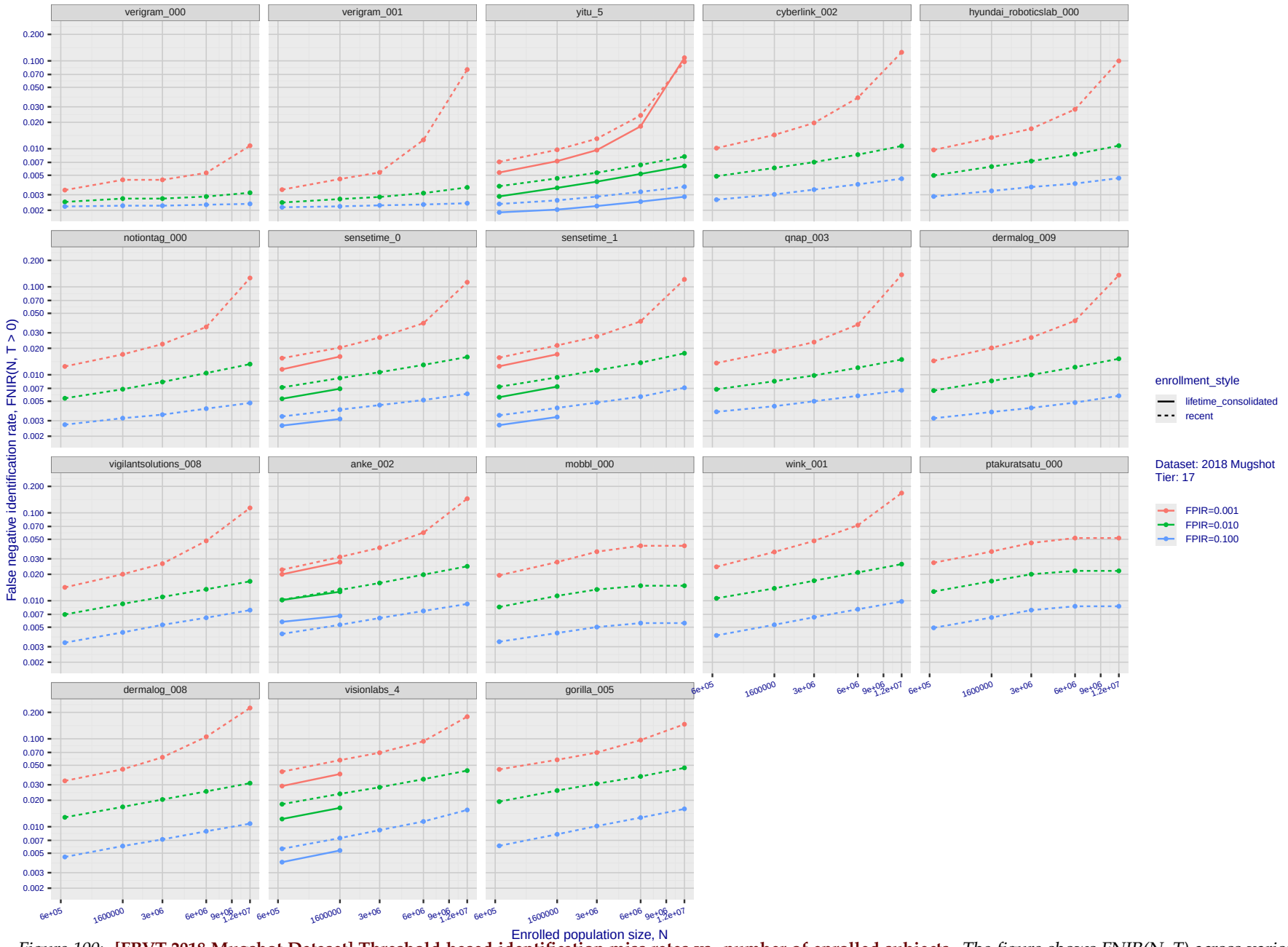

Figure 100: **[FRVT-2018 Mugshot Dataset] Threshold-based identification miss rates vs. number of enrolled subjects**. *The figure shows FNIR(N, T) across various gallery sizes when the threshold is set to achieve the given FPIRs. The rank criterion is irrelevant at high thresholds as mates are always at rank 1. The results are computed from the trials listed in rows 1-10 of Table 1. Less accurate algorithms were not run on large N, so results are missing. For clarity, results are sorted and reported into tiers spanning multiple pages. The tiering criteria is complicated: First paging by FNIR(N_b, 1, 0), then sorting by median FNIR(N_b, T), N_b = 640 000.*

2026/01/09 20:40:38

FNIR(N, R, T) = False neg. identification rate
FPIR(N, T) = False pos. identification rate
N = Num. enrolled subjects
R = Num. candidates examined
T = Threshold
T = 0 → Investigation
T > 0 → Identification

This publication is available free of charge from: https://doi.org/10.6028/NIST.IR.8271

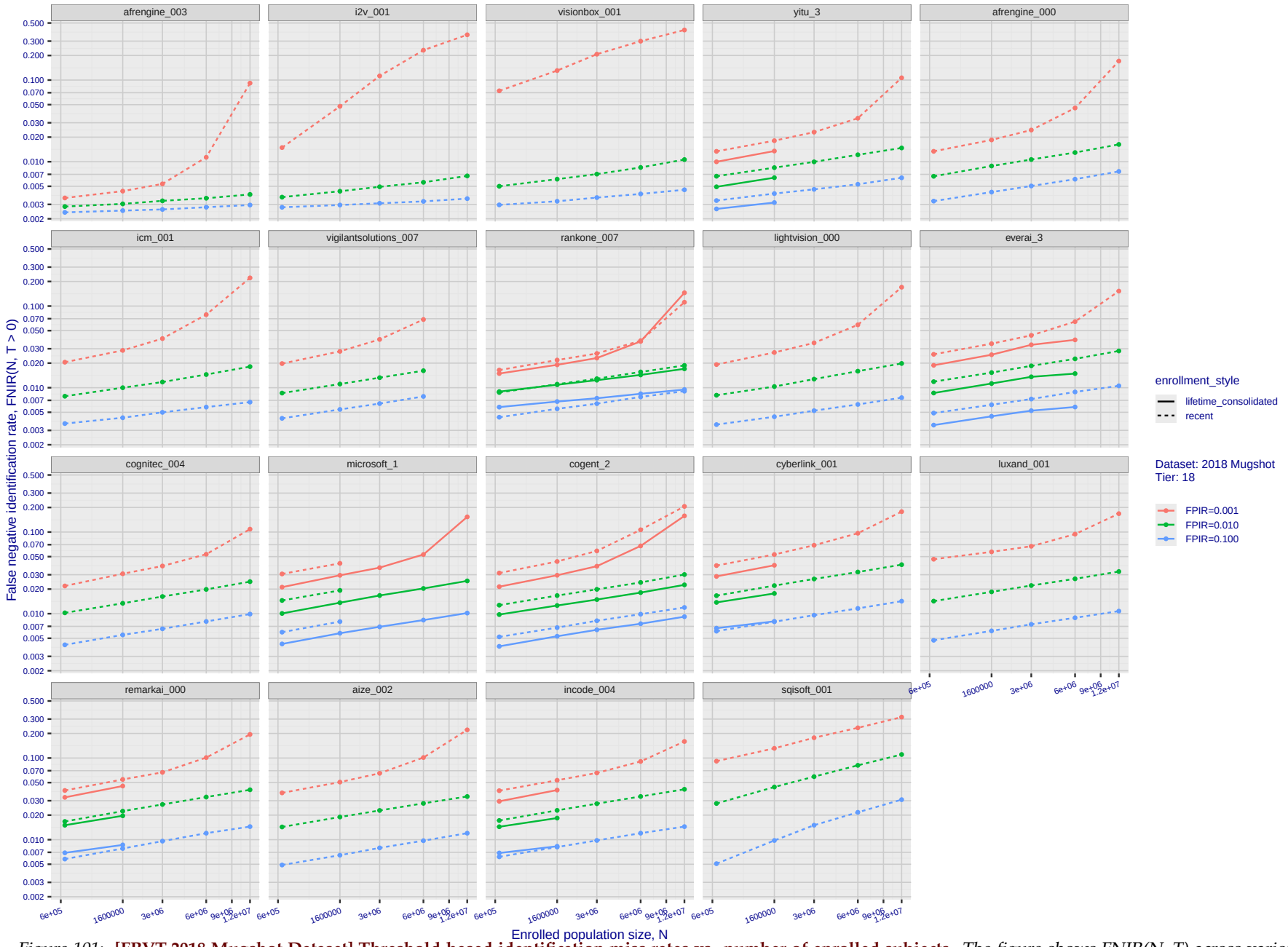

Figure 101: **[FRVT-2018 Mugshot Dataset] Threshold-based identification miss rates vs. number of enrolled subjects**. *The figure shows FNIR(N, T) across various gallery sizes when the threshold is set to achieve the given FPIRs. The rank criterion is irrelevant at high thresholds as mates are always at rank 1. The results are computed from the trials listed in rows 1-10 of Table 1. Less accurate algorithms were not run on large N, so results are missing. For clarity, results are sorted and reported into tiers spanning multiple pages. The tiering criteria is complicated: First paging by FNIR(N_b, 1, 0), then sorting by median FNIR(N_b, T), N_b = 640 000.*

2026/01/09 20:40:38

FNIR(N, R, T) = False neg. identification rate
FPIR(N, T) = False pos. identification rate

N = Num. enrolled subjects
R = Num. candidates examined

T = Threshold

T = 0 → Investigation
T > 0 → Identification

This publication is available free of charge from: https://doi.org/10.6028/NIST.IR.8271

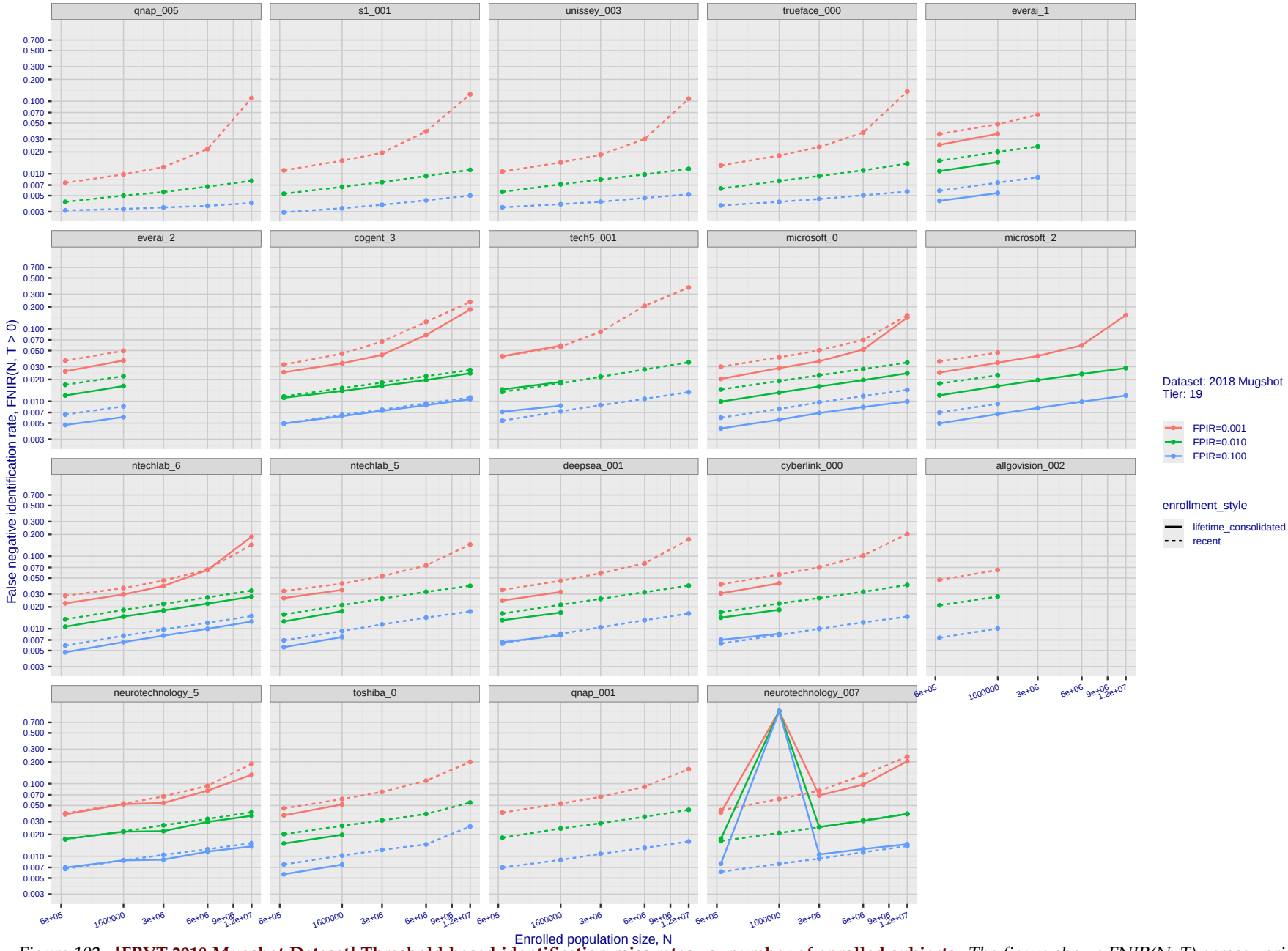

Figure 102: **[FRVT-2018 Mugshot Dataset] Threshold-based identification miss rates vs. number of enrolled subjects**. *The figure shows FNIR(N, T) across various gallery sizes when the threshold is set to achieve the given FPIRs. The rank criterion is irrelevant at high thresholds as mates are always at rank 1. The results are computed from the trials listed in rows 1-10 of Table 1. Less accurate algorithms were not run on large N, so results are missing. For clarity, results are sorted and reported into tiers spanning multiple pages. The tiering criteria is complicated: First paging by FNIR(N_b, 1, 0), then sorting by median FNIR(N_b, T), N_b = 640 000.*

This publication is available free of charge from: https://doi.org/10.6028/NIST.IR.8271

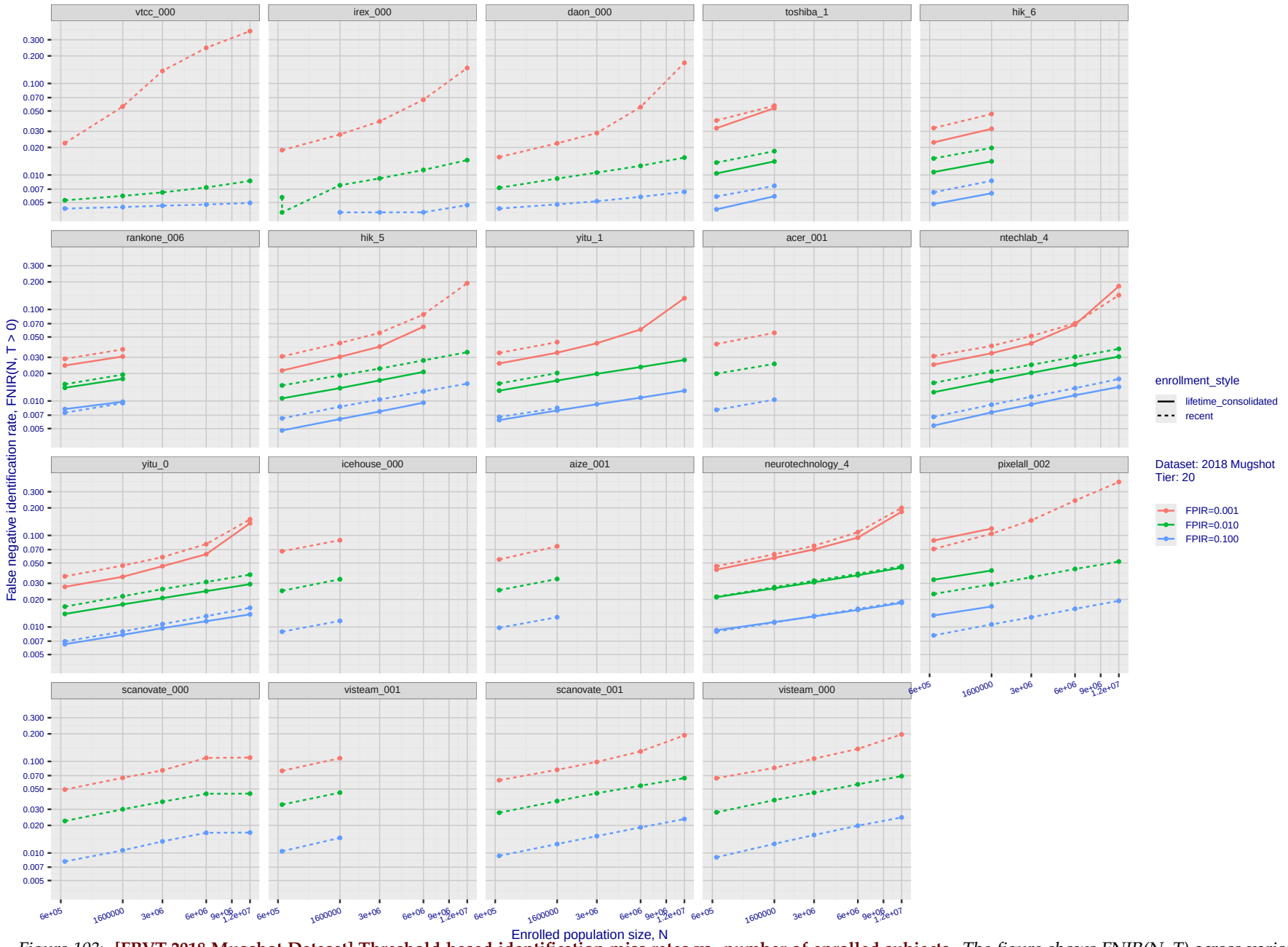

Figure 103: **[FRVT-2018 Mugshot Dataset] Threshold-based identification miss rates vs. number of enrolled subjects**. *The figure shows FNIR(N, T) across various gallery sizes when the threshold is set to achieve the given FPIRs. The rank criterion is irrelevant at high thresholds as mates are always at rank 1. The results are computed from the trials listed in rows 1-10 of Table 1. Less accurate algorithms were not run on large N, so results are missing. For clarity, results are sorted and reported into tiers spanning multiple pages. The tiering criteria is complicated: First paging by FNIR(N_b, 1, 0), then sorting by median FNIR(N_b, T), N_b = 640 000.*

2026/01/09 20:40:38
FNIR(N, R, T) = False neg. identification rate
FPIR(N, T) = False pos. identification rate
N = Num. enrolled subjects
R = Num. candidates examined
T = Threshold
T = 0 → Investigation
T > 0 → Identification

This publication is available free of charge from: https://doi.org/10.6028/NIST.IR.8271

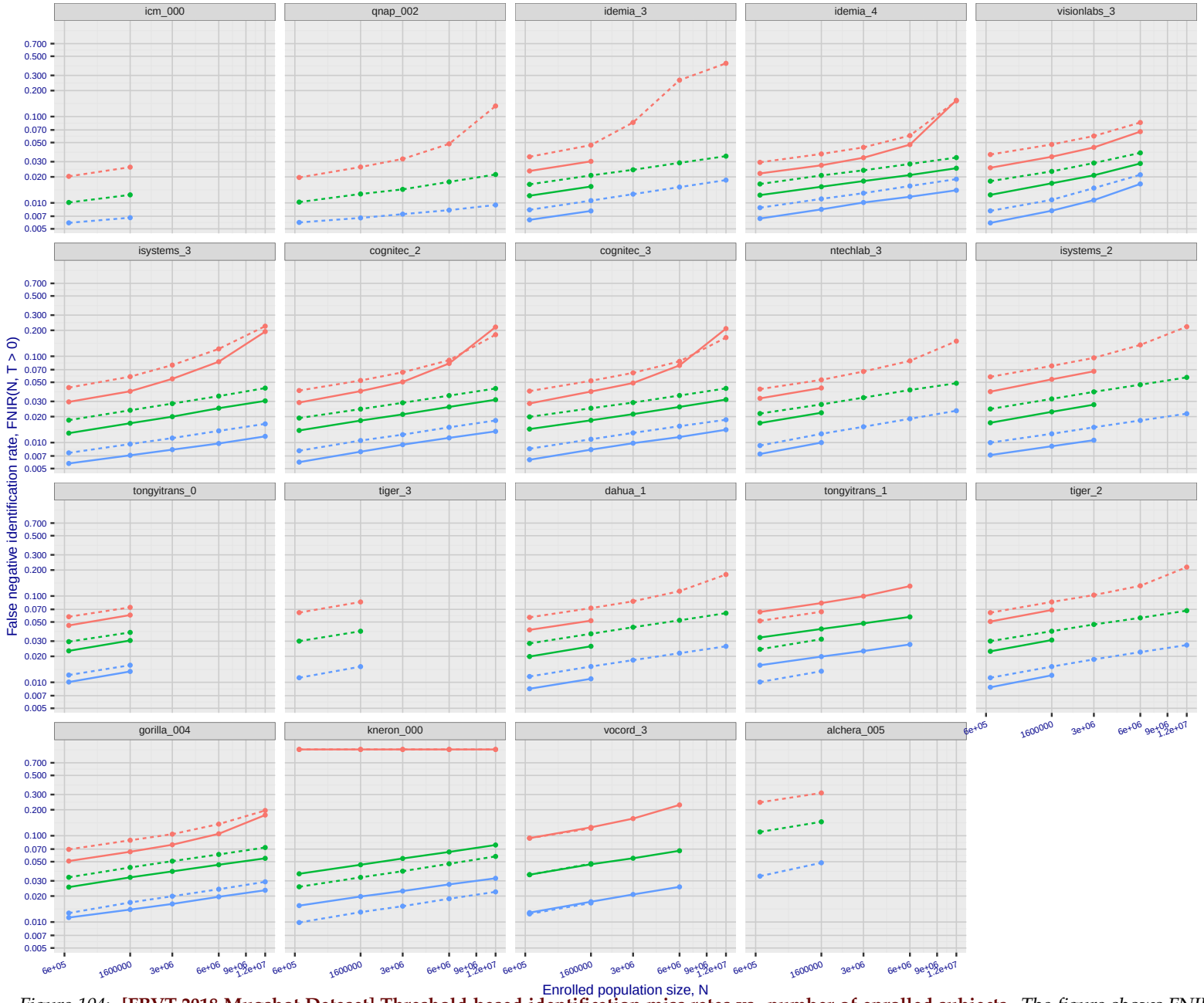

Figure 104: **[FRVT-2018 Mugshot Dataset] Threshold-based identification miss rates vs. number of enrolled subjects**. *The figure shows FNIR(N, T) across various gallery sizes when the threshold is set to achieve the given FPIRs. The rank criterion is irrelevant at high thresholds as mates are always at rank 1. The results are computed from the trials listed in rows 1-10 of Table 1. Less accurate algorithms were not run on large N, so results are missing. For clarity, results are sorted and reported into tiers spanning multiple pages. The tiering criteria is complicated: First paging by FNIR(N_b, 1, 0), then sorting by median FNIR(N_b, T), N_b = 640 000.*

FNIR(N, R, T) = False neg. identification rate
FPIR(N, T) = False pos. identification rate
N = Num. enrolled subjects
R = Num. candidates examined
T = Threshold
T = 0 → Investigation
T > 0 → Identification

This publication is available free of charge from: https://doi.org/10.6028/NIST.IR.8271

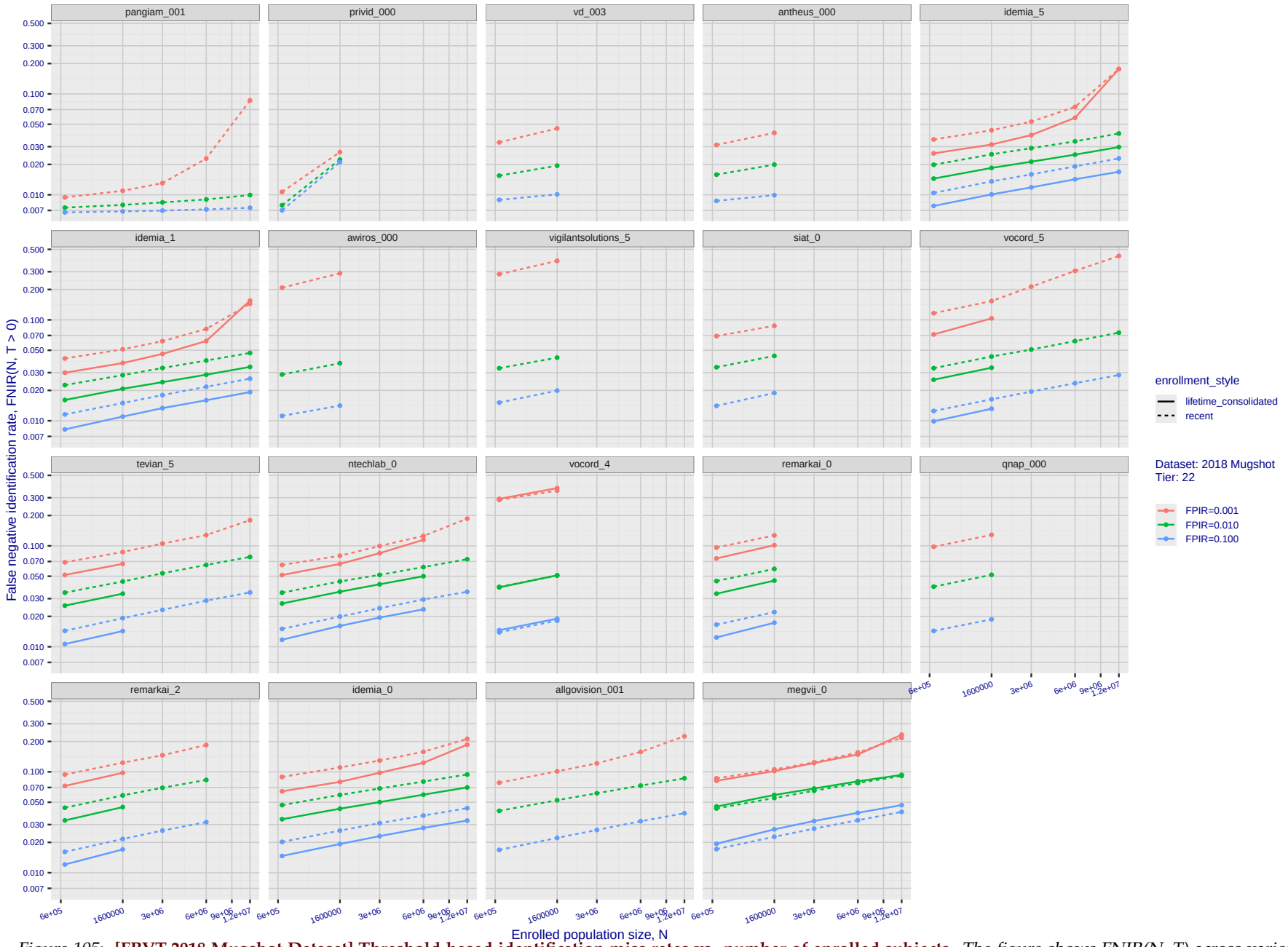

Figure 105: **[FRVT-2018 Mugshot Dataset] Threshold-based identification miss rates vs. number of enrolled subjects**. *The figure shows FNIR(N, T) across various gallery sizes when the threshold is set to achieve the given FPIRs. The rank criterion is irrelevant at high thresholds as mates are always at rank 1. The results are computed from the trials listed in rows 1-10 of Table 1. Less accurate algorithms were not run on large N, so results are missing. For clarity, results are sorted and reported into tiers spanning multiple pages. The tiering criteria is complicated: First paging by FNIR(N_b, 1, 0), then sorting by median FNIR(N_b, T), N_b = 640 000.*

2026/01/09 20:40:38

FNIR(N, R, T) = False neg. identification rate
FPIR(N, T) = False pos. identification rate
N = Num. enrolled subjects
R = Num. candidates examined
T = Threshold
T = 0 → Investigation
T > 0 → Identification

This publication is available free of charge from: https://doi.org/10.6028/NIST.IR.8271

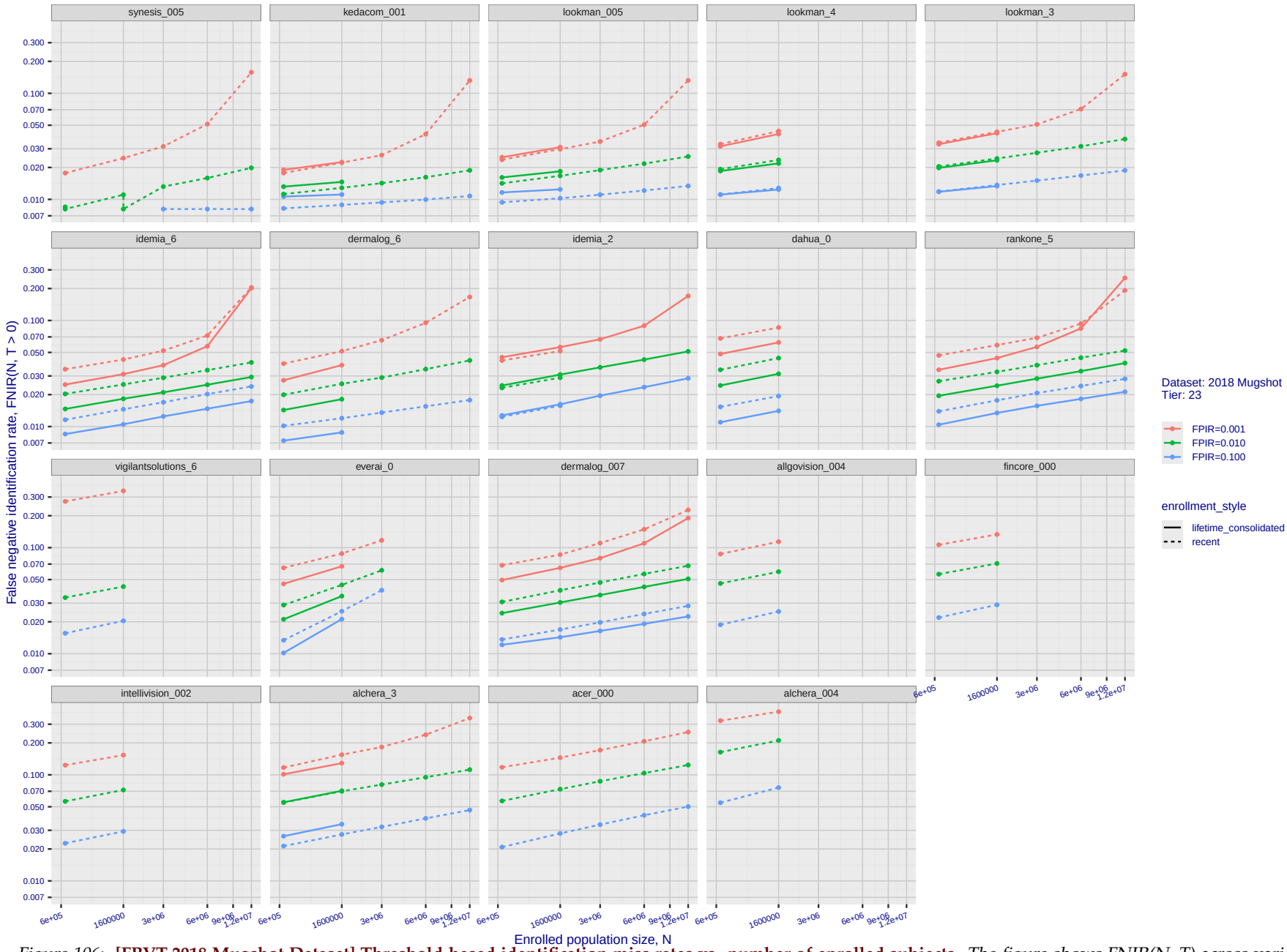

Figure 106: **[FRVT-2018 Mugshot Dataset] Threshold-based identification miss rates vs. number of enrolled subjects**. *The figure shows FNIR(N, T) across various gallery sizes when the threshold is set to achieve the given FPIRs. The rank criterion is irrelevant at high thresholds as mates are always at rank 1. The results are computed from the trials listed in rows 1-10 of Table 1. Less accurate algorithms were not run on large N, so results are missing. For clarity, results are sorted and reported into tiers spanning multiple pages. The tiering criteria is complicated: First paging by FNIR(N_b, 1, 0), then sorting by median FNIR(N_b, T), N_b = 640 000.*

2026/01/09 20:40:38

FNIR(N, R, T) = False neg. identification rate
FPIR(N, T) = False pos. identification rate
N = Num. enrolled subjects
R = Num. candidates examined
T = Threshold
T = 0 → Investigation
T > 0 → Identification

This publication is available free of charge from: https://doi.org/10.6028/NIST.IR.8271

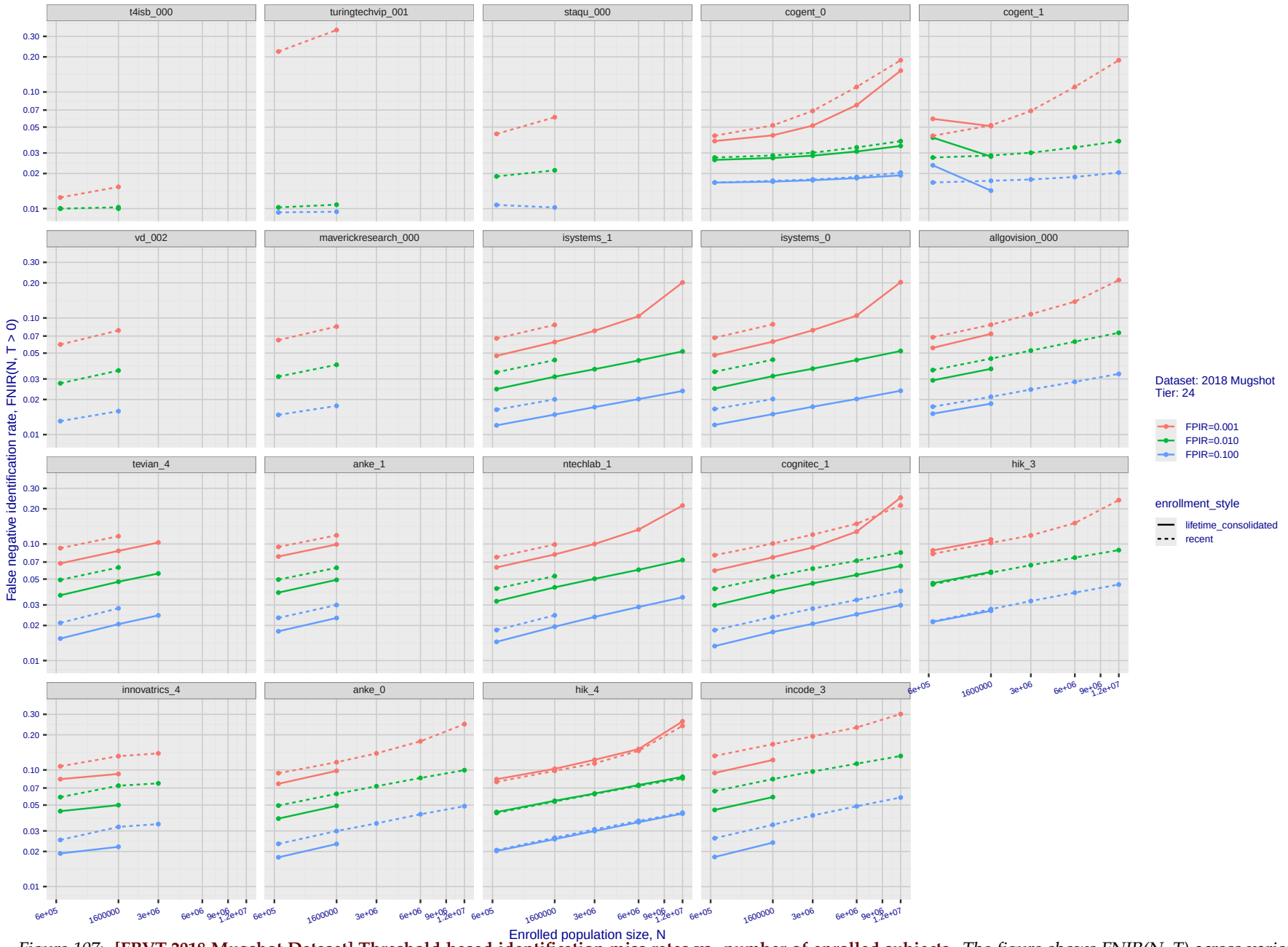

Figure 107: **[FRVT-2018 Mugshot Dataset] Threshold-based identification miss rates vs. number of enrolled subjects**. *The figure shows FNIR(N, T) across various gallery sizes when the threshold is set to achieve the given FPIRs. The rank criterion is irrelevant at high thresholds as mates are always at rank 1. The results are computed from the trials listed in rows 1-10 of Table 1. Less accurate algorithms were not run on large N, so results are missing. For clarity, results are sorted and reported into tiers spanning multiple pages. The tiering criteria is complicated: First paging by FNIR(N_b, 1, 0), then sorting by median FNIR(N_b, T), N_b = 640 000.*

This publication is available free of charge from: https://doi.org/10.6028/NIST.IR.8271

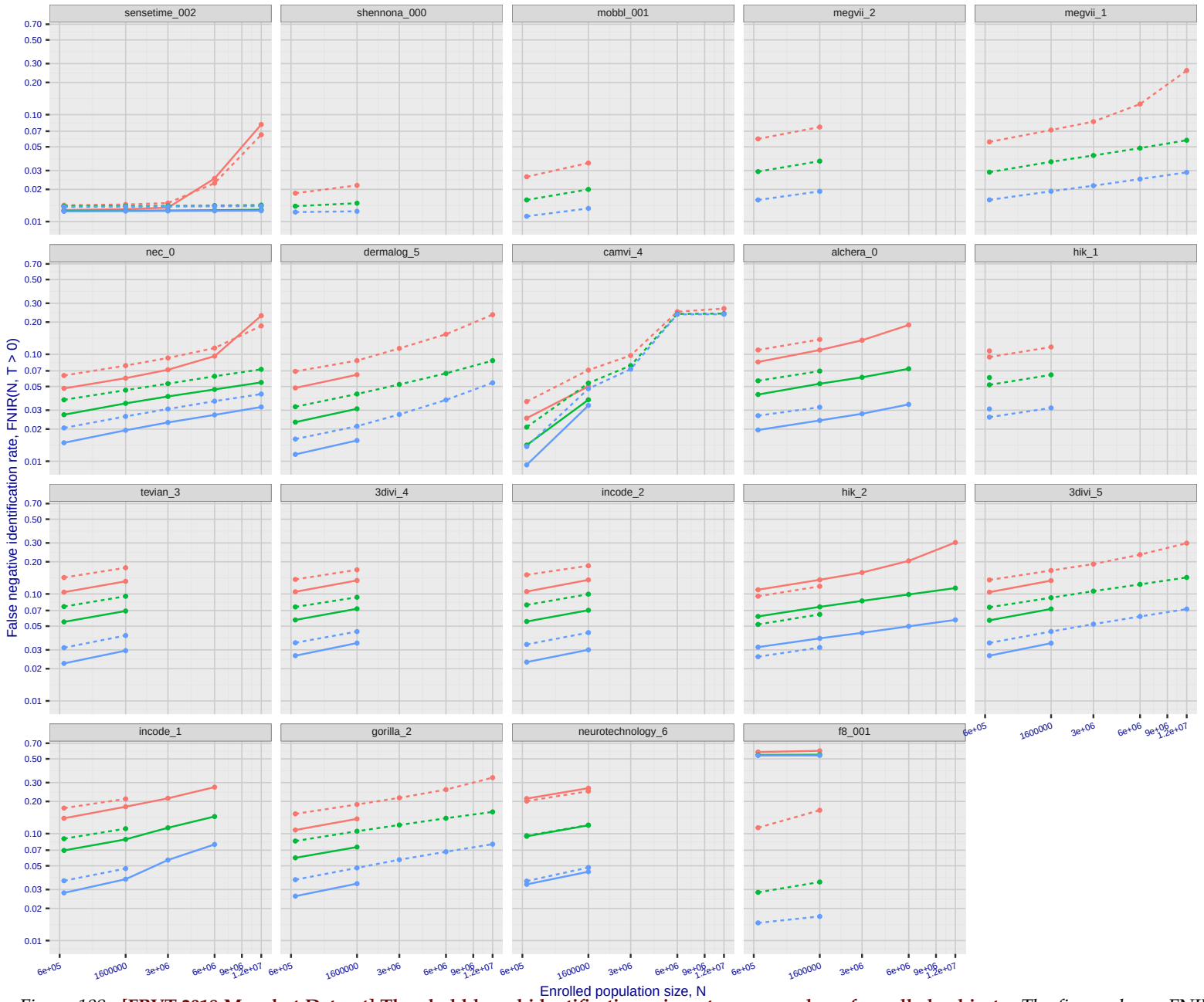

Figure 108: **[FRVT-2018 Mugshot Dataset] Threshold-based identification miss rates vs. number of enrolled subjects**. *The figure shows FNIR(N, T) across various gallery sizes when the threshold is set to achieve the given FPIRs. The rank criterion is irrelevant at high thresholds as mates are always at rank 1. The results are computed from the trials listed in rows 1-10 of Table 1. Less accurate algorithms were not run on large N, so results are missing. For clarity, results are sorted and reported into tiers spanning multiple pages. The tiering criteria is complicated: First paging by FNIR(N_b, 1, 0), then sorting by median FNIR(N_b, T), N_b = 640 000.*

This publication is available free of charge from: https://doi.org/10.6028/NIST.IR.8271

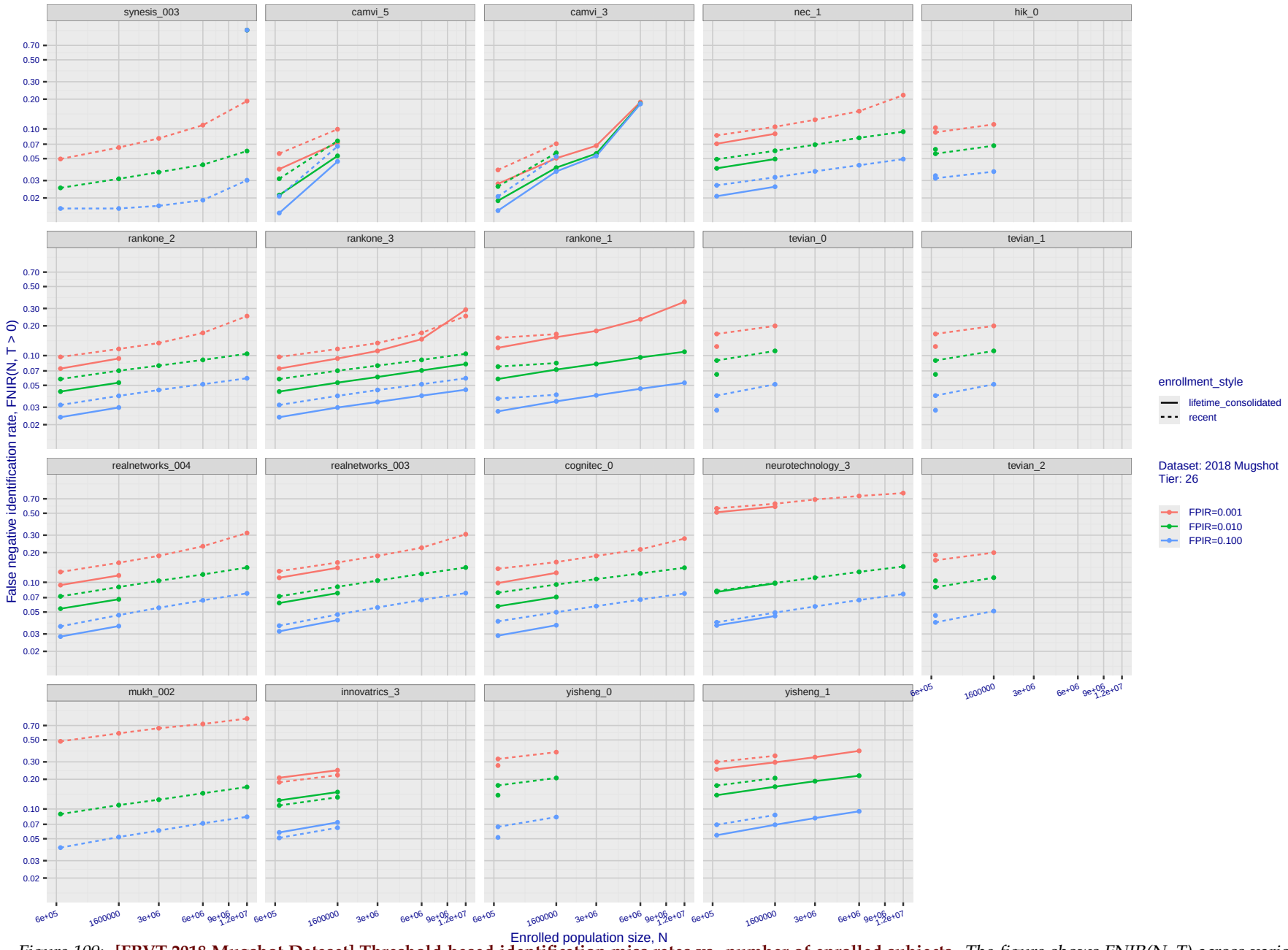

Figure 109: **[FRVT-2018 Mugshot Dataset] Threshold-based identification miss rates vs. number of enrolled subjects**. *The figure shows FNIR(N, T) across various gallery sizes when the threshold is set to achieve the given FPIRs. The rank criterion is irrelevant at high thresholds as mates are always at rank 1. The results are computed from the trials listed in rows 1-10 of Table 1. Less accurate algorithms were not run on large N, so results are missing. For clarity, results are sorted and reported into tiers spanning multiple pages. The tiering criteria is complicated: First paging by FNIR(N_b, 1, 0), then sorting by median FNIR(N_b, T), N_b = 640 000.*

2026/01/09 20:40:38

FNIR(N, R, T) = False neg. identification rate
FPIR(N, T) = False pos. identification rate
N = Num. enrolled subjects
R = Num. candidates examined
T = Threshold
T = 0 → Investigation
T > 0 → Identification

This publication is available free of charge from: https://doi.org/10.6028/NIST.IR.8271

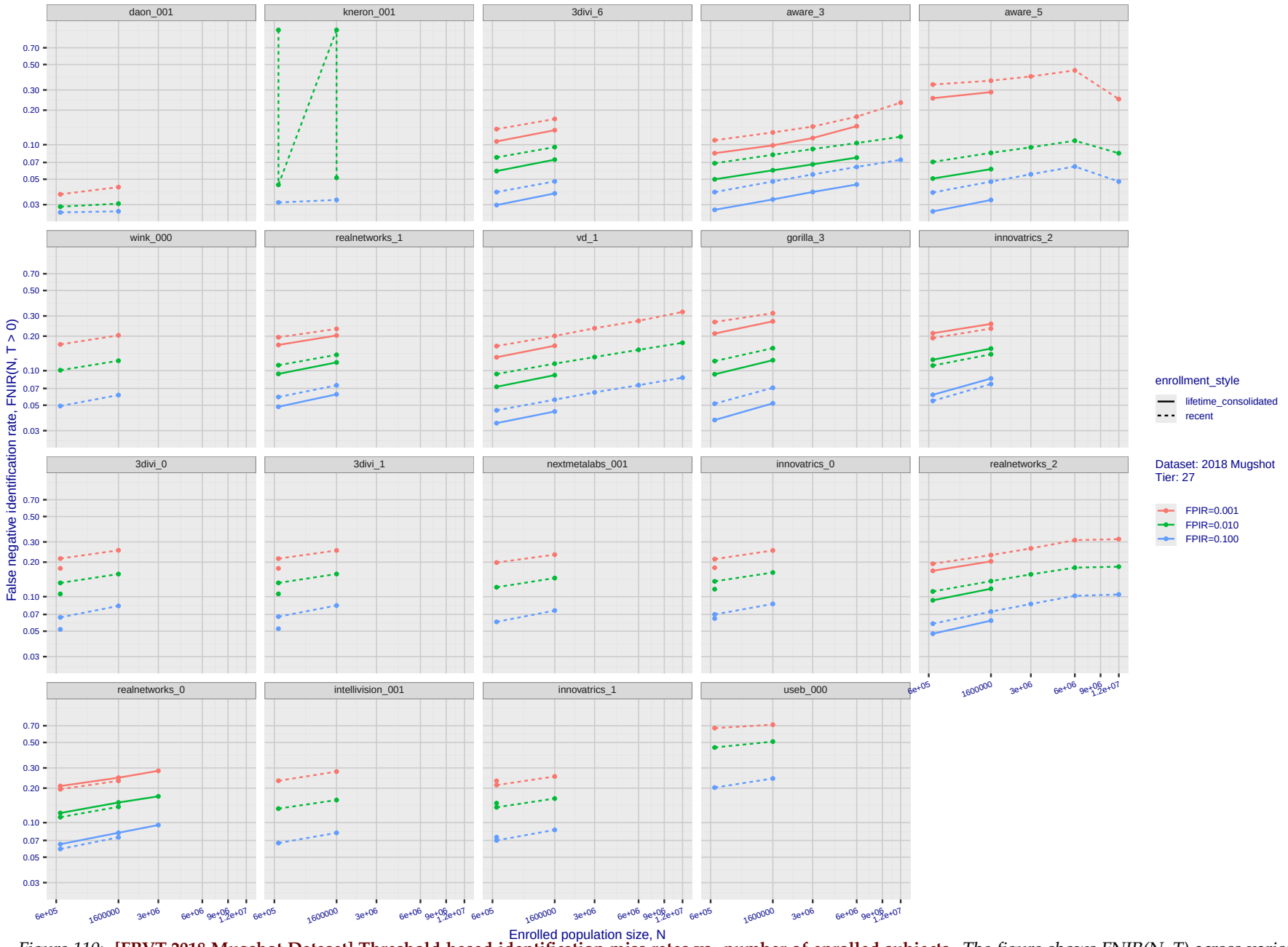

Figure 110: **[FRVT-2018 Mugshot Dataset] Threshold-based identification miss rates vs. number of enrolled subjects**. *The figure shows FNIR(N, T) across various gallery sizes when the threshold is set to achieve the given FPIRs. The rank criterion is irrelevant at high thresholds as mates are always at rank 1. The results are computed from the trials listed in rows 1-10 of Table 1. Less accurate algorithms were not run on large N, so results are missing. For clarity, results are sorted and reported into tiers spanning multiple pages. The tiering criteria is complicated: First paging by FNIR(N_b, 1, 0), then sorting by median FNIR(N_b, T), N_b = 640 000.*

2026/01/09 20:40:38

FNIR(N, R, T) = False neg. identification rate
FPIR(N, T) = False pos. identification rate

N = Num. enrolled subjects
R = Num. candidates examined

T = Threshold

T = 0 → Investigation
T > 0 → Identification

This publication is available free of charge from: https://doi.org/10.6028/NIST.IR.8271

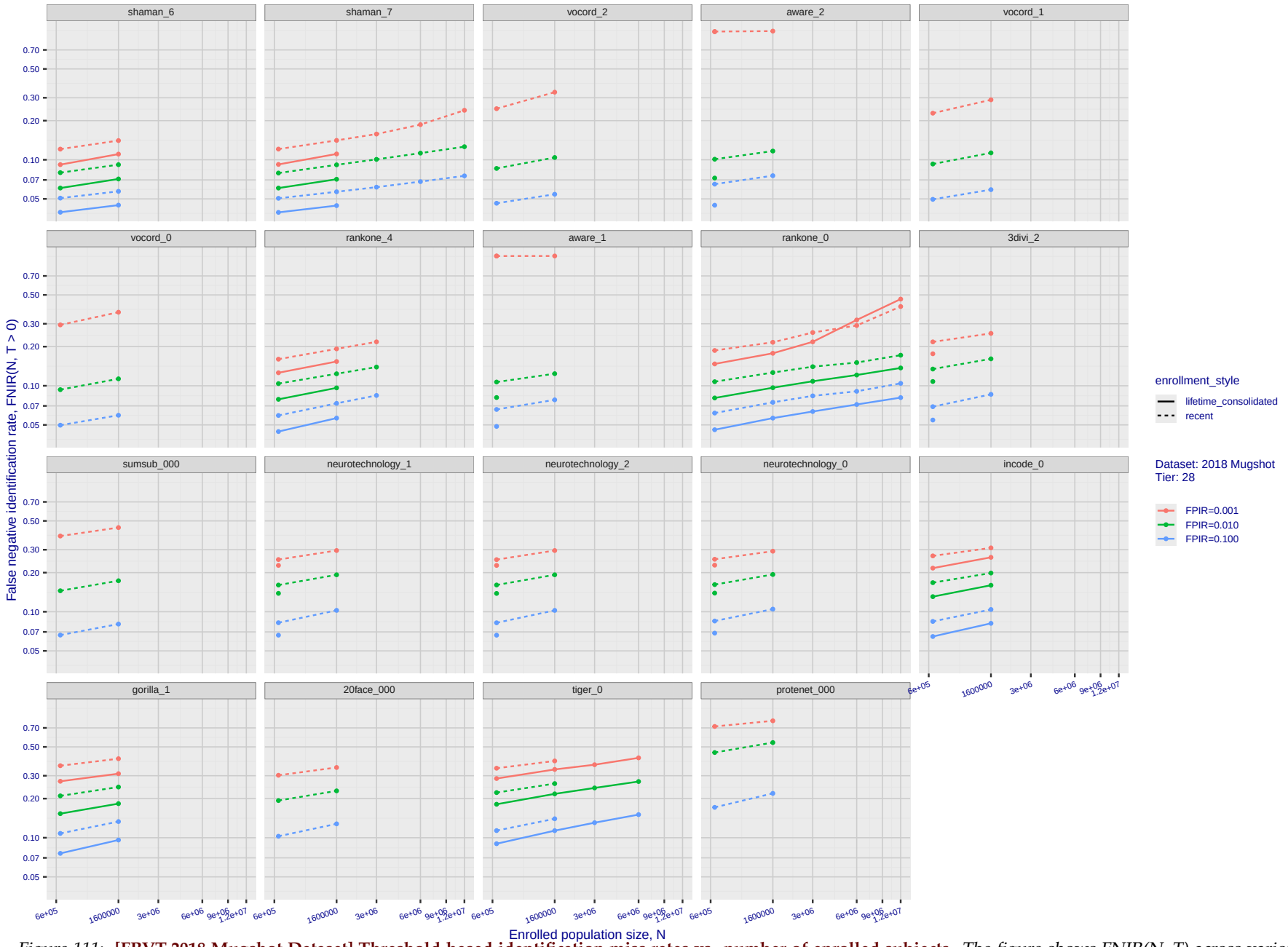

Figure 111: **[FRVT-2018 Mugshot Dataset] Threshold-based identification miss rates vs. number of enrolled subjects**. *The figure shows FNIR(N, T) across various gallery sizes when the threshold is set to achieve the given FPIRs. The rank criterion is irrelevant at high thresholds as mates are always at rank 1. The results are computed from the trials listed in rows 1-10 of Table 1. Less accurate algorithms were not run on large N, so results are missing. For clarity, results are sorted and reported into tiers spanning multiple pages. The tiering criteria is complicated: First paging by FNIR(N_b, 1, 0), then sorting by median FNIR(N_b, T), N_b = 640 000.*

2026/01/09 20:40:38

FNIR(N, R, T) = False neg. identification rate
FPIR(N, T) = False pos. identification rate

N = Num. enrolled subjects
R = Num. candidates examined

T = Threshold

T = 0 → Investigation
T > 0 → Identification

This publication is available free of charge from: https://doi.org/10.6028/NIST.IR.8271

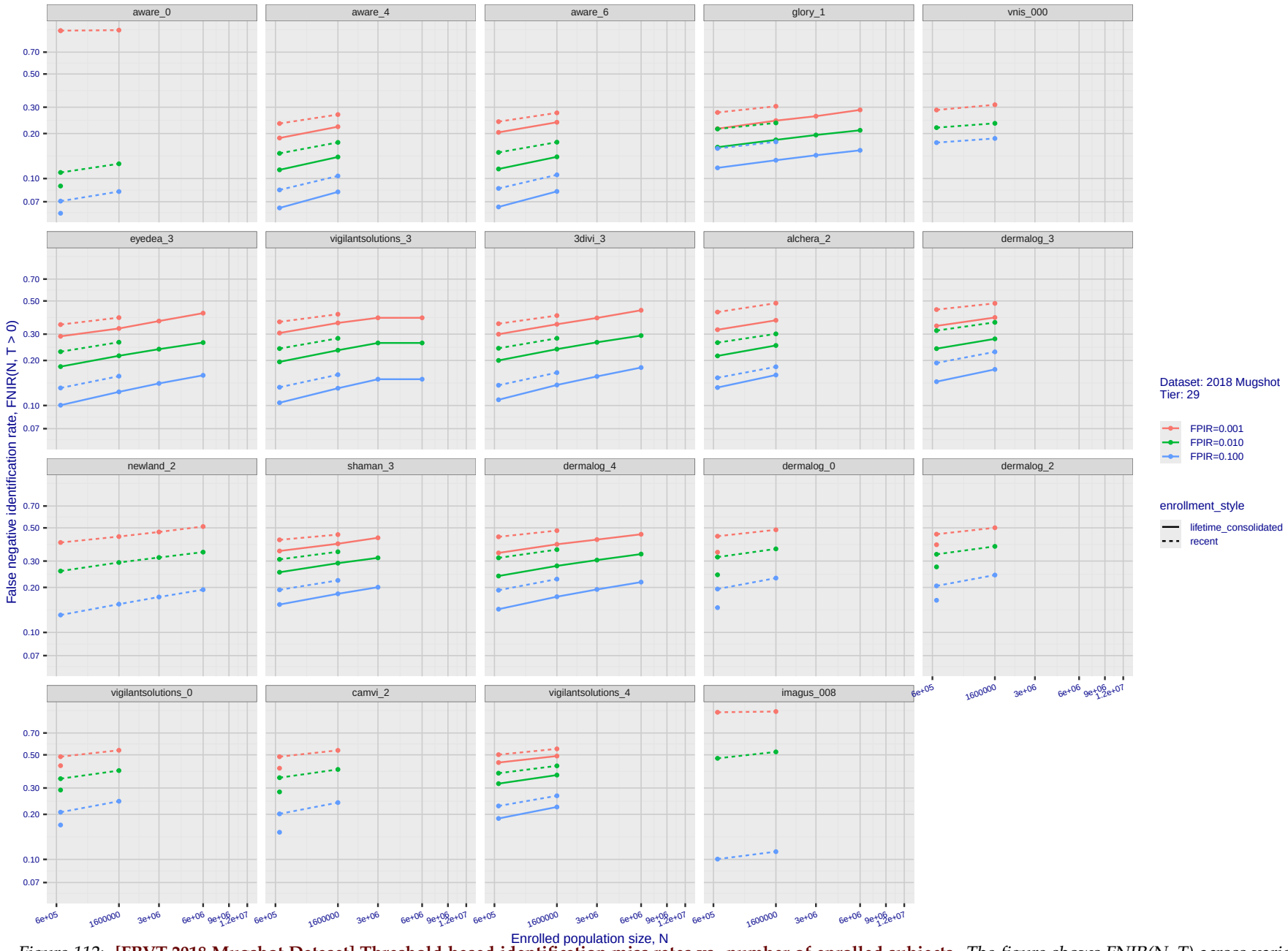

Figure 112: **[FRVT-2018 Mugshot Dataset] Threshold-based identification miss rates vs. number of enrolled subjects**. *The figure shows FNIR(N, T) across various gallery sizes when the threshold is set to achieve the given FPIRs. The rank criterion is irrelevant at high thresholds as mates are always at rank 1. The results are computed from the trials listed in rows 1-10 of Table 1. Less accurate algorithms were not run on large N, so results are missing. For clarity, results are sorted and reported into tiers spanning multiple pages. The tiering criteria is complicated: First paging by FNIR(N_b, 1, 0), then sorting by median FNIR(N_b, T), N_b = 640 000.*

This publication is available free of charge from: https://doi.org/10.6028/NIST.IR.8271

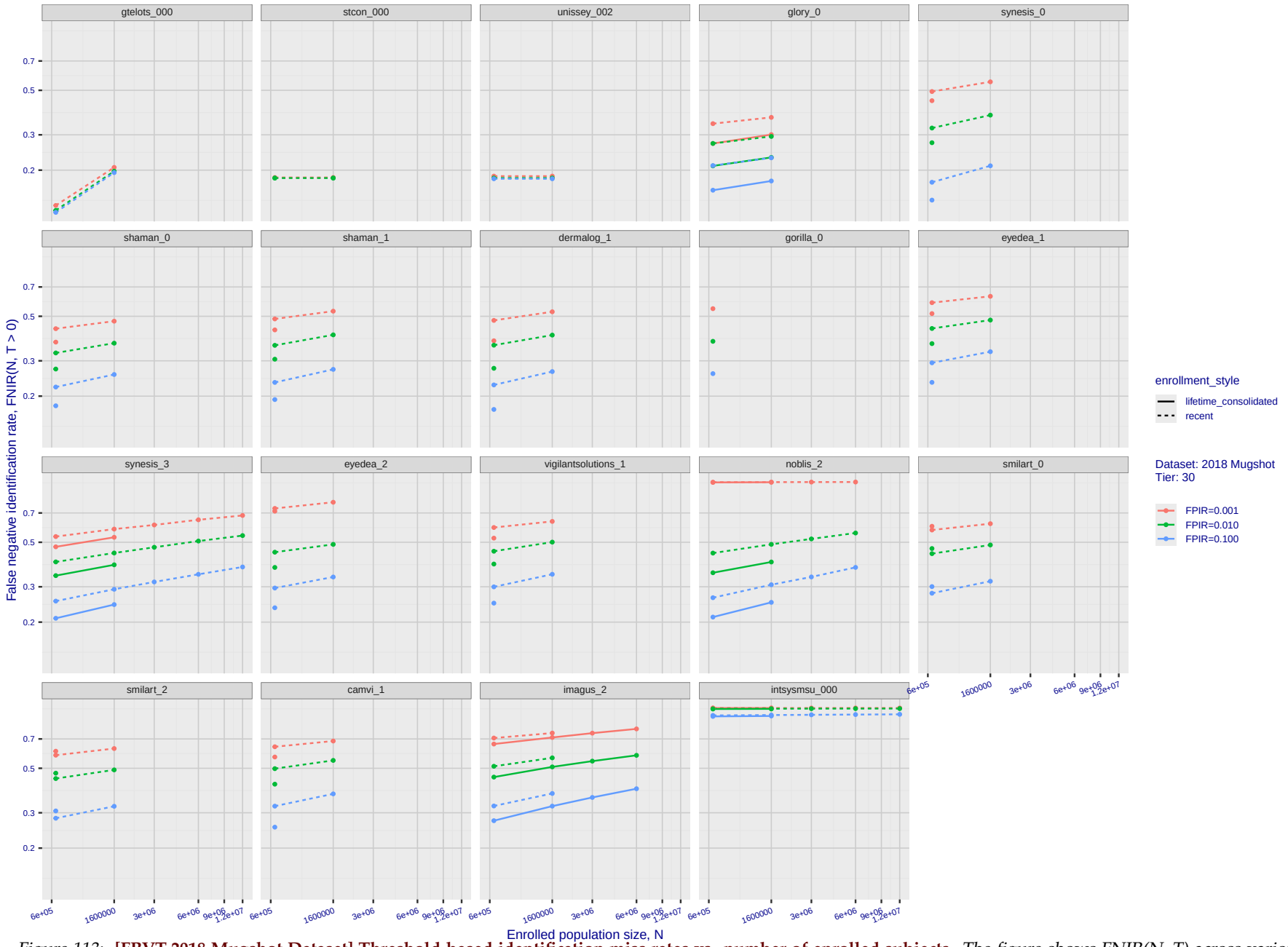

Figure 113: **[FRVT-2018 Mugshot Dataset] Threshold-based identification miss rates vs. number of enrolled subjects**. *The figure shows FNIR(N, T) across various gallery sizes when the threshold is set to achieve the given FPIRs. The rank criterion is irrelevant at high thresholds as mates are always at rank 1. The results are computed from the trials listed in rows 1-10 of Table 1. Less accurate algorithms were not run on large N, so results are missing. For clarity, results are sorted and reported into tiers spanning multiple pages. The tiering criteria is complicated: First paging by FNIR(N_b, 1, 0), then sorting by median FNIR(N_b, T), N_b = 640 000.*

2026/01/09 20:40:38

FNIR(N, R, T) = False neg. identification rate
FPIR(N, T) = False pos. identification rate
N = Num. enrolled subjects
R = Num. candidates examined
T = Threshold
T = 0 → Investigation
T > 0 → Identification

This publication is available free of charge from: https://doi.org/10.6028/NIST.IR.8271

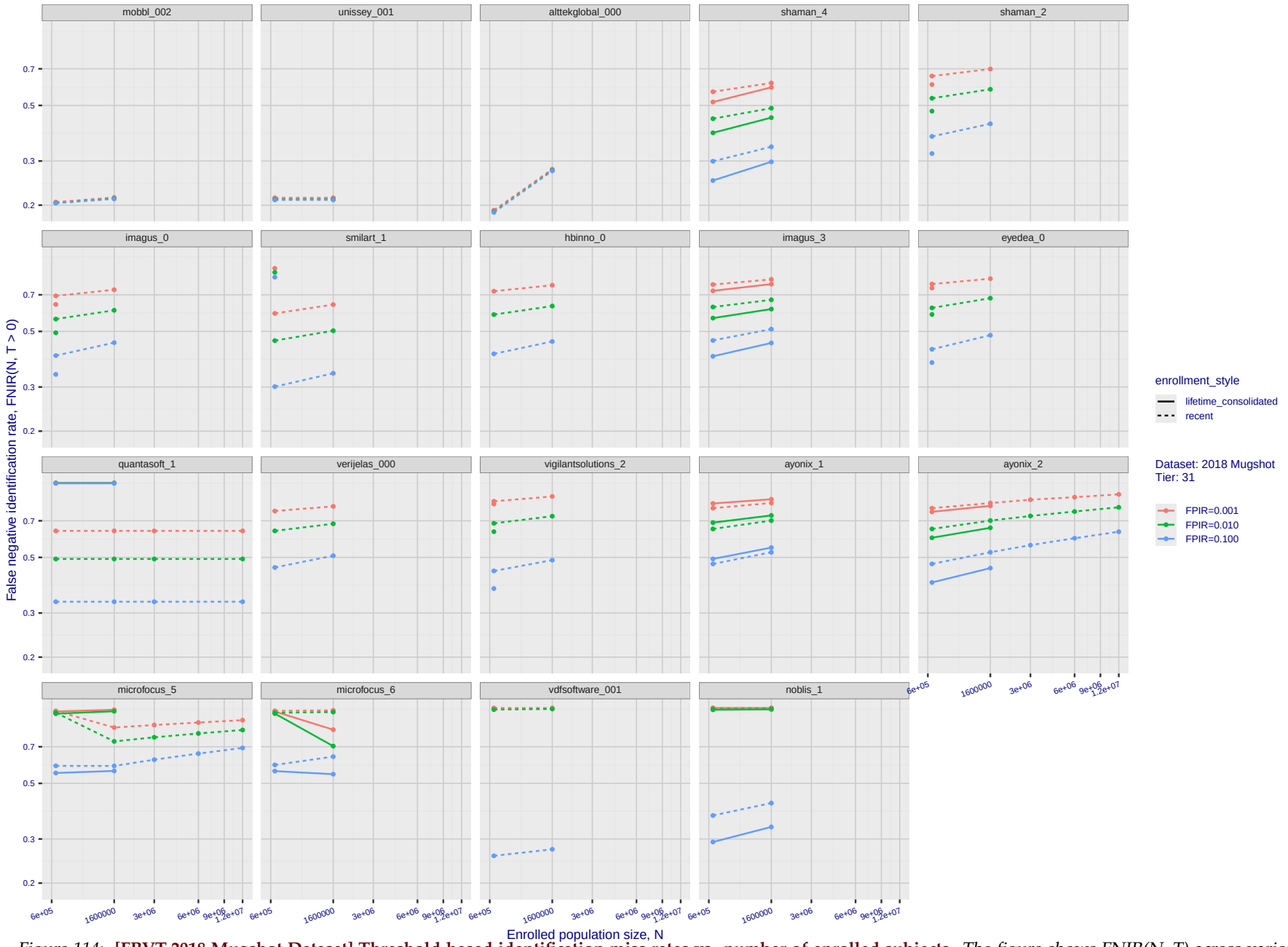

Figure 114: **[FRVT-2018 Mugshot Dataset] Threshold-based identification miss rates vs. number of enrolled subjects**. *The figure shows FNIR(N, T) across various gallery sizes when the threshold is set to achieve the given FPIRs. The rank criterion is irrelevant at high thresholds as mates are always at rank 1. The results are computed from the trials listed in rows 1-10 of Table 1. Less accurate algorithms were not run on large N, so results are missing. For clarity, results are sorted and reported into tiers spanning multiple pages. The tiering criteria is complicated: First paging by FNIR(N_b, 1, 0), then sorting by median FNIR(N_b, T), N_b = 640 000.*

2026/01/09 20:40:38

FNIR(N, R, T) = False neg. identification rate
FPIR(N, T) = False pos. identification rate
N = Num. enrolled subjects
R = Num. candidates examined
T = Threshold
T = 0 → Investigation
T > 0 → Identification

This publication is available free of charge from: https://doi.org/10.6028/NIST.IR.8271

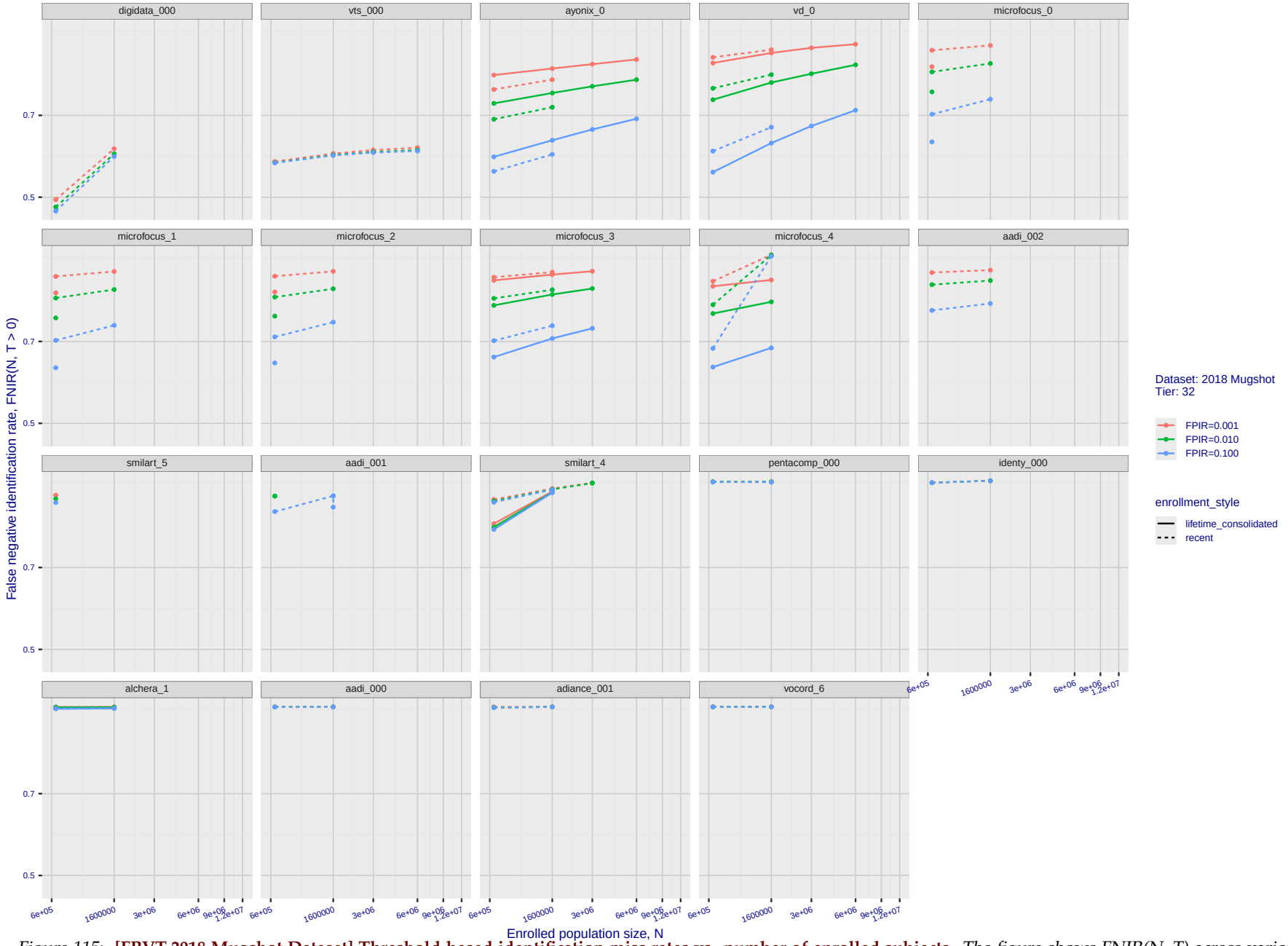

Figure 115: **[FRVT-2018 Mugshot Dataset] Threshold-based identification miss rates vs. number of enrolled subjects**. *The figure shows FNIR(N, T) across various gallery sizes when the threshold is set to achieve the given FPIRs. The rank criterion is irrelevant at high thresholds as mates are always at rank 1. The results are computed from the trials listed in rows 1-10 of Table 1. Less accurate algorithms were not run on large N, so results are missing. For clarity, results are sorted and reported into tiers spanning multiple pages. The tiering criteria is complicated: First paging by FNIR(N_b, 1, 0), then sorting by median FNIR(N_b, T), N_b = 640 000.*

2026/01/09 20:40:38
FNIR(N, R, T) = False neg. identification rate
FPIR(N, T) = False pos. identification rate
N = Num. enrolled subjects
R = Num. candidates examined
T = Threshold
T = 0 → Investigation
T > 0 → Identification

2026/01/09	FNIR(N, R, T) =	False neg. identification rate	N = Num. enrolled subjects	T = Threshold	$T = 0 \rightarrow$ Investigation
20:40:38	FPIR(N, T) =	False pos. identification rate	R = Num. candidates examined		$T > 0 \rightarrow$ Identification

This publication is available free of charge from: https://doi.org/10.6028/NIST.IR.8271

This publication is available free of charge from: https://doi.org/10.6028/NIST.IR.8271

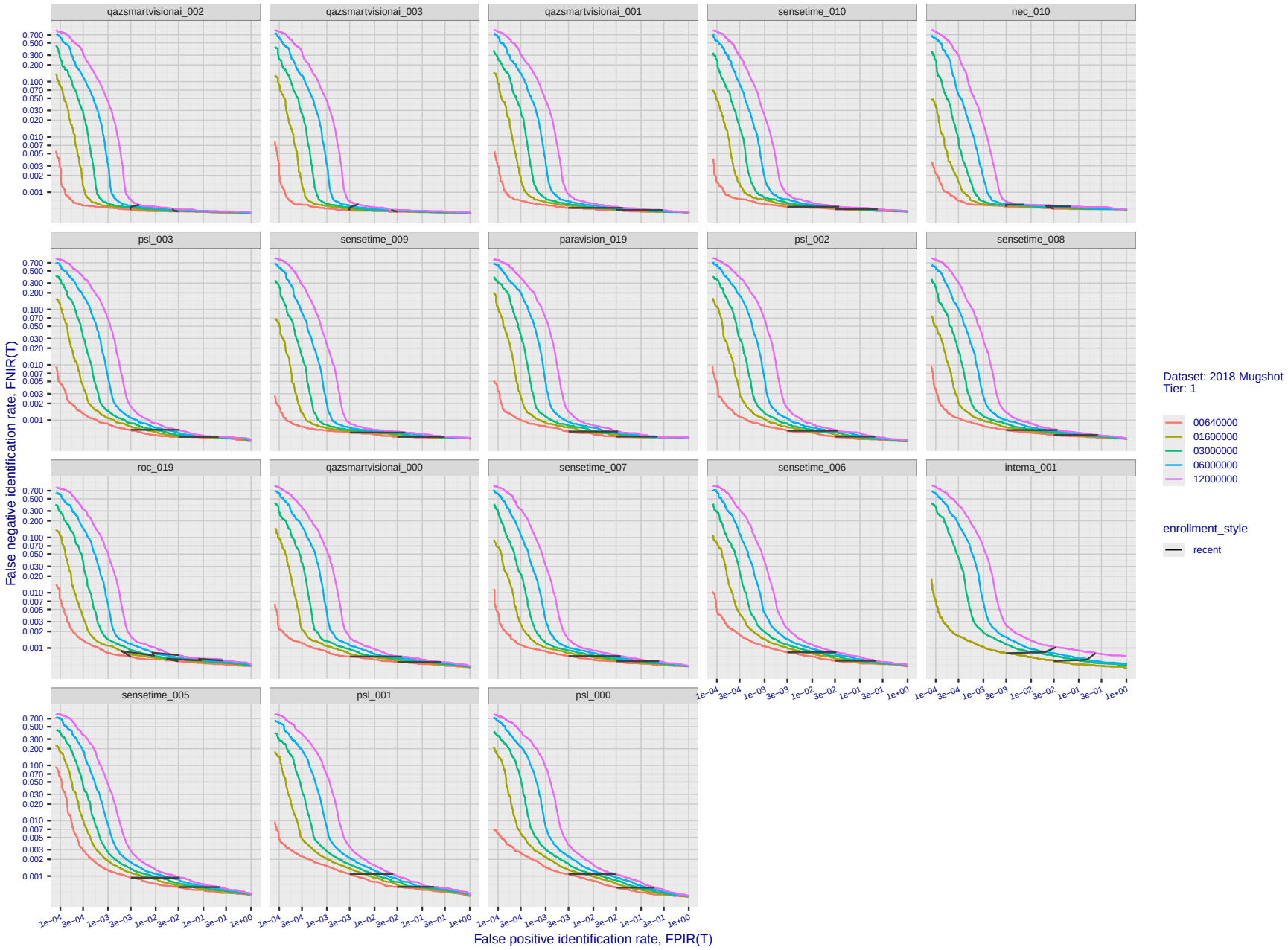

Figure 116: **[FRVT-2018 Mugshot Dataset] Identification miss rates vs. false positive rates**. *The figure shows miss rates FNIR(N, L, T) as a function of FPIR(N, T), with N ranging from 640 000 to 12 000 000 as noted in rows 1-10 of Table 1. These error tradeoff characteristics are useful for applications where a threshold must be elevated to limit false positives, such as when human reviewer labor is not matched to the volume of searches. Dark lines join points of equal threshold: If horizontal, FPIR(T) rises with N, and mate scores are independent of N. Other algorithms adjust scores in an attempt to make FPIR independent of N.*

2026/01/09 20:40:38
FNIR(N, R, T) = False neg. identification rate
FPIR(N, T) = False pos. identification rate
N = Num. enrolled subjects
R = Num. candidates examined
T = Threshold
T = 0 → Investigation
T > 0 → Identification

This publication is available free of charge from: https://doi.org/10.6028/NIST.IR.8271

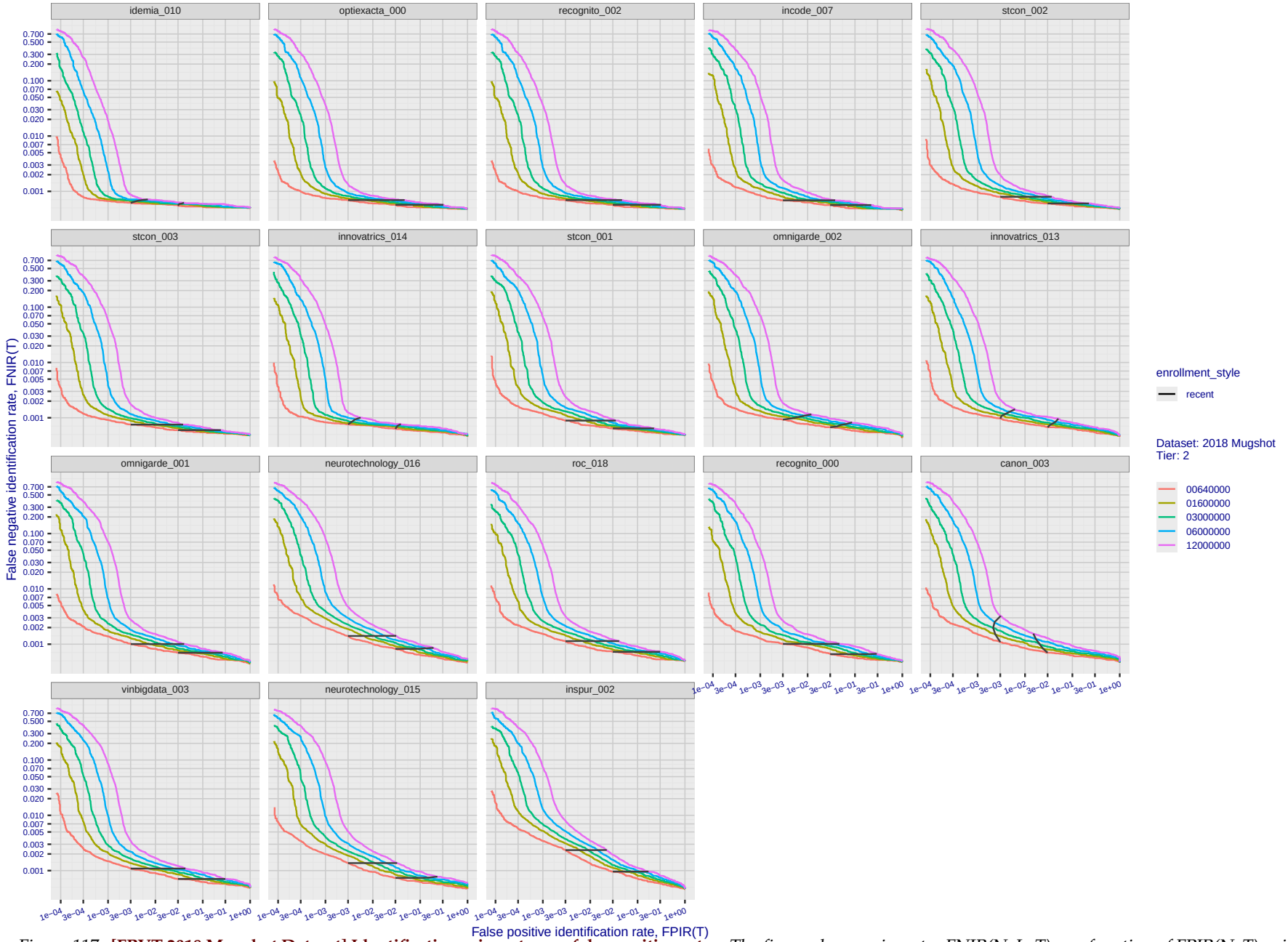

Figure 117: **[FRVT-2018 Mugshot Dataset] Identification miss rates vs. false positive rates**. *The figure shows miss rates FNIR(N, L, T) as a function of FPIR(N, T), with N ranging from 640 000 to 12 000 000 as noted in rows 1-10 of Table 1. These error tradeoff characteristics are useful for applications where a threshold must be elevated to limit false positives, such as when human reviewer labor is not matched to the volume of searches. Dark lines join points of equal threshold: If horizontal, FPIR(T) rises with N, and mate scores are independent of N. Other algorithms adjust scores in an attempt to make FPIR independent of N.*

2026/01/09 20:40:38
FNIR(N, R, T) = False neg. identification rate
FPIR(N, T) = False pos. identification rate
N = Num. enrolled subjects
R = Num. candidates examined
T = Threshold
T = 0 → Investigation
T > 0 → Identification

This publication is available free of charge from: https://doi.org/10.6028/NIST.IR.8271

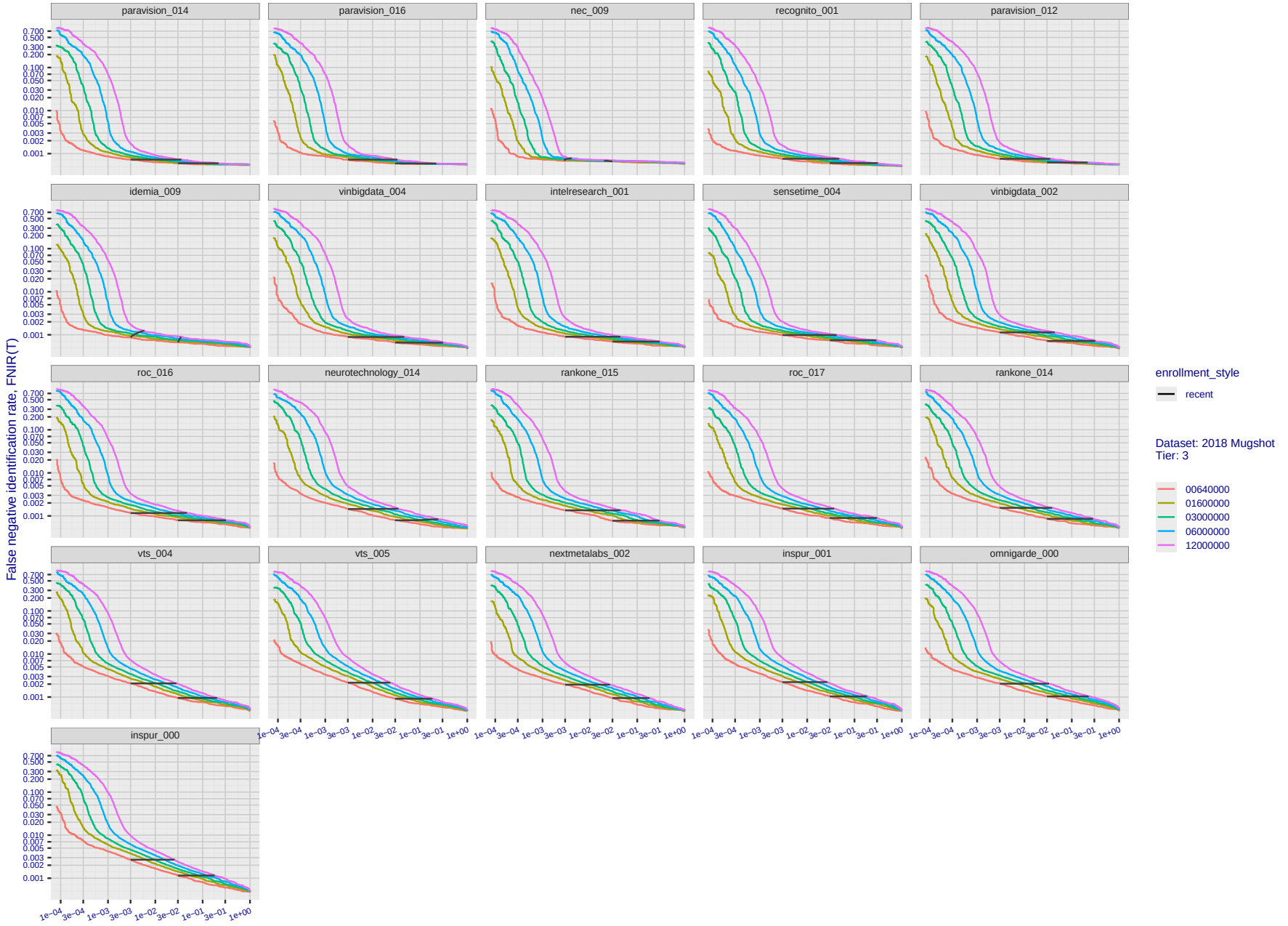

Figure 118: **[FRVT-2018 Mugshot Dataset] Identification miss rates vs. false positive rates**. *The figure shows miss rates FNIR(N, L, T) as a function of FPIR(N, T), with N ranging from 640 000 to 12 000 000 as noted in rows 1-10 of Table 1. These error tradeoff characteristics are useful for applications where a threshold must be elevated to limit false positives, such as when human reviewer labor is not matched to the volume of searches. Dark lines join points of equal threshold: If horizontal, FPIR(T) rises with N, and mate scores are independent of N. Other algorithms adjust scores in an attempt to make FPIR independent of N.*

2026/01/09 20:40:38
FNIR(N, R, T) = False neg. identification rate
FPIR(N, T) = False pos. identification rate
N = Num. enrolled subjects
R = Num. candidates examined
T = Threshold
T = 0 → Investigation
T > 0 → Identification

This publication is available free of charge from: https://doi.org/10.6028/NIST.IR.8271

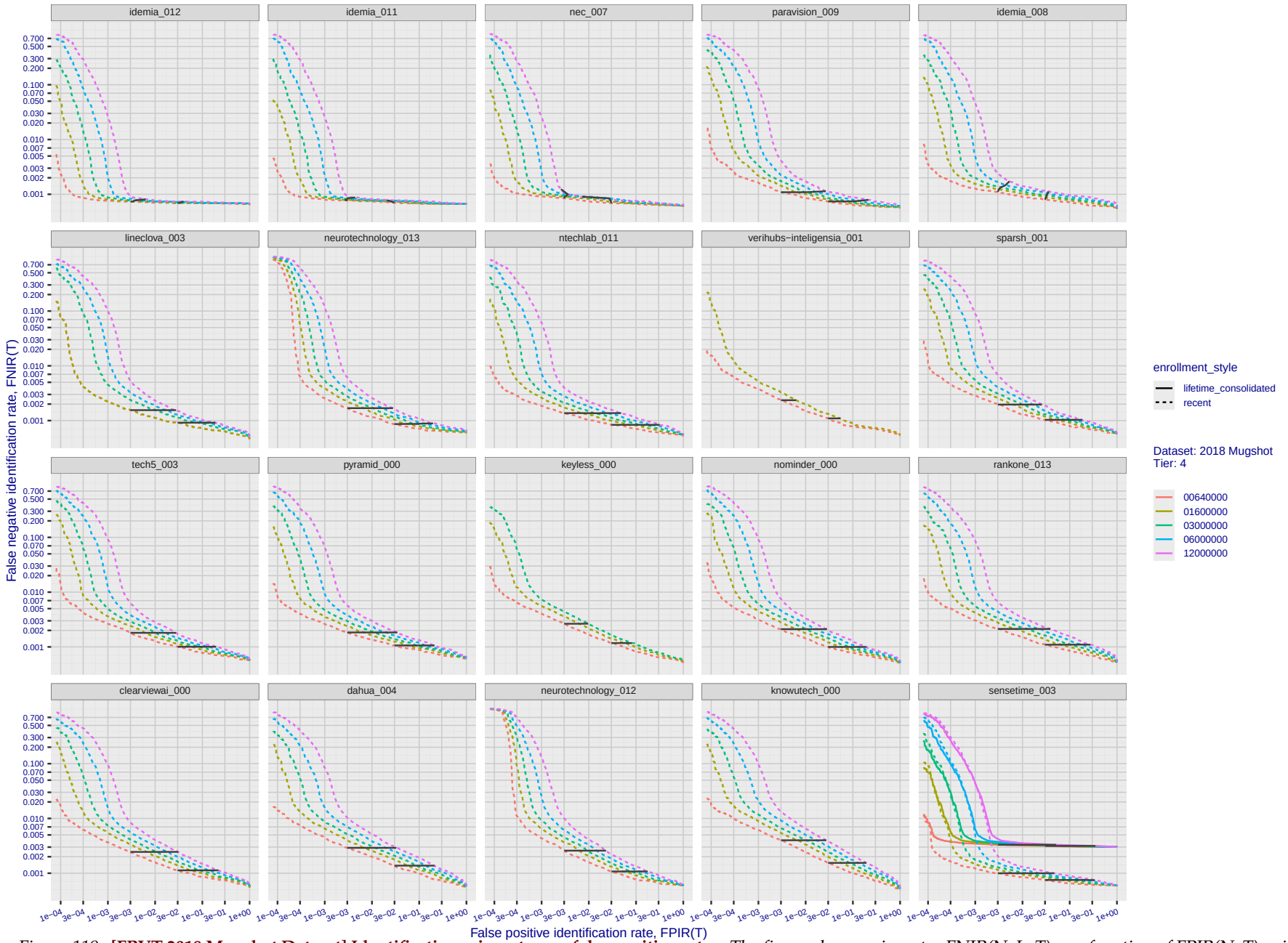

Figure 119: **[FRVT-2018 Mugshot Dataset] Identification miss rates vs. false positive rates**. *The figure shows miss rates FNIR(N, L, T) as a function of FPIR(N, T), with N ranging from 640 000 to 12 000 000 as noted in rows 1-10 of Table 1. These error tradeoff characteristics are useful for applications where a threshold must be elevated to limit false positives, such as when human reviewer labor is not matched to the volume of searches. Dark lines join points of equal threshold: If horizontal, FPIR(T) rises with N, and mate scores are independent of N. Other algorithms adjust scores in an attempt to make FPIR independent of N.*

2026/01/09 20:40:38

FNIR(N, R, T) = False neg. identification rate
FPIR(N, T) = False pos. identification rate

N = Num. enrolled subjects
R = Num. candidates examined

T = Threshold

T = 0 → Investigation
T > 0 → Identification

This publication is available free of charge from: https://doi.org/10.6028/NIST.IR.8271

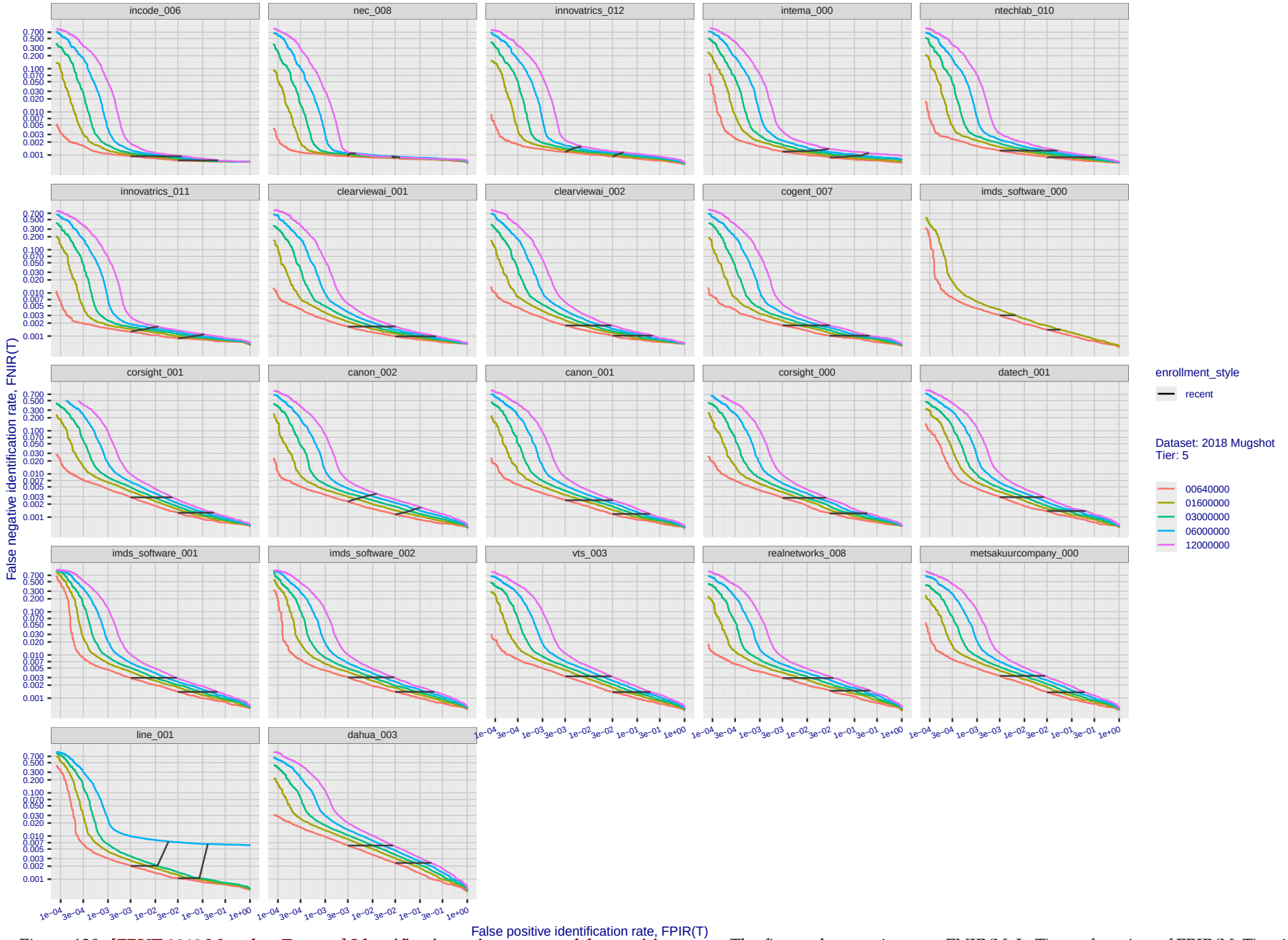

Figure 120: **[FRVT-2018 Mugshot Dataset] Identification miss rates vs. false positive rates**. *The figure shows miss rates FNIR(N, L, T) as a function of FPIR(N, T), with N ranging from 640 000 to 12 000 000 as noted in rows 1-10 of Table 1. These error tradeoff characteristics are useful for applications where a threshold must be elevated to limit false positives, such as when human reviewer labor is not matched to the volume of searches. Dark lines join points of equal threshold: If horizontal, FPIR(T) rises with N, and mate scores are independent of N. Other algorithms adjust scores in an attempt to make FPIR independent of N.*

2026/01/09 20:40:38
FNIR(N, R, T) = False neg. identification rate
FPIR(N, T) = False pos. identification rate
N = Num. enrolled subjects
R = Num. candidates examined
T = Threshold
T = 0 → Investigation
T > 0 → Identification

This publication is available free of charge from: https://doi.org/10.6028/NIST.IR.8271

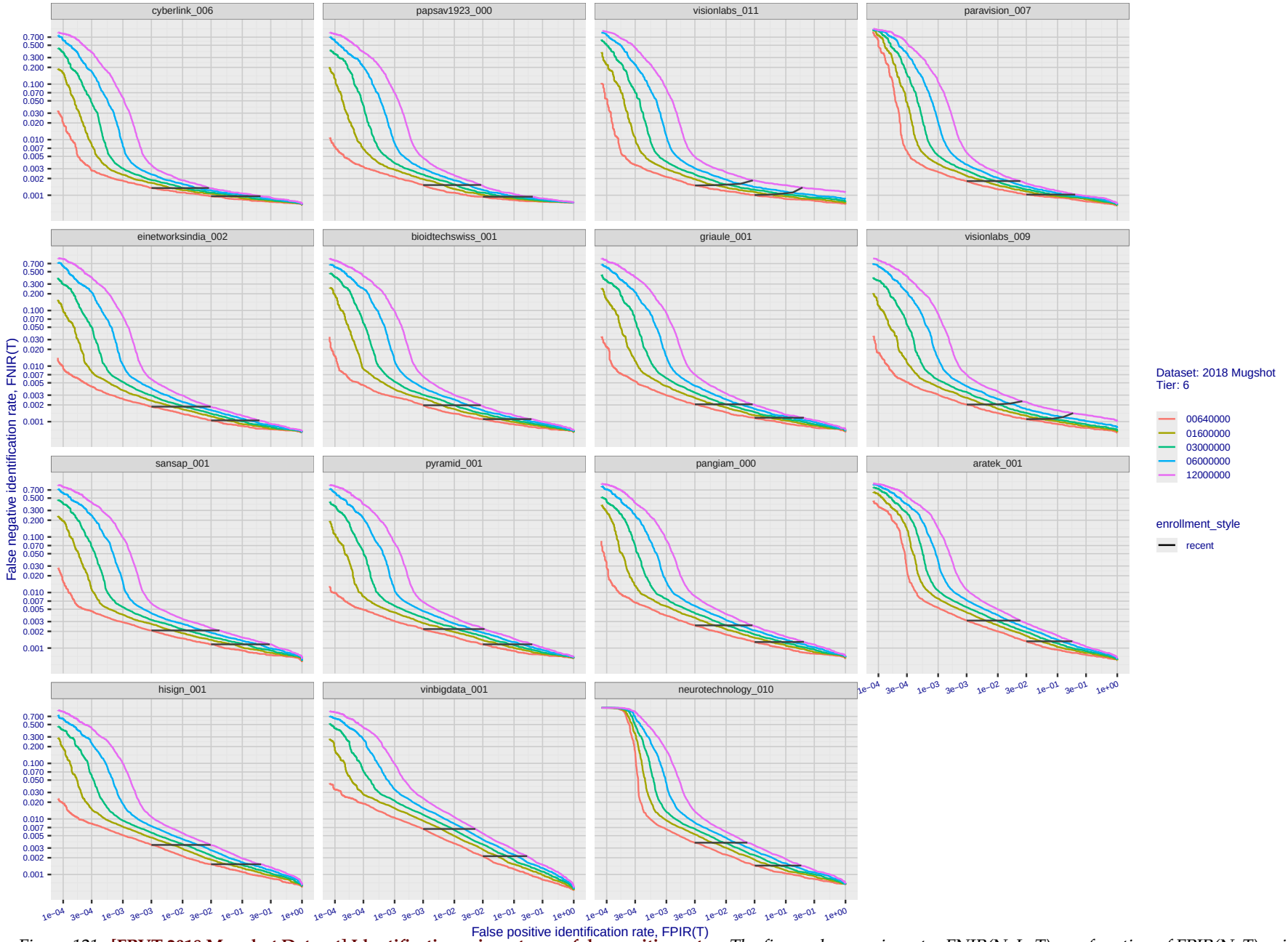

Figure 121: **[FRVT-2018 Mugshot Dataset] Identification miss rates vs. false positive rates**. *The figure shows miss rates FNIR(N, L, T) as a function of FPIR(N, T), with N ranging from 640 000 to 12 000 000 as noted in rows 1-10 of Table 1. These error tradeoff characteristics are useful for applications where a threshold must be elevated to limit false positives, such as when human reviewer labor is not matched to the volume of searches. Dark lines join points of equal threshold: If horizontal, FPIR(T) rises with N, and mate scores are independent of N. Other algorithms adjust scores in an attempt to make FPIR independent of N.*

2026/01/09 20:40:38
FNIR(N, R, T) = False neg. identification rate
FPIR(N, T) = False pos. identification rate
N = Num. enrolled subjects
R = Num. candidates examined
T = Threshold
T = 0 → Investigation
T > 0 → Identification

This publication is available free of charge from: https://doi.org/10.6028/NIST.IR.8271

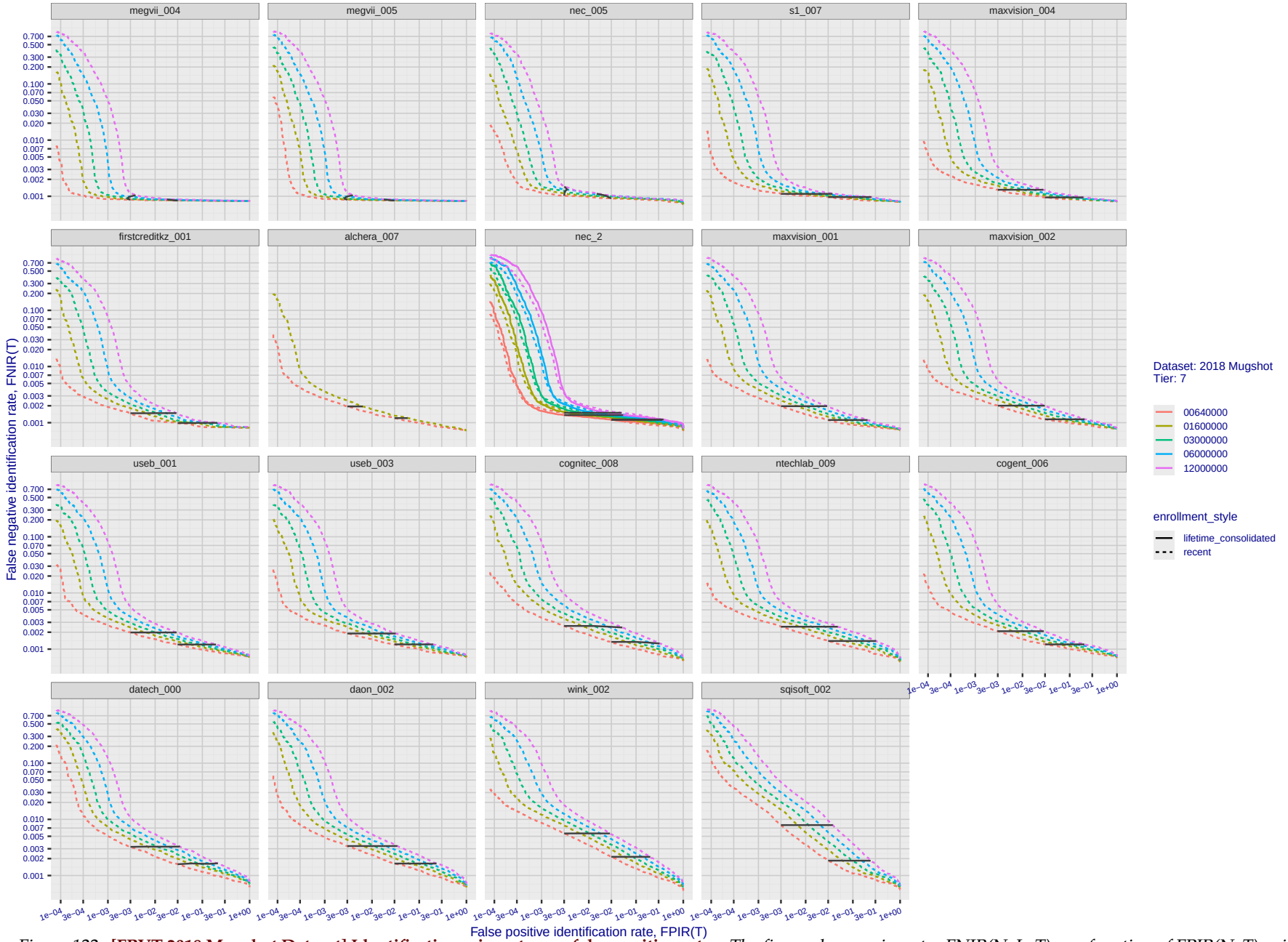

Figure 122: **[FRVT-2018 Mugshot Dataset] Identification miss rates vs. false positive rates**. *The figure shows miss rates FNIR(N, L, T) as a function of FPIR(N, T), with N ranging from 640 000 to 12 000 000 as noted in rows 1-10 of Table 1. These error tradeoff characteristics are useful for applications where a threshold must be elevated to limit false positives, such as when human reviewer labor is not matched to the volume of searches. Dark lines join points of equal threshold: If horizontal, FPIR(T) rises with N, and mate scores are independent of N. Other algorithms adjust scores in an attempt to make FPIR independent of N.*

2026/01/09 20:40:38
FNIR(N, R, T) = False neg. identification rate
FPIR(N, T) = False pos. identification rate
N = Num. enrolled subjects
R = Num. candidates examined
T = Threshold
T = 0 → Investigation
T > 0 → Identification

This publication is available free of charge from: https://doi.org/10.6028/NIST.IR.8271

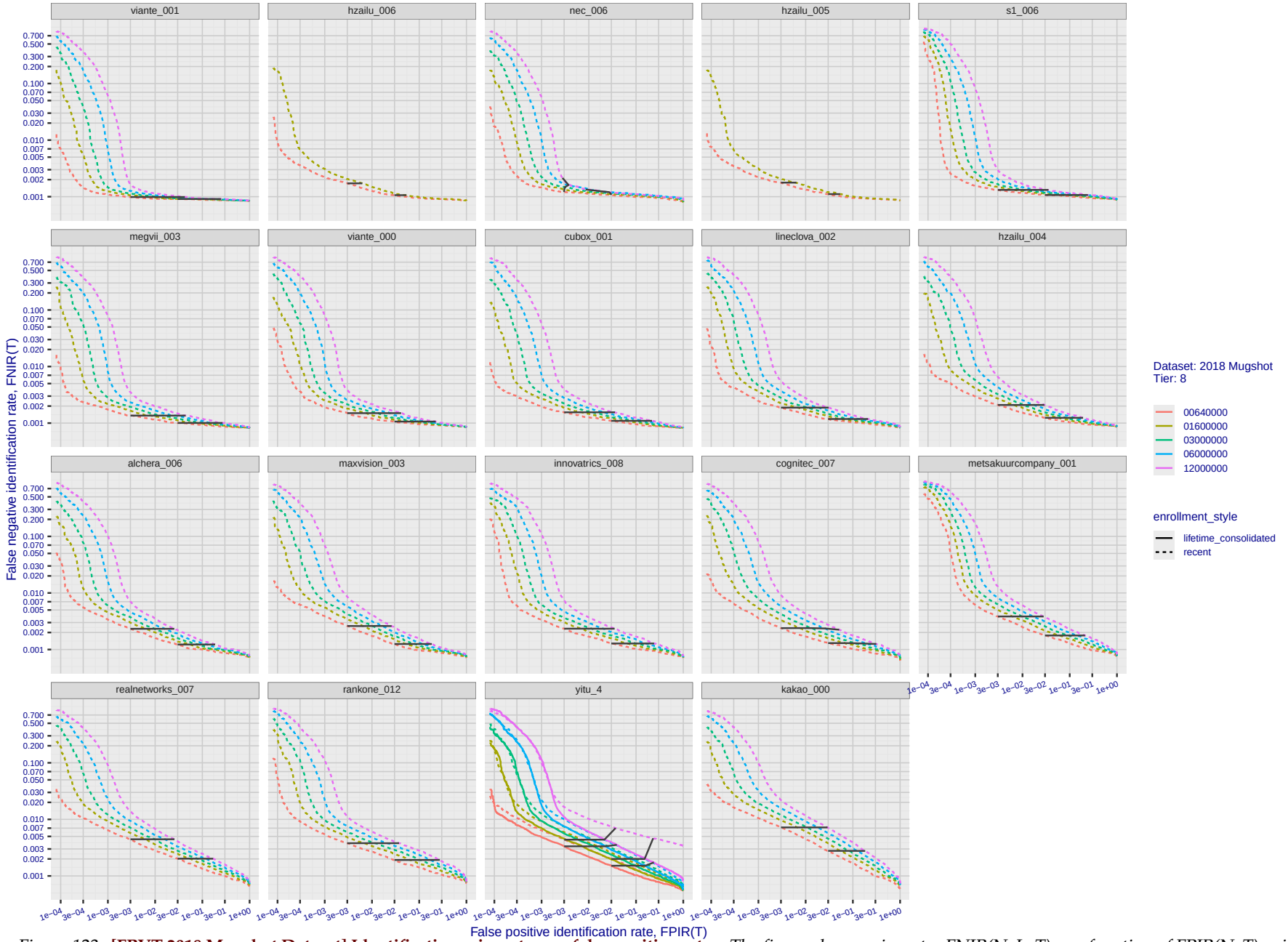

Figure 123: **[FRVT-2018 Mugshot Dataset] Identification miss rates vs. false positive rates**. *The figure shows miss rates FNIR(N, L, T) as a function of FPIR(N, T), with N ranging from 640 000 to 12 000 000 as noted in rows 1-10 of Table 1. These error tradeoff characteristics are useful for applications where a threshold must be elevated to limit false positives, such as when human reviewer labor is not matched to the volume of searches. Dark lines join points of equal threshold: If horizontal, FPIR(T) rises with N, and mate scores are independent of N. Other algorithms adjust scores in an attempt to make FPIR independent of N.*

2026/01/09 20:40:38

FNIR(N, R, T) = False neg. identification rate
FPIR(N, T) = False pos. identification rate

N = Num. enrolled subjects
R = Num. candidates examined

T = Threshold

T = 0 → Investigation
T > 0 → Identification

This publication is available free of charge from: https://doi.org/10.6028/NIST.IR.8271

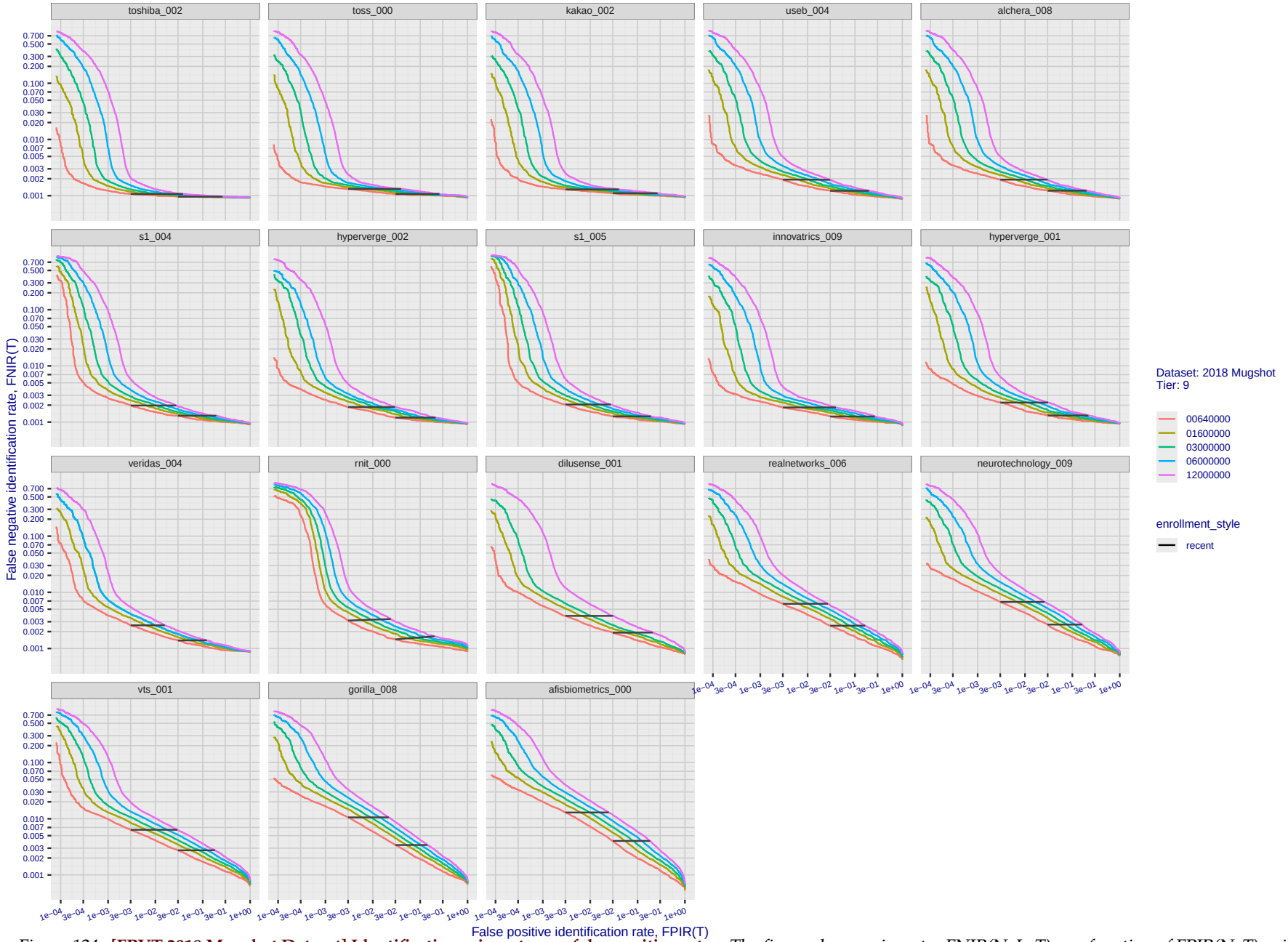

Figure 124: **[FRVT-2018 Mugshot Dataset] Identification miss rates vs. false positive rates**. *The figure shows miss rates FNIR(N, L, T) as a function of FPIR(N, T), with N ranging from 640 000 to 12 000 000 as noted in rows 1-10 of Table 1. These error tradeoff characteristics are useful for applications where a threshold must be elevated to limit false positives, such as when human reviewer labor is not matched to the volume of searches. Dark lines join points of equal threshold: If horizontal, FPIR(T) rises with N, and mate scores are independent of N. Other algorithms adjust scores in an attempt to make FPIR independent of N.*

2026/01/09 20:40:38
FNIR(N, R, T) = False neg. identification rate
FPIR(N, T) = False pos. identification rate
N = Num. enrolled subjects
R = Num. candidates examined
T = Threshold
T = 0 → Investigation
T > 0 → Identification

This publication is available free of charge from: https://doi.org/10.6028/NIST.IR.8271

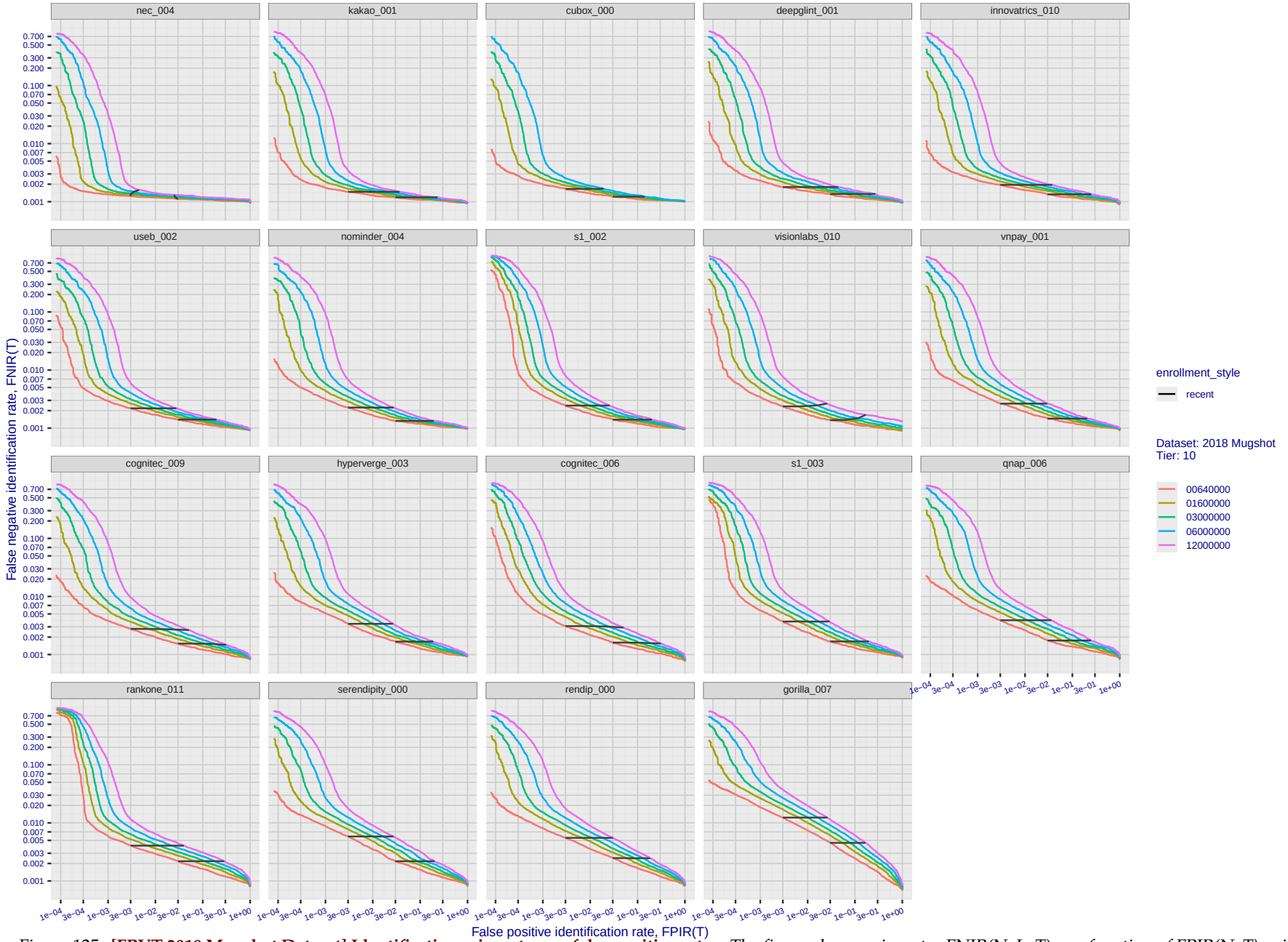

Figure 125: **[FRVT-2018 Mugshot Dataset] Identification miss rates vs. false positive rates**. *The figure shows miss rates FNIR(N, L, T) as a function of FPIR(N, T), with N ranging from 640 000 to 12 000 000 as noted in rows 1-10 of Table 1. These error tradeoff characteristics are useful for applications where a threshold must be elevated to limit false positives, such as when human reviewer labor is not matched to the volume of searches. Dark lines join points of equal threshold: If horizontal, FPIR(T) rises with N, and mate scores are independent of N. Other algorithms adjust scores in an attempt to make FPIR independent of N.*

2026/01/09 20:40:38
FNIR(N, R, T) = False neg. identification rate
FPIR(N, T) = False pos. identification rate
N = Num. enrolled subjects
R = Num. candidates examined
T = Threshold
T = 0 → Investigation
T > 0 → Identification

This publication is available free of charge from: https://doi.org/10.6028/NIST.IR.8271

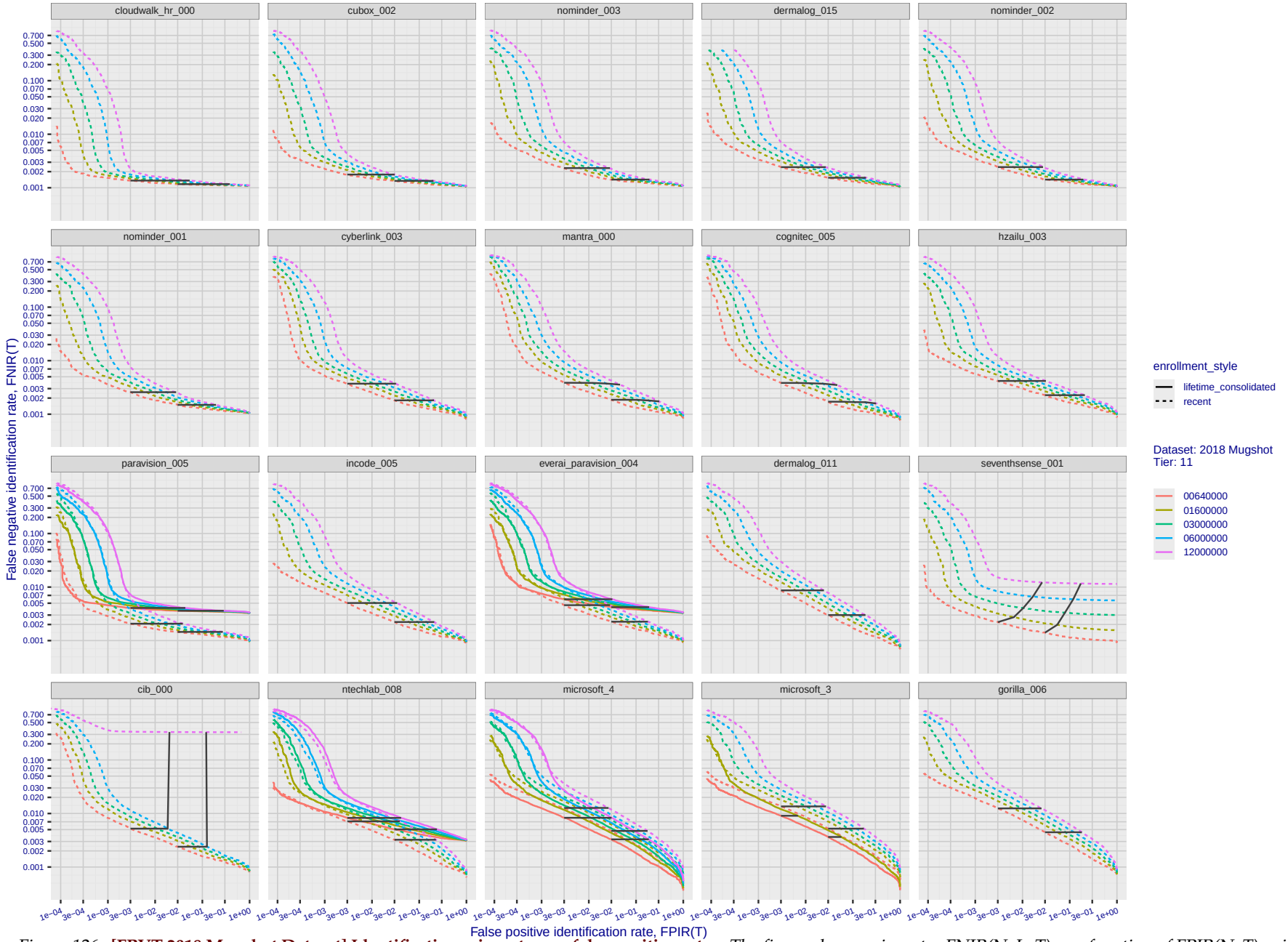

Figure 126: **[FRVT-2018 Mugshot Dataset] Identification miss rates vs. false positive rates**. *The figure shows miss rates FNIR(N, L, T) as a function of FPIR(N, T), with N ranging from 640 000 to 12 000 000 as noted in rows 1-10 of Table 1. These error tradeoff characteristics are useful for applications where a threshold must be elevated to limit false positives, such as when human reviewer labor is not matched to the volume of searches. Dark lines join points of equal threshold: If horizontal, FPIR(T) rises with N, and mate scores are independent of N. Other algorithms adjust scores in an attempt to make FPIR independent of N.*

2026/01/09 20:40:38

FNIR(N, R, T) = False neg. identification rate
FPIR(N, T) = False pos. identification rate

N = Num. enrolled subjects
R = Num. candidates examined

T = Threshold

T = 0 → Investigation
T > 0 → Identification

This publication is available free of charge from: https://doi.org/10.6028/NIST.IR.8271

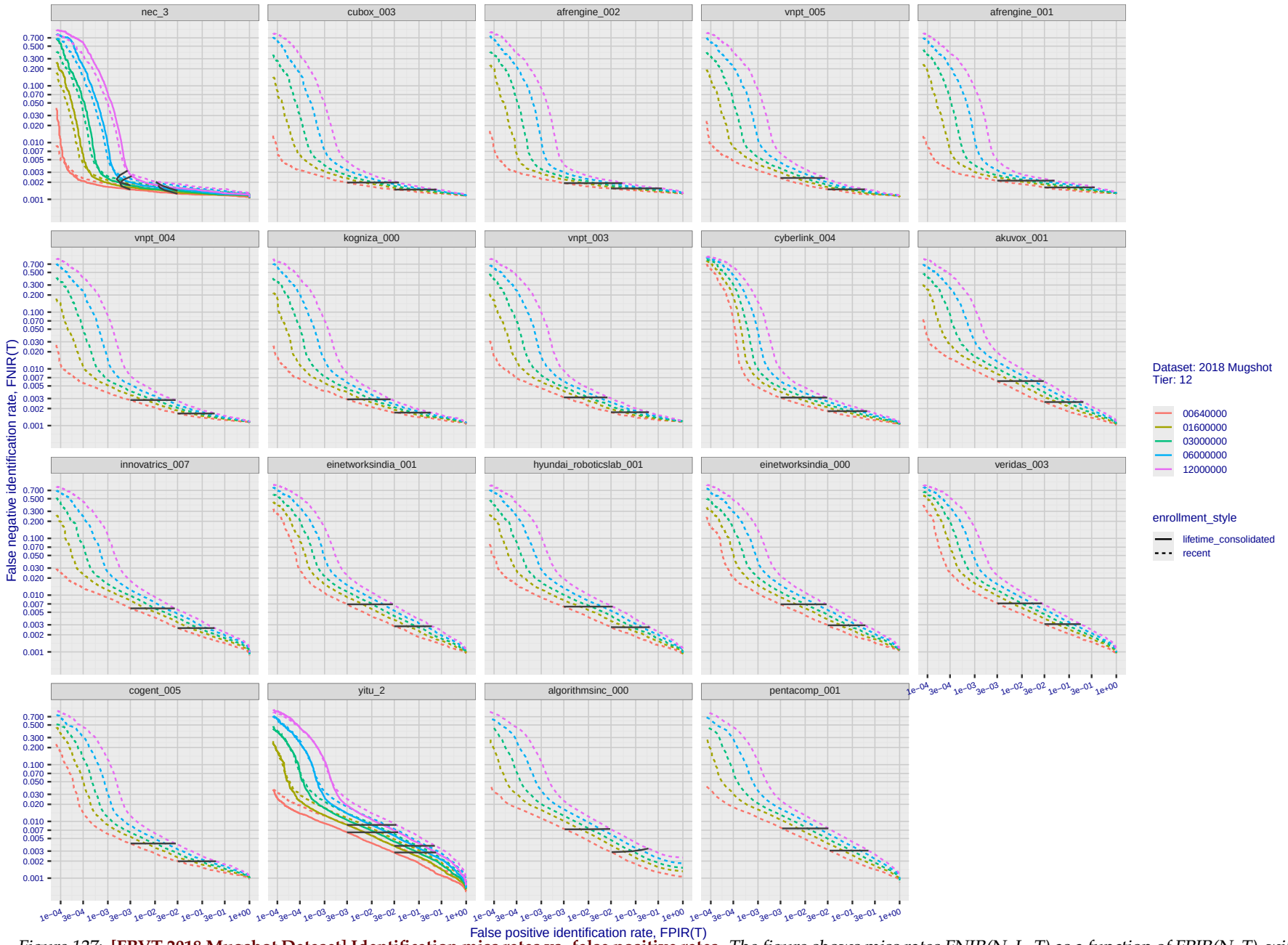

Figure 127: **[FRVT-2018 Mugshot Dataset] Identification miss rates vs. false positive rates**. *The figure shows miss rates FNIR(N, L, T) as a function of FPIR(N, T), with N ranging from 640 000 to 12 000 000 as noted in rows 1-10 of Table 1. These error tradeoff characteristics are useful for applications where a threshold must be elevated to limit false positives, such as when human reviewer labor is not matched to the volume of searches. Dark lines join points of equal threshold: If horizontal, FPIR(T) rises with N, and mate scores are independent of N. Other algorithms adjust scores in an attempt to make FPIR independent of N.*

2026/01/09 20:40:38
FNIR(N, R, T) = False neg. identification rate
FPIR(N, T) = False pos. identification rate
N = Num. enrolled subjects
R = Num. candidates examined
T = Threshold
T = 0 → Investigation
T > 0 → Identification

This publication is available free of charge from: https://doi.org/10.6028/NIST.IR.8271

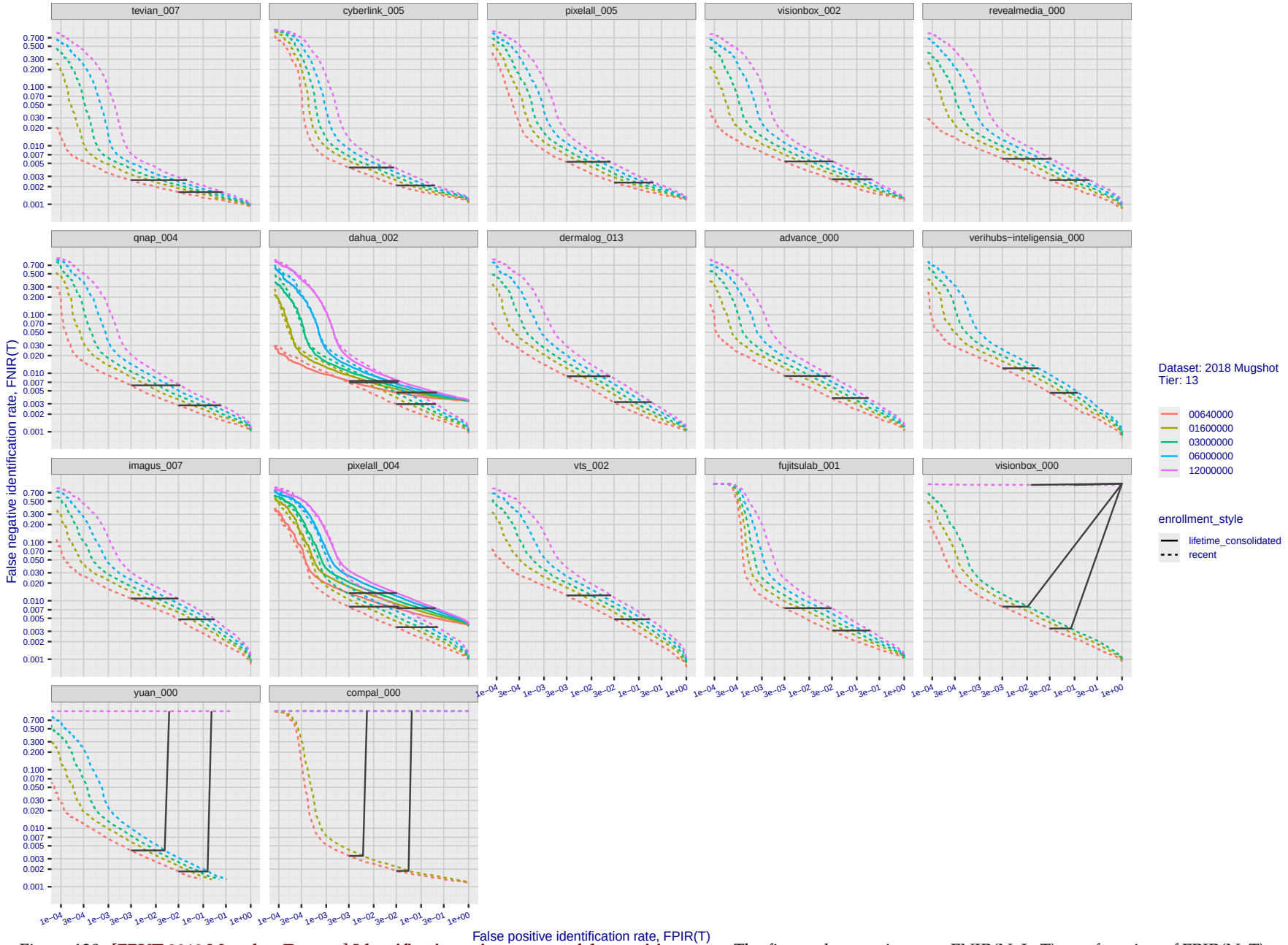

Figure 128: **[FRVT-2018 Mugshot Dataset] Identification miss rates vs. false positive rates**. *The figure shows miss rates FNIR(N, L, T) as a function of FPIR(N, T), with N ranging from 640 000 to 12 000 000 as noted in rows 1-10 of Table 1. These error tradeoff characteristics are useful for applications where a threshold must be elevated to limit false positives, such as when human reviewer labor is not matched to the volume of searches. Dark lines join points of equal threshold: If horizontal, FPIR(T) rises with N, and mate scores are independent of N. Other algorithms adjust scores in an attempt to make FPIR independent of N.*

2026/01/09 20:40:38
FNIR(N, R, T) = False neg. identification rate
FPIR(N, T) = False pos. identification rate
N = Num. enrolled subjects
R = Num. candidates examined
T = Threshold
T = 0 → Investigation
T > 0 → Identification

This publication is available free of charge from: https://doi.org/10.6028/NIST.IR.8271

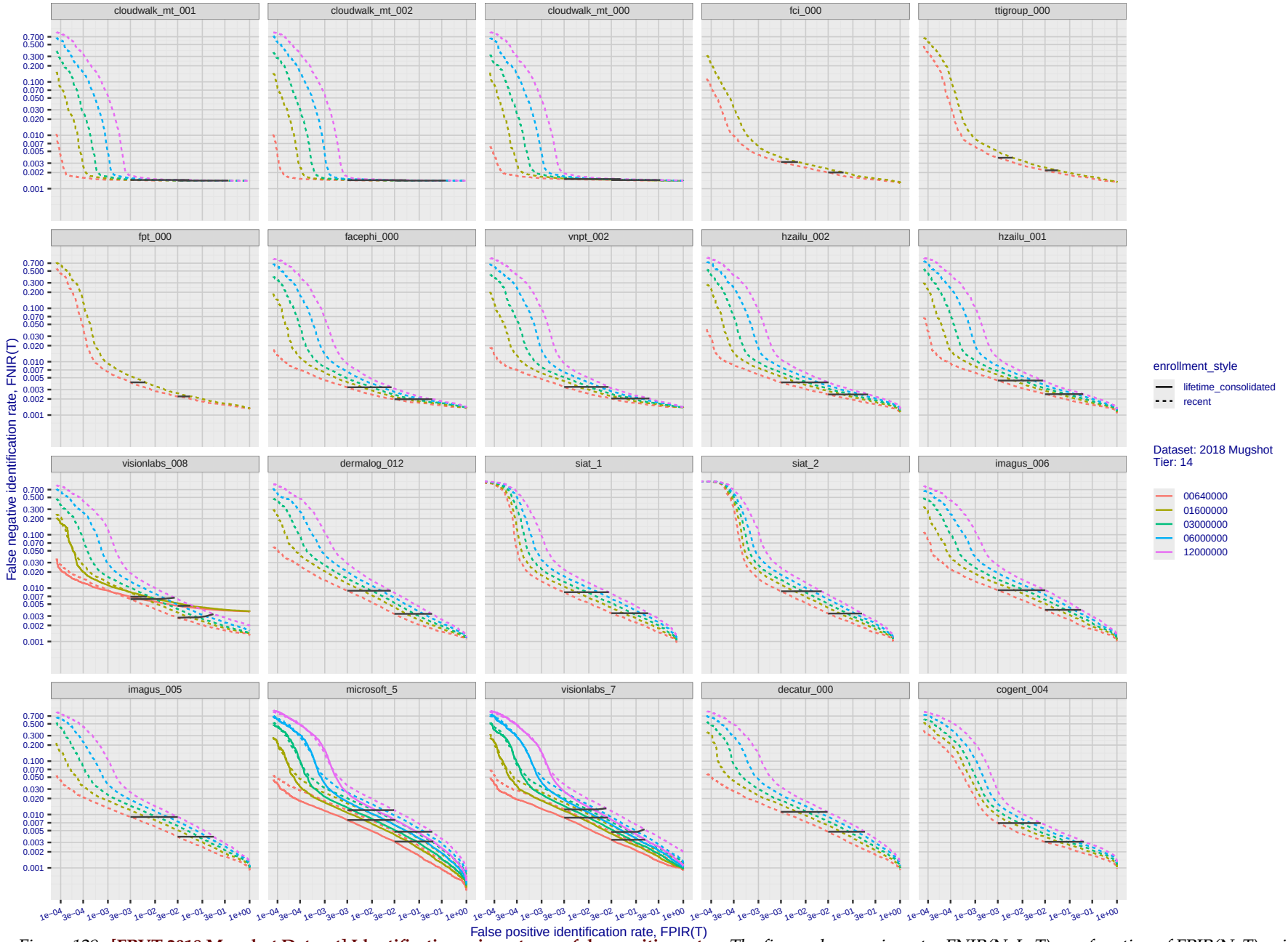

Figure 129: **[FRVT-2018 Mugshot Dataset] Identification miss rates vs. false positive rates**. *The figure shows miss rates FNIR(N, L, T) as a function of FPIR(N, T), with N ranging from 640 000 to 12 000 000 as noted in rows 1-10 of Table 1. These error tradeoff characteristics are useful for applications where a threshold must be elevated to limit false positives, such as when human reviewer labor is not matched to the volume of searches. Dark lines join points of equal threshold: If horizontal, FPIR(T) rises with N, and mate scores are independent of N. Other algorithms adjust scores in an attempt to make FPIR independent of N.*

2026/01/09
20:40:38

FNIR(N, R, T) = False neg. identification rate
FPIR(N, T) = False pos. identification rate

N = Num. enrolled subjects
R = Num. candidates examined

T = Threshold

T = 0 → Investigation
T > 0 → Identification

This publication is available free of charge from: https://doi.org/10.6028/NIST.IR.8271

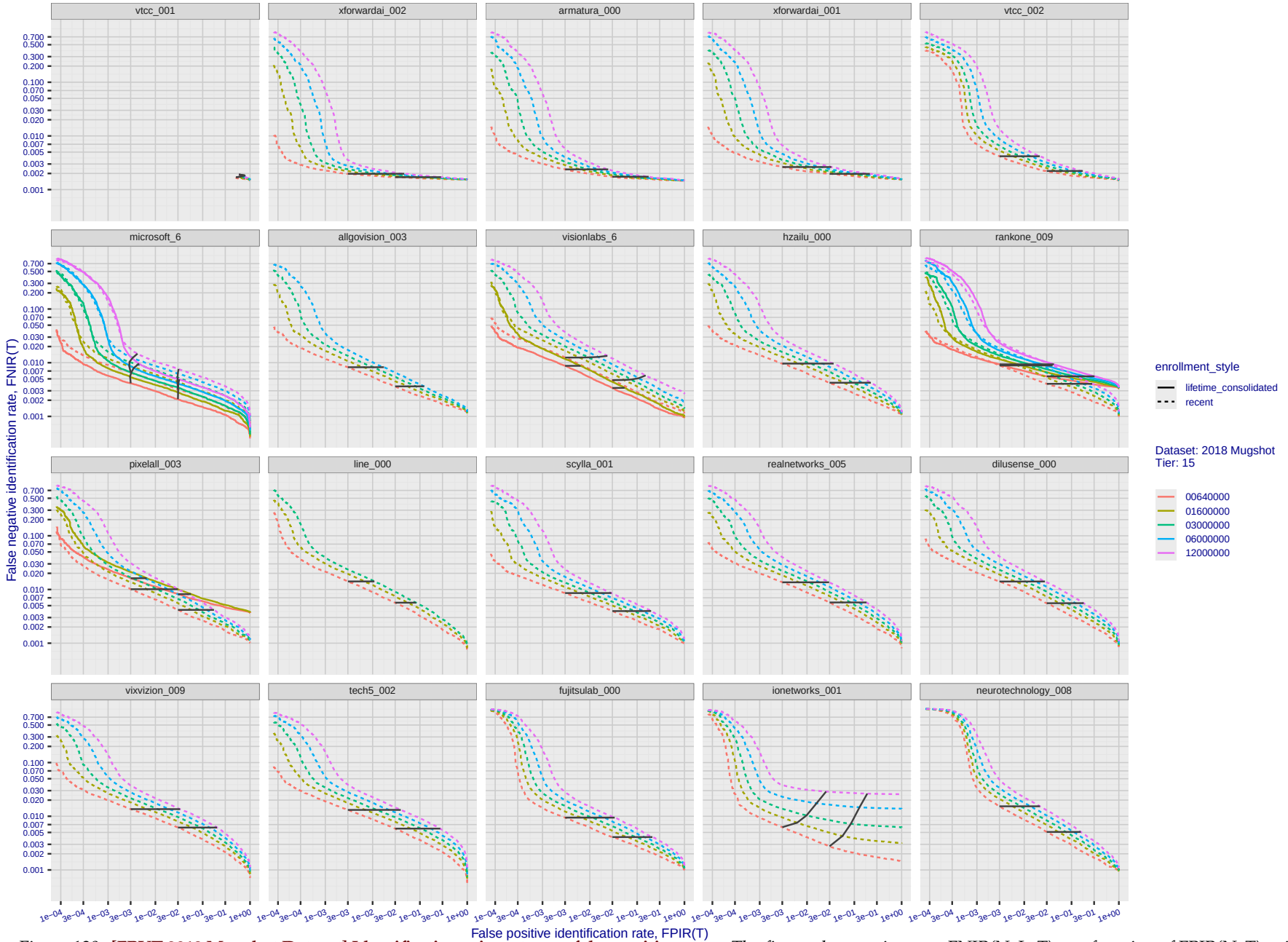

Figure 130: **[FRVT-2018 Mugshot Dataset] Identification miss rates vs. false positive rates**. *The figure shows miss rates FNIR(N, L, T) as a function of FPIR(N, T), with N ranging from 640 000 to 12 000 000 as noted in rows 1-10 of Table 1. These error tradeoff characteristics are useful for applications where a threshold must be elevated to limit false positives, such as when human reviewer labor is not matched to the volume of searches. Dark lines join points of equal threshold: If horizontal, FPIR(T) rises with N, and mate scores are independent of N. Other algorithms adjust scores in an attempt to make FPIR independent of N.*

2026/01/09 20:40:38

FNIR(N, R, T) = False neg. identification rate
FPIR(N, T) = False pos. identification rate

N = Num. enrolled subjects
R = Num. candidates examined

T = Threshold

T = 0 → Investigation
T > 0 → Identification

This publication is available free of charge from: https://doi.org/10.6028/NIST.IR.8271

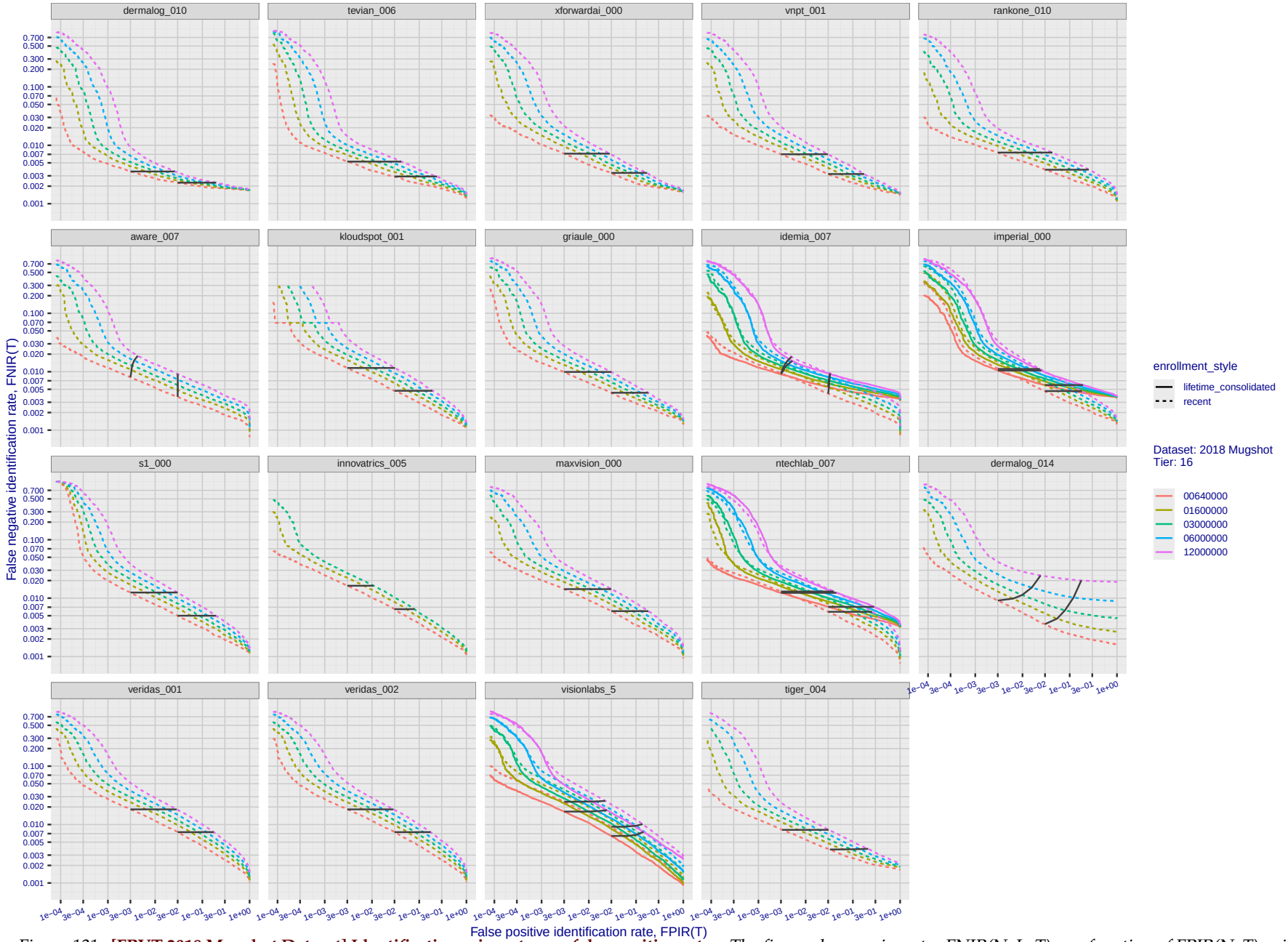

Figure 131: **[FRVT-2018 Mugshot Dataset] Identification miss rates vs. false positive rates**. *The figure shows miss rates FNIR(N, L, T) as a function of FPIR(N, T), with N ranging from 640 000 to 12 000 000 as noted in rows 1-10 of Table 1. These error tradeoff characteristics are useful for applications where a threshold must be elevated to limit false positives, such as when human reviewer labor is not matched to the volume of searches. Dark lines join points of equal threshold: If horizontal, FPIR(T) rises with N, and mate scores are independent of N. Other algorithms adjust scores in an attempt to make FPIR independent of N.*

2026/01/09 20:40:38
FNIR(N, R, T) = False neg. identification rate
FPIR(N, T) = False pos. identification rate
N = Num. enrolled subjects
R = Num. candidates examined
T = Threshold
T = 0 → Investigation
T > 0 → Identification

This publication is available free of charge from: https://doi.org/10.6028/NIST.IR.8271

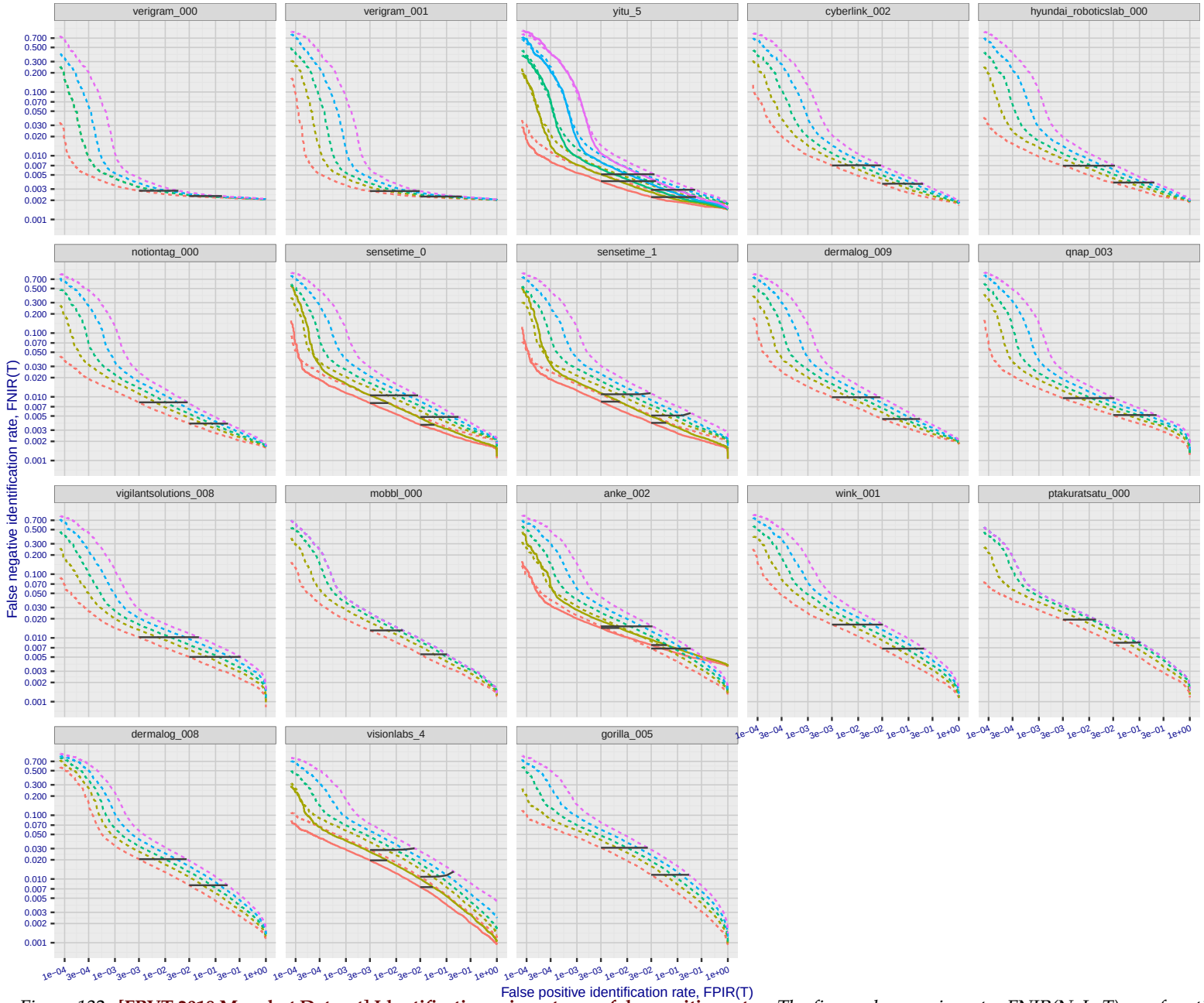

Figure 132: **[FRVT-2018 Mugshot Dataset] Identification miss rates vs. false positive rates**. *The figure shows miss rates FNIR(N, L, T) as a function of FPIR(N, T), with N ranging from 640 000 to 12 000 000 as noted in rows 1-10 of Table 1. These error tradeoff characteristics are useful for applications where a threshold must be elevated to limit false positives, such as when human reviewer labor is not matched to the volume of searches. Dark lines join points of equal threshold: If horizontal, FPIR(T) rises with N, and mate scores are independent of N. Other algorithms adjust scores in an attempt to make FPIR independent of N.*

2026/01/09 20:40:38
FNIR(N, R, T) = False neg. identification rate
FPIR(N, T) = False pos. identification rate
N = Num. enrolled subjects
R = Num. candidates examined
T = Threshold
T = 0 → Investigation
T > 0 → Identification

This publication is available free of charge from: https://doi.org/10.6028/NIST.IR.8271

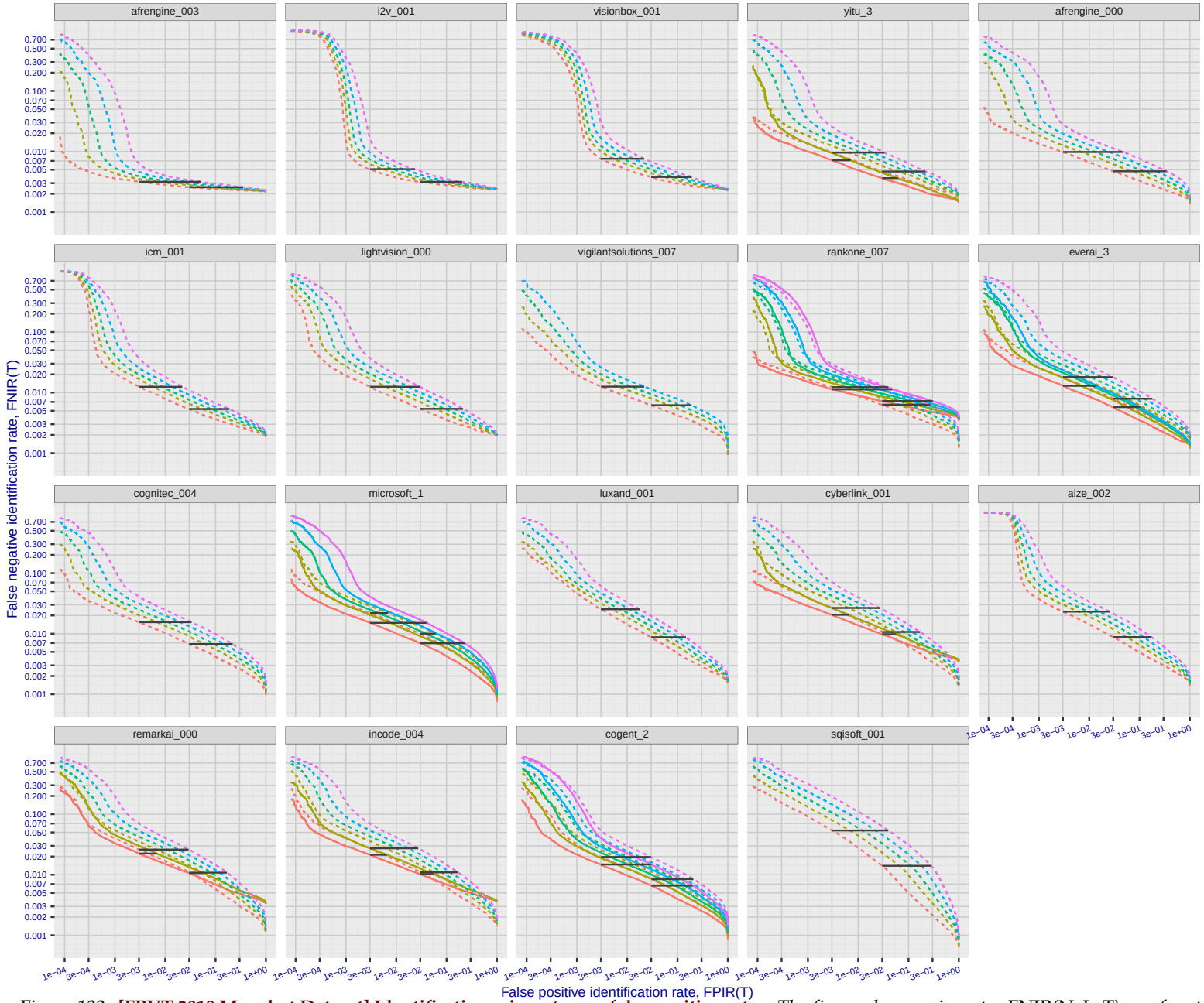

Figure 133: **[FRVT-2018 Mugshot Dataset] Identification miss rates vs. false positive rates**. *The figure shows miss rates FNIR(N, L, T) as a function of FPIR(N, T), with N ranging from 640 000 to 12 000 000 as noted in rows 1-10 of Table 1. These error tradeoff characteristics are useful for applications where a threshold must be elevated to limit false positives, such as when human reviewer labor is not matched to the volume of searches. Dark lines join points of equal threshold: If horizontal, FPIR(T) rises with N, and mate scores are independent of N. Other algorithms adjust scores in an attempt to make FPIR independent of N.*

2026/01/09 20:40:38
FNIR(N, R, T) = False neg. identification rate
FPIR(N, T) = False pos. identification rate
N = Num. enrolled subjects
R = Num. candidates examined
T = Threshold
T = 0 → Investigation
T > 0 → Identification

This publication is available free of charge from: https://doi.org/10.6028/NIST.IR.8271

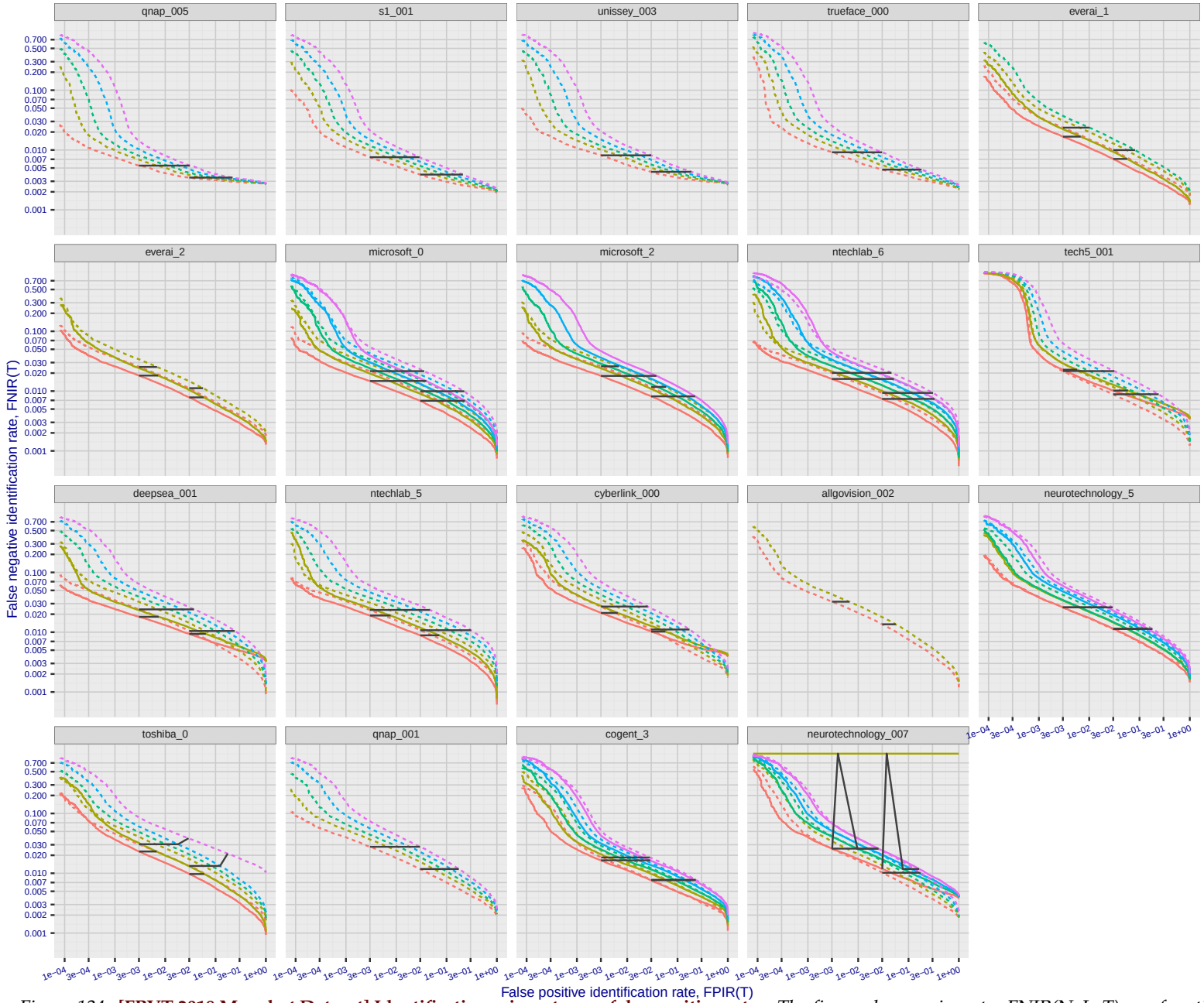

Figure 134: **[FRVT-2018 Mugshot Dataset] Identification miss rates vs. false positive rates**. *The figure shows miss rates FNIR(N, L, T) as a function of FPIR(N, T), with N ranging from 640 000 to 12 000 000 as noted in rows 1-10 of Table 1. These error tradeoff characteristics are useful for applications where a threshold must be elevated to limit false positives, such as when human reviewer labor is not matched to the volume of searches. Dark lines join points of equal threshold: If horizontal, FPIR(T) rises with N, and mate scores are independent of N. Other algorithms adjust scores in an attempt to make FPIR independent of N.*

2026/01/09 20:40:38
FNIR(N, R, T) = False neg. identification rate
FPIR(N, T) = False pos. identification rate
N = Num. enrolled subjects
R = Num. candidates examined
T = Threshold
T = 0 → Investigation
T > 0 → Identification

This publication is available free of charge from: https://doi.org/10.6028/NIST.IR.8271

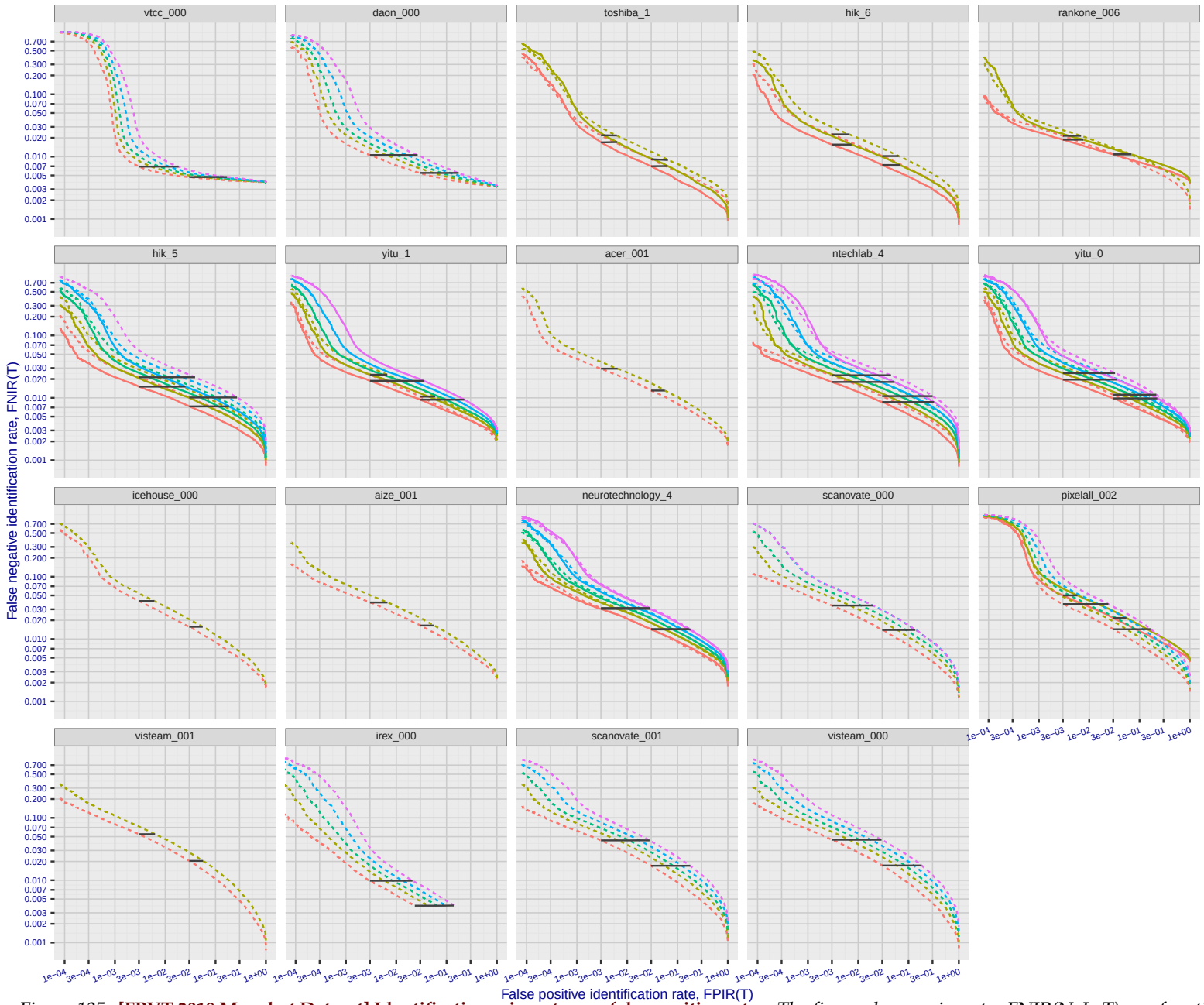

Figure 135: **[FRVT-2018 Mugshot Dataset] Identification miss rates vs. false positive rates**. *The figure shows miss rates FNIR(N, L, T) as a function of FPIR(N, T), with N ranging from 640 000 to 12 000 000 as noted in rows 1-10 of Table 1. These error tradeoff characteristics are useful for applications where a threshold must be elevated to limit false positives, such as when human reviewer labor is not matched to the volume of searches. Dark lines join points of equal threshold: If horizontal, FPIR(T) rises with N, and mate scores are independent of N. Other algorithms adjust scores in an attempt to make FPIR independent of N.*

2026/01/09 20:40:38

FNIR(N, R, T) = False neg. identification rate
FPIR(N, T) = False pos. identification rate

N = Num. enrolled subjects
R = Num. candidates examined

T = Threshold

T = 0 → Investigation
T > 0 → Identification

This publication is available free of charge from: https://doi.org/10.6028/NIST.IR.8271

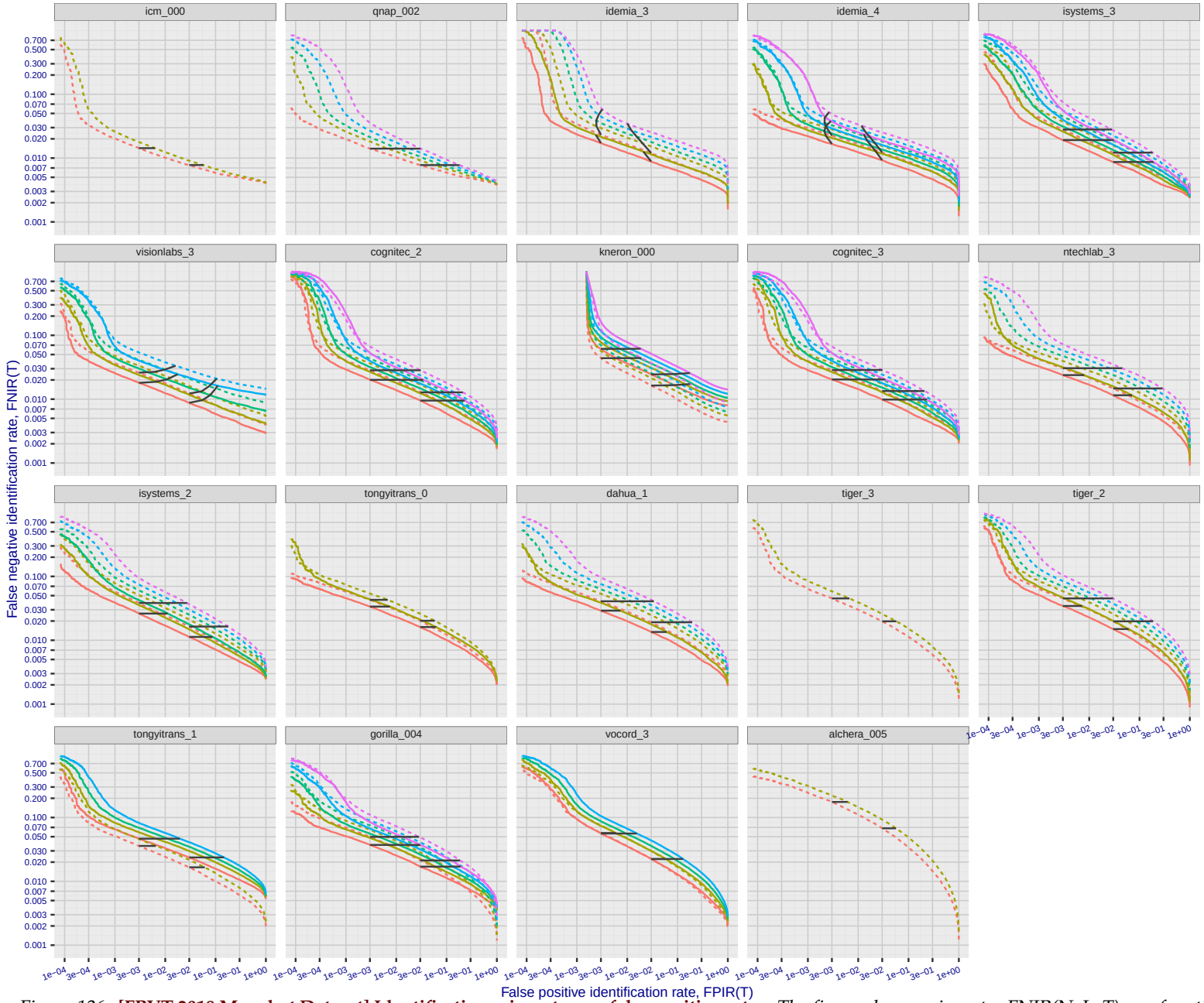

Figure 136: **[FRVT-2018 Mugshot Dataset] Identification miss rates vs. false positive rates**. *The figure shows miss rates FNIR(N, L, T) as a function of FPIR(N, T), with N ranging from 640 000 to 12 000 000 as noted in rows 1-10 of Table 1. These error tradeoff characteristics are useful for applications where a threshold must be elevated to limit false positives, such as when human reviewer labor is not matched to the volume of searches. Dark lines join points of equal threshold: If horizontal, FPIR(T) rises with N, and mate scores are independent of N. Other algorithms adjust scores in an attempt to make FPIR independent of N.*

This publication is available free of charge from: https://doi.org/10.6028/NIST.IR.8271

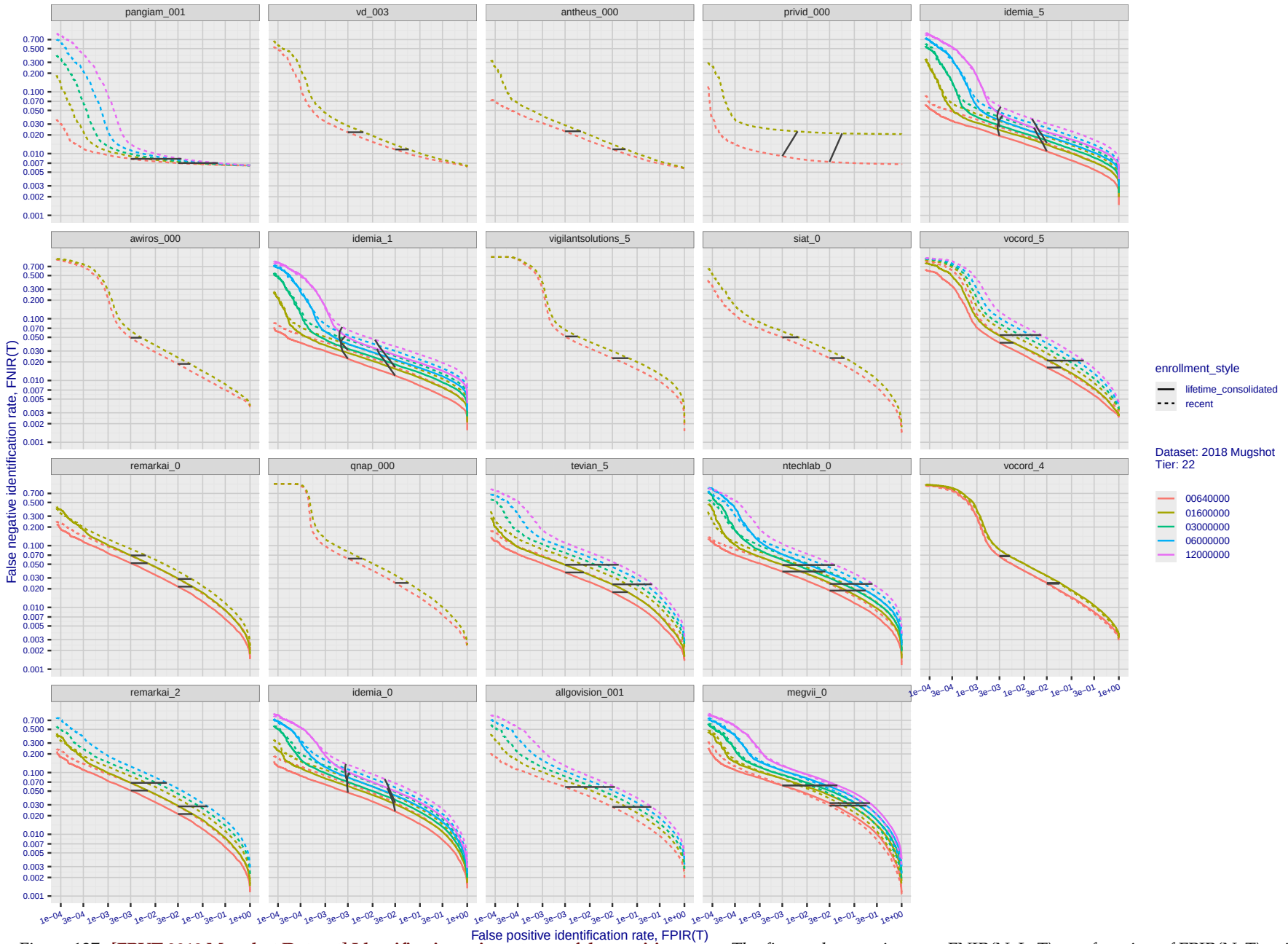

Figure 137: **[FRVT-2018 Mugshot Dataset] Identification miss rates vs. false positive rates**. *The figure shows miss rates FNIR(N, L, T) as a function of FPIR(N, T), with N ranging from 640 000 to 12 000 000 as noted in rows 1-10 of Table 1. These error tradeoff characteristics are useful for applications where a threshold must be elevated to limit false positives, such as when human reviewer labor is not matched to the volume of searches. Dark lines join points of equal threshold: If horizontal, FPIR(T) rises with N, and mate scores are independent of N. Other algorithms adjust scores in an attempt to make FPIR independent of N.*

2026/01/09 20:40:38
FNIR(N, R, T) = False neg. identification rate
FPIR(N, T) = False pos. identification rate
N = Num. enrolled subjects
R = Num. candidates examined
T = Threshold
T = 0 → Investigation
T > 0 → Identification

This publication is available free of charge from: https://doi.org/10.6028/NIST.IR.8271

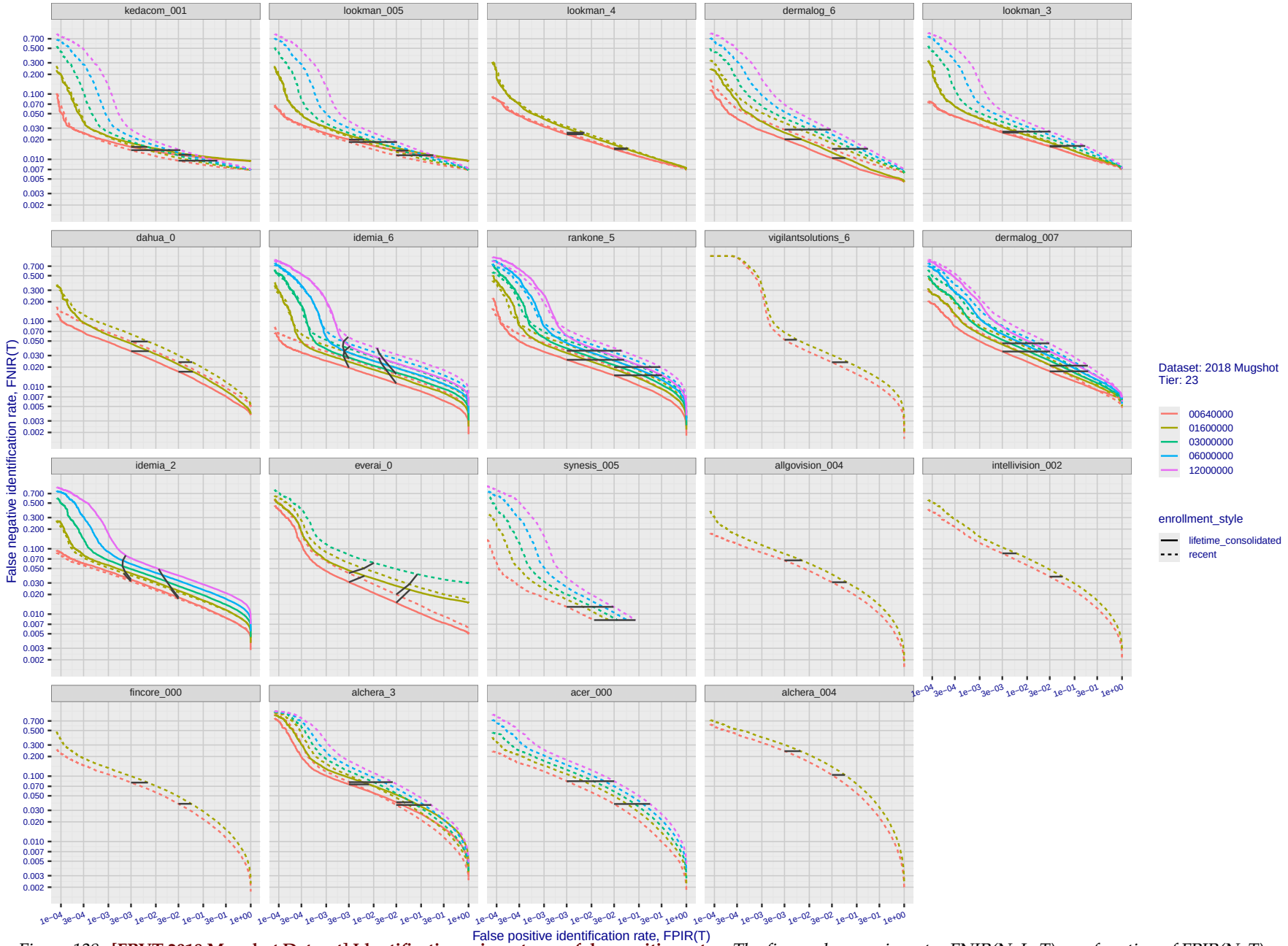

Figure 138: **[FRVT-2018 Mugshot Dataset] Identification miss rates vs. false positive rates**. *The figure shows miss rates FNIR(N, L, T) as a function of FPIR(N, T), with N ranging from 640 000 to 12 000 000 as noted in rows 1-10 of Table 1. These error tradeoff characteristics are useful for applications where a threshold must be elevated to limit false positives, such as when human reviewer labor is not matched to the volume of searches. Dark lines join points of equal threshold: If horizontal, FPIR(T) rises with N, and mate scores are independent of N. Other algorithms adjust scores in an attempt to make FPIR independent of N.*

2026/01/09 20:40:38
FNIR(N, R, T) = False neg. identification rate
FPIR(N, T) = False pos. identification rate
N = Num. enrolled subjects
R = Num. candidates examined
T = Threshold
T = 0 → Investigation
T > 0 → Identification

This publication is available free of charge from: https://doi.org/10.6028/NIST.IR.8271

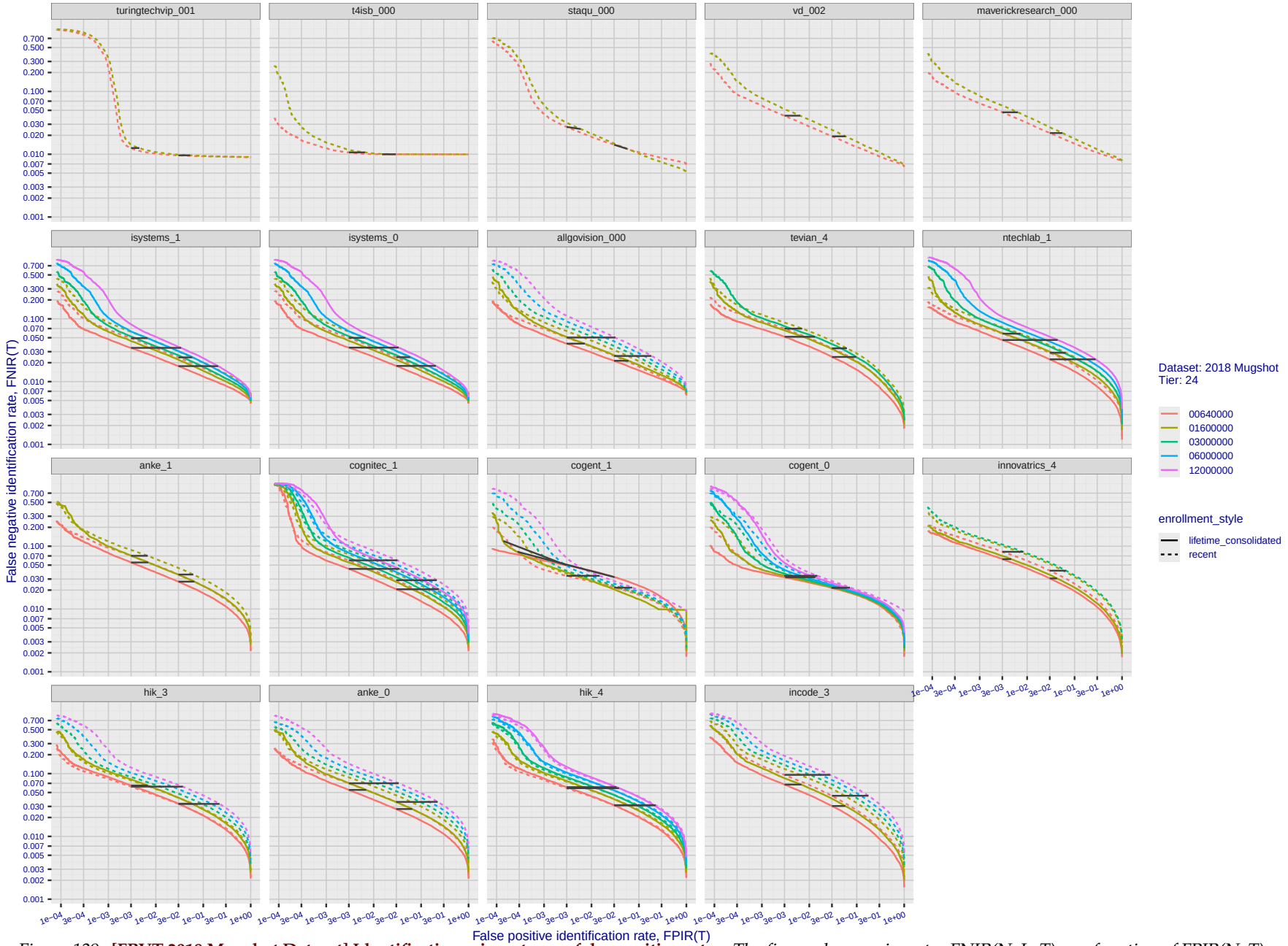

Figure 139: **[FRVT-2018 Mugshot Dataset] Identification miss rates vs. false positive rates**. *The figure shows miss rates FNIR(N, L, T) as a function of FPIR(N, T), with N ranging from 640 000 to 12 000 000 as noted in rows 1-10 of Table 1. These error tradeoff characteristics are useful for applications where a threshold must be elevated to limit false positives, such as when human reviewer labor is not matched to the volume of searches. Dark lines join points of equal threshold: If horizontal, FPIR(T) rises with N, and mate scores are independent of N. Other algorithms adjust scores in an attempt to make FPIR independent of N.*

2026/01/09 20:40:38
FNIR(N, R, T) = False neg. identification rate
FPIR(N, T) = False pos. identification rate
N = Num. enrolled subjects
R = Num. candidates examined
T = Threshold
T = 0 → Investigation
T > 0 → Identification

This publication is available free of charge from: https://doi.org/10.6028/NIST.IR.8271

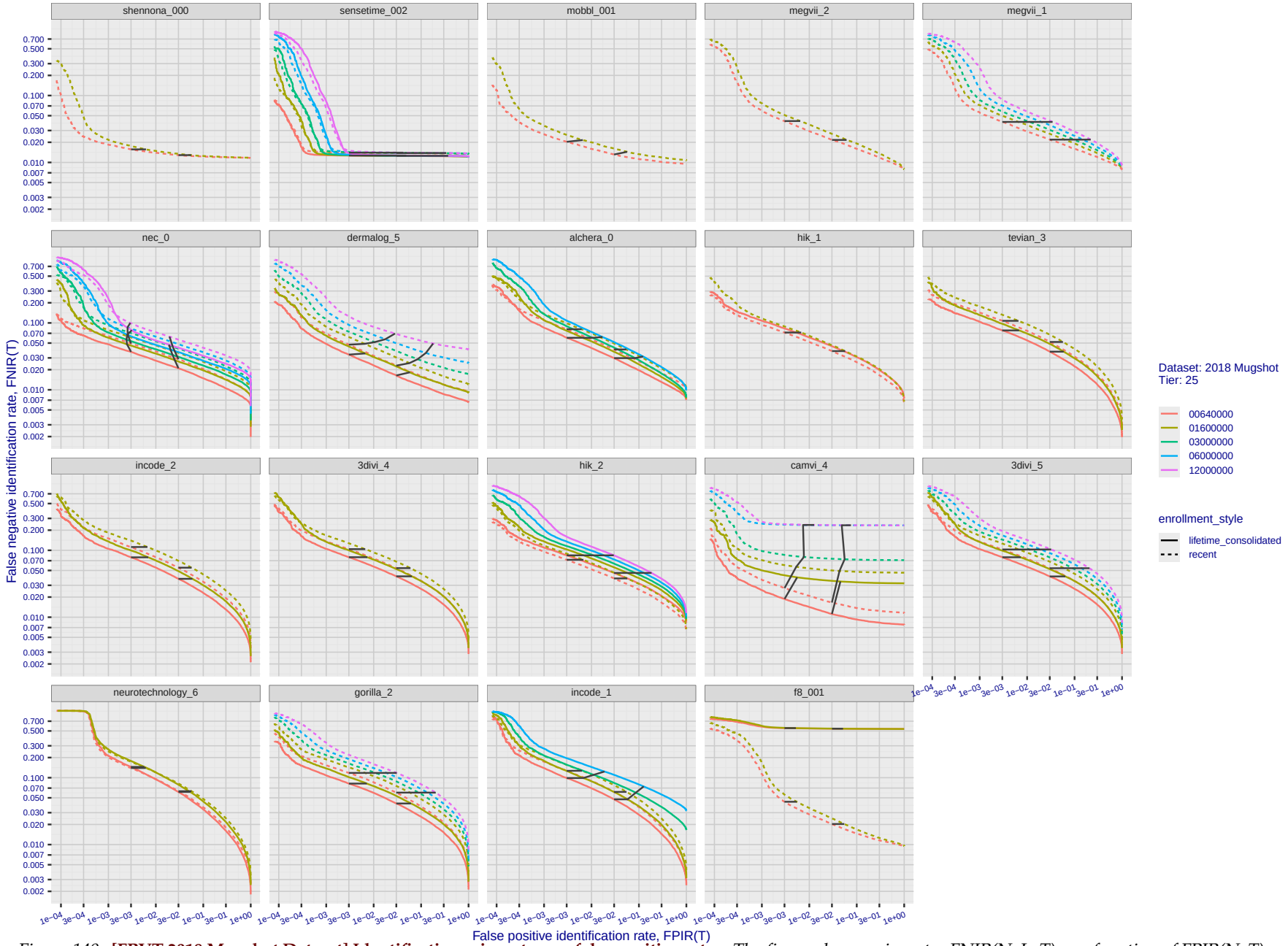

Figure 140: **[FRVT-2018 Mugshot Dataset] Identification miss rates vs. false positive rates**. *The figure shows miss rates FNIR(N, L, T) as a function of FPIR(N, T), with N ranging from 640 000 to 12 000 000 as noted in rows 1-10 of Table 1. These error tradeoff characteristics are useful for applications where a threshold must be elevated to limit false positives, such as when human reviewer labor is not matched to the volume of searches. Dark lines join points of equal threshold: If horizontal, FPIR(T) rises with N, and mate scores are independent of N. Other algorithms adjust scores in an attempt to make FPIR independent of N.*

2026/01/09 20:40:38
FNIR(N, R, T) = False neg. identification rate
FPIR(N, T) = False pos. identification rate
N = Num. enrolled subjects
R = Num. candidates examined
T = Threshold
T = 0 → Investigation
T > 0 → Identification

This publication is available free of charge from: https://doi.org/10.6028/NIST.IR.8271

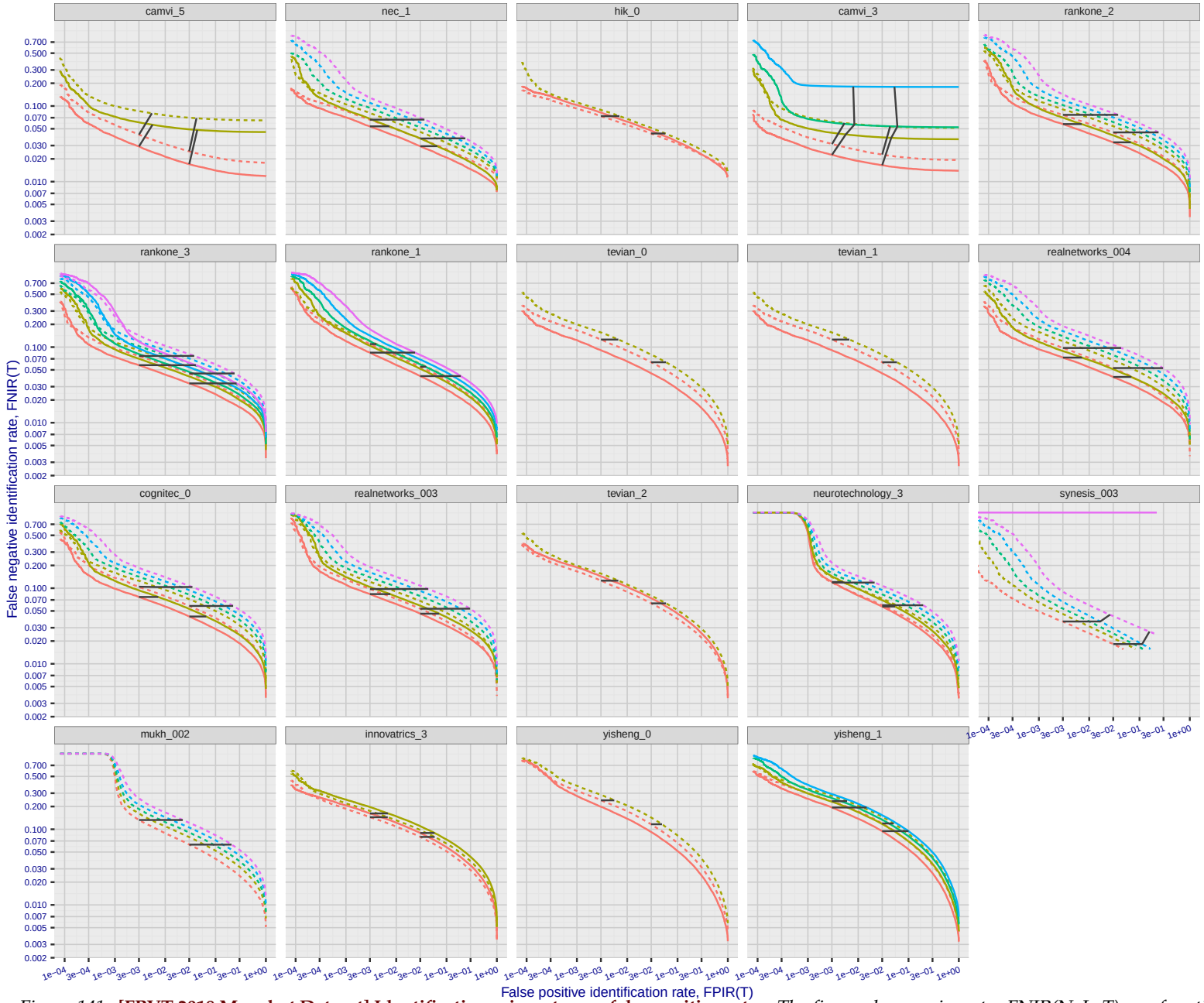

Figure 141: **[FRVT-2018 Mugshot Dataset] Identification miss rates vs. false positive rates**. *The figure shows miss rates FNIR(N, L, T) as a function of FPIR(N, T), with N ranging from 640 000 to 12 000 000 as noted in rows 1-10 of Table 1. These error tradeoff characteristics are useful for applications where a threshold must be elevated to limit false positives, such as when human reviewer labor is not matched to the volume of searches. Dark lines join points of equal threshold: If horizontal, FPIR(T) rises with N, and mate scores are independent of N. Other algorithms adjust scores in an attempt to make FPIR independent of N.*

2026/01/09 20:40:38
FNIR(N, R, T) = False neg. identification rate
FPIR(N, T) = False pos. identification rate
N = Num. enrolled subjects
R = Num. candidates examined
T = Threshold
T = 0 → Investigation
T > 0 → Identification

This publication is available free of charge from: https://doi.org/10.6028/NIST.IR.8271

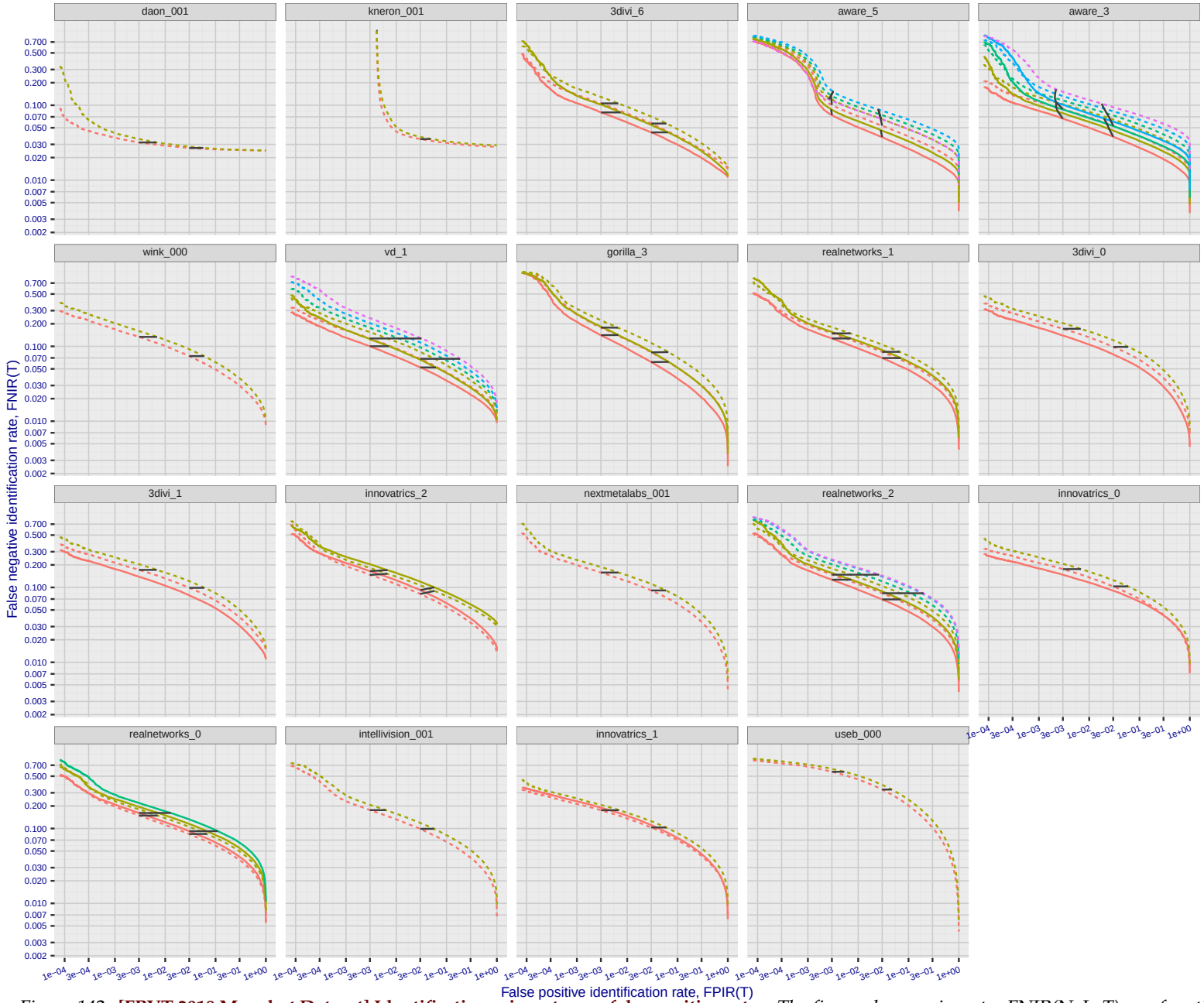

Figure 142: **[FRVT-2018 Mugshot Dataset] Identification miss rates vs. false positive rates**. *The figure shows miss rates FNIR(N, L, T) as a function of FPIR(N, T), with N ranging from 640 000 to 12 000 000 as noted in rows 1-10 of Table 1. These error tradeoff characteristics are useful for applications where a threshold must be elevated to limit false positives, such as when human reviewer labor is not matched to the volume of searches. Dark lines join points of equal threshold: If horizontal, FPIR(T) rises with N, and mate scores are independent of N. Other algorithms adjust scores in an attempt to make FPIR independent of N.*

2026/01/09
20:40:38

FNIR(N, R, T) = False neg. identification rate
FPIR(N, T) = False pos. identification rate

N = Num. enrolled subjects
R = Num. candidates examined

T = Threshold

T = 0 → Investigation
T > 0 → Identification

This publication is available free of charge from: https://doi.org/10.6028/NIST.IR.8271

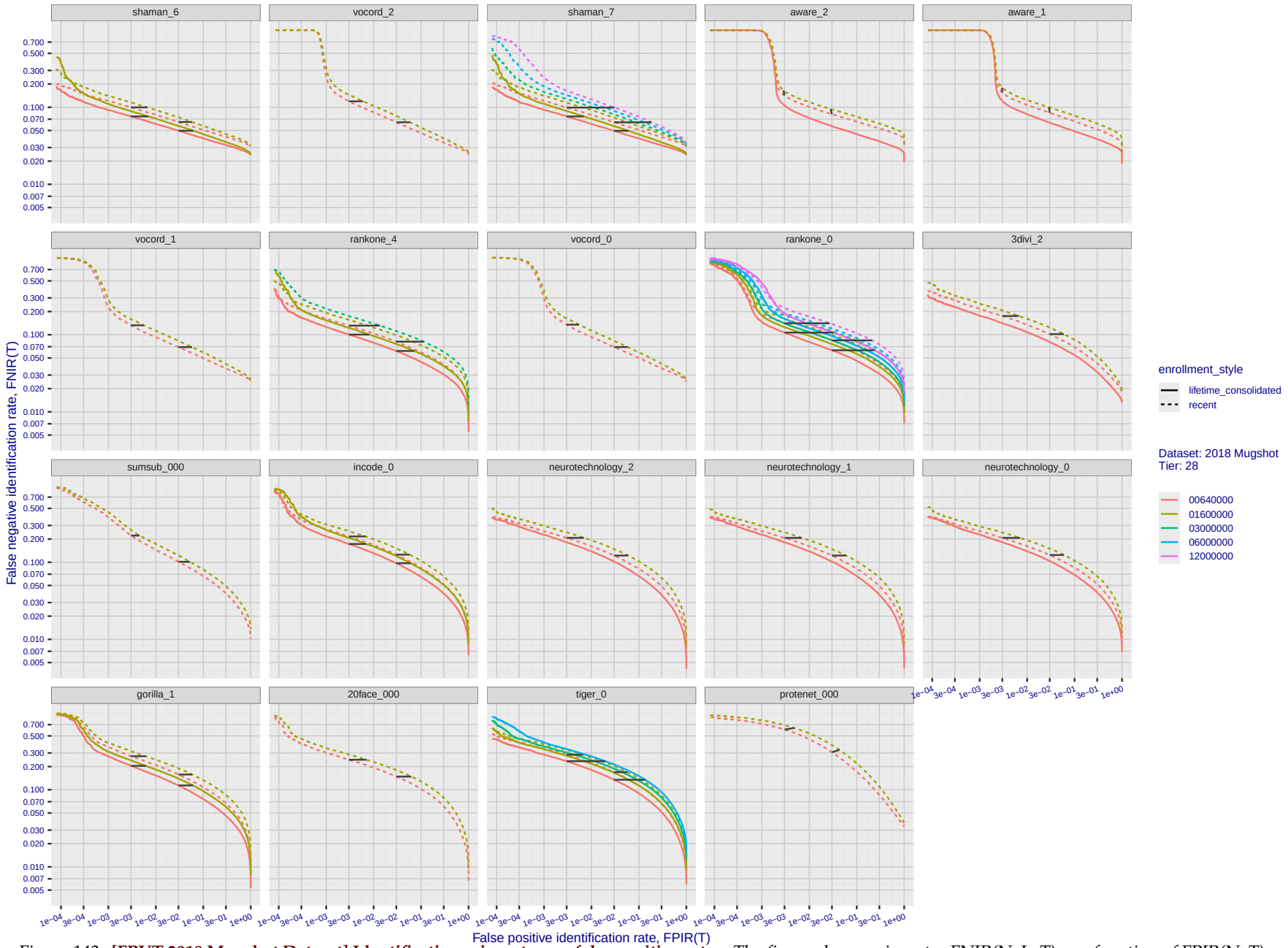

Figure 143: **[FRVT-2018 Mugshot Dataset] Identification miss rates vs. false positive rates**. *The figure shows miss rates FNIR(N, L, T) as a function of FPIR(N, T), with N ranging from 640 000 to 12 000 000 as noted in rows 1-10 of Table 1. These error tradeoff characteristics are useful for applications where a threshold must be elevated to limit false positives, such as when human reviewer labor is not matched to the volume of searches. Dark lines join points of equal threshold: If horizontal, FPIR(T) rises with N, and mate scores are independent of N. Other algorithms adjust scores in an attempt to make FPIR independent of N.*

2026/01/09 20:40:38

FNIR(N, R, T) = False neg. identification rate
FPIR(N, T) = False pos. identification rate

N = Num. enrolled subjects
R = Num. candidates examined

T = Threshold

T = 0 → Investigation
T > 0 → Identification

This publication is available free of charge from: https://doi.org/10.6028/NIST.IR.8271

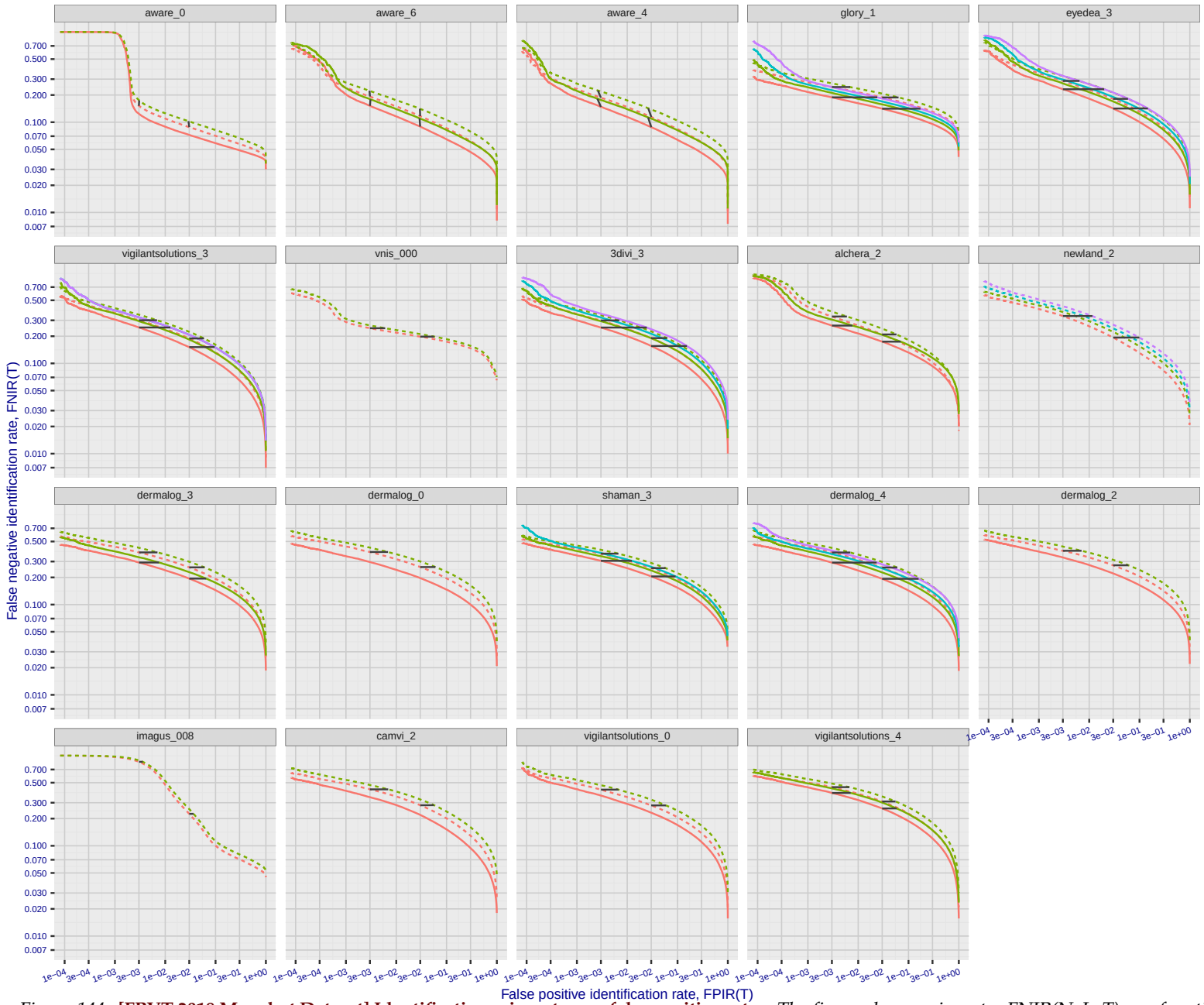

Figure 144: **[FRVT-2018 Mugshot Dataset] Identification miss rates vs. false positive rates**. *The figure shows miss rates FNIR(N, L, T) as a function of FPIR(N, T), with N ranging from 640 000 to 12 000 000 as noted in rows 1-10 of Table 1. These error tradeoff characteristics are useful for applications where a threshold must be elevated to limit false positives, such as when human reviewer labor is not matched to the volume of searches. Dark lines join points of equal threshold: If horizontal, FPIR(T) rises with N, and mate scores are independent of N. Other algorithms adjust scores in an attempt to make FPIR independent of N.*

2026/01/09 20:40:38

FNIR(N, R, T) = False neg. identification rate
FPIR(N, T) = False pos. identification rate

N = Num. enrolled subjects
R = Num. candidates examined

T = Threshold

T = 0 → Investigation
T > 0 → Identification

This publication is available free of charge from: https://doi.org/10.6028/NIST.IR.8271

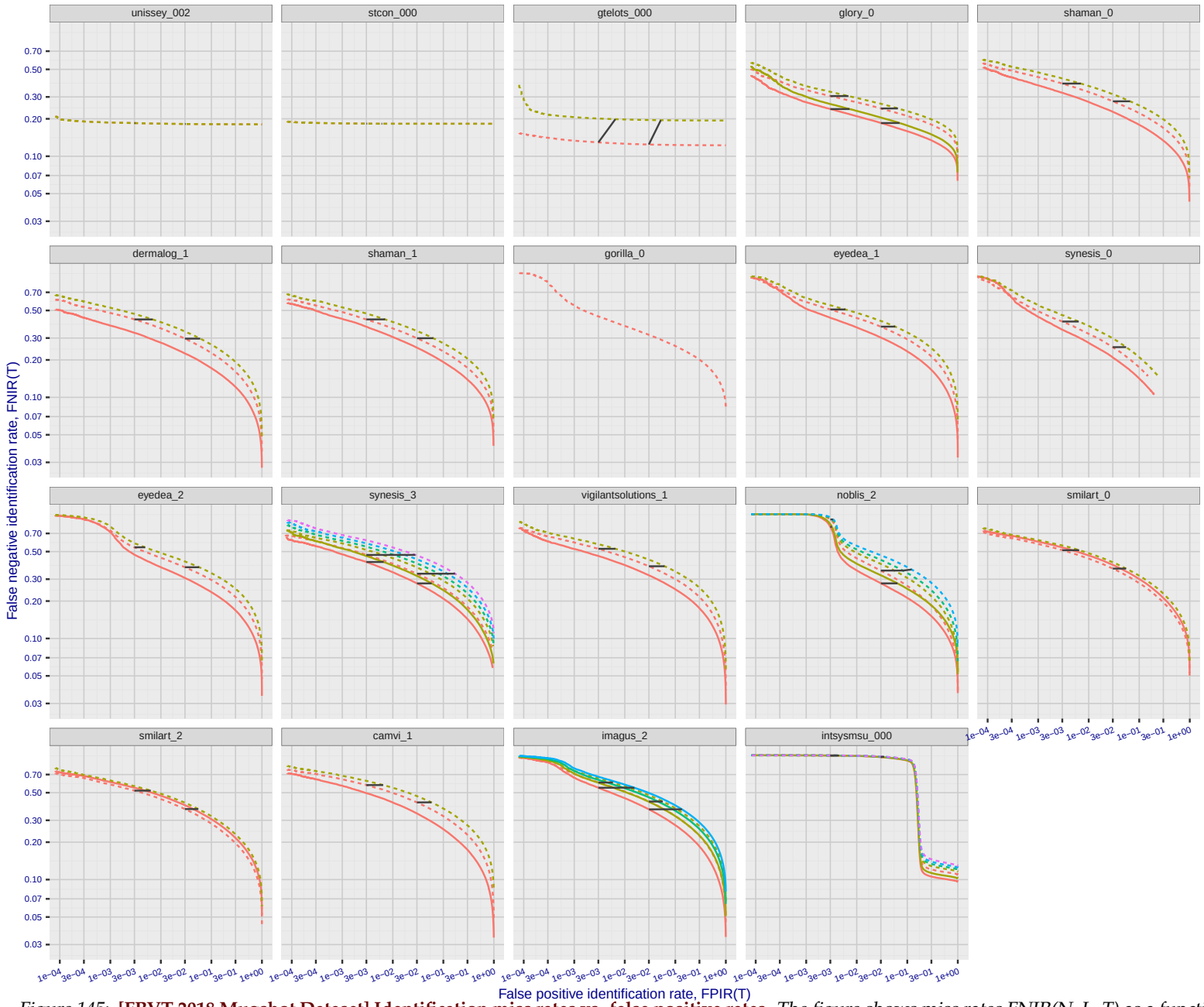

Figure 145: **[FRVT-2018 Mugshot Dataset] Identification miss rates vs. false positive rates**. *The figure shows miss rates FNIR(N, L, T) as a function of FPIR(N, T), with N ranging from 640 000 to 12 000 000 as noted in rows 1-10 of Table 1. These error tradeoff characteristics are useful for applications where a threshold must be elevated to limit false positives, such as when human reviewer labor is not matched to the volume of searches. Dark lines join points of equal threshold: If horizontal, FPIR(T) rises with N, and mate scores are independent of N. Other algorithms adjust scores in an attempt to make FPIR independent of N.*

2026/01/09 20:40:38

FNIR(N, R, T) = False neg. identification rate
FPIR(N, T) = False pos. identification rate

N = Num. enrolled subjects
R = Num. candidates examined

T = Threshold

T = 0 → Investigation
T > 0 → Identification

This publication is available free of charge from: https://doi.org/10.6028/NIST.IR.8271

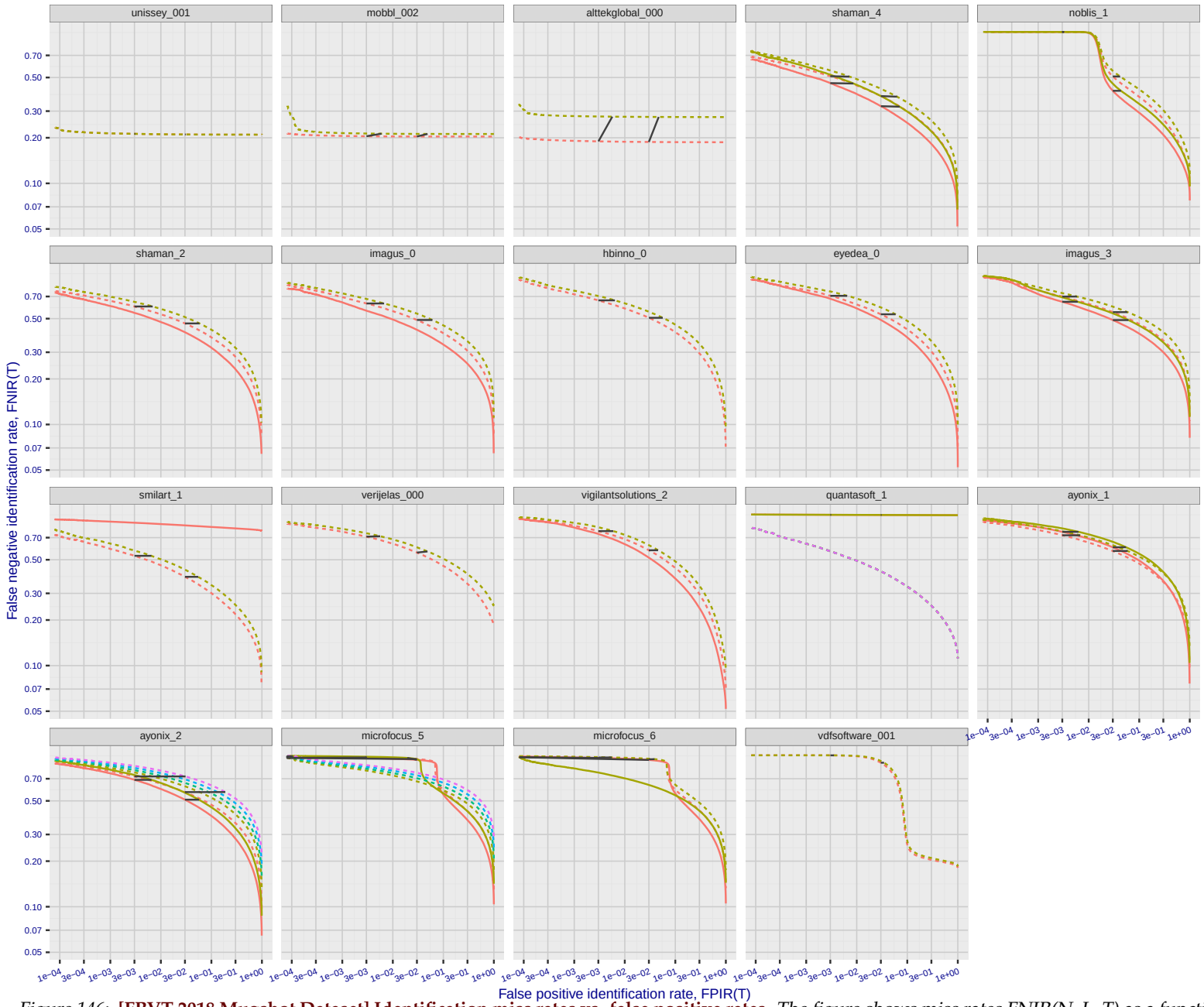

Figure 146: **[FRVT-2018 Mugshot Dataset] Identification miss rates vs. false positive rates**. *The figure shows miss rates FNIR(N, L, T) as a function of FPIR(N, T), with N ranging from 640 000 to 12 000 000 as noted in rows 1-10 of Table 1. These error tradeoff characteristics are useful for applications where a threshold must be elevated to limit false positives, such as when human reviewer labor is not matched to the volume of searches. Dark lines join points of equal threshold: If horizontal, FPIR(T) rises with N, and mate scores are independent of N. Other algorithms adjust scores in an attempt to make FPIR independent of N.*

2026/01/09 20:40:38

FNIR(N, R, T) = False neg. identification rate
FPIR(N, T) = False pos. identification rate

N = Num. enrolled subjects
R = Num. candidates examined

T = Threshold

T = 0 → Investigation
T > 0 → Identification

This publication is available free of charge from: https://doi.org/10.6028/NIST.IR.8271

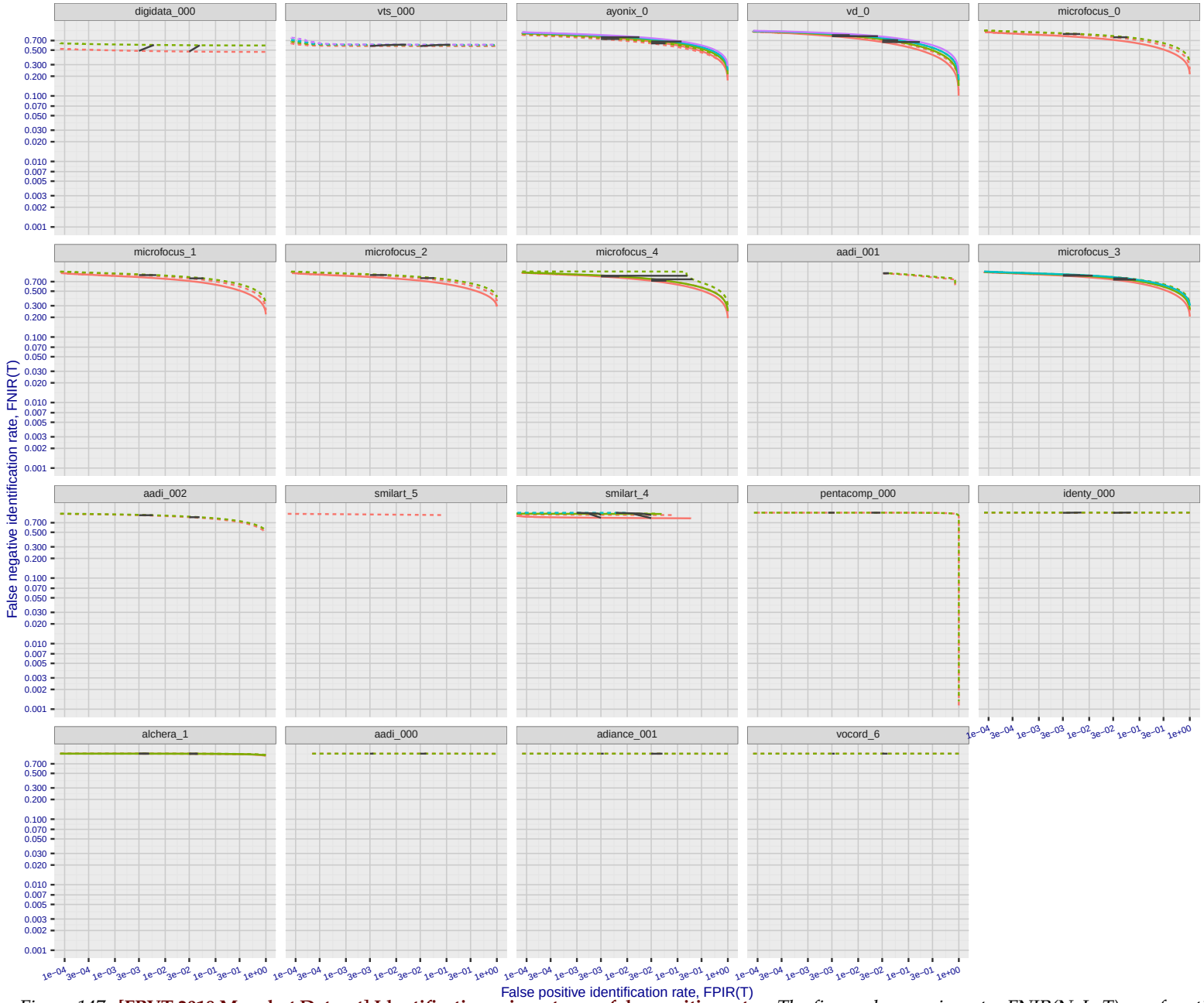

Figure 147: **[FRVT-2018 Mugshot Dataset] Identification miss rates vs. false positive rates**. *The figure shows miss rates FNIR(N, L, T) as a function of FPIR(N, T), with N ranging from 640 000 to 12 000 000 as noted in rows 1-10 of Table 1. These error tradeoff characteristics are useful for applications where a threshold must be elevated to limit false positives, such as when human reviewer labor is not matched to the volume of searches. Dark lines join points of equal threshold: If horizontal, FPIR(T) rises with N, and mate scores are independent of N. Other algorithms adjust scores in an attempt to make FPIR independent of N.*

2026/01/09 20:40:38
FNIR(N, R, T) = False neg. identification rate
FPIR(N, T) = False pos. identification rate
N = Num. enrolled subjects
R = Num. candidates examined
T = Threshold
T = 0 → Investigation
T > 0 → Identification

Appendix B Effect of time-lapse: Accuracy after face ageing

This publication is available free of charge from: https://doi.org/10.6028/NIST.IR.8271

This publication is available free of charge from: https://doi.org/10.6028/NIST.IR.8271

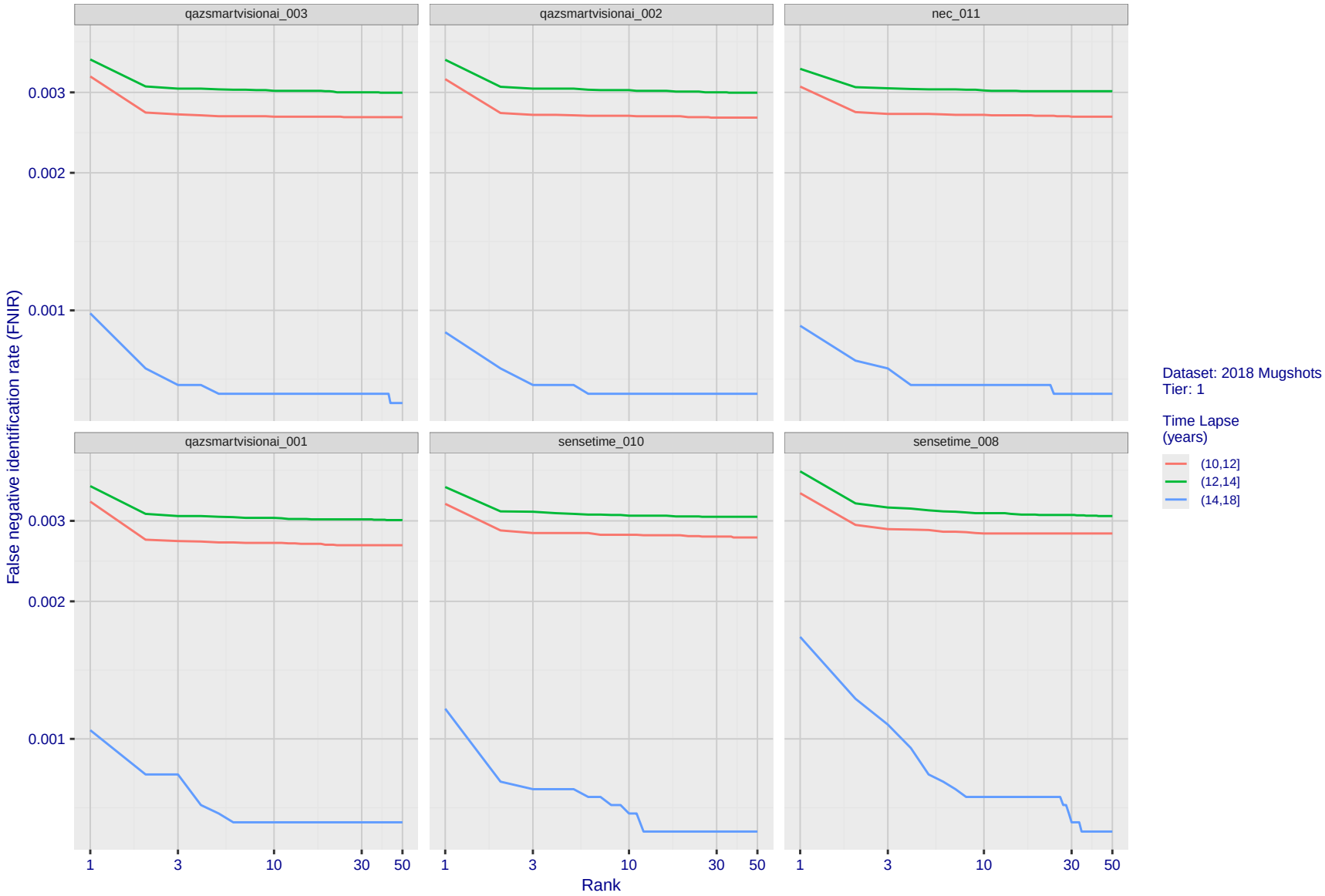

Figure 148: **[FRVT-2018 Mugshot Ageing Dataset] Identification miss rates vs. rank by time-elapsed**. *The oldest image of each individual is enrolled. Thereafter, all more recent images are searched. Miss rates are computed over all searches noted in row 17 of Table 1 and binned by number of years between search and initial enrollment.*

2026/01/09 20:40:38
FNIR(N, R, T) = False neg. identification rate
FPIR(N, T) = False pos. identification rate
N = Num. enrolled subjects
R = Num. candidates examined
T = Threshold
T = 0 → Investigation
T > 0 → Identification

This publication is available free of charge from: https://doi.org/10.6028/NIST.IR.8271

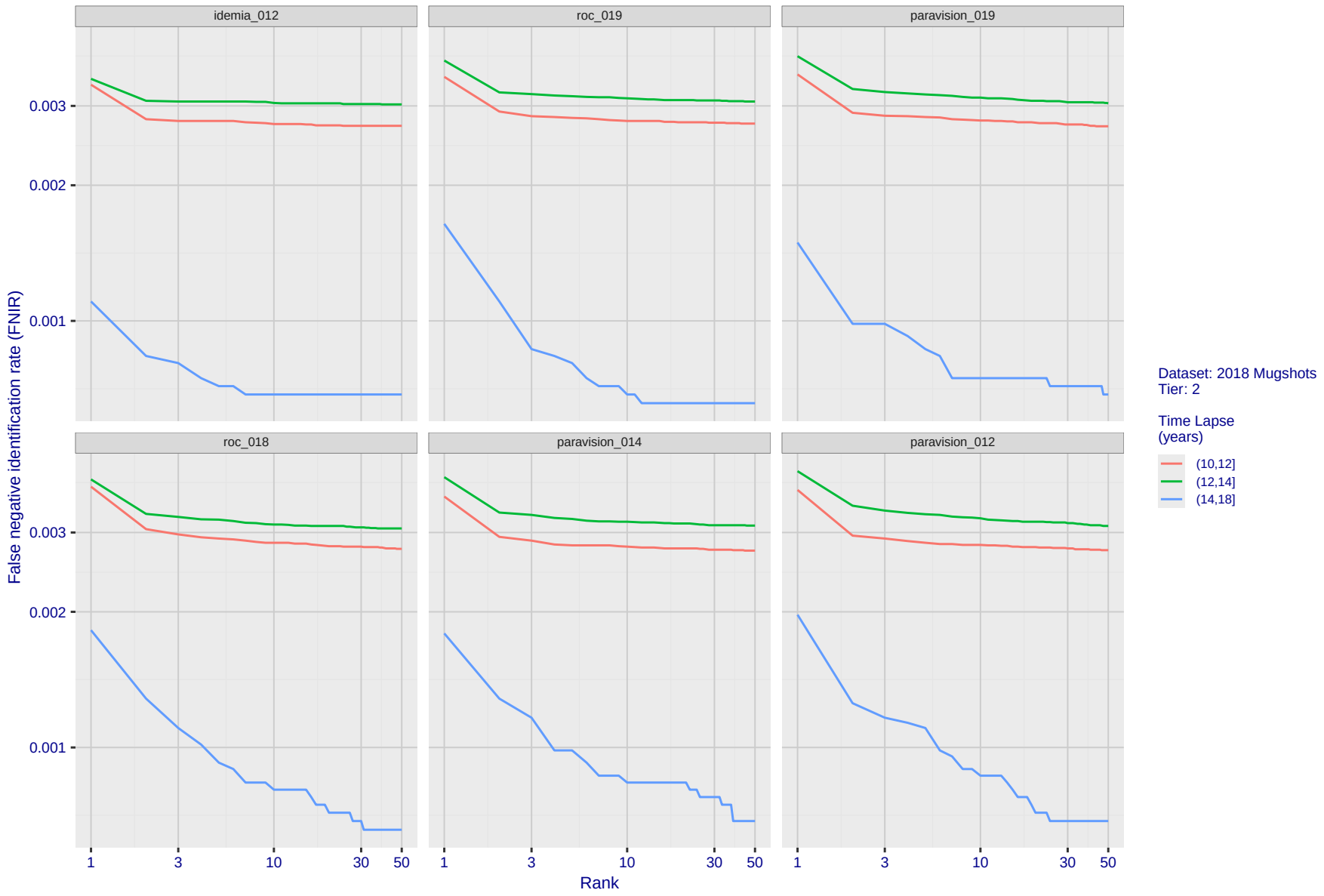

Figure 149: **[FRVT-2018 Mugshot Ageing Dataset] Identification miss rates vs. rank by time-elapsed**. *The oldest image of each individual is enrolled. Thereafter, all more recent images are searched. Miss rates are computed over all searches noted in row 17 of Table 1 and binned by number of years between search and initial enrollment.*

This publication is available free of charge from: https://doi.org/10.6028/NIST.IR.8271

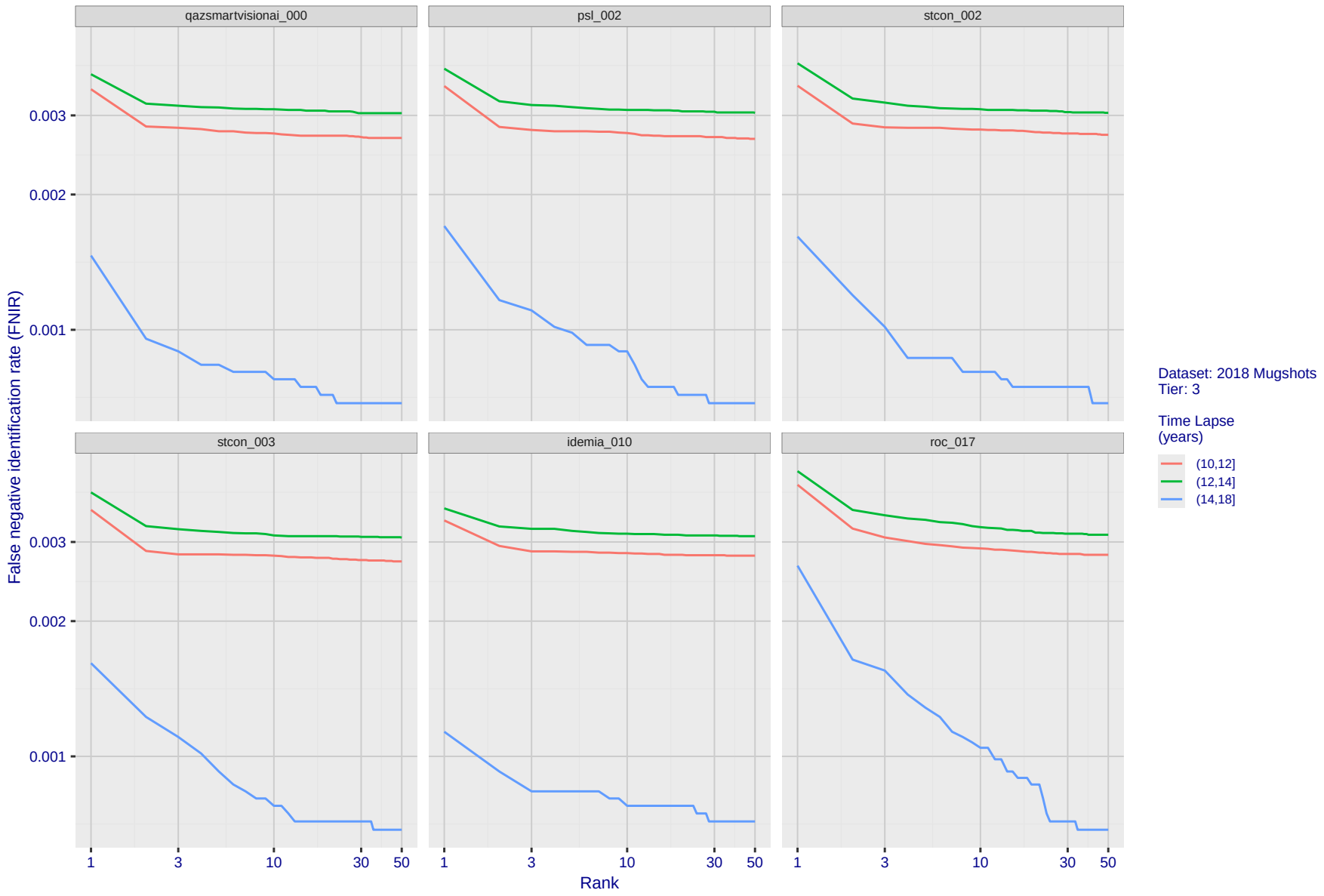

Figure 150: **[FRVT-2018 Mugshot Ageing Dataset] Identification miss rates vs. rank by time-elapsed**. *The oldest image of each individual is enrolled. Thereafter, all more recent images are searched. Miss rates are computed over all searches noted in row 17 of Table 1 and binned by number of years between search and initial enrollment.*

2026/01/09 20:40:38
FNIR(N, R, T) = False neg. identification rate
FPIR(N, T) = False pos. identification rate
N = Num. enrolled subjects
R = Num. candidates examined
T = Threshold
T = 0 → Investigation
T > 0 → Identification

This publication is available free of charge from: https://doi.org/10.6028/NIST.IR.8271

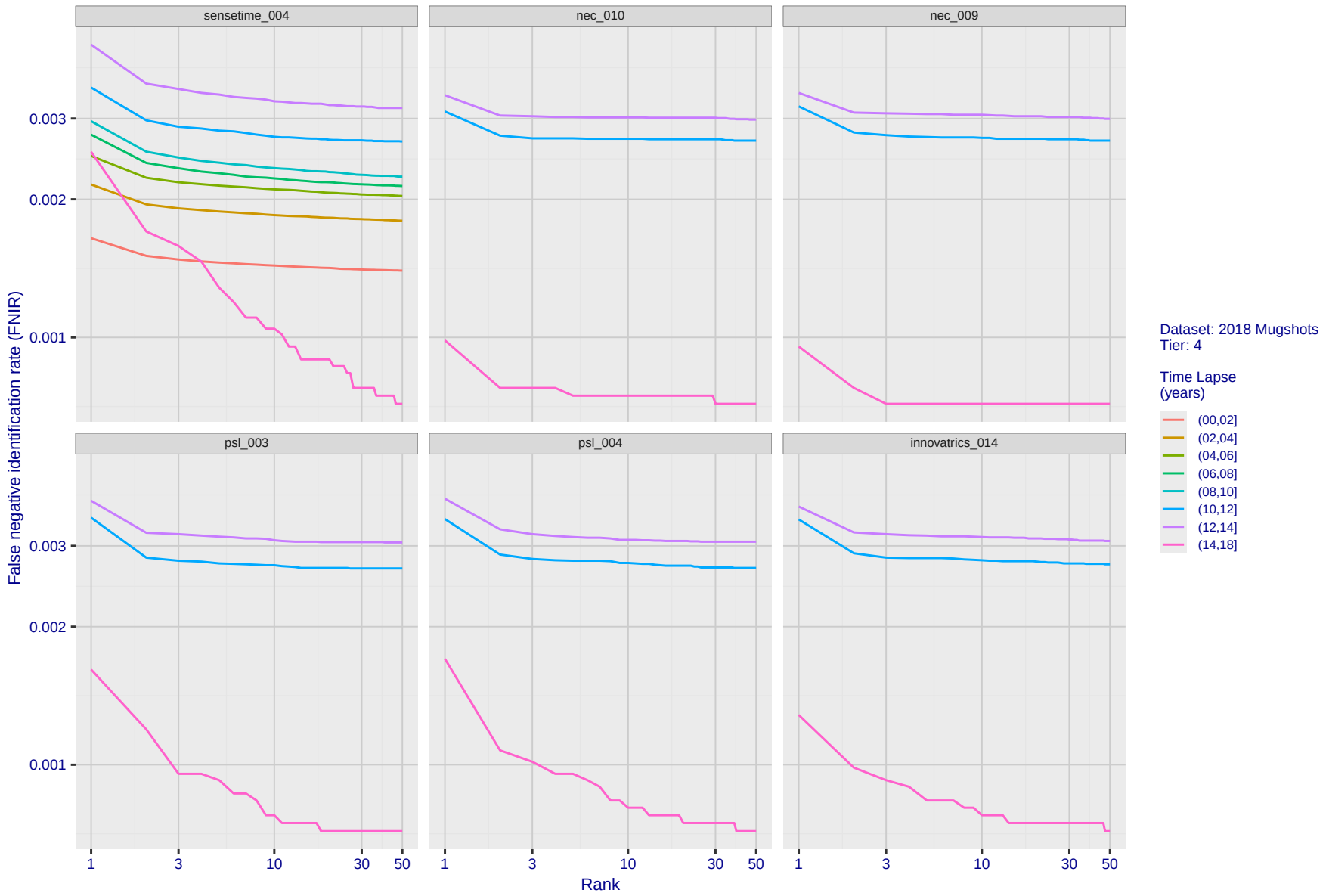

Figure 151: **[FRVT-2018 Mugshot Ageing Dataset] Identification miss rates vs. rank by time-elapsed**. *The oldest image of each individual is enrolled. Thereafter, all more recent images are searched. Miss rates are computed over all searches noted in row 17 of Table 1 and binned by number of years between search and initial enrollment.*

2026/01/09 20:40:38
FNIR(N, R, T) = False neg. identification rate
FPIR(N, T) = False pos. identification rate
N = Num. enrolled subjects
R = Num. candidates examined
T = Threshold
T = 0 → Investigation
T > 0 → Identification

This publication is available free of charge from: https://doi.org/10.6028/NIST.IR.8271

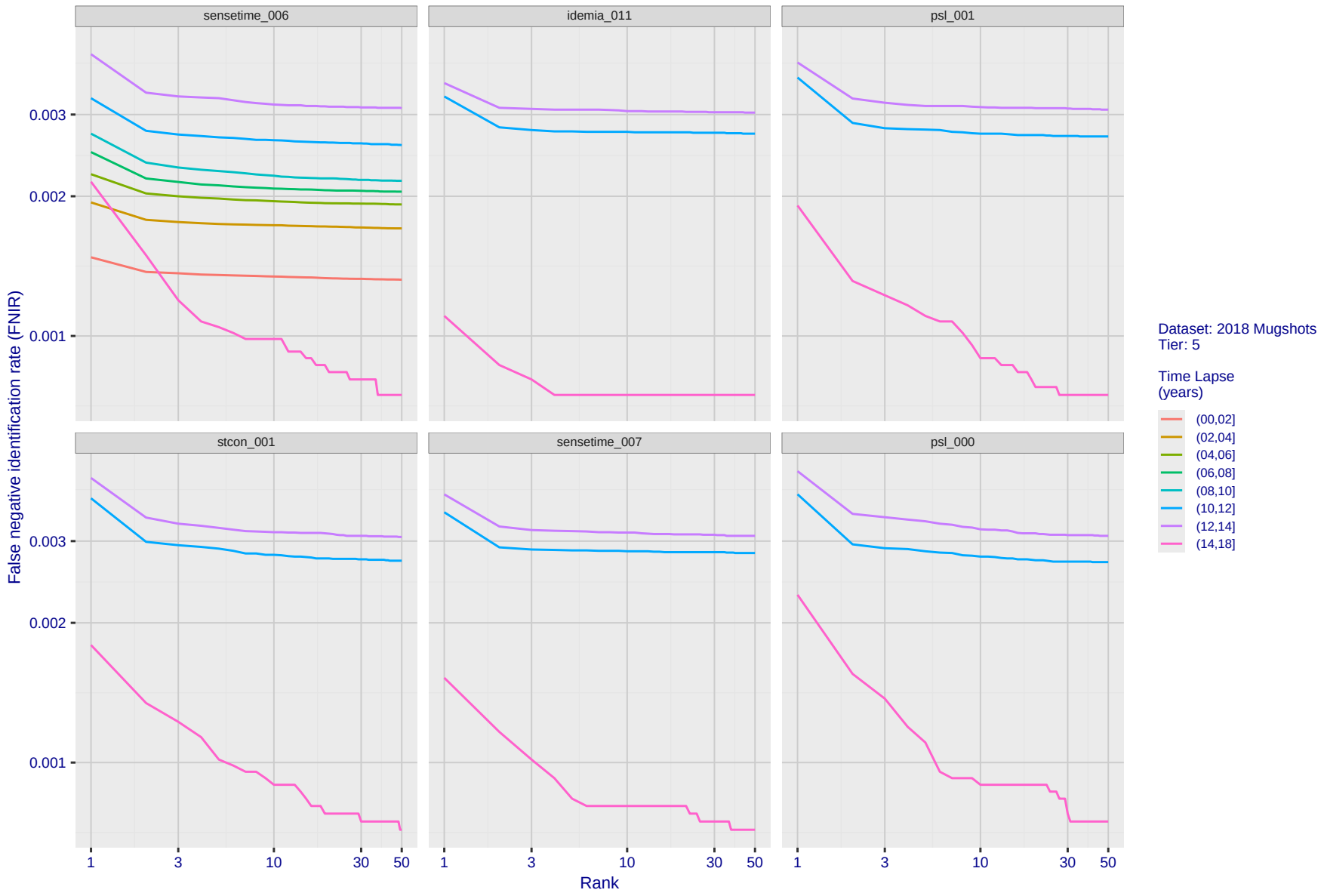

Figure 152: **[FRVT-2018 Mugshot Ageing Dataset] Identification miss rates vs. rank by time-elapsed**. *The oldest image of each individual is enrolled. Thereafter, all more recent images are searched. Miss rates are computed over all searches noted in row 17 of Table 1 and binned by number of years between search and initial enrollment.*

2026/01/09 20:40:38

FNIR(N, R, T) = False neg. identification rate
FPIR(N, T) = False pos. identification rate

N = Num. enrolled subjects
R = Num. candidates examined

T = Threshold

T = 0 → Investigation
T > 0 → Identification

This publication is available free of charge from: https://doi.org/10.6028/NIST.IR.8271

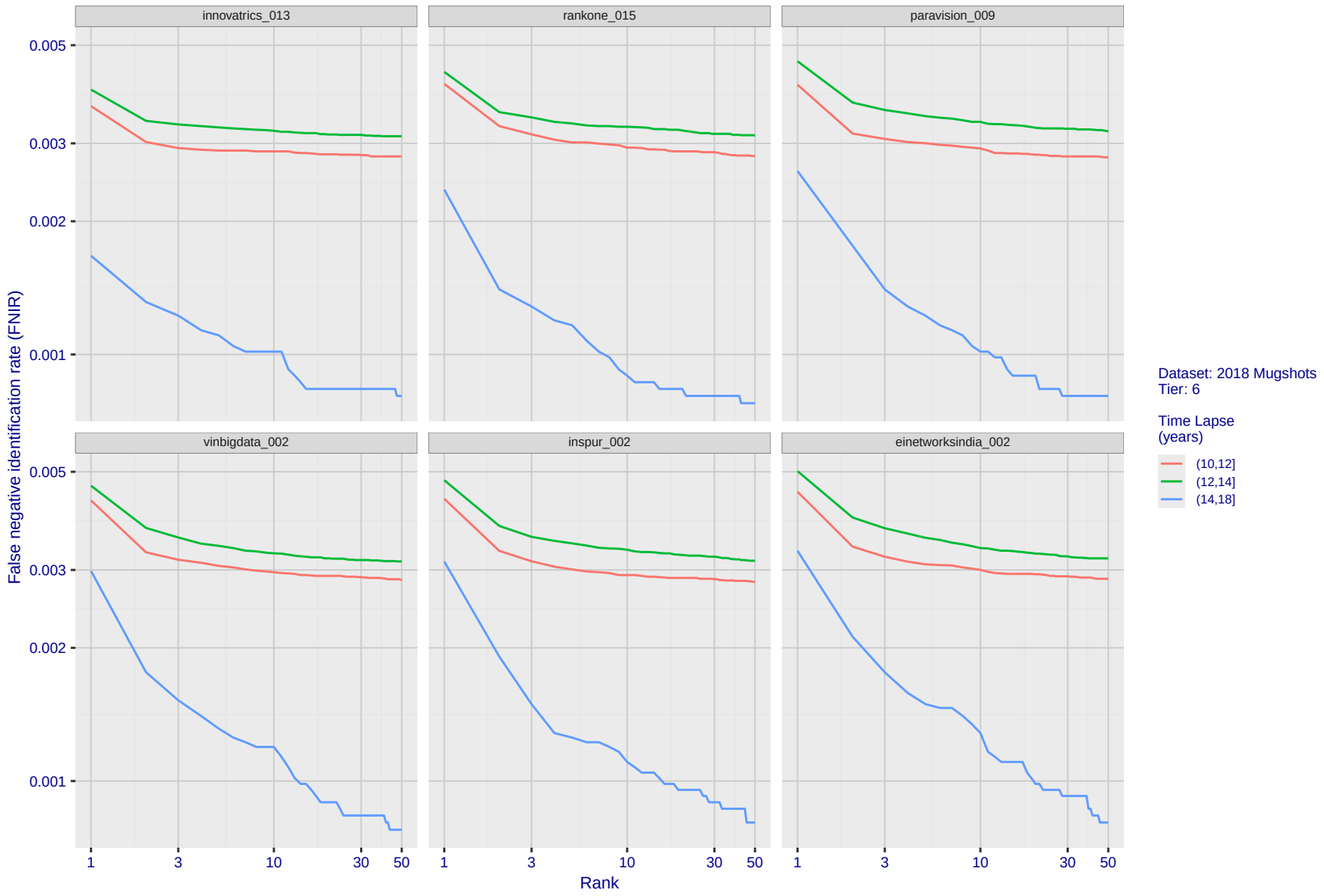

Figure 153: **[FRVT-2018 Mugshot Ageing Dataset] Identification miss rates vs. rank by time-elapsed**. *The oldest image of each individual is enrolled. Thereafter, all more recent images are searched. Miss rates are computed over all searches noted in row 17 of Table 1 and binned by number of years between search and initial enrollment.*

2026/01/09
20:40:38

FNIR(N, R, T) = False neg. identification rate
FPIR(N, T) = False pos. identification rate

N = Num. enrolled subjects
R = Num. candidates examined

T = Threshold

T = 0 → Investigation
T > 0 → Identification

This publication is available free of charge from: https://doi.org/10.6028/NIST.IR.8271

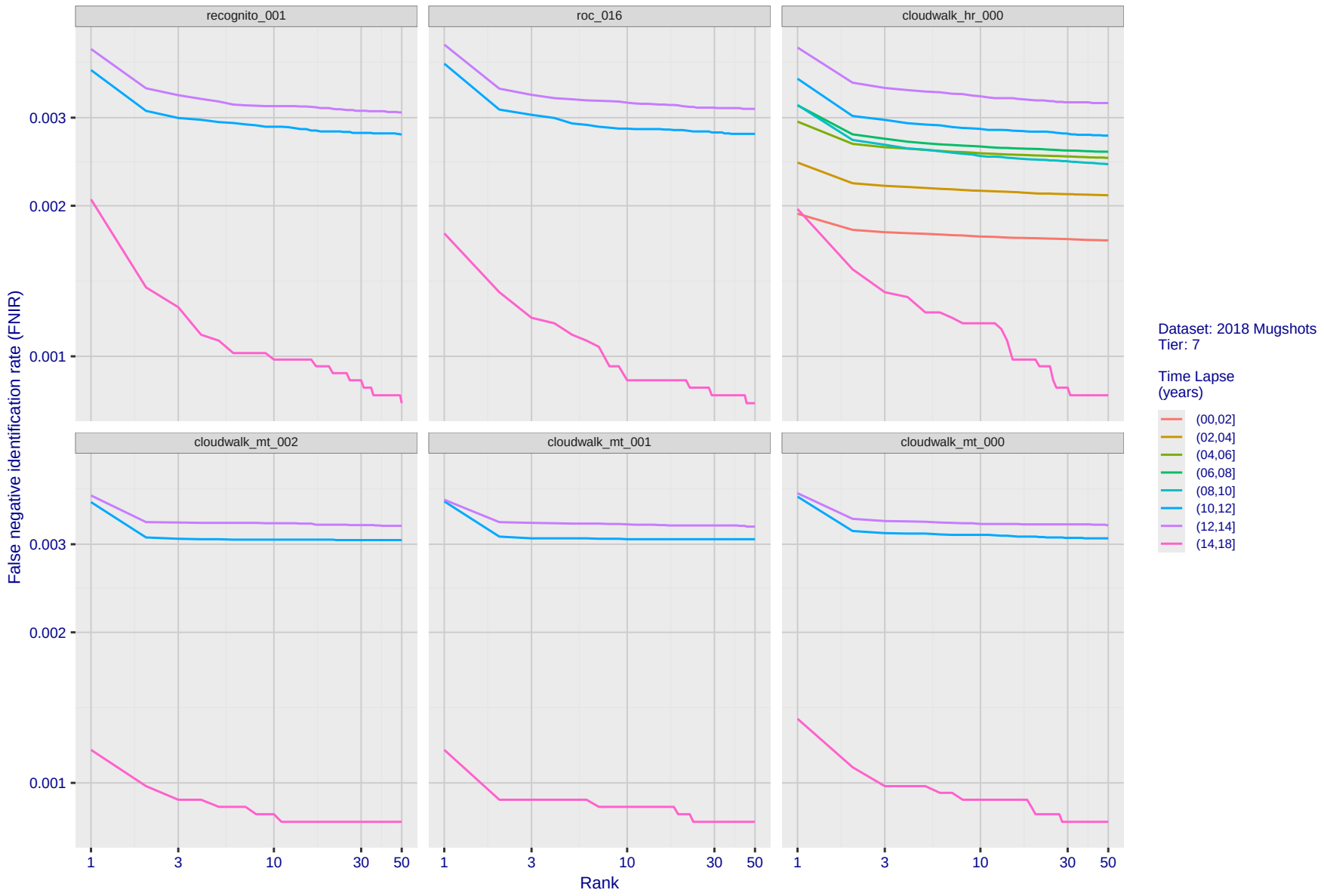

Figure 154: **[FRVT-2018 Mugshot Ageing Dataset] Identification miss rates vs. rank by time-elapsed**. *The oldest image of each individual is enrolled. Thereafter, all more recent images are searched. Miss rates are computed over all searches noted in row 17 of Table 1 and binned by number of years between search and initial enrollment.*

2026/01/09 20:40:38

FNIR(N, R, T) = False neg. identification rate
FPIR(N, T) = False pos. identification rate

N = Num. enrolled subjects
R = Num. candidates examined

T = Threshold

T = 0 → Investigation
T > 0 → Identification

This publication is available free of charge from: https://doi.org/10.6028/NIST.IR.8271

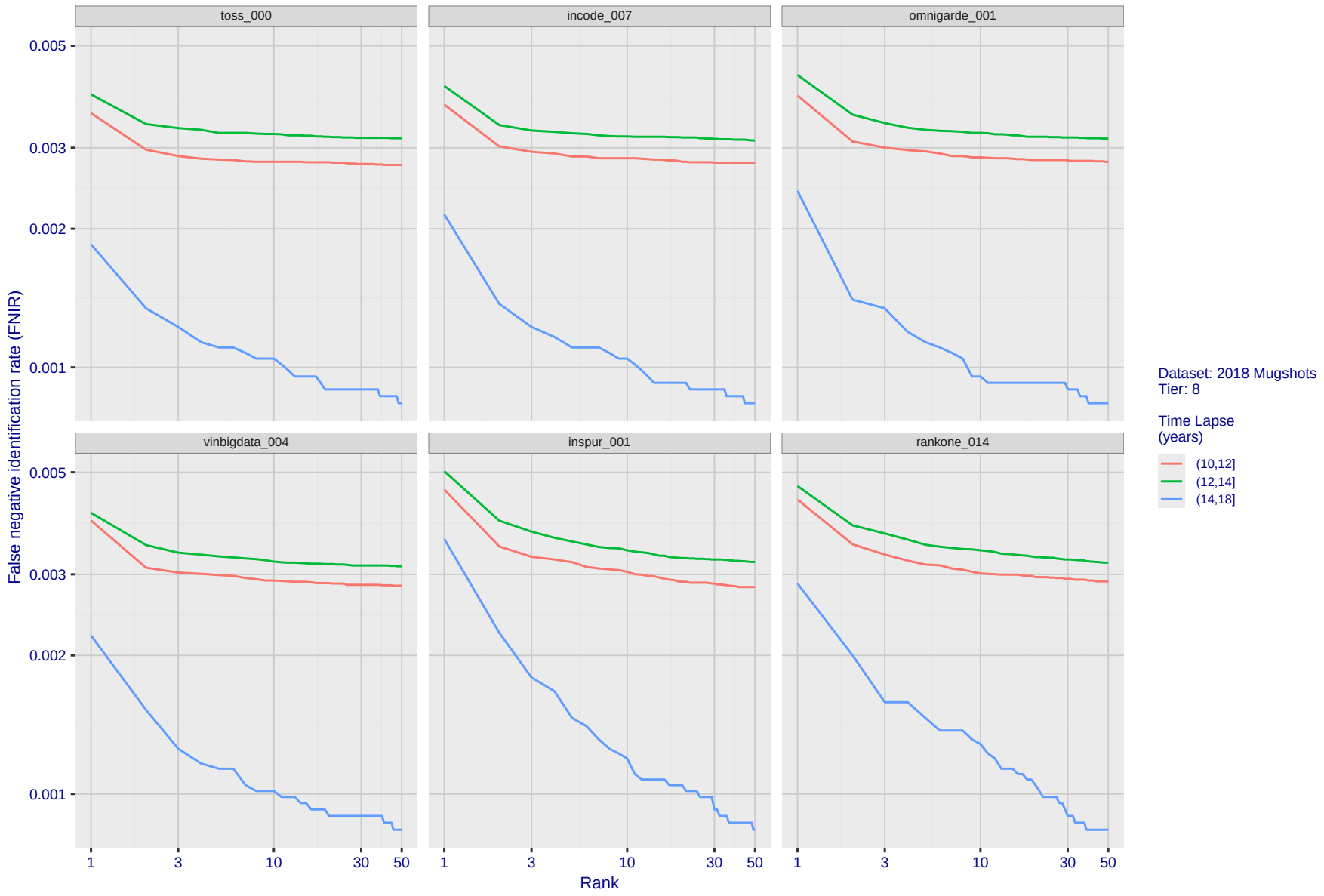

Figure 155: **[FRVT-2018 Mugshot Ageing Dataset] Identification miss rates vs. rank by time-elapsed**. *The oldest image of each individual is enrolled. Thereafter, all more recent images are searched. Miss rates are computed over all searches noted in row 17 of Table 1 and binned by number of years between search and initial enrollment.*

2026/01/09 20:40:38
FNIR(N, R, T) = False neg. identification rate
FPIR(N, T) = False pos. identification rate
N = Num. enrolled subjects
R = Num. candidates examined
T = Threshold
T = 0 → Investigation
T > 0 → Identification

This publication is available free of charge from: https://doi.org/10.6028/NIST.IR.8271

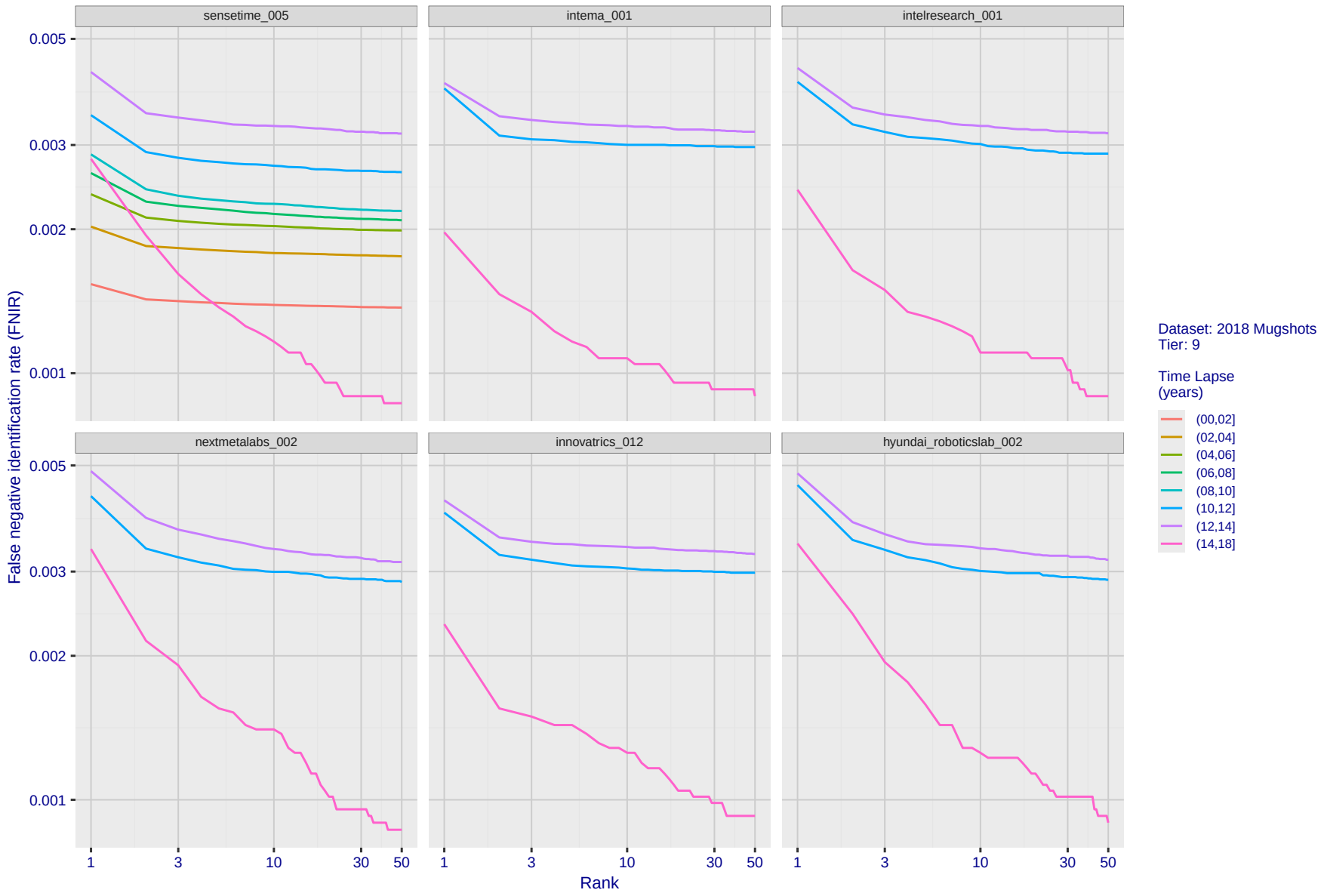

Figure 156: **[FRVT-2018 Mugshot Ageing Dataset] Identification miss rates vs. rank by time-elapsed**. *The oldest image of each individual is enrolled. Thereafter, all more recent images are searched. Miss rates are computed over all searches noted in row 17 of Table 1 and binned by number of years between search and initial enrollment.*

2026/01/09 20:40:38
FNIR(N, R, T) = False neg. identification rate
FPIR(N, T) = False pos. identification rate
N = Num. enrolled subjects
R = Num. candidates examined
T = Threshold
T = 0 → Investigation
T > 0 → Identification

This publication is available free of charge from: https://doi.org/10.6028/NIST.IR.8271

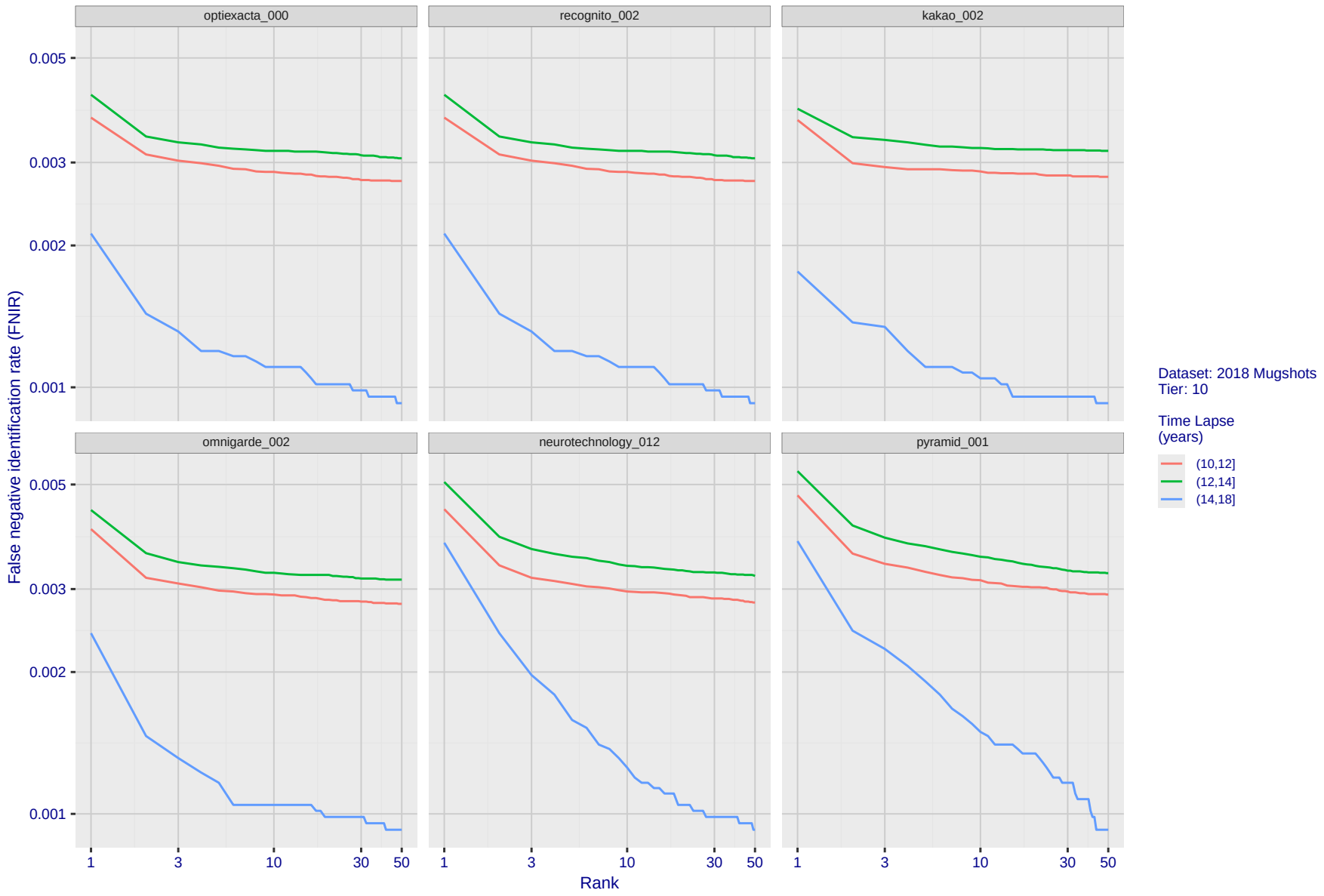

Figure 157: **[FRVT-2018 Mugshot Ageing Dataset] Identification miss rates vs. rank by time-elapsed**. *The oldest image of each individual is enrolled. Thereafter, all more recent images are searched. Miss rates are computed over all searches noted in row 17 of Table 1 and binned by number of years between search and initial enrollment.*

2026/01/09 20:40:38
FNIR(N, R, T) = False neg. identification rate
FPIR(N, T) = False pos. identification rate
N = Num. enrolled subjects
R = Num. candidates examined
T = Threshold
T = 0 → Investigation
T > 0 → Identification

This publication is available free of charge from: https://doi.org/10.6028/NIST.IR.8271

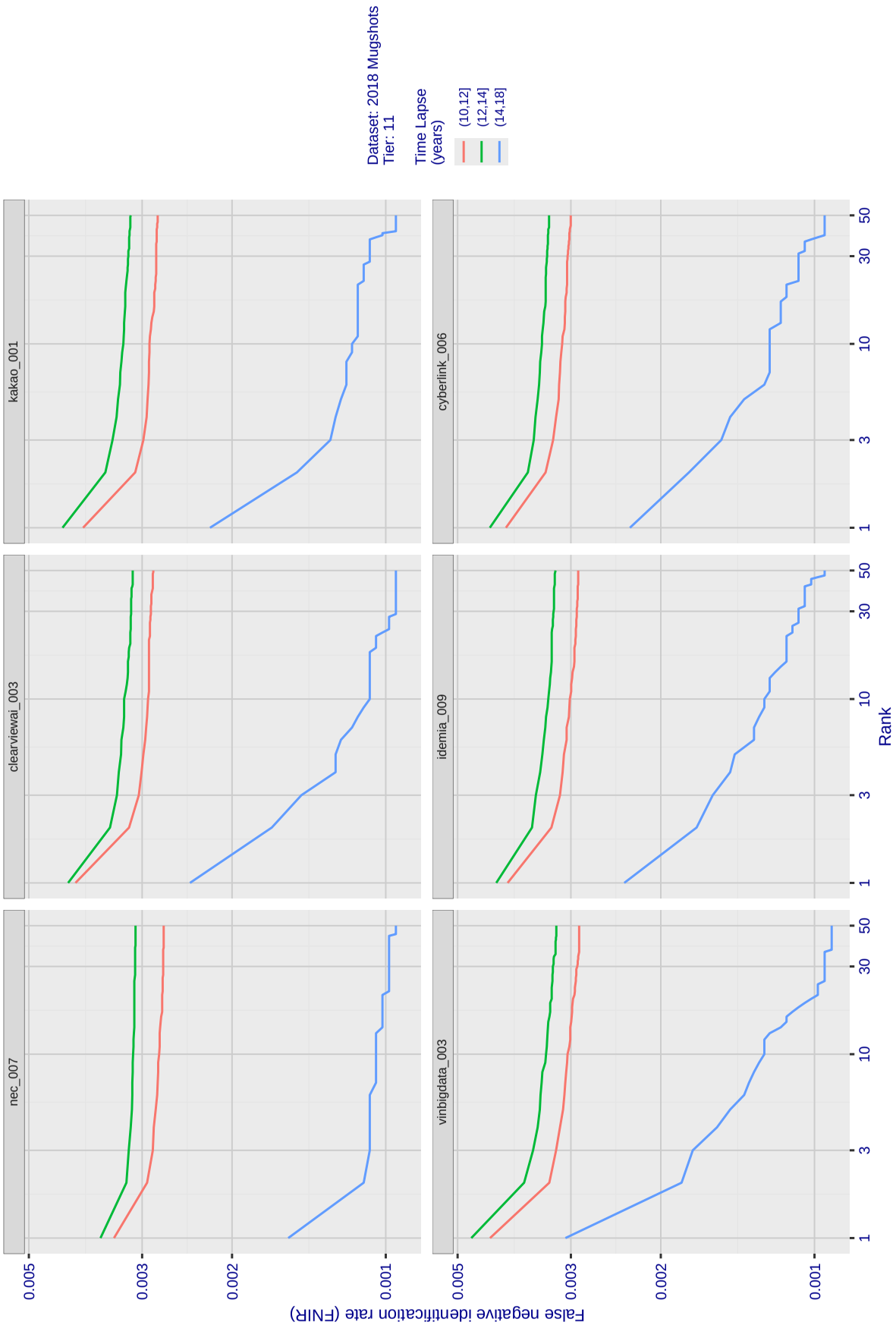

Figure 158: **[FRVT-2018 Mugshot Ageing Dataset] Identification miss rates vs. rank by time-elapsed.** *The oldest image of each individual is enrolled. Thereafter, all more recent images are searched. Miss rates are computed over all searches noted in row 17 of Table 1 and binned by number of years between search and initial enrollment.*

This publication is available free of charge from: https://doi.org/10.6028/NIST.IR.8271

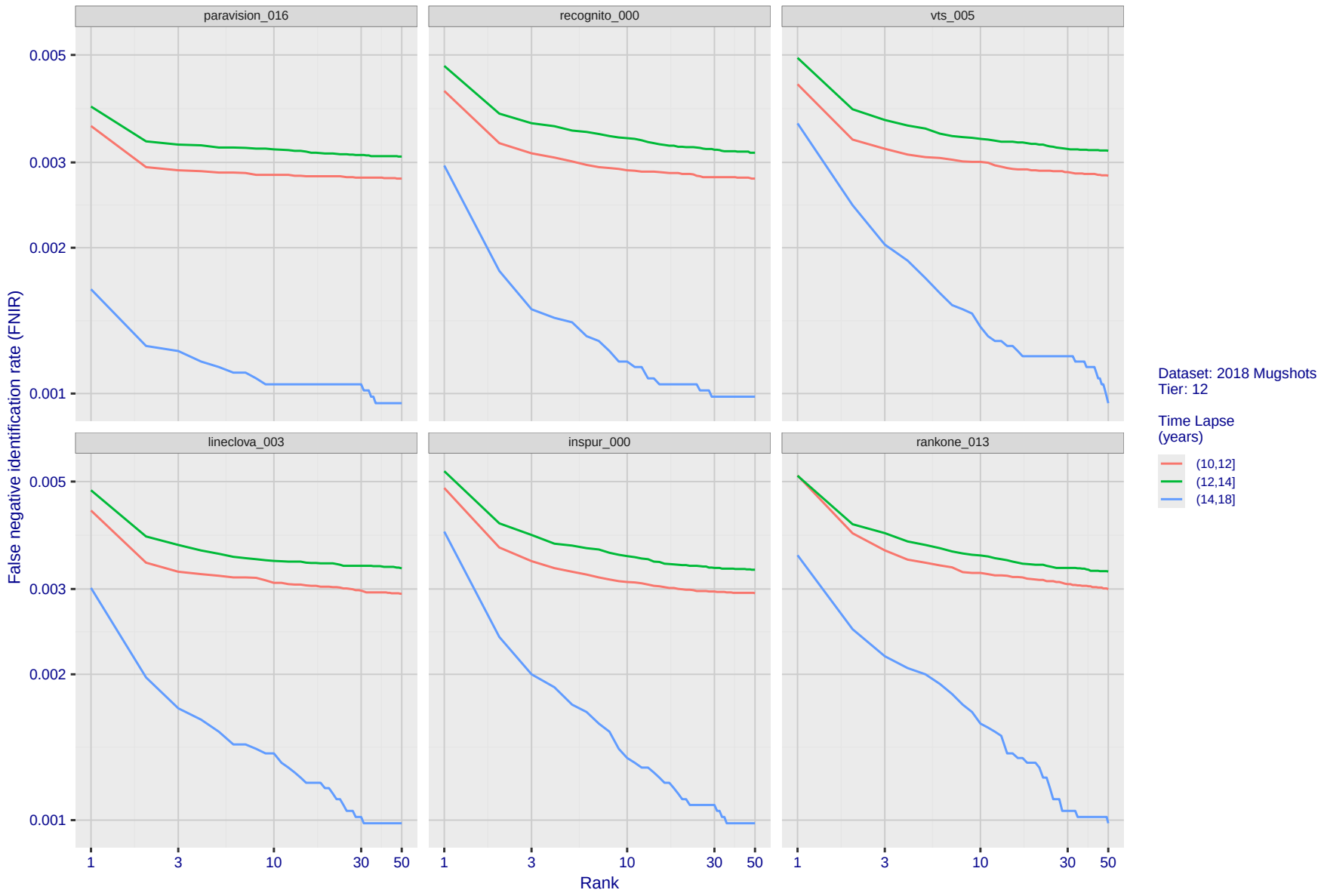

Figure 159: **[FRVT-2018 Mugshot Ageing Dataset] Identification miss rates vs. rank by time-elapsed**. *The oldest image of each individual is enrolled. Thereafter, all more recent images are searched. Miss rates are computed over all searches noted in row 17 of Table 1 and binned by number of years between search and initial enrollment.*

2026/01/09 20:40:38
FNIR(N, R, T) = False neg. identification rate
FPIR(N, T) = False pos. identification rate
N = Num. enrolled subjects
R = Num. candidates examined
T = Threshold
T = 0 → Investigation
T > 0 → Identification

This publication is available free of charge from: https://doi.org/10.6028/NIST.IR.8271

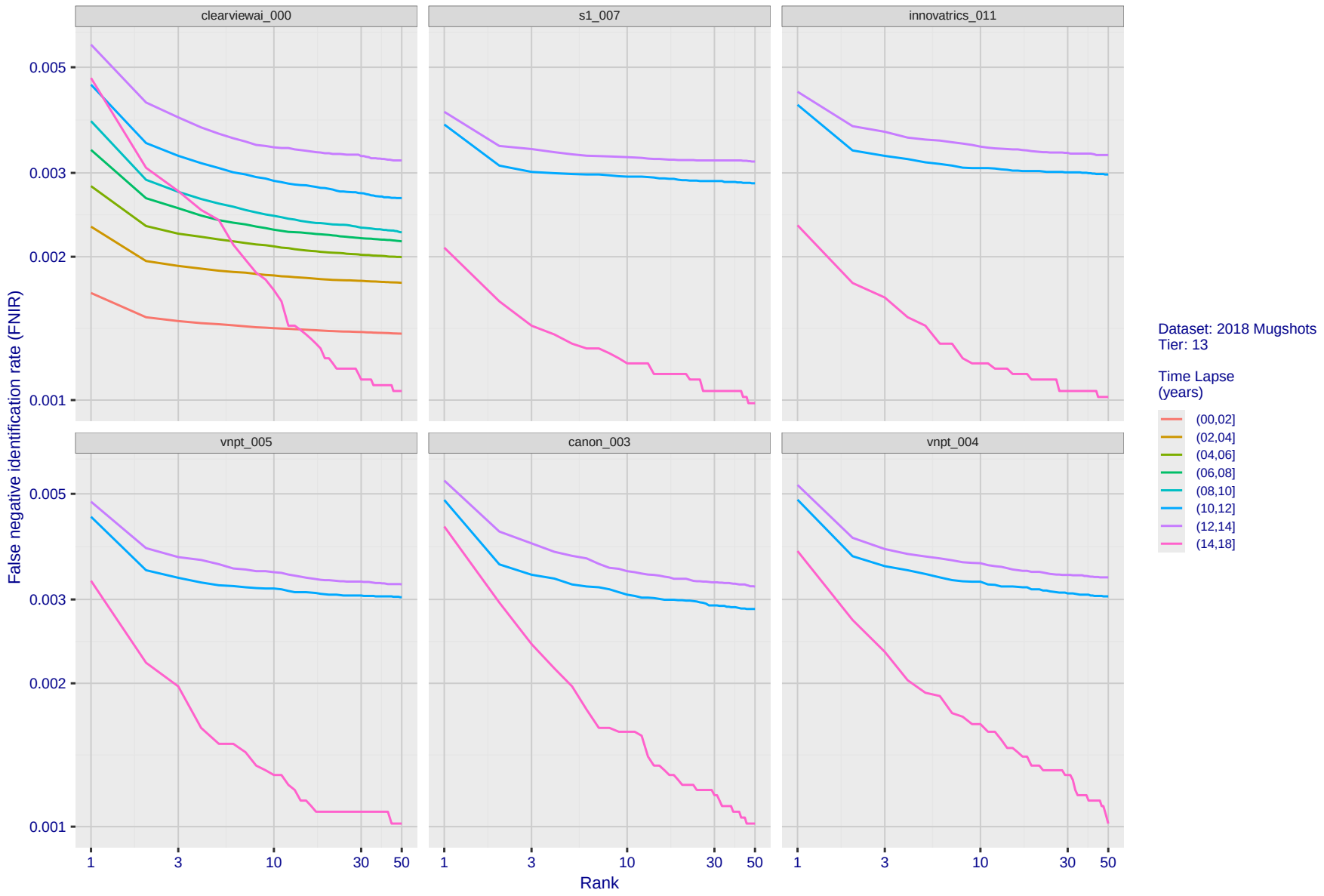

Figure 160: **[FRVT-2018 Mugshot Ageing Dataset] Identification miss rates vs. rank by time-elapsed**. *The oldest image of each individual is enrolled. Thereafter, all more recent images are searched. Miss rates are computed over all searches noted in row 17 of Table 1 and binned by number of years between search and initial enrollment.*

2026/01/09 20:40:38
FNIR(N, R, T) = False neg. identification rate
FPIR(N, T) = False pos. identification rate
N = Num. enrolled subjects
R = Num. candidates examined
T = Threshold
T = 0 → Investigation
T > 0 → Identification

This publication is available free of charge from: https://doi.org/10.6028/NIST.IR.8271

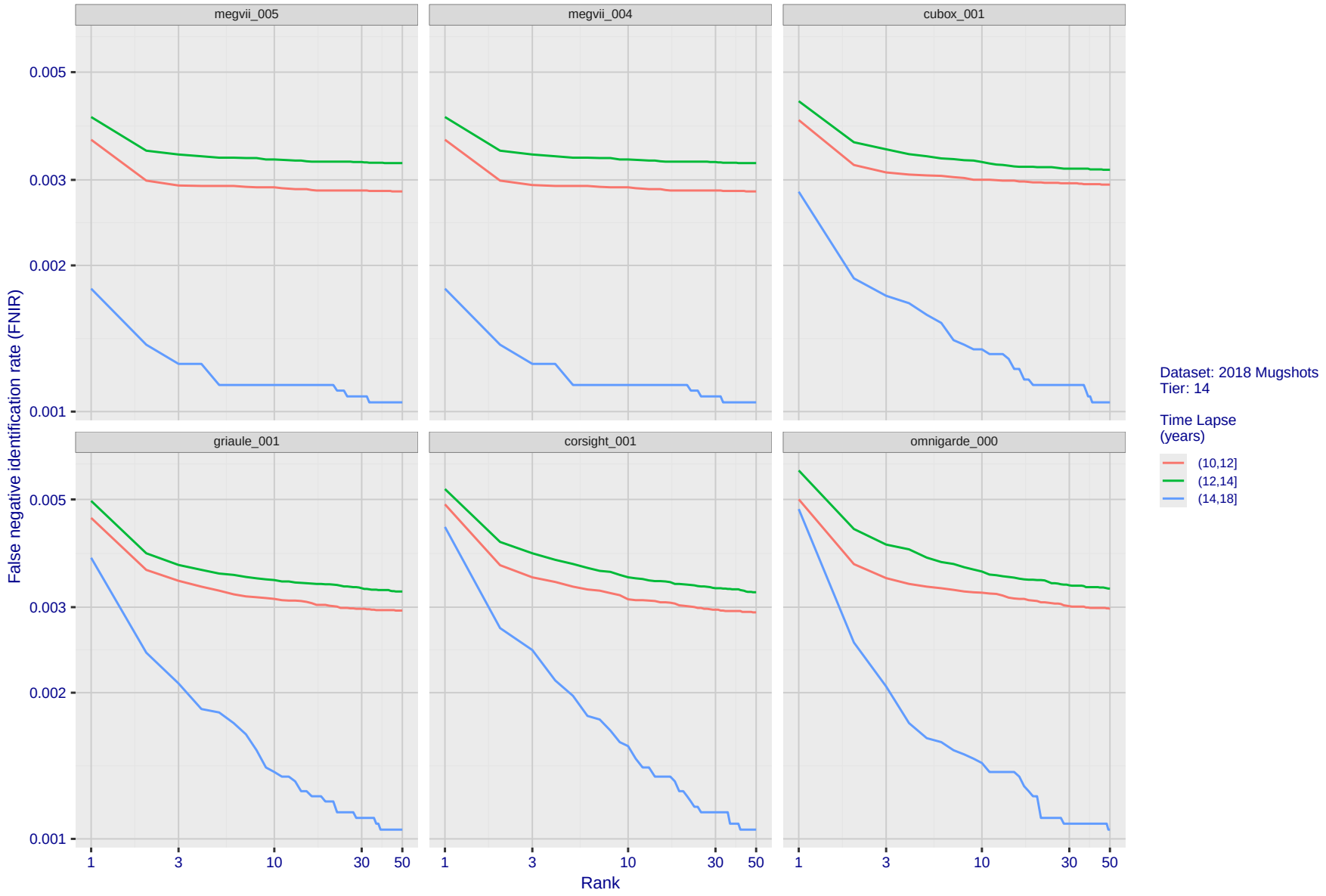

Figure 161: **[FRVT-2018 Mugshot Ageing Dataset] Identification miss rates vs. rank by time-elapsed**. *The oldest image of each individual is enrolled. Thereafter, all more recent images are searched. Miss rates are computed over all searches noted in row 17 of Table 1 and binned by number of years between search and initial enrollment.*

2026/01/09 20:40:38
FNIR(N, R, T) = False neg. identification rate
FPIR(N, T) = False pos. identification rate
N = Num. enrolled subjects
R = Num. candidates examined
T = Threshold
T = 0 → Investigation
T > 0 → Identification

This publication is available free of charge from: https://doi.org/10.6028/NIST.IR.8271

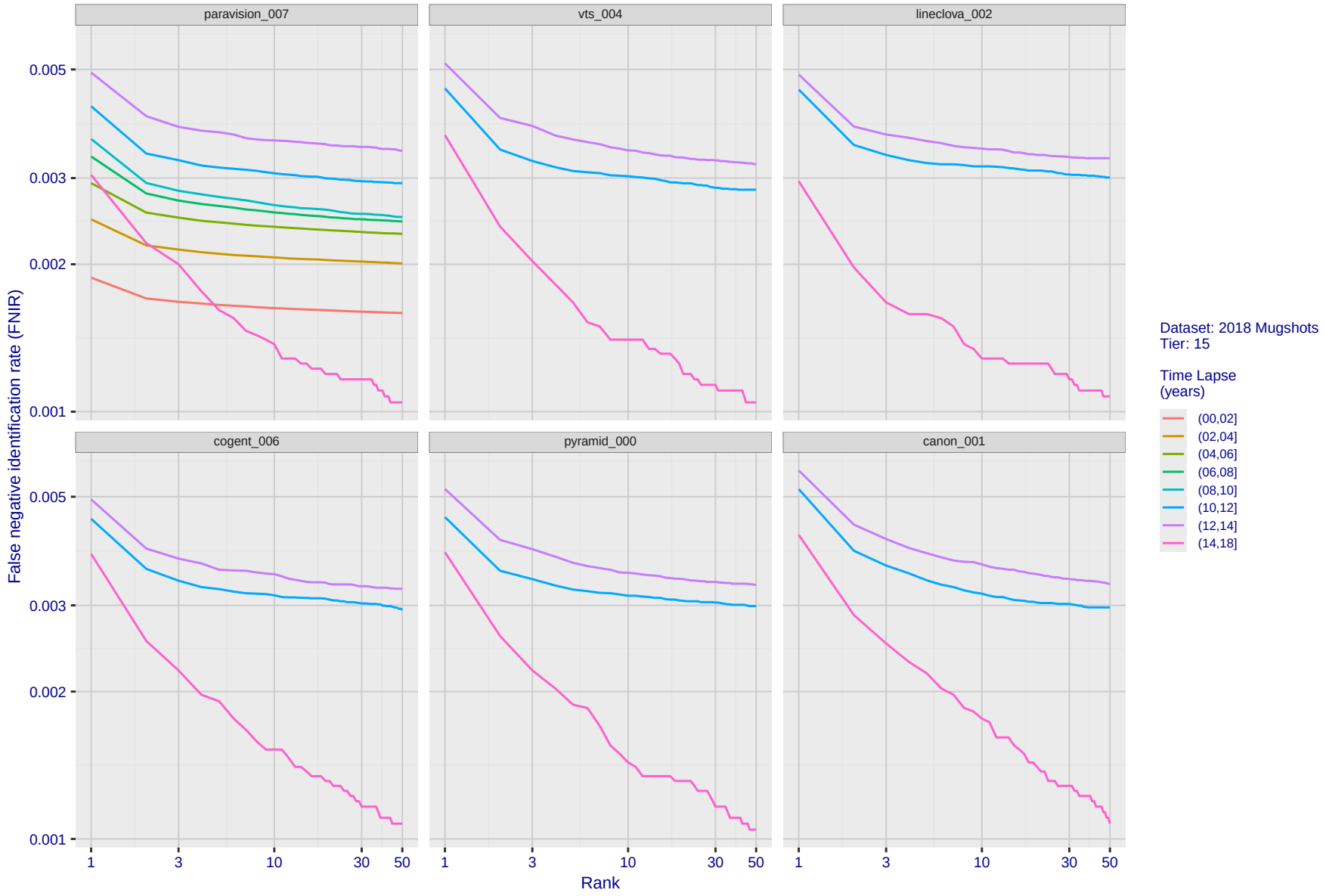

Figure 162: **[FRVT-2018 Mugshot Ageing Dataset] Identification miss rates vs. rank by time-elapsed**. *The oldest image of each individual is enrolled. Thereafter, all more recent images are searched. Miss rates are computed over all searches noted in row 17 of Table 1 and binned by number of years between search and initial enrollment.*

2026/01/09 20:40:38
FNIR(N, R, T) = False neg. identification rate
FPIR(N, T) = False pos. identification rate
N = Num. enrolled subjects
R = Num. candidates examined
T = Threshold
T = 0 → Investigation
T > 0 → Identification

This publication is available free of charge from: https://doi.org/10.6028/NIST.IR.8271

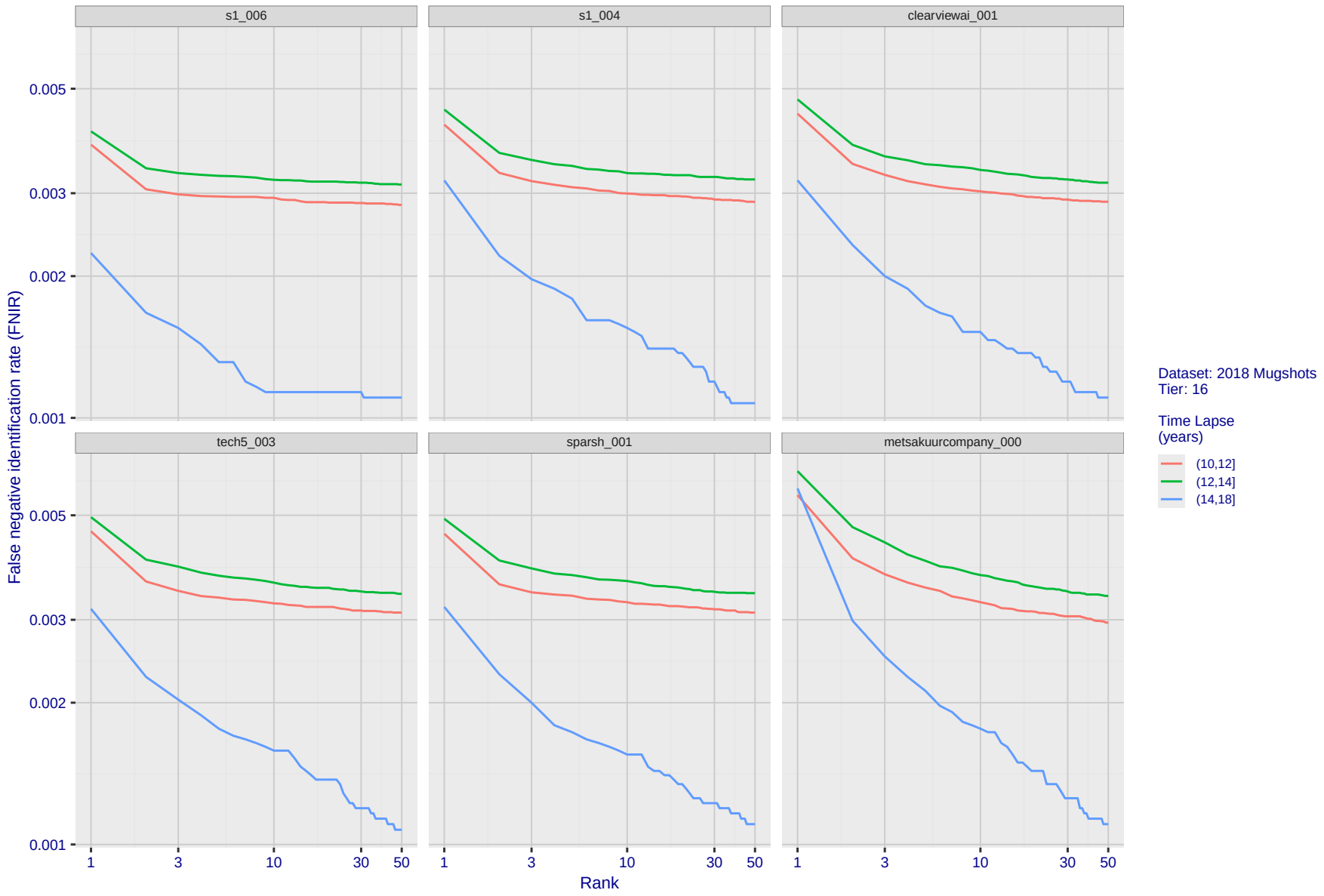

Figure 163: **[FRVT-2018 Mugshot Ageing Dataset] Identification miss rates vs. rank by time-elapsed**. *The oldest image of each individual is enrolled. Thereafter, all more recent images are searched. Miss rates are computed over all searches noted in row 17 of Table 1 and binned by number of years between search and initial enrollment.*

2026/01/09 20:40:38
FNIR(N, R, T) = False neg. identification rate
FPIR(N, T) = False pos. identification rate
N = Num. enrolled subjects
R = Num. candidates examined
T = Threshold
T = 0 → Investigation
T > 0 → Identification

This publication is available free of charge from: https://doi.org/10.6028/NIST.IR.8271

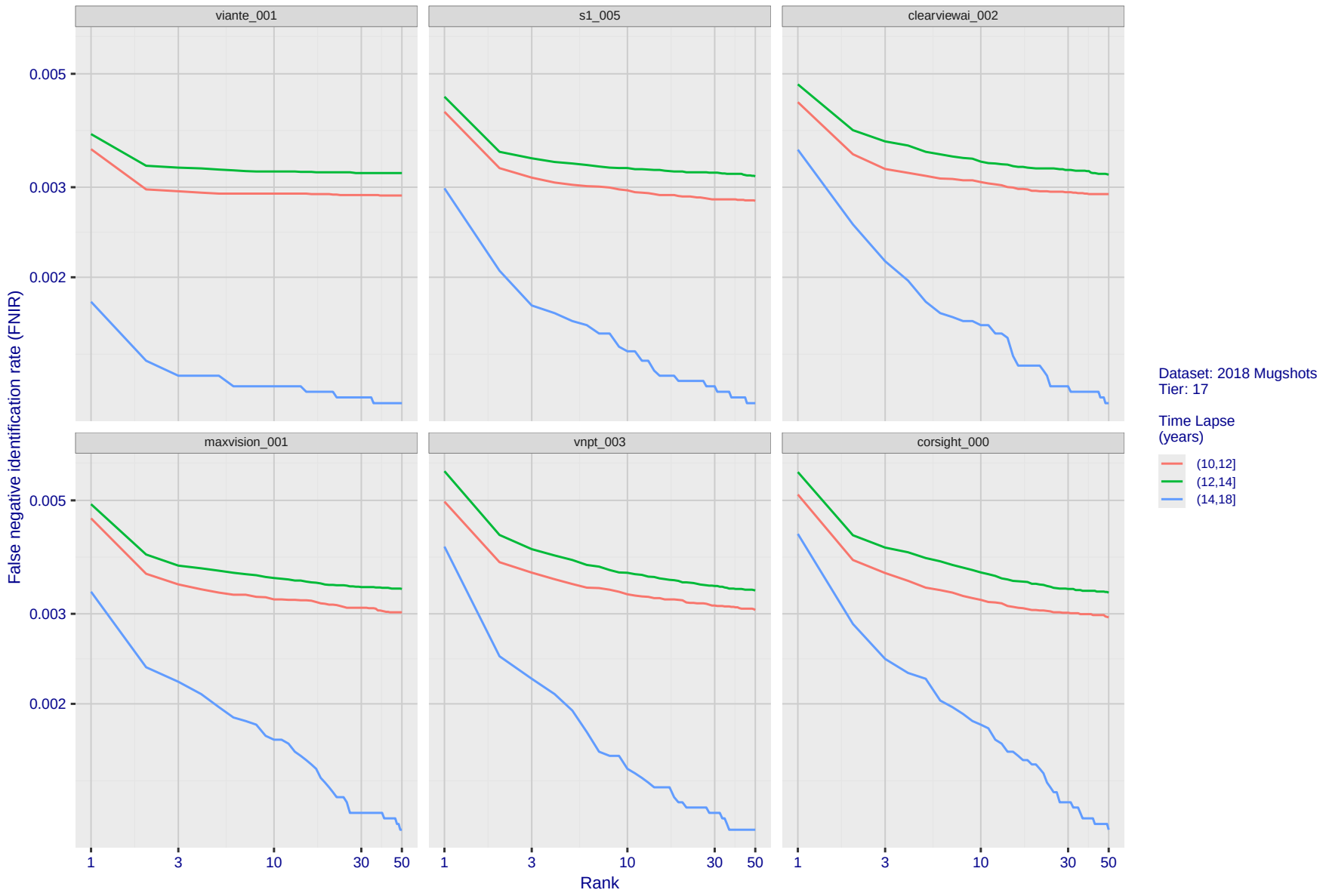

Figure 164: **[FRVT-2018 Mugshot Ageing Dataset] Identification miss rates vs. rank by time-elapsed**. *The oldest image of each individual is enrolled. Thereafter, all more recent images are searched. Miss rates are computed over all searches noted in row 17 of Table 1 and binned by number of years between search and initial enrollment.*

2026/01/09 20:40:38
FNIR(N, R, T) = False neg. identification rate
FPIR(N, T) = False pos. identification rate
N = Num. enrolled subjects
R = Num. candidates examined
T = Threshold
T = 0 → Investigation
T > 0 → Identification

This publication is available free of charge from: https://doi.org/10.6028/NIST.IR.8271

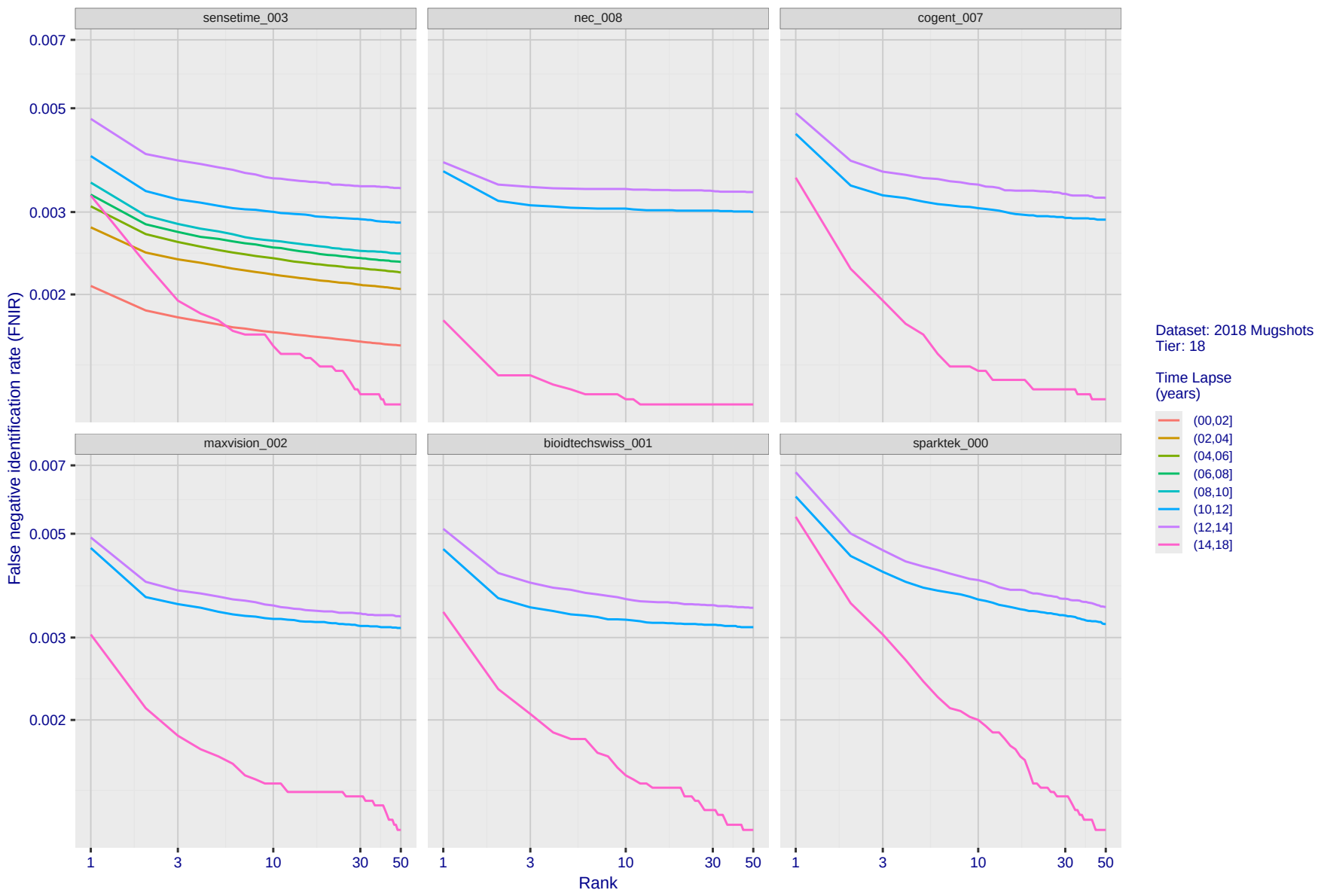

Figure 165: **[FRVT-2018 Mugshot Ageing Dataset] Identification miss rates vs. rank by time-elapsed**. *The oldest image of each individual is enrolled. Thereafter, all more recent images are searched. Miss rates are computed over all searches noted in row 17 of Table 1 and binned by number of years between search and initial enrollment.*

2026/01/09 20:40:38

FNIR(N, R, T) = False neg. identification rate
FPIR(N, T) = False pos. identification rate

N = Num. enrolled subjects
R = Num. candidates examined

T = Threshold

T = 0 → Investigation
T > 0 → Identification

This publication is available free of charge from: https://doi.org/10.6028/NIST.IR.8271

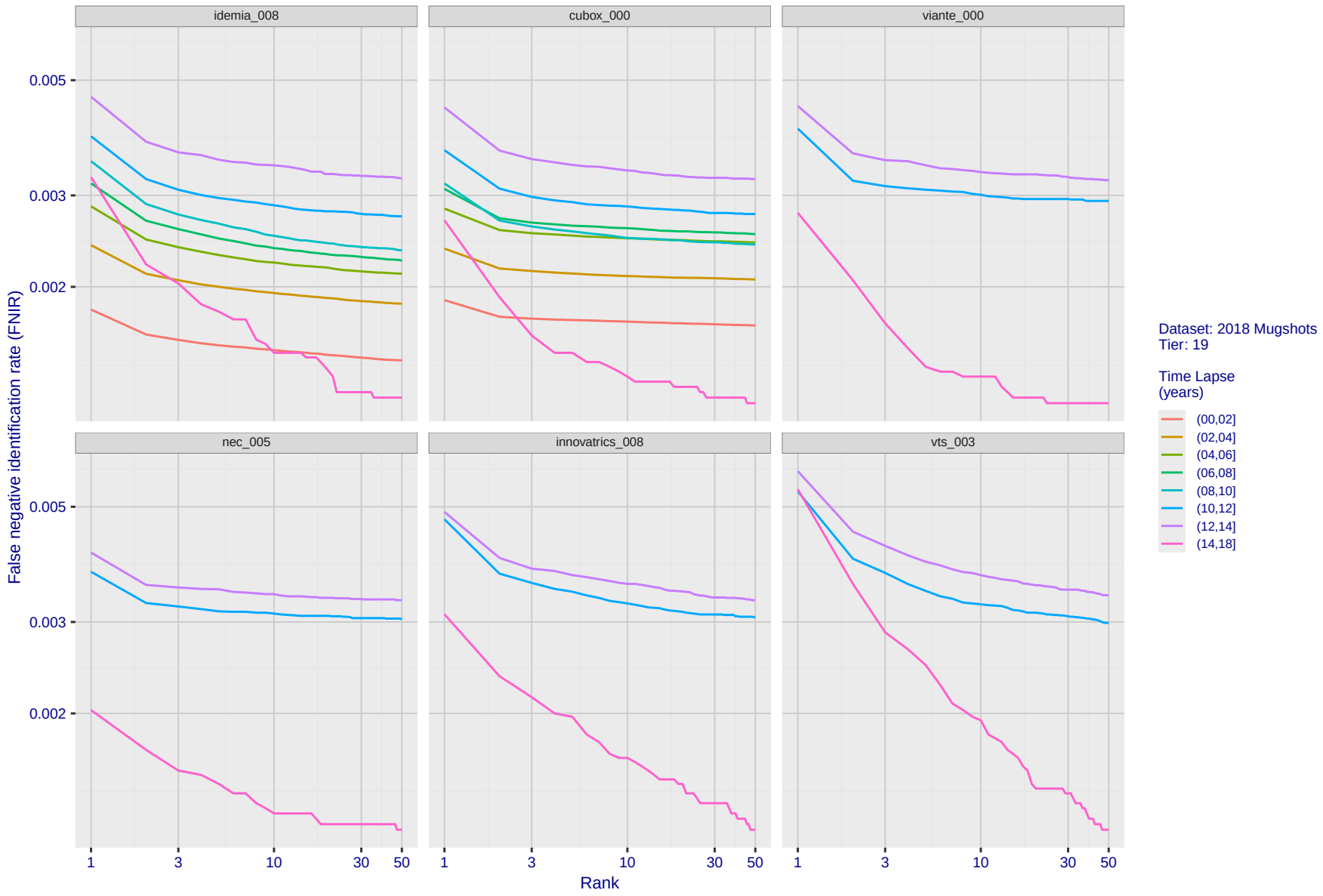

Figure 166: **[FRVT-2018 Mugshot Ageing Dataset] Identification miss rates vs. rank by time-elapsed**. *The oldest image of each individual is enrolled. Thereafter, all more recent images are searched. Miss rates are computed over all searches noted in row 17 of Table 1 and binned by number of years between search and initial enrollment.*

2026/01/09 20:40:38
FNIR(N, R, T) = False neg. identification rate
FPIR(N, T) = False pos. identification rate
N = Num. enrolled subjects
R = Num. candidates examined
T = Threshold
T = 0 → Investigation
T > 0 → Identification

This publication is available free of charge from: https://doi.org/10.6028/NIST.IR.8271

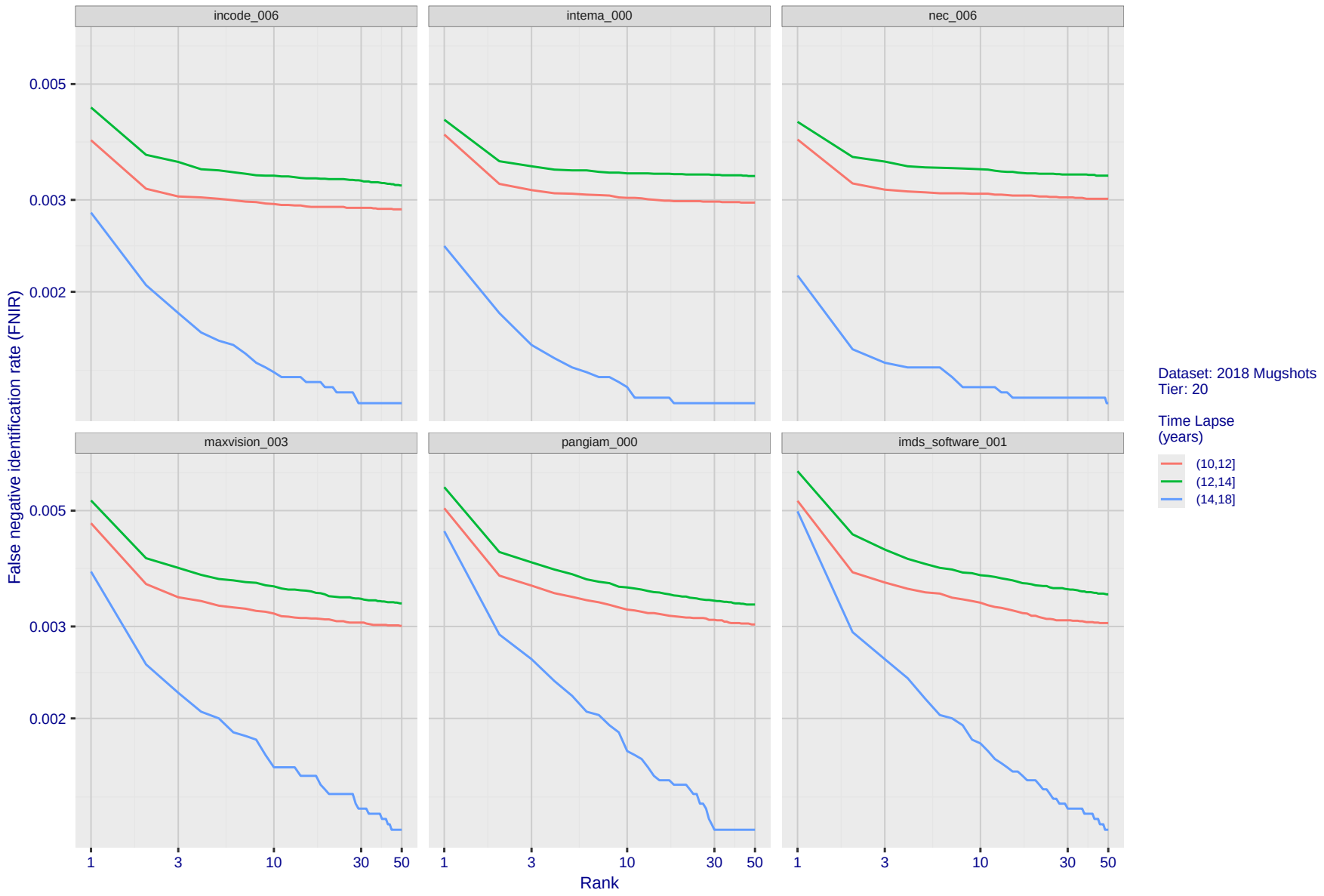

Figure 167: **[FRVT-2018 Mugshot Ageing Dataset] Identification miss rates vs. rank by time-elapsed**. *The oldest image of each individual is enrolled. Thereafter, all more recent images are searched. Miss rates are computed over all searches noted in row 17 of Table 1 and binned by number of years between search and initial enrollment.*

2026/01/09 20:40:38
FNIR(N, R, T) = False neg. identification rate
FPIR(N, T) = False pos. identification rate
N = Num. enrolled subjects
R = Num. candidates examined
T = Threshold
T = 0 → Investigation
T > 0 → Identification

This publication is available free of charge from: https://doi.org/10.6028/NIST.IR.8271

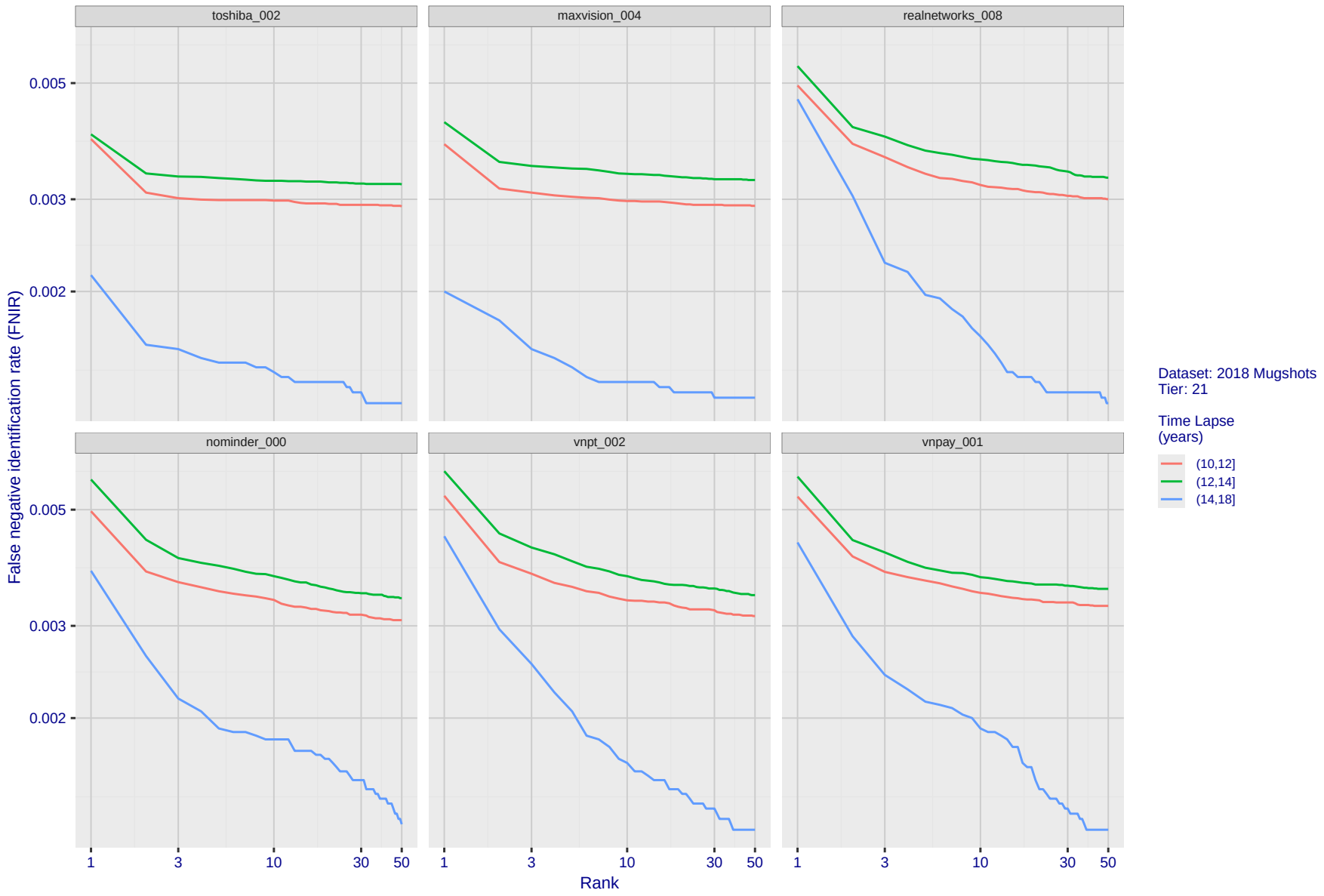

Figure 168: **[FRVT-2018 Mugshot Ageing Dataset] Identification miss rates vs. rank by time-elapsed**. *The oldest image of each individual is enrolled. Thereafter, all more recent images are searched. Miss rates are computed over all searches noted in row 17 of Table 1 and binned by number of years between search and initial enrollment.*

2026/01/09 20:40:38
FNIR(N, R, T) = False neg. identification rate
FPIR(N, T) = False pos. identification rate
N = Num. enrolled subjects
R = Num. candidates examined
T = Threshold
T = 0 → Investigation
T > 0 → Identification

This publication is available free of charge from: https://doi.org/10.6028/NIST.IR.8271

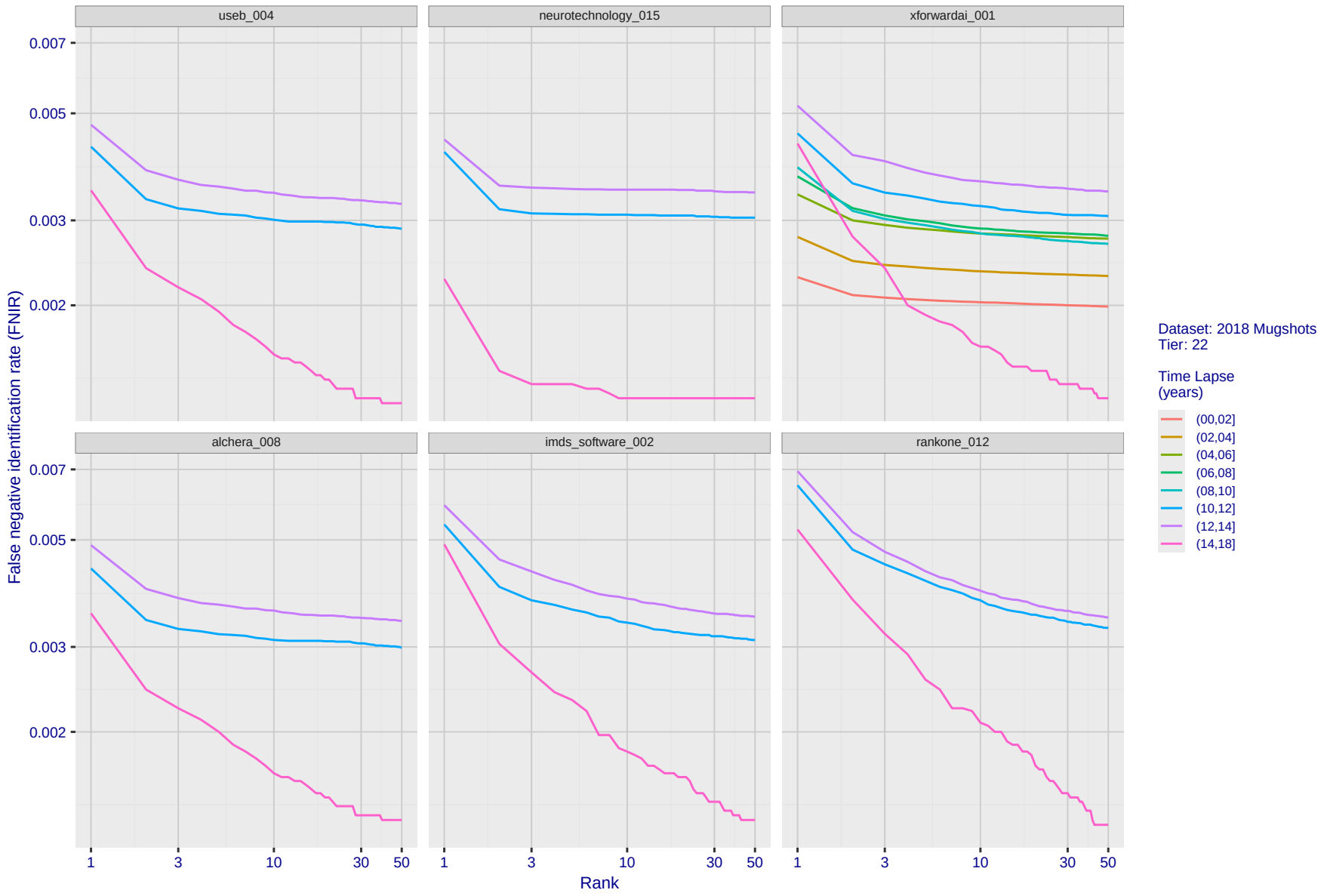

Figure 169: **[FRVT-2018 Mugshot Ageing Dataset] Identification miss rates vs. rank by time-elapsed**. *The oldest image of each individual is enrolled. Thereafter, all more recent images are searched. Miss rates are computed over all searches noted in row 17 of Table 1 and binned by number of years between search and initial enrollment.*

2026/01/09 20:40:38

FNIR(N, R, T) = False neg. identification rate
FPIR(N, T) = False pos. identification rate

N = Num. enrolled subjects
R = Num. candidates examined

T = Threshold

T = 0 → Investigation
T > 0 → Identification

This publication is available free of charge from: https://doi.org/10.6028/NIST.IR.8271

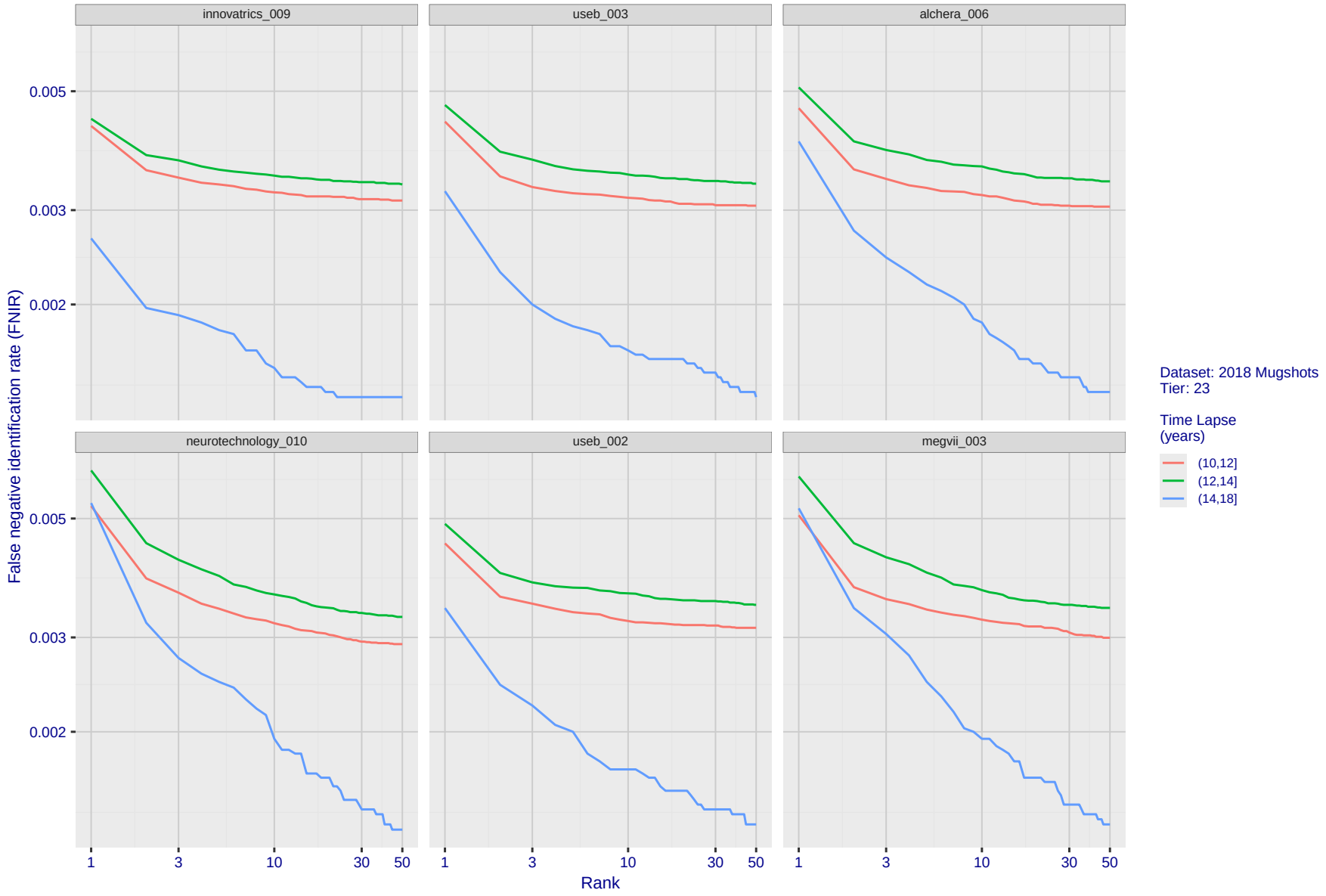

Figure 170: **[FRVT-2018 Mugshot Ageing Dataset] Identification miss rates vs. rank by time-elapsed**. *The oldest image of each individual is enrolled. Thereafter, all more recent images are searched. Miss rates are computed over all searches noted in row 17 of Table 1 and binned by number of years between search and initial enrollment.*

2026/01/09 20:40:38
FNIR(N, R, T) = False neg. identification rate
FPIR(N, T) = False pos. identification rate
N = Num. enrolled subjects
R = Num. candidates examined
T = Threshold
T = 0 → Investigation
T > 0 → Identification

This publication is available free of charge from: https://doi.org/10.6028/NIST.IR.8271

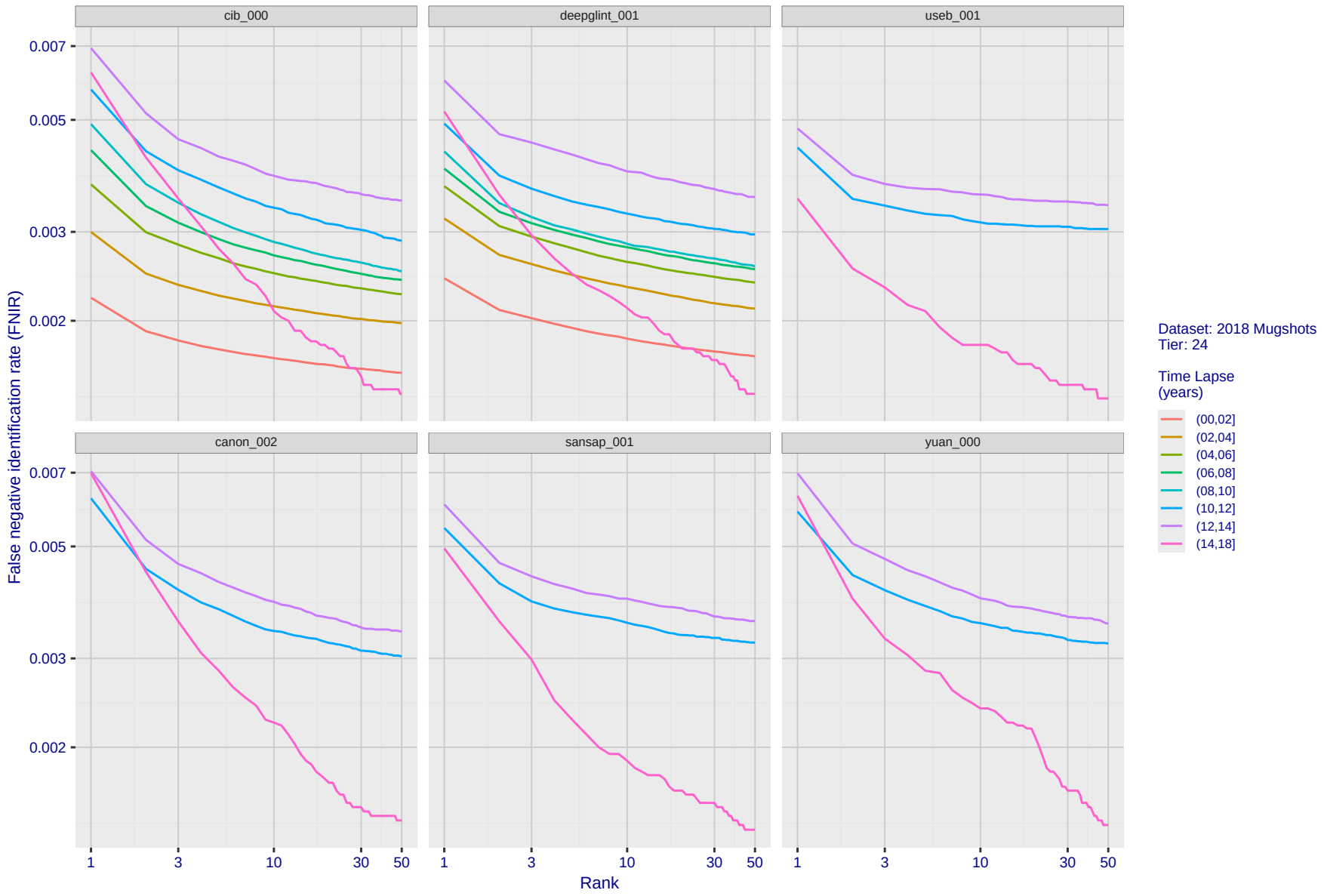

Figure 171: **[FRVT-2018 Mugshot Ageing Dataset] Identification miss rates vs. rank by time-elapsed**. *The oldest image of each individual is enrolled. Thereafter, all more recent images are searched. Miss rates are computed over all searches noted in row 17 of Table 1 and binned by number of years between search and initial enrollment.*

2026/01/09 20:40:38
FNIR(N, R, T) = False neg. identification rate
FPIR(N, T) = False pos. identification rate
N = Num. enrolled subjects
R = Num. candidates examined
T = Threshold
T = 0 → Investigation
T > 0 → Identification

This publication is available free of charge from: https://doi.org/10.6028/NIST.IR.8271

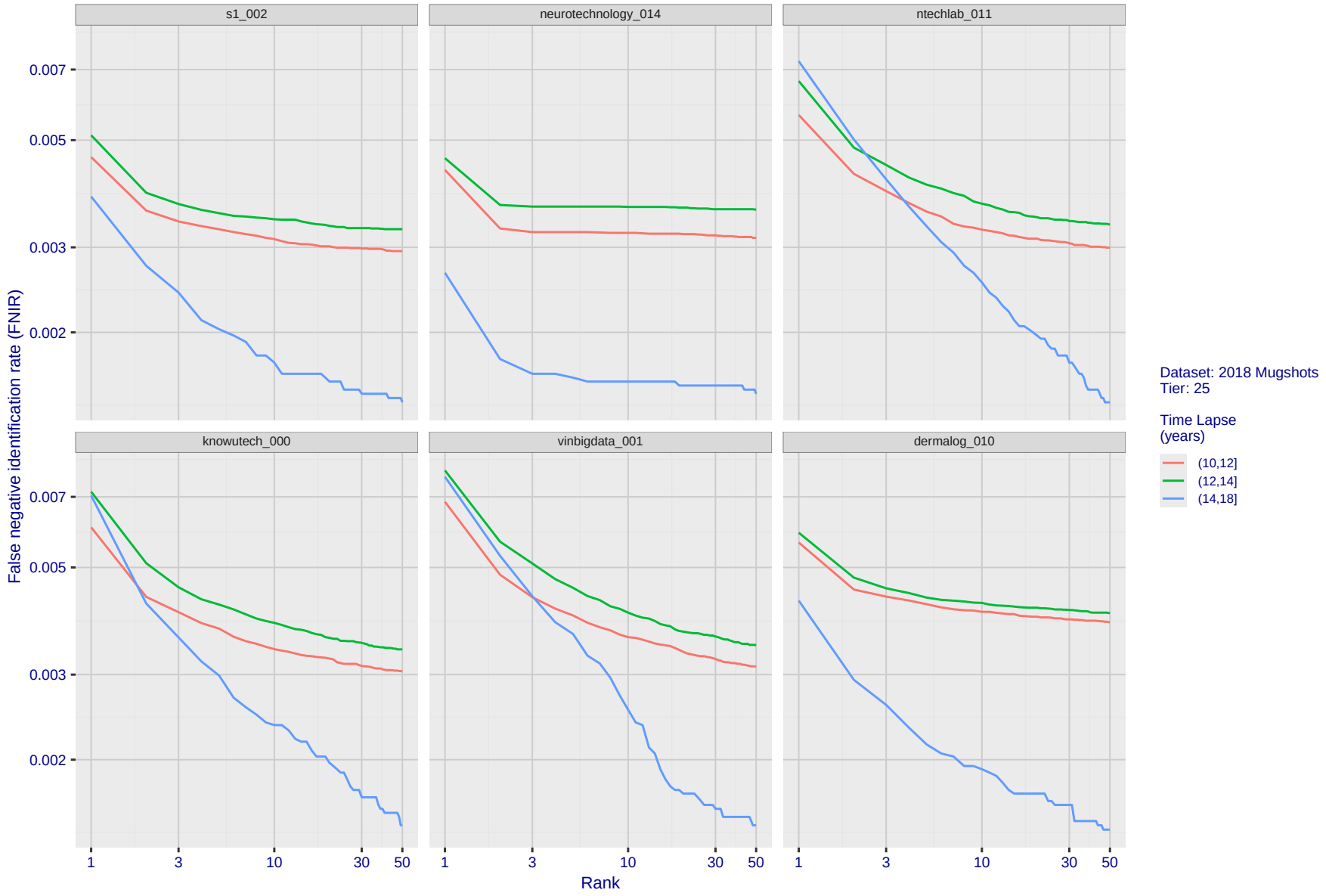

Figure 172: **[FRVT-2018 Mugshot Ageing Dataset] Identification miss rates vs. rank by time-elapsed**. *The oldest image of each individual is enrolled. Thereafter, all more recent images are searched. Miss rates are computed over all searches noted in row 17 of Table 1 and binned by number of years between search and initial enrollment.*

2026/01/09 20:40:38
FNIR(N, R, T) = False neg. identification rate
FPIR(N, T) = False pos. identification rate
N = Num. enrolled subjects
R = Num. candidates examined
T = Threshold
T = 0 → Investigation
T > 0 → Identification

This publication is available free of charge from: https://doi.org/10.6028/NIST.IR.8271

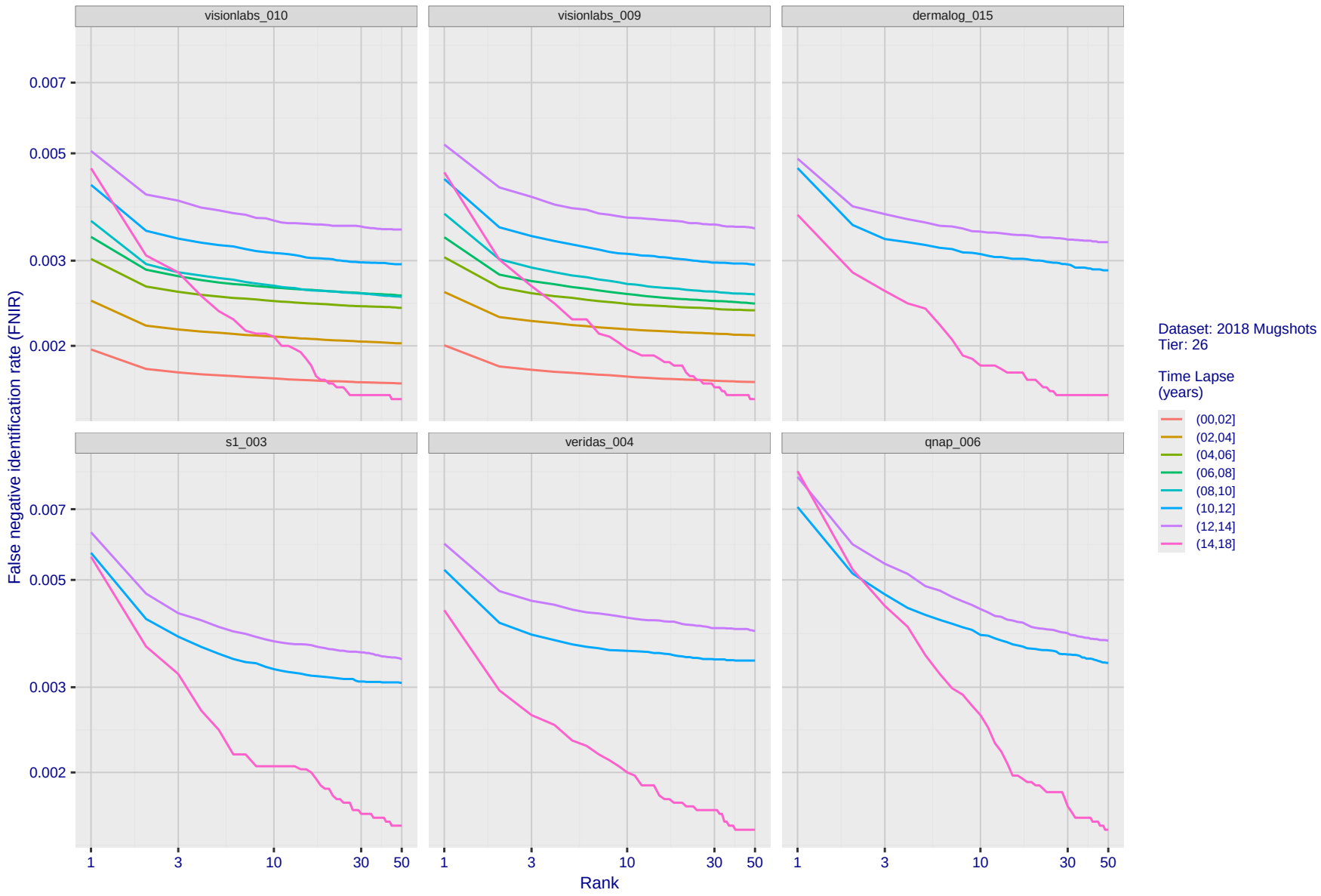

Figure 173: **[FRVT-2018 Mugshot Ageing Dataset] Identification miss rates vs. rank by time-elapsed**. *The oldest image of each individual is enrolled. Thereafter, all more recent images are searched. Miss rates are computed over all searches noted in row 17 of Table 1 and binned by number of years between search and initial enrollment.*

2026/01/09 20:40:38
FNIR(N, R, T) = False neg. identification rate
FPIR(N, T) = False pos. identification rate
N = Num. enrolled subjects
R = Num. candidates examined
T = Threshold
T = 0 → Investigation
T > 0 → Identification

This publication is available free of charge from: https://doi.org/10.6028/NIST.IR.8271

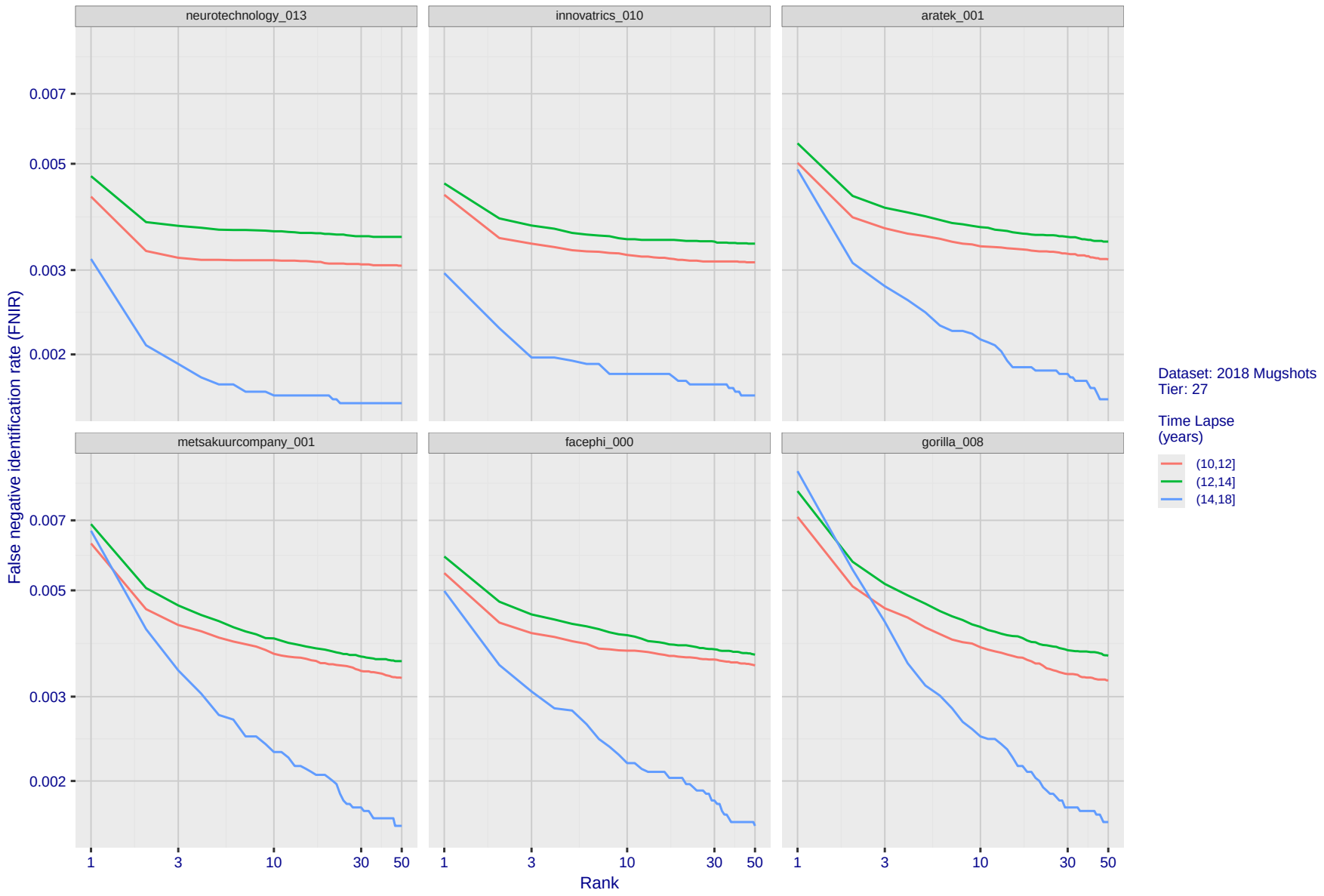

Figure 174: **[FRVT-2018 Mugshot Ageing Dataset] Identification miss rates vs. rank by time-elapsed**. *The oldest image of each individual is enrolled. Thereafter, all more recent images are searched. Miss rates are computed over all searches noted in row 17 of Table 1 and binned by number of years between search and initial enrollment.*

2026/01/09
20:40:38

FNIR(N, R, T) = False neg. identification rate
FPIR(N, T) = False pos. identification rate

N = Num. enrolled subjects
R = Num. candidates examined

T = Threshold

T = 0 → Investigation
T > 0 → Identification

This publication is available free of charge from: https://doi.org/10.6028/NIST.IR.8271

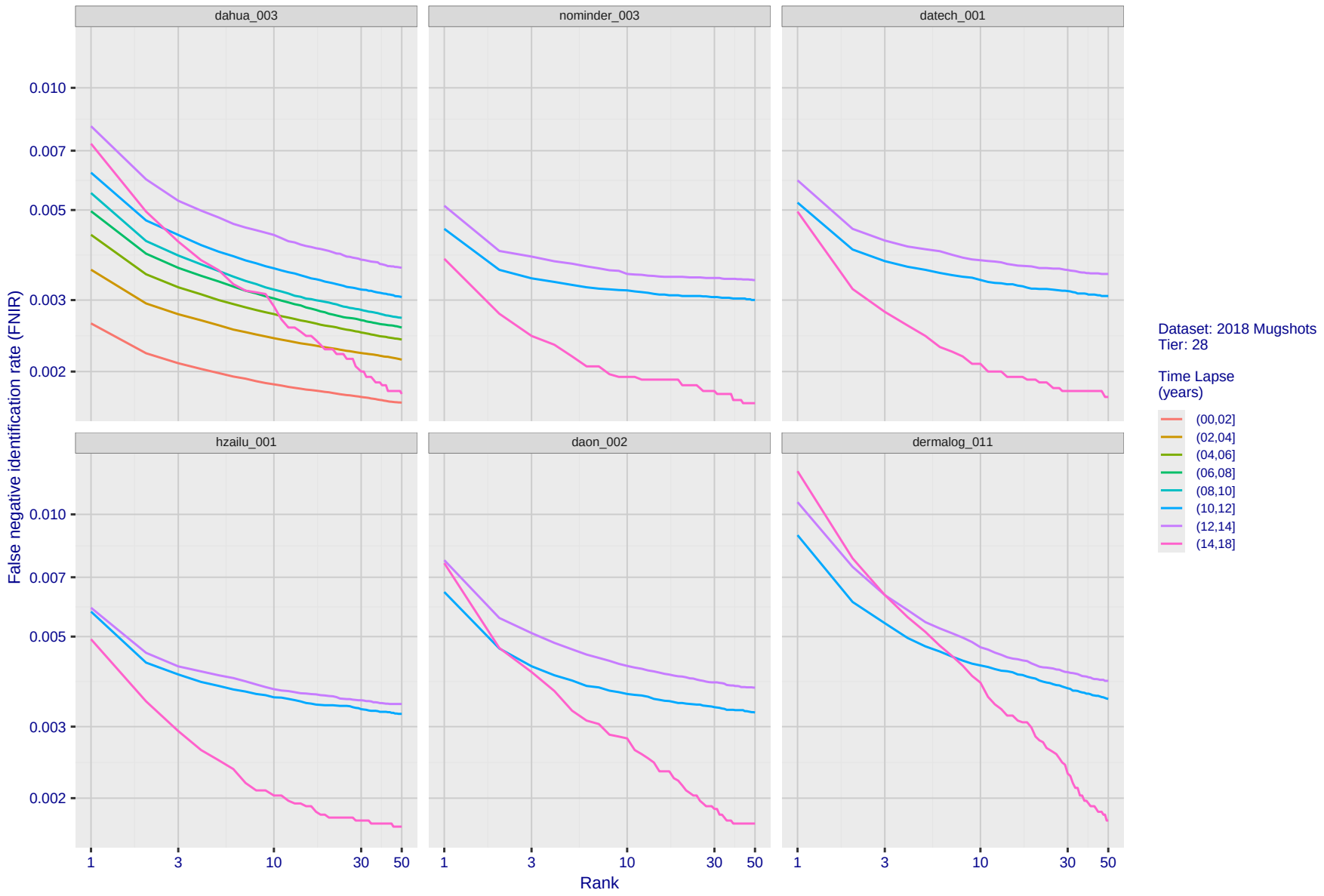

Figure 175: **[FRVT-2018 Mugshot Ageing Dataset] Identification miss rates vs. rank by time-elapsed**. *The oldest image of each individual is enrolled. Thereafter, all more recent images are searched. Miss rates are computed over all searches noted in row 17 of Table 1 and binned by number of years between search and initial enrollment.*

2026/01/09 20:40:38
FNIR(N, R, T) = False neg. identification rate
FPIR(N, T) = False pos. identification rate
N = Num. enrolled subjects
R = Num. candidates examined
T = Threshold
T = 0 → Investigation
T > 0 → Identification

This publication is available free of charge from: https://doi.org/10.6028/NIST.IR.8271

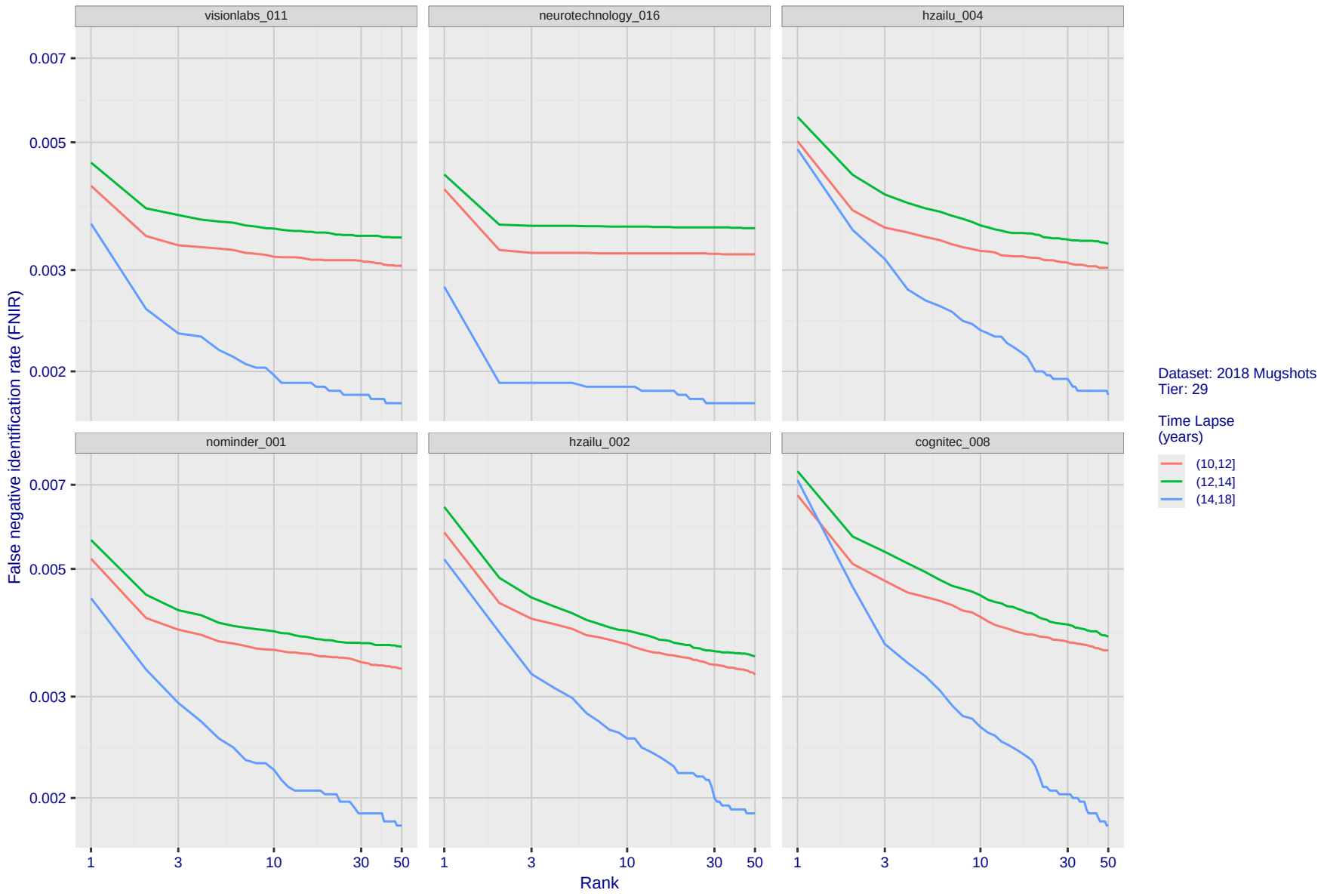

Figure 176: **[FRVT-2018 Mugshot Ageing Dataset] Identification miss rates vs. rank by time-elapsed**. *The oldest image of each individual is enrolled. Thereafter, all more recent images are searched. Miss rates are computed over all searches noted in row 17 of Table 1 and binned by number of years between search and initial enrollment.*

2026/01/09 20:40:38
FNIR(N, R, T) = False neg. identification rate
FPIR(N, T) = False pos. identification rate
N = Num. enrolled subjects
R = Num. candidates examined
T = Threshold
T = 0 → Investigation
T > 0 → Identification

This publication is available free of charge from: https://doi.org/10.6028/NIST.IR.8271

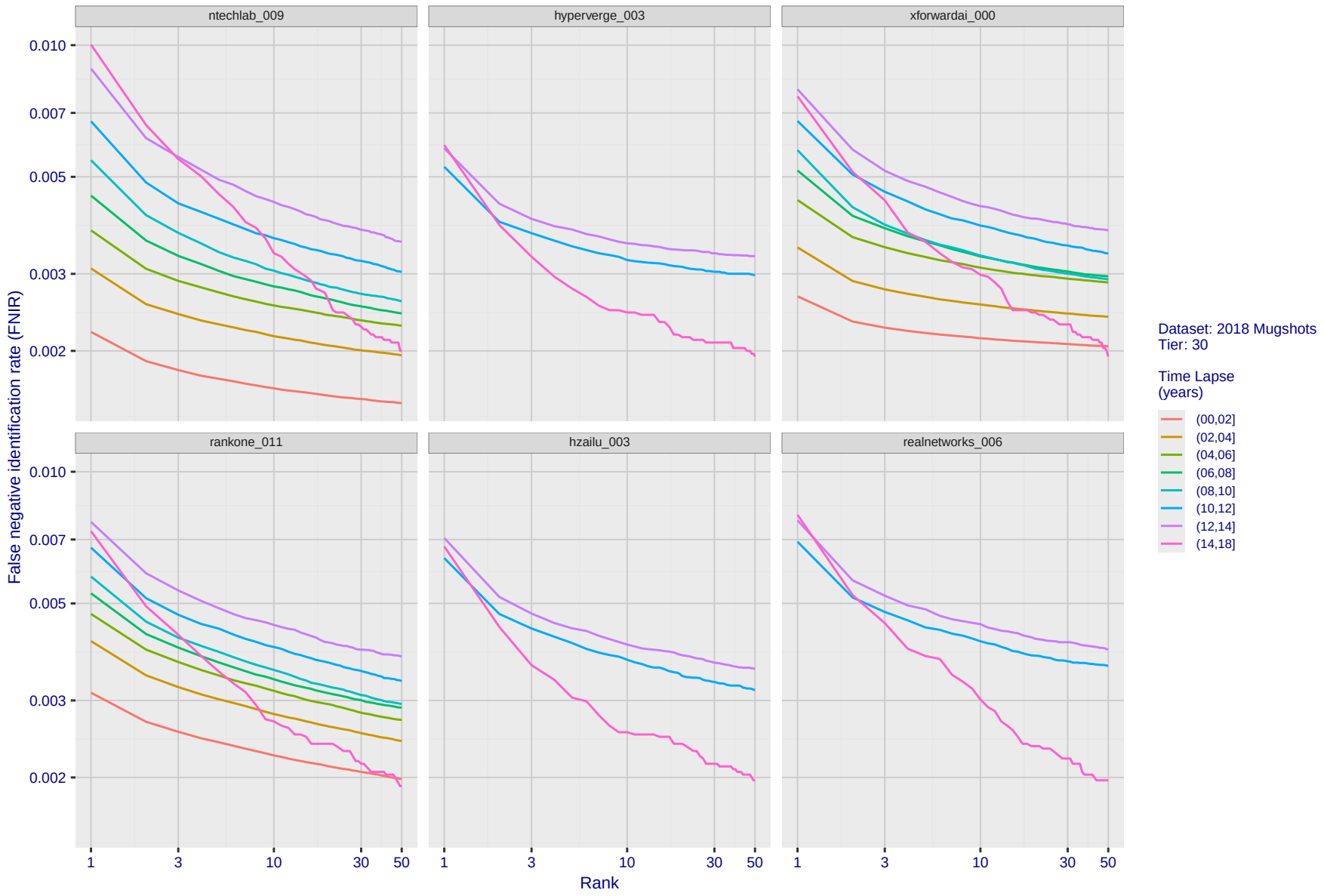

Figure 177: **[FRVT-2018 Mugshot Ageing Dataset] Identification miss rates vs. rank by time-elapsed**. *The oldest image of each individual is enrolled. Thereafter, all more recent images are searched. Miss rates are computed over all searches noted in row 17 of Table 1 and binned by number of years between search and initial enrollment.*

2026/01/09 20:40:38
FNIR(N, R, T) = False neg. identification rate
FPIR(N, T) = False pos. identification rate
N = Num. enrolled subjects
R = Num. candidates examined
T = Threshold
T = 0 → Investigation
T > 0 → Identification

This publication is available free of charge from: https://doi.org/10.6028/NIST.IR.8271

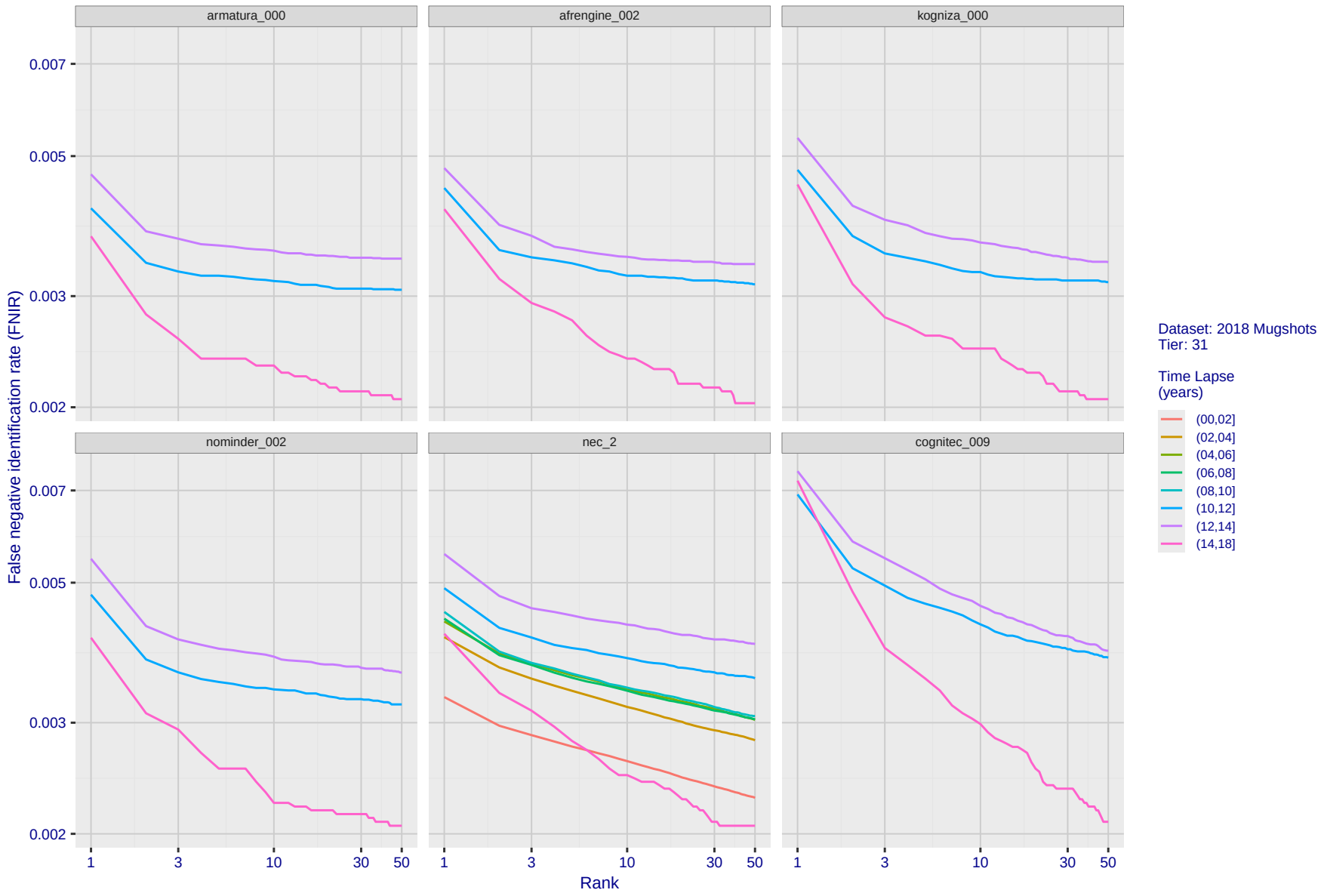

Figure 178: **[FRVT-2018 Mugshot Ageing Dataset] Identification miss rates vs. rank by time-elapsed**. *The oldest image of each individual is enrolled. Thereafter, all more recent images are searched. Miss rates are computed over all searches noted in row 17 of Table 1 and binned by number of years between search and initial enrollment.*

2026/01/09 20:40:38
FNIR(N, R, T) = False neg. identification rate
FPIR(N, T) = False pos. identification rate
N = Num. enrolled subjects
R = Num. candidates examined
T = Threshold
T = 0 → Investigation
T > 0 → Identification

This publication is available free of charge from: https://doi.org/10.6028/NIST.IR.8271

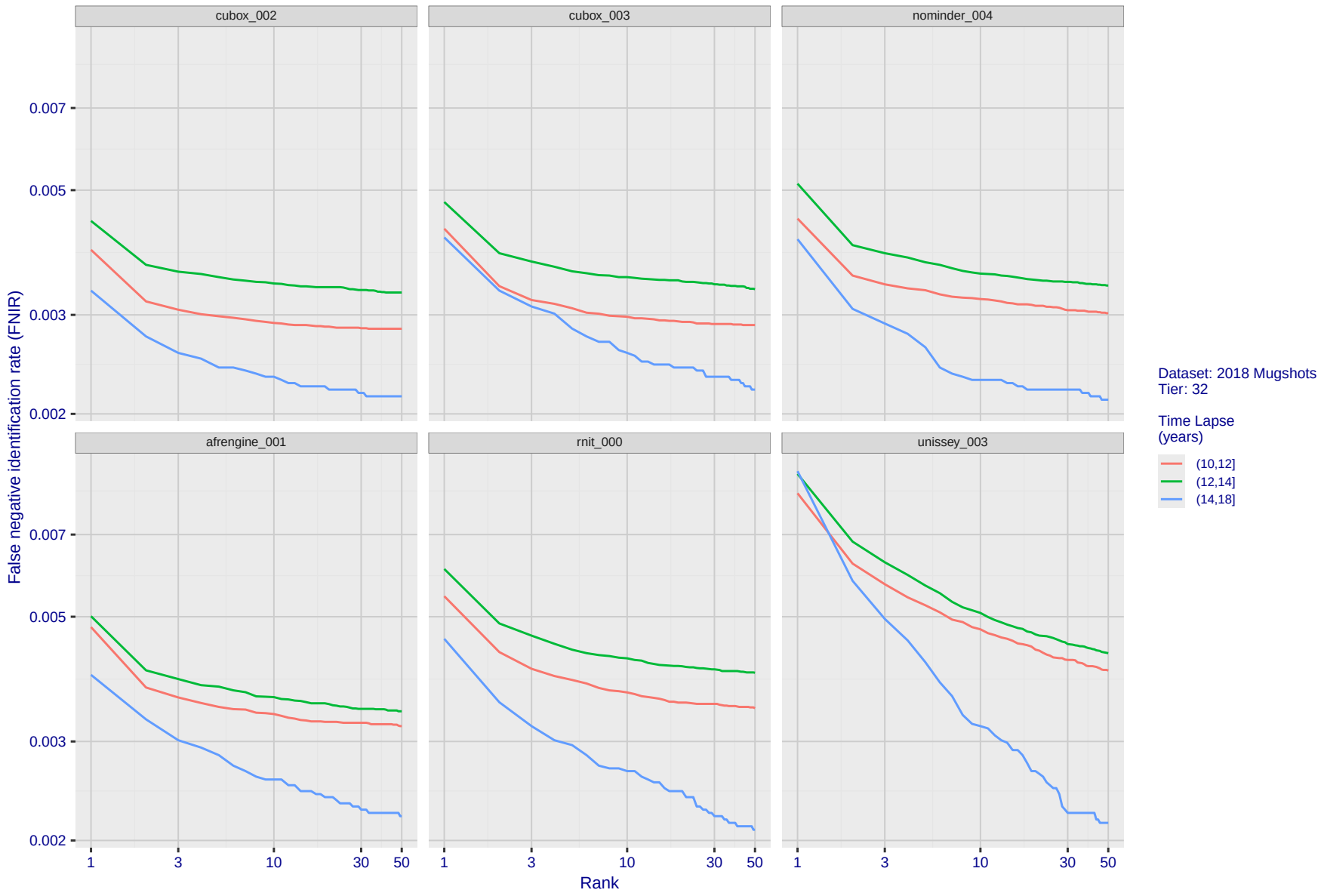

Figure 179: **[FRVT-2018 Mugshot Ageing Dataset] Identification miss rates vs. rank by time-elapsed**. *The oldest image of each individual is enrolled. Thereafter, all more recent images are searched. Miss rates are computed over all searches noted in row 17 of Table 1 and binned by number of years between search and initial enrollment.*

2026/01/09 20:40:38
FNIR(N, R, T) = False neg. identification rate
FPIR(N, T) = False pos. identification rate
N = Num. enrolled subjects
R = Num. candidates examined
T = Threshold
T = 0 → Investigation
T > 0 → Identification

This publication is available free of charge from: https://doi.org/10.6028/NIST.IR.8271

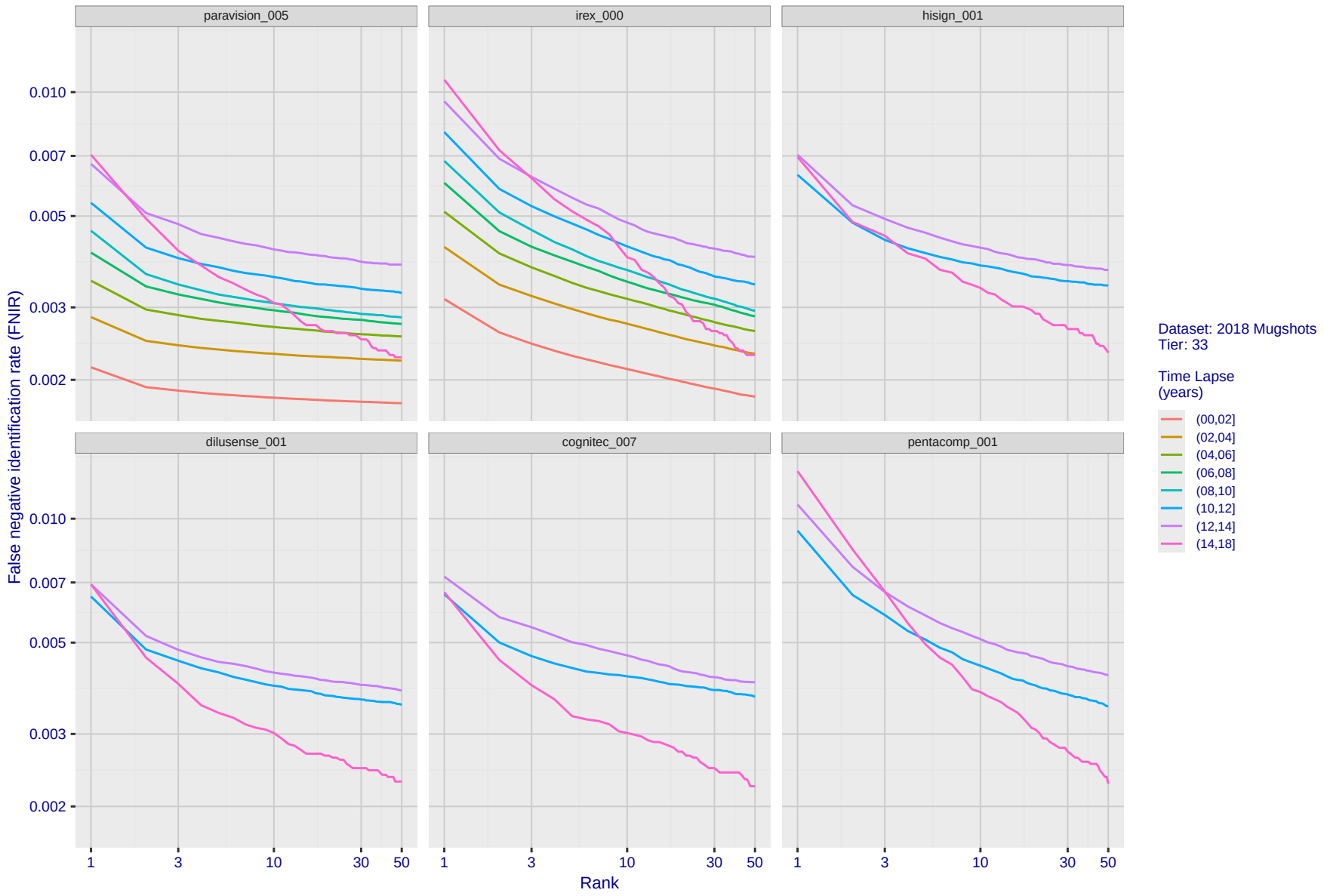

Figure 180: **[FRVT-2018 Mugshot Ageing Dataset] Identification miss rates vs. rank by time-elapsed**. *The oldest image of each individual is enrolled. Thereafter, all more recent images are searched. Miss rates are computed over all searches noted in row 17 of Table 1 and binned by number of years between search and initial enrollment.*

2026/01/09 20:40:38
FNIR(N, R, T) = False neg. identification rate
FPIR(N, T) = False pos. identification rate
N = Num. enrolled subjects
R = Num. candidates examined
T = Threshold
T = 0 → Investigation
T > 0 → Identification

This publication is available free of charge from: https://doi.org/10.6028/NIST.IR.8271

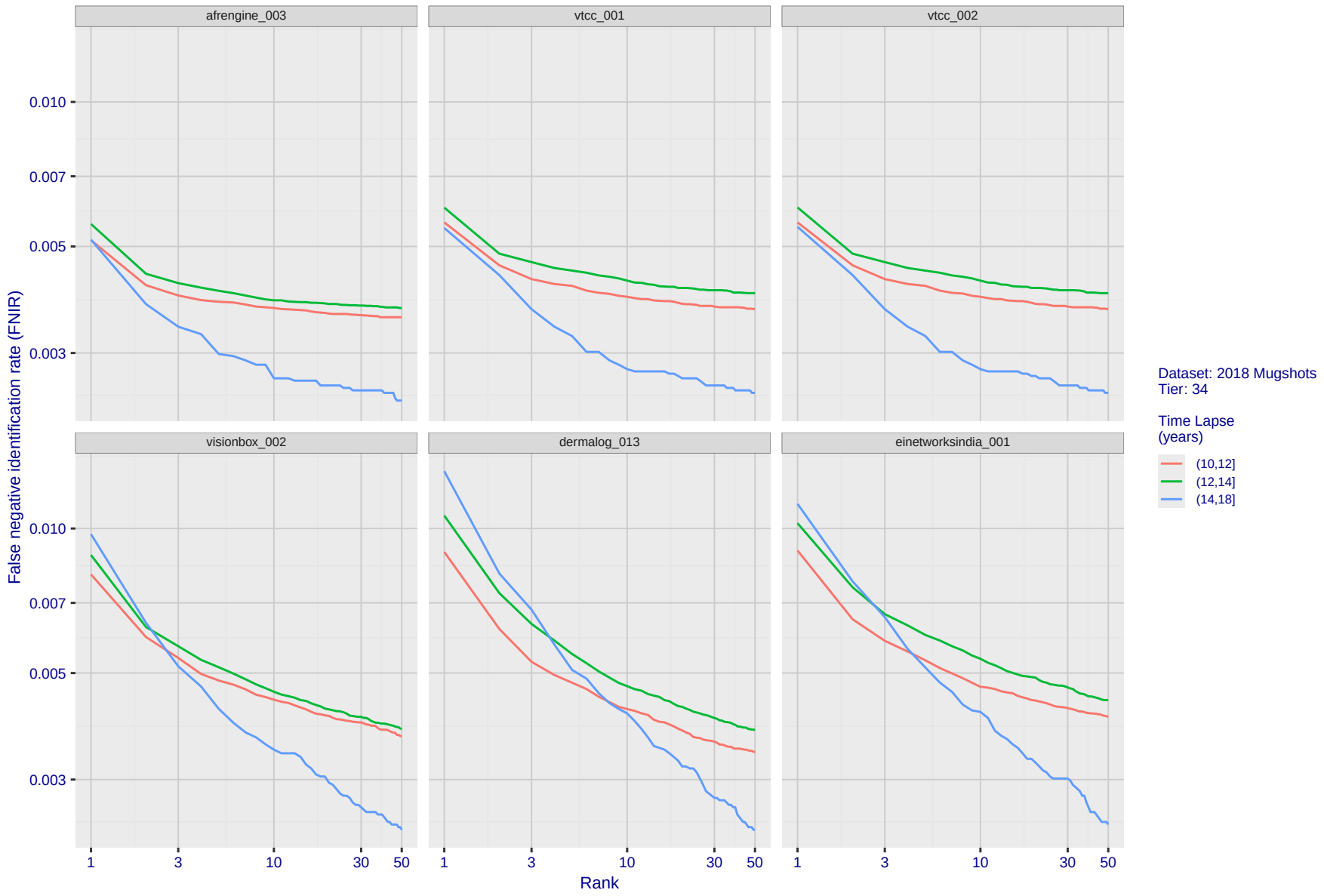

Figure 181: **[FRVT-2018 Mugshot Ageing Dataset] Identification miss rates vs. rank by time-elapsed**. *The oldest image of each individual is enrolled. Thereafter, all more recent images are searched. Miss rates are computed over all searches noted in row 17 of Table 1 and binned by number of years between search and initial enrollment.*

2026/01/09 20:40:38
FNIR(N, R, T) = False neg. identification rate
FPIR(N, T) = False pos. identification rate
N = Num. enrolled subjects
R = Num. candidates examined
T = Threshold
T = 0 → Investigation
T > 0 → Identification

This publication is available free of charge from: https://doi.org/10.6028/NIST.IR.8271

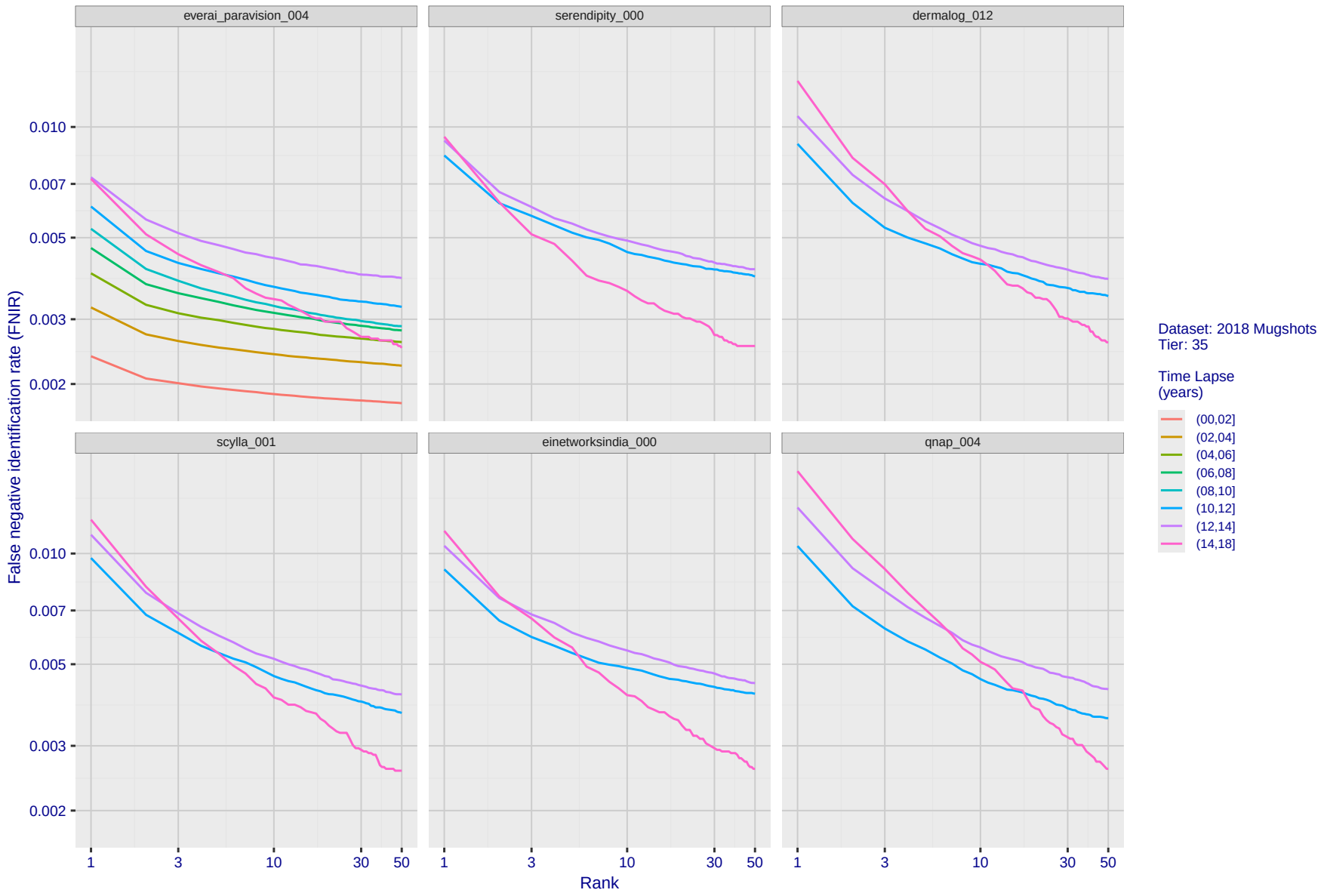

Figure 182: **[FRVT-2018 Mugshot Ageing Dataset] Identification miss rates vs. rank by time-elapsed**. *The oldest image of each individual is enrolled. Thereafter, all more recent images are searched. Miss rates are computed over all searches noted in row 17 of Table 1 and binned by number of years between search and initial enrollment.*

2026/01/09 20:40:38
FNIR(N, R, T) = False neg. identification rate
FPIR(N, T) = False pos. identification rate
N = Num. enrolled subjects
R = Num. candidates examined
T = Threshold
T = 0 → Investigation
T > 0 → Identification

This publication is available free of charge from: https://doi.org/10.6028/NIST.IR.8271

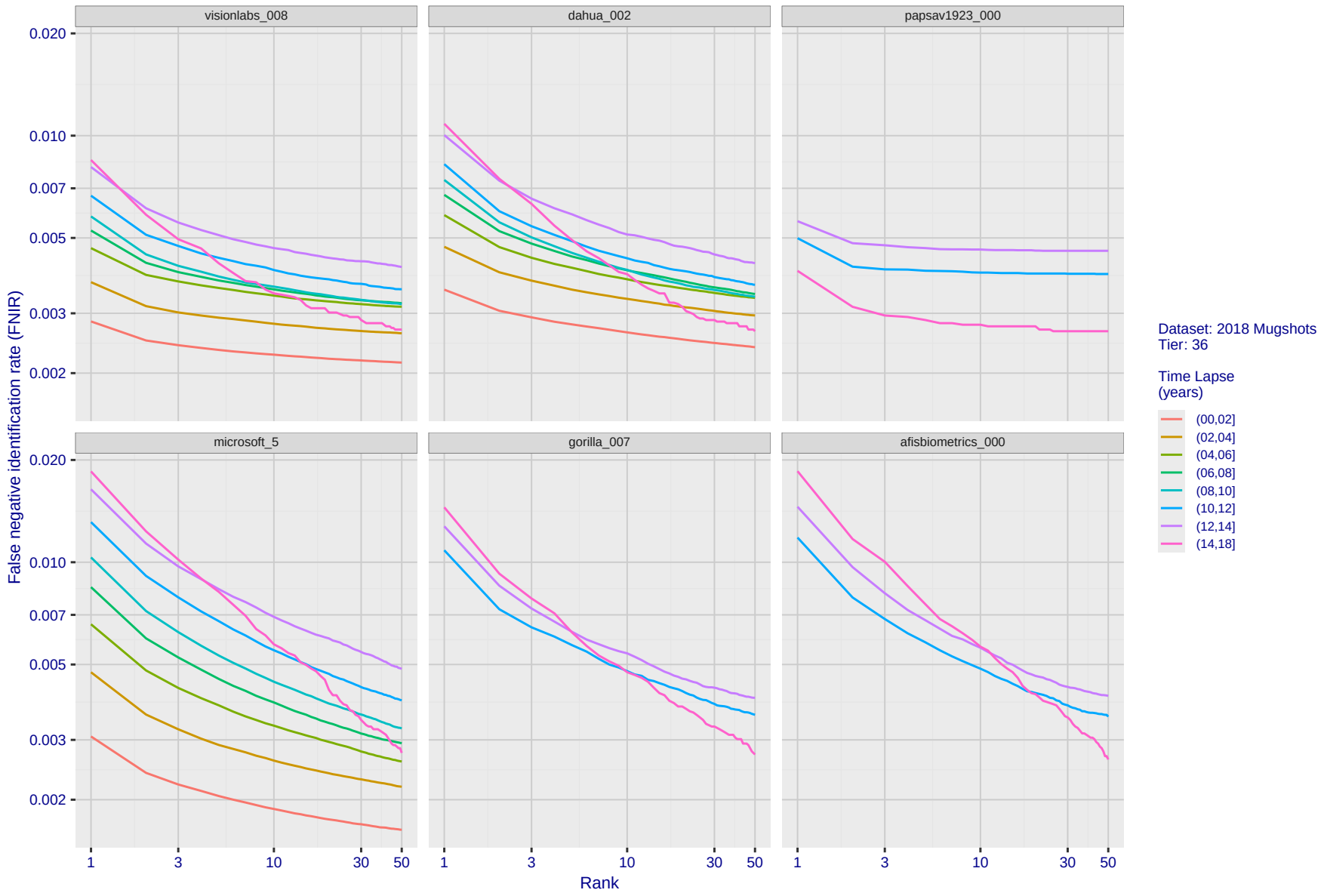

Figure 183: **[FRVT-2018 Mugshot Ageing Dataset] Identification miss rates vs. rank by time-elapsed**. *The oldest image of each individual is enrolled. Thereafter, all more recent images are searched. Miss rates are computed over all searches noted in row 17 of Table 1 and binned by number of years between search and initial enrollment.*

2026/01/09 20:40:38
FNIR(N, R, T) = False neg. identification rate
FPIR(N, T) = False pos. identification rate
N = Num. enrolled subjects
R = Num. candidates examined
T = Threshold
T = 0 → Investigation
T > 0 → Identification

This publication is available free of charge from: https://doi.org/10.6028/NIST.IR.8271

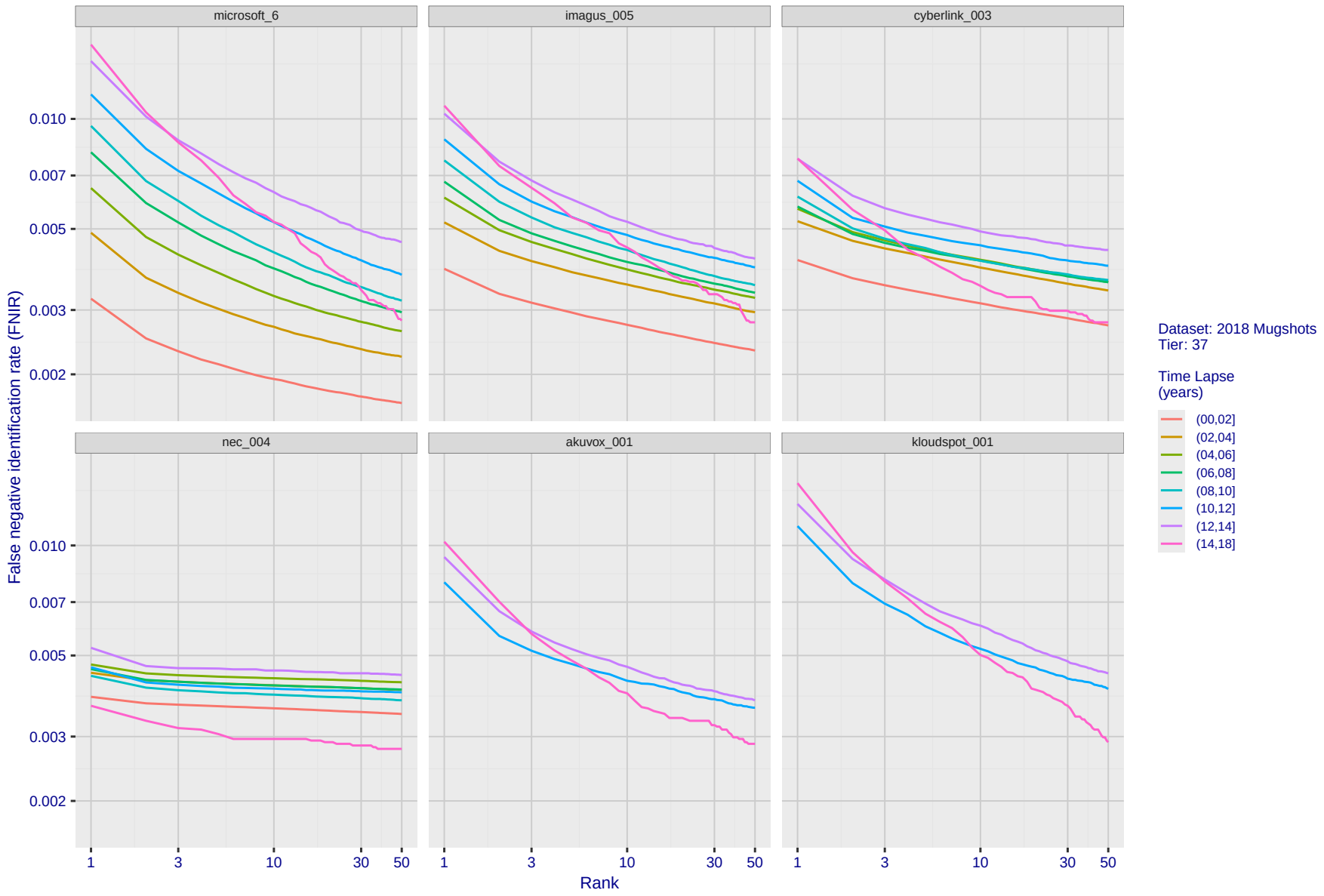

Figure 184: **[FRVT-2018 Mugshot Ageing Dataset] Identification miss rates vs. rank by time-elapsed**. *The oldest image of each individual is enrolled. Thereafter, all more recent images are searched. Miss rates are computed over all searches noted in row 17 of Table 1 and binned by number of years between search and initial enrollment.*

2026/01/09 20:40:38
FNIR(N, R, T) = False neg. identification rate
FPIR(N, T) = False pos. identification rate
N = Num. enrolled subjects
R = Num. candidates examined
T = Threshold
T = 0 → Investigation
T > 0 → Identification

This publication is available free of charge from: https://doi.org/10.6028/NIST.IR.8271

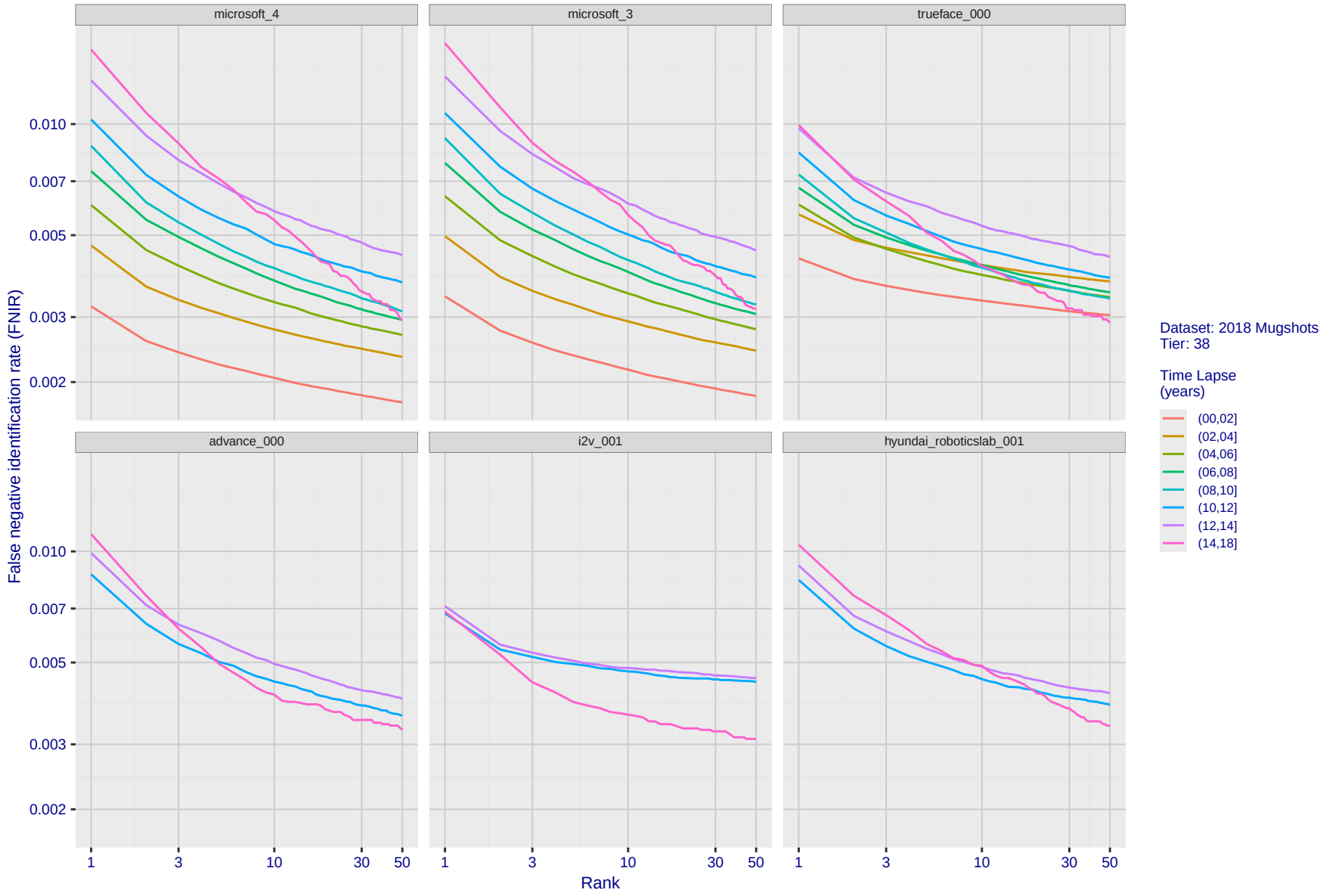

Figure 185: **[FRVT-2018 Mugshot Ageing Dataset] Identification miss rates vs. rank by time-elapsed**. *The oldest image of each individual is enrolled. Thereafter, all more recent images are searched. Miss rates are computed over all searches noted in row 17 of Table 1 and binned by number of years between search and initial enrollment.*

2026/01/09 20:40:38
FNIR(N, R, T) = False neg. identification rate
FPIR(N, T) = False pos. identification rate
N = Num. enrolled subjects
R = Num. candidates examined
T = Threshold
T = 0 → Investigation
T > 0 → Identification

This publication is available free of charge from: https://doi.org/10.6028/NIST.IR.8271

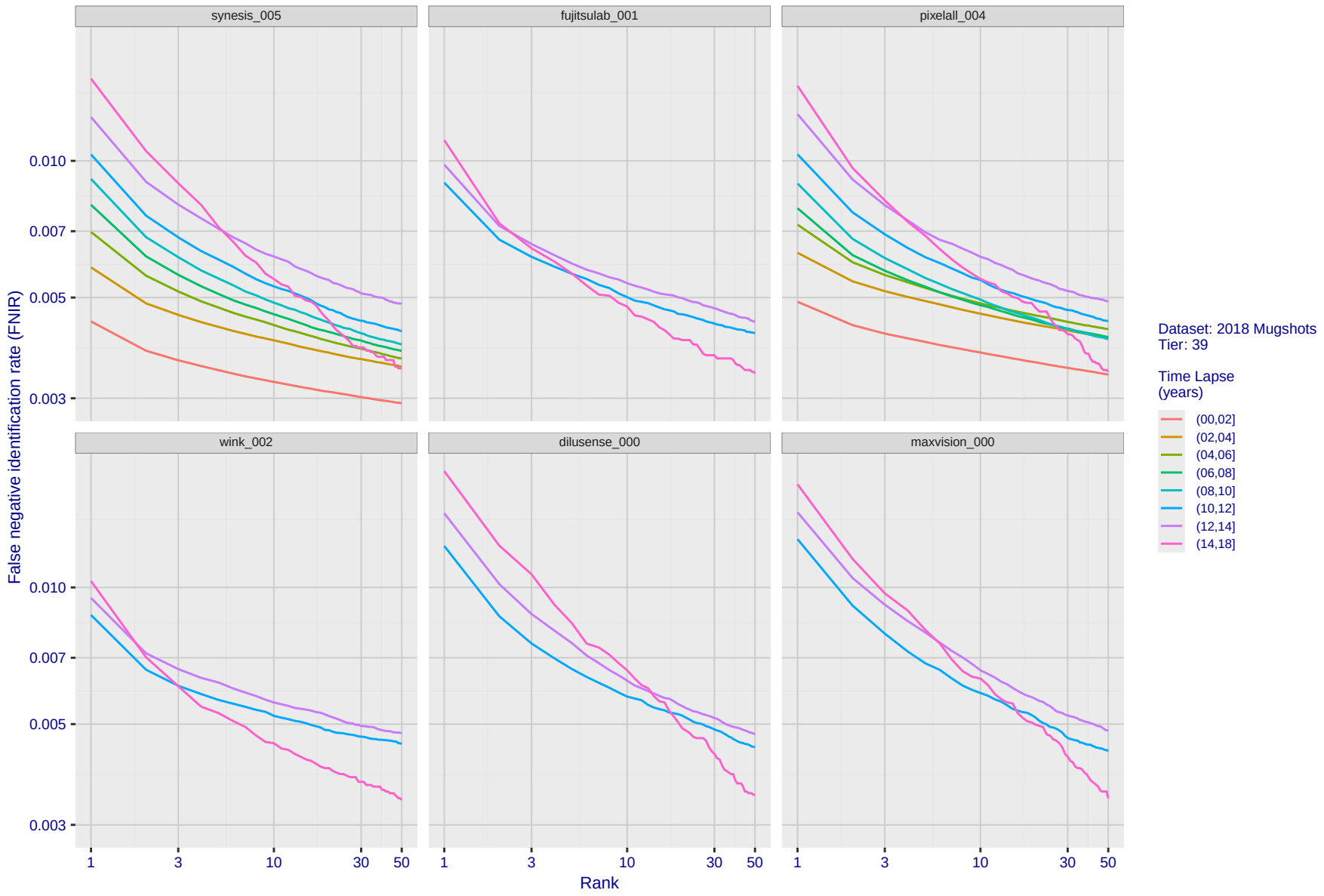

Figure 186: **[FRVT-2018 Mugshot Ageing Dataset] Identification miss rates vs. rank by time-elapsed**. *The oldest image of each individual is enrolled. Thereafter, all more recent images are searched. Miss rates are computed over all searches noted in row 17 of Table 1 and binned by number of years between search and initial enrollment.*

2026/01/09 20:40:38
FNIR(N, R, T) = False neg. identification rate
FPIR(N, T) = False pos. identification rate
N = Num. enrolled subjects
R = Num. candidates examined
T = Threshold
T = 0 → Investigation
T > 0 → Identification

This publication is available free of charge from: https://doi.org/10.6028/NIST.IR.8271

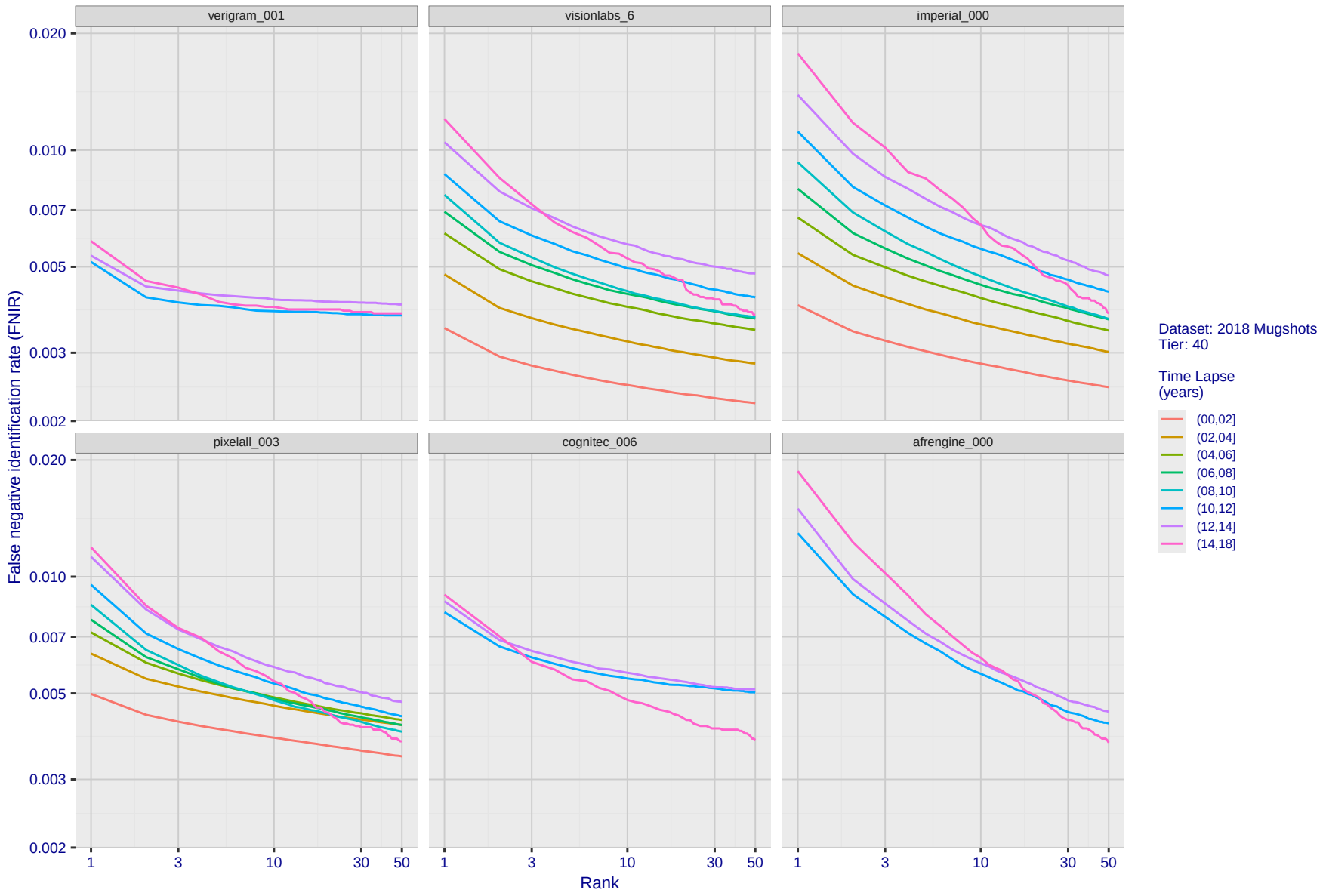

Figure 187: **[FRVT-2018 Mugshot Ageing Dataset] Identification miss rates vs. rank by time-elapsed**. *The oldest image of each individual is enrolled. Thereafter, all more recent images are searched. Miss rates are computed over all searches noted in row 17 of Table 1 and binned by number of years between search and initial enrollment.*

2026/01/09 20:40:38
FNIR(N, R, T) = False neg. identification rate
FPIR(N, T) = False pos. identification rate
N = Num. enrolled subjects
R = Num. candidates examined
T = Threshold
T = 0 → Investigation
T > 0 → Identification

This publication is available free of charge from: https://doi.org/10.6028/NIST.IR.8271

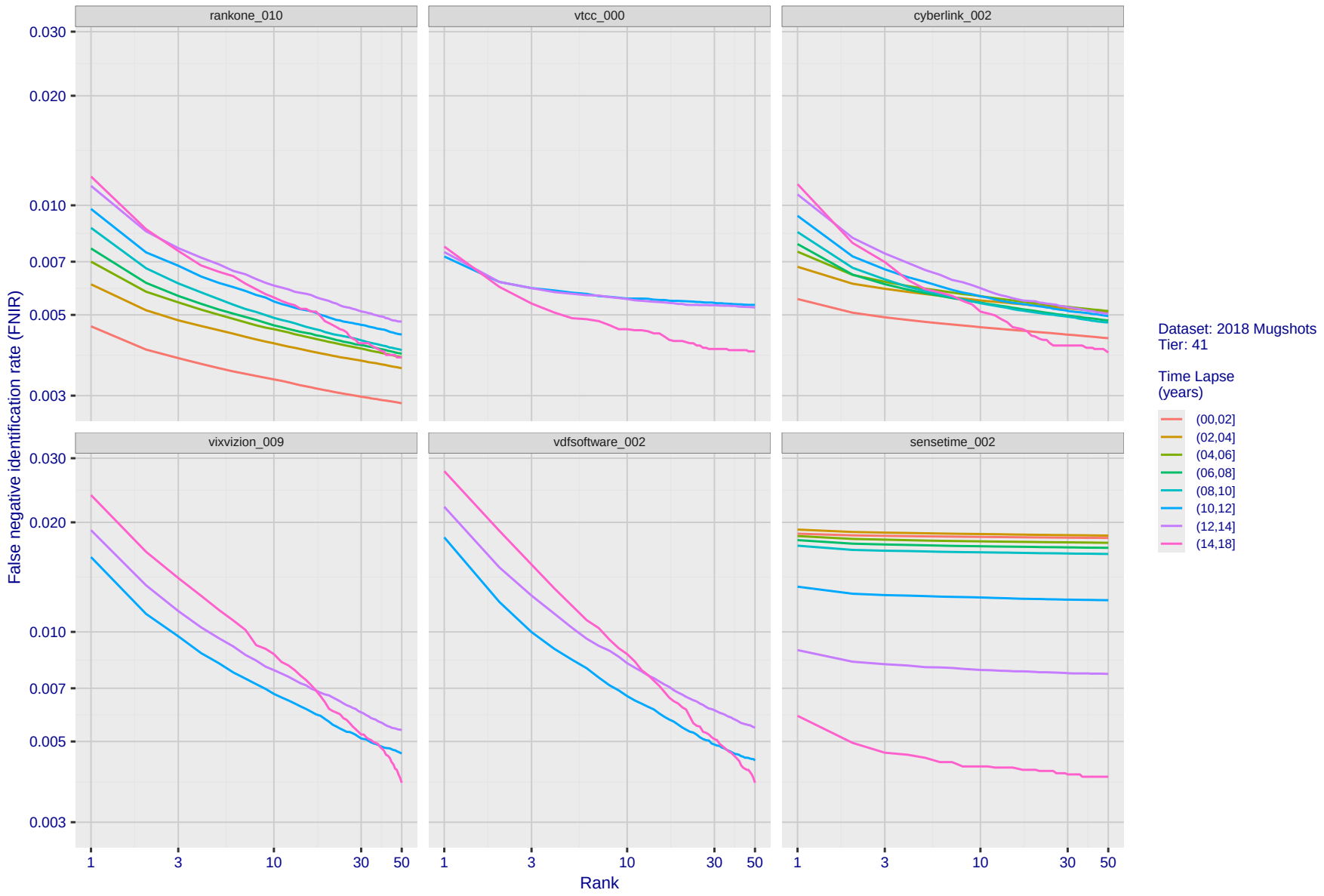

Figure 188: **[FRVT-2018 Mugshot Ageing Dataset] Identification miss rates vs. rank by time-elapsed**. *The oldest image of each individual is enrolled. Thereafter, all more recent images are searched. Miss rates are computed over all searches noted in row 17 of Table 1 and binned by number of years between search and initial enrollment.*

2026/01/09 20:40:38
FNIR(N, R, T) = False neg. identification rate
FPIR(N, T) = False pos. identification rate
N = Num. enrolled subjects
R = Num. candidates examined
T = Threshold
T = 0 → Investigation
T > 0 → Identification

This publication is available free of charge from: https://doi.org/10.6028/NIST.IR.8271

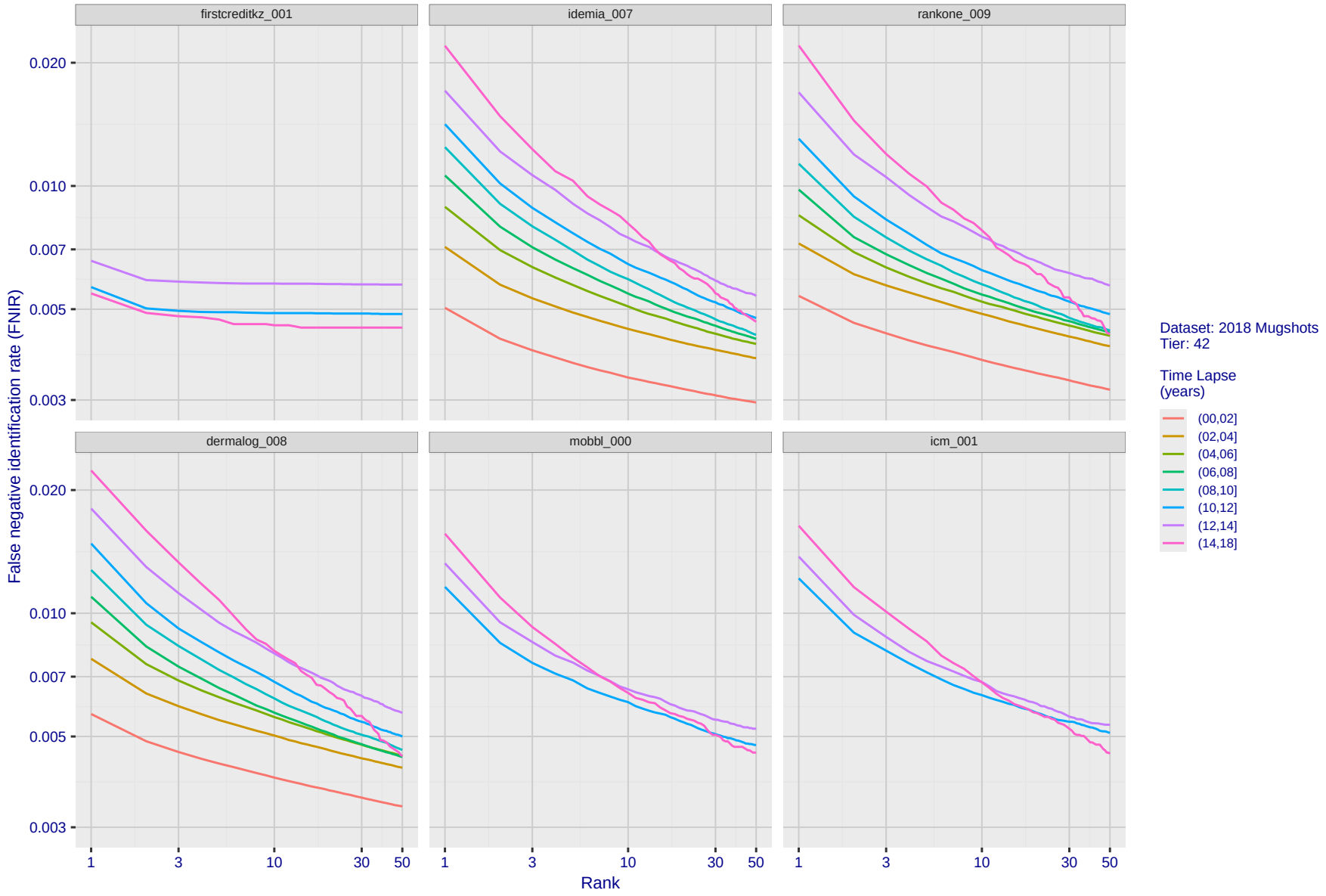

Figure 189: **[FRVT-2018 Mugshot Ageing Dataset] Identification miss rates vs. rank by time-elapsed**. *The oldest image of each individual is enrolled. Thereafter, all more recent images are searched. Miss rates are computed over all searches noted in row 17 of Table 1 and binned by number of years between search and initial enrollment.*

2026/01/09 20:40:38
FNIR(N, R, T) = False neg. identification rate
FPIR(N, T) = False pos. identification rate
N = Num. enrolled subjects
R = Num. candidates examined
T = Threshold
T = 0 → Investigation
T > 0 → Identification

This publication is available free of charge from: https://doi.org/10.6028/NIST.IR.8271

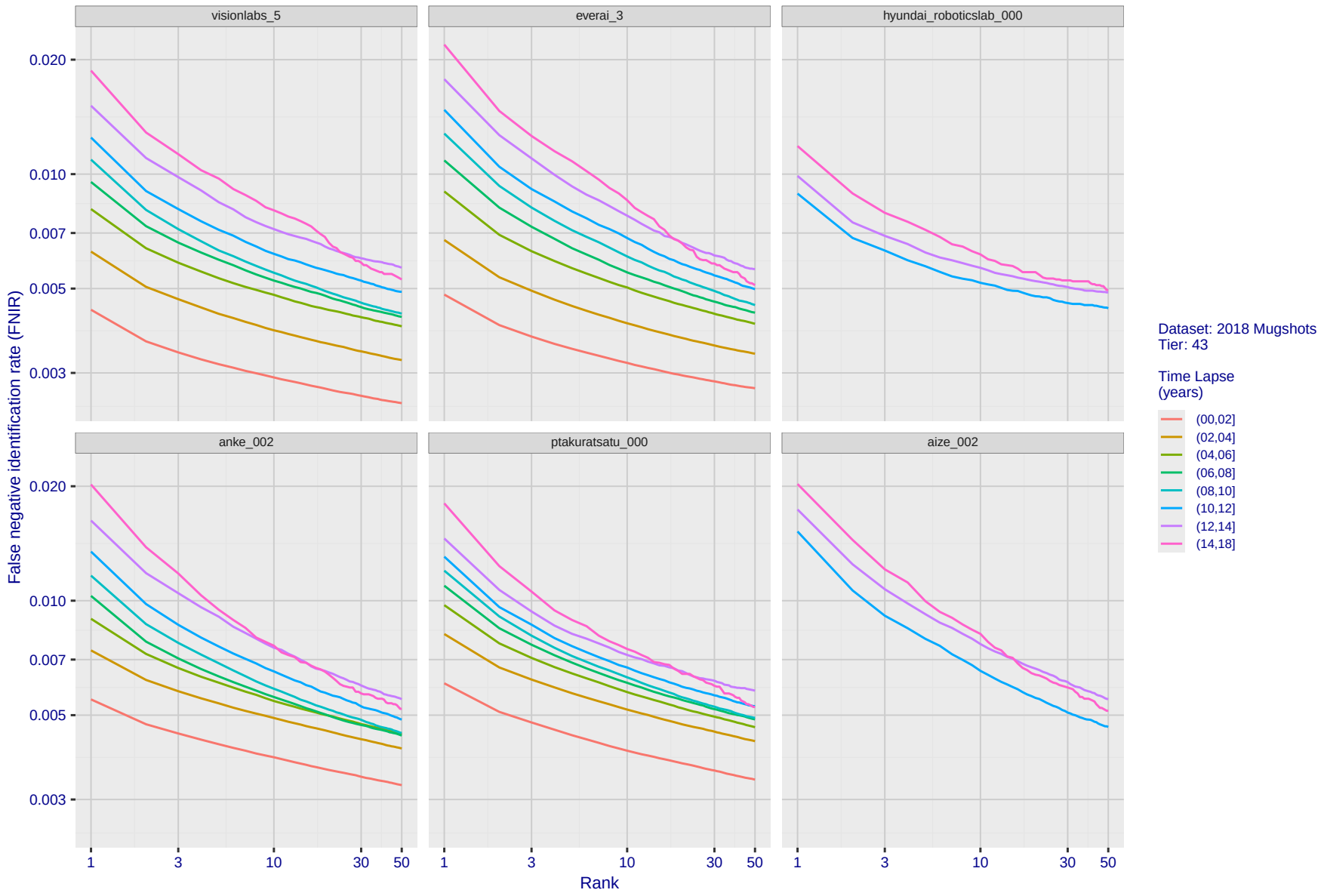

Figure 190: **[FRVT-2018 Mugshot Ageing Dataset] Identification miss rates vs. rank by time-elapsed**. *The oldest image of each individual is enrolled. Thereafter, all more recent images are searched. Miss rates are computed over all searches noted in row 17 of Table 1 and binned by number of years between search and initial enrollment.*

2026/01/09 20:40:38
FNIR(N, R, T) = False neg. identification rate
FPIR(N, T) = False pos. identification rate
N = Num. enrolled subjects
R = Num. candidates examined
T = Threshold
T = 0 → Investigation
T > 0 → Identification

This publication is available free of charge from: https://doi.org/10.6028/NIST.IR.8271

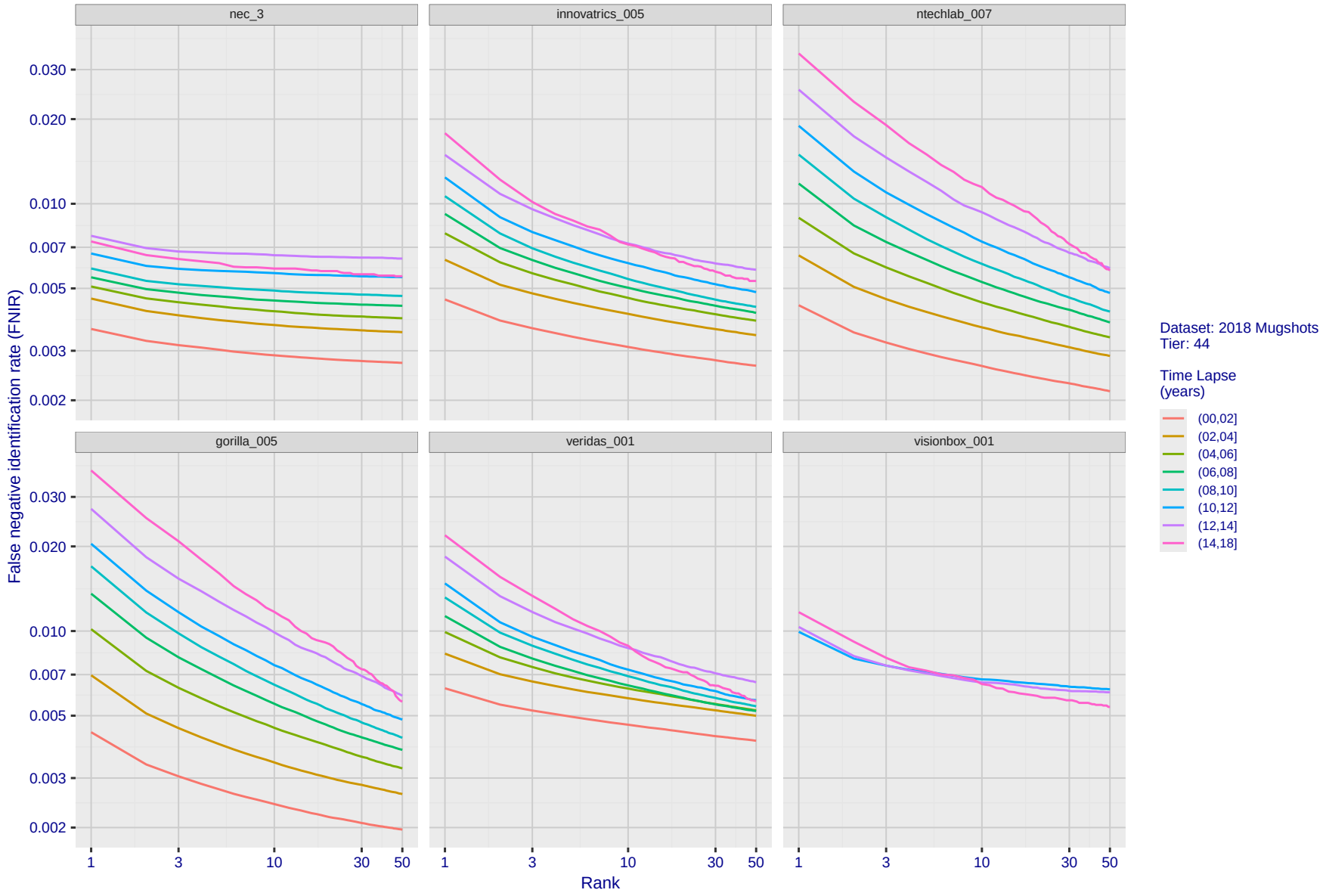

Figure 191: **[FRVT-2018 Mugshot Ageing Dataset] Identification miss rates vs. rank by time-elapsed**. *The oldest image of each individual is enrolled. Thereafter, all more recent images are searched. Miss rates are computed over all searches noted in row 17 of Table 1 and binned by number of years between search and initial enrollment.*

2026/01/09 20:40:38
FNIR(N, R, T) = False neg. identification rate
FPIR(N, T) = False pos. identification rate
N = Num. enrolled subjects
R = Num. candidates examined
T = Threshold
T = 0 → Investigation
T > 0 → Identification

This publication is available free of charge from: https://doi.org/10.6028/NIST.IR.8271

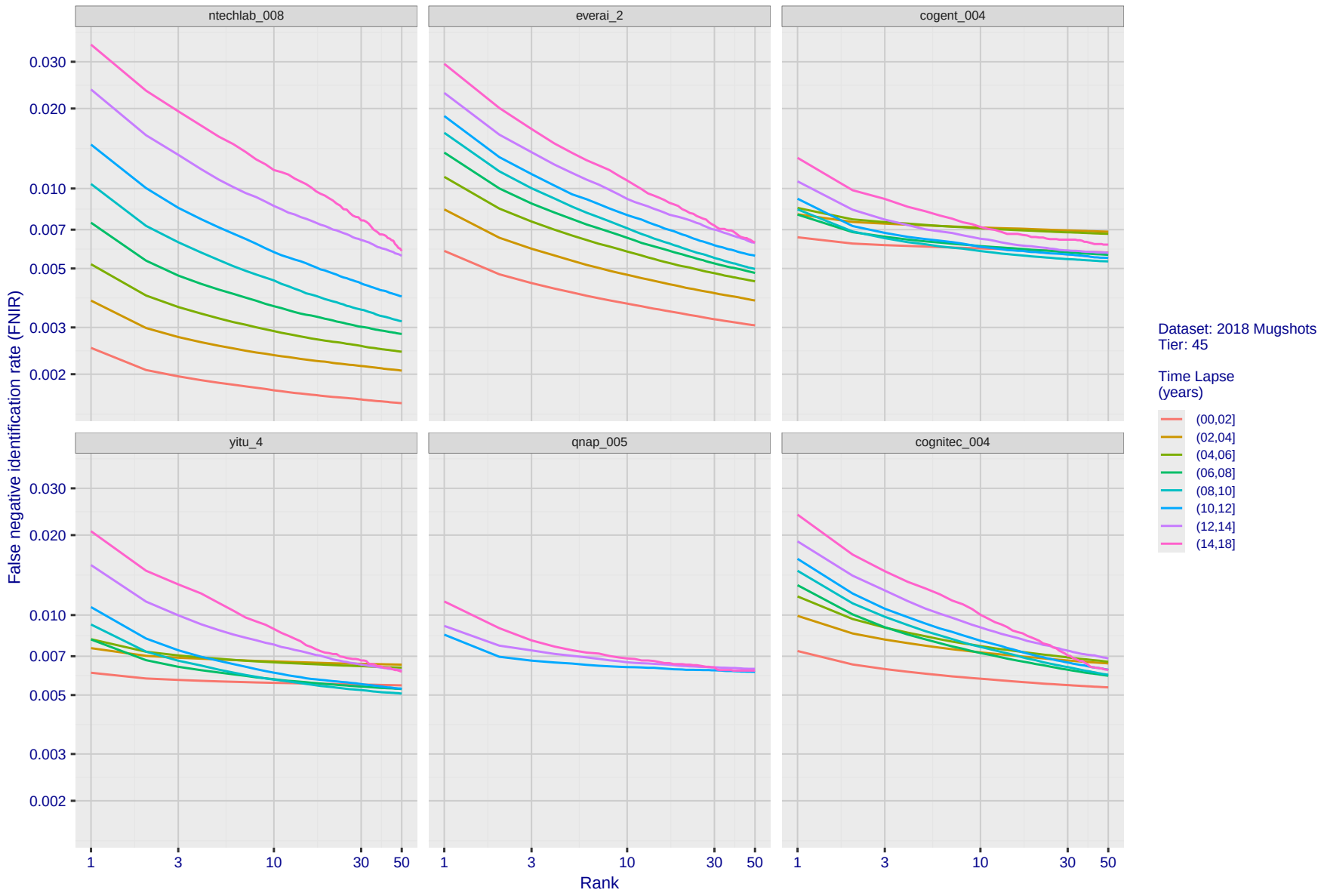

Figure 192: **[FRVT-2018 Mugshot Ageing Dataset] Identification miss rates vs. rank by time-elapsed**. *The oldest image of each individual is enrolled. Thereafter, all more recent images are searched. Miss rates are computed over all searches noted in row 17 of Table 1 and binned by number of years between search and initial enrollment.*

2026/01/09 20:40:38
FNIR(N, R, T) = False neg. identification rate
FPIR(N, T) = False pos. identification rate
N = Num. enrolled subjects
R = Num. candidates examined
T = Threshold
T = 0 → Investigation
T > 0 → Identification

This publication is available free of charge from: https://doi.org/10.6028/NIST.IR.8271

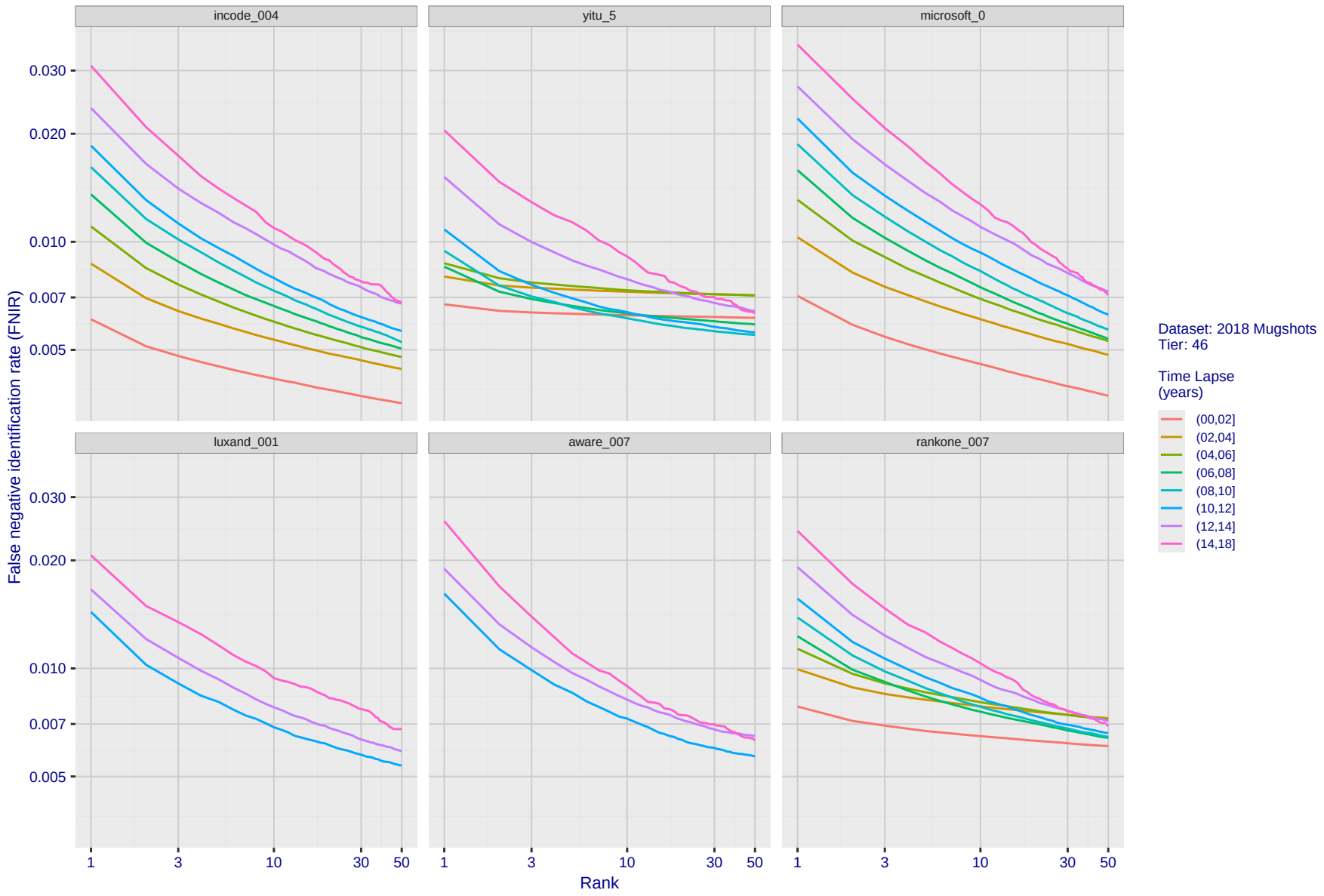

Figure 193: **[FRVT-2018 Mugshot Ageing Dataset] Identification miss rates vs. rank by time-elapsed**. *The oldest image of each individual is enrolled. Thereafter, all more recent images are searched. Miss rates are computed over all searches noted in row 17 of Table 1 and binned by number of years between search and initial enrollment.*

2026/01/09 20:40:38
FNIR(N, R, T) = False neg. identification rate
FPIR(N, T) = False pos. identification rate
N = Num. enrolled subjects
R = Num. candidates examined
T = Threshold
T = 0 → Investigation
T > 0 → Identification

This publication is available free of charge from: https://doi.org/10.6028/NIST.IR.8271

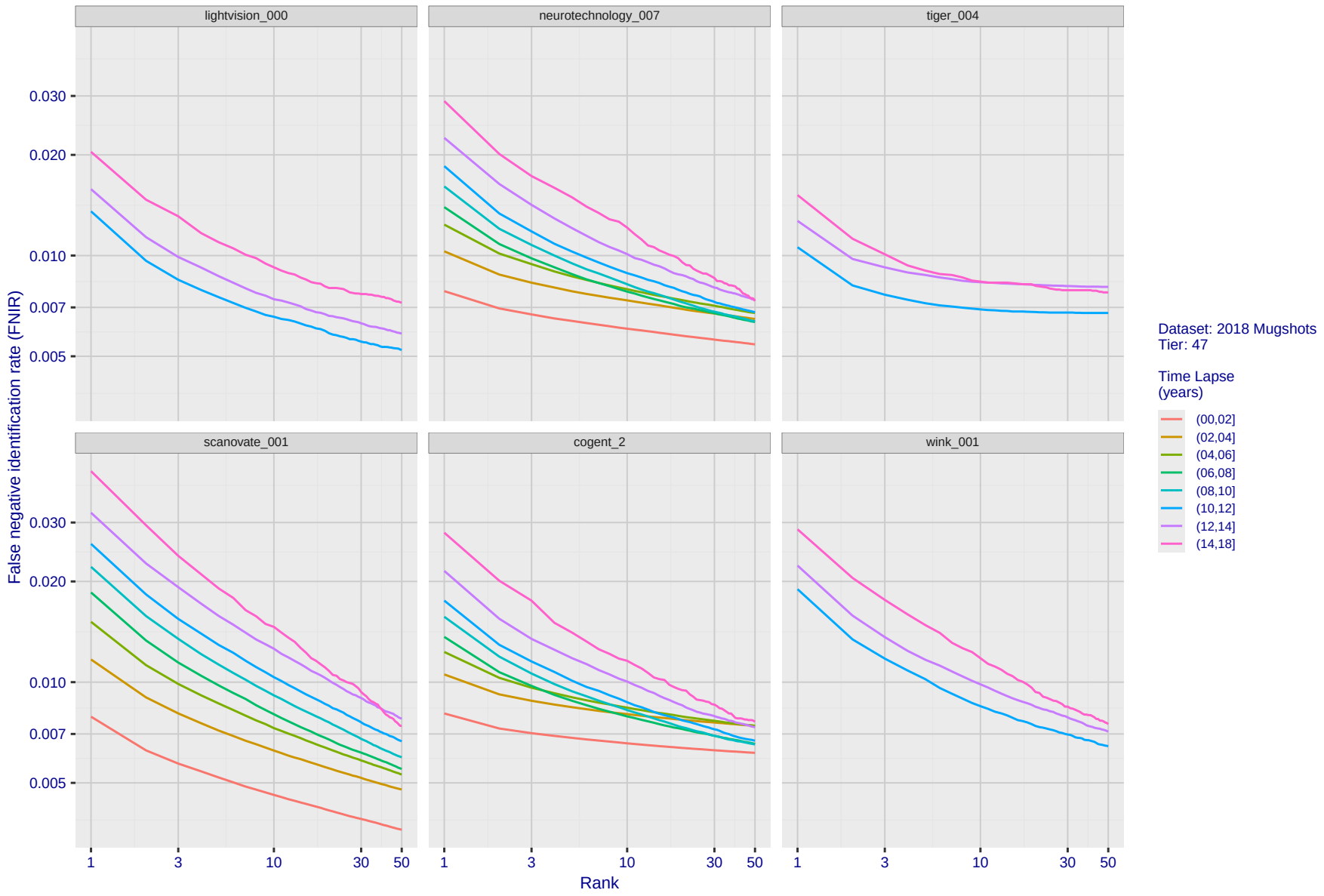

Figure 194: **[FRVT-2018 Mugshot Ageing Dataset] Identification miss rates vs. rank by time-elapsed**. *The oldest image of each individual is enrolled. Thereafter, all more recent images are searched. Miss rates are computed over all searches noted in row 17 of Table 1 and binned by number of years between search and initial enrollment.*

2026/01/09
20:40:38

FNIR(N, R, T) = False neg. identification rate
FPIR(N, T) = False pos. identification rate

N = Num. enrolled subjects
R = Num. candidates examined

T = Threshold

T = 0 → Investigation
T > 0 → Identification

This publication is available free of charge from: https://doi.org/10.6028/NIST.IR.8271

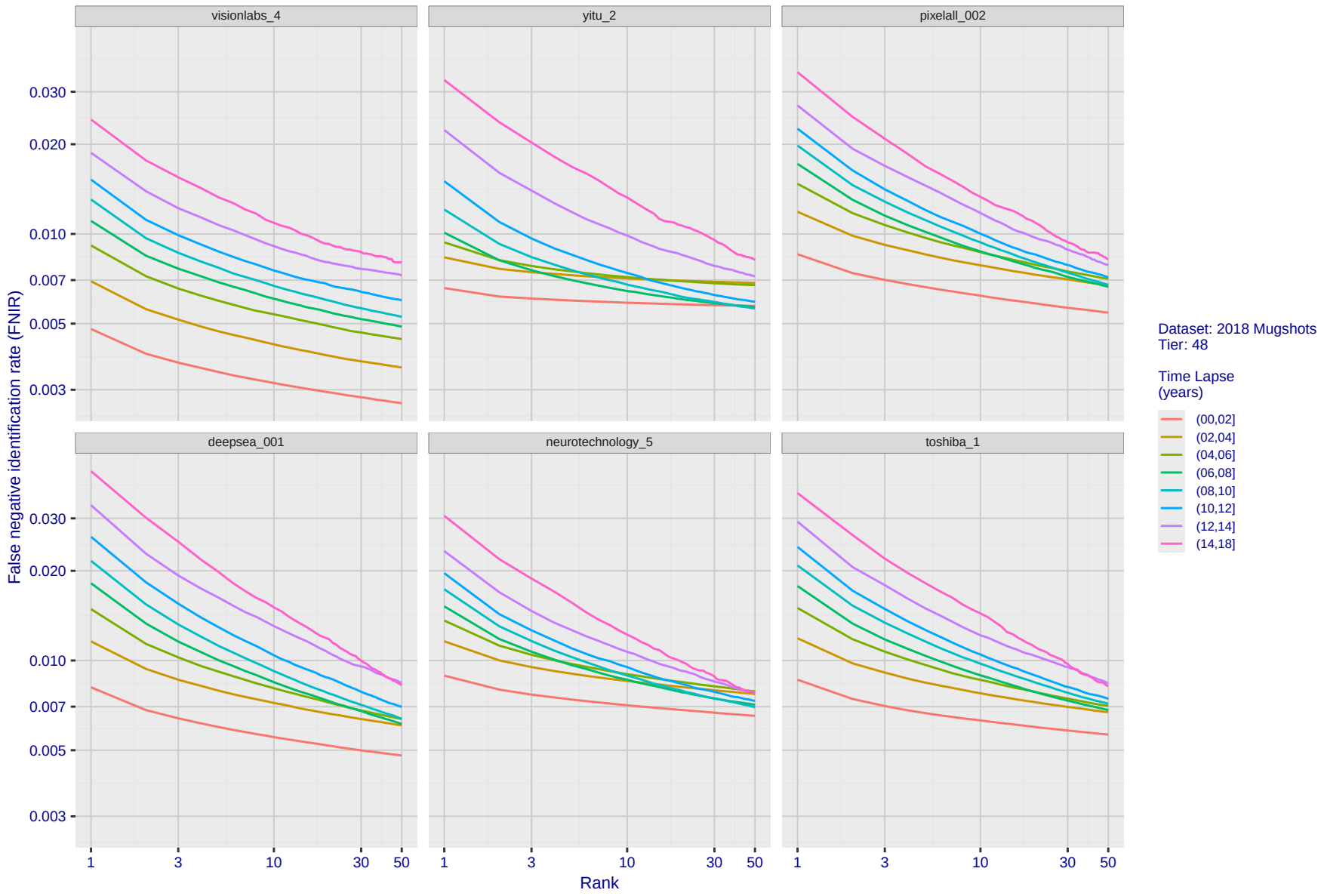

Figure 195: **[FRVT-2018 Mugshot Ageing Dataset] Identification miss rates vs. rank by time-elapsed**. *The oldest image of each individual is enrolled. Thereafter, all more recent images are searched. Miss rates are computed over all searches noted in row 17 of Table 1 and binned by number of years between search and initial enrollment.*

2026/01/09 20:40:38
FNIR(N, R, T) = False neg. identification rate
FPIR(N, T) = False pos. identification rate
N = Num. enrolled subjects
R = Num. candidates examined
T = Threshold
T = 0 → Investigation
T > 0 → Identification

This publication is available free of charge from: https://doi.org/10.6028/NIST.IR.8271

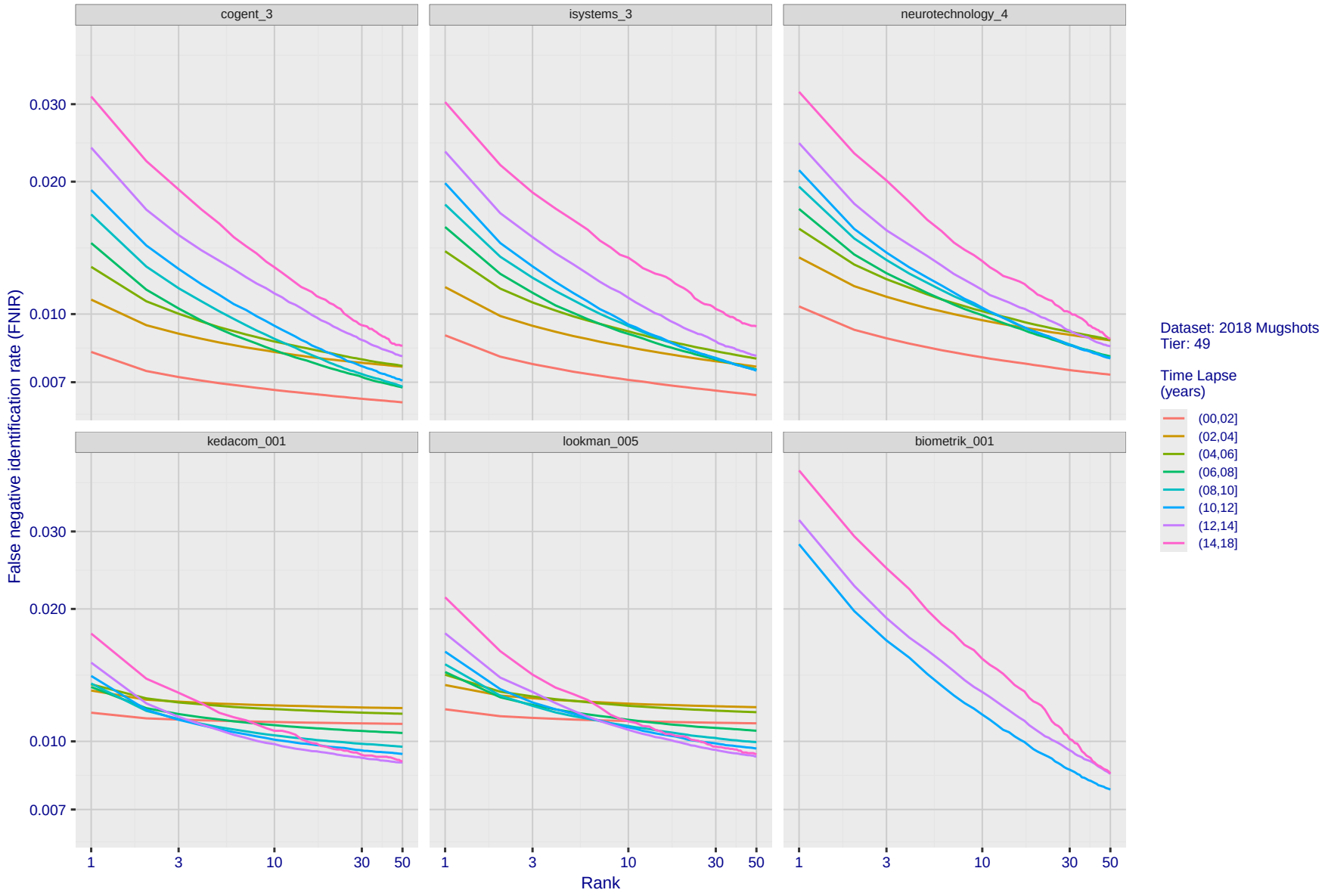

Figure 196: **[FRVT-2018 Mugshot Ageing Dataset] Identification miss rates vs. rank by time-elapsed**. *The oldest image of each individual is enrolled. Thereafter, all more recent images are searched. Miss rates are computed over all searches noted in row 17 of Table 1 and binned by number of years between search and initial enrollment.*

2026/01/09 20:40:38
FNIR(N, R, T) = False neg. identification rate
FPIR(N, T) = False pos. identification rate
N = Num. enrolled subjects
R = Num. candidates examined
T = Threshold
T = 0 → Investigation
T > 0 → Identification

This publication is available free of charge from: https://doi.org/10.6028/NIST.IR.8271

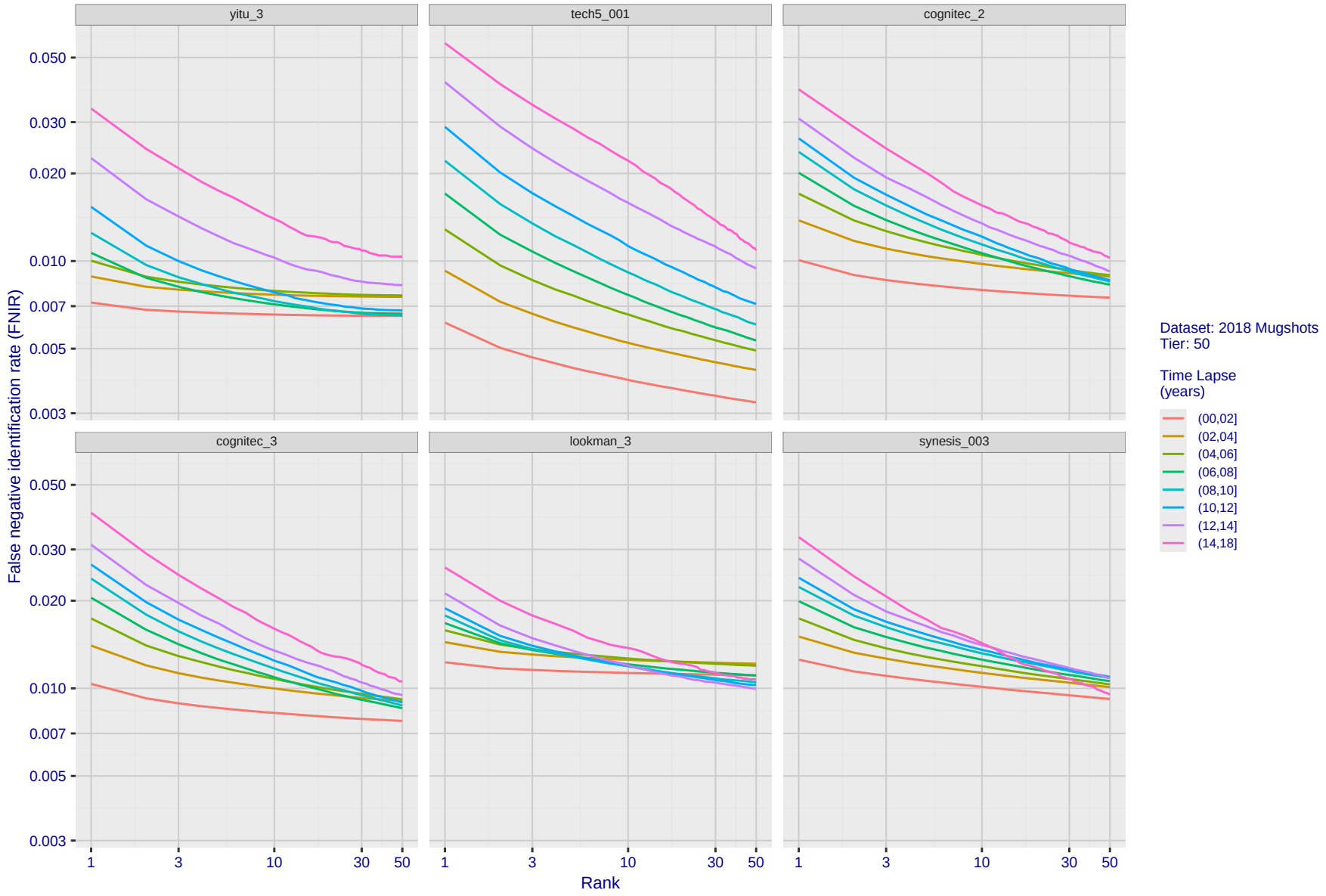

Figure 197: **[FRVT-2018 Mugshot Ageing Dataset] Identification miss rates vs. rank by time-elapsed**. *The oldest image of each individual is enrolled. Thereafter, all more recent images are searched. Miss rates are computed over all searches noted in row 17 of Table 1 and binned by number of years between search and initial enrollment.*

2026/01/09 20:40:38
FNIR(N, R, T) = False neg. identification rate
FPIR(N, T) = False pos. identification rate
N = Num. enrolled subjects
R = Num. candidates examined
T = Threshold
T = 0 → Investigation
T > 0 → Identification

This publication is available free of charge from: https://doi.org/10.6028/NIST.IR.8271

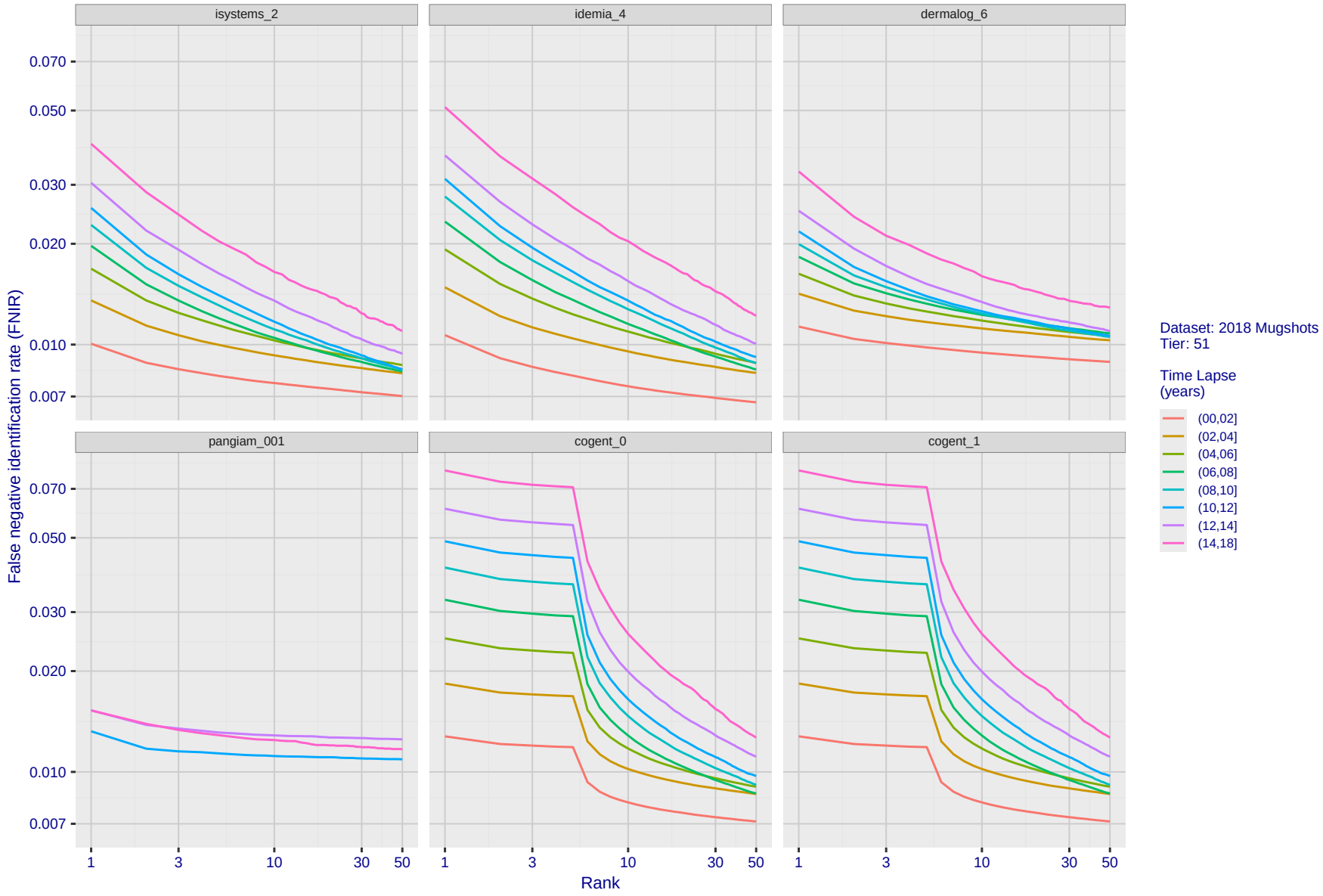

Figure 198: **[FRVT-2018 Mugshot Ageing Dataset] Identification miss rates vs. rank by time-elapsed**. *The oldest image of each individual is enrolled. Thereafter, all more recent images are searched. Miss rates are computed over all searches noted in row 17 of Table 1 and binned by number of years between search and initial enrollment.*

2026/01/09 20:40:38
FNIR(N, R, T) = False neg. identification rate
FPIR(N, T) = False pos. identification rate
N = Num. enrolled subjects
R = Num. candidates examined
T = Threshold
T = 0 → Investigation
T > 0 → Identification

This publication is available free of charge from: https://doi.org/10.6028/NIST.IR.8271

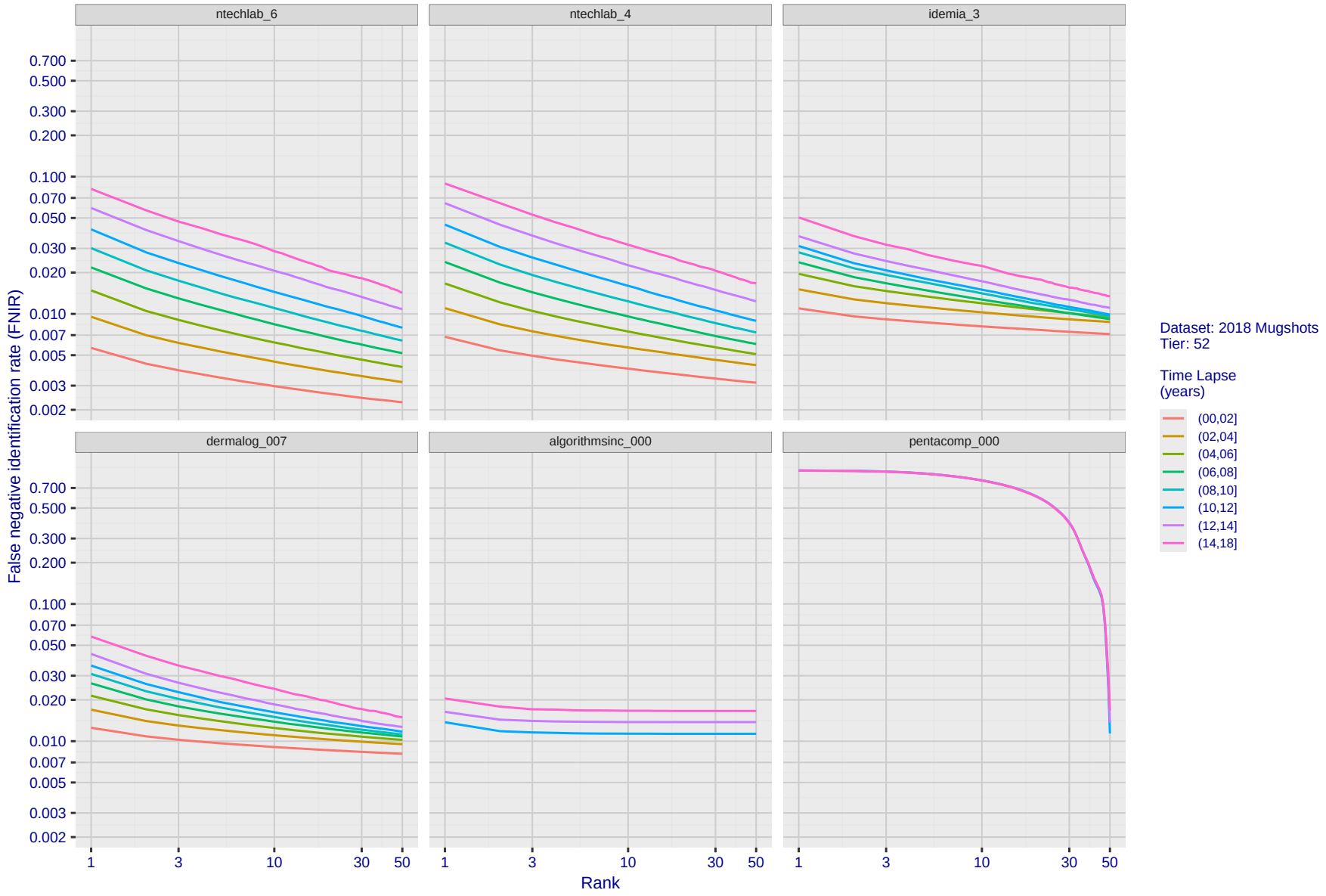

Figure 199: **[FRVT-2018 Mugshot Ageing Dataset] Identification miss rates vs. rank by time-elapsed**. *The oldest image of each individual is enrolled. Thereafter, all more recent images are searched. Miss rates are computed over all searches noted in row 17 of Table 1 and binned by number of years between search and initial enrollment.*

2026/01/09 20:40:38
FNIR(N, R, T) = False neg. identification rate
FPIR(N, T) = False pos. identification rate
N = Num. enrolled subjects
R = Num. candidates examined
T = Threshold
T = 0 → Investigation
T > 0 → Identification

This publication is available free of charge from: https://doi.org/10.6028/NIST.IR.8271

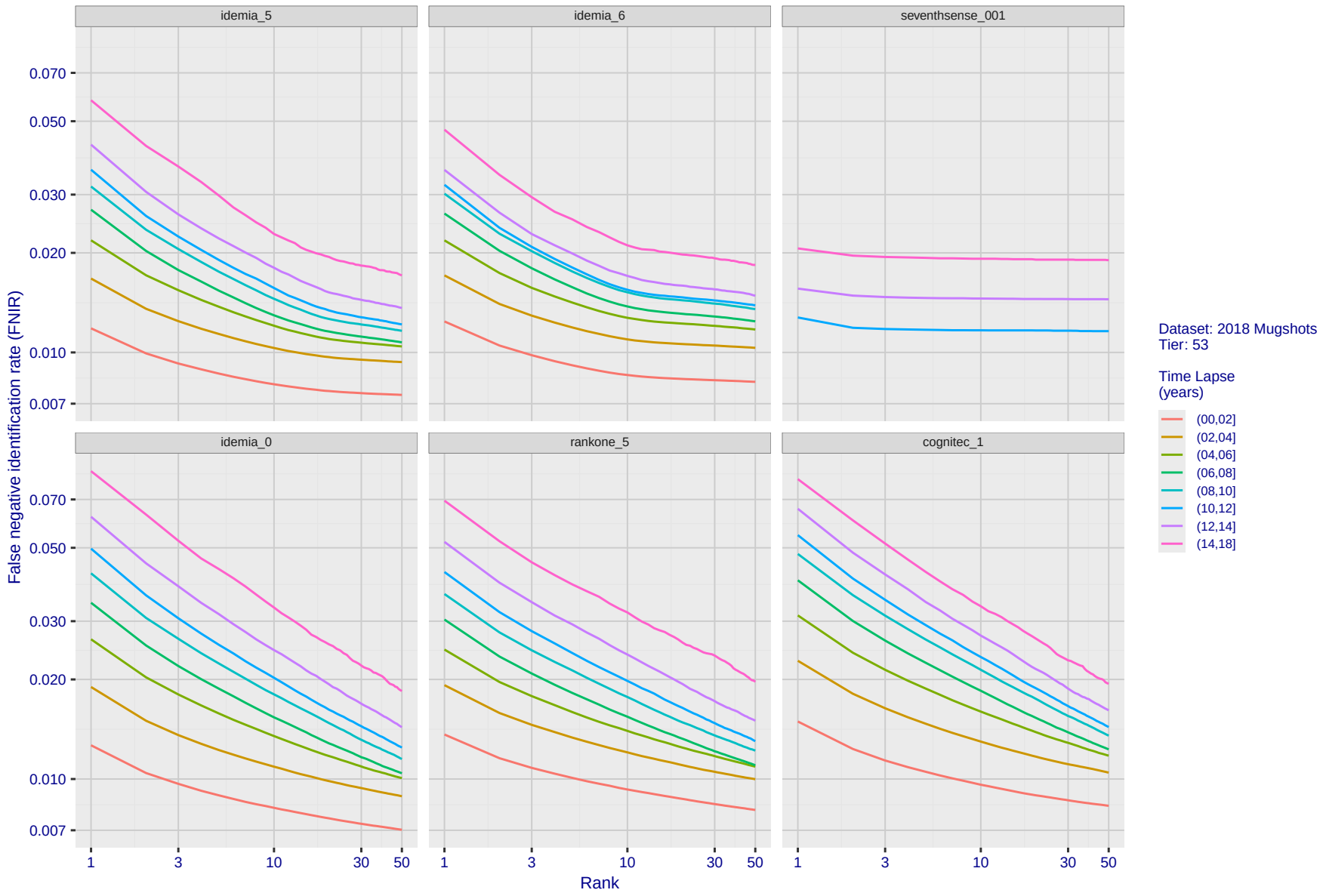

Figure 200: **[FRVT-2018 Mugshot Ageing Dataset] Identification miss rates vs. rank by time-elapsed**. *The oldest image of each individual is enrolled. Thereafter, all more recent images are searched. Miss rates are computed over all searches noted in row 17 of Table 1 and binned by number of years between search and initial enrollment.*

2026/01/09
20:40:38

FNIR(N, R, T) = False neg. identification rate
FPIR(N, T) = False pos. identification rate

N = Num. enrolled subjects
R = Num. candidates examined

T = Threshold

T = 0 → Investigation
T > 0 → Identification

This publication is available free of charge from: https://doi.org/10.6028/NIST.IR.8271

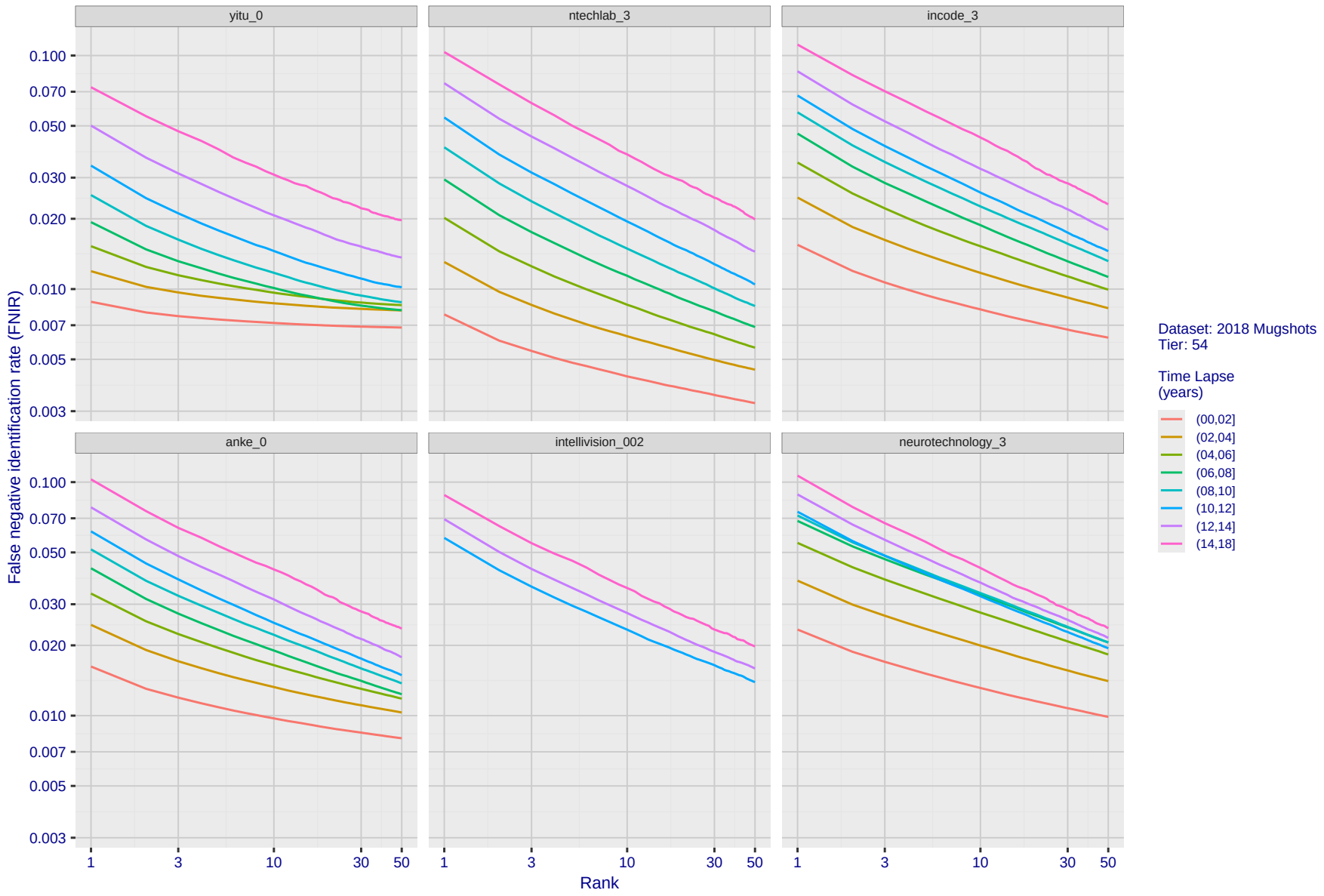

Figure 201: **[FRVT-2018 Mugshot Ageing Dataset] Identification miss rates vs. rank by time-elapsed**. *The oldest image of each individual is enrolled. Thereafter, all more recent images are searched. Miss rates are computed over all searches noted in row 17 of Table 1 and binned by number of years between search and initial enrollment.*

2026/01/09 20:40:38
FNIR(N, R, T) = False neg. identification rate
FPIR(N, T) = False pos. identification rate
N = Num. enrolled subjects
R = Num. candidates examined
T = Threshold
T = 0 → Investigation
T > 0 → Identification

This publication is available free of charge from: https://doi.org/10.6028/NIST.IR.8271

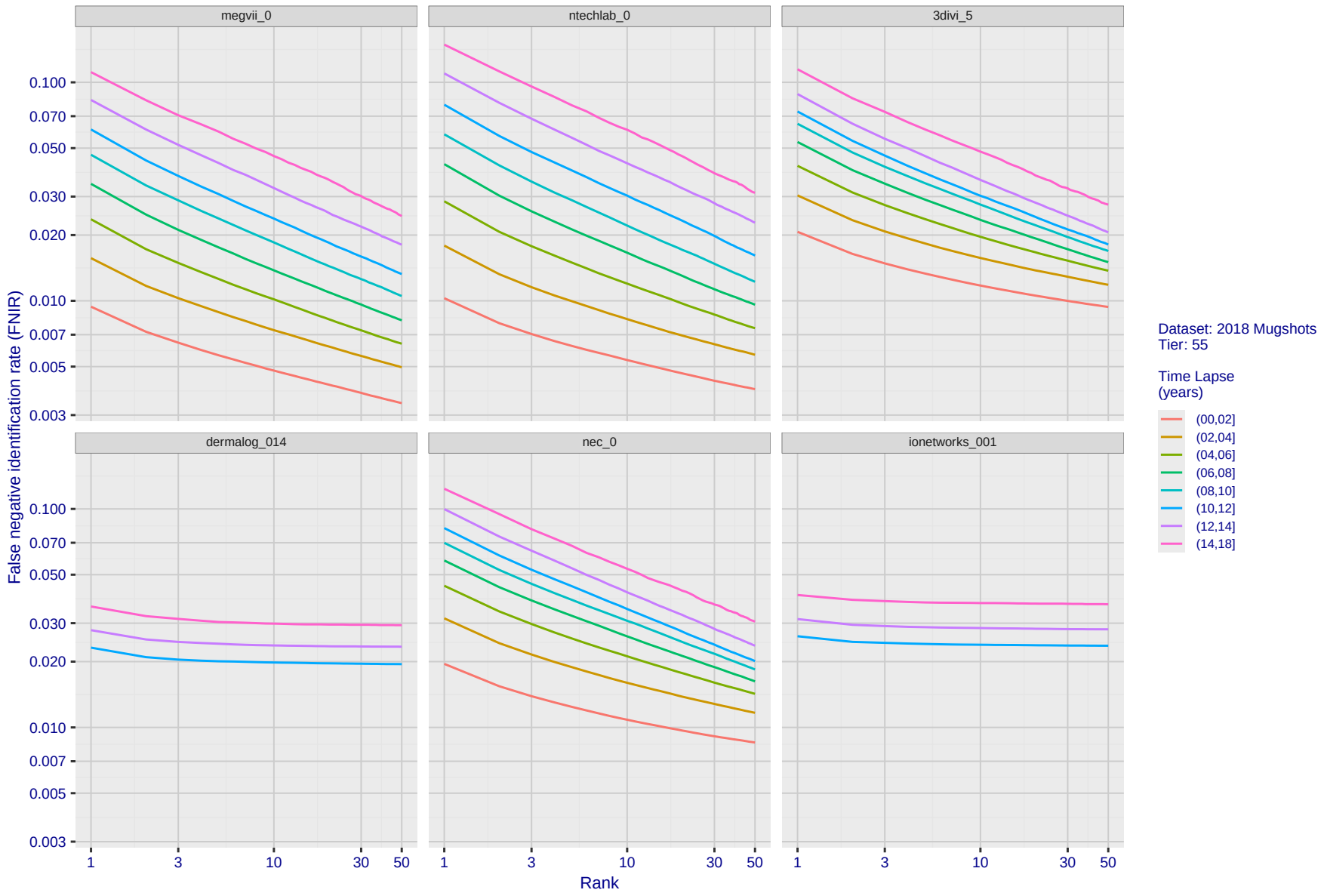

Figure 202: **[FRVT-2018 Mugshot Ageing Dataset] Identification miss rates vs. rank by time-elapsed**. *The oldest image of each individual is enrolled. Thereafter, all more recent images are searched. Miss rates are computed over all searches noted in row 17 of Table 1 and binned by number of years between search and initial enrollment.*

2026/01/09 20:40:38
FNIR(N, R, T) = False neg. identification rate
FPIR(N, T) = False pos. identification rate
N = Num. enrolled subjects
R = Num. candidates examined
T = Threshold
T = 0 → Investigation
T > 0 → Identification

This publication is available free of charge from: https://doi.org/10.6028/NIST.IR.8271

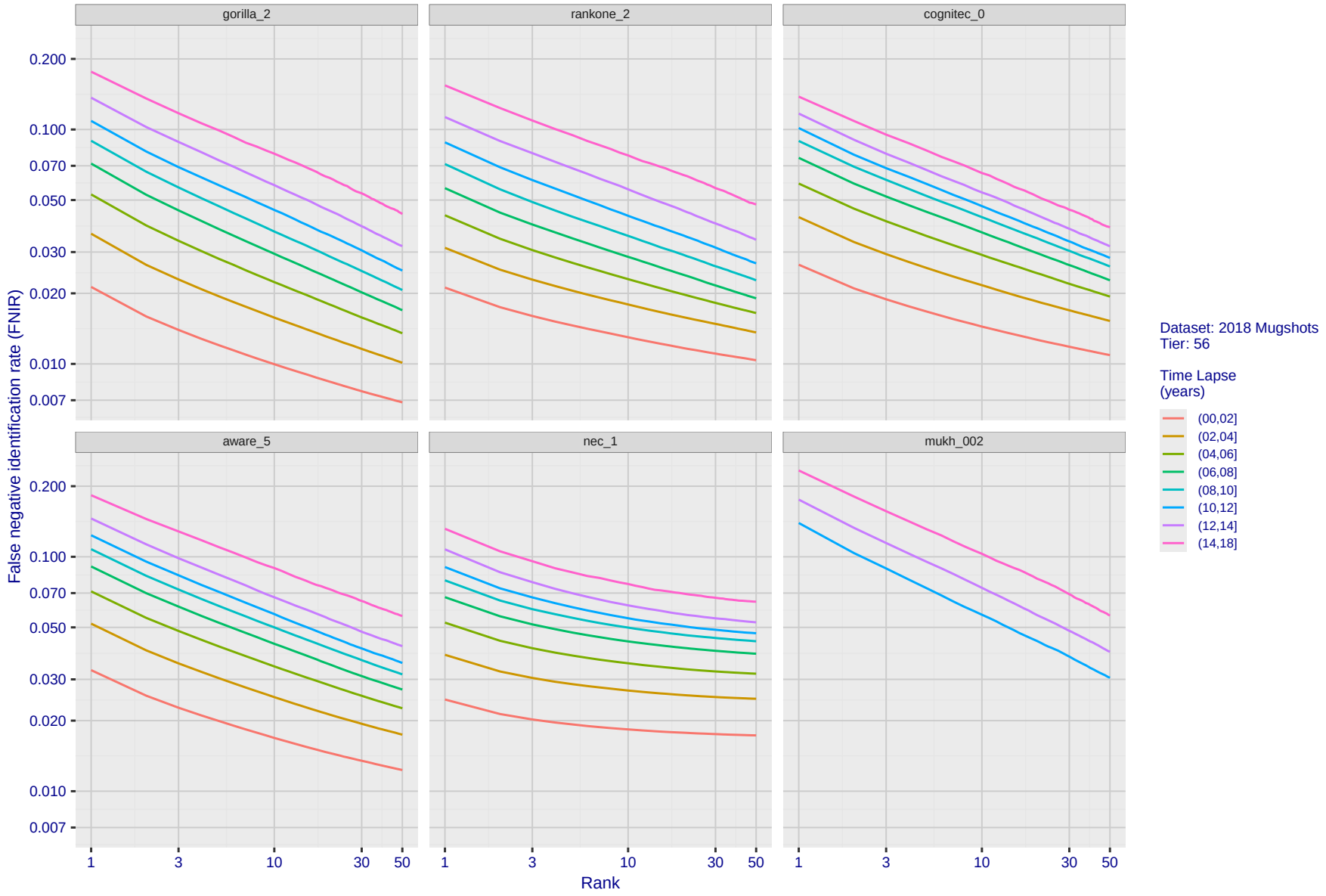

Figure 203: **[FRVT-2018 Mugshot Ageing Dataset] Identification miss rates vs. rank by time-elapsed**. *The oldest image of each individual is enrolled. Thereafter, all more recent images are searched. Miss rates are computed over all searches noted in row 17 of Table 1 and binned by number of years between search and initial enrollment.*

2026/01/09 20:40:38
FNIR(N, R, T) = False neg. identification rate
FPIR(N, T) = False pos. identification rate
N = Num. enrolled subjects
R = Num. candidates examined
T = Threshold
T = 0 → Investigation
T > 0 → Identification

This publication is available free of charge from: https://doi.org/10.6028/NIST.IR.8271

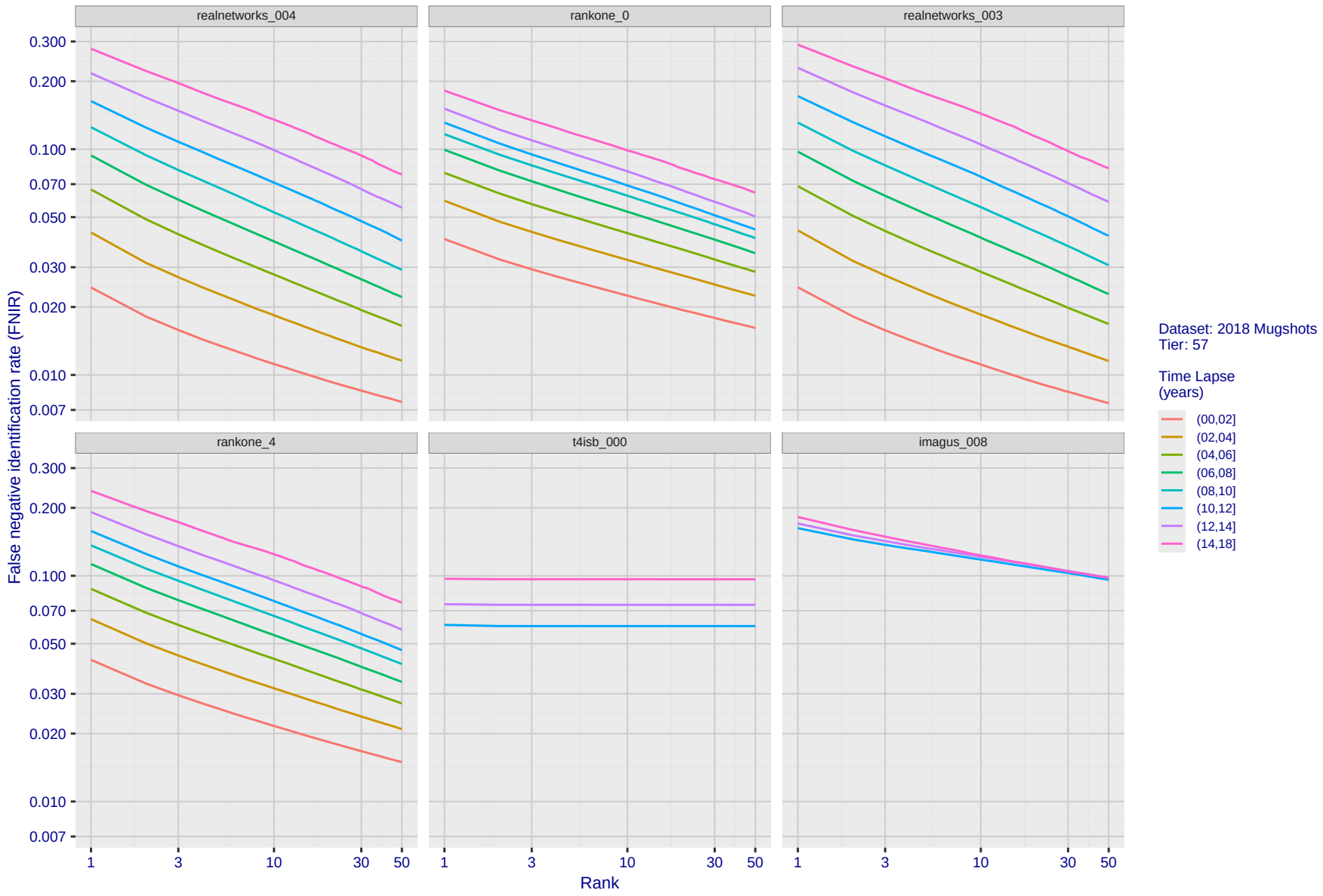

Figure 204: **[FRVT-2018 Mugshot Ageing Dataset] Identification miss rates vs. rank by time-elapsed**. *The oldest image of each individual is enrolled. Thereafter, all more recent images are searched. Miss rates are computed over all searches noted in row 17 of Table 1 and binned by number of years between search and initial enrollment.*

2026/01/09 20:40:38
FNIR(N, R, T) = False neg. identification rate
FPIR(N, T) = False pos. identification rate
N = Num. enrolled subjects
R = Num. candidates examined
T = Threshold
T = 0 → Investigation
T > 0 → Identification

This publication is available free of charge from: https://doi.org/10.6028/NIST.IR.8271

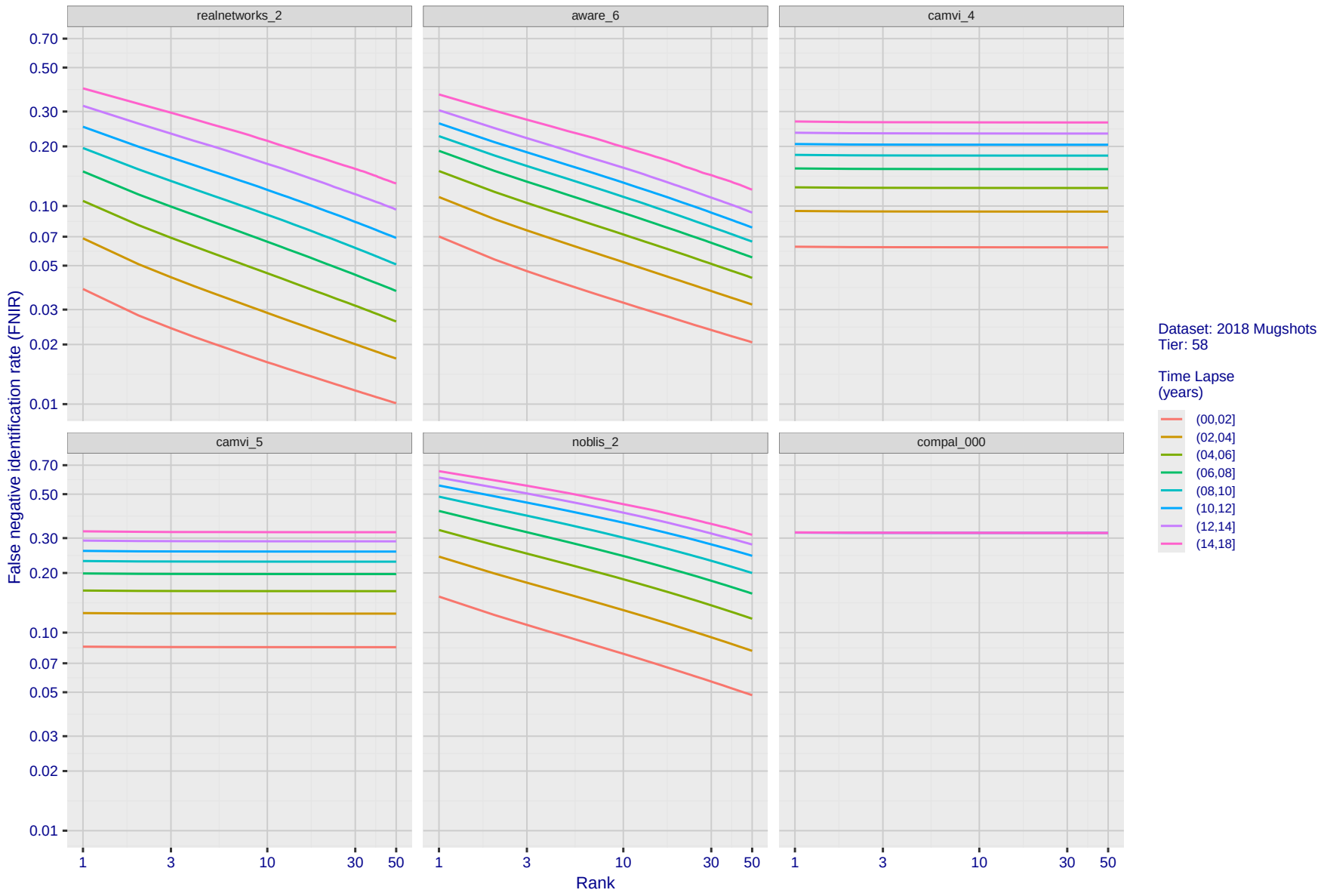

Figure 205: **[FRVT-2018 Mugshot Ageing Dataset] Identification miss rates vs. rank by time-elapsed**. *The oldest image of each individual is enrolled. Thereafter, all more recent images are searched. Miss rates are computed over all searches noted in row 17 of Table 1 and binned by number of years between search and initial enrollment.*

2026/01/09 20:40:38
FNIR(N, R, T) = False neg. identification rate
FPIR(N, T) = False pos. identification rate
N = Num. enrolled subjects
R = Num. candidates examined
T = Threshold
T = 0 → Investigation
T > 0 → Identification

This publication is available free of charge from: https://doi.org/10.6028/NIST.IR.8271

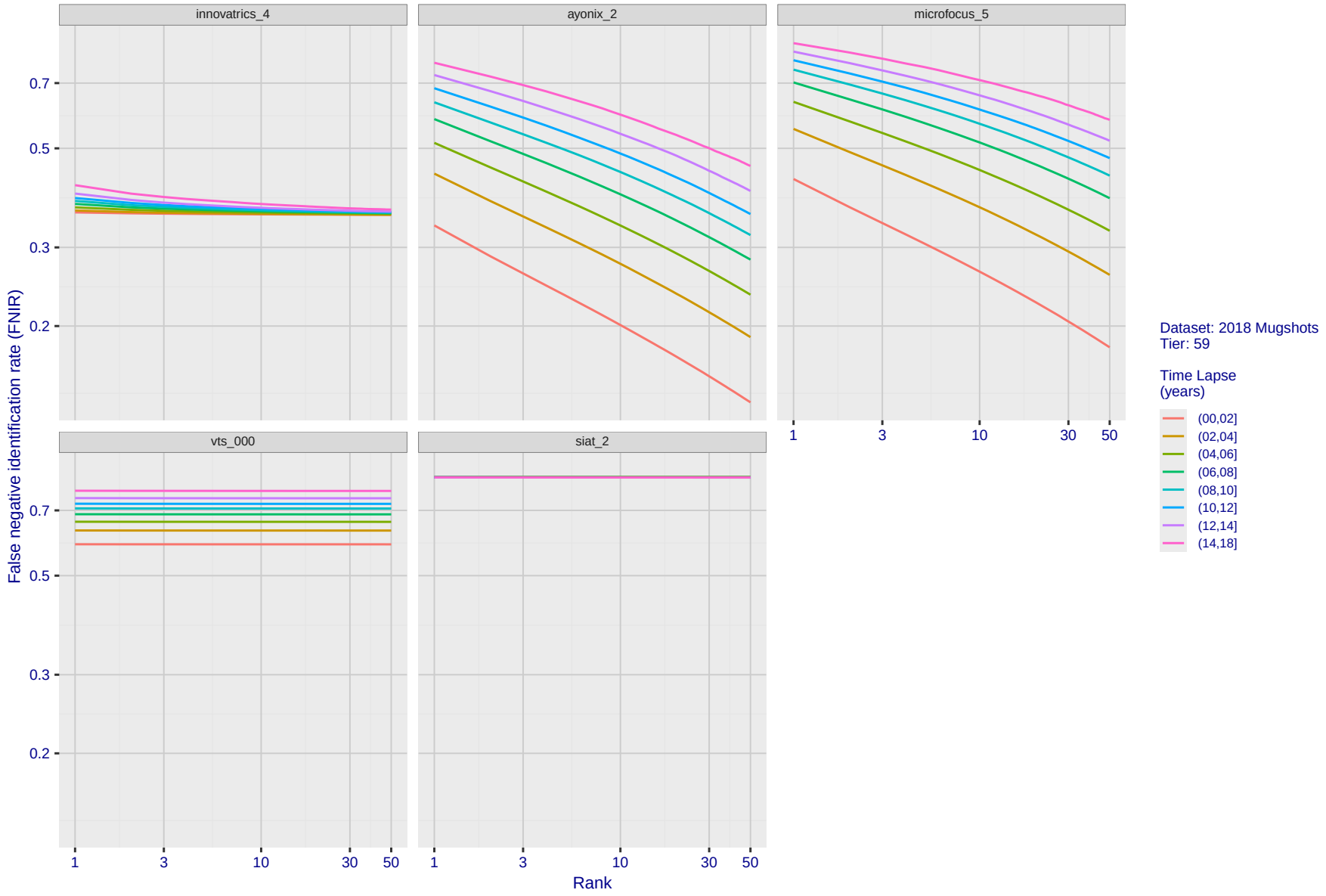

Figure 206: **[FRVT-2018 Mugshot Ageing Dataset] Identification miss rates vs. rank by time-elapsed**. *The oldest image of each individual is enrolled. Thereafter, all more recent images are searched. Miss rates are computed over all searches noted in row 17 of Table 1 and binned by number of years between search and initial enrollment.*

2026/01/09 20:40:38

FNIR(N, R, T) = False neg. identification rate
FPIR(N, T) = False pos. identification rate

N = Num. enrolled subjects
R = Num. candidates examined

T = Threshold

T = 0 → Investigation
T > 0 → Identification

2026/01/09	FNIR(N, R, T) =	False neg. identification rate	N = Num. enrolled subjects	T = Threshold	$T = 0 \rightarrow$ Investigation
20:40:38	FPIR(N, T) =	False pos. identification rate	R = Num. candidates examined		$T > 0 \rightarrow$ Identification

This publication is available free of charge from: https://doi.org/10.6028/NIST.IR.8271

This publication is available free of charge from: https://doi.org/10.6028/NIST.IR.8271

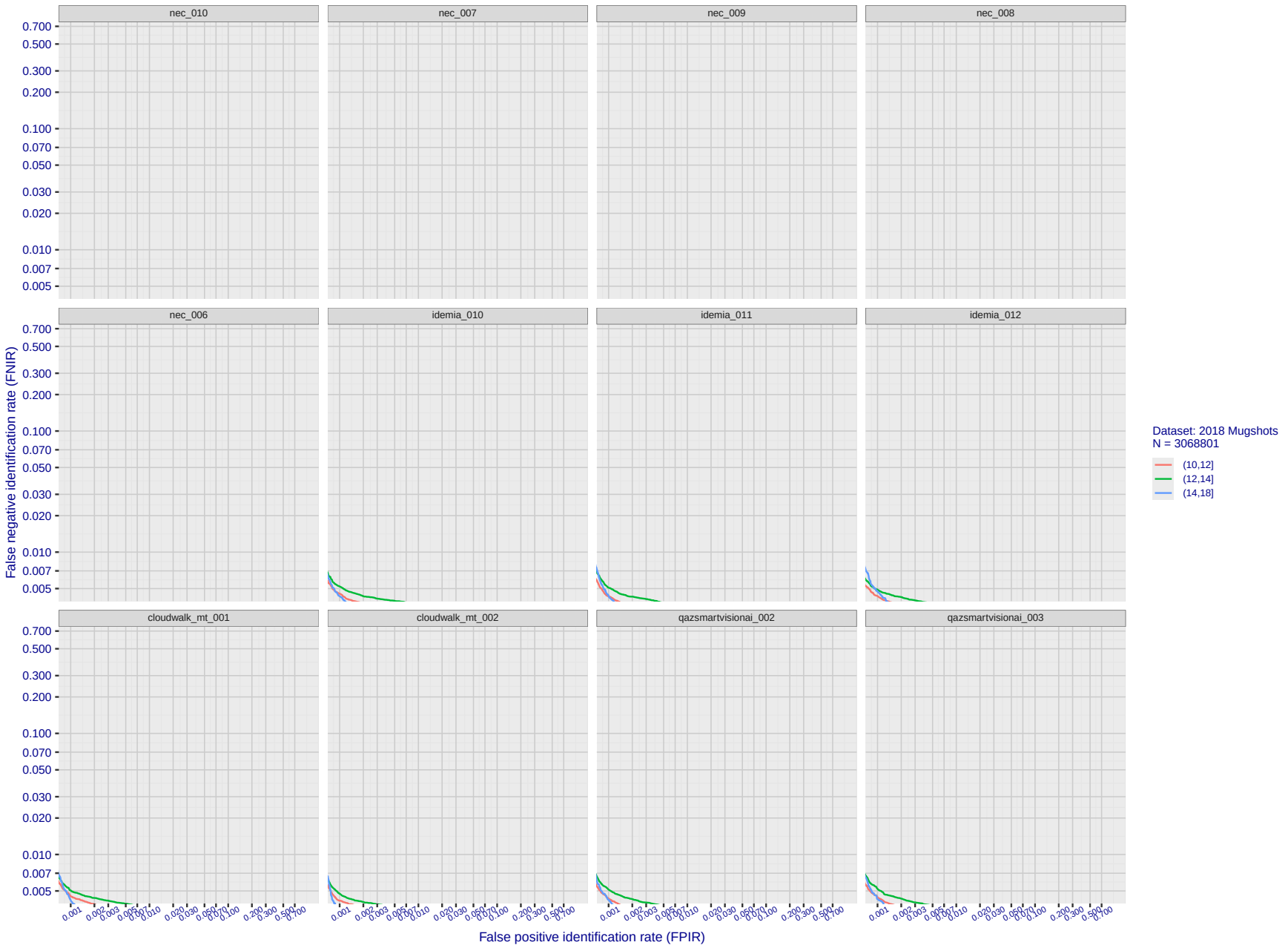

Figure 207: **[FRVT-2018 Mugshot Ageing Dataset] Identification miss rates vs. FPIR by time-elapsed**. *The oldest image of each individual is enrolled. Thereafter, all more recent images are searched. Miss rates are computed over all searches noted in row 17 of Table 1 and binned by number of years between search and initial enrollment. FPIR is computed from the same FRVT 2018 non-mates noted in row 3 of Table 1 with N = 3 000 000.*

2026/01/09 20:40:38
FNIR(N, R, T) = False neg. identification rate
FPIR(N, T) = False pos. identification rate
N = Num. enrolled subjects
R = Num. candidates examined
T = Threshold
T = 0 → Investigation
T > 0 → Identification

This publication is available free of charge from: https://doi.org/10.6028/NIST.IR.8271

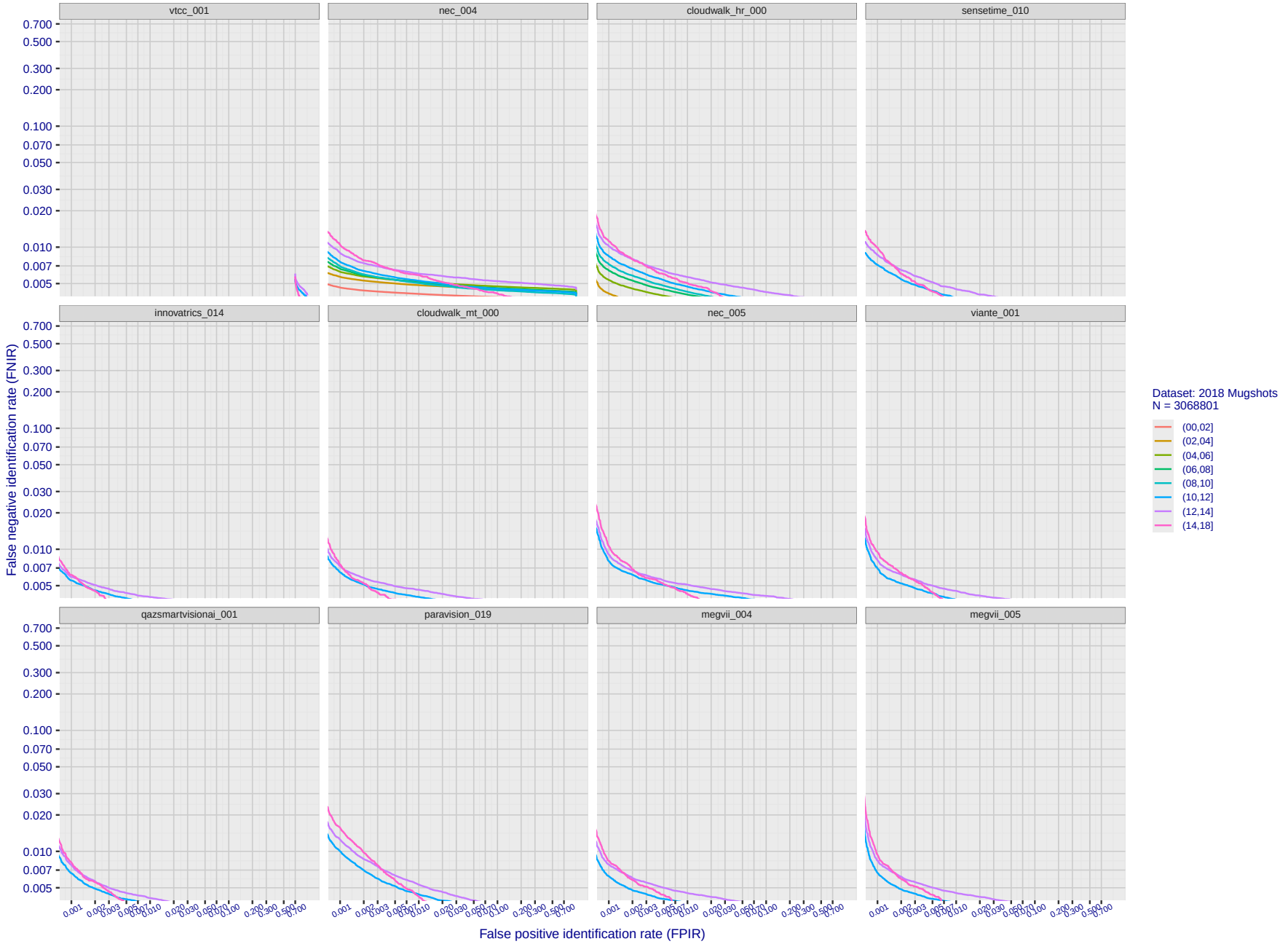

Figure 208: **[FRVT-2018 Mugshot Ageing Dataset] Identification miss rates vs. FPIR by time-elapsed**. *The oldest image of each individual is enrolled. Thereafter, all more recent images are searched. Miss rates are computed over all searches noted in row 17 of Table 1 and binned by number of years between search and initial enrollment. FPIR is computed from the same FRVT 2018 non-mates noted in row 3 of Table 1 with N = 3 000 000.*

2026/01/09 20:40:38

FNIR(N, R, T) = False neg. identification rate
FPIR(N, T) = False pos. identification rate

N = Num. enrolled subjects
R = Num. candidates examined

T = Threshold

T = 0 → Investigation
T > 0 → Identification

This publication is available free of charge from: https://doi.org/10.6028/NIST.IR.8271

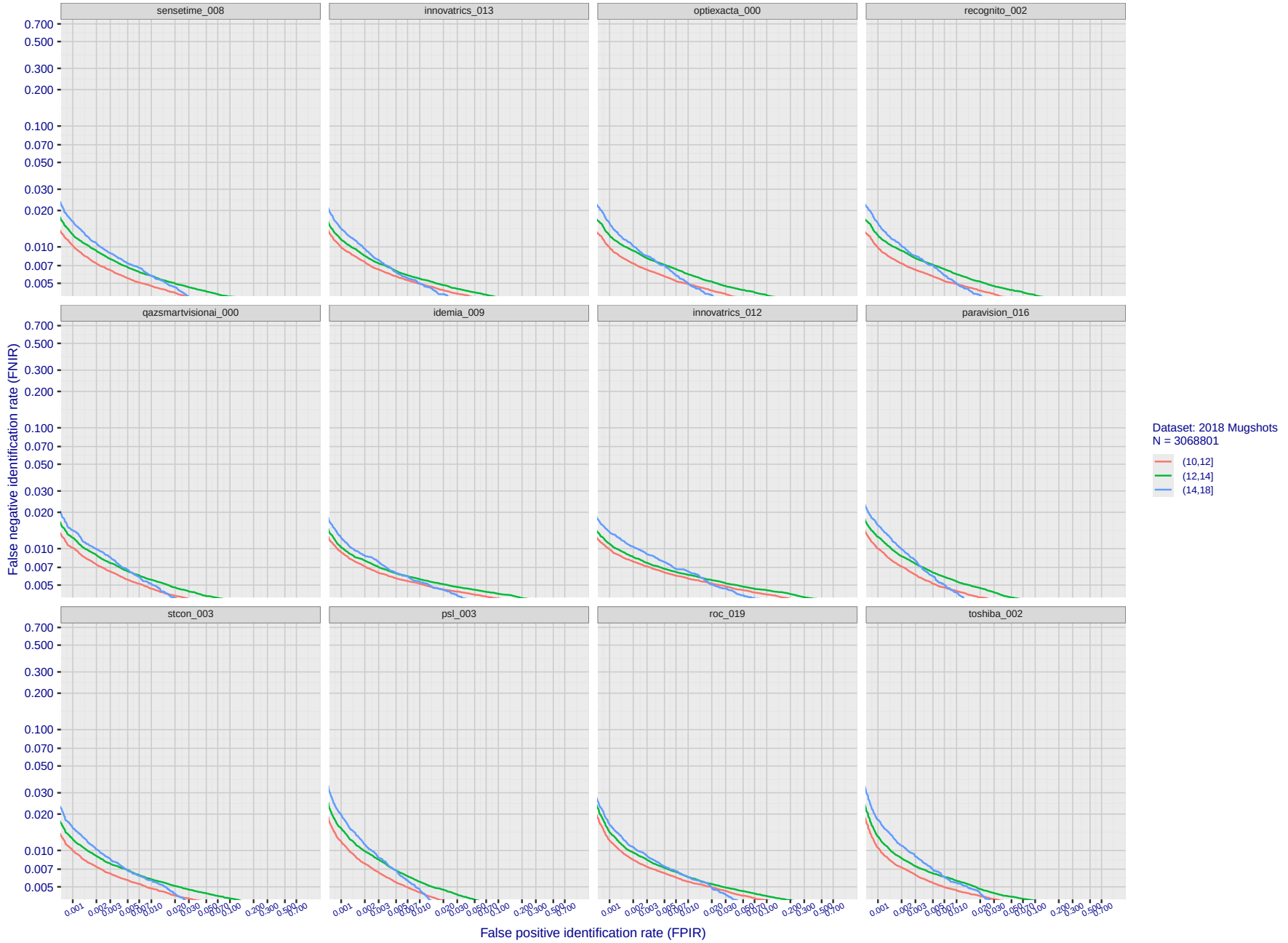

Figure 209: **[FRVT-2018 Mugshot Ageing Dataset] Identification miss rates vs. FPIR by time-elapsed**. *The oldest image of each individual is enrolled. Thereafter, all more recent images are searched. Miss rates are computed over all searches noted in row 17 of Table 1 and binned by number of years between search and initial enrollment. FPIR is computed from the same FRVT 2018 non-mates noted in row 3 of Table 1 with N = 3 000 000.*

2026/01/09 20:40:38
FNIR(N, R, T) = False neg. identification rate
FPIR(N, T) = False pos. identification rate
N = Num. enrolled subjects
R = Num. candidates examined
T = Threshold
T = 0 → Investigation
T > 0 → Identification

This publication is available free of charge from: https://doi.org/10.6028/NIST.IR.8271

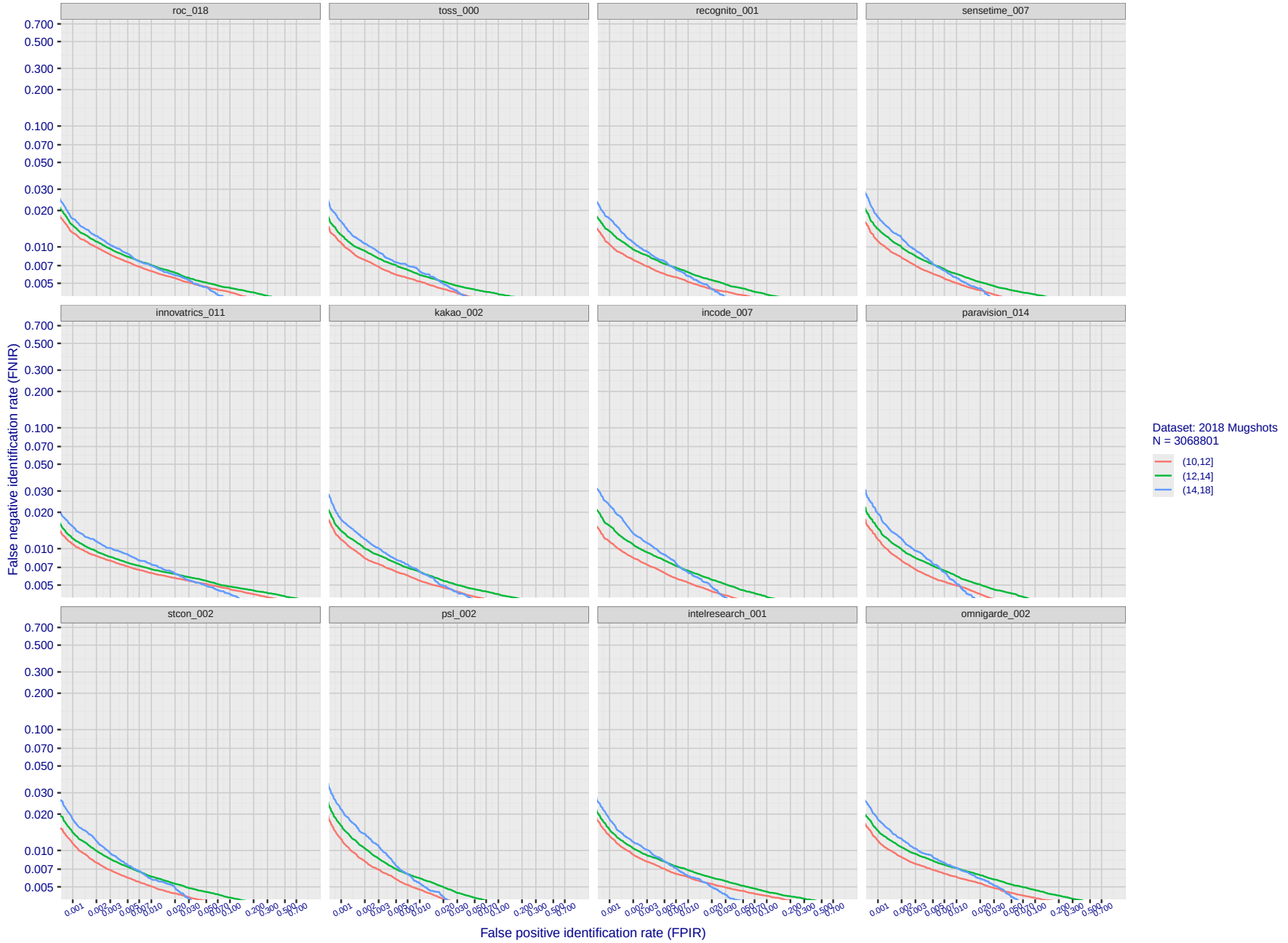

Figure 210: **[FRVT-2018 Mugshot Ageing Dataset] Identification miss rates vs. FPIR by time-elapsed**. *The oldest image of each individual is enrolled. Thereafter, all more recent images are searched. Miss rates are computed over all searches noted in row 17 of Table 1 and binned by number of years between search and initial enrollment. FPIR is computed from the same FRVT 2018 non-mates noted in row 3 of Table 1 with N = 3 000 000.*

2026/01/09 20:40:38
FNIR(N, R, T) = False neg. identification rate
FPIR(N, T) = False pos. identification rate
N = Num. enrolled subjects
R = Num. candidates examined
T = Threshold
T = 0 → Investigation
T > 0 → Identification

This publication is available free of charge from: https://doi.org/10.6028/NIST.IR.8271

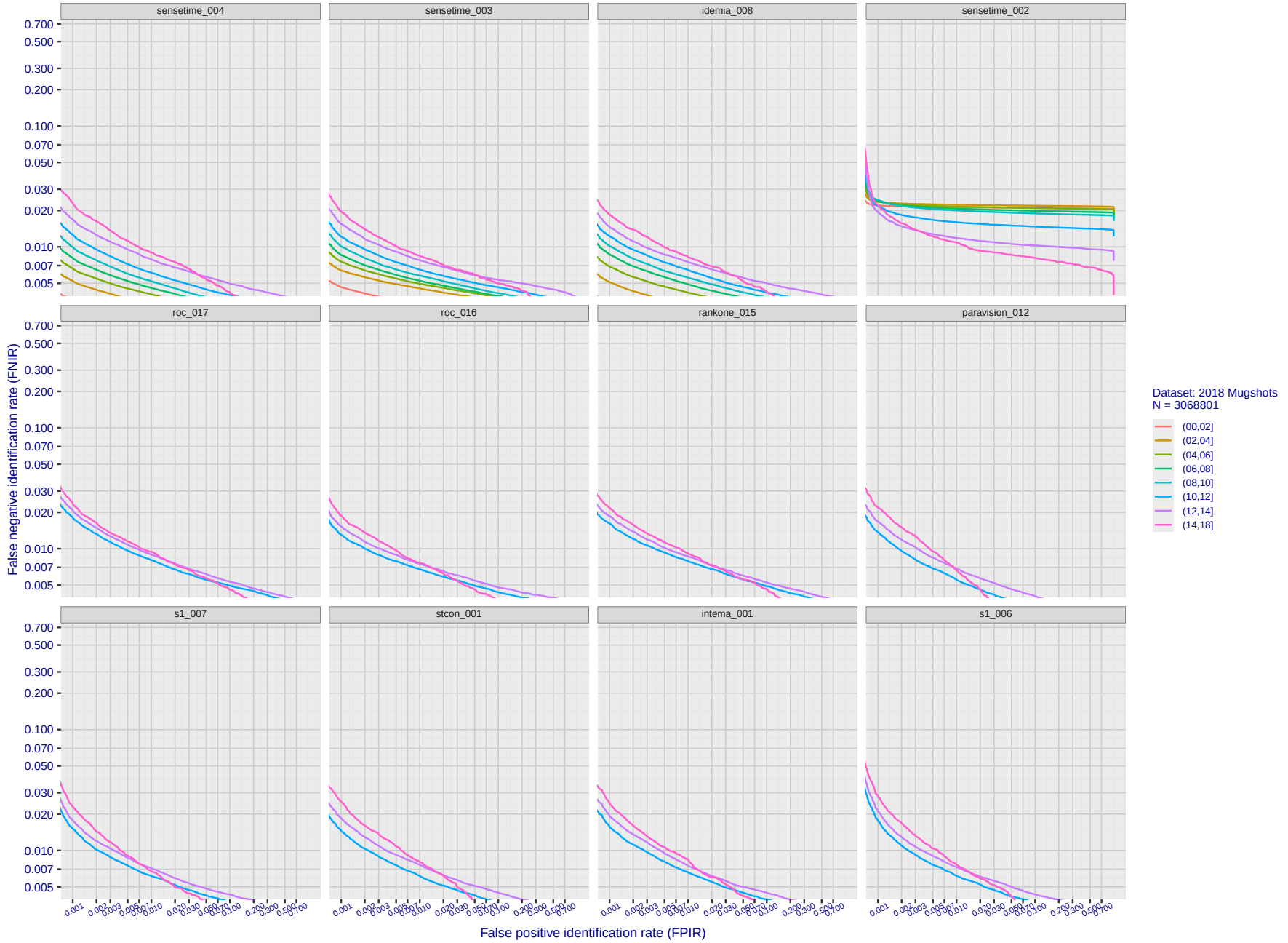

Figure 211: **[FRVT-2018 Mugshot Ageing Dataset] Identification miss rates vs. FPIR by time-elapsed**. *The oldest image of each individual is enrolled. Thereafter, all more recent images are searched. Miss rates are computed over all searches noted in row 17 of Table 1 and binned by number of years between search and initial enrollment. FPIR is computed from the same FRVT 2018 non-mates noted in row 3 of Table 1 with N = 3 000 000.*

This publication is available free of charge from: https://doi.org/10.6028/NIST.IR.8271

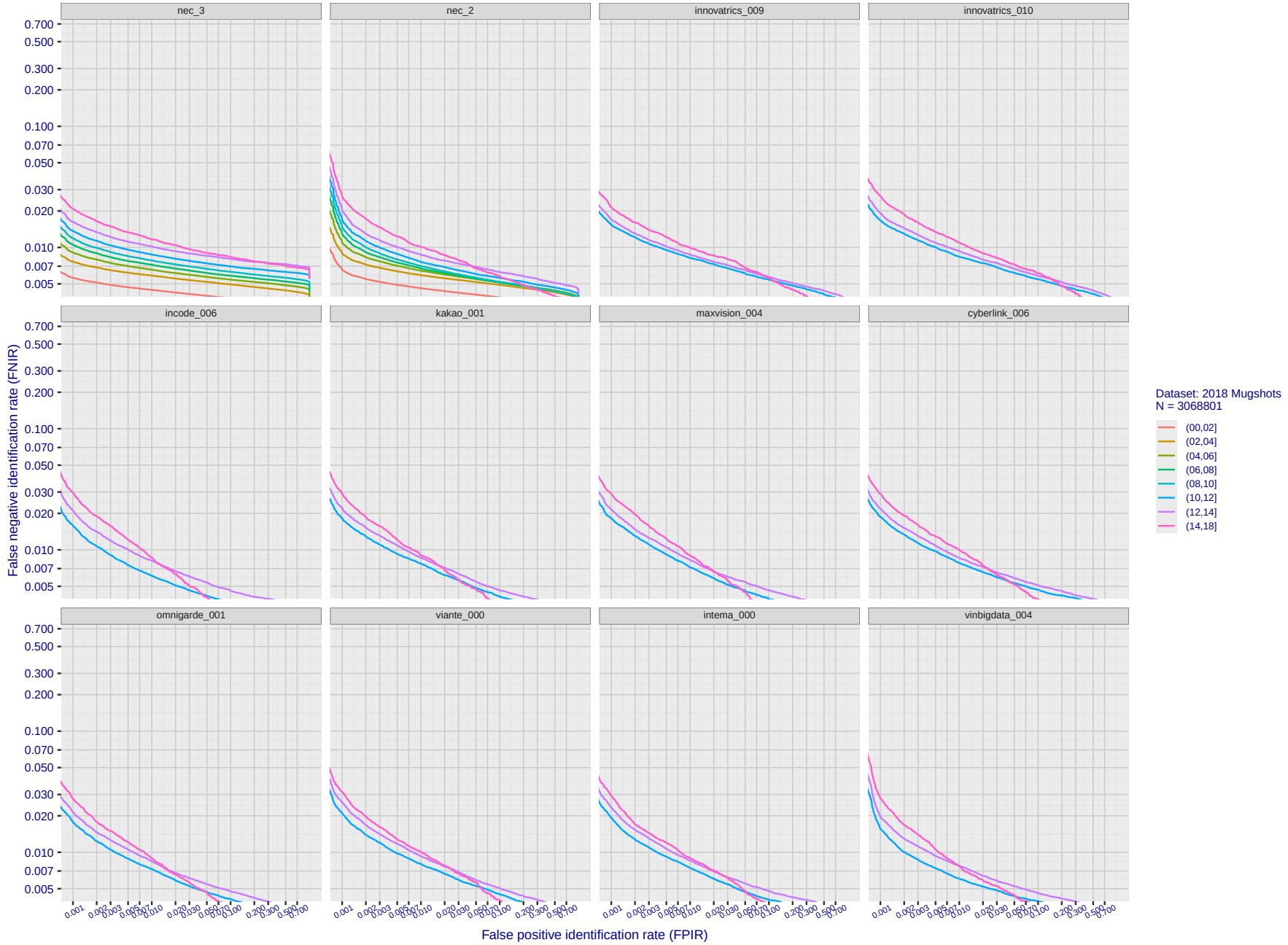

Figure 212: **[FRVT-2018 Mugshot Ageing Dataset] Identification miss rates vs. FPIR by time-elapsed**. *The oldest image of each individual is enrolled. Thereafter, all more recent images are searched. Miss rates are computed over all searches noted in row 17 of Table 1 and binned by number of years between search and initial enrollment. FPIR is computed from the same FRVT 2018 non-mates noted in row 3 of Table 1 with N = 3 000 000.*

This publication is available free of charge from: https://doi.org/10.6028/NIST.IR.8271

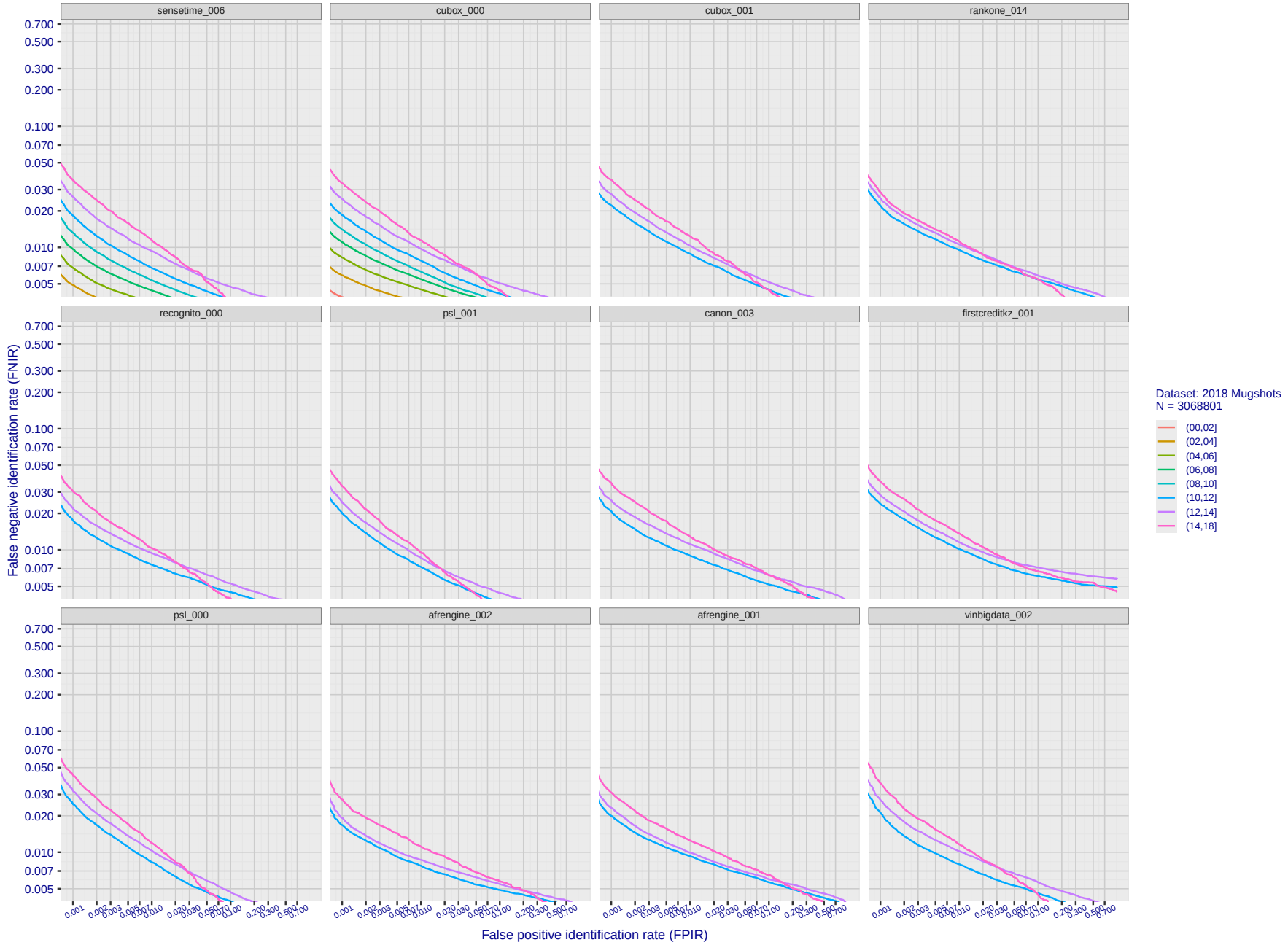

Figure 213: **[FRVT-2018 Mugshot Ageing Dataset] Identification miss rates vs. FPIR by time-elapsed**. *The oldest image of each individual is enrolled. Thereafter, all more recent images are searched. Miss rates are computed over all searches noted in row 17 of Table 1 and binned by number of years between search and initial enrollment. FPIR is computed from the same FRVT 2018 non-mates noted in row 3 of Table 1 with N = 3 000 000.*

2026/01/09 20:40:38
FNIR(N, R, T) = False neg. identification rate
FPIR(N, T) = False pos. identification rate
N = Num. enrolled subjects
R = Num. candidates examined
T = Threshold
T = 0 → Investigation
T > 0 → Identification

This publication is available free of charge from: https://doi.org/10.6028/NIST.IR.8271

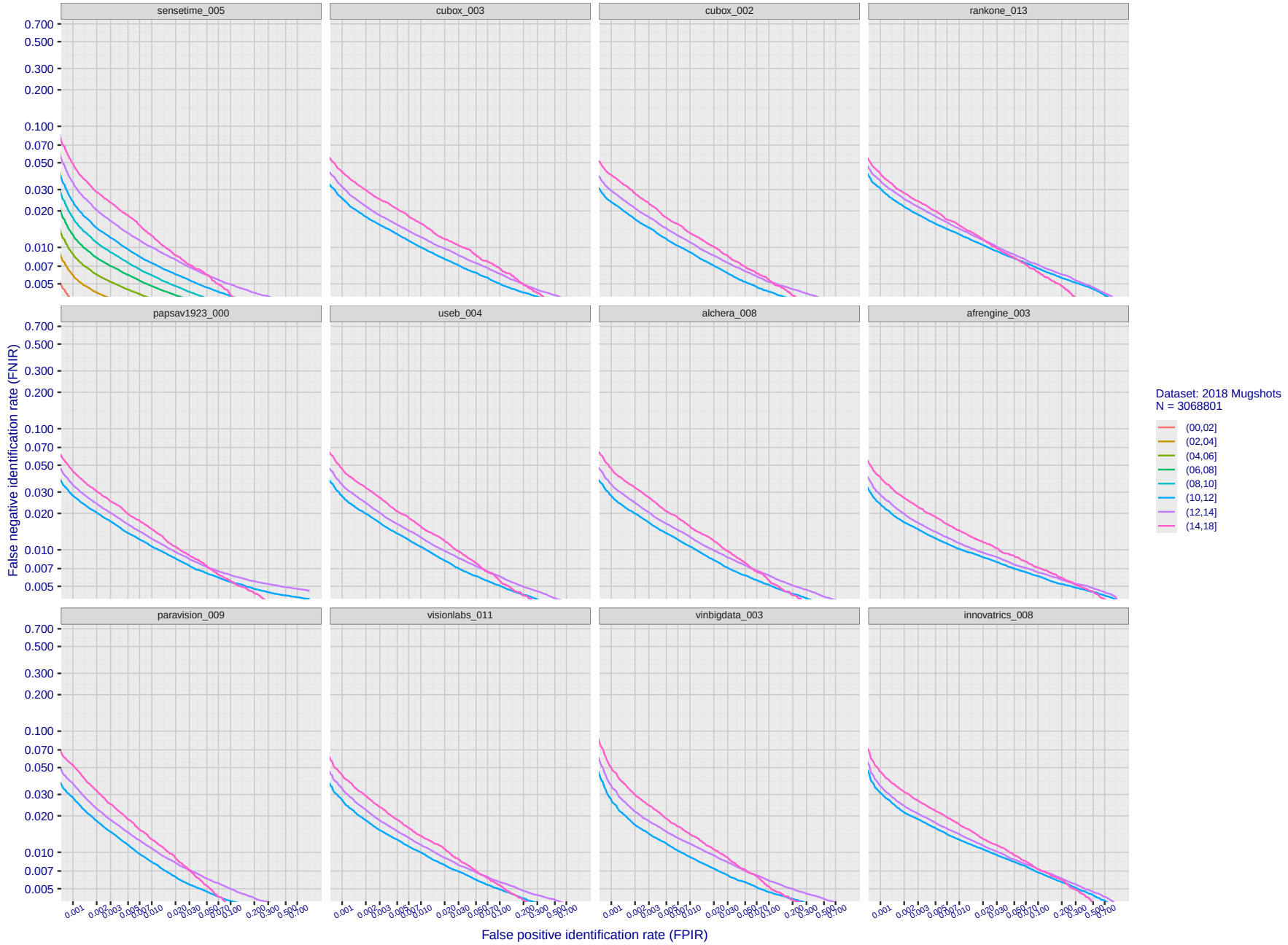

Figure 214: **[FRVT-2018 Mugshot Ageing Dataset] Identification miss rates vs. FPIR by time-elapsed**. *The oldest image of each individual is enrolled. Thereafter, all more recent images are searched. Miss rates are computed over all searches noted in row 17 of Table 1 and binned by number of years between search and initial enrollment. FPIR is computed from the same FRVT 2018 non-mates noted in row 3 of Table 1 with N = 3 000 000.*

2026/01/09 20:40:38
FNIR(N, R, T) = False neg. identification rate
FPIR(N, T) = False pos. identification rate
N = Num. enrolled subjects
R = Num. candidates examined
T = Threshold
T = 0 → Investigation
T > 0 → Identification

This publication is available free of charge from: https://doi.org/10.6028/NIST.IR.8271

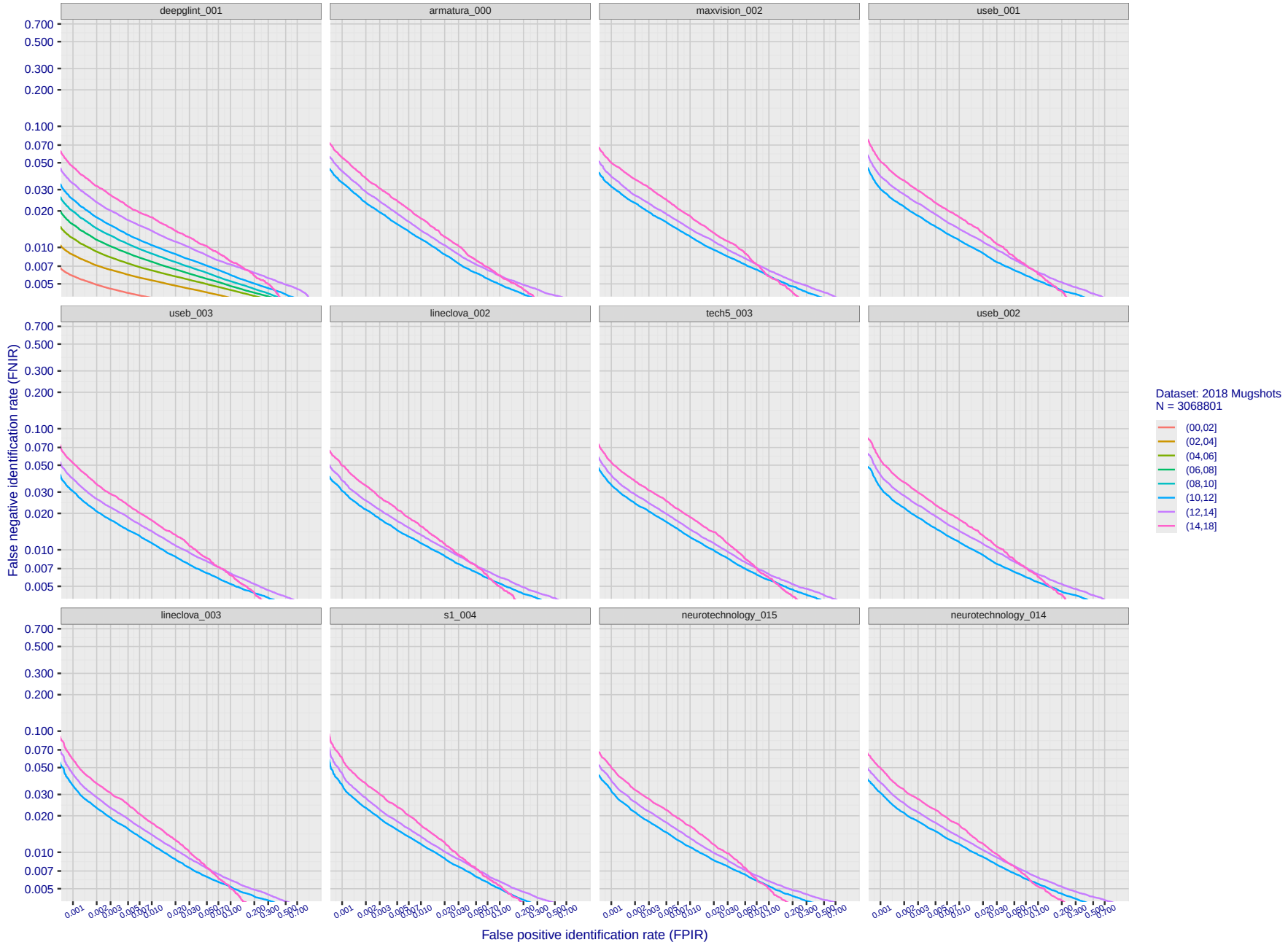

Figure 215: **[FRVT-2018 Mugshot Ageing Dataset] Identification miss rates vs. FPIR by time-elapsed**. *The oldest image of each individual is enrolled. Thereafter, all more recent images are searched. Miss rates are computed over all searches noted in row 17 of Table 1 and binned by number of years between search and initial enrollment. FPIR is computed from the same FRVT 2018 non-mates noted in row 3 of Table 1 with N = 3 000 000.*

2026/01/09 20:40:38
FNIR(N, R, T) = False neg. identification rate
FPIR(N, T) = False pos. identification rate
N = Num. enrolled subjects
R = Num. candidates examined
T = Threshold
T = 0 → Investigation
T > 0 → Identification

This publication is available free of charge from: https://doi.org/10.6028/NIST.IR.8271

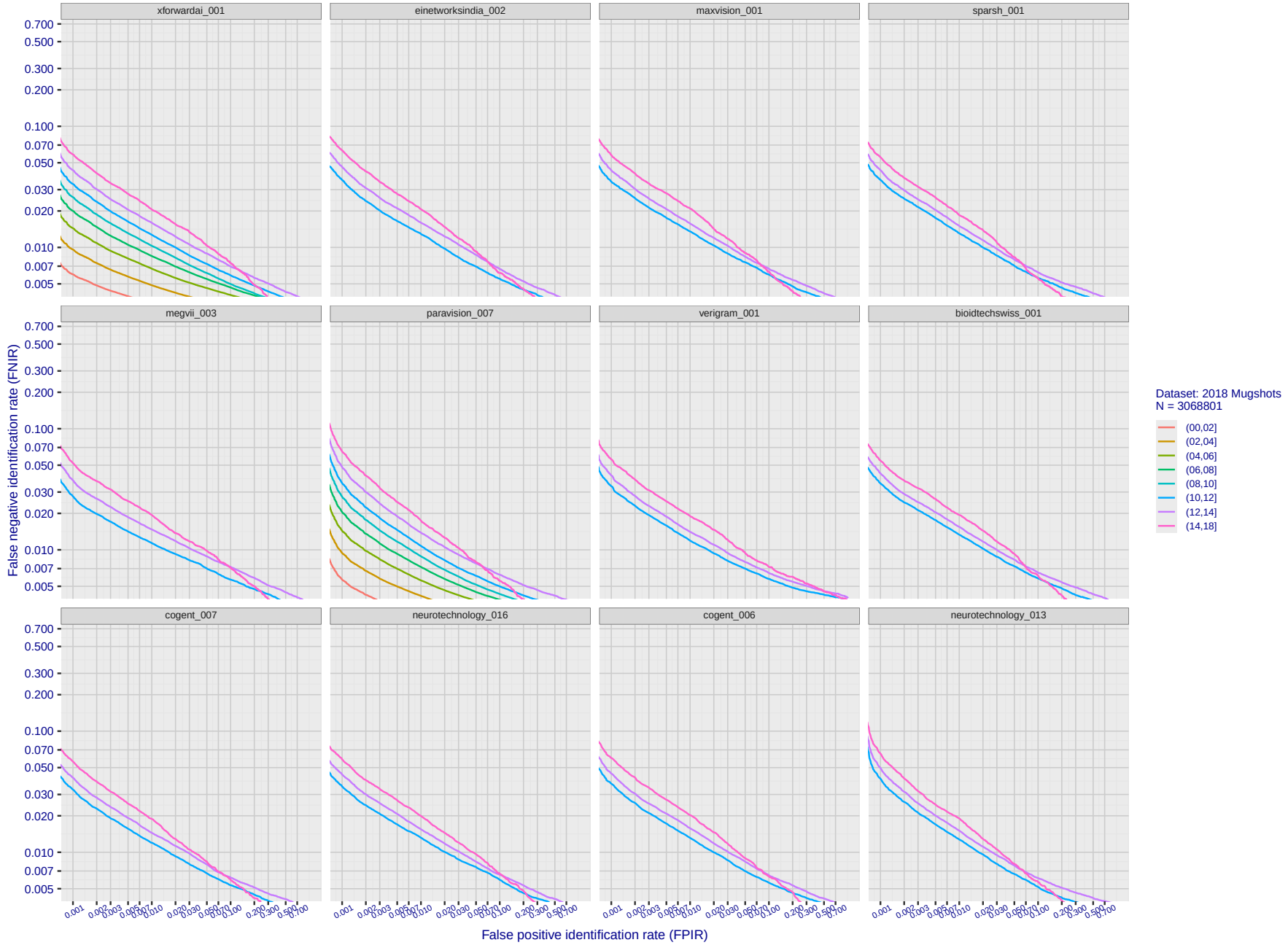

Figure 216: **[FRVT-2018 Mugshot Ageing Dataset] Identification miss rates vs. FPIR by time-elapsed**. *The oldest image of each individual is enrolled. Thereafter, all more recent images are searched. Miss rates are computed over all searches noted in row 17 of Table 1 and binned by number of years between search and initial enrollment. FPIR is computed from the same FRVT 2018 non-mates noted in row 3 of Table 1 with N = 3 000 000.*

2026/01/09 20:40:38

FNIR(N, R, T) = False neg. identification rate
FPIR(N, T) = False pos. identification rate

N = Num. enrolled subjects
R = Num. candidates examined

T = Threshold

T = 0 → Investigation
T > 0 → Identification

This publication is available free of charge from: https://doi.org/10.6028/NIST.IR.8271

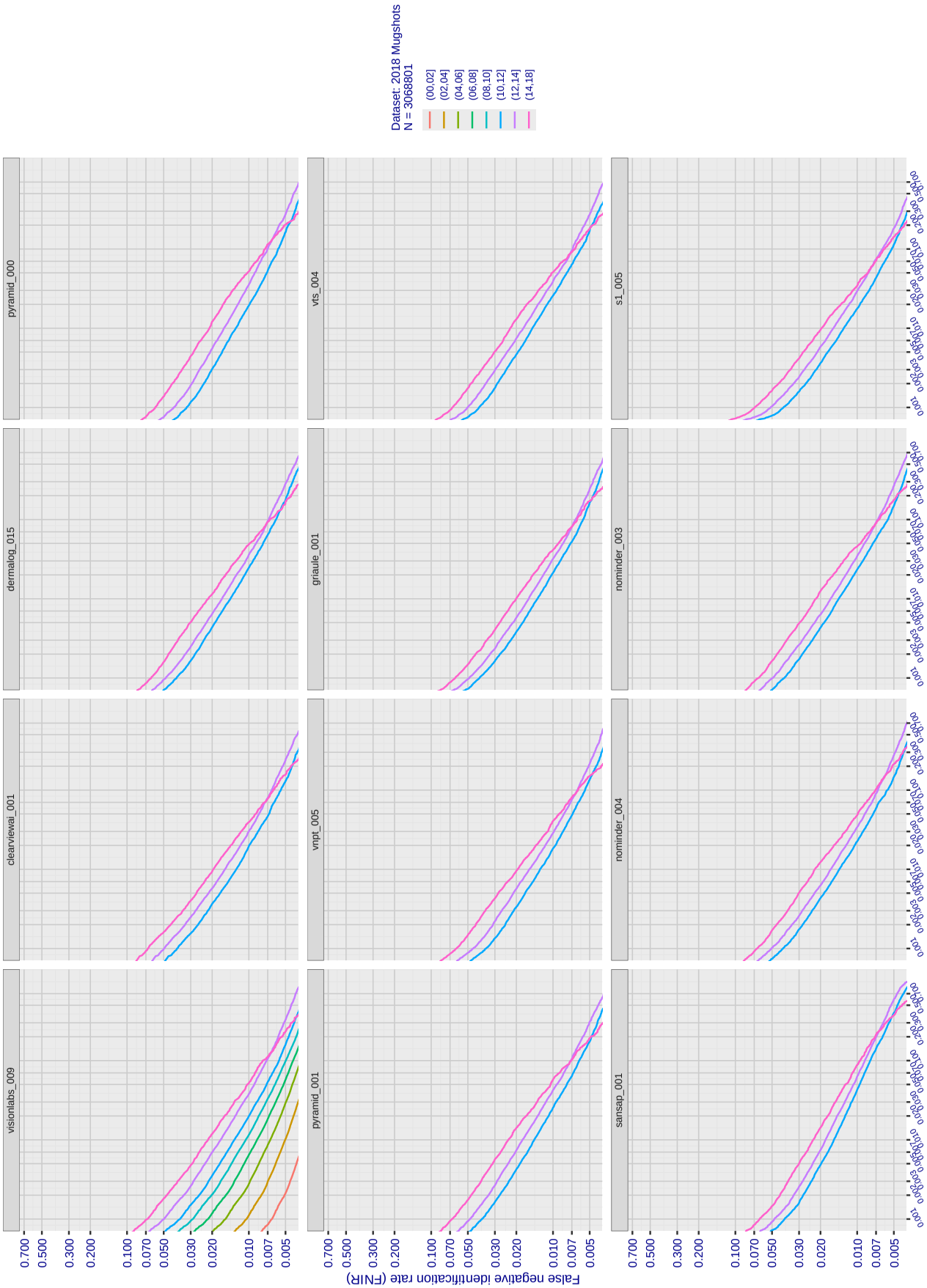

Figure 217: **[FRVT-2018 Mugshot Ageing Dataset] Identification miss rates vs. FPIR by time-elapsed.** *The oldest image of each individual is enrolled. Thereafter, all more recent images are searched. Miss rates are computed over all searches noted in row 17 of Table 1 and binned by number of years between search and initial enrollment. FPIR is computed from the same FRVT 2018 non-mates noted in row 3 of Table 1 with N = 3 000 000.*

This publication is available free of charge from: https://doi.org/10.6028/NIST.IR.8271

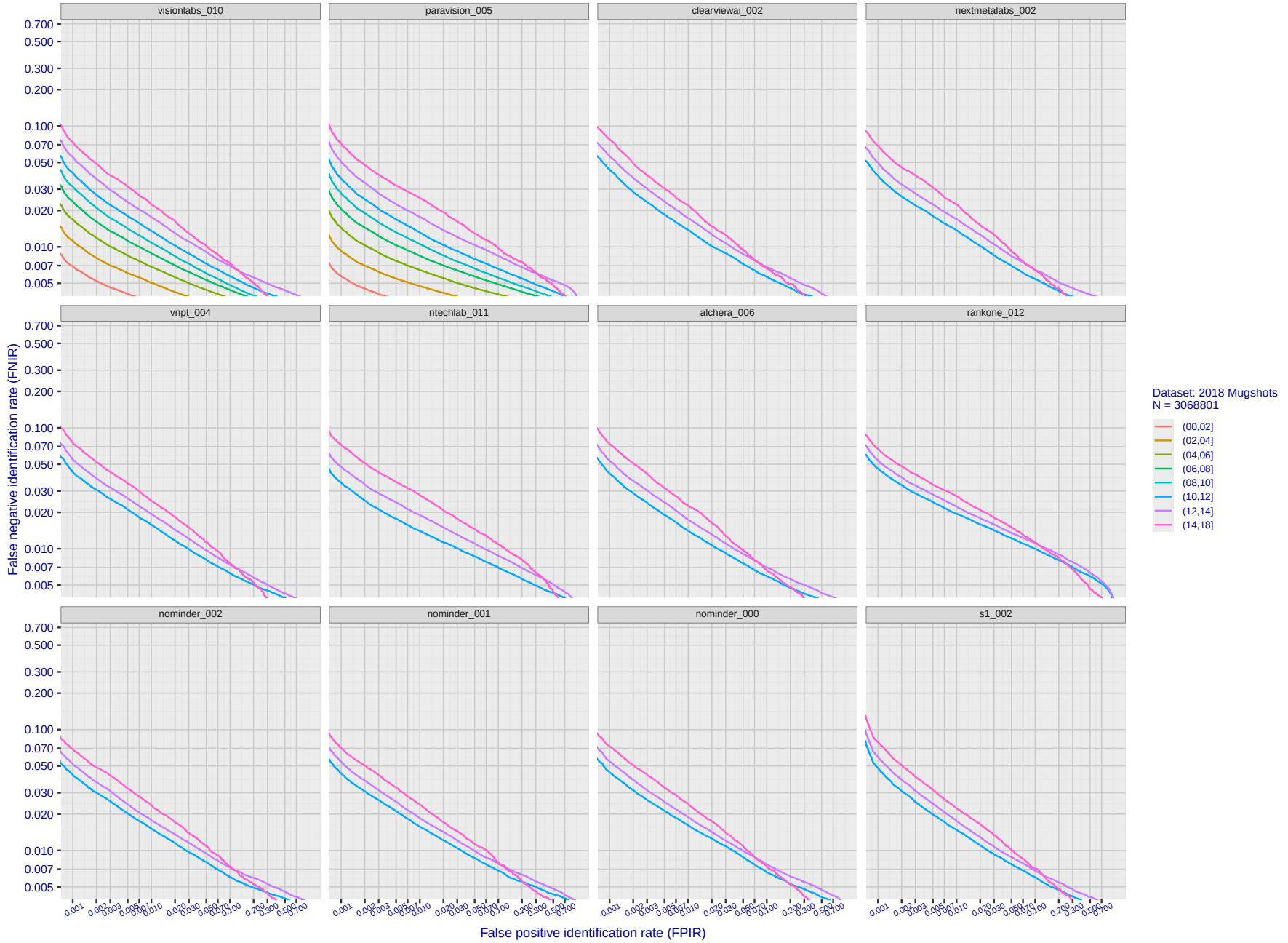

Figure 218: **[FRVT-2018 Mugshot Ageing Dataset] Identification miss rates vs. FPIR by time-elapsed**. *The oldest image of each individual is enrolled. Thereafter, all more recent images are searched. Miss rates are computed over all searches noted in row 17 of Table 1 and binned by number of years between search and initial enrollment. FPIR is computed from the same FRVT 2018 non-mates noted in row 3 of Table 1 with N = 3 000 000.*

2026/01/09 20:40:38

FNIR(N, R, T) = False neg. identification rate
FPIR(N, T) = False pos. identification rate
N = Num. enrolled subjects
R = Num. candidates examined
T = Threshold
T = 0 → Investigation
T > 0 → Identification

This publication is available free of charge from: https://doi.org/10.6028/NIST.IR.8271

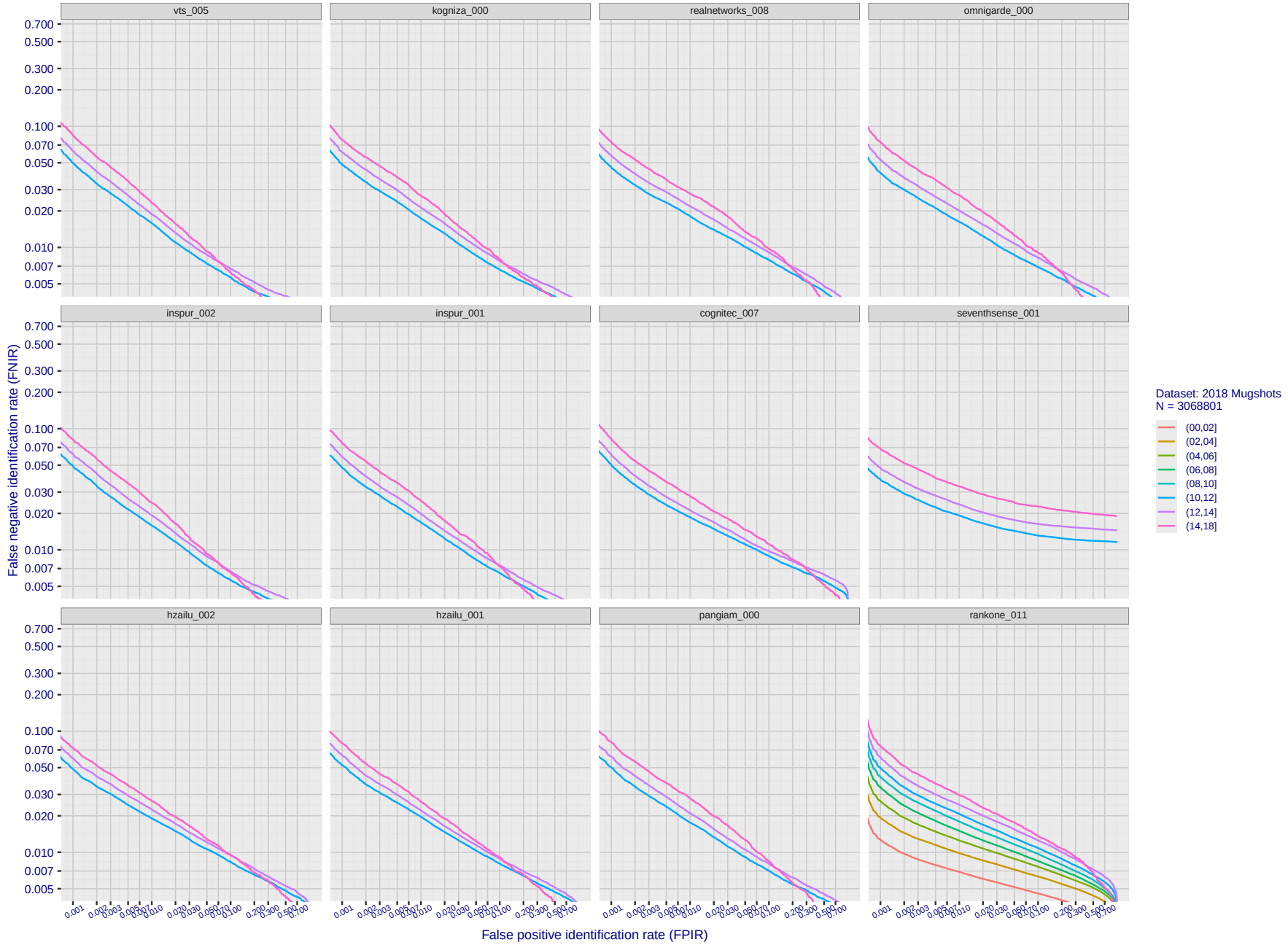

Figure 219: **[FRVT-2018 Mugshot Ageing Dataset] Identification miss rates vs. FPIR by time-elapsed**. *The oldest image of each individual is enrolled. Thereafter, all more recent images are searched. Miss rates are computed over all searches noted in row 17 of Table 1 and binned by number of years between search and initial enrollment. FPIR is computed from the same FRVT 2018 non-mates noted in row 3 of Table 1 with N = 3 000 000.*

FNIR(N, R, T) = False neg. identification rate
FPIR(N, T) = False pos. identification rate
N = Num. enrolled subjects
R = Num. candidates examined
T = Threshold
T = 0 → Investigation
T > 0 → Identification

2026/01/09
20:40:38

This publication is available free of charge from: https://doi.org/10.6028/NIST.IR.8271

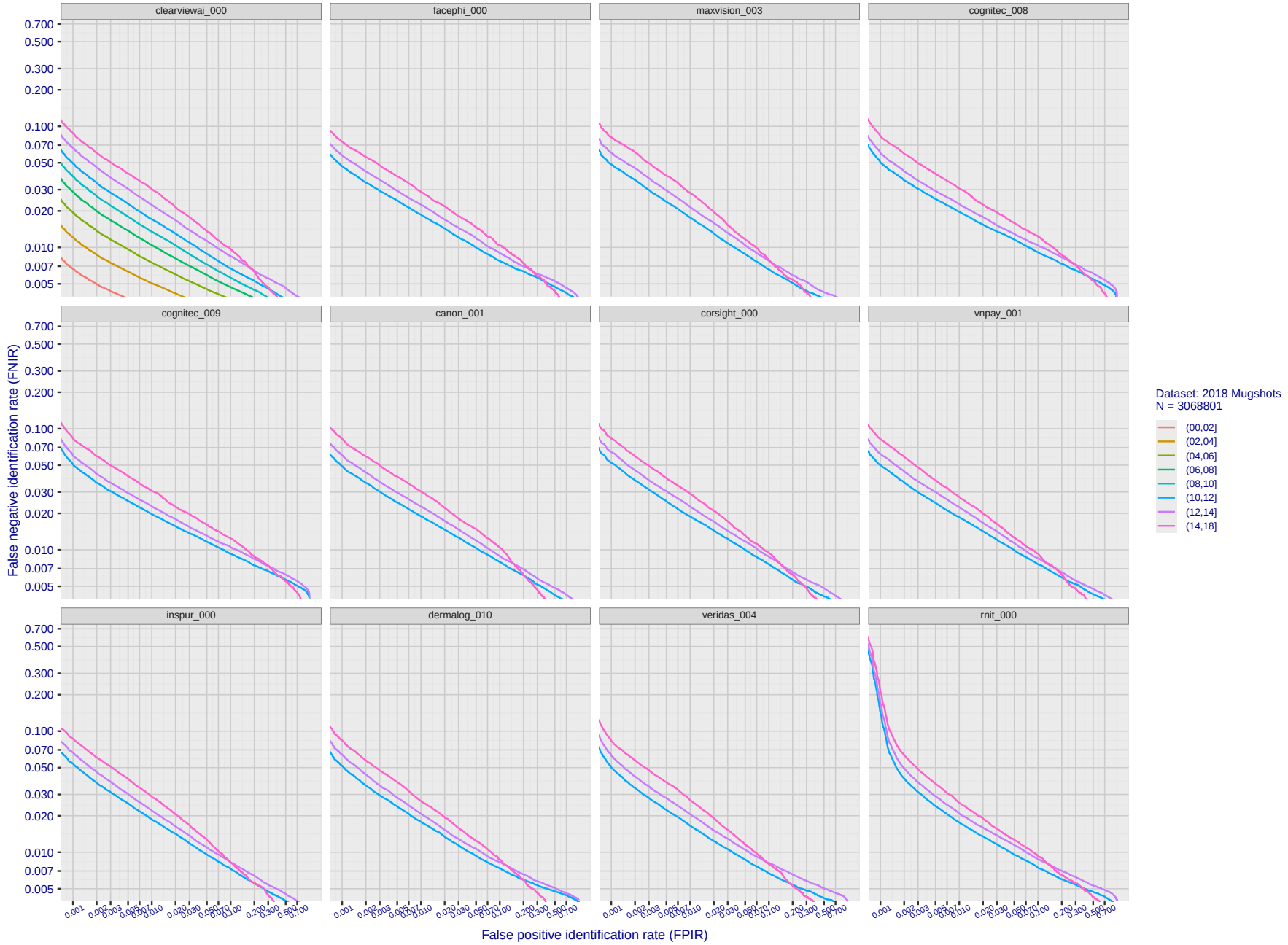

Figure 220: **[FRVT-2018 Mugshot Ageing Dataset] Identification miss rates vs. FPIR by time-elapsed**. *The oldest image of each individual is enrolled. Thereafter, all more recent images are searched. Miss rates are computed over all searches noted in row 17 of Table 1 and binned by number of years between search and initial enrollment. FPIR is computed from the same FRVT 2018 non-mates noted in row 3 of Table 1 with N = 3 000 000.*

2026/01/09 20:40:38
FNIR(N, R, T) = False neg. identification rate
FPIR(N, T) = False pos. identification rate
N = Num. enrolled subjects
R = Num. candidates examined
T = Threshold
T = 0 → Investigation
T > 0 → Identification

This publication is available free of charge from: https://doi.org/10.6028/NIST.IR.8271

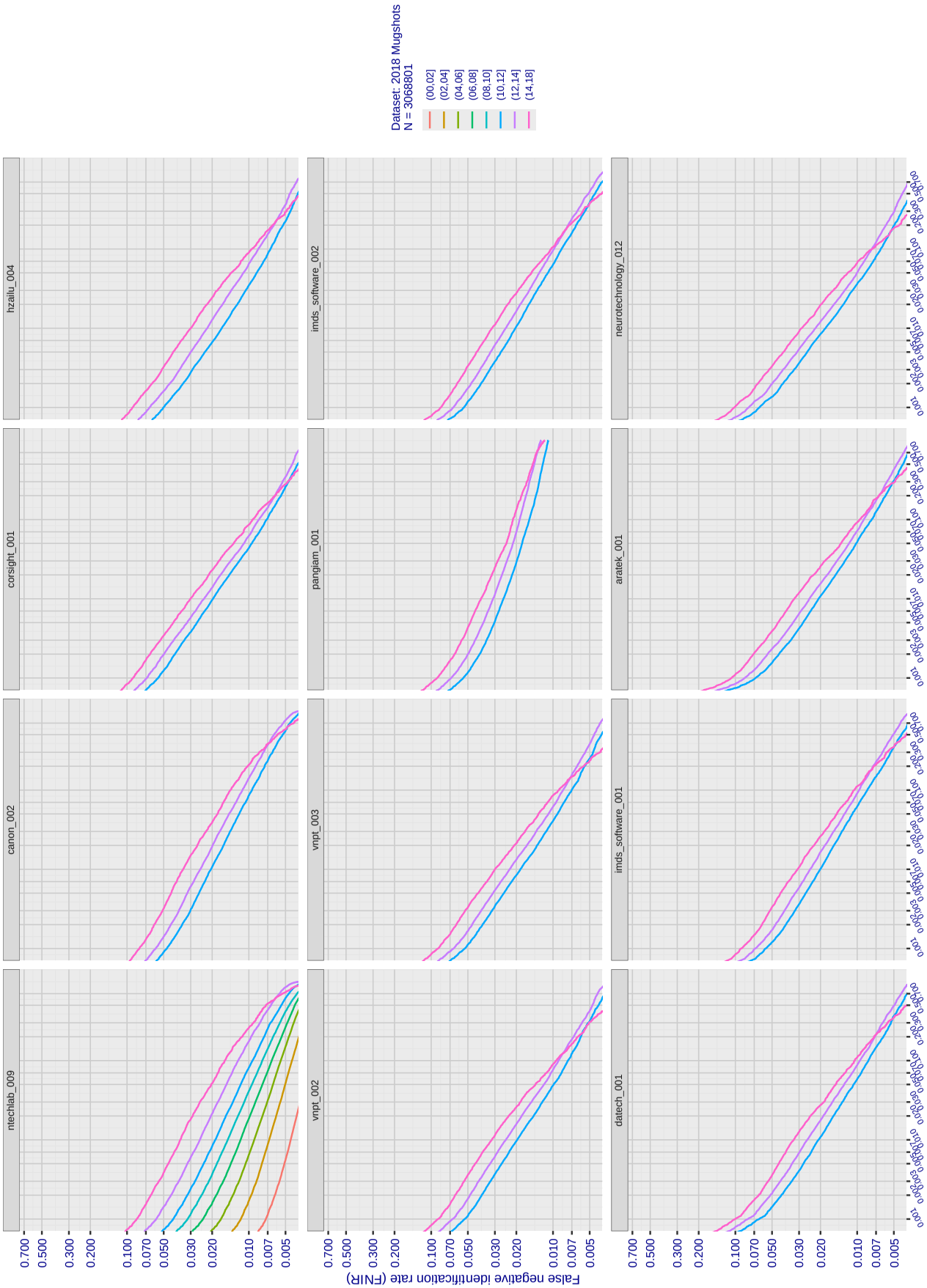

Figure 221: **[FRVT-2018 Mugshot Ageing Dataset] Identification miss rates vs. FPIR by time-elapsed.** *The oldest image of each individual is enrolled. Thereafter, all more recent images are searched. Miss rates are computed over all searches noted in row 17 of Table 1 and binned by number of years between search and initial enrollment. FPIR is computed from the same FRVT 2018 non-mates noted in row 3 of Table 1 with N = 3 000 000.*

This publication is available free of charge from: https://doi.org/10.6028/NIST.IR.8271

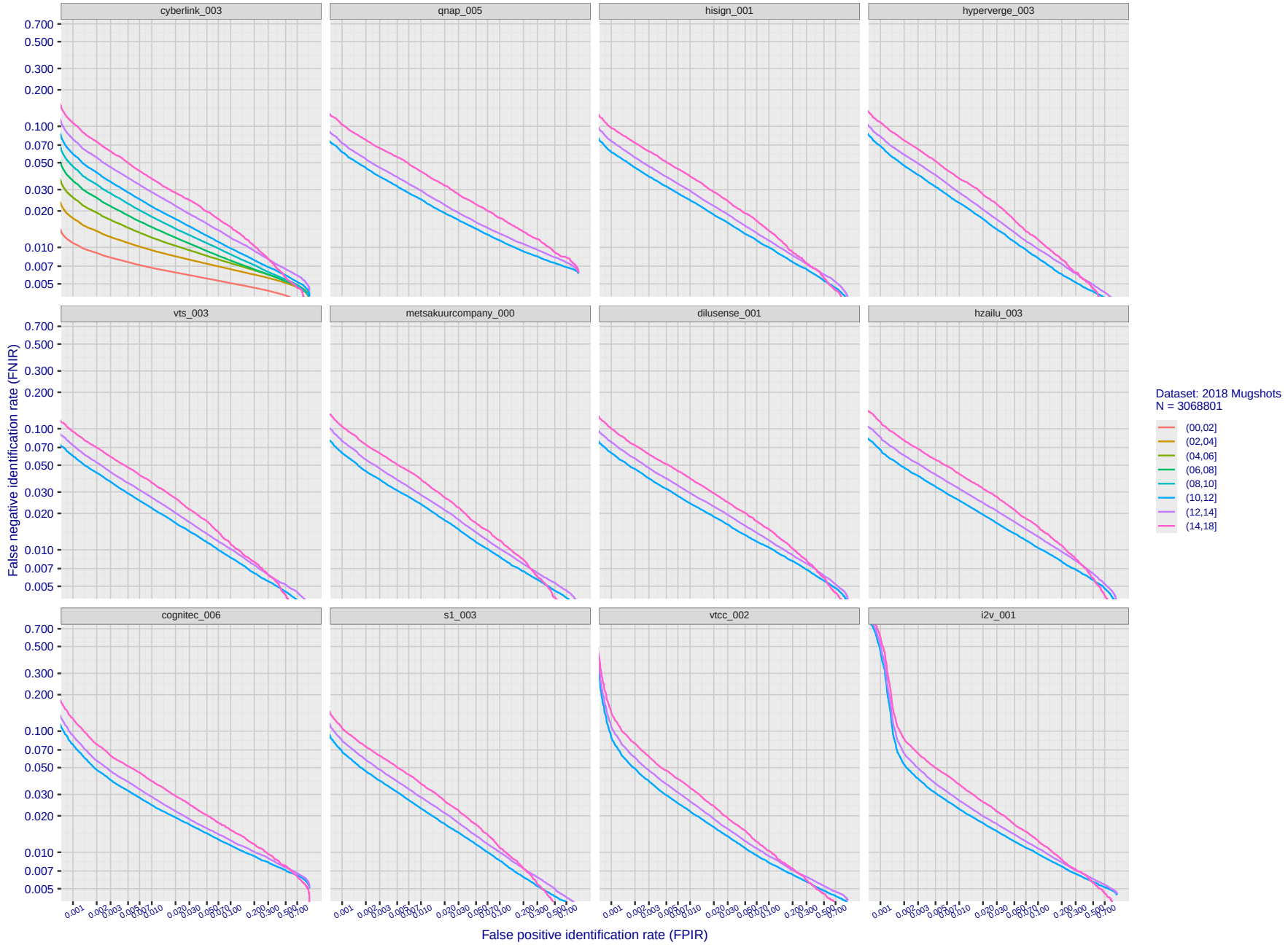

Figure 222: **[FRVT-2018 Mugshot Ageing Dataset] Identification miss rates vs. FPIR by time-elapsed**. *The oldest image of each individual is enrolled. Thereafter, all more recent images are searched. Miss rates are computed over all searches noted in row 17 of Table 1 and binned by number of years between search and initial enrollment. FPIR is computed from the same FRVT 2018 non-mates noted in row 3 of Table 1 with N = 3 000 000.*

2026/01/09 20:40:38
FNIR(N, R, T) = False neg. identification rate
FPIR(N, T) = False pos. identification rate
N = Num. enrolled subjects
R = Num. candidates examined
T = Threshold
T = 0 → Investigation
T > 0 → Identification

This publication is available free of charge from: https://doi.org/10.6028/NIST.IR.8271

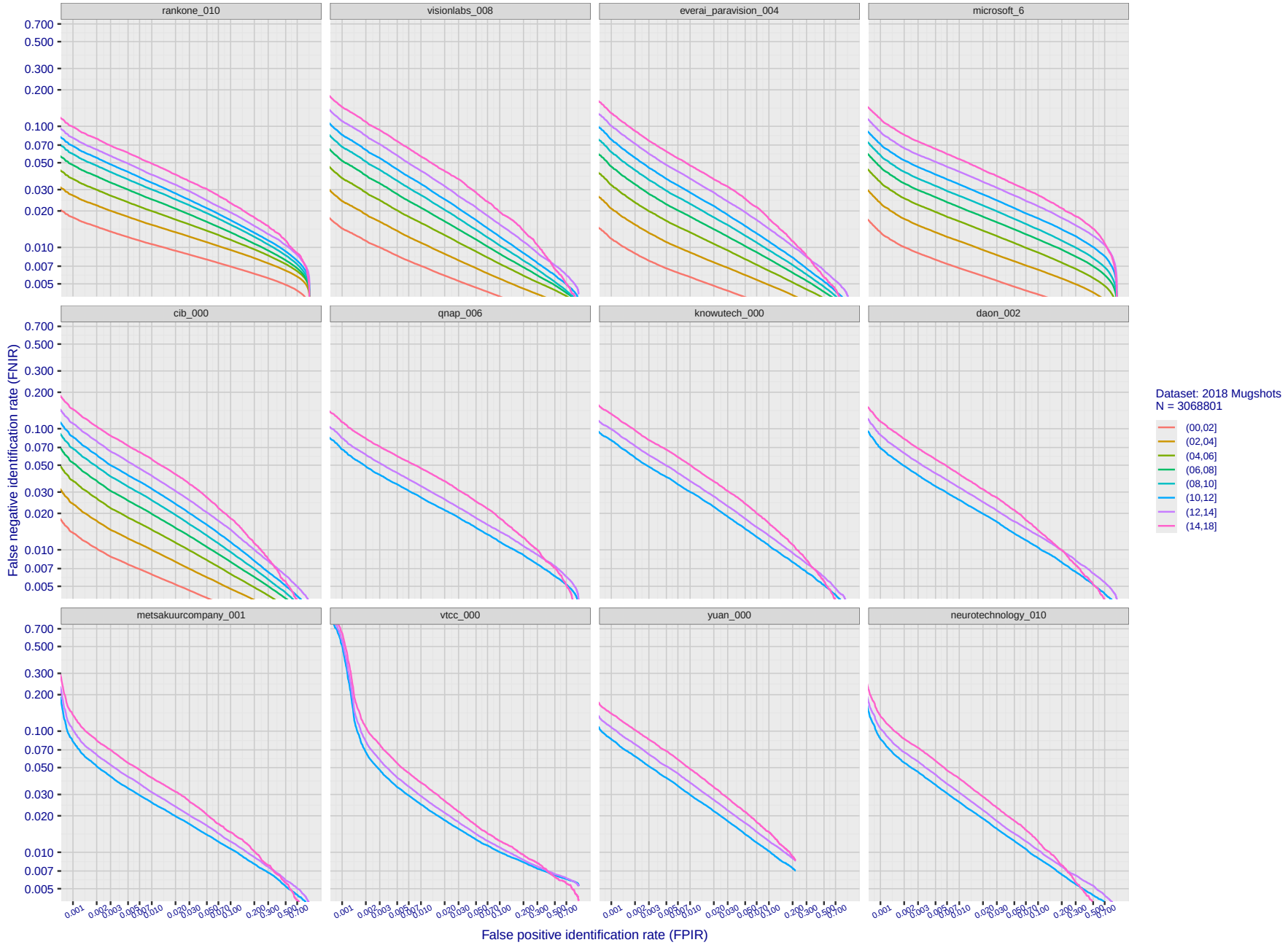

Figure 223: **[FRVT-2018 Mugshot Ageing Dataset] Identification miss rates vs. FPIR by time-elapsed**. *The oldest image of each individual is enrolled. Thereafter, all more recent images are searched. Miss rates are computed over all searches noted in row 17 of Table 1 and binned by number of years between search and initial enrollment. FPIR is computed from the same FRVT 2018 non-mates noted in row 3 of Table 1 with N = 3 000 000.*

This publication is available free of charge from: https://doi.org/10.6028/NIST.IR.8271

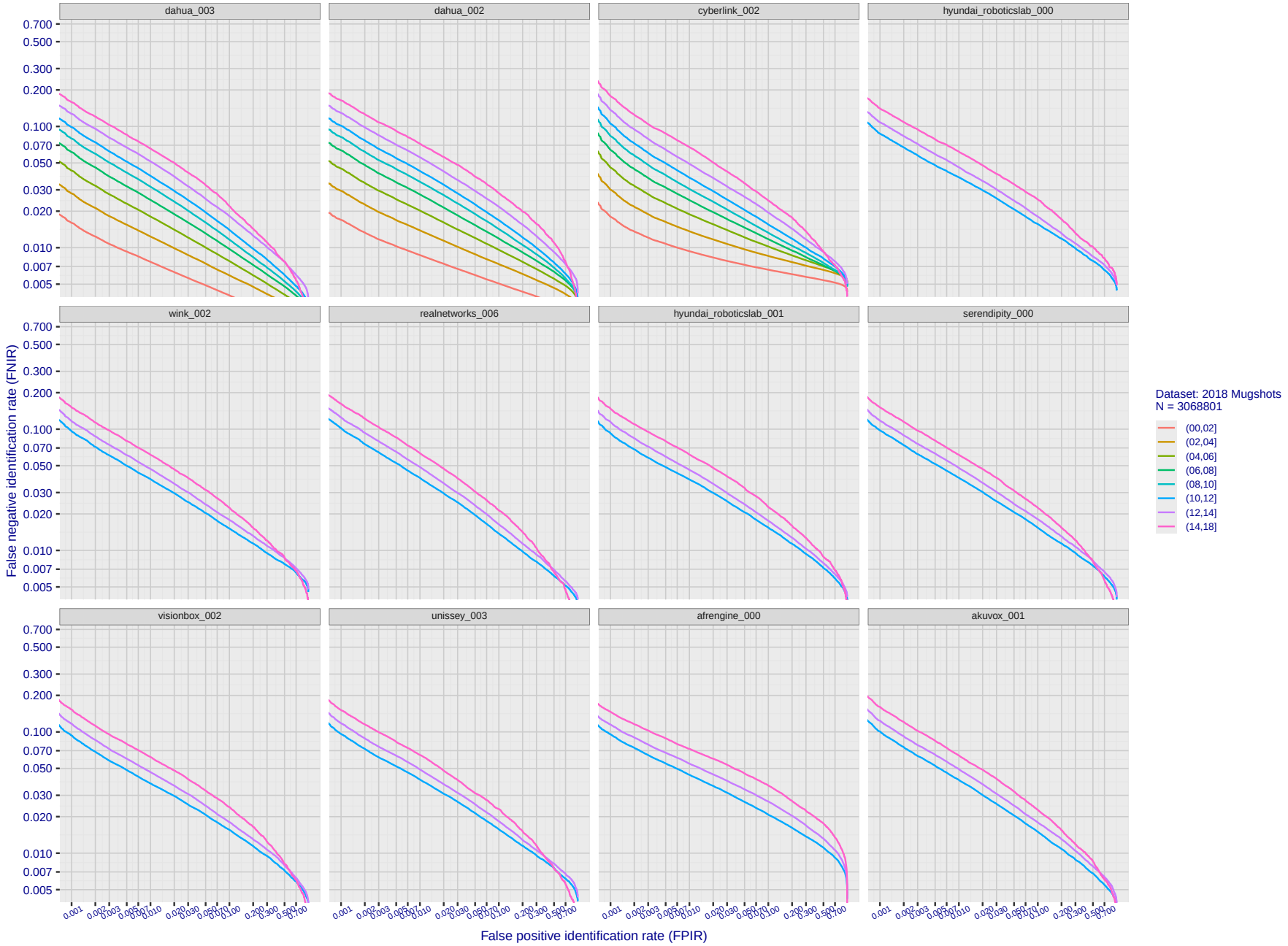

Figure 224: **[FRVT-2018 Mugshot Ageing Dataset] Identification miss rates vs. FPIR by time-elapsed**. *The oldest image of each individual is enrolled. Thereafter, all more recent images are searched. Miss rates are computed over all searches noted in row 17 of Table 1 and binned by number of years between search and initial enrollment. FPIR is computed from the same FRVT 2018 non-mates noted in row 3 of Table 1 with N = 3 000 000.*

This publication is available free of charge from: https://doi.org/10.6028/NIST.IR.8271

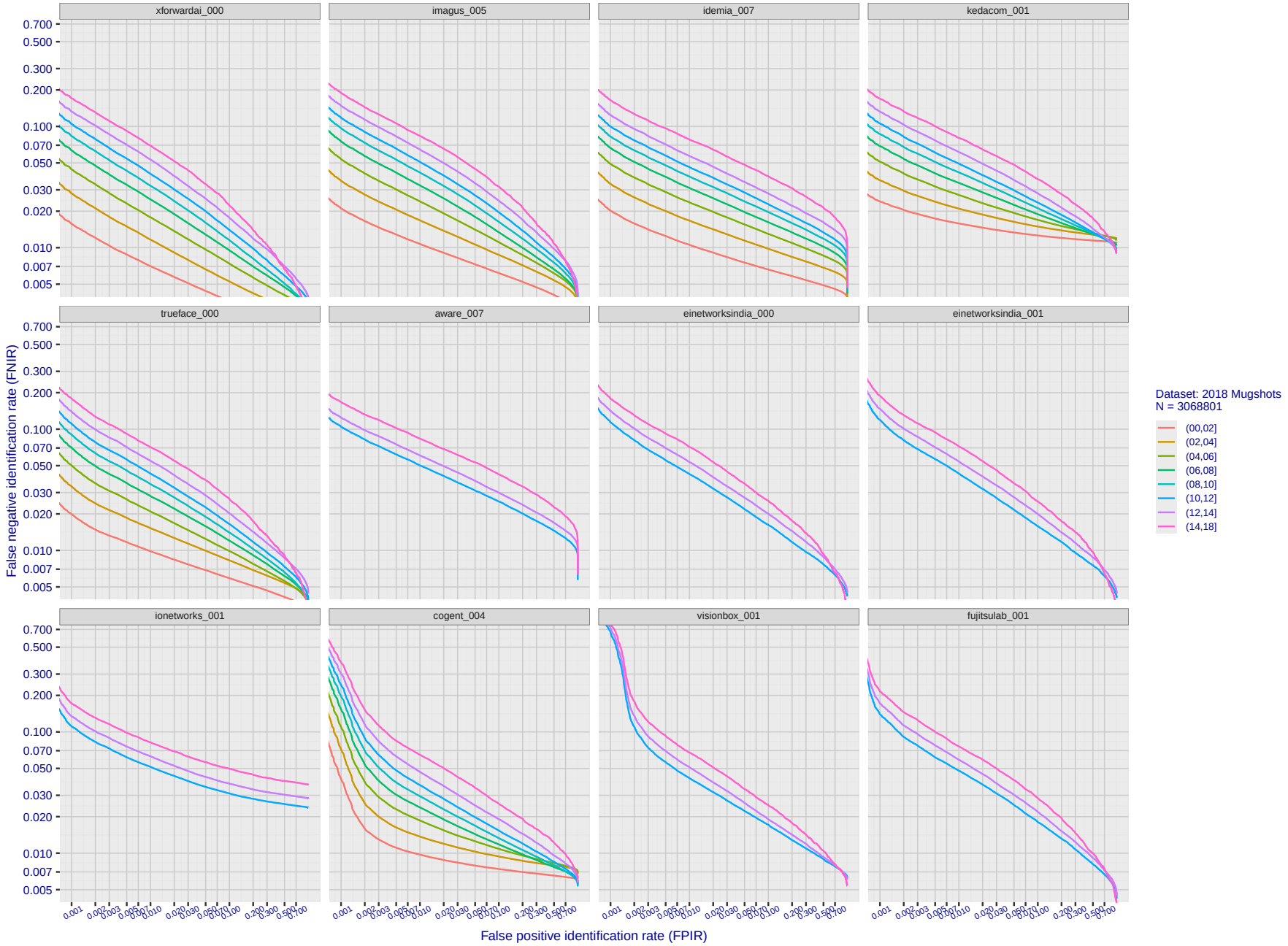

Figure 225: **[FRVT-2018 Mugshot Ageing Dataset] Identification miss rates vs. FPIR by time-elapsed**. *The oldest image of each individual is enrolled. Thereafter, all more recent images are searched. Miss rates are computed over all searches noted in row 17 of Table 1 and binned by number of years between search and initial enrollment. FPIR is computed from the same FRVT 2018 non-mates noted in row 3 of Table 1 with N = 3 000 000.*

This publication is available free of charge from: https://doi.org/10.6028/NIST.IR.8271

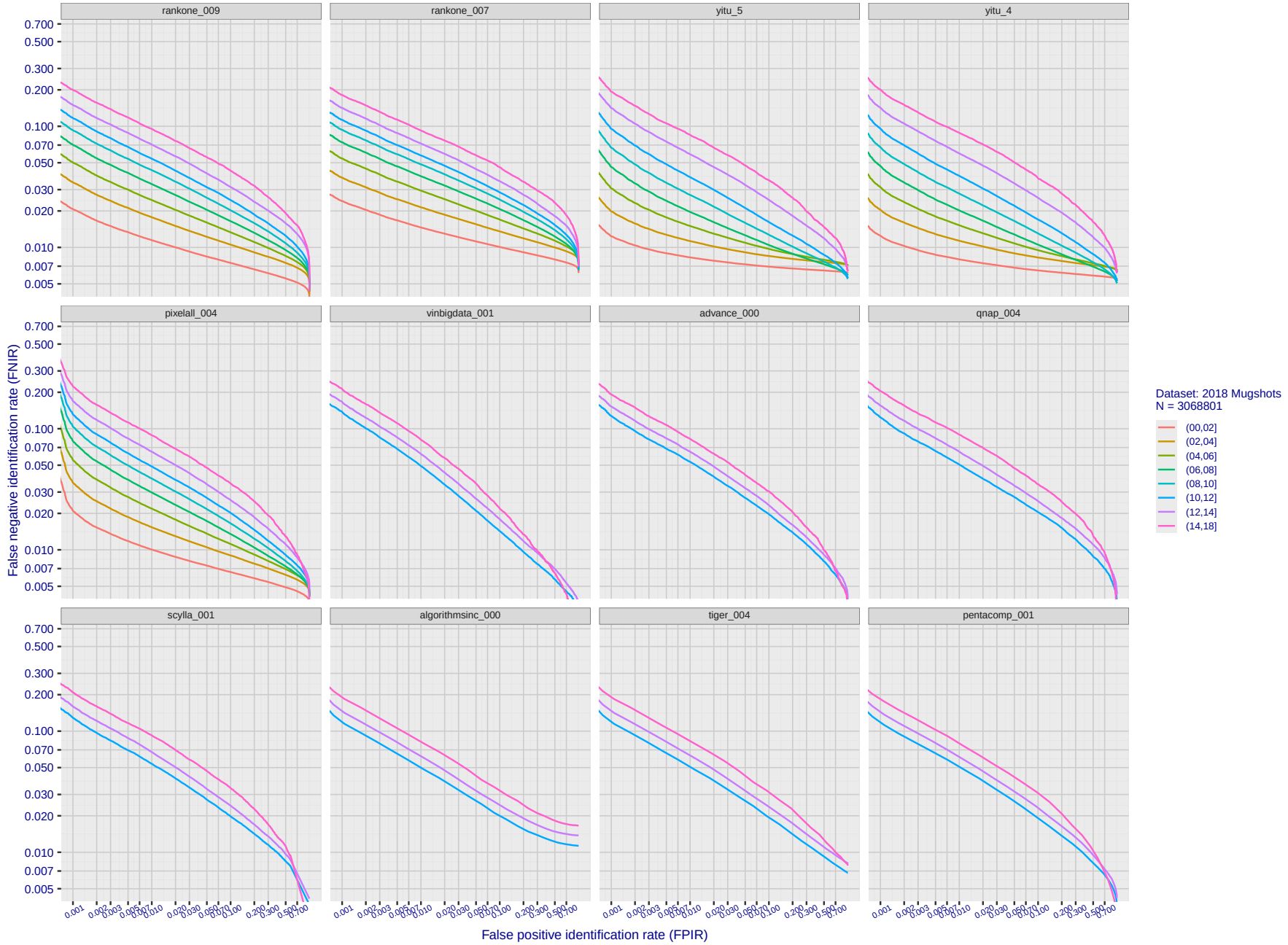

Figure 226: **[FRVT-2018 Mugshot Ageing Dataset] Identification miss rates vs. FPIR by time-elapsed**. *The oldest image of each individual is enrolled. Thereafter, all more recent images are searched. Miss rates are computed over all searches noted in row 17 of Table 1 and binned by number of years between search and initial enrollment. FPIR is computed from the same FRVT 2018 non-mates noted in row 3 of Table 1 with N = 3 000 000.*

2026/01/09 20:40:38
FNIR(N, R, T) = False neg. identification rate
FPIR(N, T) = False pos. identification rate
N = Num. enrolled subjects
R = Num. candidates examined
T = Threshold
T = 0 → Investigation
T > 0 → Identification

This publication is available free of charge from: https://doi.org/10.6028/NIST.IR.8271

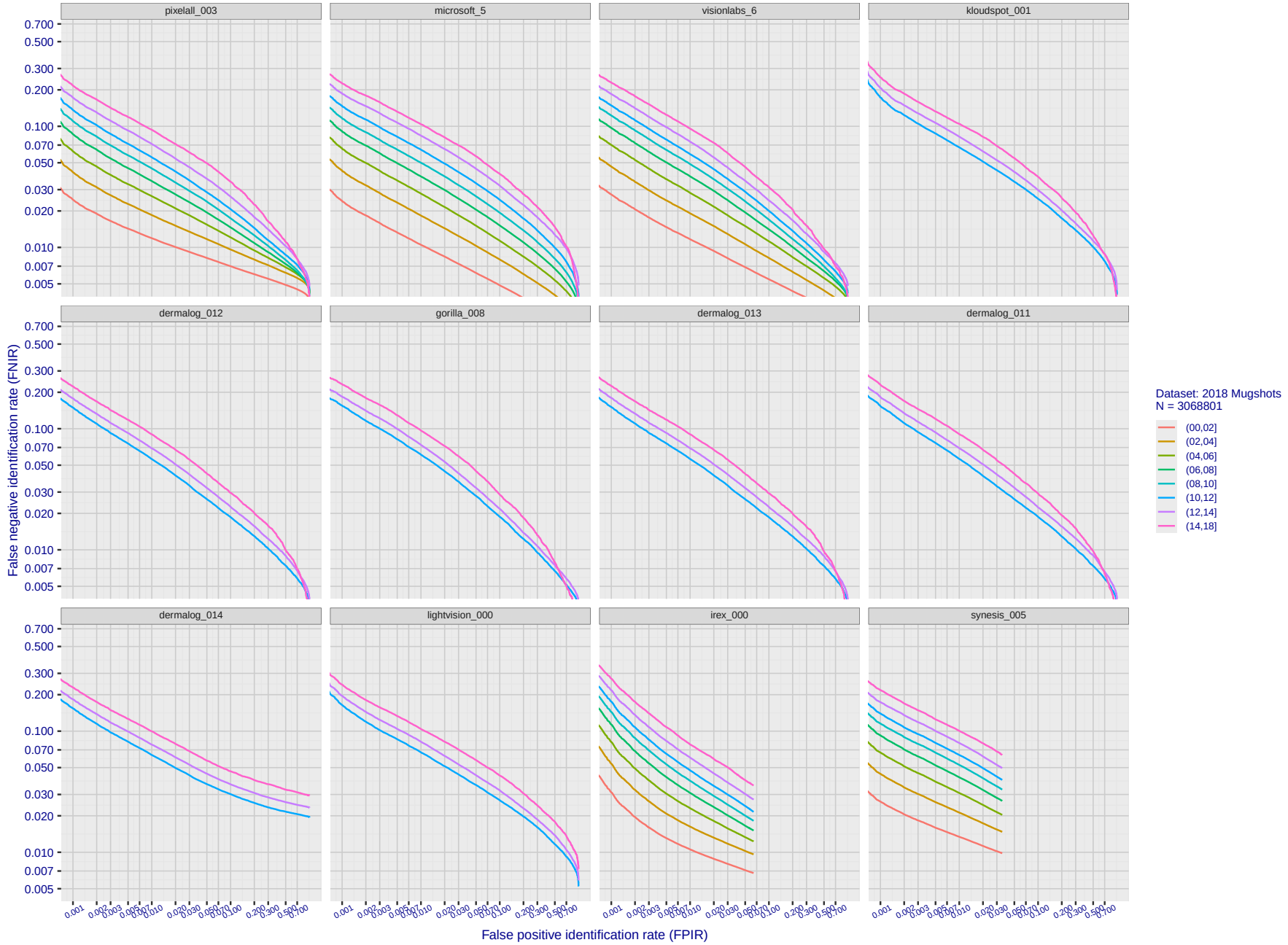

Figure 227: **[FRVT-2018 Mugshot Ageing Dataset] Identification miss rates vs. FPIR by time-elapsed**. *The oldest image of each individual is enrolled. Thereafter, all more recent images are searched. Miss rates are computed over all searches noted in row 17 of Table 1 and binned by number of years between search and initial enrollment. FPIR is computed from the same FRVT 2018 non-mates noted in row 3 of Table 1 with N = 3 000 000.*

This publication is available free of charge from: https://doi.org/10.6028/NIST.IR.8271

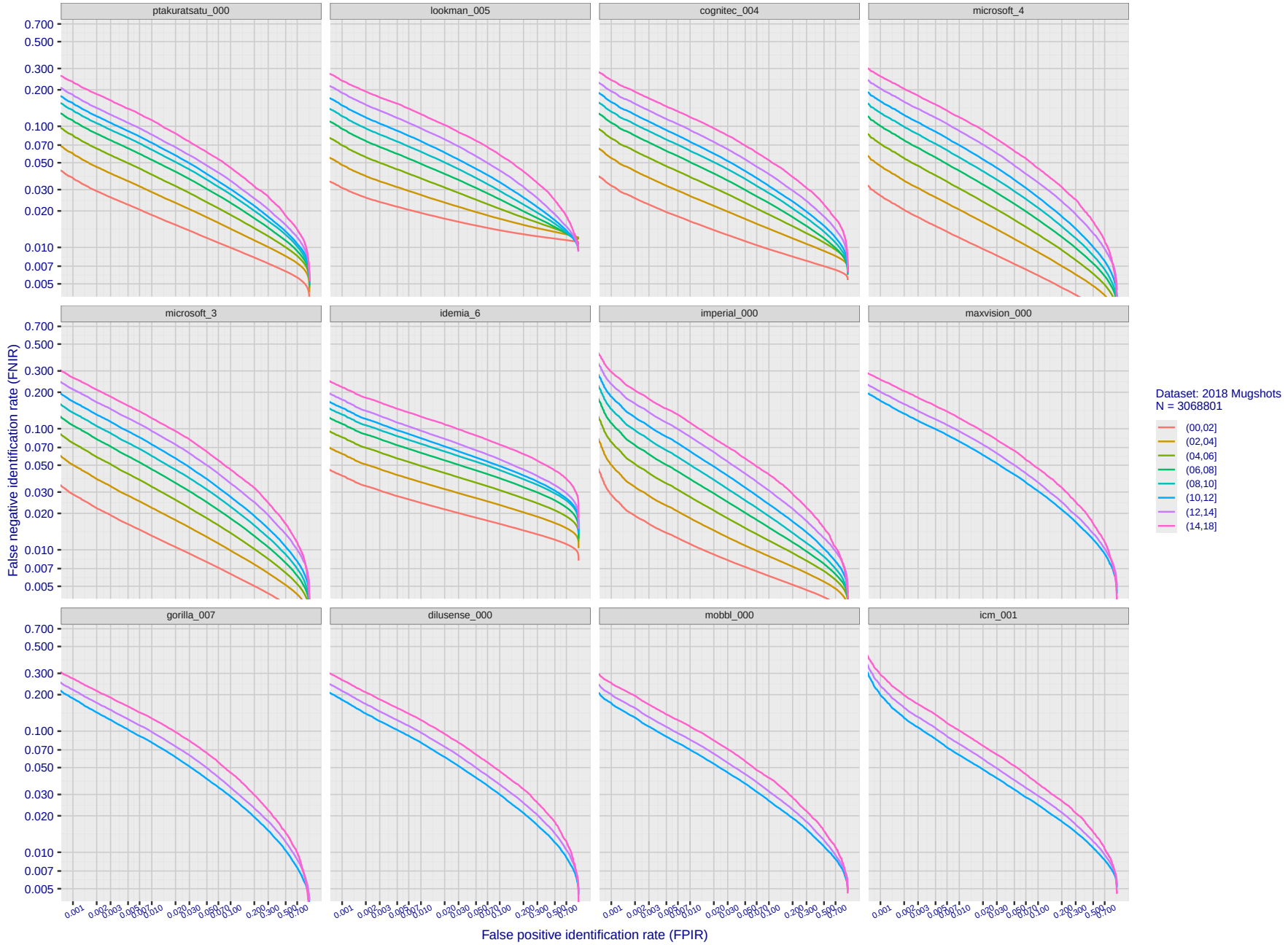

Figure 228: **[FRVT-2018 Mugshot Ageing Dataset] Identification miss rates vs. FPIR by time-elapsed**. *The oldest image of each individual is enrolled. Thereafter, all more recent images are searched. Miss rates are computed over all searches noted in row 17 of Table 1 and binned by number of years between search and initial enrollment. FPIR is computed from the same FRVT 2018 non-mates noted in row 3 of Table 1 with N = 3 000 000.*

2026/01/09 20:40:38
FNIR(N, R, T) = False neg. identification rate
FPIR(N, T) = False pos. identification rate
N = Num. enrolled subjects
R = Num. candidates examined
T = Threshold
T = 0 → Investigation
T > 0 → Identification

This publication is available free of charge from: https://doi.org/10.6028/NIST.IR.8271

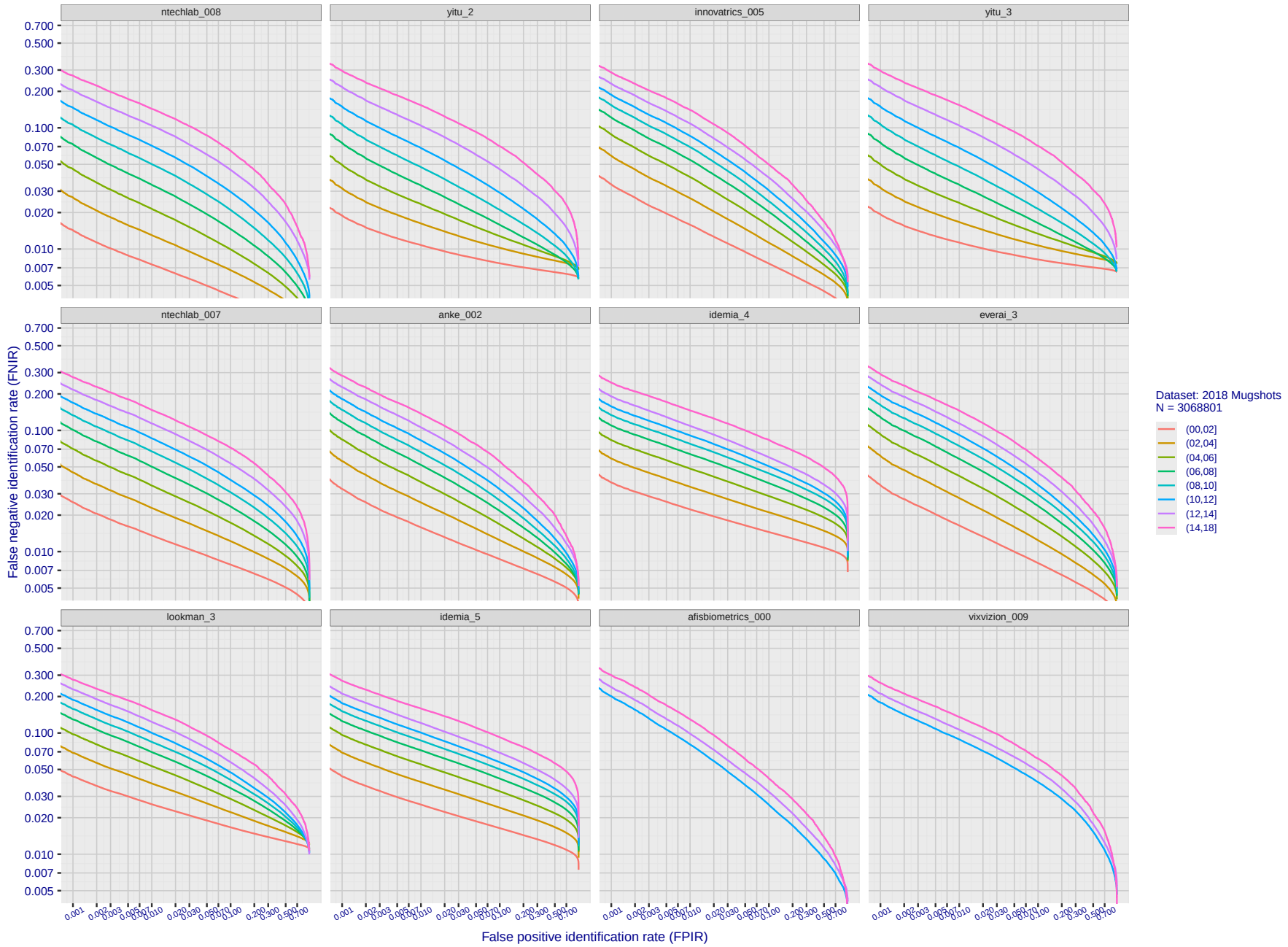

Figure 229: **[FRVT-2018 Mugshot Ageing Dataset] Identification miss rates vs. FPIR by time-elapsed**. *The oldest image of each individual is enrolled. Thereafter, all more recent images are searched. Miss rates are computed over all searches noted in row 17 of Table 1 and binned by number of years between search and initial enrollment. FPIR is computed from the same FRVT 2018 non-mates noted in row 3 of Table 1 with N = 3 000 000.*

2026/01/09 20:40:38

FNIR(N, R, T) = False neg. identification rate
FPIR(N, T) = False pos. identification rate

N = Num. enrolled subjects
R = Num. candidates examined

T = Threshold

T = 0 → Investigation
T > 0 → Identification

This publication is available free of charge from: https://doi.org/10.6028/NIST.IR.8271

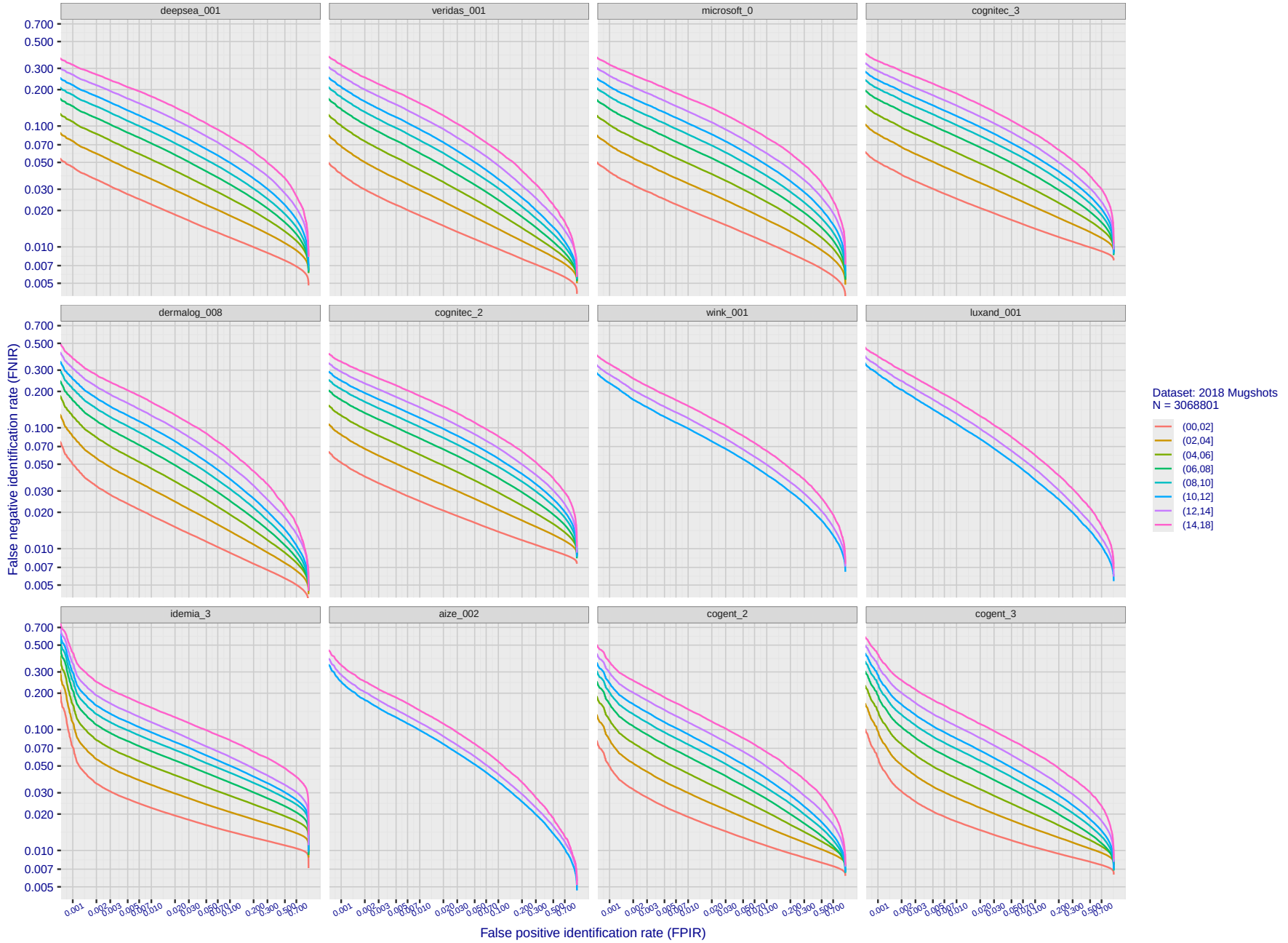

Figure 230: **[FRVT-2018 Mugshot Ageing Dataset] Identification miss rates vs. FPIR by time-elapsed**. *The oldest image of each individual is enrolled. Thereafter, all more recent images are searched. Miss rates are computed over all searches noted in row 17 of Table 1 and binned by number of years between search and initial enrollment. FPIR is computed from the same FRVT 2018 non-mates noted in row 3 of Table 1 with N = 3 000 000.*

2026/01/09 20:40:38

FNIR(N, R, T) = False neg. identification rate
FPIR(N, T) = False pos. identification rate

N = Num. enrolled subjects
R = Num. candidates examined

T = Threshold

T = 0 → Investigation
T > 0 → Identification

This publication is available free of charge from: https://doi.org/10.6028/NIST.IR.8271

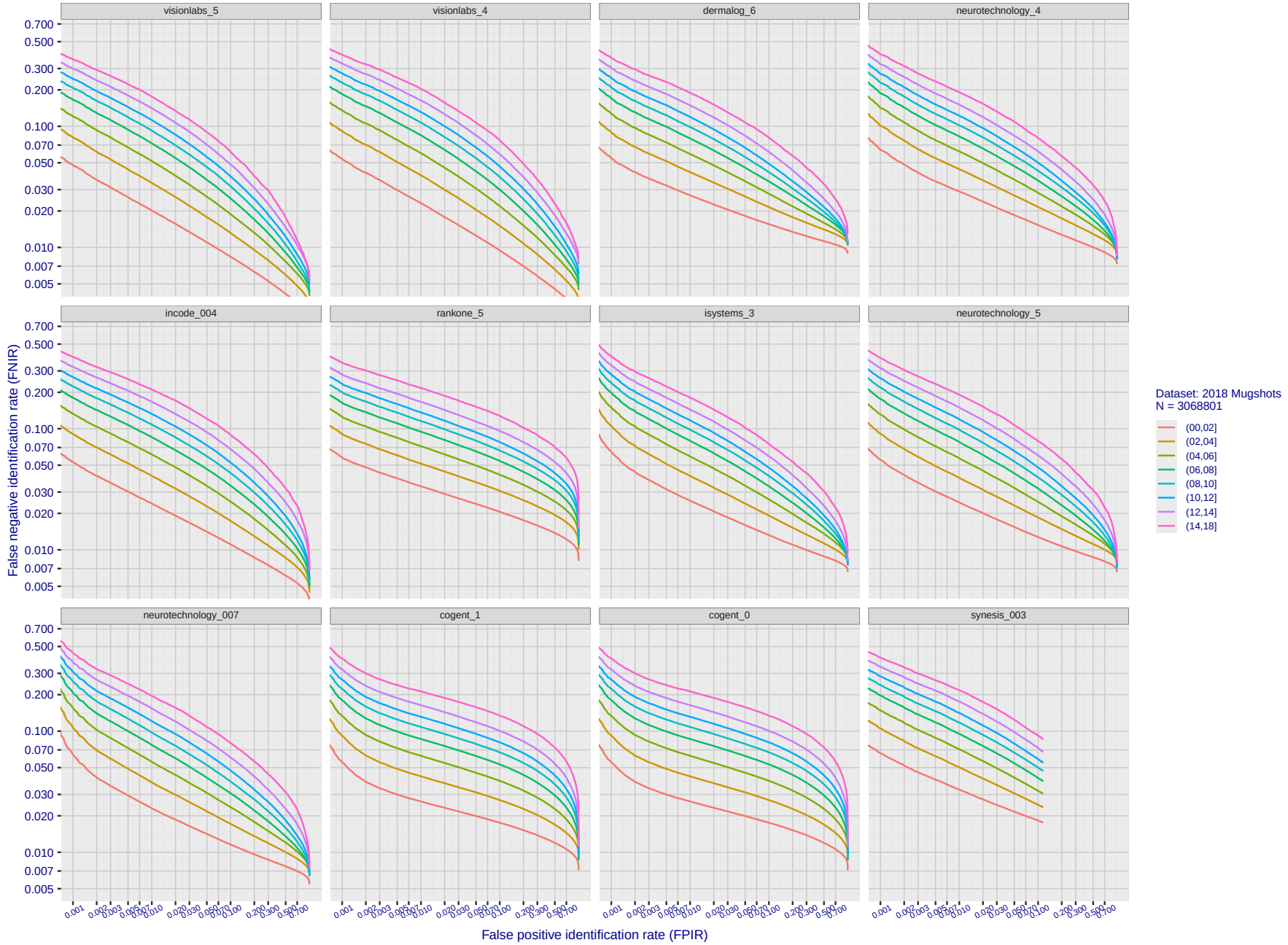

Figure 231: **[FRVT-2018 Mugshot Ageing Dataset] Identification miss rates vs. FPIR by time-elapsed**. *The oldest image of each individual is enrolled. Thereafter, all more recent images are searched. Miss rates are computed over all searches noted in row 17 of Table 1 and binned by number of years between search and initial enrollment. FPIR is computed from the same FRVT 2018 non-mates noted in row 3 of Table 1 with N = 3 000 000.*

2026/01/09 20:40:38
FNIR(N, R, T) = False neg. identification rate
FPIR(N, T) = False pos. identification rate
N = Num. enrolled subjects
R = Num. candidates examined
T = Threshold
T = 0 → Investigation
T > 0 → Identification

This publication is available free of charge from: https://doi.org/10.6028/NIST.IR.8271

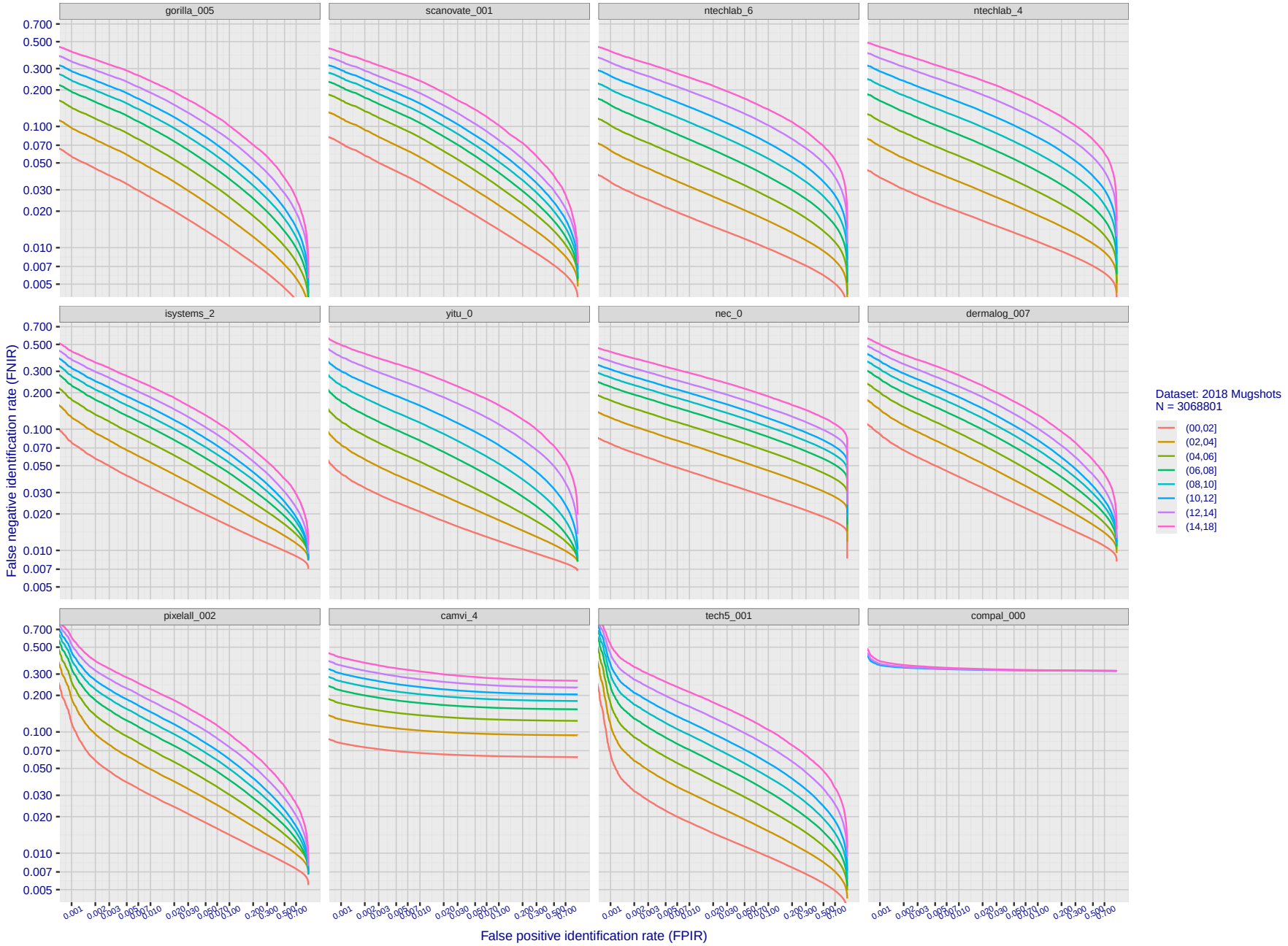

Figure 232: **[FRVT-2018 Mugshot Ageing Dataset] Identification miss rates vs. FPIR by time-elapsed**. *The oldest image of each individual is enrolled. Thereafter, all more recent images are searched. Miss rates are computed over all searches noted in row 17 of Table 1 and binned by number of years between search and initial enrollment. FPIR is computed from the same FRVT 2018 non-mates noted in row 3 of Table 1 with N = 3 000 000.*

2026/01/09 20:40:38
FNIR(N, R, T) = False neg. identification rate
FPIR(N, T) = False pos. identification rate
N = Num. enrolled subjects
R = Num. candidates examined
T = Threshold
T = 0 → Investigation
T > 0 → Identification

This publication is available free of charge from: https://doi.org/10.6028/NIST.IR.8271

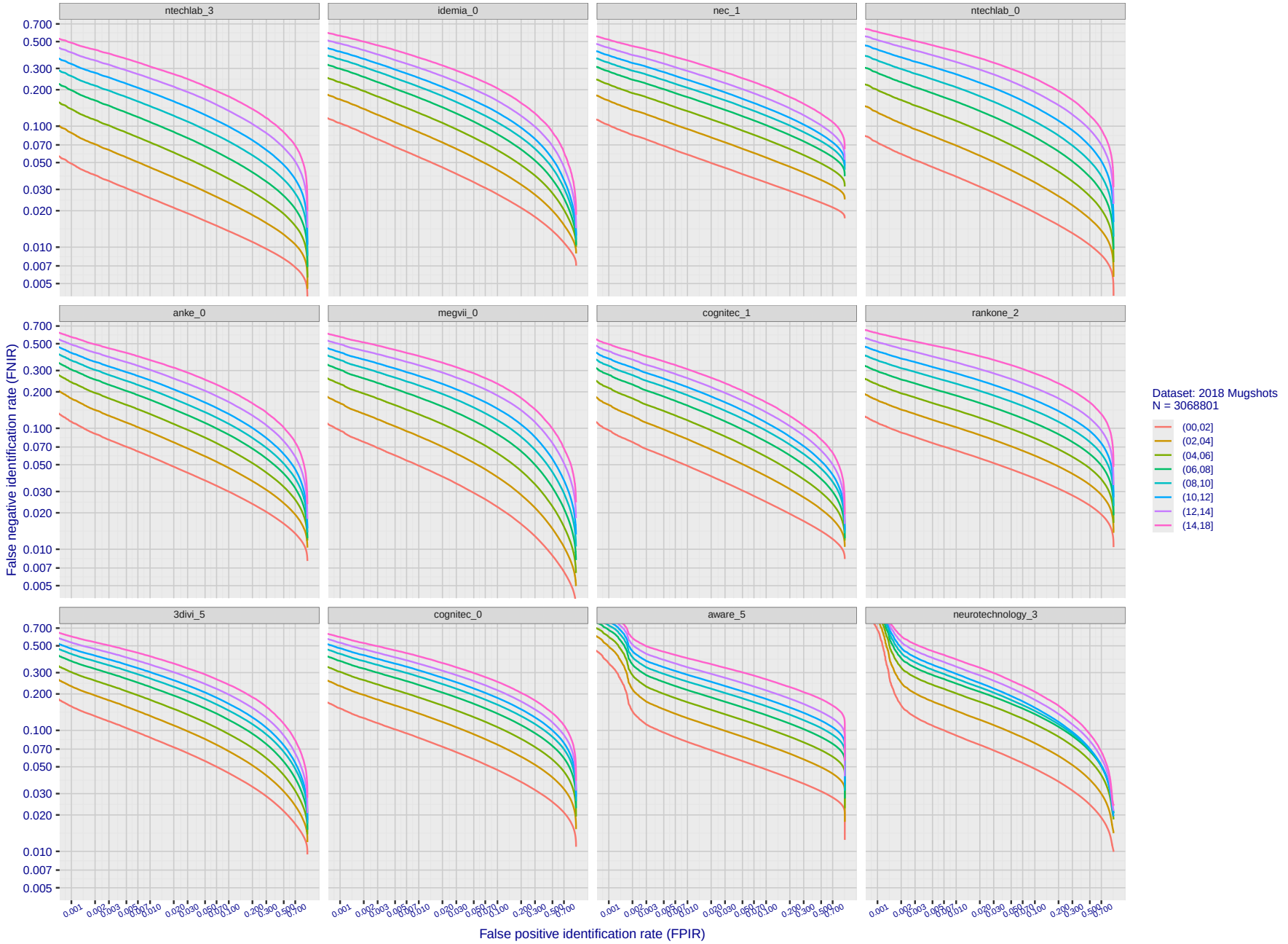

Figure 233: **[FRVT-2018 Mugshot Ageing Dataset] Identification miss rates vs. FPIR by time-elapsed**. *The oldest image of each individual is enrolled. Thereafter, all more recent images are searched. Miss rates are computed over all searches noted in row 17 of Table 1 and binned by number of years between search and initial enrollment. FPIR is computed from the same FRVT 2018 non-mates noted in row 3 of Table 1 with N = 3 000 000.*

2026/01/09 20:40:38
FNIR(N, R, T) = False neg. identification rate
FPIR(N, T) = False pos. identification rate
N = Num. enrolled subjects
R = Num. candidates examined
T = Threshold
T = 0 → Investigation
T > 0 → Identification

This publication is available free of charge from: https://doi.org/10.6028/NIST.IR.8271

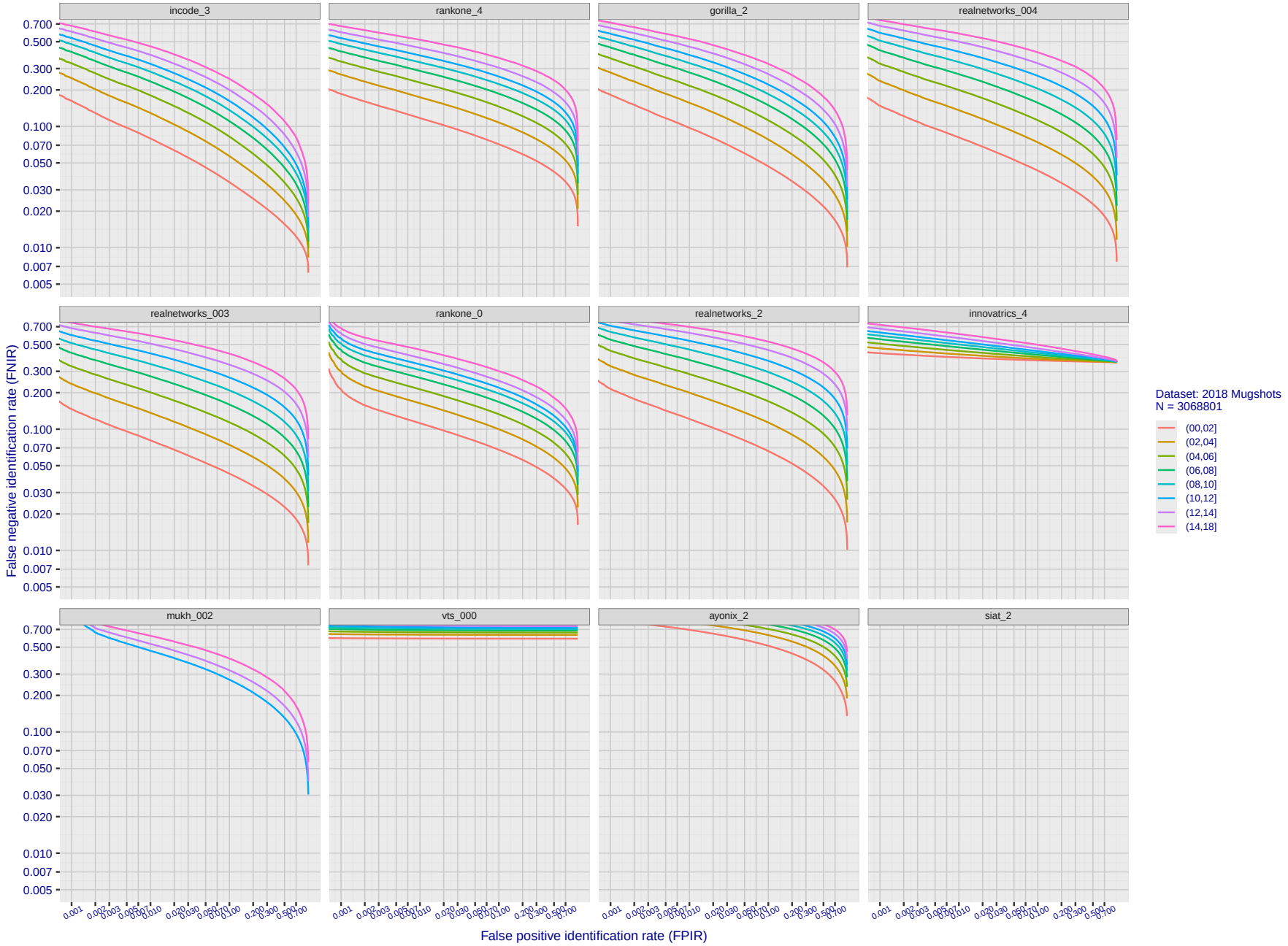

Figure 234: **[FRVT-2018 Mugshot Ageing Dataset] Identification miss rates vs. FPIR by time-elapsed**. *The oldest image of each individual is enrolled. Thereafter, all more recent images are searched. Miss rates are computed over all searches noted in row 17 of Table 1 and binned by number of years between search and initial enrollment. FPIR is computed from the same FRVT 2018 non-mates noted in row 3 of Table 1 with N = 3 000 000.*

2026/01/09 20:40:38
FNIR(N, R, T) = False neg. identification rate
FPIR(N, T) = False pos. identification rate
N = Num. enrolled subjects
R = Num. candidates examined
T = Threshold
T = 0 → Investigation
T > 0 → Identification

This publication is available free of charge from: https://doi.org/10.6028/NIST.IR.8271

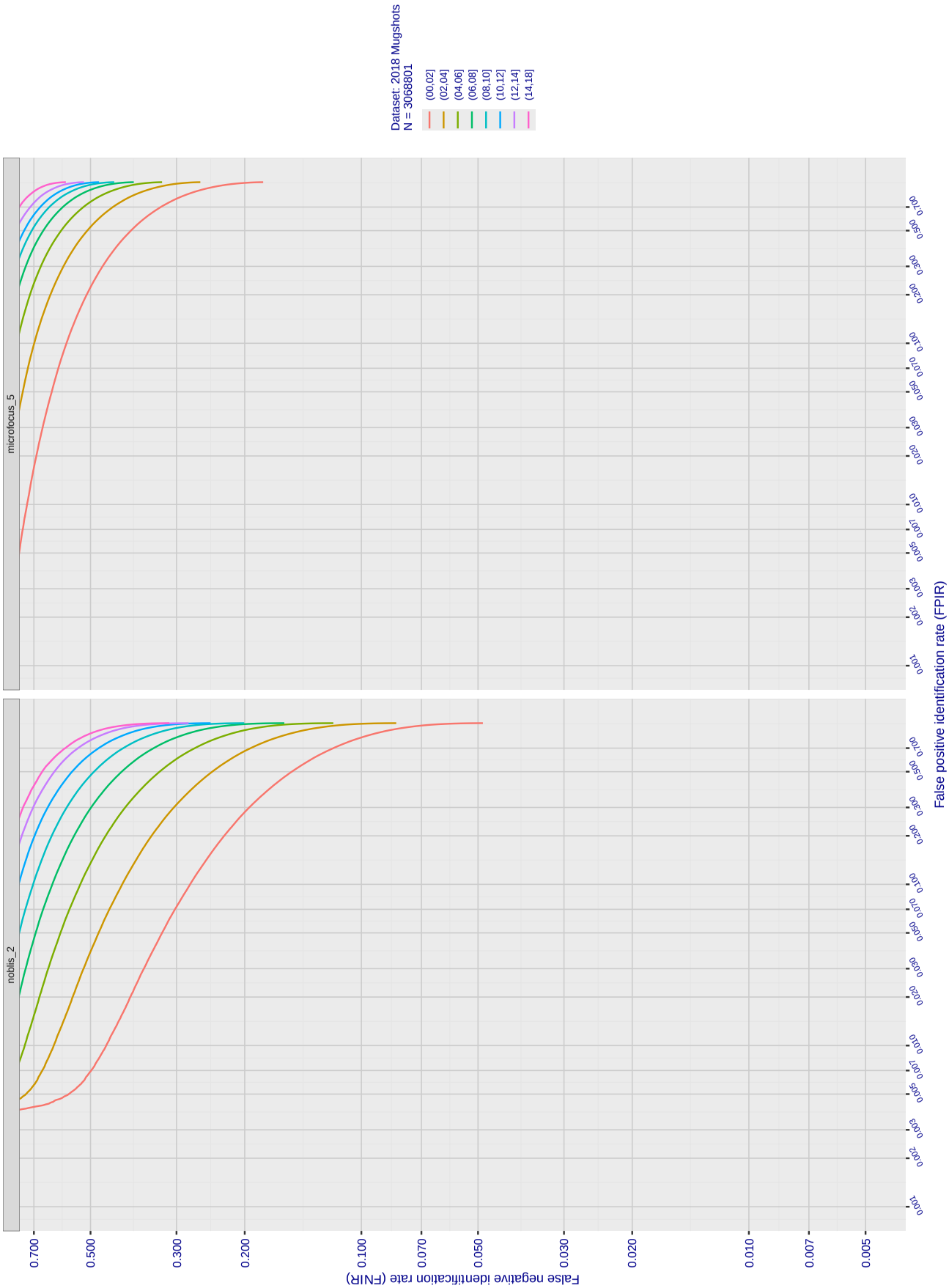

Figure 235: **[FRVT-2018 Mugshot Ageing Dataset] Identification miss rates vs. FPIR by time-elapsed.** *The oldest image of each individual is enrolled. Thereafter, all more recent images are searched. Miss rates are computed over all searches noted in row 17 of Table 1 and binned by number of years between search and initial enrollment. FPIR is computed from the same FRVT 2018 non-mates noted in row 3 of Table 1 with N = 3 000 000.*

2026/01/09	FNIR(N, R, T) =	False neg. identification rate	N = Num. enrolled subjects	T = Threshold	$T = 0 \rightarrow$ Investigation
20:40:38	FPIR(N, T) =	False pos. identification rate	R = Num. candidates examined		$T > 0 \rightarrow$ Identification

This publication is available free of charge from: https://doi.org/10.6028/NIST.IR.8271

This publication is available free of charge from: https://doi.org/10.6028/NIST.IR.8271

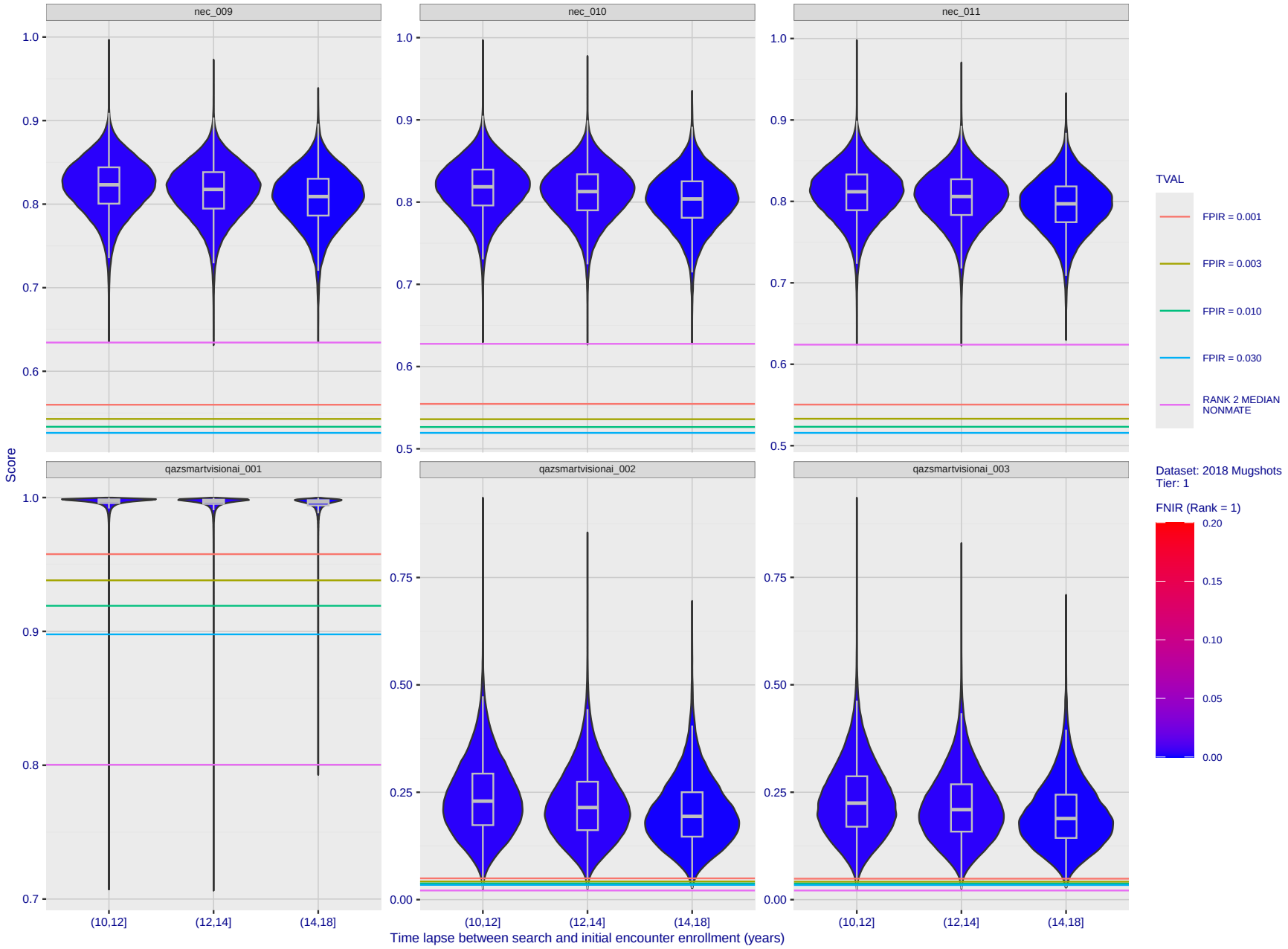

Figure 236: **[FRVT-2018 Mugshot Ageing Dataset] Native mate scores vs. time-elapsed**. *The oldest image of each individual is enrolled. Thereafter, all more recent images are searched. Mated score distributions are computed over all searches noted in row 17 of Table 1 binned by number of years between search and initial enrollment.*

2026/01/09 20:40:38
FNIR(N, R, T) = False neg. identification rate
FPIR(N, T) = False pos. identification rate
N = Num. enrolled subjects
R = Num. candidates examined
T = Threshold
T = 0 → Investigation
T > 0 → Identification

This publication is available free of charge from: https://doi.org/10.6028/NIST.IR.8271

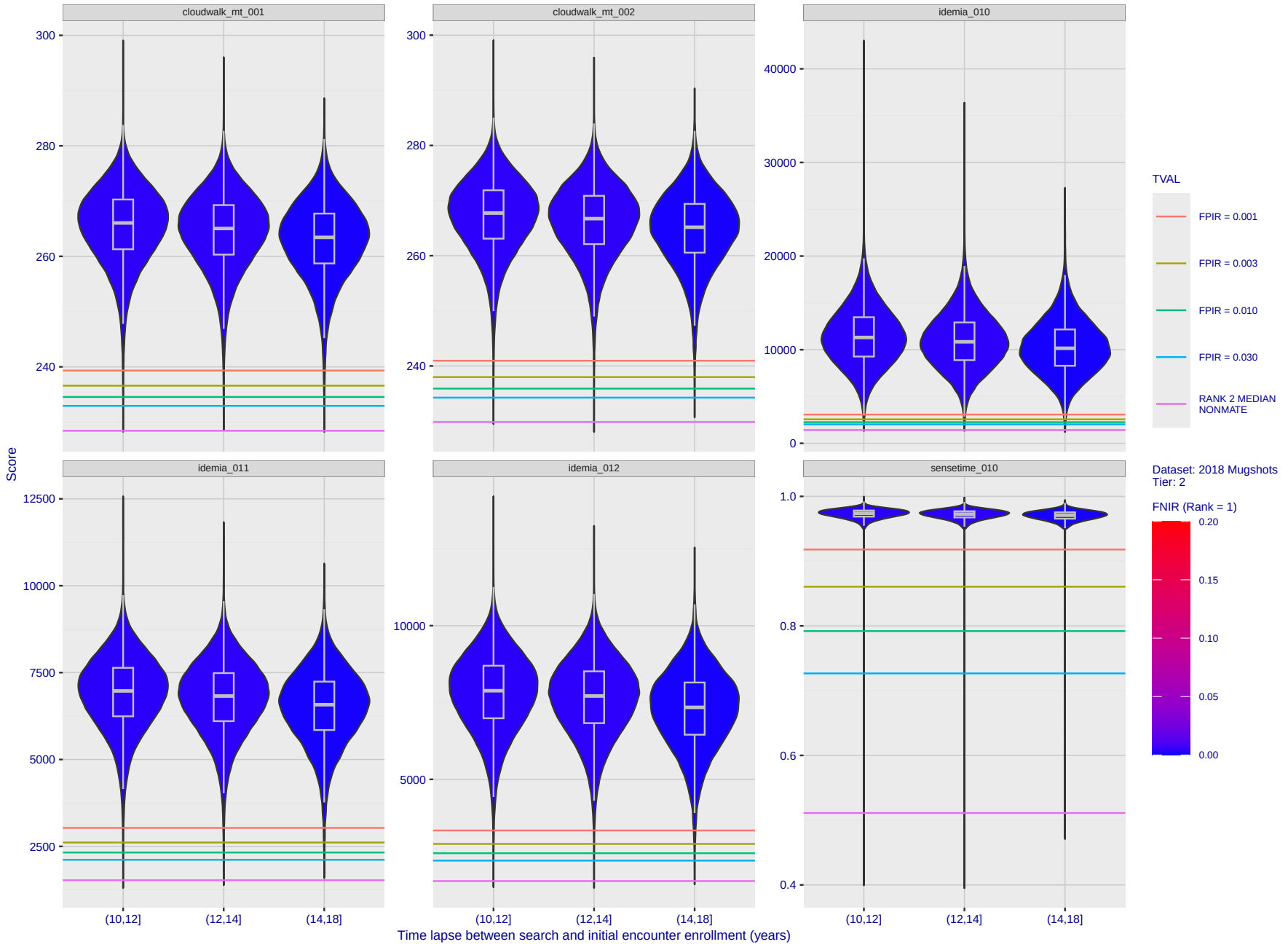

Figure 237: **[FRVT-2018 Mugshot Ageing Dataset] Native mate scores vs. time-elapsed**. *The oldest image of each individual is enrolled. Thereafter, all more recent images are searched. Mated score distributions are computed over all searches noted in row 17 of Table 1 binned by number of years between search and initial enrollment.*

This publication is available free of charge from: https://doi.org/10.6028/NIST.IR.8271

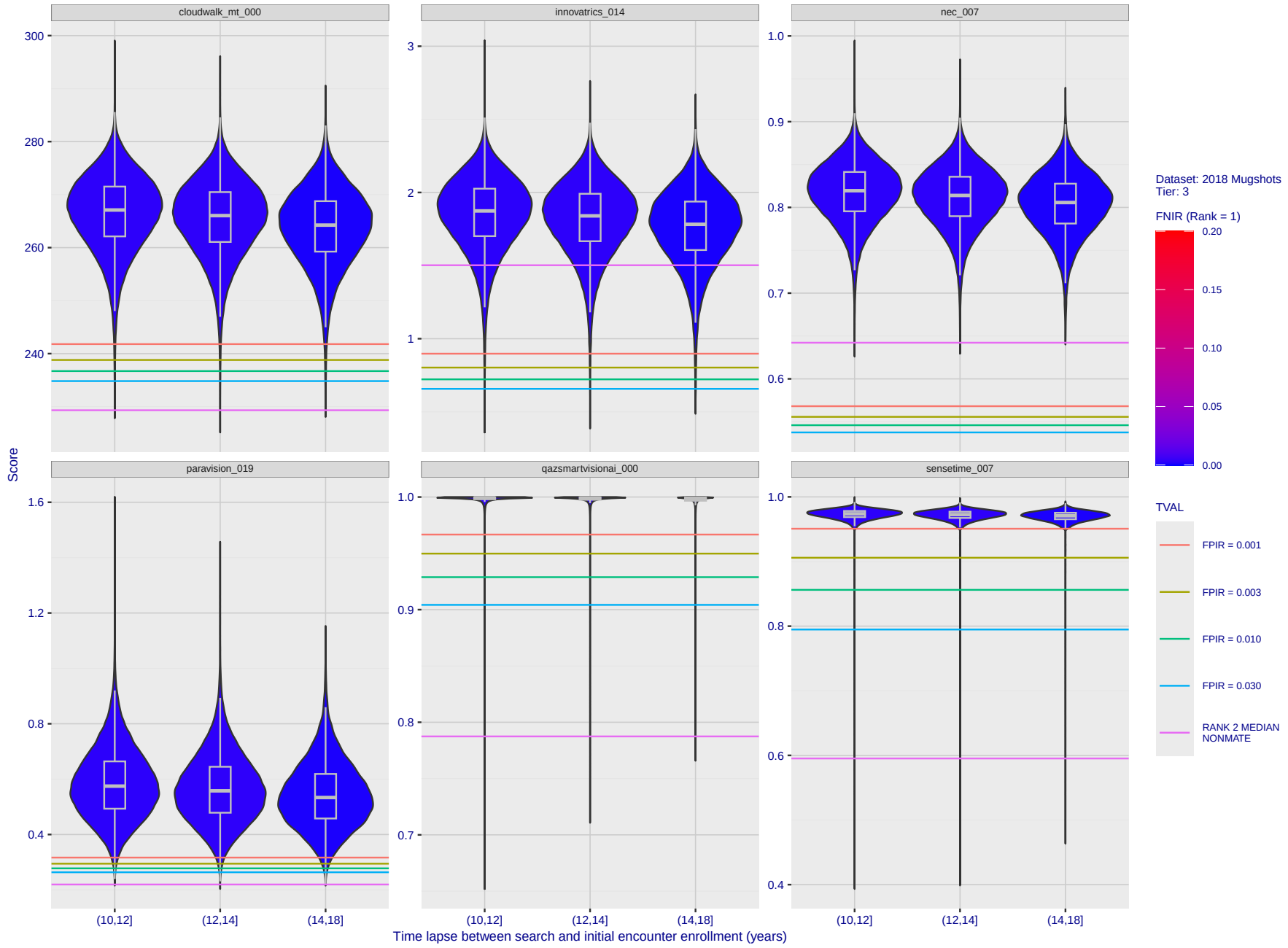

Figure 238: **[FRVT-2018 Mugshot Ageing Dataset] Native mate scores vs. time-elapsed**. *The oldest image of each individual is enrolled. Thereafter, all more recent images are searched. Mated score distributions are computed over all searches noted in row 17 of Table 1 binned by number of years between search and initial enrollment.*

This publication is available free of charge from: https://doi.org/10.6028/NIST.IR.8271

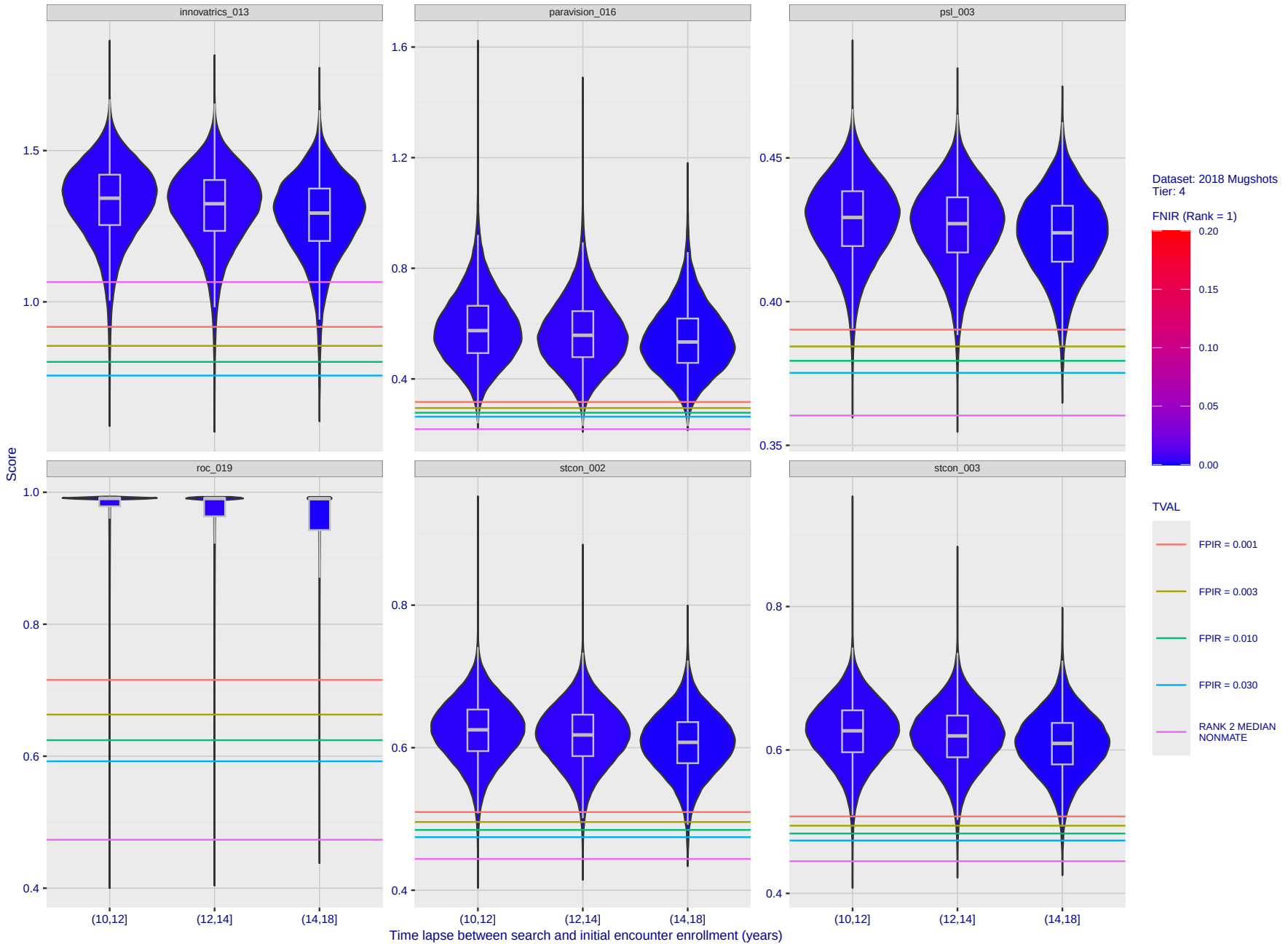

Figure 239: **[FRVT-2018 Mugshot Ageing Dataset] Native mate scores vs. time-elapsed**. *The oldest image of each individual is enrolled. Thereafter, all more recent images are searched. Mated score distributions are computed over all searches noted in row 17 of Table 1 binned by number of years between search and initial enrollment.*

2026/01/09 20:40:38
FNIR(N, R, T) = False neg. identification rate
FPIR(N, T) = False pos. identification rate
N = Num. enrolled subjects
R = Num. candidates examined
T = Threshold
T = 0 → Investigation
T > 0 → Identification

This publication is available free of charge from: https://doi.org/10.6028/NIST.IR.8271

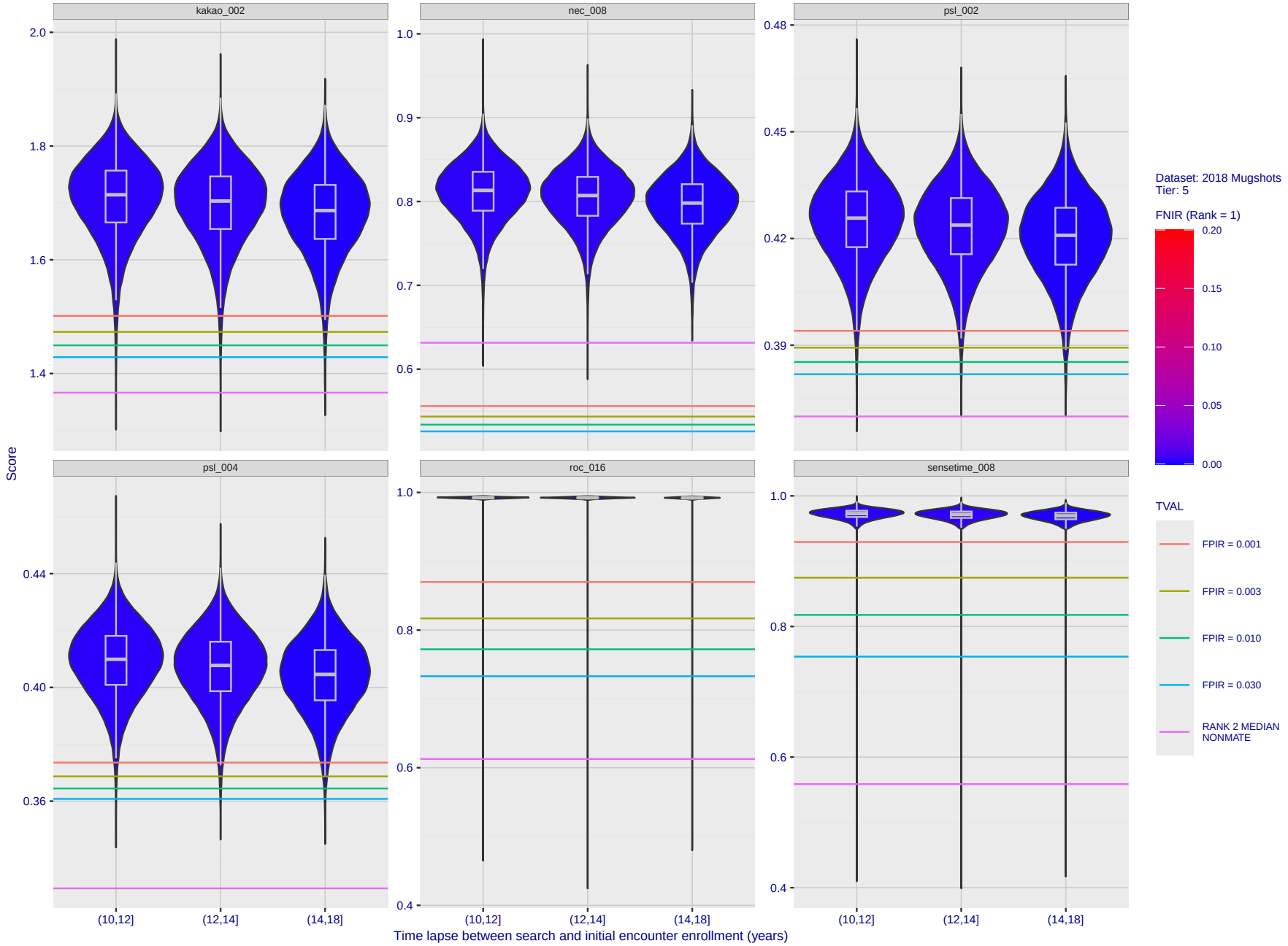

Figure 240: **[FRVT-2018 Mugshot Ageing Dataset] Native mate scores vs. time-elapsed**. *The oldest image of each individual is enrolled. Thereafter, all more recent images are searched. Mated score distributions are computed over all searches noted in row 17 of Table 1 binned by number of years between search and initial enrollment.*

This publication is available free of charge from: https://doi.org/10.6028/NIST.IR.8271

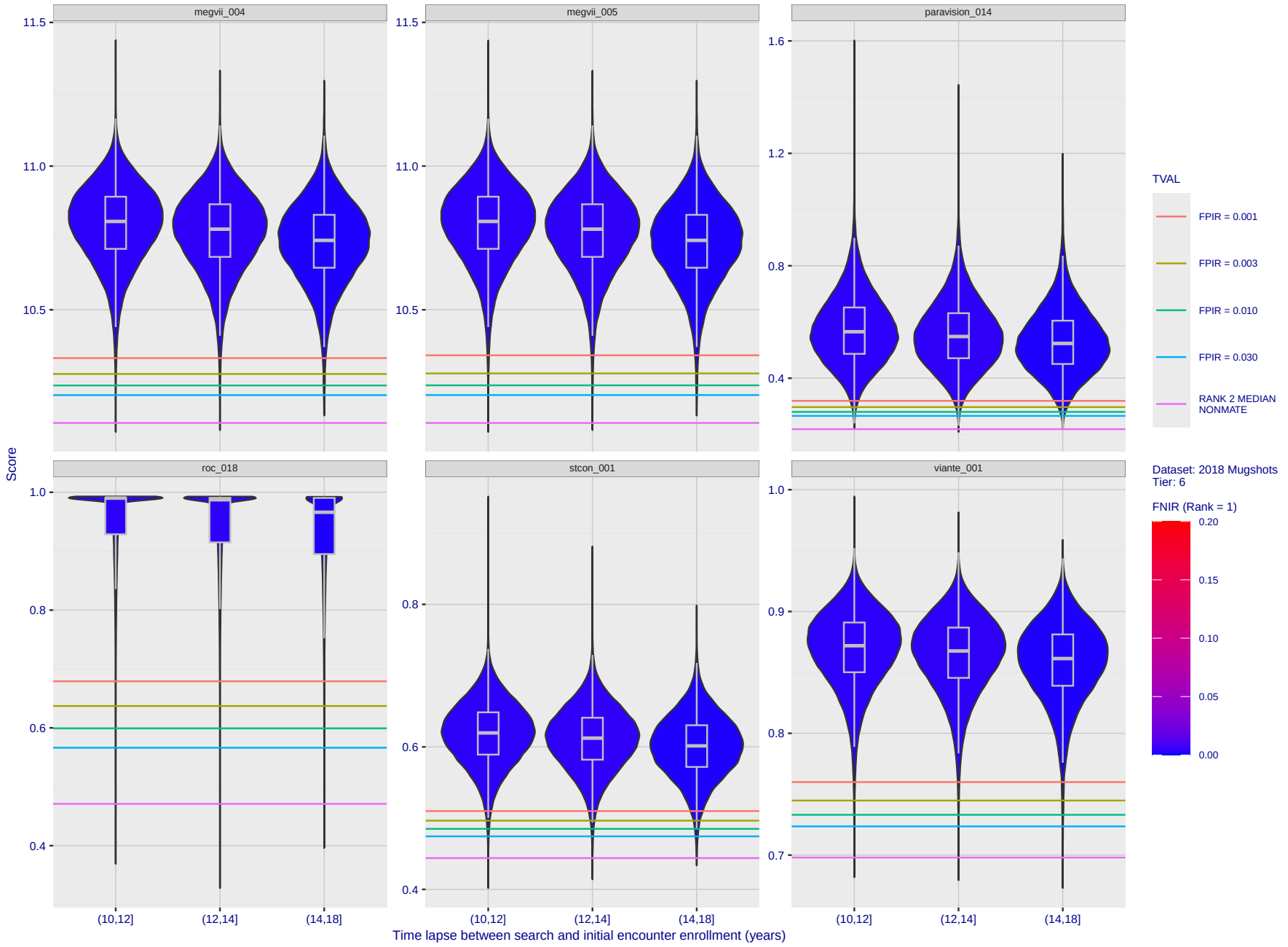

Figure 241: **[FRVT-2018 Mugshot Ageing Dataset] Native mate scores vs. time-elapsed**. *The oldest image of each individual is enrolled. Thereafter, all more recent images are searched. Mated score distributions are computed over all searches noted in row 17 of Table 1 binned by number of years between search and initial enrollment.*

2026/01/09 20:40:38

FNIR(N, R, T) = False neg. identification rate
FPIR(N, T) = False pos. identification rate

N = Num. enrolled subjects
R = Num. candidates examined

T = Threshold

T = 0 → Investigation
T > 0 → Identification

This publication is available free of charge from: https://doi.org/10.6028/NIST.IR.8271

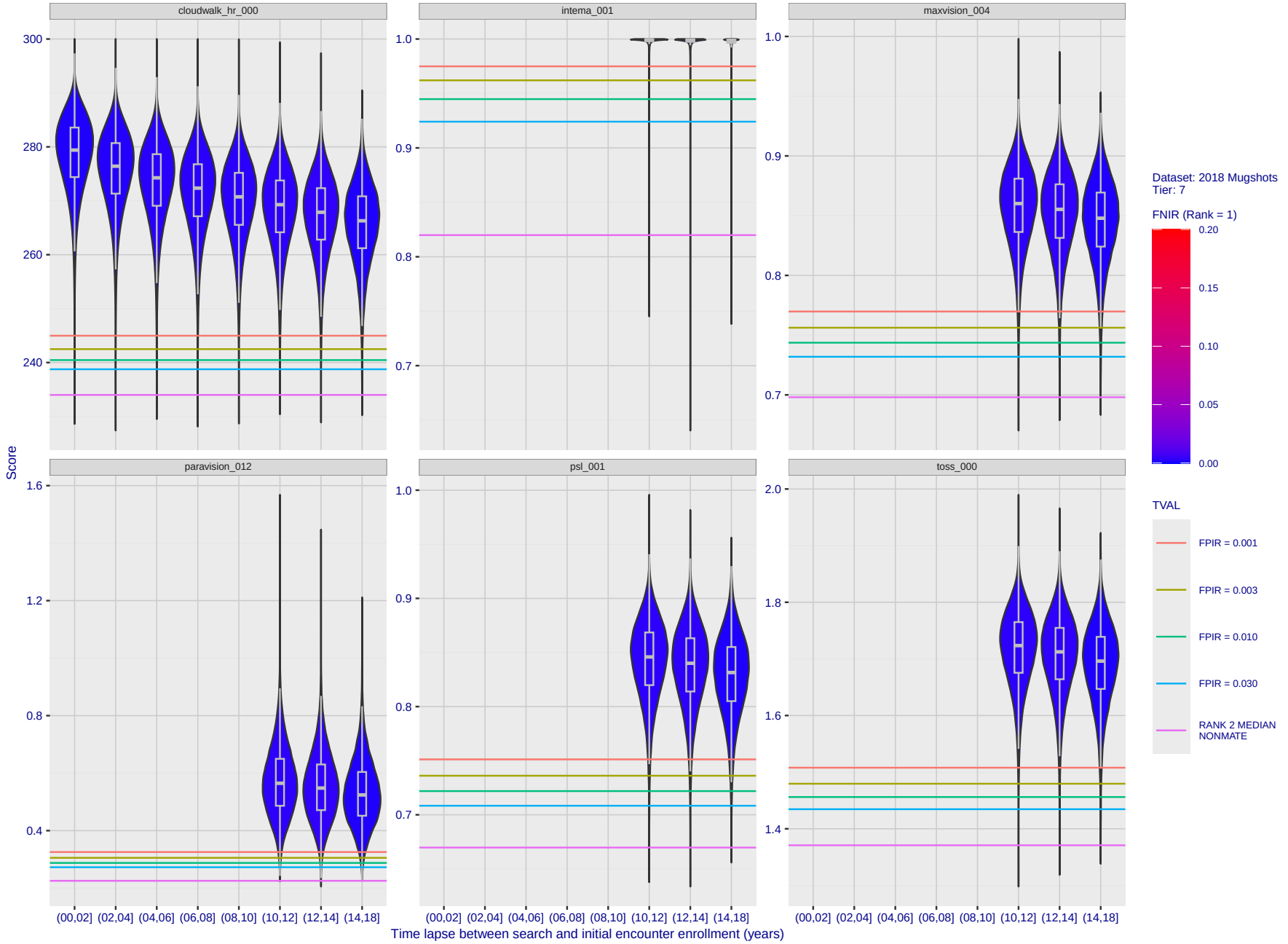

Figure 242: **[FRVT-2018 Mugshot Ageing Dataset] Native mate scores vs. time-elapsed**. *The oldest image of each individual is enrolled. Thereafter, all more recent images are searched. Mated score distributions are computed over all searches noted in row 17 of Table 1 binned by number of years between search and initial enrollment.*

This publication is available free of charge from: https://doi.org/10.6028/NIST.IR.8271

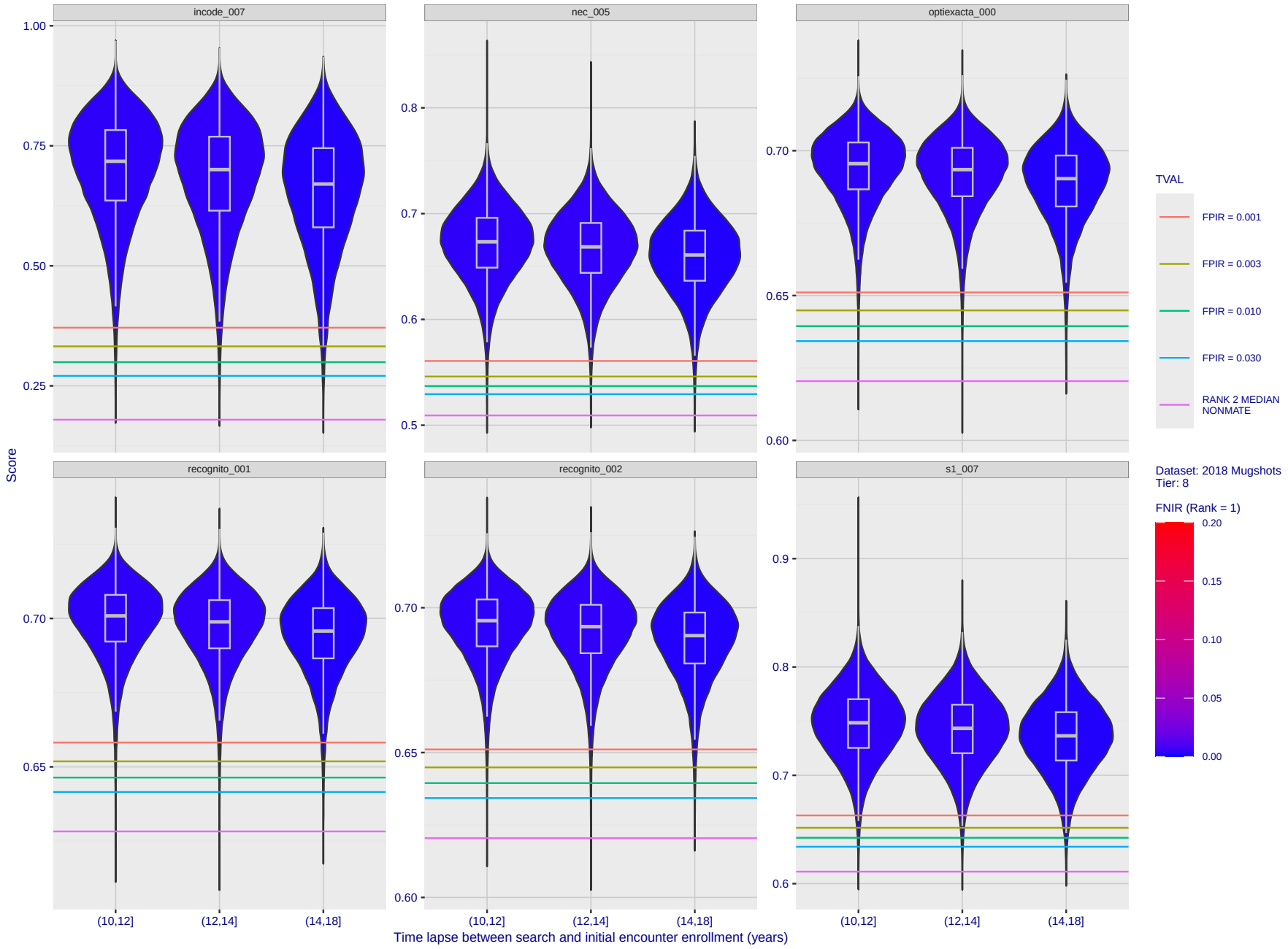

Figure 243: **[FRVT-2018 Mugshot Ageing Dataset] Native mate scores vs. time-elapsed**. *The oldest image of each individual is enrolled. Thereafter, all more recent images are searched. Mated score distributions are computed over all searches noted in row 17 of Table 1 binned by number of years between search and initial enrollment.*

2026/01/09 20:40:38
FNIR(N, R, T) = False neg. identification rate
FPIR(N, T) = False pos. identification rate
N = Num. enrolled subjects
R = Num. candidates examined
T = Threshold
T = 0 → Investigation
T > 0 → Identification

This publication is available free of charge from: https://doi.org/10.6028/NIST.IR.8271

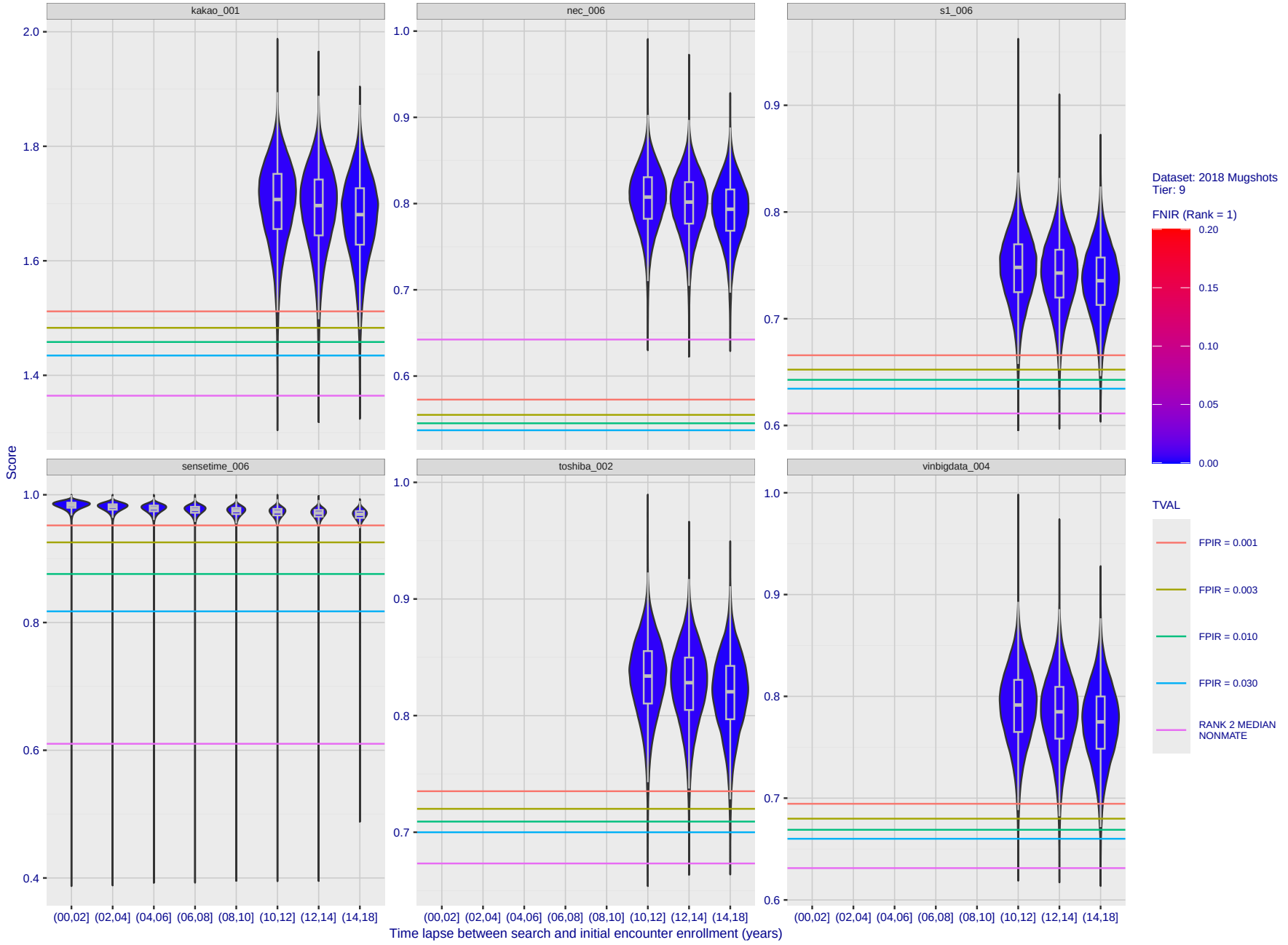

Figure 244: **[FRVT-2018 Mugshot Ageing Dataset] Native mate scores vs. time-elapsed**. *The oldest image of each individual is enrolled. Thereafter, all more recent images are searched. Mated score distributions are computed over all searches noted in row 17 of Table 1 binned by number of years between search and initial enrollment.*

2026/01/09 20:40:38
FNIR(N, R, T) = False neg. identification rate
FPIR(N, T) = False pos. identification rate
N = Num. enrolled subjects
R = Num. candidates examined
T = Threshold
T = 0 → Investigation
T > 0 → Identification

This publication is available free of charge from: https://doi.org/10.6028/NIST.IR.8271

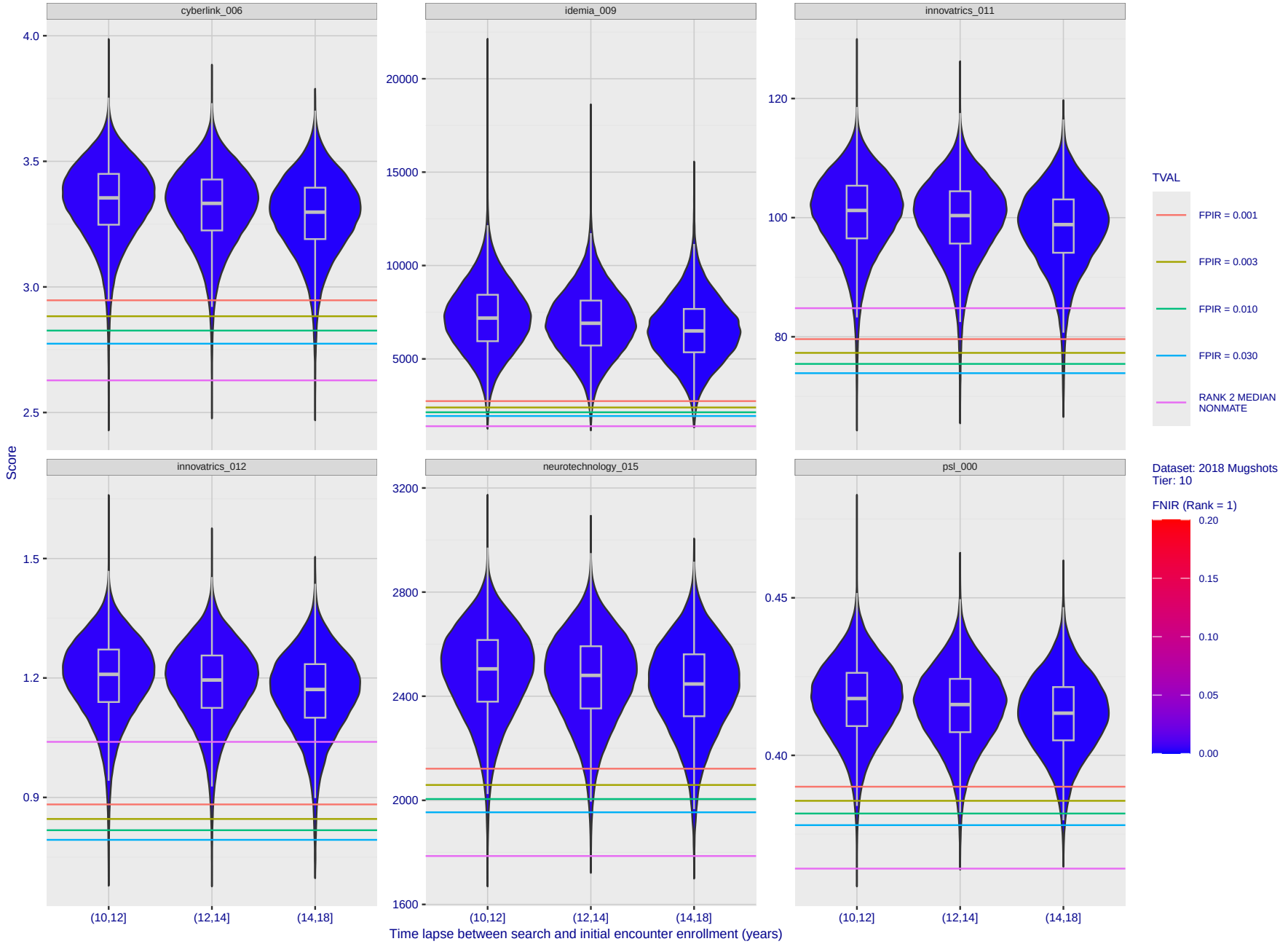

Figure 245: **[FRVT-2018 Mugshot Ageing Dataset] Native mate scores vs. time-elapsed**. *The oldest image of each individual is enrolled. Thereafter, all more recent images are searched. Mated score distributions are computed over all searches noted in row 17 of Table 1 binned by number of years between search and initial enrollment.*

2026/01/09 20:40:38
FNIR(N, R, T) = False neg. identification rate
FPIR(N, T) = False pos. identification rate
N = Num. enrolled subjects
R = Num. candidates examined
T = Threshold
T = 0 → Investigation
T > 0 → Identification

This publication is available free of charge from: https://doi.org/10.6028/NIST.IR.8271

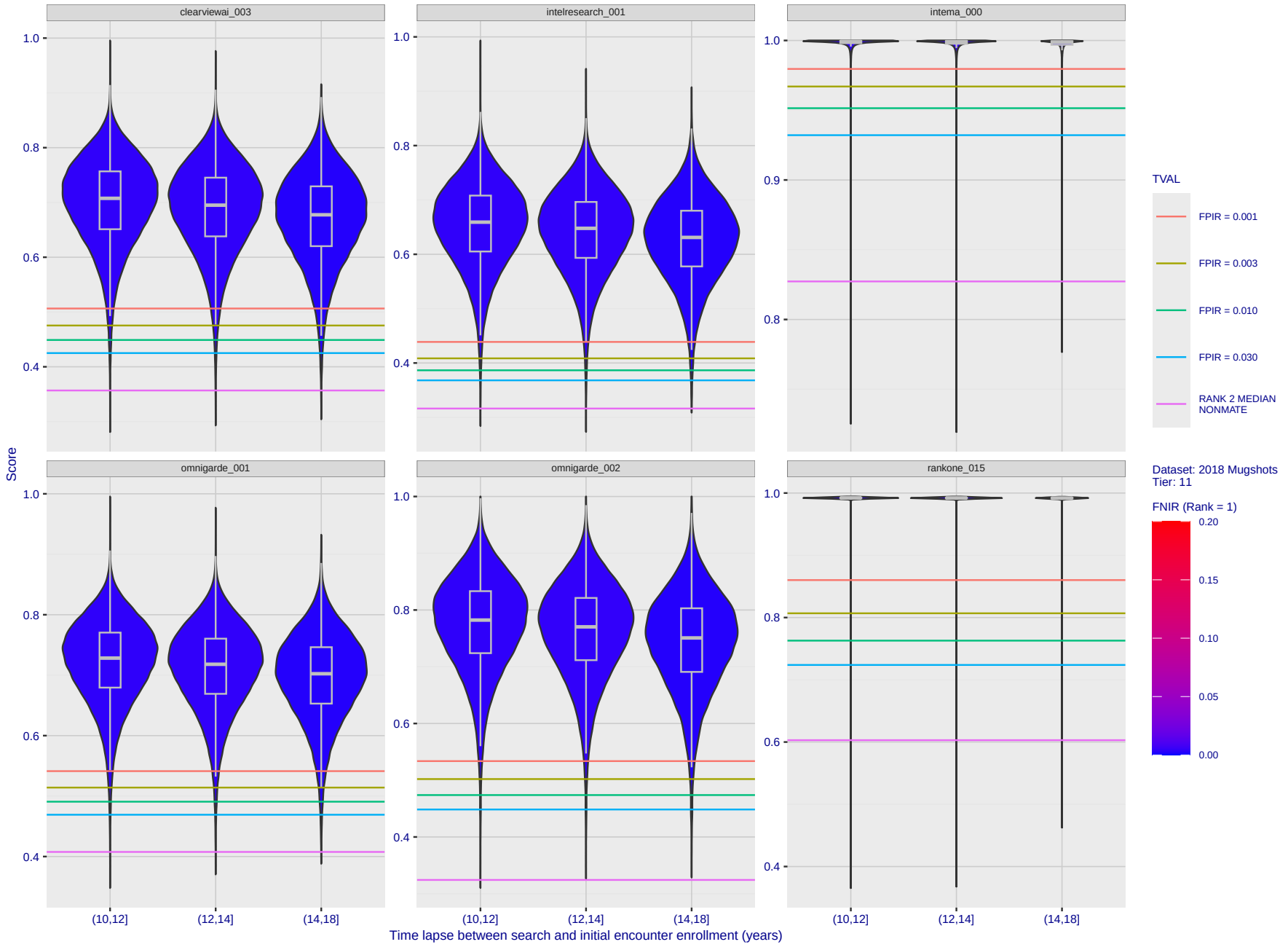

Figure 246: **[FRVT-2018 Mugshot Ageing Dataset] Native mate scores vs. time-elapsed**. *The oldest image of each individual is enrolled. Thereafter, all more recent images are searched. Mated score distributions are computed over all searches noted in row 17 of Table 1 binned by number of years between search and initial enrollment.*

This publication is available free of charge from: https://doi.org/10.6028/NIST.IR.8271

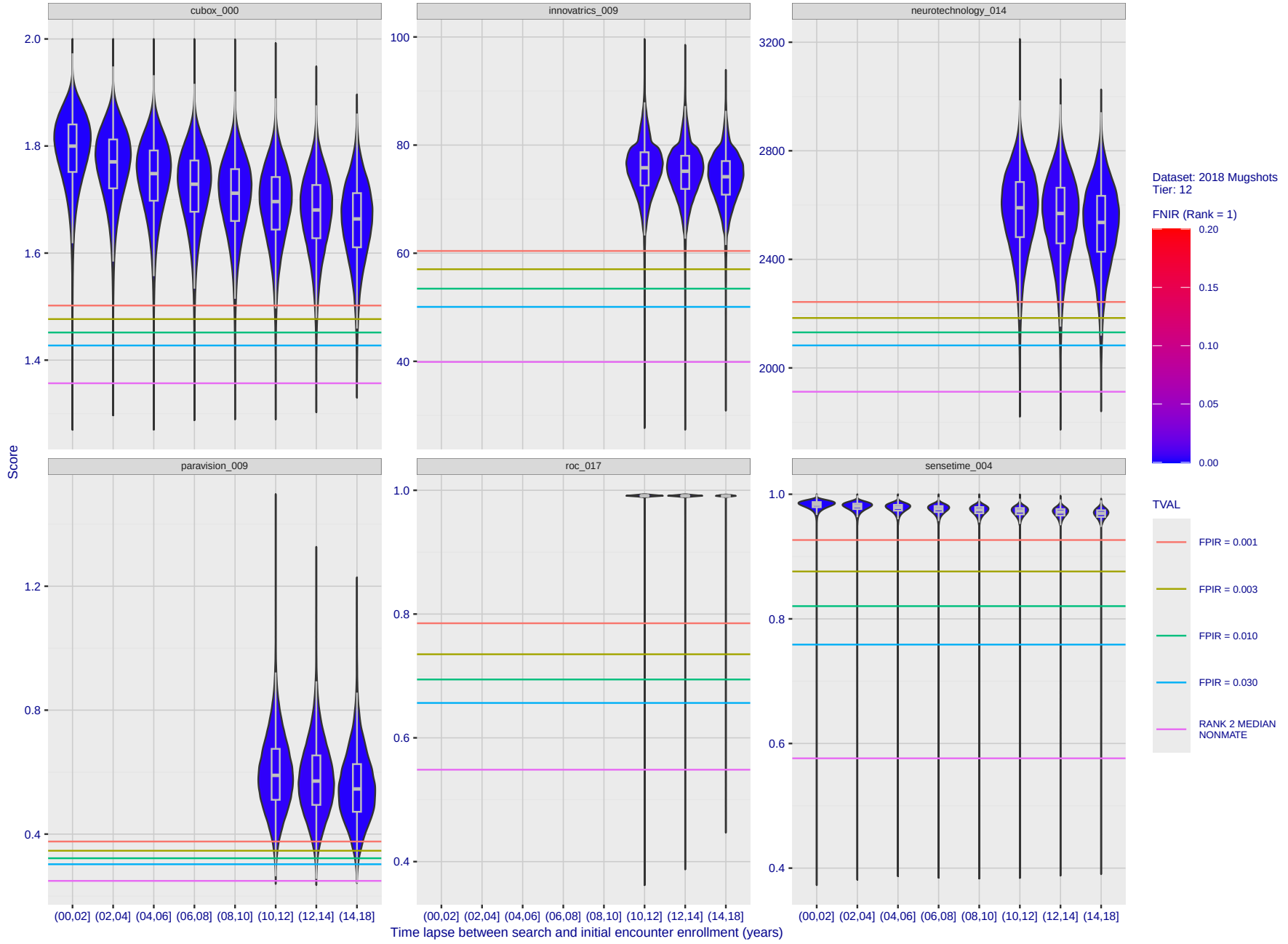

Figure 247: **[FRVT-2018 Mugshot Ageing Dataset] Native mate scores vs. time-elapsed**. *The oldest image of each individual is enrolled. Thereafter, all more recent images are searched. Mated score distributions are computed over all searches noted in row 17 of Table 1 binned by number of years between search and initial enrollment.*

This publication is available free of charge from: https://doi.org/10.6028/NIST.IR.8271

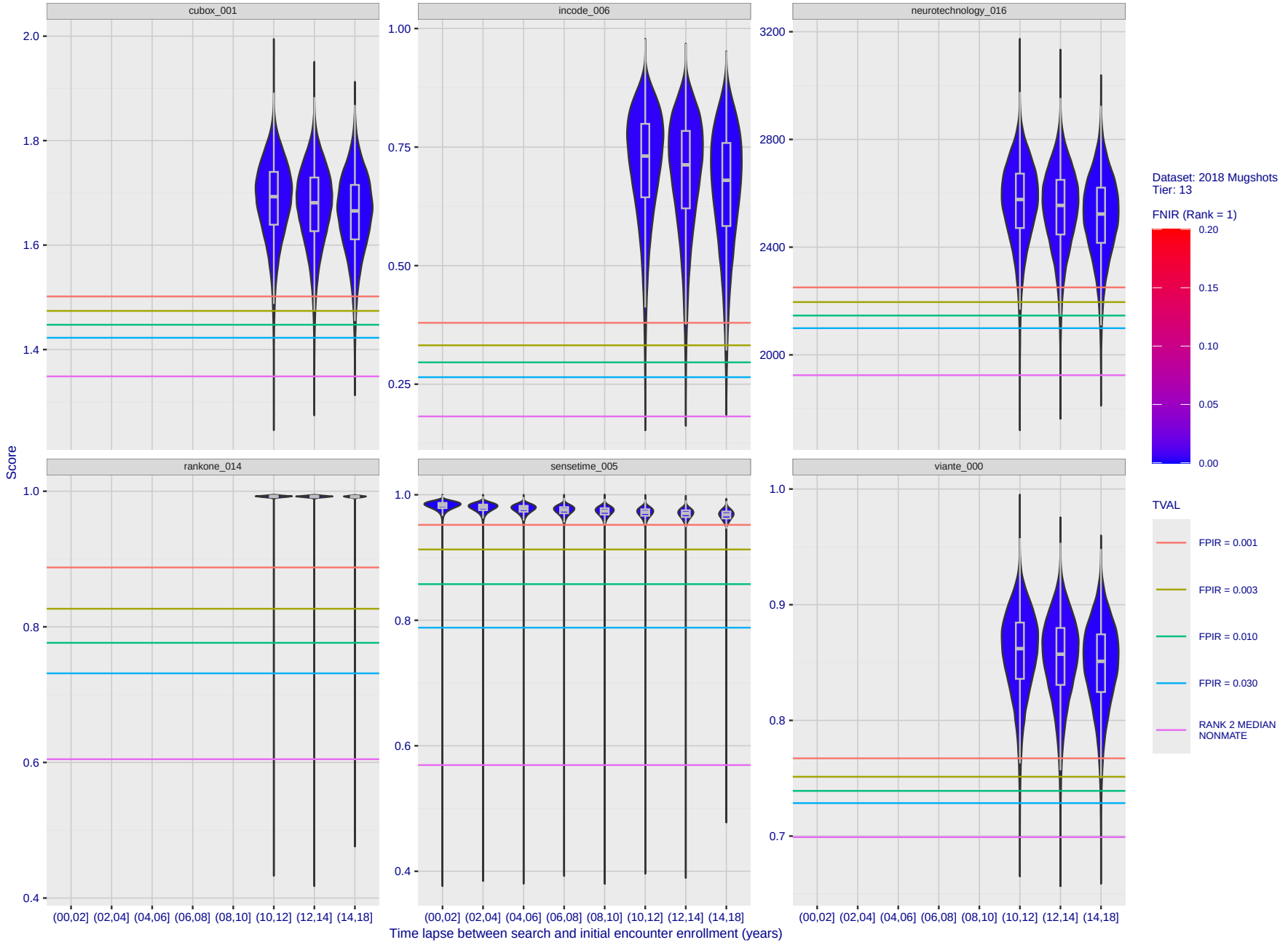

Figure 248: **[FRVT-2018 Mugshot Ageing Dataset] Native mate scores vs. time-elapsed**. *The oldest image of each individual is enrolled. Thereafter, all more recent images are searched. Mated score distributions are computed over all searches noted in row 17 of Table 1 binned by number of years between search and initial enrollment.*

This publication is available free of charge from: https://doi.org/10.6028/NIST.IR.8271

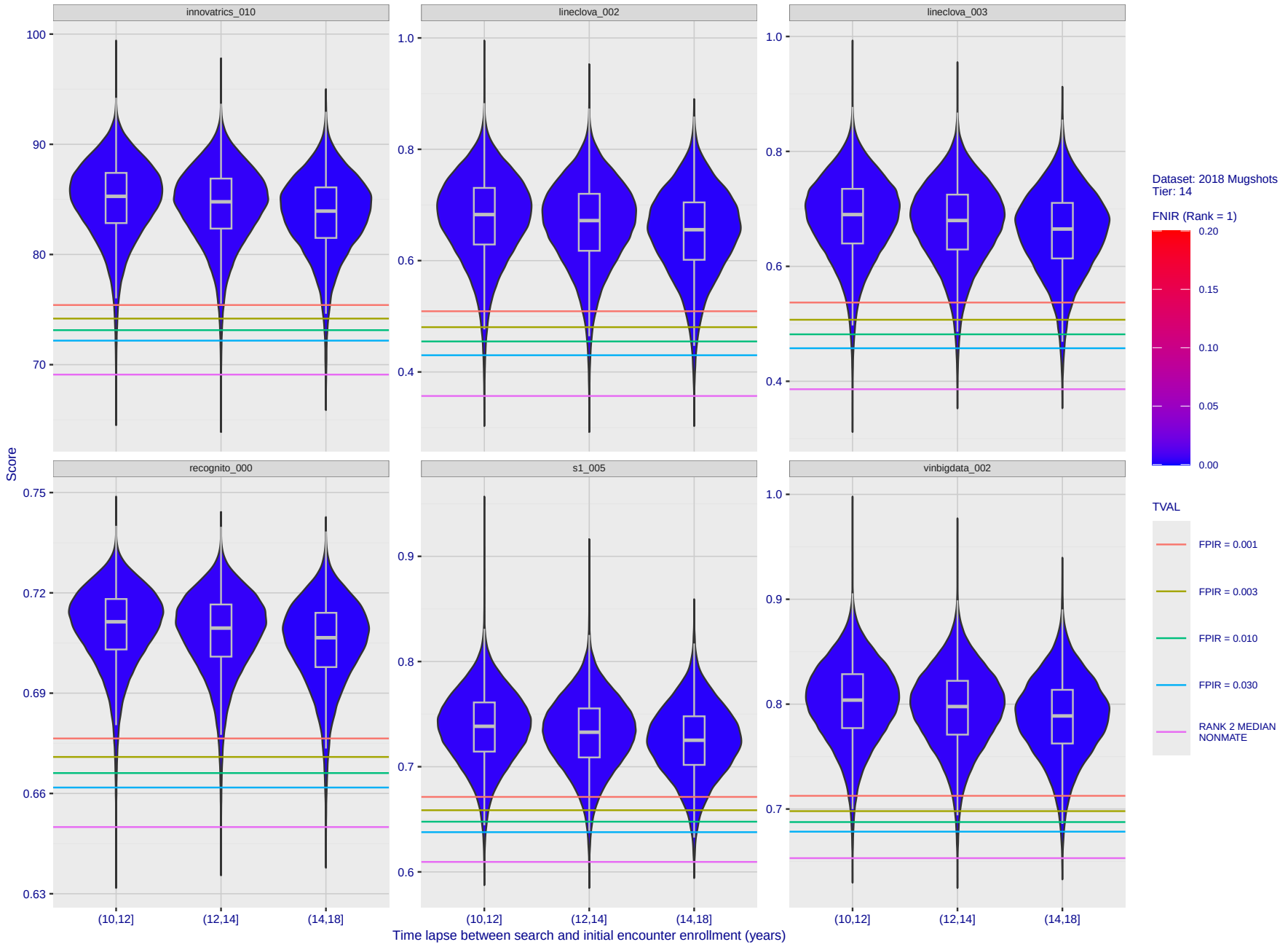

Figure 249: **[FRVT-2018 Mugshot Ageing Dataset] Native mate scores vs. time-elapsed**. *The oldest image of each individual is enrolled. Thereafter, all more recent images are searched. Mated score distributions are computed over all searches noted in row 17 of Table 1 binned by number of years between search and initial enrollment.*

This publication is available free of charge from: https://doi.org/10.6028/NIST.IR.8271

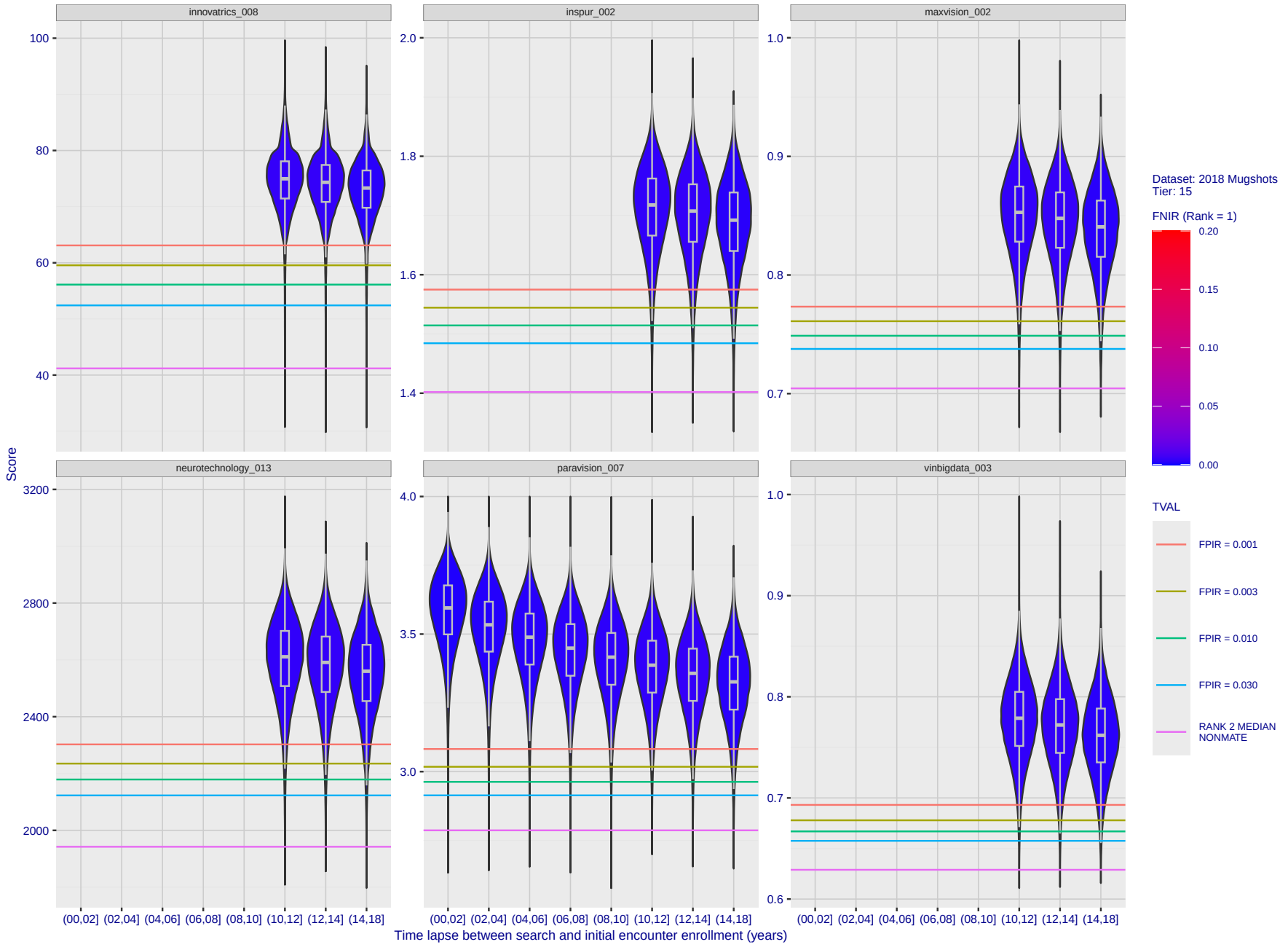

Figure 250: **[FRVT-2018 Mugshot Ageing Dataset] Native mate scores vs. time-elapsed**. *The oldest image of each individual is enrolled. Thereafter, all more recent images are searched. Mated score distributions are computed over all searches noted in row 17 of Table 1 binned by number of years between search and initial enrollment.*

This publication is available free of charge from: https://doi.org/10.6028/NIST.IR.8271

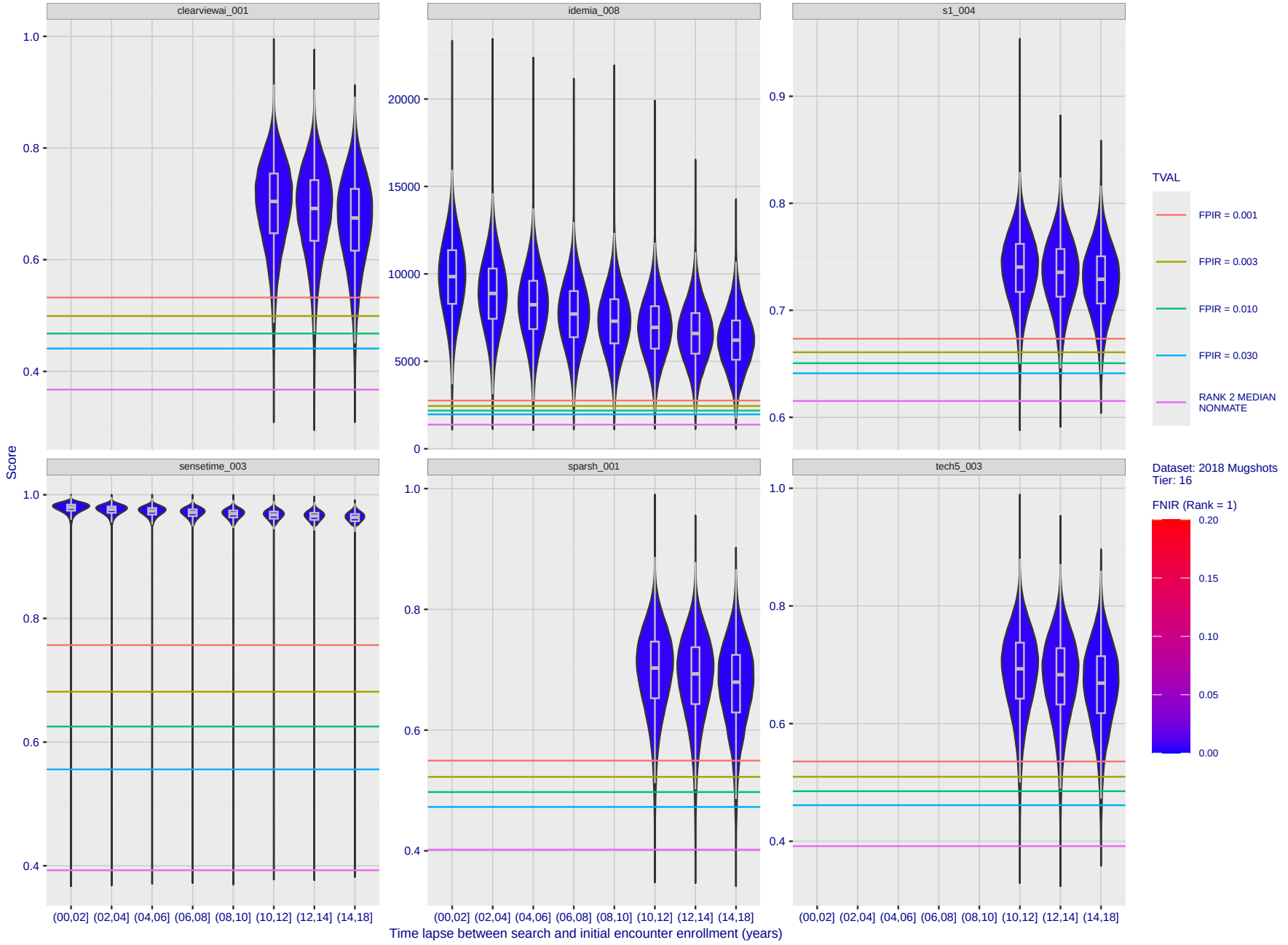

Figure 251: **[FRVT-2018 Mugshot Ageing Dataset] Native mate scores vs. time-elapsed**. *The oldest image of each individual is enrolled. Thereafter, all more recent images are searched. Mated score distributions are computed over all searches noted in row 17 of Table 1 binned by number of years between search and initial enrollment.*

2026/01/09 20:40:38
FNIR(N, R, T) = False neg. identification rate
FPIR(N, T) = False pos. identification rate
N = Num. enrolled subjects
R = Num. candidates examined
T = Threshold
T = 0 → Investigation
T > 0 → Identification

This publication is available free of charge from: https://doi.org/10.6028/NIST.IR.8271

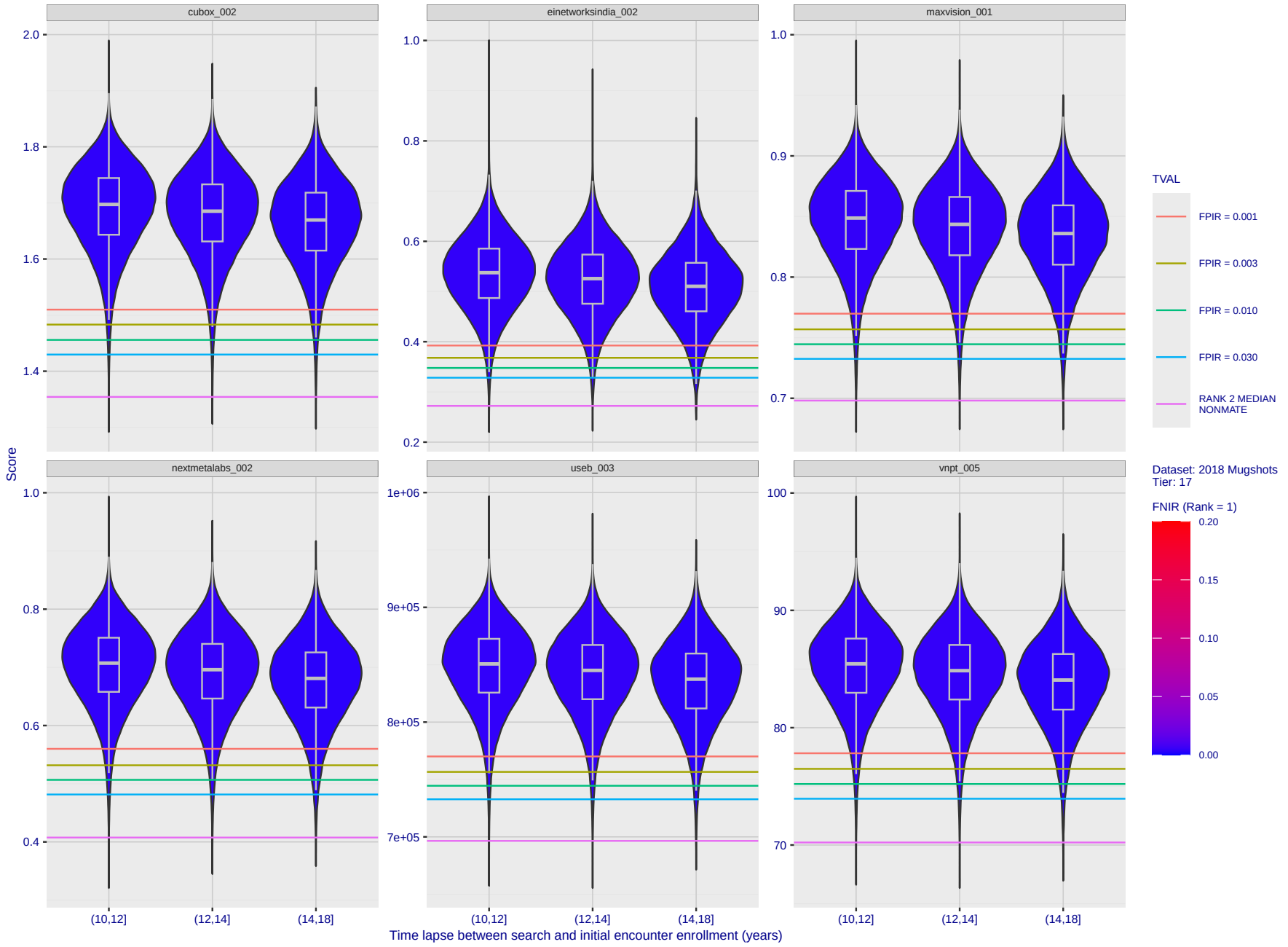

Figure 252: **[FRVT-2018 Mugshot Ageing Dataset] Native mate scores vs. time-elapsed**. *The oldest image of each individual is enrolled. Thereafter, all more recent images are searched. Mated score distributions are computed over all searches noted in row 17 of Table 1 binned by number of years between search and initial enrollment.*

2026/01/09 20:40:38
FNIR(N, R, T) = False neg. identification rate
FPIR(N, T) = False pos. identification rate
N = Num. enrolled subjects
R = Num. candidates examined
T = Threshold
T = 0 → Investigation
T > 0 → Identification

This publication is available free of charge from: https://doi.org/10.6028/NIST.IR.8271

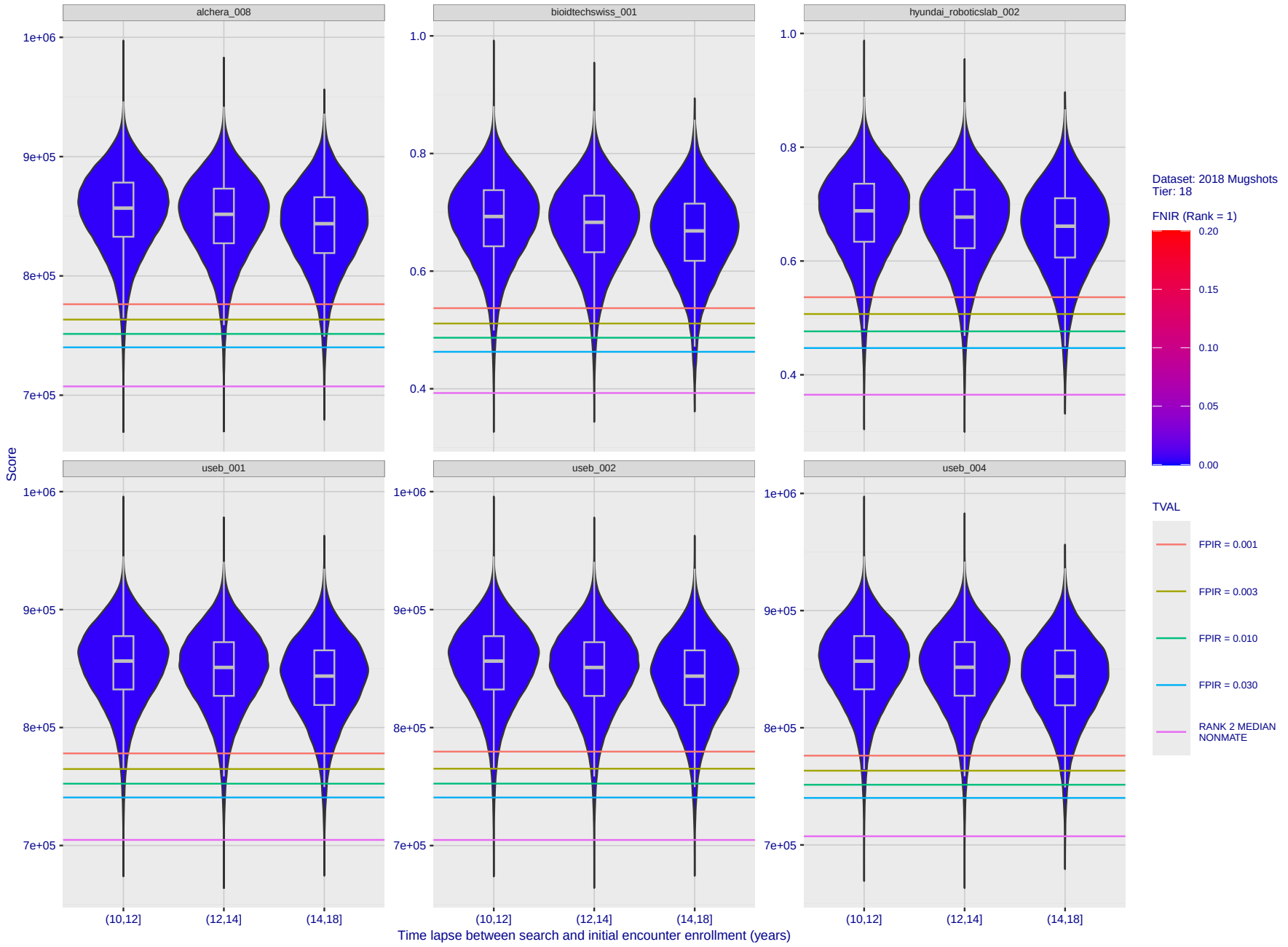

Figure 253: **[FRVT-2018 Mugshot Ageing Dataset] Native mate scores vs. time-elapsed**. *The oldest image of each individual is enrolled. Thereafter, all more recent images are searched. Mated score distributions are computed over all searches noted in row 17 of Table 1 binned by number of years between search and initial enrollment.*

This publication is available free of charge from: https://doi.org/10.6028/NIST.IR.8271

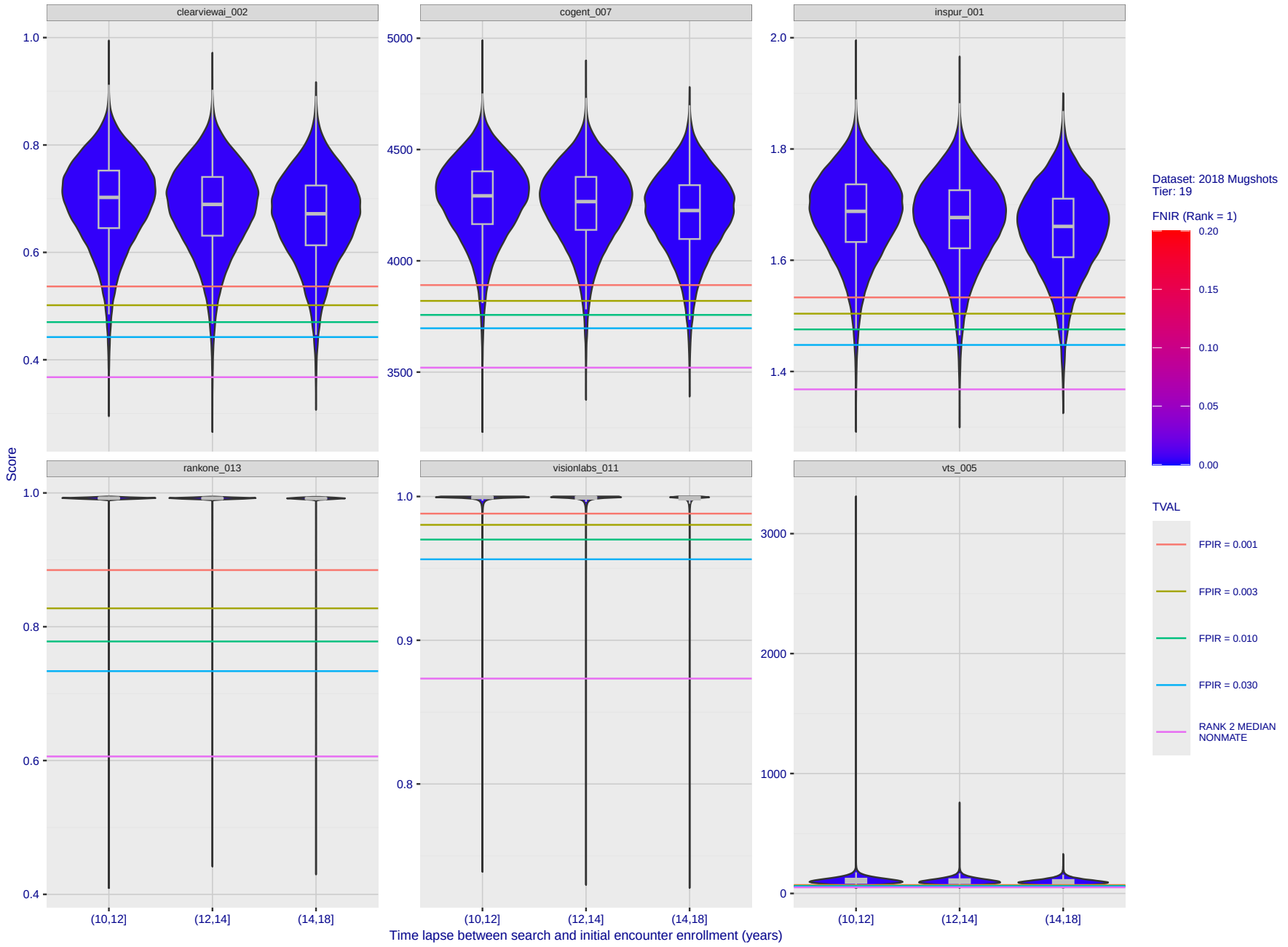

Figure 254: **[FRVT-2018 Mugshot Ageing Dataset] Native mate scores vs. time-elapsed**. *The oldest image of each individual is enrolled. Thereafter, all more recent images are searched. Mated score distributions are computed over all searches noted in row 17 of Table 1 binned by number of years between search and initial enrollment.*

This publication is available free of charge from: https://doi.org/10.6028/NIST.IR.8271

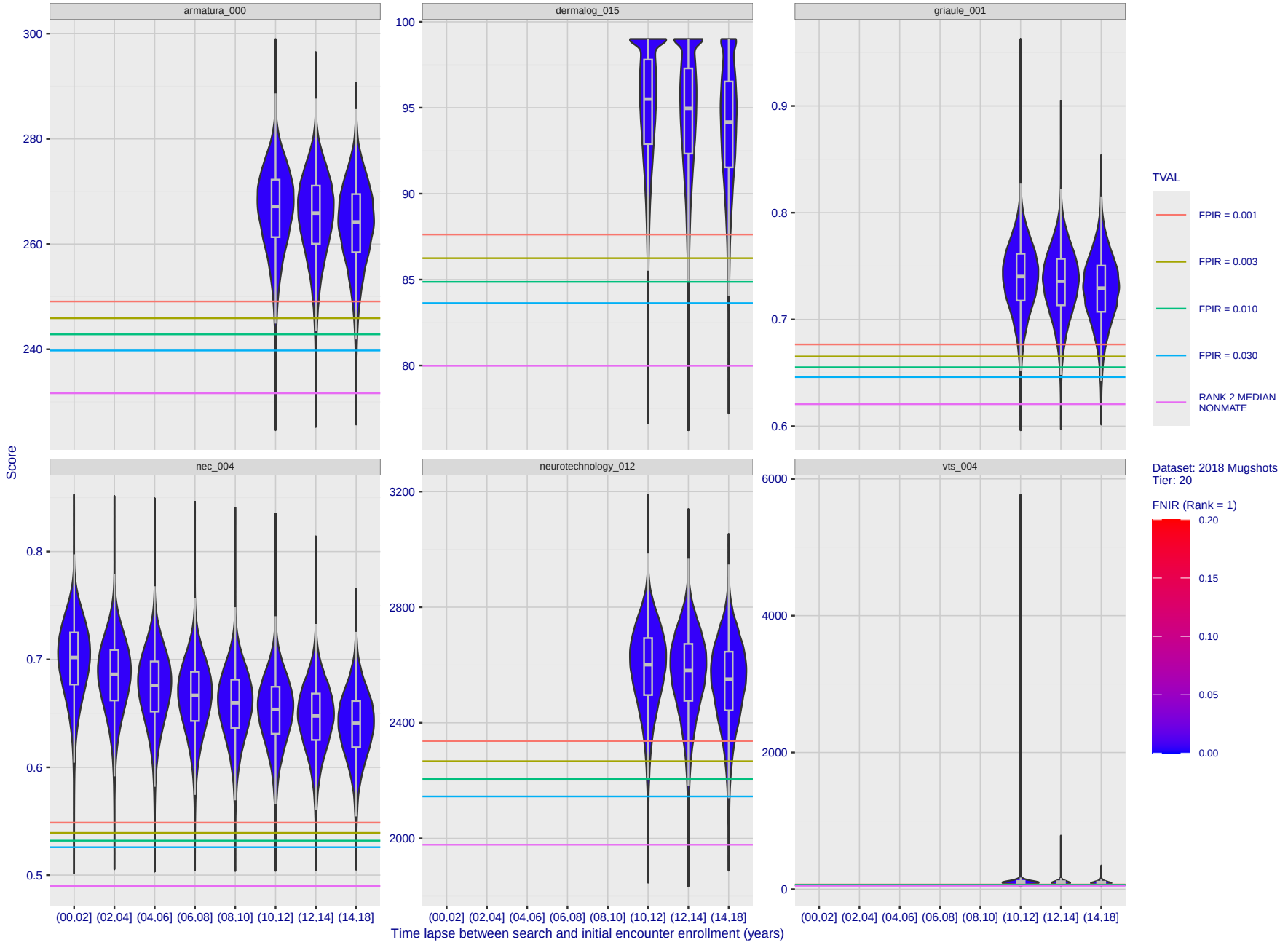

Figure 255: **[FRVT-2018 Mugshot Ageing Dataset] Native mate scores vs. time-elapsed**. *The oldest image of each individual is enrolled. Thereafter, all more recent images are searched. Mated score distributions are computed over all searches noted in row 17 of Table 1 binned by number of years between search and initial enrollment.*

2026/01/09 20:40:38
FNIR(N, R, T) = False neg. identification rate
FPIR(N, T) = False pos. identification rate
N = Num. enrolled subjects
R = Num. candidates examined
T = Threshold
T = 0 → Investigation
T > 0 → Identification

This publication is available free of charge from: https://doi.org/10.6028/NIST.IR.8271

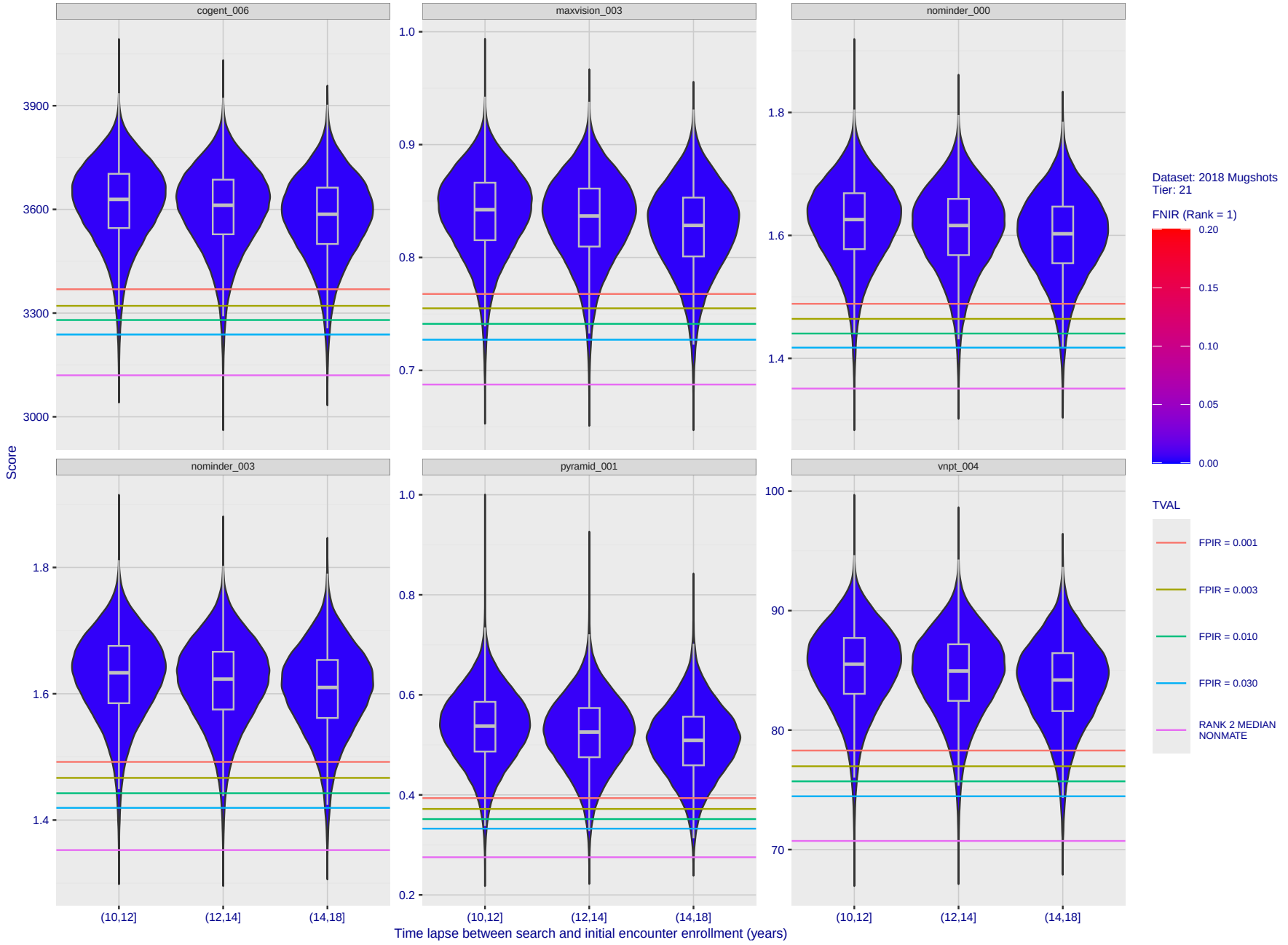

Figure 256: **[FRVT-2018 Mugshot Ageing Dataset] Native mate scores vs. time-elapsed**. *The oldest image of each individual is enrolled. Thereafter, all more recent images are searched. Mated score distributions are computed over all searches noted in row 17 of Table 1 binned by number of years between search and initial enrollment.*

2026/01/09 20:40:38
FNIR(N, R, T) = False neg. identification rate
FPIR(N, T) = False pos. identification rate
N = Num. enrolled subjects
R = Num. candidates examined
T = Threshold
T = 0 → Investigation
T > 0 → Identification

This publication is available free of charge from: https://doi.org/10.6028/NIST.IR.8271

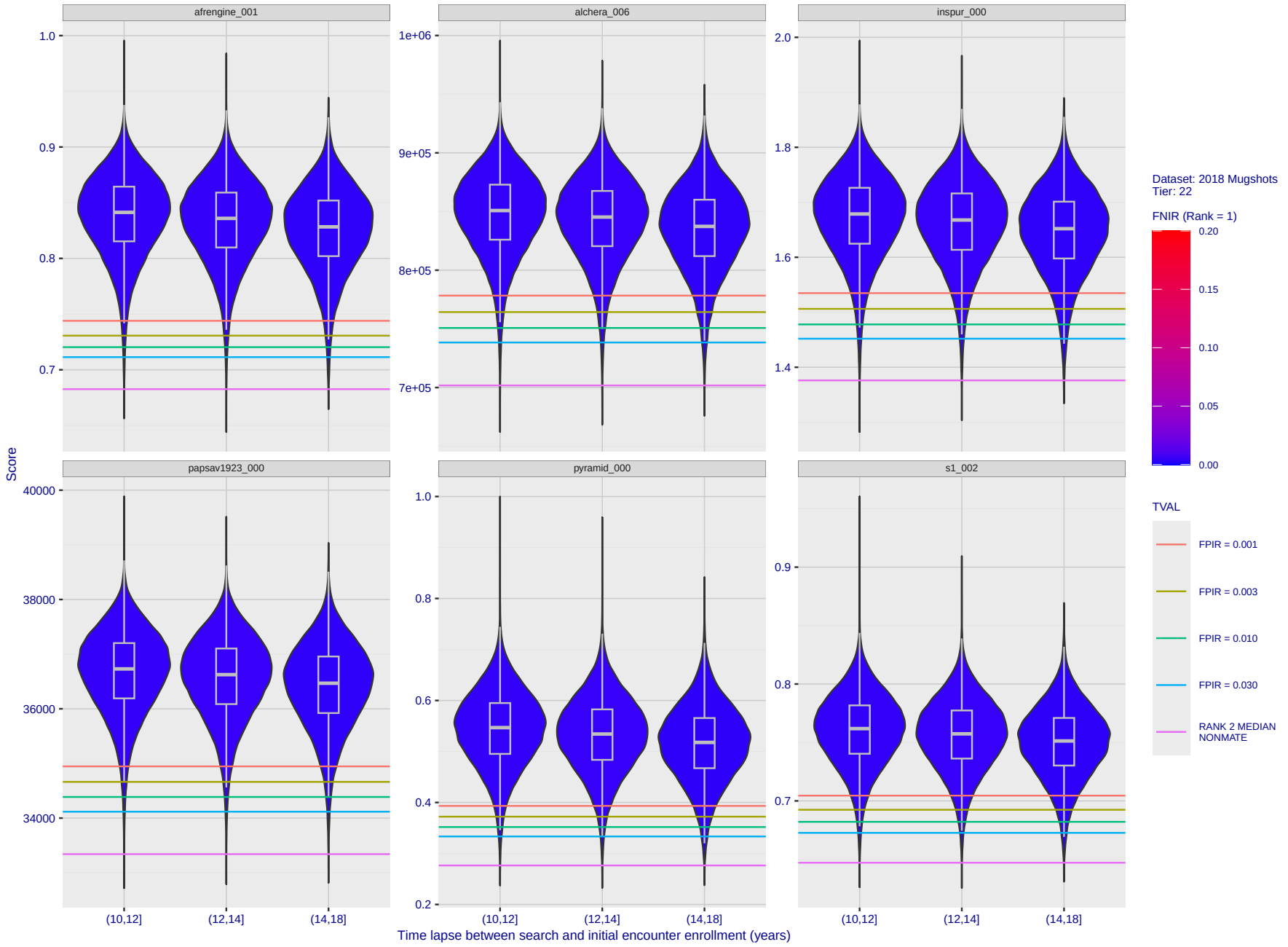

Figure 257: **[FRVT-2018 Mugshot Ageing Dataset] Native mate scores vs. time-elapsed**. *The oldest image of each individual is enrolled. Thereafter, all more recent images are searched. Mated score distributions are computed over all searches noted in row 17 of Table 1 binned by number of years between search and initial enrollment.*

This publication is available free of charge from: https://doi.org/10.6028/NIST.IR.8271

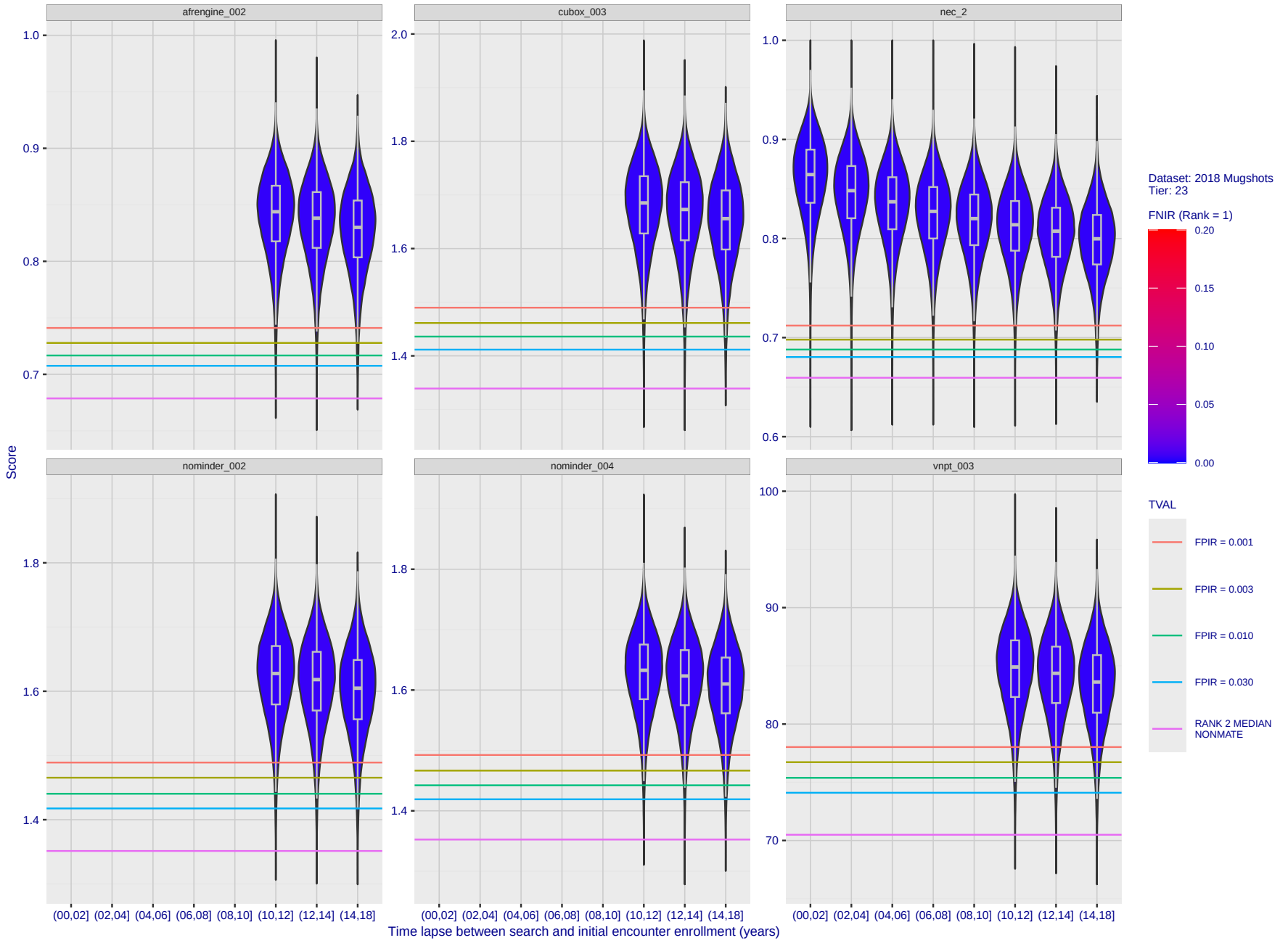

Figure 258: **[FRVT-2018 Mugshot Ageing Dataset] Native mate scores vs. time-elapsed**. *The oldest image of each individual is enrolled. Thereafter, all more recent images are searched. Mated score distributions are computed over all searches noted in row 17 of Table 1 binned by number of years between search and initial enrollment.*

2026/01/09 20:40:38
FNIR(N, R, T) = False neg. identification rate
FPIR(N, T) = False pos. identification rate
N = Num. enrolled subjects
R = Num. candidates examined
T = Threshold
T = 0 → Investigation
T > 0 → Identification

This publication is available free of charge from: https://doi.org/10.6028/NIST.IR.8271

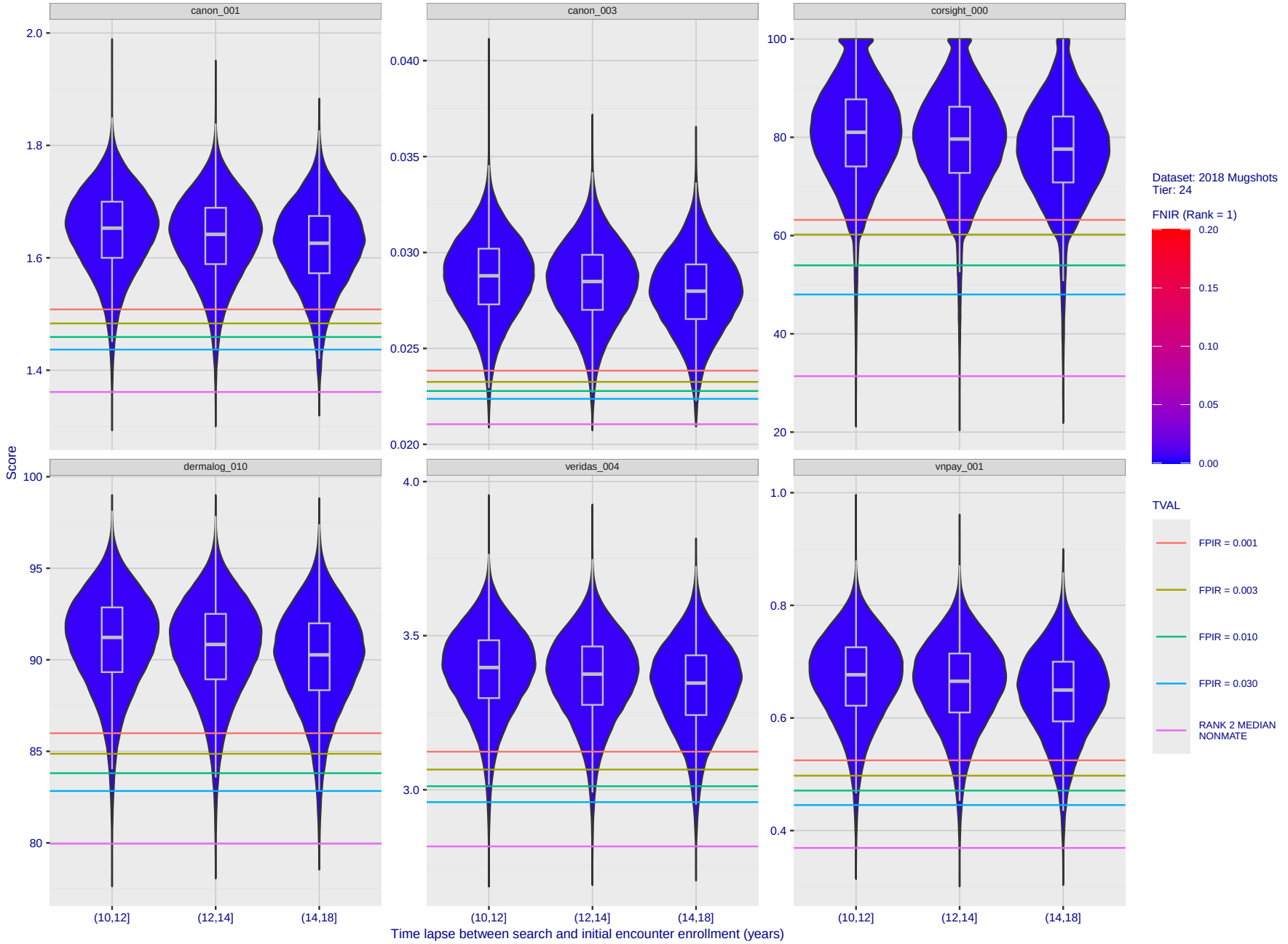

Figure 259: **[FRVT-2018 Mugshot Ageing Dataset] Native mate scores vs. time-elapsed**. *The oldest image of each individual is enrolled. Thereafter, all more recent images are searched. Mated score distributions are computed over all searches noted in row 17 of Table 1 binned by number of years between search and initial enrollment.*

2026/01/09 20:40:38
FNIR(N, R, T) = False neg. identification rate
FPIR(N, T) = False pos. identification rate
N = Num. enrolled subjects
R = Num. candidates examined
T = Threshold
T = 0 → Investigation
T > 0 → Identification

This publication is available free of charge from: https://doi.org/10.6028/NIST.IR.8271

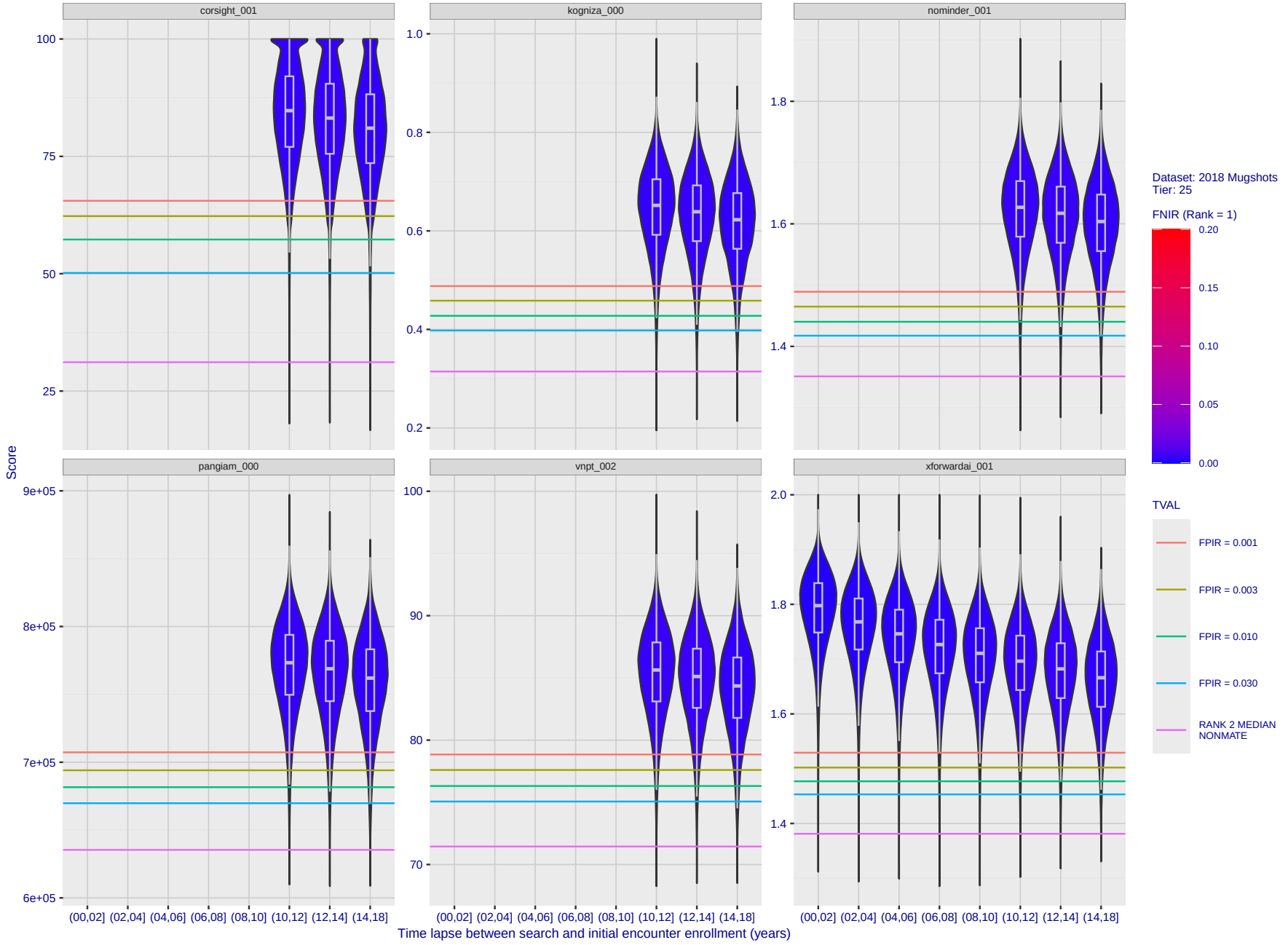

Figure 260: **[FRVT-2018 Mugshot Ageing Dataset] Native mate scores vs. time-elapsed**. *The oldest image of each individual is enrolled. Thereafter, all more recent images are searched. Mated score distributions are computed over all searches noted in row 17 of Table 1 binned by number of years between search and initial enrollment.*

This publication is available free of charge from: https://doi.org/10.6028/NIST.IR.8271

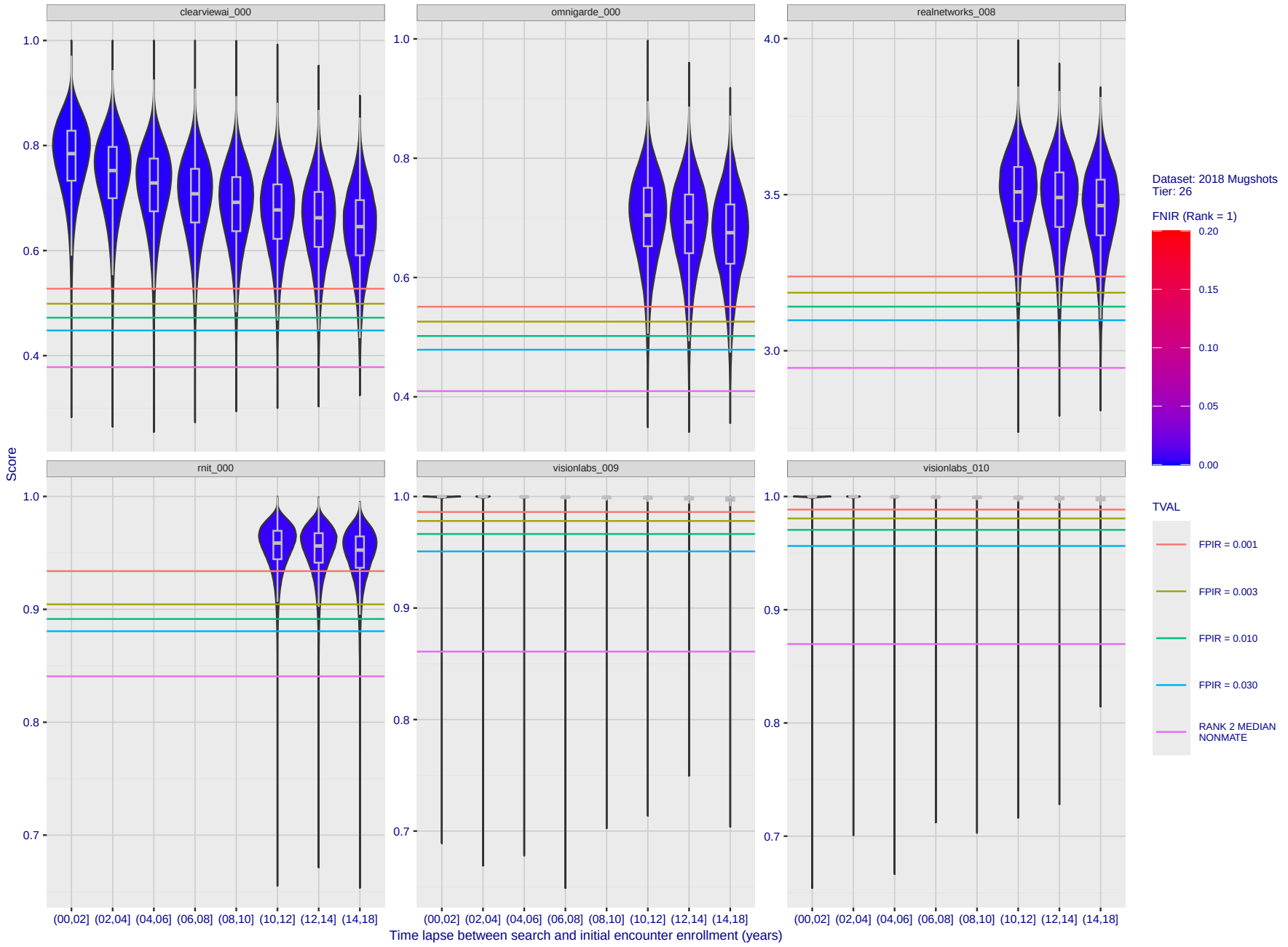

Figure 261: **[FRVT-2018 Mugshot Ageing Dataset] Native mate scores vs. time-elapsed**. *The oldest image of each individual is enrolled. Thereafter, all more recent images are searched. Mated score distributions are computed over all searches noted in row 17 of Table 1 binned by number of years between search and initial enrollment.*

2026/01/09 20:40:38
FNIR(N, R, T) = False neg. identification rate
FPIR(N, T) = False pos. identification rate
N = Num. enrolled subjects
R = Num. candidates examined
T = Threshold
T = 0 → Investigation
T > 0 → Identification

This publication is available free of charge from: https://doi.org/10.6028/NIST.IR.8271

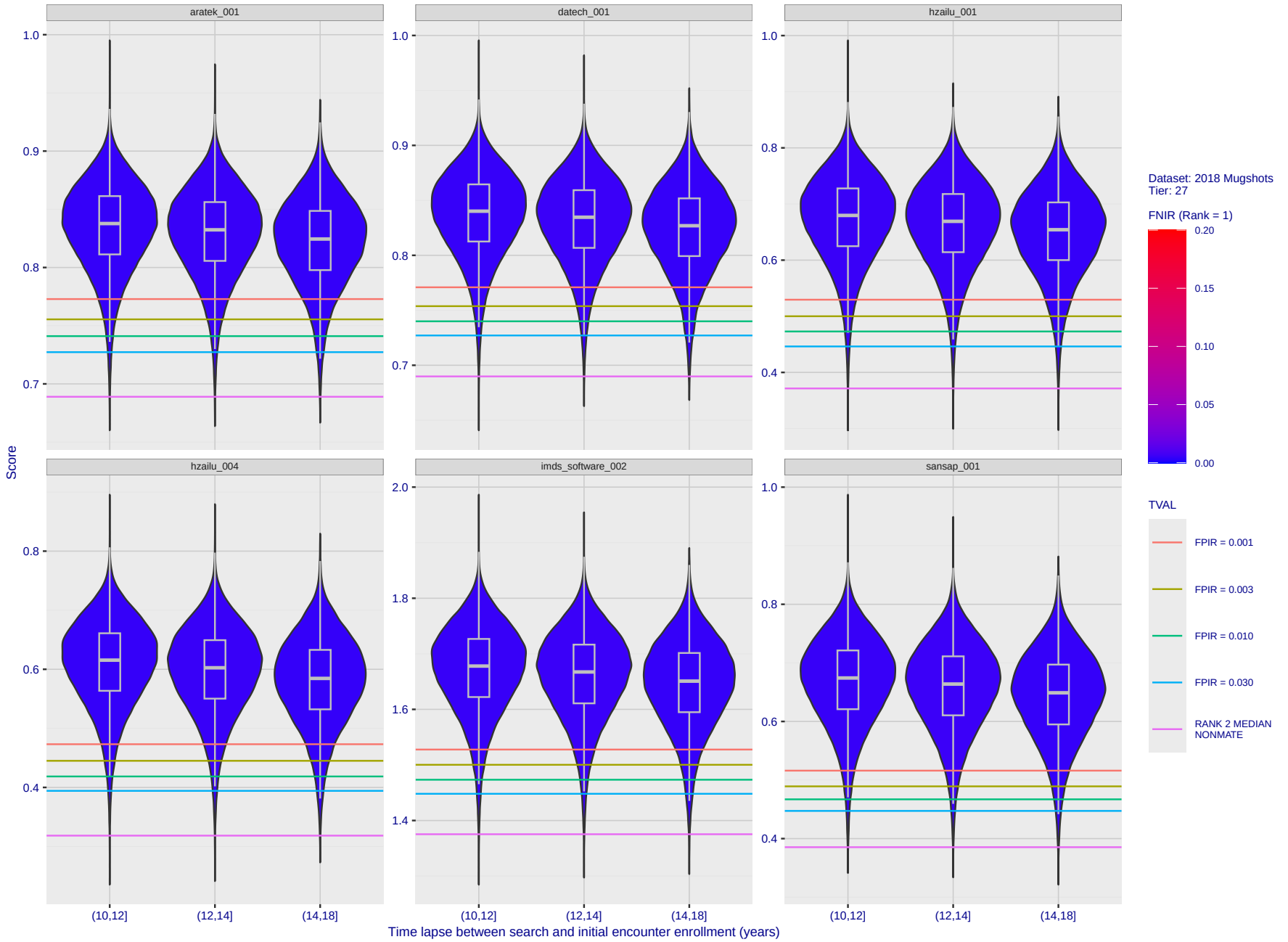

Figure 262: **[FRVT-2018 Mugshot Ageing Dataset] Native mate scores vs. time-elapsed**. *The oldest image of each individual is enrolled. Thereafter, all more recent images are searched. Mated score distributions are computed over all searches noted in row 17 of Table 1 binned by number of years between search and initial enrollment.*

2026/01/09 20:40:38
FNIR(N, R, T) = False neg. identification rate
FPIR(N, T) = False pos. identification rate
N = Num. enrolled subjects
R = Num. candidates examined
T = Threshold
T = 0 → Investigation
T > 0 → Identification

This publication is available free of charge from: https://doi.org/10.6028/NIST.IR.8271

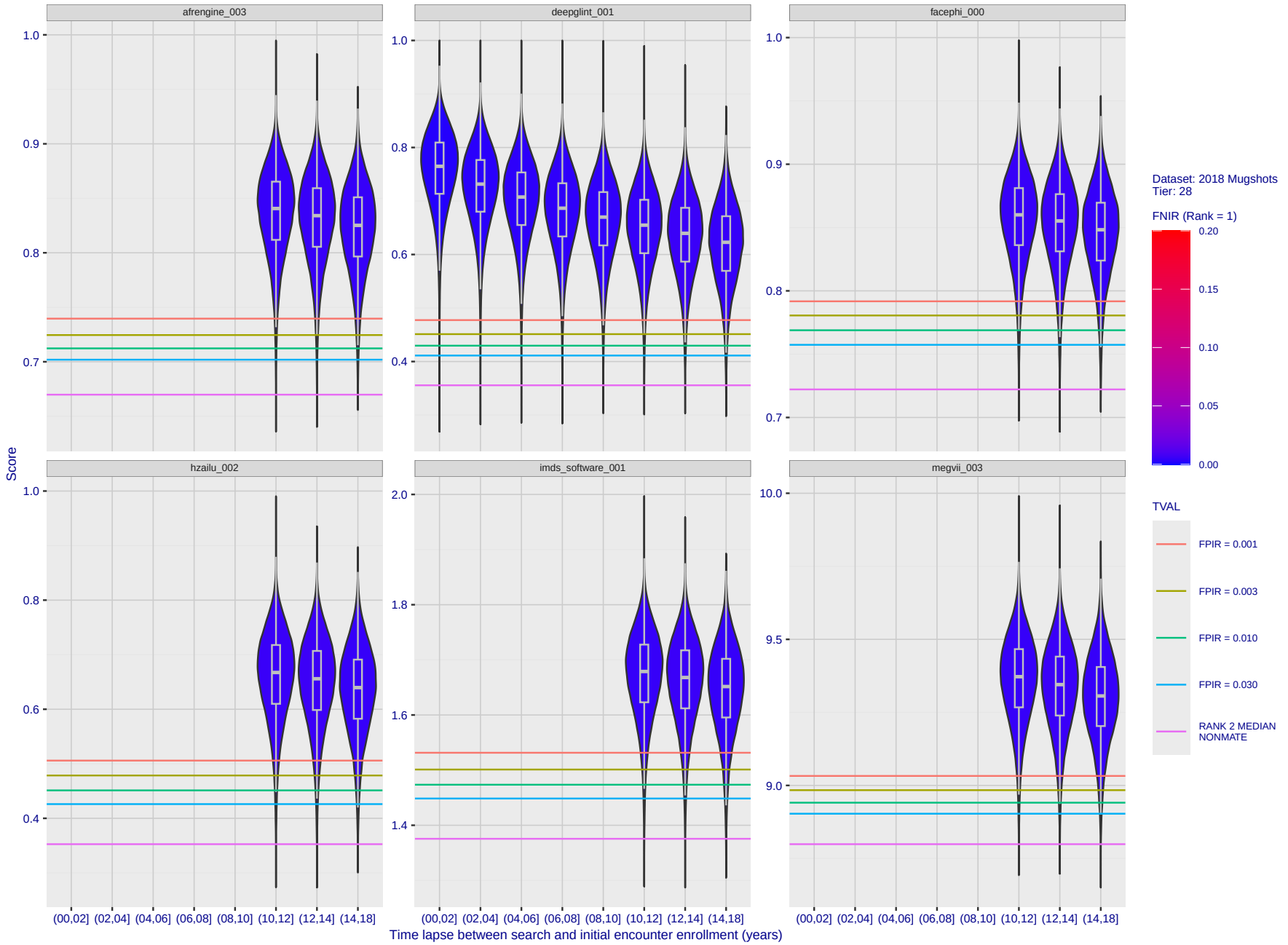

Figure 263: **[FRVT-2018 Mugshot Ageing Dataset] Native mate scores vs. time-elapsed**. *The oldest image of each individual is enrolled. Thereafter, all more recent images are searched. Mated score distributions are computed over all searches noted in row 17 of Table 1 binned by number of years between search and initial enrollment.*

2026/01/09 20:40:38
FNIR(N, R, T) = False neg. identification rate
FPIR(N, T) = False pos. identification rate
N = Num. enrolled subjects
R = Num. candidates examined
T = Threshold
T = 0 → Investigation
T > 0 → Identification

This publication is available free of charge from: https://doi.org/10.6028/NIST.IR.8271

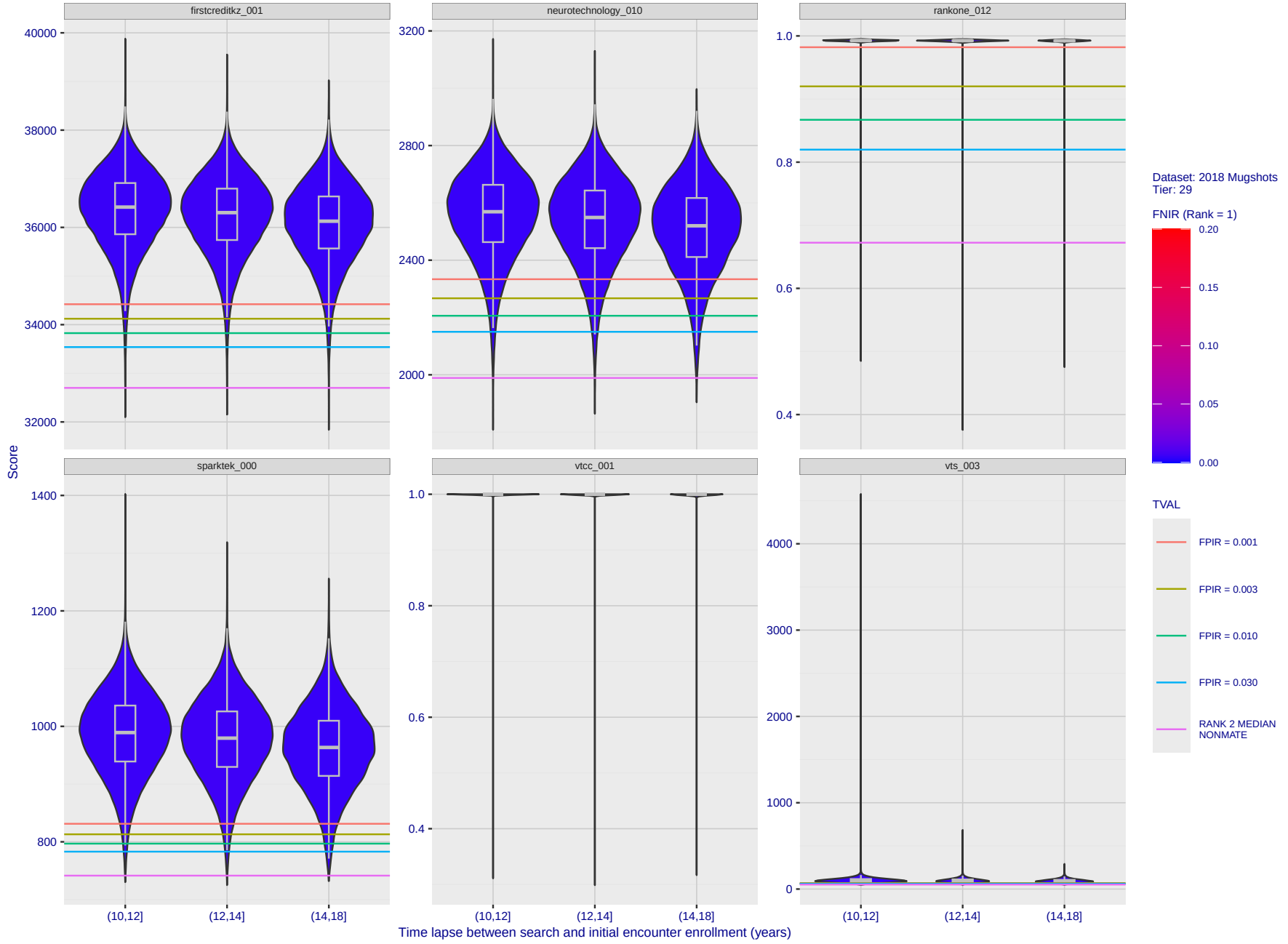

Figure 264: **[FRVT-2018 Mugshot Ageing Dataset] Native mate scores vs. time-elapsed**. *The oldest image of each individual is enrolled. Thereafter, all more recent images are searched. Mated score distributions are computed over all searches noted in row 17 of Table 1 binned by number of years between search and initial enrollment.*

This publication is available free of charge from: https://doi.org/10.6028/NIST.IR.8271

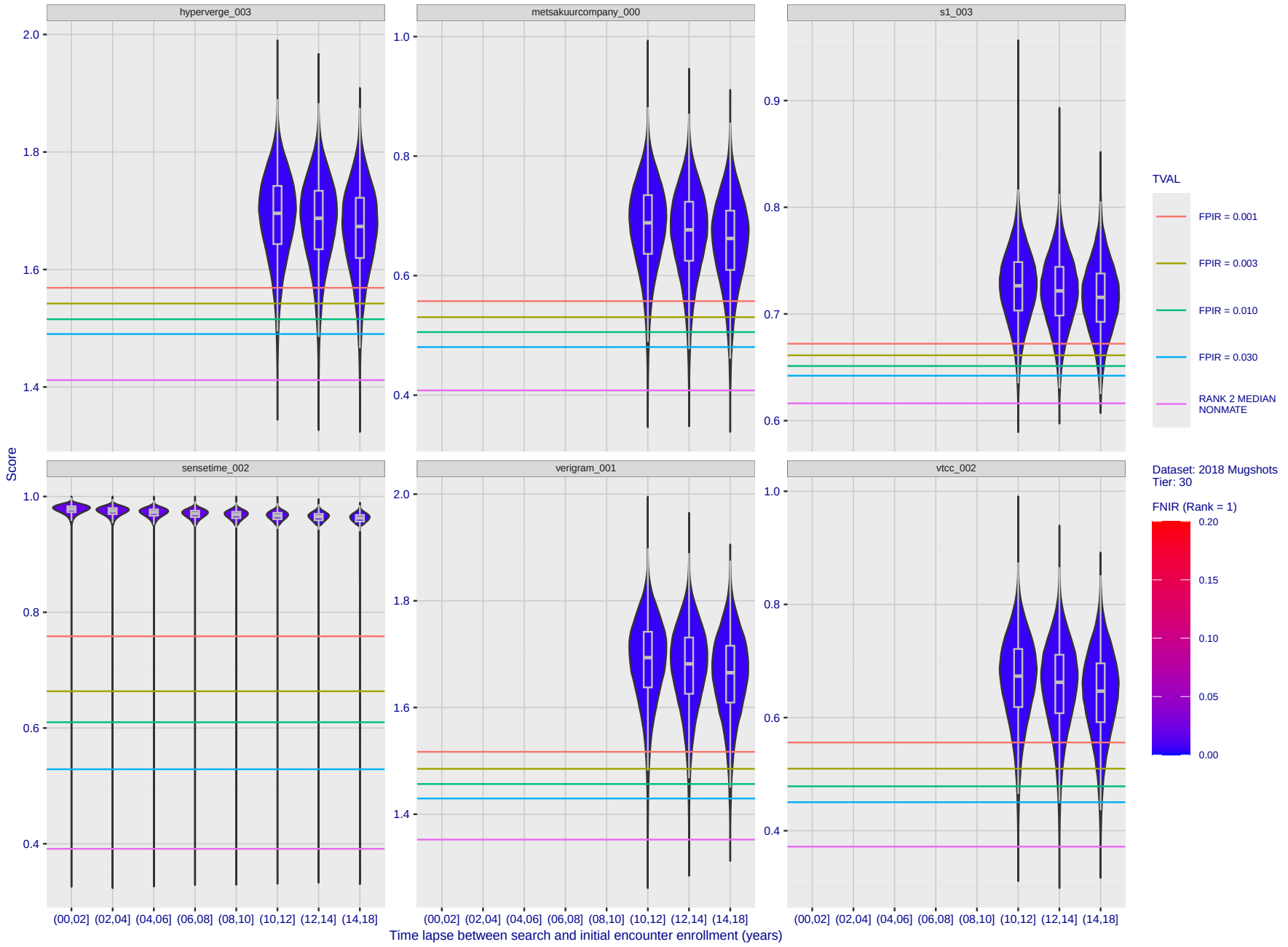

Figure 265: **[FRVT-2018 Mugshot Ageing Dataset] Native mate scores vs. time-elapsed**. *The oldest image of each individual is enrolled. Thereafter, all more recent images are searched. Mated score distributions are computed over all searches noted in row 17 of Table 1 binned by number of years between search and initial enrollment.*

This publication is available free of charge from: https://doi.org/10.6028/NIST.IR.8271

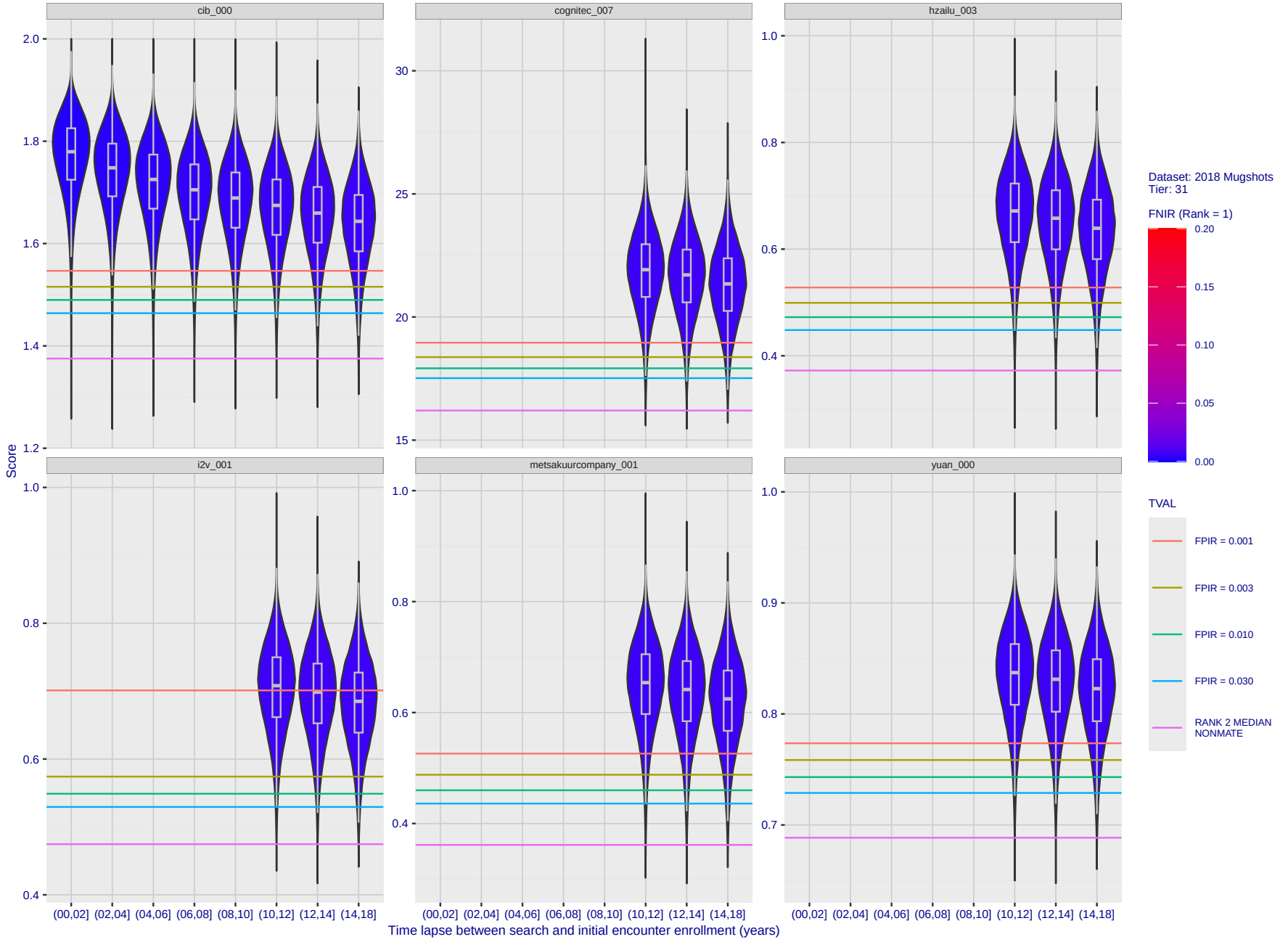

Figure 266: **[FRVT-2018 Mugshot Ageing Dataset] Native mate scores vs. time-elapsed**. *The oldest image of each individual is enrolled. Thereafter, all more recent images are searched. Mated score distributions are computed over all searches noted in row 17 of Table 1 binned by number of years between search and initial enrollment.*

This publication is available free of charge from: https://doi.org/10.6028/NIST.IR.8271

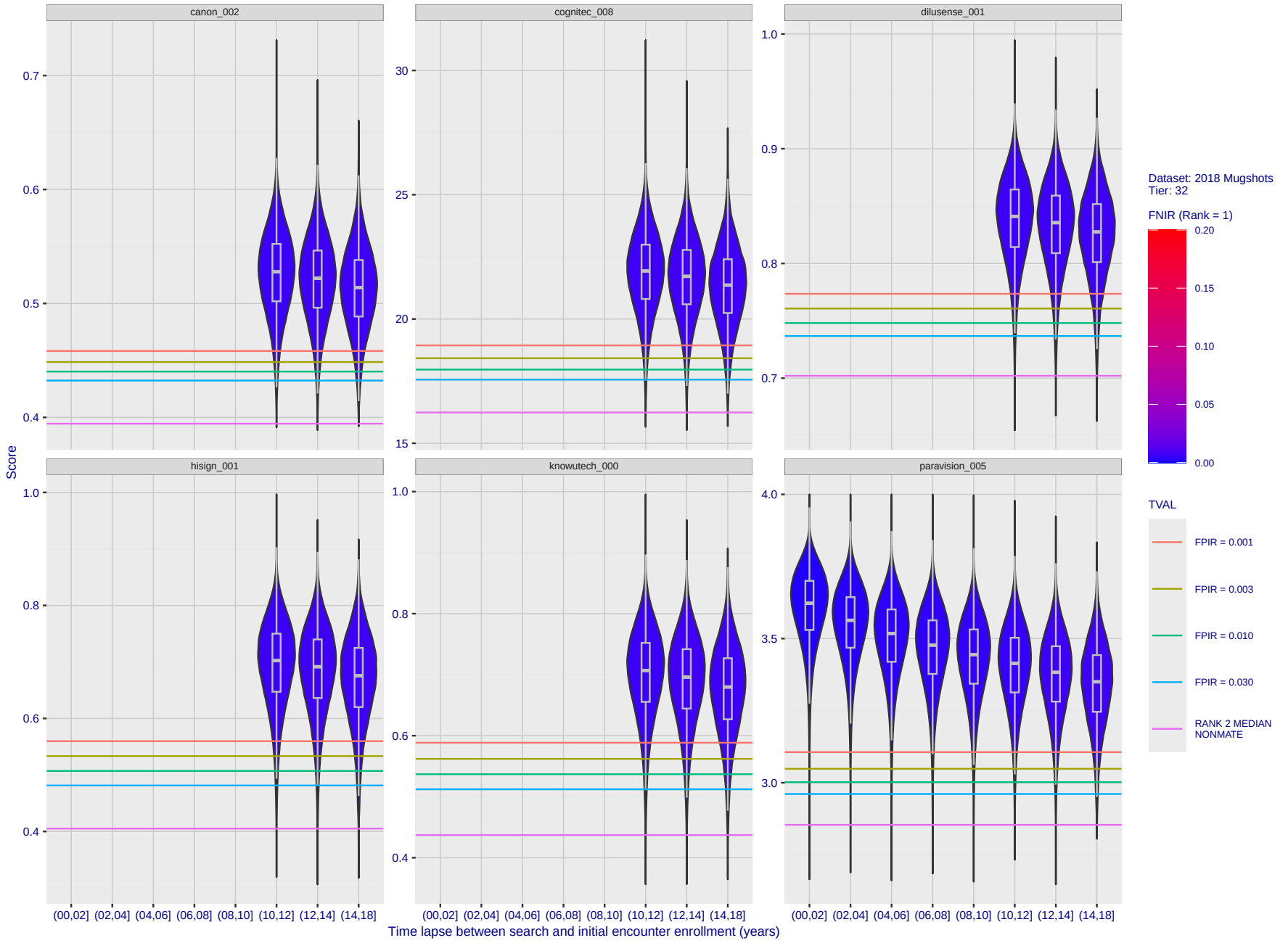

Figure 267: **[FRVT-2018 Mugshot Ageing Dataset] Native mate scores vs. time-elapsed**. *The oldest image of each individual is enrolled. Thereafter, all more recent images are searched. Mated score distributions are computed over all searches noted in row 17 of Table 1 binned by number of years between search and initial enrollment.*

2026/01/09 20:40:38

FNIR(N, R, T) = False neg. identification rate
FPIR(N, T) = False pos. identification rate

N = Num. enrolled subjects
R = Num. candidates examined

T = Threshold

T = 0 → Investigation
T > 0 → Identification

This publication is available free of charge from: https://doi.org/10.6028/NIST.IR.8271

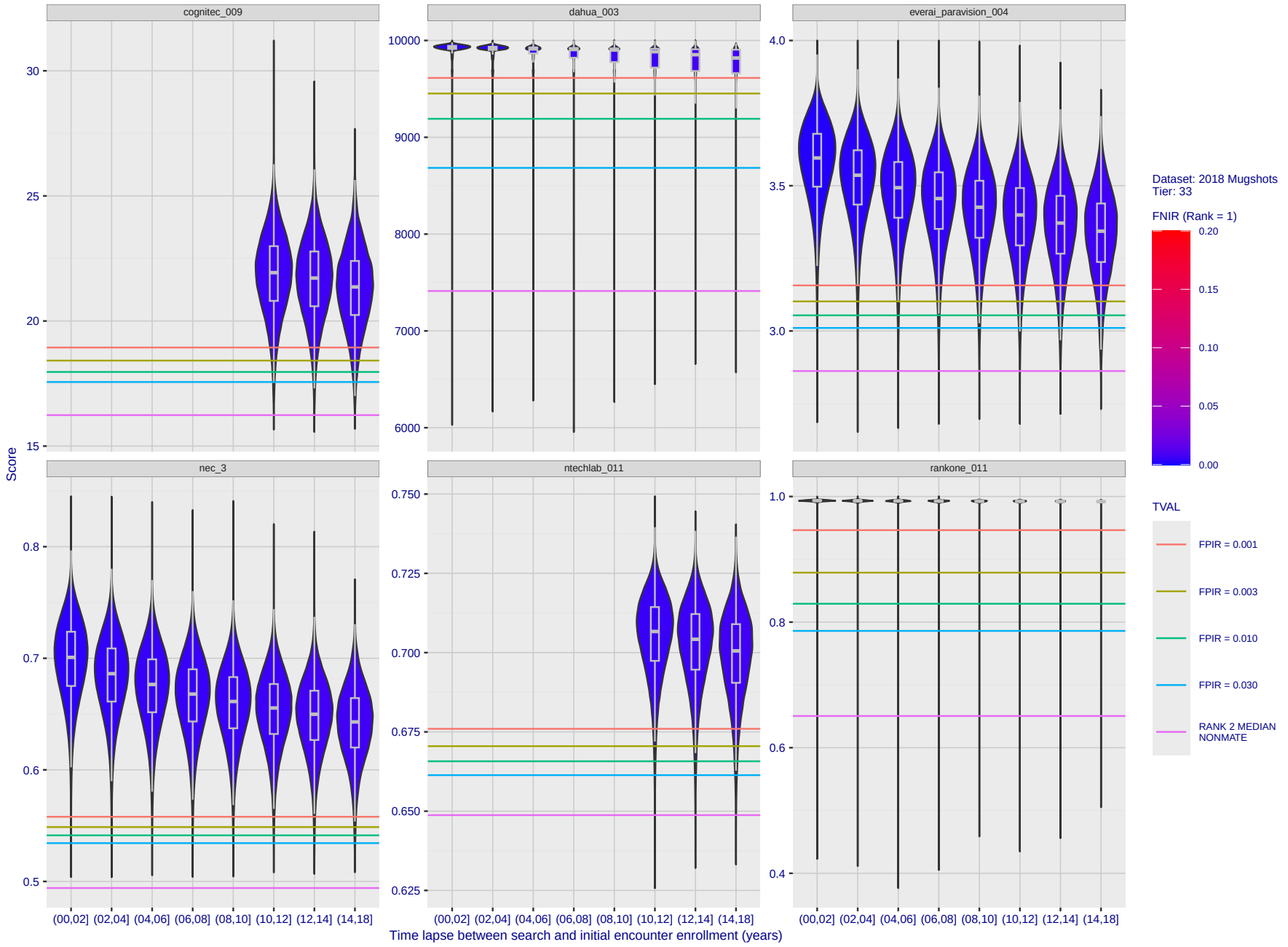

Figure 268: **[FRVT-2018 Mugshot Ageing Dataset] Native mate scores vs. time-elapsed**. *The oldest image of each individual is enrolled. Thereafter, all more recent images are searched. Mated score distributions are computed over all searches noted in row 17 of Table 1 binned by number of years between search and initial enrollment.*

2026/01/09 20:40:38

FNIR(N, R, T) = False neg. identification rate
FPIR(N, T) = False pos. identification rate

N = Num. enrolled subjects
R = Num. candidates examined

T = Threshold

T = 0 → Investigation
T > 0 → Identification

This publication is available free of charge from: https://doi.org/10.6028/NIST.IR.8271

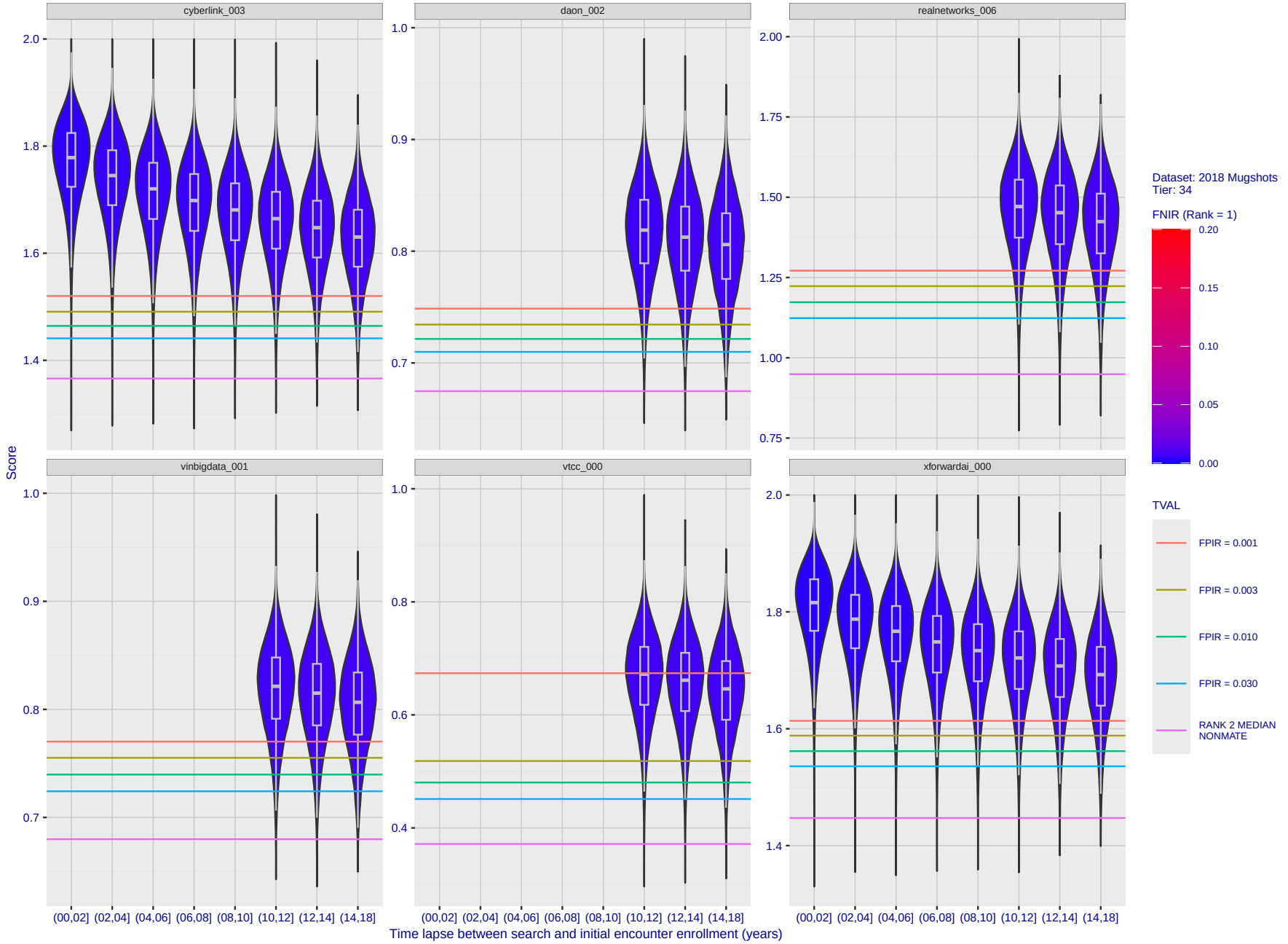

Figure 269: **[FRVT-2018 Mugshot Ageing Dataset] Native mate scores vs. time-elapsed**. *The oldest image of each individual is enrolled. Thereafter, all more recent images are searched. Mated score distributions are computed over all searches noted in row 17 of Table 1 binned by number of years between search and initial enrollment.*

This publication is available free of charge from: https://doi.org/10.6028/NIST.IR.8271

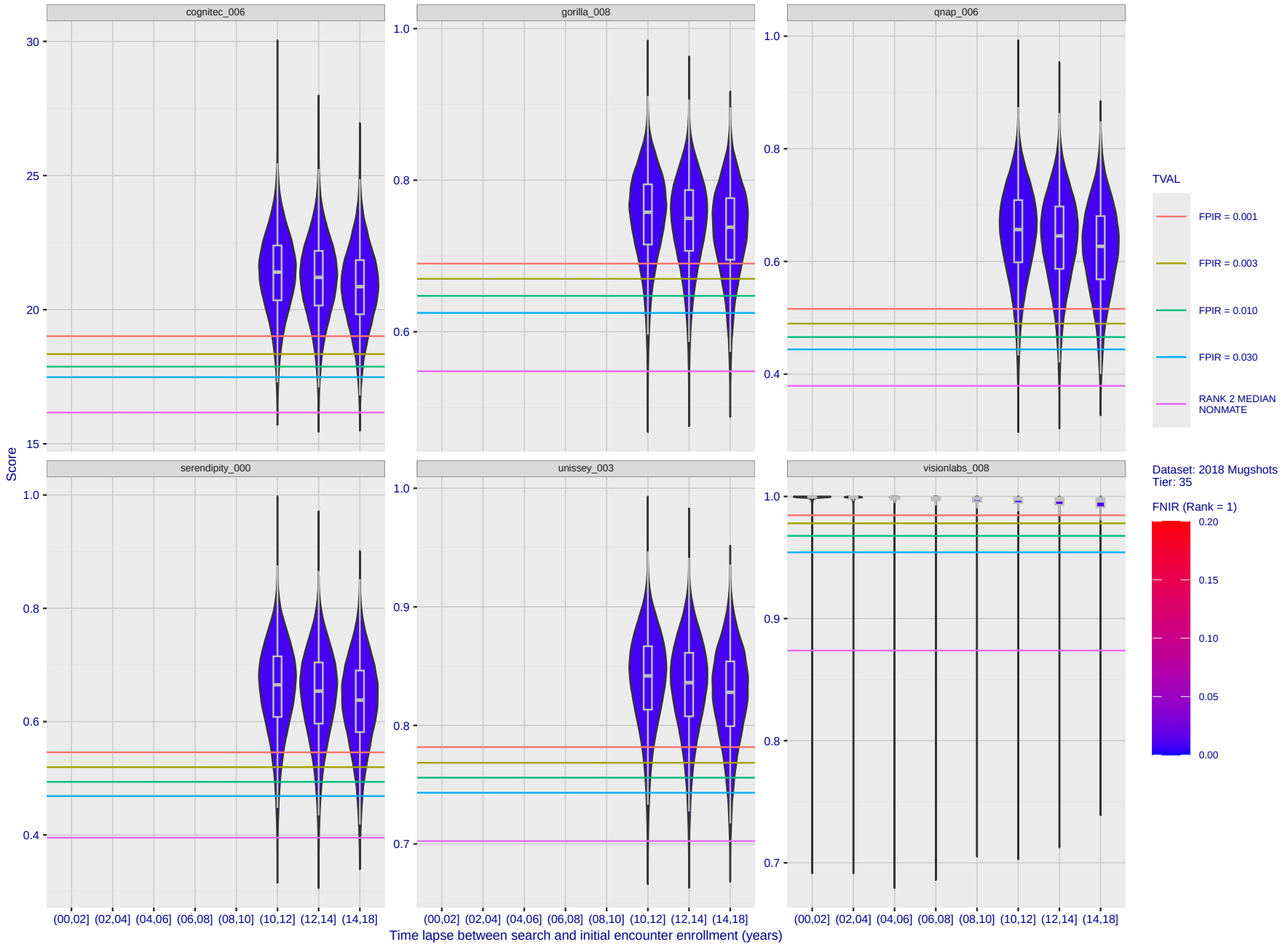

Figure 270: **[FRVT-2018 Mugshot Ageing Dataset] Native mate scores vs. time-elapsed**. *The oldest image of each individual is enrolled. Thereafter, all more recent images are searched. Mated score distributions are computed over all searches noted in row 17 of Table 1 binned by number of years between search and initial enrollment.*

2026/01/09 20:40:38
FNIR(N, R, T) = False neg. identification rate
FPIR(N, T) = False pos. identification rate
N = Num. enrolled subjects
R = Num. candidates examined
T = Threshold
T = 0 → Investigation
T > 0 → Identification

This publication is available free of charge from: https://doi.org/10.6028/NIST.IR.8271

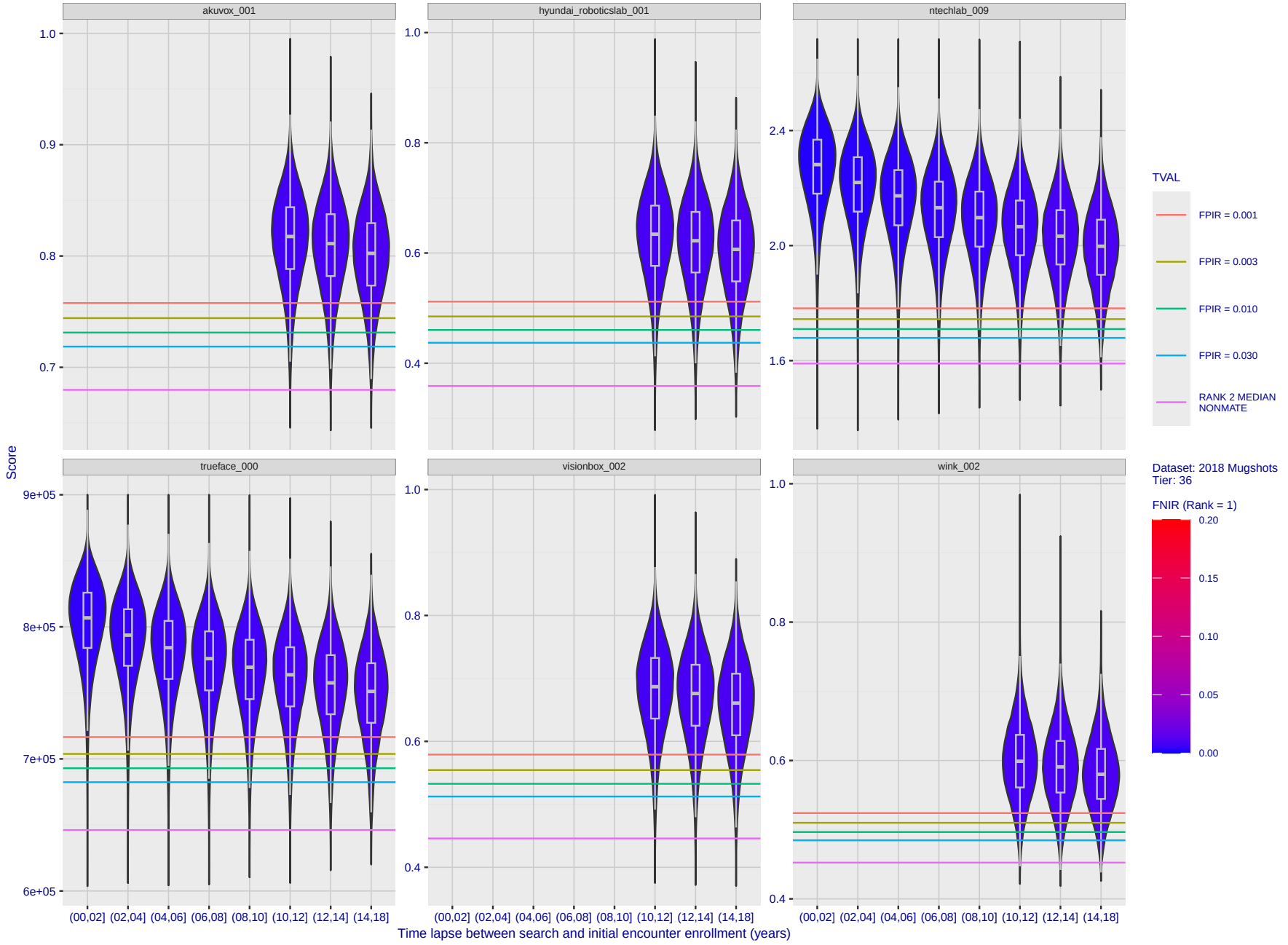

Figure 271: **[FRVT-2018 Mugshot Ageing Dataset] Native mate scores vs. time-elapsed**. *The oldest image of each individual is enrolled. Thereafter, all more recent images are searched. Mated score distributions are computed over all searches noted in row 17 of Table 1 binned by number of years between search and initial enrollment.*

This publication is available free of charge from: https://doi.org/10.6028/NIST.IR.8271

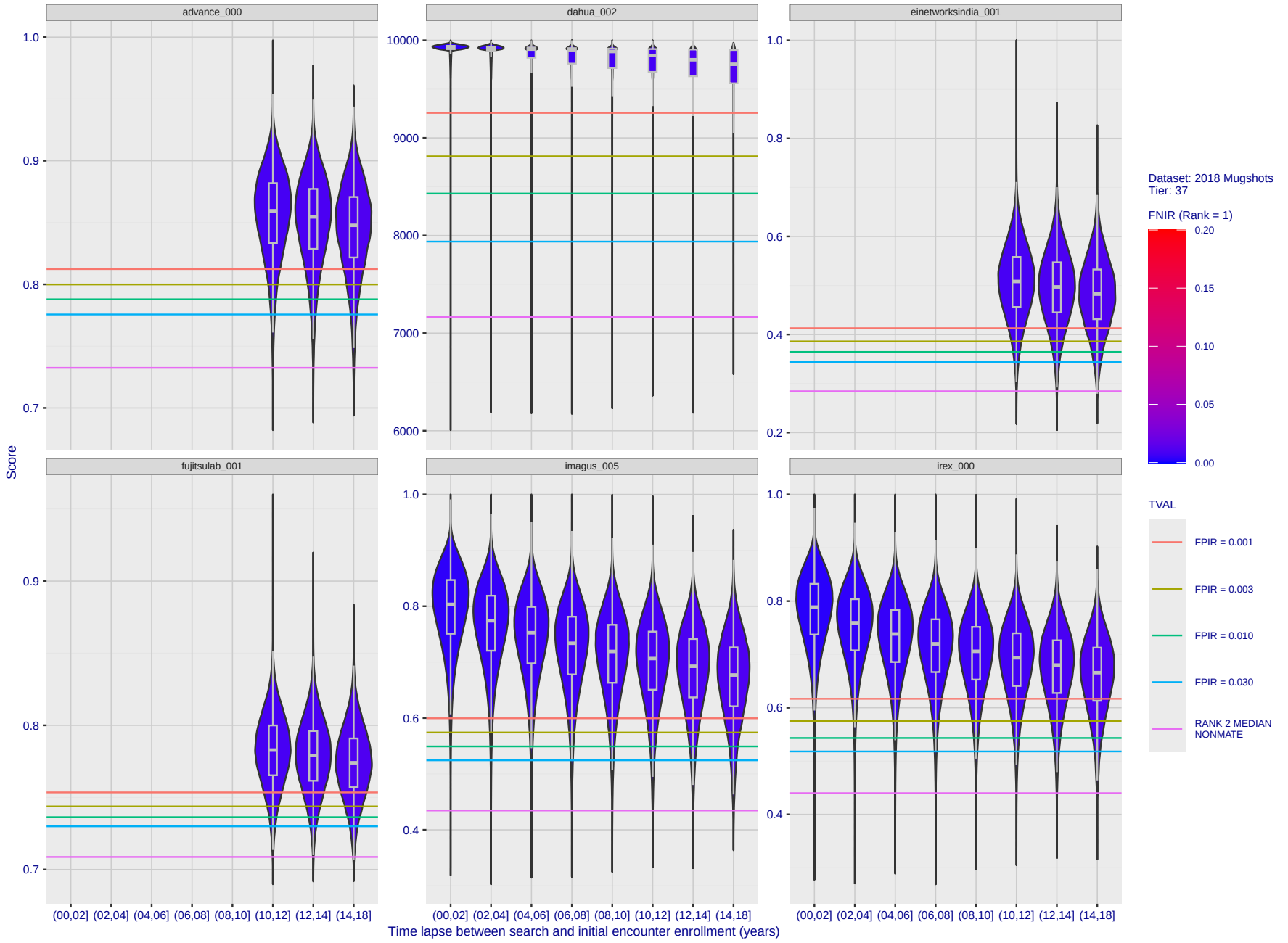

Figure 272: **[FRVT-2018 Mugshot Ageing Dataset] Native mate scores vs. time-elapsed**. *The oldest image of each individual is enrolled. Thereafter, all more recent images are searched. Mated score distributions are computed over all searches noted in row 17 of Table 1 binned by number of years between search and initial enrollment.*

This publication is available free of charge from: https://doi.org/10.6028/NIST.IR.8271

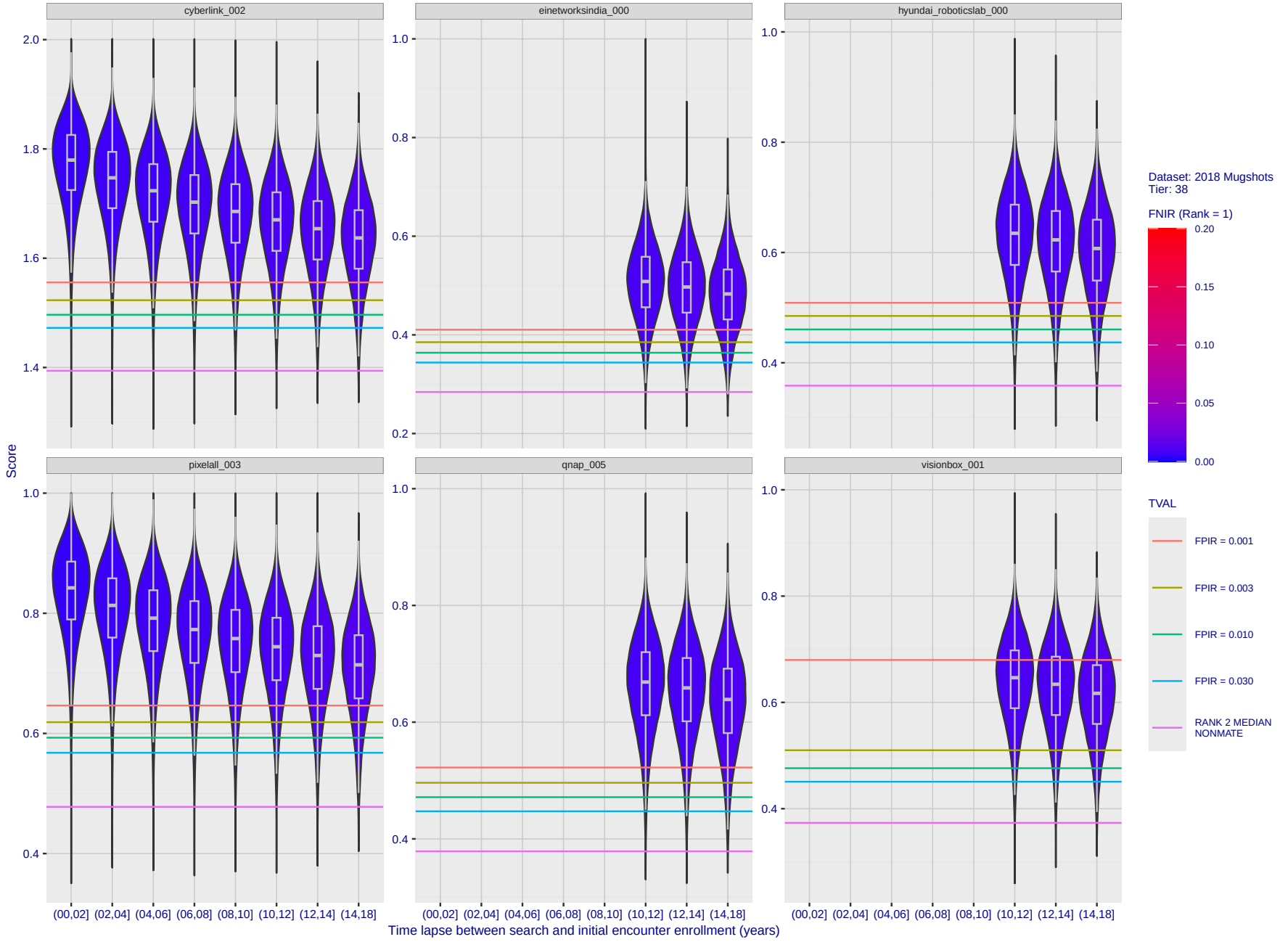

Figure 273: **[FRVT-2018 Mugshot Ageing Dataset] Native mate scores vs. time-elapsed**. *The oldest image of each individual is enrolled. Thereafter, all more recent images are searched. Mated score distributions are computed over all searches noted in row 17 of Table 1 binned by number of years between search and initial enrollment.*

2026/01/09 20:40:38
FNIR(N, R, T) = False neg. identification rate
FPIR(N, T) = False pos. identification rate
N = Num. enrolled subjects
R = Num. candidates examined
T = Threshold
T = 0 → Investigation
T > 0 → Identification

This publication is available free of charge from: https://doi.org/10.6028/NIST.IR.8271

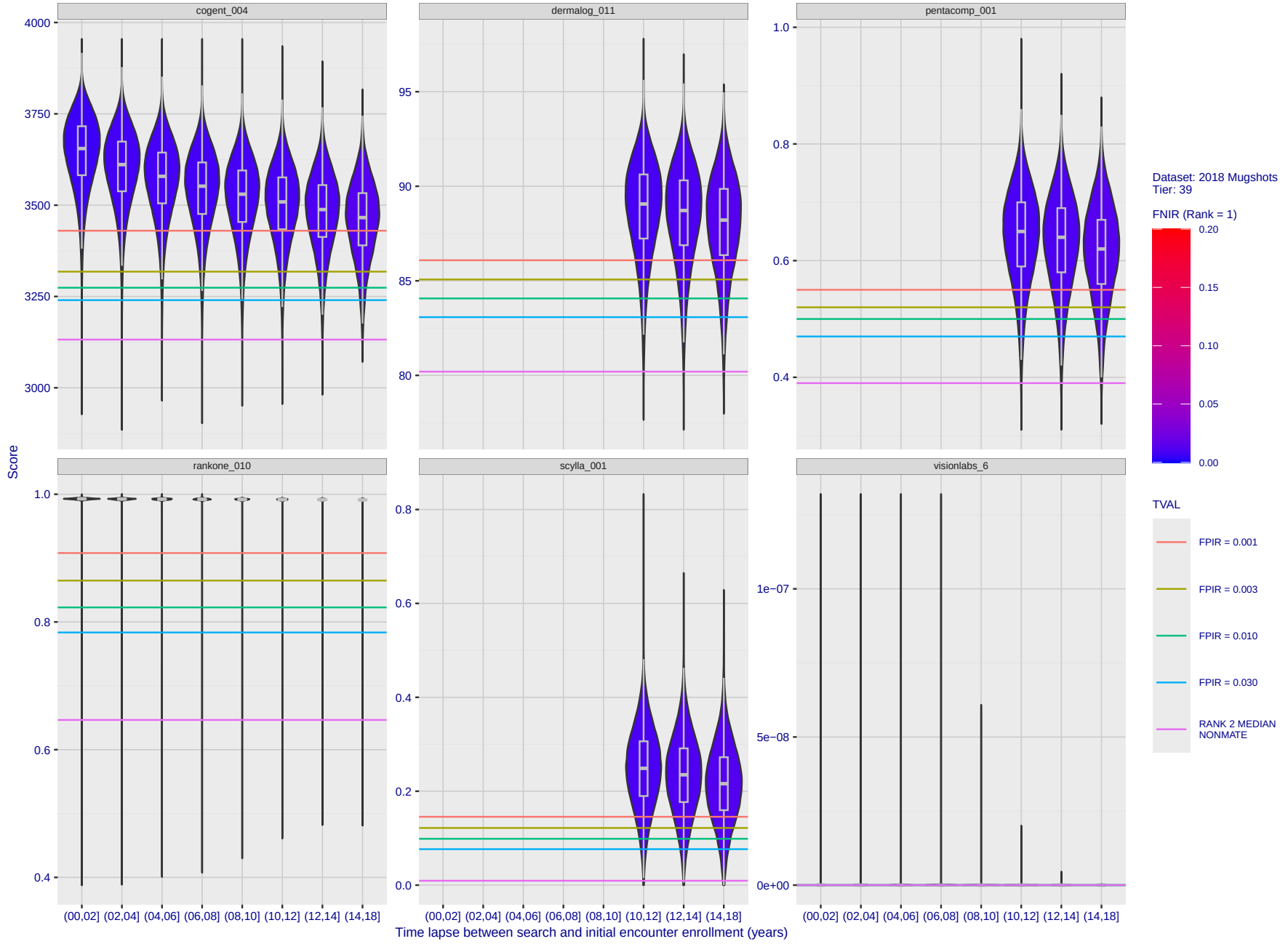

Figure 274: **[FRVT-2018 Mugshot Ageing Dataset] Native mate scores vs. time-elapsed**. *The oldest image of each individual is enrolled. Thereafter, all more recent images are searched. Mated score distributions are computed over all searches noted in row 17 of Table 1 binned by number of years between search and initial enrollment.*

This publication is available free of charge from: https://doi.org/10.6028/NIST.IR.8271

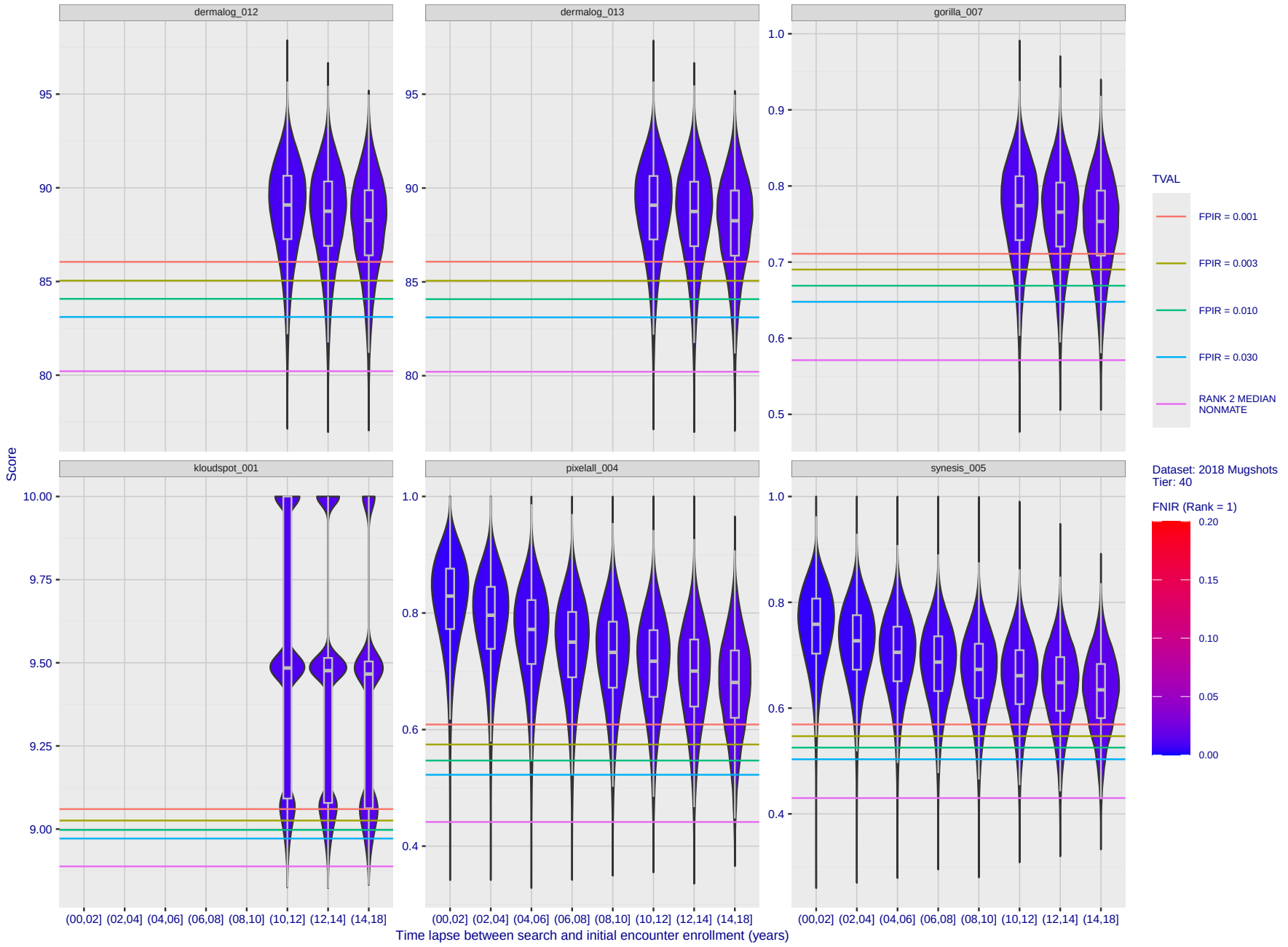

Figure 275: **[FRVT-2018 Mugshot Ageing Dataset] Native mate scores vs. time-elapsed**. *The oldest image of each individual is enrolled. Thereafter, all more recent images are searched. Mated score distributions are computed over all searches noted in row 17 of Table 1 binned by number of years between search and initial enrollment.*

This publication is available free of charge from: https://doi.org/10.6028/NIST.IR.8271

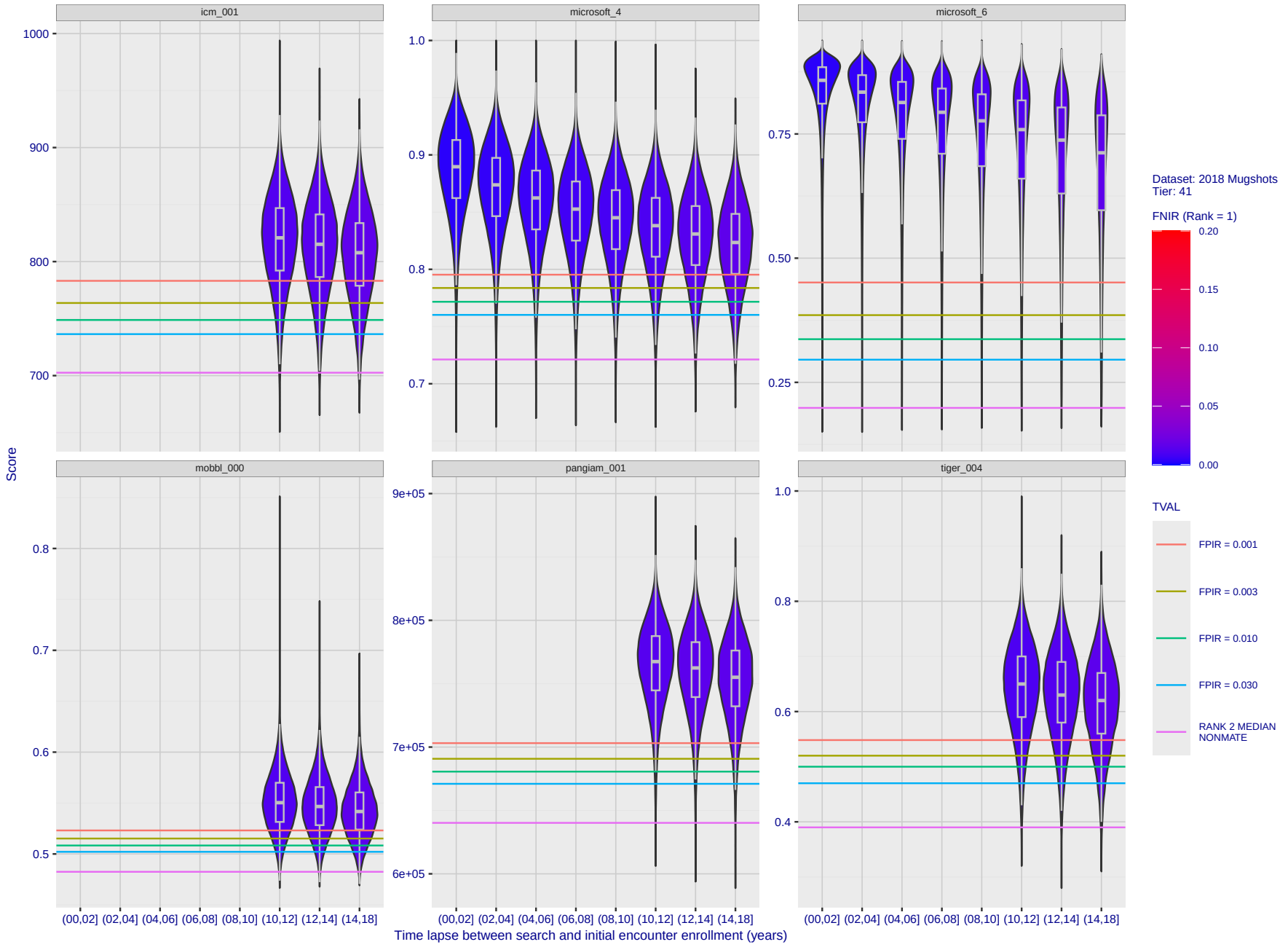

Figure 276: **[FRVT-2018 Mugshot Ageing Dataset] Native mate scores vs. time-elapsed**. *The oldest image of each individual is enrolled. Thereafter, all more recent images are searched. Mated score distributions are computed over all searches noted in row 17 of Table 1 binned by number of years between search and initial enrollment.*

2026/01/09 20:40:38
FNIR(N, R, T) = False neg. identification rate
FPIR(N, T) = False pos. identification rate
N = Num. enrolled subjects
R = Num. candidates examined
T = Threshold
T = 0 → Investigation
T > 0 → Identification

This publication is available free of charge from: https://doi.org/10.6028/NIST.IR.8271

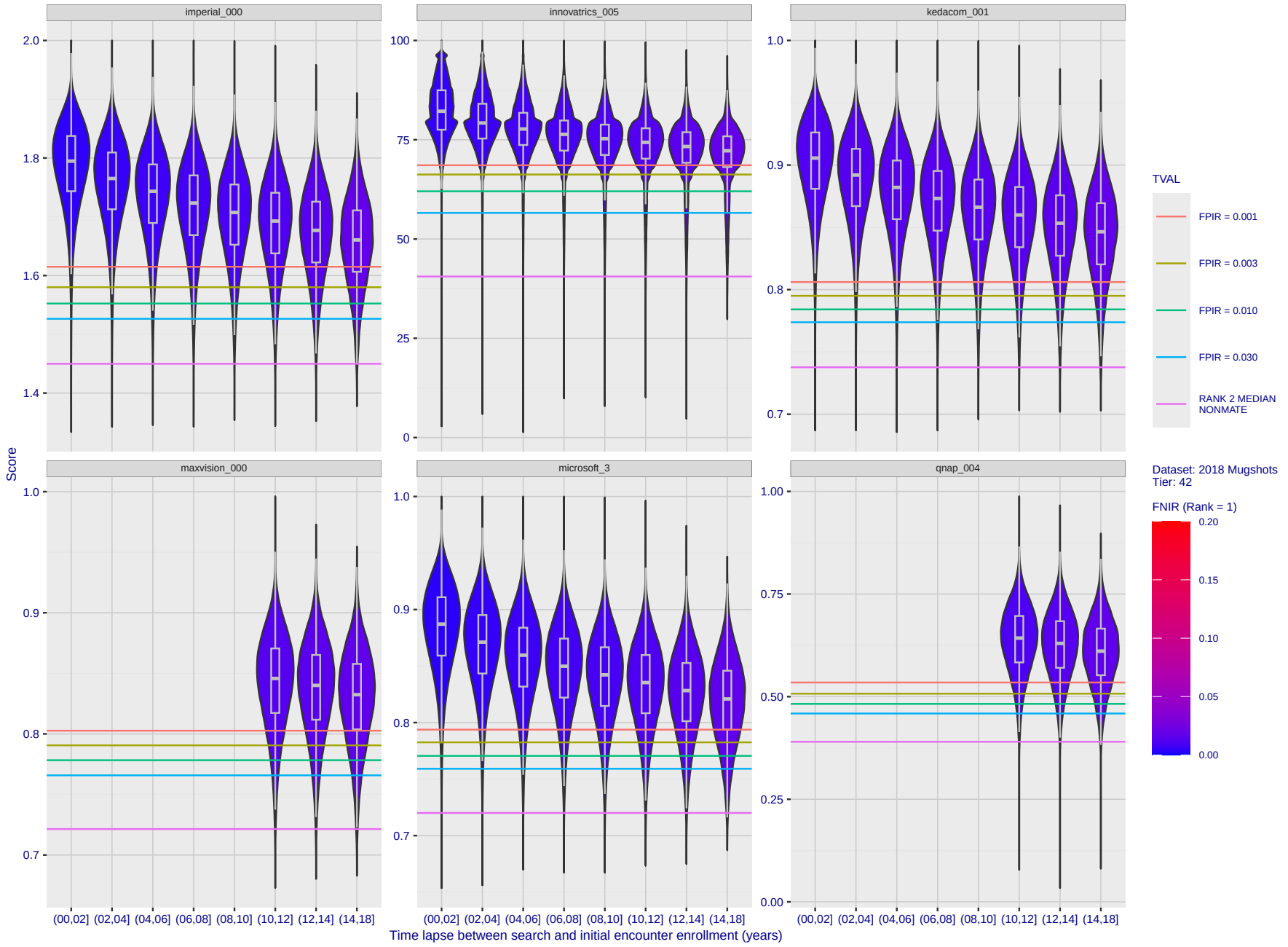

Figure 277: **[FRVT-2018 Mugshot Ageing Dataset] Native mate scores vs. time-elapsed**. *The oldest image of each individual is enrolled. Thereafter, all more recent images are searched. Mated score distributions are computed over all searches noted in row 17 of Table 1 binned by number of years between search and initial enrollment.*

2026/01/09 20:40:38
FNIR(N, R, T) = FPIR(N, T) = False neg. identification rate / False pos. identification rate
N = Num. enrolled subjects
R = Num. candidates examined
T = Threshold
T = 0 → Investigation
T > 0 → Identification

This publication is available free of charge from: https://doi.org/10.6028/NIST.IR.8271

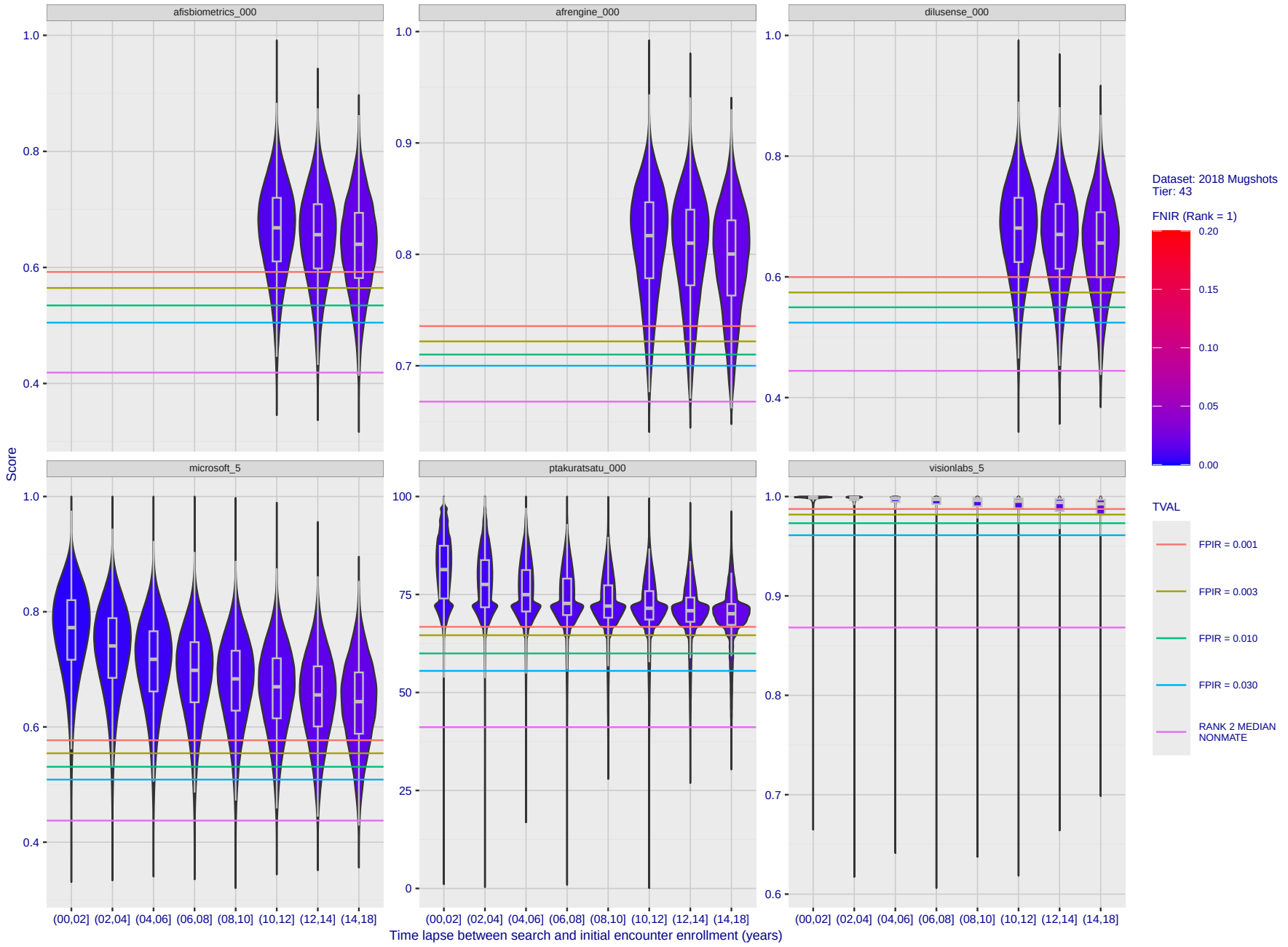

Figure 278: **[FRVT-2018 Mugshot Ageing Dataset] Native mate scores vs. time-elapsed**. *The oldest image of each individual is enrolled. Thereafter, all more recent images are searched. Mated score distributions are computed over all searches noted in row 17 of Table 1 binned by number of years between search and initial enrollment.*

This publication is available free of charge from: https://doi.org/10.6028/NIST.IR.8271

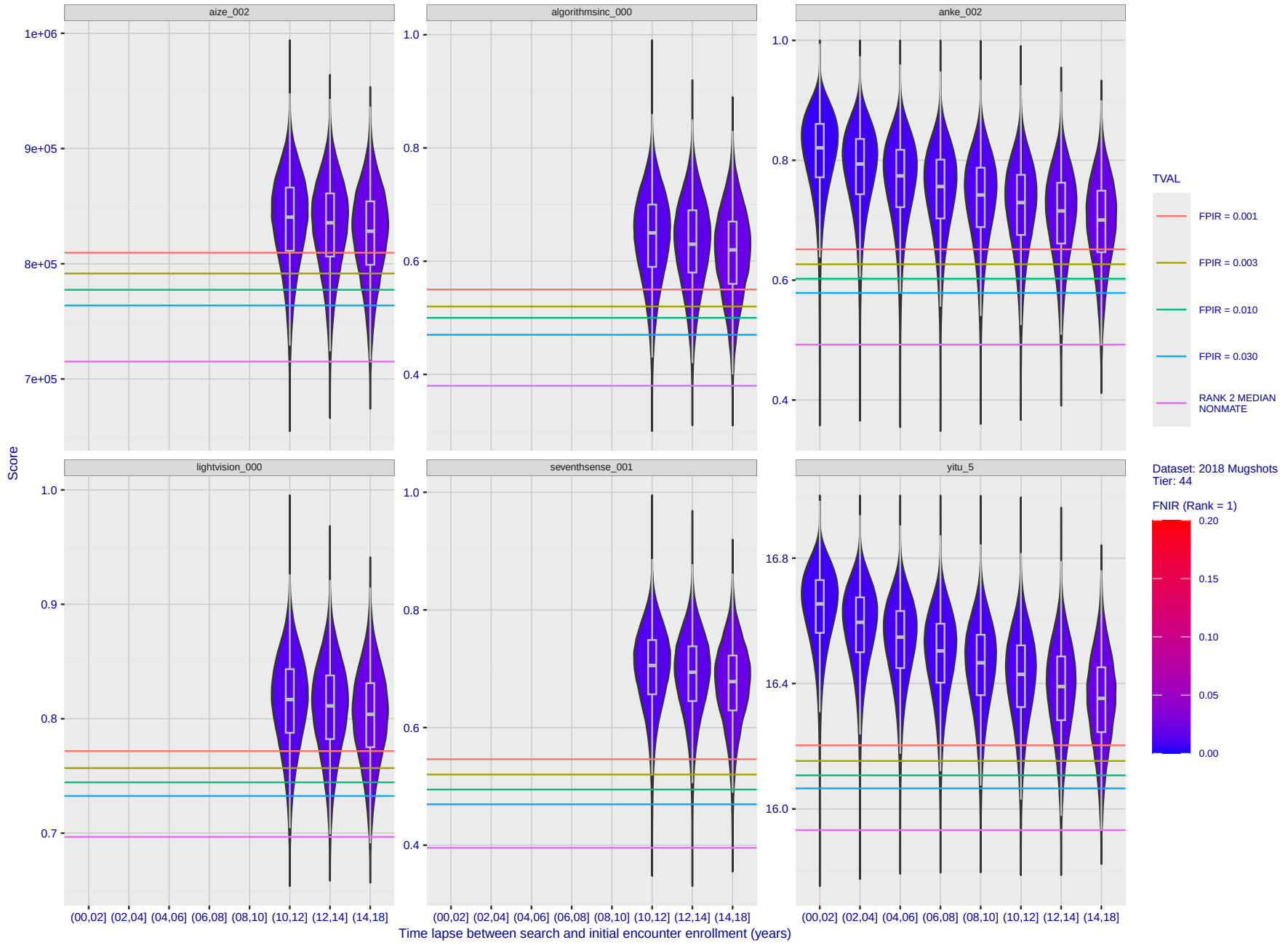

Figure 279: **[FRVT-2018 Mugshot Ageing Dataset] Native mate scores vs. time-elapsed**. *The oldest image of each individual is enrolled. Thereafter, all more recent images are searched. Mated score distributions are computed over all searches noted in row 17 of Table 1 binned by number of years between search and initial enrollment.*

2026/01/09 20:40:38
FNIR(N, R, T) = False neg. identification rate
FPIR(N, T) = False pos. identification rate
N = Num. enrolled subjects
R = Num. candidates examined
T = Threshold
T = 0 → Investigation
T > 0 → Identification

This publication is available free of charge from: https://doi.org/10.6028/NIST.IR.8271

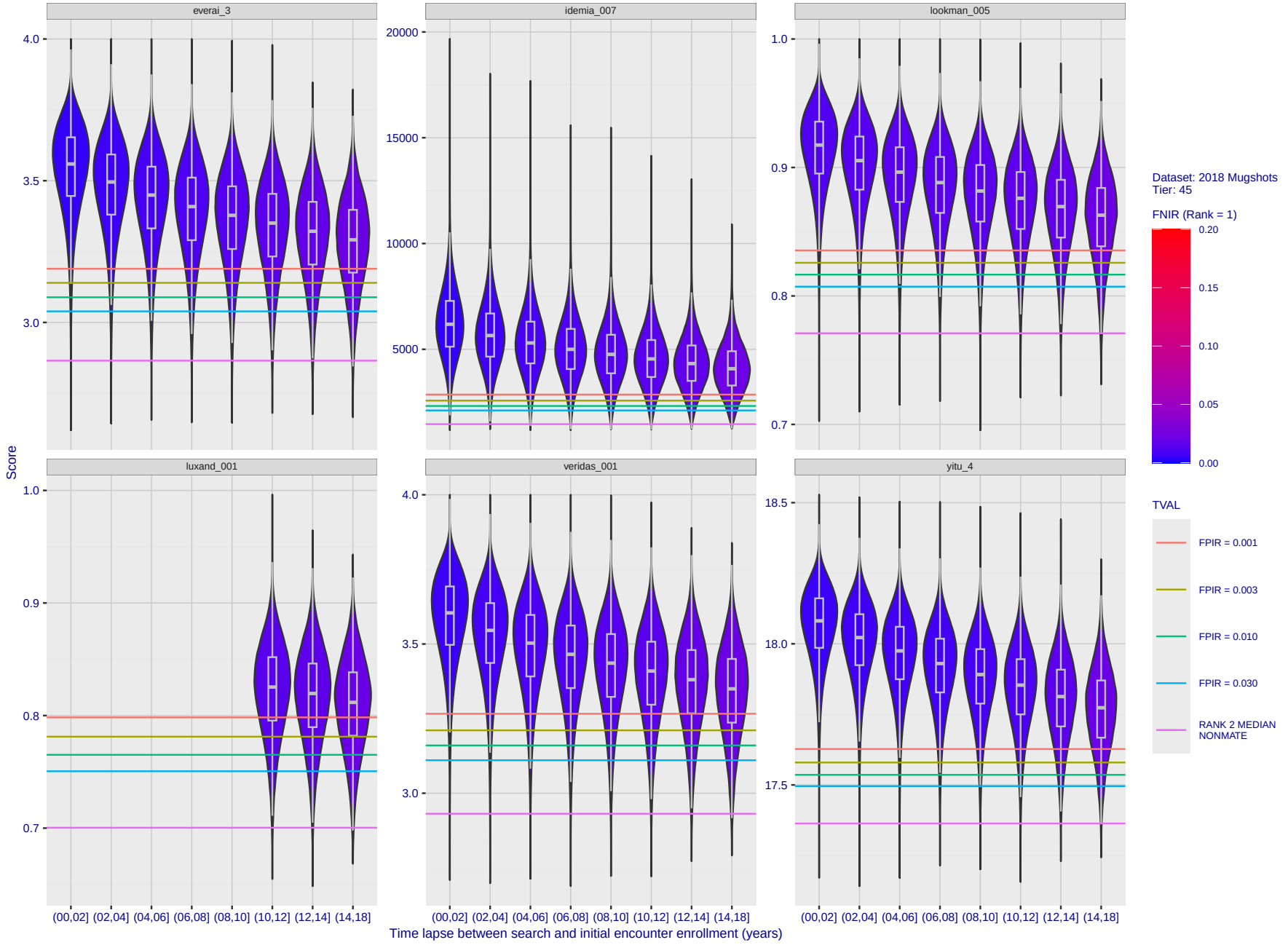

Figure 280: **[FRVT-2018 Mugshot Ageing Dataset] Native mate scores vs. time-elapsed**. *The oldest image of each individual is enrolled. Thereafter, all more recent images are searched. Mated score distributions are computed over all searches noted in row 17 of Table 1 binned by number of years between search and initial enrollment.*

This publication is available free of charge from: https://doi.org/10.6028/NIST.IR.8271

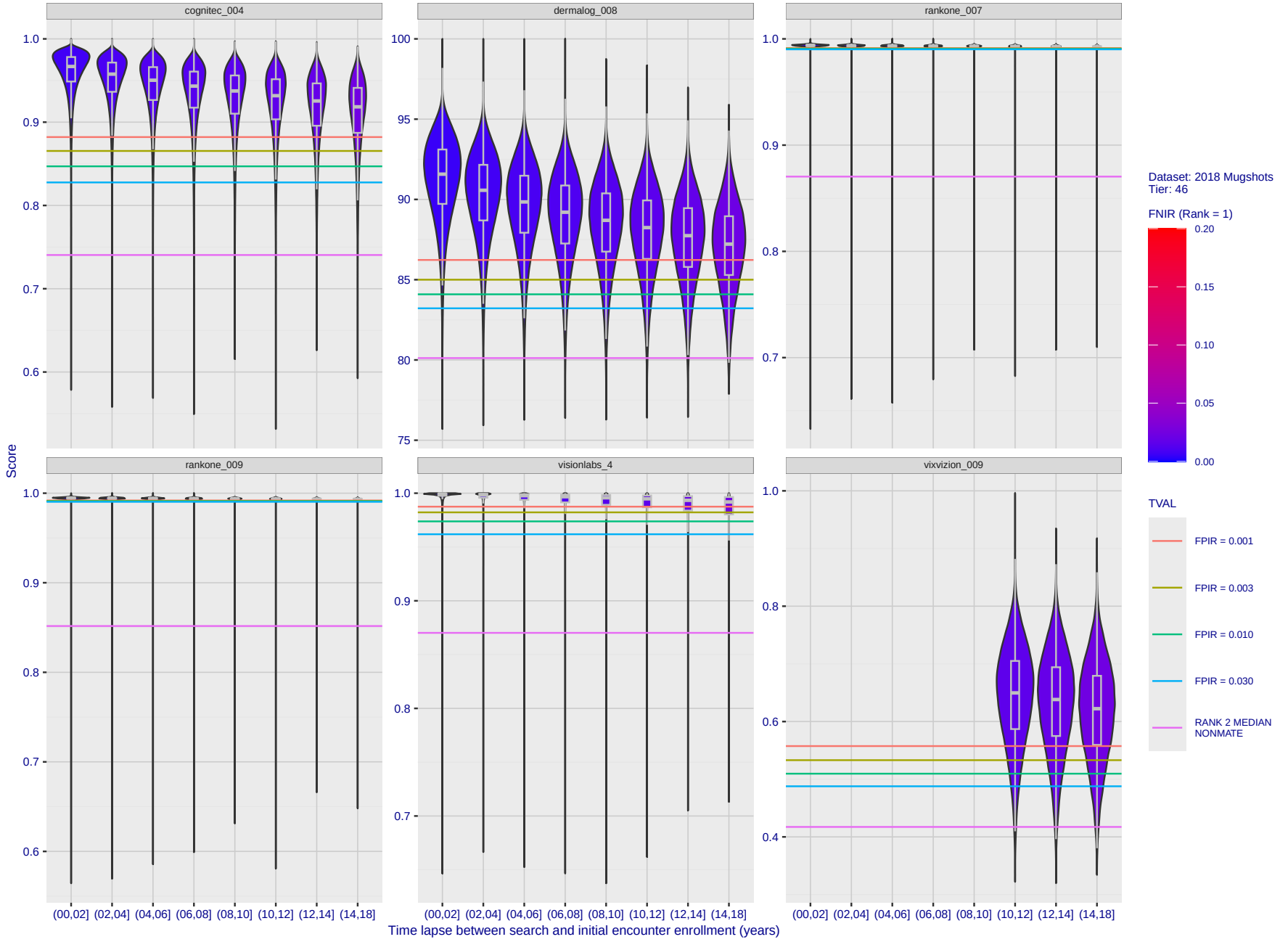

Figure 281: **[FRVT-2018 Mugshot Ageing Dataset] Native mate scores vs. time-elapsed**. *The oldest image of each individual is enrolled. Thereafter, all more recent images are searched. Mated score distributions are computed over all searches noted in row 17 of Table 1 binned by number of years between search and initial enrollment.*

This publication is available free of charge from: https://doi.org/10.6028/NIST.IR.8271

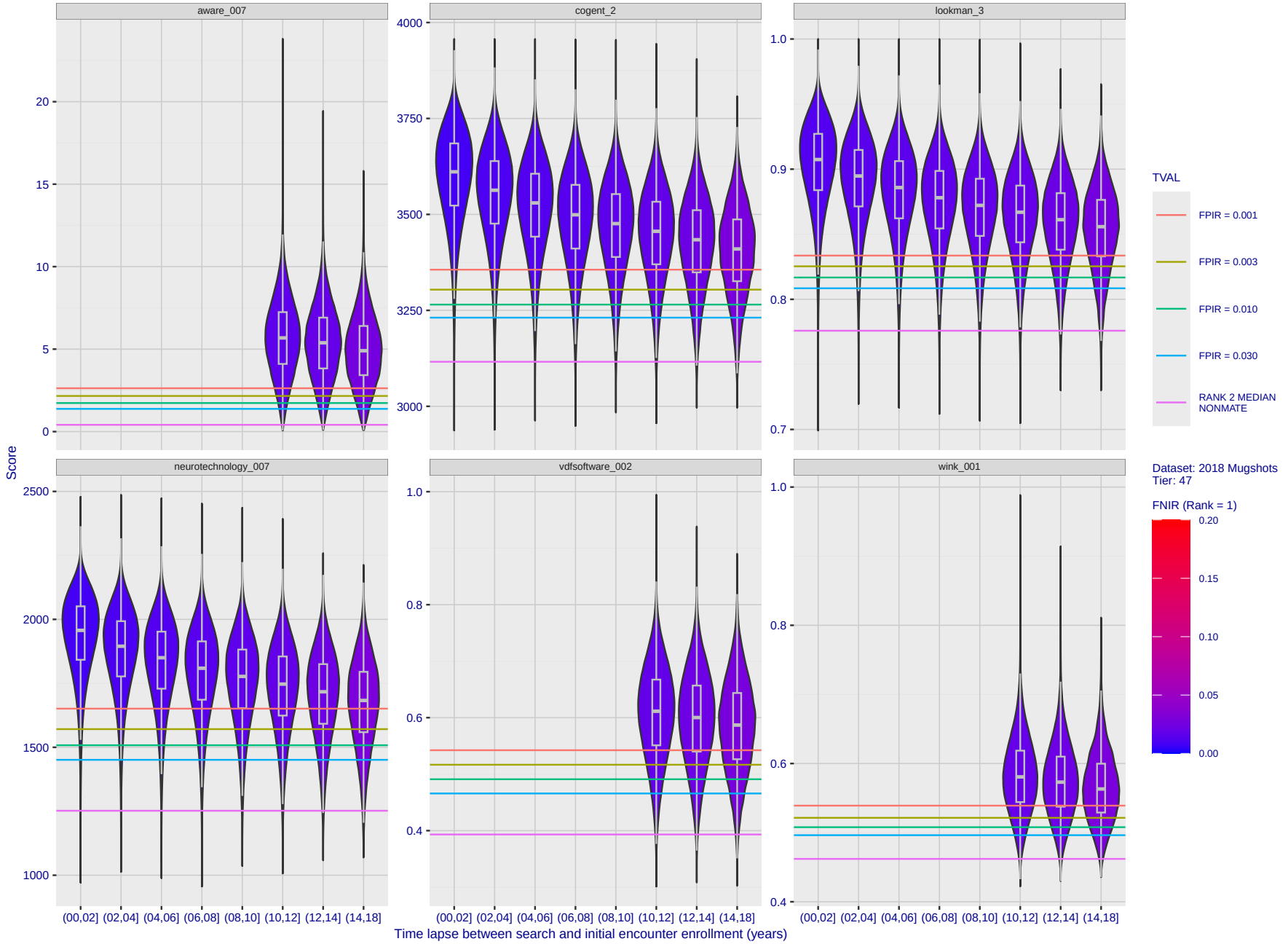

Figure 282: **[FRVT-2018 Mugshot Ageing Dataset] Native mate scores vs. time-elapsed**. *The oldest image of each individual is enrolled. Thereafter, all more recent images are searched. Mated score distributions are computed over all searches noted in row 17 of Table 1 binned by number of years between search and initial enrollment.*

2026/01/09 20:40:38
FNIR(N, R, T) = False neg. identification rate
FPIR(N, T) = False pos. identification rate
N = Num. enrolled subjects
R = Num. candidates examined
T = Threshold
T = 0 → Investigation
T > 0 → Identification

This publication is available free of charge from: https://doi.org/10.6028/NIST.IR.8271

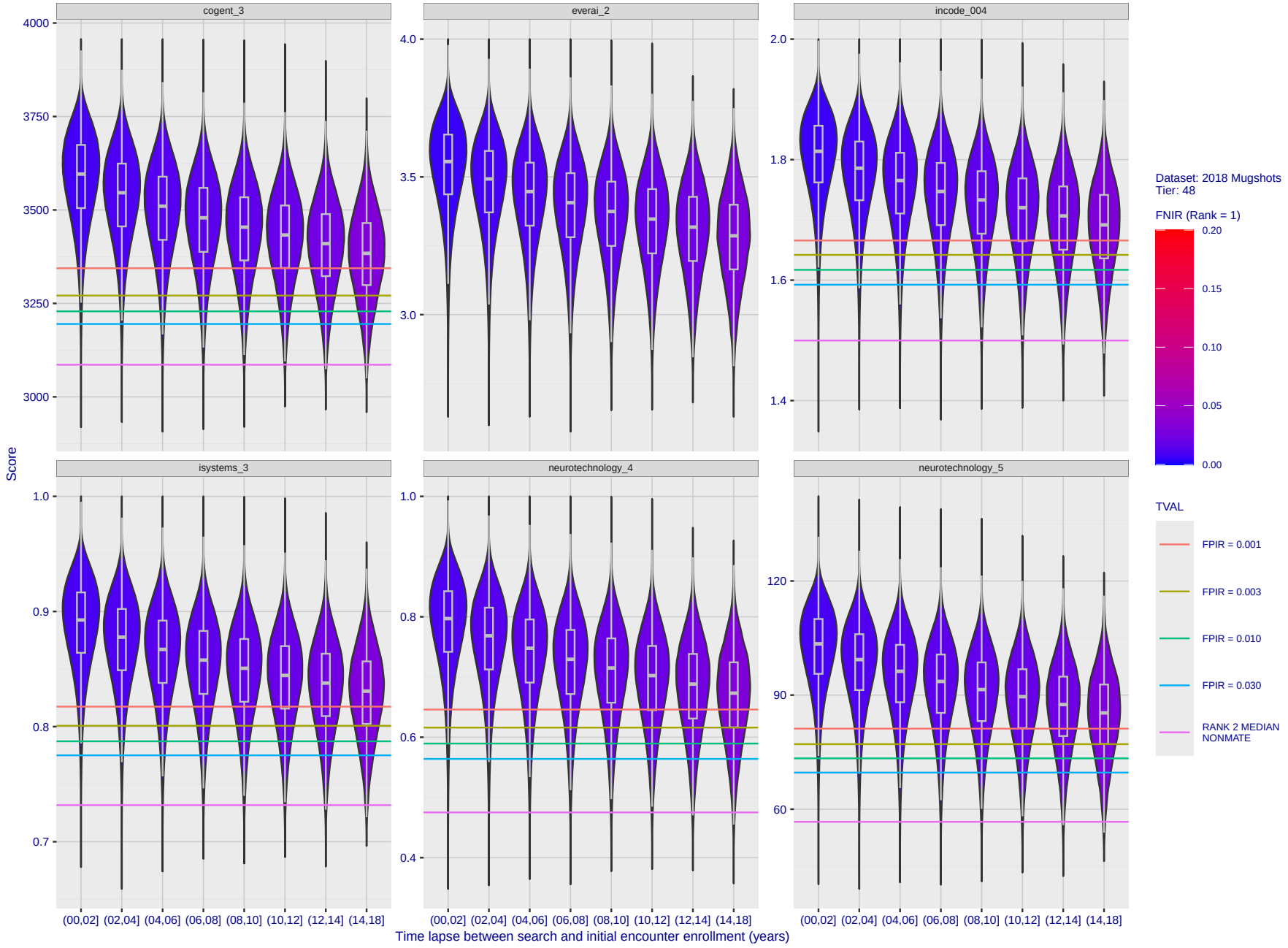

Figure 283: **[FRVT-2018 Mugshot Ageing Dataset] Native mate scores vs. time-elapsed**. *The oldest image of each individual is enrolled. Thereafter, all more recent images are searched. Mated score distributions are computed over all searches noted in row 17 of Table 1 binned by number of years between search and initial enrollment.*

2026/01/09 20:40:38

FNIR(N, R, T) = False neg. identification rate
FPIR(N, T) = False pos. identification rate

N = Num. enrolled subjects
R = Num. candidates examined

T = Threshold

T = 0 → Investigation
T > 0 → Identification

This publication is available free of charge from: https://doi.org/10.6028/NIST.IR.8271

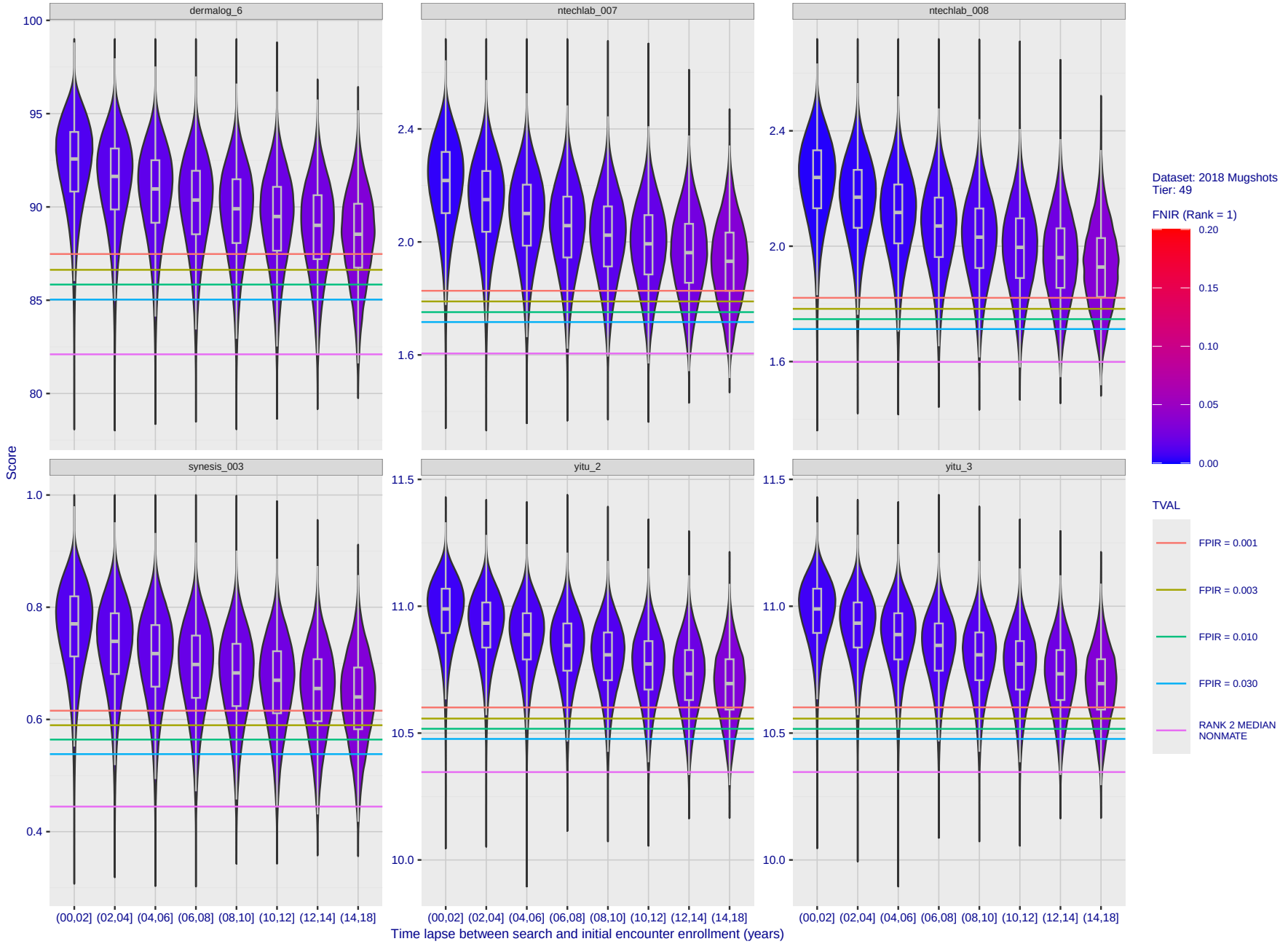

Figure 284: **[FRVT-2018 Mugshot Ageing Dataset] Native mate scores vs. time-elapsed**. *The oldest image of each individual is enrolled. Thereafter, all more recent images are searched. Mated score distributions are computed over all searches noted in row 17 of Table 1 binned by number of years between search and initial enrollment.*

This publication is available free of charge from: https://doi.org/10.6028/NIST.IR.8271

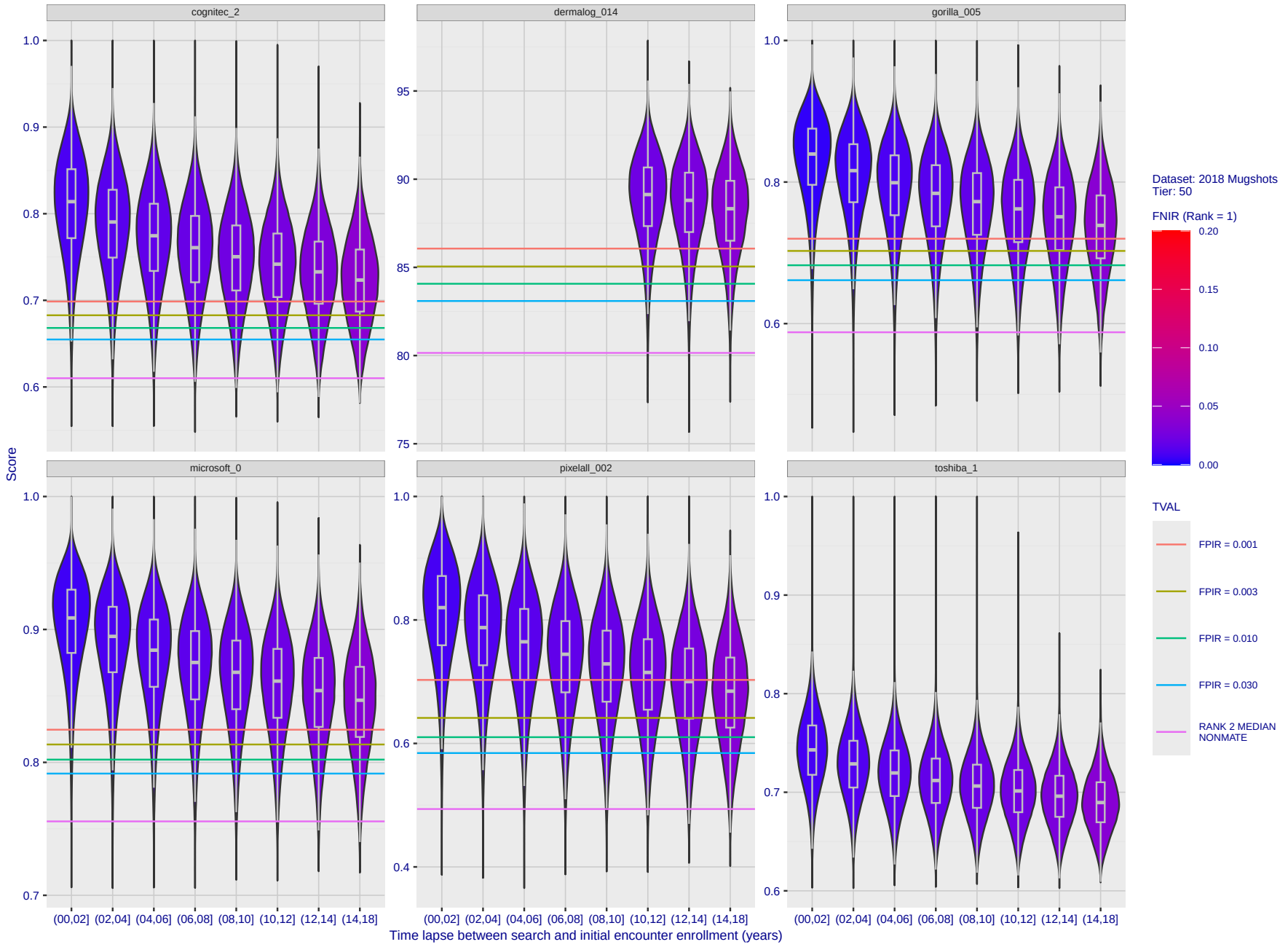

Figure 285: **[FRVT-2018 Mugshot Ageing Dataset] Native mate scores vs. time-elapsed**. *The oldest image of each individual is enrolled. Thereafter, all more recent images are searched. Mated score distributions are computed over all searches noted in row 17 of Table 1 binned by number of years between search and initial enrollment.*

2026/01/09 20:40:38
FNIR(N, R, T) = False neg. identification rate
FPIR(N, T) = False pos. identification rate
N = Num. enrolled subjects
R = Num. candidates examined
T = Threshold
T = 0 → Investigation
T > 0 → Identification

This publication is available free of charge from: https://doi.org/10.6028/NIST.IR.8271

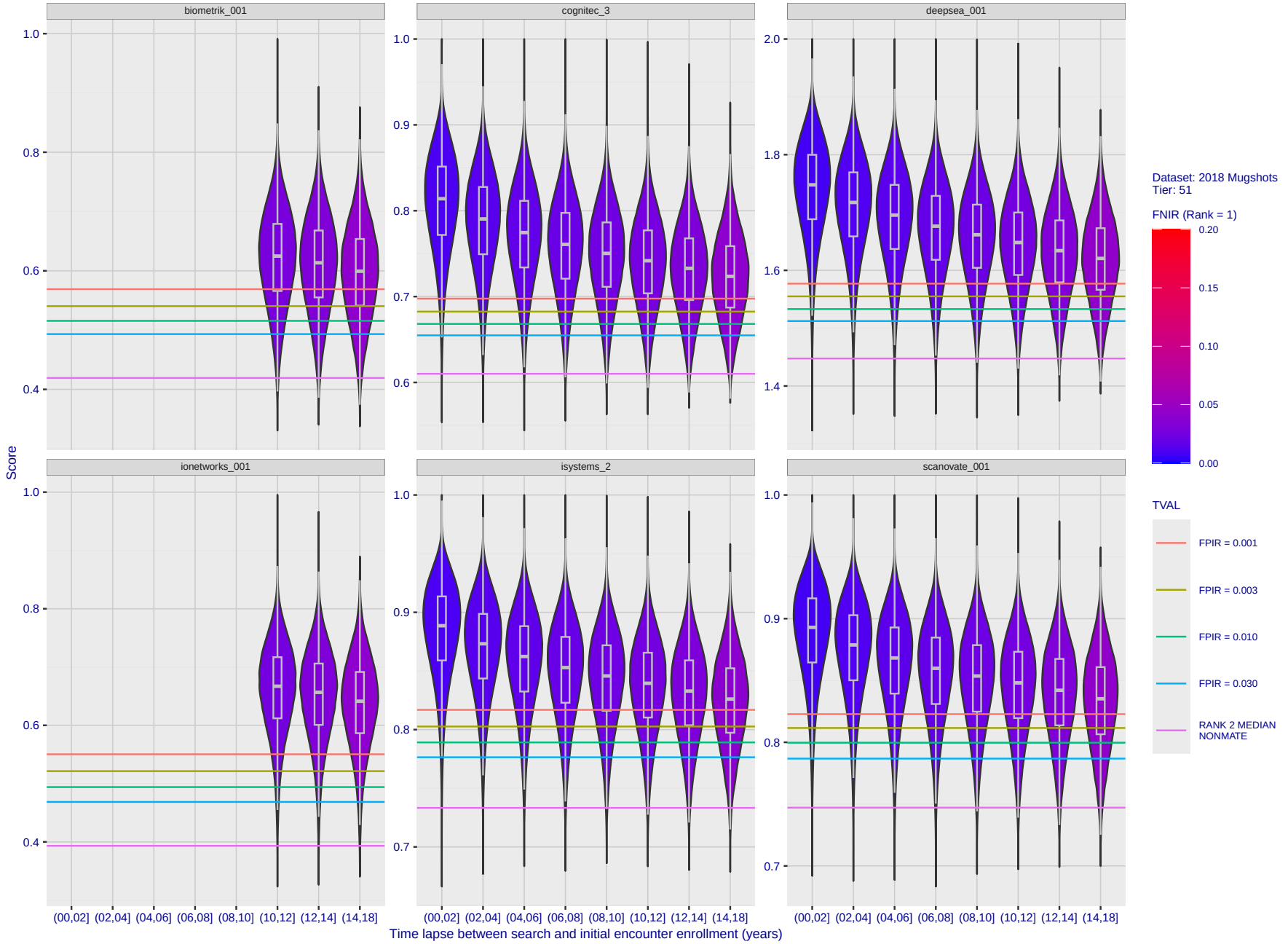

Figure 286: **[FRVT-2018 Mugshot Ageing Dataset] Native mate scores vs. time-elapsed**. *The oldest image of each individual is enrolled. Thereafter, all more recent images are searched. Mated score distributions are computed over all searches noted in row 17 of Table 1 binned by number of years between search and initial enrollment.*

This publication is available free of charge from: https://doi.org/10.6028/NIST.IR.8271

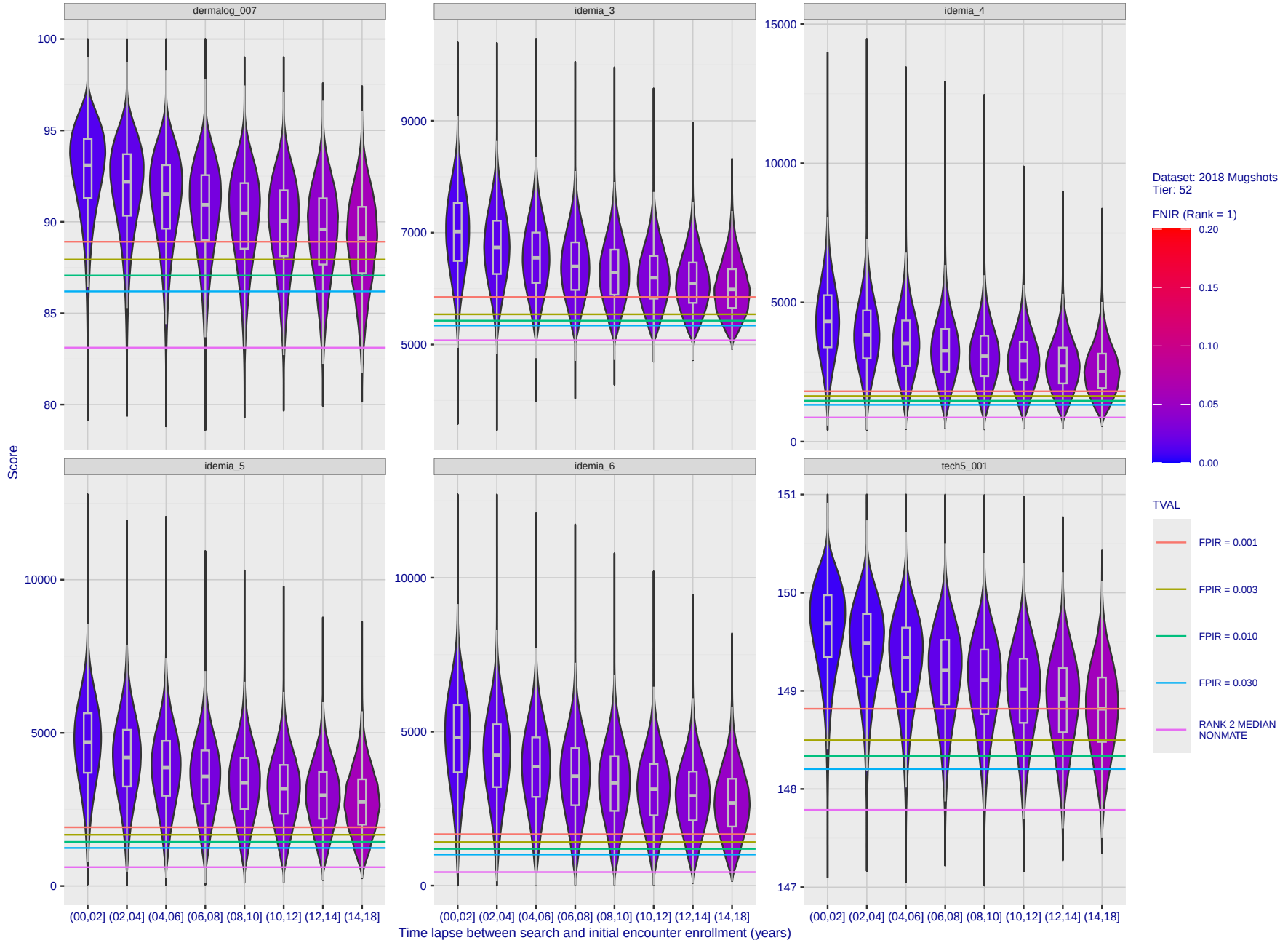

Figure 287: **[FRVT-2018 Mugshot Ageing Dataset] Native mate scores vs. time-elapsed**. *The oldest image of each individual is enrolled. Thereafter, all more recent images are searched. Mated score distributions are computed over all searches noted in row 17 of Table 1 binned by number of years between search and initial enrollment.*

2026/01/09 20:40:38
FNIR(N, R, T) = False neg. identification rate
FPIR(N, T) = False pos. identification rate
N = Num. enrolled subjects
R = Num. candidates examined
T = Threshold
T = 0 → Investigation
T > 0 → Identification

This publication is available free of charge from: https://doi.org/10.6028/NIST.IR.8271

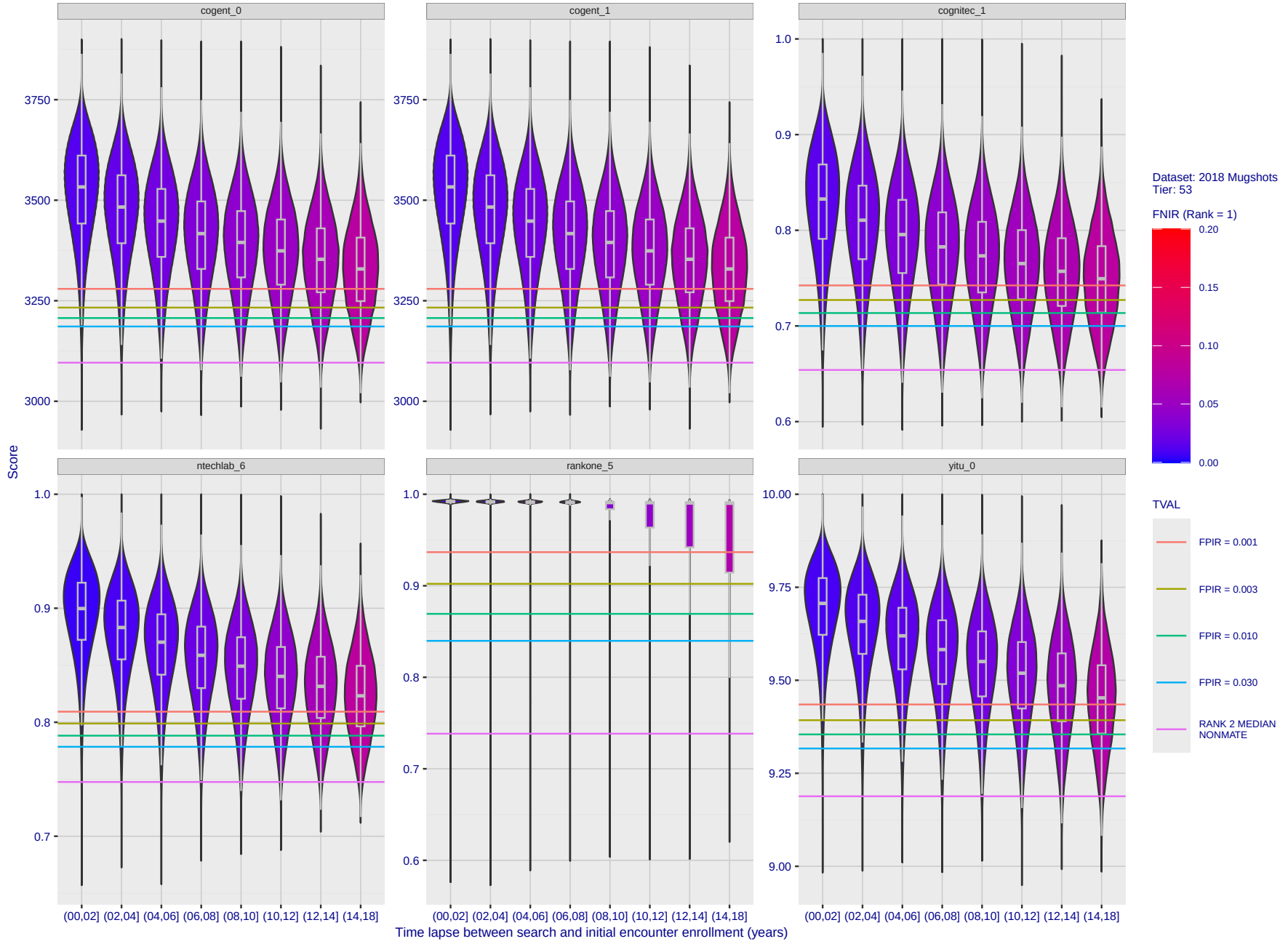

Figure 288: **[FRVT-2018 Mugshot Ageing Dataset] Native mate scores vs. time-elapsed**. *The oldest image of each individual is enrolled. Thereafter, all more recent images are searched. Mated score distributions are computed over all searches noted in row 17 of Table 1 binned by number of years between search and initial enrollment.*

2026/01/09 20:40:38

FNIR(N, R, T) = False neg. identification rate
FPIR(N, T) = False pos. identification rate

N = Num. enrolled subjects
R = Num. candidates examined

T = Threshold

T = 0 → Investigation
T > 0 → Identification

This publication is available free of charge from: https://doi.org/10.6028/NIST.IR.8271

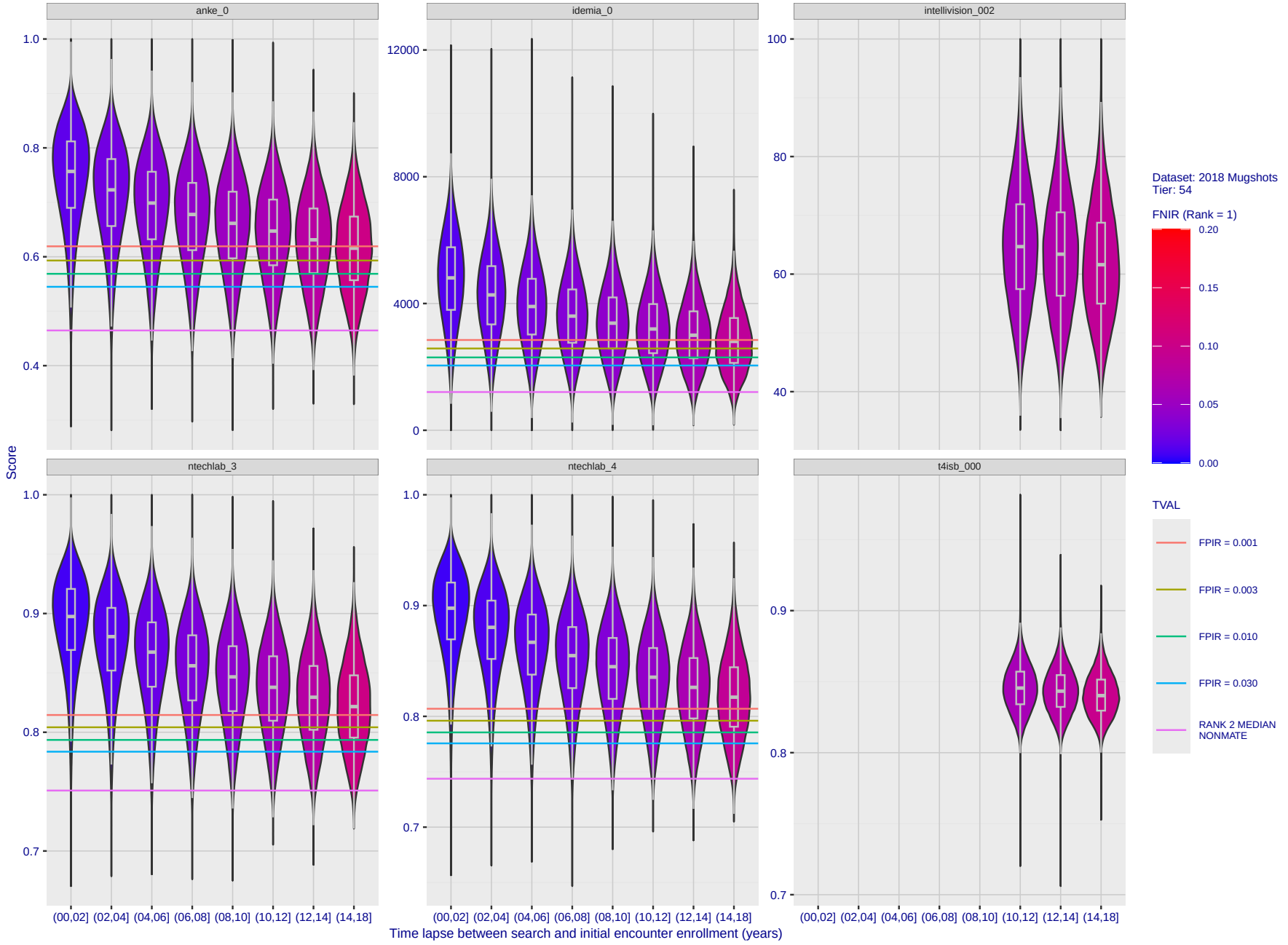

Figure 289: **[FRVT-2018 Mugshot Ageing Dataset] Native mate scores vs. time-elapsed**. *The oldest image of each individual is enrolled. Thereafter, all more recent images are searched. Mated score distributions are computed over all searches noted in row 17 of Table 1 binned by number of years between search and initial enrollment.*

2026/01/09 20:40:38
FNIR(N, R, T) = False neg. identification rate
FPIR(N, T) = False pos. identification rate
N = Num. enrolled subjects
R = Num. candidates examined
T = Threshold
T = 0 → Investigation
T > 0 → Identification

This publication is available free of charge from: https://doi.org/10.6028/NIST.IR.8271

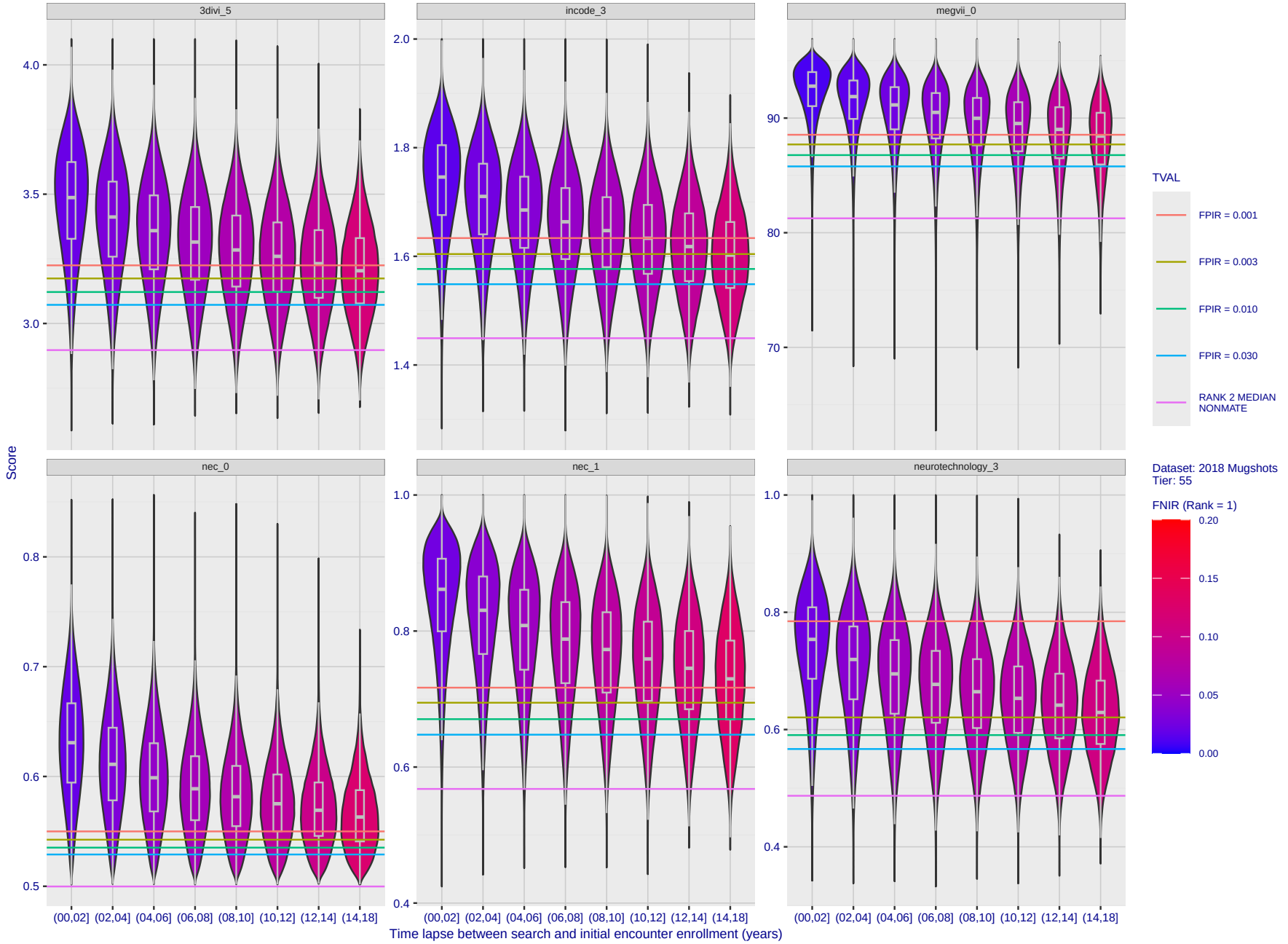

Figure 290: **[FRVT-2018 Mugshot Ageing Dataset] Native mate scores vs. time-elapsed**. *The oldest image of each individual is enrolled. Thereafter, all more recent images are searched. Mated score distributions are computed over all searches noted in row 17 of Table 1 binned by number of years between search and initial enrollment.*

This publication is available free of charge from: https://doi.org/10.6028/NIST.IR.8271

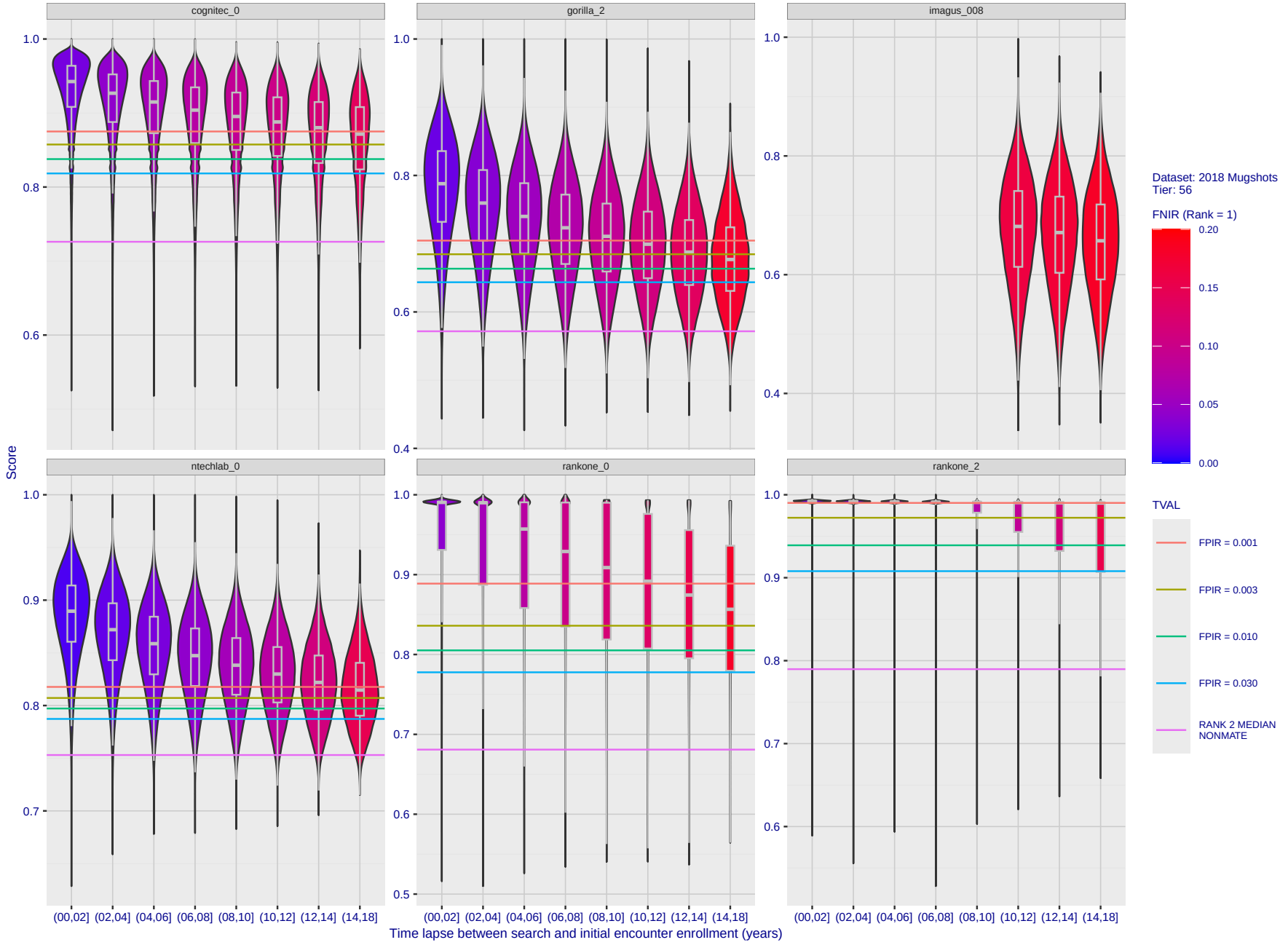

Figure 291: **[FRVT-2018 Mugshot Ageing Dataset] Native mate scores vs. time-elapsed**. *The oldest image of each individual is enrolled. Thereafter, all more recent images are searched. Mated score distributions are computed over all searches noted in row 17 of Table 1 binned by number of years between search and initial enrollment.*

2026/01/09 20:40:38
FNIR(N, R, T) = False neg. identification rate
FPIR(N, T) = False pos. identification rate
N = Num. enrolled subjects
R = Num. candidates examined
T = Threshold
T = 0 → Investigation
T > 0 → Identification

This publication is available free of charge from: https://doi.org/10.6028/NIST.IR.8271

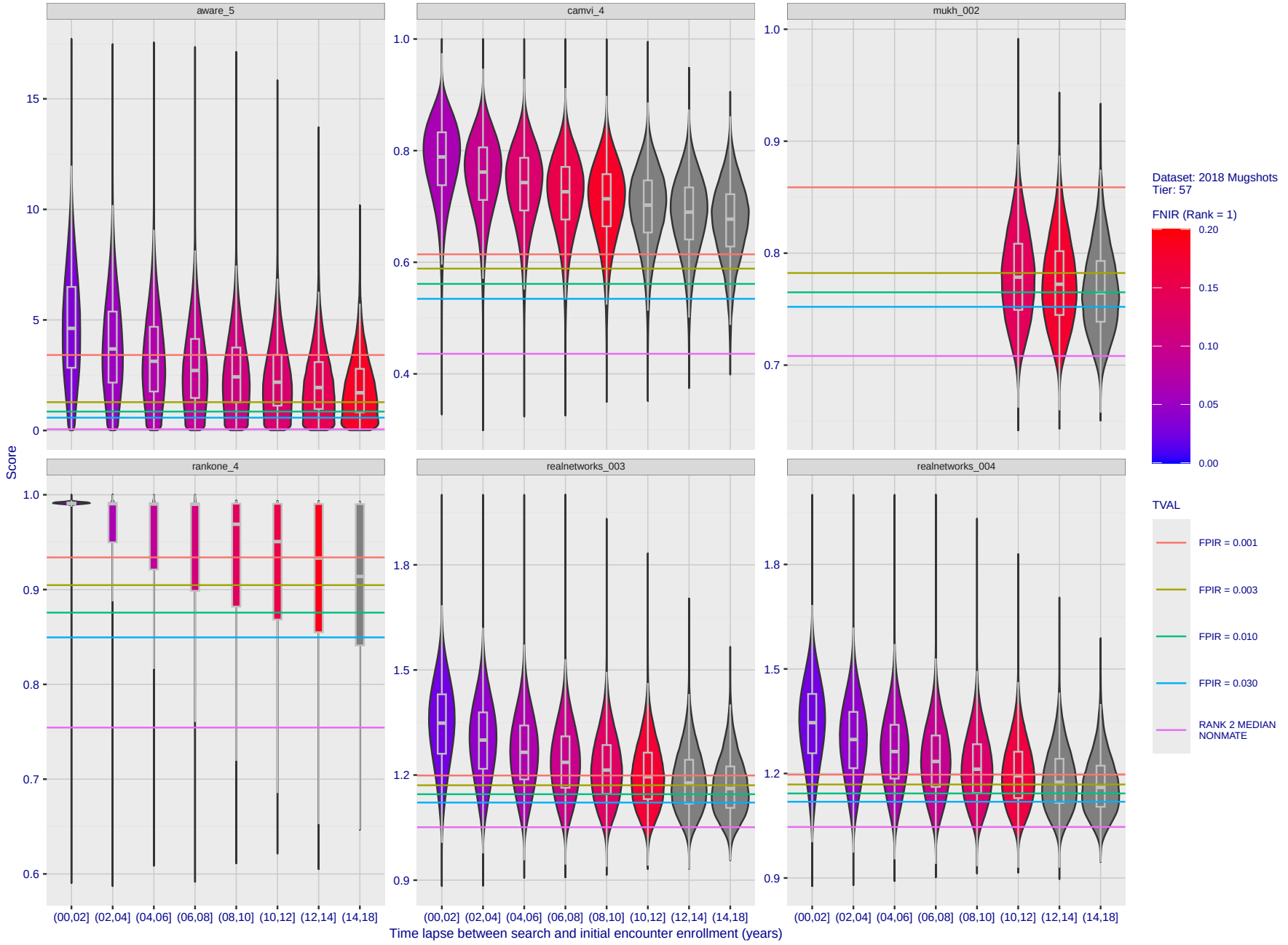

Figure 292: **[FRVT-2018 Mugshot Ageing Dataset] Native mate scores vs. time-elapsed**. *The oldest image of each individual is enrolled. Thereafter, all more recent images are searched. Mated score distributions are computed over all searches noted in row 17 of Table 1 binned by number of years between search and initial enrollment.*

2026/01/09 20:40:38
FNIR(N, R, T) = False neg. identification rate
FPIR(N, T) = False pos. identification rate
N = Num. enrolled subjects
R = Num. candidates examined
T = Threshold
T = 0 → Investigation
T > 0 → Identification

This publication is available free of charge from: https://doi.org/10.6028/NIST.IR.8271

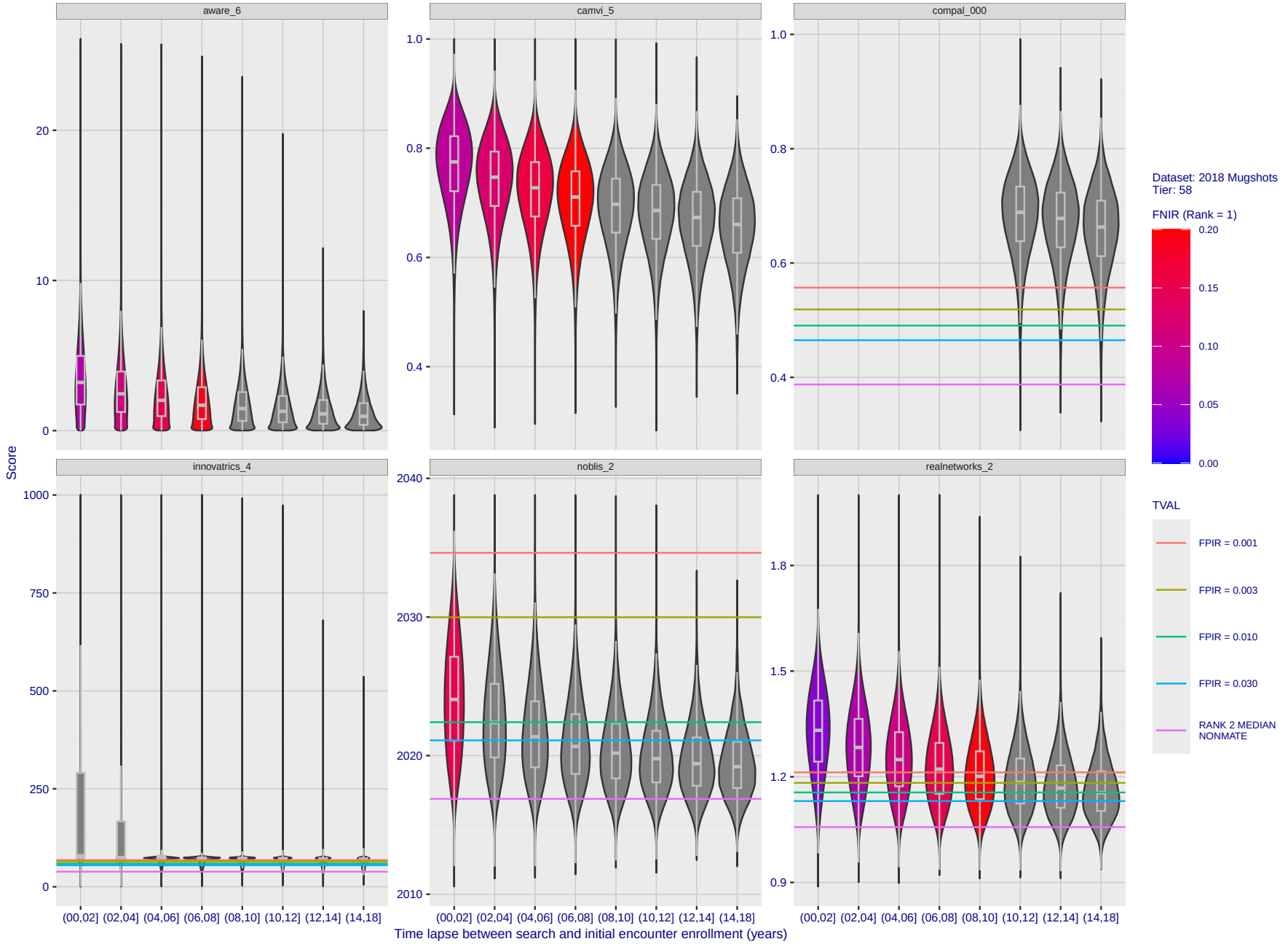

Figure 293: **[FRVT-2018 Mugshot Ageing Dataset] Native mate scores vs. time-elapsed**. *The oldest image of each individual is enrolled. Thereafter, all more recent images are searched. Mated score distributions are computed over all searches noted in row 17 of Table 1 binned by number of years between search and initial enrollment.*

2026/01/09 20:40:38

FNIR(N, R, T) = False neg. identification rate
FPIR(N, T) = False pos. identification rate

N = Num. enrolled subjects
R = Num. candidates examined

T = Threshold

T = 0 → Investigation
T > 0 → Identification

This publication is available free of charge from: https://doi.org/10.6028/NIST.IR.8271

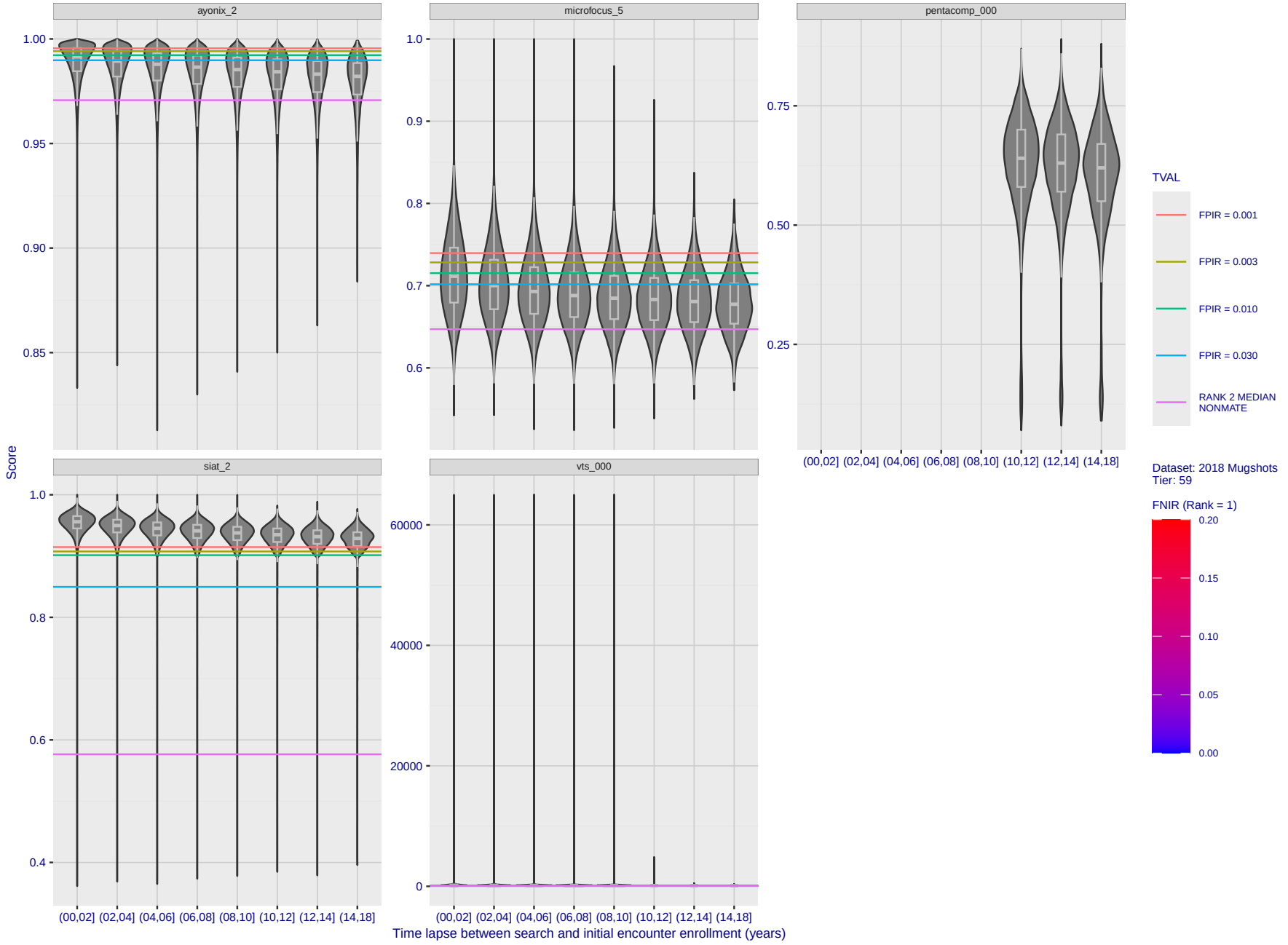

Figure 294: **[FRVT-2018 Mugshot Ageing Dataset] Native mate scores vs. time-elapsed**. *The oldest image of each individual is enrolled. Thereafter, all more recent images are searched. Mated score distributions are computed over all searches noted in row 17 of Table 1 binned by number of years between search and initial enrollment.*

2026/01/09 20:40:38
FNIR(N, R, T) = False neg. identification rate
FPIR(N, T) = False pos. identification rate
N = Num. enrolled subjects
R = Num. candidates examined
T = Threshold
T = 0 → Investigation
T > 0 → Identification

Appendix C Effect of enrolling multiple images

This publication is available free of charge from: https://doi.org/10.6028/NIST.IR.8271

This publication is available free of charge from: https://doi.org/10.6028/NIST.IR.8271

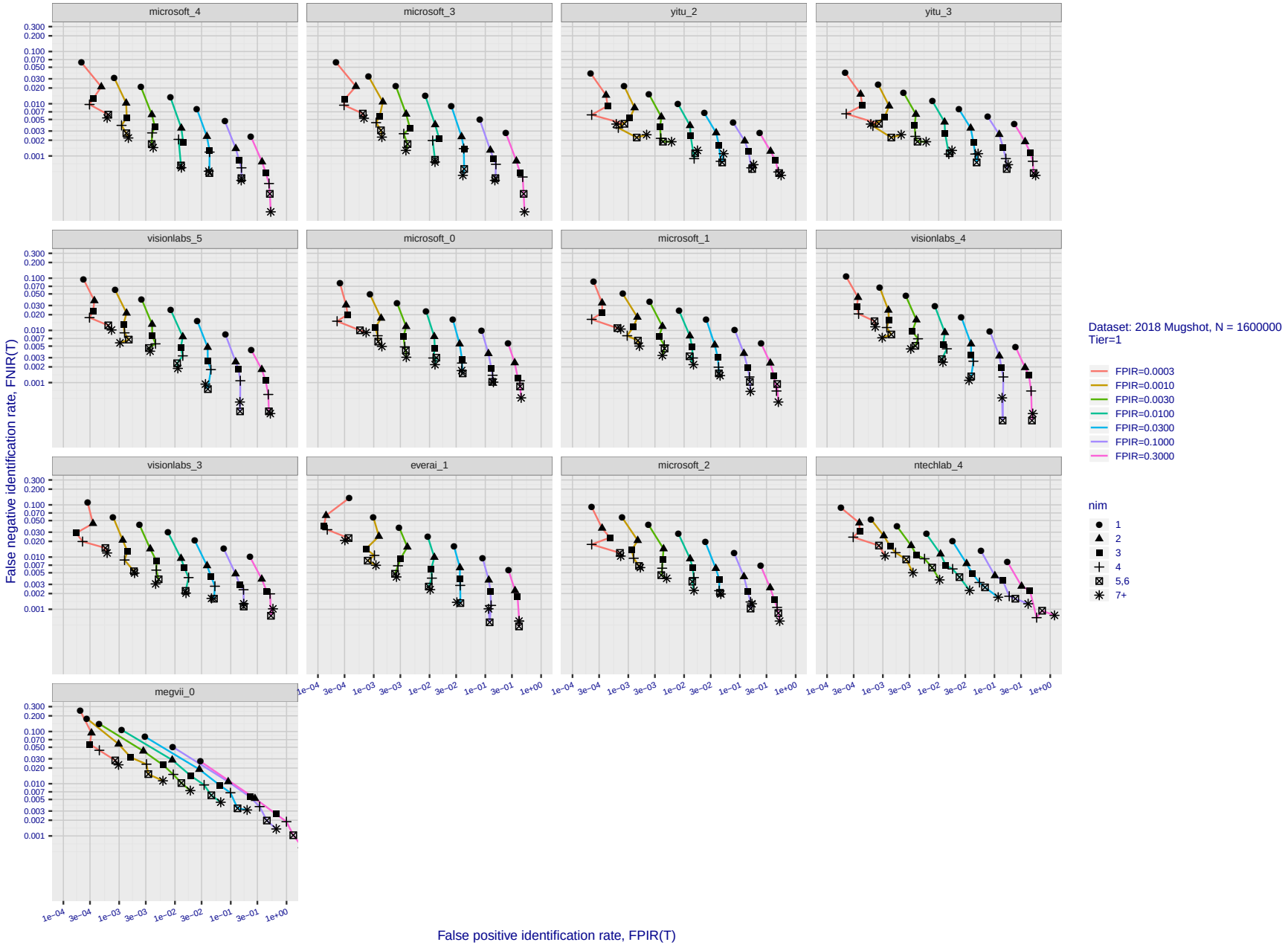

Figure 295: **[FRVT-2018 Mugshot Dataset] Effect of enrolling multiple images for each identity**. *The plot shows an identification miss rates vs. false positive rates, at seven operating thresholds. The enrolled population size is fixed. The images are enrolled with lifetime-consolidation - see section 2.3.*

2026/01/09 20:40:38
FNIR(N, R, T) = False neg. identification rate
FPIR(N, T) = False pos. identification rate
N = Num. enrolled subjects
R = Num. candidates examined
T = Threshold
T = 0 → Investigation
T > 0 → Identification

This publication is available free of charge from: https://doi.org/10.6028/NIST.IR.8271

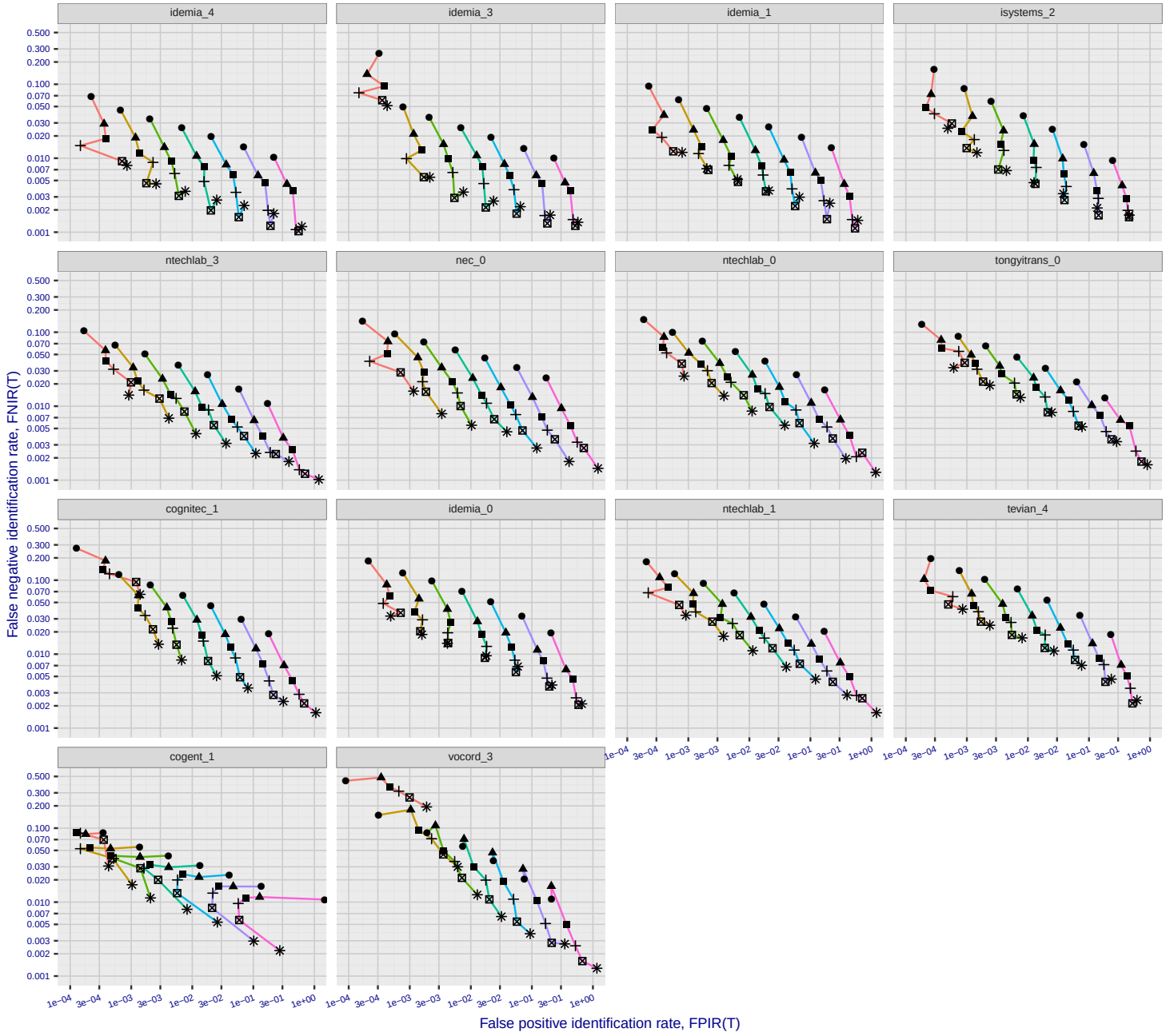

Figure 296: **[FRVT-2018 Mugshot Dataset] Effect of enrolling multiple images for each identity**. *The plot shows an identification miss rates vs. false positive rates, at seven operating thresholds. The enrolled population size is fixed. The images are enrolled with lifetime-consolidation - see section 2.3.*

2026/01/09 20:40:38

FNIR(N, R, T) = False neg. identification rate
FPIR(N, T) = False pos. identification rate

N = Num. enrolled subjects
R = Num. candidates examined

T = Threshold

T = 0 → Investigation
T > 0 → Identification

This publication is available free of charge from: https://doi.org/10.6028/NIST.IR.8271

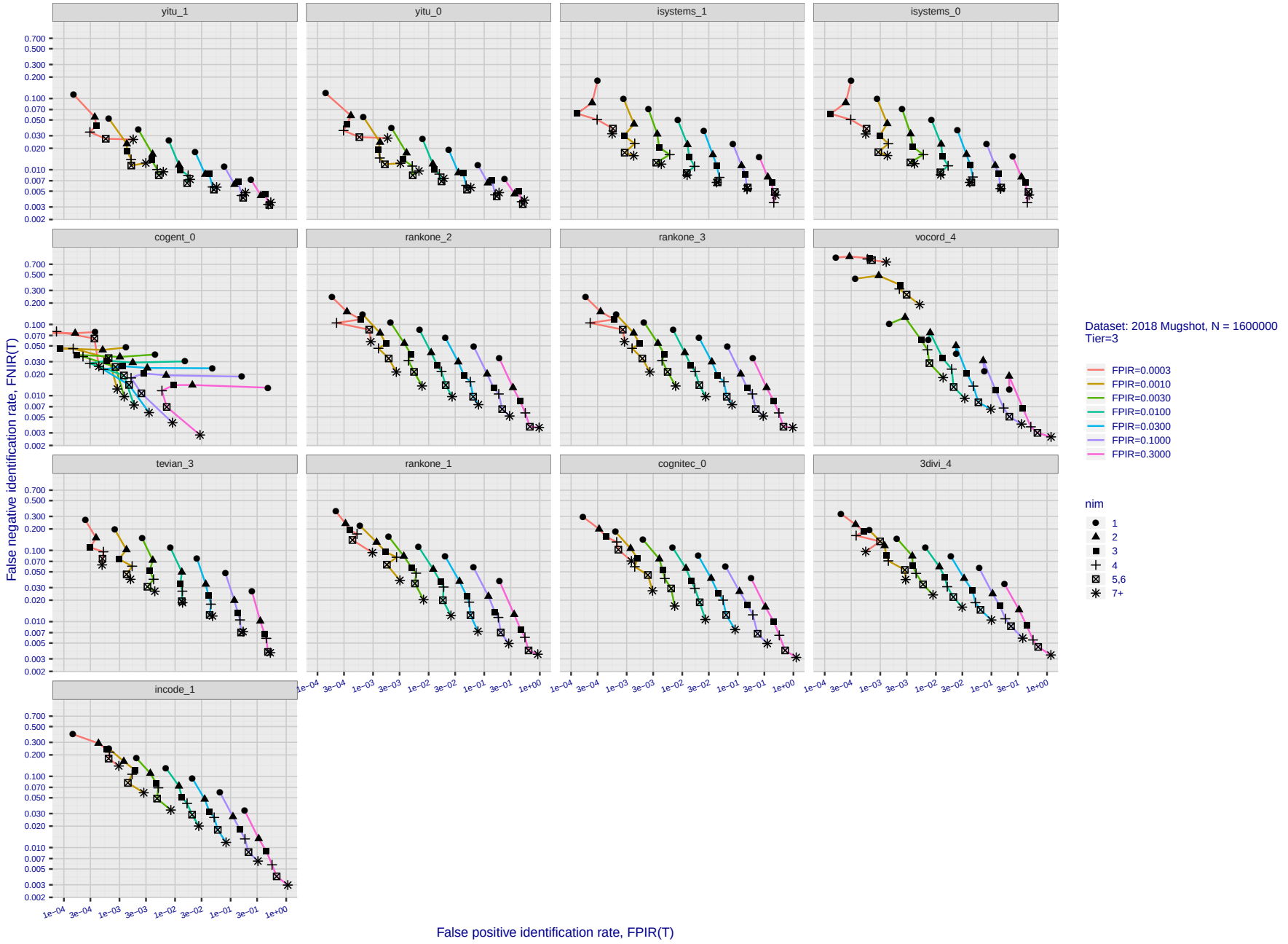

Figure 297: **[FRVT-2018 Mugshot Dataset] Effect of enrolling multiple images for each identity**. *The plot shows an identification miss rates vs. false positive rates, at seven operating thresholds. The enrolled population size is fixed. The images are enrolled with lifetime-consolidation - see section 2.3.*

2026/01/09 20:40:38

FNIR(N, R, T) = False neg. identification rate
FPIR(N, T) = False pos. identification rate

N = Num. enrolled subjects
R = Num. candidates examined

T = Threshold

T = 0 → Investigation
T > 0 → Identification

This publication is available free of charge from: https://doi.org/10.6028/NIST.IR.8271

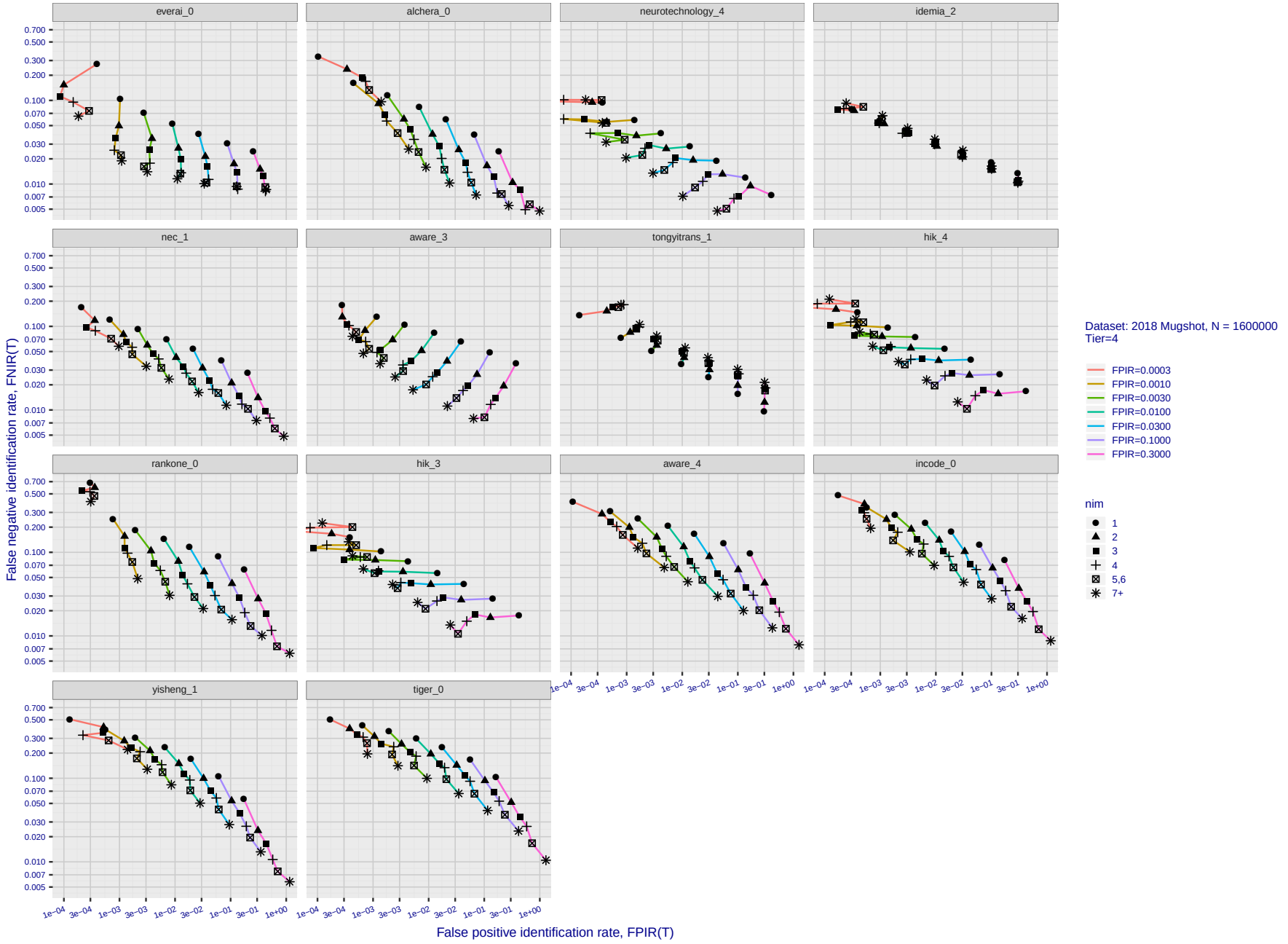

Figure 298: **[FRVT-2018 Mugshot Dataset] Effect of enrolling multiple images for each identity**. *The plot shows an identification miss rates vs. false positive rates, at seven operating thresholds. The enrolled population size is fixed. The images are enrolled with lifetime-consolidation - see section 2.3.*

2026/01/09 20:40:38

FNIR(N, R, T) = False neg. identification rate
FPIR(N, T) = False pos. identification rate

N = Num. enrolled subjects
R = Num. candidates examined

T = Threshold

T = 0 → Investigation
T > 0 → Identification

This publication is available free of charge from: https://doi.org/10.6028/NIST.IR.8271

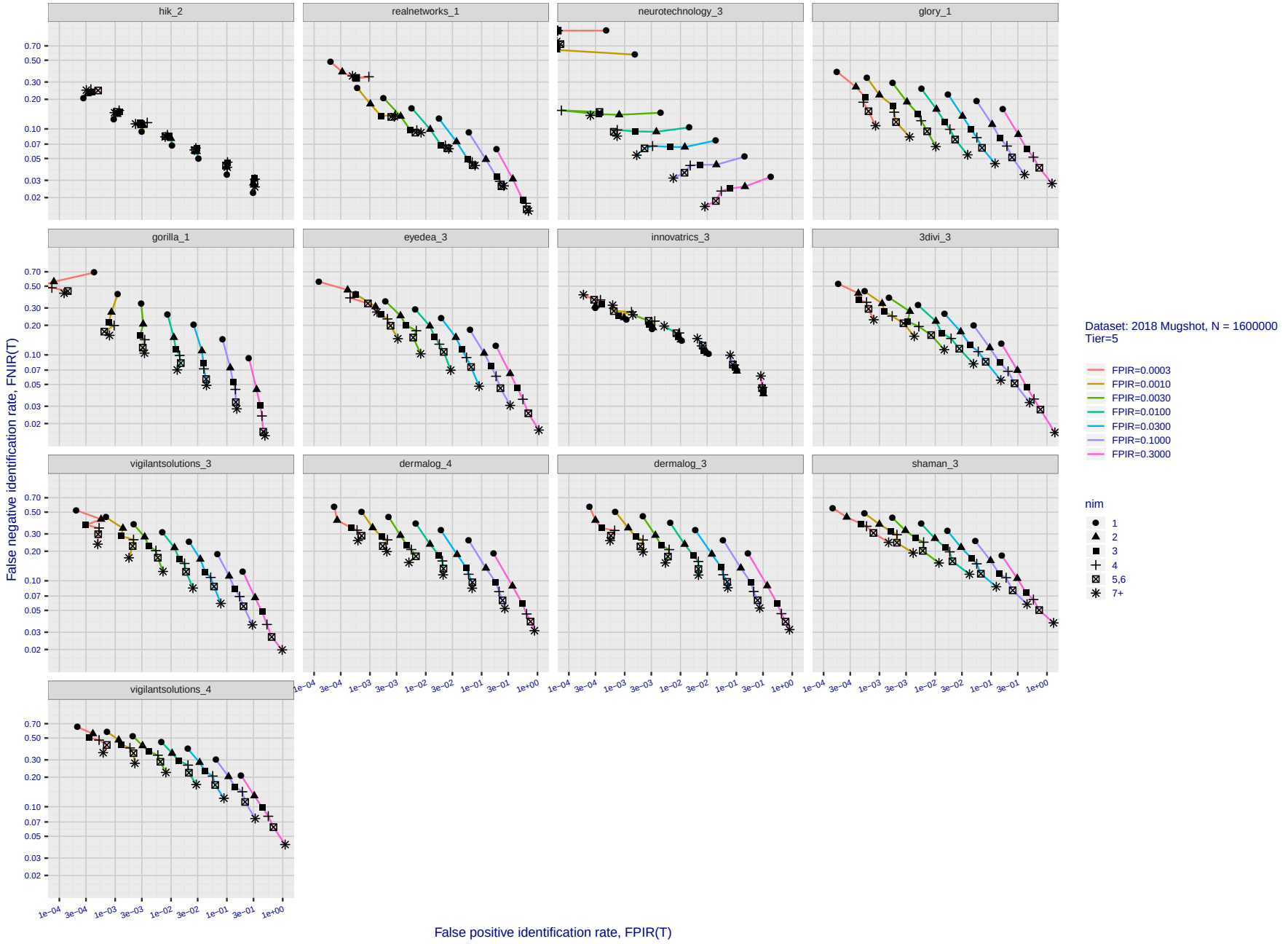

Figure 299: **[FRVT-2018 Mugshot Dataset] Effect of enrolling multiple images for each identity**. *The plot shows an identification miss rates vs. false positive rates, at seven operating thresholds. The enrolled population size is fixed. The images are enrolled with lifetime-consolidation - see section 2.3.*

2026/01/09 20:40:38

FNIR(N, R, T) = False neg. identification rate
FPIR(N, T) = False pos. identification rate

N = Num. enrolled subjects
R = Num. candidates examined

T = Threshold

T = 0 → Investigation
T > 0 → Identification

This publication is available free of charge from: https://doi.org/10.6028/NIST.IR.8271

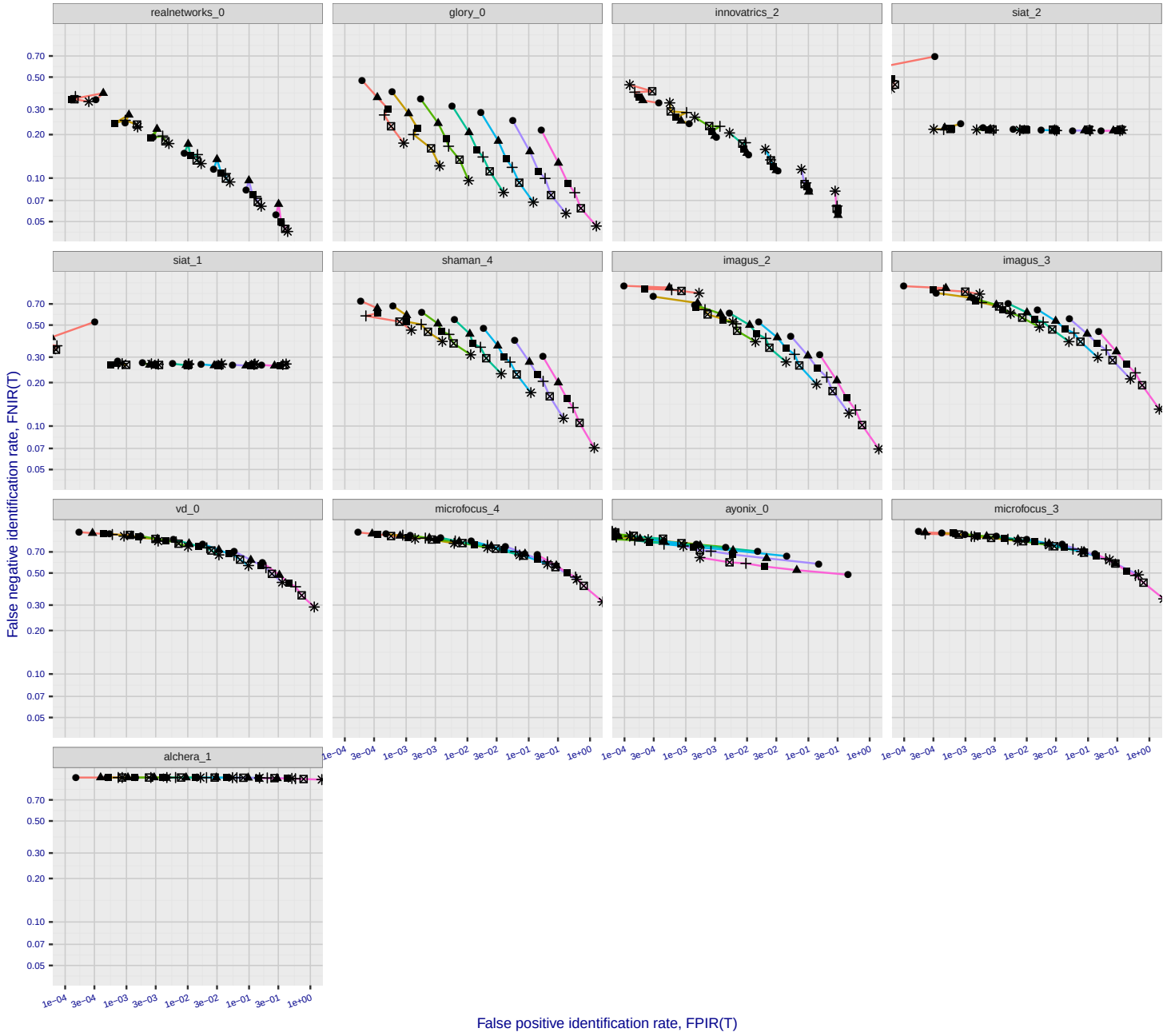

Figure 300: **[FRVT-2018 Mugshot Dataset] Effect of enrolling multiple images for each identity**. *The plot shows an identification miss rates vs. false positive rates, at seven operating thresholds. The enrolled population size is fixed. The images are enrolled with lifetime-consolidation - see section 2.3.*

2026/01/09 20:40:38
FNIR(N, R, T) = False neg. identification rate
FPIR(N, T) = False pos. identification rate
N = Num. enrolled subjects
R = Num. candidates examined
T = Threshold
T = 0 → Investigation
T > 0 → Identification

Appendix D Accuracy with poor quality webcam images

This publication is available free of charge from: https://doi.org/10.6028/NIST.IR.8271

2026/01/09	FNIR(N, R, T) =	False neg. identification rate	N = Num. enrolled subjects	T = Threshold	$T = 0 \rightarrow$ Investigation
20:40:38	FPIR(N, T) =	False pos. identification rate	R = Num. candidates examined		$T > 0 \rightarrow$ Identification

This publication is available free of charge from: https://doi.org/10.6028/NIST.IR.8271

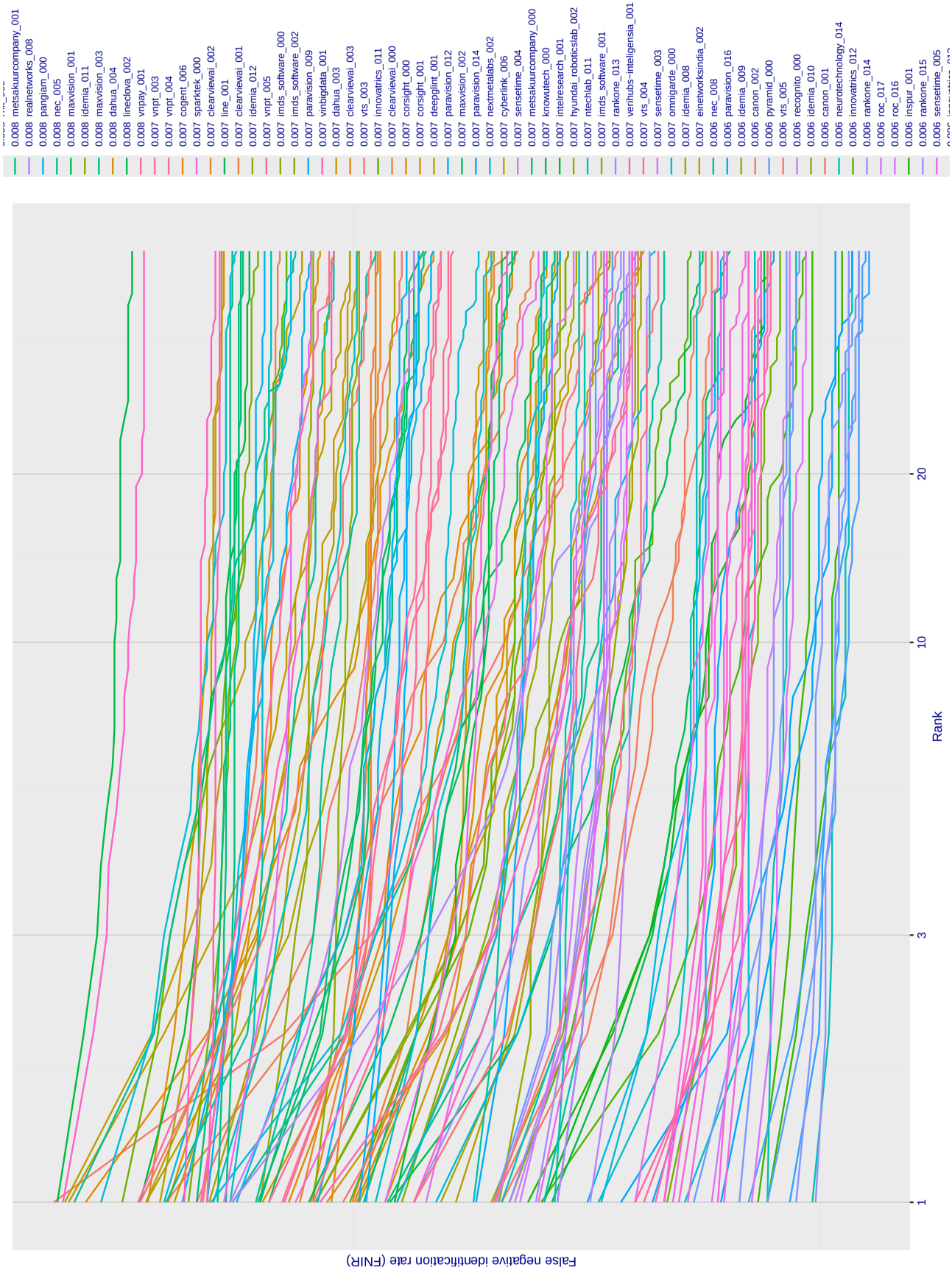

Figure 301: **[Webcam Dataset] Identification miss rates vs. rank.** *The results apply to cross-domain recognition in which webcams are searched against enrolled mugshots. The FNIR values are higher than those for mugshot-mugshot identification due to low image resolution, lighting and less constrained subject pose in webcam images - see Figure 6.*

This publication is available free of charge from: https://doi.org/10.6028/NIST.IR.8271

This publication is available free of charge from: https://doi.org/10.6028/NIST.IR.8271

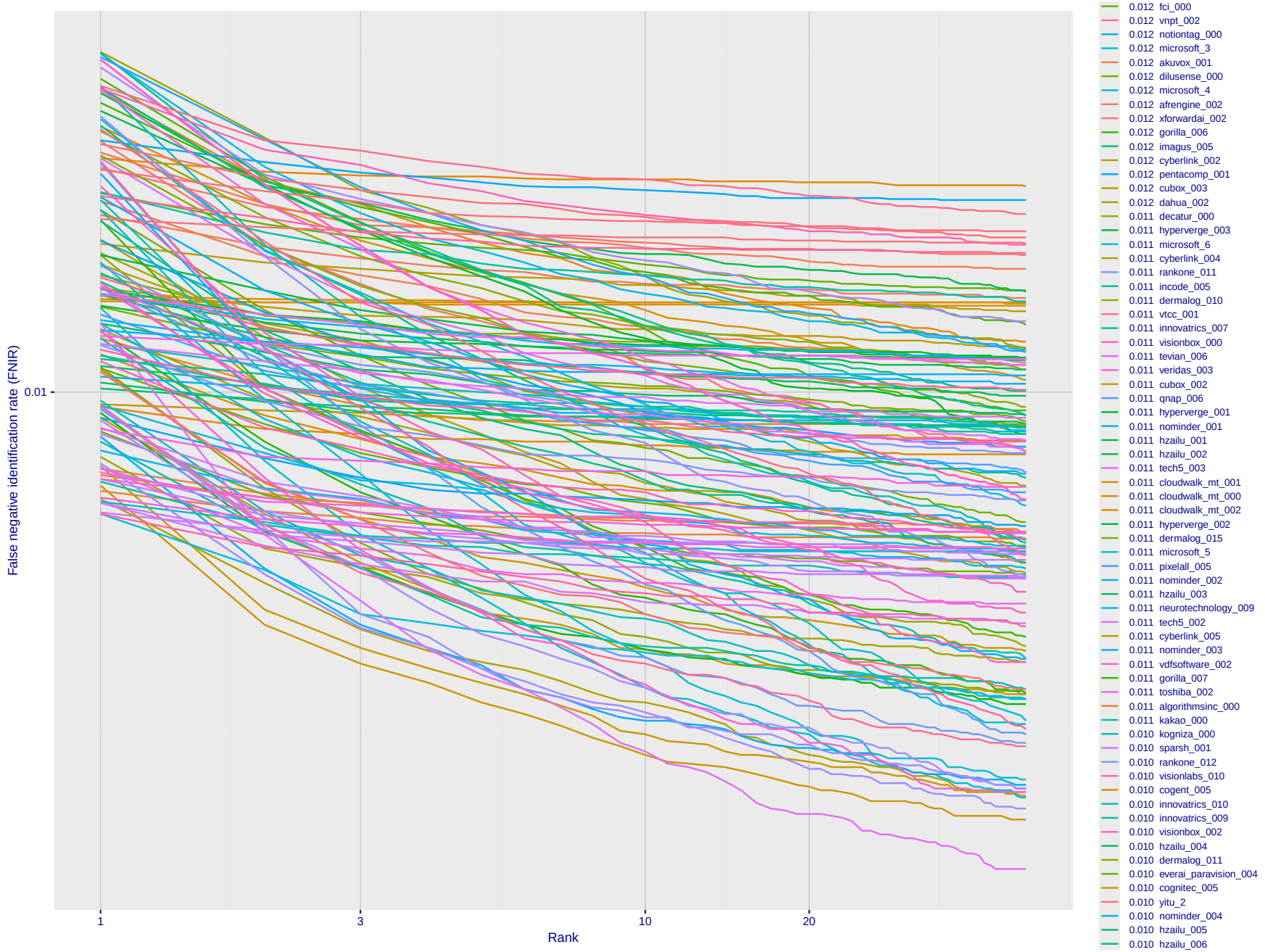

2026/01/09 20:40:38

FNIR(N, R, T) = False neg. identification rate
FPIR(N, T) = False pos. identification rate

N = Num. enrolled subjects
R = Num. candidates examined

T = Threshold

T = 0 → Investigation
T > 0 → Identification

Figure 302: **[Webcam Dataset] Identification miss rates vs. rank**. *The results apply to cross-domain recognition in which webcams are searched against enrolled mugshots. The FNIR values are higher than those for mugshot-mugshot identification due to low image resolution, lighting and less constrained subject pose in webcam images - see Figure 6.*

This publication is available free of charge from: https://doi.org/10.6028/NIST.IR.8271

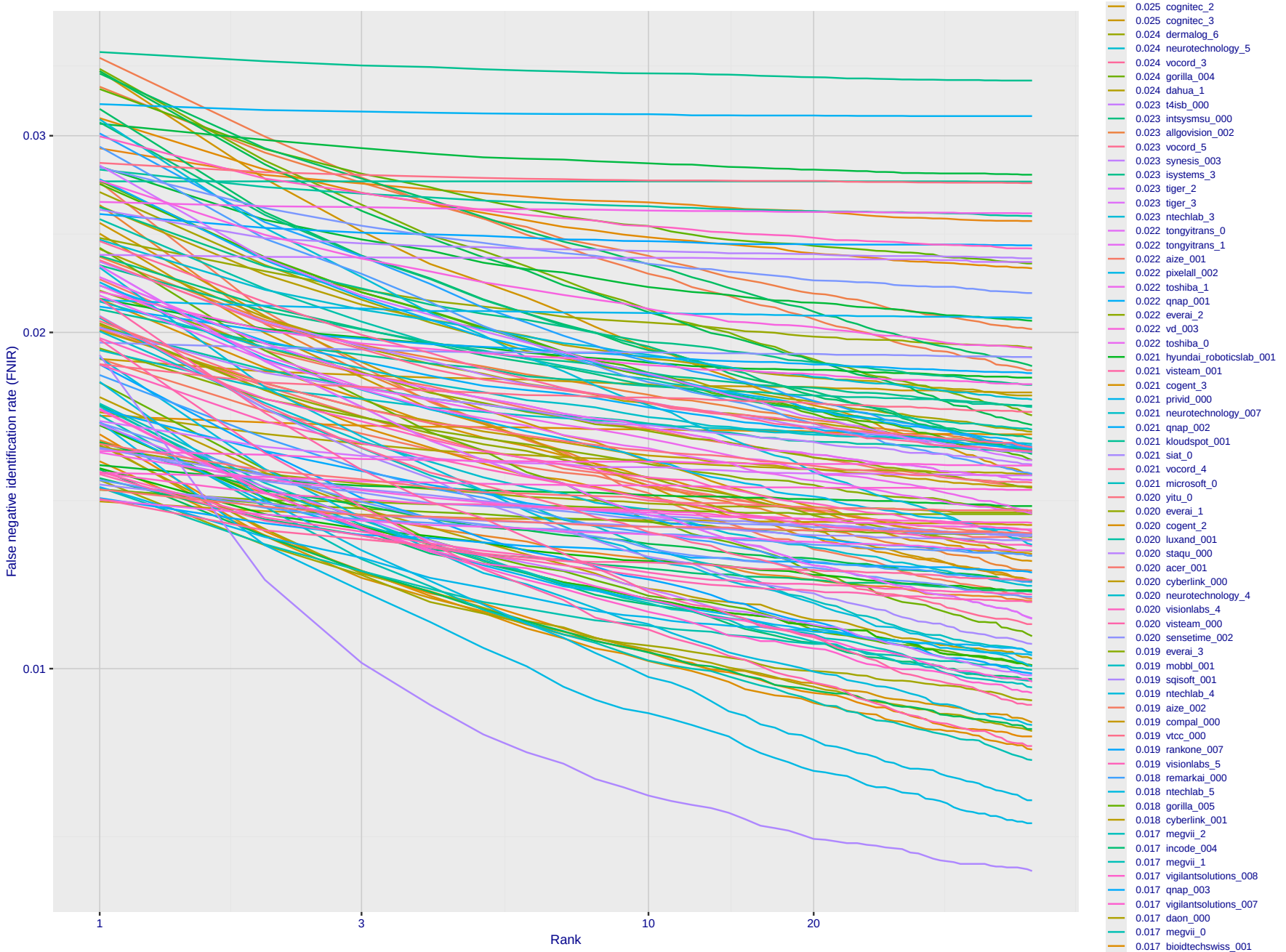

Figure 303: **[Webcam Dataset] Identification miss rates vs. rank**. *The results apply to cross-domain recognition in which webcams are searched against enrolled mugshots. The FNIR values are higher than those for mugshot-mugshot identification due to low image resolution, lighting and less constrained subject pose in webcam images - see Figure 6.*

2026/01/09 20:40:38

FNIR(N, R, T) = False neg. identification rate
FPIR(N, T) = False pos. identification rate

N = Num. enrolled subjects
R = Num. candidates examined

T = Threshold

T = 0 → Investigation
T > 0 → Identification

This publication is available free of charge from: https://doi.org/10.6028/NIST.IR.8271

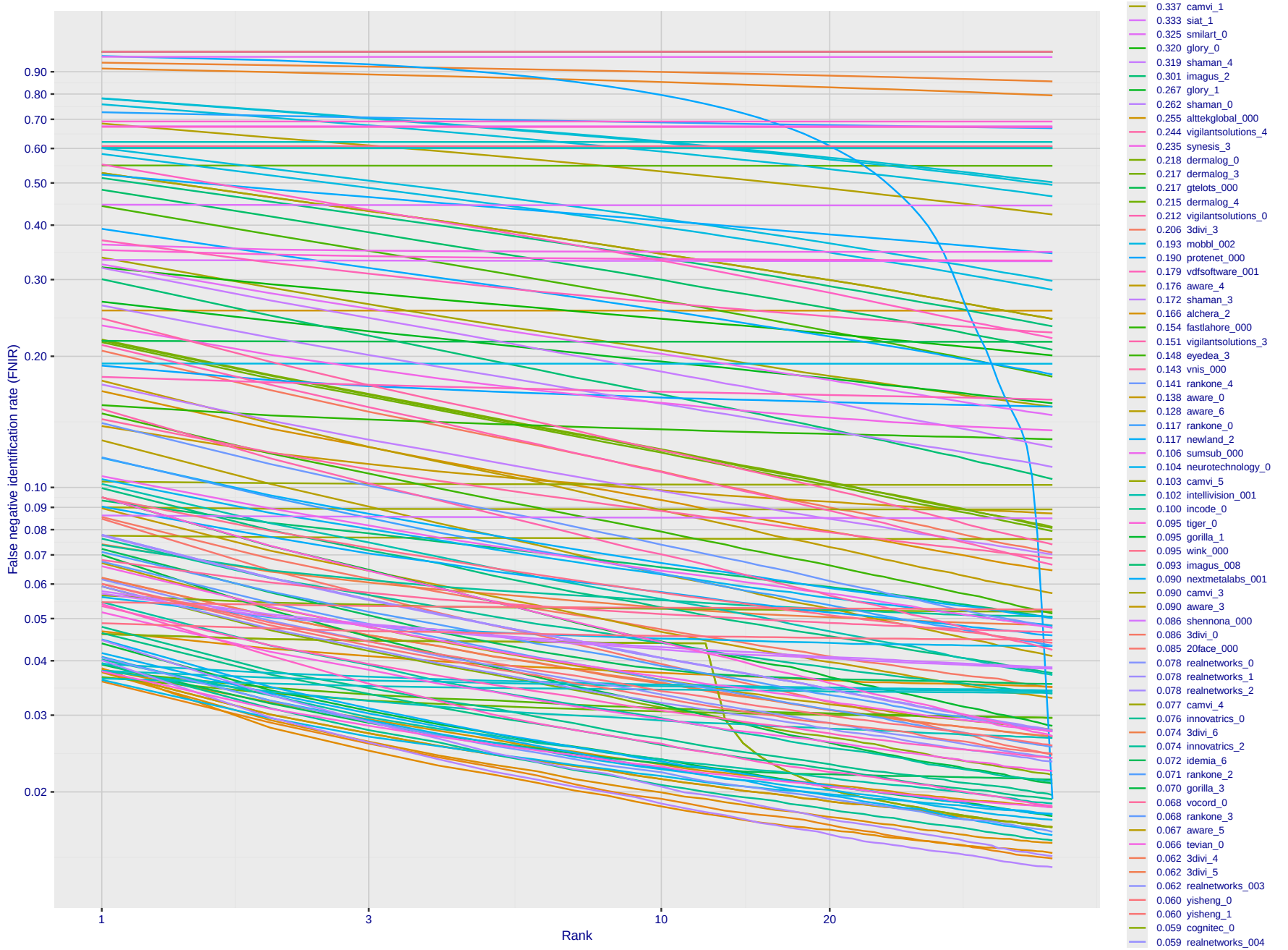

Figure 304: **[Webcam Dataset] Identification miss rates vs. rank**. *The results apply to cross-domain recognition in which webcams are searched against enrolled mugshots. The FNIR values are higher than those for mugshot-mugshot identification due to low image resolution, lighting and less constrained subject pose in webcam images - see Figure 6.*

2026/01/09 20:40:38
FNIR(N, R, T) = FPIR(N, T) =
False neg. identification rate
False pos. identification rate
N = Num. enrolled subjects
R = Num. candidates examined
T = Threshold
T = 0 → Investigation
T > 0 → Identification

2026/01/09	FNIR(N, R, T) =	False neg. identification rate	N = Num. enrolled subjects	T = Threshold	$T = 0 \rightarrow$ Investigation
20:40:38	FPIR(N, T) =	False pos. identification rate	R = Num. candidates examined		$T > 0 \rightarrow$ Identification

This publication is available free of charge from: https://doi.org/10.6028/NIST.IR.8271

This publication is available free of charge from: https://doi.org/10.6028/NIST.IR.8271

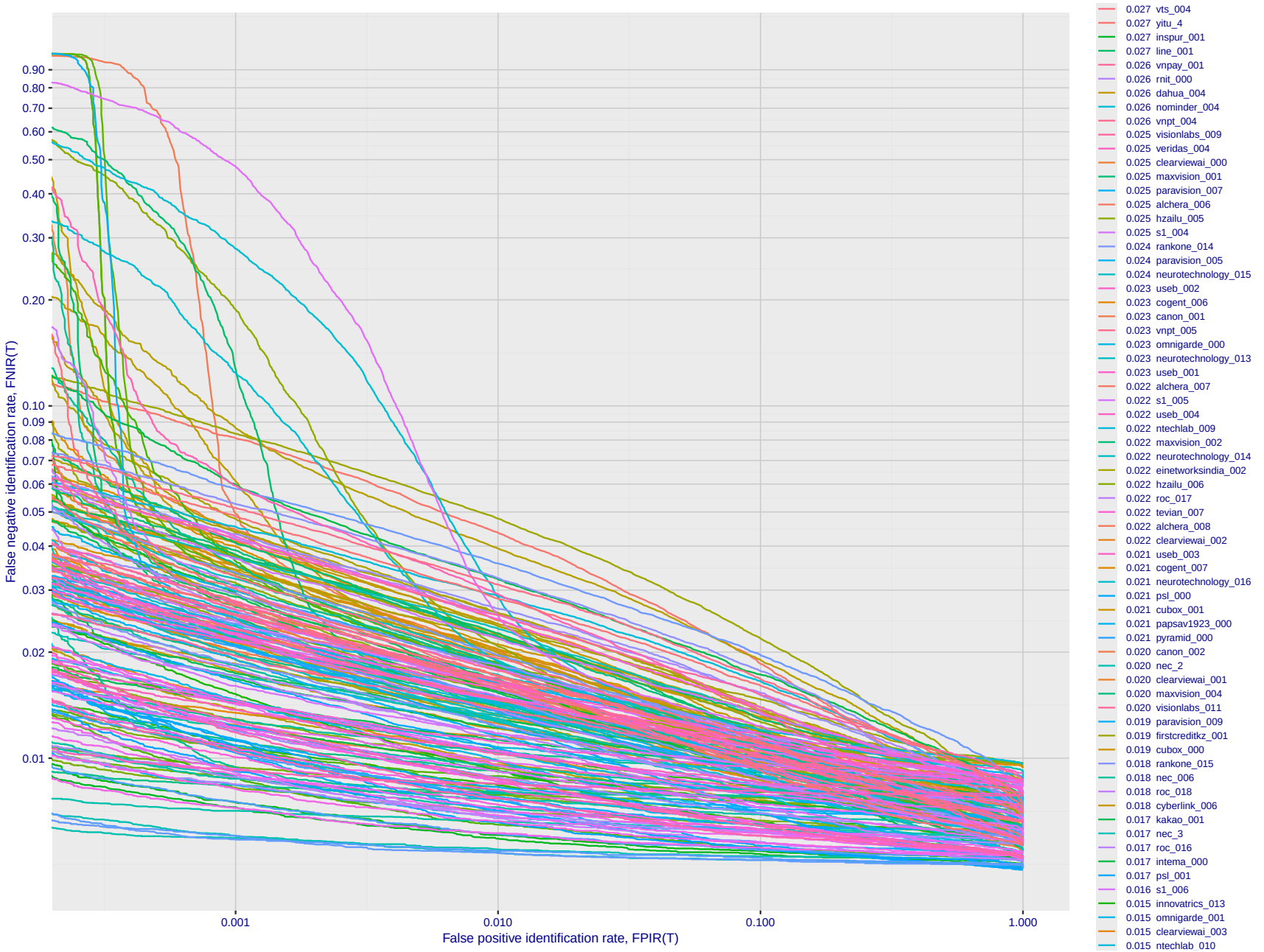

Figure 305: **[Webcam Dataset] Identification miss rates vs. false positive rates**. *The results apply to cross-domain recognition in which webcams are searched against enrolled mugshots. The FNIR values are higher than those for mugshot-mugshot identification due to low image resolution, lighting and less constrained subject pose in webcam images - see Figure 6.*

2026/01/09 20:40:38

FNIR(N, R, T) = False neg. identification rate
FPIR(N, T) = False pos. identification rate

N = Num. enrolled subjects
R = Num. candidates examined

T = Threshold

T = 0 → Investigation
T > 0 → Identification

This publication is available free of charge from: https://doi.org/10.6028/NIST.IR.8271

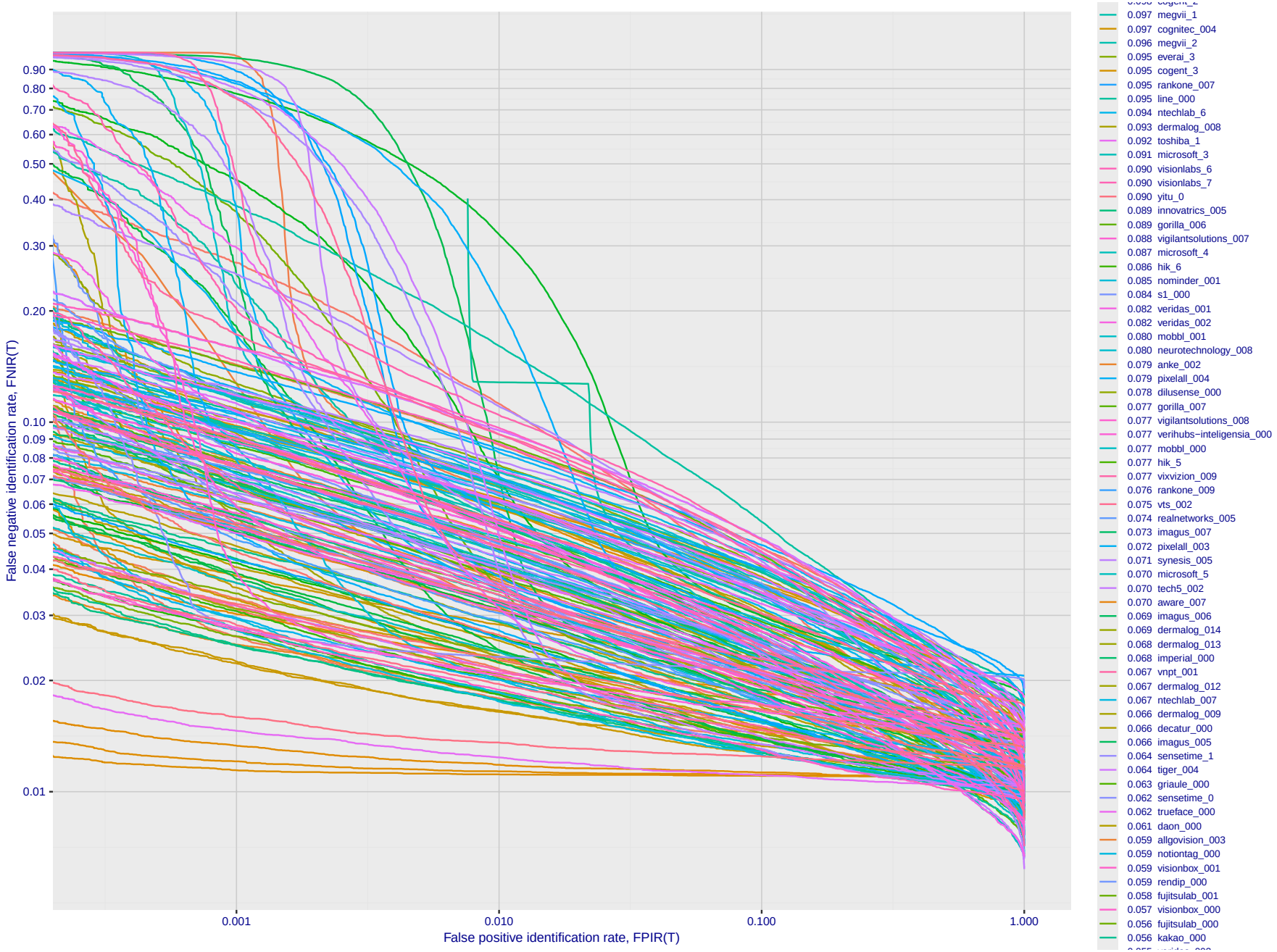

Figure 306: **[Webcam Dataset] Identification miss rates vs. false positive rates**. *The results apply to cross-domain recognition in which webcams are searched against enrolled mugshots. The FNIR values are higher than those for mugshot-mugshot identification due to low image resolution, lighting and less constrained subject pose in webcam images - see Figure 6.*

2026/01/09 20:40:38
FNIR(N, R, T) = False neg. identification rate
FPIR(N, T) = False pos. identification rate
N = Num. enrolled subjects
R = Num. candidates examined
T = Threshold
T = 0 → Investigation
T > 0 → Identification

This publication is available free of charge from: https://doi.org/10.6028/NIST.IR.8271

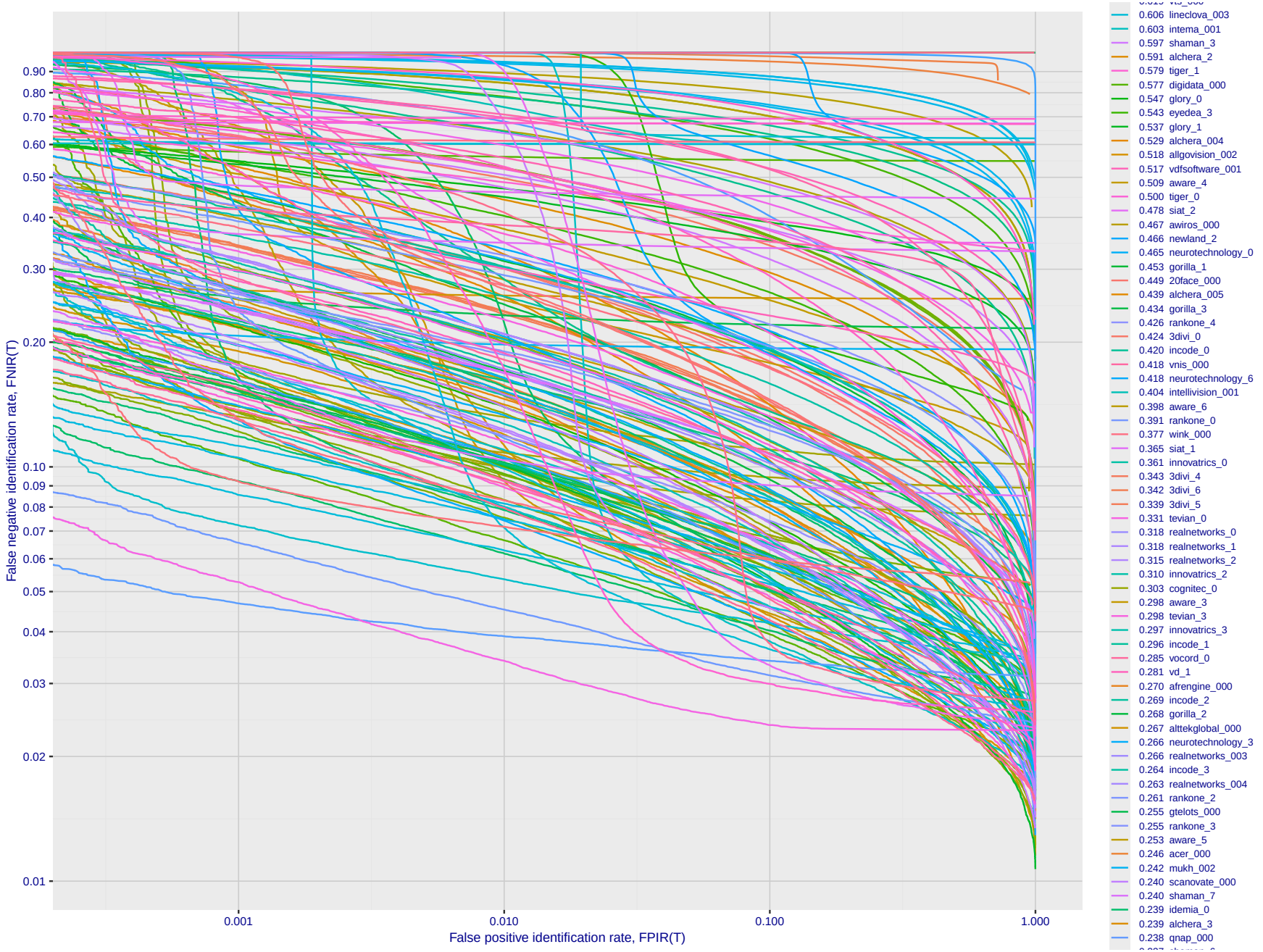

Figure 307: **[Webcam Dataset] Identification miss rates vs. false positive rates**. *The results apply to cross-domain recognition in which webcams are searched against enrolled mugshots. The FNIR values are higher than those for mugshot-mugshot identification due to low image resolution, lighting and less constrained subject pose in webcam images - see Figure 6.*

2026/01/09 20:40:38
FNIR(N, R, T) = False neg. identification rate
FPIR(N, T) = False pos. identification rate
N = Num. enrolled subjects
R = Num. candidates examined
T = Threshold
T = 0 → Investigation
T > 0 → Identification

Appendix E Accuracy for profile-view to frontal recognition

Figures 308 - 310 gives accuracy results for searching 100 000 mated and 100 000 non-mated profile-view images against the same FRVT 2018 frontal enrollment dataset, N = 1 600 000, used in the main mugshot trials. This experiment corresponds to row-13 of Table 1. An example of profile-view image is given in Figure 7.

This publication is available free of charge from: https://doi.org/10.6028/NIST.IR.8271

This publication is available free of charge from: https://doi.org/10.6028/NIST.IR.8271

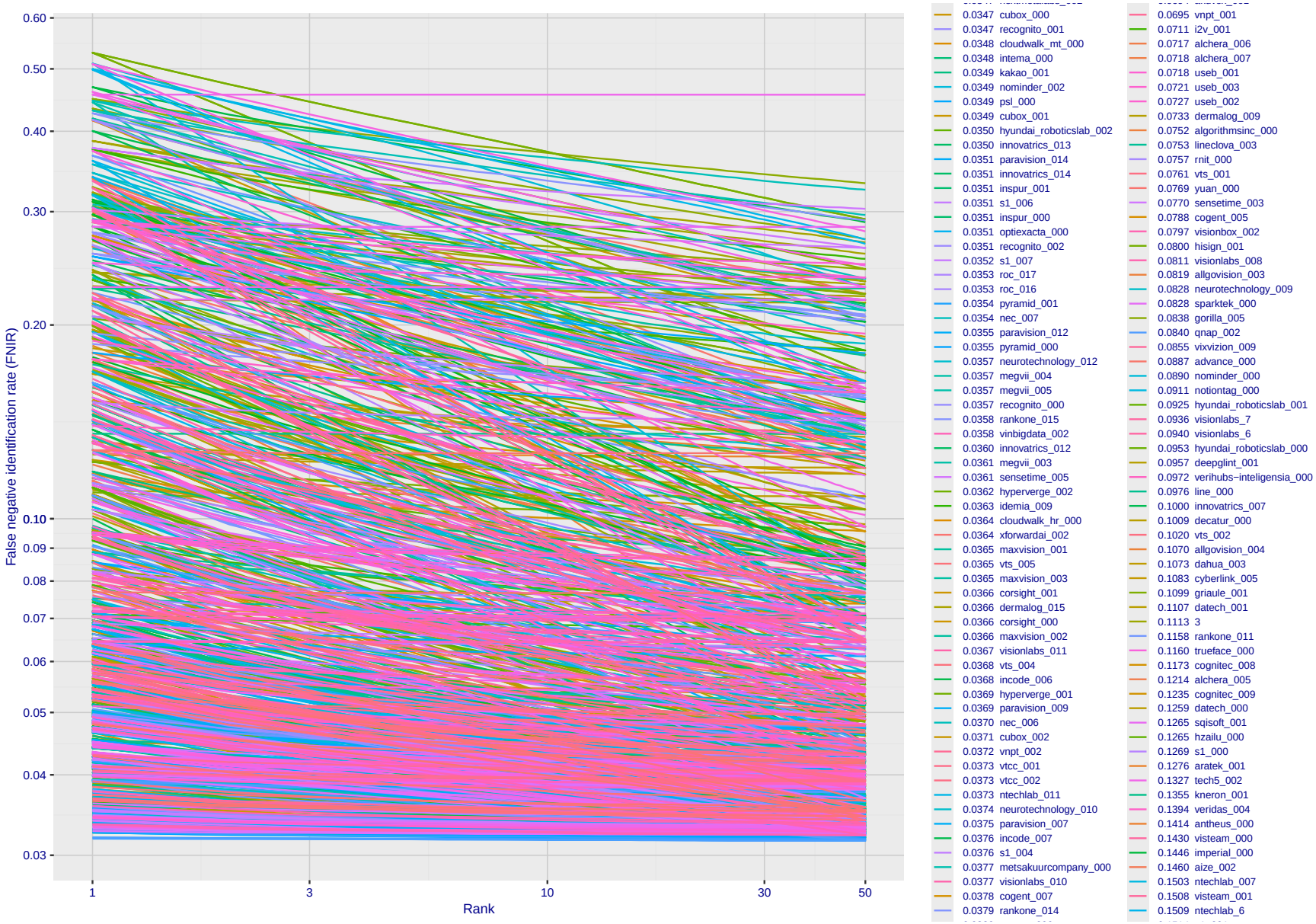

Figure 308: **[Mugshot and profile-view dataset] Rank-based accuracy**. *For some of the more accurate Phase 3 algorithms the figure plots error tradeoff characteristics for frontal and profile-view searches into an enrolled set of N = 1 600 000 frontal images. Note that some algorithms fail on profile-view images with FNIR → 1 - this evaluation did not ask developers to provide profile-view capability. Some algorithms, on the other hand, give FNIR approaching that for frontal-view searches using c. 2010 algorithms. The best result is that 91% of profile-view searches yield the correct mate at rank 1, and better than 94% in the top-50 candidates.*

This publication is available free of charge from: https://doi.org/10.6028/NIST.IR.8271

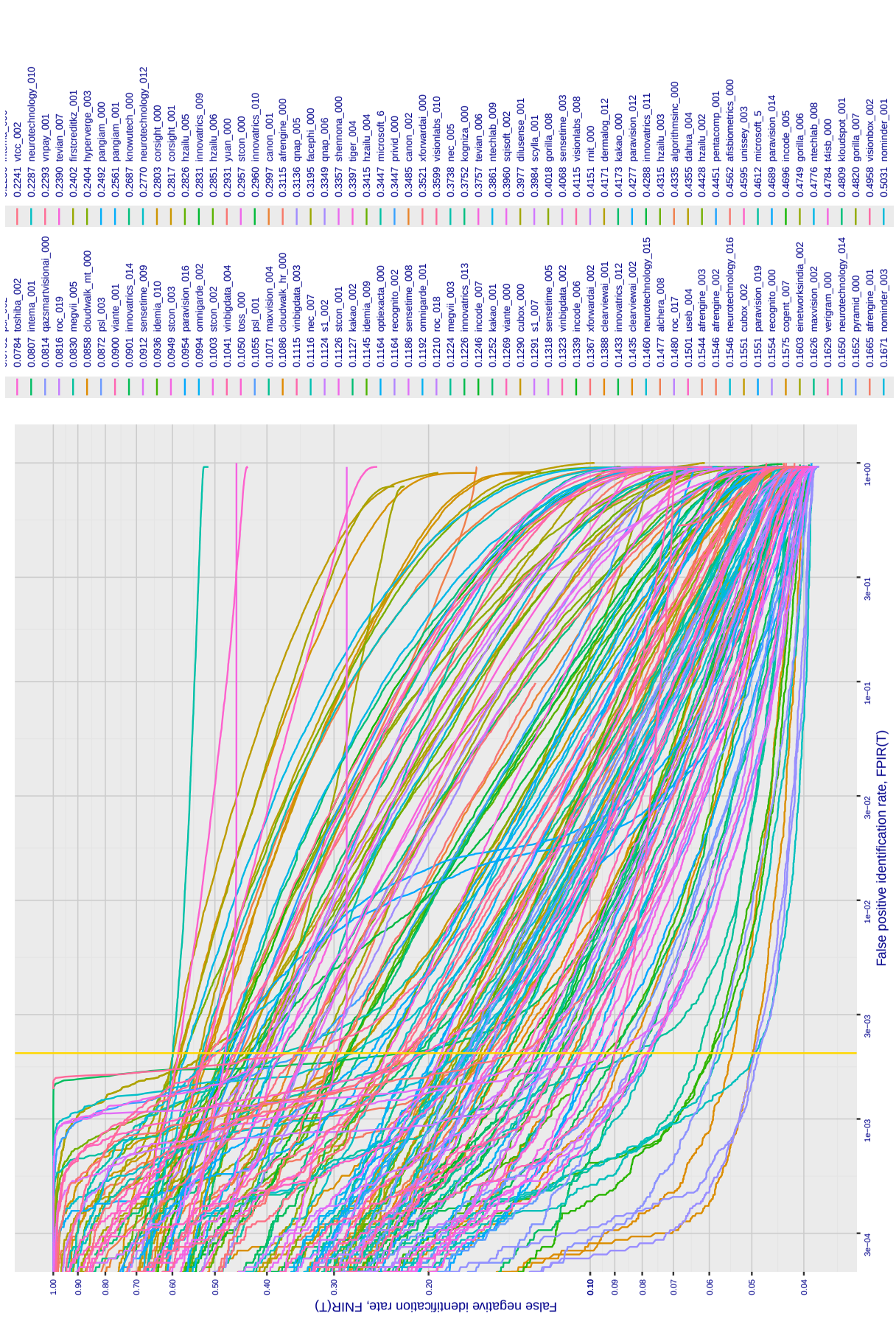

Figure 309: **[Mugshot and profile-view dataset] Threshold-based accuracy**. *For some of the more accurate Phase 3 algorithms the figure plots error tradeoff characteristics for frontal and profile-view searches into an enrolled set of N = 1 600 000 frontal images. Note that some algorithms fail on profile-view images with FNIR → 1 - this evaluation did not ask developers to provide profile-view capability. Some algorithms, on the other hand, give FNIR approaching that for frontal-view searches using c. 2010 algorithms.*

This publication is available free of charge from: https://doi.org/10.6028/NIST.IR.8271

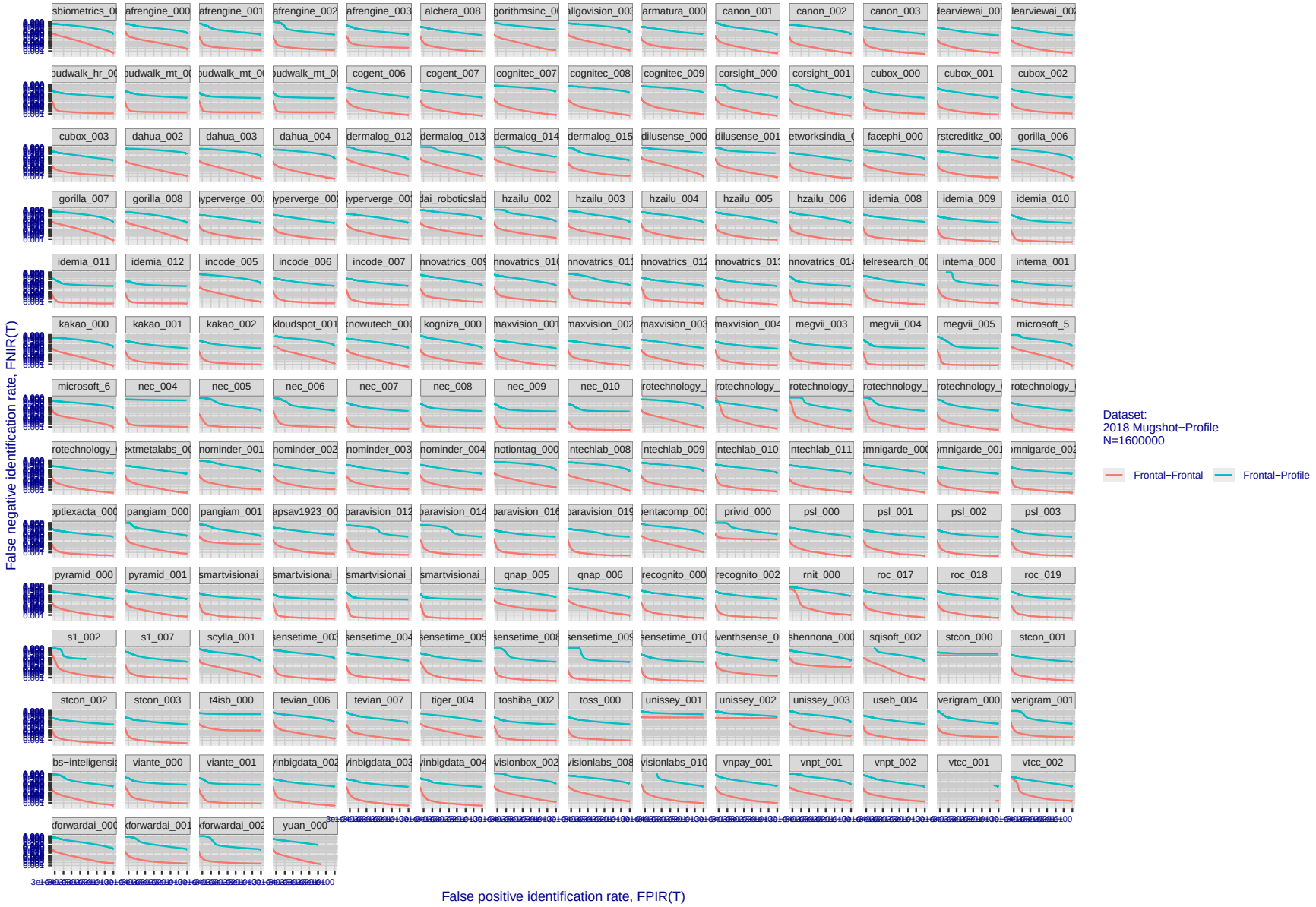

Figure 310: **[Mugshot and profile-view dataset] Speed-accuracy tradeoff**. *For some of the more accurate Phase 3 algorithms the figure plots error tradeoff characteristics for frontal and profile-view searches into an enrolled set of N = 1 600 000 frontal images. Some algorithms fail on profile-view images with FNIR → 1 - this evaluation did not ask developers to provide profile-view capability. Some algorithms, on the other hand, give FNIR approaching that for frontal-view searches using c. 2010 algorithms. Blue lines connect points of equal threshold from which it is evident that some algorithms would give markedly higher false positive outcomes if profile-view images were searched in a system configured for frontal searches. This would be a vulnerability in an access control system.*

2026/01/09 20:40:38

FNIR(N, R, T) = FPIR(N, T) =

False neg. identification rate
False pos. identification rate

N = Num. enrolled subjects
R = Num. candidates examined

T = Threshold

T = 0 → Investigation
T > 0 → Identification

Appendix F Search duration

As in and prior tests, this section documents search speeds spanning three orders of magnitude. In applications where search volumes are high enough, this will have implications for hardware requirements especially for large N or when search duration is appreciably larger than the time it takes to prepare a template from the search image(s). Further, given very large (and growing) operational databases, the scalability of algorithms is important. It has been reported previously [8] that search duration can scale sublinearly with enrolled population size N. Further there has been considerable recent research on indexing, exact [13] and approximate nearest neighbor search [1,13] and fast-search [14,16].

Figure 311 charts the search duration measurements presented earlier in Tables 2 - 4.

- Most algorithms scale linearly. For those in that category, there is a wide range in speed with search durations ranging from 82 milliseconds for a 12 million gallery (for NEC-3) to more than 40 seconds (for Yitu-3, Toshiba-2) and even higher for less accurate algorithms.
- Some developers (Camvi, Dermalog, EverAI, Innovatrics, and Visionlabs) provide algorithms whose template search durations grow approimately logarithmically i.e. $T(N)\tilde{a}\log N$ with the constant a varying between implementations. In the figure this model is fit using the point $T(1) = 0$, and $T(640\,000)$. This very sublinear behaviour affords extremely fast search times in very large galleries. One caveat for the sublinear algorithms is that their fast-search data structures can require considerable computation time - on the order of hours - for N in the millions, and this scales mildy super-linearly, i.e. $O(N^b), b > 1$. There are exceptions: the Camvi algorithms take minutes; and Innvovatrics' scale sublinearly.

This publication is available free of charge from: https://doi.org/10.6028/NIST.IR.8271

2026/01/09 20:40:38	FNIR(N, R, T) = FPIR(N, T) =	False neg. identification rate False pos. identification rate	N = Num. enrolled subjects R = Num. candidates examined	T = Threshold	$T = 0 \rightarrow$ Investigation $T > 0 \rightarrow$ Identification

This publication is available free of charge from: https://doi.org/10.6028/NIST.IR.8271

This publication is available free of charge from: https://doi.org/10.6028/NIST.IR.8271

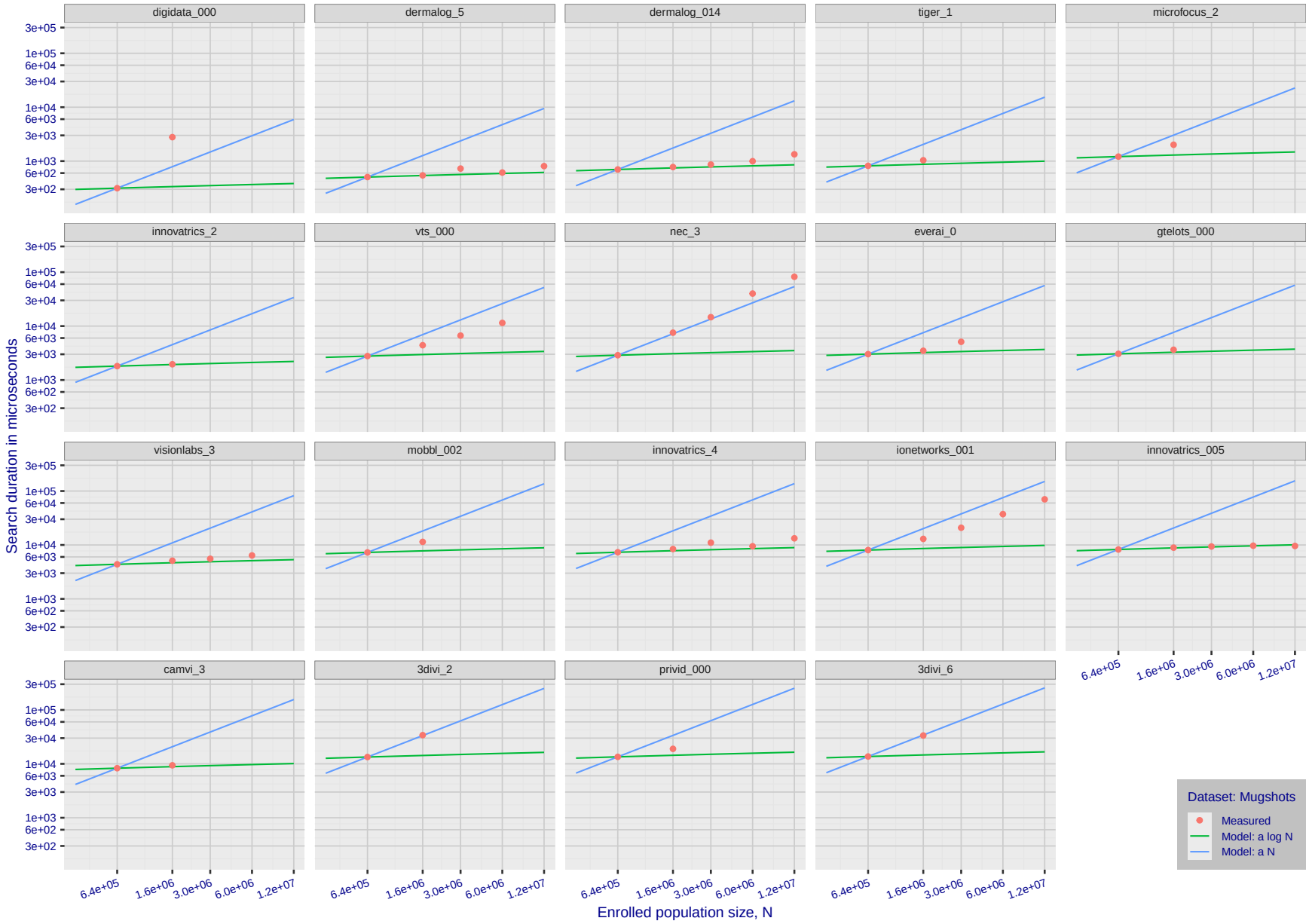

Figure 311: **[Mugshot Dataset] Search duration vs. enrolled population size**. *In red are the actual point durations measured on a single c. 2016 core. The blue shows linear growth from $N = 640\,000$. The green line shows logathmic growth from that point to $N = 1\,600\,000$. Note the sublinear growth from algorithms from Camvi, Dermalog, EverAI, Innovatrics, and Visionlabs. The tiger_1 algorithm is also sublinear, but inaccurate and inoperable at $N \geq 3000000$. This capability sometimes comes at the additional expense of converting a linear gallery data structure into whatever fast-search data structure is used. Note that search times are sometimes dominated by the template generation times shown in Table 45.*

2026/01/09 20:40:38
FNIR(N, R, T) = False neg. identification rate
FPIR(N, T) = False pos. identification rate
N = Num. enrolled subjects
R = Num. candidates examined
T = Threshold
T = 0 → Investigation
T > 0 → Identification

This publication is available free of charge from: https://doi.org/10.6028/NIST.IR.8271

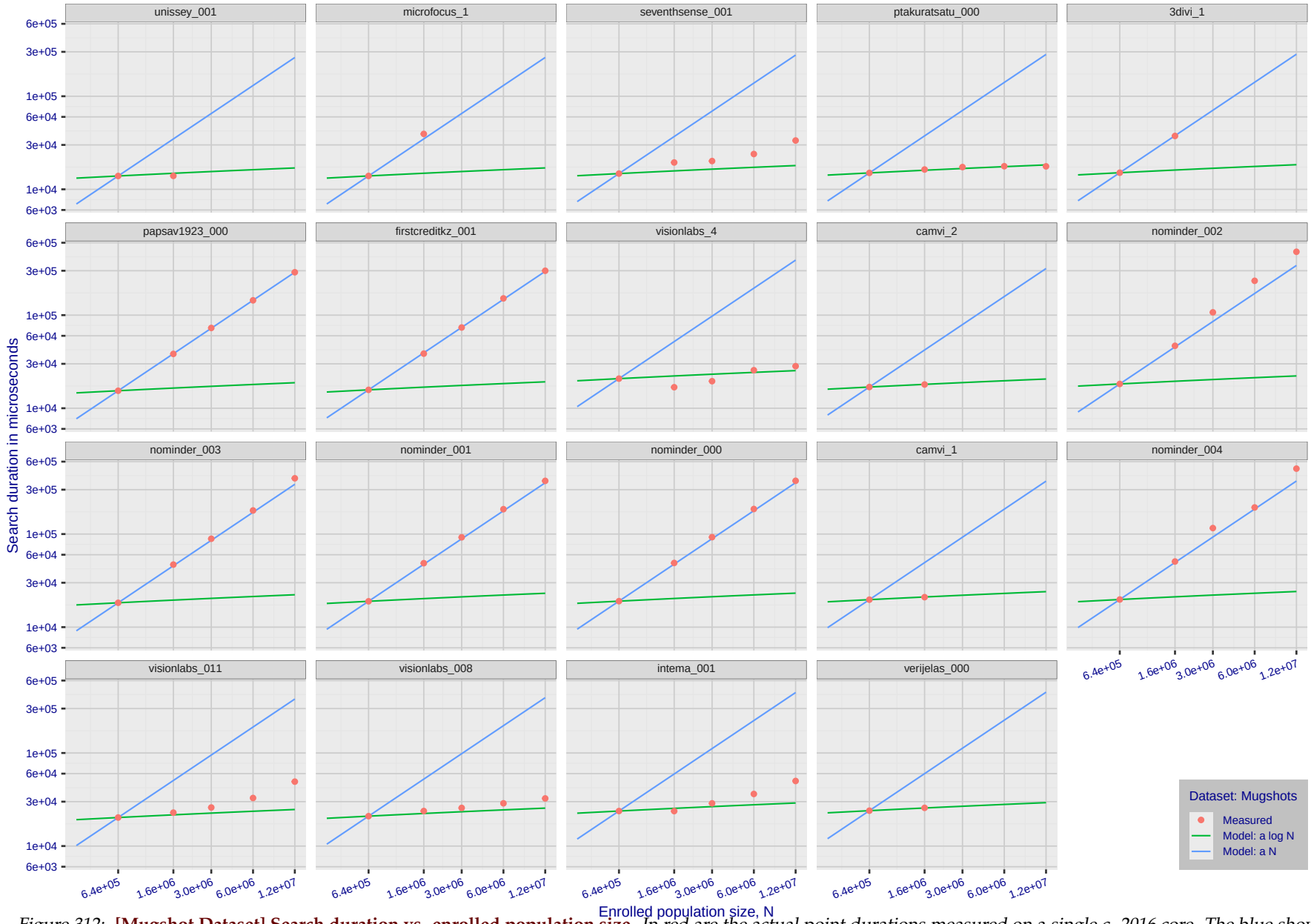

Figure 312: **[Mugshot Dataset] Search duration vs. enrolled population size**. *In red are the actual point durations measured on a single c. 2016 core. The blue shows linear growth from $N = 640\,000$. The green line shows logathmic growth from that point to $N = 1\,600\,000$. Note the sublinear growth from algorithms from Camvi, Dermalog, EverAI, Innovatrics, and Visionlabs. The tiger_1 algorithm is also sublinear, but inaccurate and inoperable at $N \geq 3000000$. This capability sometimes comes at the additional expense of converting a linear gallery data structure into whatever fast-search data structure is used. Note that search times are sometimes dominated by the template generation times shown in Table 45.*

2026/01/09 20:40:38

FNIR(N, R, T) = False neg. identification rate
FPIR(N, T) = False pos. identification rate
N = Num. enrolled subjects
R = Num. candidates examined
T = Threshold
T = 0 → Investigation
T > 0 → Identification

This publication is available free of charge from: https://doi.org/10.6028/NIST.IR.8271

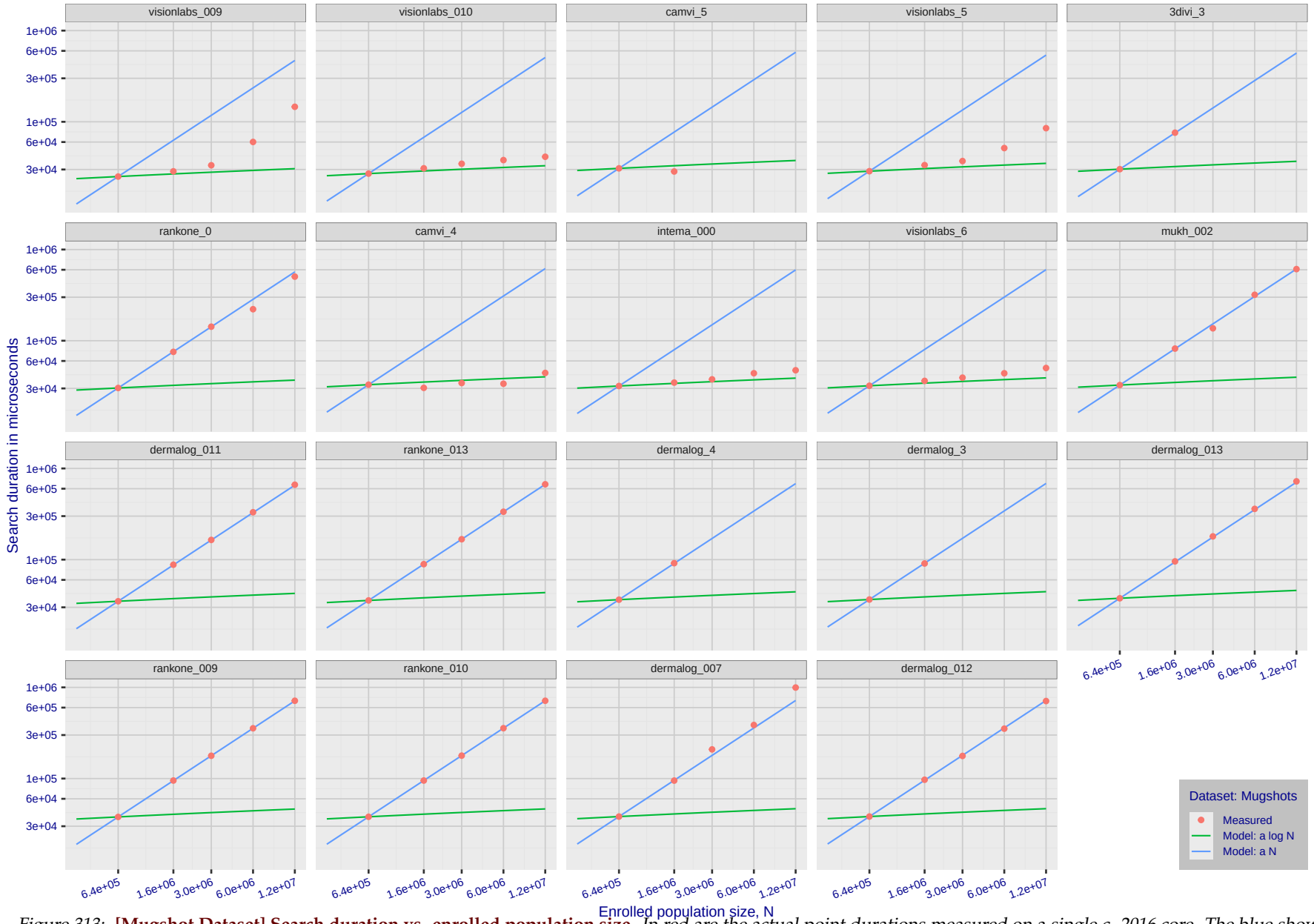

Figure 313: **[Mugshot Dataset] Search duration vs. enrolled population size**. *In red are the actual point durations measured on a single c. 2016 core. The blue shows linear growth from $N = 640\,000$. The green line shows logathmic growth from that point to $N = 1\,600\,000$. Note the sublinear growth from algorithms from Camvi, Dermalog, EverAI, Innovatrics, and Visionlabs. The tiger_1 algorithm is also sublinear, but inaccurate and inoperable at $N \geq 3000000$. This capability sometimes comes at the additional expense of converting a linear gallery data structure into whatever fast-search data structure is used. Note that search times are sometimes dominated by the template generation times shown in Table 45.*

2026/01/09 20:40:38

FNIR(N, R, T) = False neg. identification rate
FPIR(N, T) = False pos. identification rate

N = Num. enrolled subjects
R = Num. candidates examined

T = Threshold

T = 0 → Investigation
T > 0 → Identification

This publication is available free of charge from: https://doi.org/10.6028/NIST.IR.8271

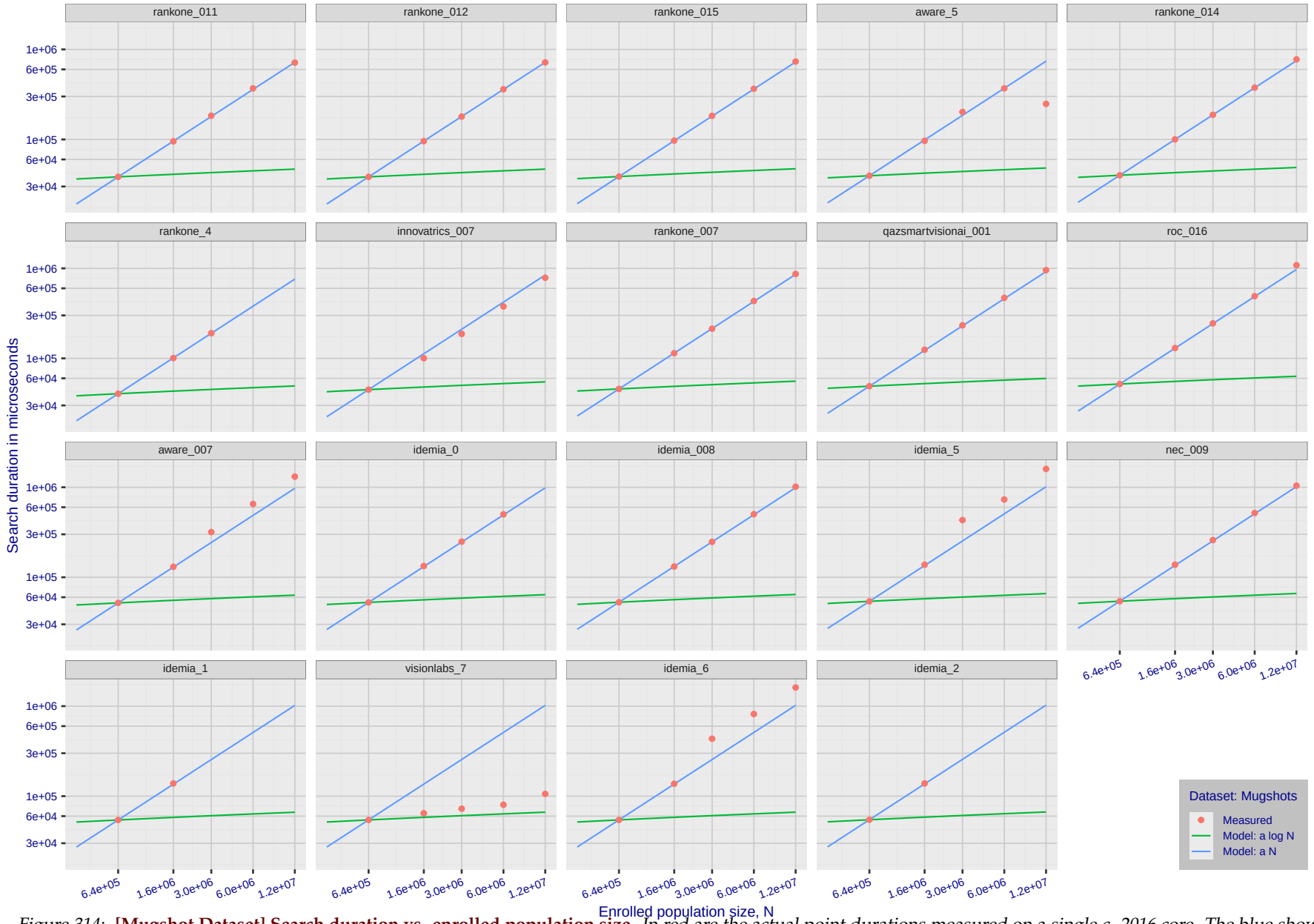

Figure 314: **[Mugshot Dataset] Search duration vs. enrolled population size**. *In red are the actual point durations measured on a single c. 2016 core. The blue shows linear growth from $N = 640\,000$. The green line shows logathmic growth from that point to $N = 1\,600\,000$. Note the sublinear growth from algorithms from Camvi, Dermalog, EverAI, Innovatrics, and Visionlabs. The tiger_1 algorithm is also sublinear, but inaccurate and inoperable at $N \geq 3000000$. This capability sometimes comes at the additional expense of converting a linear gallery data structure into whatever fast-search data structure is used. Note that search times are sometimes dominated by the template generation times shown in Table 45.*

2026/01/09 20:40:38

FNIR(N, R, T) = False neg. identification rate
FPIR(N, T) = False pos. identification rate

N = Num. enrolled subjects
R = Num. candidates examined

T = Threshold

T = 0 → Investigation
T > 0 → Identification

This publication is available free of charge from: https://doi.org/10.6028/NIST.IR.8271

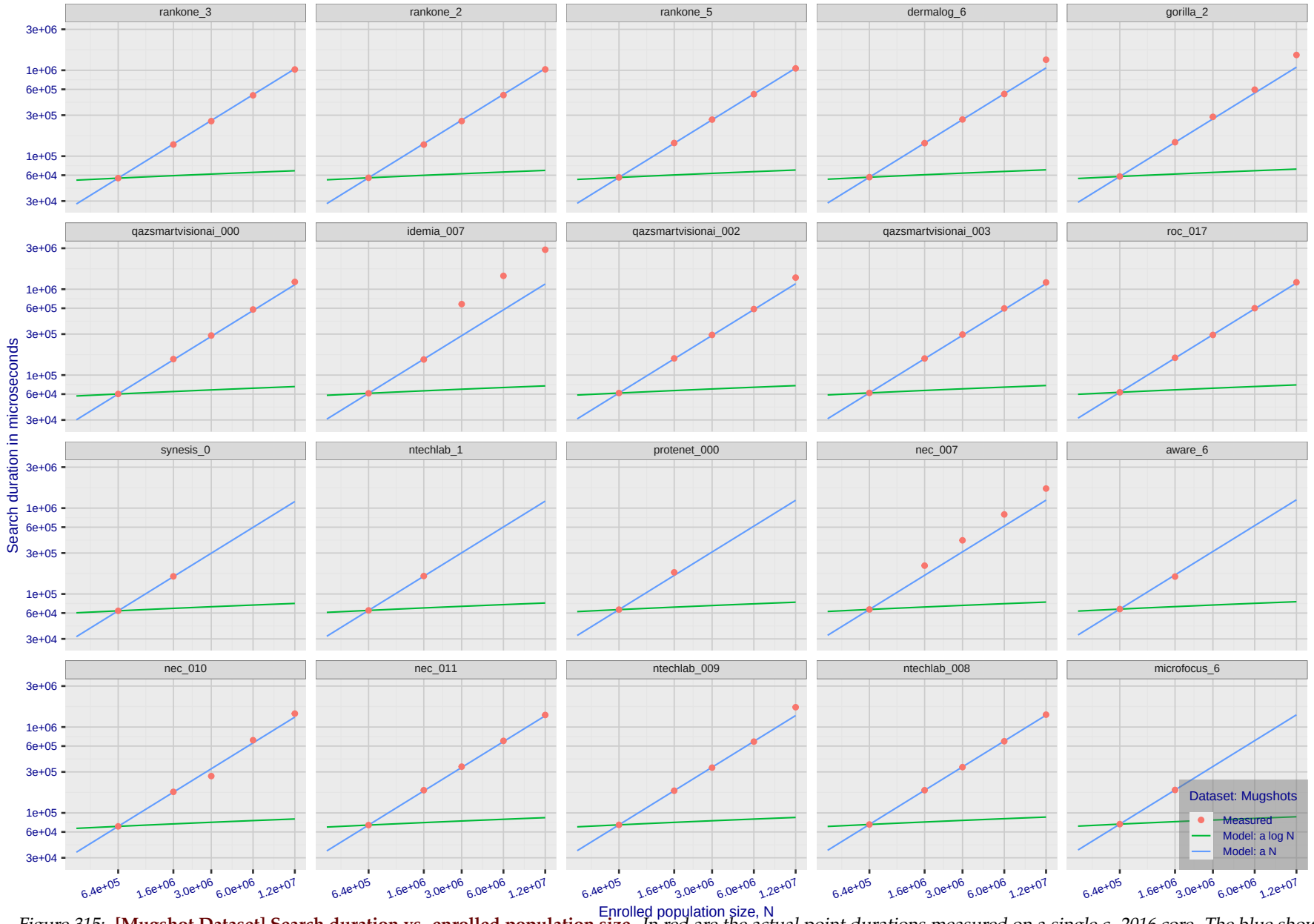

Figure 315: **[Mugshot Dataset] Search duration vs. enrolled population size**. *In red are the actual point durations measured on a single c. 2016 core. The blue shows linear growth from $N = 640\,000$. The green line shows logathmic growth from that point to $N = 1\,600\,000$. Note the sublinear growth from algorithms from Camvi, Dermalog, EverAI, Innovatrics, and Visionlabs. The tiger_1 algorithm is also sublinear, but inaccurate and inoperable at $N \geq 3000000$. This capability sometimes comes at the additional expense of converting a linear gallery data structure into whatever fast-search data structure is used. Note that search times are sometimes dominated by the template generation times shown in Table 45.*

2026/01/09 20:40:38

FNIR(N, R, T) = False neg. identification rate
FPIR(N, T) = False pos. identification rate

N = Num. enrolled subjects
R = Num. candidates examined

T = Threshold

T = 0 → Investigation
T > 0 → Identification

This publication is available free of charge from: https://doi.org/10.6028/NIST.IR.8271

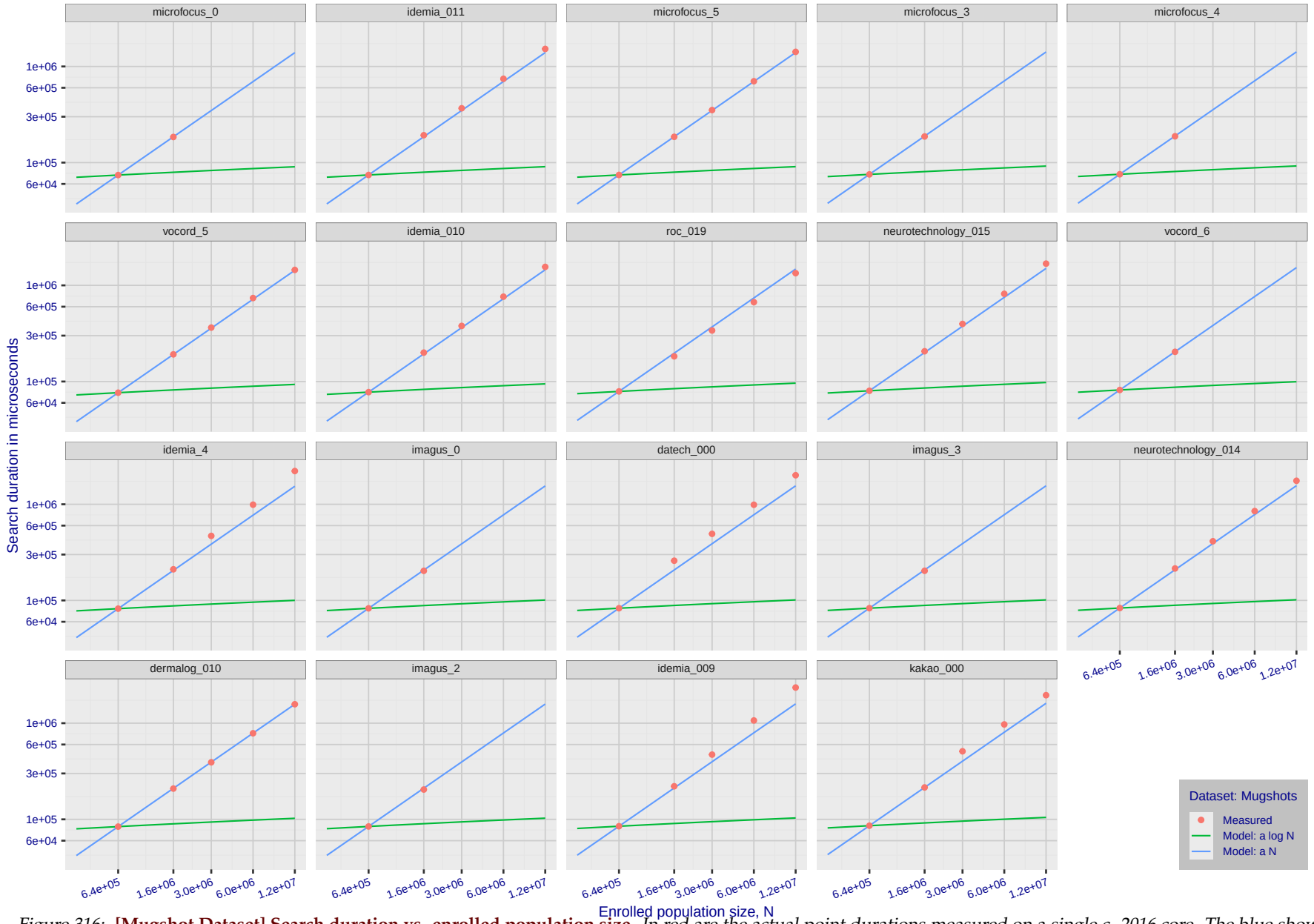

Figure 316: **[Mugshot Dataset] Search duration vs. enrolled population size**. *In red are the actual point durations measured on a single c. 2016 core. The blue shows linear growth from $N = 640\,000$. The green line shows logathmic growth from that point to $N = 1\,600\,000$. Note the sublinear growth from algorithms from Camvi, Dermalog, EverAI, Innovatrics, and Visionlabs. The tiger_1 algorithm is also sublinear, but inaccurate and inoperable at $N \geq 3000000$. This capability sometimes comes at the additional expense of converting a linear gallery data structure into whatever fast-search data structure is used. Note that search times are sometimes dominated by the template generation times shown in Table 45.*

2026/01/09 20:40:38

FNIR(N, R, T) = False neg. identification rate
FPIR(N, T) = False pos. identification rate

N = Num. enrolled subjects
R = Num. candidates examined

T = Threshold

T = 0 → Investigation
T > 0 → Identification

This publication is available free of charge from: https://doi.org/10.6028/NIST.IR.8271

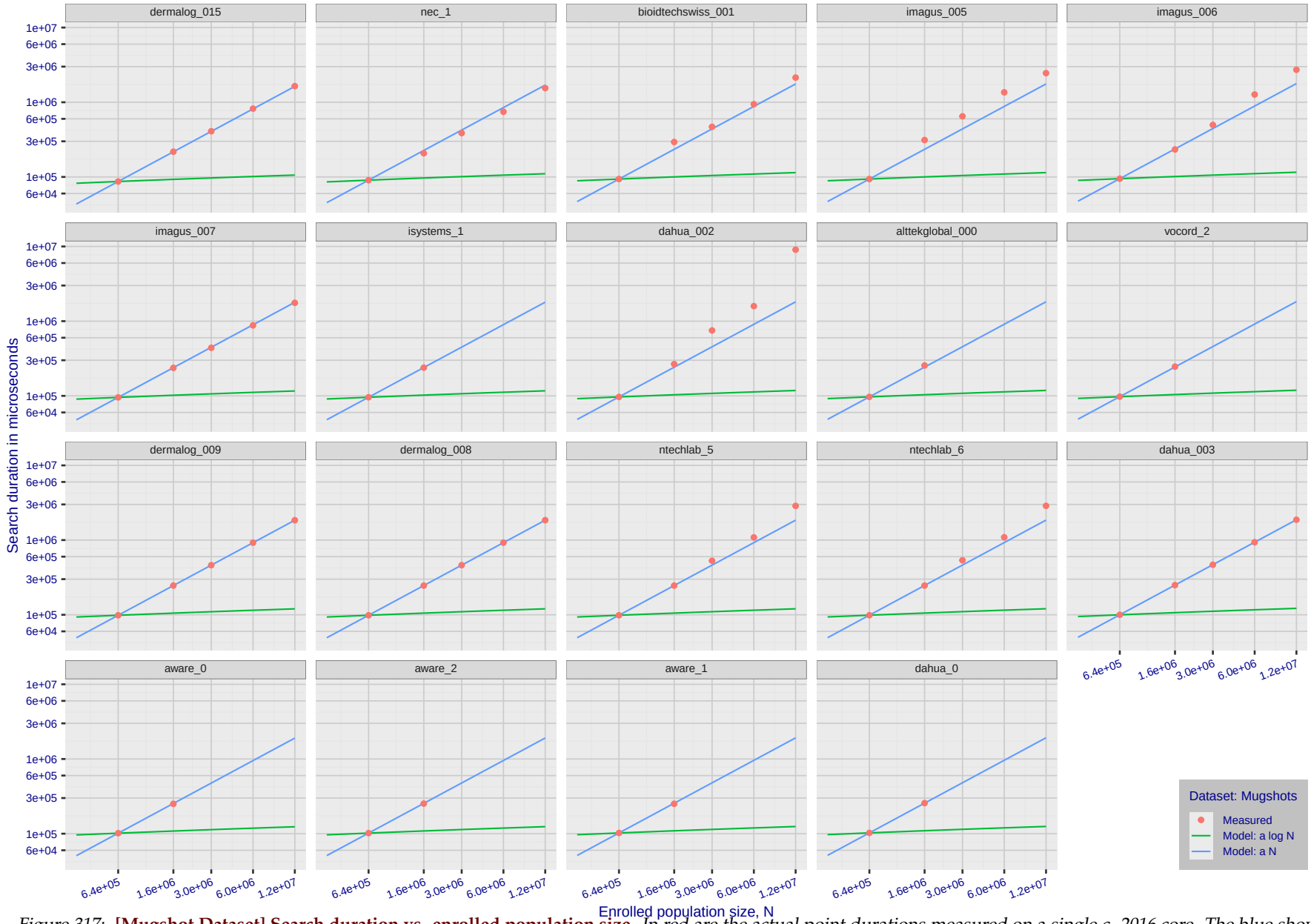

Figure 317: **[Mugshot Dataset] Search duration vs. enrolled population size**. *In red are the actual point durations measured on a single c. 2016 core. The blue shows linear growth from $N = 640\,000$. The green line shows logathmic growth from that point to $N = 1\,600\,000$. Note the sublinear growth from algorithms from Camvi, Dermalog, EverAI, Innovatrics, and Visionlabs. The tiger_1 algorithm is also sublinear, but inaccurate and inoperable at $N \geq 3000000$. This capability sometimes comes at the additional expense of converting a linear gallery data structure into whatever fast-search data structure is used. Note that search times are sometimes dominated by the template generation times shown in Table 45.*

2026/01/09 20:40:38

FNIR(N, R, T) = False neg. identification rate
FPIR(N, T) = False pos. identification rate

N = Num. enrolled subjects
R = Num. candidates examined

T = Threshold

T = 0 → Investigation
T > 0 → Identification

This publication is available free of charge from: https://doi.org/10.6028/NIST.IR.8271

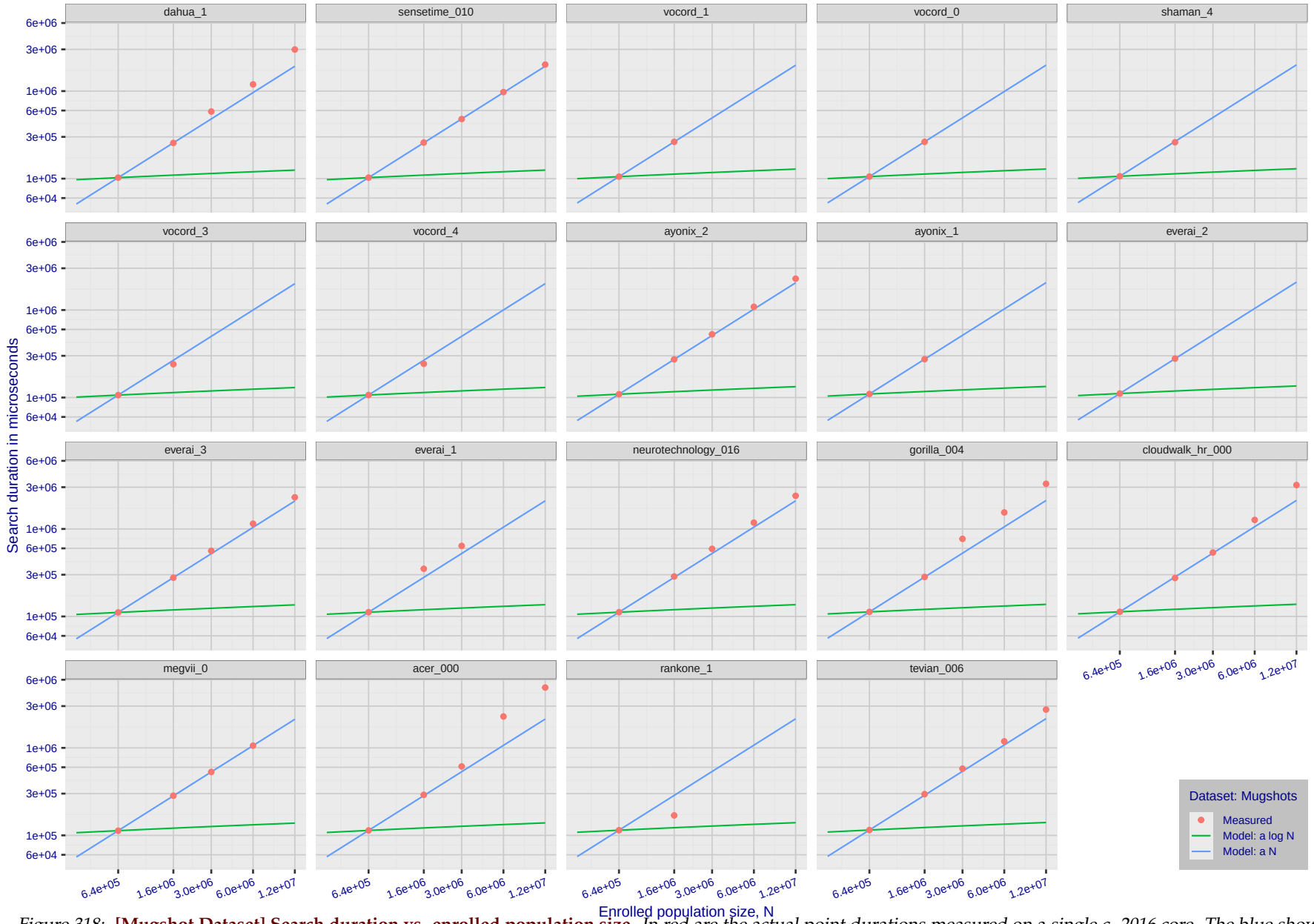

Figure 318: **[Mugshot Dataset] Search duration vs. enrolled population size**. *In red are the actual point durations measured on a single c. 2016 core. The blue shows linear growth from $N = 640\,000$. The green line shows logathmic growth from that point to $N = 1\,600\,000$. Note the sublinear growth from algorithms from Camvi, Dermalog, EverAI, Innovatrics, and Visionlabs. The tiger_1 algorithm is also sublinear, but inaccurate and inoperable at $N \geq 3000000$. This capability sometimes comes at the additional expense of converting a linear gallery data structure into whatever fast-search data structure is used. Note that search times are sometimes dominated by the template generation times shown in Table 45.*

2026/01/09 20:40:38

FNIR(N, R, T) = False neg. identification rate
FPIR(N, T) = False pos. identification rate

N = Num. enrolled subjects
R = Num. candidates examined

T = Threshold

T = 0 → Investigation
T > 0 → Identification

This publication is available free of charge from: https://doi.org/10.6028/NIST.IR.8271

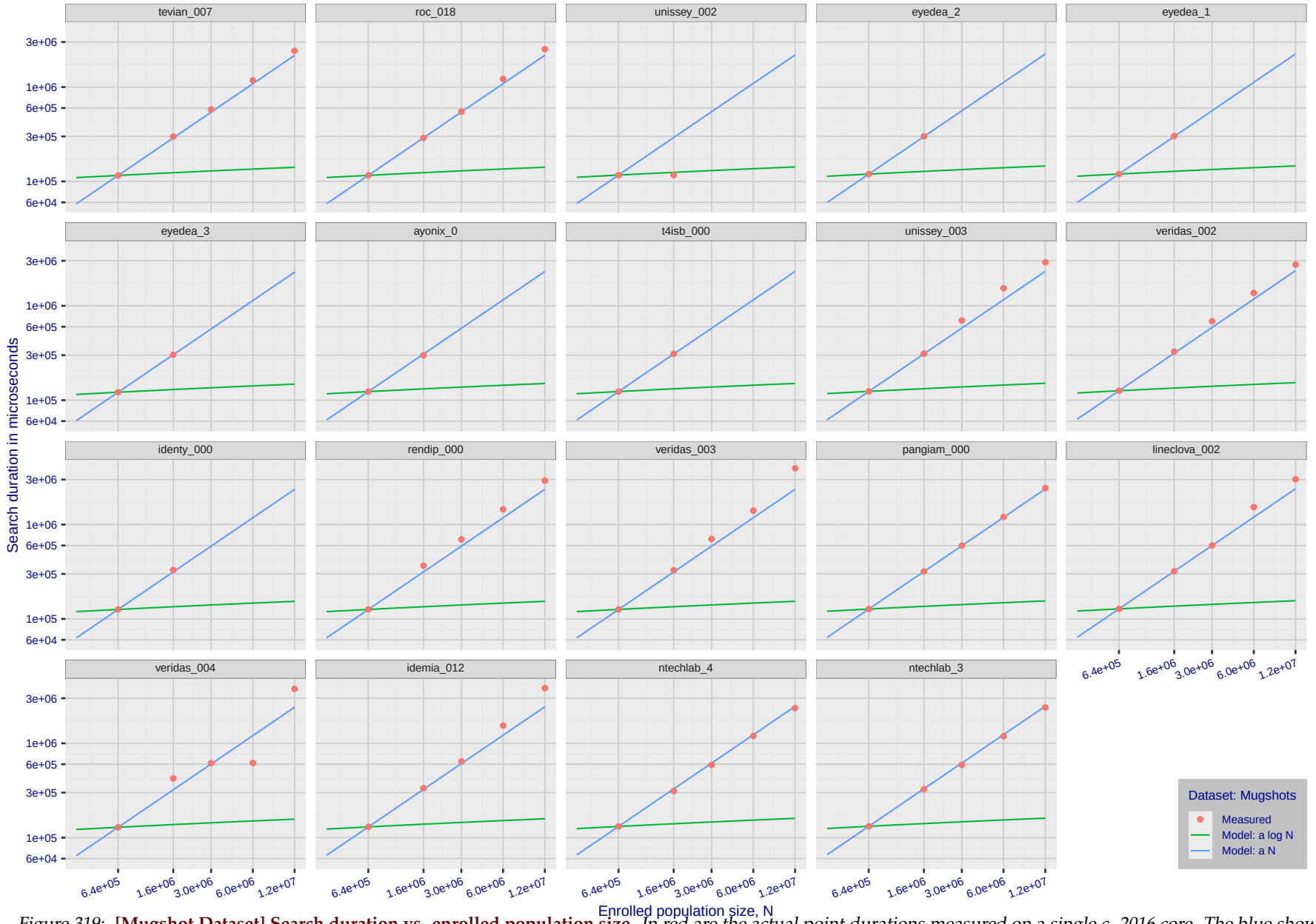

Figure 319: **[Mugshot Dataset] Search duration vs. enrolled population size**. *In red are the actual point durations measured on a single c. 2016 core. The blue shows linear growth from $N = 640\,000$. The green line shows logathmic growth from that point to $N = 1\,600\,000$. Note the sublinear growth from algorithms from Camvi, Dermalog, EverAI, Innovatrics, and Visionlabs. The tiger_1 algorithm is also sublinear, but inaccurate and inoperable at $N \geq 3000000$. This capability sometimes comes at the additional expense of converting a linear gallery data structure into whatever fast-search data structure is used. Note that search times are sometimes dominated by the template generation times shown in Table 45.*

2026/01/09 20:40:38
FNIR(N, R, T) = False neg. identification rate
FPIR(N, T) = False pos. identification rate
N = Num. enrolled subjects
R = Num. candidates examined
T = Threshold
T = 0 → Investigation
T > 0 → Identification

This publication is available free of charge from: https://doi.org/10.6028/NIST.IR.8271

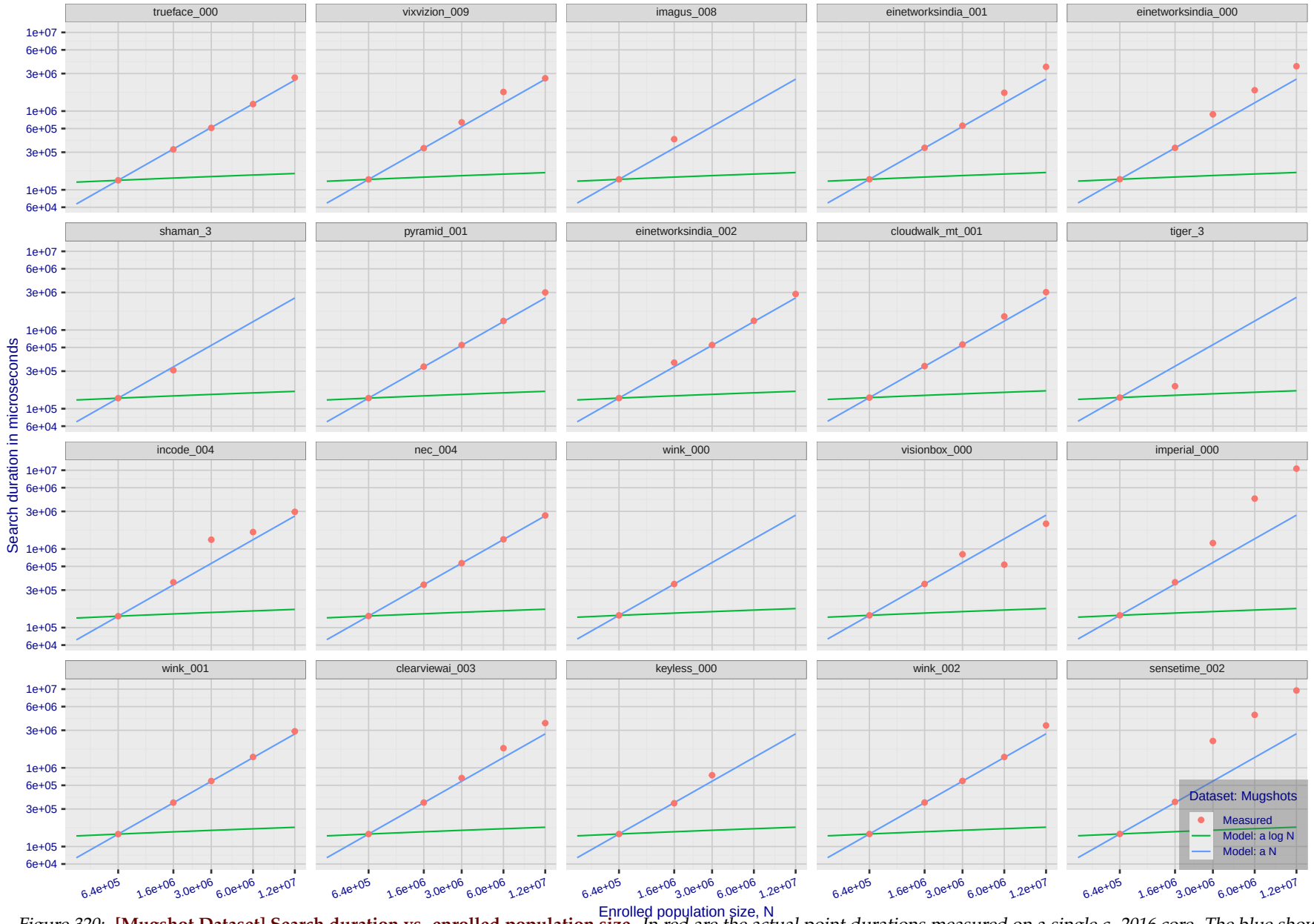

Figure 320: **[Mugshot Dataset] Search duration vs. enrolled population size**. *In red are the actual point durations measured on a single c. 2016 core. The blue shows linear growth from $N = 640\,000$. The green line shows logathmic growth from that point to $N = 1\,600\,000$. Note the sublinear growth from algorithms from Camvi, Dermalog, EverAI, Innovatrics, and Visionlabs. The tiger_1 algorithm is also sublinear, but inaccurate and inoperable at $N \geq 3000000$. This capability sometimes comes at the additional expense of converting a linear gallery data structure into whatever fast-search data structure is used. Note that search times are sometimes dominated by the template generation times shown in Table 45.*

2026/01/09 20:40:38
FNIR(N, R, T) = False neg. identification rate
FPIR(N, T) = False pos. identification rate
N = Num. enrolled subjects
R = Num. candidates examined
T = Threshold
T = 0 → Investigation
T > 0 → Identification

This publication is available free of charge from: https://doi.org/10.6028/NIST.IR.8271

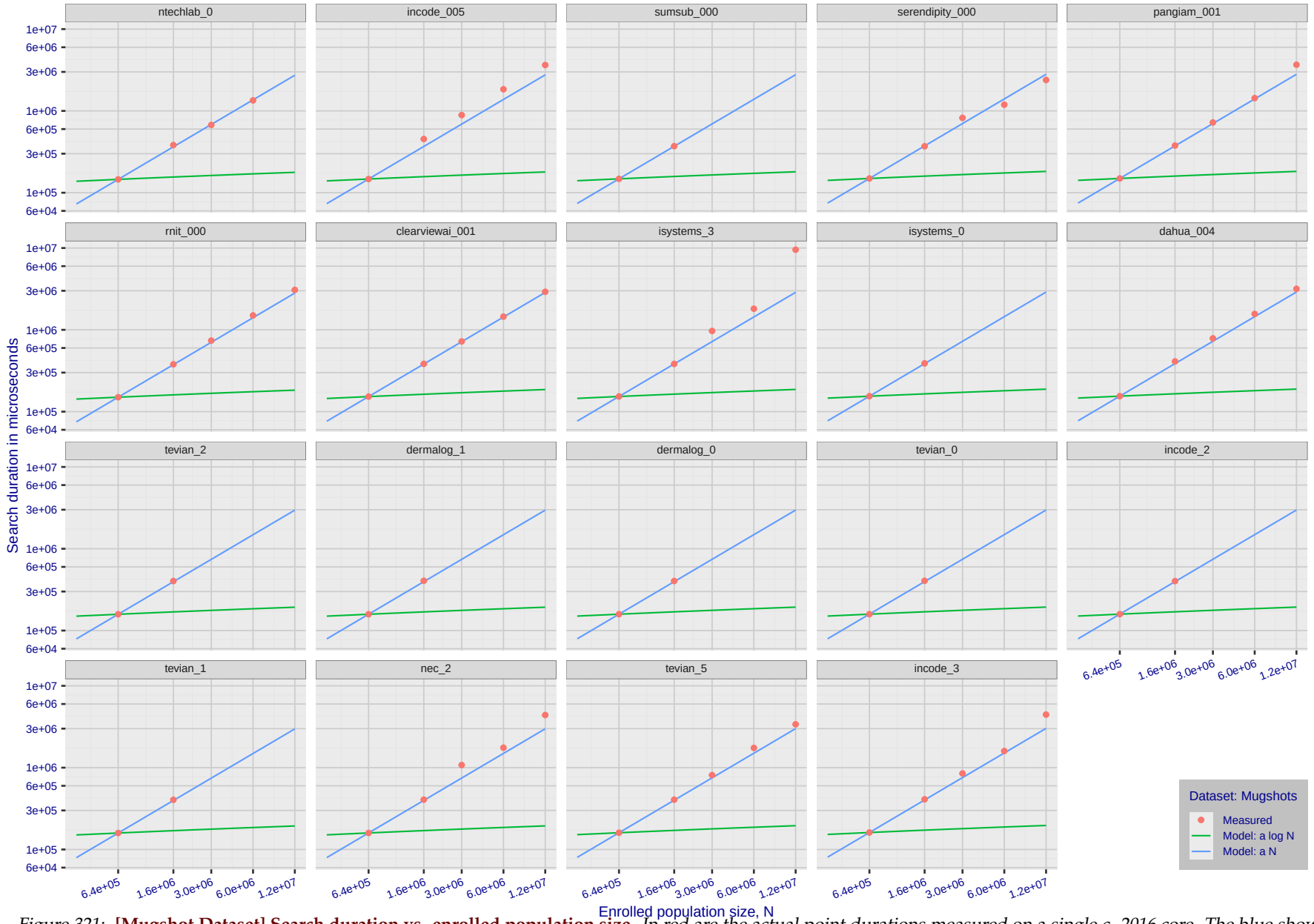

Figure 321: **[Mugshot Dataset] Search duration vs. enrolled population size**. *In red are the actual point durations measured on a single c. 2016 core. The blue shows linear growth from $N = 640\,000$. The green line shows logathmic growth from that point to $N = 1\,600\,000$. Note the sublinear growth from algorithms from Camvi, Dermalog, EverAI, Innovatrics, and Visionlabs. The tiger_1 algorithm is also sublinear, but inaccurate and inoperable at $N \geq 3000000$. This capability sometimes comes at the additional expense of converting a linear gallery data structure into whatever fast-search data structure is used. Note that search times are sometimes dominated by the template generation times shown in Table 45.*

2026/01/09 20:40:38
FNIR(N, R, T) = False neg. identification rate
FPIR(N, T) = False pos. identification rate
N = Num. enrolled subjects
R = Num. candidates examined
T = Threshold
T = 0 → Investigation
T > 0 → Identification

This publication is available free of charge from: https://doi.org/10.6028/NIST.IR.8271

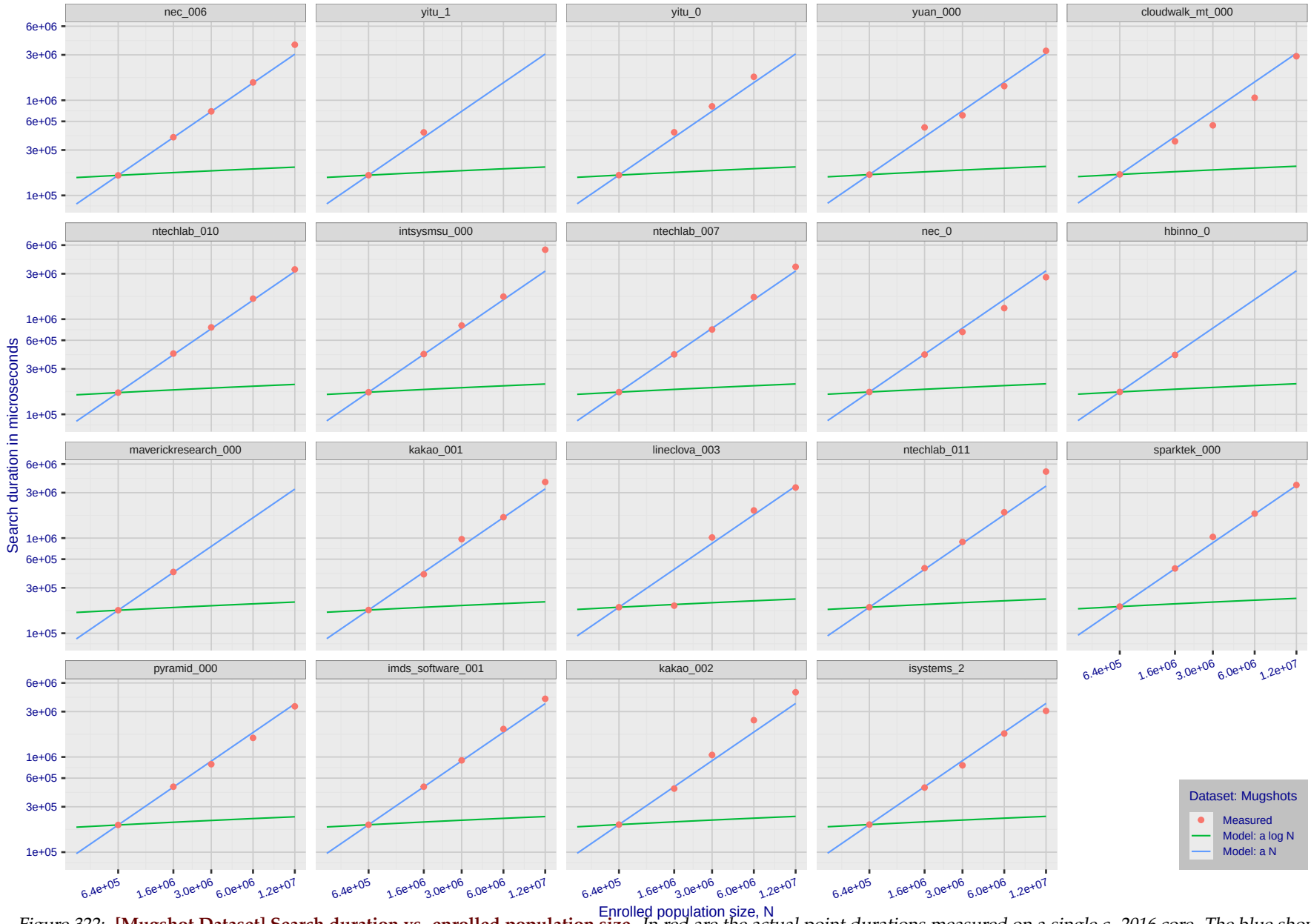

Figure 322: **[Mugshot Dataset] Search duration vs. enrolled population size**. *In red are the actual point durations measured on a single c. 2016 core. The blue shows linear growth from $N = 640\,000$. The green line shows logathmic growth from that point to $N = 1\,600\,000$. Note the sublinear growth from algorithms from Camvi, Dermalog, EverAI, Innovatrics, and Visionlabs. The tiger_1 algorithm is also sublinear, but inaccurate and inoperable at $N \geq 3000000$. This capability sometimes comes at the additional expense of converting a linear gallery data structure into whatever fast-search data structure is used. Note that search times are sometimes dominated by the template generation times shown in Table 45.*

This publication is available free of charge from: https://doi.org/10.6028/NIST.IR.8271

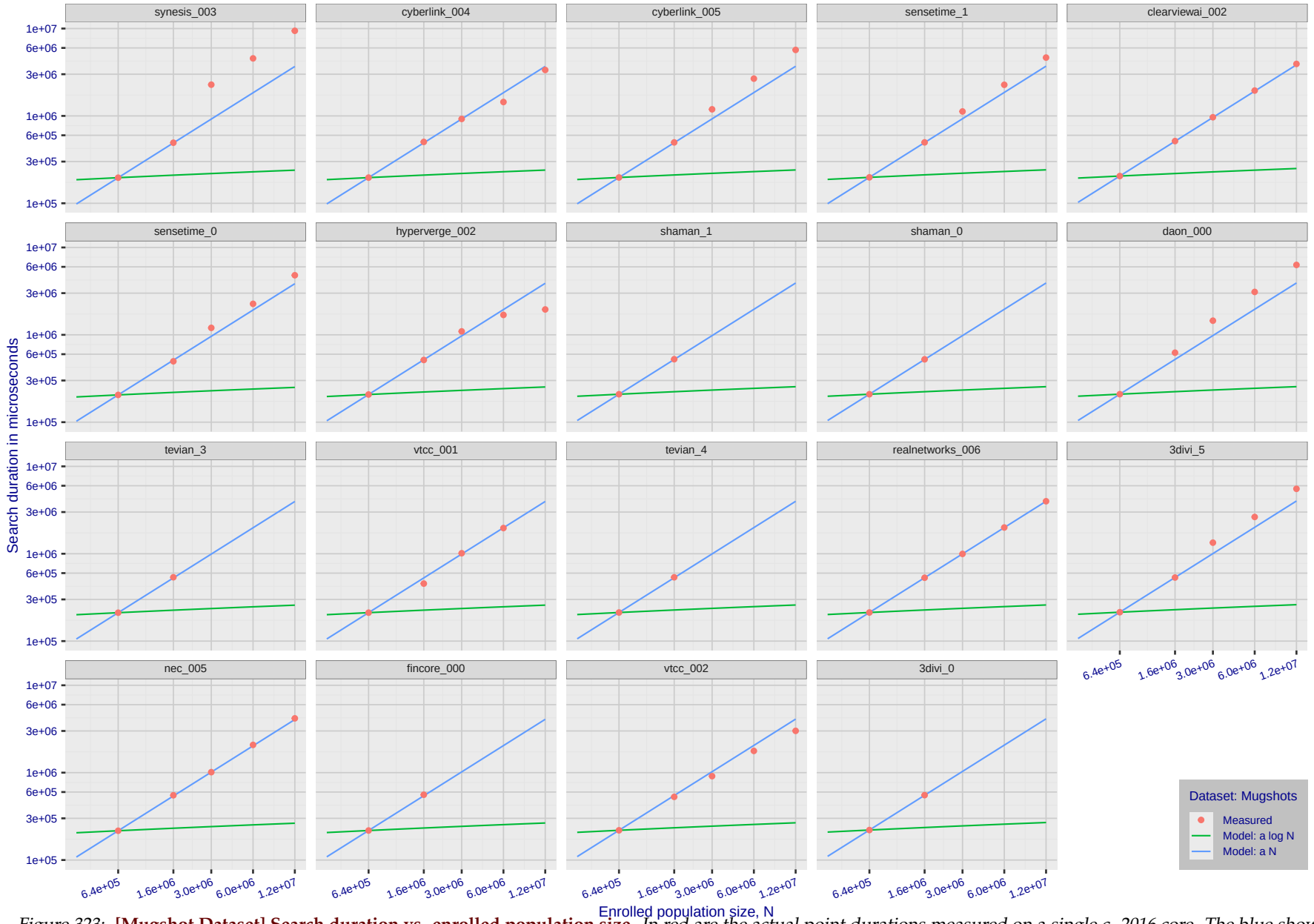

Figure 323: **[Mugshot Dataset] Search duration vs. enrolled population size**. *In red are the actual point durations measured on a single c. 2016 core. The blue shows linear growth from $N = 640\,000$. The green line shows logathmic growth from that point to $N = 1\,600\,000$. Note the sublinear growth from algorithms from Camvi, Dermalog, EverAI, Innovatrics, and Visionlabs. The tiger_1 algorithm is also sublinear, but inaccurate and inoperable at $N \geq 3000000$. This capability sometimes comes at the additional expense of converting a linear gallery data structure into whatever fast-search data structure is used. Note that search times are sometimes dominated by the template generation times shown in Table 45.*

2026/01/09 20:40:38

FNIR(N, R, T) = False neg. identification rate
FPIR(N, T) = False pos. identification rate
N = Num. enrolled subjects
R = Num. candidates examined
T = Threshold
T = 0 → Investigation
T > 0 → Identification

This publication is available free of charge from: https://doi.org/10.6028/NIST.IR.8271

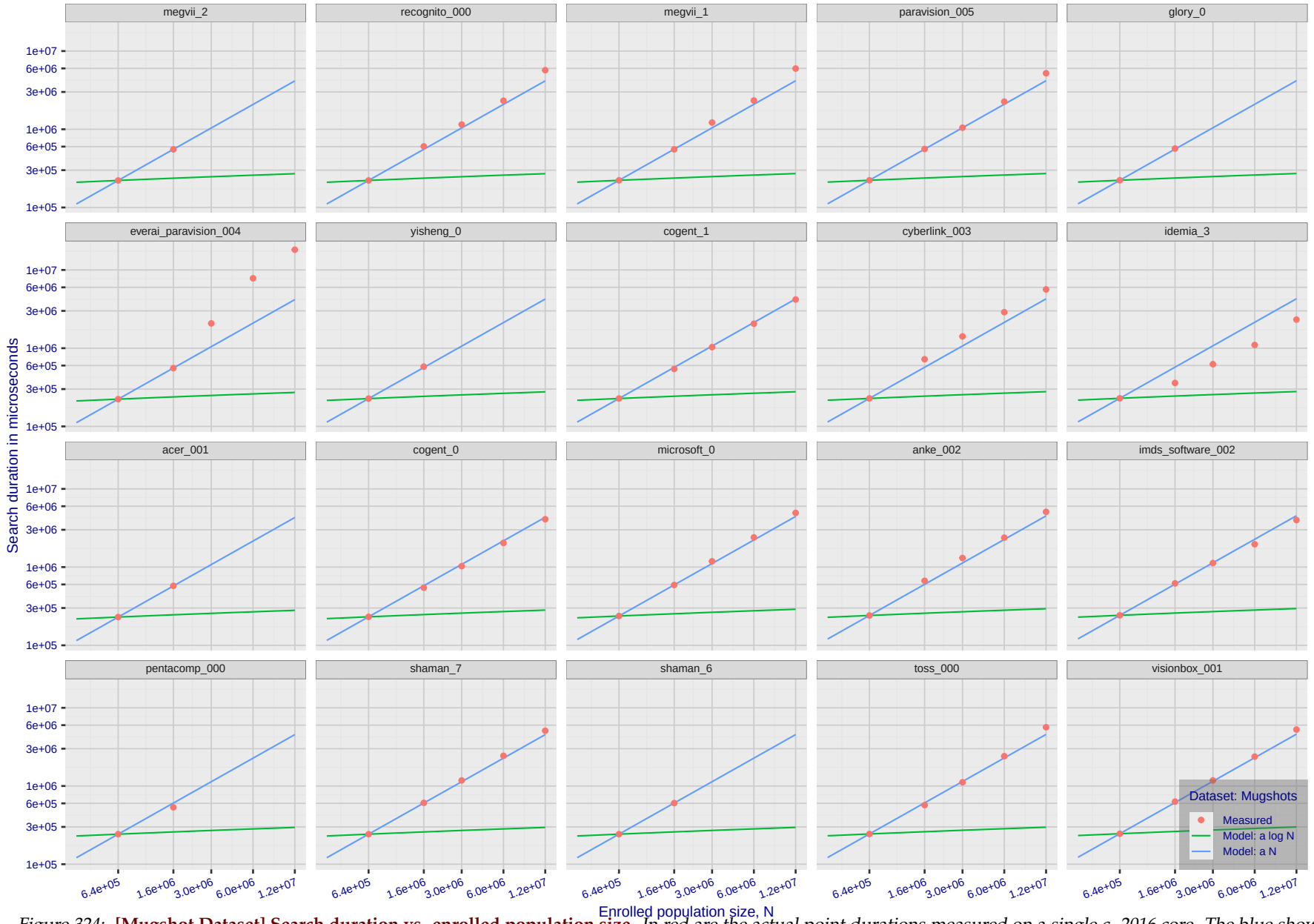

Figure 324: **[Mugshot Dataset] Search duration vs. enrolled population size**. *In red are the actual point durations measured on a single c. 2016 core. The blue shows linear growth from $N = 640\,000$. The green line shows logathmic growth from that point to $N = 1\,600\,000$. Note the sublinear growth from algorithms from Camvi, Dermalog, EverAI, Innovatrics, and Visionlabs. The tiger_1 algorithm is also sublinear, but inaccurate and inoperable at $N \geq 3000000$. This capability sometimes comes at the additional expense of converting a linear gallery data structure into whatever fast-search data structure is used. Note that search times are sometimes dominated by the template generation times shown in Table 45.*

2026/01/09 20:40:38
FNIR(N, R, T) = False neg. identification rate
FPIR(N, T) = False pos. identification rate
N = Num. enrolled subjects
R = Num. candidates examined
T = Threshold
T = 0 → Investigation
T > 0 → Identification

This publication is available free of charge from: https://doi.org/10.6028/NIST.IR.8271

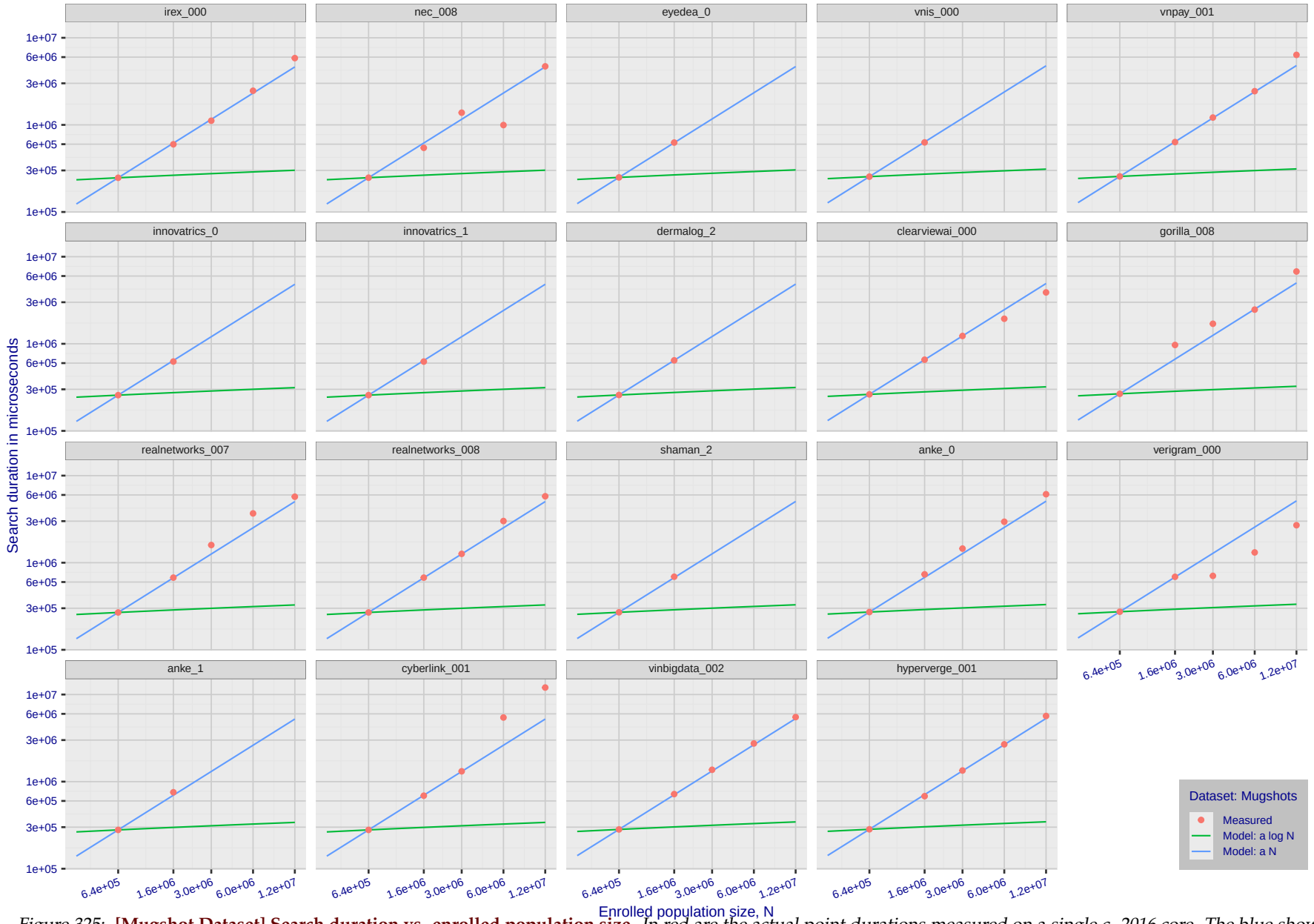

Figure 325: **[Mugshot Dataset] Search duration vs. enrolled population size**. *In red are the actual point durations measured on a single c. 2016 core. The blue shows linear growth from $N = 640\,000$. The green line shows logathmic growth from that point to $N = 1\,600\,000$. Note the sublinear growth from algorithms from Camvi, Dermalog, EverAI, Innovatrics, and Visionlabs. The tiger_1 algorithm is also sublinear, but inaccurate and inoperable at $N \geq 3000000$. This capability sometimes comes at the additional expense of converting a linear gallery data structure into whatever fast-search data structure is used. Note that search times are sometimes dominated by the template generation times shown in Table 45.*

2026/01/09 20:40:38
FNIR(N, R, T) = False neg. identification rate
FPIR(N, T) = False pos. identification rate
N = Num. enrolled subjects
R = Num. candidates examined
T = Threshold
T = 0 → Investigation
T > 0 → Identification

This publication is available free of charge from: https://doi.org/10.6028/NIST.IR.8271

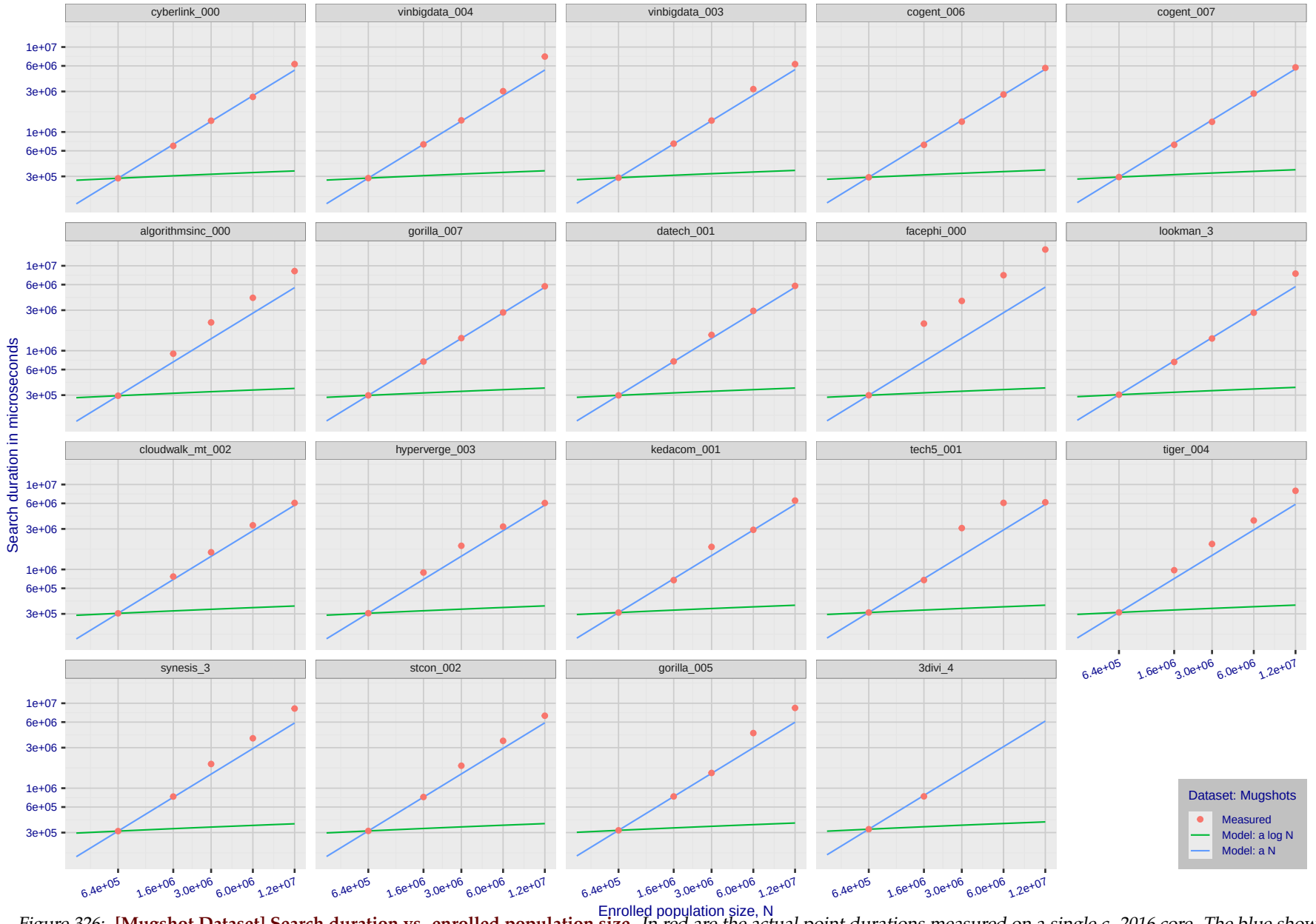

Figure 326: **[Mugshot Dataset] Search duration vs. enrolled population size**. *In red are the actual point durations measured on a single c. 2016 core. The blue shows linear growth from $N = 640\,000$. The green line shows logathmic growth from that point to $N = 1\,600\,000$. Note the sublinear growth from algorithms from Camvi, Dermalog, EverAI, Innovatrics, and Visionlabs. The tiger_1 algorithm is also sublinear, but inaccurate and inoperable at $N \geq 3000000$. This capability sometimes comes at the additional expense of converting a linear gallery data structure into whatever fast-search data structure is used. Note that search times are sometimes dominated by the template generation times shown in Table 45.*

2026/01/09 20:40:38

FNIR(N, R, T) = False neg. identification rate
FPIR(N, T) = False pos. identification rate

N = Num. enrolled subjects
R = Num. candidates examined

T = Threshold

T = 0 → Investigation
T > 0 → Identification

This publication is available free of charge from: https://doi.org/10.6028/NIST.IR.8271

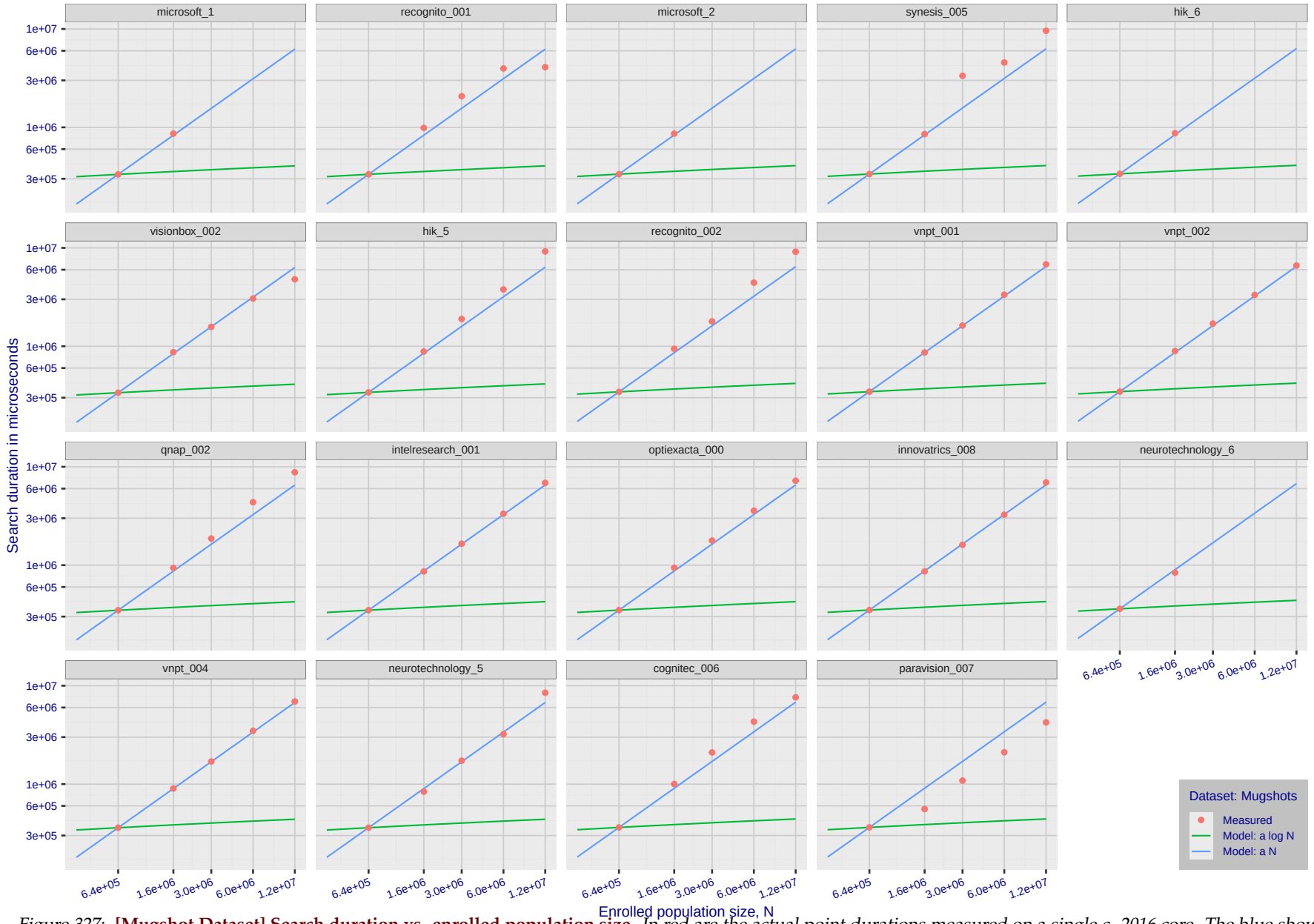

Figure 327: **[Mugshot Dataset] Search duration vs. enrolled population size**. *In red are the actual point durations measured on a single c. 2016 core. The blue shows linear growth from $N = 640\,000$. The green line shows logathmic growth from that point to $N = 1\,600\,000$. Note the sublinear growth from algorithms from Camvi, Dermalog, EverAI, Innovatrics, and Visionlabs. The tiger_1 algorithm is also sublinear, but inaccurate and inoperable at $N \geq 3000000$. This capability sometimes comes at the additional expense of converting a linear gallery data structure into whatever fast-search data structure is used. Note that search times are sometimes dominated by the template generation times shown in Table 45.*

2026/01/09 20:40:38

FNIR(N, R, T) = False neg. identification rate
FPIR(N, T) = False pos. identification rate

N = Num. enrolled subjects
R = Num. candidates examined

T = Threshold

T = 0 → Investigation
T > 0 → Identification

This publication is available free of charge from: https://doi.org/10.6028/NIST.IR.8271

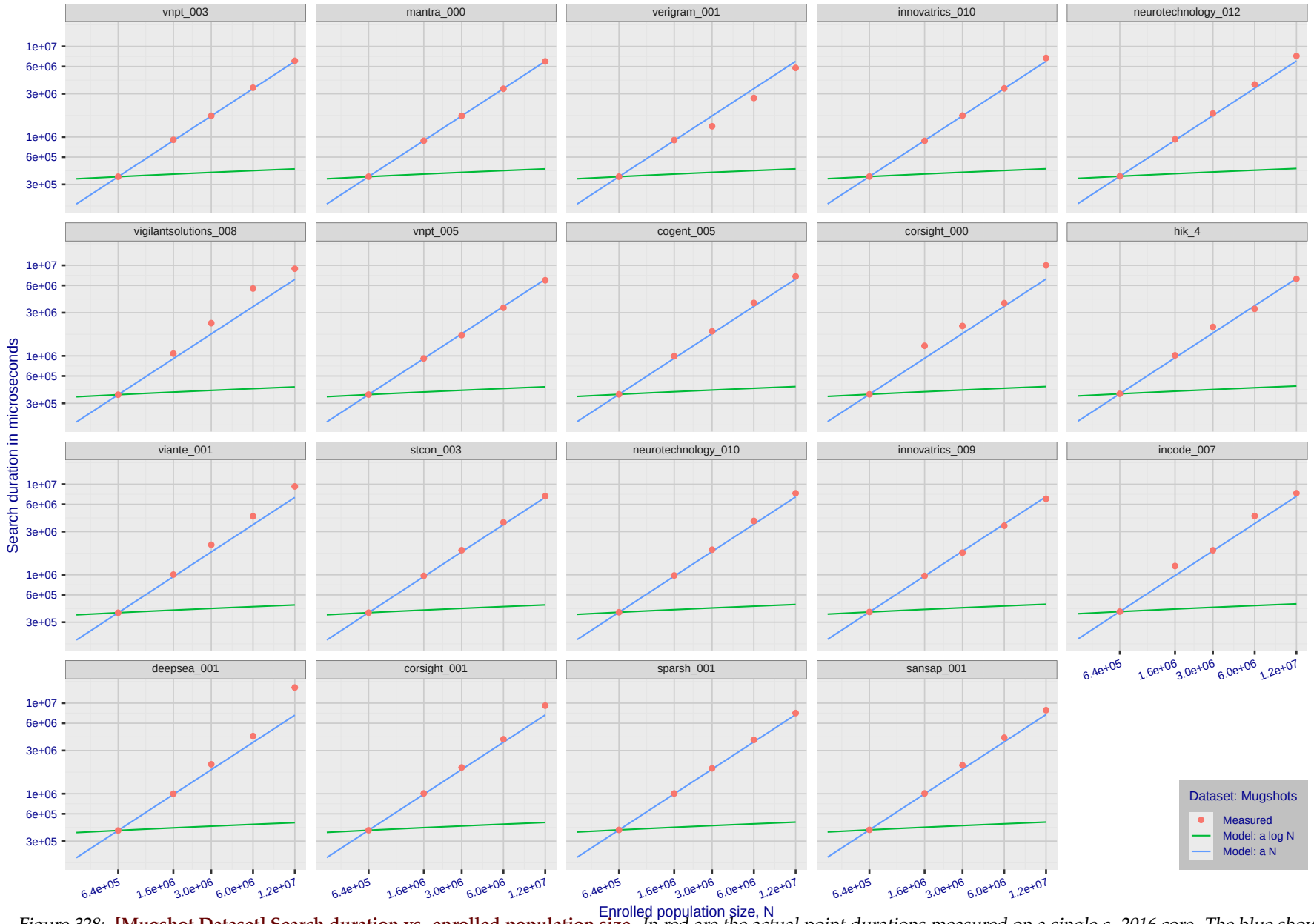

Figure 328: **[Mugshot Dataset] Search duration vs. enrolled population size**. *In red are the actual point durations measured on a single c. 2016 core. The blue shows linear growth from $N = 640\,000$. The green line shows logathmic growth from that point to $N = 1\,600\,000$. Note the sublinear growth from algorithms from Camvi, Dermalog, EverAI, Innovatrics, and Visionlabs. The tiger_1 algorithm is also sublinear, but inaccurate and inoperable at $N \geq 3000000$. This capability sometimes comes at the additional expense of converting a linear gallery data structure into whatever fast-search data structure is used. Note that search times are sometimes dominated by the template generation times shown in Table 45.*

2026/01/09 20:40:38
FNIR(N, R, T) = False neg. identification rate
FPIR(N, T) = False pos. identification rate
N = Num. enrolled subjects
R = Num. candidates examined
T = Threshold
T = 0 → Investigation
T > 0 → Identification

This publication is available free of charge from: https://doi.org/10.6028/NIST.IR.8271

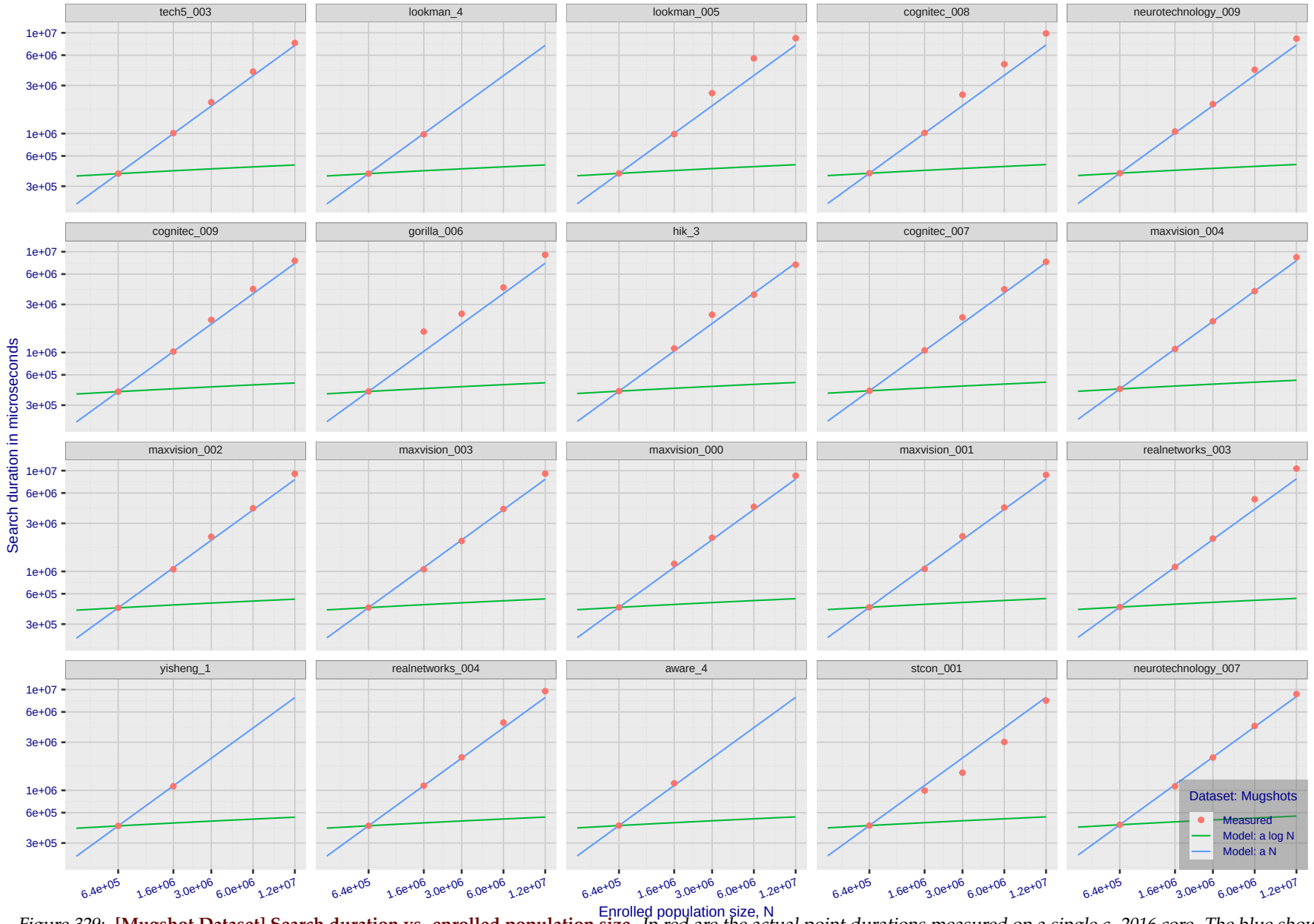

Figure 329: **[Mugshot Dataset] Search duration vs. enrolled population size**. *In red are the actual point durations measured on a single c. 2016 core. The blue shows linear growth from $N = 640\,000$. The green line shows logathmic growth from that point to $N = 1\,600\,000$. Note the sublinear growth from algorithms from Camvi, Dermalog, EverAI, Innovatrics, and Visionlabs. The tiger_1 algorithm is also sublinear, but inaccurate and inoperable at $N \geq 3000000$. This capability sometimes comes at the additional expense of converting a linear gallery data structure into whatever fast-search data structure is used. Note that search times are sometimes dominated by the template generation times shown in Table 45.*

2026/01/09 20:40:38

FNIR(N, R, T) = False neg. identification rate
FPIR(N, T) = False pos. identification rate

N = Num. enrolled subjects
R = Num. candidates examined

T = Threshold

T = 0 → Investigation
T > 0 → Identification

This publication is available free of charge from: https://doi.org/10.6028/NIST.IR.8271

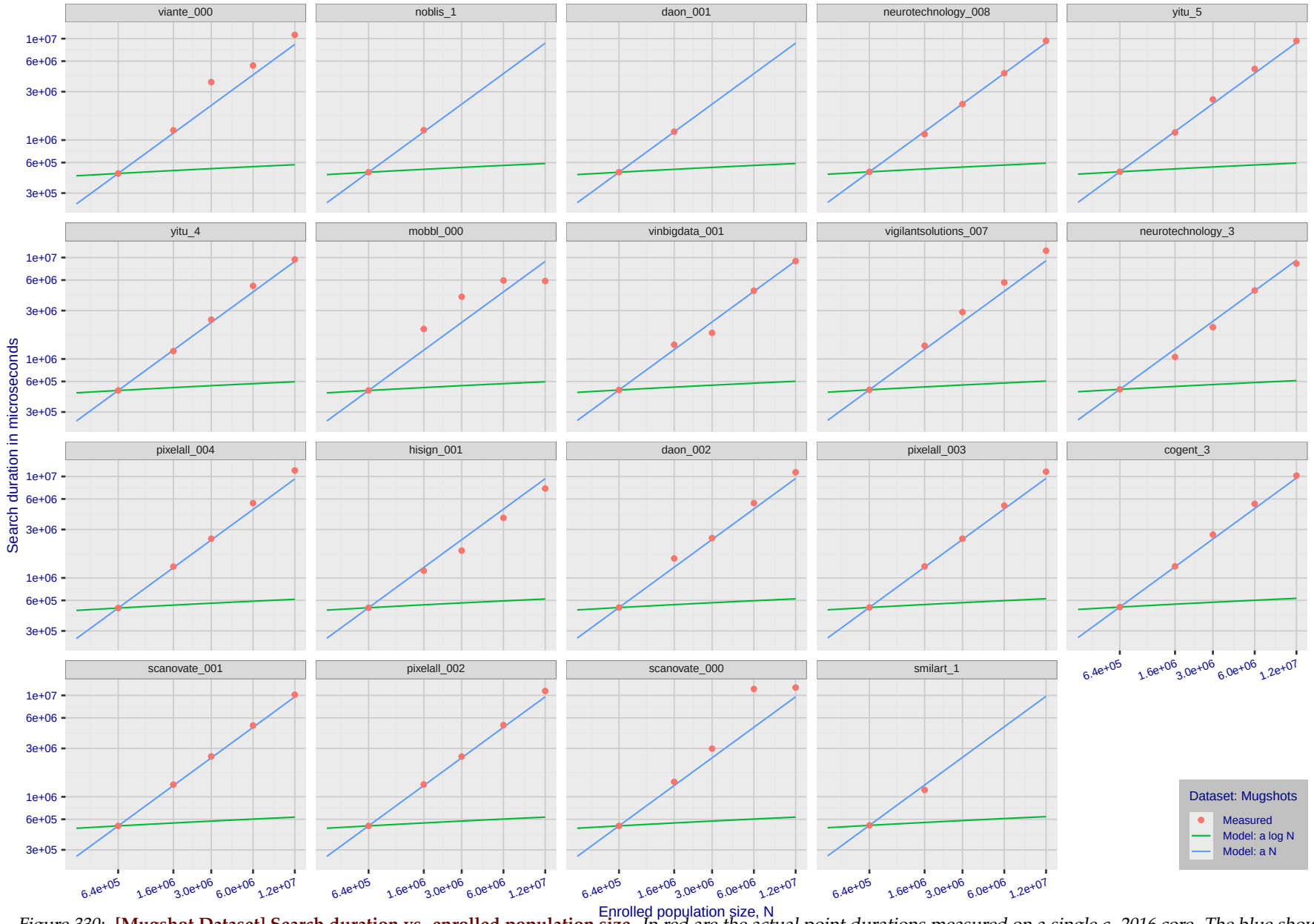

Figure 330: **[Mugshot Dataset] Search duration vs. enrolled population size**. *In red are the actual point durations measured on a single c. 2016 core. The blue shows linear growth from $N = 640\,000$. The green line shows logathmic growth from that point to $N = 1\,600\,000$. Note the sublinear growth from algorithms from Camvi, Dermalog, EverAI, Innovatrics, and Visionlabs. The tiger_1 algorithm is also sublinear, but inaccurate and inoperable at $N \geq 3000000$. This capability sometimes comes at the additional expense of converting a linear gallery data structure into whatever fast-search data structure is used. Note that search times are sometimes dominated by the template generation times shown in Table 45.*

2026/01/09 20:40:38

FNIR(N, R, T) = False neg. identification rate
FPIR(N, T) = False pos. identification rate

N = Num. enrolled subjects
R = Num. candidates examined

T = Threshold

T = 0 → Investigation
T > 0 → Identification

This publication is available free of charge from: https://doi.org/10.6028/NIST.IR.8271

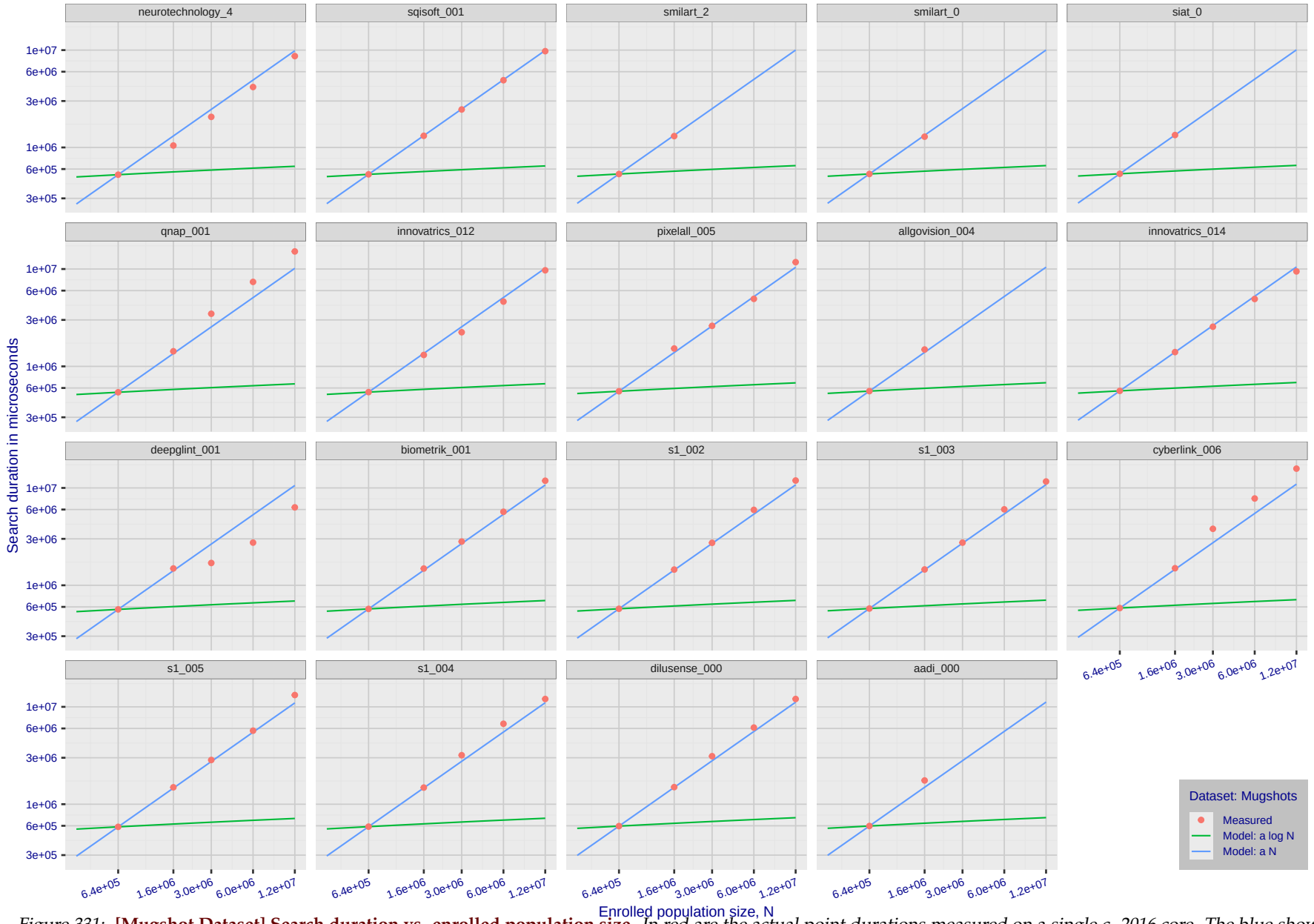

Figure 331: **[Mugshot Dataset] Search duration vs. enrolled population size**. *In red are the actual point durations measured on a single c. 2016 core. The blue shows linear growth from $N = 640\,000$. The green line shows logathmic growth from that point to $N = 1\,600\,000$. Note the sublinear growth from algorithms from Camvi, Dermalog, EverAI, Innovatrics, and Visionlabs. The tiger_1 algorithm is also sublinear, but inaccurate and inoperable at $N \geq 3000000$. This capability sometimes comes at the additional expense of converting a linear gallery data structure into whatever fast-search data structure is used. Note that search times are sometimes dominated by the template generation times shown in Table 45.*

2026/01/09 20:40:38
FNIR(N, R, T) = False neg. identification rate
FPIR(N, T) = False pos. identification rate
N = Num. enrolled subjects
R = Num. candidates examined
T = Threshold
T = 0 → Investigation
T > 0 → Identification

This publication is available free of charge from: https://doi.org/10.6028/NIST.IR.8271

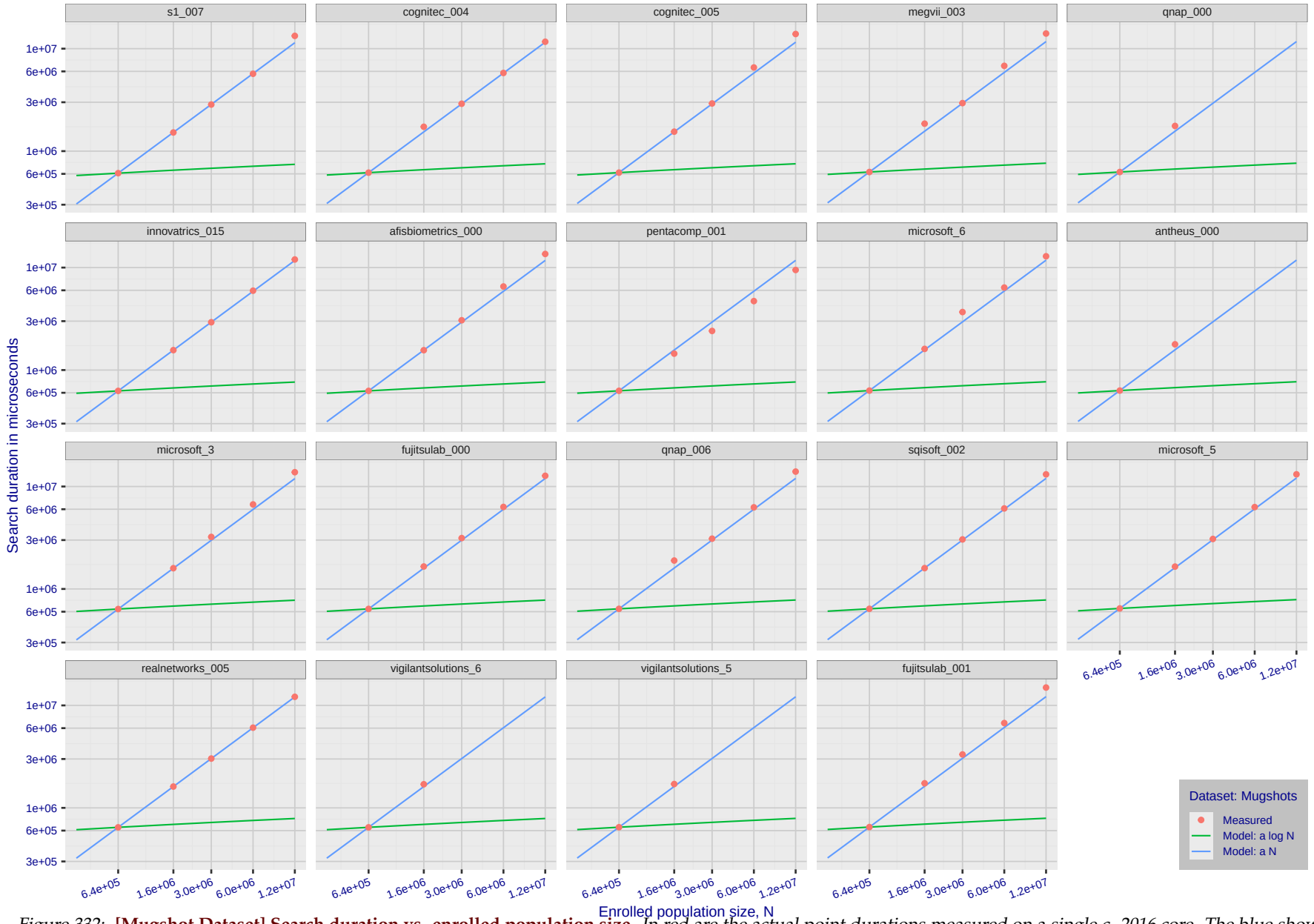

Figure 332: **[Mugshot Dataset] Search duration vs. enrolled population size**. *In red are the actual point durations measured on a single c. 2016 core. The blue shows linear growth from $N = 640\,000$. The green line shows logathmic growth from that point to $N = 1\,600\,000$. Note the sublinear growth from algorithms from Camvi, Dermalog, EverAI, Innovatrics, and Visionlabs. The tiger_1 algorithm is also sublinear, but inaccurate and inoperable at $N \geq 3000000$. This capability sometimes comes at the additional expense of converting a linear gallery data structure into whatever fast-search data structure is used. Note that search times are sometimes dominated by the template generation times shown in Table 45.*

2026/01/09 20:40:38

FNIR(N, R, T) = False neg. identification rate
FPIR(N, T) = False pos. identification rate

N = Num. enrolled subjects
R = Num. candidates examined

T = Threshold

T = 0 → Investigation
T > 0 → Identification

This publication is available free of charge from: https://doi.org/10.6028/NIST.IR.8271

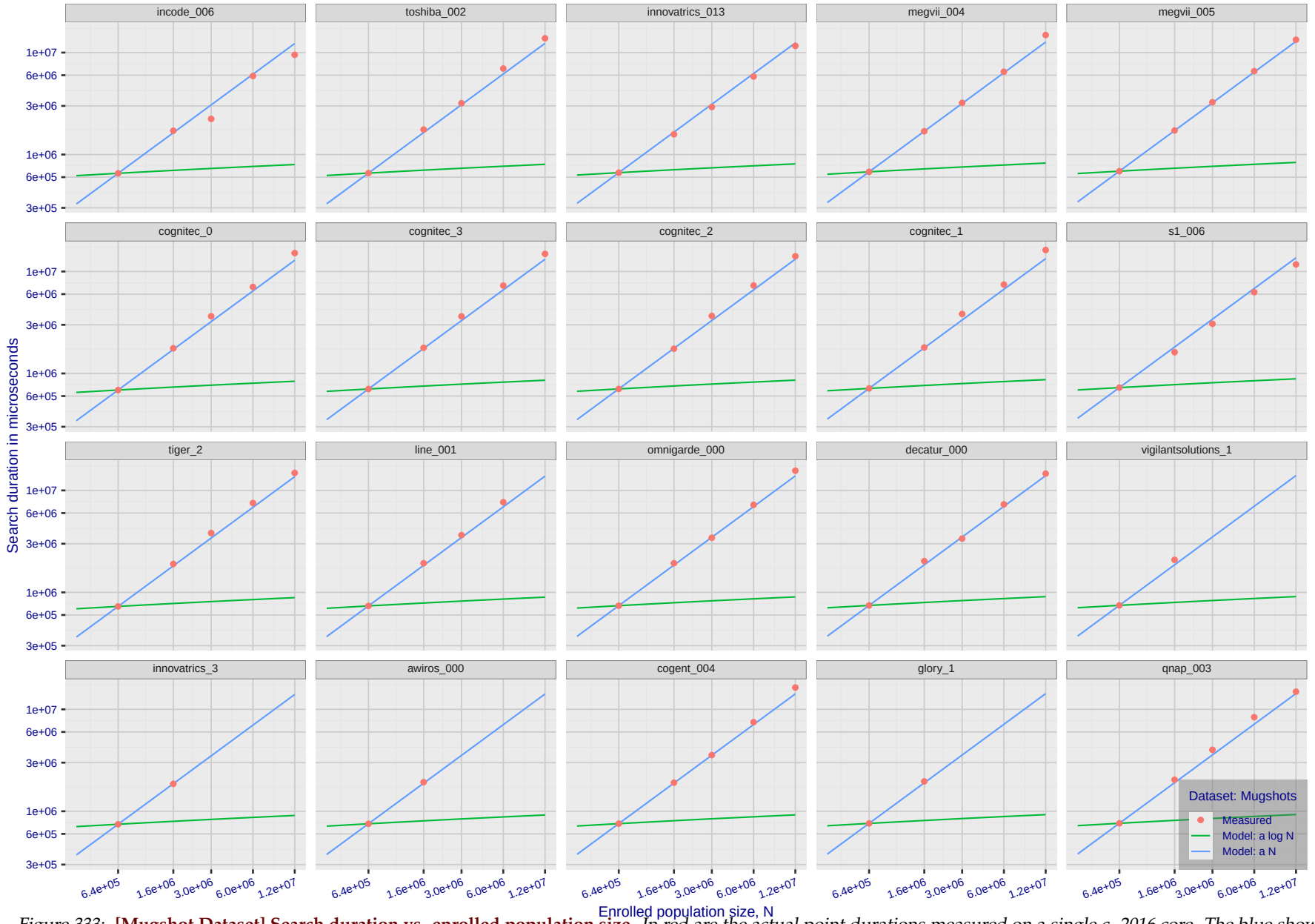

Figure 333: **[Mugshot Dataset] Search duration vs. enrolled population size**. *In red are the actual point durations measured on a single c. 2016 core. The blue shows linear growth from $N = 640\,000$. The green line shows logathmic growth from that point to $N = 1\,600\,000$. Note the sublinear growth from algorithms from Camvi, Dermalog, EverAI, Innovatrics, and Visionlabs. The tiger_1 algorithm is also sublinear, but inaccurate and inoperable at $N \geq 3000000$. This capability sometimes comes at the additional expense of converting a linear gallery data structure into whatever fast-search data structure is used. Note that search times are sometimes dominated by the template generation times shown in Table 45.*

2026/01/09 20:40:38

FNIR(N, R, T) = False neg. identification rate
FPIR(N, T) = False pos. identification rate

N = Num. enrolled subjects
R = Num. candidates examined

T = Threshold

T = 0 → Investigation
T > 0 → Identification

This publication is available free of charge from: https://doi.org/10.6028/NIST.IR.8271

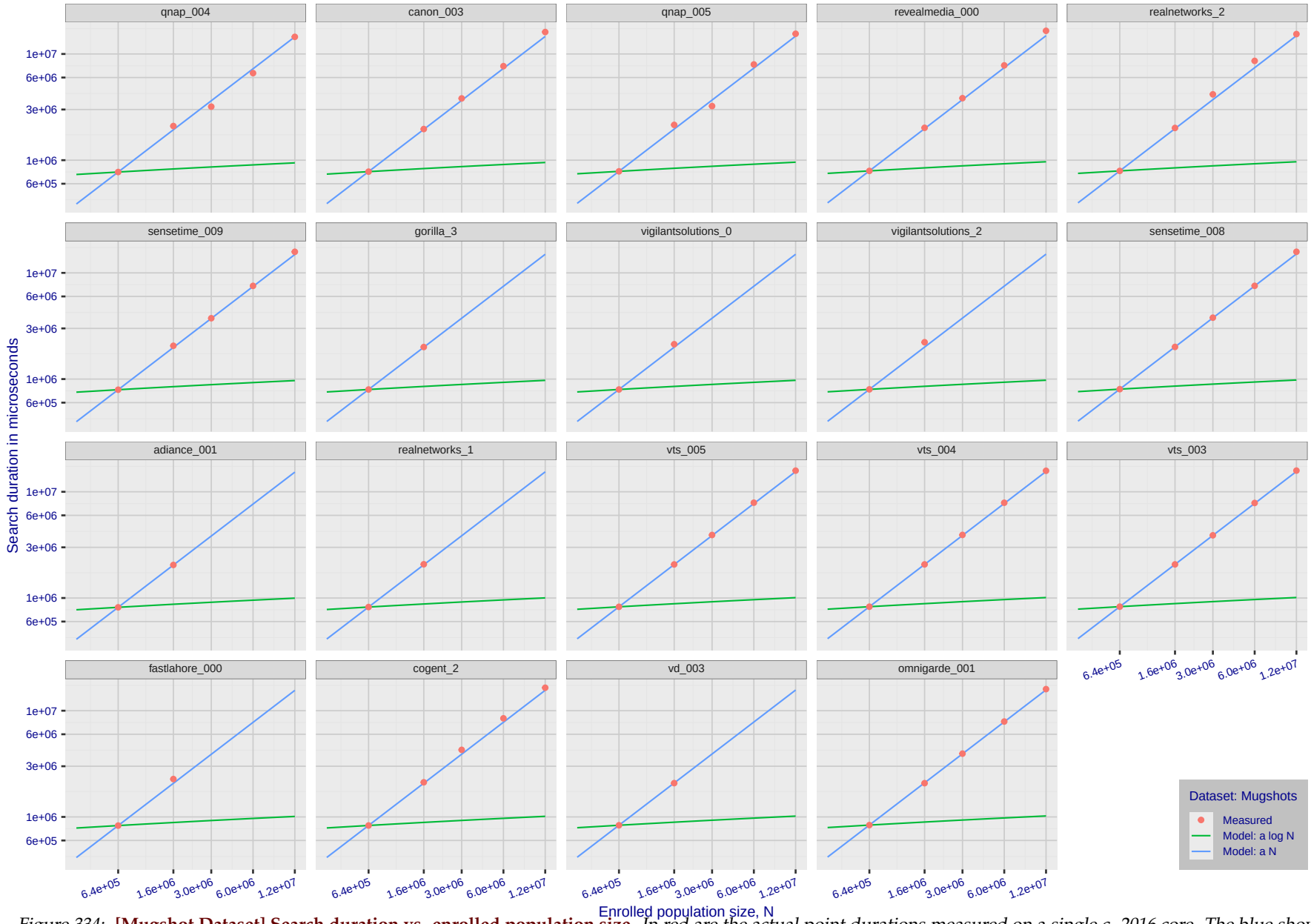

Figure 334: **[Mugshot Dataset] Search duration vs. enrolled population size**. *In red are the actual point durations measured on a single c. 2016 core. The blue shows linear growth from $N = 640\,000$. The green line shows logathmic growth from that point to $N = 1\,600\,000$. Note the sublinear growth from algorithms from Camvi, Dermalog, EverAI, Innovatrics, and Visionlabs. The tiger_1 algorithm is also sublinear, but inaccurate and inoperable at $N \geq 3000000$. This capability sometimes comes at the additional expense of converting a linear gallery data structure into whatever fast-search data structure is used. Note that search times are sometimes dominated by the template generation times shown in Table 45.*

2026/01/09 20:40:38

FNIR(N, R, T) = False neg. identification rate
FPIR(N, T) = False pos. identification rate

N = Num. enrolled subjects
R = Num. candidates examined

T = Threshold

T = 0 → Investigation
T > 0 → Identification

This publication is available free of charge from: https://doi.org/10.6028/NIST.IR.8271

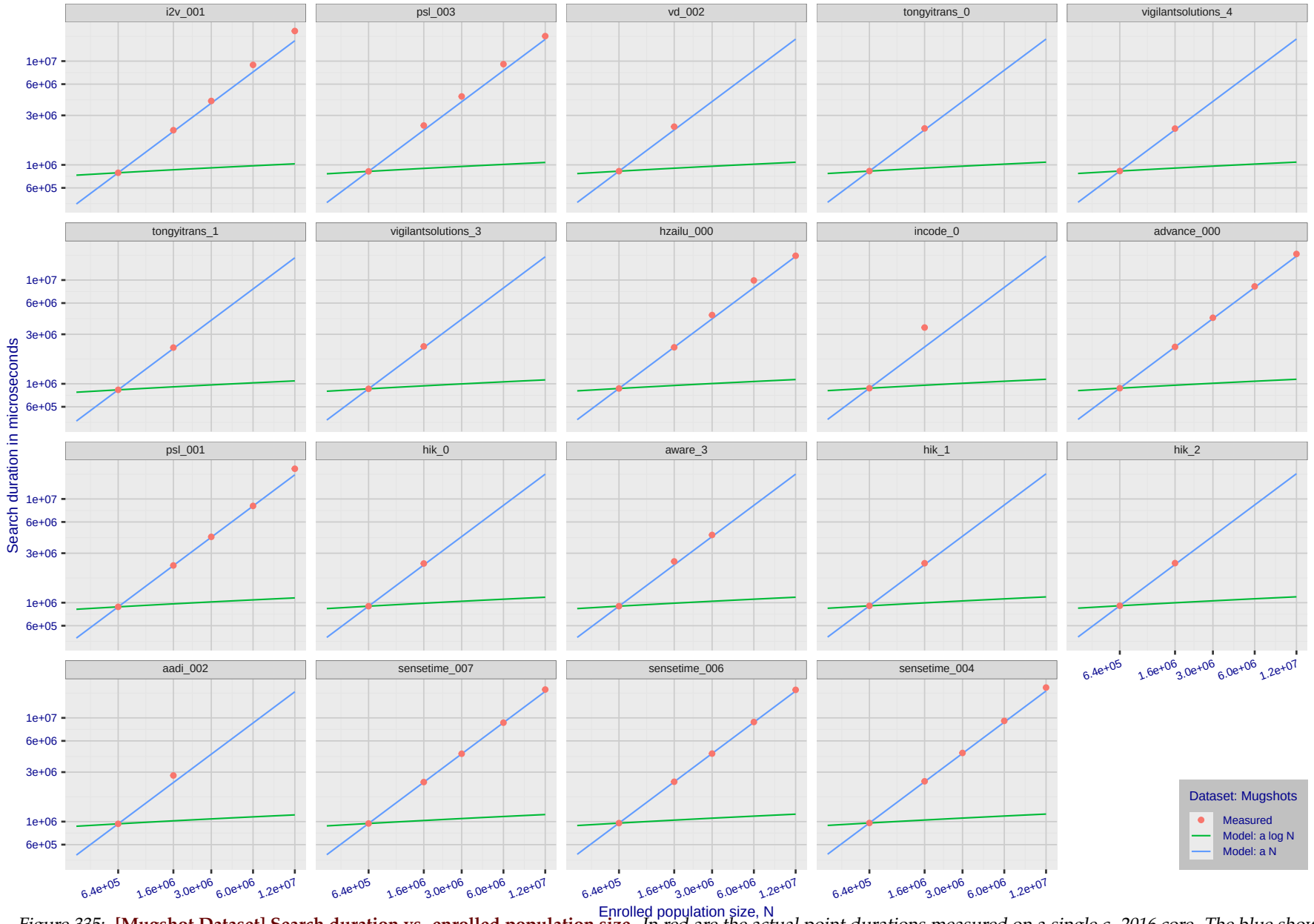

Figure 335: **[Mugshot Dataset] Search duration vs. enrolled population size**. *In red are the actual point durations measured on a single c. 2016 core. The blue shows linear growth from $N = 640\,000$. The green line shows logathmic growth from that point to $N = 1\,600\,000$. Note the sublinear growth from algorithms from Camvi, Dermalog, EverAI, Innovatrics, and Visionlabs. The tiger_1 algorithm is also sublinear, but inaccurate and inoperable at $N \geq 3000000$. This capability sometimes comes at the additional expense of converting a linear gallery data structure into whatever fast-search data structure is used. Note that search times are sometimes dominated by the template generation times shown in Table 45.*

2026/01/09 20:40:38

FNIR(N, R, T) = False neg. identification rate
FPIR(N, T) = False pos. identification rate

N = Num. enrolled subjects
R = Num. candidates examined

T = Threshold

T = 0 → Investigation
T > 0 → Identification

This publication is available free of charge from: https://doi.org/10.6028/NIST.IR.8271

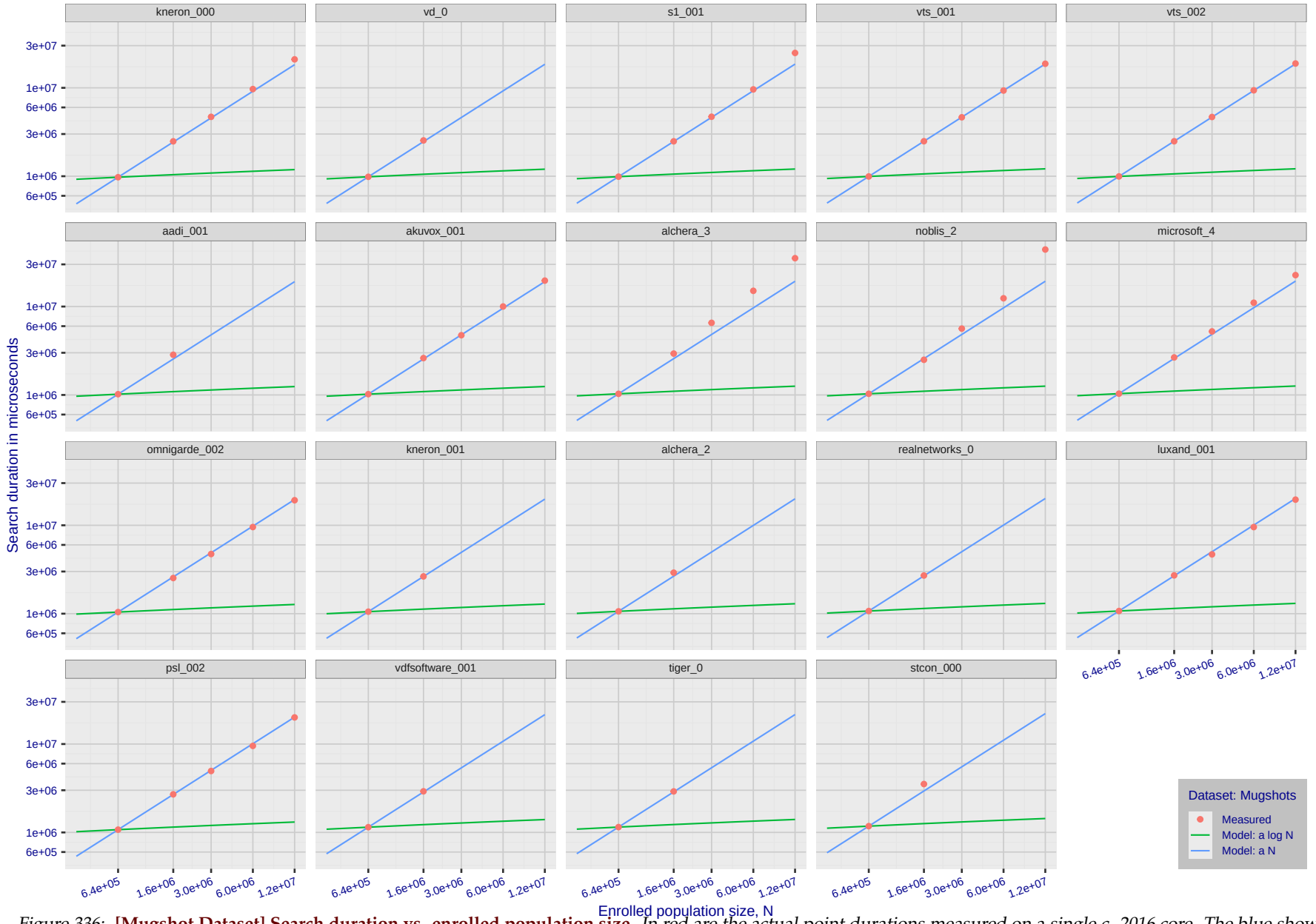

Figure 336: **[Mugshot Dataset] Search duration vs. enrolled population size**. *In red are the actual point durations measured on a single c. 2016 core. The blue shows linear growth from $N = 640\,000$. The green line shows logathmic growth from that point to $N = 1\,600\,000$. Note the sublinear growth from algorithms from Camvi, Dermalog, EverAI, Innovatrics, and Visionlabs. The tiger_1 algorithm is also sublinear, but inaccurate and inoperable at $N \geq 3000000$. This capability sometimes comes at the additional expense of converting a linear gallery data structure into whatever fast-search data structure is used. Note that search times are sometimes dominated by the template generation times shown in Table 45.*

2026/01/09 20:40:38
FNIR(N, R, T) = False neg. identification rate
FPIR(N, T) = False pos. identification rate
N = Num. enrolled subjects
R = Num. candidates examined
T = Threshold
T = 0 → Investigation
T > 0 → Identification

This publication is available free of charge from: https://doi.org/10.6028/NIST.IR.8271

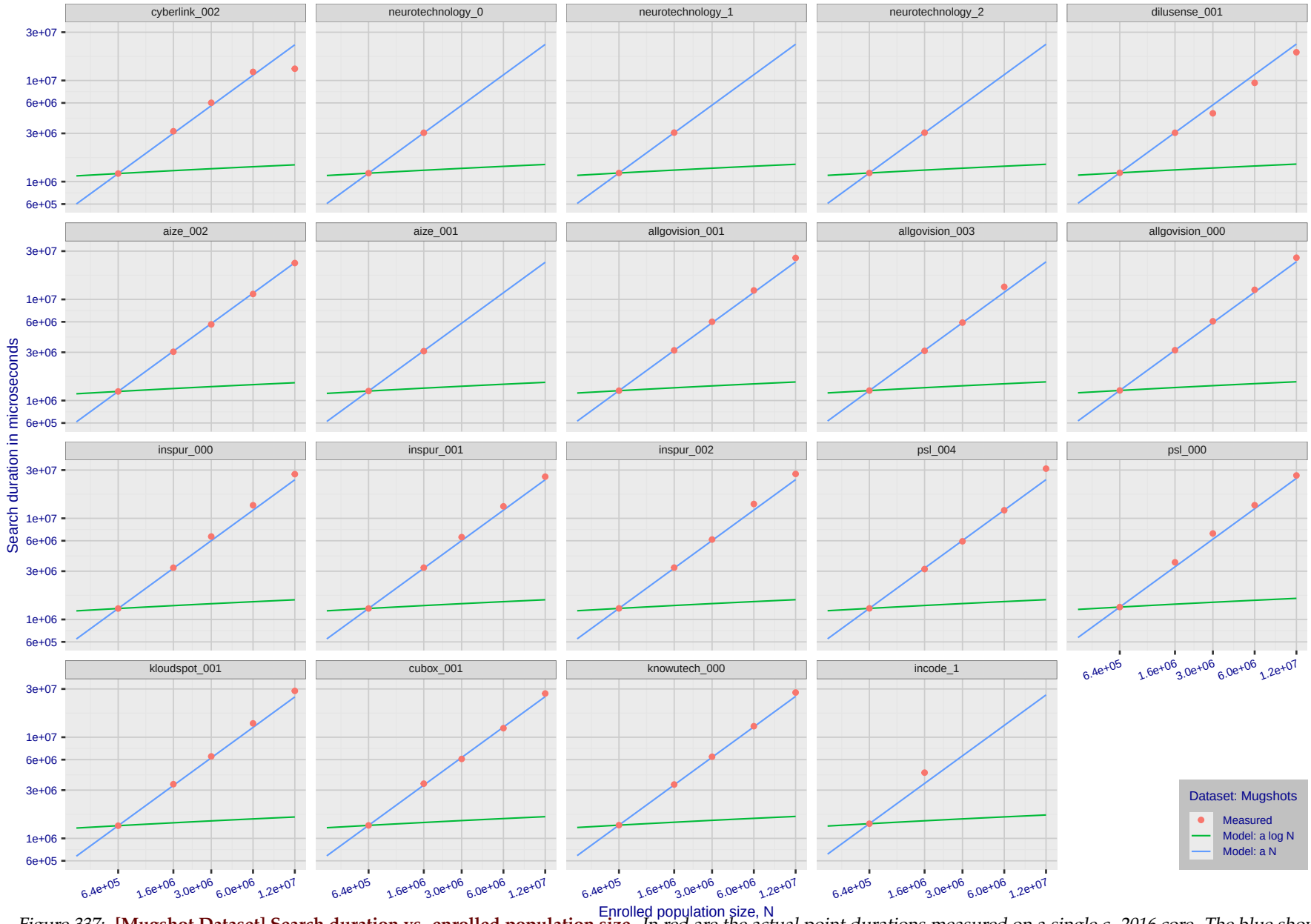

Figure 337: **[Mugshot Dataset] Search duration vs. enrolled population size**. *In red are the actual point durations measured on a single c. 2016 core. The blue shows linear growth from $N = 640\,000$. The green line shows logathmic growth from that point to $N = 1\,600\,000$. Note the sublinear growth from algorithms from Camvi, Dermalog, EverAI, Innovatrics, and Visionlabs. The tiger_1 algorithm is also sublinear, but inaccurate and inoperable at $N \geq 3000000$. This capability sometimes comes at the additional expense of converting a linear gallery data structure into whatever fast-search data structure is used. Note that search times are sometimes dominated by the template generation times shown in Table 45.*

2026/01/09 20:40:38

FNIR(N, R, T) = False neg. identification rate
FPIR(N, T) = False pos. identification rate
N = Num. enrolled subjects
R = Num. candidates examined
T = Threshold
T = 0 → Investigation
T > 0 → Identification

This publication is available free of charge from: https://doi.org/10.6028/NIST.IR.8271

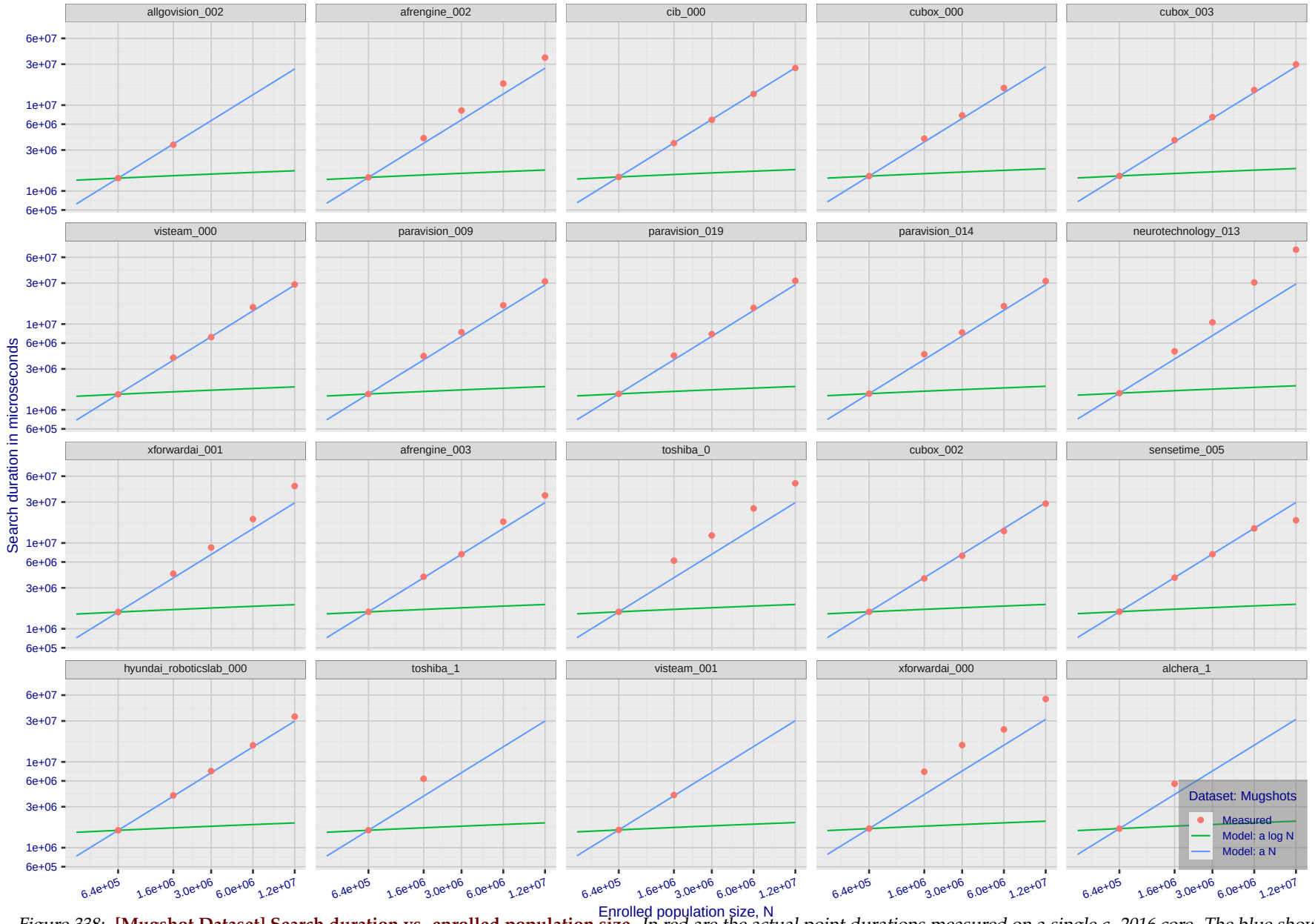

Figure 338: **[Mugshot Dataset] Search duration vs. enrolled population size**. *In red are the actual point durations measured on a single c. 2016 core. The blue shows linear growth from $N = 640\,000$. The green line shows logathmic growth from that point to $N = 1\,600\,000$. Note the sublinear growth from algorithms from Camvi, Dermalog, EverAI, Innovatrics, and Visionlabs. The tiger_1 algorithm is also sublinear, but inaccurate and inoperable at $N \geq 3000000$. This capability sometimes comes at the additional expense of converting a linear gallery data structure into whatever fast-search data structure is used. Note that search times are sometimes dominated by the template generation times shown in Table 45.*

2026/01/09 20:40:38

FNIR(N, R, T) = False neg. identification rate
FPIR(N, T) = False pos. identification rate

N = Num. enrolled subjects
R = Num. candidates examined

T = Threshold

T = 0 → Investigation
T > 0 → Identification

This publication is available free of charge from: https://doi.org/10.6028/NIST.IR.8271

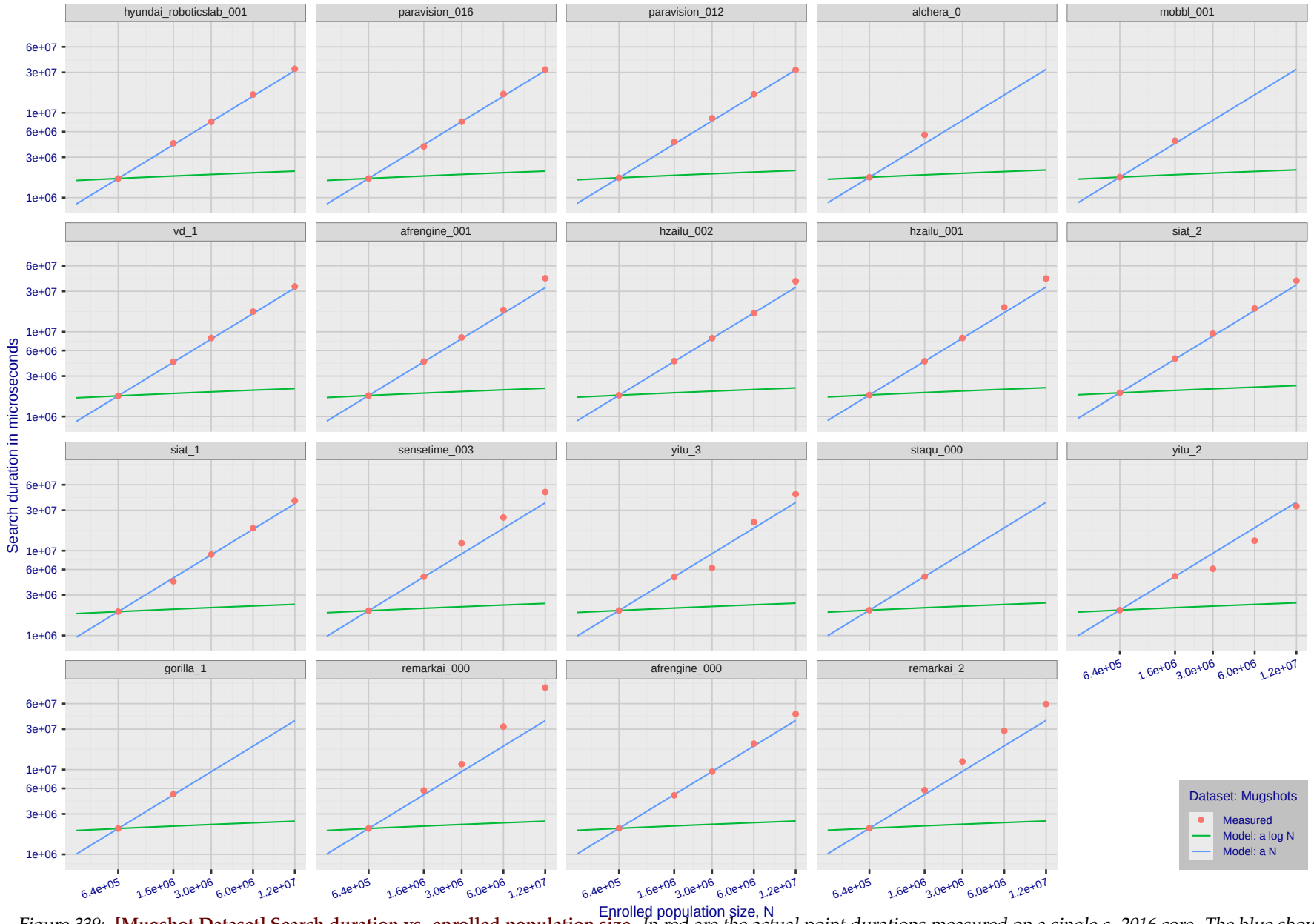

Figure 339: **[Mugshot Dataset] Search duration vs. enrolled population size**. *In red are the actual point durations measured on a single c. 2016 core. The blue shows linear growth from $N = 640\,000$. The green line shows logathmic growth from that point to $N = 1\,600\,000$. Note the sublinear growth from algorithms from Camvi, Dermalog, EverAI, Innovatrics, and Visionlabs. The tiger_1 algorithm is also sublinear, but inaccurate and inoperable at $N \geq 3000000$. This capability sometimes comes at the additional expense of converting a linear gallery data structure into whatever fast-search data structure is used. Note that search times are sometimes dominated by the template generation times shown in Table 45.*

2026/01/09 20:40:38
FNIR(N, R, T) = False neg. identification rate
FPIR(N, T) = False pos. identification rate
N = Num. enrolled subjects
R = Num. candidates examined
T = Threshold
T = 0 → Investigation
T > 0 → Identification

This publication is available free of charge from: https://doi.org/10.6028/NIST.IR.8271

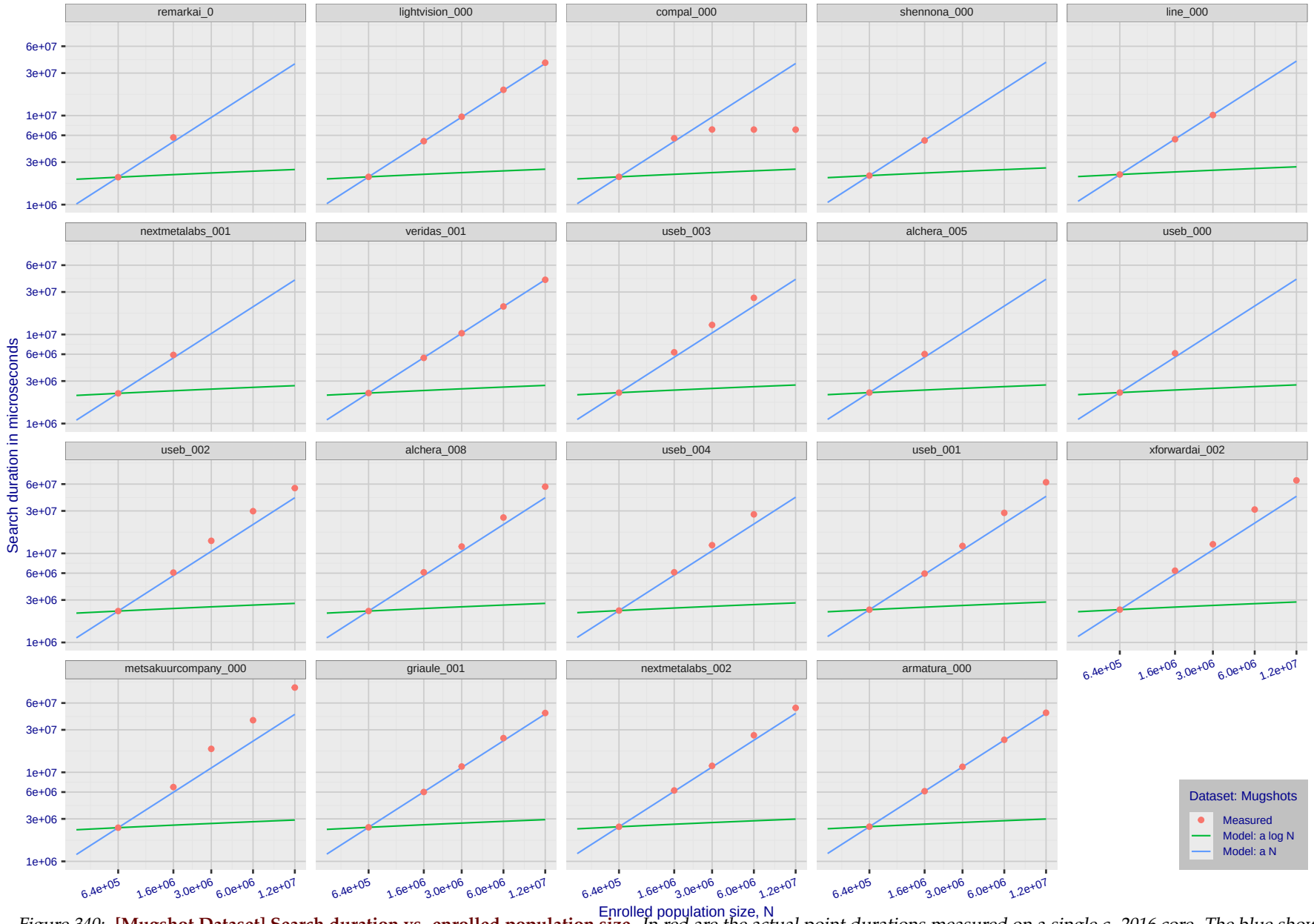

Figure 340: **[Mugshot Dataset] Search duration vs. enrolled population size**. *In red are the actual point durations measured on a single c. 2016 core. The blue shows linear growth from $N = 640\,000$. The green line shows logathmic growth from that point to $N = 1\,600\,000$. Note the sublinear growth from algorithms from Camvi, Dermalog, EverAI, Innovatrics, and Visionlabs. The tiger_1 algorithm is also sublinear, but inaccurate and inoperable at $N \geq 3000000$. This capability sometimes comes at the additional expense of converting a linear gallery data structure into whatever fast-search data structure is used. Note that search times are sometimes dominated by the template generation times shown in Table 45.*

2026/01/09 20:40:38
FNIR(N, R, T) = False neg. identification rate
FPIR(N, T) = False pos. identification rate
N = Num. enrolled subjects
R = Num. candidates examined
T = Threshold
T = 0 → Investigation
T > 0 → Identification

This publication is available free of charge from: https://doi.org/10.6028/NIST.IR.8271

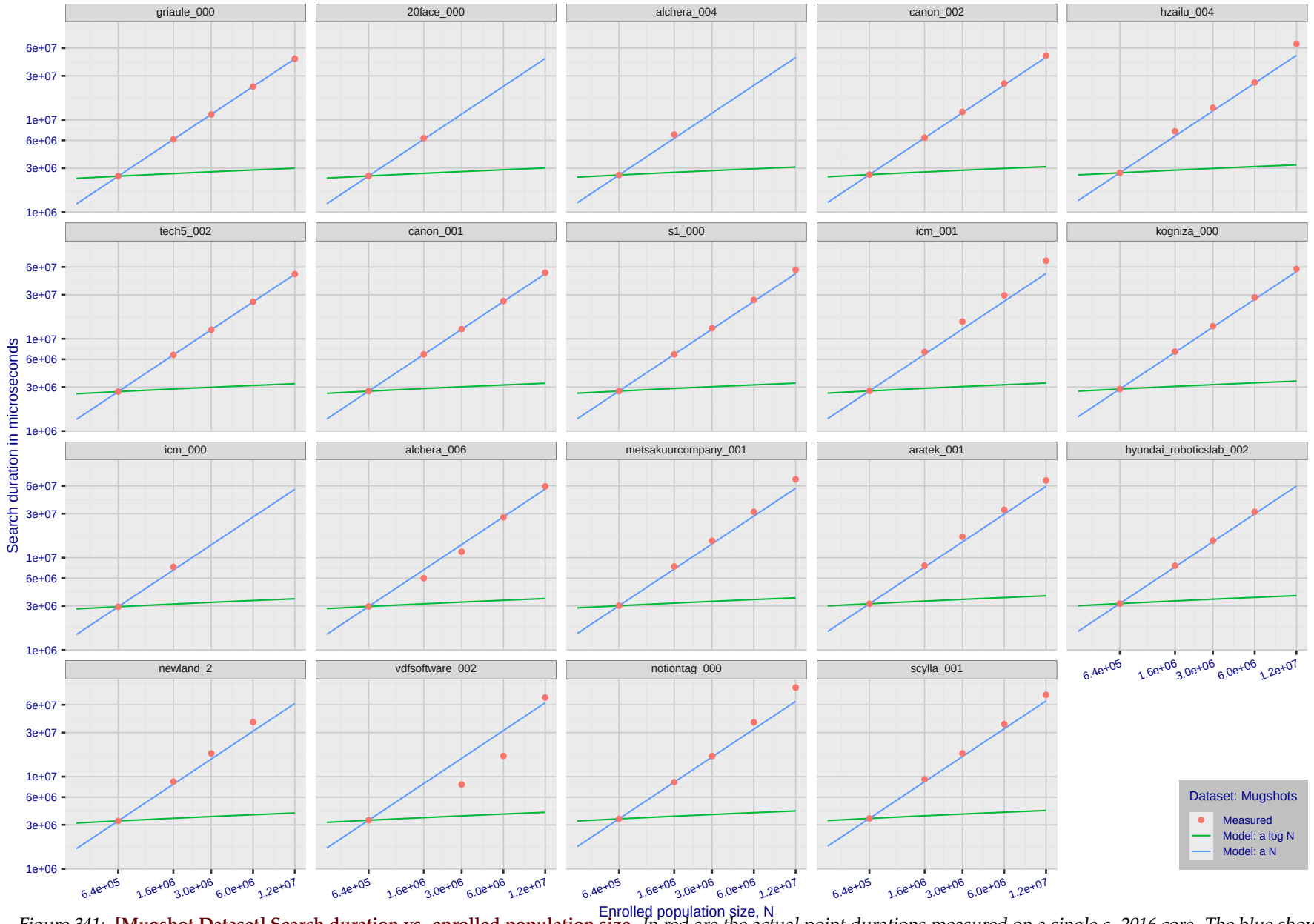

Figure 341: **[Mugshot Dataset] Search duration vs. enrolled population size**. *In red are the actual point durations measured on a single c. 2016 core. The blue shows linear growth from $N = 640\,000$. The green line shows logathmic growth from that point to $N = 1\,600\,000$. Note the sublinear growth from algorithms from Camvi, Dermalog, EverAI, Innovatrics, and Visionlabs. The tiger_1 algorithm is also sublinear, but inaccurate and inoperable at $N \geq 3000000$. This capability sometimes comes at the additional expense of converting a linear gallery data structure into whatever fast-search data structure is used. Note that search times are sometimes dominated by the template generation times shown in Table 45.*

This publication is available free of charge from: https://doi.org/10.6028/NIST.IR.8271

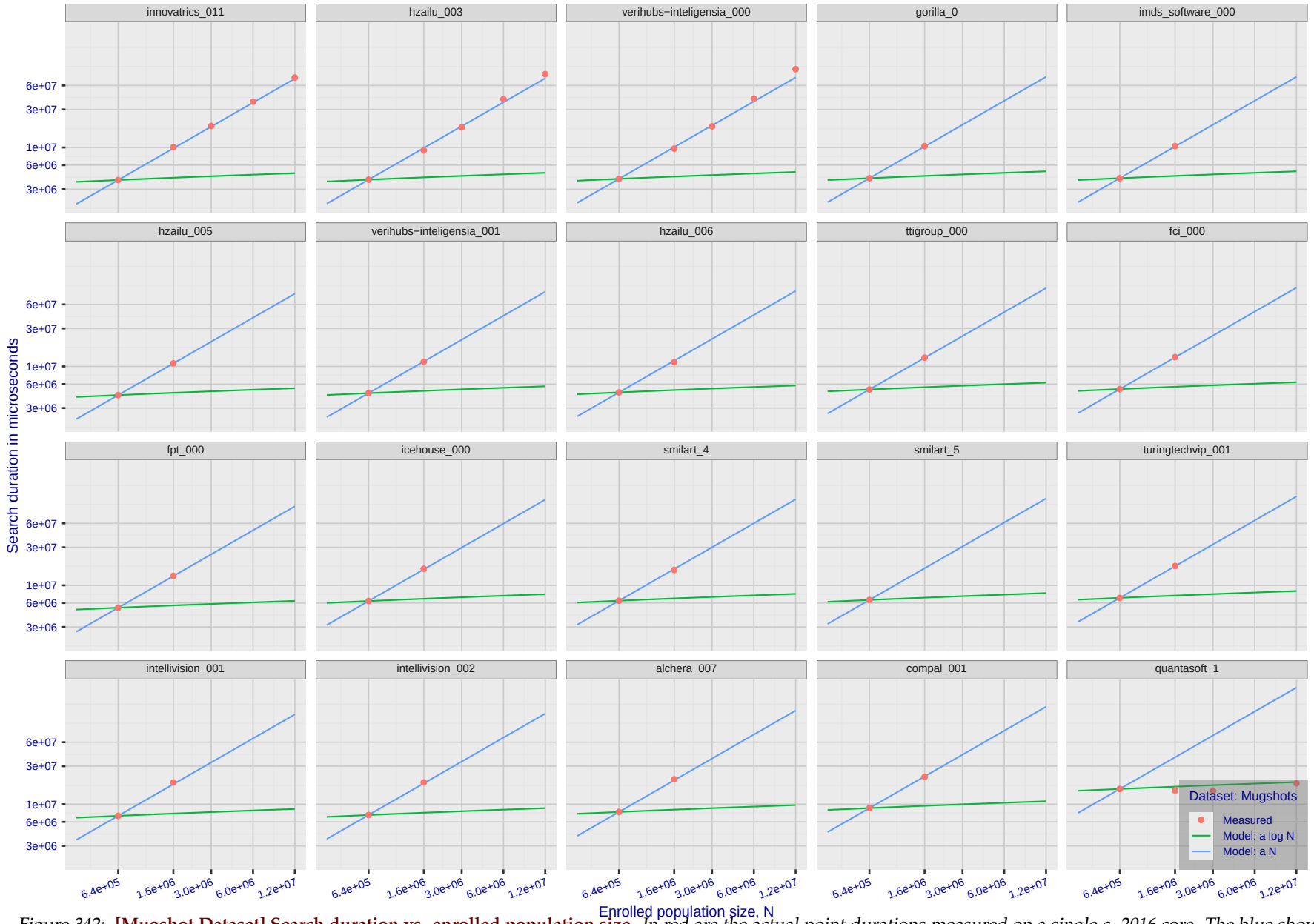

Figure 342: **[Mugshot Dataset] Search duration vs. enrolled population size**. *In red are the actual point durations measured on a single c. 2016 core. The blue shows linear growth from $N = 640\,000$. The green line shows logathmic growth from that point to $N = 1\,600\,000$. Note the sublinear growth from algorithms from Camvi, Dermalog, EverAI, Innovatrics, and Visionlabs. The tiger_1 algorithm is also sublinear, but inaccurate and inoperable at $N \geq 3000000$. This capability sometimes comes at the additional expense of converting a linear gallery data structure into whatever fast-search data structure is used. Note that search times are sometimes dominated by the template generation times shown in Table 45.*

2026/01/09 20:40:38

FNIR(N, R, T) = False neg. identification rate
FPIR(N, T) = False pos. identification rate

N = Num. enrolled subjects
R = Num. candidates examined

T = Threshold

T = 0 → Investigation
T > 0 → Identification

This publication is available free of charge from: https://doi.org/10.6028/NIST.IR.8271

Figure 343: **[Mugshot Dataset] Search duration vs. enrolled population size**. *In red are the actual point durations measured on a single c. 2016 core. The blue shows linear growth from $N = 640\,000$. The green line shows logathmic growth from that point to $N = 1\,600\,000$. Note the sublinear growth from algorithms from Camvi, Dermalog, EverAI, Innovatrics, and Visionlabs. The tiger_1 algorithm is also sublinear, but inaccurate and inoperable at $N \geq 3000000$. This capability sometimes comes at the additional expense of converting a linear gallery data structure into whatever fast-search data structure is used. Note that search times are sometimes dominated by the template generation times shown in Table 45.*

Appendix G Gallery Insertion Timing

This publication is available free of charge from: https://doi.org/10.6028/NIST.IR.8271

This publication is available free of charge from: https://doi.org/10.6028/NIST.IR.8271

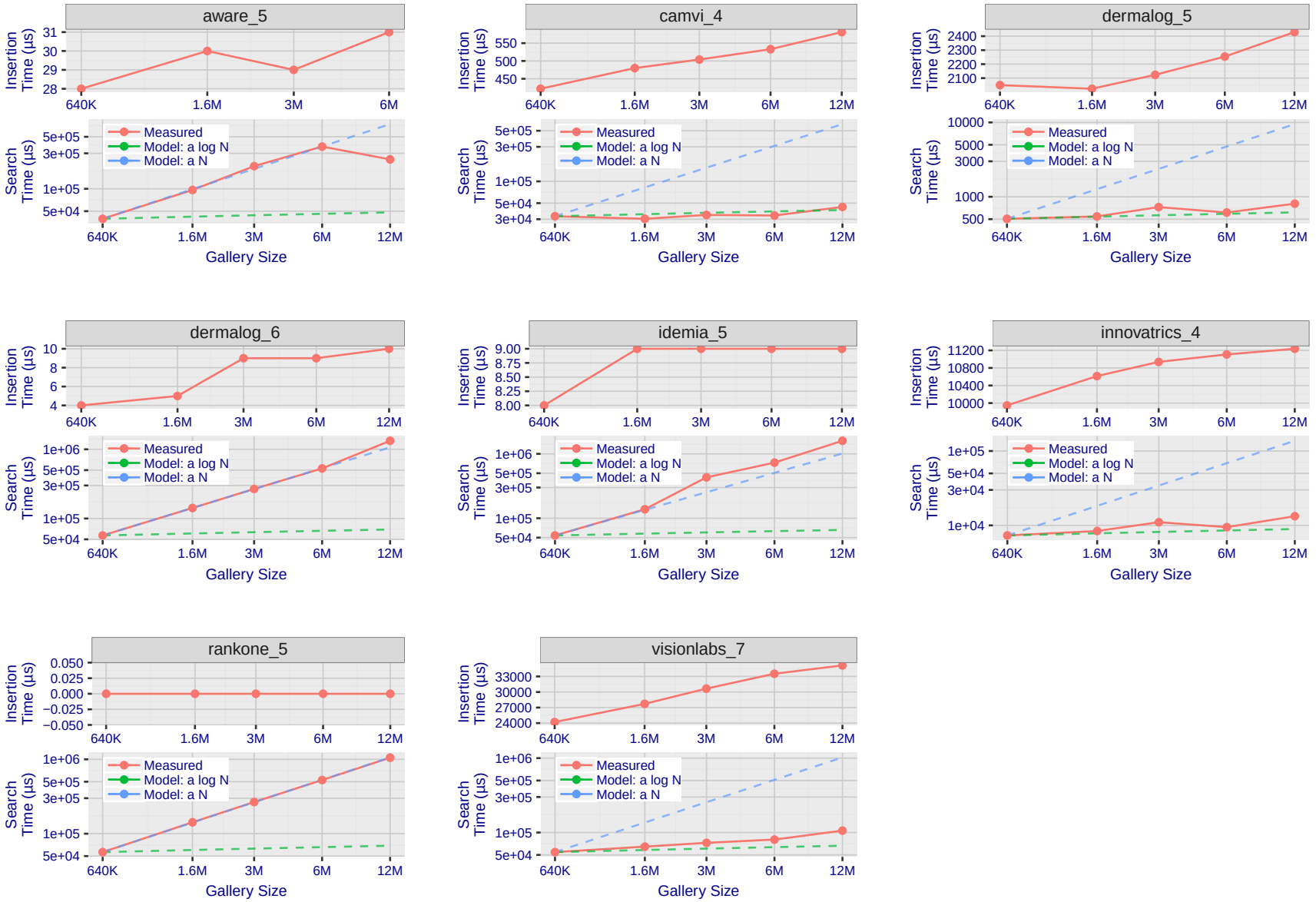

Figure 344: **[Mugshot Dataset] Gallery insertion duration vs. enrolled population size**. *This chart plots the time it takes to insert a single template into a finalized gallery, illustrated over increasing gallery sizes. For reference, search times on finalized galleries of corresponding sizes are plotted right underneath. Gallery insertion time plots were generated on algorithms that 1) successfully implemented gallery insertion with no errors and 2) that were run on galleries with N up to* 12 000 000. *Generally, only the more accurate algorithms were run on galleries with N up to* 12 000 000.

2026/01/09 20:40:38

FNIR(N, R, T) = False neg. identification rate
FPIR(N, T) = False pos. identification rate

N = Num. enrolled subjects
R = Num. candidates examined

T = Threshold

T = 0 → Investigation
T > 0 → Identification

This publication is available free of charge from: https://doi.org/10.6028/NIST.IR.8271

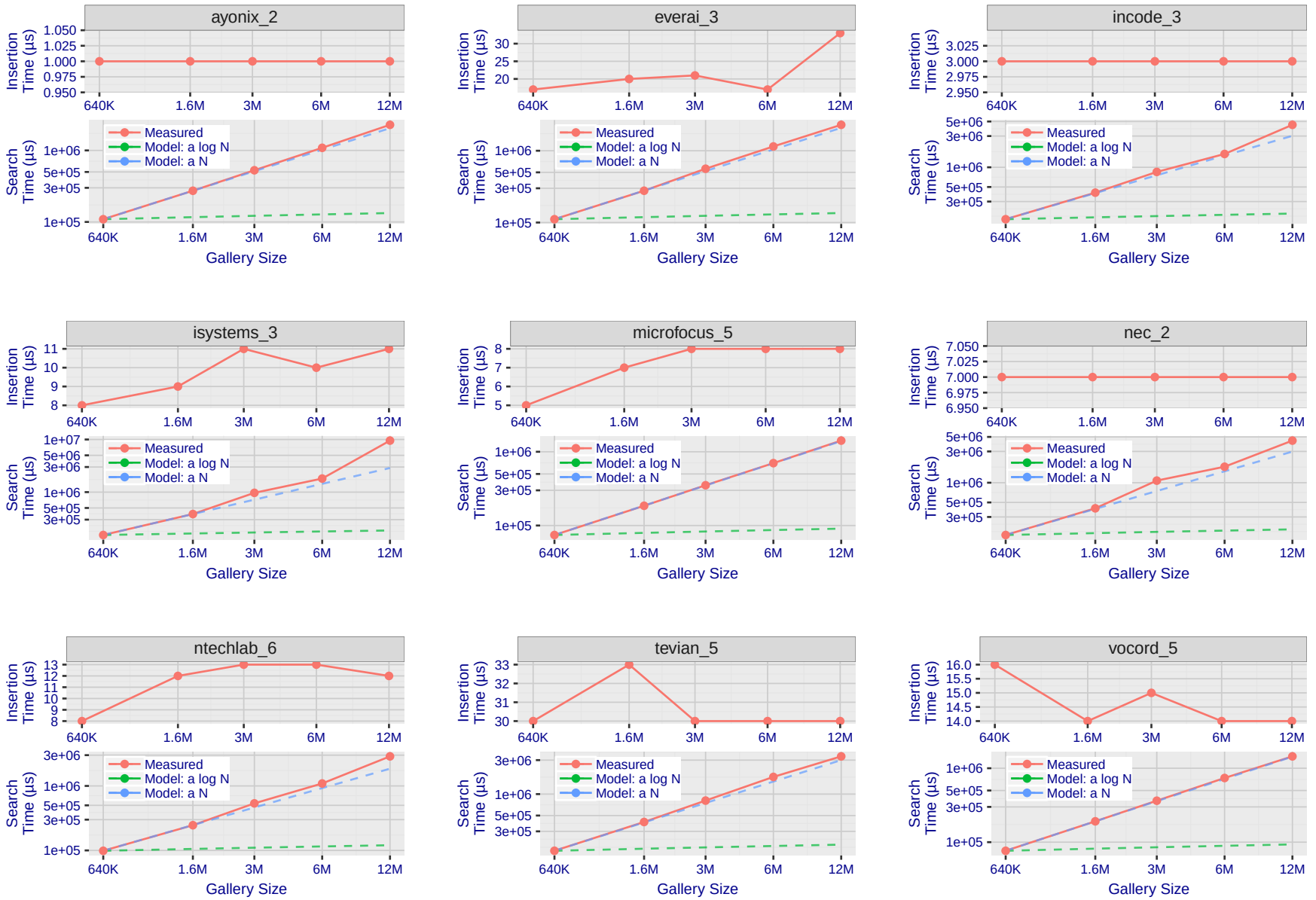

Figure 345: **[Mugshot Dataset] Gallery insertion duration vs. enrolled population size**. *This chart plots the time it takes to insert a single template into a finalized gallery, illustrated over increasing gallery sizes. For reference, search times on finalized galleries of corresponding sizes are plotted right underneath. Gallery insertion time plots were generated on algorithms that 1) successfully implemented gallery insertion with no errors and 2) that were run on galleries with N up to* 12 000 000. *Generally, only the more accurate algorithms were run on galleries with N up to* 12 000 000.

2026/01/09 20:40:38
FNIR(N, R, T) = False neg. identification rate
FPIR(N, T) = False pos. identification rate
N = Num. enrolled subjects
R = Num. candidates examined
T = Threshold
T = 0 → Investigation
T > 0 → Identification

This publication is available free of charge from: https://doi.org/10.6028/NIST.IR.8271

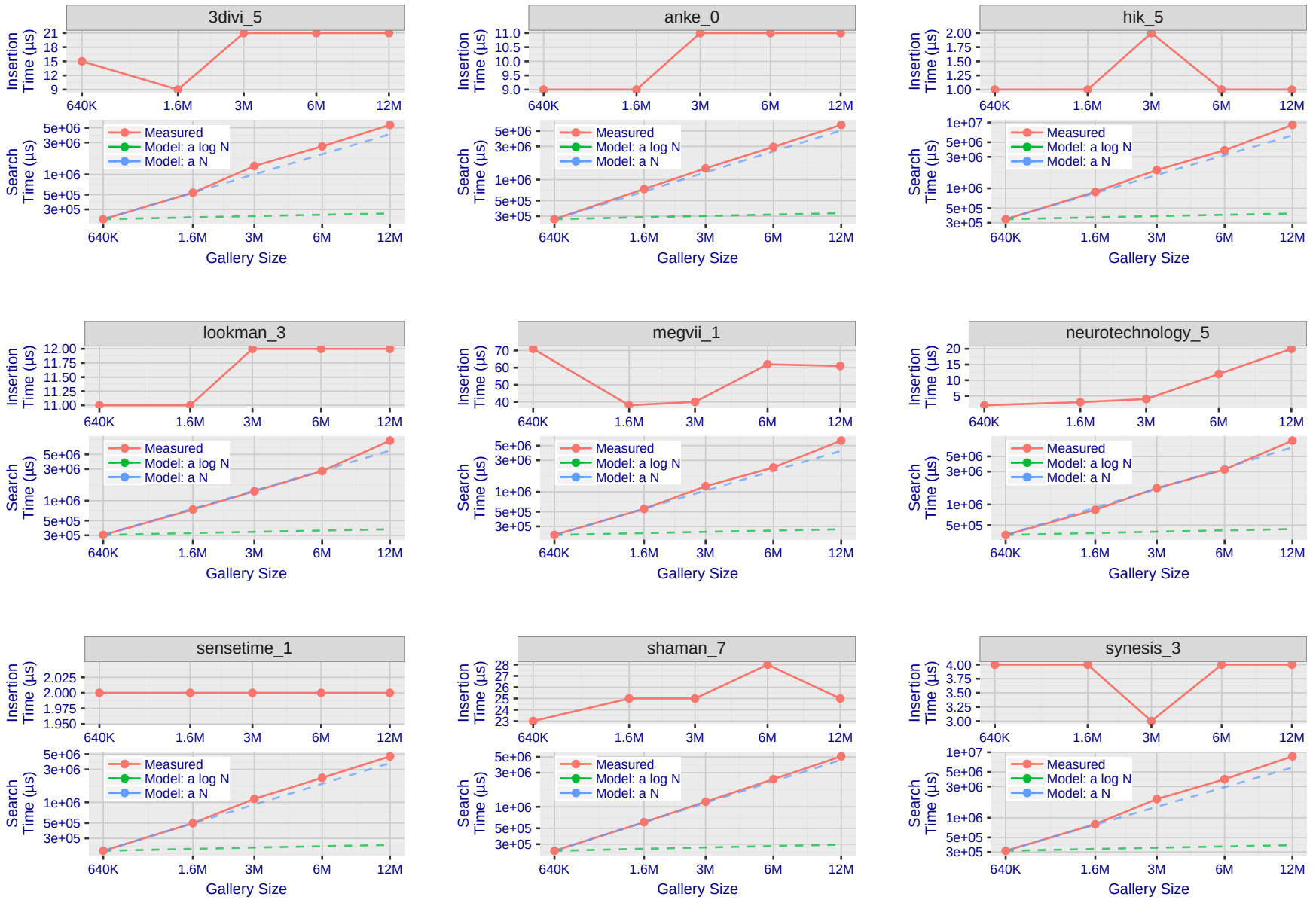

Figure 346: **[Mugshot Dataset] Gallery insertion duration vs. enrolled population size**. *This chart plots the time it takes to insert a single template into a finalized gallery, illustrated over increasing gallery sizes. For reference, search times on finalized galleries of corresponding sizes are plotted right underneath. Gallery insertion time plots were generated on algorithms that 1) successfully implemented gallery insertion with no errors and 2) that were run on galleries with N up to* 12 000 000. *Generally, only the more accurate algorithms were run on galleries with N up to* 12 000 000.

2026/01/09 20:40:38
FNIR(N, R, T) = False neg. identification rate
FPIR(N, T) = False pos. identification rate
N = Num. enrolled subjects
R = Num. candidates examined
T = Threshold
T = 0 → Investigation
T > 0 → Identification

This publication is available free of charge from: https://doi.org/10.6028/NIST.IR.8271

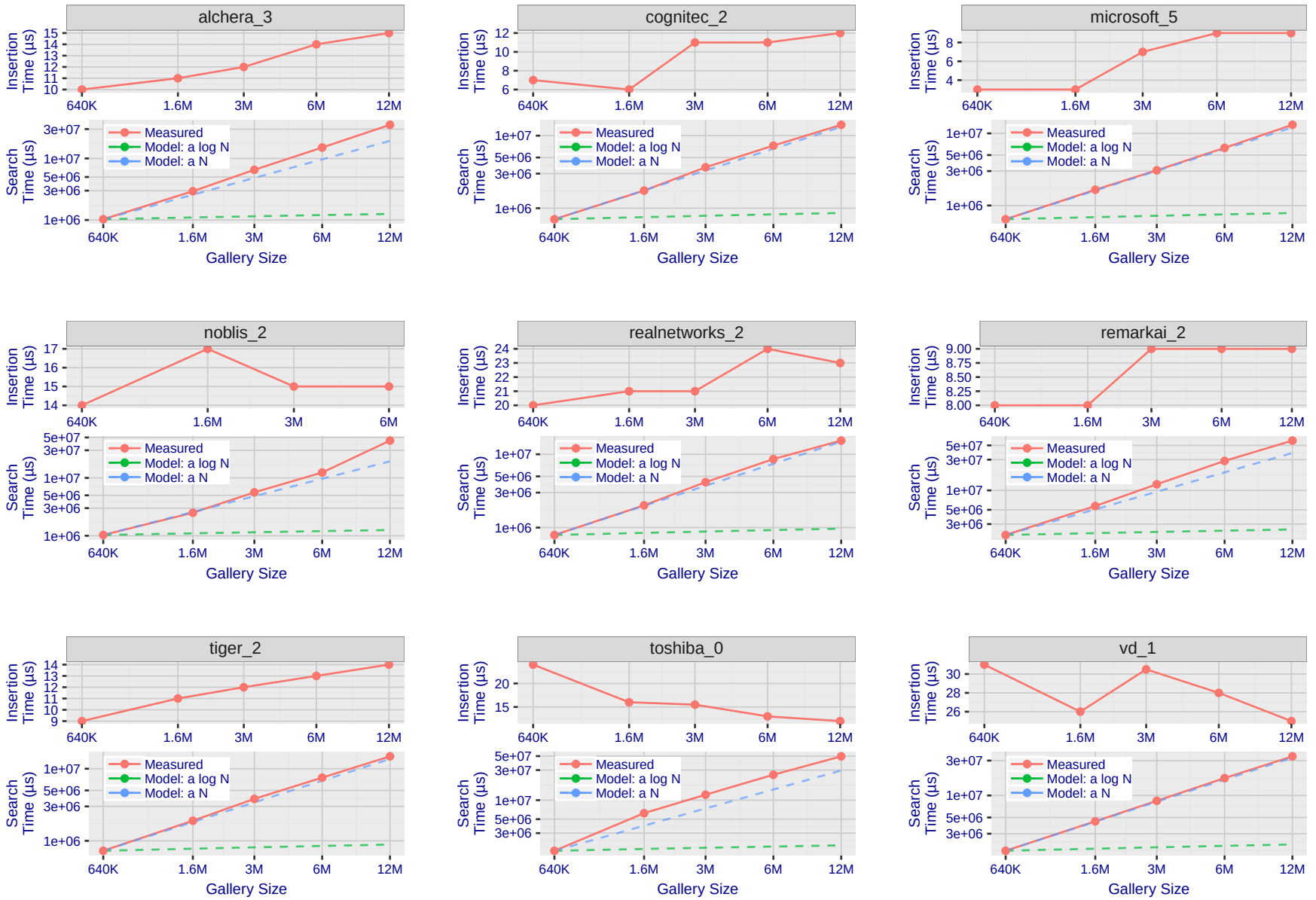

Figure 347: **[Mugshot Dataset] Gallery insertion duration vs. enrolled population size**. *This chart plots the time it takes to insert a single template into a finalized gallery, illustrated over increasing gallery sizes. For reference, search times on finalized galleries of corresponding sizes are plotted right underneath. Gallery insertion time plots were generated on algorithms that 1) successfully implemented gallery insertion with no errors and 2) that were run on galleries with N up to* 12 000 000. *Generally, only the more accurate algorithms were run on galleries with N up to* 12 000 000.

2026/01/09 20:40:38
FNIR(N, R, T) = False neg. identification rate N = Num. enrolled subjects T = Threshold T = 0 → Investigation
FPIR(N, T) = False pos. identification rate R = Num. candidates examined T > 0 → Identification

References

[1] Artem Babenko and Victor Lempitsky. Efficient indexing of billion-scale datasets of deep descriptors. In *The IEEE Conference on Computer Vision and Pattern Recognition (CVPR)*, June 2016.

[2] L. Best-Rowden and A. K. Jain. Longitudinal study of automatic face recognition. *IEEE Transactions on Pattern Analysis and Machine Intelligence*, 40(1):148–162, Jan 2018.

[3] Blumstein, Cohen, Roth, and Visher, editors. *Random parameter stochastic models of criminal careers*. National Academy of Sciences Press, 1986.

[4] Thomas P. Bonczar and Lauren E. Glaze. Probation and parole in the united statesm 2007, statistical tables. Technical report, Bureau of Justice Statistics, December 2008.

[5] White D., Kemp R. I., Jenkins R., Matheson M, and Burton A. M. Passport officers' errors in face matching. *PLoS ONE*, 9(8), 2014. e103510. doi:10.1371/journal. pone.0103510.

[6] P. Grother, G. W. Quinn, and P. J. Phillips. Evaluation of 2d still-image face recognition algorithms. NIST Interagency Report 7709, National Institute of Standards and Technology, 8 2010. http://face.nist.gov/mbe as MBE2010 FRVT2010.

[7] P. J. Grother, R. J. Micheals, and P. J. Phillips. Performance metrics for the frvt 2002 evaluation. In *Proceedings of Audio and Video Based Person Authentication Conference (AVBPA)*, June 2003.

[8] Patrick Grother and Mei Ngan. Interagency report 8009, performance of face identification algorithms. *Face Recognition Vendor Test (FRVT)*, May 2014.

[9] Patrick Grother, George Quinn, and Mei Ngan. Face in video evaluation (five) face recognition of non-cooperative subjects. Interagency Report 8173, National Institute of Standards and Technology, March 2017. https://doi.org/10.6028/NIST.IR.8173.

[10] Patrick Grother, George W. Quinn, and Mei Ngan. Face recognition vendor test - still face image and video concept, evaluation plan and api. Technical report, National Institute of Standards and Technology, 7 2013. http://biometrics.nist.gov/cs_links/face/frvt/frvt2012/NIST_FRVT2012_api_Aug15.pdf.

[11] K. He, X. Zhang, S. Ren, and J. Sun. Deep residual learning for image recognition. In *2016 IEEE Conference on Computer Vision and Pattern Recognition (CVPR)*, pages 770–778, June 2016.

[12] Gary B. Huang, Manu Ramesh, Tamara Berg, and Erik Learned-Miller. Labeled faces in the wild: A database for studying face recognition in unconstrained environments. Technical Report 07-49, University of Massachusetts, Amherst, October 2007.

[13] Masato Ishii, Hitoshi Imaoka, and Atsushi Sato. Fast k-nearest neighbor search for face identification using bounds of residual score. In *2017 12th IEEE International Conference on Automatic Face & Gesture Recognition (FG 2017)*, pages 194–199, Los Alamitos, CA, USA, May 2017. IEEE Computer Society.

[14] Jeff Johnson, Matthijs Douze, and Hervé Jégou. Billion-scale similarity search with gpus. *CoRR*, abs/1702.08734, 2017.

This publication is available free of charge from: https://doi.org/10.6028/NIST.IR.8271

[15] Ira Kemelmacher-Shlizerman, Steven M. Seitz, Daniel Miller, and Evan Brossard. The megaface benchmark: 1 million faces for recognition at scale. *CoRR*, abs/1512.00596, 2015.

[16] Yury A. Malkov and D. A. Yashunin. Efficient and robust approximate nearest neighbor search using hierarchical navigable small world graphs. *CoRR*, abs/1603.09320, 2016.

[17] Joyce A. Martin, Brady E. Hamilton, Michelle J.K. Osterman, Anne K. Driscoll, , and Patrick Drake. National vital statistics reports. Technical Report 8, Centers for Disease Control and Prevention, National Center for Health Statistics, National Vital Statistics System, Division of Vital Statistics, November 2018.

[18] O. M. Parkhi, A. Vedaldi, and A. Zisserman. Deep face recognition. In *British Machine Vision Conference*, 2015.

[19] P. Jonathon Phillips, Amy N. Yates, Ying Hu, Carina A. Hahn, Eilidh Noyes, Kelsey Jackson, Jacqueline G. Cavazos, Géraldine Jeckeln, Rajeev Ranjan, Swami Sankaranarayanan, Jun-Cheng Chen, Carlos D. Castillo, Rama Chellappa, David White, and Alice J. O'Toole. Face recognition accuracy of forensic examiners, superrecognizers, and face recognition algorithms. *Proceedings of the National Academy of Sciences*, 115(24):6171–6176, 2018.

[20] Florian Schroff, Dmitry Kalenichenko, and James Philbin. Facenet: A unified embedding for face recognition and clustering. *CoRR*, abs/1503.03832, 2015.

[21] Jeroen Smits and Christiaan Monden. Twinning across the developing world. *PLOS ONE*, 6(9):1–5, 09 2011.

[22] Yaniv Taigman, Ming Yang, Marc'Aurelio Ranzato, and Lior Wolf. Deepface: Closing the gap to human-level performance in face verification. In *Proceedings of the 2014 IEEE Conference on Computer Vision and Pattern Recognition*, CVPR '14, pages 1701–1708, Washington, DC, USA, 2014. IEEE Computer Society.

[23] A. Towler, R. I. Kemp, and D White. *Unfamiliar face matching systems in applied settings*. Nova Science, 2017.

[24] Working Group 3. Ed. M. Werner. *ISO/IEC 19794-5 Information Technology - Biometric Data Interchange Formats - Part 5: Face image data*. JTC1 :: SC37, 2 edition, 2011. http://webstore.ansi.org.

[25] David White, James D. Dunn, Alexandra C. Schmid, and Richard I. Kemp. Error rates in users of automatic face recognition software. *PLoS ONE*, 10:1–14, October 2015.

[26] Bradford Wing and R. Michael McCabe. Special publication 500-271: American national standard for information systems data format for the interchange of fingerprint, facial, and other biometric information part 1. Technical report, NIST, September 2015. ANSI/NIST ITL 1-2015.

[27] Andreas Wolf. Portrait quality - (reference facial images for mrtd). Technical report, ICAO, April 2018.

[28] D. Yadav, N. Kohli, P. Pandey, R. Singh, M. Vatsa, and A. Noore. Effect of illicit drug abuse on face recognition. In *2016 IEEE Winter Conference on Applications of Computer Vision (WACV)*, pages 1–7, Los Alamitos, CA, USA, mar 2016. IEEE Computer Society.

This publication is available free of charge from: https://doi.org/10.6028/NIST.IR.8271